NUREG/CR-5395
EPRI/NP-6480
BAW-2062
Vol. 4

Multiloop Integral System Test (MIST): Final Report

Test Group 32, SBLOCA With Altered Leak and HPI Configurations

Prepared by J. R. Gloudemans/B&W

Prepared for
U.S. Nuclear Regulatory
Commission
and
Electric Power Research Institute
and
Babcock & Wilcox Owners Group

AVAILABILITY NOTICE

Availability of Reference Materials Cited in NRC Publications

Most documents cited in NRC publications will be available from one of the following sources:

1. The NRC Public Document Room, 2120 L Street, NW, Lower Level, Washington, DC 20555

2. The Superintendent of Documents, U.S. Government Printing Office, P.O. Box 37082, Washington, DC 20013-7082

3. The National Technical Information Service, Springfield, VA 22161

Although the listing that follows represents the majority of documents cited in NRC publications, it is not intended to be exhaustive.

Referenced documents available for inspection and copying for a fee from the NRC Public Document Room include NRC correspondence and internal NRC memoranda; NRC Office of Inspection and Enforcement bulletins, circulars, information notices, inspection and investigation notices; Licensee Event Reports; vendor reports and correspondence; Commission papers; and applicant and licensee documents and correspondence.

The following documents in the NUREG series are available for purchase from the GPO Sales Program: formal NRC staff and contractor reports, NRC-sponsored conference proceedings, and NRC booklets and brochures. Also available are Regulatory Guides, NRC regulations in the *Code of Federal Regulations*, and *Nuclear Regulatory Commission Issuances*.

Documents available from the National Technical Information Service include NUREG series reports and technical reports prepared by other federal agencies and reports prepared by the Atomic Energy Commission, forerunner agency to the Nuclear Regulatory Commission.

Documents available from public and special technical libraries include all open literature items, such as books, journal and periodical articles, and transactions. *Federal Register* notices, federal and state legislation, and congressional reports can usually be obtained from these libraries.

Documents such as theses, dissertations, foreign reports and translations, and non-NRC conference proceedings are available for purchase from the organization sponsoring the publication cited.

Single copies of NRC draft reports are available free, to the extent of supply, upon written request to the Office of Information Resources Management, Distribution Section, U.S. Nuclear Regulatory Commission, Washington, DC 20555.

Copies of industry codes and standards used in a substantive manner in the NRC regulatory process are maintained at the NRC Library, 7920 Norfolk Avenue, Bethesda, Maryland, and are available there for reference use by the public. Codes and standards are usually copyrighted and may be purchased from the originating organization or, if they are American National Standards, from the American National Standards Institute, 1430 Broadway, New York, NY 10018.

DISCLAIMER NOTICE

NUREG/CR-5395
EPRI/NP-6480
BAW-2062
Vol. 4

Multiloop Integral System Test (MIST): Final Report

Test Group 32, SBLOCA With Altered Leak and HPI Configurations

Date Published: July 1989

Principal Author
J. R. Gloudemans

Major Contributors

ARC		NPD
D. P. Birmingham	T. F. Habib	G. O. Geissler
J. E. Blake	F. Karimi-Azad	K. W. Turner
H. R. Carter	C. G. Koksal	
M. T. Childerson	T. E. Moskal	
R. P. Ferron	G. C. Rush	

Prepared by

Babcock & Wilcox
Nuclear Power Division
3315 Old Forest Road
Lynchburg, VA 24506-0935

Babcock & Wilcox
Research and Development Division
Alliance Research Center
1562 Beeson Street
Alliance, OH 44601

Prepared for

Division of Systems Research
Office of Nuclear Regulatory Research
U. S. Nuclear Regulatory Commission
Washington, DC 20555
NRC FINs B8909, D1734

Electric Power Research Institute
P. O. Box 10412
Palo Alto, CA 94303

Babcock & Wilcox Owners Group
P. O. Box 10935
Lynchburg, VA 24506-0935

For sale by the Superintendent of Documents, U.S. Government Printing Office
Washington, D.C. 20402

ABSTRACT

The multiloop integral system test (MIST) is part of a multiphase program started in 1983 to address small-break loss-of-coolant accidents (SBLOCAs) specific to Babcock & Wilcox-designed plants. MIST is sponsored by the U.S. Nuclear Regulatory Commission, the Babcock & Wilcox Owners Group, the Electric Power Research Institute, and Babcock & Wilcox. The unique features of the Babcock & Wilcox design, specifically the hot leg U-bends and steam generators, prevented the use of existing integral system data or existing integral system facilities to address the thermal-hydraulic SBLOCA questions. MIST and two other supporting facilities were specifically designed and constructed for this program, and an existing facility -- the once-through integral system (OTIS) -- was also used. Data from MIST and the other facilities will be used to benchmark the adequacy of system codes, such as RELAP-5 and TRAC, for predicting abnormal plant transients.

The MIST program is reported in 11 volumes. The program is summarized in Volume 1; Volumes 2 through 8 describe groups of tests by test type; Volume 9 presents inter-group comparisons; Volume 10 provides comparisons between the calculations of RELAP5 MOD2 and MIST observations, and Volume 11 presents the later, "Phase 4" tests. This is Volume 4, pertaining to Test Group 32, Altered Leak and HPI Configurations. The specifications, conduct, observations, and results of these tests are described herein.

CONTENTS

Contents (Cont'd)

List of Tables

List of Figures

Figures (Cont'd)

Figures 5.2.21 through 5.2.30: 0 to 80 Minutes

Figures 5.2.31 through 5.2.34: 0 to End of Test

Figures (Cont'd)

Figures (Cont'd)

Figures (Cont'd)

Figures (Cont'd)

EXECUTIVE SUMMARY

Introduction

The multiloop integral system test (MIST) was a scaled 2-by-4 (2 hot legs and 4 cold legs) physical model of a Babcock & Wilcox (B&W), lowered-loop, nuclear steam supply system (NSSS). MIST was designed to operate at typical plant pressures and temperatures. Experimental data obtained from this facility during post-small-break loss-of-coolant accident (SBLOCA) testing are used for computer code benchmarking. The MIST interactions are of intrinsic interest because they may provide insight into expected plant behavior. MIST was necessarily atypical of a plant in certain important respects, however. The MIST interactions therefore are not to be applied directly to a plant.

MIST consisted of two 19-tube, once-through steam generators, a reactor, a pressurizer, 2 hot legs, and 4 cold legs with scaled reactor coolant pumps. Other loop components included a closed secondary system, 4 simulated reactor vessel vent valves (RVVVs), a pressurizer power-operated relief valve (PORV), hot leg and reactor vessel upper head vents, high-pressure injection (HPI), core flood system, and critical flow orifices for scaled leak simulation. Guard heaters, used in conjunction with passive insulation to reduce model heat loss, were used on all primary system components as well as the steam generator secondaries. MIST is illustrated in Figure 1.

Boundary Systems

The MIST boundary systems were sized to power-scale the plant boundary conditions. HPI and auxiliary feedwater (AFW) characteristics were based on composite plant characteristics. Scaled model vents were included in both hot legs and in the reactor vessel upper head. Leaks were located in the cold leg suction and discharge piping, and the upper and lower elevations of steam generator B (for tube rupture simulation). The desired vent and leak flows were obtained using power-scaled restrictors.

Heat Losses and Guard Heaters

MIST was designed to minimize heat losses from the reactor coolant system. Fin effects (instrument penetrations through the insulation) were minimized by using 1/2-inch penetrations for most of the instrumentation. Heat losses due to conduction through component supports were minimized by designing the supports to reduce the cross-sectional area and placing insulating blocks between load-bearing surfaces. The reactor coolant system piping and vessels were covered with passive insulation, active insulation (or guard heaters), and an outer-sealed jacket (to prevent chimney effects). The guard heaters were divided into 42 zones, each controlled by a zonal temperature difference and pipe metal temperature.

Instrumentation

MIST had approximately 850 instruments. These instruments were interfaced to a computer-controlled, high-speed data acquisition system. MIST instrumentation consisted of measurements of temperature, pressure, and differential pressure. Fluid level and phase indications were provided by optical viewports, conductivity probes, differential pressures, and gamma densitometers. Mass flow rates at the system boundaries were measured using Coriolis flowmeters and weigh scales. Loop mass flow rates were measured using venturis or turbines.

Transient Test Program

The MIST transient tests were defined to generate integral system data for code benchmarking. The transient test series was divided into the following seven groups:

- Mapping
- Boundary systems
- Leak and HPI configurations
- HPI-PORV cooling (feed and bleed)
- Steam generator tube rupture
- Noncondensible gas (NCG) and venting
- Reactor coolant pump (RCP) operation

The mapping tests were intended to examine the initial post-SBLOCA transient interactions. In these tests, the primary system inventory was carefully controlled and slowly varied to allow the examination of the normally rapid and overlapping post-SBLOCA events.

The leak and HPI configurations were varied singly in Test Group 32. Each of these tests was based on the nominal boundary system characteristics of Test Group 31. These nominal characteristics included a scaled 10-cm^2 cold leg B1 leak; full HPI capacity; automatic and independent RVVV actuation on differential pressure; automatic guard heater control; constant steam generator level control, after the initial refill of the secondary sides; and symmetric steam generator cooldown based on the difference between the core-exit fluid temperature and the steam generator secondary saturation temperature.

Two off-nominal leak sizes were tested in Group 32, a scaled 5-cm^2 leak and a scaled 50-cm^2 leak. The (10-cm^2) leak location was also varied in two tests, namely cold leg suction rather than discharge and a PORV break. In one test, the leak was isolated at the time perceived to be least desirable, i.e. when the hot leg levels were below the U-bend spillover elevation but above the steam generators. Half-capacity HPI was used in the sixth and final test of Group 32. The base test to which the Group 32 Tests are to be compared is the Nominal Repeat Test of Group 31, Test 311000.

The leak size variations demonstrated a variety of primary system depressurization mechanisms. The loop remained full throughout most of the 5-cm^2 leak transient. The primary system was cooled through continuing single-phase natural circulation heat transfer. The primary system was depressurized primarily through the automatic throttling of the high-pressure injection flow rate to maintain a subcooling margin of 75F at the core exit. Several modes of depressurization were encountered with a 10-cm^2 break. The most persistent mode was through the HPI condensation of the core steam production coupled with leak-HPI cooling. The 50-cm^2 leak transient, on the other hand, depressurized directly through the break volumetric discharge.

The test transients with varied leak locations were quite similar. HPI-leak cooling was operative with the cold leg suction break. This cooling mechanism offset core power by discharging relatively warm fluid out the break.

The subcooled HPI fluid was heated as it condensed core steam (transported to the downcomer through the RVVVs). The relatively warm fluid frequently traversed the cold leg piping in liquid-liquid counterflow; that is, the warmer fluid travelled backward along the top of the sloping cold leg discharge piping and the HPI-cooled fluid flowed forward along the bottom. One loop remain d full and the core exit fluid remained subcooled with the simulated PORV break. The primary system thus depressurized through the PORV volumetric discharge, primary-to-secondary heat transfer in the full loop plus intermittent activity in the voided loop, and HPI throttling to maintain the core exit fluid subcooling margin.

The isolated leak test repeated the boundary system controls of the Nominal Repeat Test (311000) until leak isolation at 30 minutes. The initial transients were virtually identical. Upon leak isolation, the primary system abruptly began to refill and to repressurize. The repressurization was halted when the hot leg levels achieved the U-bend spillover elevation and a two-loop cooldown began.

The cold leg discharge piping voided in the test using half-capacity HPI. The break mass flow rate thus decreased towards the HPI flow rate, and the vapor discharged by the break offset the decreased condensation capability of the reduced HPI flow rate. This interaction was an example of the inherent system resiliency observed repeatedly in Test Group 32. The system conditions generally realigned to offset imposed boundary system changes. In each test, the primary system ultimately depressurized, the total primary system fluid mass stabilized and began to increase, and the core remained cooled.

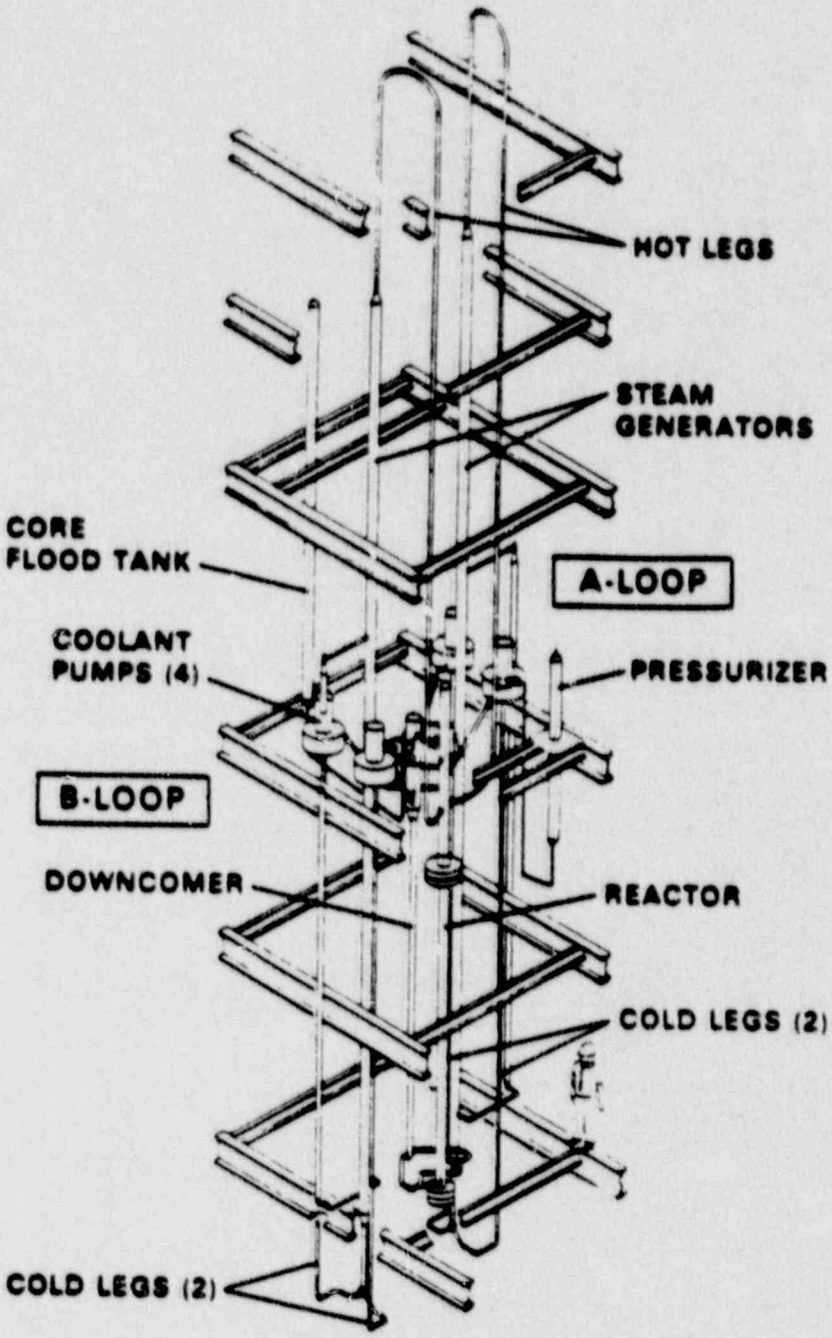

Figure 1. Reactor Coolant System -- Multiloop Integral System Test (MIST)

1. INTRODUCTION

The multiloop integral system test (MIST) was a scaled 2-by-4 (2 hot legs and 4 cold legs) physical model of a Babcock & Wilcox (B&W), lowered-loop, nuclear steam supply system (NSSS). MIST was sponsored by the U.S. Nuclear Regulatory Commission, the B&W Owners Group, the Electric Power Research Institute, and B&W. The MIST results are presented in the following eleven volumes:

1. Summary
2. Mapping Tests, Group
3. SBLOCA Tests With Varied Boundary Conditions, Group 31
4. SBLOCA Tests With Altered Leak and HPI Configuration, Group 32
5. HPI-PORV Cooling Tests, Group 33
6. Steam Generator Tube Rupture Tests, Group 34
7. Noncondensible Gas and Venting Tests, Group 35
8. Pump Operation Tests, Group 36, and Core Uncovery Test 3801
9. Inter-Group Comparisons
10. RELAP5/MOD2 Calculations Versus MIST Observations
11. Phase 4 Tests

The Group 32 tests with altered leak and HPI configurations are reported herein.

The MIST design, features, and instruments are outlined in section 2. The Group 32 Test Specifications are provided in section 3; the six tests of Group 32 varied the leak and HPI configurations. The following configurations were examined singly:

Leak size

Leak location

Leak isolation status

HPI capacity

The control of these tests as well as instrument performance is described in section 4. Section 5 provides a brief narrative description of each test, inter-test comparisons, and a summary of major observations. The base test for Group 32 is the Nominal Repeat Test from Group 31; this test is described in detail in section 5.2. The observations are summarized in section 5.7. Key data plots are provided with each test. A complete plot set for each test is provided in the enclosed microfiche; these plots are indexed in Appendix A of Volume 9.

The six tests of Group 32, as well as Repeat Nominal SBLOCA Test 3110, are summarized in Figures 1.1 through 1.7. The key events and timing of each test are shown on traces of primary system pressure versus primary system total fluid mass.

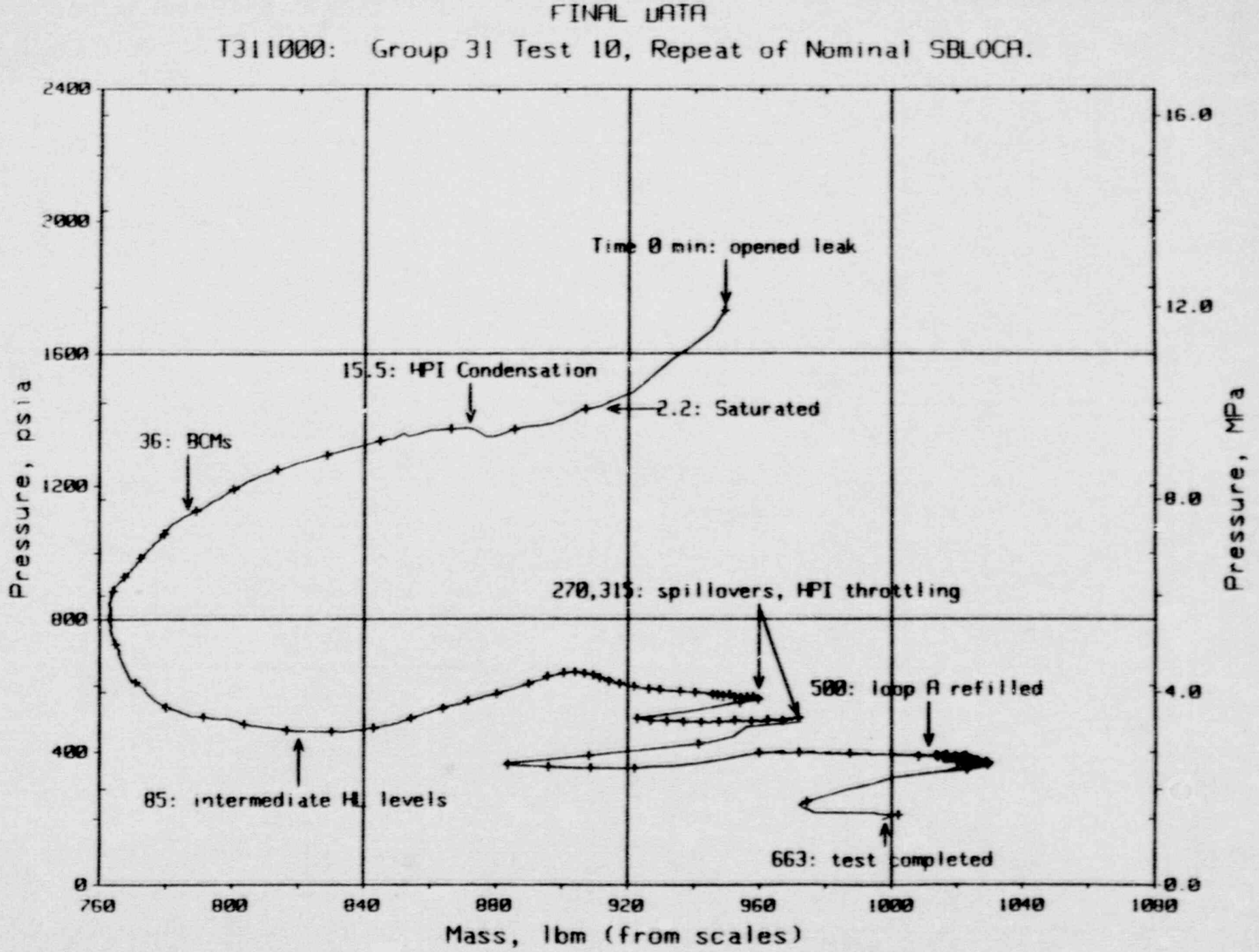

Figure 1.1 Primary System Pressure Vs Primary System Total Fluid Mass

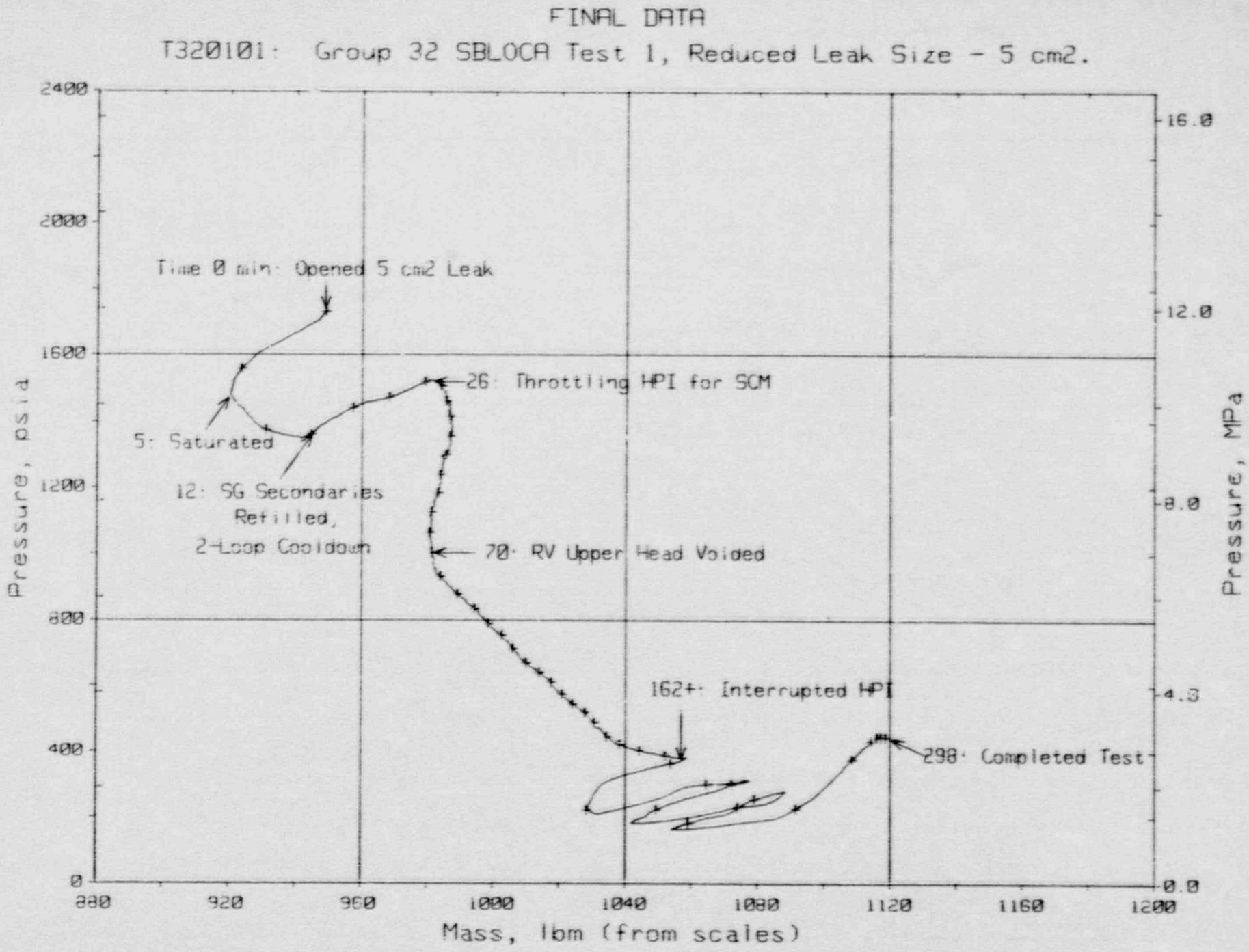

Figure 1.2 Primary System Pressure Vs Primary System Total Fluid Mass

Fri Aug 19 09:09:27 1988

PPvPM

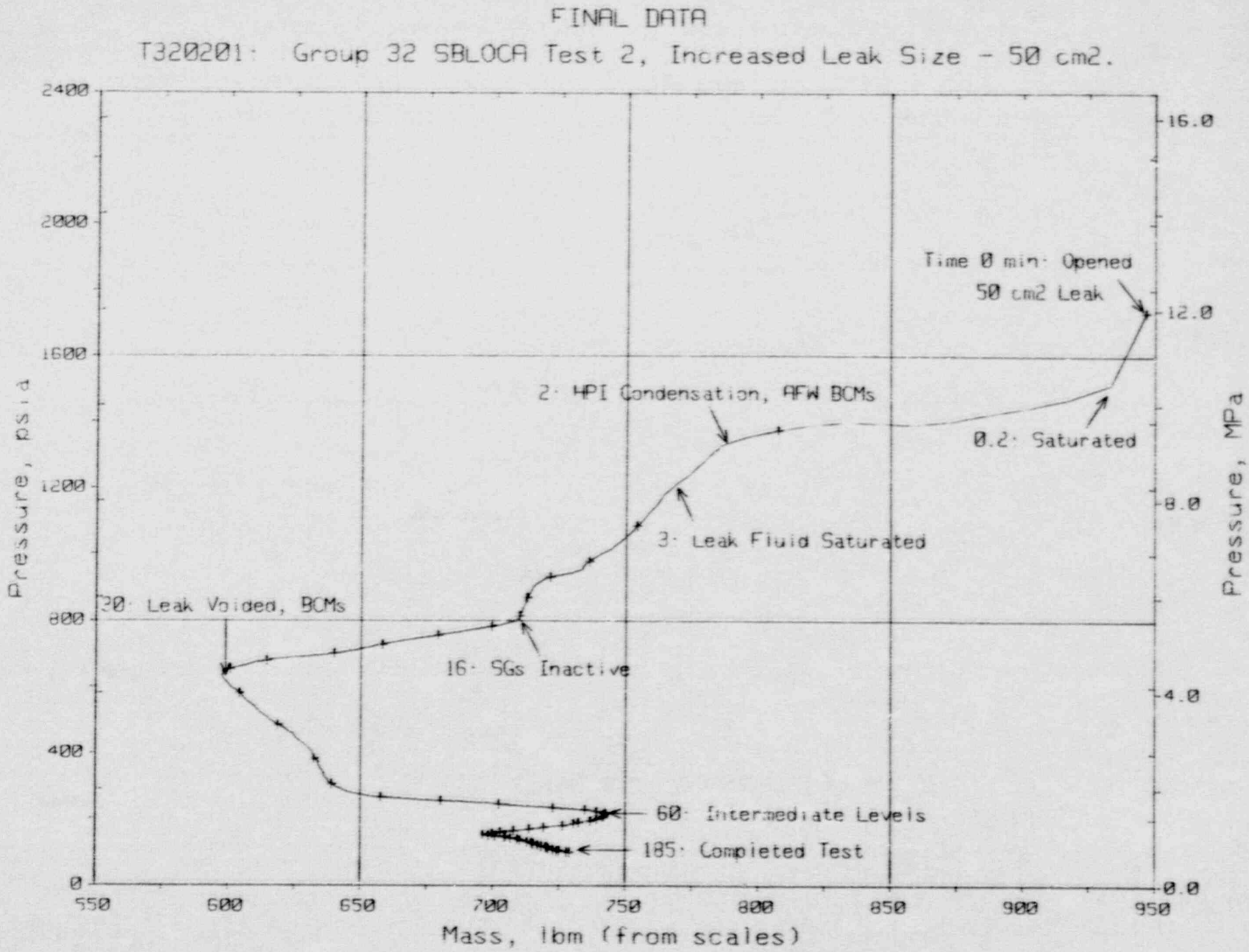

Figure 1.3 Primary System Pressure Vs Primary System Total Fluid Mass

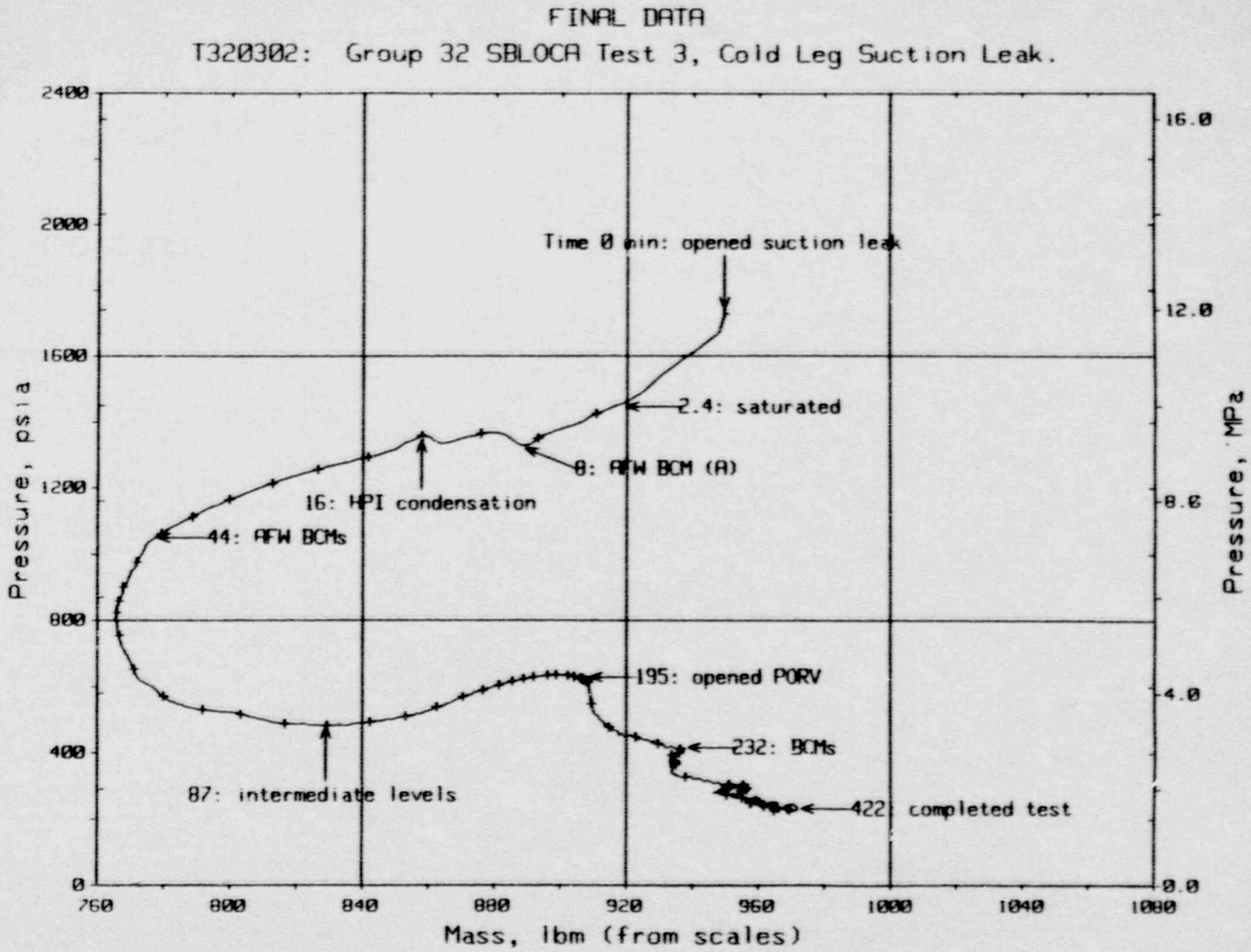

Figure 1.4 Primary System Pressure Vs Primary System Total Fluid Mass

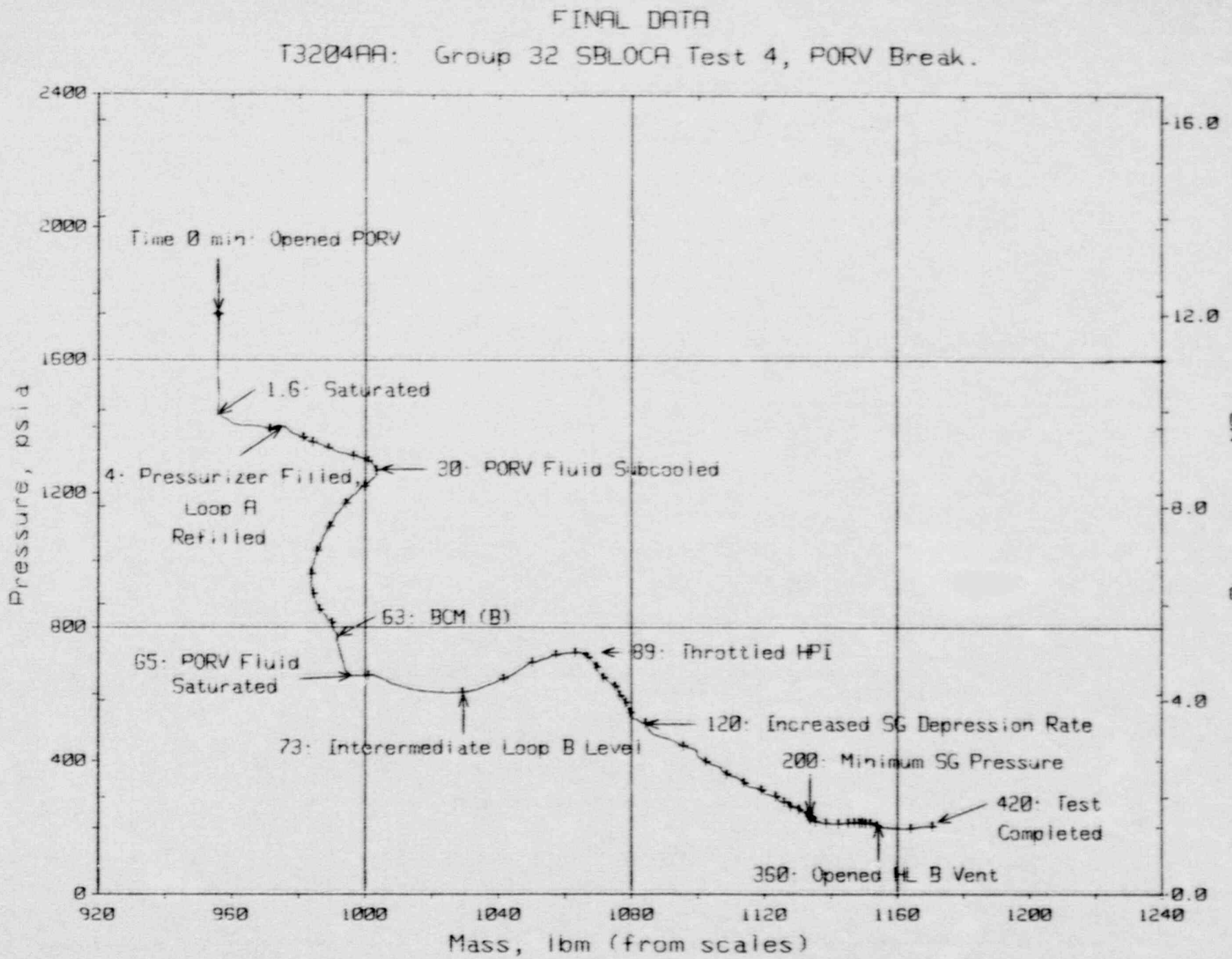

Figure 1.5 Primary System Pressure Vs Primary System Total Fluid Mass

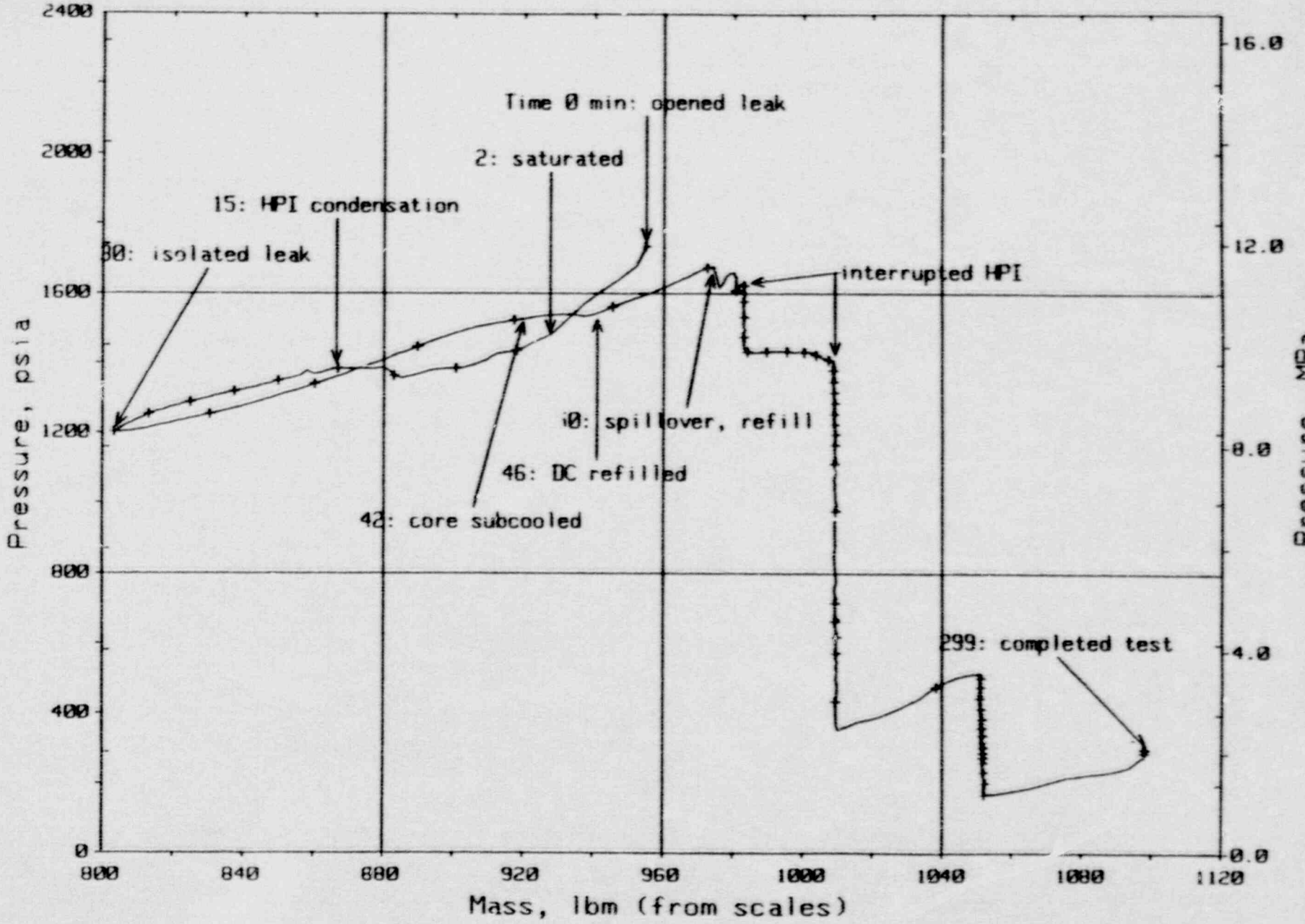

Figure 1.6 Primary System Pressure Vs Primary System Total Fluid Mass

Tue May 3 15:14:41 1988

PPvPM

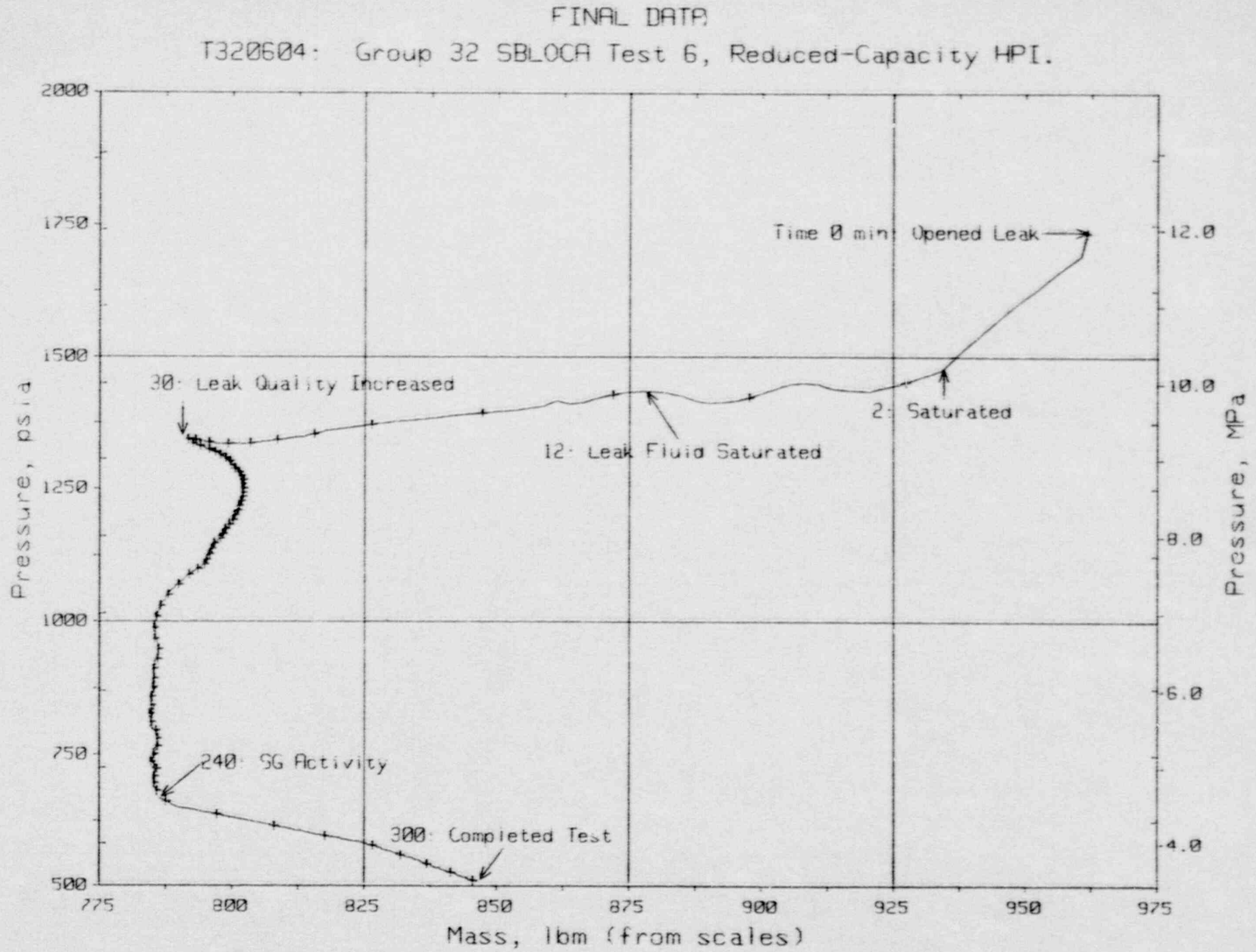

Figure 1.7 Primary System Pressure Vs Primary System Total Fluid Mass

Fri Aug 19 08:34:09 1988

PPvPM

2. FACILITY DESCRIPTION

2.1. Introduction

MIST was a scaled, 2-by-4 (2 hot legs and 4 cold legs) model of a B&W, lowered-loop, nuclear steam supply system (NSSS). MIST was designed to operate at typical plant pressures and temperatures. Experimental data obtained from this facility during post-SBLOCA testing are used for computer code benchmarking.

The reactor coolant system of MIST was scaled according to the following criteria, listed in order of decreasing priority: elevation, post-SBLOCA flow phenomena, component volume, and irrecoverable pressure drop. MIST consisted of two 19-tube, once-through steam generators; reactor; pressurizer; 2 hot legs; and 4 cold legs, each with a scaled reactor coolant pump.

Other loop components in MIST included a closed secondary system, 4 simulated reactor vessel vent valves (RVVVs), a pressurizer power-operated relief valve (PORV), hot leg vents and reactor vessel upper-head vents, high-pressure injection (HPI), core flood system, and critical flow orifices for scaled leak simulation. Guard heaters, used in conjunction with passive insulation to reduce model heat loss, were included on the steam generator secondaries and on all primary coolant components. The system was also capable of noncondensible gas addition at selected loop sites.

The approximately 850 MIST instruments were interfaced to a computer-controlled, high-speed data acquisition system. MIST instrumentation consisted of measurements of temperature, pressure, and differential pressure. Fluid level and phase indications were provided by optical viewports, gamma densitometers, conductivity probes, and differential pressures. Mass flow rates in the circulation loop were measured using venturis and a cooled

thermocouple, and at the system boundaries using Coriolis flowmeters and weigh scales.

2.2. MIST Design

MIST was a scaled, full-pressure, experimental facility arranged to represent the B&W lowered-loop plant design. Like the plant, MIST was a 2-by-4 arrangement with 2 hot legs and 4 cold legs, as shown in Figure 2.1. MIST was designed for prototypical fluid conditions, with emphasis on being leak-tight and minimizing heat loss.

The scaling of MIST followed the approach and priorities used for OTIS[1]: that is, elevation, post-SBLOCA phenomenon, component and piping volumes, and irrecoverable pressure losses. MIST retained full plant elevations throughout the primary system and the steam generator secondaries. Only the elevations of several non-flow regions were compromised, primarily to optimize power-to-volume scaling. Key interfaces were maintained -- these included the hot leg U-bend spillover, upper and lower tubesheets of the steam generator (secondary faces), cold leg low point, pump discharge, cold and hot leg nozzles, core (throughout), and points of emergency core cooling system (ECCS) injection.

Two-phase behavior during voiding of the hot leg U-bend and flow interruption was sufficiently prototypical; that is, both the plant and the model were expected to encounter phase separation early in the post-SBLOCA transient. The MIST hot leg pipes were large enough to admit bubbly flow.

Fluid volume was 40% larger than power-to-volume scaling would dictate; the hot legs, cold legs, and upper downcomer were oversized. This atypicality was imposed by the previously described two-phase requirements and by considering component irrecoverable pressure losses. The excess volume of the hot leg slowed the rate of level decrease for power-scaled draining and similarly retarded the rate of level increase for power-scaled injection. Although the excess volume of loop fluid delayed system heatup and cooldown, this effect was usually minor compared to the long-term impact on system energy of leak-HPI cooling. The concentration of excess volume in the piping runs decreased fluid velocities in the hot legs and cold legs and therefore

lengthened the transit time of loop fluid. Irrecoverable pressure drops were well preserved.

The MIST core and steam generators were full-length subsections of their plant counterparts. As shown on Figure 2.2, the core consisted of a 7-by-7 array of 45 full-length, 0.430-inch-diameter heater rods and four simulated incore guide tubes. Plant-typical fuel pin pitch and grid geometry were used. The simulated rods were capable of full-scale power output but were limited to approximately 10% of scaled power for the planned MIST testing. (The ratio of plant power to MIST power was 817:1.) A fixed, axial heat flux profile and a flat, radial heat flux profile were used. The axial peak-to-average flux ratio was 1.25:1.

The steam generators, shown in Figure 2.3, each contained 19 full-length tubes. The tubing diameter (5/8-inch OD), material, and triangular pitch of the tube bundle (7/8 inch, tube centerline to centerline) were prototypical. The geometry of the tube support plates (TSPs) was similar to that of the plant TSPs and provided equivalent flow areas and irrecoverable pressure losses. The MIST steam generators contained 16 TSPs, versus 15 in the plant. The flow holes of the MIST TSPs were drilled rather than broached. Also, the thicknesses of the MIST and plant steam generator tubesheets were unequal.

The hot legs used 2.5-inch, schedule-80 piping (2.32-inch ID). This diameter admitted bubbly flow and approximated the irrecoverable pressure loss of a plant hot leg. With the schedule-80 piping, the metal-to-fluid volume ratio in MIST was only 20% greater than that of the plant. The horizontal runs in the hot leg were approximately 1 foot long to accommodate the gamma densitometers. The pipe diameters of the hot leg U-bends maintained the pipe diameters of the hot leg risers and stubs. The radii of curvature of the hot leg U-bends were 1.61 ft. This curvature was chosen to match the horizontal displacement between the riser and stub while preserving the elevation of the U-bend spillover and approximating a power-scaled U-bend volume. Phase separation at the U-bend was predicted to occur at and below approximately 18% of scaled full power in MIST, versus 8% in the plant.[2] Beyond the U-bend, the hot leg piping in the model extended 12 feet, versus 1.5 feet in the plant, to span the height of the inlet plenum for the plant steam generator.

The four cold legs preserved elevation throughout. Two-inch, schedule-80 piping (1.939-inch ID) was used primarily to match irrecoverable pressure drop. This piping size also preserved the cold-leg Froude number, which influenced the mixing of the HPI and RVVV fluid streams. The cold leg horizontal piping runs were shortened, but the slope of the plant cold leg discharge piping was approximately maintained. HPI was injected into the sloping pipes at the appropriate elevation; the diameter of the model HPI nozzle was selected to preserve the ratio of fluid momentum between the cold leg and HPI.

A model reactor coolant pump was mounted in each cold leg. Suction and discharge orientations were prototypical. The pumps delivered single-phase scaled flows at plant-typical heads, allowed for simulated pump bumps by matching the plant pump spinup and coastdown times, and permitted operation under single- and two-phase conditions. The specific speeds of the model pumps were only one-tenth of those of the plant pumps. Therefore, the two-phase characteristics of the model pumps did not simulate those of the plant pumps.

The MIST reactor vessel employed an external annular downcomer. Inter-cold leg coupling was restricted toward that of a plant by using fins in the downcomer annulus to form quadrants, as shown in Figure 2.4. The annular gap was 1.4 inches and the gap at each fin was 0.4 inches. Each downcomer quadrant was connected to a separate RVVV simulation and a cold leg. The two core flood tank nozzles were each located at an interface between two downcomer quadrants.

The geometry of the model downcomer was annular down to the elevation of the top of the core. Just above the top of the core, the downcomer was gradually reconfigured to form a single pipe for the remaining elevation. The lower downcomer region obtained approximately the power-scaled fluid volume over the elevation of the core. Four model RVVVs were used to simulate eight plant valves. The MIST RVVVs could be controlled individually or in unison. Individual controllers provided automatic actuation of the valves on the upper plenum to downcomer-quadrant pressure differences. The MIST RVVVs thus approximated the head-flow response of the plant valves.[3] However, partially

open operation was not possible in MIST; therefore, the detailed valve dynamics of the plant swing check valves were absent.

The MIST pressurizer was power-to-volume scaled. It contained heaters, spray, and a PORV. The lower pressurizer elevations were prototypical, as were those of the surge line. The model pressurizer height was reduced from that of the plant to increase its diameter, thus lessening atypical fluid stratification and the likelihood of spray impinging on the vessel wall.

One core flood tank was used in MIST. This tank was power-to-volume scaled to represent the two plant tanks. The model tank was installed vertically, with the bottom of the tank at a prototypical elevation. The injection line from the tank to the nozzles on the downcomer was sized to preserve plant-typical irrecoverable losses, and the nozzles were sized to maintain the plant ratio of (core-flood) injected fluid momentum to the downcomer fluid momentum.

2.3. Boundary Systems

The MIST boundary systems were sized to power-scale the plant boundary conditions. HPI and auxiliary feedwater (AFW) head-flow characteristics were based on composite plant characteristics. Model vents were included in both hot legs and in the reactor vessel upper head. Controlled leaks were located in the cold leg suction and discharge piping and at the upper and lower elevations of steam generator B (for tube rupture simulation). The desired vent and leak flow rates were obtained using critical flow orifices of power-scaled areas.

A steam generator tube rupture was simulated by opening a flow circuit across either the upper or the lower tubesheet of steam generator B. This circuit is shown in Figure 2.5. It consisted of a flow control orifice, isolation valves, and measurements of fluid temperature and differential pressure. The tube rupture simulation flow circuit did not preserve the complex flow path geometry of an actual tube rupture.

2.4. Heat Losses and Guard Heaters

MIST was designed to minimize heat losses from the reactor coolant system. Fin effects (instrument penetrations through the insulation) were minimized by using 1/4-inch penetrations for most of the instrumentation. Heat losses

due to conduction through component supports were minimized by designing the supports to reduce the cross-sectional area and by placing ceramic blocks between load-bearing surfaces. The reactor coolant system piping and components were covered with passive insulation, guard heaters, and a sealed outer jacket (to prevent chimney effects). The insulation arrangement is illustrated in Figure 2.6. The guard heaters were divided into 42 zones, each controlled by a zonal temperature difference and a pipe metal temperature. This system provided differential temperature control as a function of temperature. A detailed finite-difference analysis of the insulation system indicated that heat loss was strongly dependent on metal temperature and weakly related to fluid state. The control temperature difference required to minimize heat losses was determined experimentally at several loop temperatures.

However, the guard heaters did not compensate for all the loop heat losses. For example, large local losses at the gamma densitometers and viewports were not compensated. Had these local losses been compensated, the requisite increased metal temperatures would have generated atypically large metal stored energies as well as undesirable local effects. The total MIST primary system heat loss at 650F was approximately 18 kW or 0.55% of scaled full power. The post-trip core power commonly simulated in MIST ranged from 3.5 down to 1% of scaled full power; the uncompensated heat losses of 0.55% of scaled full power thus represented from 16 to 55% of these post-trip power levels. Core power was increased to offset these uncompensated heat losses.

2.5. Instrumentation

The MIST instrumentation was selected and distributed based on the input from experimenters and code analysts. This instrument selection process considered the needs of code benchmarking, indications of thermal-hydraulic phenomena, and system closure.

The approximately 850 MIST instruments were interfaced to a computer-controlled, high-speed, data acquisition system. MIST instrumentation consisted of measurements of temperature, pressure, and differential pressure. Fluid level and phase indications were provided by optical viewports, conductivity probes, differential pressures, and gamma densitometers. Mass flow measurements at the system boundaries were made using Coriolis flowmeters and weigh

scales. Mass flow rate measurements in the loop were performed with venturis or turbines. Tables 2.1 and 2.2 provide a summary of the MIST instrumentation by component and instrument type.

The largest grouping of instrumentation was in the two steam generators. About 250, or 30%, of the instruments were located in these two components. The steam generator instrumentation provided for the measurement of fluid temperature, metal and differential temperature, total guard heater power, differential pressure, gauge pressure, and conductivity (for void determination). The allocation of instruments to the steam generators resulted from the judgement that observations of AFW wetting effects and steam generator heat transfer were of major importance. Several other local and multidimensional phenomena were also of considerable interest: noncondensible gas blanketing of primary tubes, intermittent radial advancement of condensation fronts in the region of the AFW nozzle, and boiler-condenser heat transfer in the region of the secondary pool.

The core and RVVV instrumentation measured fluid temperature, metal and differential temperature, total guard heater and core power, conductivity (for void determination), and gauge and differential pressures. The core instrument distribution concentrated on the axially varying parameters. A flat, radial heat flux profile was used in the core, and radial maldistribution of inlet flow was expected to result in only minor variations of enthalpy. Therefore, the majority of the incore temperature instrumentation was located in a single, interior flow channel. Radial temperature variations at the core outlet were recorded, but with a limited number of instruments. The core instrument allocation provided core heat input, inlet and exit fluid properties, and fluid gradients within the reactor vessel. In addition, collapsed levels and regional void fractions were available. The vent valve mass flow rates were obtained by synthesizing RVVV differential pressures, valve positions, and indications of fluid state.

Downcomer instruments measured fluid temperature, metal and differential temperature, total guard heater power, and differential pressures. Forty fluid thermocouples were concentrated in the upper downcomer, detailing mixing information for the RVVV, core flood, and cold leg fluid streams. Six additional fluid thermocouples were spaced uniformly in the lower downcomer

to indicate the extent of mixing as the fluid left the upper downcomer. The downcomer flow rate was measured using a venturi and a cooled thermocouple probe.

Table 2.1 MIST Instrumentation by Component

Component	Number of Instruments
Cold legs	164
Core flood	7
Hot legs	121
Pressurizer	25
Primary boundary systems	72
Reactor vessel and core	169
Steam generators	249
Steam generator feedwater and steam circuit	44
TOTAL	851

Table 2.2 MIST Instrumentation by Measurement Type

Measurement Type	Number of Instruments
Conductivity probes	36
Cooled thermocouple	12
Differential pressure	133
Differential temperature	42
Fluid temperature	381
Gamma densitometer	12
Limit switches	79
Mass flow	9
Metal temperature	69
Miscellaneous	17
Power	48
Pressure	9
Volumetric flow	4
TOTAL	851

Cold leg instrumentation provided fluid and metal temperatures, differential temperatures, total guard heater power, and differential pressures. Gamma densitometers indicated pump suction fluid density. Cold leg flow rates were measured using venturis located in the suction piping of each cold leg. For tests requiring full forced flow, turbine meters were used in place of the venturis. In addition, the reactor coolant pump power, speed, and head rise were measured. Thermocouple rakes were installed in the cold legs, upstream and downstream of the HPI injection points, to indicate thermal stratification and counterflow near the junctions of the cold legs and downcomer.

Hot leg instrumentation measured fluid and metal temperatures, differential temperatures, total guard heater power, and differential pressures. Void measurements using gamma densitometers and conductivity probes were also made. In addition, viewports provided visual data to assess the local flow regimes. The placement of the hot leg instruments provided detailed fluid temperature gradients, local void fractions, and overall collapsed level. A conductivity probe, combined with local differential pressures in the hot leg U-bend region, provided additional information regarding loop refill and spillover. Gamma densitometers in the hot leg horizontals, downstream of the reactor vessel outlet nozzles, and viewports at the 29-foot elevation and at the U-bend high points, provided information regarding fluid state and flow conditions. Viewports in the hot leg horizontals near the densitometers probed the developing flow regimes upstream of the hot leg risers.

The boundary systems, which included HPI, leaks, vents, and gas addition, were provided with fluid thermocouples, absolute and differential pressure transmitters, mass flowmeters, and weigh scales. These instruments provided mass and energy closure for the facility. Additional information regarding the design and instrumentation of MIST may be found in the Facility Specification[2] and in the Instrument Report.[4]

2.6. Conversion Factors

The key MIST conversion factors are listed below.

Power: 1% of scaled full power (2700. mW)

= 33. kW = 31.3 Btu/s

Primary Flow Rate (Total Primary System):

1% of scaled full flow (135. x 10^6 lbm/h)

= 0.46 lbm/s = 1660. lbm/h = 0.21 kg/s

Secondary Flow Rate (Total Secondary System, i.e., 2 steam generators)

1% of scaled full flow (11.3 x 10^6 lbm/h)

= 0.0384 lbm/s = 138. lbm/h = 0.0174 kg/s

MIST piping was larger than power-to-volume scaled in consideration of two-phase phenomena and hydraulic losses. Whereas the plant-to-MIST power scaling factor was 817, the corresponding volume scaling factor was 620 for the total primary system volume (CFT excluded), and 600 for the primary system excluding the pressurizer.

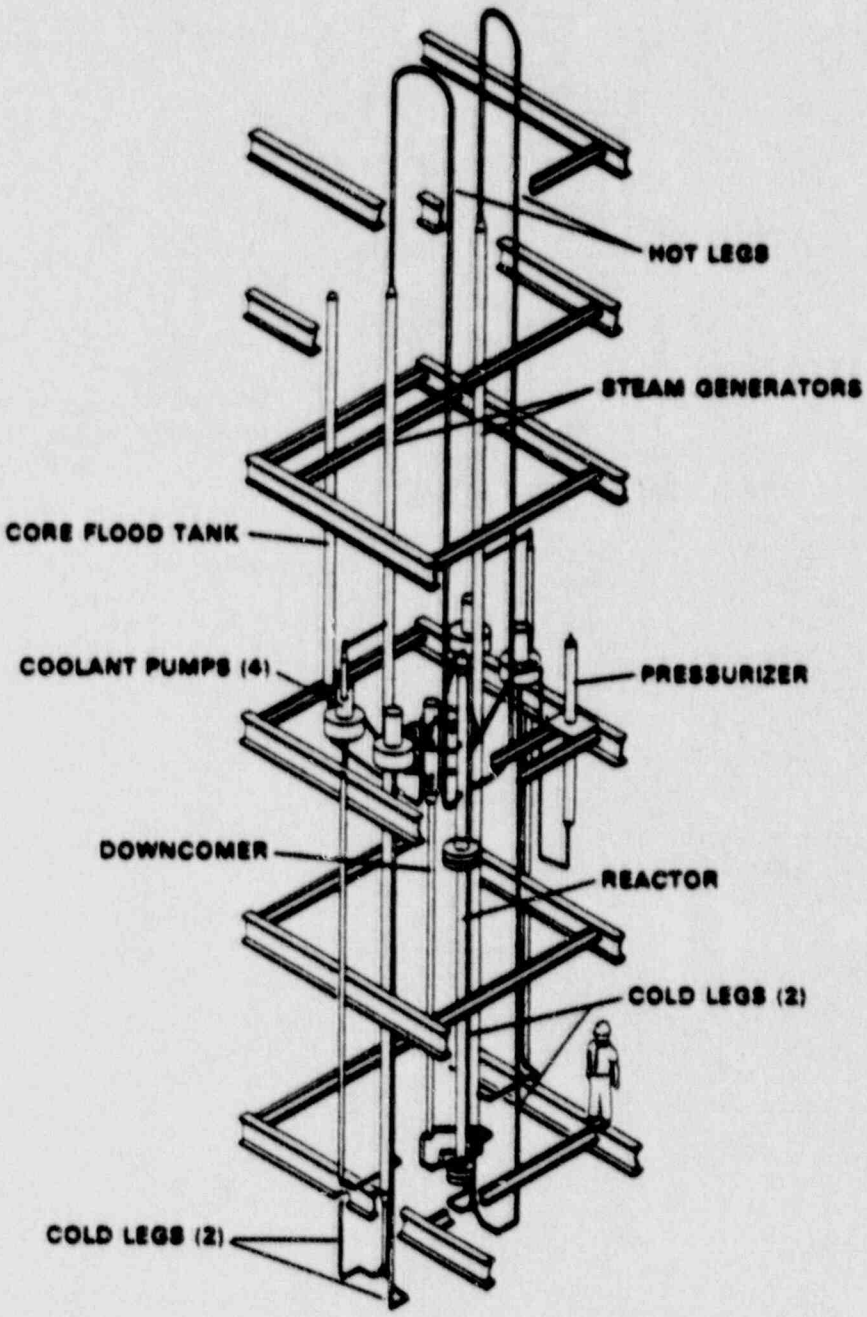

Figure 2.1. Reactor Coolant System -- MIST

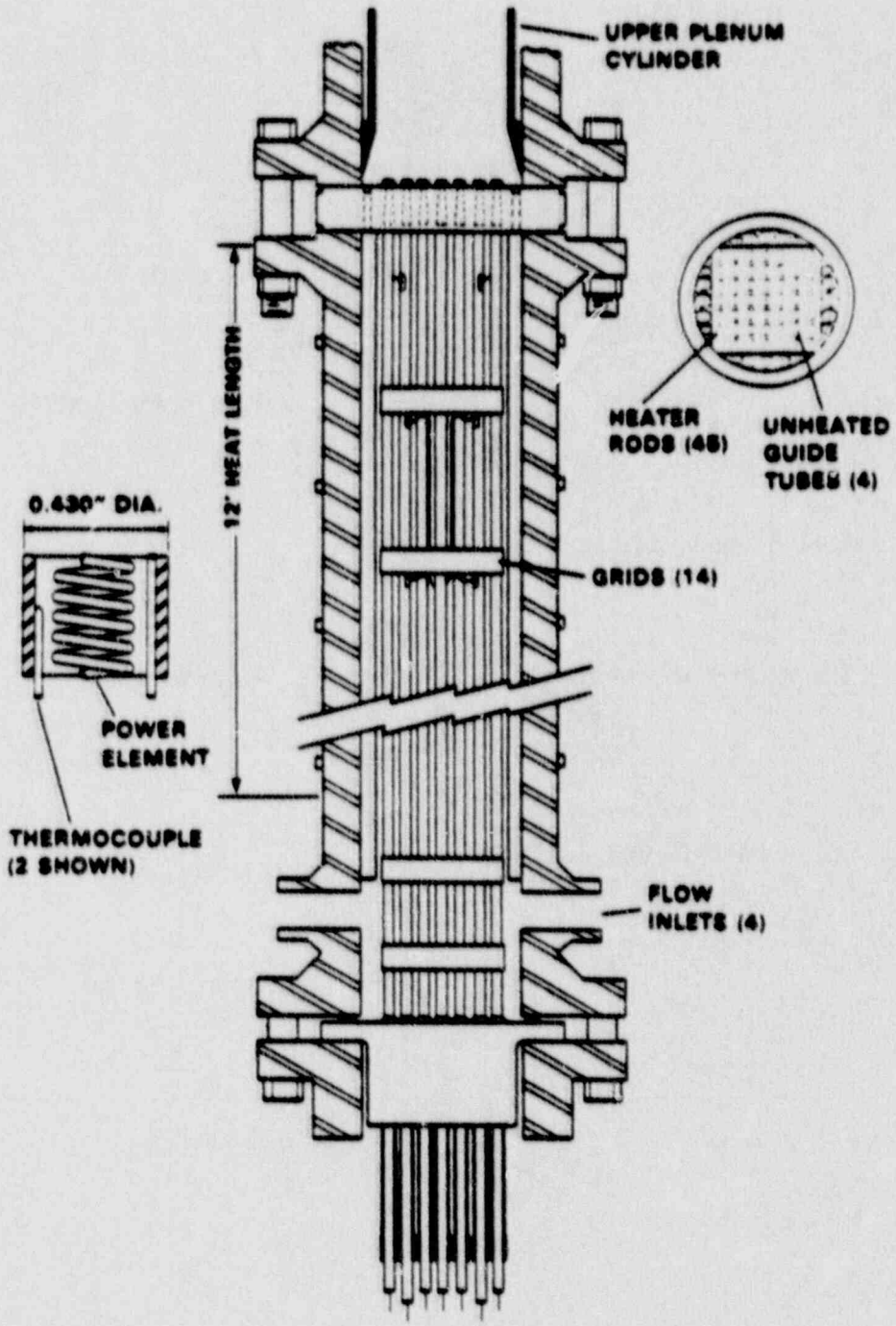

Figure 2.2. MIST Core Arrangement

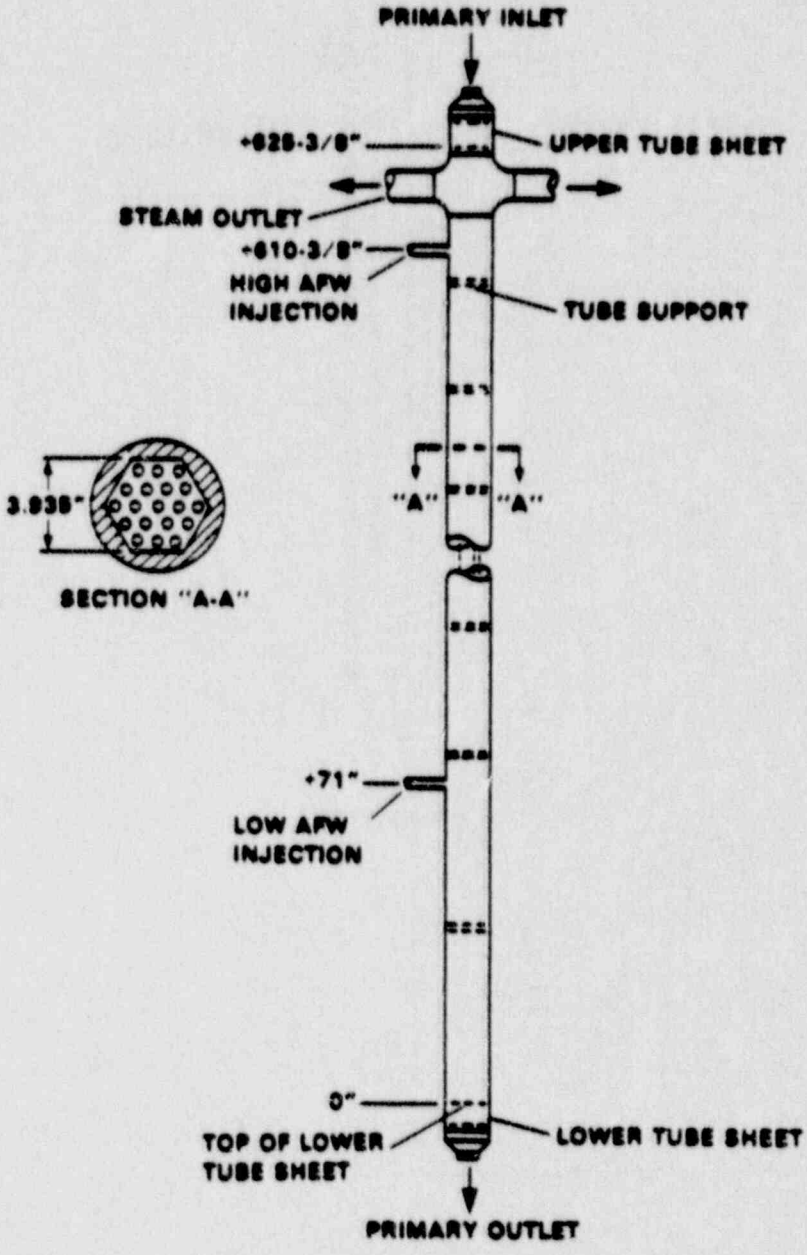

Figure 2.3. Nineteen-Tube, Once-Through Steam Generator

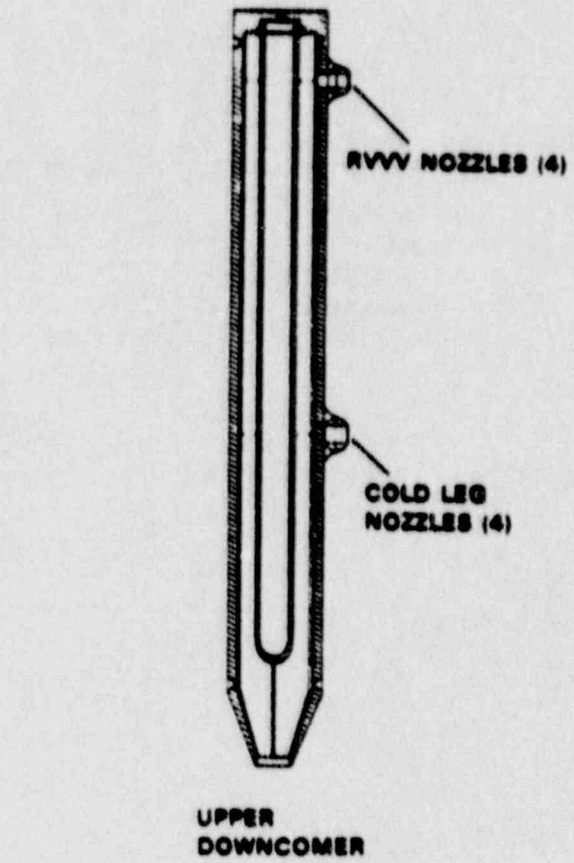

Figure 2.4. Upper Downcomer Arrangement

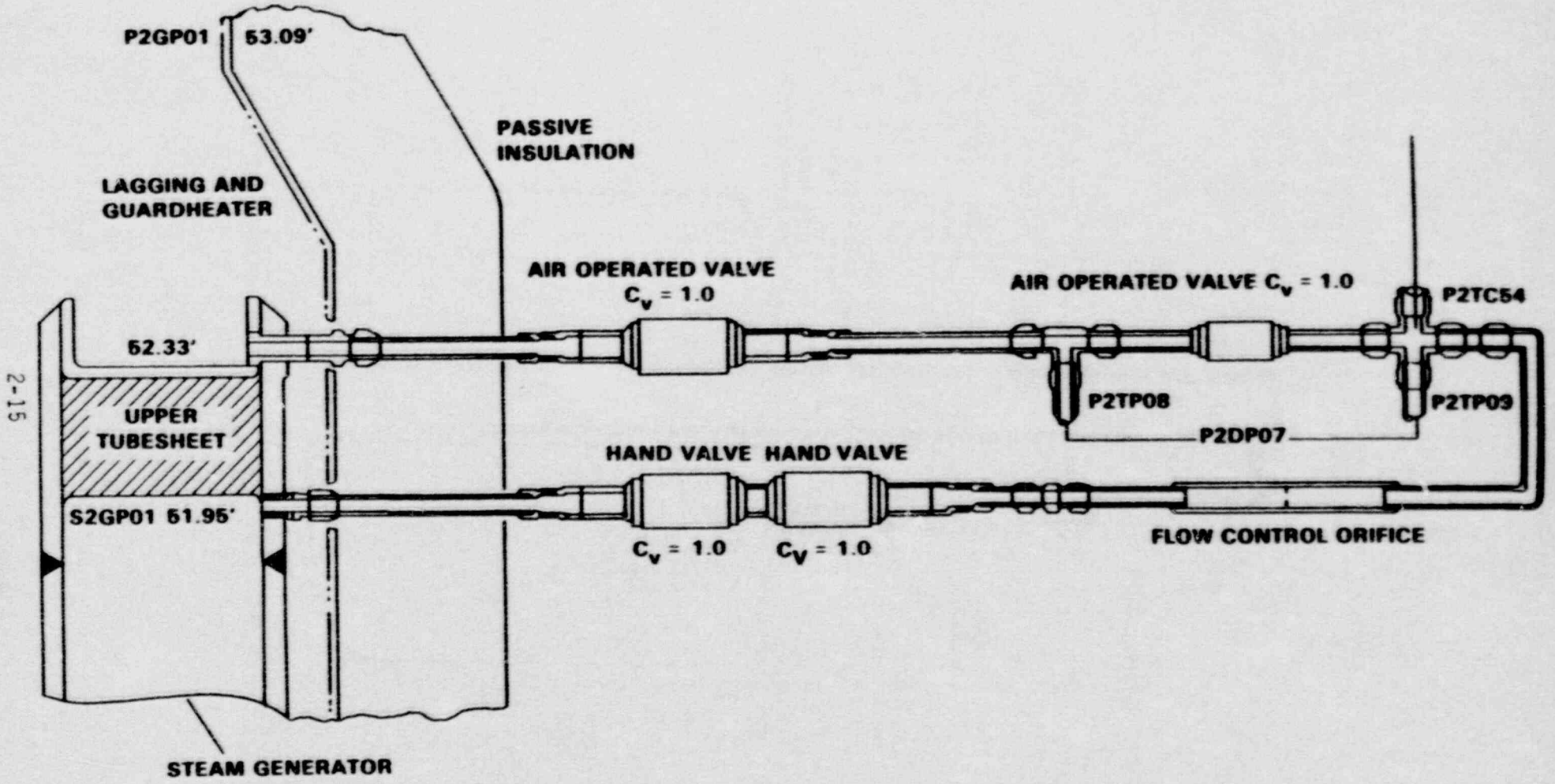

Figure 2.5 Primary-to-Secondary Tube Leak at Upper Tubesheet (Similar Arrangement at Lower Tubesheet)

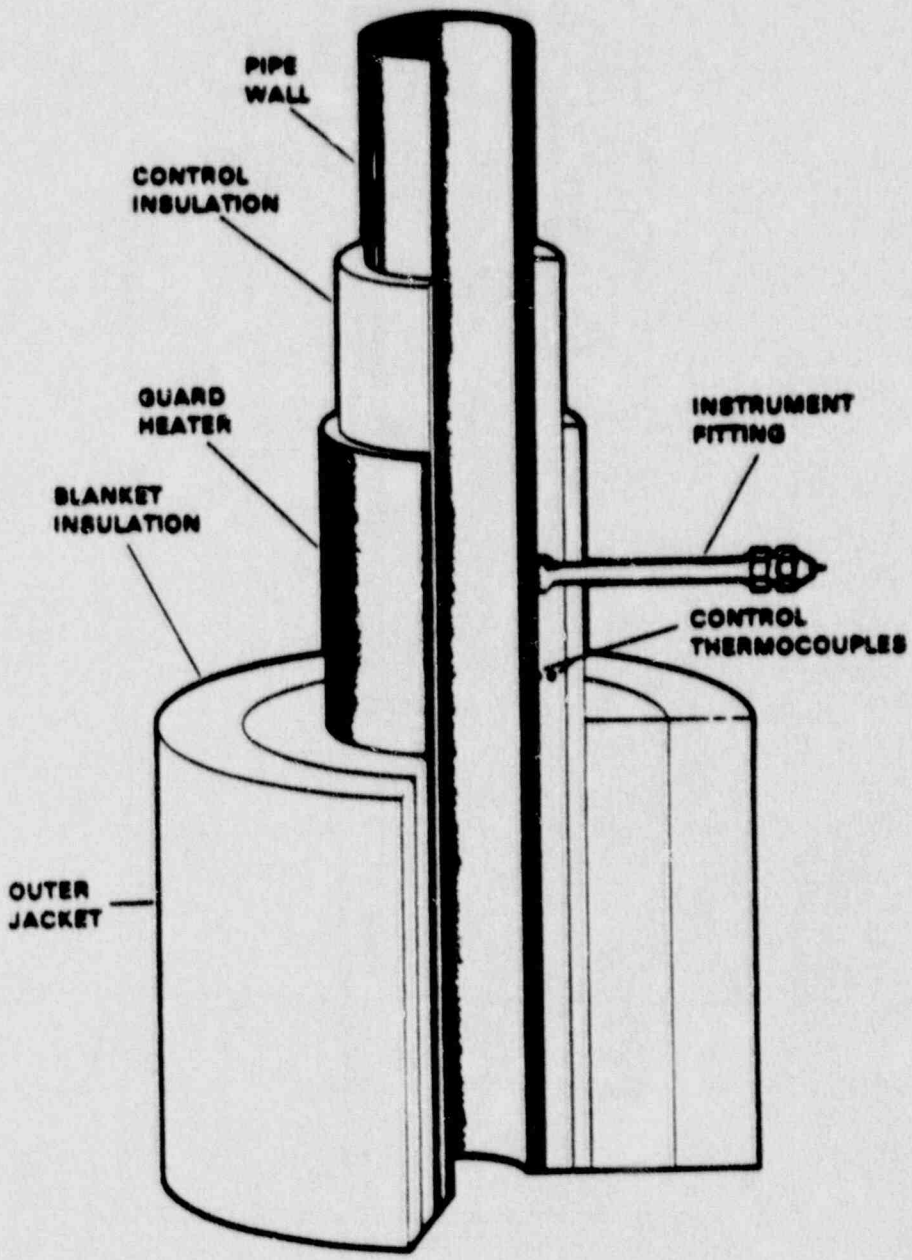

Figure 2.6 MIST Insulation Arrangement

3. TEST SPECIFICATIONS

The MIST Test Specifications[5] pertaining to the Group 32 leak and HPI configuration tests are excerpted herein. These specifications were formulated before testing, as is reflected by their tense. Test 4 (320402) was replaced by the retest numbered "3204AA," and this numbering change has been made herein.

3.1. Introduction

The leak and HPI characteristics are varied in Test Group 32. These six tests are summarized in Table 3.1.1. Section 3.1.1 presents conditions to be encountered during the Nominal Test. The variations imposed in the Group 32 tests are outlined in section 3.1.2. Subsequent sections give the purpose, description, and conduct (specifications) of each of the tests.

Tests 1 and 2 (320101 and 320201) vary break size. Full HPI capacity is nominally to be used for both tests, but either full HPI capacity or evaluation model (EM) HPI capacity will be selected and used depending on observations drawn from the Nominal Test transient. The Repeat Nominal Test (311000) uses full HPI and a scaled 10-cm^2 (cold leg B1 discharge) break. Test 6 (320604) uses EM HPI and the same break configuration. The selection between full and EM HPI thus might logically be made by comparing the results of these two tests (and Test 320604 should be performed first in Group 32). The reduced HPI capacity of Test 6 may promote primary repressurization when the HPI flow rate is insufficient to condense all of the steam being produced in the core. However, the reduced HPI capacity of Test 6 may also cause an early boiler-condenser mode (BCM) and depressurization toward the leak-HPI mass flow rate equilibrium pressure. This equilibrium pressure will be lower than in the Nominal Test, therefore the repressurization following BCM may be suppressed in Test 6. The comparison of the results of Tests 311000 and 320604 with different HPI capacities should indicate the predominant

repressurization mechanism and, therefore, the HPI characteristics of greater interest. The test specifications are summarized in Table 3.1.2.

3.1.1. Conditions During the Nominal Repeat Test (311000)

The pre-test steady-state conditions obtain an initial leak fluid temperature of 550F at ~1750 psia system pressure. The primary quickly depressurizes upon leak initiation and may stabilize as the hot leg fluid saturates. At the initial hot leg temperature of ~595F, this plateau pressure is approximately 1500 psia. The leak fluid temperature is expected to vary little during the initial rapid depressurization. There is a wide range of possible leak fluid conditions after saturation. Should the leak site uncover early in the transient, the leak fluid will saturate at a relatively high system pressure. The leak flow rate is sufficiently depressed at saturation to cause the HPI flow rate to exceed the leak flow rate. HPI-leak cooling offsets only ~1-1/2% of scaled full power, however (with saturated liquid at the leak). This decay power level is not achieved until 30 minutes after reactor trip. Until this time, the primary system will repressurize during periods of interrupted primary-to-secondary heat transfer.

The primary may gradually depressurize following saturation, due to sustained primary-to-secondary heat transfer. Such coupling is predicted by the system codes, or, the system may depressurize rapidly, after a period of weak heat transfer, due to the initiation of the AFW-BCM or pool BCM. If the leak fluid temperature remains constant, refill will begin at ~1300 psia and 550F. But the leak fluid temperature will more likely cool, primarily in response to HPI cooling but also due to the decreasing primary pressure (and hence saturation temperature). When the primary depressurizes to the initial secondary temperature, the leak flow rate remains in excess of the HPI flow rate, therefore the primary continues to lose inventory. The power offset by HPI-leak cooling is almost 2-1/2% of scaled full power. This power level is achieved 4 minutes after trip, thus little primary repressurization is expected to occur upon interruptions of primary-to-secondary heat transfer.

The primary will depressurize toward secondary pressure with continued coupling. The HPI flow rate will finally exceed the leak flow rate at 650 psia, i.e., just above the pressure at which the core flood tank (CFT) first

actuates. Refill will probably be completed in this pressure range, from 600 to 700 psia.

3.1.2. Variations of Group 32

The Group 32 tests vary the leak and HPI mass flow rates and energy transfer balances. The reduced leak size test uses only half of the nominal leak flow rate. The interruption of loop flow may be thereby delayed. System refill may begin at a much higher pressure than nominal. The increased leak size test, on the other hand, is likely to encounter CFT actuation because of the imposed excess of leak over HPI flow rates. The leak location is changed (in Test 3) to vary the leak fluid temperature response to system conditions, as well as the impact of leak flow on inter-cold leg asymmetries. The PORV break (Test 4) will discharge vapor initially. Thus, the effects of increased HPI-leak cooling will be obtained, as well as an altered distribution of system inventory between the loop and the pressurizer. The break will be isolated in Test 5. HPI-leak cooling will thus be deleted, and relatively high primary system pressures will be encountered. Finally, the effects of reduced HPI capacity will be introduced in Test 6. Whereas the Nominal Test with full HPI may have begun to refill at ~700 psia, pressures below the CFT actuation pressure may be needed to begin refill with reduced HPI capacity.

Control changes are introduced late in the transients of two tests. In Test 4, PORV break, the steam generator secondary control pressure is abruptly reduced over the final 50 psi of the controlled pressure reduction to induce steam generator activity. HPI-PORV cooling rather than hot leg venting is used during the later stages of loop refill in Test 3, cold leg suction leak.

3.2. Reduced Leak Size, Test 1 (320101)

A reduced (5- versus 10-cm^2) cold leg B1 discharge leak is used in Test 1. Full HPI capacity is nominally to be used.

3.2.1. Purpose

The reduced leak size of Test 1 (320101) will provide integral-system data with a prolonged period of intermittent loop flow. The leak-HPI (mass flow rate) equilibrium pressure is expected to be much higher than nominal, but the power offset by HPI-leak cooling will be much less than usual at equilibrium. Test 1 will thus provide data with enhanced repressurizations during

periods of interrupted primary-to-secondary heat transfer. The interactions expected during this test are described further in the following paragraphs.

3.2.2. Description

The reduced leak size test, Test 1 (320101), uses a scaled 5-cm^2 cold leg B1 discharge leak, versus 10 cm^2 in the Nominal Test. The pressure at which the HPI flow rate equals the leak flow rate is now approximately 1700 psia, versus 650 psia nominally. (The leak flow rate was estimated using the Modified Burnell correlation[6] and an equilibrium plot, as has been described in the MIST Test Specifications.[5]) But the power offset by HPI-leak cooling is only ~1-3/4% of scaled full power, which is not achieved until 20 minutes of post- trip decay.

Test 1 may thus begin to refill at a relatively high system pressure, but will experience significant repressurizations when primary-to-secondary heat transfer is interrupted. Also, the initial portions of the Test 1 transient are likely to be prolonged, compared to those of the Nominal Test, simply because of the reduced imbalance between the initial HPI and leak flow rates.

3.2.3. Conduct

A 5-cm^2 (cold leg B1 discharge) leak is to be opened to initiate Test 1, rather than the 10-cm^2 leak used in the Nominal Test. The remaining Test Specifications for Test 1 are identical to those of the Nominal Test. Test 1 is to be completed within 10 hours.

Although full HPI capacity has been specified and discussed herein, either the full or the evaluation model HPI capacity will be selected for Test 1 based on the results of the Nominal Test.

3.3. Increased Leak Size, Test 2 (320201)

Test 2 uses a 50-cm^2 cold leg B1 discharge leak, versus 10 cm^2 nominally. Full HPI capacity is nominally to be used.

3.3.1. Purpose

Test 2 (320201) will provide data for a relatively large break size. The depressurization due to leak activation will be rapid and pronounced. Although the power offset by HPI-leak cooling will be much larger than usual, the greatly increased leak flow rate will obtain sufficient system

depressurization to trigger CFT actuation. Reverse heat transfer may also be encountered. Test 2 will thus generate data through interactions that are quite unlike those expected in the nominal transient. These interactions are discussed further in the following paragraphs.

3.3.2. Description

The actuation of a 50-cm^2 leak will quickly blow down the primary to saturation and interrupt loop flow. But the leak-HPI equilibrium pressure is much lower than the initial loop saturation pressure (~1500 psia),[5] and the power offset by the magnified leak discharge rate will far exceed core power; thus, the relatively rapid loop depressurization will continue. The cold leg B1 discharge leak site may void during this period. Immediately, the leak mass flow rate will drop to the low level characterizing the critical flow of vapor; simultaneously, the power offset by this discharge will increase due to the increased leak fluid enthalpy. At and below approximately 1300 psia, the leak flow rate decrease upon flashing at the leak site will cause the HPI flow rate to exceed the leak flow rate. This revised mass balance may force the leak site fluid back to the saturated liquid state so that the HPI-leak balance is again perturbed. Thus, the leak fluid state may fluctuate with the ongoing primary depressurization.

The rapid depressurization is likely to cause the secondary pressures to exceed the primary pressure. The attendant transfer of steam generator secondary (fluid and metal) energy to the primary will slow the rate of primary depressurization. But, as the primary and secondary pressures equilibriate, the MIST steam generator secondary pressure control system will initiate a rapid depressurization of the steam generator secondaries (at about 50 psi/m) to reestablish a primary-to-secondary temperature difference. The primary depressurization will thus proceed largely unimpeded by reverse heat transfer. (The MIST steam generator secondary pressure control system is designed to maintain a positive primary-to-secondary temperature difference, simulating ATOG. Thus the MIST control system initiates a rapid steam generator secondary depressurization when the temperature difference becomes negative.)

The (full) HPI capacity is not expected to match the leak discharge flow rate even at the minimum primary system pressure for MIST testing, 200 psia.

Therefore, the primary will depressurize into the range of CFT actuation pressures, less than 600 psia. The CFT discharge will slow (and may halt) the primary depressurization. A major CFT discharge will occur. System refill is not expected to be completed; testing will be continued until the low-pressure testing limit of 200 psia is encountered.

3.3.3. Conduct

The 50-cm^2 cold leg B1 discharge leak is to be actuated at test initiation (rather than the 10-cm^2 leak used nominally). The remaining specifications of the Nominal Test apply. Note that the test initiation steps must be performed rapidly to accommodate the more rapid transient, which will be encountered in this test.

The nominal termination criteria are keyed to loop refill. Refill is not expected in Test 2, rather the primary pressure is expected to decrease to the MIST low-pressure limit for the testing of 200 psia. If the primary system pressure remains below 200 psia for 2 hours, terminate the test (enter the test-termination time into the log), close the leak, and refill the system (without regard for the limits of the scaled boundary systems) while continuing to record data. Test 2 is to be completed within 6 hours.

Although full HPI capacity has been specified and discussed herein, either full or EM HPI will be selected for Test 2 based on the results of the Nominal Test and Test 6.

3.4. Cold Leg Suction Leak, Test 3 (320302)

Test 3 (320302) uses the cold leg B1 suction leak site, rather than the cold leg B1 discharge site of the Nominal Test. HPI-PORV cooling rather than hot leg high-point vent (HPV) actuation is to be used late in the transient.

3.4.1. Purpose

Test 3 highlights the effects of leak fluid temperature on the integral system transient. Increased cold leg backflow as well as markedly asymmetric hot leg refills may occur. The impact of using HPI-PORV cooling during the later stages of refill will be observed. These interactions are discussed in the following paragraphs.

3.4.2. Description

The 10-cm^2 cold leg B1 suction leak site of Test 3 has exactly the same equilibrium characteristics as those of the cold leg discharge site used nominally. The draining and interruption transients should thus be similar to those observed in Test 310000. But events beyond interruption are increasingly sensitive to the leak fluid temperature. The cold leg suction leak site is expected to have the coldest attainable leak fluid temperature (except perhaps for a lower downcomer leak). The cooler leak fluid temperature will obtain increased leak flow rates, thereby lowering the pressure at which the leak and HPI flow rates become equal. Also, the cold leg suction leak site may promote backflow within both cold legs B2 and B1. Backflow may further reduce the leak fluid temperature by decreasing the proportion of the leak discharge flow rate that is first heated in the downcomer. Backflow tendencies will also highlight interloop asymmetries and may cause the refill of the hot legs to occur quite unequally.

The introduction of HPI-PORV cooling rather than venting should markedly alter the final stages of loop refill. The diversion of loop fluid to the pressurizer plus the PORV discharge may reactivate BCM heat transfer. The primary system should depressurize rapidly, perhaps increasing the HPI flow rate enough to overcome the increased rate of inventory depletion.

3.4.3. Conduct

A 10-cm^2 cold leg B1 suction leak, rather than the cold leg B1 discharge leak used nominally, is to be opened at test initiation. Also, HPI-PORV cooling is to be introduced late in the transient, in lieu of hot leg HPV actuation. Start HPI-PORV cooling when both steam generator primary levels have been refilled to the elevation of the steam generator upper tubesheets. HPI-PORV cooling may be started earlier in the refill phase, at the discretion of the Test Engineer, when primary-to-secondary heat transfer is interrupted. Base this decision on two criteria: both steam generator primaries have been refilled to at least 2 feet above their secondary pool elevations, and the primary system pressure is constant or increasing while the steam generator secondaries are being depressurized. Start HPI-PORV cooling by manually opening the PORV and using full HPI, automatically throttled for 75F subcooling. Continue HPI-PORV cooling in this manner through test termination. The

specifications of Test 3 are otherwise the same as those of the Nominal Test. Test 3 is to be completed within 8 hours.

3.5. PORV Break, Test 4 (3204AA)

Test 4 uses a (10-cm^2) PORV break.

3.5.1. Purpose

Test 4 will provide data with a PORV-site leak. Phenomena of interest, which are discussed in the following paragraphs, include the energy dissipation rate and system pressure response with vapor rather than liquid being discharged from the break, the displacement of loop fluid to the pressurizer, the suppression of refill due to stagnant fluid near the hot leg U-bends (HLUBs), and the interloop condition differences that result from HPI flowing up only hot leg A (toward the pressurizer surge line connection to loop A).

3.5.2. Description

The PORV-site leak location of Test 4 will obtain a vapor discharge until the pressurizer fills. Compared to the cold leg B1 discharge (liquid region) break location, the leak mass flow rate will be reduced corresponding to the critical discharge of vapor rather than liquid. The rate of energy dissipation will be similar (the increase in discharged enthalpy is offset by the decreased flow rate). The loop may lose liquid inventory faster than usual, however, because of the combined contributions of discharge from the system through the PORV and of the diversion of loop liquid to the pressurizer as the loop fluid reaches saturation.

The transient is expected to be relatively mild, with little tendency toward repressurization. Loop refill may be longer than usual, however, because of the persistence of stagnant and, therefore, uncooled fluid at the HLUBs. The flow of HPI fluid up the loop A hot leg toward the pressurizer surge line connection will cause inter-loop differences, particularly at and beyond refill. The effect of steam generator activity with the loop nearly full will be induced by increasing the primary-to-secondary temperature difference from 50 to 100F, conditions permitting. (Both temperature differences are used in the abnormal transient operating guideline.)

3.5.3. Conduct

The PORV is to be manually opened at test initiation. Begin the second test-initiation step approximately 1 minute after PORV actuation. The specifications for Test 4 are otherwise the same as those for the Nominal Test. Test conduct is to be altered late in the transient, however.

This alteration is to be used if one or both loops have been refilled to the HLUB spillover elevation or higher, when the steam generator secondary control pressure is within the pressure equivalent of 50F of the facility minimum control pressure. At this time, abruptly reduce the steam generator secondary control pressure from its current value to the minimum value. Record dense data during this control pressure reduction and the ensuing transient, if any. Continue testing in the standard manner with the usual termination criteria. Also, if the conditions (given above) for steam generator control pressure reduction are not met, delete this step and use the standard test conduct and termination criteria. Complete Test 4 within 8 hours.

3.6. Isolated Break, Test 5 (320503)

The (10-cm^2 cold leg B1 discharge) leak is to be isolated in Test 5. The precise time to isolate will be determined from the results of the Nominal Test (3109AA) and Nominal Repeat Test (310000). Isolation will occur about 20 minutes into the transient.

3.6.1. Purpose

The isolated break test will provide test reproducibility information through the early transient events. Leak isolation will provide transient (refill) data at relatively high system pressures. Should the PORV not actuate before refill spillover, data will be obtained during a prolonged natural circulation cooldown. Should the PORV actuate, data will be obtained through an extended primary depressurization with the PORV open.

3.6.2. Description

Test 5 replicates the Nominal Test transient through the initial events -- depressurization, HLUB saturation, intermittent circulation, and flow interruption. This test thus provides an indication of test reproducibility

through the early events. Following flow interruption and heat transfer decoupling of the primary and secondaries, the leak is to be isolated. The primary will repressurize rather rapidly due to both the compression of the voided loop volumes by HPI and the elimination of the heat removal due to HPI-leak cooling. Should refill, spillover, and hence, recoupling occur before the PORV actuation pressure is reached, refill should be completed relatively rapidly. (In a similar OTIS test, spillover and coupling occurred at a primary pressure that was more than 500 psi below the PORV actuation pressure.) The remaining primary cooldown and depressurization (to the test termination conditions) will then occur in single-phase natural circulation and will involve HPI throttling.

Should the PORV actuate before spillover and recoupling, however, the subsequent events will be substantially different. Upon a PORV actuation, the MIST operator is to manually open the PORV and keep it open until the primary depressurizes to within 100 psi of the secondary pressure. Such an event will obtain a fairly long period of HPI-PORV cooling and may even persist until the steam generator secondaries attain the MIST low-pressure limit (~100 psia). PORV closure should then obtain a relatively rapid rate of loop refill. System pressure is not likely to reach the PORV setpoint a second time.

3.6.3. Conduct

The isolated leak test, Test 5 (320503), is to be initiated exactly as the Nominal Test. Approximately 20 minutes after leak actuation, the leak is to be closed and kept closed. The exact time at which the leak is to be isolated will be determined from the results of the Nominal Test. The time that is perceived to be least propitious will be selected, i.e., after loop flow interruption and decoupling (of primary-to-secondary heat transfer), and before the primary levels have descended into either steam generator (whereupon primary depressurization by BCM could occur).

Test conduct following leak isolation is the same as for the Nominal Test. Test 5 is to be completed within 8 hours.

3.7. Reduced HPI Capacity, Test 6 (320604)

The reduced HPI capacity of the evaluation model is used with a 10-cm^2 cold leg B1 discharge (nominal) break in Test 6.

3.7.1. Purpose

The reduced HPI capacity test, Test 6, will generate integral system data with insufficient HPI flow rates to condense the core vapor production until relatively late in the transient. Extensive system voiding and perhaps an early occurrence of the BCM will be observed. Loop refill will be prolonged.

3.7.2. Description

The EM HPI capacity to be used in Test 6 is about half that of full HPI. This difference has two major effects on system conditions compared to those of the Nominal Test. The pressure at which the HPI and leak flow rates become equal is much reduced and is below the CFT actuation pressure. Also, due to the reduced HPI flow rate, the amount of vapor that can be condensed by HPI cooling is proportionally reduced. Using full HPI capacity, HPI can condense the vapor produced by about 2-1/2% of scaled full power for system pressures ranging from 1000 to 1500 psia (the HPI flow rate reduction with increasing pressure is offset by the increased enthalpy change from injection to saturation). The condensation capacity with the EM HPI characteristics is thus approximately 1-1/4% of scaled full power, which is not achieved until ~1 hour after reactor trip.

The reduced HPI transient will thus be characterized by increased voiding from the onset. The reactor vessel level will rapidly drop to the hot leg nozzle elevation, releasing relatively large amounts of vapor to the hot legs. The accompanying primary pressure variations will be magnified, but the BCM depressurization may occur early in the transient, when the primary level first descends to the steam generator elevation.

The BCM depressurization will be accompanied by extensive primary voiding and by lower-than-usual primary levels, particularly in the reactor vessel and downcomer. Refill will be relatively prolonged, may accompany CFT actuation, and might encounter the primary low-pressure limit for testing (200 psia).

3.7.3. Conduct

The evaluation model HPI characteristics (rather than full HPI) are to be introduced during test initiation (in step 2, which immediately precedes loop saturation). The test specifications are otherwise those of the Nominal Test. If the MIST primary low-pressure limit for testing (200 psia) is encountered during the transient, terminate the test by entering the termination time in the log and refilling the loop (without regard for boundary system characteristics) while continuing to record data. Test 6 is to be completed within 6 hours.

Table 3.1.1 Leak-HPI Configuration Tests, Group 32

Test Number	Description	Variable	Value	Nominal Value
1 320101	Reduced leak size	Leak size, cm^2	5	10
2 320201	Increased leak size	Leak size, cm^2	50	10
3 320302	CLS leak	Leak location	B1-CLS	B1-CLD
4 3204AA	PORV break	Leak location	PORV	B1-CLD
5 320503	Isolated leak	Break isolation	Isolated during flow interruption phase (see text)	Uniso-lated
6 320604	Reduced HPI capacity	HPI capacity	Evaluation model	Full

Table 3.1.2 Leak-HPI Test Specifications

The Nominal specifications are those of MIST Nominal Test (3109AA) and the Nominal Repeat Test (311000).

Nominal Specification	Specification(s) Different from Nominal
PRE-TEST STEADY-STATE CONDITIONS	None
TEST INITIATION STEP 1	
1. Break actuation, open: 10-cm^2 cold leg B1 discharge	• Reduced leak size Test 1 (320101): 5-cm^2 cold leg B1 discharge • Increased leak size Test 2 (320201): 50-cm^2 cold leg B1 discharge • CLS leak Test 3 (320302): 10-cm^2 PORV
2. Record test-initiation time	None
3. Verify that the pressurizer heaters trip on low pressurizer level	• PORV break Test 4 (3204AA): manually deenergize pressurizer main heaters
TEST INITIATION STEP 2	
1. Activate HPI with full capacity	• Reduced HPI capacity Test 6 (320604): evaluation model
2. Adjust steam generator control level to 31.6 ft	None
3. Initiate core power decay ramp	None
4. Transfer RVVVs to auto/independent @ 0.125/0.04 psi	None
5. Transfer steam generator secondary pressure control to ATOG	None
CONTROL DURING TESTING	
1. HPI	
a. Head-flow (auto) = full	• Reduced HPI capacity Test 6 (320604): evaluation model
b. Throttling (auto & manual)	• CLS leak Test 3 (320302): HPI-PORV cooling late in the refill phase

Table 3.1.2 Leak-HPI Test Specifications (Cont'd)

Nominal Specification	Specification(s) Different from Nominal
2. Steam generator level (auto @ 31.6 ft)	None
3. AFW flow as required to maintain steam generator level	None
4. Core power decay	None
5. Steam generator secondary pressure control	• PORV break Test 4 (3204AA): see text
6. Primary depressurization: Open PORV @ 2350 psia	• PORV break Test 4 (3204AA): maintain PORV open
7. CFT isolation (auto on low level, manual on subcooling)	• CLS leak Test 3 (320302): HPI-PORV cooling late in the refill phase
8. Venting (hot leg HPVs)	
9. Leak isolation	
Maintain unisolated	• Break isolation Test 5 (320503): isolate at stall
TEST TERMINATION CRITERIA	None
(Note low-pressure termination criteria)	
DATA REQUIREMENTS	None
ACCEPTANCE CRITERIA	None
MAXIMUM TEST DURATION	
8 hours	• Reduced leak size Test 1 (320101): 10h
	• Increased leak size Test 2 (320201) and reduced HPI capacity Test 6 (320604): 6h

4. PERFORMANCE

The acceptability of each test was determined by examining both the conduct of the test and the performance of the measurement systems. The acceptance criteria for each test were defined in the corresponding test procedure, which was based on the MIST Test Specifications.[5] Any condition, action, or measurement that did not meet the acceptance criteria was evaluated for its impact on test acceptability. The tests reported herein are only those that were determined to be acceptable. Any specific deviations of these tests from the acceptance criteria are described in this section.

The review of test conduct included the following checks for each test:

- System conditions and stability just prior to test initiation
- Sequence and timing of the test initiation actions
- Performance of the manual and automatic control functions
- Test termination criteria and the sequence of actions

The impact of out-of-specification conditions or actions was assessed. The deviations of those tests that were determined to be acceptable are described in section 4.1.

The following pretest and post-test data qualification checks were performed for each test:

- The acquisition of the critical measurements
- The operation of the measurement systems within their calibrated range
- The acquisition of instrument readings within their expected range of operation
- Self-consistent measurements, considering both comparable measurements and derived quantities

The appropriate measurement uncertainties were used to assess the individual measurements. The impact of the individual out-of-specification conditions was assessed. The deviations of the critical measurements of those tests that were determined to be acceptable are noted in section 4.2.

4.1. Conduct

The operation of the control systems and manual interactions during the test transients are discussed in sections 4.1.1 through 4.1.4.

4.1.1. Initial Conditions

Initial conditions for the tests were defined by the governing test procedure, ARC-TP-670, and actual values from each test are repeated in Table 4.1.1. All initial conditions were met except for the core flood tank initial pressure in Test 320201, which was 0.29 psi above the allowable limit. For reference, this value is underlined in the table. This deviation did not impact test acceptability.

4.1.2. Test Initiation

The test initiation actions associated with steam generator secondary fill, HPI, core power decay ramp, RVVV control, and abnormal transient operating guideline (ATOG) steam pressure control were performed acceptably for all the tests in this group. Secondary fill, HPI, and core power decay were verifiable from the data, and were performed for each test within 20 seconds of one another. Initiation of HPI flow in Tests 3204AA and 320604 was not observed within the 20-second window. The delay in HPI flow initiation was associated with the time required to pressurize the accumulator in the HPI supply circuit.

4.1.3. Control During Testing

The performance of automatic control systems and manual interactions during the test transients is described in this section. The controls for HPI, CFT, pressurizer main heaters, AFW to steam generators A and B, core power, PORV, ATOG steam pressure control, and level control for steam generators A and B performed acceptably for all the tests in this group except as noted in the following text. The time referred to in the discussion is referenced to the test zero time, which is defined as the time of leak initiation.

Steam Generator Secondary Level Control

Constant steam generator level control was used in all the tests. Constant level control was performed to maintain the levels at 31.6 ± 1 ft. Performance of the steam generator level control was acceptable during all the tests. During Tests 320101, 320201, 320302, 3204AA, and 320503, steam generator level controls deviated from the desired control tolerance as summarized below.

At 20 minutes in Test 320101, the steam generator A and B secondary levels dropped about 9 and 3 inches below the desired control band, respectively. At 25 minutes, the generator B level rose about 2 inches above the desired control band. Each of these deviations lasted for about 3 minutes.

During Test 320201, the loop A secondary level exceeded the acceptable band for 18 minutes starting at 29 minutes. These deviations were caused by an ATOG-triggered blowdown of 50 psi/min. The maximum and minimum levels during this time were 34.3 and 28.8 ft, respectively. The loop B secondary level also responded to the 50 psi/min blowdown with a maximum and minimum level of 34.2 and 27.9 ft, respectively.

During Test 320302, the steam generator A level control experienced five isolated excursions above and below the 31.6 ± 1 ft acceptance control band. The worst deviation occurred at about 230 minutes when the level decreased to about 29.2 ft. Leakage across the feedwater control valve caused the secondary level to exceed the desired upper limit of 32.6 ft at 393 minutes and continued to the time of test termination at 420 minutes. The steam generator level increased at a rate of about 1 ft/h, causing the level to increase to 33.1 ft at the time of test termination. The steam generator B level control showed only isolated deviations outside the level control band. The largest deviation occurred at 233 minutes when the level reached 29.4 ft.

During Tests 3204AA and 320503, the steam generator A level control experienced short deviations (5 minutes maximum) of less than 0.3 ft from the allowable control band of 31.6 ± 1 ft.

ATOG Steam Pressure Control

The performance of the ATOG steam pressure control was examined using the temperature difference between the core outlet and the maximum of the two

steam generator secondary saturation temperatures. According to the temperature difference, DT, the following control was required:

1. If the DT was greater than or equal to 5OF, secondary steam pressure control was maintained constant.

2. If the DT was less than 50 but greater than OF, a secondary cooldown rate of 100F/h was activated and maintained until the DT increased to 5OF at which time constant pressure control was invoked.

3. If the DT was less than or equal to OF, a secondary depressurization rate of 50 psi/min was to be imposed on the secondary pressure setpoints and maintained until the DT increased to 5OF.

ATOG steam pressure control was used in all the tests. Control mode 1 was encountered during all the tests except Test 320101. Control mode 2 was encountered during all the tests. Control mode 3 was activated only during Test 320201. The control system performed as intended during all the tests. The isolated control anomalies are summarized below.

During the activation of control mode 1, and when the secondary was decoupled from the primary due to the absence of steam generator heat transfer, the secondary pressure in generator A decreased about 20 to 50 psi/h during the tests. This depressurization resulted from heat loss in steam generator A and leakage in the feedwater valve. The secondary pressure in generator B dropped at about 30 psi/h during Test 320302, about 90 psi/h during Test 320604, and about 125 psi/h during Test 320503. The large depressurization was caused by steam leakage that triggered intermittent feedwater activations to maintain constant level control. During Tests 320201 and 3204AA, control mode 1 was activated during the test initiation. As a result of AFW additions during steam generator fill, the secondaries depressurized below the control setpoint. The pressure control setpoint was properly maintained during this time. Control mode 1 performed acceptably.

During the activation of control mode 2, at a secondary pressure below about 120 psia, the 100F/h cooldown was not achieved as intended. At this low pressure, the pressure differential between the steam generator and condenser was too low to attain the steam flow rate required to cool at the rate of 100F/h. In Test 320101, control mode 2 was activated during the initiation period. During the secondary fill period, secondary pressures dropped quickly as the generators were overcooled by AFW, thereby masking the

cooldown of 100F/h. During Test 320302 at 260 minutes when control mode 2 was activated, steam generator B began depressurizing, as required, in response to the control differential temperature decreasing below 50F. Generator A did not begin depressurizing until about 20 minutes later. The delay in the generator A depressurization resulted from an error in the Network 90 control system input table. This caused the control setpoint to increase in value, thus delaying the initiation time of the cooldown ramp. With the exception of this delay in generator A depressurization, performance of control mode 2 was acceptable.

During the activation of control mode 3 in Test 320201, the depressurization rate of 50 psi/min could not be achieved at low secondary pressure. As with the control mode of 100F/h, at reduced steam generator pressure, the required steam flow rate could not be obtained to achieve the 50 psi/min depressurization. Control performance was acceptable.

Steam Generator Auxiliary Feedwater

In all the tests, the AFW control performed as intended, maintaining the feedwater flow rate at the head/flow characteristic during the secondary fill transient. The AFW to generators A and B achieved the required flow rate, and remained within 10 to 15 lbm/h (1.3 to 1.9%) of the required head/flow characteristic during the level increase from 5 to 31.6 ft.

During Test 320604, the AFW flow rate to steam generator A exceeded the desired head/flow curve by 17 lbm/h (2%) as the feedwater was terminated.

Power-Operated Relief Valve

For all the tests in this group, primary pressure remained below the actuation pressure of 2350 psia, and with the exception of Tests 320302 and 3204AA, the PORV never opened. During Test 320302, the PORV was opened as required under manual control to initiate HPI/PORV cooling when the level in the two steam generators refilled to the elevation of the upper tubesheets, 52.1 ft. During Test 3204AA, the PORV was operated as required under manual control to initiate the test. The PORV was used from 196 to 424 minutes and from 0 to 434 minutes in Tests 320302 and 3204AA, respectively.

High-Pressure Injection

Automatic and manual control of HPI was performed as follows:

1. Maintenance of the head/flow characteristic for all times when subcooling was less than 7OF.

2. Automatic HPI throttling to control subcooling to between 70 and 8OF.

3. Manual HPI shut off when subcooling increased to 10OF and returned to automatic when subcooling decreased to 5OF (3 times). HPI was left on automatic subcooling control when subcooling reached 10OF for the fourth time.

4. Manual throttling of HPI to maintain a pressurizer level of 21.4 ± 0.5 ft.

During all the tests in this group, control of HPI was performed as required. With the exception of Test 320604, all the tests were performed using "full capacity" HPI. Test 320604 was performed using "evaluation model" HPI as the head/flow characteristic. Control anomalies observed in the tests are summarized below.

During the activation of control mode 4 in Test 320101, HPI flow exceeded the desired head/flow curve by up to 48 lbm/h. This action occurred when HPI flow was restarted in automatic throttling after subcooling decreased to 5OF.

During the activation of control mode 4 in Test 320503, HPI flow was manually reduced and then stopped to control the pressurizer level. From 70 to 90 minutes, HPI was restarted and the water level in the pressurizer was controlled to 22.0 ± 0.1 ft. The procedure specified that the level should be controlled to 21.4 ± 0.5 ft. This difference did not impact test performance.

The "evaluation model" HPI used in Test 320604 required a lower pump speed for control. This lower speed delayed the HPI flow initiation about 100 seconds from the time that the HPI pump was activated, reflecting the increased time to pressurize the accumulator in the HPI circuit. HPI flow exceeded the desired head/flow curve by 50 lbm/h (22%) when the flow was initiated.

Core Flood Tank

Manual and automatic operation of the core flood tank isolation valves was acceptable for all the tests in this group. The CFT water inventory discharged to the loop during all the tests except Tests 320101 and 320503. During Tests 320101 and 320503, the CFT isolation valves were manually closed as specified when the primary pressure decreased below 600 psia and core outlet subcooling exceeded 50F. During Test 3204AA, the CFT was manually isolated after it discharged to the loop.

During Test 320201, the CFT automatic low-level control was activated, causing the isolation valves to close when the CFT level reached 26.3 ft. This level was 0.17 ft lower than the specified lower limit of 26.5 ft. The difference did not impact test acceptability.

Pressurizer Main Heaters

The pressurizer main heaters were automatically deenergized on low pressurizer level at test initiation for each test except Test 3204AA. During Test 3204AA, the pressurizer main heaters were manually deenergized at test initiation, as required. The control for pressurizer main heater power, PZWM04, was manually set to zero power in all the tests as required.

Core Power

The core power control performed satisfactorily during each test. The maximum deviation of the measured core power was 3.5 kW (3.9%) from the intended core power decay curve during the tests in this series.

4.1.4. Termination

Test termination activities were acceptable for all the tests in this group. Tests 320302 and 3204AA were terminated on the basis of a maximum elapsed time of 7 hours. Test 320604 was terminated based on a maximum elapsed time of 5 hours. Tests 320101 and 320503 were terminated based on 2 hours of core outlet subcooling of at least 50F and a primary system pressure of less than 400 psia. Test 320201 was terminated based on 2 hours of primary pressure less than 200 psia. In all cases, the loop was refilled and the reactor vessel upper head void was removed prior to the termination of saving data. Termination activities for all the tests were performed as required.

4.2. Instruments

Each of the six tests in the Group 32 series used a common set of instrumentation. The critical instruments in this set are defined in Table 4.2.1. The measurements obtained from the instrumentation were checked to assure acceptable operation during the tests. Checks on instrument measurements were performed by computer-automated data qualification activities and manual examination of the analysis plots. Data qualification activities for each test in Group 32 were performed at steady-state, pre-test initial conditions, during the test transient, and after test termination as summarized below:

Check	Purpose	Time of Performance		
		Before Test	During Test	After Test
NOREAD	Definition of instruments not acquiring data	x	x	x
ANDCHK	Calibration check of the Analogic data acquisition system	x		x
ZEROS	Zero check of instrument transmitters	x		x
RANGE	Validity of instrument measurement as compared to expected range	x	x	x
CONSIS	Instrument and derived quantity consistency check	x	x	x

As a result of these manual and automatic data qualification checks applied to the measurements and derived quantities in the test data base, the critical instruments identified in Table 4.2.2 were determined to be invalid during all or part of the test. In most instances, there was sufficient redundancy in the group of critical instruments so that the individual failure did not violate the requirements of the critical instrument list. In the other cases, the existence of the failed critical instrument did not warrant repeating the test.

For the 18 conductivity probes identified by Note 3, the measurement system error was not identified until after the test series was completed. In this instance, the void fraction obtained from neighboring differential pressure measurements provided sufficient backup except for the reactor vessel probes,

RVCP01-04. The absence of these measurements did not warrant repeating the test.

Prior to and after completion of the test, a "zero" reading was obtained for all differential pressure and pressure transmitters, mass flowmeters, weigh tank load cells, and reactor core voltage and current measurements. For those critical instruments that failed the zero check (defined in the Immediate Report for each test), the magnitude of the failure was small enough that measurement performance was not degraded to a condition that warranted repeating the test. The instrumentation performance during these tests was fully acceptable based upon this check.

RVVV Performance

The behavior of the RVVVs was reviewed using limit switch data. The RVVVs performed symmetrically in most of the Group 32 tests. The exceptions were Test 1, in which the individual RVVVs exhibited diverse behavior, and Test 3. In Test 3, RVVV A2 appeared to actuate more frequently than the other RVVVs and to stay open longer. The characteristics of the RVVV differential pressure (DP) transmitters have been examined for each of the Group 32 tests. The responses to the initial DP increase were compared among the transmitters using high-speed data. The performance of the RVVV DP transmitters was determined to be satisfactory for each of the Group 32 tests.

Table 4.1.1 Test Initial Conditions

(Underlined entries are our of specifications, and are discussed in the text.)

System	Parameter	VTAB	Units	Desired	Tolerance	Actual Values 320101	320201	320302	3204AA	320503	320604
Primary											
	Pressure	RVGP01	psia	1750*		1731	1733	1727	1738	1732	1734
	Hot leg subcooling	*	F	22.0	± 2.0	23.8	23.6	23.1	23.8	23.8	23.9
	Core power	RVWM20	kW	128.7	± 1.65	128.3	128.1	128.5	128.7	128.2	127.9
	Pressurizer level	PZLV20	ft	23.0 and varying less than ± 0.6 ft/h.	± 0.2	22.9 and steady.	22.9 and steady.	23.1 and steady.	23.1 and steady.	22.8 and steady.	22.8 and steady.
	Pressurizer surge line fluid temperature	PZTC01	F	Match H1TC11	± 5	H1TC11 + 0.1	H1TC11 - 0.5	H1TC11 - 2.8	H1TC11 - 1.2	H1TC11 - 3.1	H1TC11 + 0.7
	Fluid/metal temperatures	**	F	Varying less than 3F/h for fluid and 10F/h for metal during a 30-minute interval.		acceptable	acceptable	acceptable	acceptable	acceptable	acceptable
Secondary											
	Pressure	S1GP01 S2GP01	psia	1010	± 10	1014 1015	1014 1014	1014 1015	1013 1015	1014 1015	1013 1015

Table 4.1.1 Test Initial Conditions (Cont'd)

System	Parameter	VTAB	Units	Desired	Tolerance	Actual Values					
						320101	320201	320302	3204AA	320503	320604
	Level	S1LV20	ft	5.0	± 1.0	5.5	4.7	4.8	5.1	5.5	5.1
		S2LV20				5.4	5.0	5.1	5.0	5.6	4.8
	Feedwater temperature	SFRT01	F	110	± 20	120.4	116.6	120.3	114.2	121.6	112.5
		SFRT02				121.2	117.5	121.0	115.3	122.5	113.1
Core Flood Tank											
	Pressure	CFGP01	psia	600	± 10	600.8	610.3	602.6	593.8	599.2	600.1
	Level	CFLV20	ft	42.8	± 0.3	43.0	42.7	42.9	42.9	42.9	43.0

*Pressure was adjusted to yield a hot leg subcooling of 22 ± 2F as given by the difference between H1TC11 and RVRF20 (the saturation temperature based on RVGP01).

**The following fluid and metal temperature measurements were used to define steady state (minimum time interval of 30 minutes without test operator manual control adjustments):

Fluid: H1RT01, H2RT01, P1RT02, P2RT02.
Metal: P1MT01, P2MT01, C1MT04, C2MT04, C3MT04, C4MT04, RVMT24, RVMT25.

Table 4.2.1 Critical Instruments for the Group 32 Test Series

Component	Instrument Type	Critical Instruments
Reactor vessel	Ammeter	RVAM01
	Conductivity probe	RVCP01-04
	Differential pressure transmitter	RVDP01,RVDP03-09
	Differential temperature	RVDT01-04,-23
	Pressure transmitter	RVGP01
	Limit switch	RVLS01-04
	Metal thermocouple	RVMT01-04,-23
		RVMT05-22 (12 of 18)
	Fluid thermocouple	RVTC01,02,RVTC16-20
		RVTC03-15 (9 of 13)
		RVTC21-23 (2 of 3)
	Voltmeter	RVVM01
Hot legs	Conductivity probe	H1CP01-10 (5 of 10)
		H2CP01-10 (5 of 10)
	Differential pressure transmitter	H1DP01,-04,-09-12,-14
		H2DP01,-04,-09-12,-14,-16
	Differential temperature	H1DT01-04
		H2DT01-04
	Limit switch	H1LS01,H2LS01
	Metal thermocouple	H1MT01-04
		H2MT01-04
	Resistance temperature detector	H1RT01 or H1TC01,
		H2RT01 or H2TC01
	Fluid thermocouple	H1TC02-09 (5 of 8)
		H2TC02-09 (5 of 8)
		H1TC10-12 (1 of 3)
		H2TC10-12 (1 of 3)
		H1TC13-19 (5 of 7)
		H2TC13-19 (5 of 7)
Steam generator A	Differential pressure transmitter	P1DP04,S1DP01,S1DP03
	Differential temperature	S1DT01-05
	Pressure transmitter	P1GP01,S1GP01
	Metal thermocouple	S1MT01-05
	Resistance temperature detector	P1RT01,02
	Fluid thermocouple	P1TC01-03,-13-16,-23-26,
		-33,-34,-35,-36
		(10 of 15)
		P1TC18,-27,-28,-37,-38
		(3 of 5)
		P1TC09-12,-19-22,-29-32
		(8 of 12)
		S1TC01,-02,-26 (2 of 3)
		S1TC03-12 (7 of 10)
		S1TC13-23,-25 (8 of 12)
		S1TC24

Table 4.2.1 Critical Instruments for the Group 32 Test Series (Cont'd)

Component	Instrument Type	Critical Instruments
Steam generator B	Conductivity probe	S2CP01-12 (6 of 12)
	Differential pressure transmitter	P2DP06,S2DP01,S2DP12
		S2DP02-11 (5 of 10)
	Differential temperature	S2DT01-05
	Pressure transmitter	P2GP01,S2GP01
	Metal thermocouple	S2MT01-05
	Resistance temperature detector	P2RT01,-02
	Fluid thermocouple	P2TC01-13 (9 of 13)
		P2TC14-28 (10 of 15)
		P2TC29-43 (10 of 15)
		P2TC44-53 (7 of 10)
		S2TC01-08,-55 (6 of 9)
		S2TC09-19 (7 of 11)
		S2TC20-33,-54 (10 of 15)
		S2TC34-53 (13 of 20)
Cold legs (n=1,2,3,4)	Differential pressure transmitter	C1DP01,C2DP01,C2DP09
		CnDP02,-03,-04,-06,-07, -08
	Differential temperature	CnDT01-03
	Metal thermocouples	CnMT01-03
	Resistance temperature detector	CnRT01,-02
	Fluid thermocouple	CnTC02
		CnTC03-06 (3 of 4)
		CnTC07-10 (3 of 4)
		CnTC11-14 (3 of 4)
Reactor vessel downcomer	Differential pressure transmitter	DCDP01,-02,-05-08
	Differential temperature	DCDT01-03
	Metal thermocouple	DCMT01-03
	Resistance temperature detector	DCRT01
	Fluid thermocouple	DCTC01-04
		DCTC05-12 (5 of 8)
		DCTC13-40 (19 of 28)
		DCTC41-46 (4 of 6)
Pressurizer	Differential pressure transmitter	PZDP01,-02
	Differential temperature	PZDT01,-02
	Pressure transmitter	PZGP01
	Metal thermocouple	PZMT01,-02
	Resistance temperature detector	PZRT01 or PZTC09
	Fluid thermocouple	PZTC01,-02
		PZTC04-08 (4 of 5)
	Power controller	PZWM04
HPI	Differential pressure transmitter	HPDP01
	Flowmeter	HPMM01-05
	Fluid thermocouple	HPTC01

Table 4.2.1 Critical Instruments for the Group 32 Test Series (Cont'd)

Component	Instrument Type	Critical Instruments
Single-phase vent system	Load cell	V1LC01,-02 (not for 320402)
	Limit switch	V1LS01,-02 (not for 320402)
		V1LS03 (320302 only)
		V1LS04 (320101 only)
		V1LS05 (320503 and 320604 only)
		V1LS06 (320201 only)
	Fluid thermocouple	V1TC01 (320302 only)
		V1TC02 (not for 320302 and 320402)
	Flowmeter	V1MM01 (not for 320402)
Leak enthalpy	Pressure transmitter	LQGP01 (not for 320302 and 320402)
	Flowmeter	LQMM01 (not for 320302 and 320402)
	Fluid thermocouple	LQTC01-04 (not for 320302 and 320402)
Two-phase vent system	Load cell	V2LC01-04
	Limit switch	V2LS03-06
	Flowmeter	V2MM01-03
	Fluid thermocouple	V2TC01-04
Core flood tank	Differential pressure transmitter	CFDP01
	Pressure transmitter	CFGP01
	Limit switch	CFLS01,-02 (1 of 2)
	Fluid thermocouple	CFTC01
Gas addition	Fluid thermocouple	GATC02-04 (1 of 3)
Feedwater circuit	Differential pressure transmitter	SFDP01-06
	Resistance temperature detector	SFRT01,-02
Steam circuit	Differential pressure transmitter	SSDP01-06
	Resistance temperature detector	SSRT01,-02
	Fluid temperature	SSTC01-03 (1 of 2)
		SSTC02,-04 (1 of 2)
Miscel-laneous	Resistance temperature Detector shunt	MSRF01
	Reference oven temperature	MSTC01-07

Table 4.2.2 Critical Instruments Not Available for the Group 32 Test Series

Instrument	Description	320101	320201	320302	3204AA	320503	320604	Backup Available
CFLS01	Limit switch on loop A header isolation valve	x	x	x	x	x	x	Yes
C1TC04	Pump suction fluid temperature at 2.36 ft	x	x	x	x	x	x	Yes
C3TC07	Pump discharge rake fluid temperature at 25.08 ft	*		**				Yes
H2CP09	Hot leg fluid conductivity probe at 66.78 ft	x	x	x	x	x	x	Yes
P1TC30	Generator A primary fluid temperature at 50.56 ft	x	x	x	x	x	x	Yes
P1TC35	Generator A primary fluid temperature at 39.08 ft	x	x	x	x	x	x	Yes
P2TC12	Generator B primary fluid temperature at 49.50 ft	x	x	x	x	x	x	Yes
RVTC07	Core fluid temperature (mid-bundle) at 13.15 ft	x	x	x	x	x	x	Yes
S1TC04	Generator A secondary fluid temperature at 11.07 ft	x	x	x	x	x	x	Yes
S1TC16	Generator A secondary fluid temperature at 38.19 ft	x	x	x	x	x	x	Yes
S1TC19	Generator A secondary fluid temperature at 41.28 ft	x	x	x		x	x	Yes

Table 4.2.2 Critical Instruments Not Available for the Group 32 Test Series (Cont'd)

Instrument	Description	320101	320201	320302	3204AA	320503	320604	Backup Available
S2TC12	Generator B secondary fluid temperature at 14.27 ft	x	x	x		x	x	Yes
S2TC13	Generator B secondary fluid temperature at 20.19 ft	x	x	x		x	x	Yes
S2TC16	Generator B secondary fluid temperature at 26.27 ft	x	x	x		x	x	Yes
S2TC24	Generator B secondary fluid temperature at 38.19 ft	x	x	x		x	x	Yes
V2MM03	Hot leg high point vent mass flowmeter		x					No
H2CP05	Hot leg fluid conductivity probe at 50.68 ft				x			Yes
H2CP07	Hot leg fluid conductivity probe at 63.56 ft				x			Yes
RVCP01-04	Reactor vessel fluid conductivity probes	***	***	***	***	***	***	No
S2CP01-12	Generator B secondary conductivity probes	***	***	***	***	***	***	No
H1CP01-02	Hot leg fluid conductivity probes	***	***	***	***	***	***	Yes

*Unavailable after 270 minutes.

**Unavailable from 413 to 449 minutes.

***Raw data obtained with these conductivity probes cannot be processed due to a measurement problem observed after completing these tests.

5. OBSERVATIONS

Group 32 observations are arranged by like variations. For example, tests using varied leak sizes are described and compared in section 5.3, and those having off-nominal leak locations are described in section 5.4. These discussions are preceded by generic information, in section 5.1, and by a detailed description of the base test for Group 32, Nominal Repeat Test 311000, in section 5.2. The observations are summarized in section 5.7; general observations, inter-test comparisons, and noteworthy observations are addressed.

5.1. Introduction

The Group 32 tests varied leak and HPI characteristics, as described in section 5.1.1. Their initial conditions were similar, as discussed in section 5.1.2. The timing of the test-initiating actions and the early events and conditions is discussed in sections 5.1.3 and 5.1.4.

5.1.1. Description of Test Group 32

Test Group 32 consisted of six tests varying either leak or HPI characteristics. These tests are listed in Table 5.1.1; also shown are their single-digit identifiers used herein, for example, Test 1 refers to 320101. The Group 32 tests were conducted after 13 July 86, therefore their reference test with nominal conditions was the Nominal Repeat Test, Test 10 of Group 31.

5.1.2. Initial Conditions

The initial conditions were virtually identical among the Group 32 tests, Table 5.1.2. In each of the tests, the reactor vessel fluid temperature at the RVVVs was approximately 2F higher than the core exit fluid temperature, and the fluid temperature at the top of the reactor vessel was about 1F lower. These small differences may reflect heat loss and guard heating

effects, but they are so small as to be near the uncertainty of the fluid temperature measurements.

The hot leg inlet and steam generator primary inlet fluid temperatures were nearly constant among tests and between loops. Beyond the steam generators, the loop A fluid temperatures at the steam generator primary outlet and reactor coolant pumps (RCPs) were generally 1F less than those of loop B. The cold leg flow rates also evidenced inter-loop differences. The loop A cold leg flow rates were on the order of 0.1 to 0.2% of scaled full cold leg flow rate, or 4% of the initial flow rate, less than those of loop B. The order of flow rates, from lowest to highest, was loops A2, A1, B2, and B1 in each of the Group 32 tests. The downcomer flow rate was approximately 0.2% of scaled full flow less than the total cold leg flow rate. Based on feed and steaming rates, steam generator A was slightly more active than steam generator B, also in each of the tests.

5.1.3. Timing of Test-Initiating Actions

Table 5.1.3 indicates the timing of the test-initiating actions. The activation of the appropriate primary system discharge limit switch defined "zero" time. The accompanying indications such as leak flow rate, leak fluid temperature increase, and primary system depressurization occurred either as the discharge limit switch activated or by the next data scan, at 0.08 minutes or 5 seconds. The exception was the PORV flow rate in Test 4, which was first observed at 1.25 minutes. Based on the primary fluid mass decrease and primary system depressurization, both of which occurred at time 0, the PORV flow rate delay apparently reflects the deadband of the flow measurement system.

The remaining test-initiating event timing was keyed to the depletion of the pressurizer fluid inventory and was thus dependent on the specific boundary conditions tested. For example, events were delayed in Test 1 with a reduced leak size, and accelerated in Test 2 with an increased leak size. The timing of the activation of AFW, the core power reduction ramp, and the RVVVs was generally tightly grouped in each test. The HPI isolation valves opened at approximately the same time as the effects of these three initiating actions were observed, but HPI flow rate to the loop was delayed somewhat by the time required (20 to 30 seconds) to pressurize the HPI system accumulations. The

exception occurred in Test 6. Because of the reduced HPI capacity used in Test 6, more than 1.5 minutes were required to pressurize the HPI system, thus delaying the time of first HPI delivery to the loop.

5.1.4. Early Events and Conditions

Early conditions and events are indicated in Table 5.1.4. The rates shown on this table were obtained just after the respective system-initiating transient had subsided, thus the entries are only approximate. The inter-test variation of leak flow rates (considering the tests having a cold leg leak) was in approximate correspondence to leak size. The initial primary system depressurization rates varied even more than the break flow area. For example, the depressurization rate in Test 1, with a 5-cm^2 break area, was less than one-third of those of the tests having a 10-cm^2 cold leg break. The timing of the restabilization of primary system pressure (as the loop fluid approached saturation) was similarly responsive to break flow area. The saturation temperature corresponding to the stabilization pressure, 591 to 600F, reflected the initial hot leg temperature as well as the outsurge of the relatively warm pressurizer fluid. The AFW system response was similar among the Group 32 tests, the steam generator secondaries refilled at 3.6 to 3.8 ft/min. (In Nominal Repeat Test 3110, the feed to steam generator A was slightly less responsive than the feed to steam generator B.)

Table 5.1.1 Group 32 Tests

Number	Identifier	Description	Date	Duration, Min.
1	320101	Reduced leak size, 5 cm^2	7/20/86	298
2	320201	Increased leak size, 50 cm^2	7/22/86	185
3	320302	Leak location: cold leg suction	7/15/86	422
4	3204AA	Leak location: PORV break	8/26/86	420
5	320503	Isolated leak	7/19/86	299
6	320604	Reduced HPI	7/14/86	300
—	—	—	—	—
10	311000	Nominal Repeat	9/3/86	663

Table 5.1.2 Initial Conditions

Test:	3201 5 cm^2	3202 50 cm^2	3203 Suction	3204 PORV	3205 Isolated	3206 HPI/2	3110 Nominal	Group 32 Min.	Max.
Pressure, psia									
Reactor vessel	1730	1730	1725	1735	1730	1730	1730	1725	1735
Steam generator secondaries (A and B)	1015	1015	1015	1015	1015	1015	1015	1015	1015
Temperature, F									
Core region									
Inlet	545.5	546	546	545.5	545.5	546	545	545.5	546
12.1 ft	576	577	576.5	576	576	576	576	576	577
14.2 ft	584.5	585	585	585	585	584	585	584	585
Exit	592	592	592	593	592	592	593	592	593
Reactor vessel									
@ RVVVs	594	594	594.5	594.5	594	594	594	594	594.5
RV top	591	591	591	591.5	591	591	591	591	591.5
Saturation	615.6	615.8	615.5	616.2	615.6	615.7	615.5	615.5	616.2
Hot Leg Inlet									
A	591	591	591	591	591	591	591	591	591
B	591	591	591.5	591	591	591	591	591	591.5
Steam generator inlet									
A	591	591	591	591	591	591	591	591	591
B	591	591	591.5	591	591	591	591	591	591.5

Table 5.1.2 Initial Conditions (Cont'd)

Test:	3201 5 cm^2	3202 50 cm^2	3203 Suction	3204 PORV	3205 Isolated	3206 HPI/2	3110 Nominal	Group 32 Min.	Group 32 Max.
Steam generator outlet									
A	550	550.3	550	549	549.5	550	549	549	550.3
B	551	551	551	551	550.5	551	550	550.5	551
RCP									
A1 and 2	546	546	546	546	545	546	546	545	546
B1 and 2	547	547	547	547	546.5	547	547	546.5	547
Lower DC	546	546	546	546	545	546	546	545	546
Secondaries									
Feed	125	117	120	115	122	113	114	113	125
Saturation	546	546	546	546	546	546	546	546	546
Steam	579	580	580	580	579	580	579	579	580
Level, ft									
Pressurizer	22.9	22.8	23.6	23.0	22.8	22.8	23.0	22.8	23.6
Steam generator secondaries (A and B)	6.4	4.8	~5	5	5.5	4.9	5.2	5	6.4
Flow rates, %*									
Cold Leg									
A1	4.12	4.08	4.09	4.11	4.10	4.10	4.09	4.08	4.12
A2	4.06	4.02	4.03	4.04	4.04	4.03	4.01	4.02	4.06
B1	4.23	4.24	4.23	4.25	4.25	4.22	4.25	4.22	4.25
B2	4.14	4.15	4.14	4.15	4.14	4.13	4.15	4.13	4.15
Average	4.10	4.12	4.12	4.14	4.13	4.12	4.12	4.12	4.14
Downcomer	3.95	3.93	3.93	3.94	3.94	3.93	3.93	3.93	3.95

Table 5.1.2 Initial Conditions (Cont'd)

Test:	3201 5 cm^2	3202 50 cm^2	3203 Suction	3204 PORV	3205 Isolated	3206 HPI/2	3110 Nominal	Group 32 Min.	Max.
Secondaries									
Steam generator A feed	2.36 ±0.05	2.3	2.32 ±0.04	2.34	2.35 ±0.04	2.31 ±0.04	2.30	2.3	2.36
Steam generator A steam	2.33 ±0.13	2.3	2.30 ±0.06	2.33	2.32 ±0.07	2.30 ±0.08	2.31	2.3	2.33
Steam generator B feed	2.23 ±0.02	2.2	2.22 ±0.02	2.22	2.24 ±0.02	2.16 ±0.02	2.20	2.2	2.24
Steam generator B steam	2.25 ±0.01	2.3	2.27 ±0.03	2.24	2.26 ±0.01	2.20 ±0.02	2.26	2.2	2.27
Temperature differences, F									
SCM	24	24	24	23	24	24	23	23	24
Core Rise	46.3	46.5	46	46.6	46.5	46	46.8	46	46.6
Steam generator A drop	41.2	41	41	41.4	41	41.2	41.5	41	41.4
Steam generator B drop	40.1	40.4	40	40.4	40.3	39.8	40.5	39.8	40.5
Core power, kW	130	128	128	128	128	128	128	128	130

*Cold leg flow rates are % of scaled full cold leg flow, downcomer flow rates are % of the scaled full downcomer flow rate, and secondary flow rates are % of scaled full steam generator secondary flow rate.

Table 5.1.3 Timing of Test-Initiating Actions

Times are in minutes.

Test:	3201 5 cm^2	3202 50 cm^2	3203 Suction	3204 PORV	3205 Isolated	3206 HPI/2	3110 Nominal
Leak actuation							
Leak flow rate increase	0	0	0	1.3	0	0	0.08
Leak limit switch activation	0	0	0	0	0	0	0
Primary fluid mass decrease	0	0	0.08	0	0	0	0.08
Leak fluid temperature increase	0	0	0	--	0	0	0.08
Primary system pressure decrease	0	0	0.08	0	0	0	0.08
Leak fluid enthalpy increase	0	0	--	--	0	0	0.08
Auxiliary feedwater							
AFW flow rate increase	4.4	0.6	2.2	1.0	1.9	1.8	2.0
Steam generator levels increase	4.4	0.6	2.2	1.0	1.9	1.8	2.0
Core power decrease	4.5	0.7	2.3	1.2	~2	2.0	2.2
RVVVs							
Limit switches actuate	4.5	0.8	2.25 to 2.33	1.2, 2*	2.0	2.0, 2.5*	2.1
Bracketing temperatures respond	4.6	0.8	2.3	1.2	2.1	2.0	2.2

Table 5.1.3 Timing of Test-Initiating Actions (Cont'd)

Test:	3201 5 cm^2	3202 50 cm^2	3203 Suction	3204 PORV	3205 Isolated	3206 HPI/2	3110 Nominal
HPI							
HPI limit switches activate	4.4	0.7	2.2	1.1	1.9	1.9	2.1
HPI flow rate increase	4.8	0.9	2.5	1.6	2.2	3.6	2.4

*In Tests 4 and 6, the RVVVs opened at the first time listed, then closed briefly and opened again at the second time listed.

Table 5.1.4 Initial Events and Conditions

Rates are those immediately after the actuation pulse has subsided and are only approximate.

Test:	3201 5 cm^2	3202 50 cm^2	3203 Suction	3204 PORV	3205 Isolated	3206 HPI/2	3110 Nominal
Leak							
Flow rate, lbm/h	380	>3430	820	0 to 130	950	950	870
Fluid temperature, F	540	550	550	---	548	550	540
Fluid enthalpy, Btu/lbm	500	580	---	---	540	525	520
Rate of primary system depressurization, psi/min	34	1700	100	180	100	125	115
AFW flow rate, % of full steam generator secondary flow rate	9.8	~10	9.8	10.3	~10	~10	~10*
Rate of steam generator secondary level rise, ft/min	3.6	3.8	3.8	3.6	3.8	3.8	3.8
HPI							
Flow rate, lbm/h	510	520	490	520	500	220	510
Temperature, F	90	100	90	80	90	85	80
Primary system pressure begins to stabilize							
Time, min	5.1	0.2	2.4	1.6	2.1	2.15	2.2
Pressure, psia	1470	1550	1450	1440	1470	1470	1470
Corresponding saturation temperature, F	594	601	594	591	594	594	594

*In Test 311000, the steam generator B AFW stabilized at 2.08 minutes, the steam generator A AFW stabilized at approximately 2.6 minutes.

5.2. Nominal Repeat Test 311000

The Group 31 and 32 tests had the same nominal conditions, namely those of Nominal Test 3109AA and Nominal Repeat Test 311000. Test 3109AA has been described in detail in the Group 31 Report, as have the differences between Tests 9 and 10. As was explained in that discussion, the (10-cm^2 cold leg B1 discharge) leak flow area increased approximately 6% between 12 and 13 July 1986. Nominal Test 3109AA was performed before this area change, and Nominal Repeat Test 311000 was performed after the change. All the Group 32 tests were performed after the change, therefore Nominal Repeat Test 311000 provides the nominal conditions for Test Group 32. Test 311000 is described below. The discussion is ordered chronologically according to the following groups of interactions:

5.2.1 Test Initiation Through Loop Flow Interruption

5.2.2 Primary System Depressurization, 15 to 80 Minutes

5.2.3 Equilibrium and Gradual Hot Leg Refill

5.2.4 Spillovers Through Test Termination, Times Beyond 270 Minutes

5.2.1. Test Initiation Through Loop Flow Interruption

Leak Actuation

Upon leak actuation defining time zero, the leak flow rate began to register, stabilizing near 900 lbm/h (Figure 5.2.1), and the leak fluid temperature abruptly rose from the ambient temperature to 540F. The primary system began to depressurize at 115 psi/min from 1730 psia (Figure 5.2.2). The core exit fluid subcooling margin (SCM) descended from 23F (Figure 5.2.3) in response to the depressurization. The cold leg flow rates varied little, but the downcomer flow rate decreased abruptly, from 6500 to 5800 lbm/h, in response to the imposition of the cold leg B1 discharge leak (Figure 5.2.4 and 5.2.5). The core fluid temperature increased as the core flow rate decreased, warming from 593F at test initiation to 596F at 1 minute (Figure 5.2.6). Whereas the loop B hot leg fluid temperatures rose sequentially in response to the increased core exit fluid temperature, the loop A hot leg fluid temperatures responded quite differently. The pressurizer outsurge accompanying leak actuation first displaced the relatively cold surge line (and pressurizer

bottom) fluid into the hot leg A riser, then reheated the A riser as the initially saturated pressurizer fluid entered the hot leg. The timing and extent of these fluid temperature swings were key to the loop A versus B interruption and, hence, to the subsequent interactions.

Saturation of Loop A

The coldest surge line fluid passed into the hot leg A riser at 0.2 minutes, reached 47 ft in hot leg A at 0.65 minutes, and attained the A U-bend at 1.15 minutes (Figure 5.2.6). The fluid cooling diminished with the traversed hot leg length; the successive minimum temperatures were thus 583F near the surge line-to-hot leg A connection, 586F at 47 ft, and 588.5F at the hot leg A U-bend. Following the passage of this colder fluid, the subsequent reheating of the hot leg A fluid, due to the outsurge of the relatively warm pressurizer fluid inventory, was more rapid than the ongoing heating of the hot leg B fluid. This more rapid heatup rate of the hot leg A fluid combined with the decreasing primary saturation temperature (due to depressurization) obtained saturation of the loop A fluid before loop B. The loop A fluid near the surge line connection peaked just above 596F, at 1.5 minutes; at this time, the primary saturation temperature had decreased to 601F from 615.5F initially. The hot leg A riser fluid at 47 ft thus reached 595F and saturated at 2 minutes, followed by the hot leg A U-bend fluid at 2.15 minutes. The primary system pressure stabilized at 1470 psia. The loop B U-bend fluid saturated only 15 seconds later, at 2.4 minutes (Figure 5.2.6). But the preceding loop A saturation had already had a significant impact on inter-loop conditions.

Interruption of Loop A Flow

The hot leg A upper riser void fractions increased abruptly to approximately 10% at 2.1 minutes (Figure 5.2.7), whereas the loop B voiding was delayed and suppressed (Figure 5.2.8). The riser fluid density decrease caused the loop A flow rate to increase, followed by loop B (Figures 5.2.4 and 5.2.5). The resulting core flow increase cooled the core exit fluid, reversing the earlier trend (Figure 5.2.6). The core exit cooling reached the nozzle elevation at 2.2 minutes and traversed the hot leg inlets at 2.4 minutes. But the loop A flow rate had already begun to decrease, thus the cooling trend affected mostly the loop B hot leg fluid. The reduction of the loop flow rate, which caused this asymmetric cooling, was governed by U-bend

voiding. The hot leg A riser collapsed liquid level first indicated voiding at 1.9 minutes, the remaining levels (A stub, B riser and stub) first decreased near 2.2 minutes (Figure 5.2.9). Whereas the riser void fractions subsided after their initial increase (Figure 5.2.7 and 5.2.8), the U-bend void fraction increases persisted (Figure 5.2.10). The hot leg A U-bend void fractions (both upstream and downstream of the U-bend) began to increase at 2.15 minutes, the corresponding loop B void fractions increased at 2.4 minutes. The loop A hot leg U-bend upstream void fraction began to stabilize at 2.4 minutes after an increase of 7%, the corresponding B void fraction trend occurred at 2.5 minutes after an increase of 5%. As the U-bend spillover elevations began to be uncovered, the corresponding loop flow rates abruptly began to decrease and the stub levels (beyond the U-bends) began to drop relatively rapidly (Figure 5.2.9). (As the loop flow rates declined, the levels bracketing the U-bend realigned to compensate for the decreased flow losses in that loop.) The loop A flow rates remained virtually stagnated beyond 3.6 minutes, whereas the loop B flow rates first decreased to 1000 lbm/h and then increased (Figures 5.2.4 and 5.2.5).

Second Set of Test-Initiating Actions

The second set of test-initiating actions was performed as the loop fluid began to void and as the loop A flow increased and then stagnated. The steam generator secondary control levels were increased, causing the feed rates to both generators to increase to approximately 10% of the scaled full (per steam generator) secondary flow rate at 2.0 minutes (Figure 5.2.11). The steam generator A feed rate increase lagged that of steam generator B. The RVVV limit switches activated at 2.1 minutes (Figure 5.2.12), followed by changes of the fluid temperatures bracketing the valves, in response to the transfer of their control from manually closed to automatic/independent. Core power began to decrease at 2.2 minutes as the core power decay simulation was activated. The HPI isolation valves actuated at 2.1 minutes. The MIST HPI system, unlike the plant HPI systems, included accumulators. HPI flow to the loop was delayed until 2.4 minutes (Figure 5.2.1) by the requisite pressurization of the MIST HPI system accumulators.

Divergence of Downcomer Fluid Temperatures

The downcomer fluid temperatures diverged markedly in response to the actuations of the RVVVs and HPI. The upper downcomer fluid temperatures, sequentially downward from the elevation of the RVVVs, increased toward saturation starting at 2.15 minutes (Figure 5.2.13). The lower downcomer temperatures, in sequence from the cold leg nozzle elevation downward, decreased in response to HPI cooling starting at 2.5 minutes. The densification of the lower downcomer fluid in consort with the RVVV opening augmented the flow rate through the downcomer and the core.

Divergence of Cold Leg Nozzle Fluid Temperatures

The temperature across the core rose from 34F at 2.8 minutes to 58F at 3.8 minutes as the lower downcomer and core inlet fluid cooled (Figure 5.2.14). The cold leg nozzle fluid temperature distributions indicated the combined effects of loop flow rate, HPI cooling, and heatup of the upper downcomer fluid through RVVV discharge. The nozzle temperatures in each of the four cold legs dropped abruptly at 2.5 minutes (Figures 5.2.15 and 5.2.16), as HPI cooling took effect. Beyond 2.6 minutes, the cold leg nozzle fluid temperatures began to diverge among the cold legs in response to the unequal cold leg flow rates. The loop A flow rates declined after 2.4 minutes whereas the loop B flow rates peaked at 2.6 minutes. Therefore, the HPI flow rate was a greater portion of the nozzle flow in loop A than in loop B, HPI cooling was greater in loop A, and the loop A nozzle fluid temperatures decreased below those of loop B. The upper downcomer fluid just above the cold leg nozzle elevation began to heat toward saturation at 2.8 minutes (Figure 5.2.13). Shortly thereafter, and as the loop A flow rate continued to decline, the relatively warm upper downcomer fluid began to backflow into the cold leg A1 and A2 discharge piping, as reflected by their nozzle upper fluid temperatures (Figure 5.2.15). As the loop A cold leg flow rates virtually stagnated near 3.6 minutes, temperature differences of 100F developed across the loop A cold leg nozzles (Figures 5.2.15 and 5.2.16). The fluid temperatures near the top of the nozzles stabilized near the primary saturation temperature of 575F (Figure 5.2.15), while the fluid temperatures toward the bottom of the nozzles stabilized near 460F (Figure 5.2.16). The loop B nozzle upper and lower fluid temperatures, on the other hand, behaved similarly. The cold leg

B1 nozzle fluid temperatures, in the cold leg containing the leak, increased as its loop flow rate declined and vice versa.

Core Region Voiding

The core exit SCM had approached zero as the primary system pressure stabilized near 2.1 minutes, increased as the loop flow rates increased, and again saturated from 3.6 to 4.4 minutes as loop A stagnated and the loop B flow rate declined (Figure 5.2.3). At 3.5 minutes, the reactor vessel collapsed liquid level began to decline (Figure 5.2.17) and the uppermost incremental void fraction (24 to 29 ft) began to increase (Figure 5.2.18). Slight core region voiding was also in evidence.

Hot Leg B Heating, Voiding, and Interruption

Intermittent loop B flow predominated the system interactions from 5 to 15 minutes. The loop A U-bend remained voided (Figures 5.2.7 and 5.2.9) and loop A flow remained inactive (Figure 5.2.4). The driving interactions were the (inverse) relation between loop flow and core fluid temperature rise, and the several-minute transit time between the core exit and the hot leg (B) U-bend. Loop B flow rate minimums occurred at 3.7, 7.2, and approximately 10 minutes (Figure 5.2.5). For the first flow rate minimum, the core exit fluid temperature began to increase at 2.9 minutes, saturating at 3.8 minutes (Figure 5.2.6). The hot leg B fluid temperatures began to increase sequentially with distance up the hot leg -- inlet at 3.5 minutes, mid-height at 4.7 minutes, and U-bend at 5.1 minutes. The hot leg B flow rate increased (Figure 5.2.5) as its riser density decreased. The resulting primary-to-steam generator B heat transfer slightly enhanced the continuing primary system depressurization (Figure 5.2.2), causing the heated hot leg B riser fluid to saturate and void more readily. The hot leg B inlet fluid saturated at 4.1 minutes, the riser mid-height at 5.1 minutes, and the U-bend at 5.3 minutes (Figure 5.2.6). The hot leg B riser began voiding at 5.0 minutes (Figure 5.2.8), and the U-bend void fraction increased from 5.2 to 6.5 minutes (Figure 5.2.10). The U-bend spillover elevation apparently uncovered and the loop B flow rate began to decrease after 5.4 minutes (Figure 5.2.5).

Core Exit Subcooling

The period of enhanced loop B flow had reversed the core exit temperature trend, however. The core exit fluid subcooled at 4.6 minutes, followed by the hot leg B inlet at 5.2 minutes (Figure 5.2.6). The increasing riser fluid density further retarded the loop B flow rate following its peak at 5.4 minutes. The downcomer flow rate reached a minimum value of 3300 lbm/h at 6.6 minutes (Figure 5.2.5). The decreased core flow rate caused the core fluid to reheat (Figure 5.2.6), thus beginning a second cycle of heating, voiding, and enhanced flow rate.

Steam Generator Secondary Refill

The repetitive sequence was interrupted when the steam generator secondaries had been refilled at 9.7 minutes (Figure 5.2.19). Rather than continuing to decrease but at varying rates, primary system pressure began to increase slowly from 1350 psia (Figure 5.2.2), thus suppressing hot leg riser voiding. The loop B U-bend void fraction approached 10% at 9.9 minutes (Figure 5.2.10), the loop B flow rate approximately stagnated (Figure 5.2.5), and the hot leg B riser fluid remained near saturation (Figure 5.2.6).

The reactor vessel level approached the elevation of the RVVVs at 11.4 minutes (Figure 5.2.17). The RVVVs began to discharge vapor, the primary system pressure resumed a slow decrease, and the upper downcomer began to void. As the reactor vessel and downcomer voided, the hot leg B stub level began to increase (Figure 5.2.9). The hot leg B riser level remained near the spillover elevation, therefore the loop B flow rate gradually increased (Figure 5.2.5) as the level imbalance across the loop B U-bend was reduced. The steam generator B secondary began to repressurize at 13.1 minutes (Figure 5.2.2), leading to steam generator B steaming at 14.1 minutes (Figure 5.2.11). The primary system depressurization rate increased slightly at 13.7 minutes, the loop B riser began to void gradually, and then more rapidly beyond 14.2 minutes (Figure 5.2.8). Loop B was thus reactivated as had occurred earlier, but by quite different mechanisms.

RVVV Activity

The RVVV differential pressures generally varied inversely with core flow rate (Figures 5.2.5 and 5.2.20), reflecting primarily the increased core

fluid heating and density reduction with decreased core flow. The RVVV differential pressure decrease beyond 12.5 minutes was more extensive than had occurred earlier. The downcomer was partially voided (Figure 5.2.17), thus the suppression of core region voiding (Figure 5.2.18) with loop flow reactivation countered the usual RVVV differential pressure. The pressure differences descended to the valve actuation setpoints and the valves began closing at 13.4 minutes (Figure 5.2.12). The core fluid subcooling was of short duration, however (Figure 5.2.3). The hot leg B U-bend region voids (Figure 5.2.10), loop B flow began to decrease (Figure 5.2.5), the core region fluid again began to void (Figure 5.2.18), the RVVV differential pressures rose (Figure 5.2.20), and the valves opened beyond 15.5 minutes (Figure 5.2.12).

5.2.2. Primary System Depressurization, 15 to 80 Minutes

The downcomer level resumed its descent until, at 15.7 minutes, the cold leg nozzles were uncovered (Figure 5.2.17). The key interaction during this period was the condensation of core steam, discharged through the RVVVs, by HPI. The heat capacity of the subcooled HPI was sufficient to condense the entire core steam generation rate, thus the primary system gradually depressurized. The system interactions stabilized beyond 16 minutes, following the stagnation of outer-loop flow. These conditions resembled those of Nominal Test 3109AA, which are described in detail in the Group 31 Report.

Inter-Cold Leg Flow

The loop A cold leg flow rates remained stagnant but the loop B cold legs began to interact (Figure 5.2.21). The flow directions were backward in B1 (toward the leak site from the downcomer) and forward in B2. As discussed in detail in Test 3109AA, the requisite condition for this cold leg interaction included the downcomer and steam generator primary outlet common points and a fluid density difference between the adjacent vertical cold leg suction piping lengths. Relatively cold HPI fluid was supplied to the backflowing cold leg B1; steam generator primary outlet fluid mixed with the forward-flowing cold leg B2. The leak fluid temperature, which had been quite variable, stabilized at 540F (Figure 5.2.22) as the loop B cold legs began to interact beyond 16 minutes. These cold leg flow rates attained ± 2.7% (of scaled full CL flow) at 18 minutes, and then stabilized at approximately ±

2.5% near 30 minutes. As the primary system slowly depressurized (Figure 5.2.23), the leak fluid subcooling gradually decreased from 17.5F.

Steam Generator Activity

The steam generator B secondary repressurization at 14.5 minutes raised its secondary saturation temperature to the control point, as previously noted. The core exit-to-steam generator B secondary saturation temperature difference remained near the control value of 50F, therefore the steam generator B secondary remained intermittently active (Figure 5.2.24). The steam generator B secondary was depressurized in parallel with the continuing primary system depressurization. The steam generator A secondary level dropped several feet upon its feed deactivation at 9.5 minutes, therefore its feed was reactivated to regain the specified control level. The steam generator A secondary remained depressurized (Figure 5.2.23), therefore it was not steamed and its feed was terminated at approximately 19 minutes, after the specified secondary level had been regained. The loop A steam generator primary level descended into the steam generator just as its feed was terminated (Figure 5.2.25), therefore steam generator A remained inactive.

Reactor Vessel Conditions

The brief interruption of RVVV flow ending at 15.5 minutes, followed by the cessation of loop flow, had a lingering effect on the core fluid temperature rise. The downcomer fluid cooled (sequentially) from 525 to 480F during the RVVV closures, then reheated to 490F. The core exit fluid remained saturated, therefore the core fluid temperature rise reached 95F at 17 minutes and then slowly declined with the primary system depressurization (Figure 5.2.26). The core region levels and void fractions also stabilized beyond 17.5 minutes. The downcomer collapsed liquid level remained near the cold leg nozzle elevation, and the reactor vessel level descended slowly from approximately 1 ft higher (Figure 5.2.27). The core exit region (14 to 17 ft) void fraction indicated ~15%.

Gradual Steam Generator B Depressurization, 15 to 45 Minutes

For the next half hour, from 15 minutes to 45 minutes, steam generator B was gradually depressurized with the primary system (Figure 5.2.23) to maintain the control temperature difference of 50F (core exit to secondary saturation).

At 27 minutes, the loop B steam generator primary level descended into the steam generator (Figure 5.2.25) while its feed remained mildly active. As a result, the primary system depressurization rate increased from 10 to 17 psi/min. Rather than repressurizing through primary-to-secondary heat transfer, the steam generator B secondary depressurized slightly, apparently due to the feed addition, and its controlled steaming was interrupted (Figure 5.2.24). Steam generator B evidenced increased activity beyond 36 minutes. Steam generator B began to be steamed, its feed rate was gradually increased, and its primary level, which had been declining, began to rise. The primary system depressurization rate, which had declined since the BCM near 25 minutes, again increased (Figure 5.2.23). The loop A steam generator primary level decreased more rapidly as the steam generator B heat removal increased. The loop A steam generator primary level had entered the steam generator at 18 minutes, as previously noted. Now, the primary level decreased toward the elevation of the steam generator secondary pool.

Boiler-Condenser Mode

The loop A steam generator primary level descended to the elevation of the secondary pool at 45.5 minutes (Figure 5.2.28), thus activating "pool BCM"; this is the condensation of primary system vapor within the steam generator, in the vicinity of that liquid level overlap, with the secondary level at or above the primary level. The steam generator A secondary pressure had remained constant since secondary refill. Its control temperature difference (core exit minus steam generator A secondary saturation) had decreased only gradually in response to the primary system depressurization. The steam generator A pool BCM altered these trends. The steam generator A secondary repressurized, its temperature difference dropped to the control value, and it began to be steamed at 50 minutes (Figure 5.2.24). The primary system depressurization rate, which had again dwindled since the previous steam generator B heat transfer event, now stabilized at 20 psi/min (Figure 5.2.23). The enhanced rate of primary system depressurization reduced the core exit-to-steam generator saturation temperature differences at a rate sufficient to activate both steam generators. The steam generator B steaming rate was increased, steam generator B feed was reactivated at 49 minutes, and steam generator A feed was reintroduced at 56.3 minutes and increased at 58.5

minutes (Figure 5.2.24). The reactivation of feed to steam generator A obtained sufficient heat transfer from the loop A primary fluid to alter the inter-loop levels (Figure 5.2.25). The loop A hot leg (riser and stub) levels rose whereas the relatively warm loop B levels dropped. Thus, the steam generator A pool BCM was supplanted by (steam generator A) AFW-BCM, the condensation of primary system vapor within the steam generator, in the region cooled by the (high-elevation) injection of relatively cold feed. The primary system depressurization approached 40 psi/min, reducing the primary system pressure to within 100 psi of the steam generator secondary pressures.

Start of Refill, 55 Minutes

The steam generator activity reversed the primary system mass depletion. The leak fluid subcooling decreased to less than 20F at 60 minutes. As a result of the decline of both leak fluid subcooling and primary system pressure, the leak mass flow rate decreased from 650 lbm/h at 50 minutes to 480 lbm/h at 70 minutes (Figure 5.2.29). The HPI flow rate, on the other hand, increased slightly with the primary system pressure reduction. The flow rates intersected near 55 minutes and primary system refill began.

The primary system depressurized below the CFT pressure, 600 psia, at 63.5 minutes (Figure 5.2.30). The effects of the ensuing CFT discharge were overshadowed by the ongoing steam generator activity. The rate of gain of the primary system total fluid mass (which included the CFT inventory) approached 200 lbm/h between 70 and 95 minutes, which corresponded to the maximum difference between the measured HPI and leak mass flow rates. The reactor vessel collapsed liquid level descended to 20 ft, more than 3 ft above the top of the core, during the CFT activity (Figure 5.2.27).

5.2.3. Equilibrium and Gradual Hot Leg Refill

Quasi-Equilibrium Beyond 85 Minutes

The steam generator heat transfer activity alternated between the steam generators. The primary system fluid mass increase quickly precluded steam generator heat transfer, however. The primary levels in both steam generators exceeded the upper tubesheet elevation at 85 minutes (Figure 5.2.31). The controlled depressurization of the steam generator secondaries ceased at 90 minutes (Figure 5.2.32) and feed was interrupted at 97 minutes. The steam

generator secondary pressures stabilized at 300 psia, whereas the primary system repressurized as rapidly as 7 psi/min from a minimum value of 470 psia. The leak fluid subcooling increased due to the primary system repressurization and due to the increased effects of HPI cooling. The leak flow rate thus increased dramatically (Figure 5.2.33) through the combined effects of repressurization and enhanced subcooling, and approached the slightly diminished HPI flow rate at 130 minutes. The rate of hot leg level rise thus slowed with the riser and stub levels between 55 and 58 ft (Figure 5.2.31), that is, above the steam generators but well below the U-bend spillover.

Asymmetric Hot Leg Refill

The core region level stabilized just below the RVVVs (Figure 5.2.34), then the hot leg levels began to increase at approximately 140 minutes (Figure 5.2.31). The primary system pressure also stabilized at this time (at 650 psia) and then very gradually decreased (Figure 5.2.32). Apparently, the primary system fluid volume sources and sinks were balanced near 140 minutes, and the subsequent reduction of core power lowered the primary system equilibrium pressure.

The hot leg levels ascended asymmetrically (Figure 5.2.31). In both loops, the stub levels remained a few feet below the riser levels. But the riser and stub levels rose first in loop B until 155 minutes, then the loop B levels remained almost constant while the loop A riser and stub levels rose. Just before the loop A levels achieved the spillover elevation at 270 minutes, the inter-loop level difference was approximately 6 ft. (These level indications were confirmed by the incremental level measurements and by the local fluid temperature measurements.) The 6-foot level difference was the equivalent of 2 psi, a large pressure difference compared to the forces governing natural circulation. Comparing this difference to liquid density differences, the loop A and B liquid temperatures would have to have differed by 10F throughout 60 ft of vertical piping to account for this level difference. There were no temperature differences of this magnitude over any significant vertical length of piping.

The pressurizer connection to loop A was an obvious source of inter-loop asymmetries. But the pressurizer interactions during this period of slow hot leg refill (from 110 to 270 minutes) apparently had little impact on the hot

leg fluid temperature profiles. The total pressurizer outsurge during the gradual depressurization was much smaller than the loop A hot leg excess (over loop B) corresponding to the 6-foot level difference. Thus, like the hot leg level differences that occurred during the initial draining period, the observed level differences were due to differences in vapor energy. That is, the U-bend vapor in loop B, compared to that in loop A, was sufficiently energetic to sustain the inter-loop level imbalance. The hot leg riser upper-elevation (Zone 3) guard heaters exhibited corresponding inter-loop asymmetries. The loop B Zone 3 guard heater power demand was approximately 50% greater than that of loop A (Figures 5.2.35 and 5.2.36), due to a corresponding difference of the guard heater control temperature differences. The guard heaters maintained the actual metal-to-insulation temperature differences approximately equal to the specified control values, as intended. The relatively high metal temperatures during refill may have affected the performance of the Zone 3 guard heaters, however. Whereas the Zone 3 guard heaters had been characterized up to 473F in loop A and 447F in loop B, the hot leg upper elevation metal temperatures ranges from 480 to 500F during hot leg refill. A perturbation preceded the hot leg A level increase. The hot leg A stub fluid gradually cooled toward saturation between 125 and 150 minutes (Figure 5.2.37). At 132 minutes, the hot leg A stub guard heater control temperature difference abruptly decreased (Figure 5.2.38), the guard heater was deenergized from 135 to 143 minutes (Figure 5.2.35), and the stub metal temperature decreased to the saturation temperature (Figure 5.2.39). The hot leg A vapor temperatures upstream of the U-bend remained 10 to 20F superheated (Figure 5.2.40).

Hot Leg Temperature Profiles

The hot leg liquid temperature profiles during refill (Figure 5.2.41) reflected the preceding primary system pressure trends. That is, the liquid in both hot legs had been virtually isothermal at 460F as the primary system pressure achieved its minimum value. As the hot legs refilled and the primary system repressurized, the liquid being introduced at the bottom of the hot legs became progressively warmer and the now cooler liquid was displaced upward into the hot legs. The uppermost hot leg liquid, being in contact with vapor, remained saturated. Thus, the liquid in both hot legs

was saturated at the top and bottom, but as much as 30F subcooled at the middle elevations. Rather than warming through internal circulation, the middle-elevation fluid cooled very gradually, apparently reflecting uncompensated heat losses to ambient.

Steam Generator and Core Conditions During Equilibrium

The steam generator secondaries remained largely inactive as the hot legs slowly refilled. Feed was briefly reactivated to steam generator B near 150 minutes (Figure 5.2.42) to maintain level. This reactivation caused the steam generator B secondary to depressurize slightly, but otherwise had little impact. Also near 150 minutes, the RVVVs began to actuate intermittently (Figure 5.2.43) as the core vapor generation rate became insufficient to continuously maintain the RVVV differential pressures above the closing setpoint. The core exit fluid remained saturated during the slow refill of the hot legs, but the temperature difference across the core rose as the lower downcomer and core inlet fluid cooled. This cooling occurred as the HPI condensing and cooling capacity exceeded the core vapor generation rate. The temperature difference across the core reached 217F when the system reactivated at 270 minutes.

5.2.4. Spillovers Through Test Termination

Spillover at 270 Minutes

The hot leg A riser level achieved the U-bend spillover elevation at 270 minutes (Figure 5.2.31). The previously quiescent system conditions were markedly perturbed. The displacement of loop A primary fluid caused the steam generator A secondary to pressurize (Figure 5.2.32), reactivating first its steam flow to maintain secondary pressure and then its feed flow to maintain secondary level. As the loop A level beyond the U-bend increased, the loop B riser and stub levels dropped. Also due to the displacement of primary fluid, the relatively cool core inlet fluid was transported through the core. The fluid temperature rise across the core abruptly dropped (Figure 5.2.44) while the SCM rapidly increased (Figure 5.2.45). Full HPI flow had been used since test initiation. Now the SCM exceeded the HPI throttling value, 75F, and HPI was interrupted (Figure 5.2.33). Also due to the reduction of the core exit fluid temperature, the temperature difference

between the core exit fluid and the steam generator secondary saturation temperatures (the temperature difference for secondary pressure control) became negative (Figure 5.2.45). This negative control temperature difference triggered the rapid depressurization of both steam generator secondaries. Both steam generators were subsequently depressurized to their minimum values, approximately 40 psia (Figure 5.2.32).

The spillover activity lasted only a few minutes. With HPI interrupted and with a leak flow rate almost 600 lbm/h, the hot leg A levels receded from the U-bend, loop A flow ceased, and the system conditions reverted toward those preceding the spillover. The SCM decreased to 75F at 273.5 minutes, HPI was restored, and the hot leg levels again began to rise toward the U-bend elevation. There were two lasting effects of the spillover -- lowered primary and secondary system pressures (Figure 5.2.32), and a decreased primary system total fluid energy.

Second Spillover at 315 Minutes

The hot leg A riser level again reached the spillover elevation at 315 minutes (Figure 5.2.31). The interactions during this second spillover event were much like those during the earlier event. Unlike the earlier event, however, the core region and downcomer levels rose above the RVVV elevation (Figure 5.2.34) and the core exit fluid remained subcooled. Thus, the HPI flow rate was throttled beyond 350 minutes (Figure 5.2.33). The steam generator A secondary repressurized to approximately 100 psia during the spillover activity but was not sequentially depressurized (Figure 5.2.32), apparently reflecting a control system anomaly. The loop A hot leg and steam generator primary level descended sufficiently to obtain the BCM (Figure 5.2.31).

Refill of Loop A and Test Termination

The HPI throttling (for 75F SCM) reduced the hot leg level rise rates. The loop A riser finally refilled at 495 minutes. The loop A stub level followed, at 505 minutes, and loop A remained full (Figure 5.2.31). The test was terminated at 663 minutes based on maximum test duration. At termination, loop A remained full whereas the loop B hot leg riser and steam generator primary levels remained in the vicinity of the upper tubesheet.

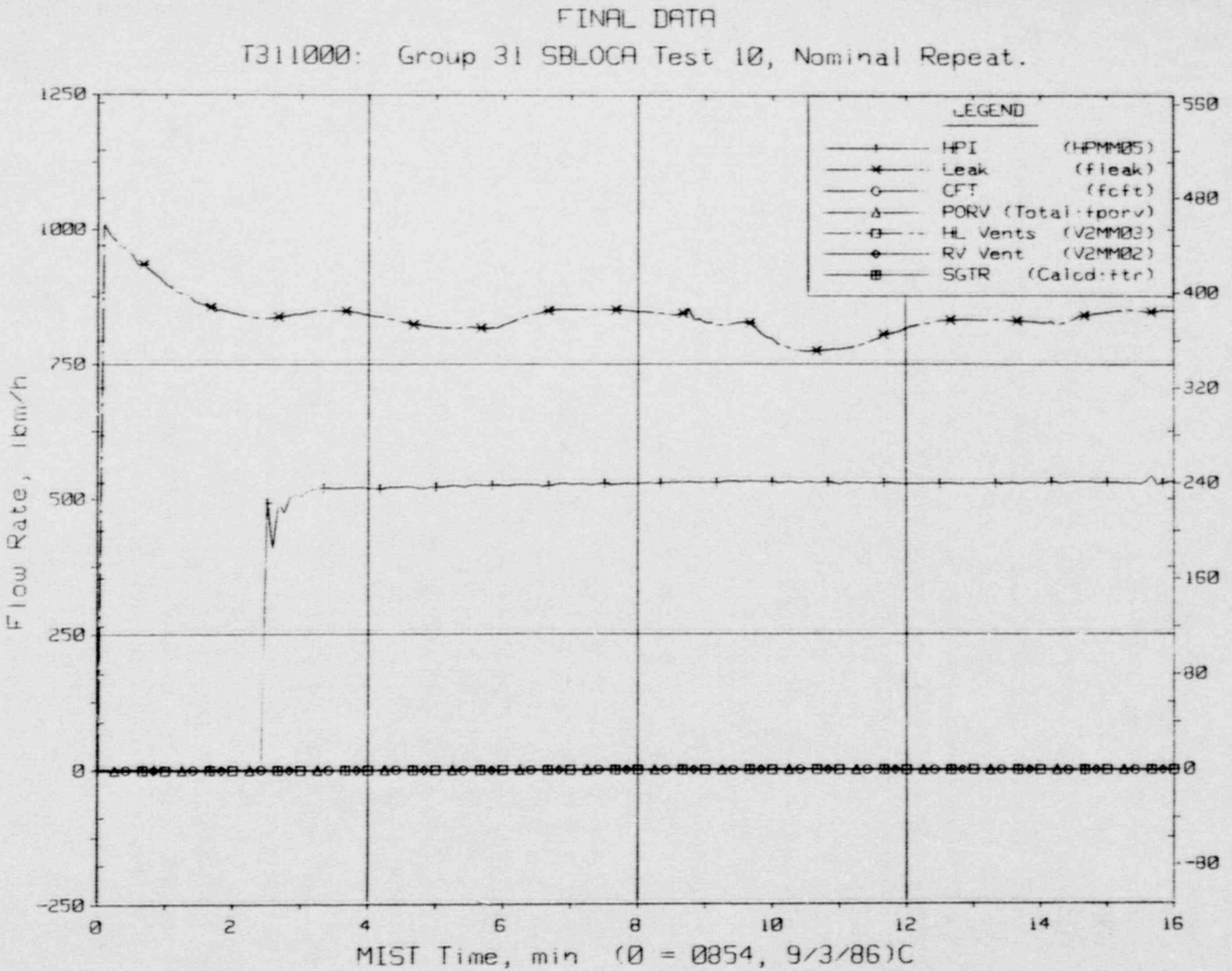

Figure 5.2.1. Primary System Boundary Flow Rates

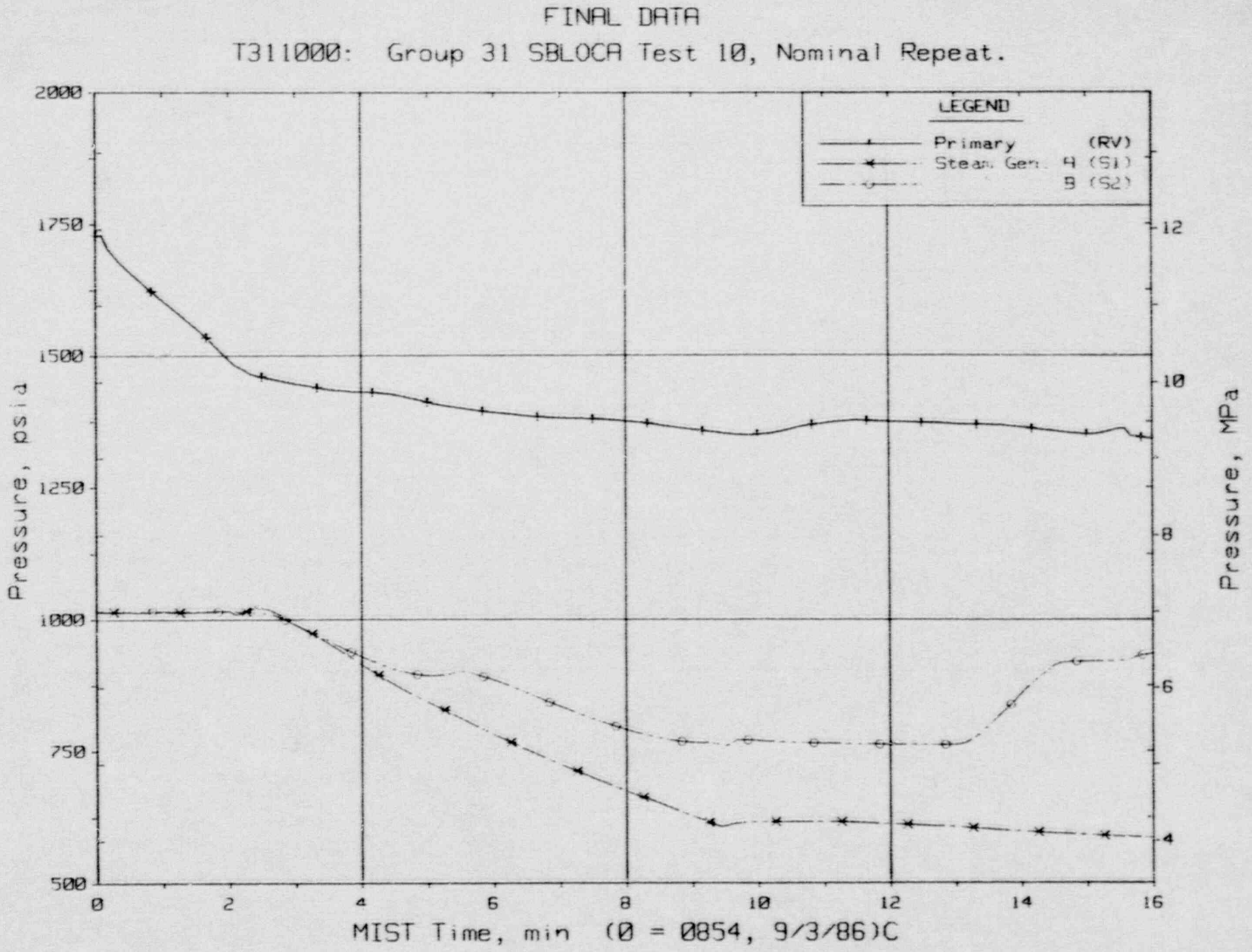

Figure 5.2.2. Primary and Secondary System Pressures (GP01s)

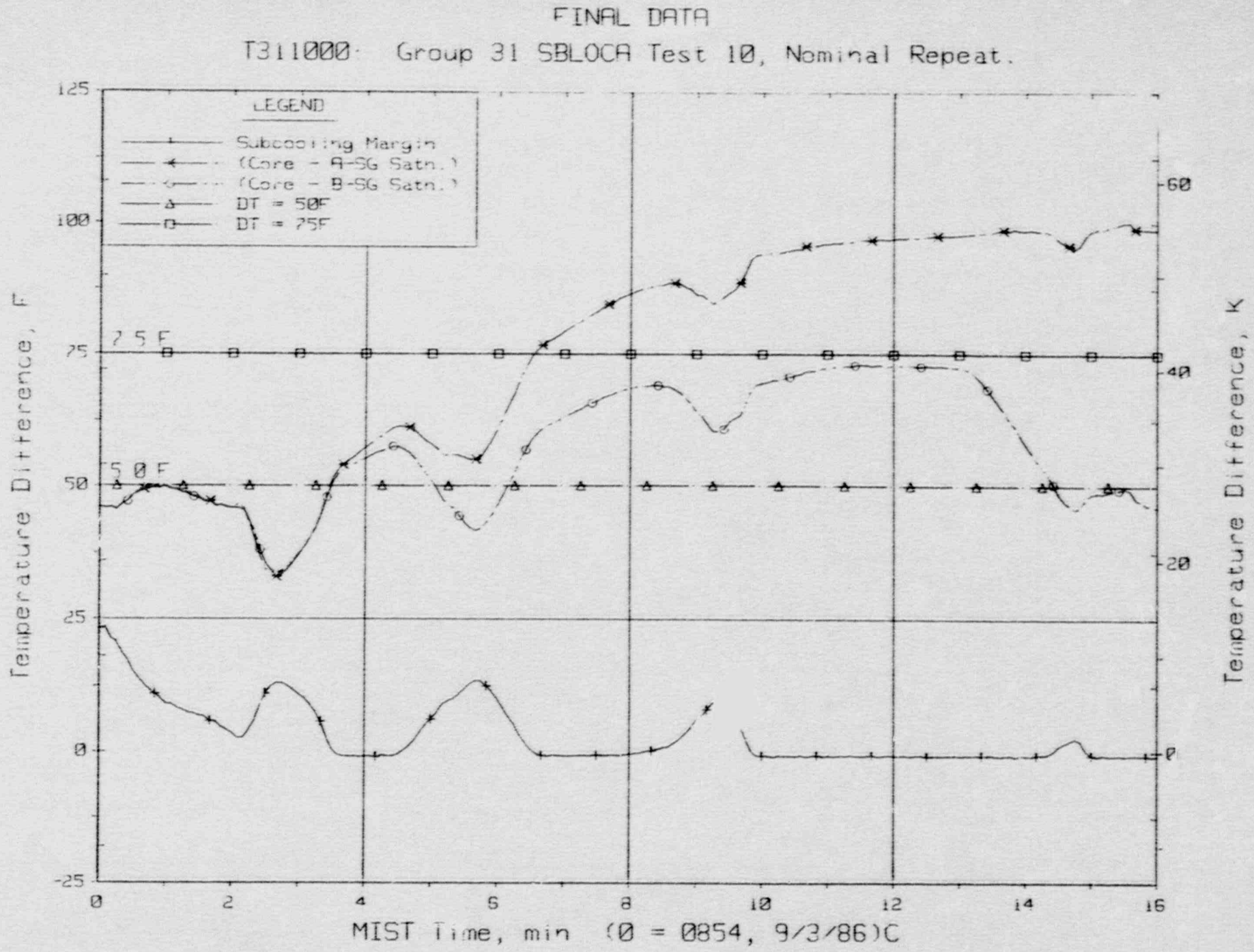

Figure 5.2.3. Control Temperature Difference

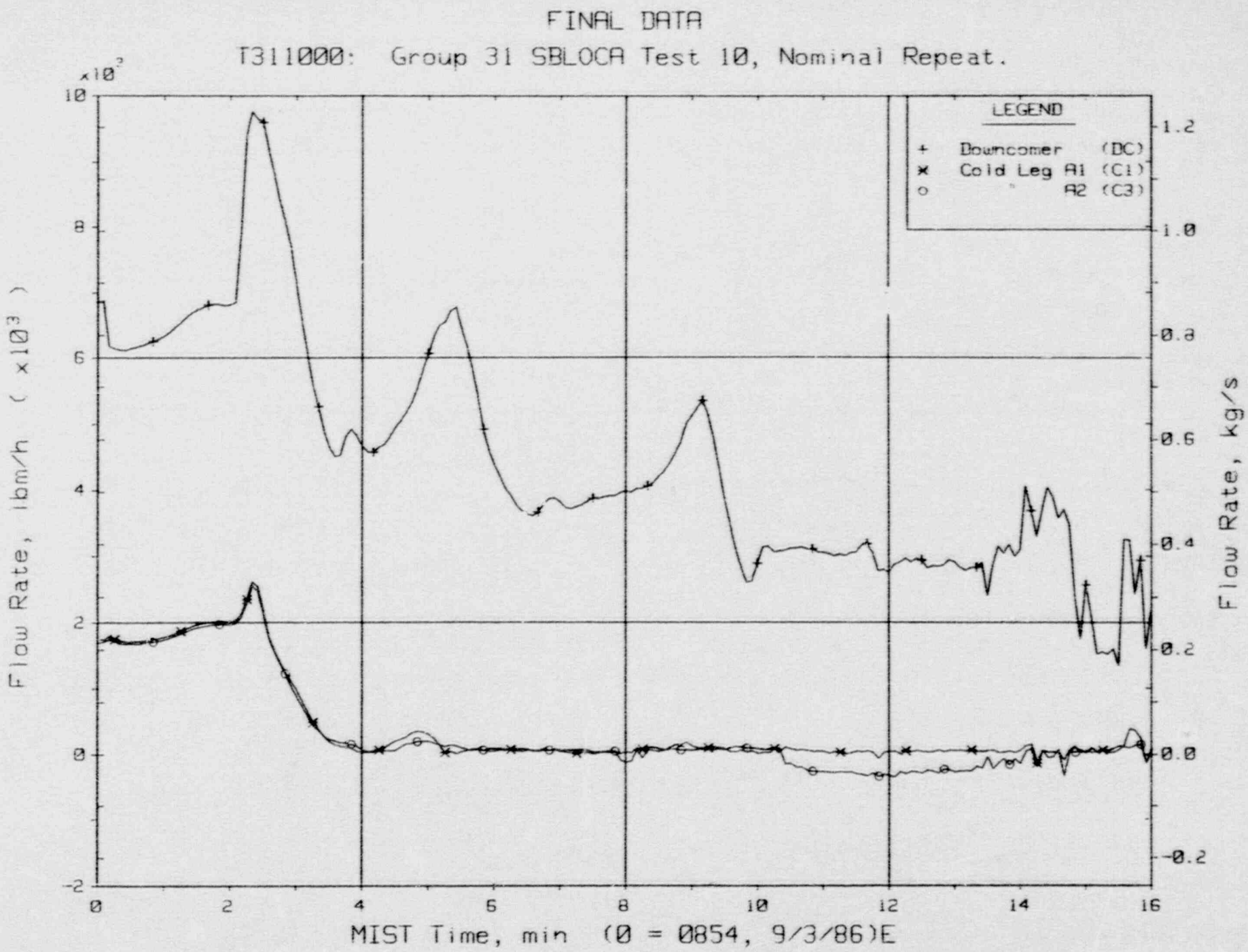

Figure 5.2.4. Primary System (Venturi) Flow Rates (VN20s)

Wed Dec 14 12:39:19 1988

PRFL1

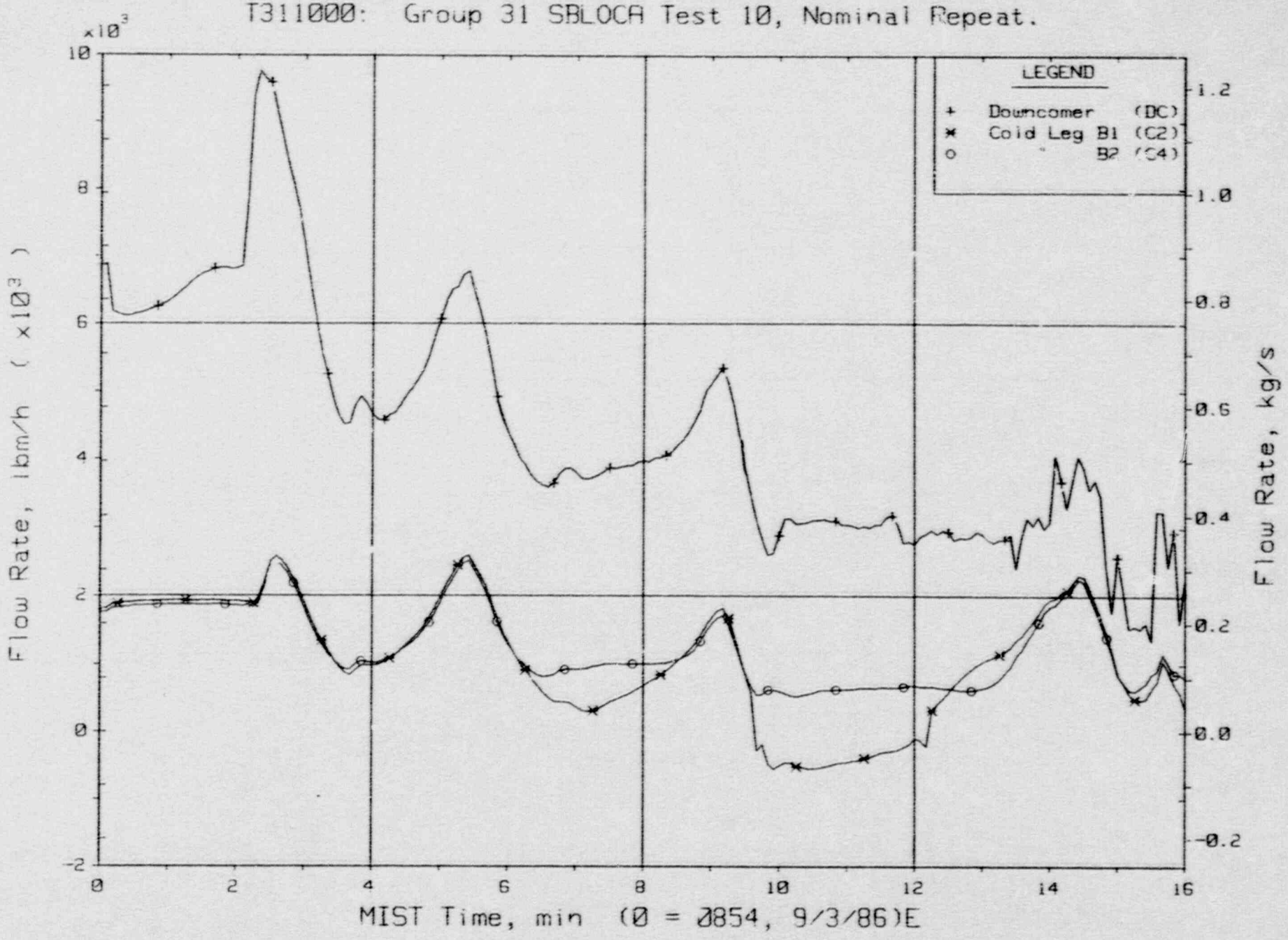

Figure 5.2.5. Primary System (Venturi) Flow Rates (VN20s)

Wed Dec 14 12:42:09 1988

PRFL2

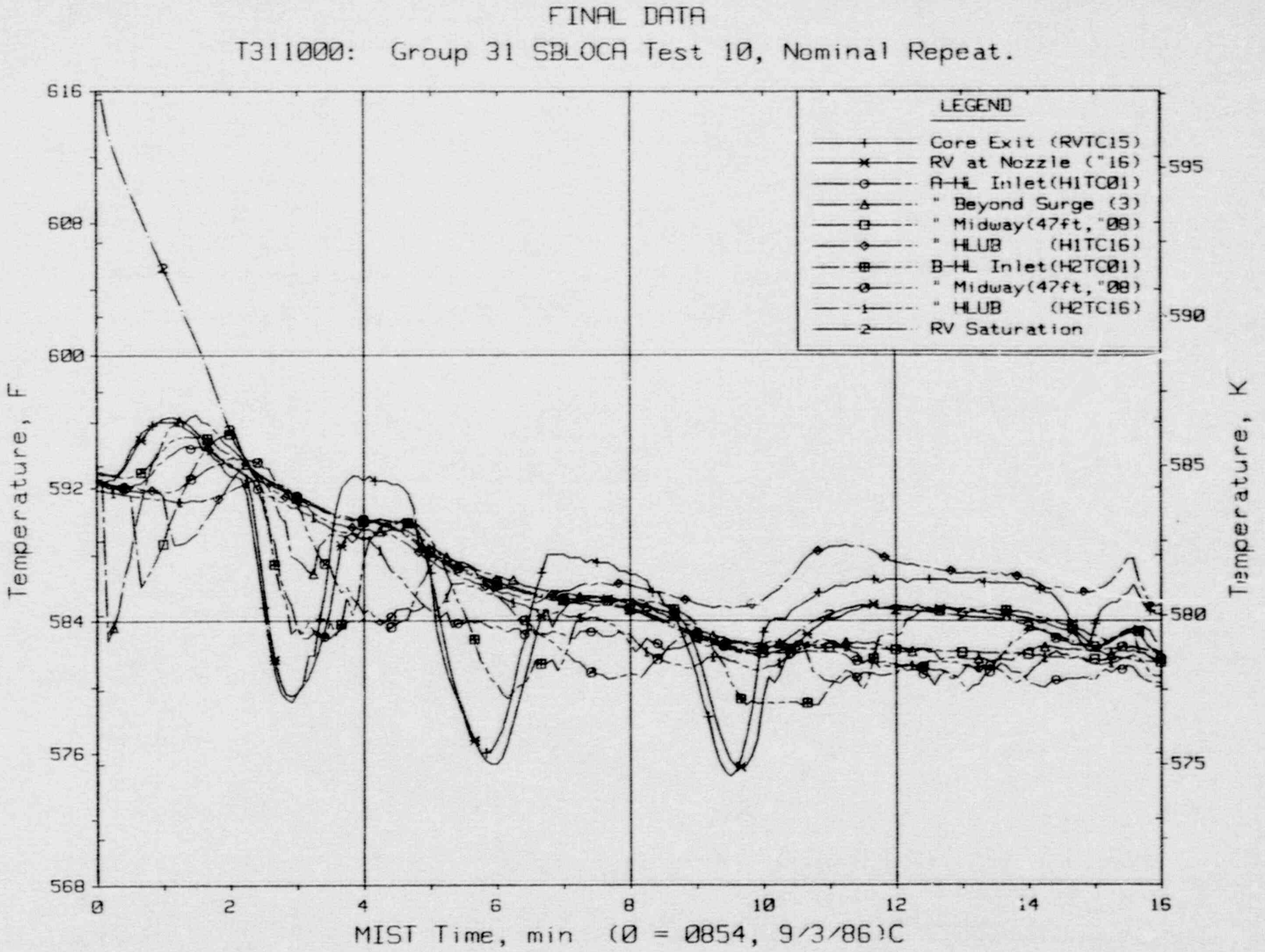

Figure 5.2.6. Composite Core Exit and Hot Leg Fluid Temperatures

Thu Jul 14 10:02:00 1988

PRKT1

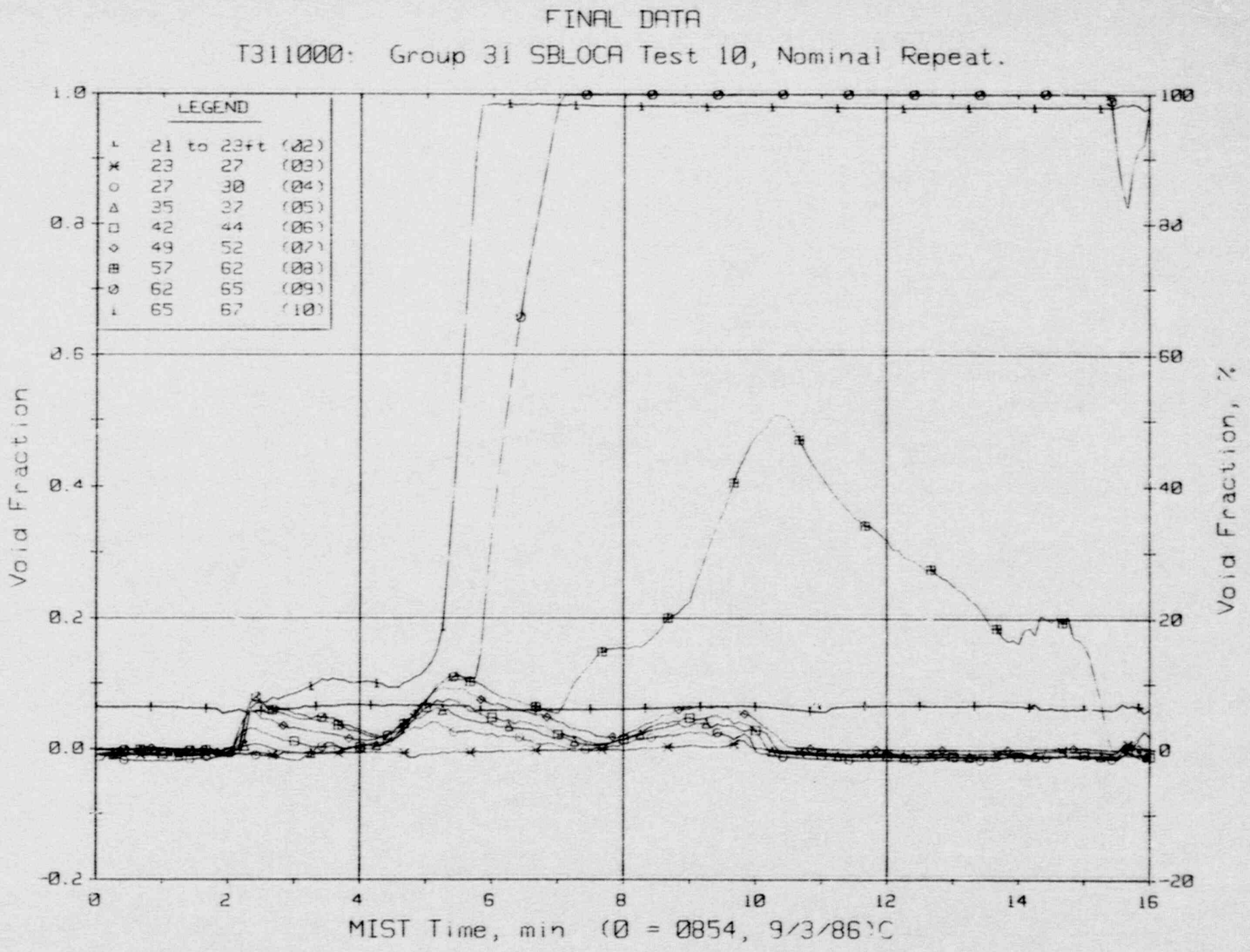

Figure 5.2.7. Hot Leg A Riser Void Fractions from Differential Pressures (HIVFs)

Thu Jul 7 10:40:06 1988

HIVF1

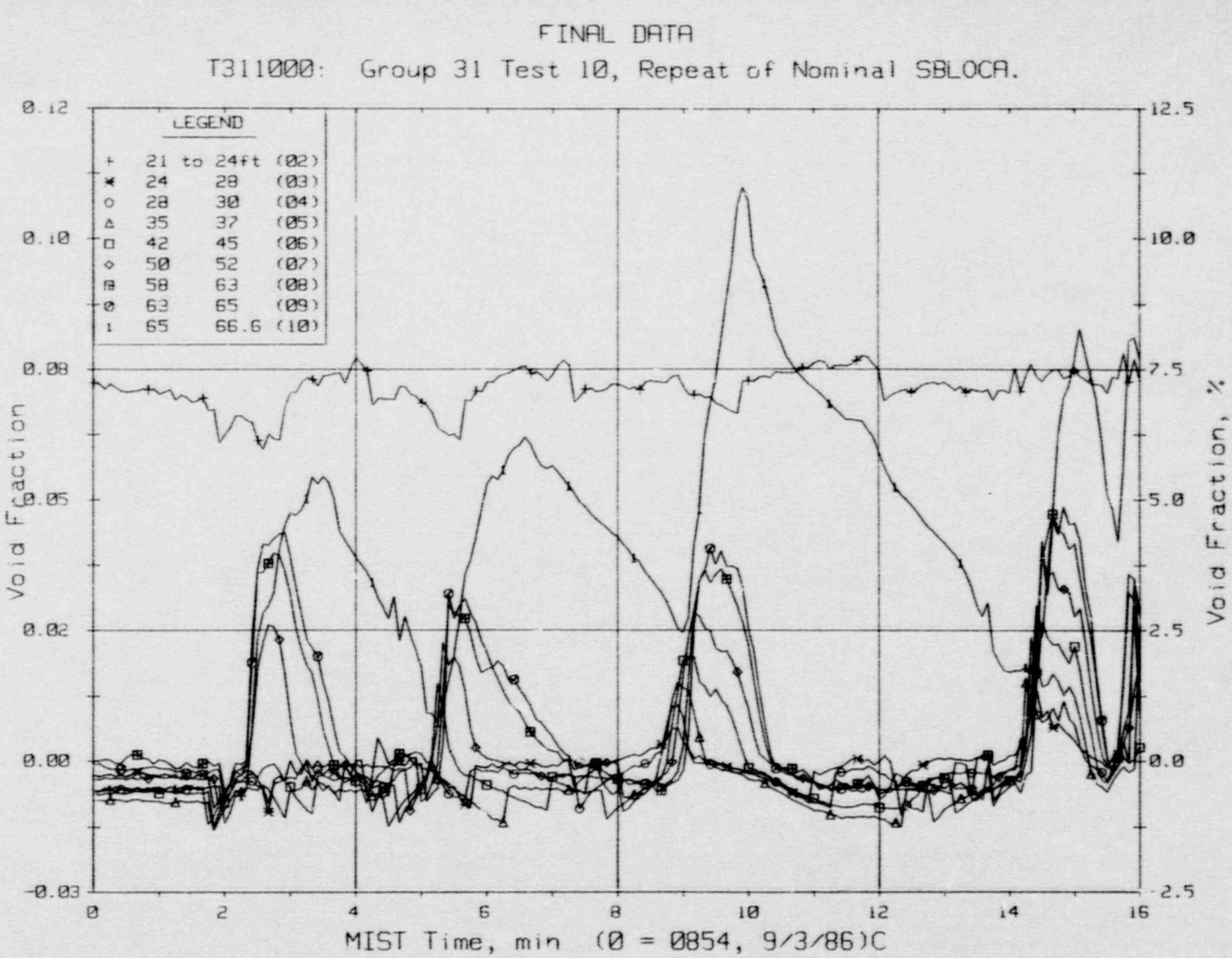

Figure 5.2.8. Hot Leg B Riser Void Fraction from Differential Pressures (H2VFs)

Wed Oct 26 11:24:03 1988

H2VF1

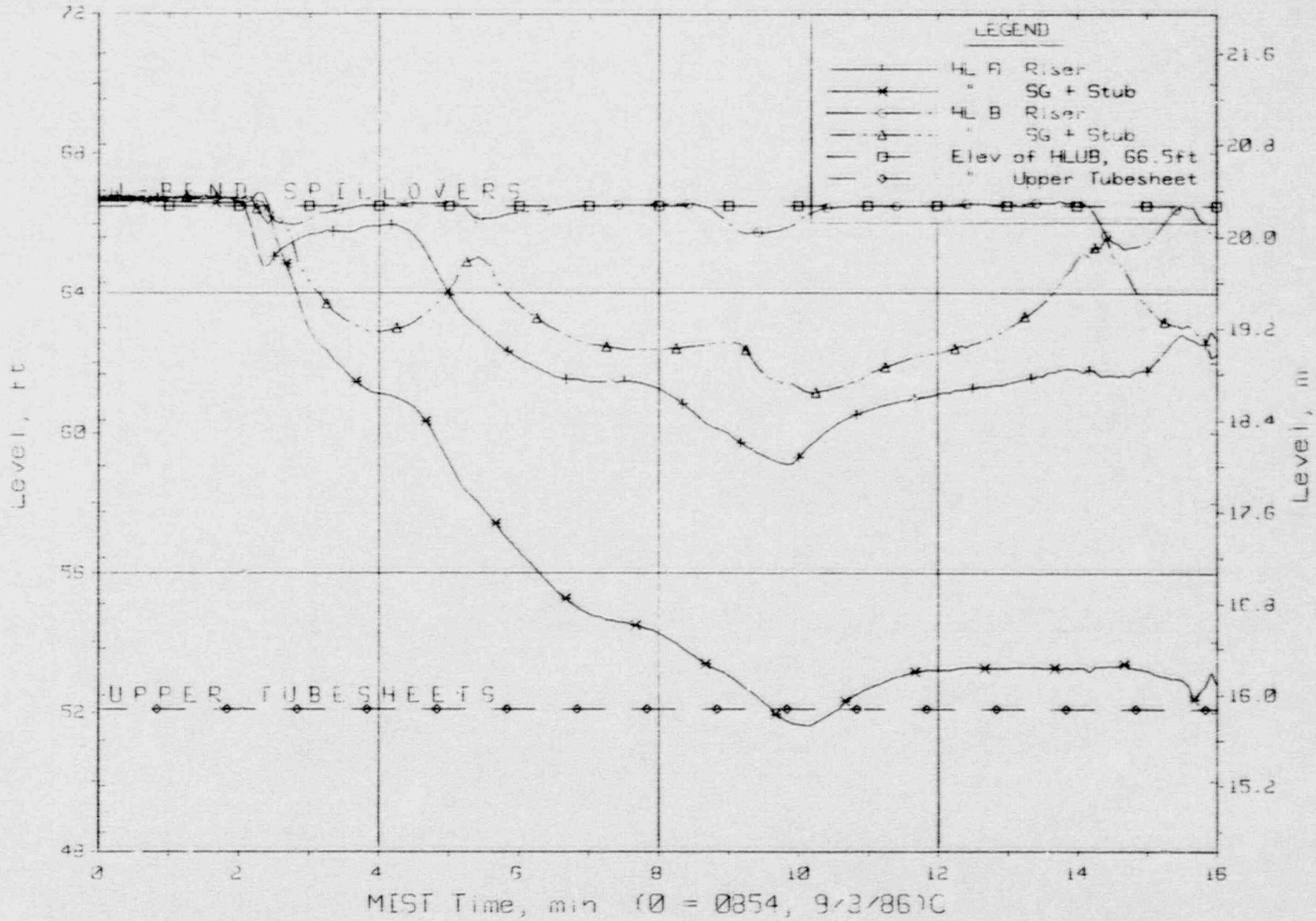

Figure 5.2.9. Hot Leg Riser and Stub Collapsed Liquid Levels

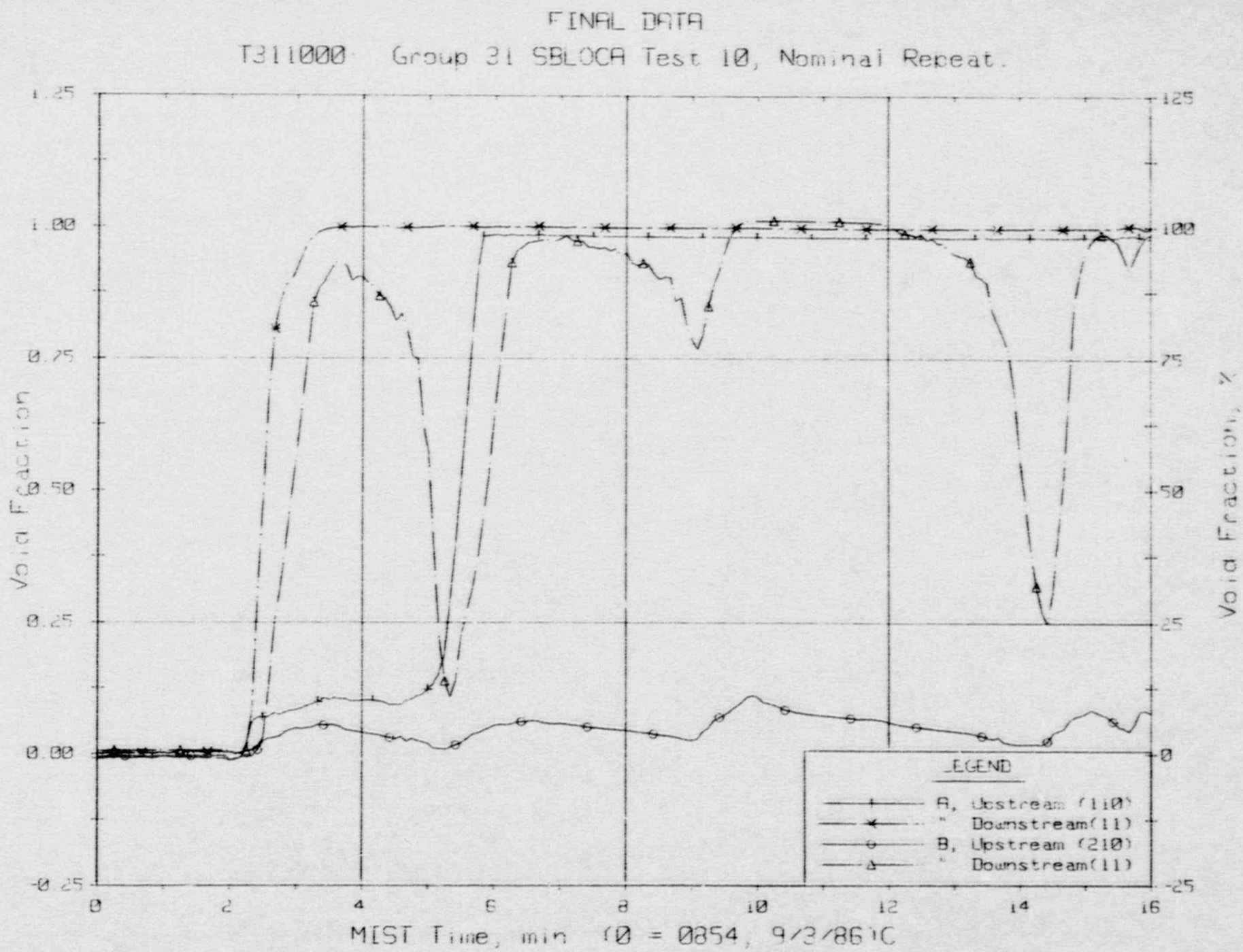

Figure 5.2.10. Hot Leg U-Bend Void Fractions from Differential Pressures (64.8 to 66.6 ft, HnVFs)

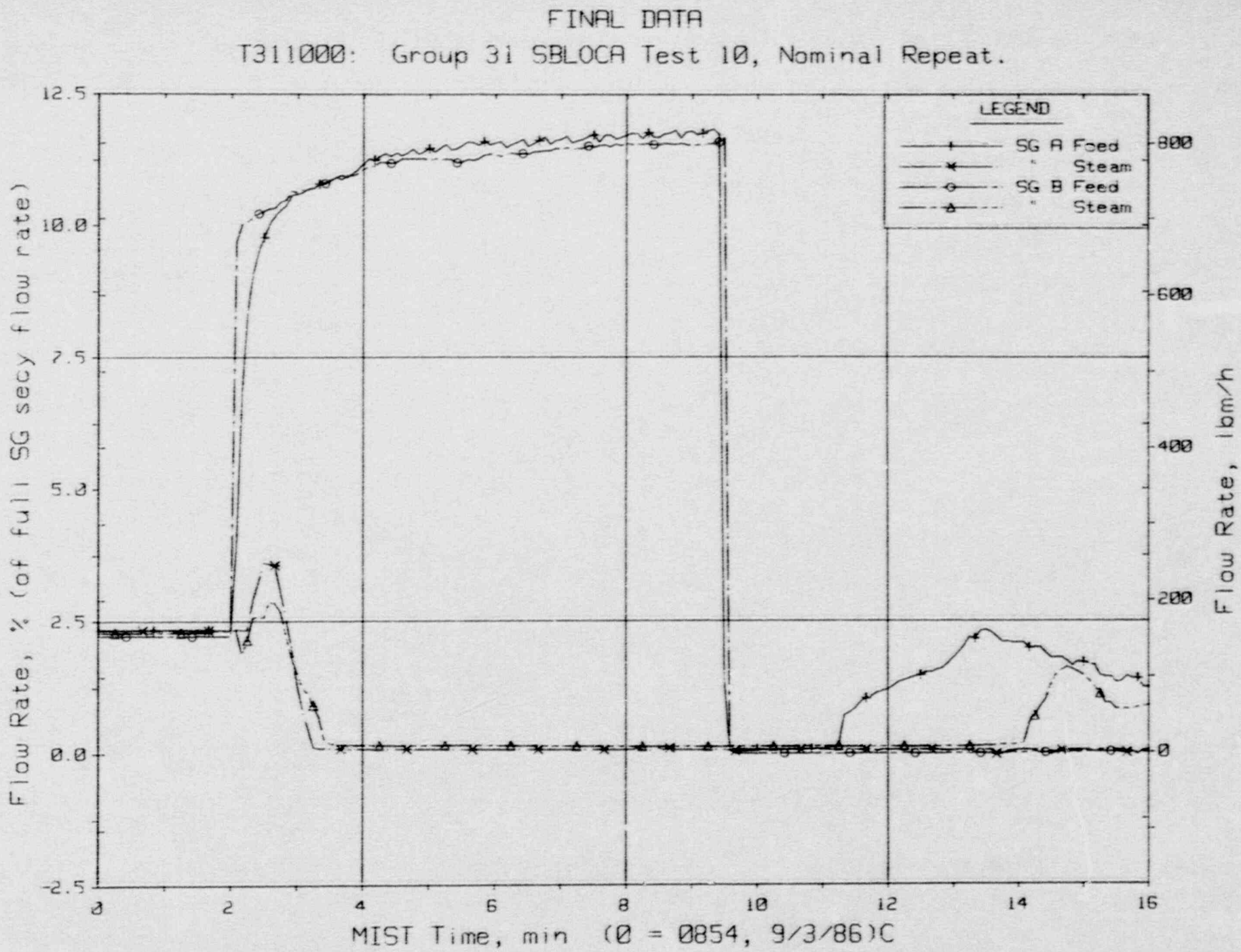

Figure 5.2.11. Secondary System Flow Rates

SGFL2

Wed Jul 6 14:22:46 1988

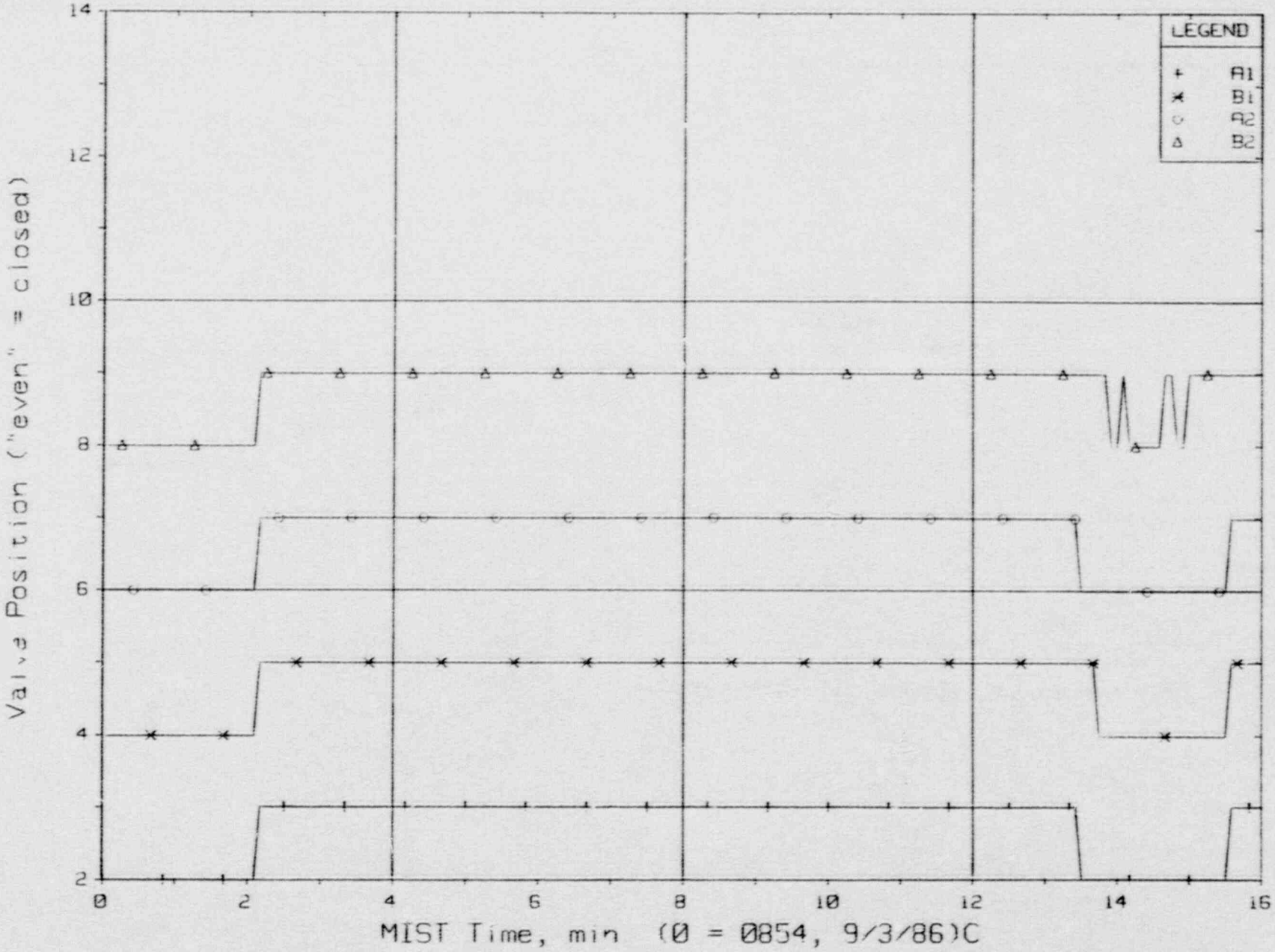

Figure 5.2.12. Reactor Vessel Vent Valve Positions

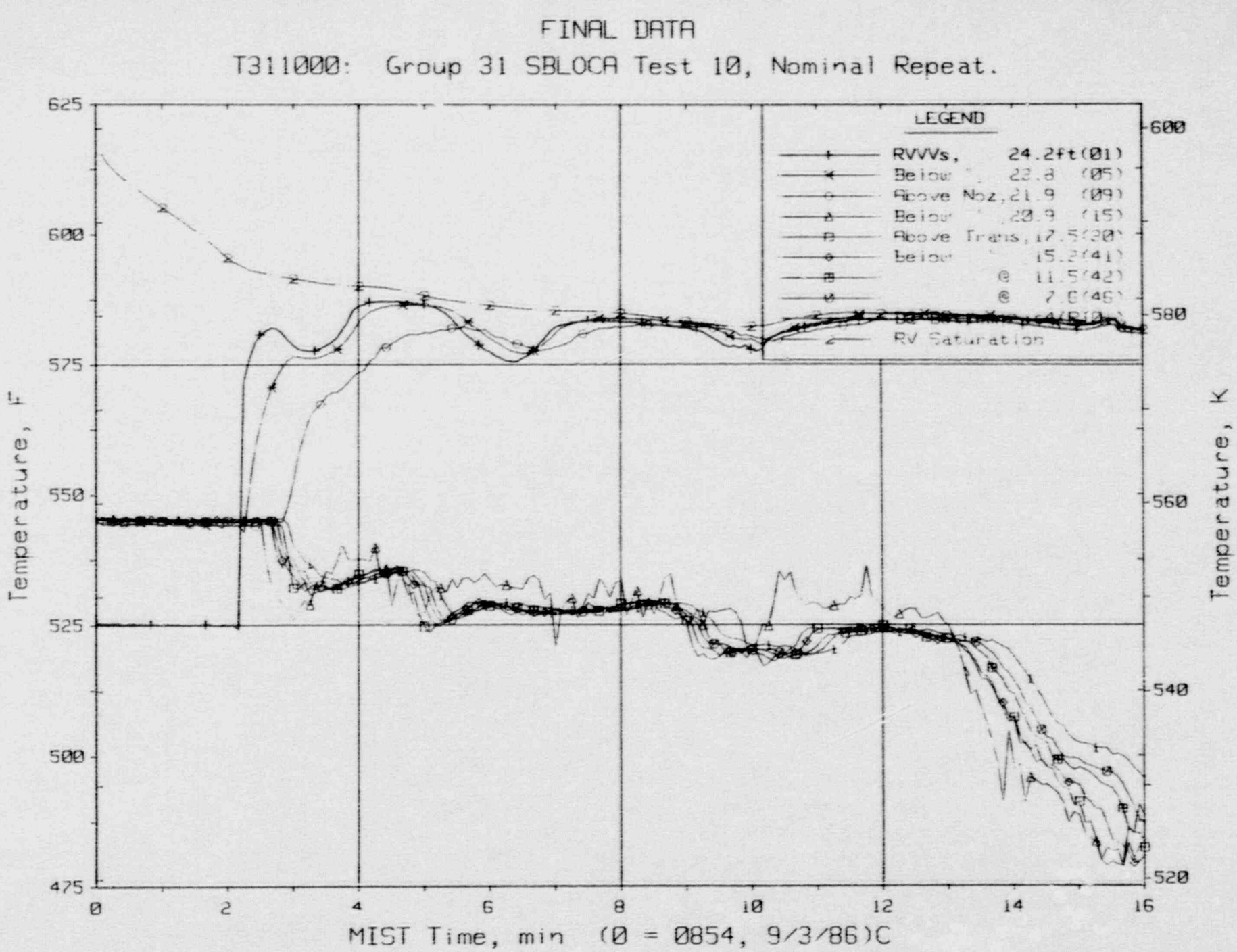

Figure 5.2.13. Downcomer Quadrant A1 Fluid Temperatures (DCTCs)

Wed Jul 6 14:27:32 1988

DCTC6

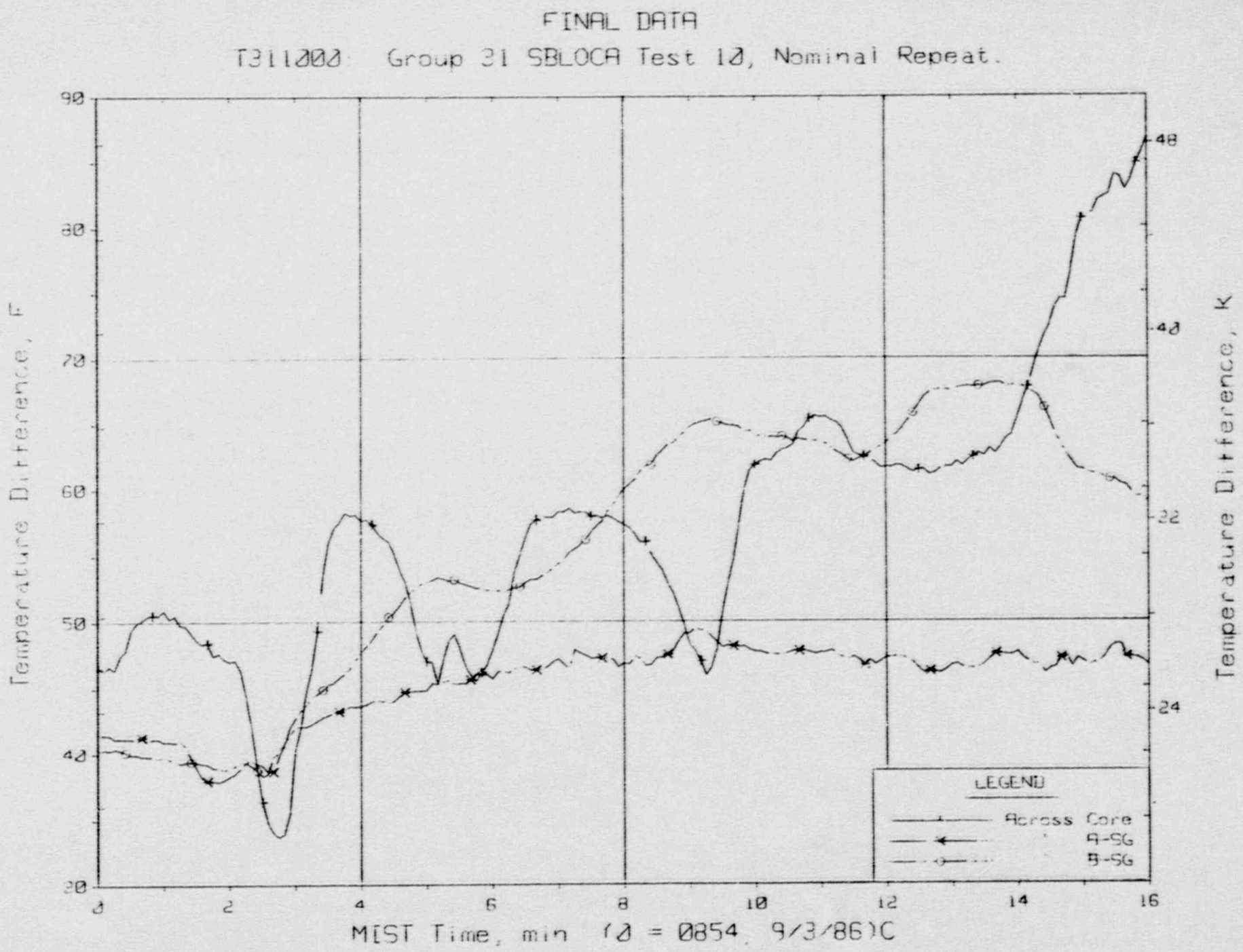

Figure 5.2.14. Key Temperature Differences

Thu Jul 7 10:42:43 1988

PRTD2

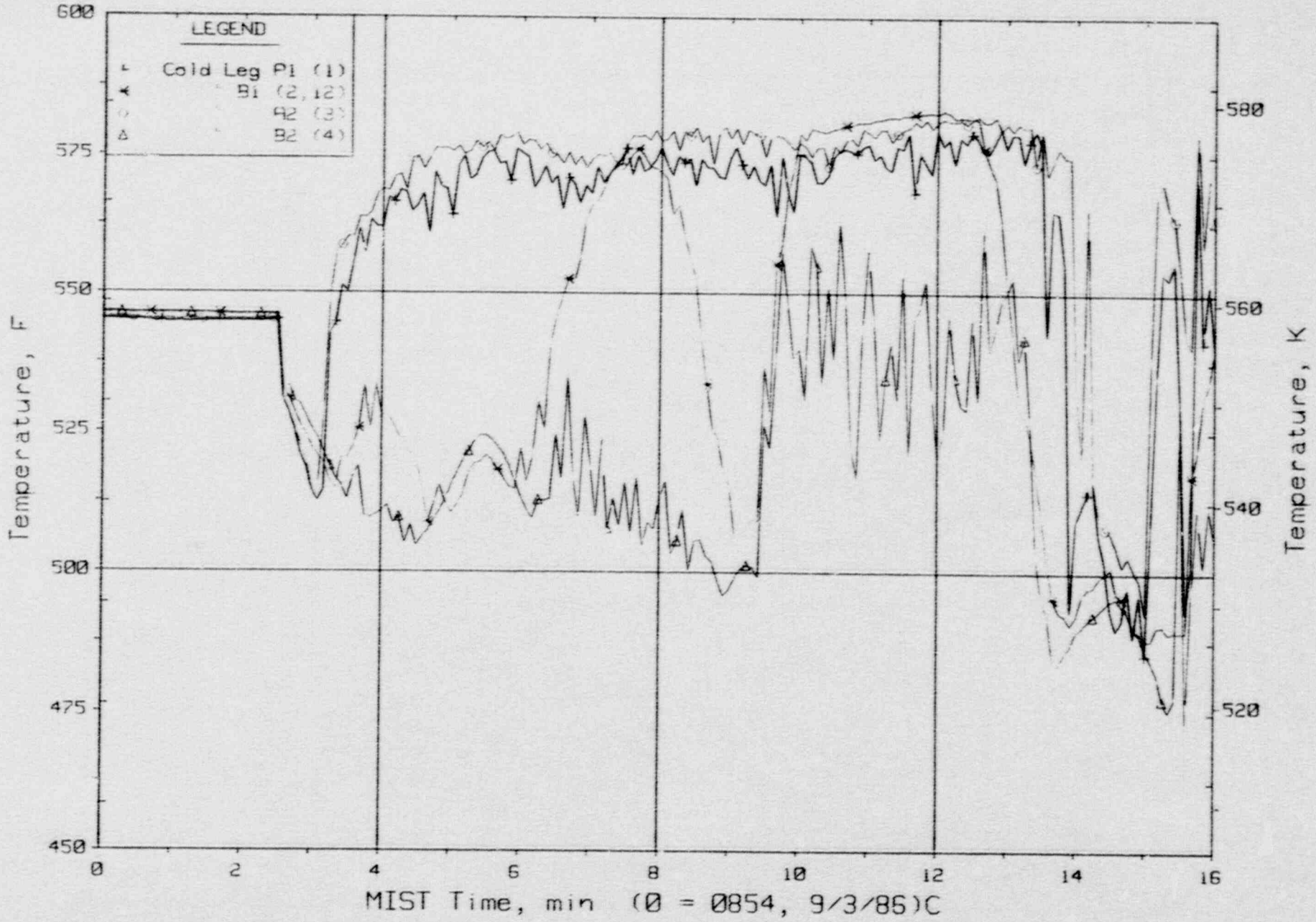

Figure 5.2.15. Cold Leg Nozzle Fluid Temperatures, Top of Rake (21.3 ft, CnTC11s)

Wed Jul 6 14:32:00 1988

CLTC1

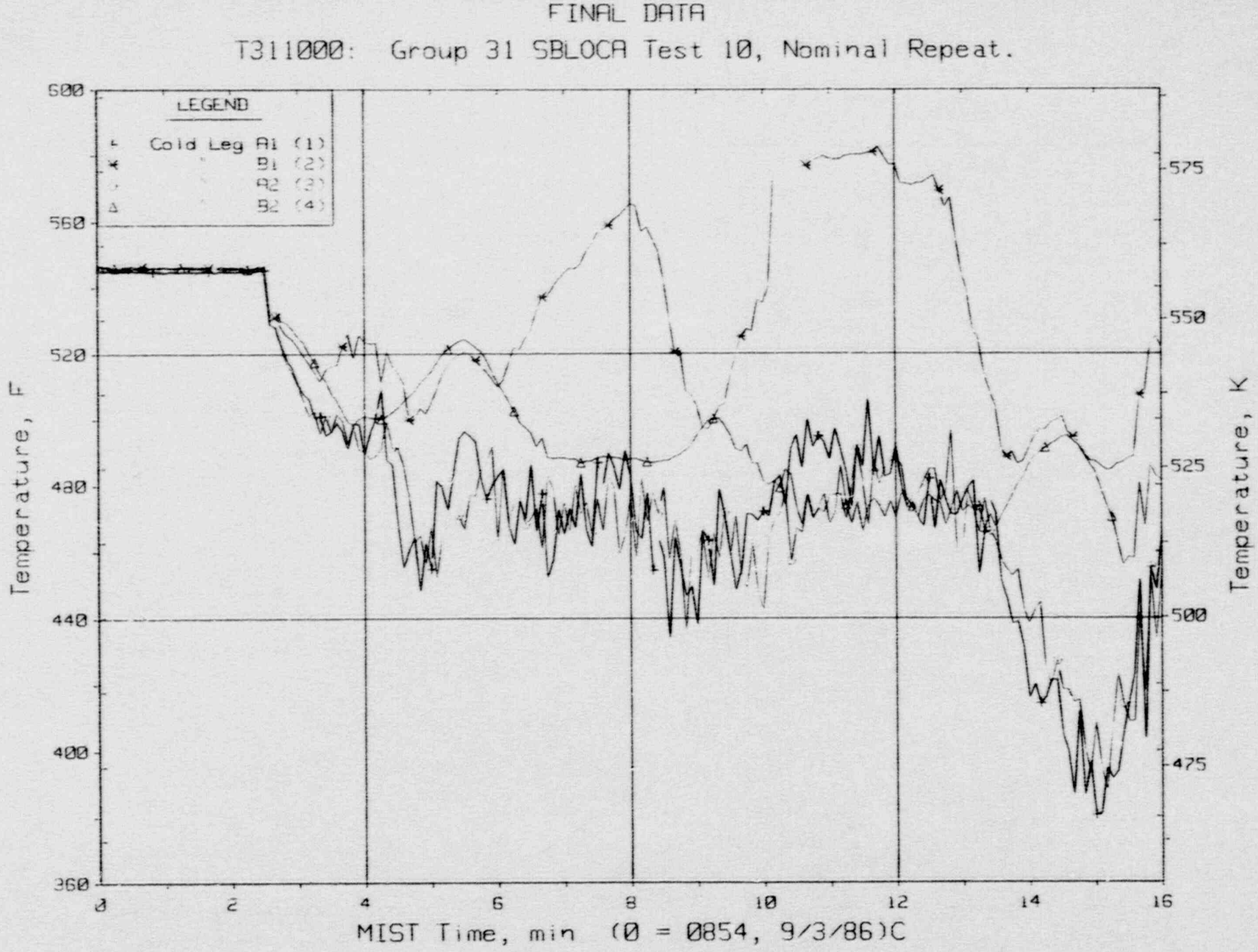

Figure 5.2.16. Cold Leg Nozzle Fluid Temperatures, Bottom of Rake (21.2 ft, CnTC14s)

Wed Jul 6 14:34:11 1988

CLTC2

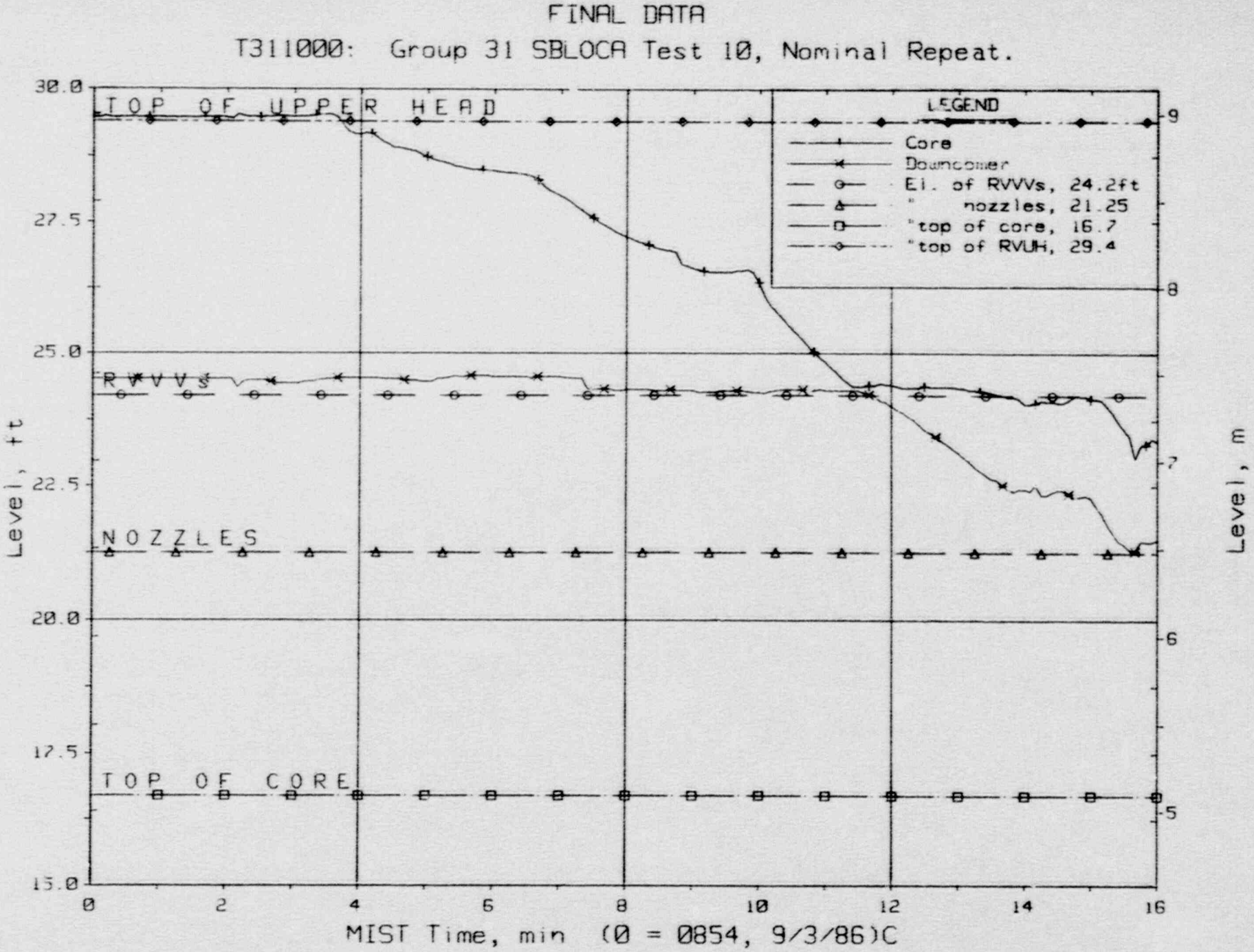

Figure 5.2.17. Core Region Collapsed Liquid Levels

Wed Jul 6 14:26:45 1988

COLV1

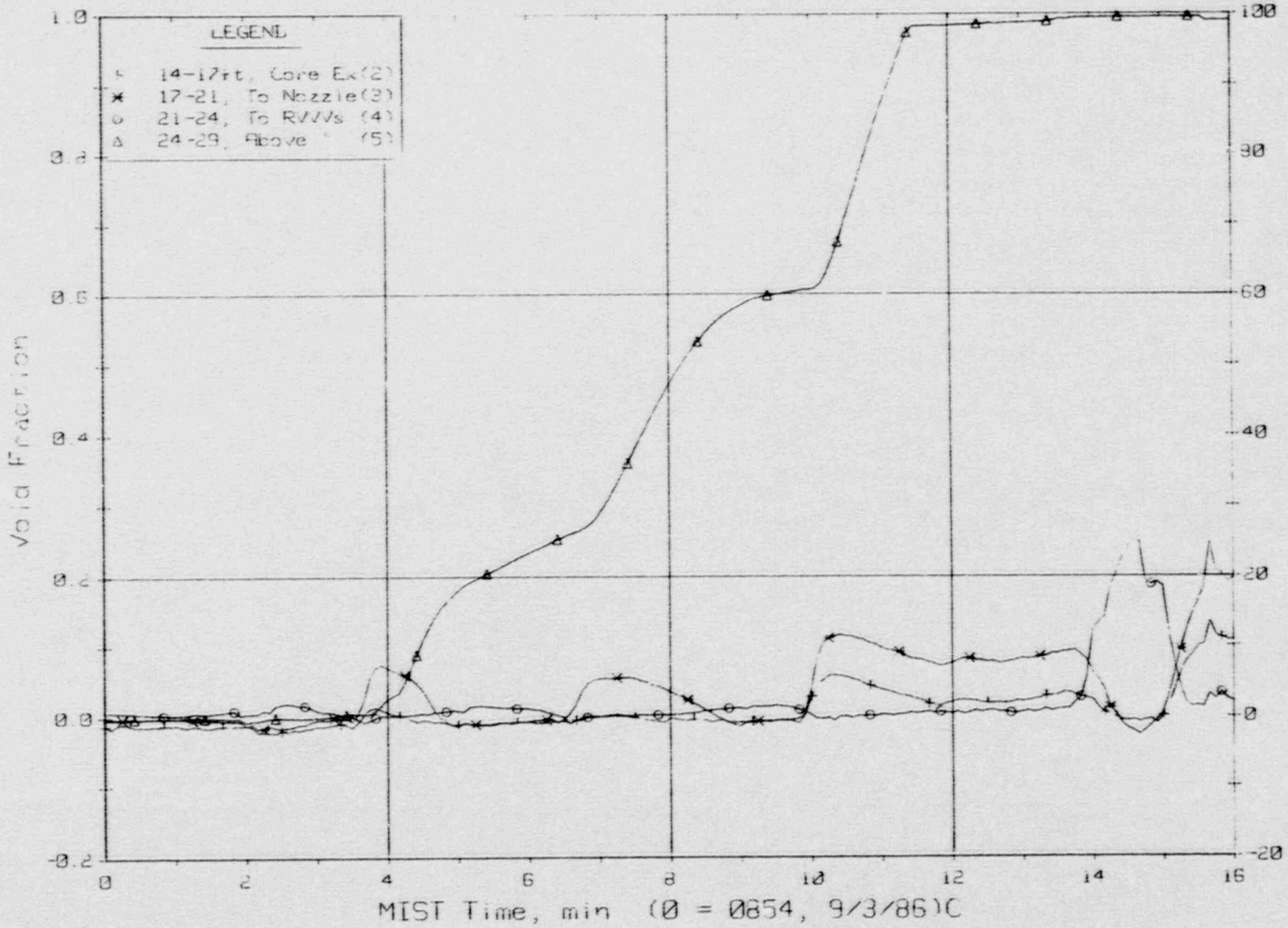

Figure 5.2.18. Reactor Vessel Void Fractions from Differential Pressures (RVVFs)

RVVF1

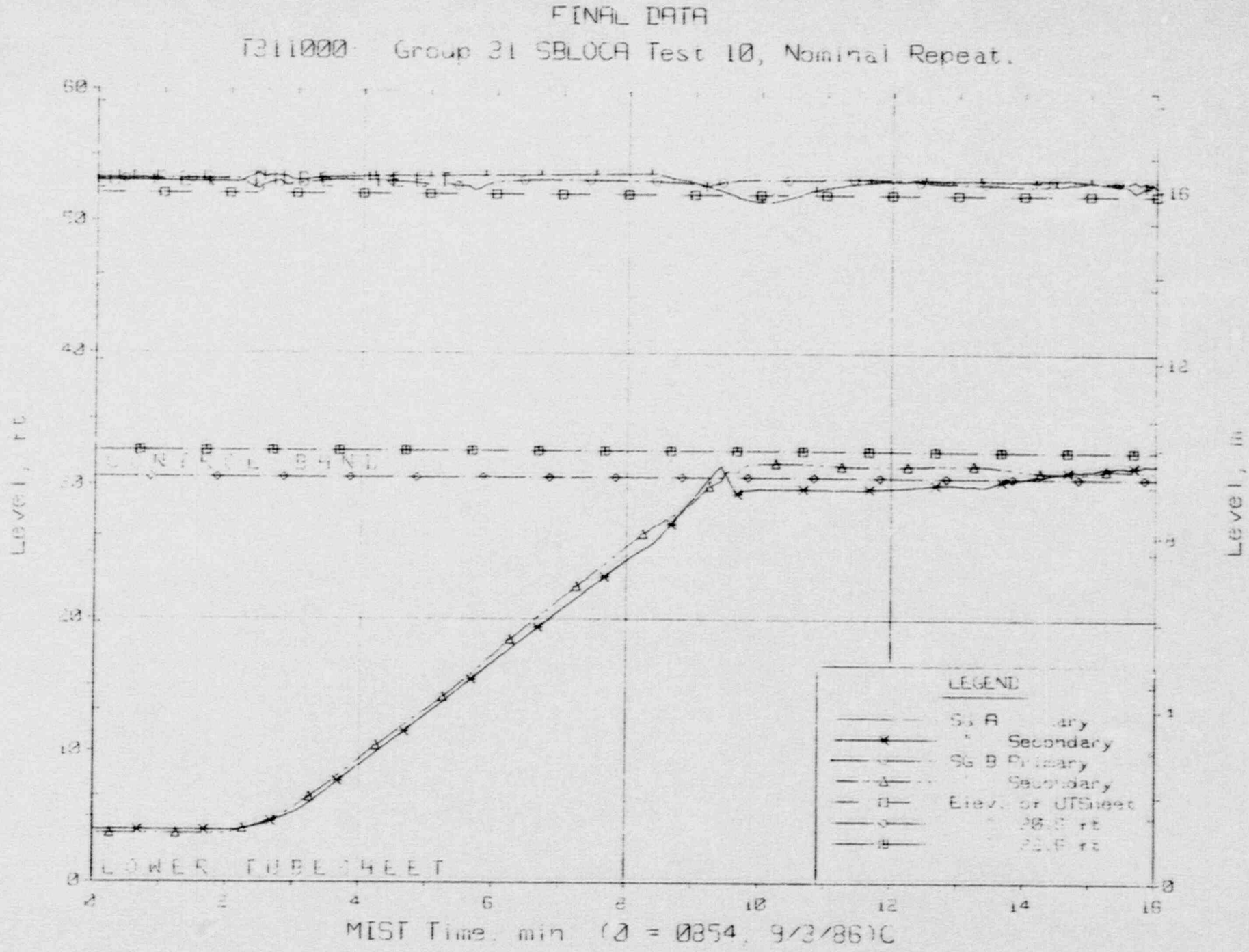

Figure 5.2.19. Steam Generator Collapsed Liquid Levels

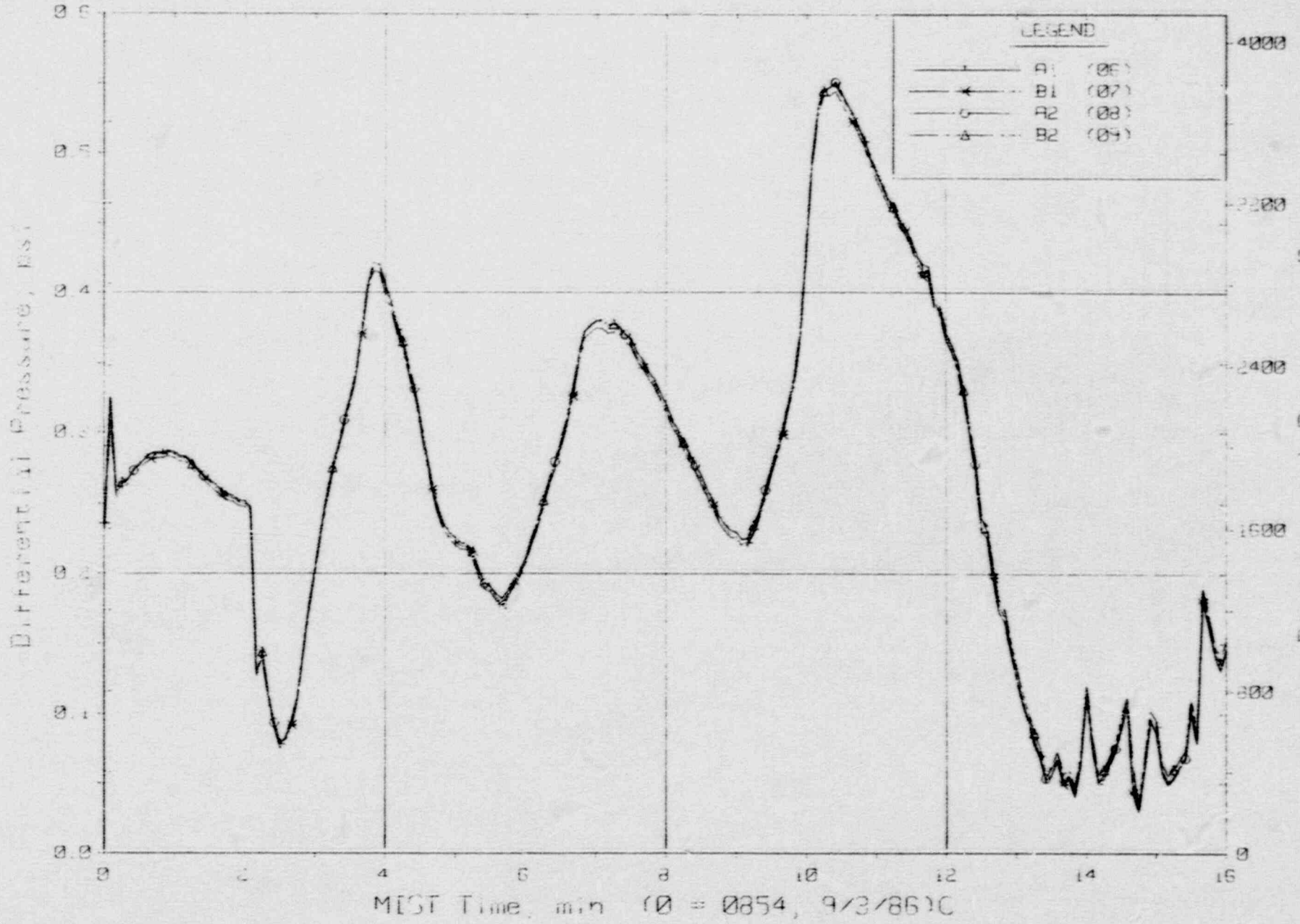

Figure 5.2.20. Reactor Vessel Vent Valve Differential Pressures (RVDPs)

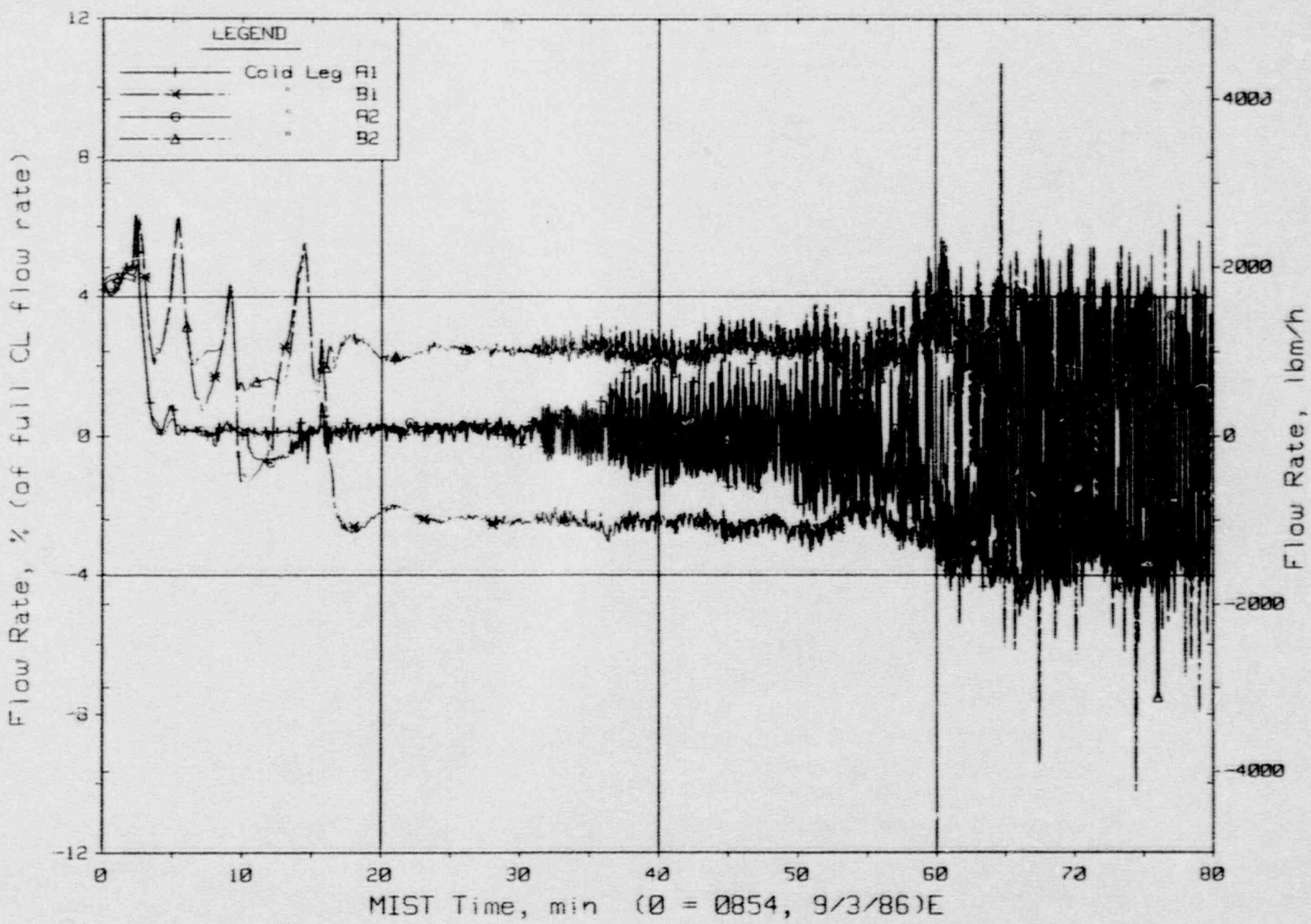

Figure 5.2.21. Cold Leg (Venturi) Flow Rates

Wed Dec 14 12:54:23 1988

CLFL2

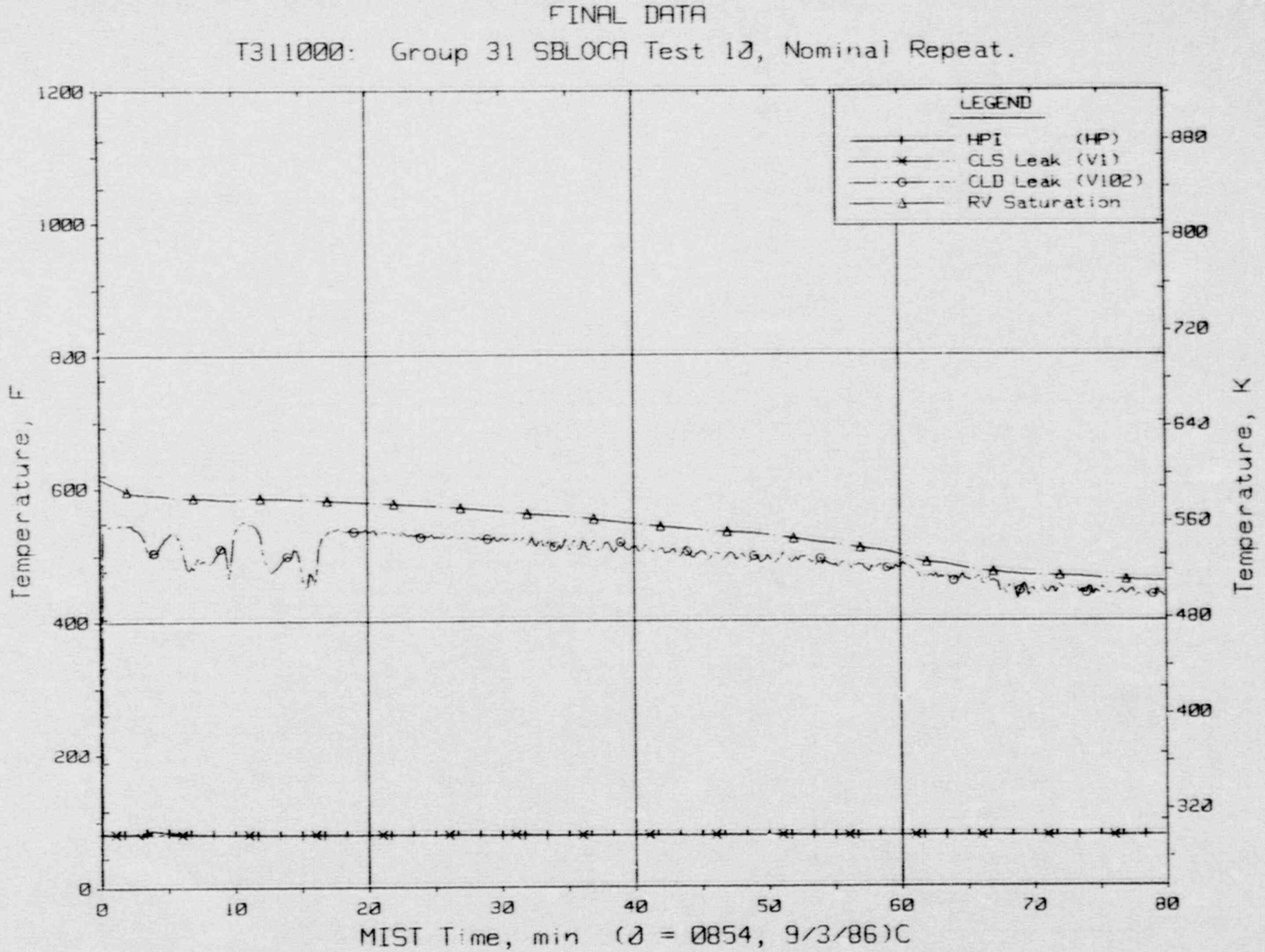

Figure 5.2.22. Single-Phase Discharge and HPI Fluid Temperatures (TCOls)

Thu Jul 7 11:08:45 1988

PRTC1

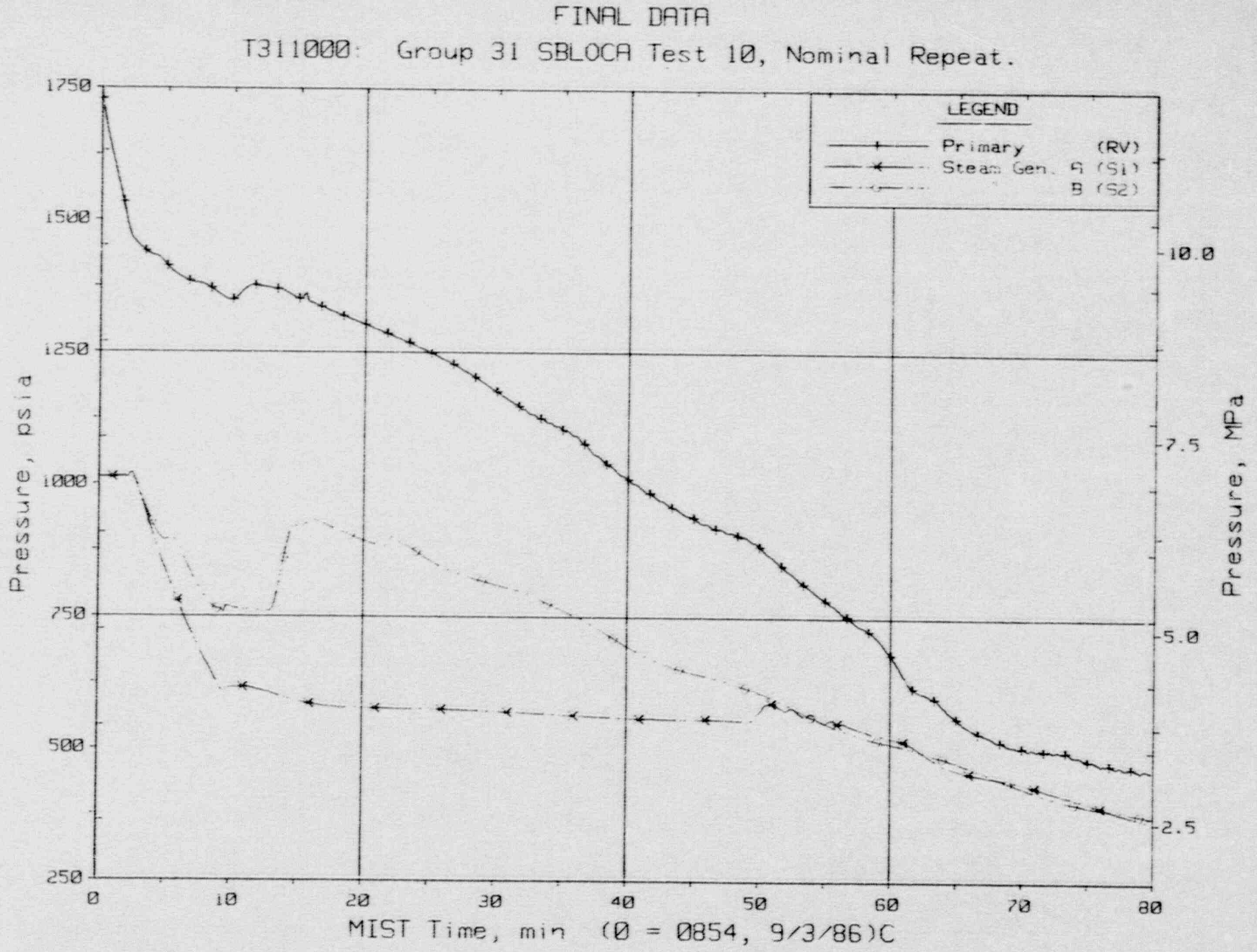

Figure 5.2.23. Primary and Secondary System Pressures (GP01s)

PSGP1

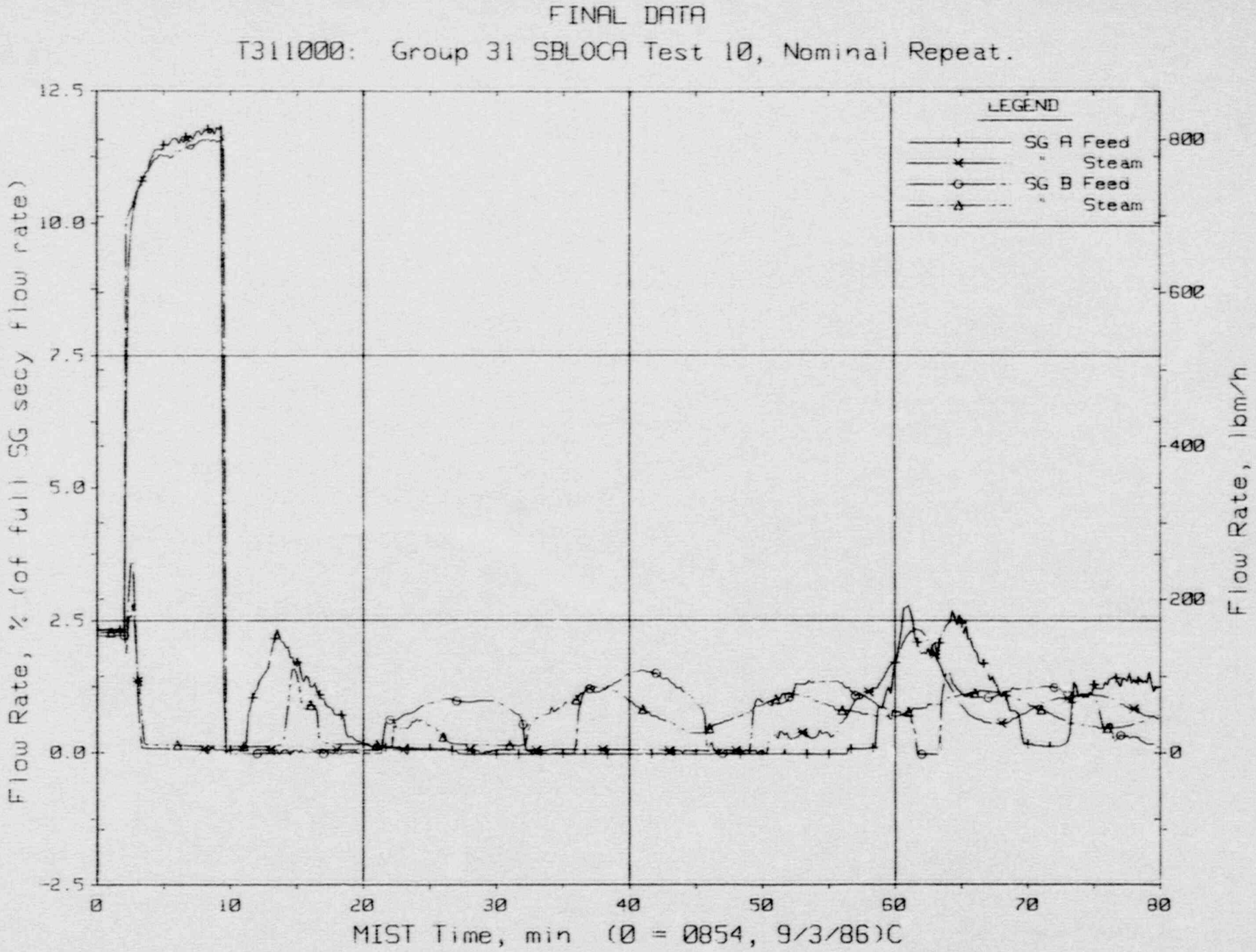

Figure 5.2.24. Secondary System Flow Rates

Wed Jul 6 14:59:47 1988

SGFL2

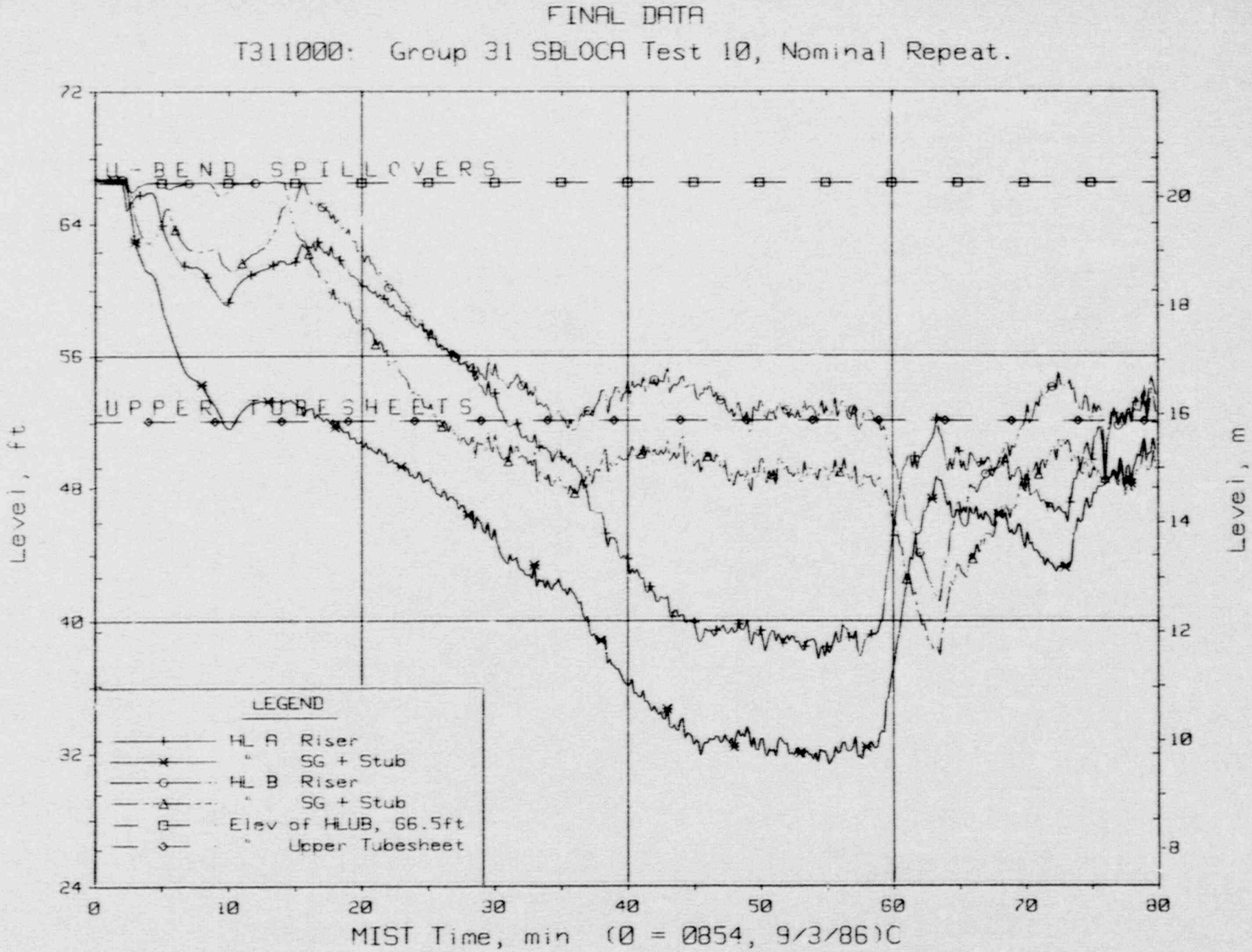

Figure 5.2.25. Hot Leg Riser and Stub Collapsed Liquid Levels

Thu Jul 7 14:28:16 1988

HLLV1

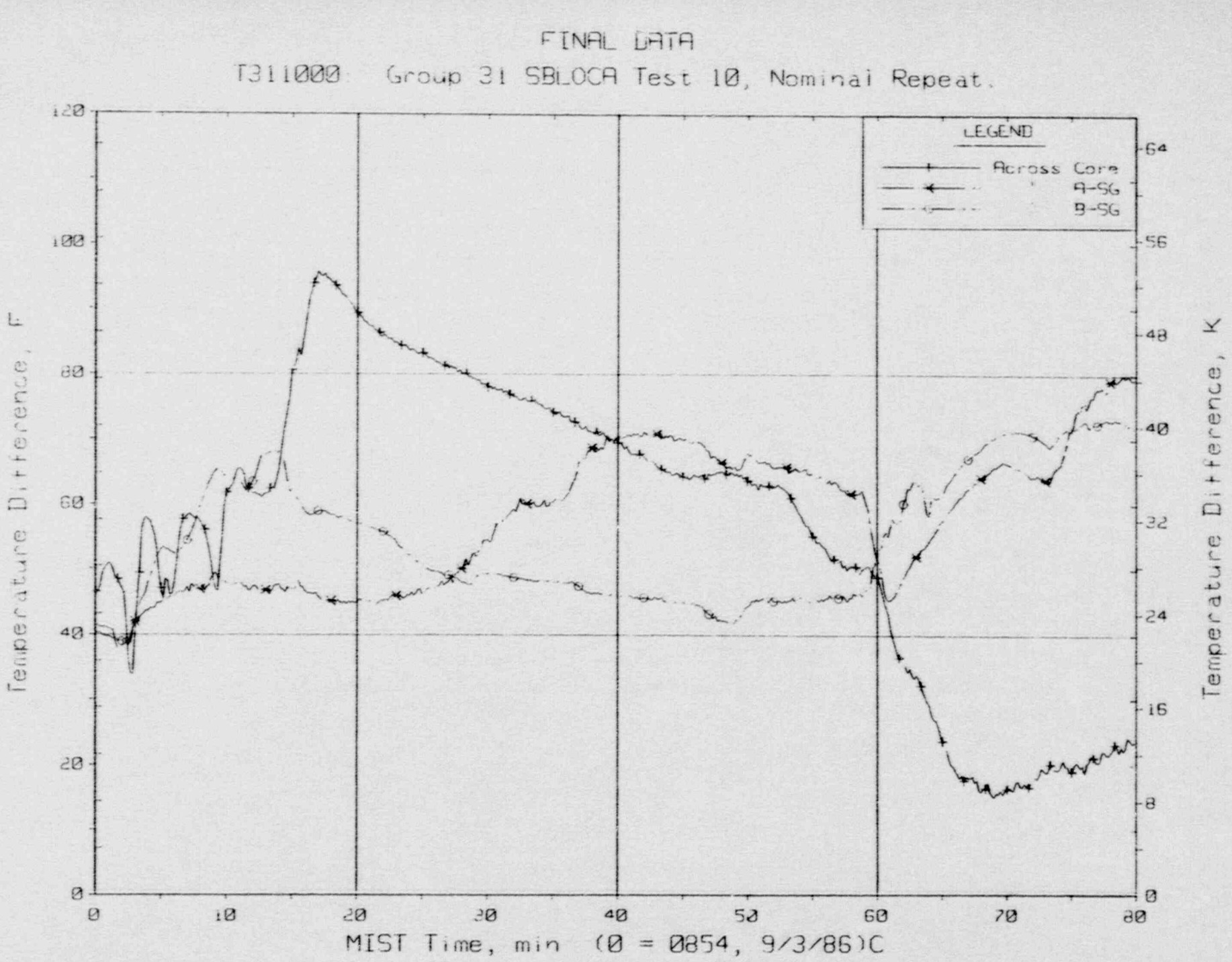

Figure 5.2.26. Key Temperature Differences

Thu Jul 7 11:15:42 1988

PRTD2

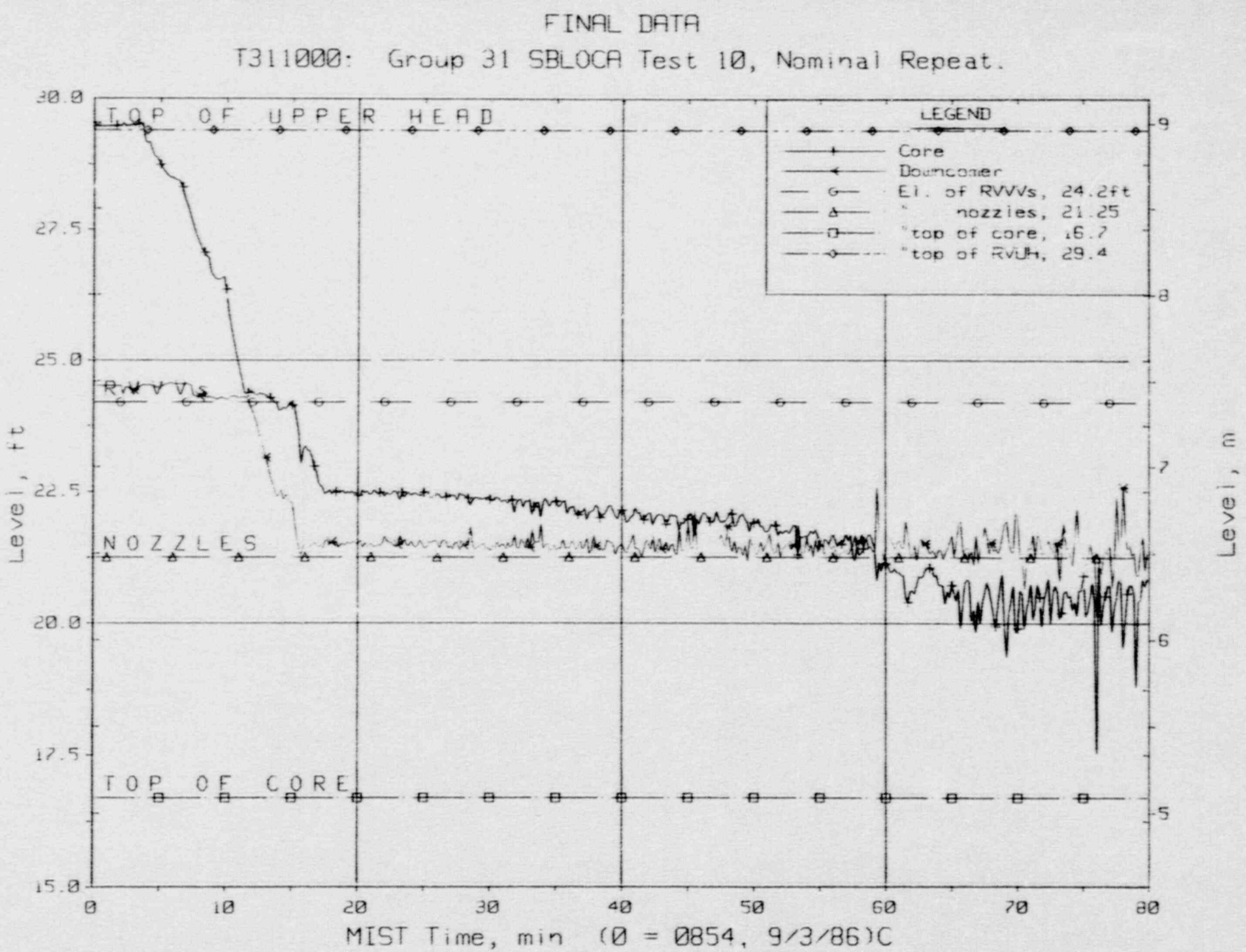

Figure 5.2.27. Core Region Collapsed Liquid Levels

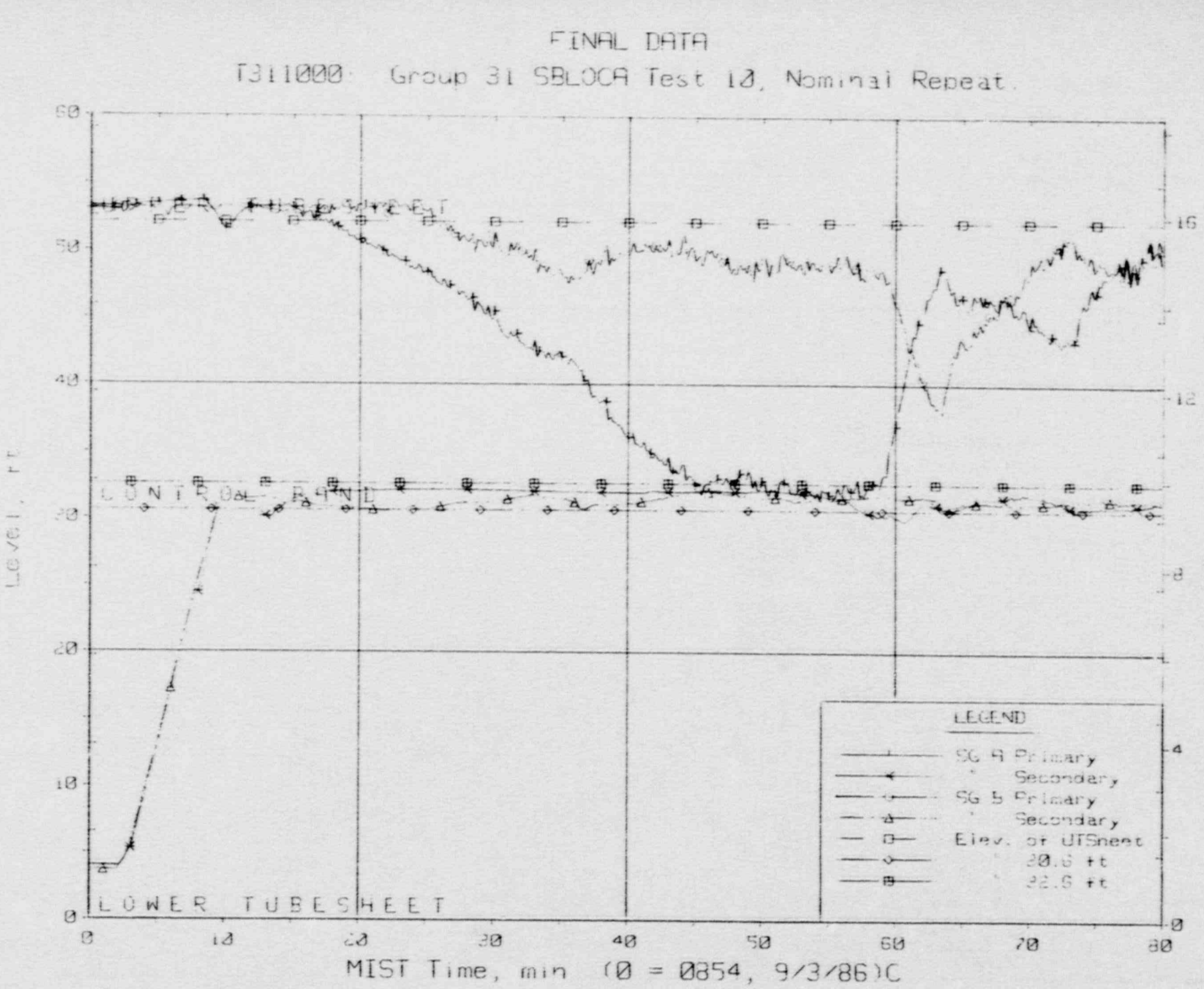

Figure 5.2.28. Steam Generator Collapsed Liquid Levels

SGLV2

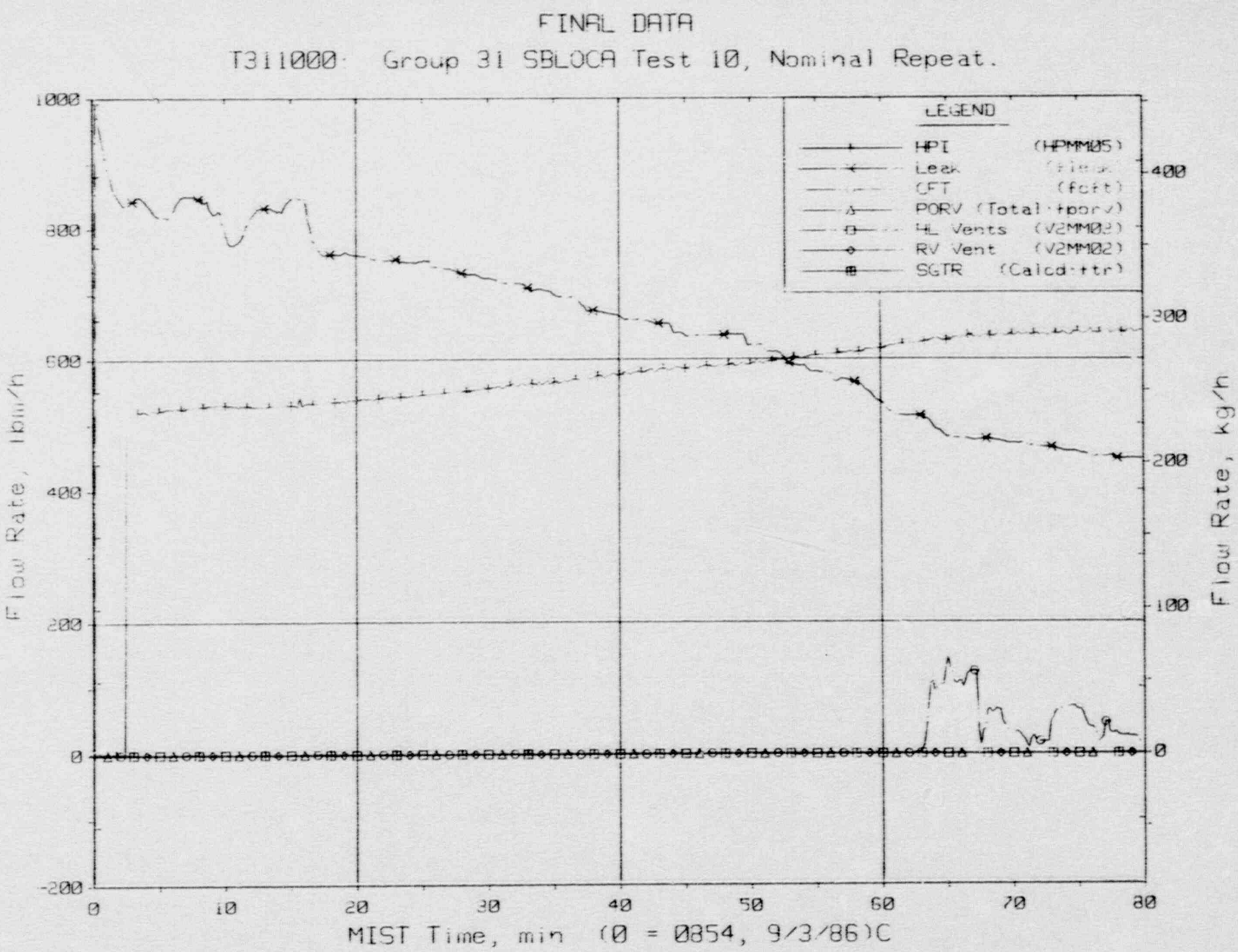

Figure 5.2.29. Primary System Boundary Flow Rates

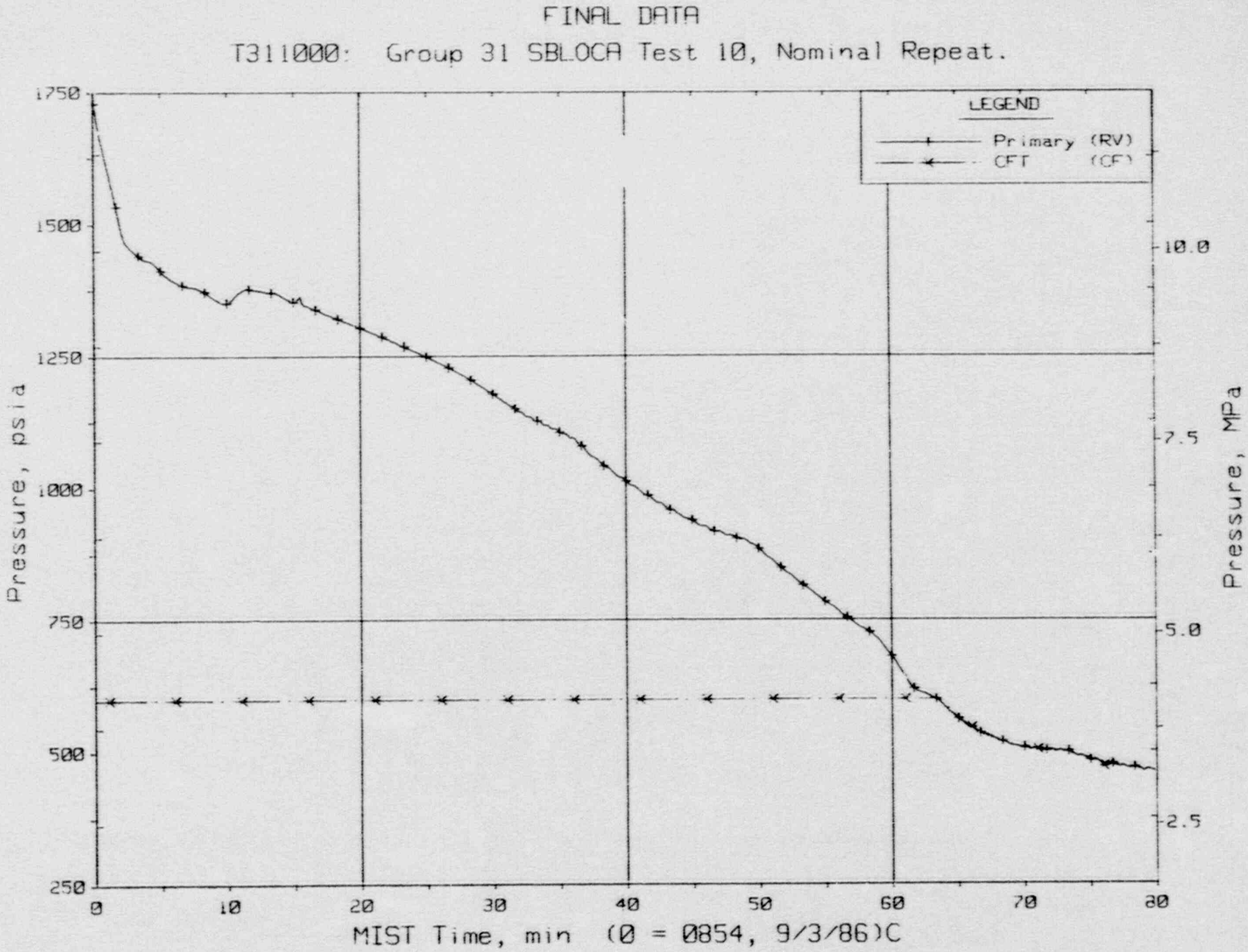

Figure 5.2.30. Primary System and Core Flood Tank Pressures (GP01s)

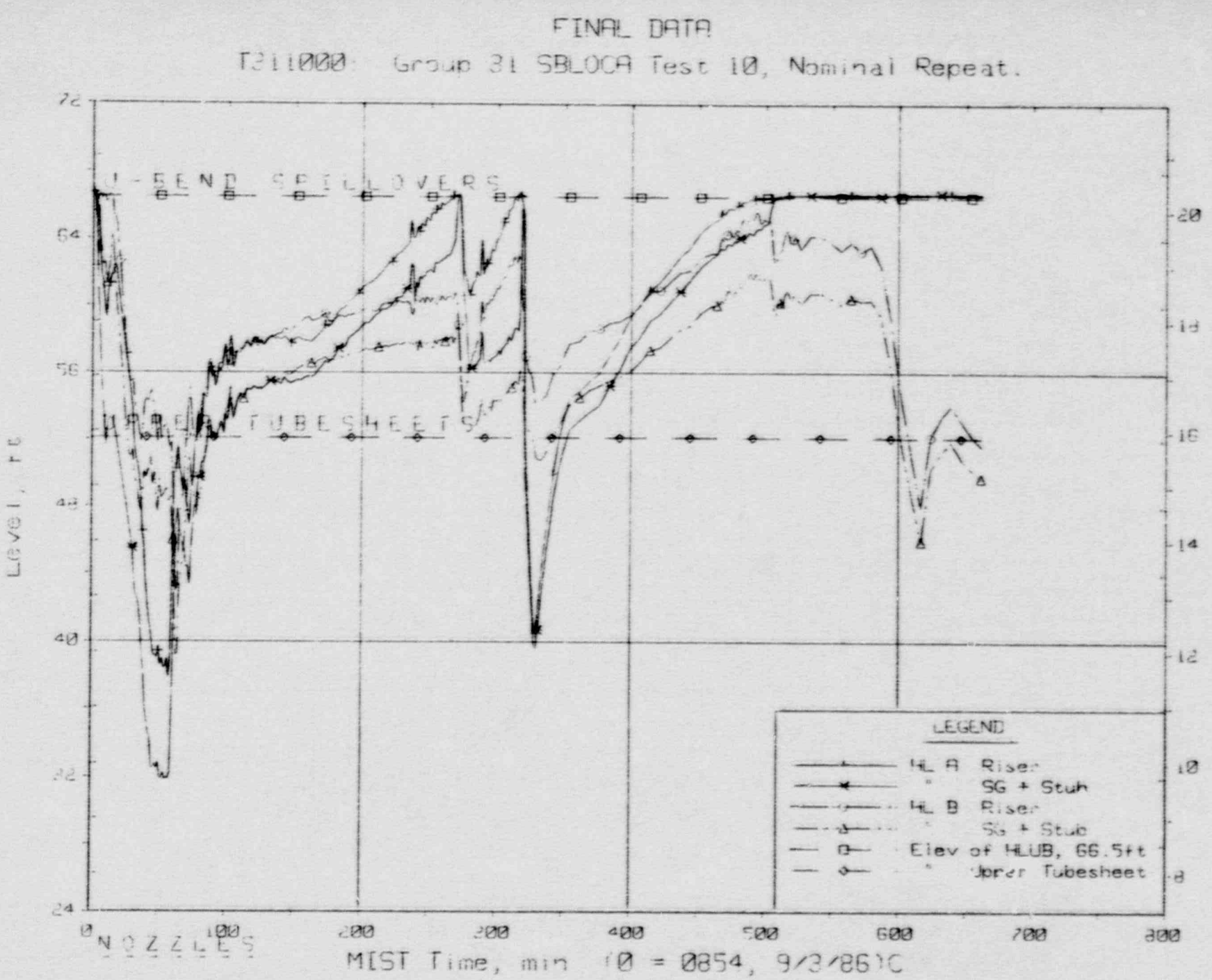

Figure 5.2.31. Hot Leg Riser and Stub Collapsed Liquid Levels

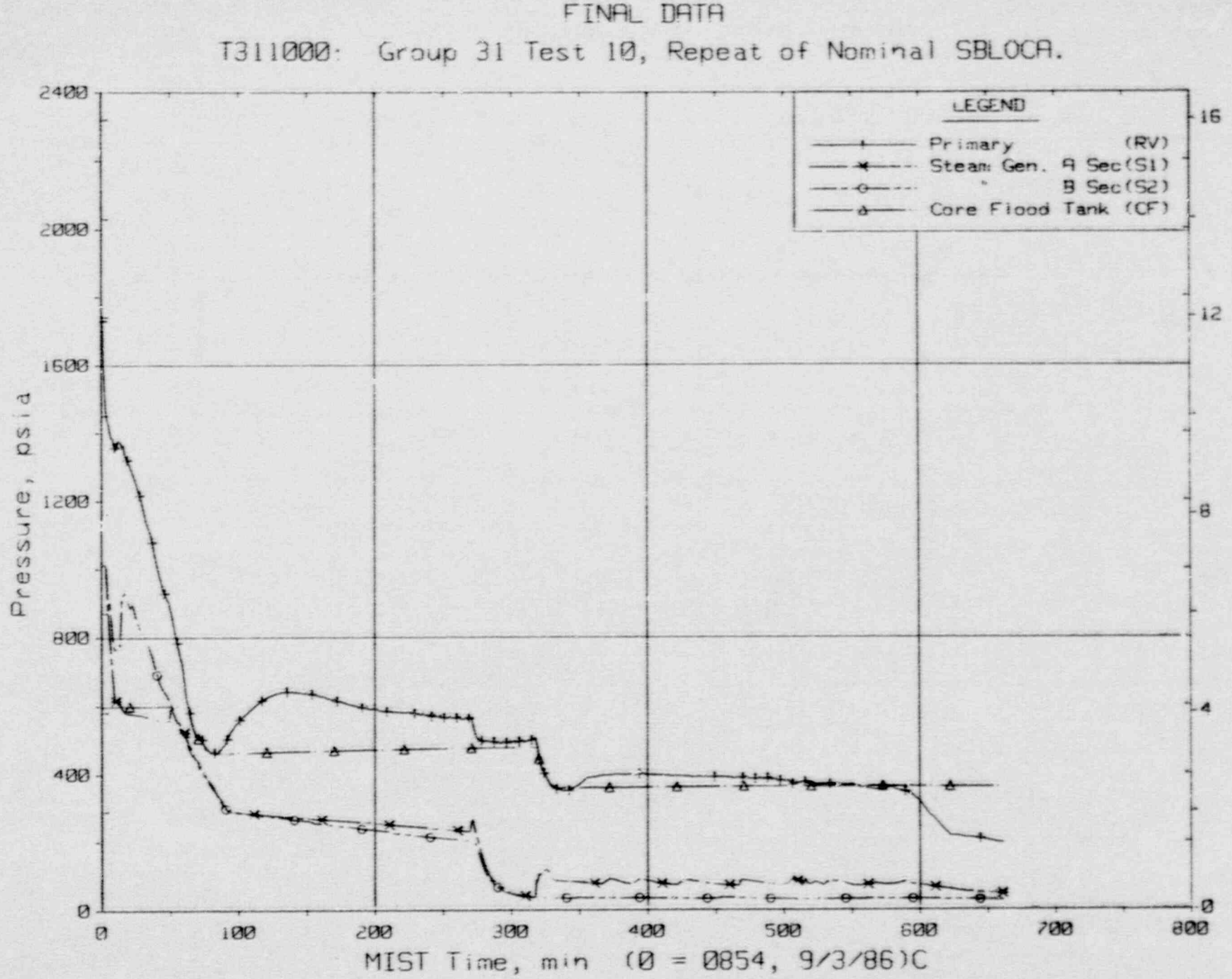

Figure 5.2.32. Primary and Secondary System and CFT Pressures (GP01s)

Wed Oct 26 11:31:51 1988

PSGP0

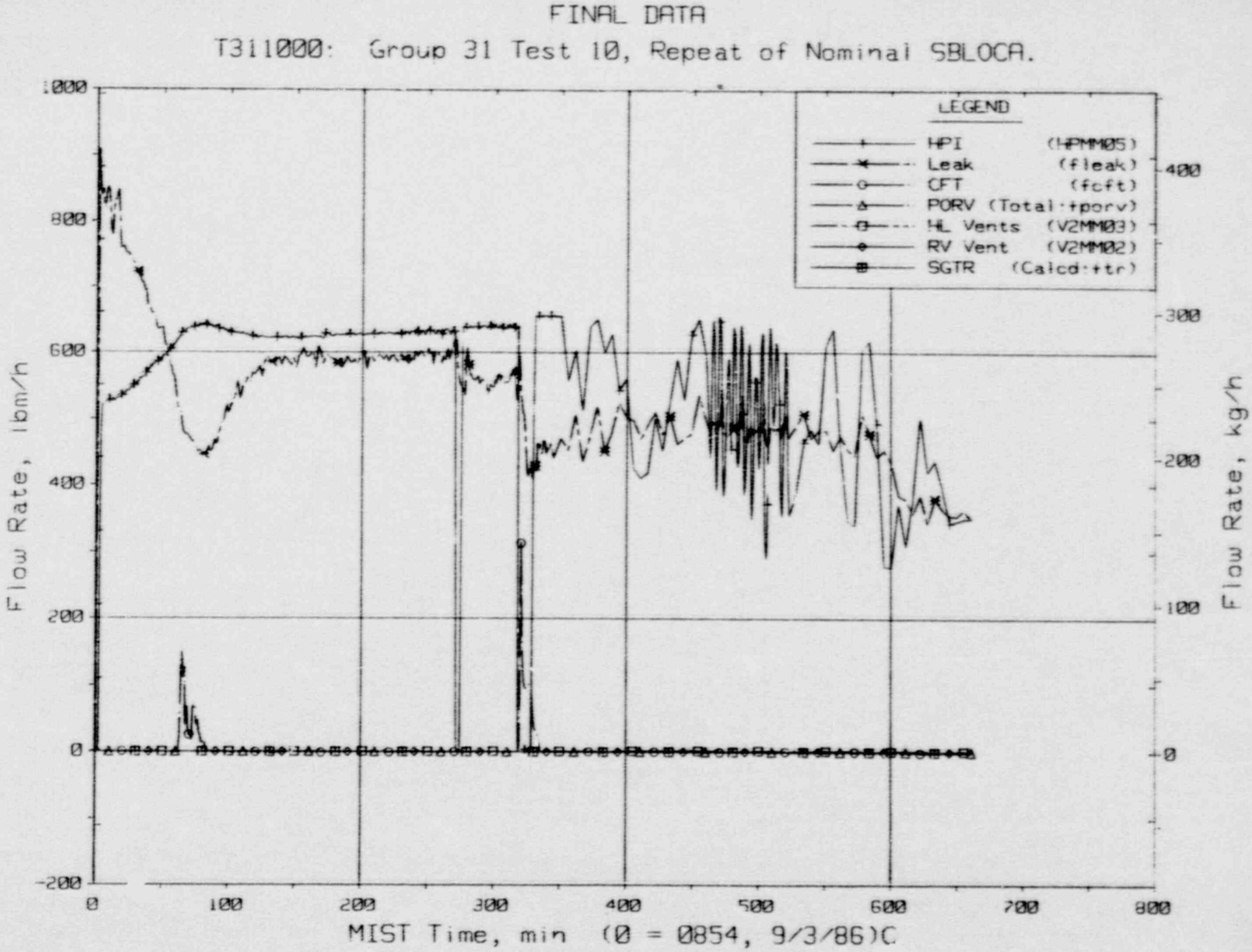

Figure 5.2.33. Primary System Boundary Flow Rates

Wed Oct 26 11:26:08 1988

PRFL3

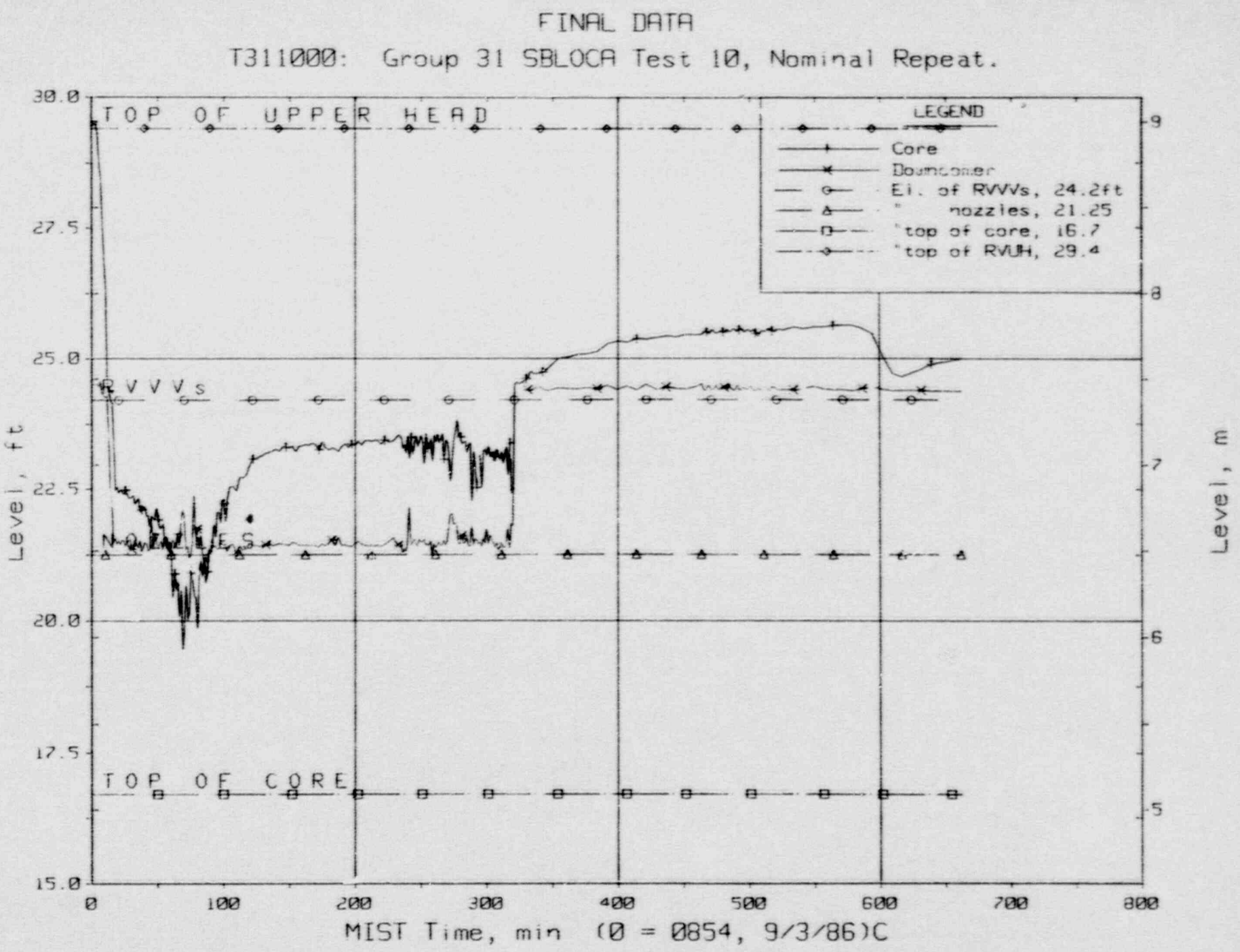

Figure 5.2.34. Core Region Collapsed Liquid Levels

Wed Jul 6 15:56:25 1988

COLV1

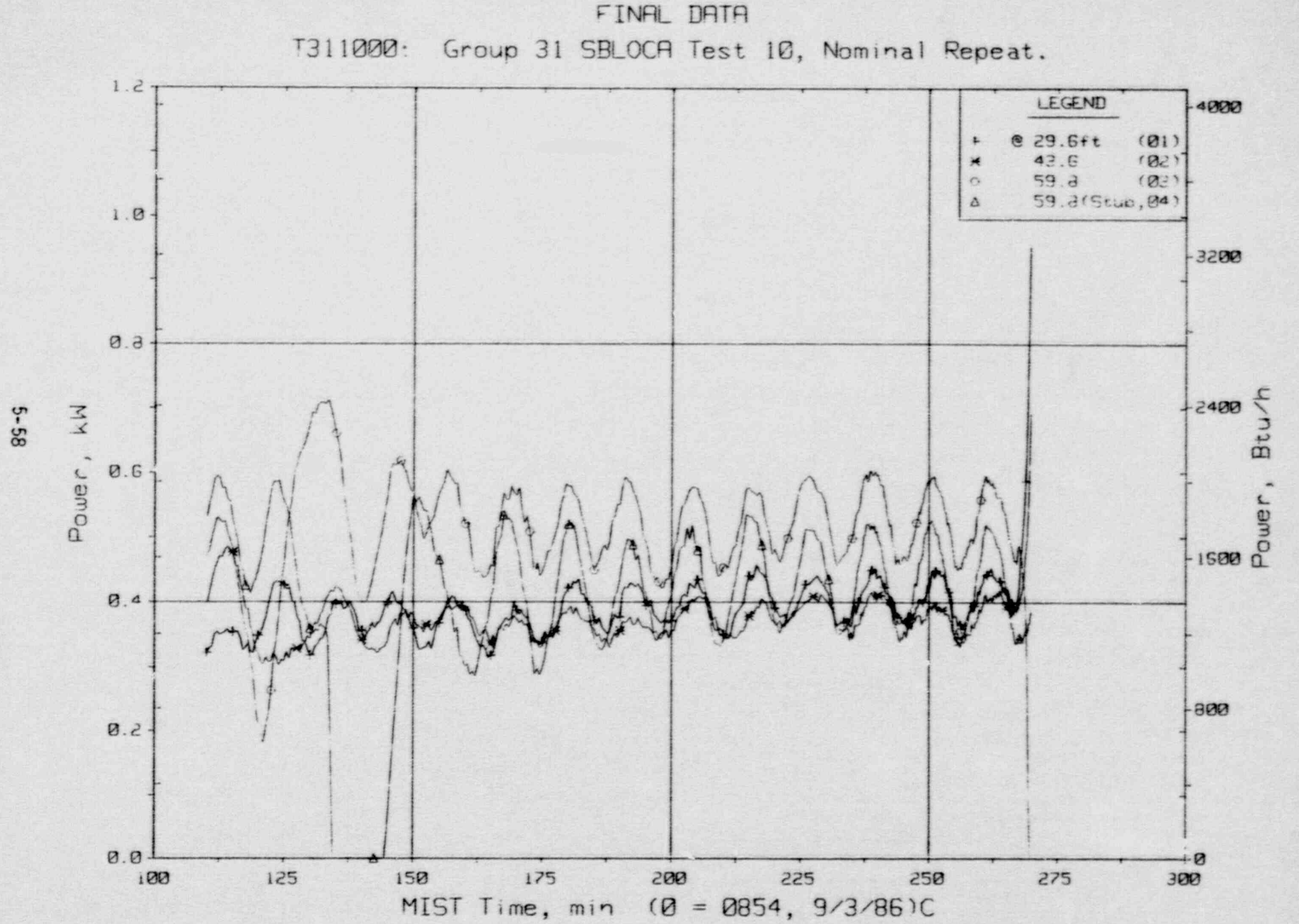

Figure 5.2.35. Hot Leg A Guard Heater Specified Power (H1WMs)

Wed Jul 6 16:00:58 1988

H1WM1

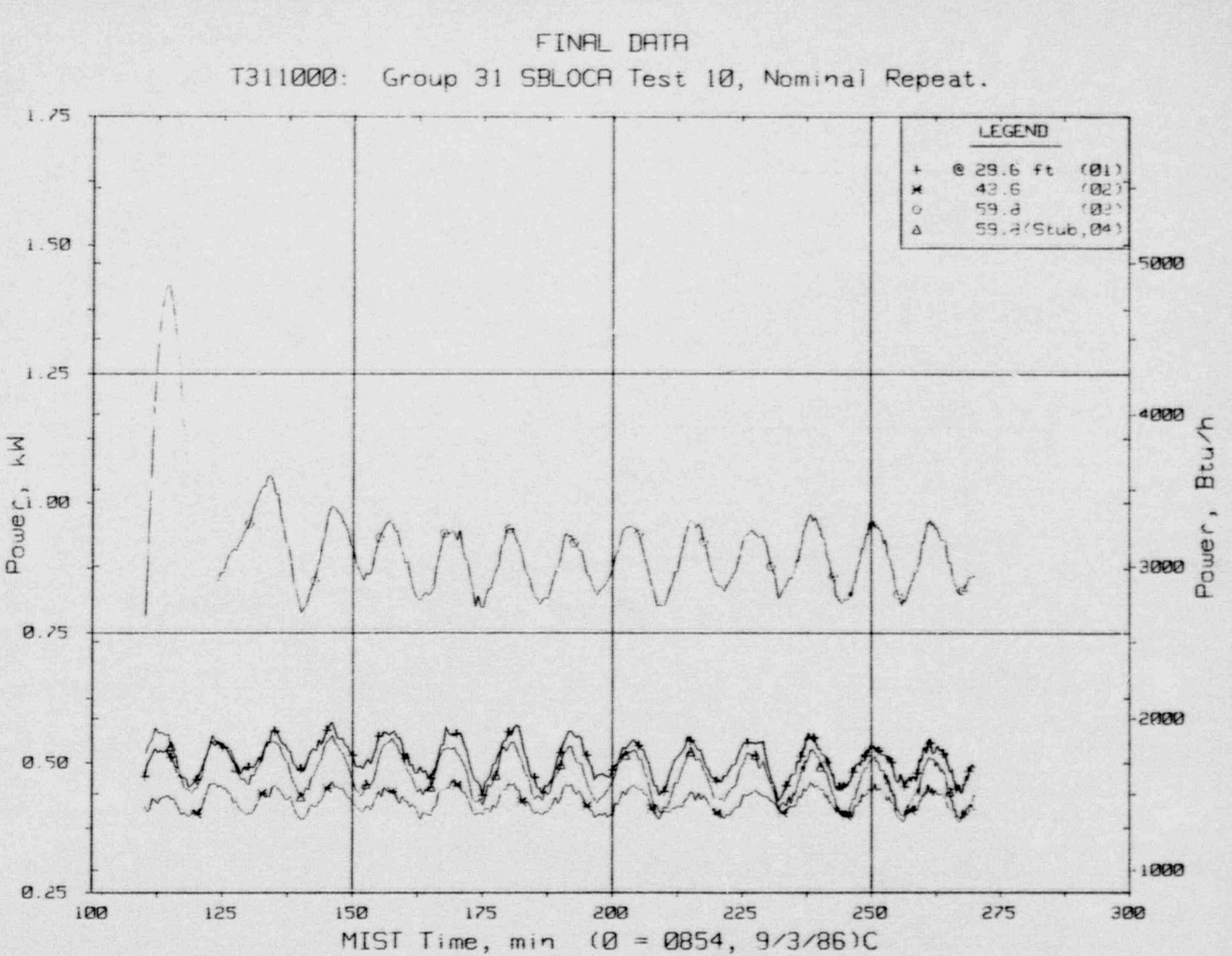

Figure 5.2.36. Hot Leg B Guard Heater Specified Power (H2WMs)

Wed Jul 6 16:02:27 1988

H2WM1

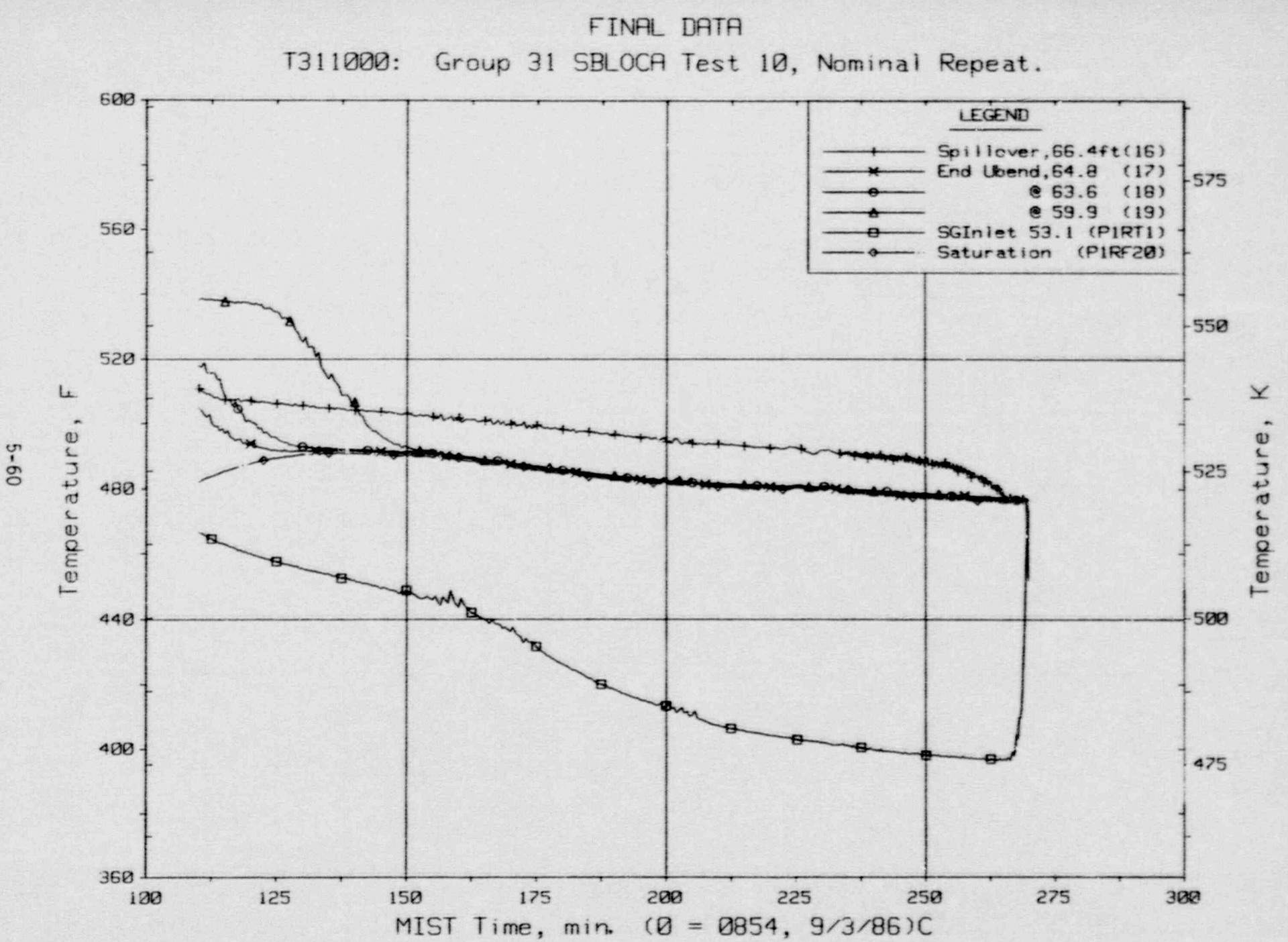

Figure 5.2.37. Hot Leg A Fluid Temperatures Beyond U-Bend (HITCs)

Thu Jul 14 10:09:35 1988

H1TC3

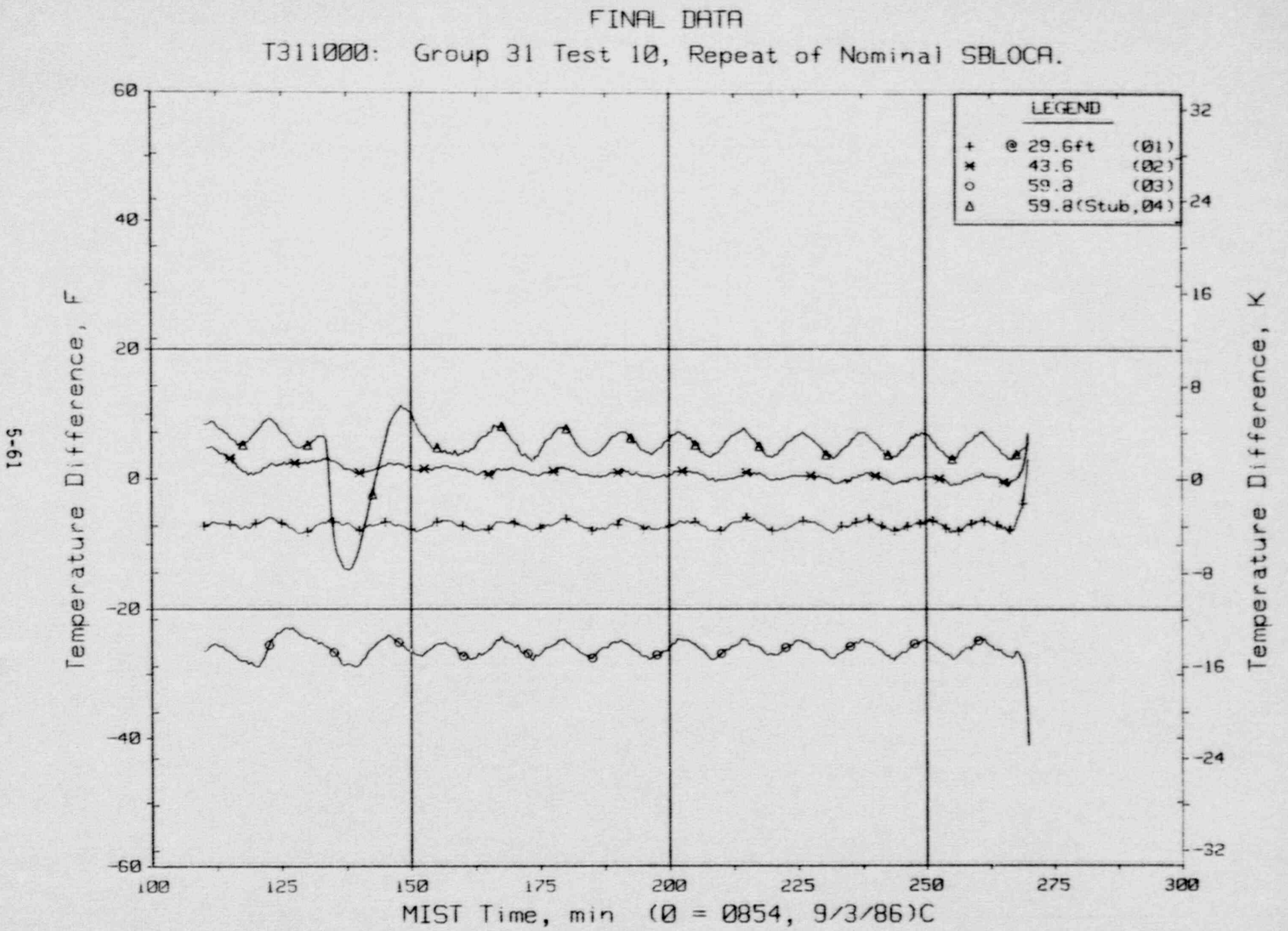

Figure 5.2.38. Hot Leg A Control Differential Temperatures (H1DTs)

Thu Oct 27 09:49:29 1988

H1DT1

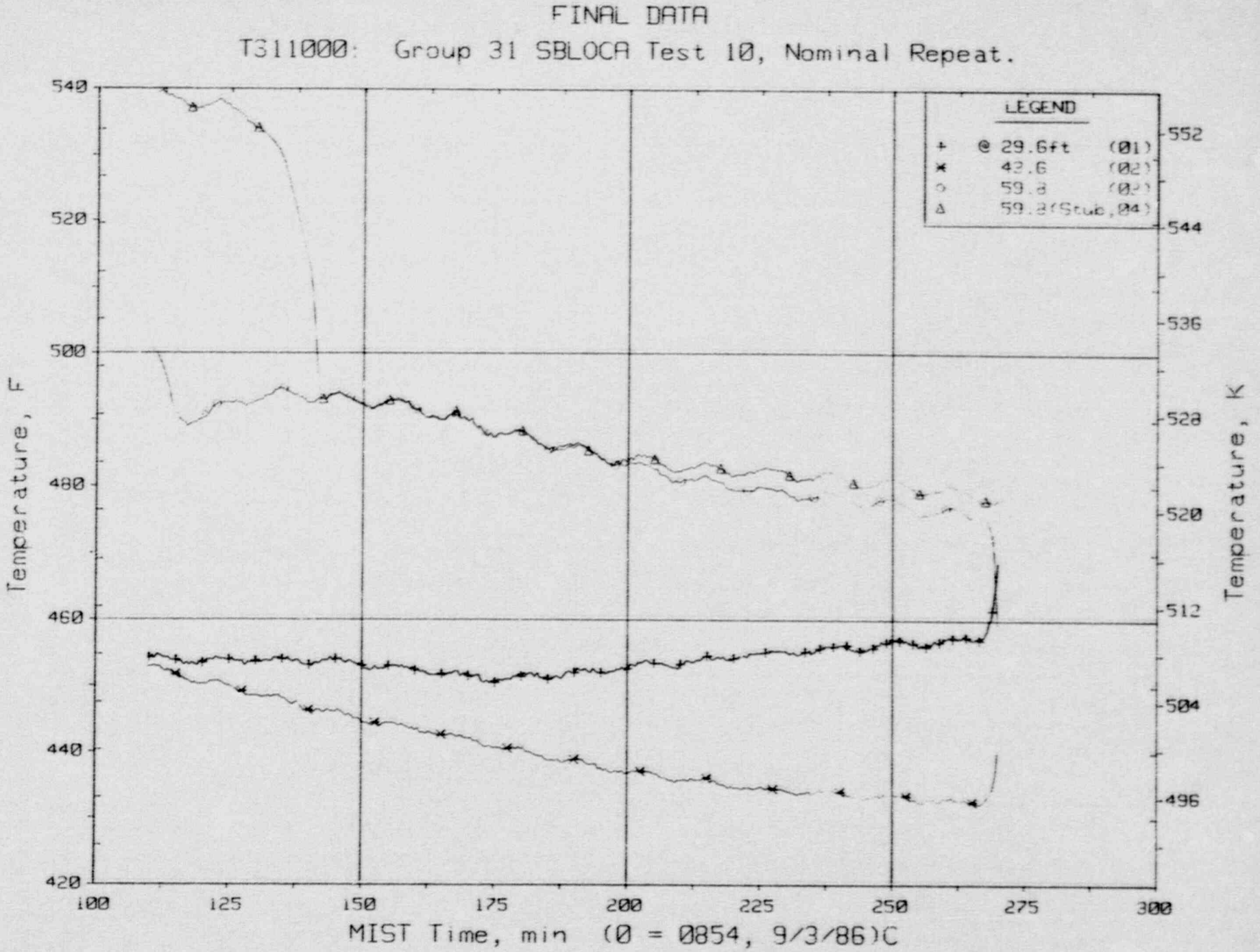

Figure 5.2.39. Hot Leg A Metal Temperatures (HlMTs)

Wed Jul 6 16:12:51 1988

HlMT1

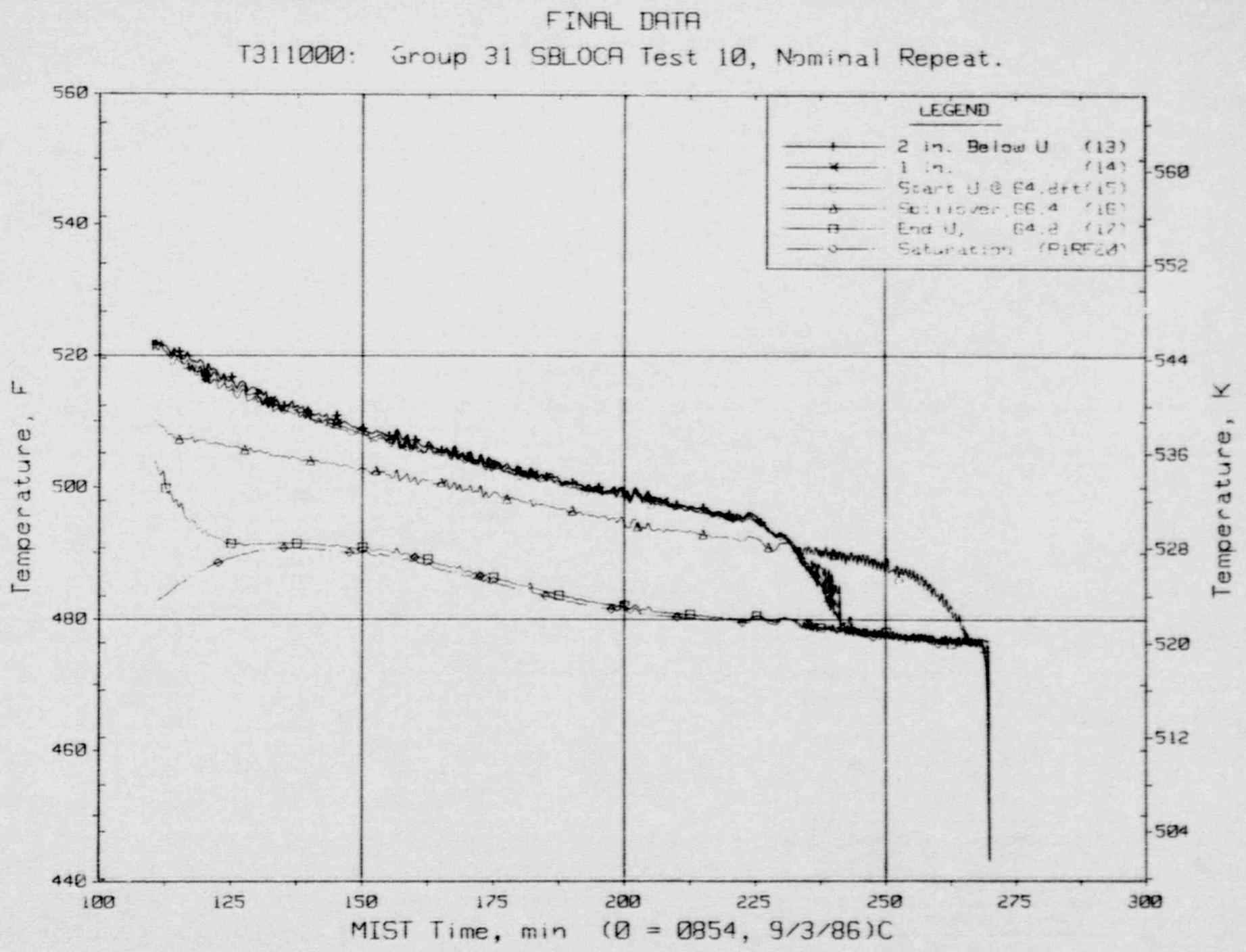

Figure 5.2.40. Hot Leg A U-Bend Fluid Temperatures (HITCs)

Wed Jul 6 16:15:39 1988

H1TC4

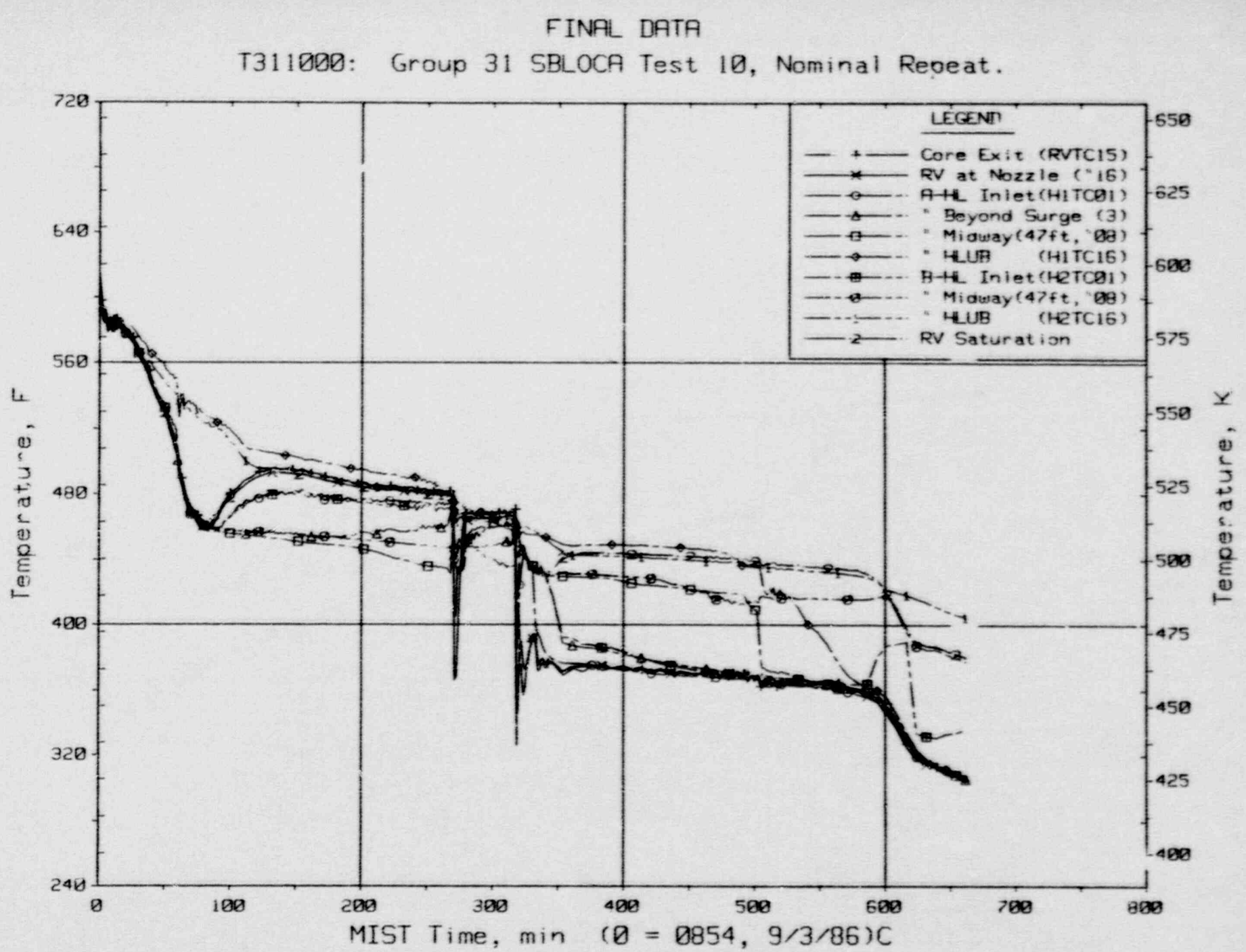

Figure 5.2.41. Composite Core Exit and Hot Leg Fluid Temperatures

Thu Jul 7 15:27:30 1988

PRKT1

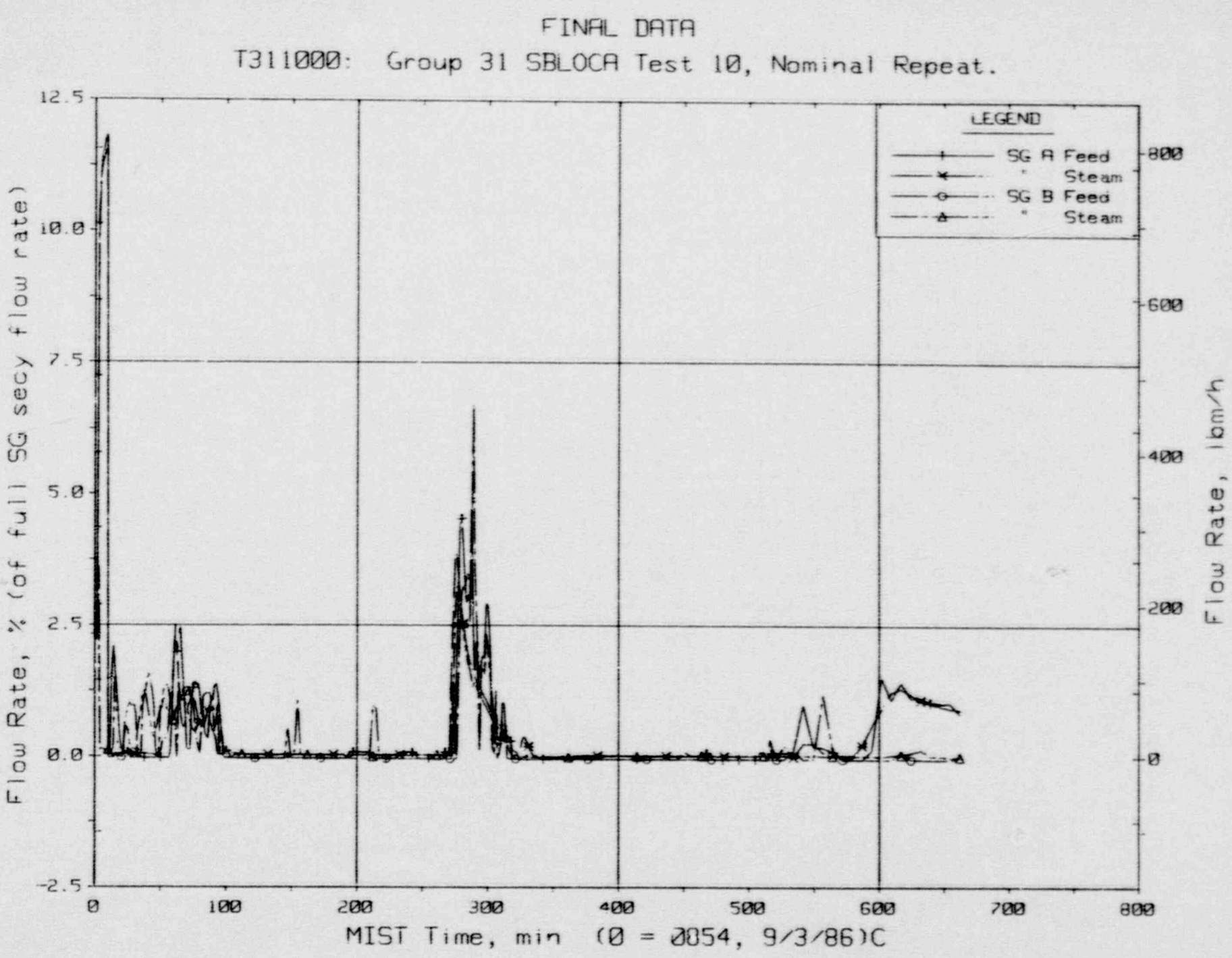

Figure 5.2.42. Secondary System Flow Rates

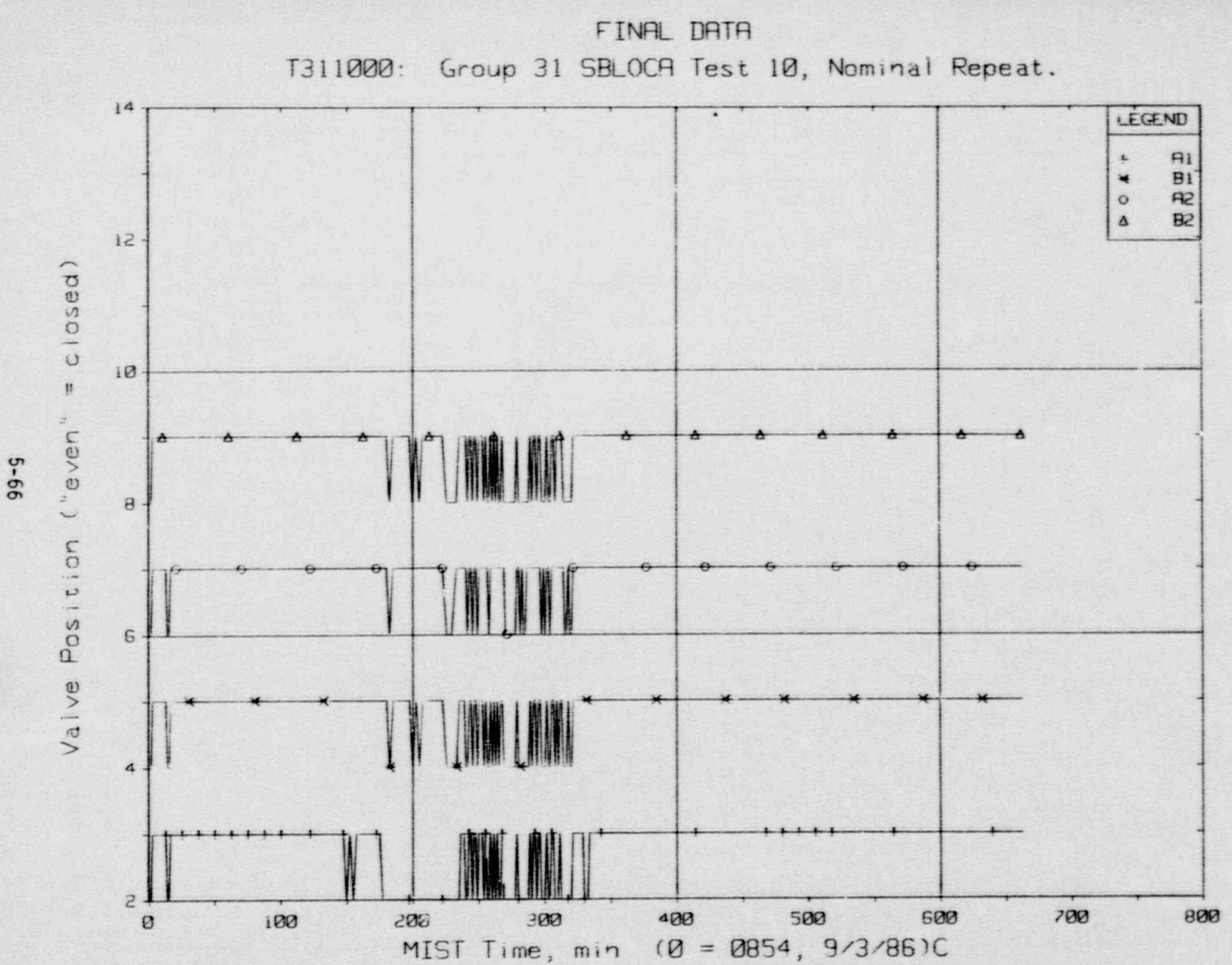

Figure 5.2.43. Reactor Vessel Vent Valve Positions

Wed Jul 6 16:26:26 1988

VVLS1

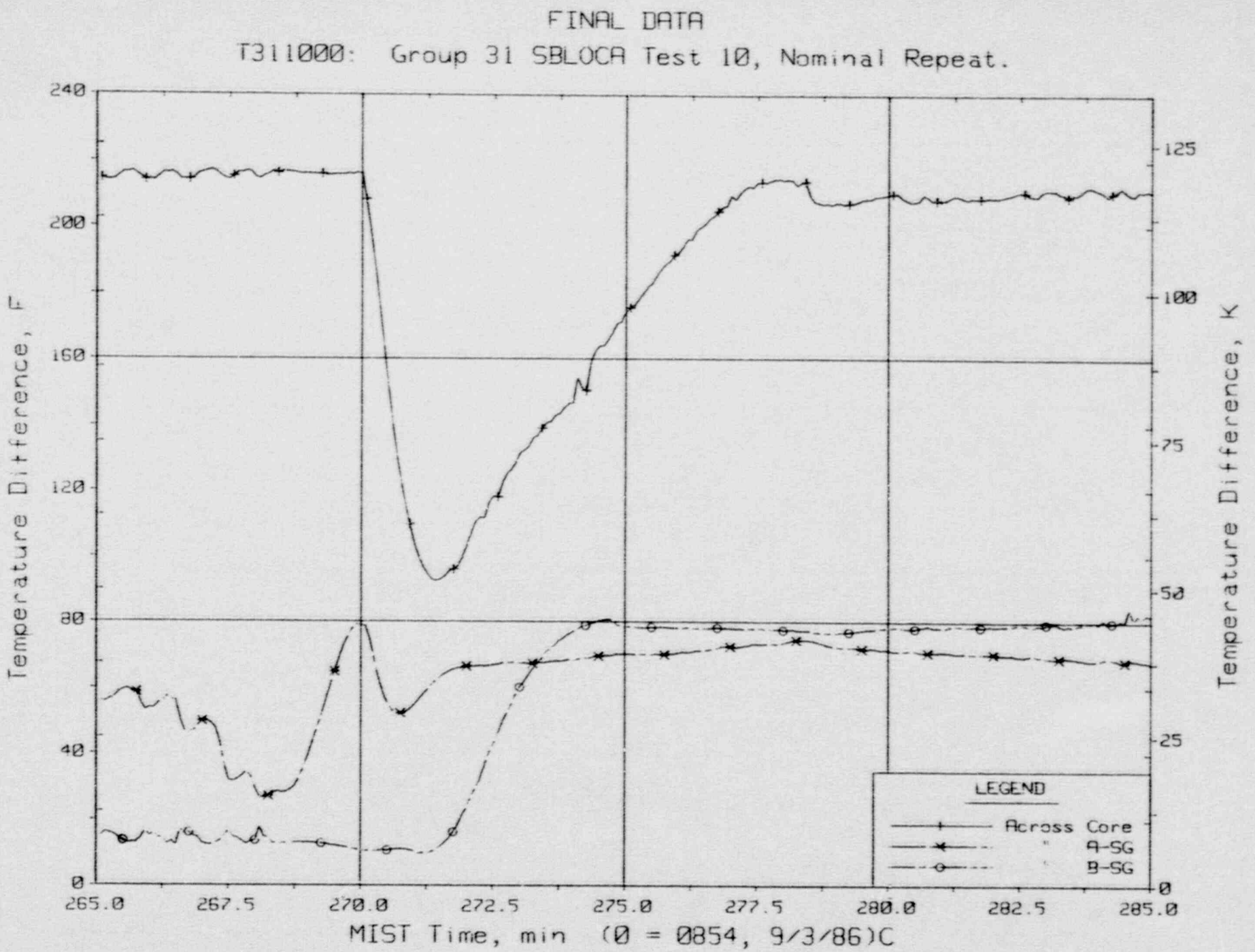

Figure 5.2.44. Key Temperature Differences

Wed Jul 6 16:49:37 1988

PRTD2

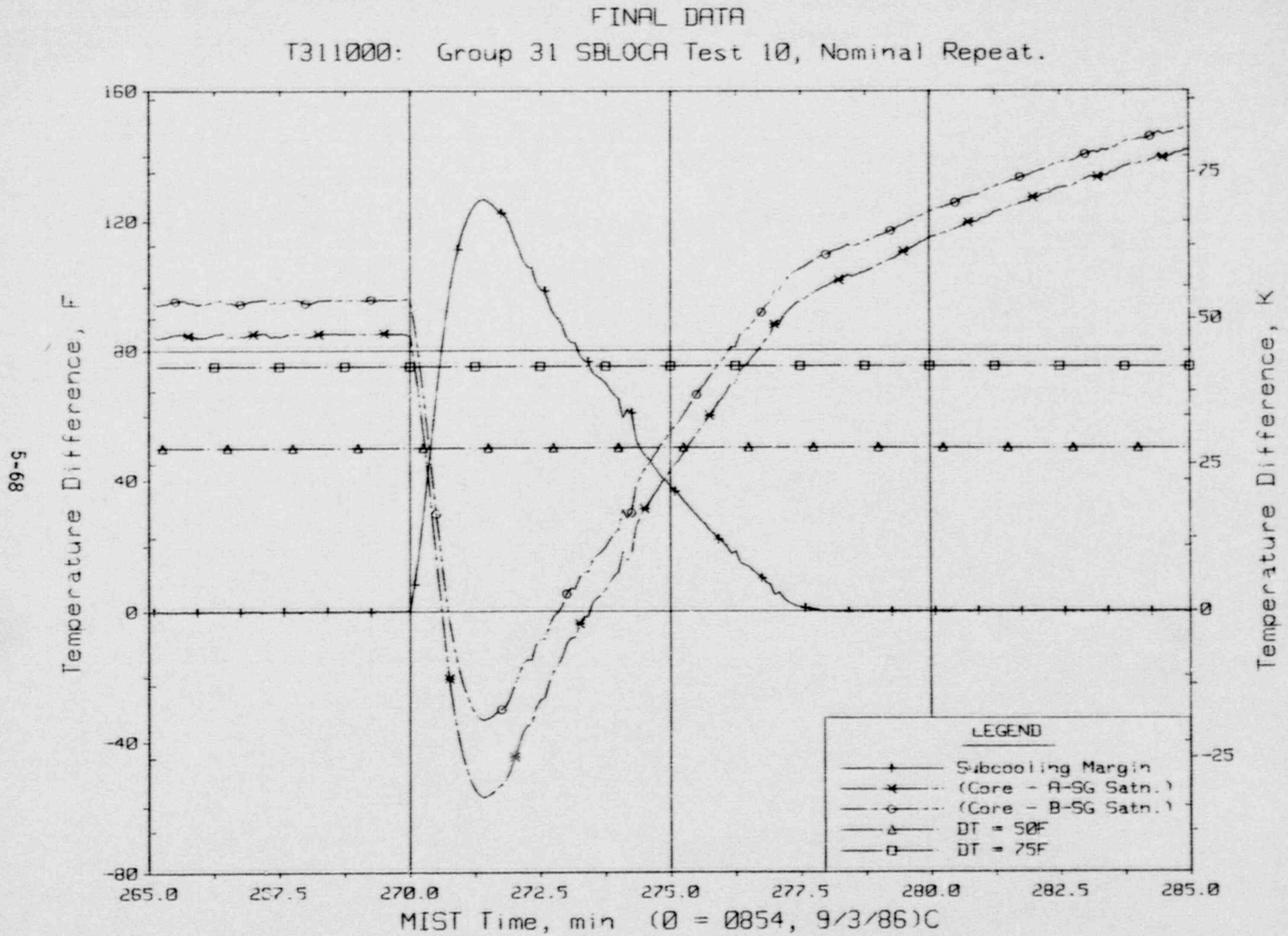

Figure 5.2.45. Control Temperature Differences

Wed Jul 6 16:52:07 1988

PRTD1

5.3. Leak Size Variations, Tests 1 and 2

The size of the cold leg B1 discharge break was varied in Tests 1 and 2. The nominal leak size was 10 cm^2 (reduced in area by the MIST power scale factor, 617). A scaled 5-cm^2 leak was used in Test 1 (320101), and a scaled 50-cm^2 leak was used in Test 2 (320201).

5.3.1. Reduced Leak Size, Test 1

A 5-cm^2 cold leg B1 discharge leak was used in Test 1 (320101). Upon leak actuation at time zero, the primary system depressurized from 1730 to 1560 psia at 4.2 minutes (Figure 5.3.1). Then, the depressurization rate increased, signifying the depletion of the saturated pressurizer fluid inventory. Just after this indication of pressurizer draining, the following effects of the second set of test-initiating actions became evident: The AFW flow rates abruptly increased at 4.4 minutes, the RVVV differential pressures abruptly decreased at 4.5 minutes, and the HPI flow rate began to increase at 4.8 minutes. These initial evolutions were delayed in approximate proportion to the decreased leak size of Test 1, 5 versus the nominal 10 cm^2.

At 5 minutes, the primary system depressurization rate slowed at 1480 psia (indicating the saturation of the loop fluid), the core exit and hot leg fluid temperatures briefly merged with the decreasing primary system saturation temperature, and the hot leg levels (particularly the loop A level downstream of the U-bend) were briefly perturbed. These level variations would usually presage interruption but the large excess of HPI over leak flow (Figure 5.3.2) refilled the hot legs and precluded interruption. Beyond 6 minutes, and for the duration of the test, the core exit and hot leg fluid temperatures remained subcooled, although the uppermost reactor vessel elevations evidenced lingering voiding from 7 to about 30 minutes.

The RVVVs opened as part of the test-indicating actions when their controls were transferred to automatic (independent) at 4.5 minutes. But the combined effects of valve actuation and the increase in AFW flow rate caused the RVVV differential pressures to abruptly decrease. The increased AFW flow rate elevated the steam generator thermal center, thereby decreasing the net loss of pressure in the outer flow loop and the RVVV differential pressure. (The "outer flow loop" was from the core outlet, through the hot legs, steam

generators, and cold legs, and back to the downcomer at the nozzle plane.) The RVVV differential pressures decreased to 0 055 psi at 5.3 minutes, and then to the vicinity of the closing setpoint, 0.04 psi, from 8 to 12 minutes (Figure 5.3.3). Although the differential pressures across the individual valves tracked together and were each within approximately 0.002 psi of the average differential pressure, the valves began to perform asymmetrically (Figure 5.3.4). The A1- and B1-RVVVs closed at 7.5 minutes, and the B2-RVVV closed at 9.5 minutes, but the A2-RVVV stayed open (all by limit switch indications). The temperature differences across the RVVVs confirmed this asymmetric performance (Figure 5.3.5). Also, the difference among coplanar fluid temperatures within the reactor vessel at the RVVV elevation increased to 13F by 13 minutes.

Several asymmetries among loop conditions occurred during this period of asymmetric RVVV operations. As was usual for tests of this group, the leak was imposed in the cold leg B1 discharge piping. Of more significance, the usual tendency to interrupt loop A in preference to loop B because of the initial pressurizer outsurge to loop A affected the loop flow distribution early in the transient (Figure 5.3.6). The flow rates in all four cold legs first increased from about 4.2 to 6% (of scaled full cold leg flow rate), apparently in response to the aforementioned AFW increase and elevated thermal centers. Then, the loop flow rates abruptly decreased, just before 7 minutes; whereas the loop B cold leg flow rates decreased toward their initial values, the loop A cold leg flow rates diminished to 3%. Because this flow rate difference was between loops A and B, rather than among individual cold legs, the difference was apparently driven by the brief and minor U-bend voiding that was observed early in the transient. In contrast, the asymmetries of vent valve behavior were among individual vent valves -- the A1- and B1-RVVVs behaved most similarly. Thus, the differing RVVV behavior was caused by the differences among actuation setpoints rather than by inter-loop condition differences.

The refill of the steam generator secondaries was completed at 12 minutes. The system conditions were responsive to the consequent termination of AFW. The cold leg flow rates dropped from 4.8 to 2.6% (of the scaled full cold leg flow rates, Figure 5.3.6), the RVVV differential pressures rose toward the

opening setpoint (Figure 5.3.3), all four RVVVs opened (the A2-RVVV had been open, Figure 5.3.4), and the downcomer flow rate diverged from the loop flow rate in response to the flow through the RVVVs. The primary system, which had gradually depressurized to 1350 psia during the refill of the steam generator secondaries, began to repressurize slowly (Figure 5.3.1). The steam generator secondaries had also been depressurized during the secondary side refill, although this depressurization was mitigated by the continuing primary-to-secondary heat transfer. The steam generator secondaries repressurized from 810 psia at 12 minutes to 875 psia at 14 minutes, with AFW interrupted. Then, the difference between the core exit fluid and the steam generator secondary saturation temperatures reached the setpoint of 50F, and the steam generators began to be depressurized by steaming to effect a cooldown of 100F/h. Both generators began to be steamed at 13.8 minutes, then feed became active to maintain level (B at 16.4 minutes, A at 17.7 minutes). The system thus became aligned for a cooldown of 100F/h with the primary in subcooled natural circulation.

The core exit subcooling margin (SCM) approached the control point of 75F at 26 minutes. This event triggered the automatic throttling of HPI (Figure 5.3.2). HPI was gradually reduced, the SCM was maintained near 75F, and the primary system pressure began to decrease (from 1525 psia at 26 minutes, Figure 5.3.1). At 40 minutes, the primary saturation temperature was reduced below the core outlet temperature at test initiation, and the reactor vessel upper head began to void (Figure 5.3.7). The voided region gradually expanded with the continuing primary system depressurization. Finally, at 70 minutes, the reactor vessel upper head void extended down to the elevation of the RVVVs and the void growth stopped. The vent valves had been performing asymmetrically, as previously discussed. This unequal operation continued after the completion of the steam generator refill at 12 minutes (at which time all the RVVVs were open, Figure 5.3.4). The differential pressures across the RVVVs gradually decreased because of the following three continuing trends:

1. HPI throttling (to limit the SCM to a maximum of 75F).
2. Core power decay.

3. The decrease of the average primary fluid temperature, and the consequent decrease of the thermal expansion coefficient of water.

In response to this decreasing differential pressure, the RVVVs closed. But, again apparently due to the differences among the RVVV closure setpoints, the RVVVs closed asymmetrically. The A1-RVVV closed at 30 minutes, the B1 at 42 minutes, the B2 at 59 minutes, and finally, the A2-RVVV closed at 77 minutes. Again, the temperature differences across the RVVVs (Figure 5.3.5) confirmed the limit switch indications of valve closures. The differential pressures (DPs) across the RVVVs increased about 0.01 psi as the individual valves closed (Figure 5.3.3). Although the variation among indicated RVVV DPs remained small, the individual DPs seemed to approximately conform to the order of closing; that is, the DP across the B1-RVVV was lowest and it closed second, the A1-RVVV DP was intermediate and it closed first, and the DPs across the A2- and B2-RVVVs were highest and they closed last. The voiding in the upper reactor vessel persisted and remained almost constant even after the last vent valve had closed at 77 minutes.

The relatively stagnant upper reactor vessel downcomer fluid saturated at 12? minutes as the primary system saturation temperature continued to decrease. The downcomer then gradually voided through the elevation of the vent valves (Figure 5.3.8, the RVVVs remained closed). During the same period, beyond approximately 125 minutes, the HPI could no longer be throttled sufficiently to maintain the 75F core exit subcooling (Figure 5.3.2). The SCM thus increased and achieved 100F at 162 minutes. The operator then stopped HPI as specified and allowed the SCM to diminish to 50F. The resulting perturbation of system conditions was evident by the indications of primary system pressure, loop flow rate, and downcomer level, but the ongoing cooldown continued unabated. The SCM reached 50F at 172 minutes, prompting the reactivation of HPI. This HPI off/on sequence was repeated two additional times, then HPI was left active as specified; the SCM then gradually increased to approximately 150F. The steam generator secondary systems approached their (MIST) minimum pressures at 200 minutes (Figure 5.3.9), thus attenuating the primary system cooldown. The test was terminated at 298 minutes because of the attainment of stable system conditions. At test termination, the primary system fluid temperatures (within the flow loop)

ranged from 258 to 292F, the primary system pressure was 450 psia, and the primary flow rates continued at about 2% of scaled full flow (Figure 5.3.10).

5.3.2. Increased Leak Size, Test 2

A 50-cm^2 cold leg B1 discharge leak was used in Test 2 (320201). The initial transient events with an increased leak size were accelerated accordingly. After leak actuation at time zero, the primary depressurized at about 1700 psi/min (Figure 5.3.11). This depressurization slowed at approximately 0.2 minutes as the primary loop fluid saturated; the core exit fluid saturated and the core region collapsed liquid level began to descend. Indications of the second set of test-initiating actions were in evidence between 0.5 and 0.8 minutes. These actions included the reset of the steam generator secondary level control point, activation of HPI, transfer of the RVVV controls to automatic/independent, activation of the core power decay simulation, and activation of the (ATOG) steam pressure control logic.

The enhanced initial primary system mass depletion rate with the 50-cm^2 break caused (broken) loop B, rather than (intact and pressurizer) loop A, to interrupt first. The relatively cold pressurizer surge line fluid continued to cool hot leg A through about 0.6 minutes (Figure 5.3.12) whereas the loop B U-bend began to decrease at 0.7 and 0.9 minutes. The steam generator secondary pressures began to diverge beyond about 1 minute (Figure 5.3.11), with the steam generator B pressure becoming lower (corresponding to the earlier interruption of loop B).

The primary system pressure stabilized near 1400 psia until 2 minutes. During this time, the core region collapsed liquid level descended through the elevation of the RVVVs and down to the hot leg nozzles, then the downcomer level descended to the same elevation (Figure 5.3.14). The hot leg riser levels rose somewhat while the stub levels (beyond the U-bends) stabilized, so the level differences across the U-bends at 2 minutes reached 7 ft (Figure 5.3.13). The loop flow rates peaked at 1 minute and then subsided. The core exit fluid briefly subcooled in response to this flow increase, then remained saturated beyond 1.4 minutes.

The core region and downcomer voiding propagated to the cold legs beyond 2 minutes (Figure 5.3.15). The (broken) cold leg B1 discharge level began to

descend, followed by the other three legs at 4 minutes. The cold leg B1 suction level began to decrease near 3 minutes. The leak site fluid saturated at 3.2 minutes, and the leak flow rate abruptly decreased (Figure 5.3.16) as the leak site fluid conditions changed from subcooled liquid to two-phase fluid. Based on the magnitude and behavior of the leak flow rate, the leak site conditions apparently approached saturated vapor beyond 4 minutes. (The actual leak mass flow rate apparently exceeded the capacity of the single-phase discharge flowmeter until 2.5 minutes -- the indicated leak flow rate remained constant at 3420 lbm/h, Figure 5.3.16.) The voiding of the leak site slowed the rate of primary system fluid mass depletion to approximately 500 lbm/h beyond 5 minutes.

The hot leg levels of both loops descended relatively rapidly beyond 2 minutes. Both steam generator primary levels descended below the elevation of the upper tubesheet (A at 2.8 minutes, B at 2.9 minutes, Figure 5.3.13), exposing the primary system vapor to the feed injection site. Secondary-side refill was only half completed, therefore the primary system depressurization was robust, approaching 200 psi/min at 3 minutes (Figure 5.3.11). The steam generator A secondary repressurized somewhat.

The combination of the continuing vent valve discharge of core-generated steam and the decreasing primary system saturation temperature caused the saturation of the core region liquid. The downcomer fluid below the cold leg nozzles saturated at 4.8 minutes (Figure 5.3.17), saturation proceeded sequentially to lower elevations, and the bottom downcomer fluid (at 1.4 ft) saturated at 6.8 minutes. The steam generator primary levels at 6 minutes increased slightly to the vicinity of the upper tubesheets, thus slowing the rate of primary system depressurization.

The refill of the steam generator secondaries was completed at 8 minutes. Feed was thus interrupted and the steam generator A and B secondary pressures stabilized at 710 and 630 psia (Figure 5.3.11). The temperature difference between the core exit fluid and the steam generator saturation temperatures remained less than the control value of 5°F, due to the continuing primary depressurization with the core exit fluid saturated. Thus, the secondary control pressure was continually reduced at a rate equivalent to a cooldown of 100F/h (Figure 5.3.18). The decreasing control pressure finally reached

the current steam generator secondary pressures at 28.5 minutes. However, before the control steaming of 100F/h could take effect, the primary system depressurization overtook that of the steam generator secondaries (Figure 5.3.11). The core exit-to-steam generator A saturation temperature difference became negative and the rapid mode of steam generator depressurization was activated. The steam generator steaming rates (Figure 5.3.19) rose to 6% (of scaled full steam generator secondary flow) and both steam generators were depressurized at approximately 50 psi/min from 30 to 35 minutes. Feed was activated at 32 minutes and reached nearly 12% (of scaled full steam generator secondary) flow. The steam generator primary levels had been gradually declining before this heat transfer event (Figure 5.3.20). The steam generator primary level had descended below the elevation of the secondary pool at 22.5 minutes, but little heat transfer had occurred because of the small temperature difference between the primary and secondary systems. The reactivation of the steam generators under these circumstances thus produced pronounced primary-to-secondary coupling. The primary system depressurized in parallel with the secondaries from 650 psia at 30 minutes to 300 psia at 40 minutes (Figure 5.3.11). The leak flow rate abruptly decreased (Figure 5.3.21) and the CFT actuated, both due to the primary system depressurization. The primary system began to refill.

The mass closure of the steam generator secondaries routinely has been evaluated by determining and comparing the mass balance using independent techniques. The "calculated" steam generator secondary fluid mass was based on the initial fluid mass and the time-integrated feed and steam flow rates, whereas the "indicated" fluid mass was determined using the measured steam generator secondary levels and fluid conditions. This comparison yielded almost exact closure through 40 minutes (Figure 5.3.22), during which time the total fluid mass in each steam generator increased from 27 to 130 lbm. However, the mass closure comparisons indicated large errors from 40 minutes to approximately 55 minutes. The indicated feed flow rate for steam generator B was zero during most of this time (Figure 5.3.19), and the indicated steaming rates of both steam generators were only on the order of 1 to 2% flow, about one-half of the feed flow rate for steam generator A during the earlier portion of this period. The steam outlet temperatures at the exits of both generators tracked together (Figure 5.3.23) and with saturation from

35 to 40 minutes. But, beyond 40 minutes, these temperatures diverged -- the steam generator B steam line temperatures indicated more than 80F subcooling at 52 minutes. Also, the steam generator B secondary level remained as much as 4 ft below the control level. from 40 to 52 minutes (Figure 5.3.24), which would have activated feed. Thus, the steam generator B feed flowmeter is deduced to have overranged from 41 to 55 minutes. Rather than the zero flow rate indicated, the actual feed flow rate to steam generator B was more than 12% flow, or 900 lbm/h. This feed flow rate was sufficient to raise the steam generator B level at more than 3 ft/min, or the equivalent of 42 ft over the 14-minute period. The actual level varied by only 11 feet, suggesting that most of the feed left steam generator B without adding to the secondary inventory.

A similar but less pronounced event occurred in steam generator A, as indicated by the relatively constant indicated fluid mass versus the increasing calculated value. The steam generator steam line flowmeter indications were converted using vapor rather than liquid properties. This situation, plus the observed subcooling of the steam generator B steam lines, suggests that much of the injected feed was diverted to the steam lines rather than contributing to the steam generator secondary fluid inventory. This redirection of AFW is postulated to have been caused by the relatively high steam flow rate associated with the blowdown of the steam generator secondaries. The upward momentum of the steam may have been sufficient to divert the feed upward and into the steam piping. As an alternative explanation, the upward velocity of steam through the flow holes in the uppermost tube support plate may have been sufficient to prevent the downflow of feed. The continuing introduction of feed filled the uppermost secondary volume and the steam lines. The result was the same in either case. Note that although a section of a plant steam generator is virtually replicated in MIST, several MIST atypicalities bear on the observed behavior. The fewer steam generator tubes and, hence, the confined interactions of the model steam generator are relevant to the observed steam line refill.

As the steam generator secondary pressures approached their minimum values, the rate of secondary depressurization gradually diminished beyond 35 minutes (Figure 5.3.11). The previously discussed feed diversion ceased at 52

minutes, apparently in response to the reduced steaming rate. The steam line subcooling decreased (Figure 5.3.23), the indicated steam generator B secondary level abruptly increased by 6 ft (Figure 5.3.24), and then the steam generator B feed flow rate came back into range (Figure 5.3.19).

The remainder of the transient was quite uneventful. The HPI and leak mass flow rates remained approximately equal, the steam generator primary levels remained near the elevation of the upper tubesheets, and the primary system gradually depressurized toward the 25-psia secondaries (Figure 5.3.25). The core flood tank was isolated at 90 minutes upon receipt of the low-level trip. The test was terminated at 187 minutes. Upon termination, the primary system pressure was 100 psia. The core exit and upper-elevation loop fluid remained saturated, the hot leg U-bend regions remained voided, and the core region levels remained in the vicinity of the nozzles.

5.3.3. Comparisons

The break size was varied in three tests with the same nominal conditions otherwise. These tests were as follows:

- Test 1 (320101) 5 cm^2
- Test 10 (311000) 10 cm^2
- Test 2 (320201) 50 cm^2

(Test 10 was the Nominal Repeat Test from Group 31.)

Each of these tests used a cold leg B1 discharge break, full HPI capacity, and the nominal steam generator controls. Their test transients were quite diverse, as discussed below.

Leak Flow Rate

The leak flow rate in Test 10 remained about twice that in Test 1 (Figure 5.3.26); that is, in the same proportion as their leak flow areas. The leak flow rate in Test 2, on the other hand, was quite variable. The initial leak flow rate in Test 2 apparently overranged the flowmeter, remaining constant at 3430 lbm/h; this was approximately four times the flow rate of Test 10, although its leak flow area was five times larger. The Test 2 leak flow rate dropped abruptly at 3 minutes as the leak-site fluid saturated. The leak flow rates with a 10- and with a 50-cm^2 break then remained almost equal

until 30 minutes. At this time, the quality at the 50-cm^2 leak increased (Figure 5.3.27) and the leak flow rate decreased further towards that of the 5-cm^2 leak.

The (modified) leak flow rate ratios, measured over predicted, remained near unity for Tests 1 and 10 (Figure 5.3.28). But the vagaries of the 50-cm^2 leak flow rate were not well predicted, thus its ratio remained oscillatory and deviated from unity.

Reactor Vessel Levels

The reactor vessel levels underscored the differences among the three transients with differing break sizes (Figure 5.3.29). With a 50-cm^2 break, the reactor vessel level quickly plummeted, exposing the RVVVs to vapor; this event allowed the condensation of vapor on the subcooled HPI fluid and saturated the break site fluid. The primary system thus depressurized relatively rapidly with a 50-cm^2 break (Figure 5.3.30), primarily through the relatively large rate of break volumetric discharge.

The reactor vessel level initially remained almost full with the 5-cm^2 break. And with a 10-cm^2 break, the reactor vessel level followed an intermediate course, exposing the RVVVs to vapor after 12 to 15 minutes.

Primary System Pressure

The primary system repressurized somewhat, after the steam generator secondaries were refilled, with the 5-cm^2 break (Figure 5.3.30). With the larger breaks, however, the primary system depressurized regularly.

The Test 2 primary system pressure decreased markedly near 30 minutes -- the primary system had depressurized more rapidly than the secondaries, triggering a rapid depressurization of the secondaries and, hence, robust primary-to-secondary heat transfer. The primary system also depressurized in Test 10 through increased primary-to-secondary heat transfer and BCM, but later repressurized (Figure 5.3.31) as the hot leg levels became intermediate (Figure 5.3.32).

Test 1 evidenced yet a third type of primary system depressurization (Figure 5.3.31). After the repressurization following the refill of the steam generator secondaries, the primary system depressurized quite regularly due

to sustained two-loop, single-phase natural circulation and the controlled steam generator secondary cooldown.

Hot Leg Levels

The hot leg levels remained full throughout virtually all of Test 1 (Figure 5.3.32). In Tests 2 and 10, on the other hand, the hot leg levels remained intermediate -- above the steam generators but below the U-bend spillover elevation -- after approximately 1-1/2 hours. The levels in Test 2 dropped precipitously during the enhanced primary system depressurization near 25 minutes, but recovered when pressure stabilized at a relatively low value.

Equilibrium

Remarkably, the primary system conditions approximately equilibrated in Test 2 much as they did in Test 10, although the break area was five times larger. The HPI flow rate and core power input of the two tests were virtually identical. The key to this seeming contradiction was the break fluid conditions. The core region level increased toward the elevation of the RVVVs in Test 10, but it remained near the top of the core in Test 2 (Figure 5.3.33). The break site fluid remained saturated with a 50-cm^2 leak whereas the break fluid was slightly subcooled with a 10-cm^2 break. The break mass flow rates thus remained approximately equal beyond 90 minutes (Figure 5.3.34). The higher volumetric flow rate with two-phase conditions at the break obtained a lower sustained pressure with the larger break (Figure 5.3.31). The lower pressure in Test 2 also contributed to its lower break mass flux.

Summary

The break size variations resulted in quite different transients. The loops remained full throughout the entire 5-cm^2 break transient. The primary system depressurized regularly through sustained natural circulation and steam generator depressurization. With a 50-cm^2 break, the break site fluid saturated and caused the primary system to depressurize relatively rapidly through the break volumetric discharge alone. The primary system depressurization overtook the controlled secondary depressurization, a rapid steam generator secondary pressure reduction was initiated, and the primary pressure plummeted through robust, two-loop BCM heat transfer and vapor

condensation. Near-equilibrium conditions were obtained with both the 10- and 50-cm^2 break, but at a lower pressure with the larger break.

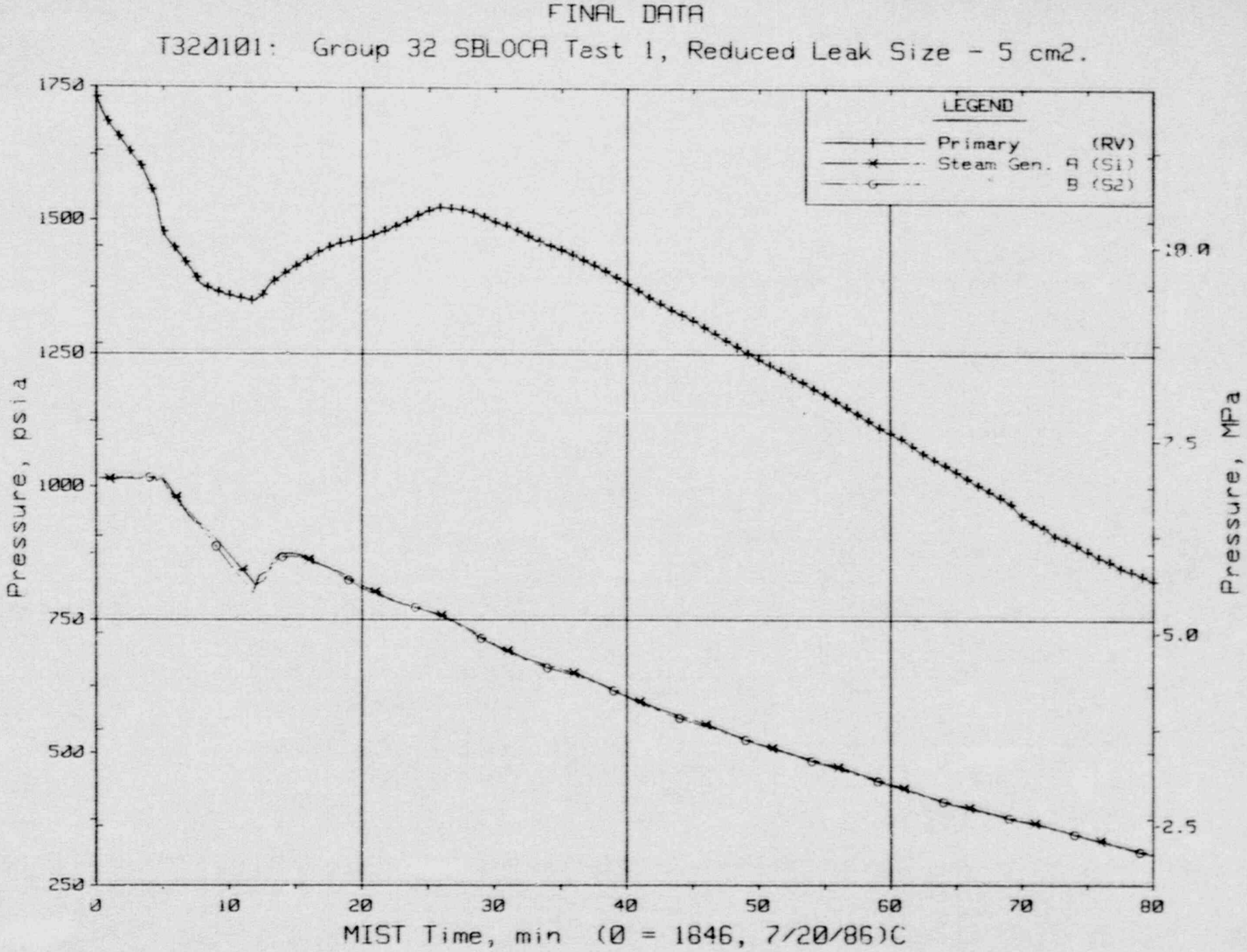

Figure 5.3.1. Primary and Secondary System Pressures (GPOIs)

Mon Oct 31 15:38:27 1988

PSGP1

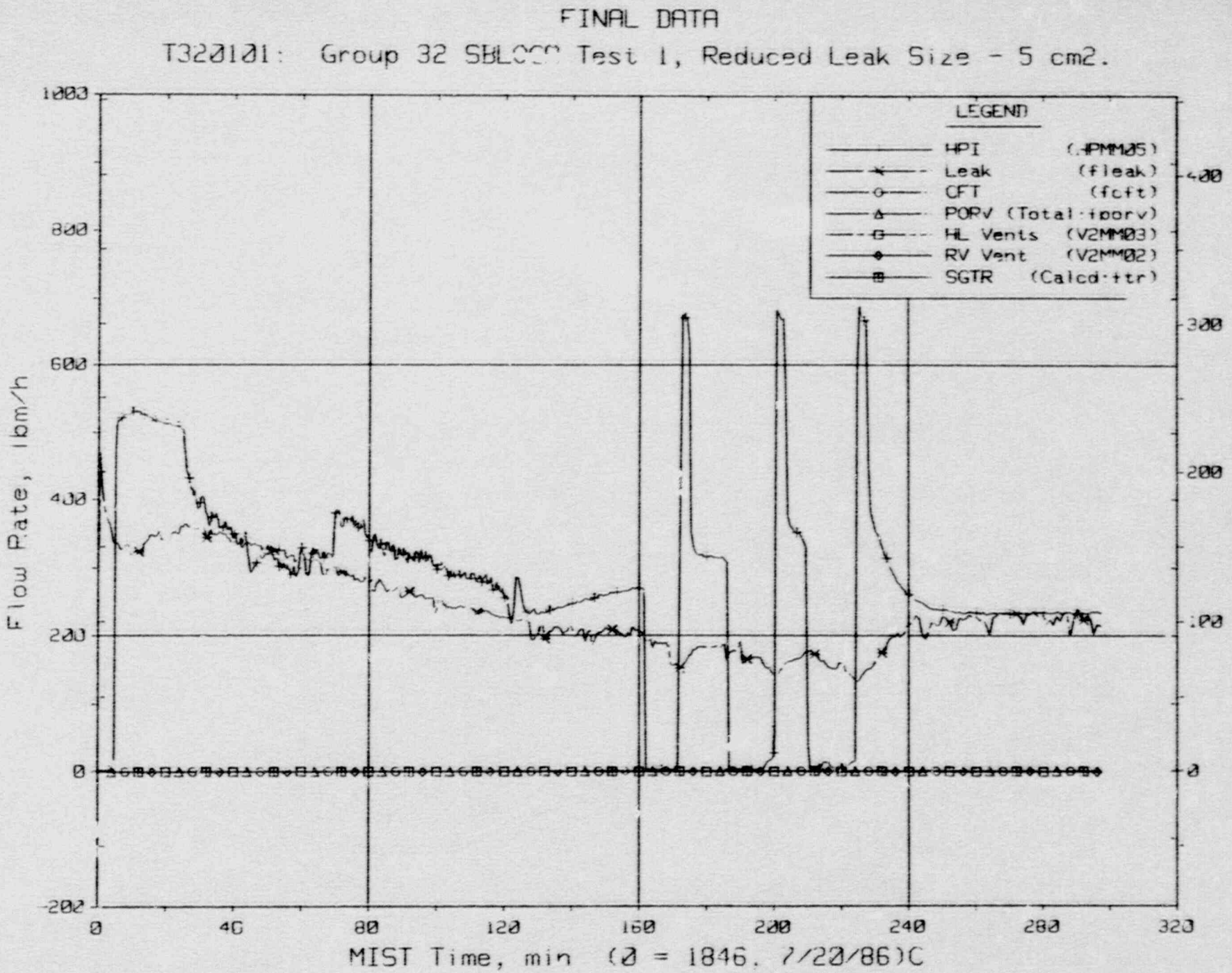

Figure 5.3.2. Primary System Boundary Flow Rates

Tue Nov 1 08:55:55 1988

PRFL3

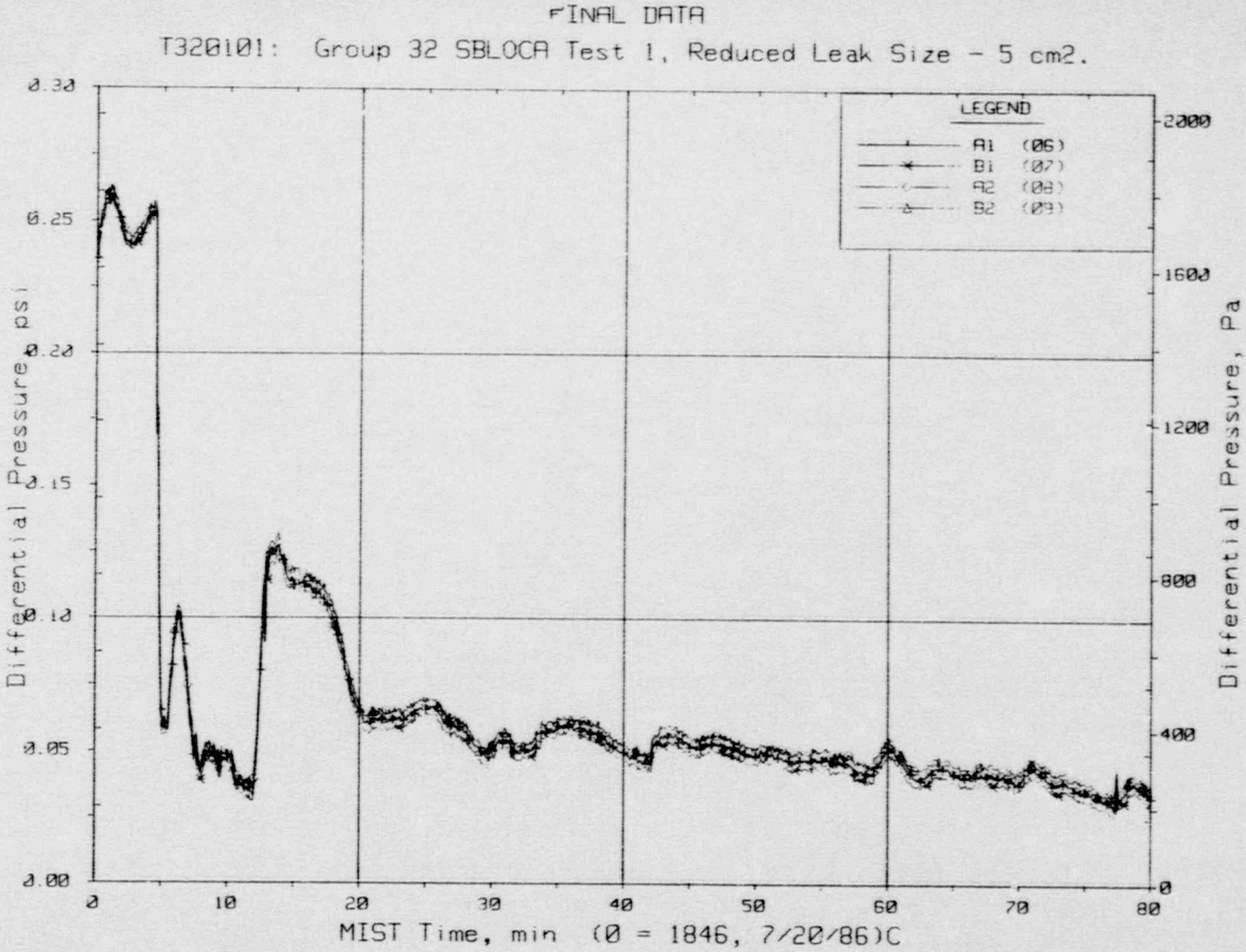

Figure 5.3.3. Reactor Vessel Vent Valve Differential Pressures (RVDPs)

Mon Oct 31 16:09:37 1988

V7DP1

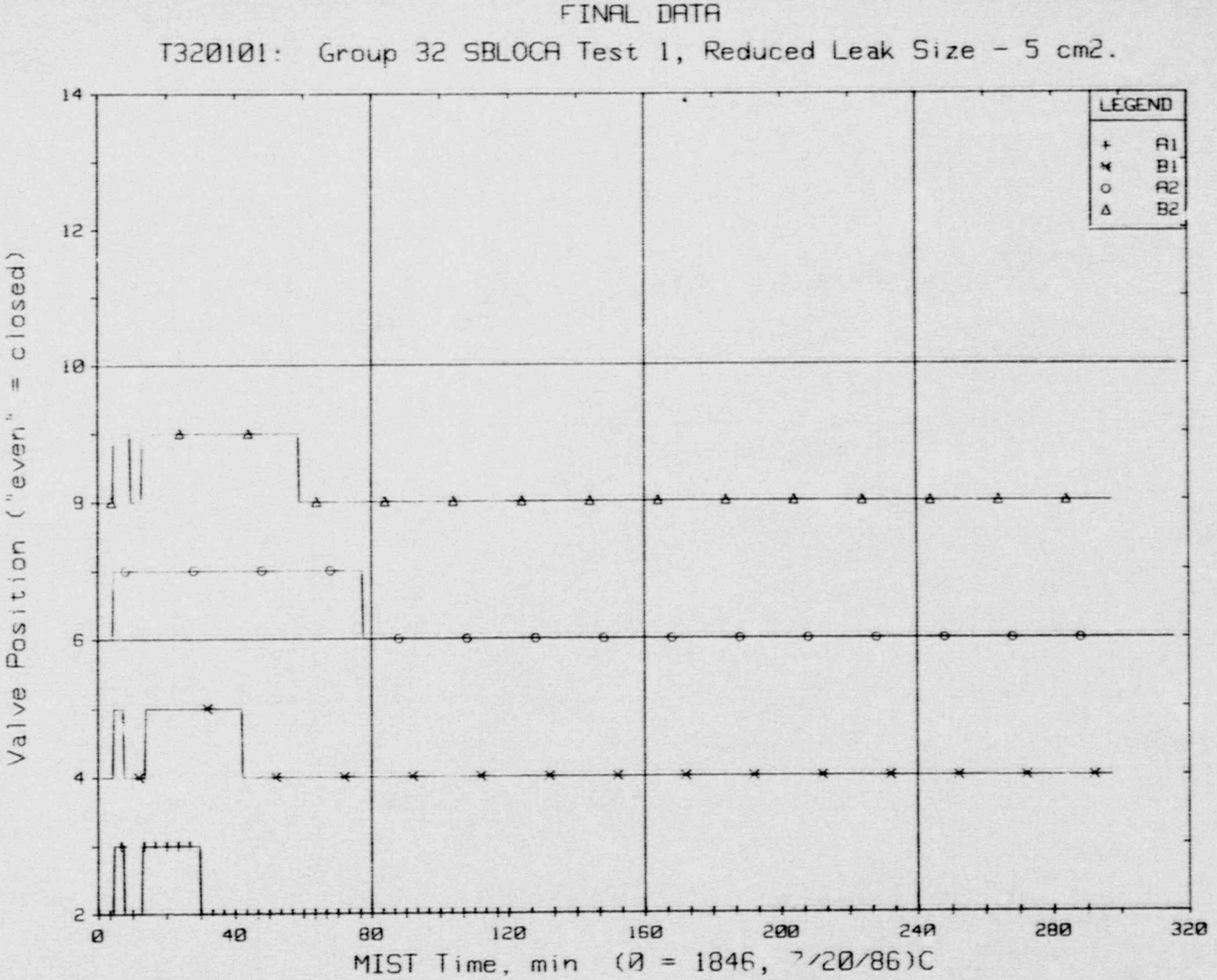

Figure 5.3.4. Reactor Vessel Vent Valve Positions

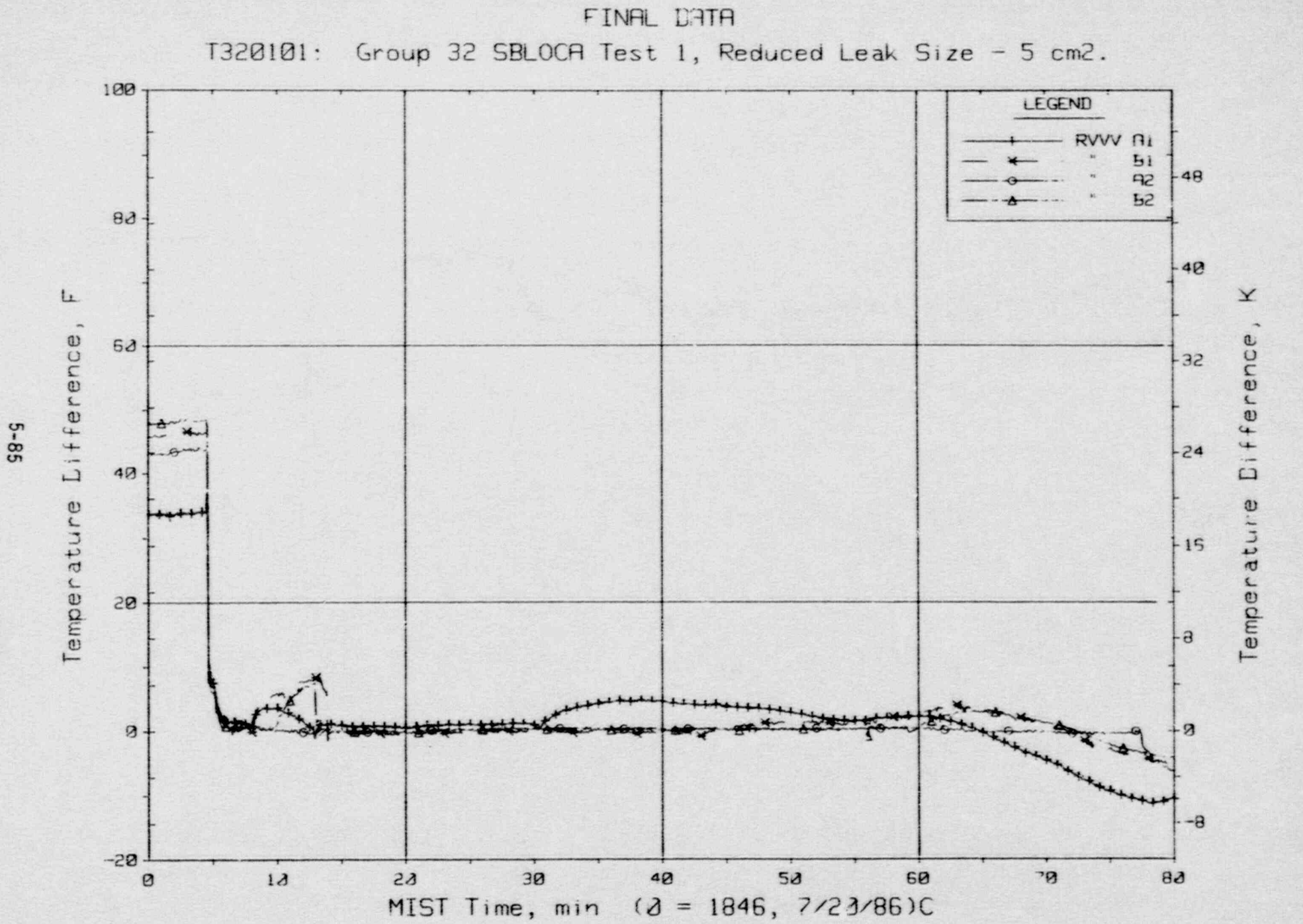

Figure 5.3.5. Temperature Differences Across Vent Valves

Mon Oct 31 16:22:37 1988

VVTD1

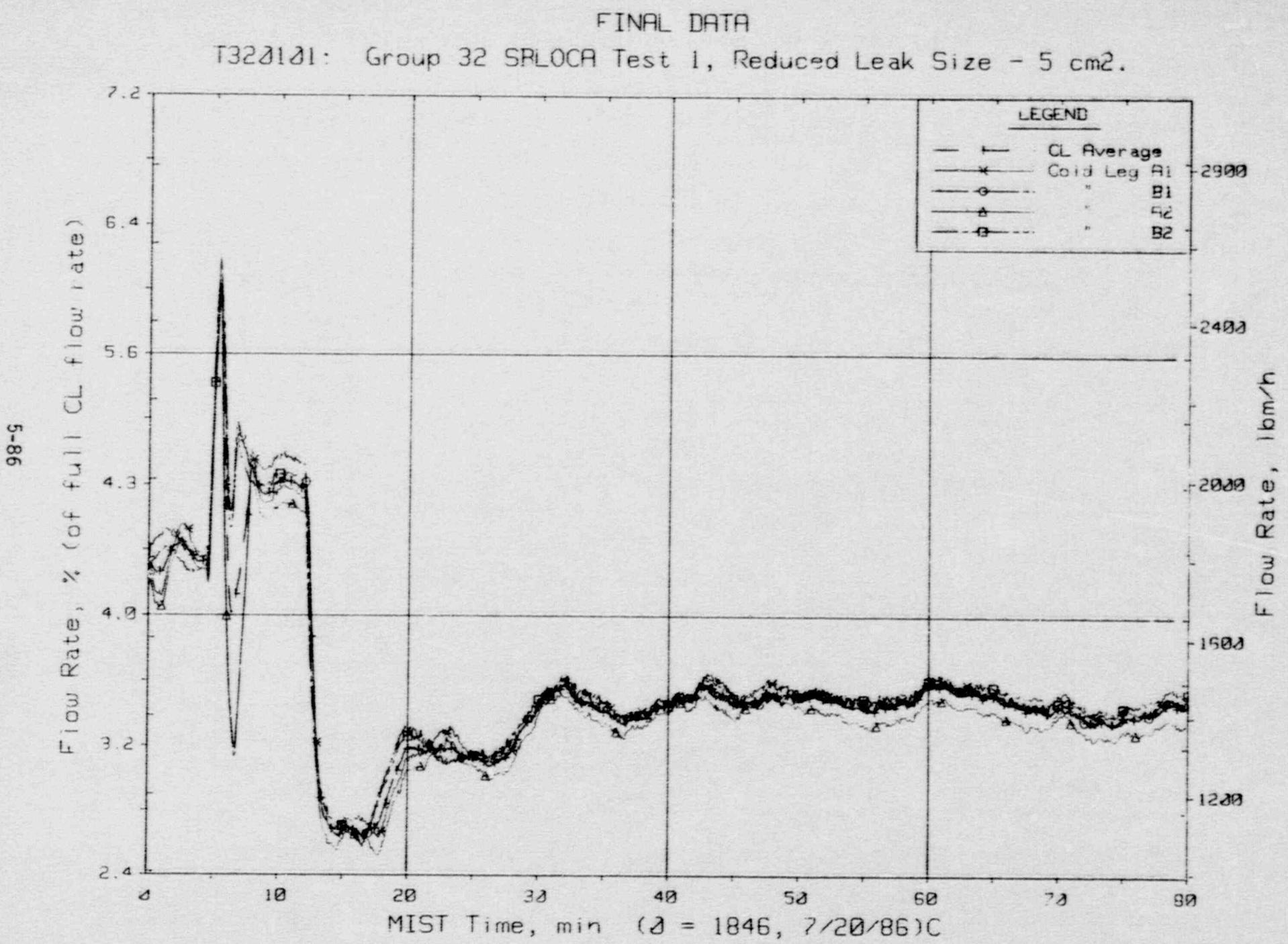

Figure 5.3.6. Cold Leg (Venturi) Flow Rates

Mon Oct 31 15:28:12 1988

CLFL1

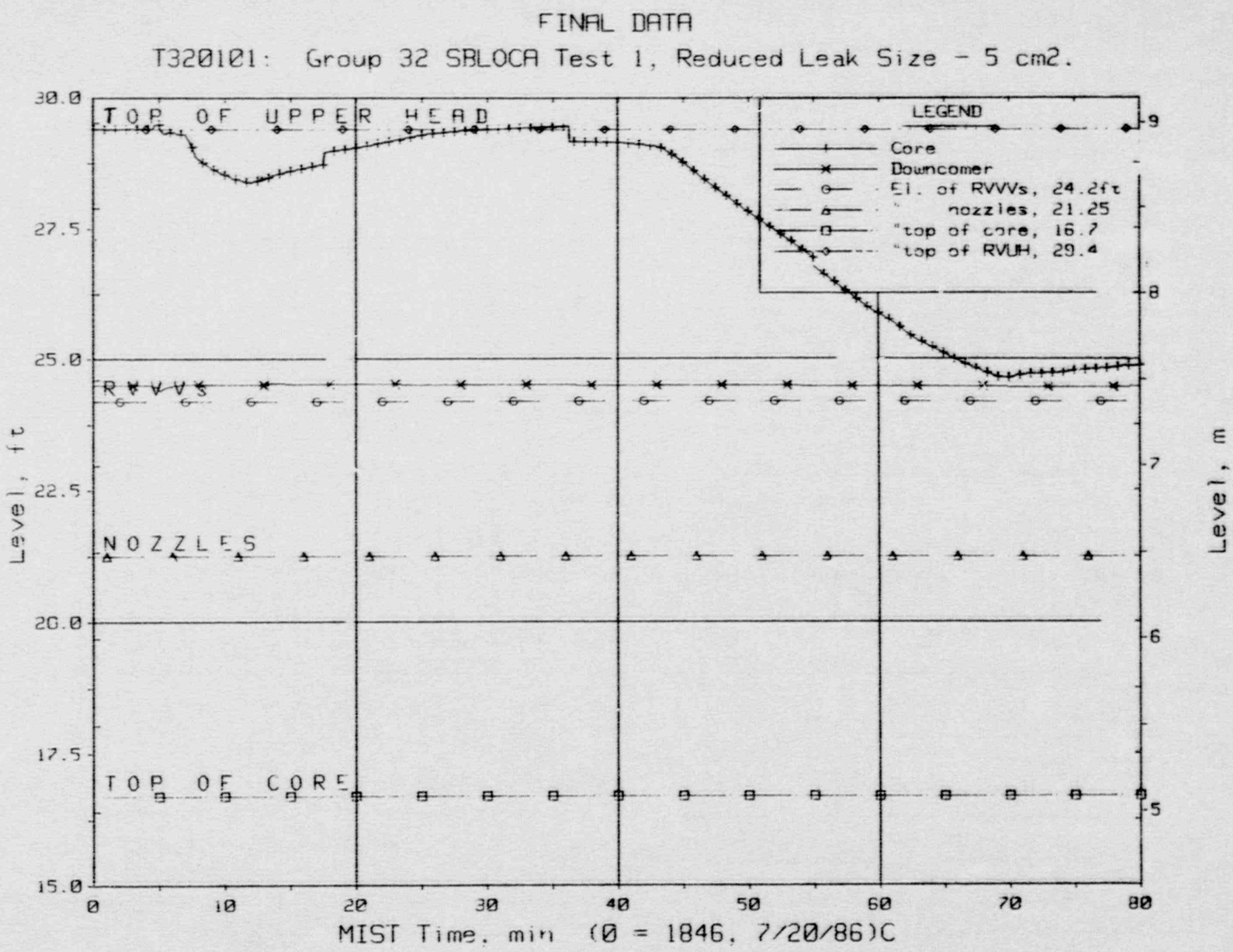

Figure 5.3.7. Core-Region Collapsed Liquid Levels

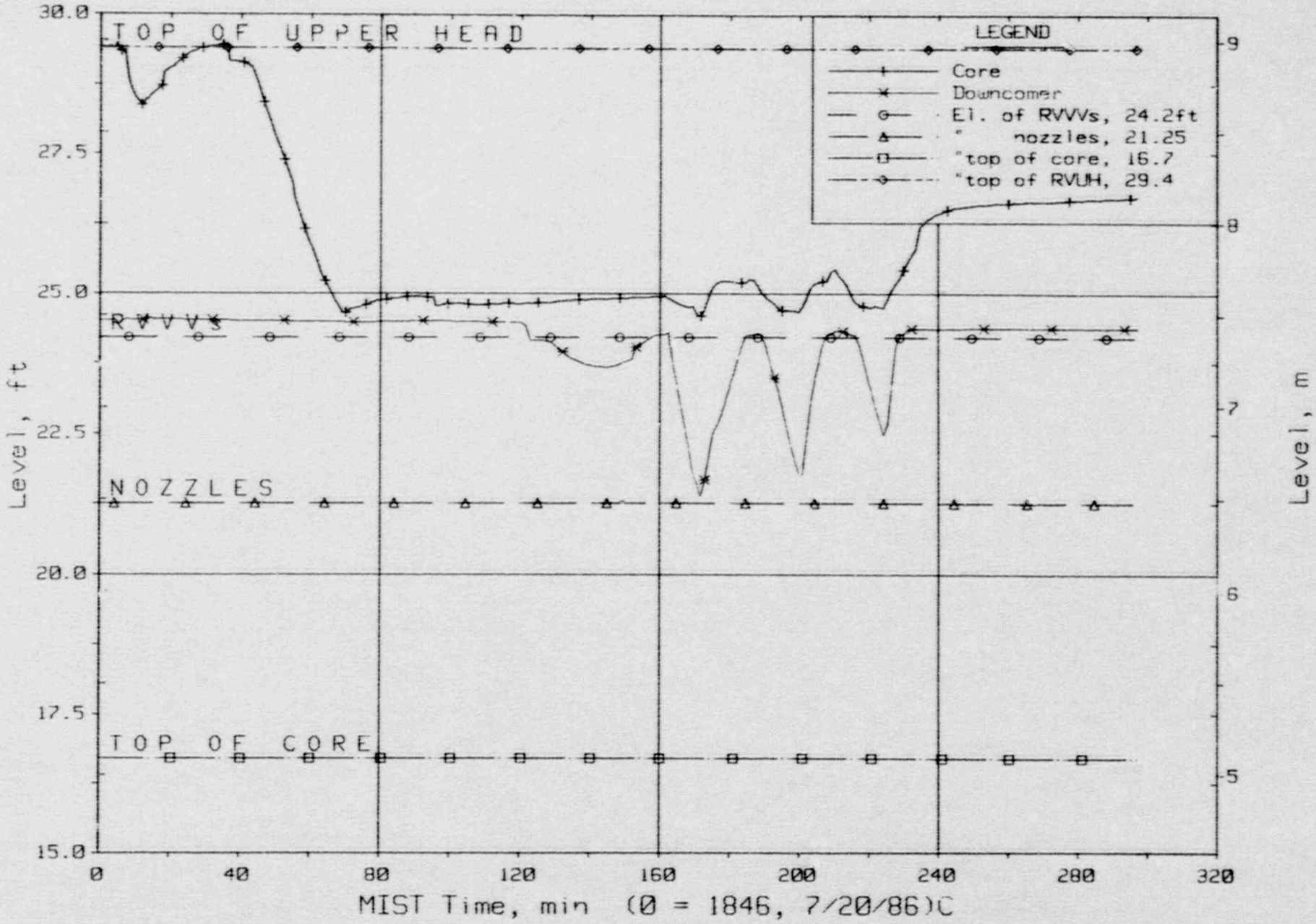

Figure 5.3.8. Core-Region Collapsed Liquid Levels

Mon Jul 11 10:43:54 1988

COLV1

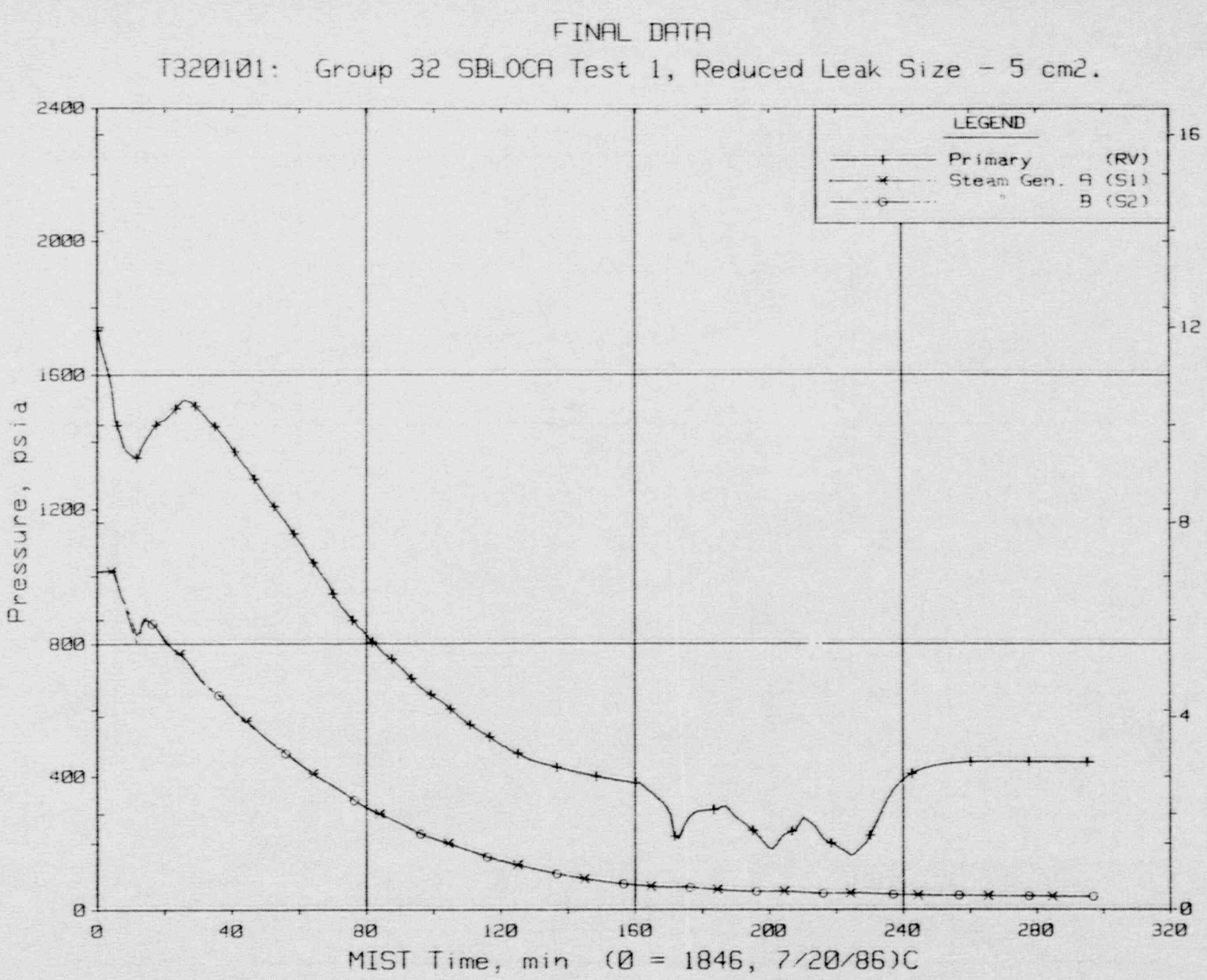

Figure 5.3.9. Primary and Secondary System Pressures (GP01s)

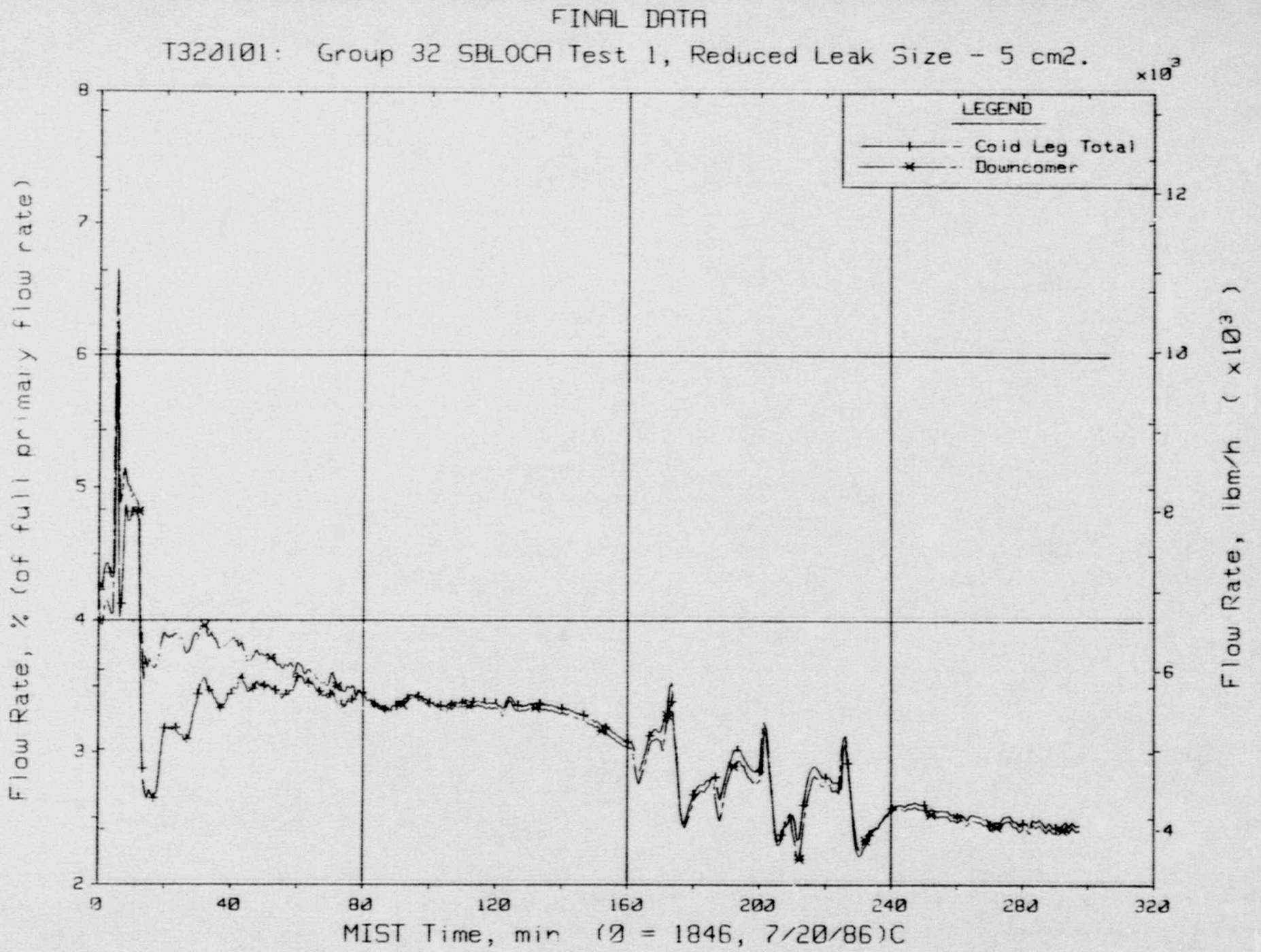

Figure 5.3.10. Primary System Flow Rates

Mon Oct 31 18:18:16 1988

PRFL7

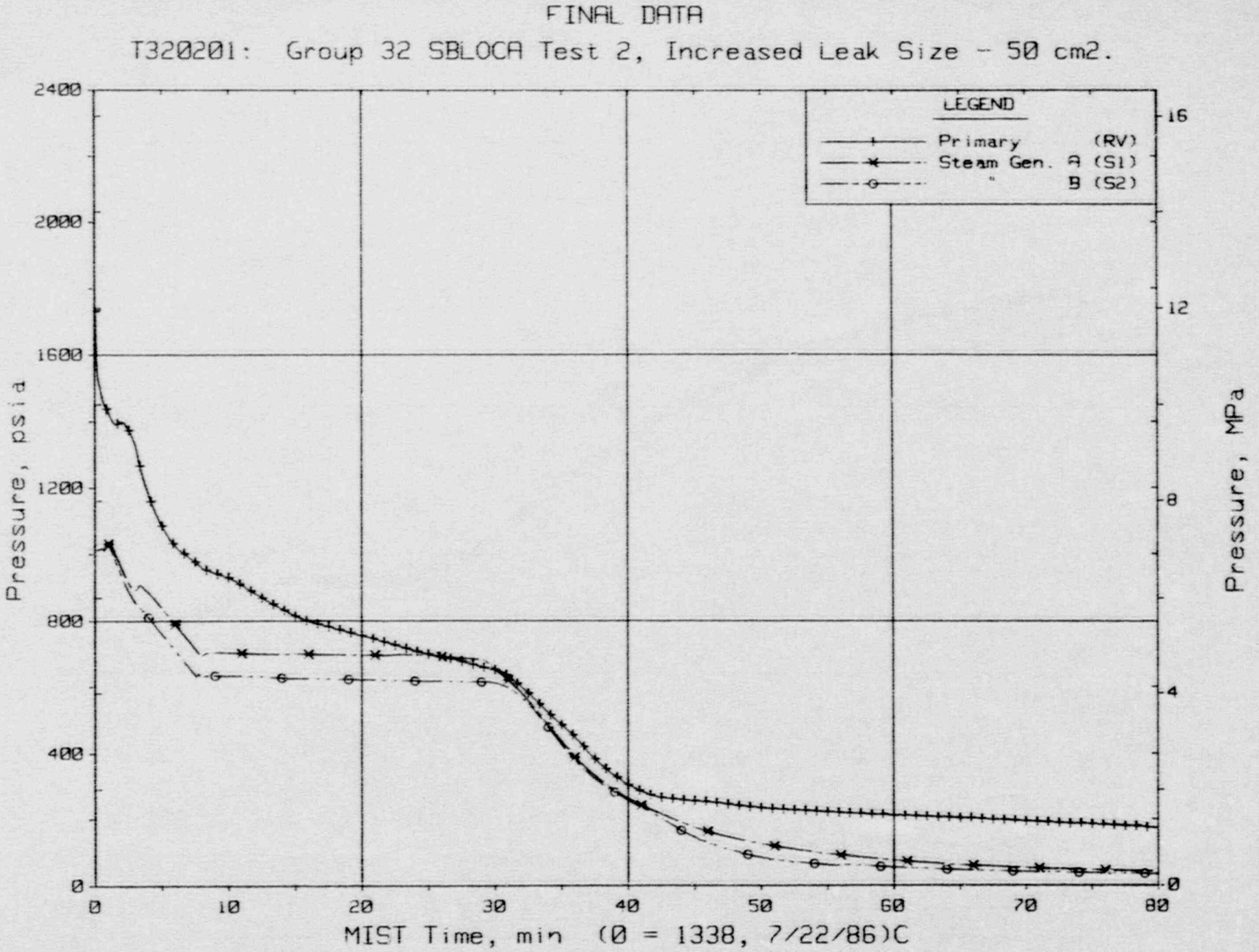

Figure 5.3.11. Primary and Secondary System Pressures (GP01s)

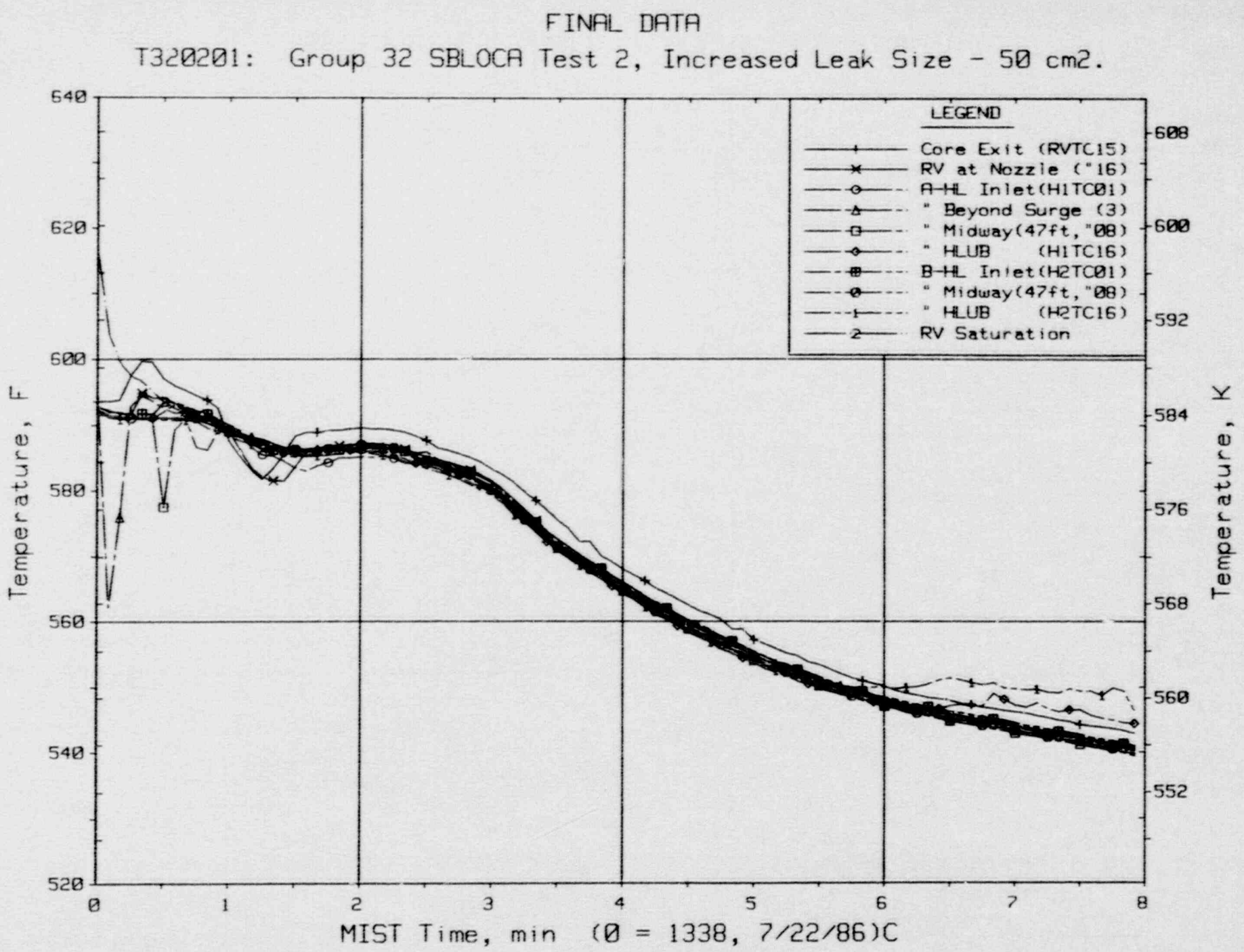

Figure 5.3.12. Composite Core Exit and Hot Leg Fluid Temperatures

Thu Jul 14 12:33:56 1988

PRKT1

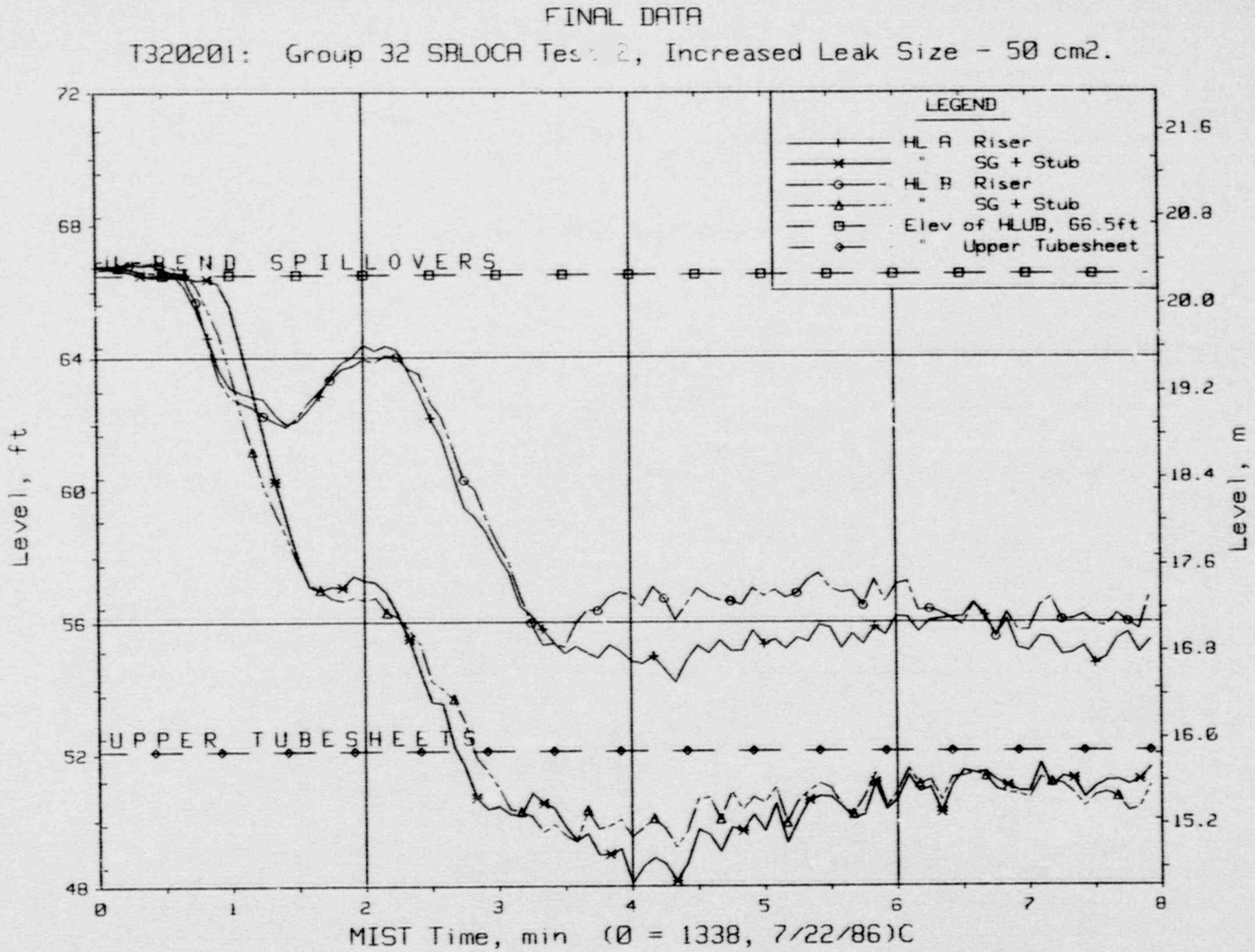

Figure 5.3.13. Hot Leg Riser and Stub Collapsed Liquid Levels

Mon Jul 11 12:46:12 1988

HLLV1

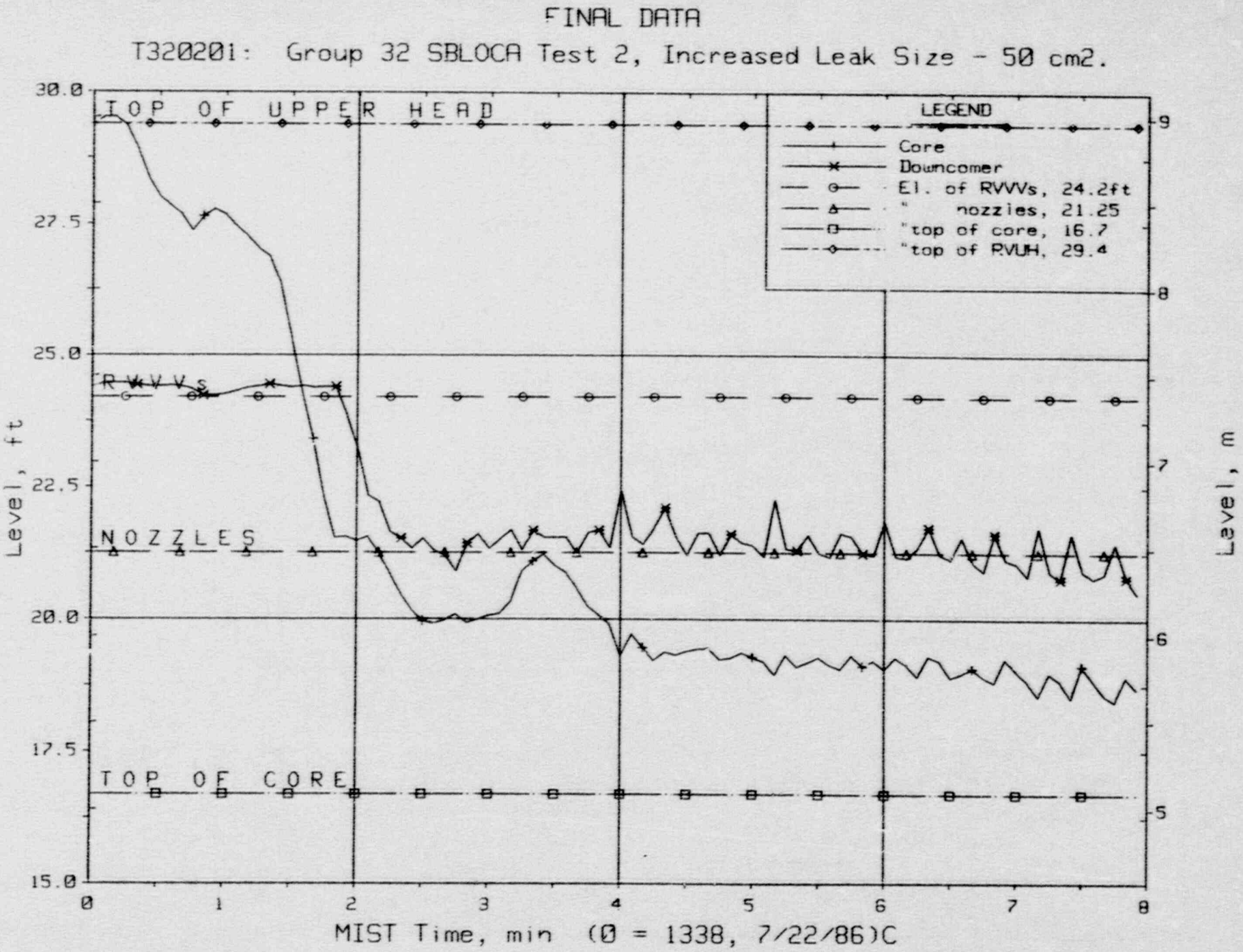

Figure 5.3.14. Core-Region Collapsed Liquid Levels

Mon Jul 11 12:49:01 1988

COLV1

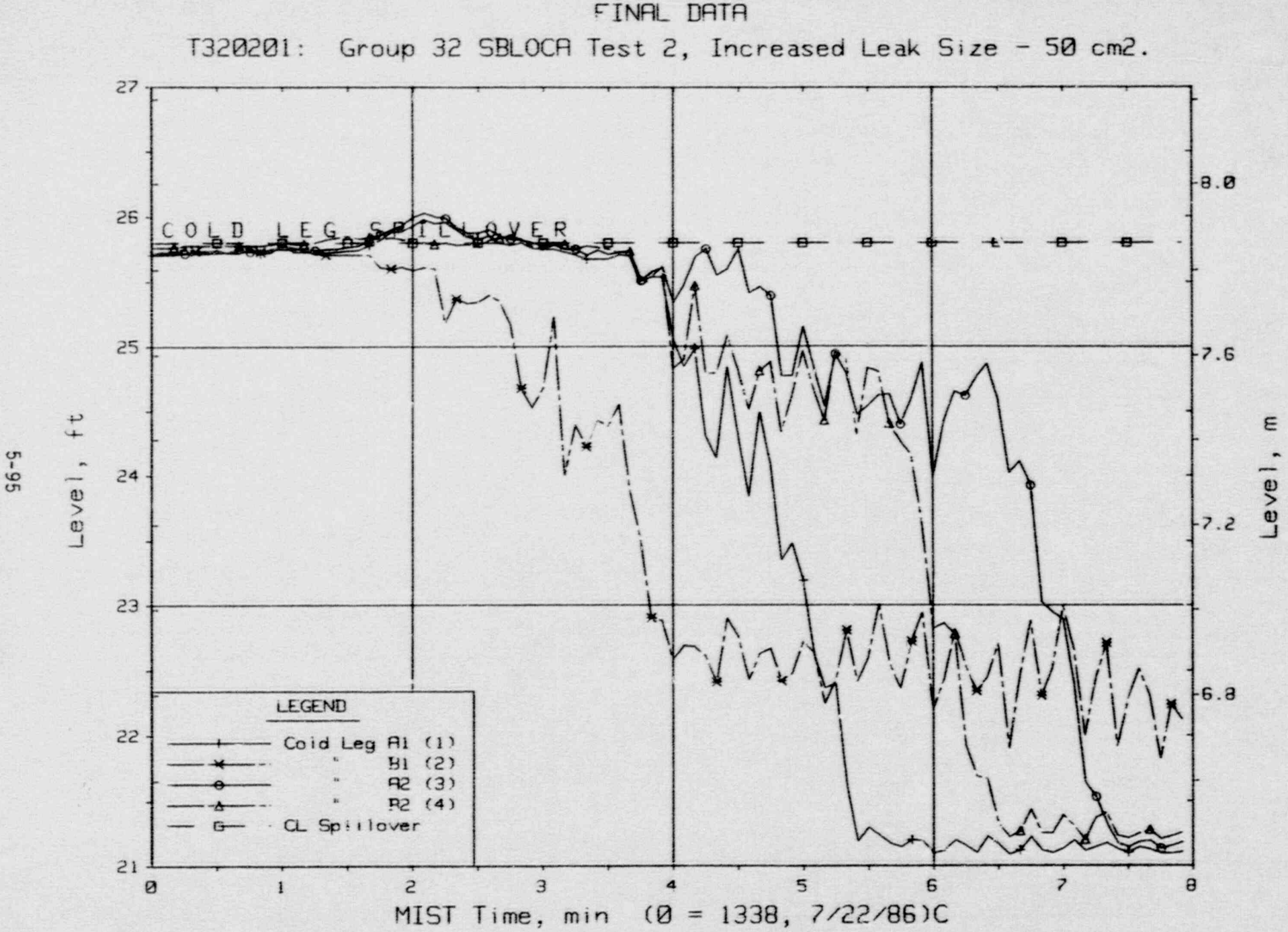

Figure 5.3.15. Cold Leg Discharge Collapsed Liquid Levels

Mon Jul 11 12:51:28 1988

CLLV5

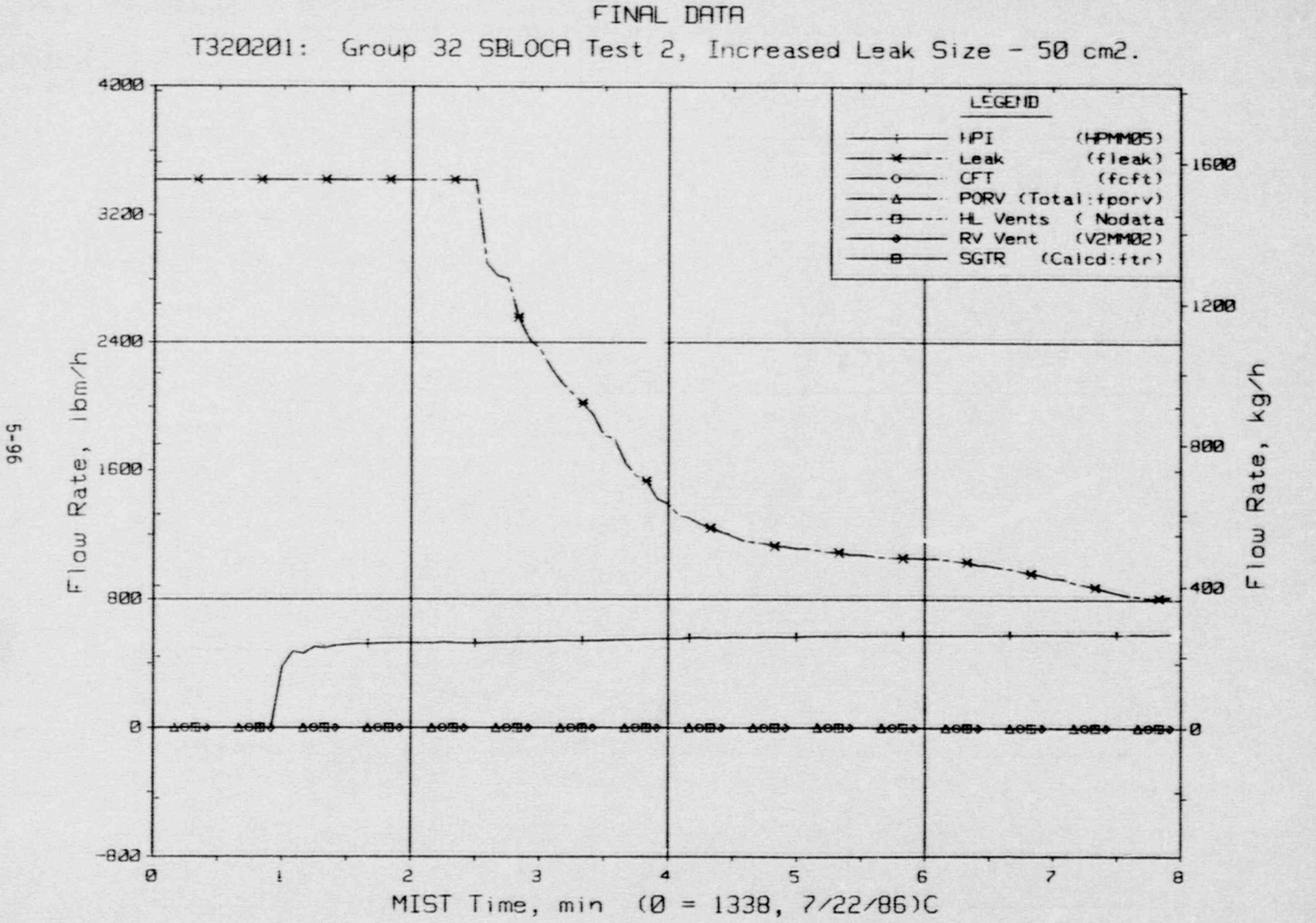

Figure 5.3.16. Primary System Boundary Flow Rates

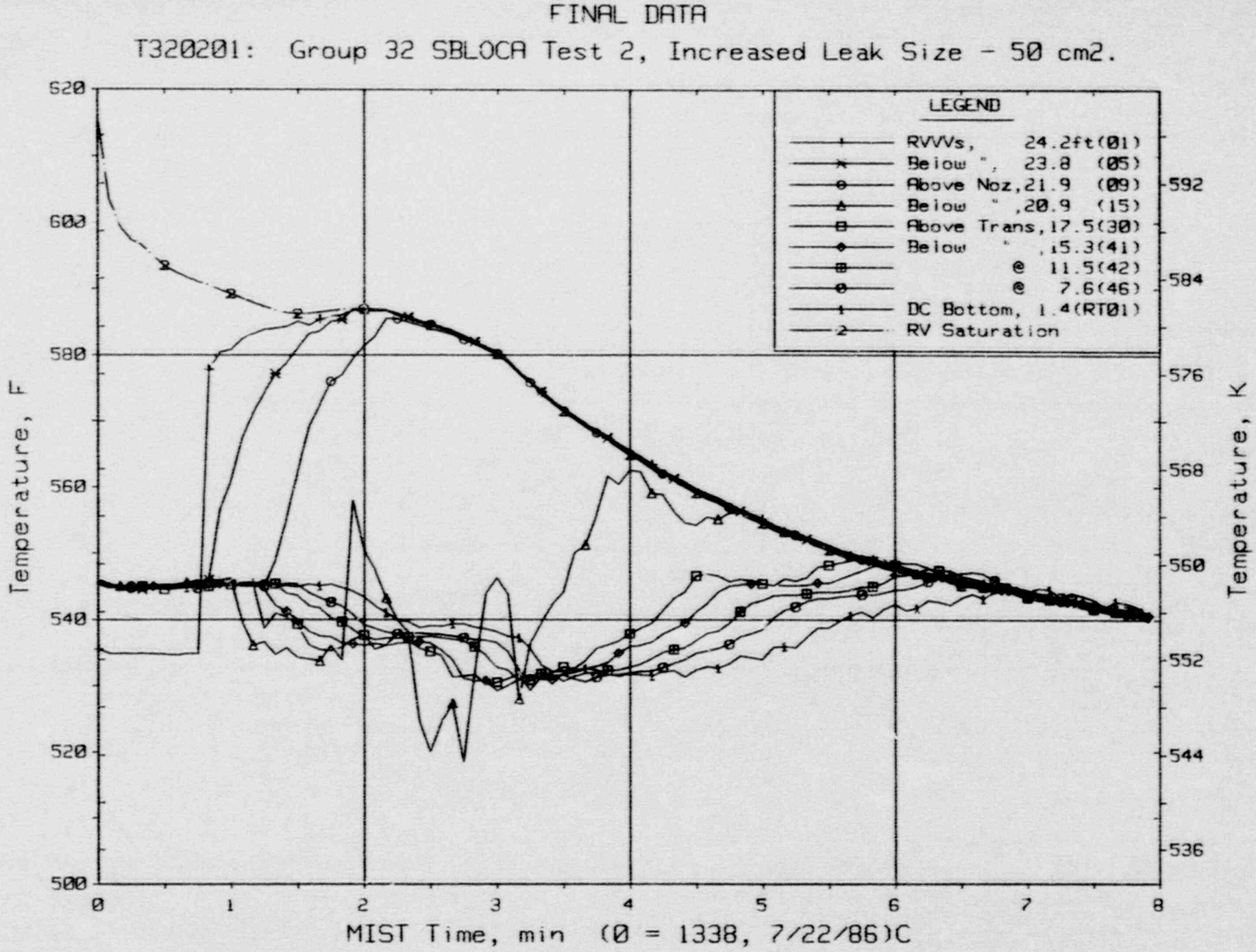

Figure 5.3.17. Downcomer Fluid Temperatures (Quadrant A1, DCTCs)

Mon Jul 11 12:56:47 1988

DCTC6

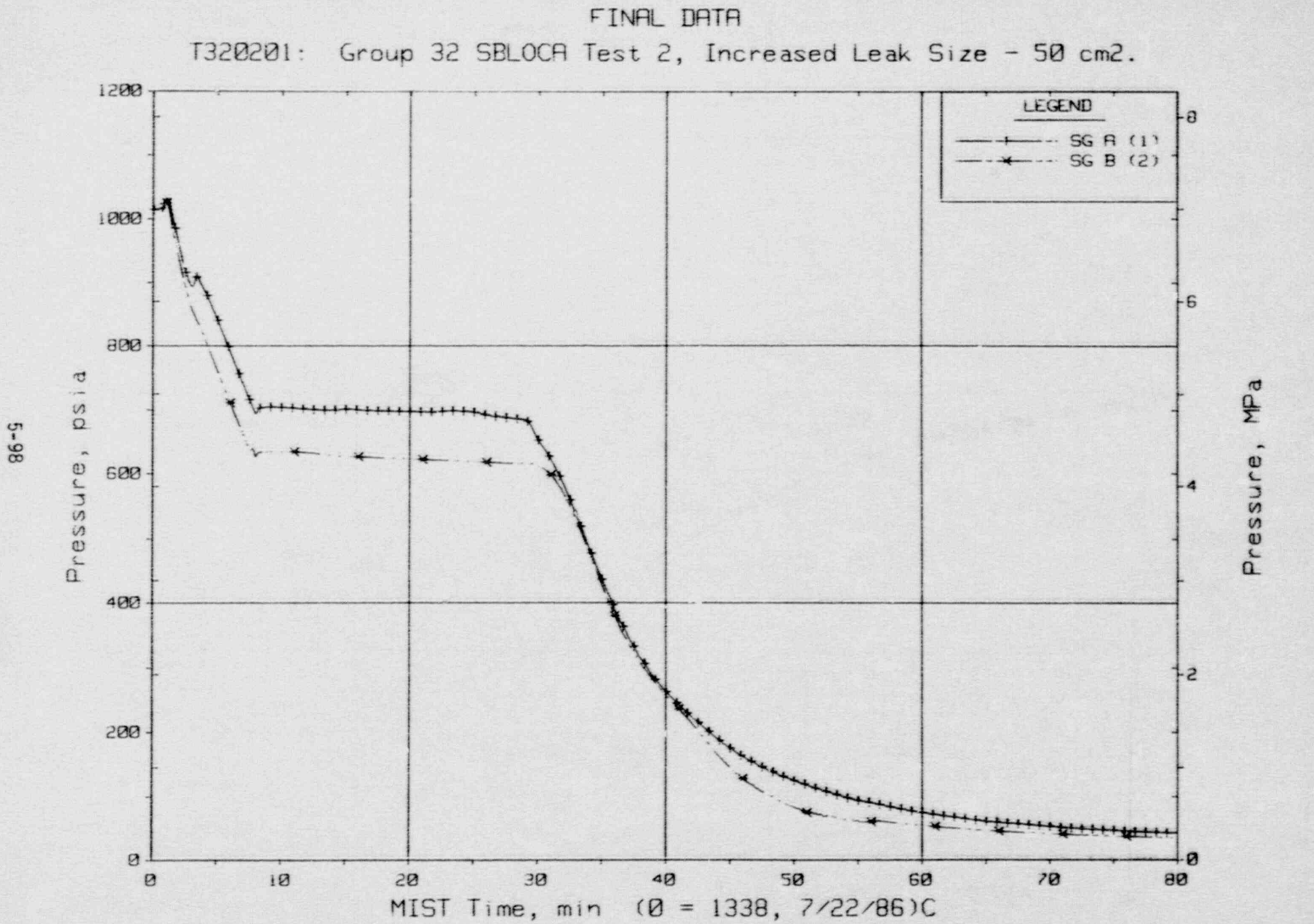

Figure 5.3.18. Steam Generator Secondary Pressures

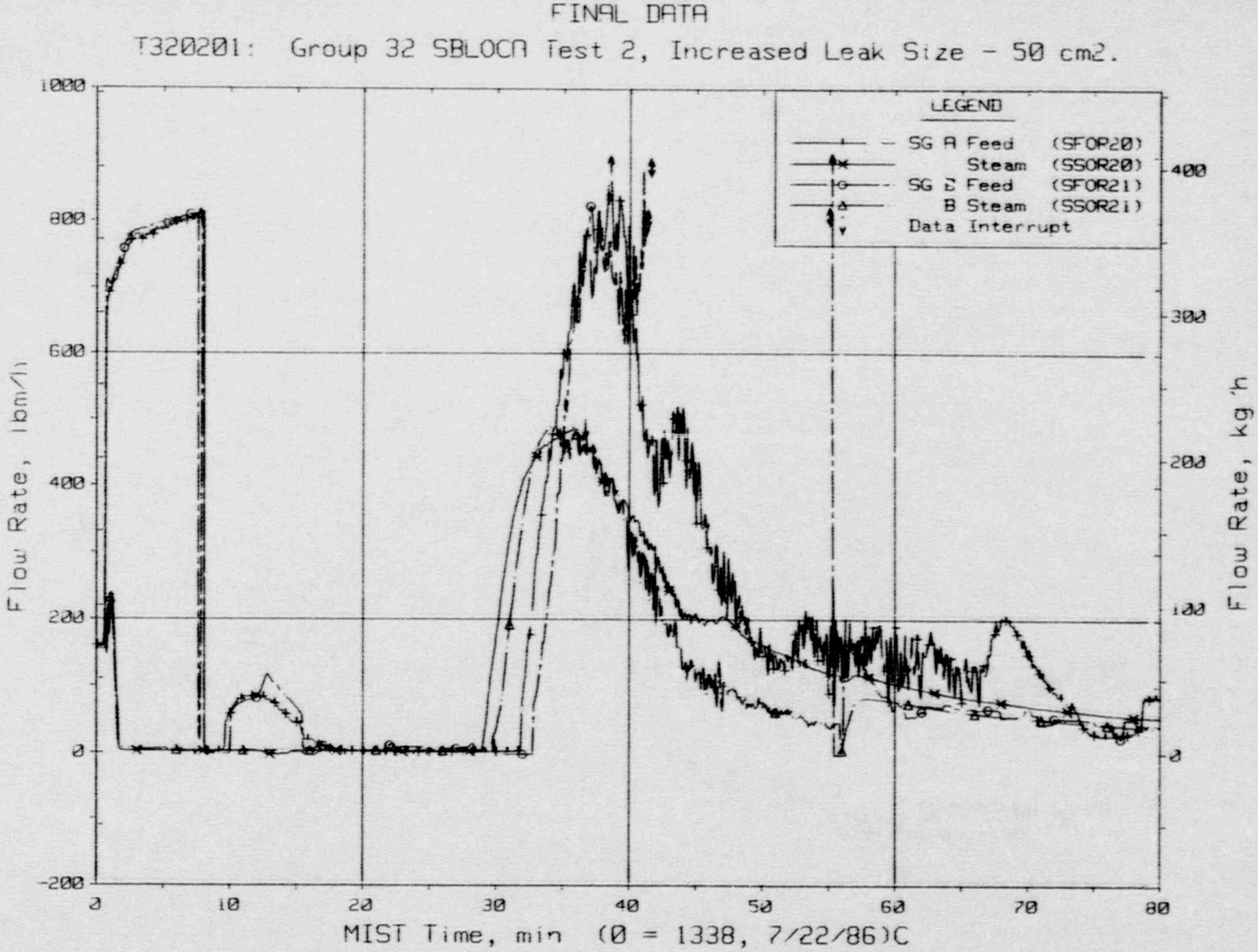

Figure 5.3.19. Secondary System Flow Rates

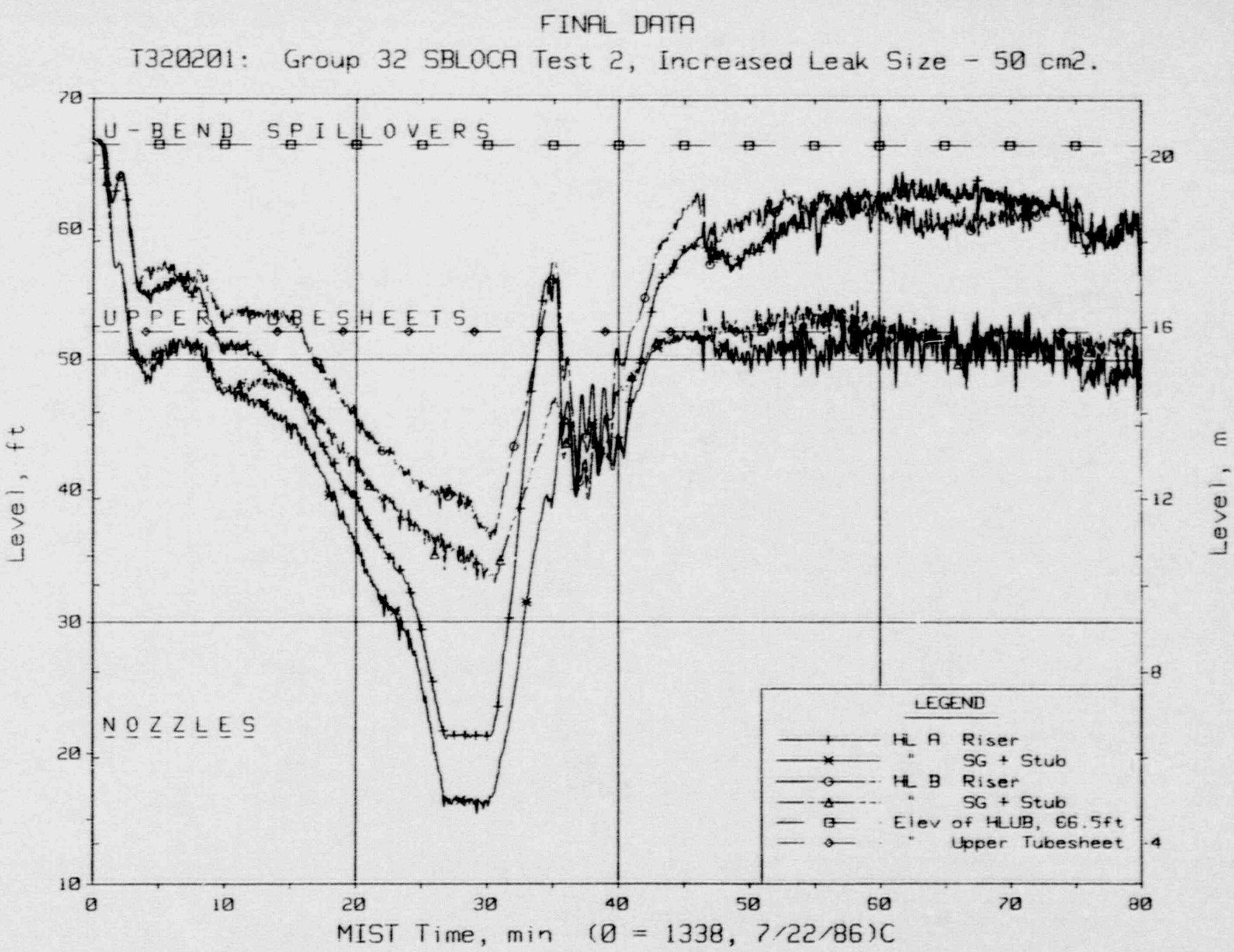

Figure 5.3.20. Hot Leg Riser and Stub Collapsed Liquid Levels

Tue Oct 18 12:19:24 1988

HLLV1

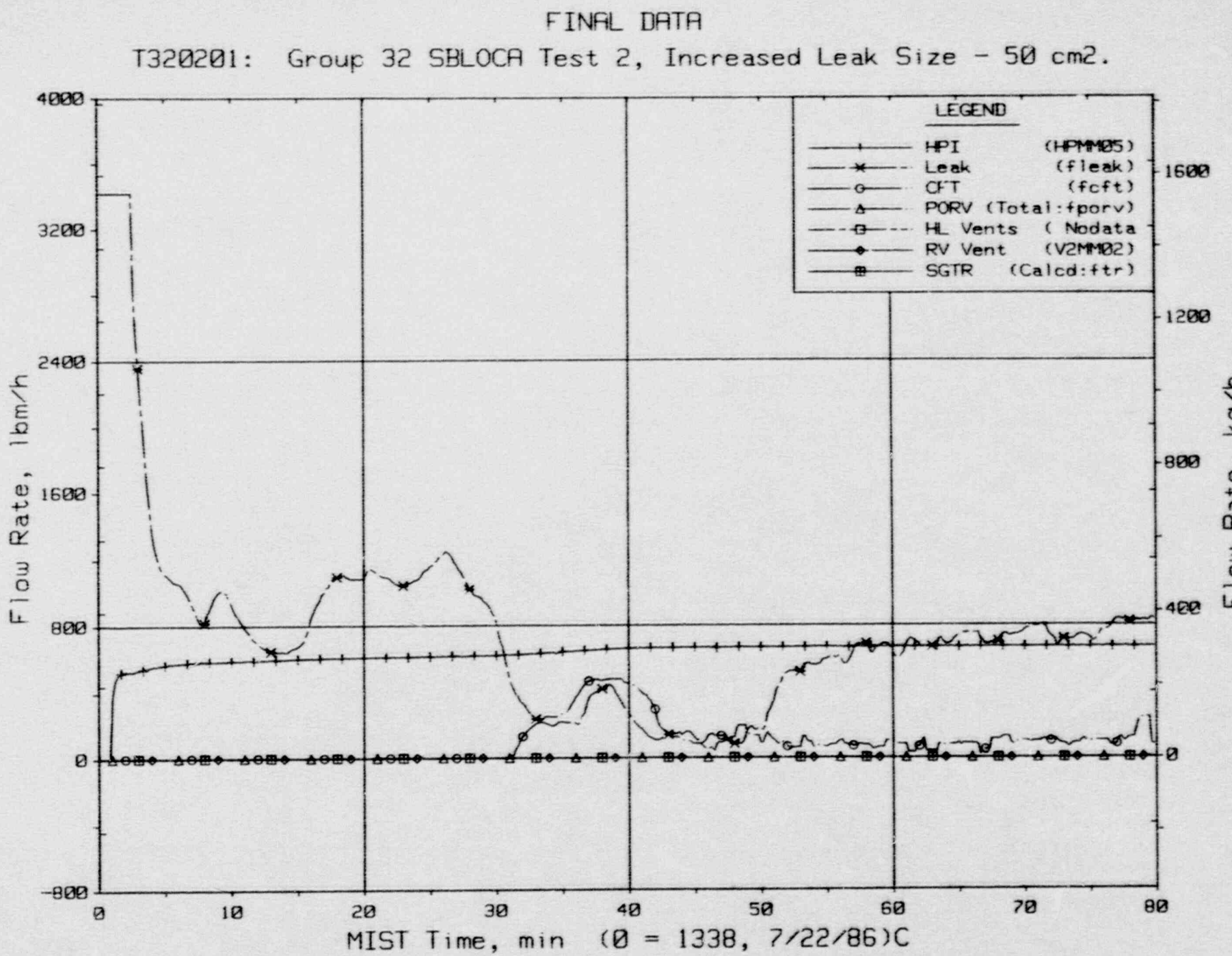

Figure 5.3.21. Primary System Boundary Flow Rates

Thu Jul 14 12:48:18 1988

PRFL3

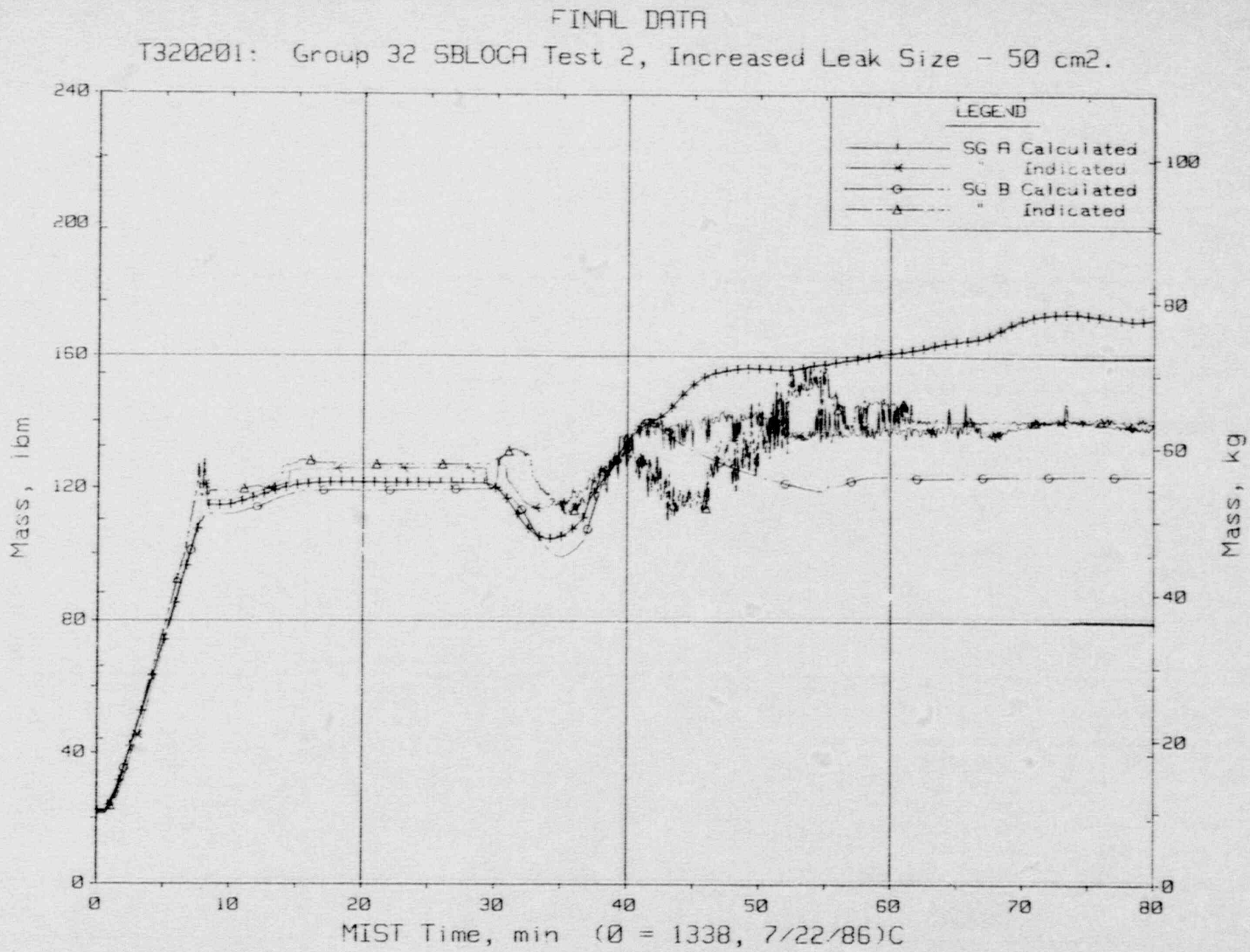

Figure 5.3.22. Steam Generator Secondary Mass Balances

Mon Jul 11 11:55:05 1988

SGML1

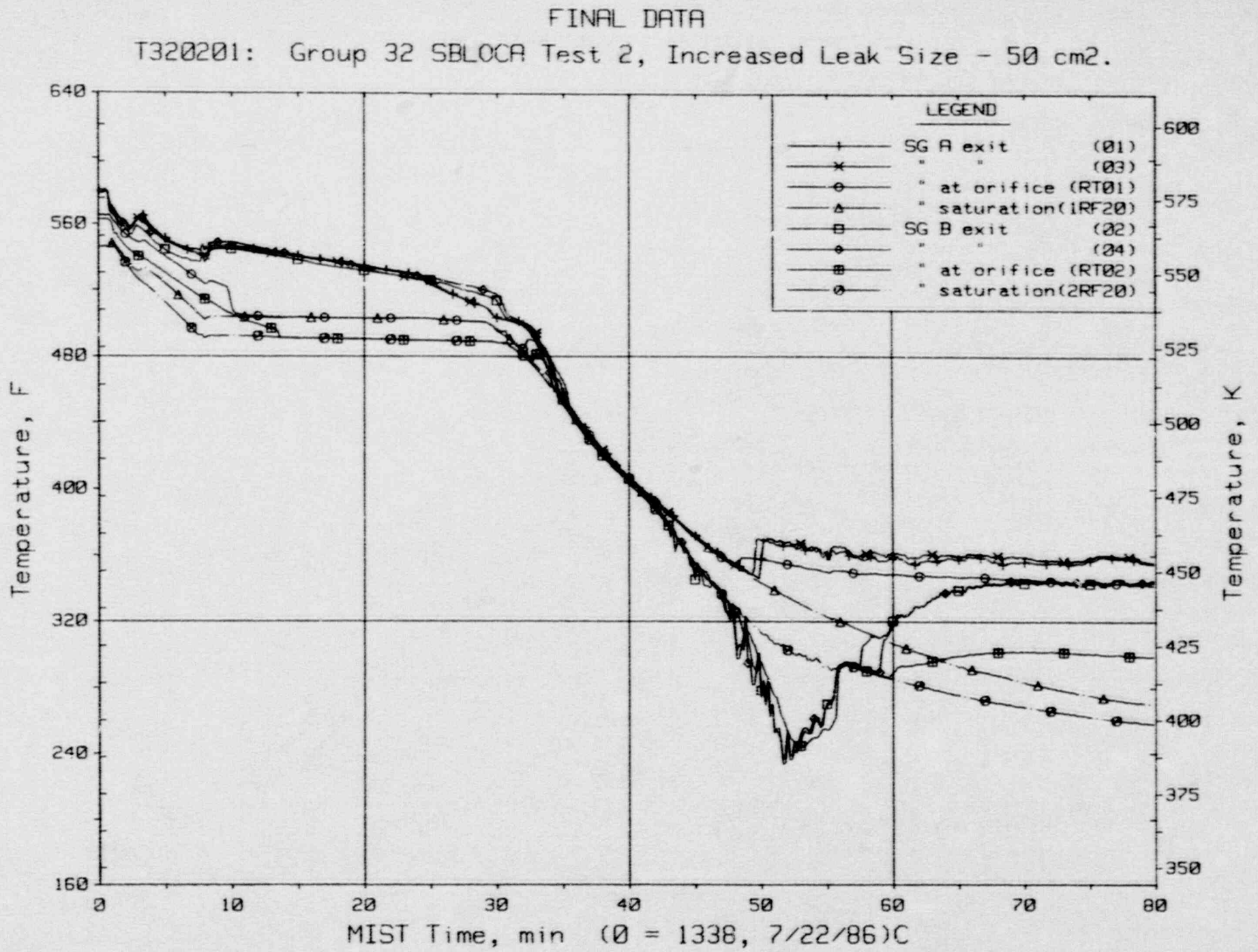

Figure 5.3.23. Steam Generator Steam Outlet Temperatures (SSTCs)

Thu Jul 14 12:53:41 1988

SGRT2

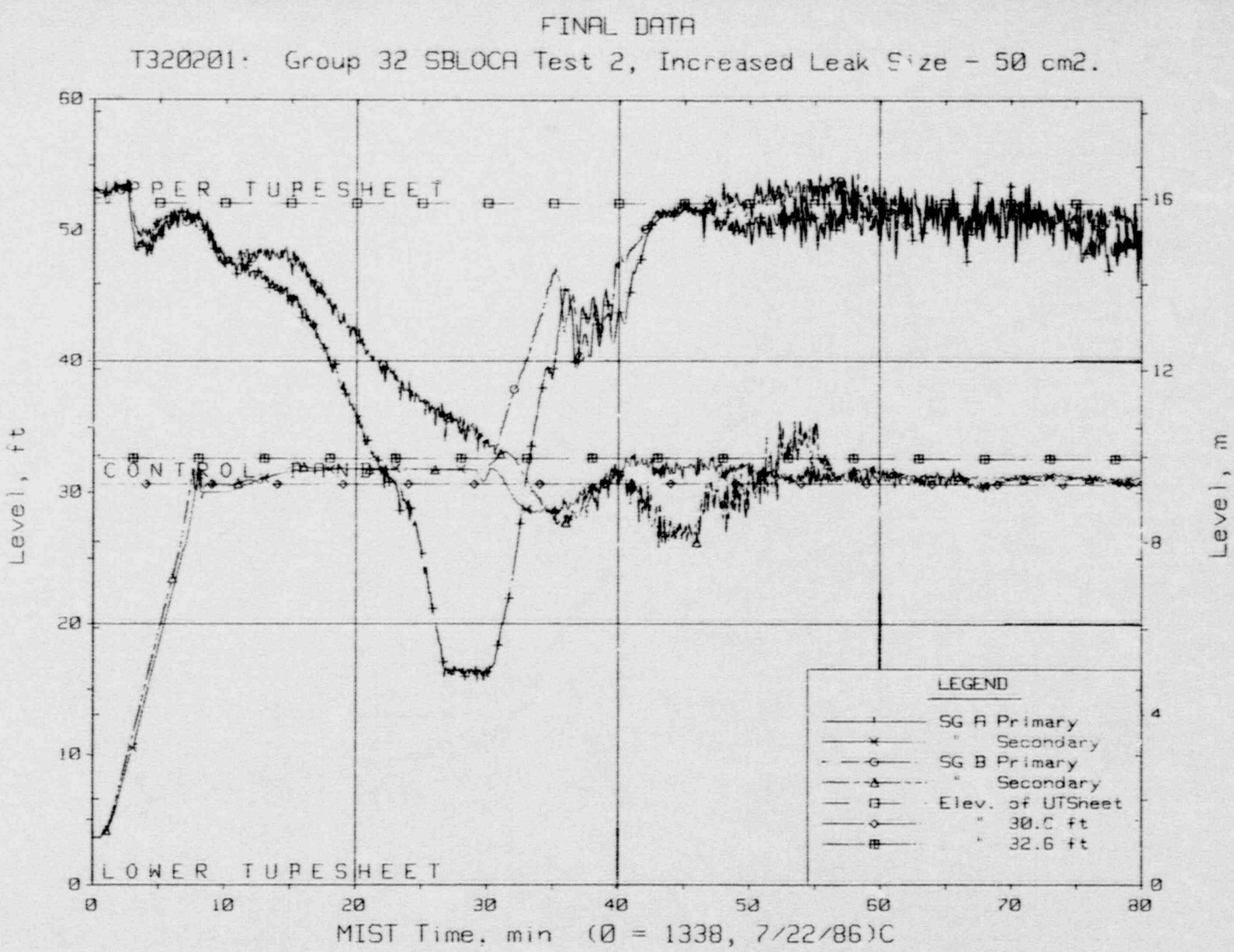

Figure 5.3.24. Steam Generator Collapsed Liquid Levels

Mon Jul 11 12:00:32 1988

SGLV2

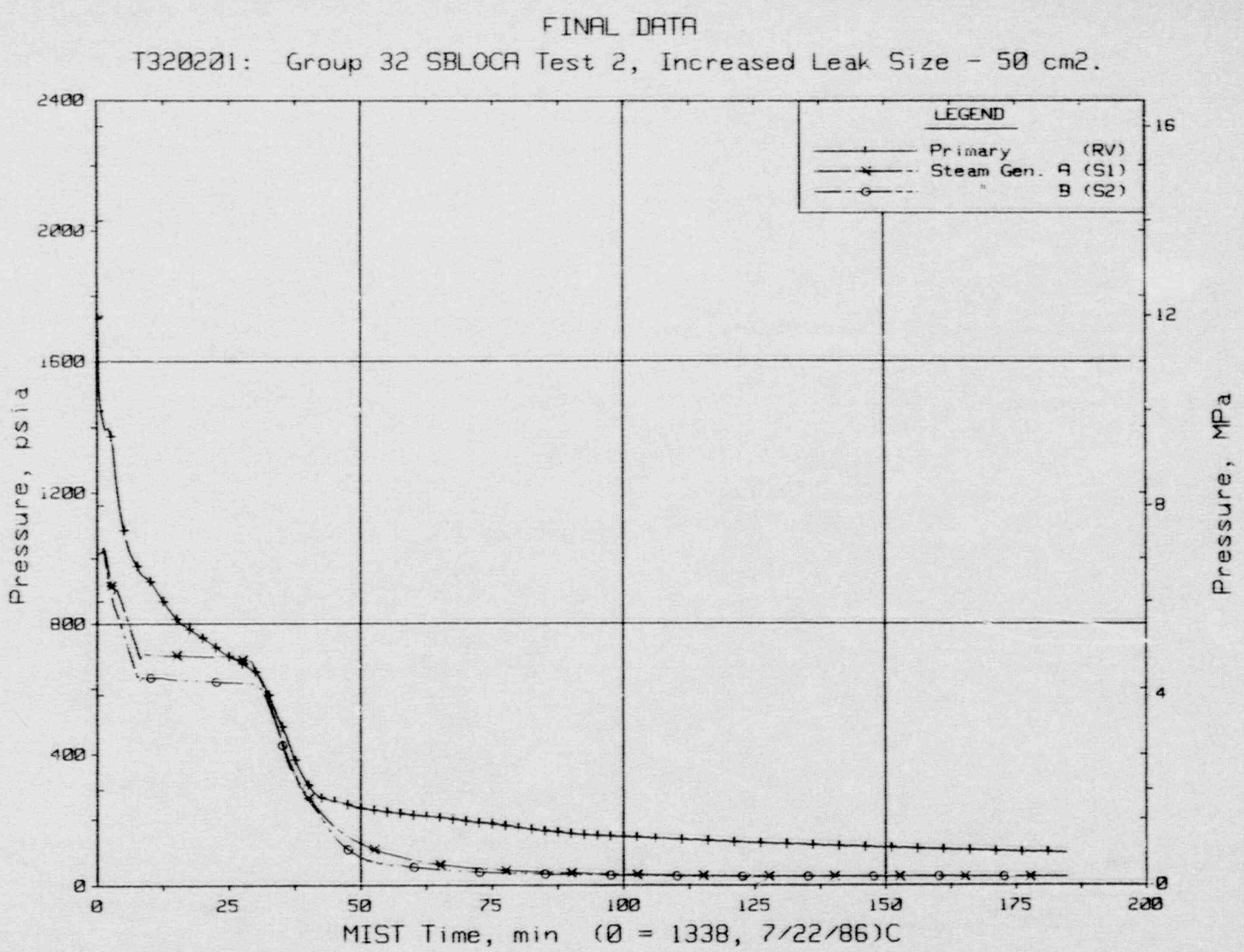

Figure 5.3.25. Primary and Secondary System Pressures

Mon Jul 11 13:32:37 1988

PSGP1

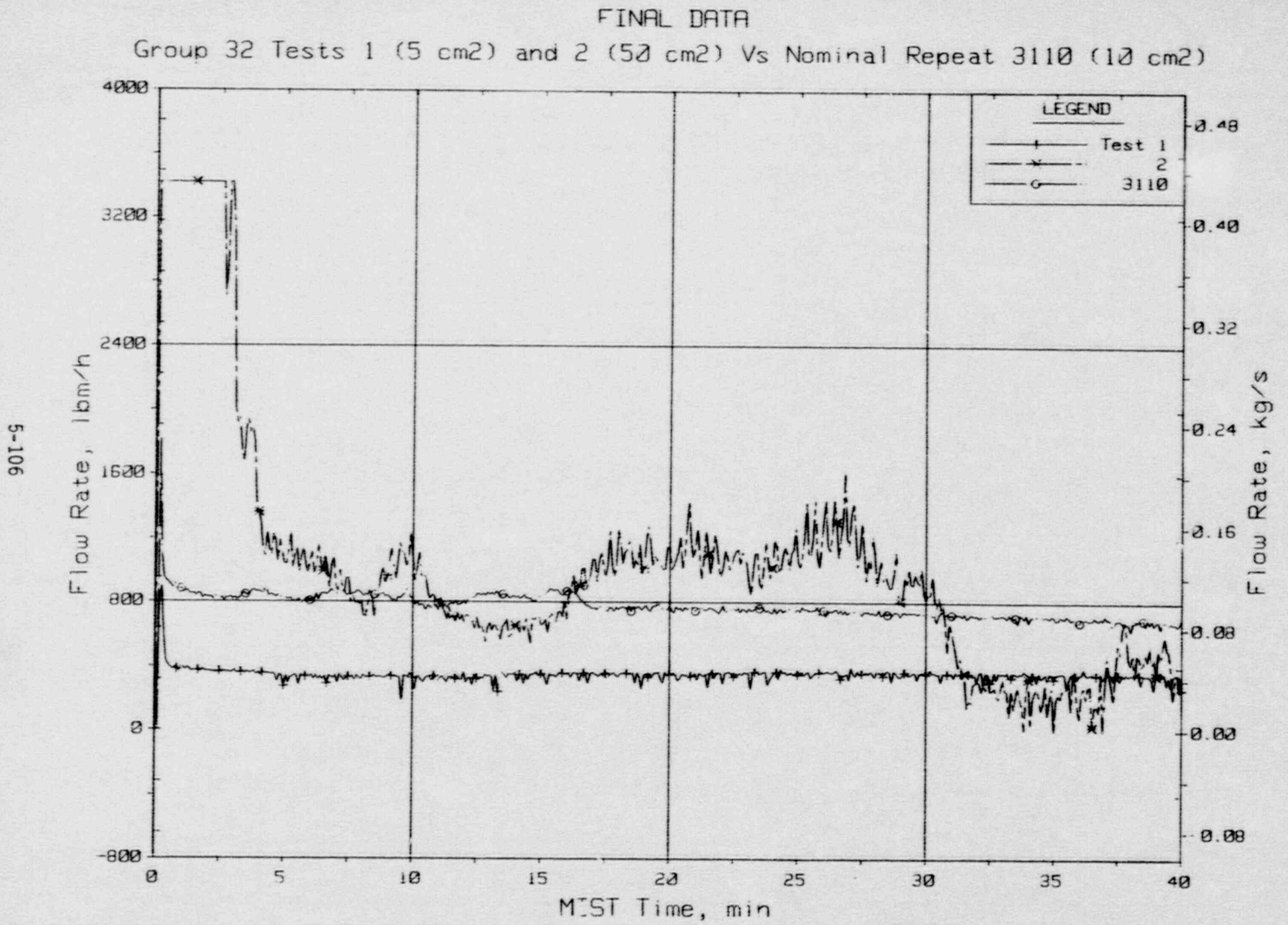

5-106

Figure 5.3.26. Leak Flow Rates

Mon Jul 11 13:48:01 1988

12PRFL3

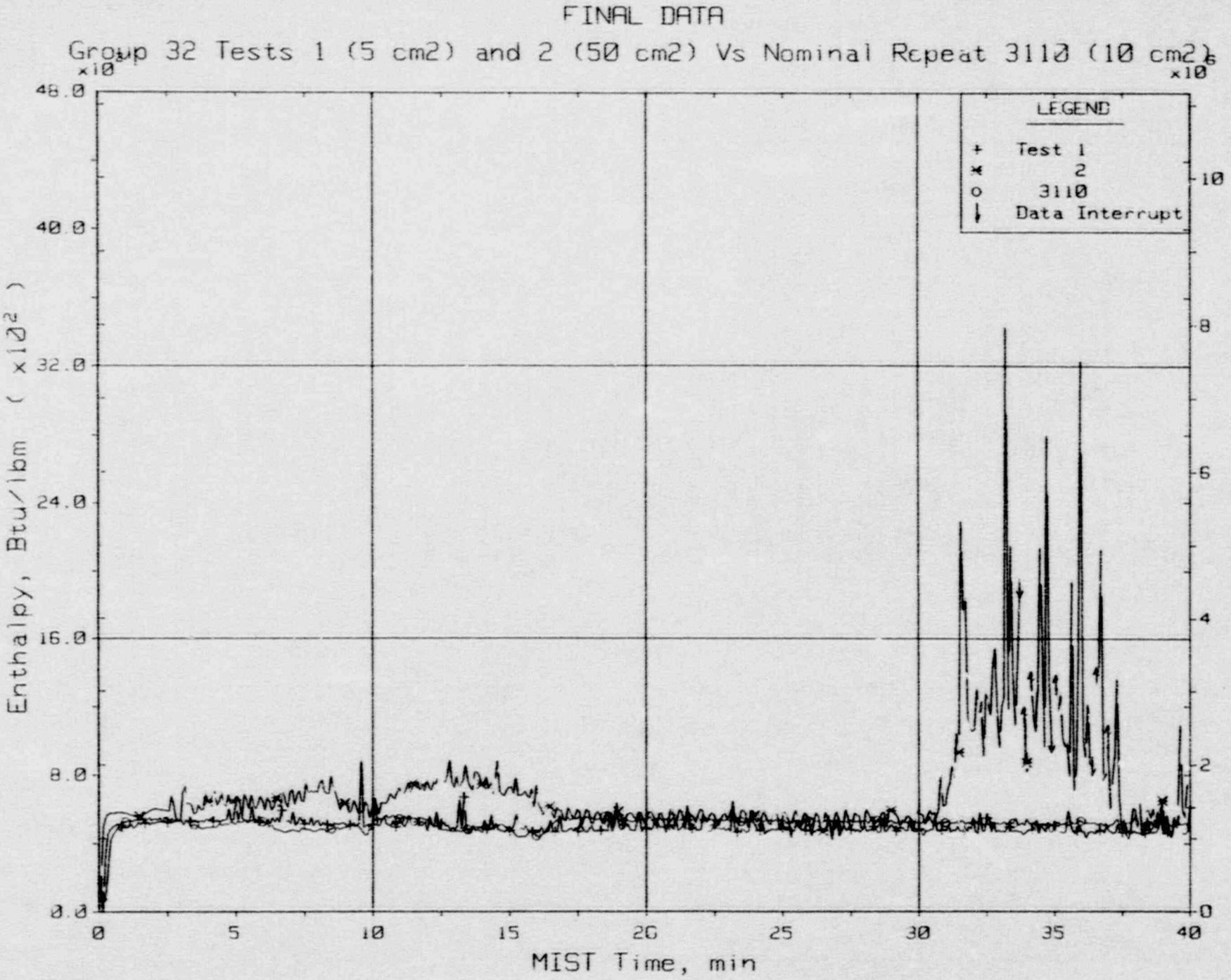

Figure 5.3.27. Single-Phase Leak Fluid Enthalpy

Mon Jul 11 13:50:28 1988

12V1EN1

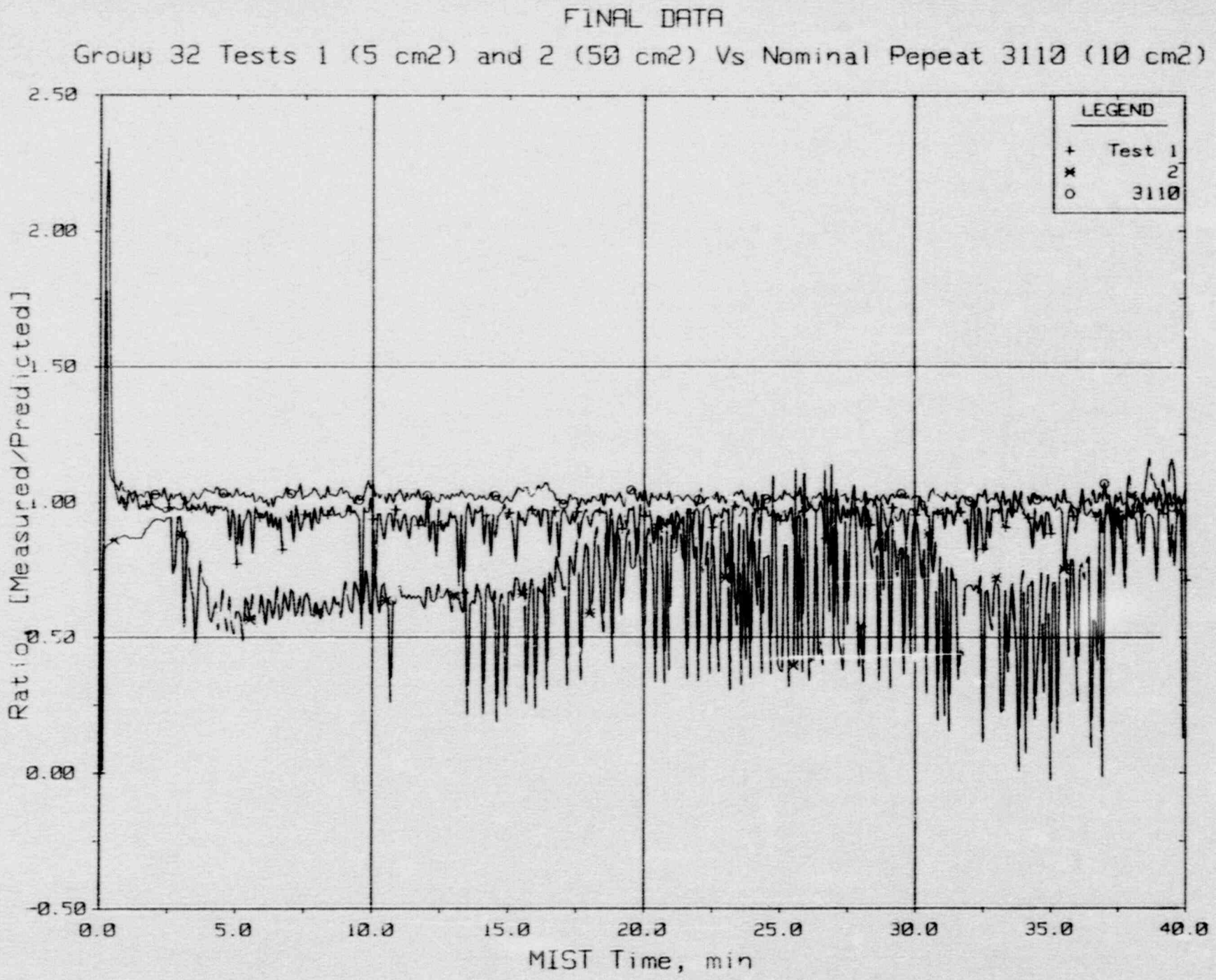

Figure 5.3.28. Modified Leak Flow Rate Ratios

Mon Jul 11 13:53:02 1988

12CRPA2

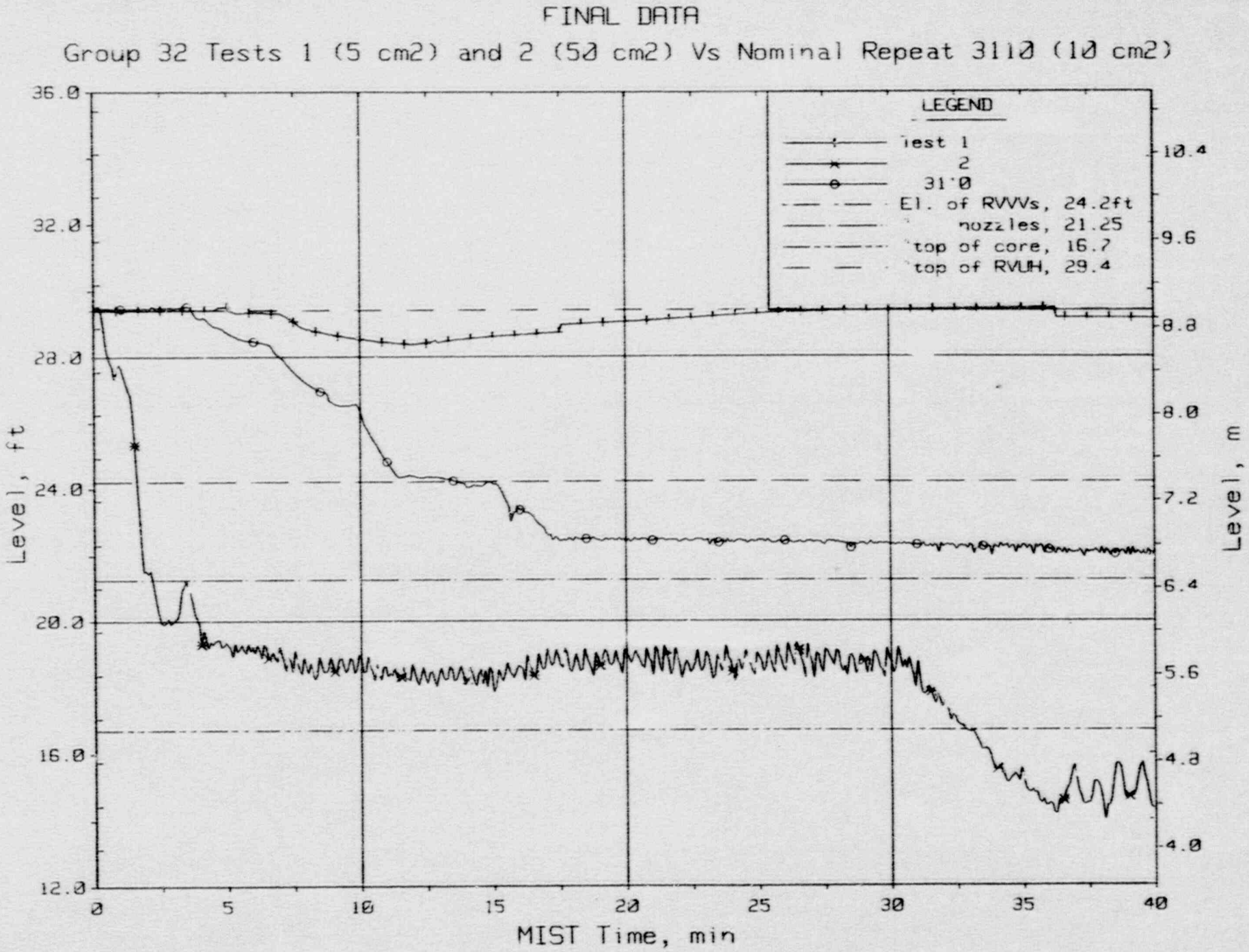

Figure 5.3.29. Reactor Vessel Collapsed Liquid Levels (RVLV20)

Mon Jul 11 13:56:10 1988

12COLV1

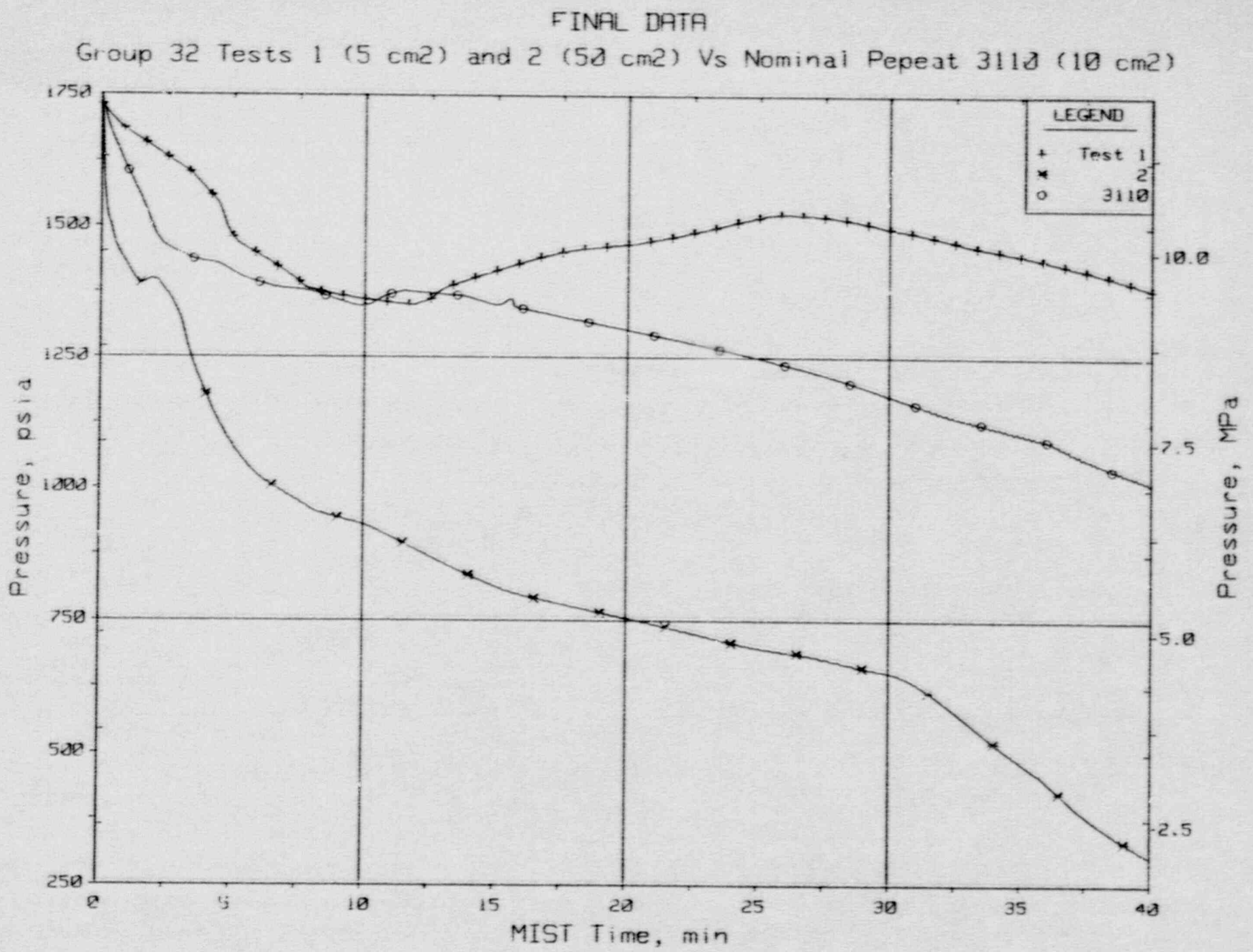

Figure 3.3.30. Reactor Vessel Pressure

Mon Jul 11 13:58:42 1988

12RVGP1

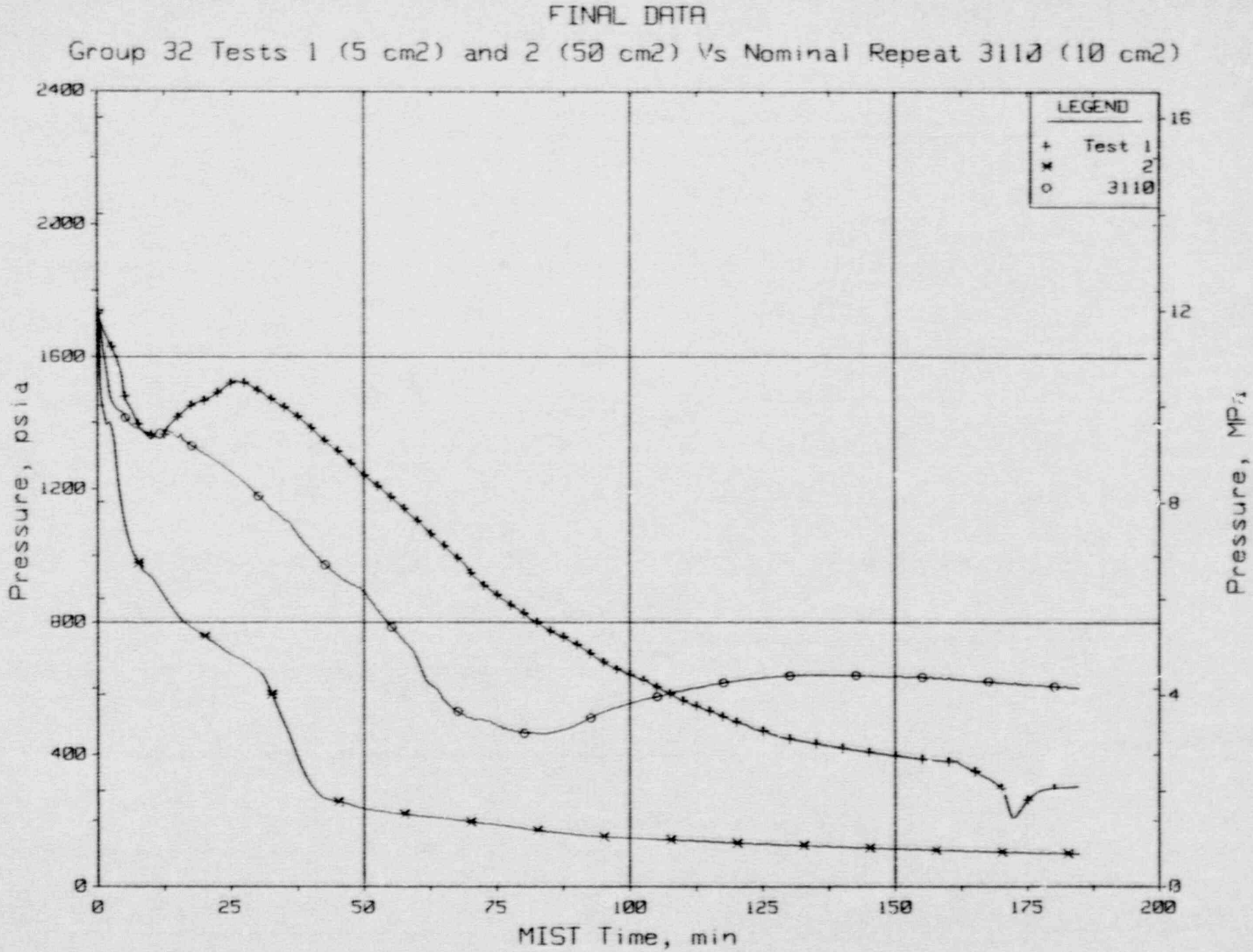

Figure 5.3.31. Reactor Vessel Pressure

Mon Jul 11 16:24:24 1988

12RVGP1

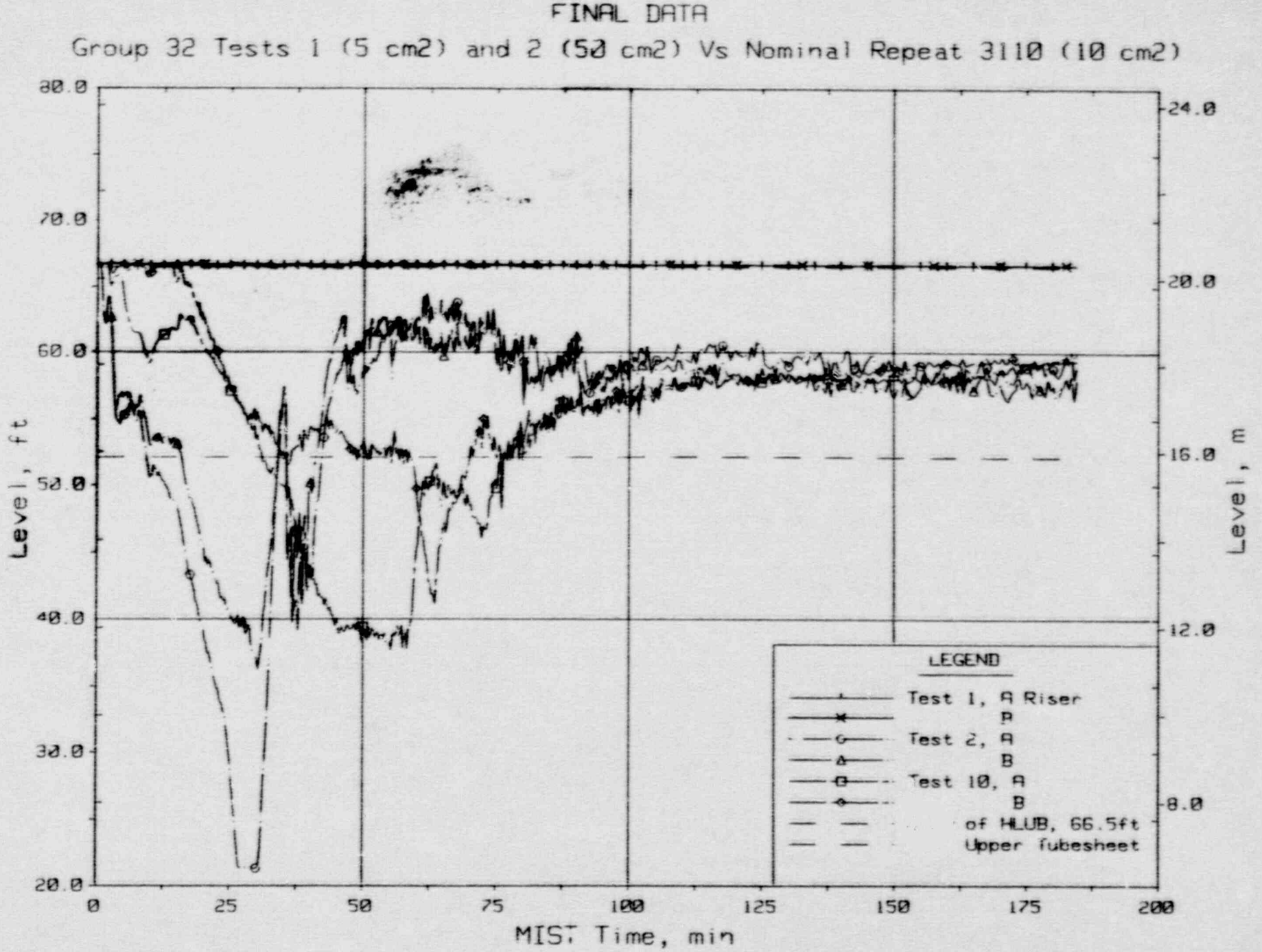

Figure 5.3.32. Hot Leg Riser Collapsed Liquid Levels

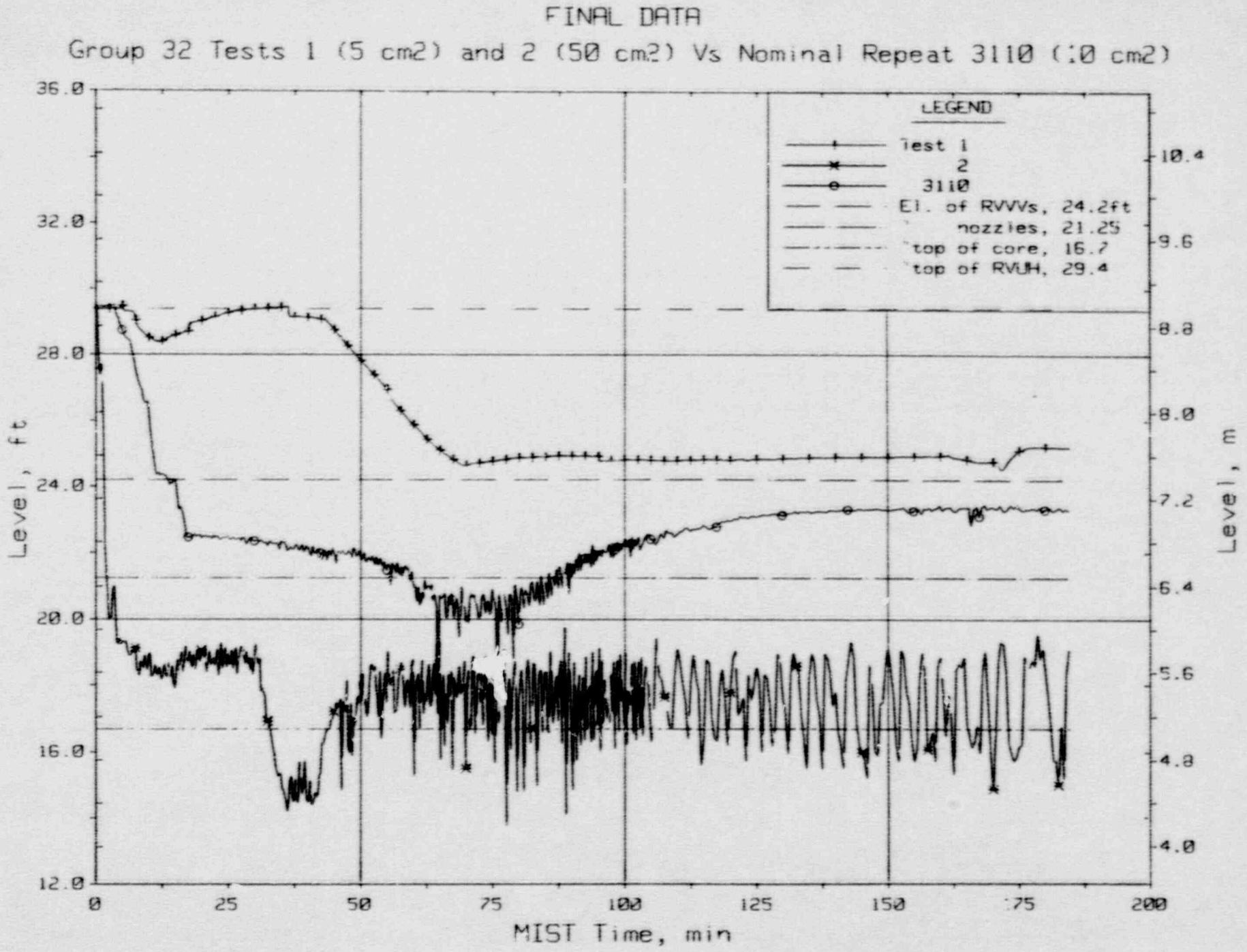

Figure 5.3.33. Reactor Vessel Collapsed Liquid Level (RVLV20)

Mon Jul 11 16:34:01 1988

12COLV1

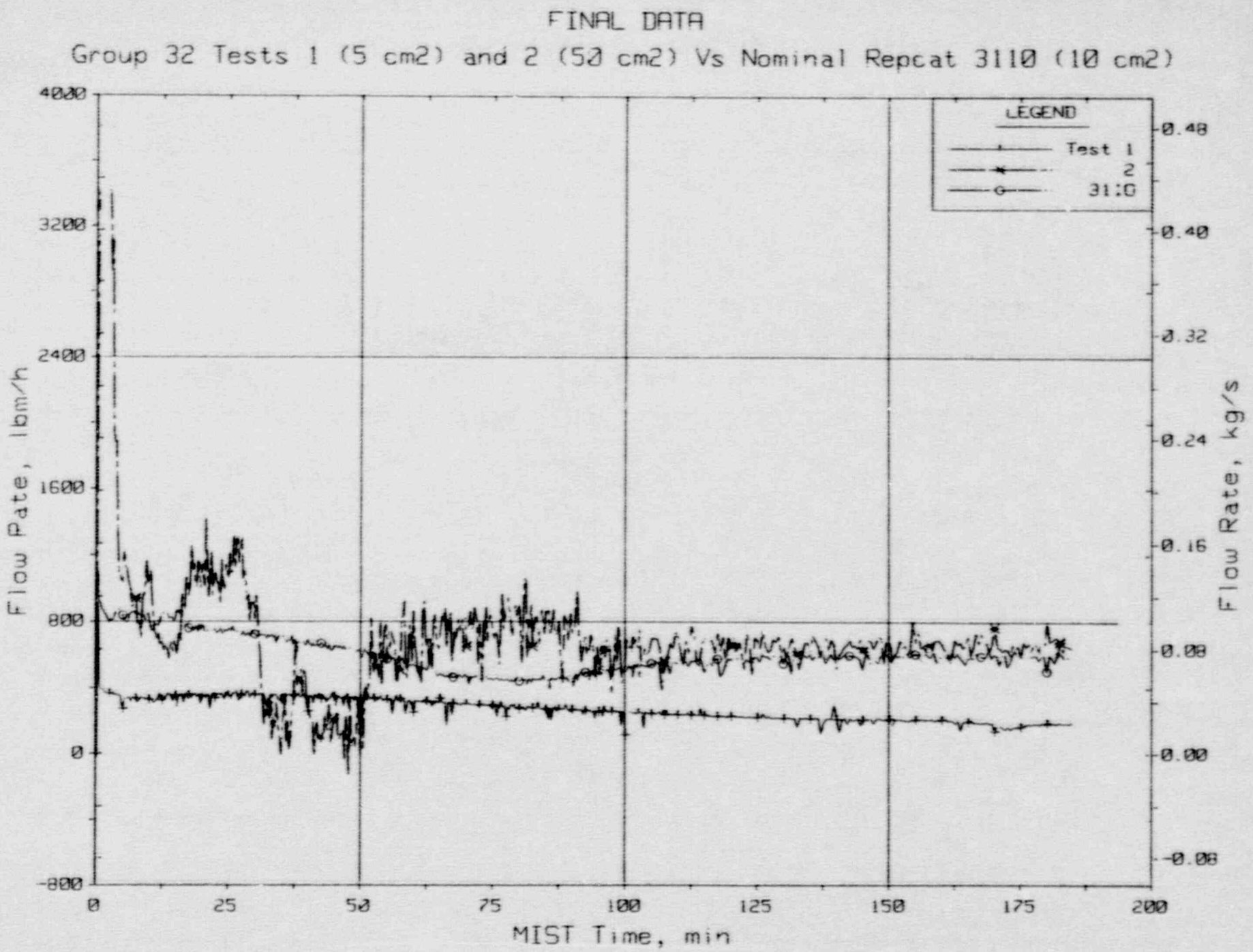

Figure 5.3.34. Leak Flow Rates

Mon Jul 11 16:27:14 1988

12PRFL3

5.4. Varied Leak Location, Tests 3 and 4

The nominally employed leak location was at the bottom of the cold leg B1 discharge piping. A cold leg B1 suction leak was employed in Test 3 (320302), and a PORV break was used in Test 4 (3204AA). These tests are described separately in sections 5.4.1 and 5.4.2, and compared in section 5.4.3.

5.4.1. Cold Leg Suction Leak, Test 3

A cold leg B1 suction leak was used in Test 3 (320302). The initial events following actuation of the cold leg suction leak were similar to those of tests having a cold leg discharge leak location. The loop fluid saturated at 2.4 minutes, causing the primary system depressurization to slow at 1450 psia. The second set of test-initiating actions was taken within seconds of primary saturation. Whereas with a discharge leak site the leak fluid temperature generally cooled due to the influence of HPI, the leak fluid temperature in Test 3 varied only slowly from the steam generator primary outlet temperature of 550F (Figure 5.4.1). The leak fluid subcooling was thereby kept small, and the net primary system mass loss early in the transient was about 240 lbm/h.

The cold leg B1 suction leak site fluid was apparently transported from the downcomer through inter-cold leg flow (backflow in B1 and forward flow in the adjacent B2 cold leg, Figure 5.4.2). The steam generator B primary outlet fluid temperature measurement at -3.2 ft was not responsive to the cold leg B1 (and B2) fluid temperature variations, indicating that the inter-cold leg flow generally did not penetrate into the steam generator. The uppermost thermocouple of the cold leg B1 nozzle rake was inoperative, therefore an estimate of the fluid temperature variation across the B1 discharge piping was hindered. The three available thermocouples in the cold leg B1 nozzle rake indicated a maximum temperature, just above the pipe centerline, which was approximately equal to the downcomer fluid temperature, and a minimum temperature at 1/4 of the pipe radius above the bottom of the pipe, which was as much as 55F less than the maximum temperature (Figure 5.4.3). Thus, it would appear that, even though the cold leg suction leak flow rate exceeded the total HPI flow rate during almost the first hour of the transient, liquid-liquid counterflow was active in the broken cold leg. HPI-cooled fluid was flowing toward the downcomer, in the lower portion of the cold leg

cross section, while relatively warm fluid from the downcomer was backflowing up the cold leg (B1). The leak fluid temperature was thus somewhat warmer than the mixed-mean temperature (obtained by weighing the cold leg B1 HPI and the upper downcomer fluid temperatures by their respective flow rate fractions at the leak site).

The core region collapsed liquid level began to evidence voiding at 4.7 minutes (Figure 5.4.4). The loop A (interrupted) steam generator primary level approached the steam generator upper tubesheet (Figure 5.4.5) while the secondary side was being refilled, between 8 and 9 minutes. The primary system depressurized slightly (Figure 5.4.6). The core exit fluid saturated at 9.3 minutes. At 9.5 minutes, feed was terminated upon completion of the secondary refill. Feed was reactivated to steam generator A at 11.8 minutes to maintain level. The primary system pressure response evidenced little heat transfer. The core region collapsed liquid level stabilized near the elevation of the RVVVs at 12 minutes, then the downcomer level descended toward the nozzle elevation (Figure 5.4.4). Between 14 and 17 minutes, loop B reactivated, steam generator B repressurized to the control point, and steam generator B steaming and feeding were reinitiated. The attendant increase of primary flow briefly subcooled the core, causing the RVVVs, which had been open, to close and to cycle. The primary system depressurized only slightly. At 16 minutes, the downcomer level stabilized at the nozzle elevation. Then, the loop B hot leg level receded from the spillover elevation (Figure 5.4.5) and steam generator B activity ceased. The core region level receded from the vent valve elevation and the RVVVs reopened. The primary system began to slowly depressurize from 1350 psia (Figure 5.4.6).

The steam generator A and B primary levels reached the steam generators at 22.5 and 29.5 minutes, but the steam generator feed and steam systems remained inactive. At 40 minutes, steam generator B began to be steamed. Feed was introduced at 43.5 minutes (Figure 5.4.7) and the resulting BCM enhanced the rate of primary system depressurization (from 1040 psia). At 58 minutes, the steam generator B secondary had been depressurized sufficiently to equate the secondary pressures, the steam generator A secondary became active, and the primary system depressurization was again enhanced (Figure

5.4.6). Beyond 1 hour, the steam generators were alternately active. The HPI flow rate first exceeded the leak flow rate at 55 minutes. The leak site fluid remained sufficiently coupled to the downcomer fluid so that the leak site fluid approached saturation during the primary system depressurization near 1 hour (Figure 5.4.1). The HPI-leak flow rate excess thereby increased, reaching some 200 lbm/h or 50% of the current leak flow rate by 70 minutes. The primary fluid mass was also increased by CFT activity near 80 minutes. Thus, the steam generator primary levels in both loops were elevated above the upper tubesheets, the steam generator activity ceased, and the primary system repressurized, attaining 640 psia beyond 2 hours (Figure 5.4.8).

The PORV was manually opened at 195 minutes. This action was taken, as specified, with both steam generator primary levels above the upper tubesheets. The primary system immediately depressurized (from 610 psia), causing the leak flow rate to decrease and reducing the temperature difference between the core exit fluid and the secondary system saturation temperatures. The pressurizer insurge caused the hot legs to deplete (Figure 5.4.9). Thus, the steam generator activity beginning at 220 minutes caused the primary system to depressurize further, from 370 psia at 232 minutes (Figure 5.4.8). The CFT again became active. The PORV was maintained open for the duration of the test, which was terminated at 422 minutes. The combined leak plus PORV mass flow rate approximated the HPI flow rate. Thus, the steam generator primary levels remained near the upper tubesheets (Figure 5.4.9) and the primary system pressure remained fairly constant. The leak site fluid gradually cooled as the lower downcomer and core inlet fluid cooled. The core exit fluid remained saturated.

5.4.2. PORV Break, Test 4

A PORV break was used in Test 4 (3204AA). The PORV was manually opened at time zero and kept open for the duration of the test. The primary system depressurized at 180 psi/min from time zero (Figure 5.4.10), but the first indication of the PORV discharge flow rate was delayed until 1.3 minutes (Figure 5.4.11). The usual second set of test-initiating actions was performed at approximately 1 minute. As a result of these actions, the steam generator feed rates increased at 1.0 minute, the RVVVs opened at 1.2 minutes, and HPI flow began to register at 1.8 minutes.

The fluid at the PORV site was initially vapor, as evidenced by the initial pressurizer level and the initial rate of PORV discharge (Figure 5.4.11), about 150 lbm/h. The (full-capacity) HPI flow rate of more than 500 lbm/h thus far exceeded the rate of PORV discharge. Therefore, the primary system gained fluid mass. The pressurizer insurge upon PORV actuation caused a net loss of loop fluid mass, however. Both hot leg levels receded from the U-bend elevation at 1.4 minutes (Figure 5.4.12), the loop flow rates peaked at 1.7 minutes and then subsided (Figure 5.4.13), and the primary system depressurization rate abruptly slowed at 1.6 minutes with a primary system pressure of 1440 psia (Figure 5.4.10). The core region collapsed liquid level began to decrease at 2.6 minutes and, simultaneously, the core exit fluid saturated.

The pressurizer filled just beyond 4 minutes. The rate of PORV discharge increased to approximately 500 lbm/h, just less than the HPI flow rate (Figure 5.4.11), apparently as the PORV site fluid changed to saturated liquid. The rate of increase of the primary system total fluid mass slowed. The primary system repressurized slightly, then began to depressurize at 4 psi/min as the loop A hot leg refilled, loop A flow and primary-to-secondary heat transfer reactivated (Figures 5.4.13 and 5.4.14 -- the steam generator secondaries were still being refilled), and the core region fluid subcooled.

The refill of the steam generator secondaries was completed beyond 8 minutes, and feed was largely interrupted. The steam generator A and B pressures, 700 and 600 psia, were well below the control pressure, but steam generator A repressurized due to the continuing loop A activity (Figure 5.4.10). Thus, steam generator A began to be steamed at 20 minutes.

The pressurizer fluid cooled upward from the bottom of the pressurizer vessel, with the continuing flow through the surge line, pressurizer, and PORV. The PORV site fluid first subcooled at 30 minutes (Figure 5.4.15), the rate of PORV discharge increased approximately 100 lbm/h (exceeding the HPI flow rate), and the rate of primary system depressurization increased to 12 psi/min.

The loop B steam generator primary level descended into the steam generator at 36 minutes (Figure 5.4.12). The steam generator B secondary remained

inactive, although the primary system depressurization rate increased to 17 psi/min. At 63 minutes, with a steam generator B primary level more than 10 feet below the AFW injection site, the steam generator control pressure (and steam generator A pressure) had been reduced to 525 psia, the current pressure in the steam generator B secondary (Figure 5.4.10). Steam generator B feed and steam were reactivated. The resulting condensation of primary system vapor increased the rate of primary system depressurization to some 70 psi/min. This primary system depressurization was short lived, however. The attendant reduction of the saturation temperature caused the PORV site fluid to saturate (Figure 5.4.15), the PORV discharge rate to abruptly decrease at 65 minutes (Figure 5.4.11), and the primary system pressure to stabilize at 650 psia. The hot leg B levels increased and the steam generator B heat transfer activity subsided. The core region collapsed liquid level just approached the RVVV elevation at this time, then it gradually rose. The PORV site fluid again subcooled at 70 minutes and the PORV discharge rate increased accordingly (Figures 5.4.11 and 5.4.15), but the increased HPI flow rate at the now-reduced primary system pressure remained greater than the PORV discharge rate. The primary system thus gradually repressurized beyond 70 minutes (Figure 5.4.10) with the reduced steam generator B activity.

The core exit subcooling margin approached the control value of 75F ($\pm$5F) at 89 minutes. This event initiated automatic throttling of HPI based on the subcooling margin (Figure 5.4.16), causing the primary system to slowly depressurize from 725 psia (Figure 5.4.17). The time-averaged HPI flow rate just exceeded the PORV flow rate. Thus, the steam generator B primary level remained near the upper tubesheet (the loop A hot leg remained full and circulating).

With at least one loop refilled to the U-bend spillover elevation and with the steam generator secondary control pressure within 50 psi of its minimum value, the operator increased the depressurization rates of the steam generator secondaries, as specified. This depressurization increase occurred at 120 minutes (Figures 5.4.17 and 5.4.18). Loop A remained full and circulating; the steam generator secondary pressures were 180 psia. The activity increased in both steam generators, the loop A primary flow rate increased, and the rate of primary system depressurization increased briefly

(Figure 5.4.17). The voided hot leg (B) inlet fluid subcooled, but its upper-elevation fluid remained saturated. The steam generator secondary depressurization rate soon slowed as the facility minimum pressure was approached. Thus, there was little net effect of the imposed increase of the depressurization rate. The loop B hot leg remained voided, and the loop A hot leg remained full and circulating. As the secondary system approached the facility minimum pressure, causing the maximum steaming rates to decrease, the primary system pressure gradually stabilized near 200 psia (Figure 5.4.19).

The operator opened the (voided) loop B hot leg high-point vent at 360 minutes. The primary system pressure was little affected by this venting, but the loop B hot leg levels, which had remained near the elevation of the upper tubesheet, began to increase at about 5 ft/h (Figure 5.4.20); this rate of refill slowed as the refill proceeded. The test was terminated at 420 minutes.

5.4.3. Comparisons

The leak location was varied in the following three tests:

10	(311000)	Cold leg B1 discharge
3	(320302)	Cold leg B1 suction
4	(3204AA)	PORV

Test 10 was the Nominal Repeat Test from Group 31. The three tests otherwise had the same nominal boundary system controls including full HPI capacity. Several control perturbations were introduced later in the tests, as described below.

Pressure

The test transients with varied leak location were surprisingly similar. Tests 3 (with the cold leg suction break) and 10 (with the cold leg discharge break) were virtually repeat tests until the boundary system controls were varied as specified. In both tests, the primary system repressurized slightly, when loop flow was interrupted, then gradually depressurized over the first hour as the steam being discharged through the RVVVs was condensed by HPI (Figure 5.4.21). With a PORV break, the primary system depressurized

relatively rapidly. This initial depressurization trend was quickly halted as the loop fluid saturated and the pressurizer filled, placing liquid rather than vapor at the PORV. Much as in Tests 3 and 10, the primary system gradually depressurized after 20 minutes in Test 4. Whereas the depressurization mechanism involved the HPI condensation of core steam in the tests with a cold leg break, the core region level remained well above the elevation of the RVVVs with a PORV break (Figure 5.4.22). The depressurization mechanism in this case was heat transfer to steam generator A plus the PORV volumetric discharge. The core exit fluid remained subcooled with the PORV break, thus repressurization tendencies due to core steam production were absent.

Fluid Mass

The primary system total fluid mass rose almost immediately with the PORV break of Test 4 and then approximately stabilized (Figure 5.4.23). The initial increase occurred while the PORV discharged vapor, thus the HPI flow exceeded the PORV flow. The total mass stabilized when liquid reached the PORV and the PORV-site fluid subsequently subcooled. The primary system mass of Test 3 paralleled that of Test 10, attesting to the similarity of leak fluid conditions in these two tests. In both tests, the total fluid mass began to increase after approximately 1 hour, after the primary system depressurizations due to BCMs.

The primary system repressurized somewhat at 1 hour, with the PORV break (Figure 5.4.24). This repressurization was preceded by BCM heat transfer in the interrupted loop B. This BCM depressurization was sufficient to increase the rate of primary system mass increase, refill the loop B hot leg riser and stub levels to an intermediate elevation, extinguish BCM, and thus cause the repressurization. The primary system subsequently again depressurized near 90 minutes when the increasing SCM triggered HPI throttling.

Equilibrium

The hot leg levels attained intermediate elevations beyond 2 hours in both Tests 3 and 10 (Figure 5.4.25). The primary system gradually repressurized to almost 650 psia in both tests. In Test 10, the loop A levels gradually rose whereas the loop B levels remained almost constant, apparently due to

differences in guard heating between the loops. The loop A levels achieved the U-bend spillover elevation near 270 minutes, thus beginning a series of spillover recouplings characterized by abrupt reductions of primary system pressure and variations of core fluid temperatures.

The near-equilibrium conditions of Test 3 (suction break) were perturbed by the manual PORV actuation at 195 minutes. The hot leg levels dropped sufficiently to trigger BCM heat transfer (Figure 5.4.25), thus the primary system depressurized earlier in Test 3 than in Test 10 (Figure 5.4.24).

Summary

Tests 3, 4, and 3110 varied leak location with otherwise similar conditions. The three transients were remarkably alike. The conditions with a cold leg suction leak were virtually identical to those with a discharge leak, attesting to the leak fluid heating accomplished by cold leg counterflow and inter cold leg flow.

Although the conditions were similar among the three tests, the interactions with a PORV break differed in nature from those with a cold leg break. The core exit fluid remained subcooled whereas, with a cold leg break, the core steam production was offset by HPI condensation. The PORV site fluid subcooled quite early in the transient, thus almost equating the PORV discharge mass flow rate to the leak mass flow rates of Tests 3 and 10. Unlike Tests 3 and 10, the cooling and depressurization mechanism in Test 4 was generally through single-phase natural circulation heat transfer to steam generator A.

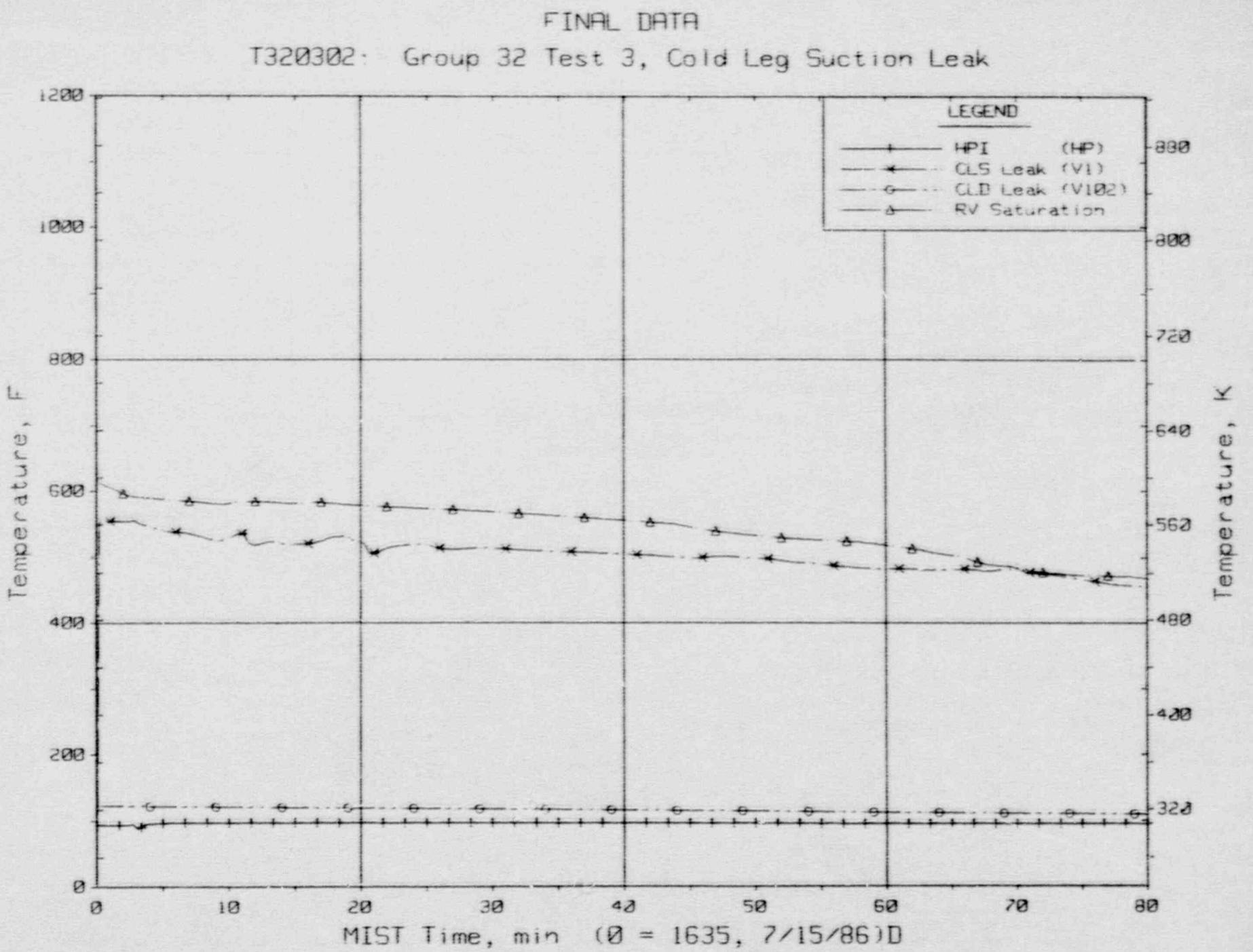

Figure 5.4.1. Single-Phase Discharge and HPI Fluid Temperatures

Tue Jul 12 12:56:31 1988

PRTC1

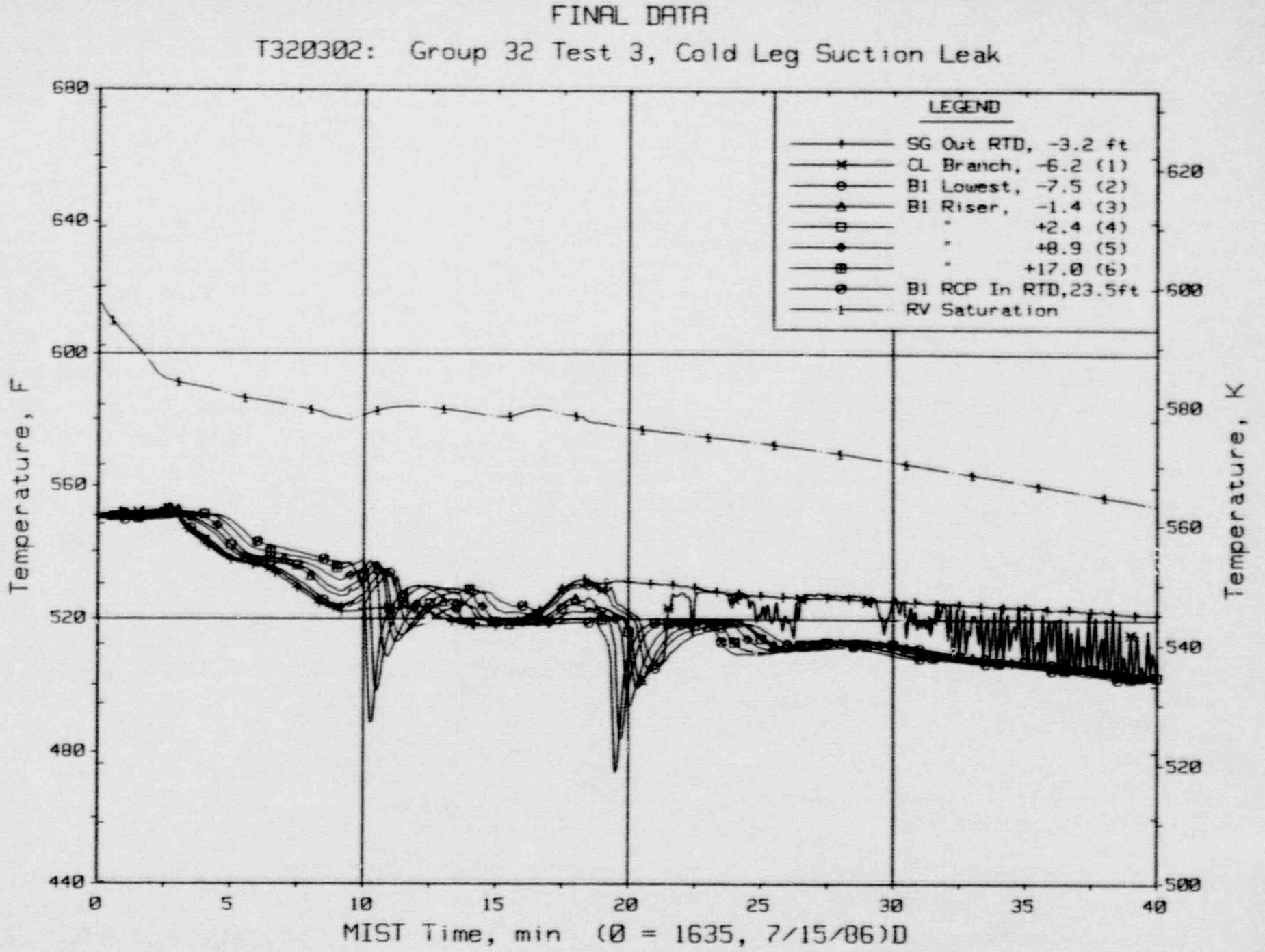

Figure 5.4.2. Cold Leg B1 Suction Fluid Temperatures (C2TCs)

Tue Jul 12 13:52:27 1988

C2TC1

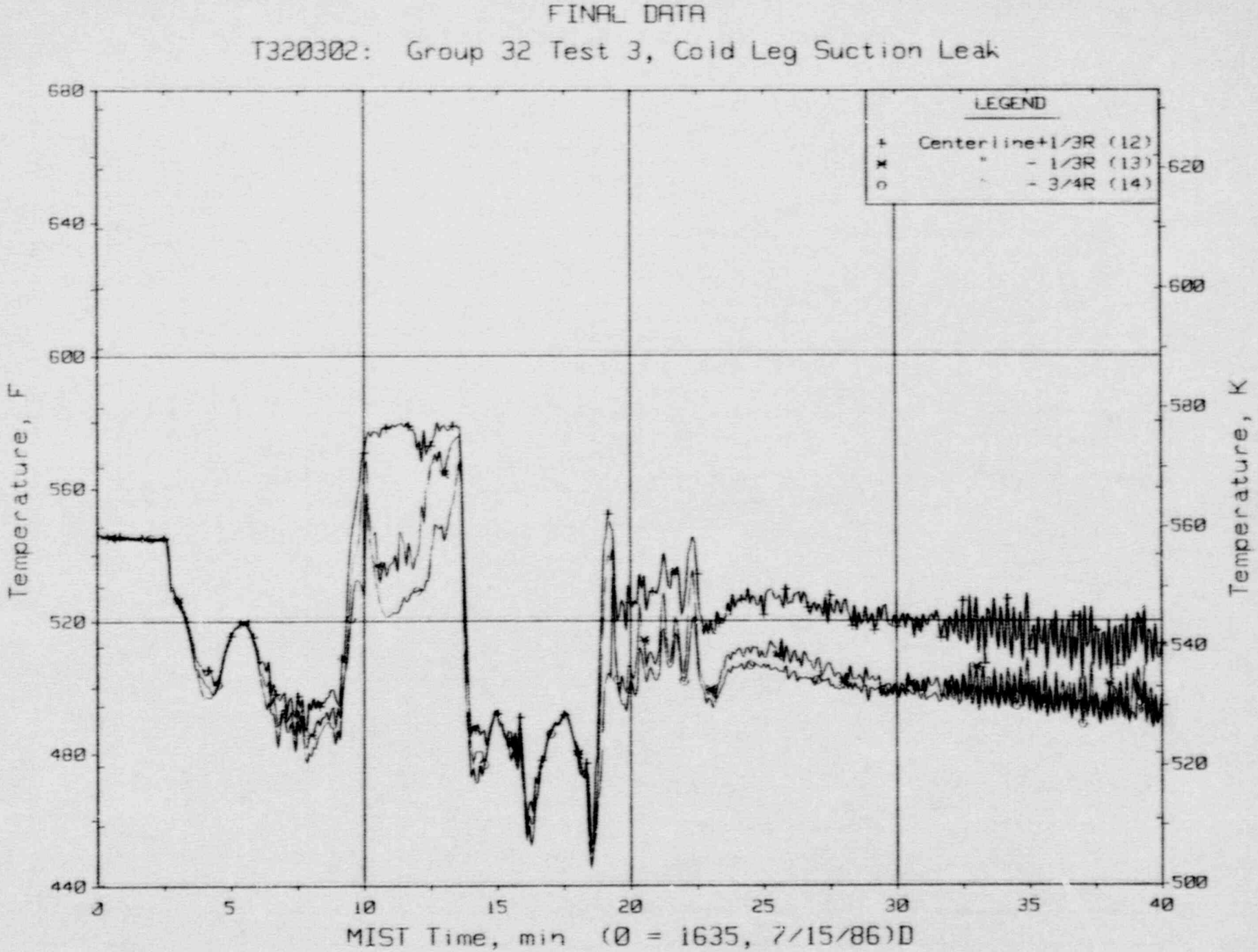

Figure 5.4.3. Cold Leg B1 Nozzle Rake Fluid Temperatures (21.2 ft, C2TCs)

Tue Jul 12 13:23:46 1988

C2TC4

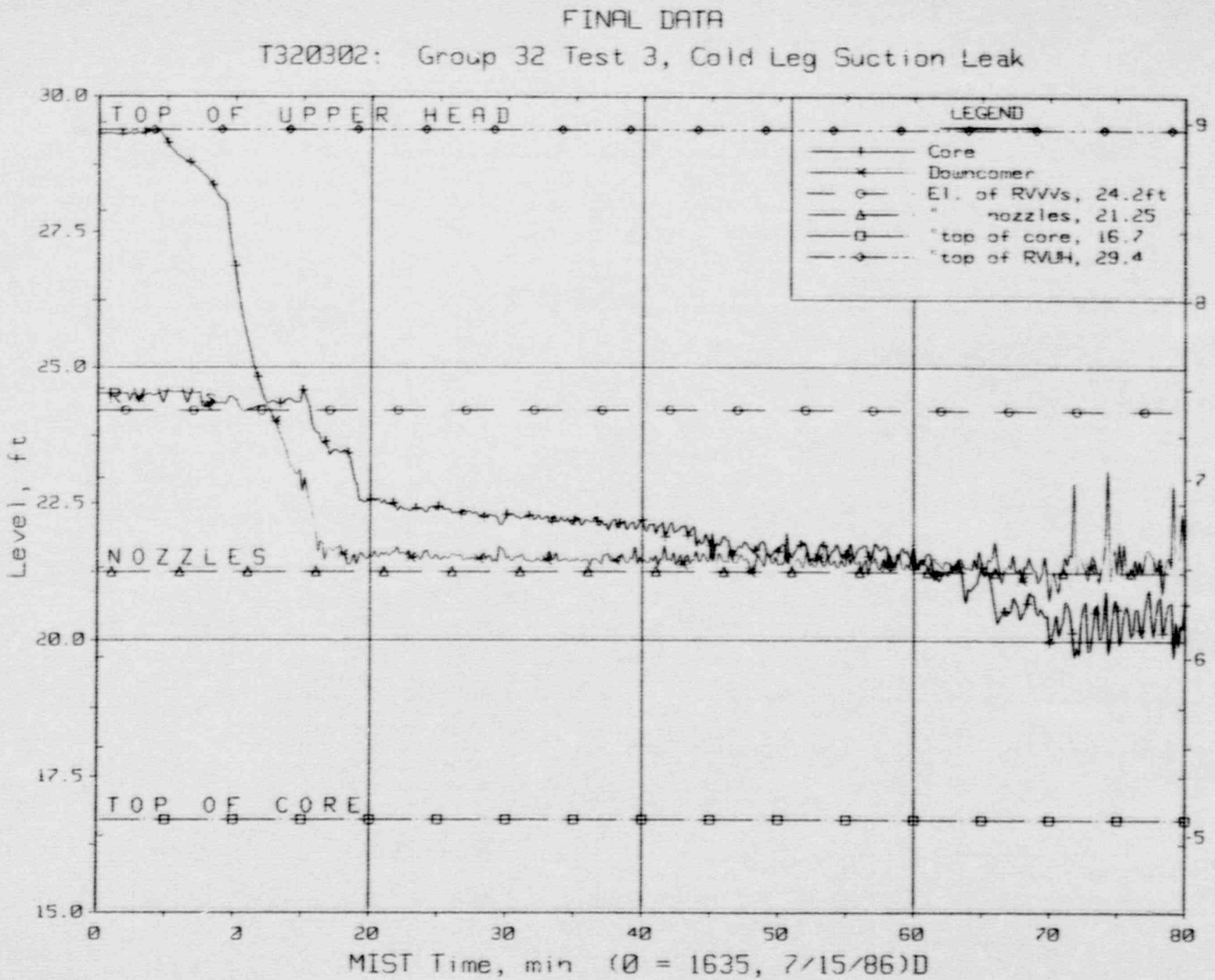

Figure 5.4.4. Core-Region Collapsed Liquid Levels

Tue Jul 12 13:02:52 1988

COLV1

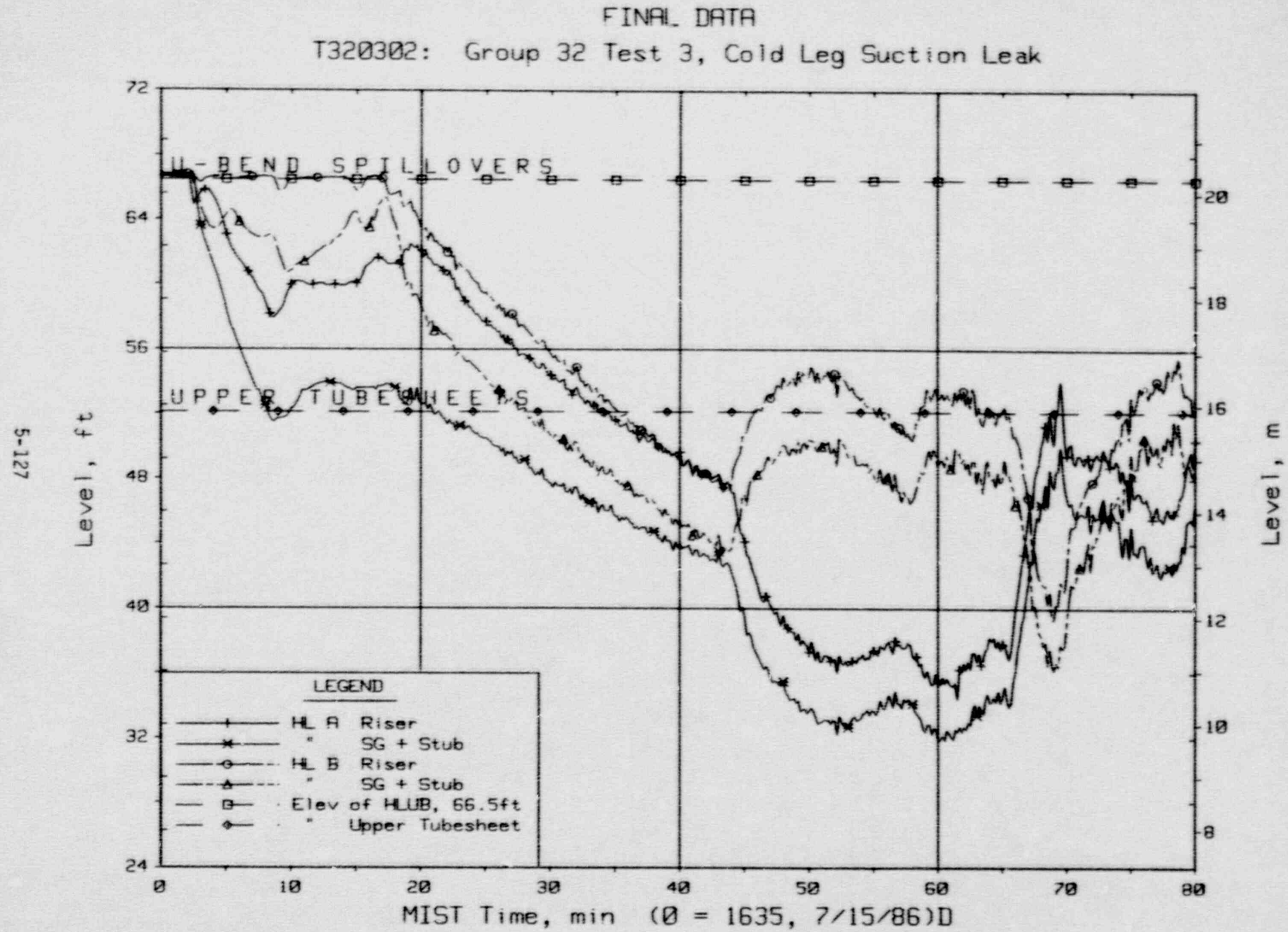

Figure 5.4.5. Hot Leg Riser and Stub Collapsed Liquid Levels

Tue Jul 12 14:41:28 1988

HLLV1

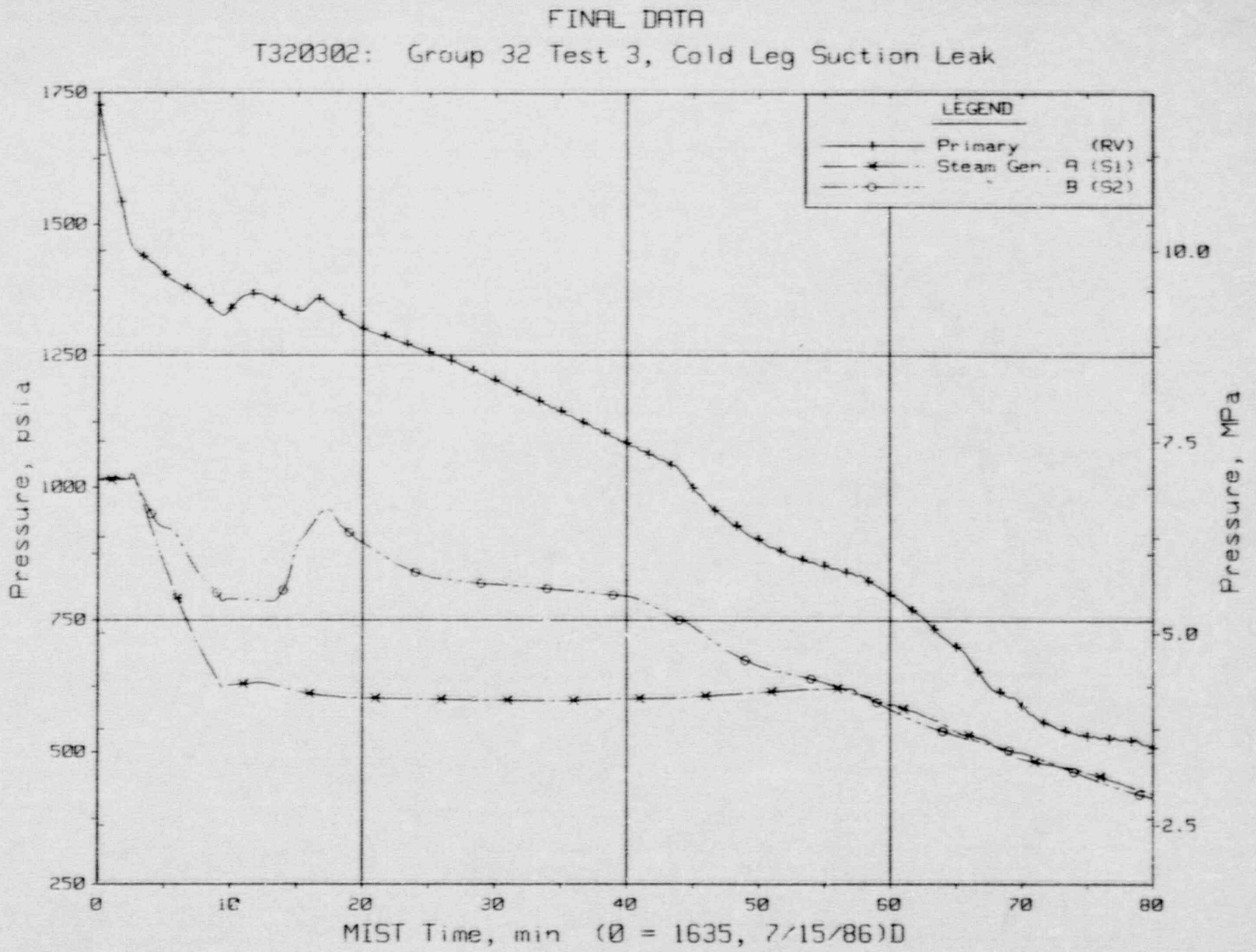

Figure 5.4.8. Primary and Secondary System Pressures (GPOIs)

Tue Jul 12 13:10:27 1988

PSGP1

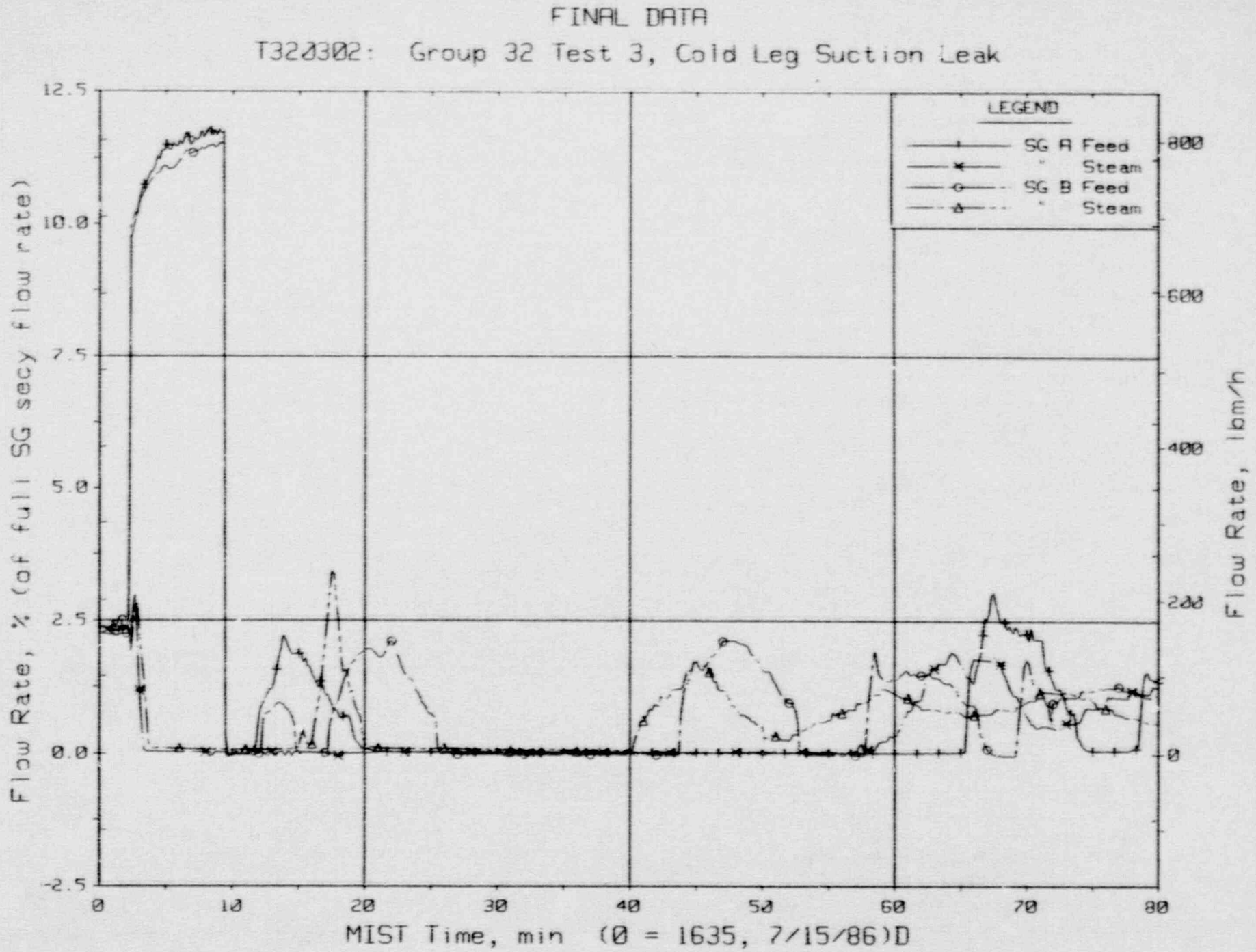

Figure 5.4.7. Secondary System Flow Rates

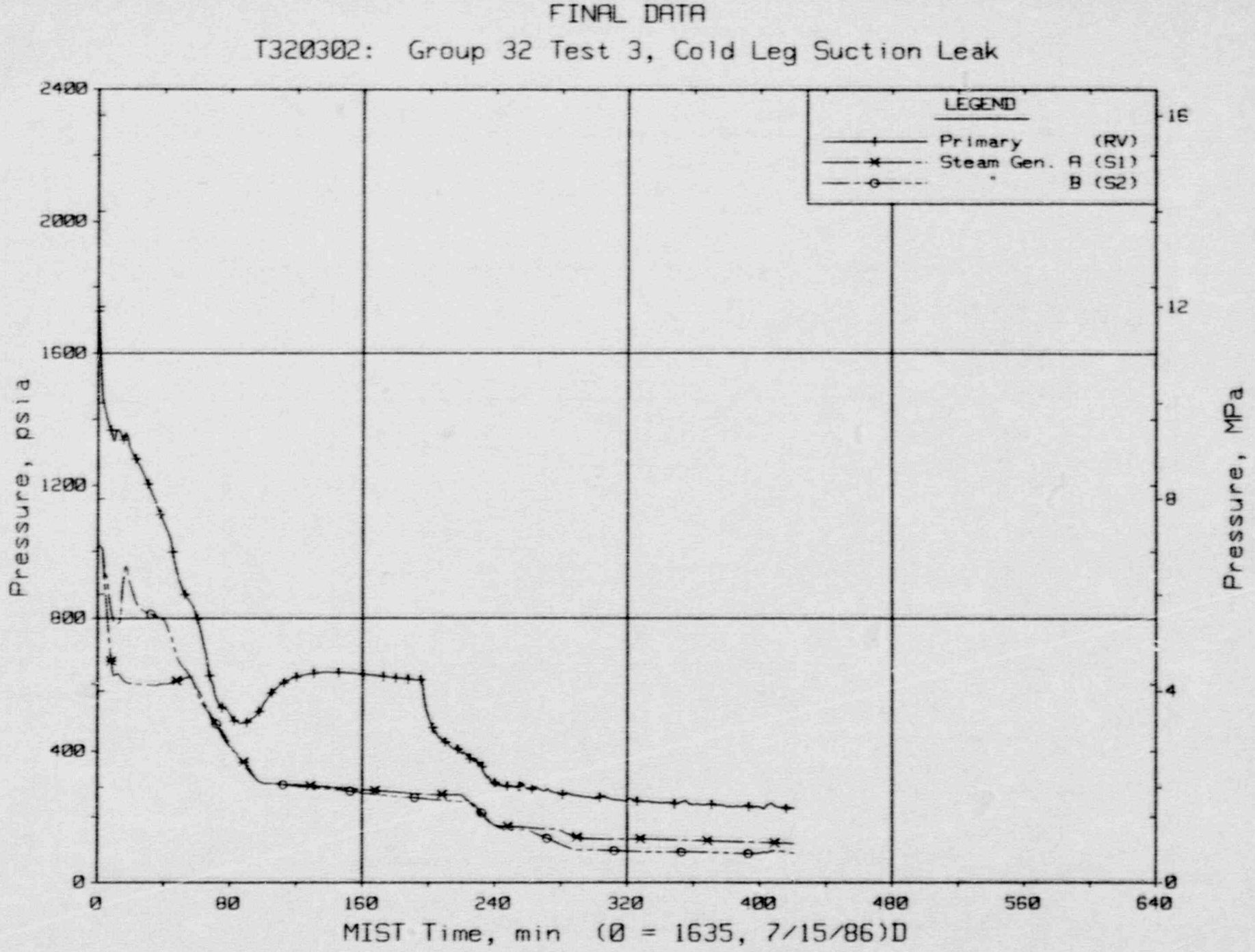

Figure 5.4.8. Primary and Secondary System Pressures (GP01s)

Tue Jul 12 13:55:45 1988

PSGP1

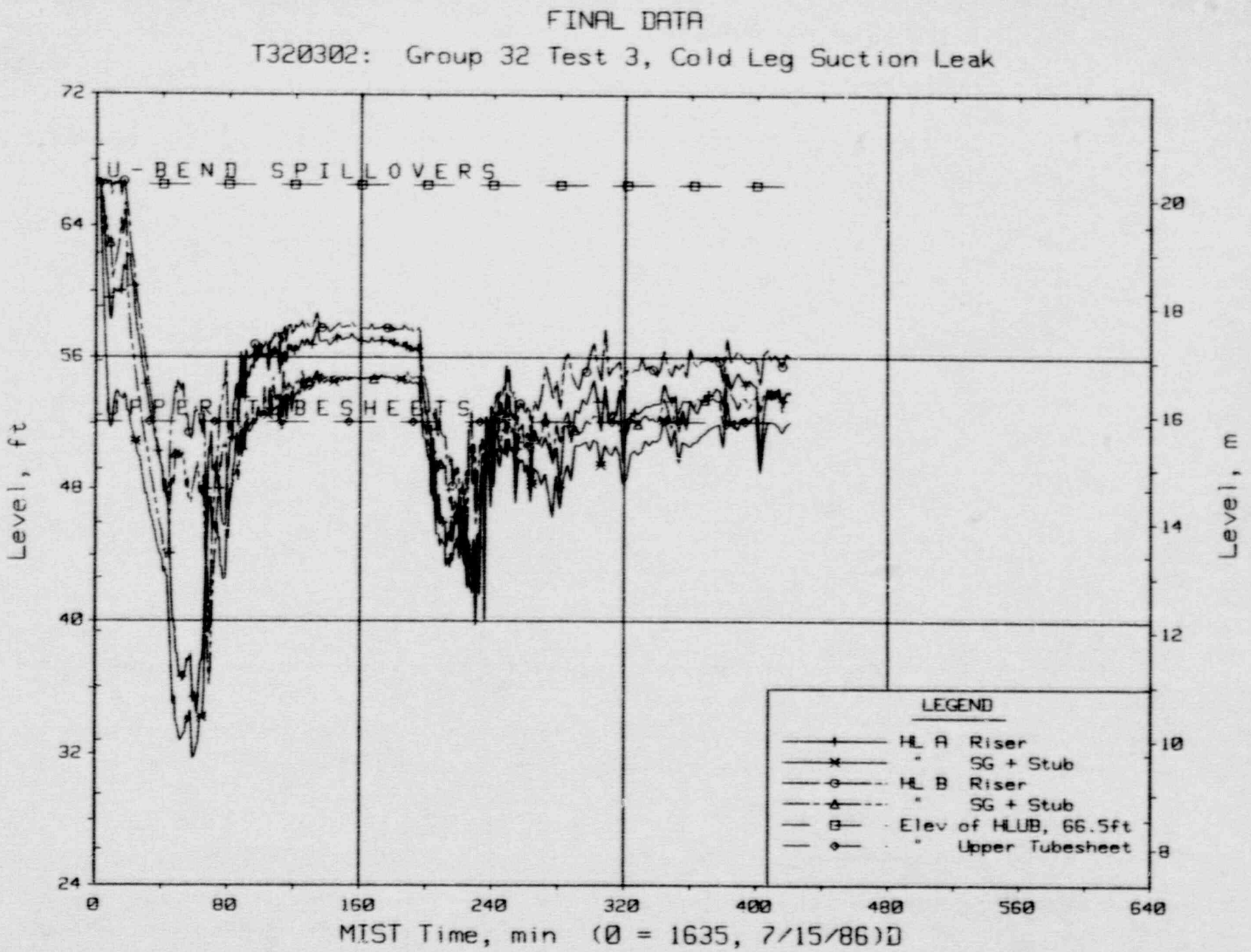

Figure 5.4.9. Hot Leg Riser and Stub Collapsed Liquid Levels

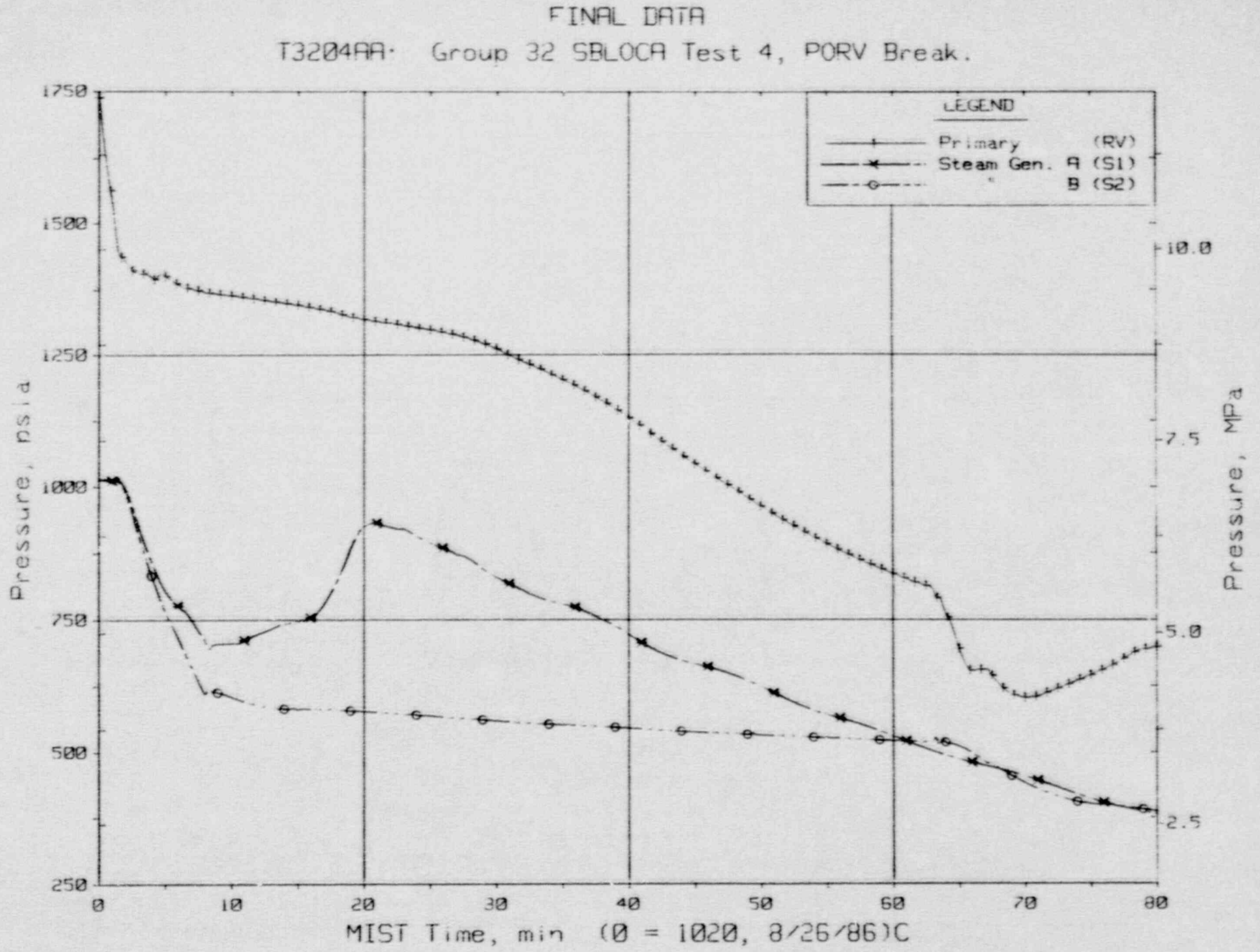

Figure 5.4.10. Primary and Secondary System Pressures (GP01s)

Mon Oct 31 15:02:0[illegible] 1988

PSGP1

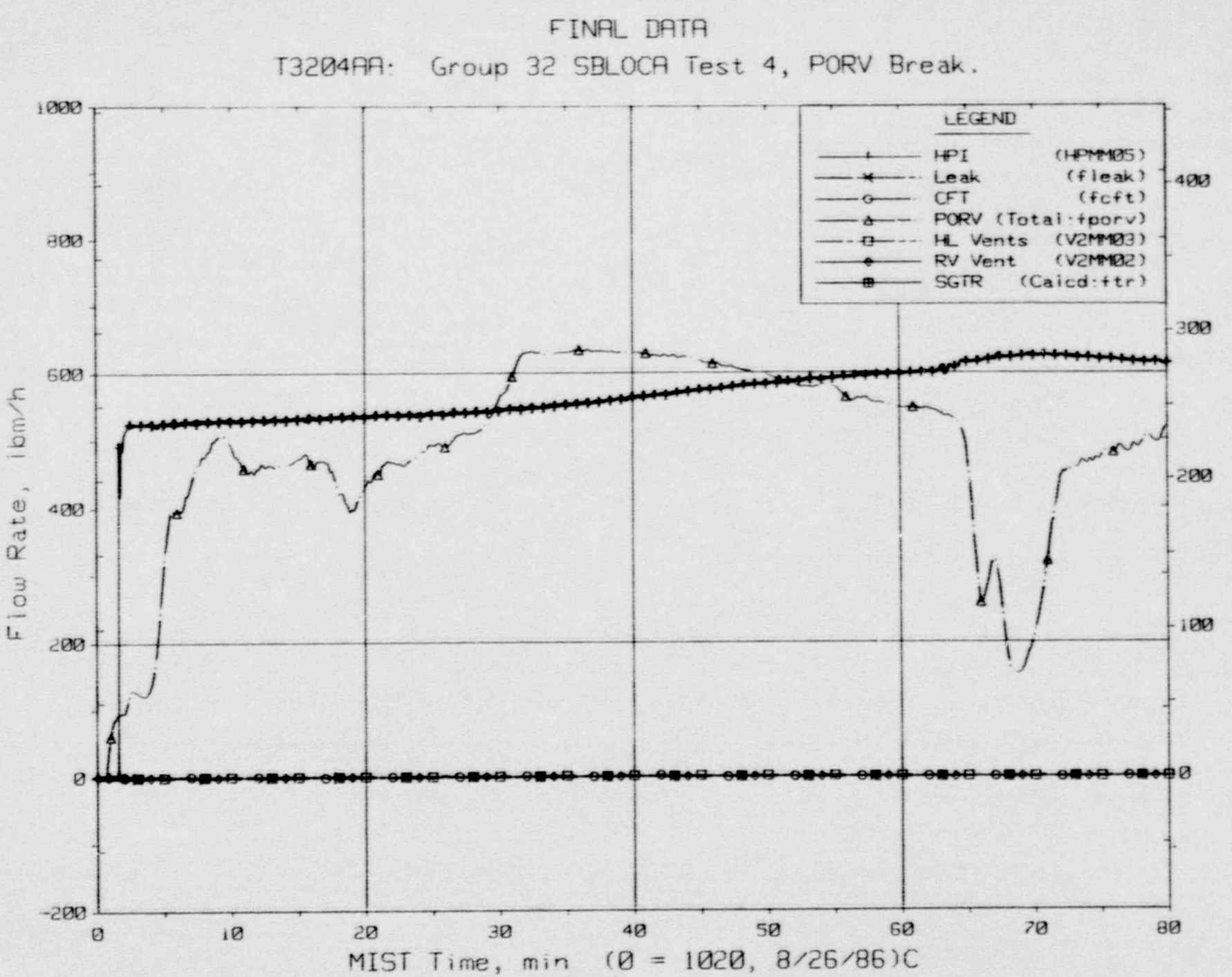

Figure 5.4.11. Primary System Boundary Flow Rates

Mon Oct 31 15:40:15 1988

PRFL3

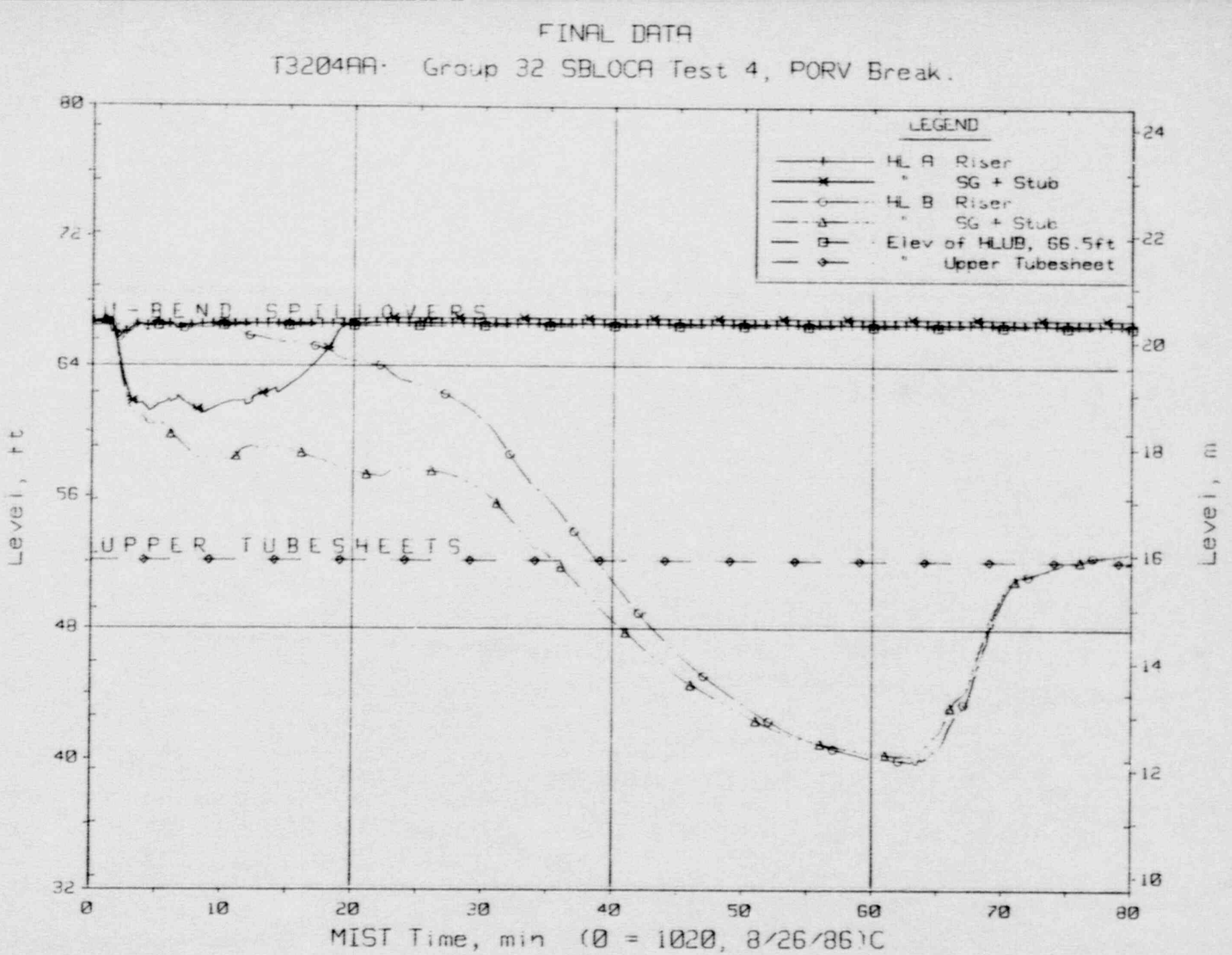

Figure 5.4.12. Hot Leg Riser and Stub Collapsed Liquid Levels

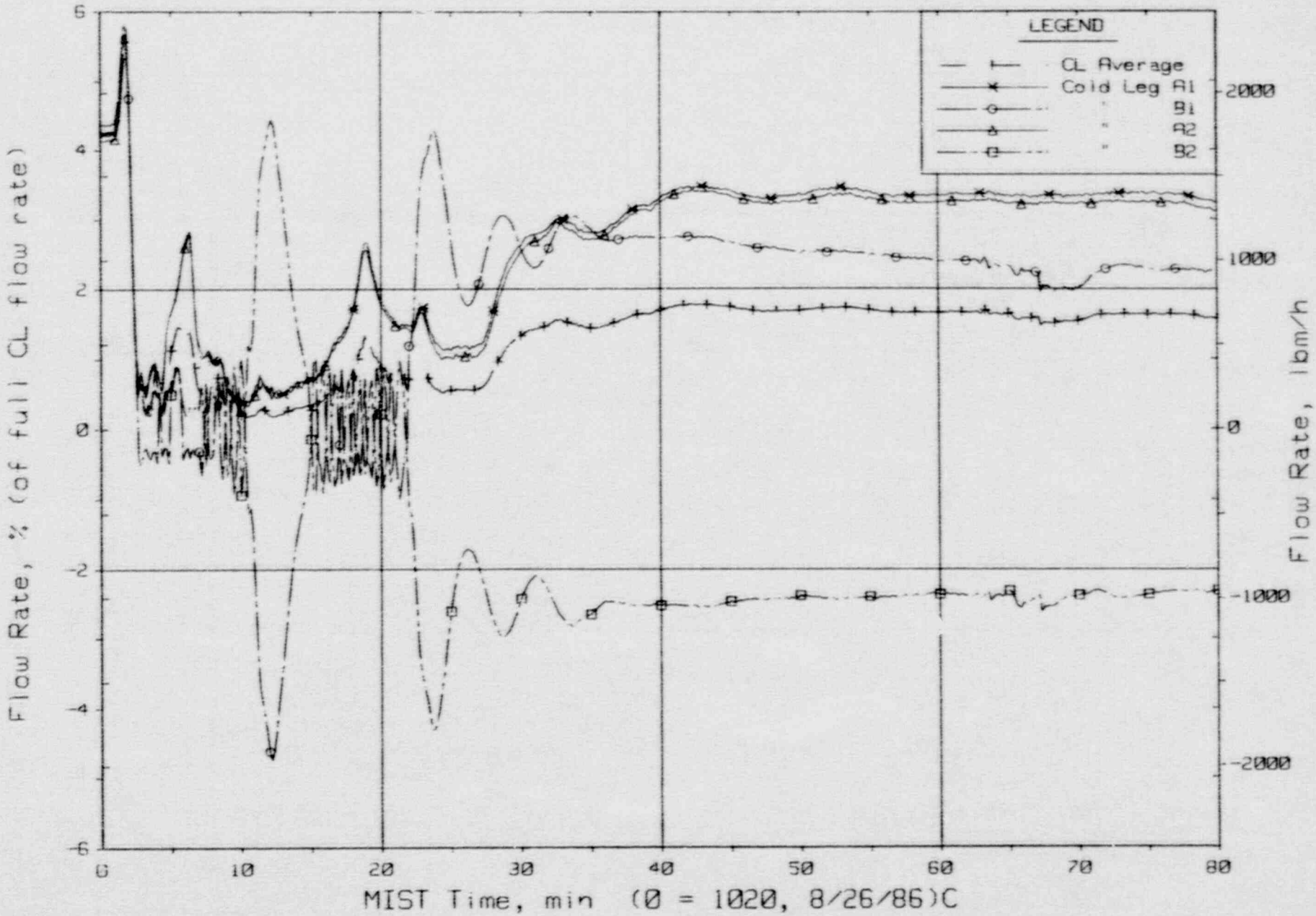

Figure 5.4.13. Cold Leg (Venturi) Flow Rates

Tue Jul 12 12:22:24 1988

CLFL1

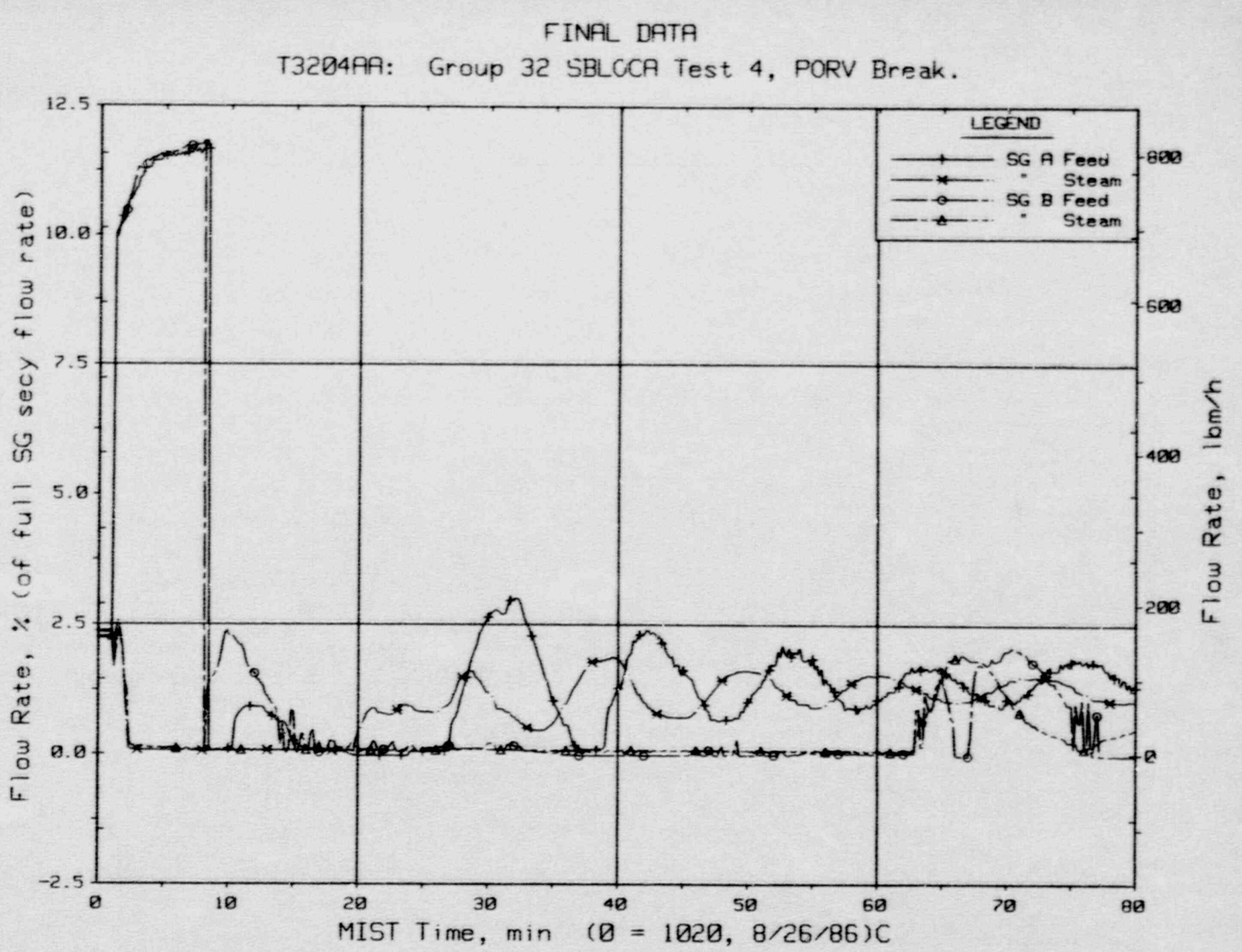

Figure 5.4.14. Secondary System Flow Rates

Tue Jul 12 13:59:28 1988

SGFL2

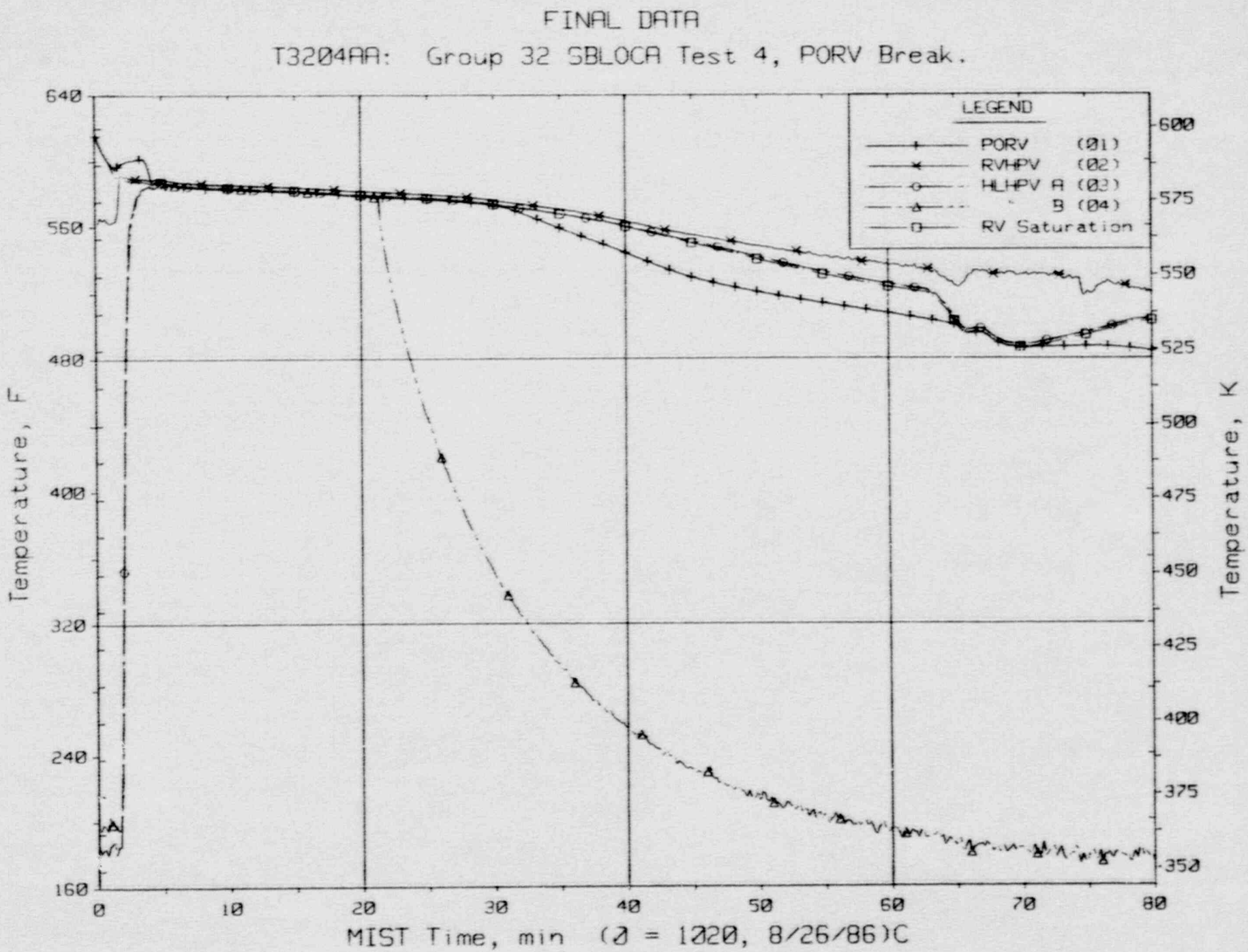

Figure 5.4.15. Two-Phase Discharge Fluid Temperatures (V2s)

Tue Jul 12 12:35:41 1988

PRTC2

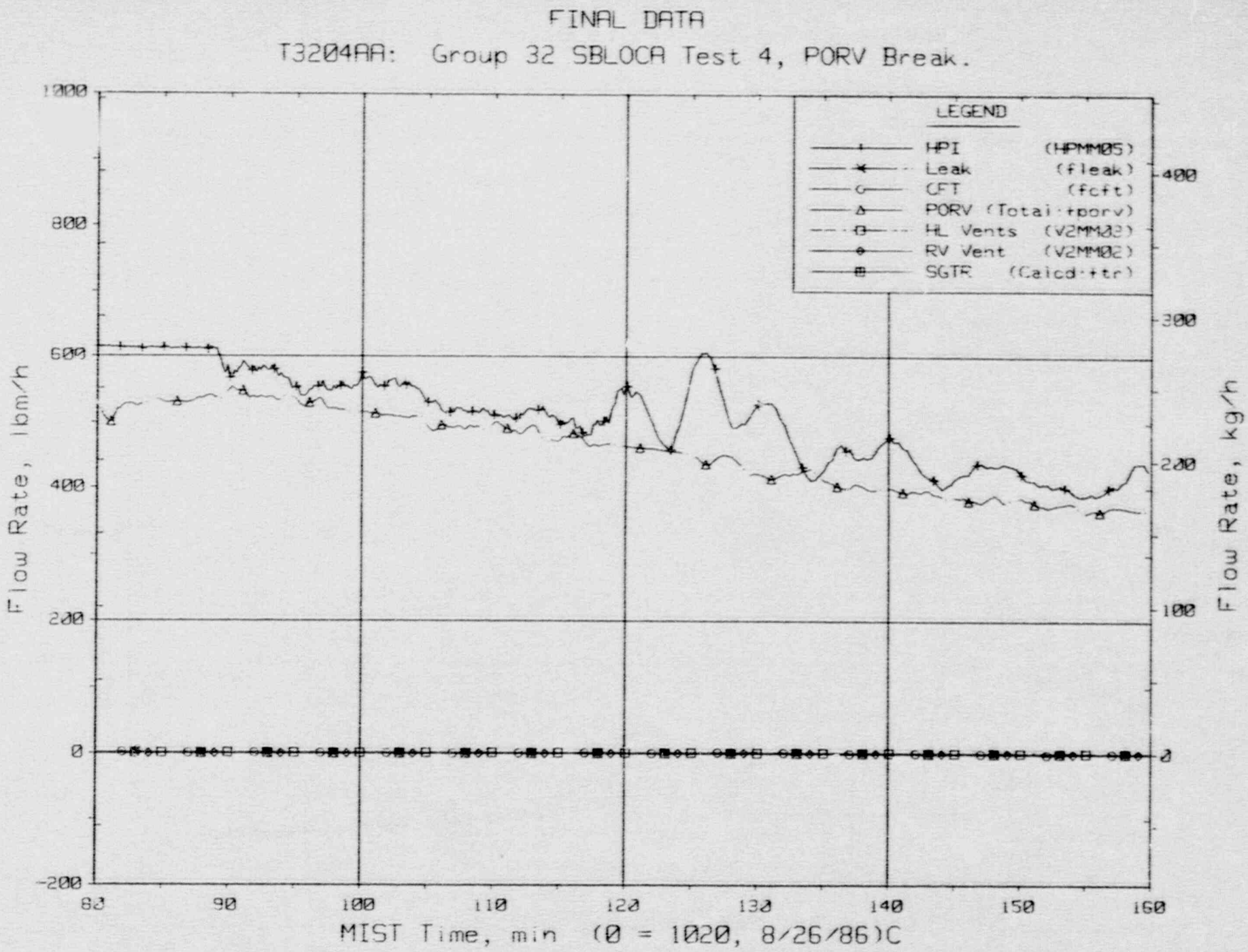

Figure 5.4.16. Primary System Boundary Flow Rates

Tue Jul 12 12:39:12 1988

PRFL3

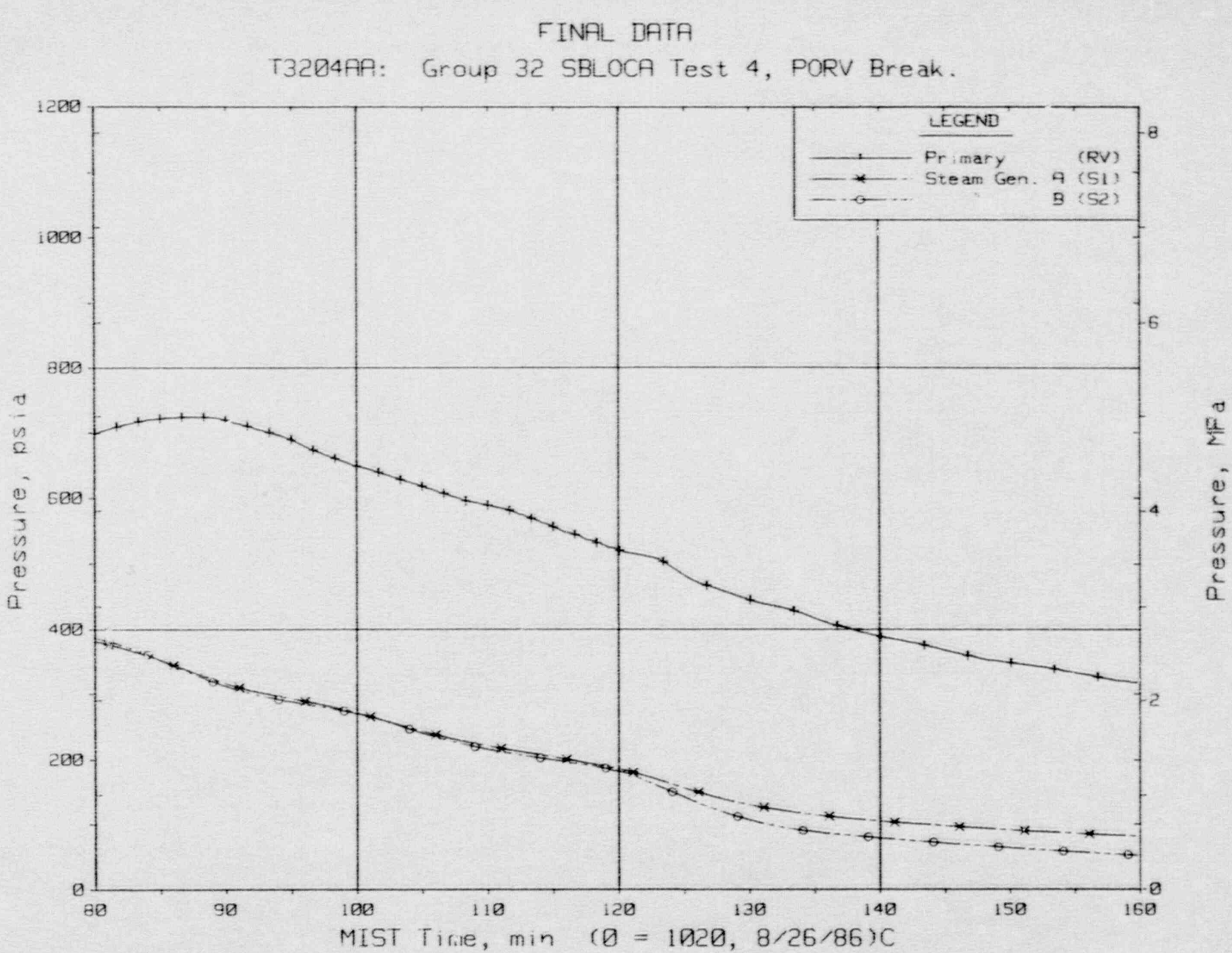

Figure 5.4.17. Primary and Secondary System Pressures (GP01s)

Tue Jul 12 12:41:43 1988

PSGP1

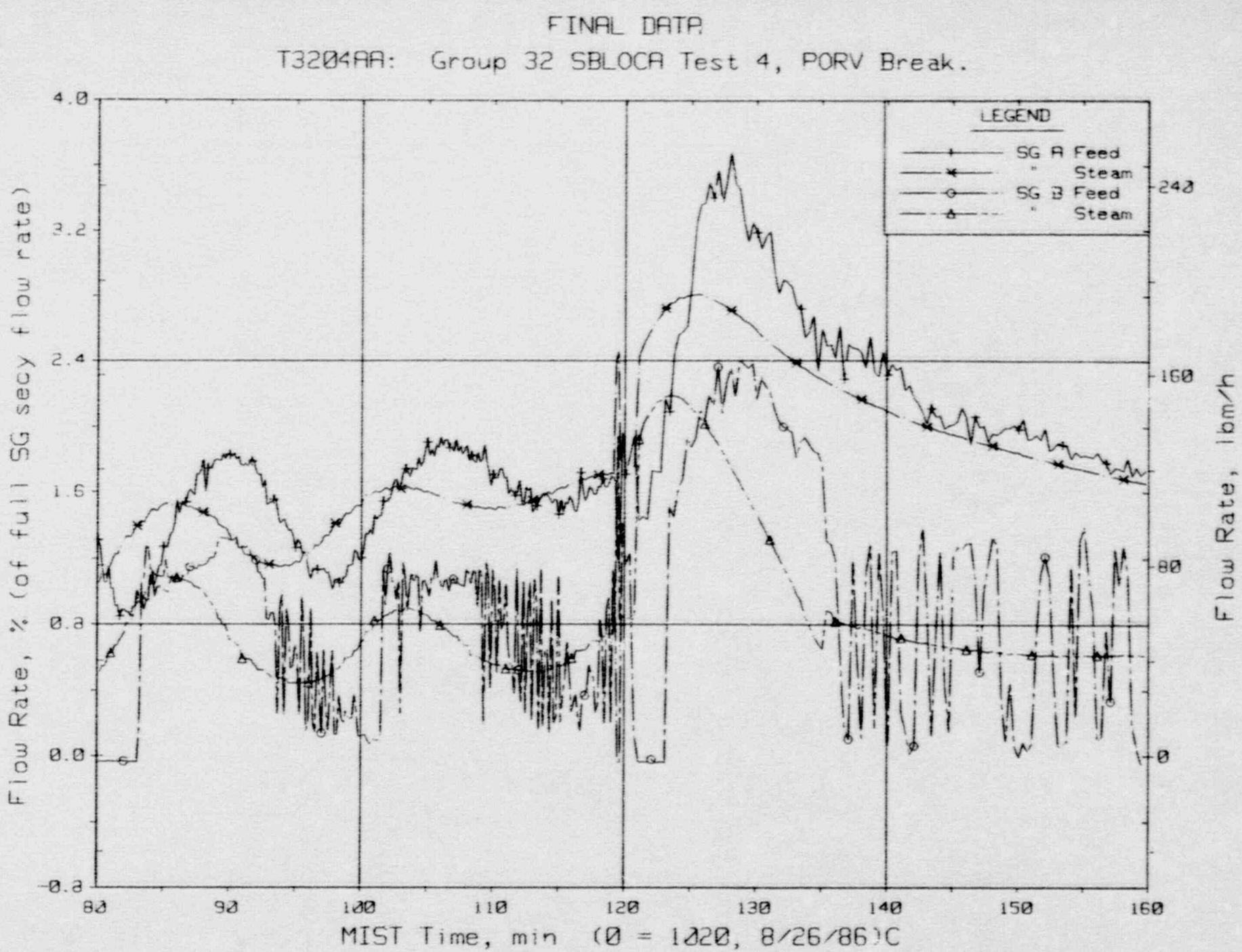

Figure 5.4.18. Secondary System Flow Rates

Tue Jul 12 12:44:48 1988

SGFL2

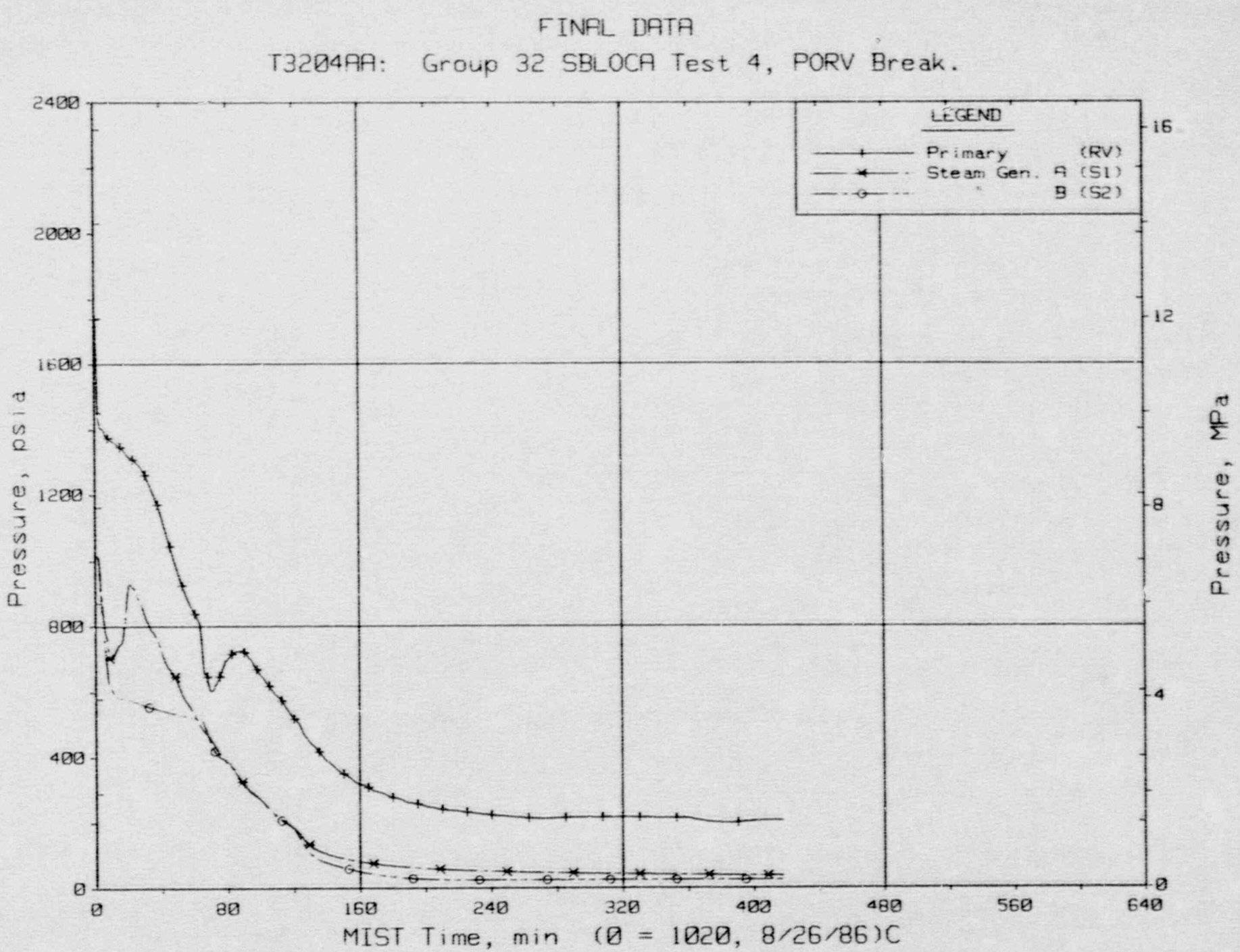

Figure 5.4.19. Primary and Secondary System Pressures (GPOIs)

Tue Jul 12 12:47:16 1988

PSGP1

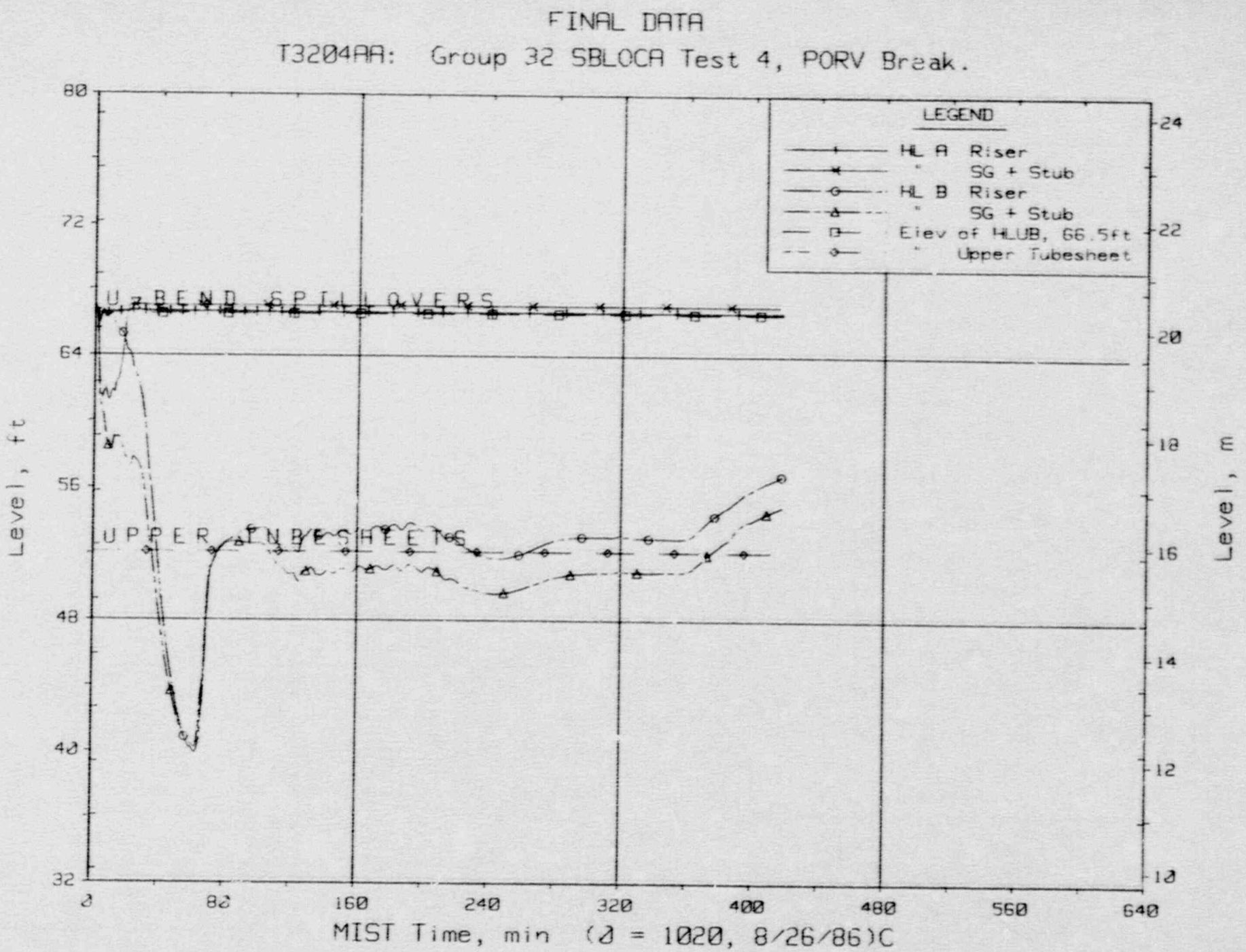

Figure 5.4.20. Hot Leg Riser and Stub Collapsed Liquid Levels

Tue Jul 12 12:58:16 1988

HLLV1

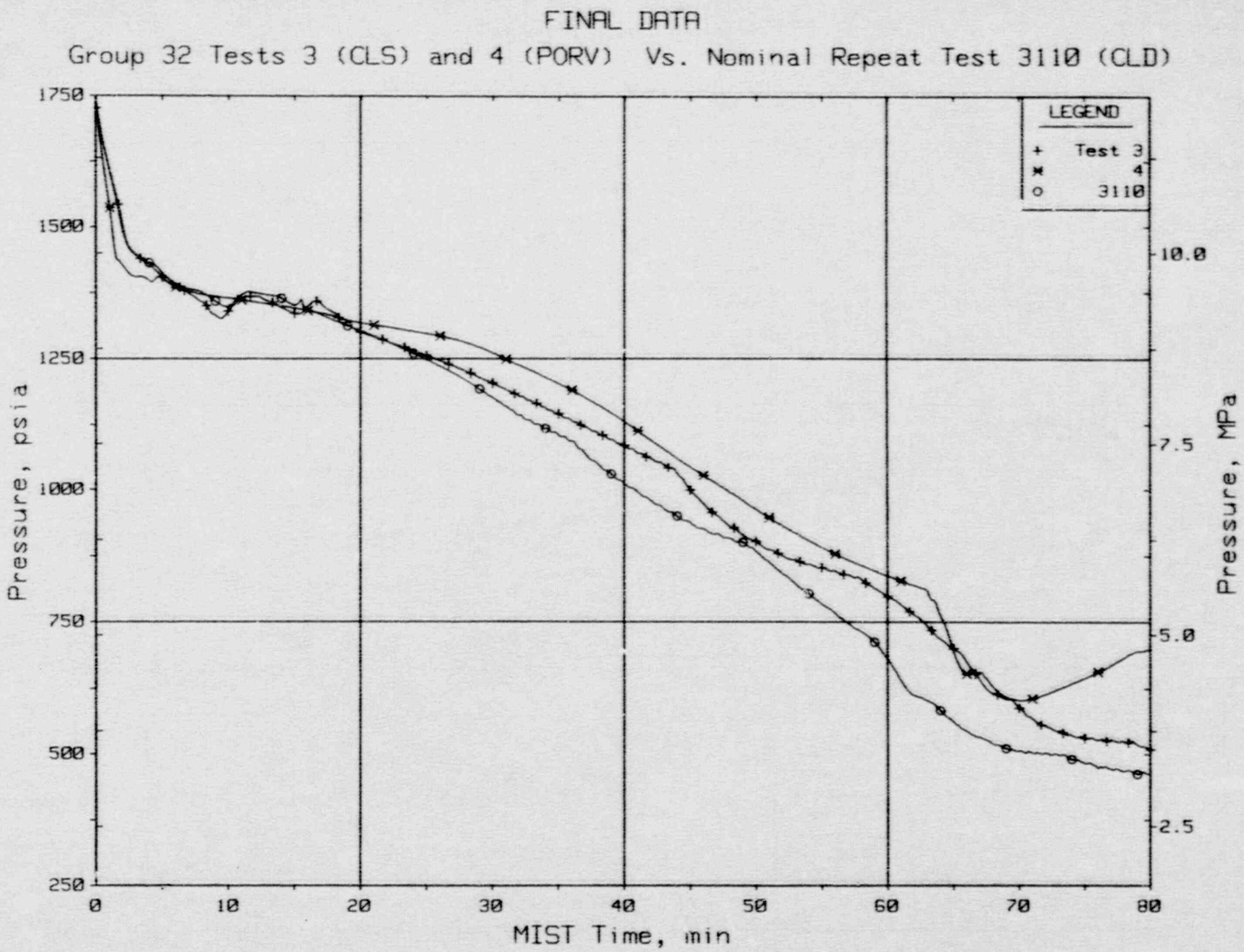

Figure 5.4.21. Reactor Vessel Pressure

Tue Jul 12 14:53:08 1988

34RVGP1

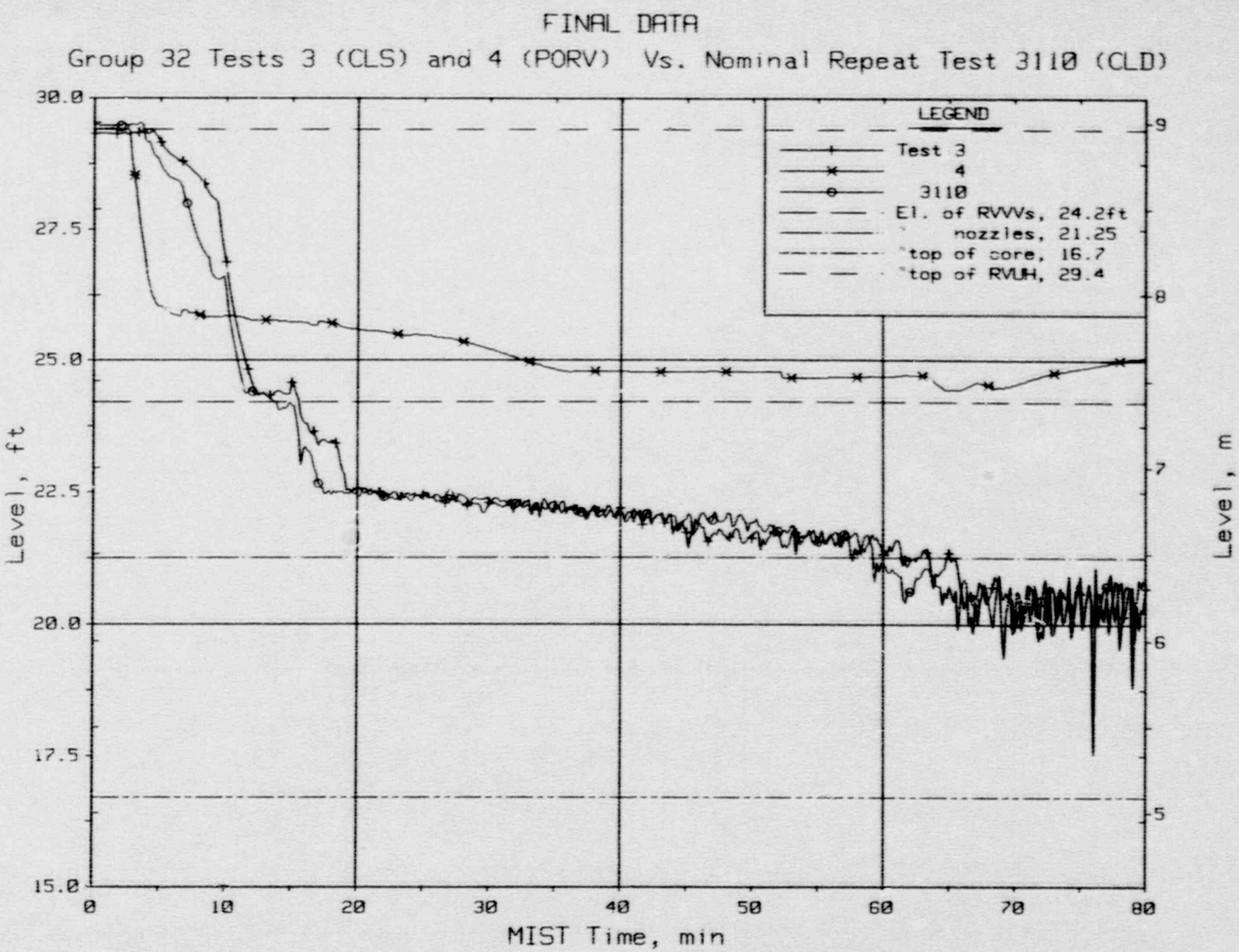

Figure 5.4.22. Reactor Vessel Collapsed Liquid Levels

Tue Jul 12 14:56:57 1988

34COLV1

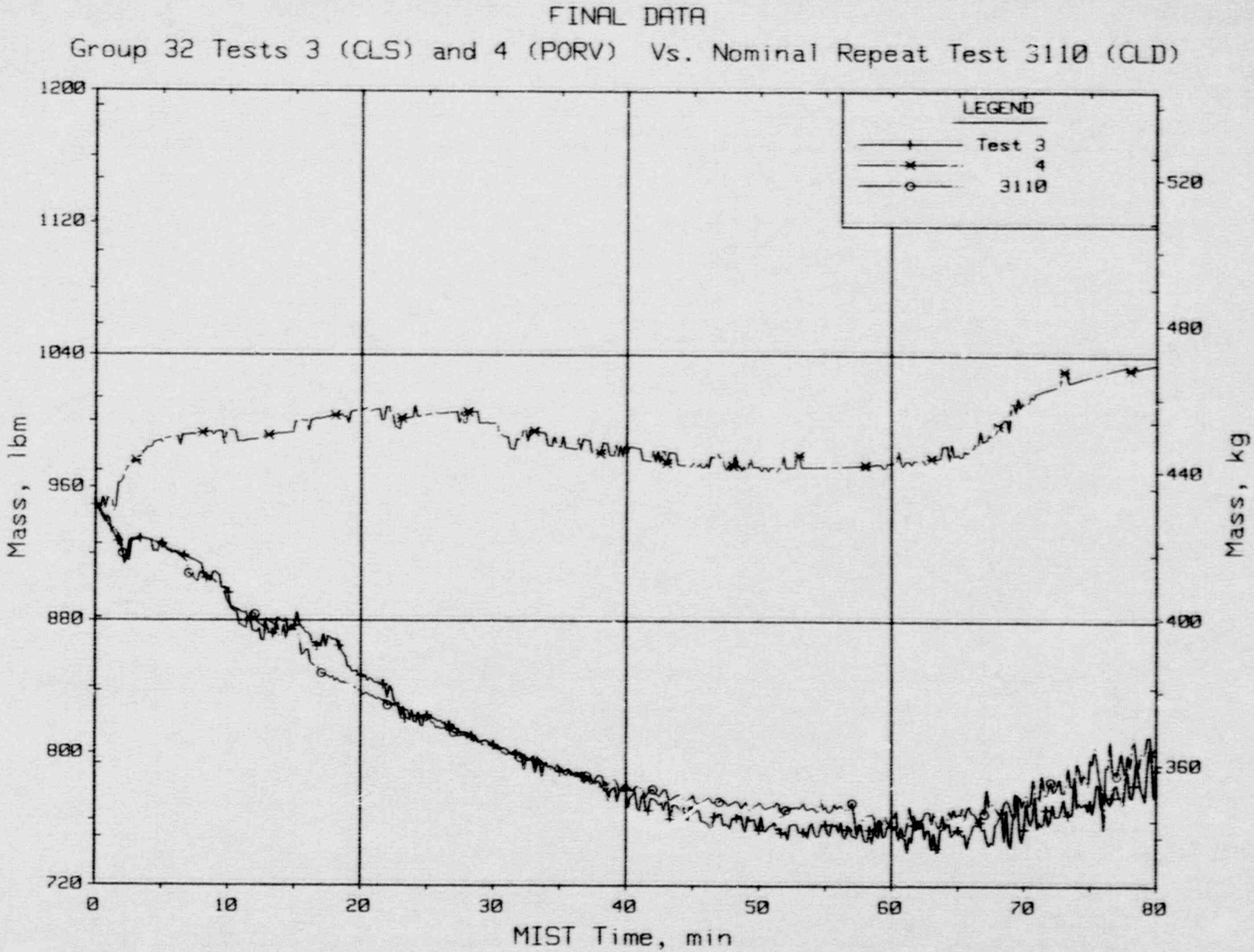

Figure 5.4.23. Primary System Total Fluid Mass (Indicated, PLML20s)

Tue Jul 12 14:59:53 1988

34PRML1

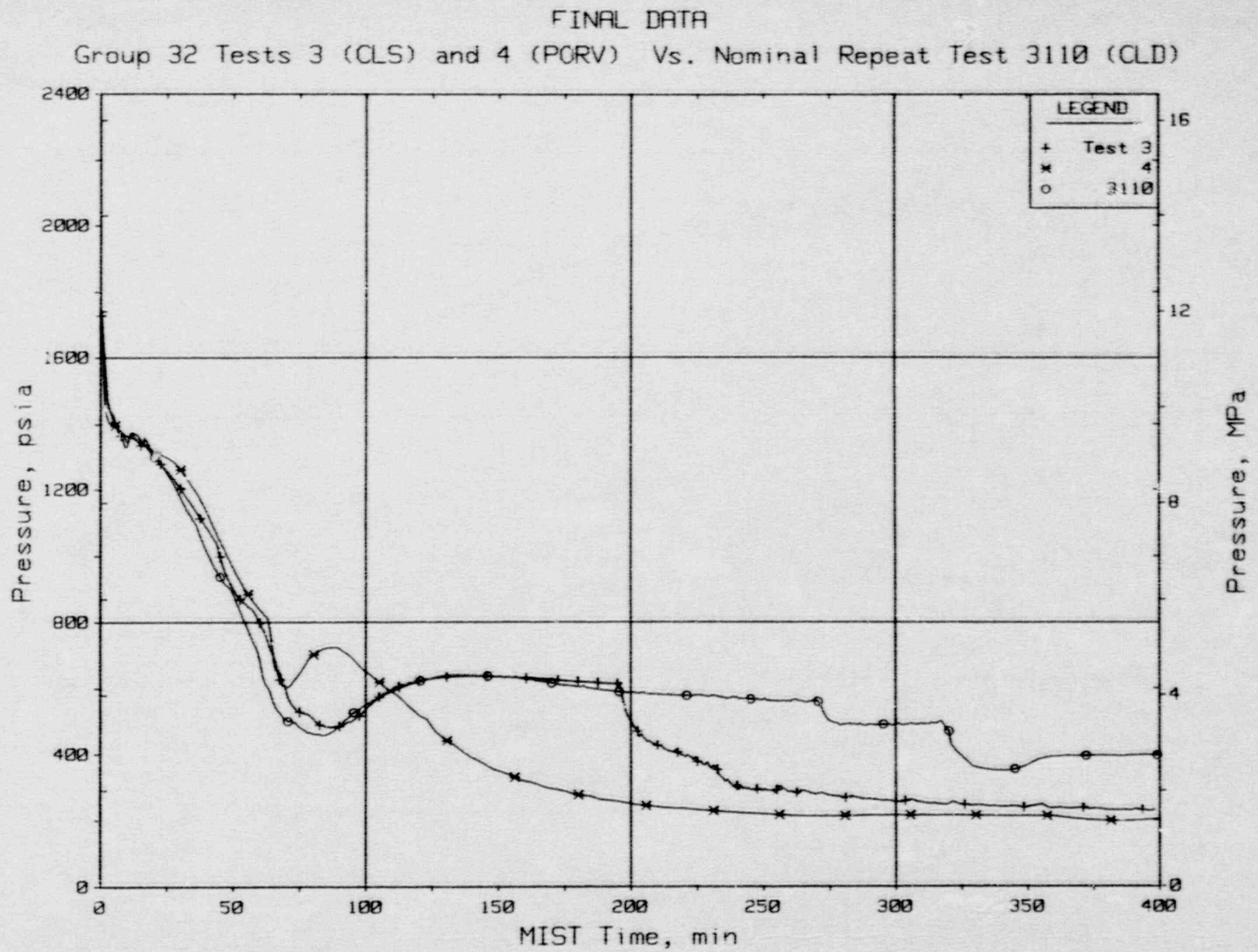

Figure 5.4.24. Reactor Vessel Pressure

Tue Jul 12 15:05:19 1988

34RVGP1

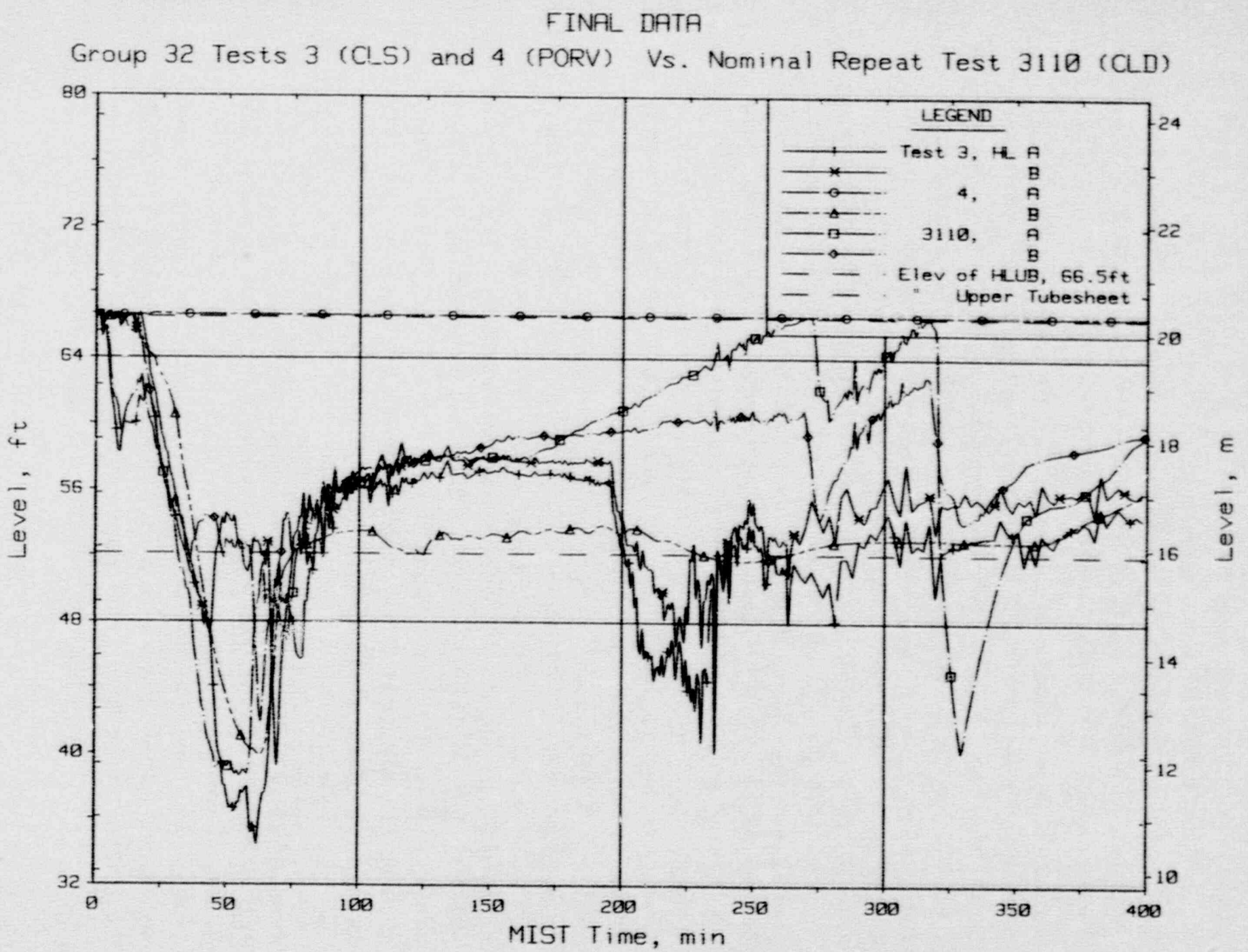

Figure 5.4.25. Hot Leg Riser Collapsed Liquid Levels

Tue Jul 12 15:09:04 1988

34HLLV1

5.5. Isolated Leak, Test 5

The 10-cm^2 cold leg B1 discharge leak was actuated and later isolated in Test 5 (320503). The initial events of Test 5 were similar to those of the other small-break tests with similar boundary conditions.

The scaled 10-cm^2 cold leg B1 discharge leak was opened at time 0. The primary system depressurized from approximately 1730 psia at approximately 100 psi/min (Figure 5.5.1). The primary depressurization rate slowed between 2 and 2.3 minutes, indicating primary fluid saturation. The second group of test-initiating actions was evidenced (RVVVs opened, feed rates increased, core power decreased, and HPI indicated). Also, the core exit and hot leg fluid approached saturation, the hot leg levels began to indicate voiding (Figure 5.5.2), the cold leg flow rates briefly increased and then decreased toward stagnation, and the steam generator secondaries began to depressurize. The core region collapsed liquid level began to recede at 3.4 minutes (Figure 5.5.3) and the core exit fluid briefly saturated. The steam generator secondary pressures began to diverge noticeably beyond 3.8 minutes and the steam generator B secondary repressurized slightly. The hot leg B riser intermittently refilled. Both steam generator secondary levels entered the control range (31.6 $\pm$ 1 ft) near 9 minutes. Feeding was terminated and the secondary pressures stabilized (A at 630 psia and B at 780 psia). The core exit fluid again saturated and generally remained at saturation. The core region collapsed liquid level briefly stabilized at 26.7 ft, then descended more rapidly than before (Figure 5.5.3). Feed was reactivated to steam generator A at 11 minutes (Figure 5.5.4) (the hot leg A primary levels remained intermediate to the steam generator and U-bend). The core region collapsed liquid level stabilized near the vent valve elevation and the downcomer began to void.

From 12.5 to 15 minutes, the steam generator B secondary repressurized toward the control point (indicating heat transfer activity). The core exit fluid briefly subcooled, the RVVVs closed (A2 intermittently), and the downcomer voided toward the nozzle elevation. After 15 minutes, both hot leg U-bends were voided and the downcomer level stabilized near the elevation of the cold leg nozzles (Figure 5.5.3). The primary system repressurized slightly, then

the RVVVs reopened. The primary system then gradually depressurized from 1370 psia (Figure 5.5.1).

The hot leg A level beyond the U-bend entered the steam generator at 21.5 minutes but the steam generator A secondary remained inactive (Figure 5.5.4). The hot leg B level followed at 27 minutes. The steam generator B feed was active at this time. Thus, the primary system depressurization rate increased somewhat (Figure 5.5.1) through the condensation of primary system vapor in steam generator B. At 30 minutes, the cold leg discharge leak was isolated, as specified.

Upon leak isolation at 30 minutes, the HPI flow rate was 550 lbm/h (Figure 5.5.5). The primary system therefore refilled and repressurized (Figures 5.5.1 through 5.5.3). The hot leg and core region levels began to increase immediately. The loop B steam generator primary level exceeded the steam generator upper tubesheet beyond 31 minutes; this occurred in loop A at 33.7 minutes. The temperature difference between the core exit fluid and the steam generator B secondary saturation (which was higher than the steam generator A saturation temperature) exceeded the control value of 50F. Thus, steam generator B steaming was halted and both steam generators became inactive (Figure 5.5.4). The fluid temperature rise across the core began to increase from 70F. The primary system began to repressurize, at approximately 30 psi/min, from 1200 psia. The pressurizer level began to rise. The middle-elevation hot leg fluid began to subcool as the primary system pressure increased, but the voided upper-elevation regions and the core exit remained saturated (Figure 5.5.6).

The downcomer and core-inlet fluid subcooling began to increase after leak closure (Figure 5.5.7). The downcomer level began to rise at 40 minutes and, at 43 minutes, the core exit fluid subcooled (Figure 5.5.6) and the primary system repressurization rate slowed. The downcomer refilled at 46 minutes, the core region level began to rise, and the primary system again began to repressurize from 1540 psia (Figure 5.5.1). But the hot leg riser levels achieved the U-bend elevation at 50 minutes (Figure 5.5.2), both steam generators became active, and the primary system repressurization was halted at 1675 psia (Figure 5.5.1). Manual HPI throttling to obtain a pressurizer level of 21.4 ft was begun (Figure 5.5.5) as the core exit subcooling margin

(SCM) exceeded 50F. The A1- and B1-RVVVs closed from 51 to 52 minutes, whereas the A2 and B2 valves remained open (Figure 5.5.8), apparently in response to the differing valve control setpoints.

The primary system cooldown quickly became established. Beyond approximately 55 minutes, each of the primary loop fluid temperatures began to cool at the secondary cooldown rate (Figures 5.5.6 and 5.5.7) of 100F/h. Between 54 and 58 minutes, the RVVVs closed in the order A1 and B1, B2, and then A2 (Figure 5.5.8). The test was relatively uneventful beyond 1 hour. HPI was throttled almost continuously and was sporadically terminated when the SCM exceeded 100F.

The primary system depressurization rate was perturbed somewhat by the changes in HPI flow (Figure 5.5.9), as were the core region and downcomer levels (Figure 5.5.10). After HPI was interrupted and the rate of primary system depressurization increased, the downcomer level descended from the elevation of the RVVVs toward the nozzle elevation. As HPI was reactivated, the downcomer level trend was reversed; this occurred at 155 and 270 minutes.

The test was terminated at 299 minutes, based on the dual criteria of an SCM greater than 50F and pressure less than 400 psia for 2 hours. At termination, the primary and secondary system pressures were 305 and 50 psia, respectively. The primary and secondary systems remained active, with primary loop fluid temperatures ranging from 265 to 300F.

Comparison

The leak was isolated at 30 minutes in Test 5. Until this event, Test 5 repeated the controls of Nominal Test 9 (3109AA) and Nominal Repeat Test 10 (311000). Comparing Tests 5 and 10, their transients were virtually indistinguishable until leak isolation. For example, they maintained similar primary system pressures (Figure 5.5.11), primary system total fluid mass and energy (Figures 5.5.12 and 5.5.13), hot leg riser levels (Figure 5.5.14), and reactor vessel levels (Figure 5.5.15). This inter-test similarity was eliminated upon leak isolation.

Whereas the Nominal Repeat Test 10 depressurized through HPI condensation of core steam and, later, through BCMs, the primary system abruptly repressurized in Test 5 (Figure 5.5.16). The hot leg riser and stub levels were near

the steam generator upper tubesheets upon leak isolation (Figure 5.5.17), thus primary-to-secondary heat transfer was quickly precluded as the levels rose after leak isolation. Also, the fluid volumetric reduction through leak discharge was eliminated upon leak isolation. The primary thus repressurized at nearly 25 psi/min, achieving 1675 psia by 50 minutes (Figure 5.5.16). At this time, the primary fluid mass increase upon leak closure obtained loop refill and a natural circulation cooldown ensued. The first refill spillover in Test 10, on the other hand, was delayed until 270 minutes (Figure 5.5.17). In summary, the Test 5 and 10 transients were nearly identical until leak isolation. Upon closure of the leak in Test 5, the primary system repressurized until loop circulation was reestablished.

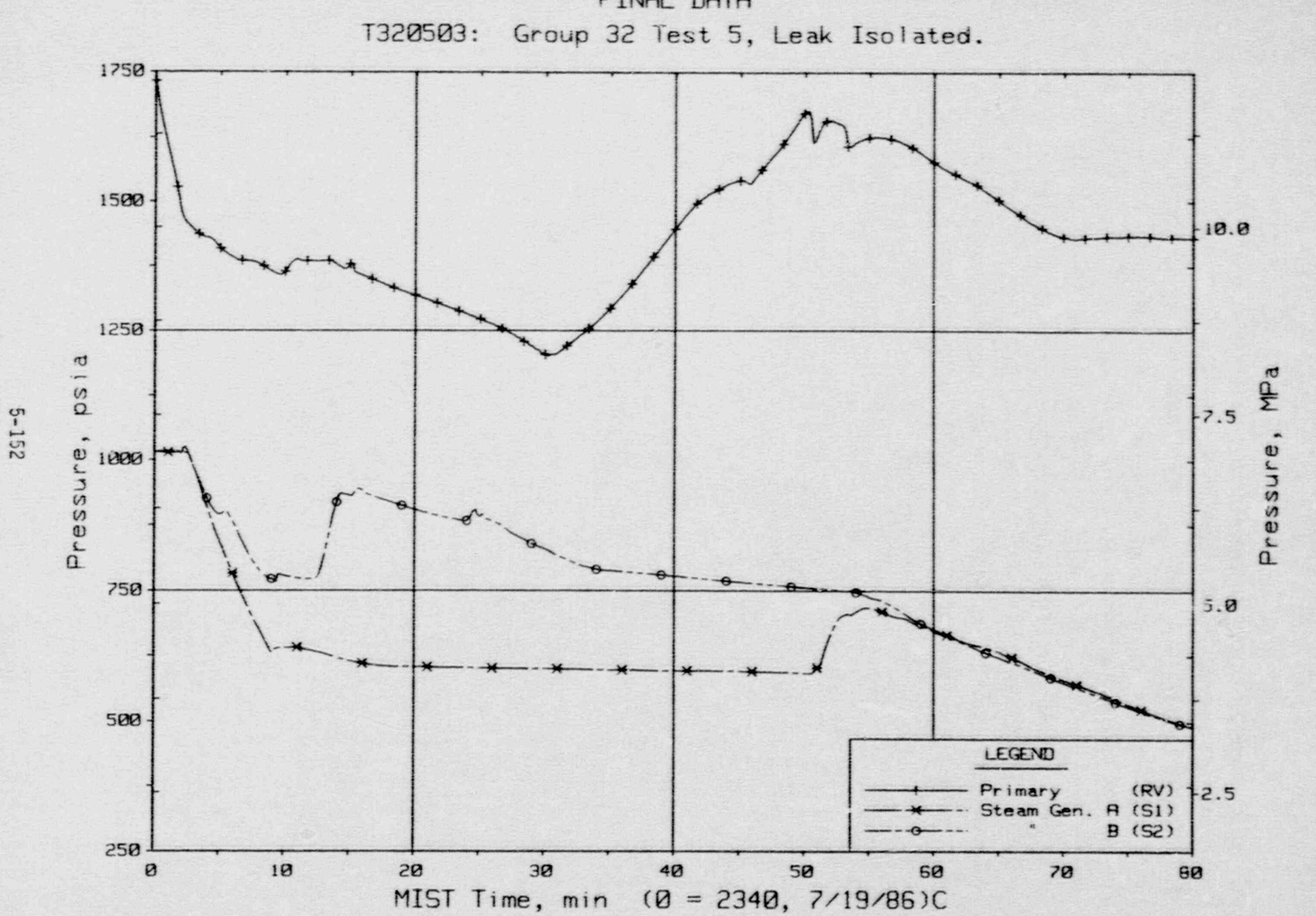

Figure 5.5.1. Primary and Secondary System Pressures (GPOIs)

Wed Jul 13 10:11:09 1988

PSGP1

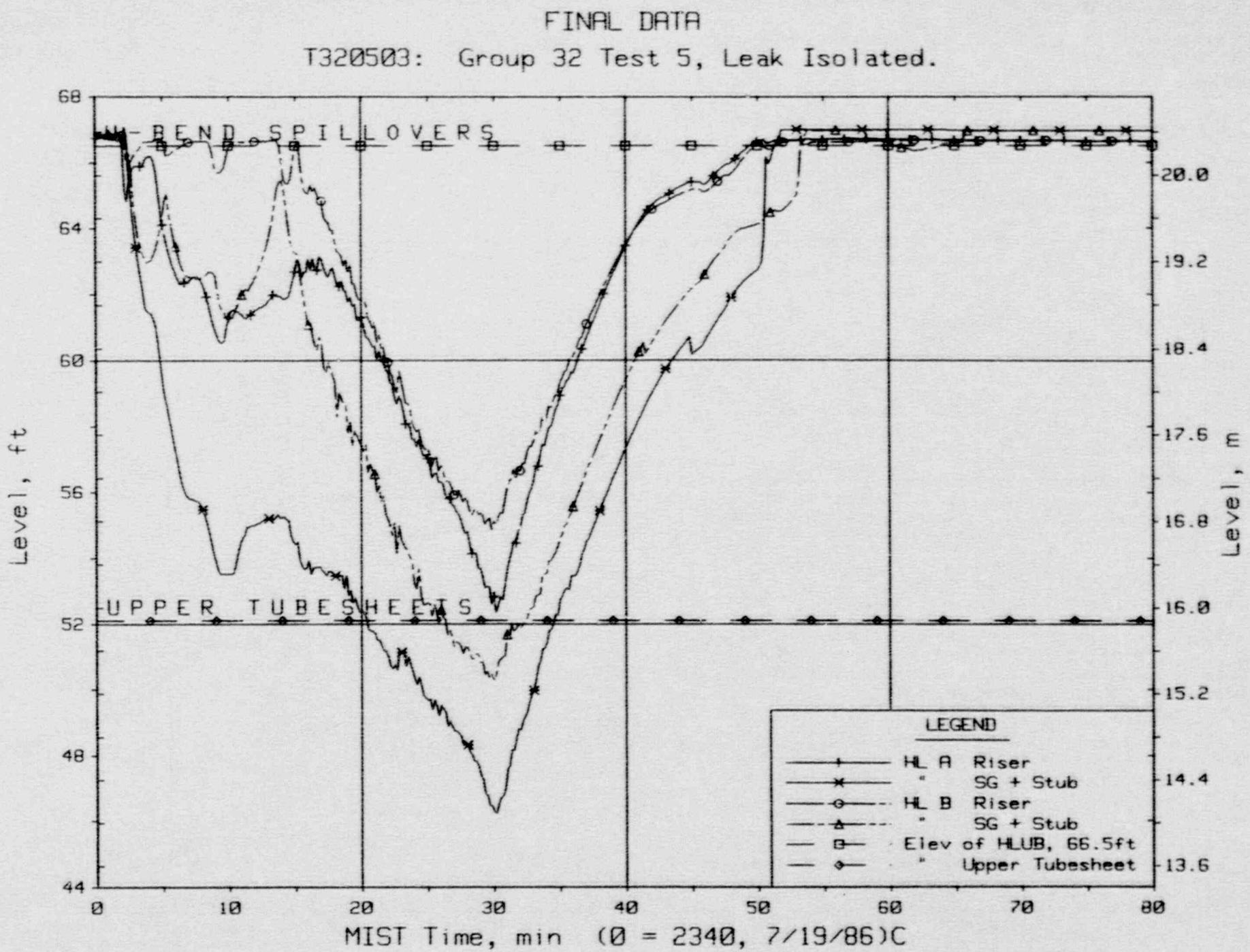

Figure 5.5.2. Hot Leg Riser and Stub Collapsed Liquid Levels

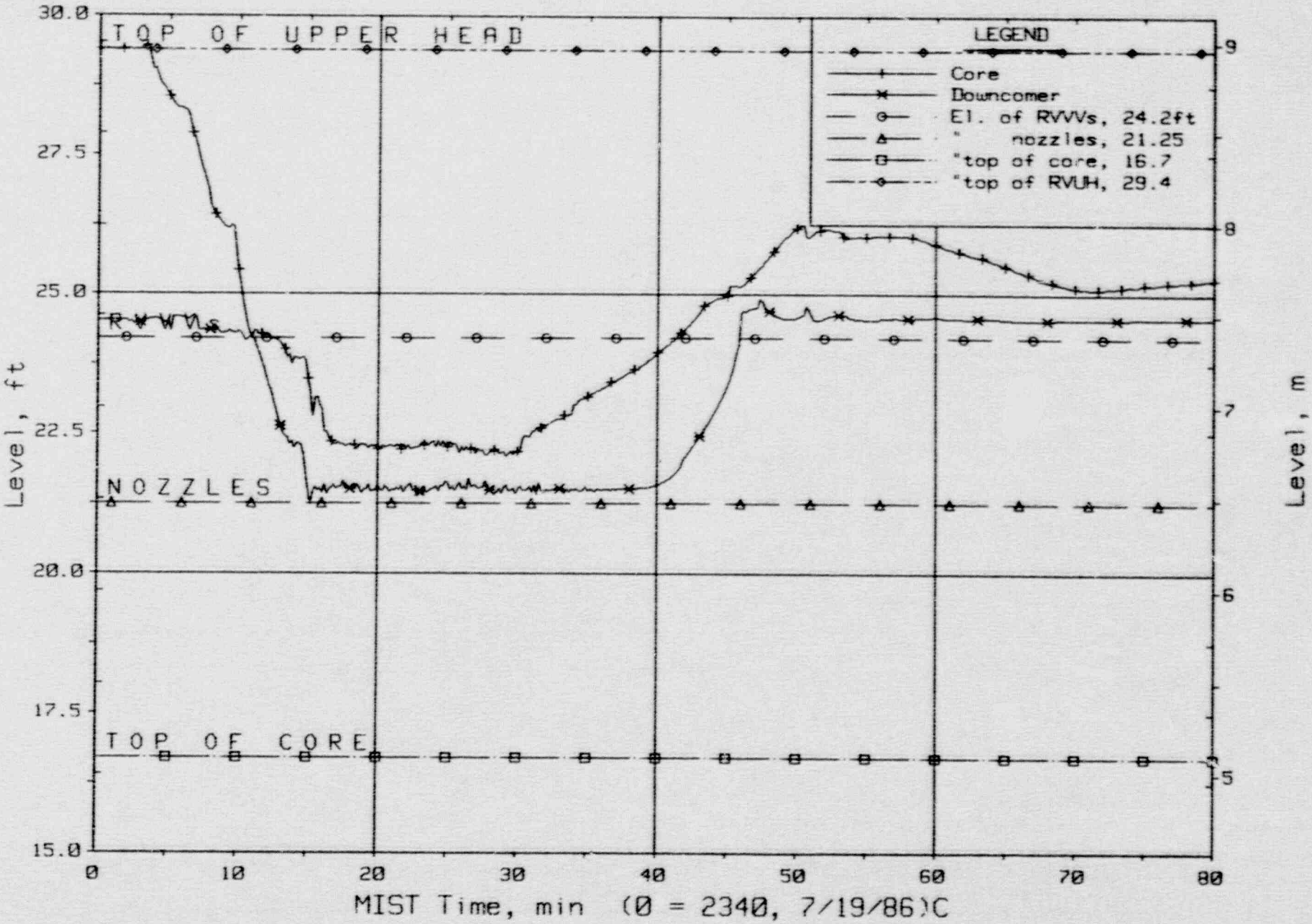

Figure 5.5.3. Core-Region Collapsed Liquid Levels

Wed Jul 13 10:49:15 1988

COLV1

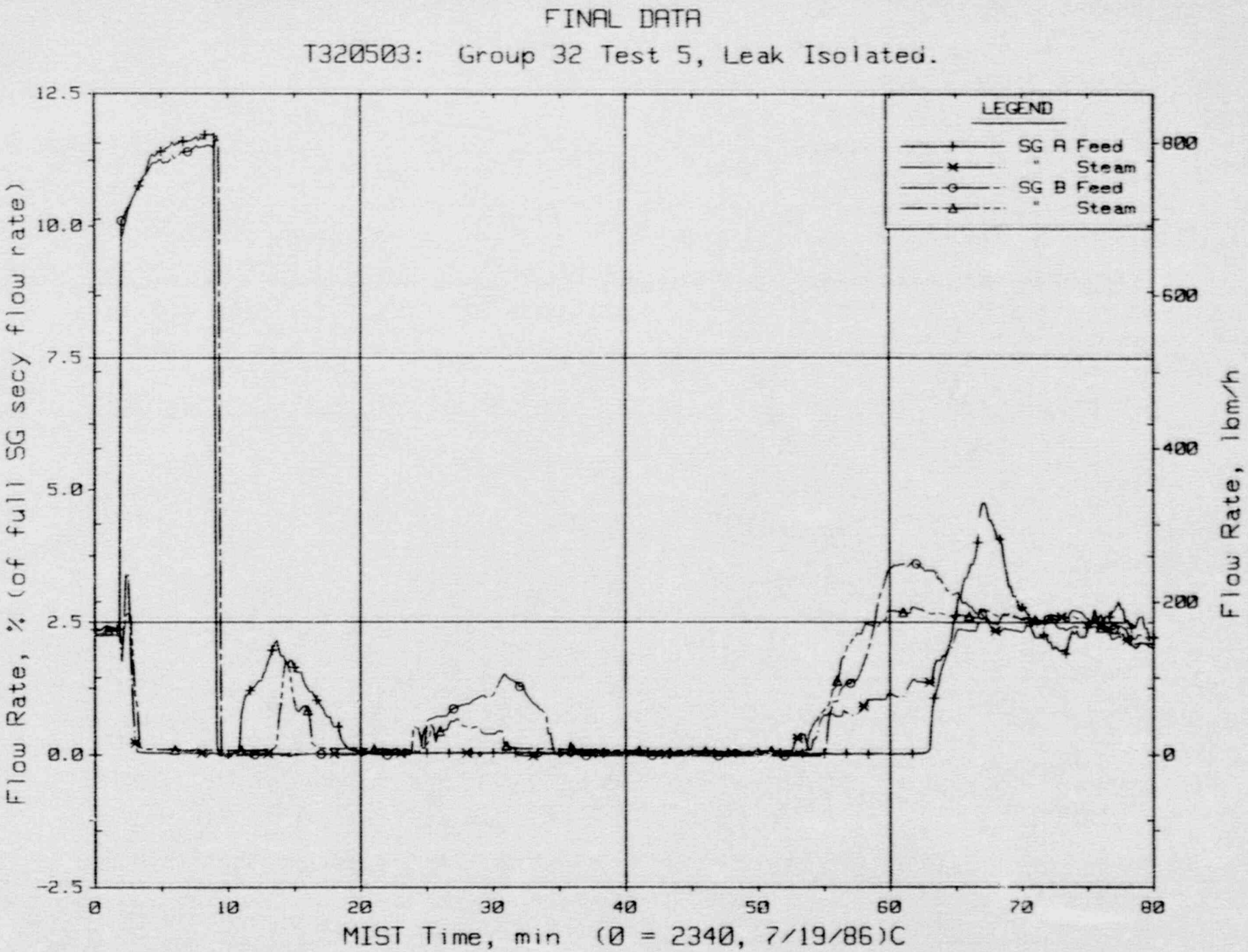

Figure 5.5.4. Secondary System Flow Rates

Wed Jul 13 10:21:37 1988

SGFL2

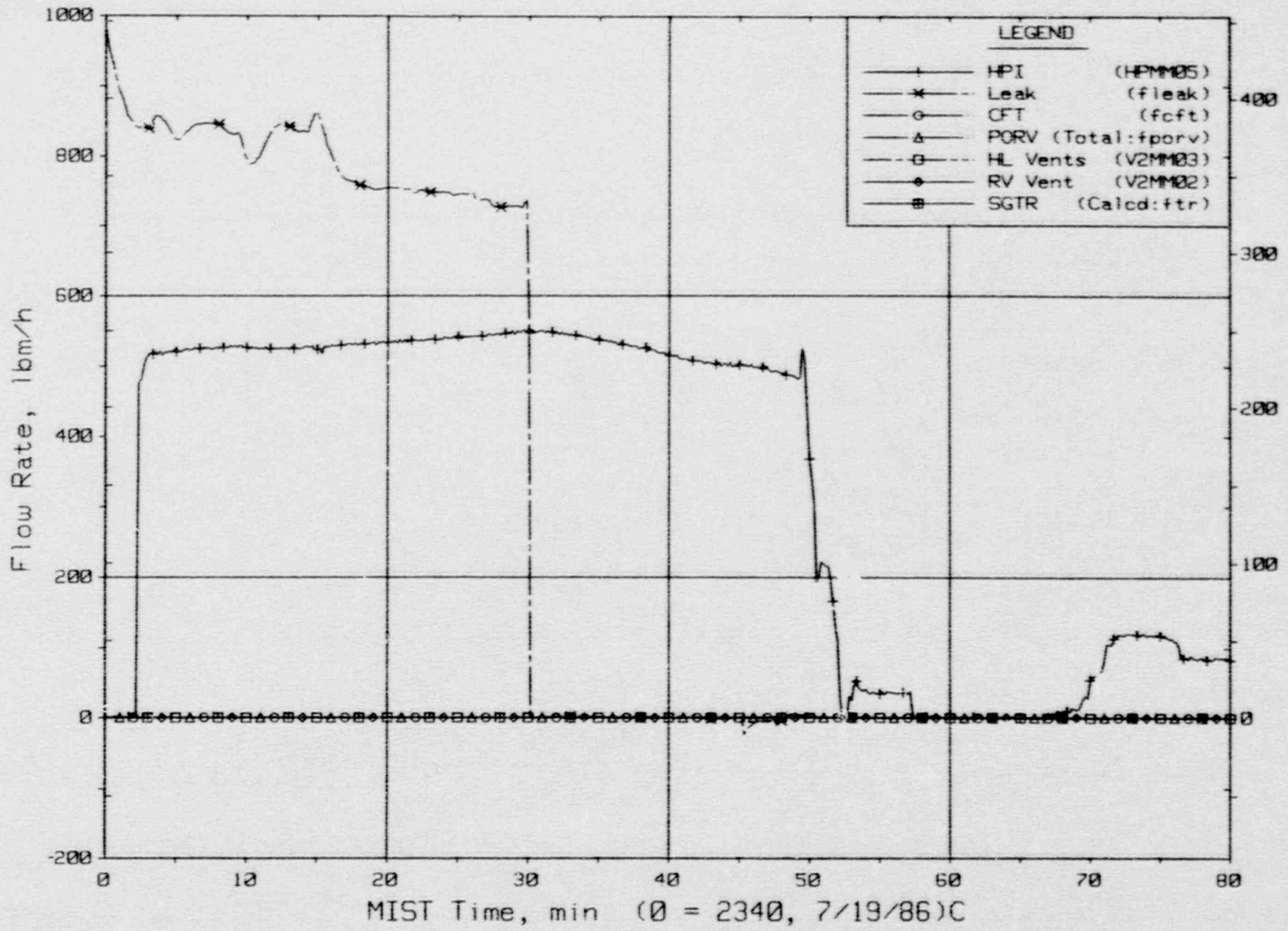

Figure 5.5.5. Primary System Boundary Flow Rates

Wed Jul 13 10:25:10 1988

PRFL3

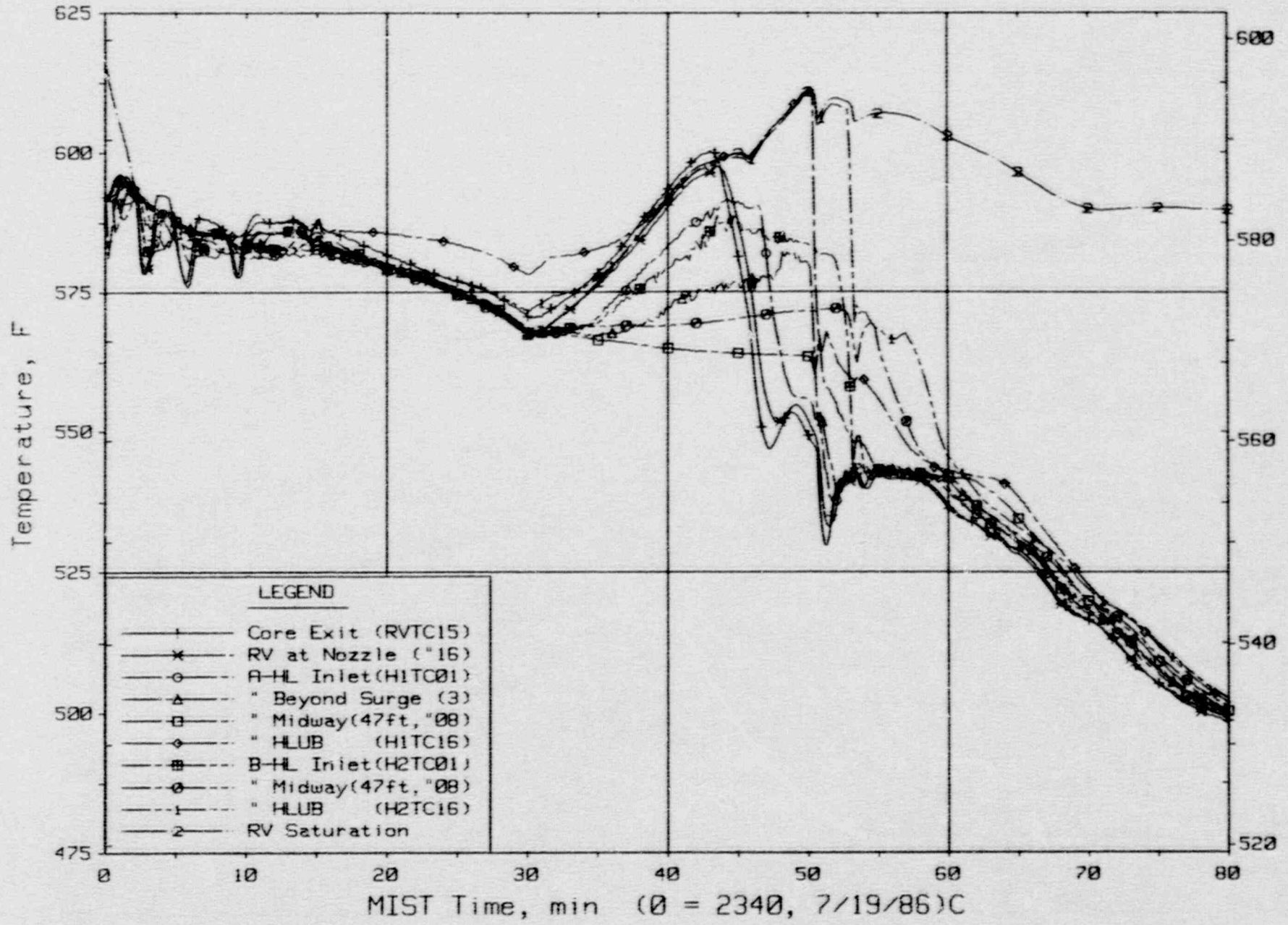

Figure 5.5.6. Composite Core Exit and Hot Leg Fluid Temperatures

Wed Jul 13 10:29:55 1988

PRKT1

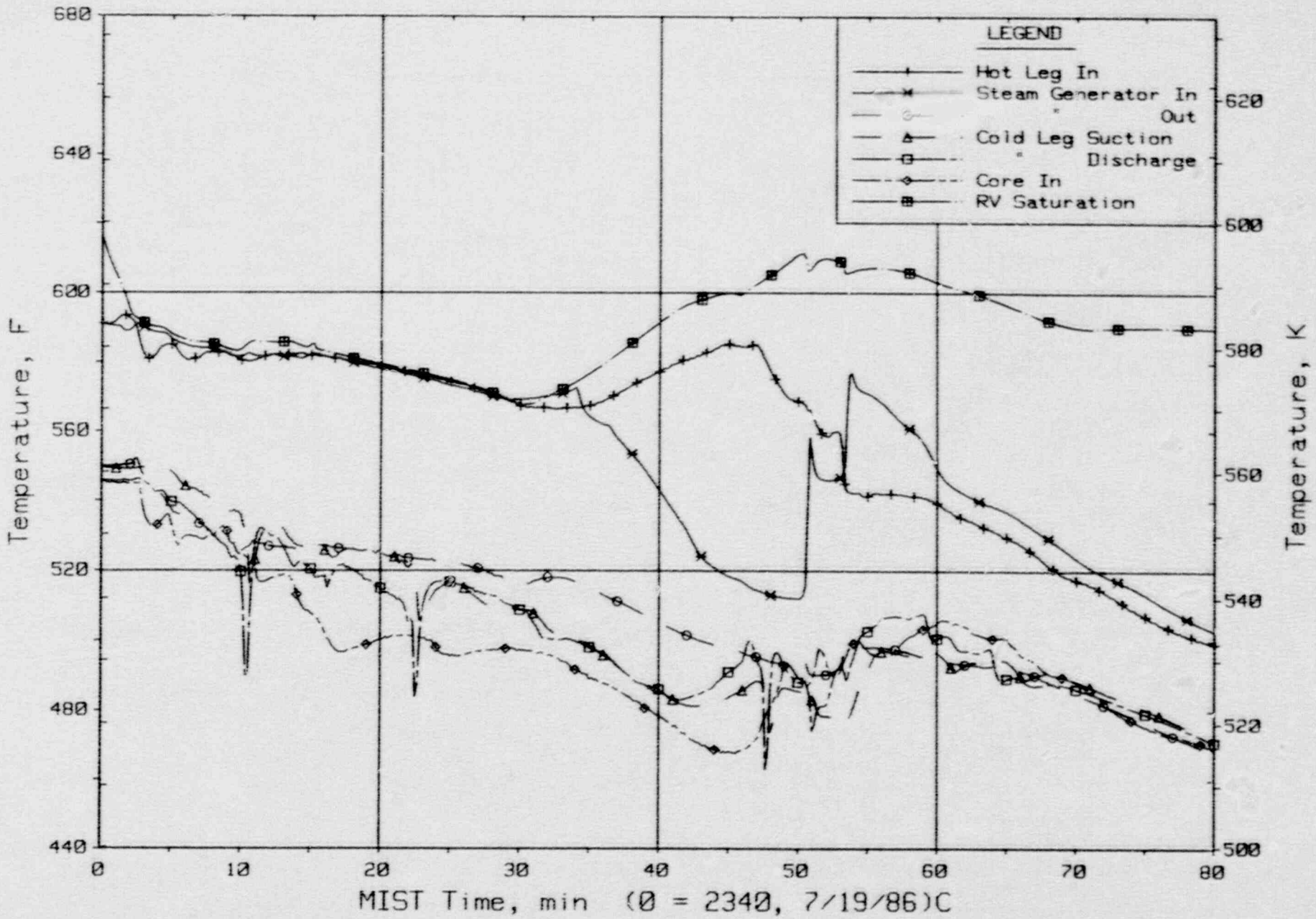

Figure 5.5.7. Average Primary Fluid Temperatures (RTDs)

Wed Jul 13 10:34:05 1988

PRAT0

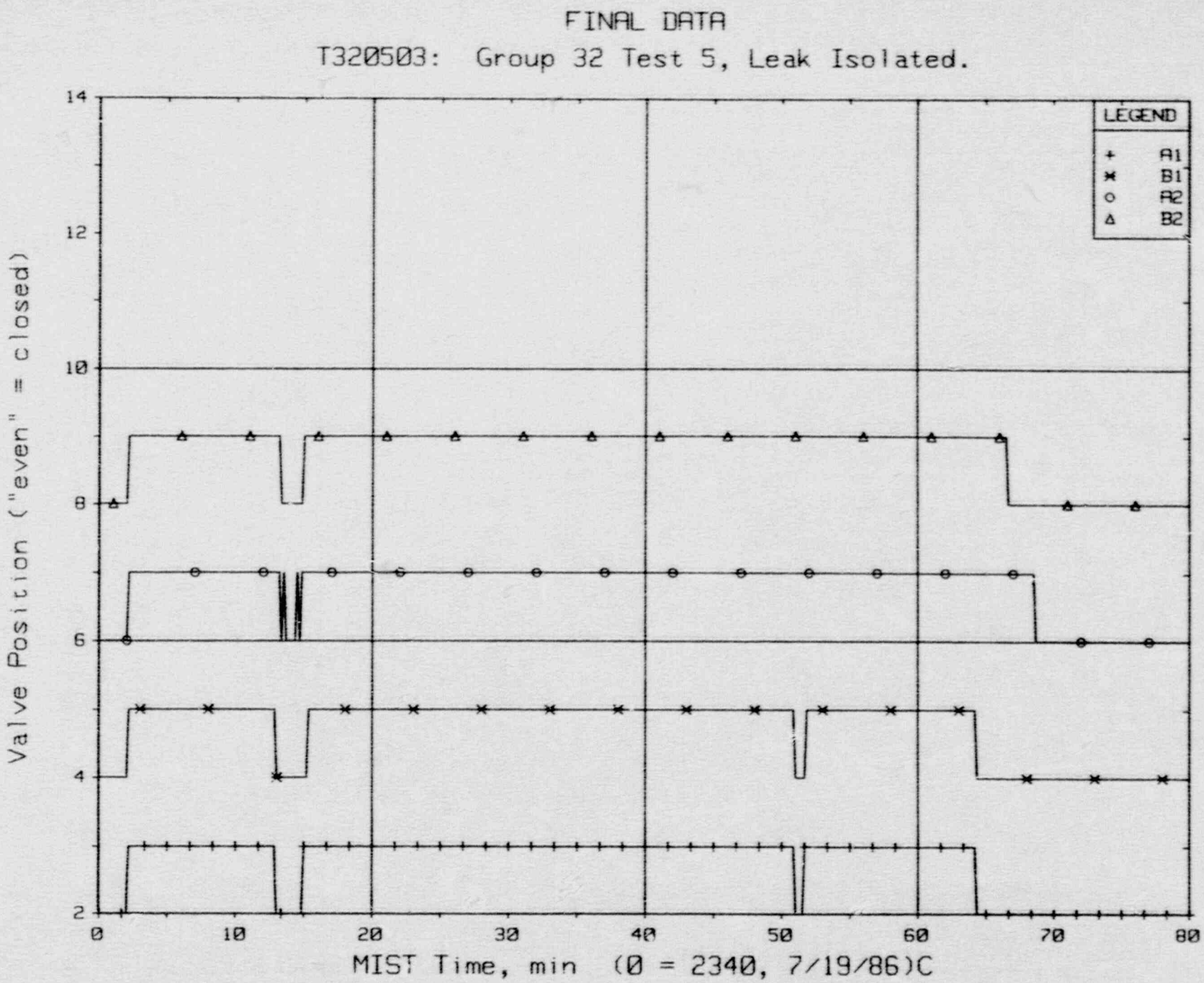

Figure 5.5.8. Reactor Vessel Vent Valve Positions

Wed Jul 13 10:37:05 1988

VVLS1

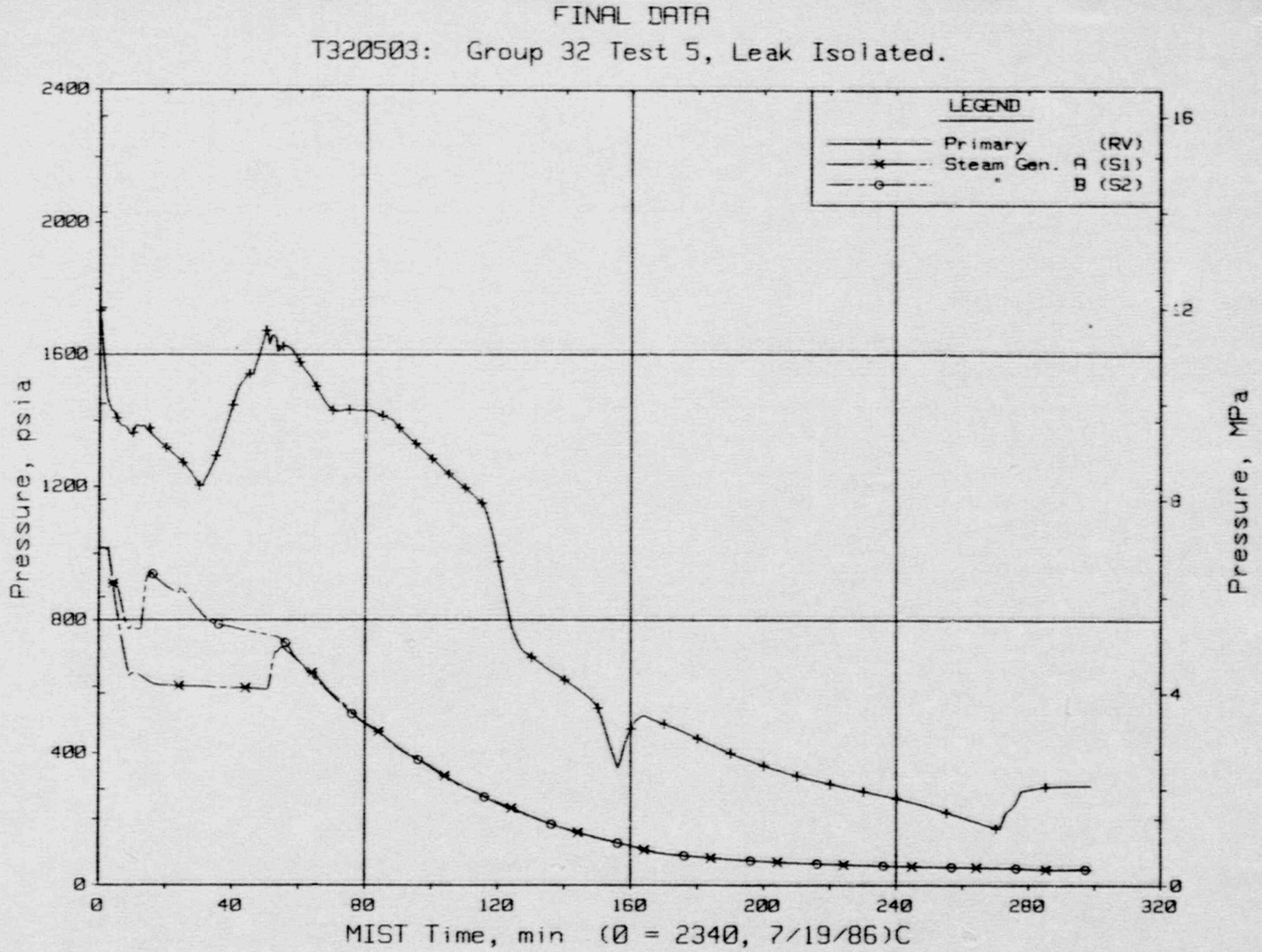

Figure 5.5.9. Primary and Secondary System Pressure (GP01s)

Wed Jul 13 10:39:24 1988

PSGP1

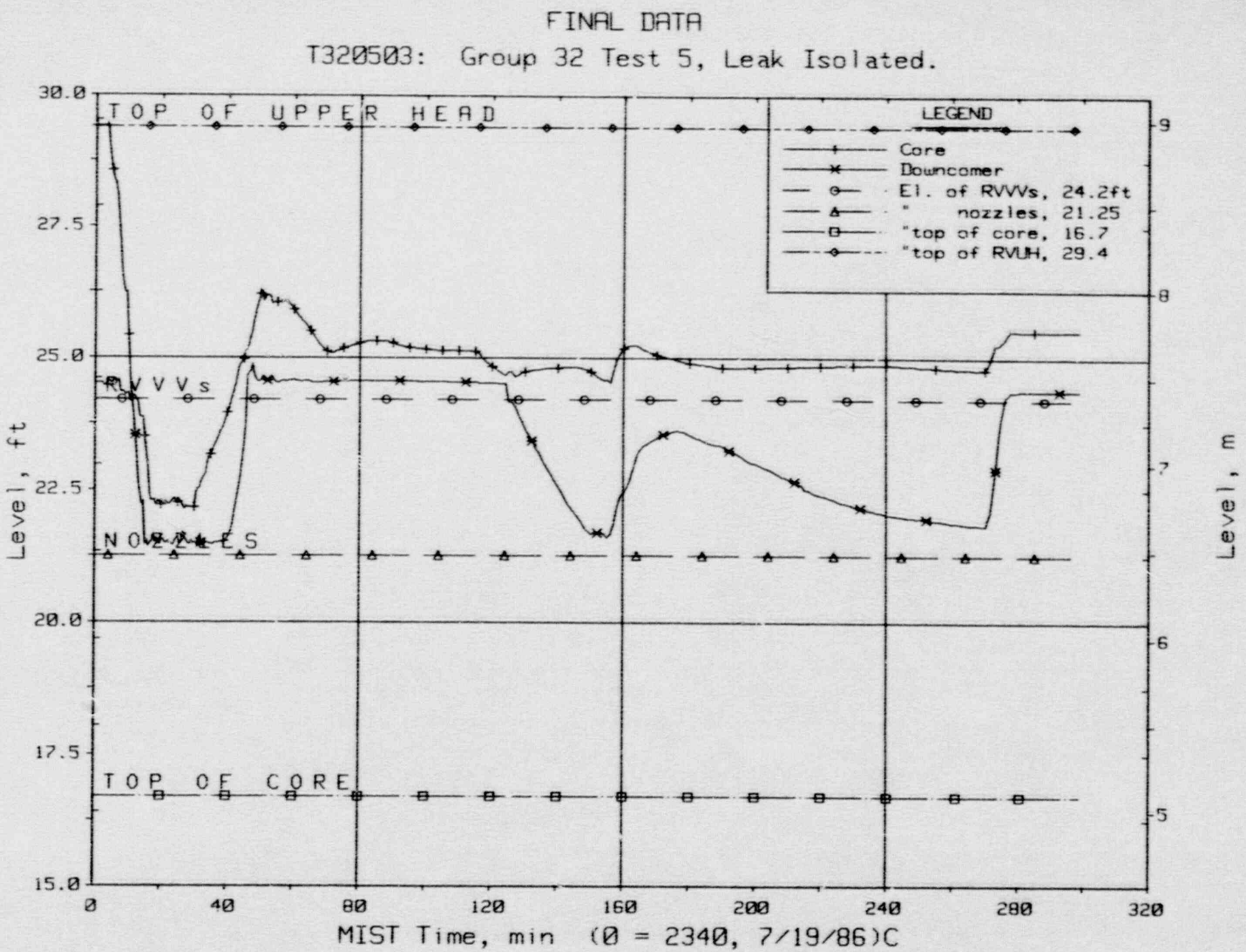

Figure 5.5.10. Core-Region Collapsed Liquid Levels

Wed Jul 13 10:42:26 1988

COLV1

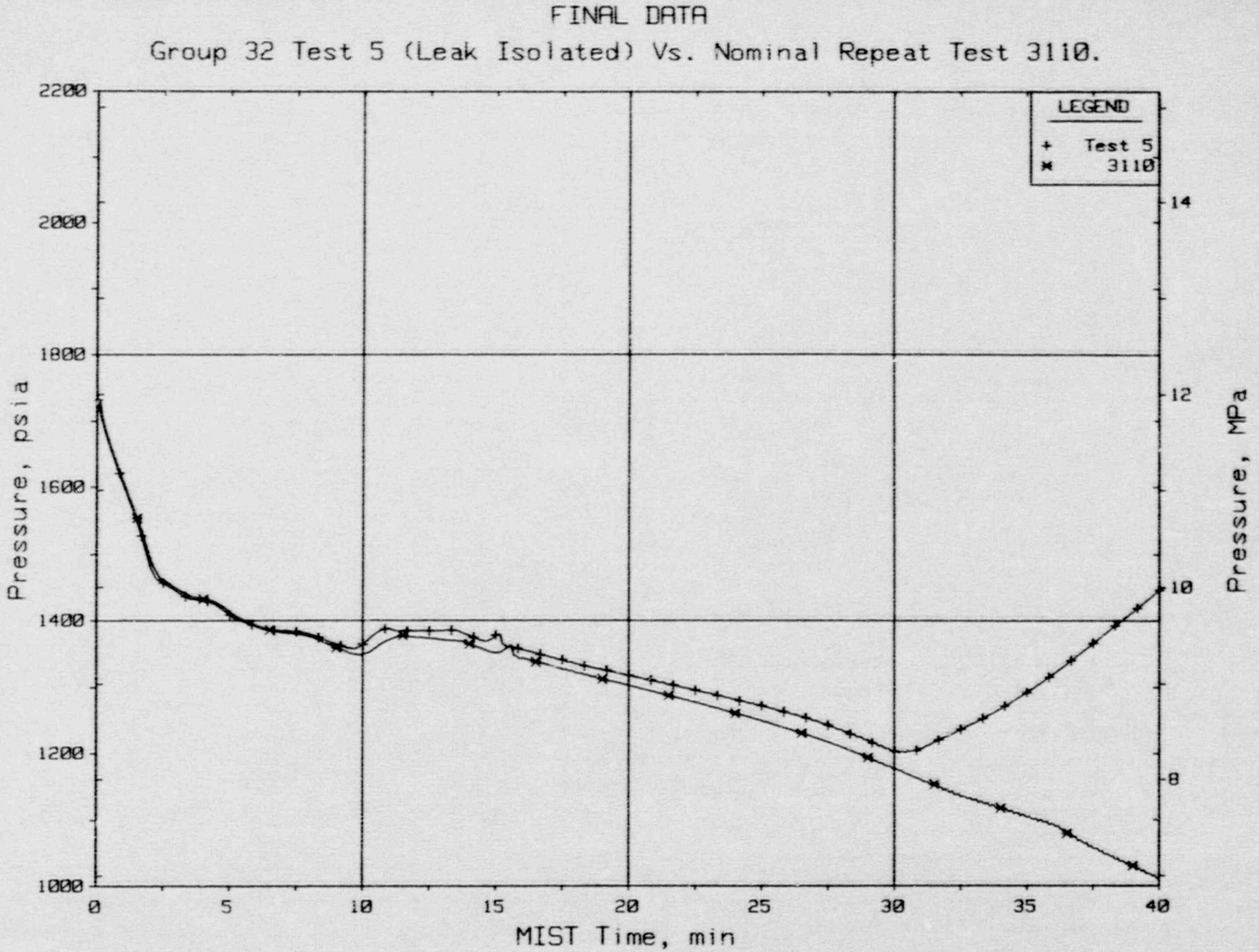

Figure 5.5.11. Reactor Vessel Pressure

Wed Jul 13 10:58:19 1988

5RVGP1

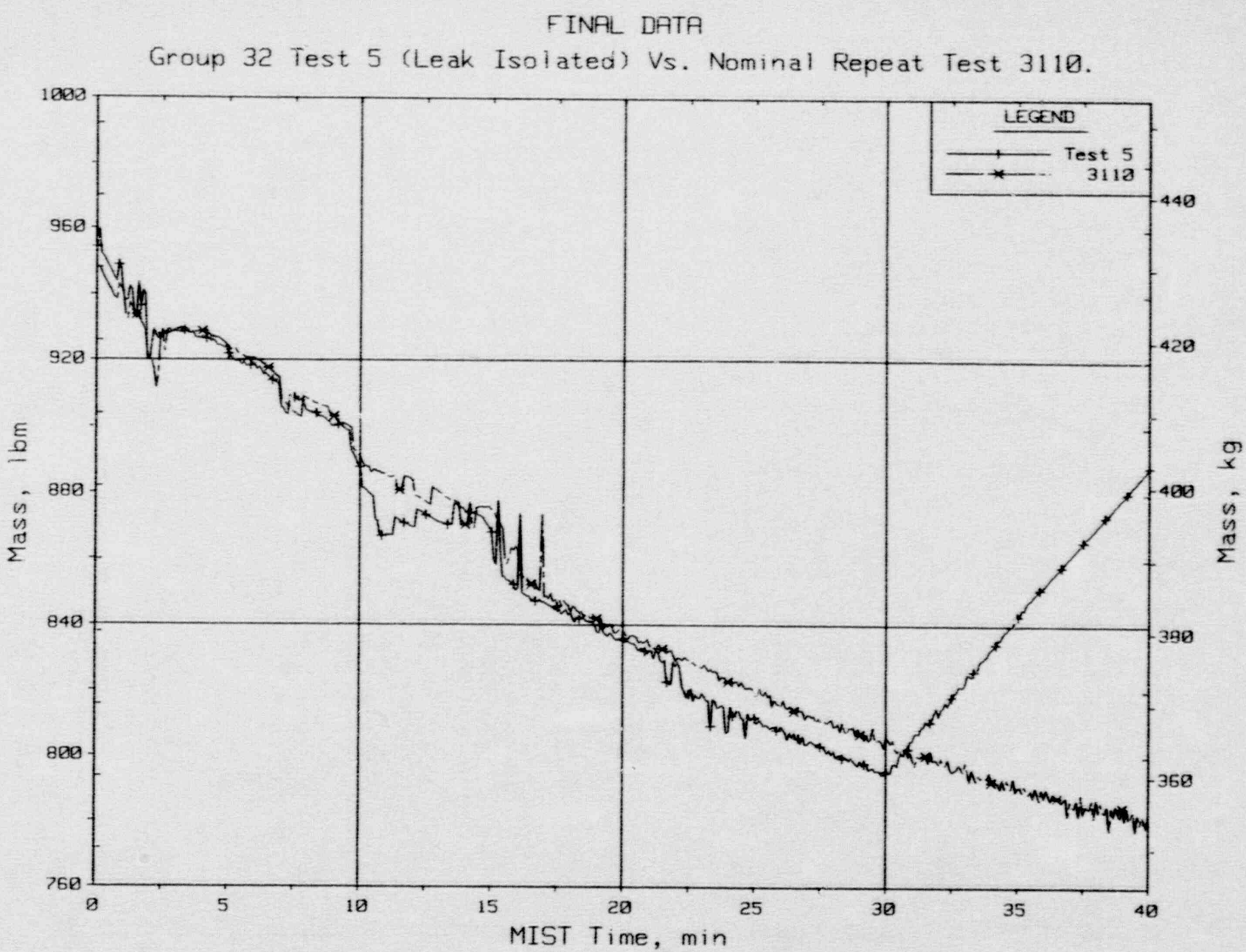

Figure 5.5.12. Primary System Total Fluid Mass (Indicated, PLML20s)

Wed Jul 13 11:00:19 1988

5PRML1

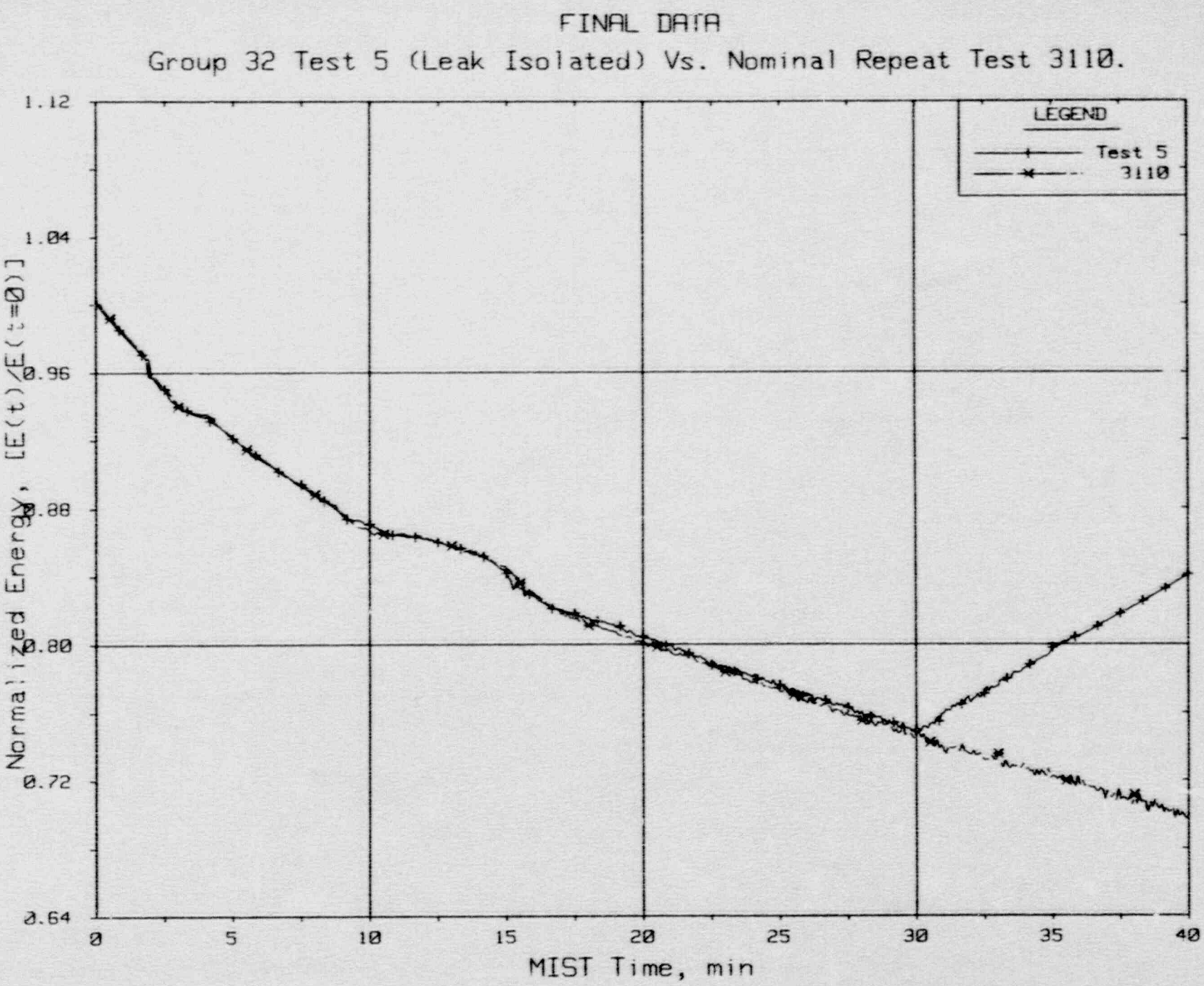

Figure 5.5.13. Primary System Indicated Total Fluid Energy

Wed Jul 13 11:02:29 1988

5PRTE1

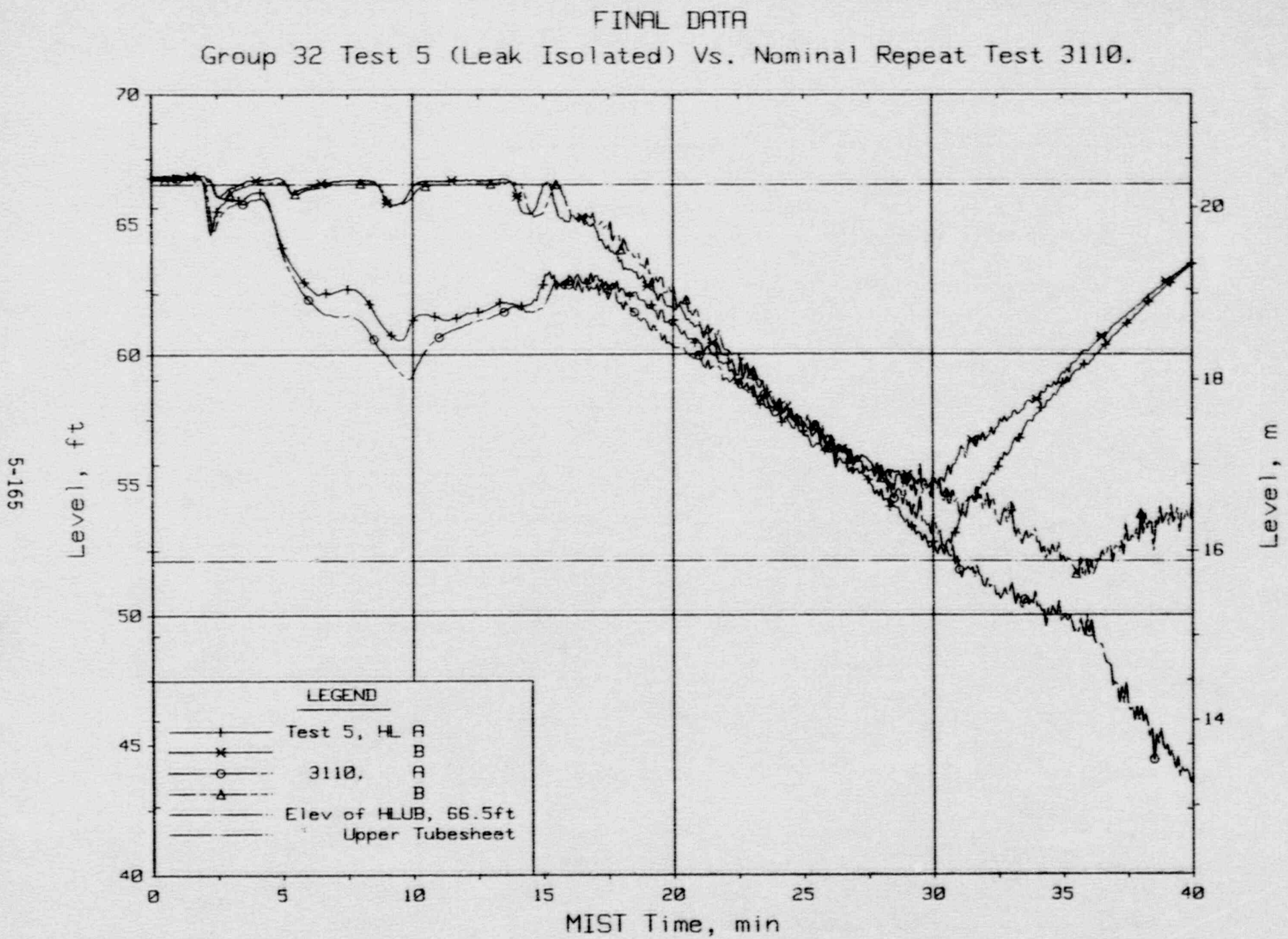

Figure 5.5.14. Hot Leg Riser Collapsed Liquid Levels

Wed Jul 13 11:05:46 1988

5HLLV1

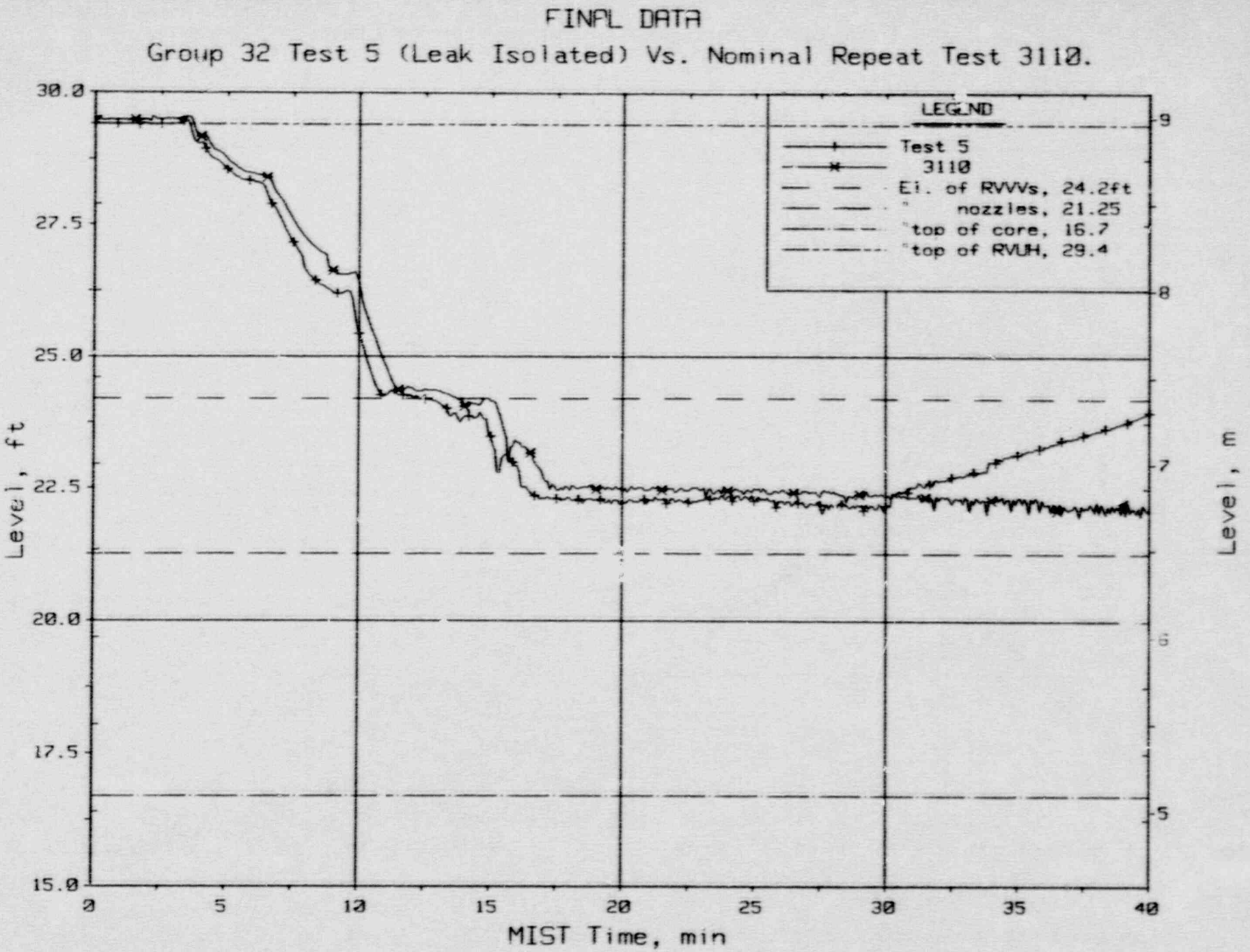

5-166

Figure 5.5.15. Reactor Vessel Collapsed Liquid Levels

Wed Jul 13 11:08:49 1988

SCOLV1

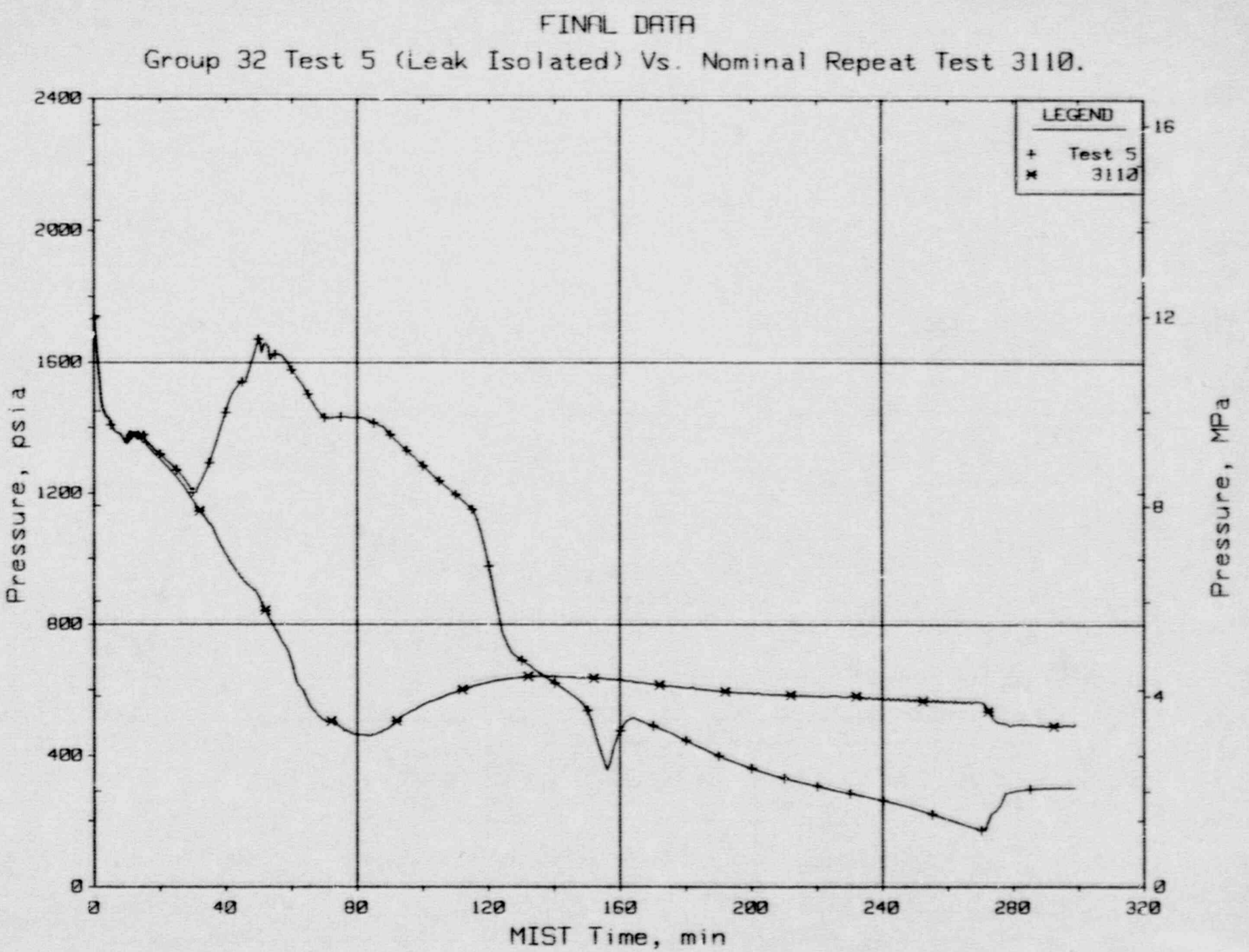

Figure 5.5.16. Reactor Vessel Pressure

Wed Jul 13 11:11:00 1988

3RVGP1

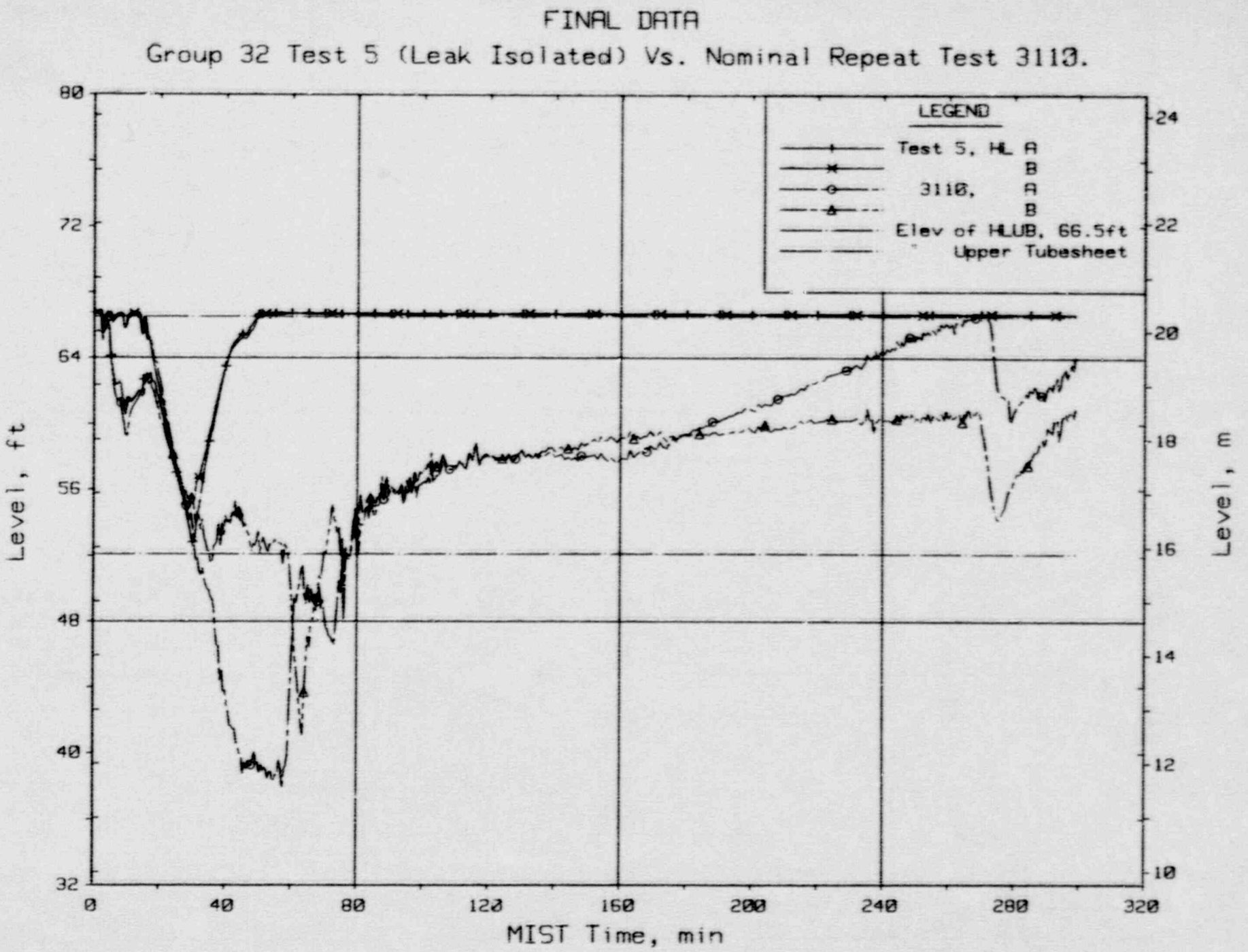

Figure 5.5.17. Hot Leg Riser Collapsed Liquid Levels

Wed Jul 13 11:14:20 1988

SHELLV1

5.6. Reduced HPI Capacity, Test 6

The reduced HPI capacity of Test 6 (320604) resulted in a delayed introduction of HPI to the loop, compared to the times of HPI introduction observed with full HPI capacity. Because of this approximately 1-minute delay (until more than 3 minutes after leak opening), and also because of the reduced injection flow rate, the initial hot leg voiding and flow interruption were rapid and quite symmetric. The hot leg riser and stub levels in both loops receded from the U-bend spillover elevation at 2 minutes (Figure 5.6.1). After two subsequent spillovers, both hot leg levels continually subsided from the spillover elevation beyond 8.6 minutes. Both steam generator secondary pressures decreased with secondary refill, although the steam generator B secondary repressurized slightly after 4 minutes due to a brief period of primary-to-secondary heat transfer (Figure 5.6.2). By 6 minutes, the reactor vessel collapsed liquid level had decreased to the elevation of the RVVVs, and both the reactor vessel (RV) and downcomer levels began to decline (Figure 5.6.3). By 9 minutes, the reactor vessel and downcomer levels reached the vicinity of the cold leg and hot leg nozzles. The refill of the steam generator secondaries was completed at 9.2 minutes. The steam generator secondary pressures then remained quite constant, indicating negligible primary-to-secondary heat transfer. The temperature difference between the core exit fluid and the steam generator saturation temperatures, which had exceeded the setpoint of 50F (for secondary depressurization) at 3 minutes, now stabilized at about 80F. The steam generators thus became relatively inactive for a prolonged period.

The continuing excess of leak flow rate over HPI flow caused the hot leg levels to decrease toward the steam generators (Figure 5.6.1). The (broken) cold leg B1 discharge piping began to void at 11.6 minutes, the leak fluid temperature abruptly increased (Figure 5.6.4) and, at 12.3 minutes, the leak flow rate decreased, indicating saturated conditions at the leak site. The excess of leak over HPI flow was thus reduced from about 600 to 200 lbm/h and the total primary system fluid mass stabilized (Figure 5.6.5). The hot leg levels stabilized and then began to slowly increase, thus precluding primary-to-secondary heat transfer through condensation of primary system vapor (BCM). Whereas the hot leg levels stabilized, the cold leg suction and

discharge levels voided sporadically between 12 and 29 minutes. At 30 minutes, the leak quality apparently increased, causing the leak flow rate to decrease further and to approximately equal the (reduced-capacity) HPI flow rate. The primary system pressure, which had been nearly constant at 1350 psia, began to diminish slowly (Figure 5.6.2) in response to the enhanced volumetric flow rate out the break. The resulting gradual primary system depressurization with negligible primary-to-secondary heat transfer was of long duration.

During the succeeding 4 hours, the steam generator B secondary depressurized somewhat (Figure 5.6.2), apparently due to steam leakage. Steam generator B depressurized at approximately 90 psi/h and generator A depressurized at half that rate, whereas the primary system depressurized at approximately 185 psi/h. Intermittent feeding of steam generator B was recorded. These feed cycles, with steaming not in evidence, increased the calculated steam generator B secondary fluid mass (Figure 5.6.6). The calculated steam generator B mass, which had been 6 lbm below that indicated after the secondary refill was completed, approximately equalled the indicated value after 2 hours. The hot leg and stub levels in both loops declined slowly after 1 hour. The U-bend downstream primary levels entered steam generators A and B at 133 and 165 minutes, but with no dramatic system response.

The hot leg high-point vents (HLHPVs) were opened by procedure after 4 hours of testing. The vents apparently had little effect on the system conditions, although certain interactions occurred near the time at which the HLHPVs were opened. Steam generator B was fed from 235 to 241 minutes (Figure 5.6.7) to maintain its secondary level. The loop B hot leg riser and stub levels, which had been fairly constant, began to increase. As the steam generator B primary level transcended the elevation of the upper tubesheet near 240 minutes (the time at which the HLHPVs were opened), the loop B U-bend fluid temperature began to decrease at a slower rate than the primary saturation temperature, and thus superheated. Also as the steam generator B feeding began at 235 minutes, the leak flow rate decreased noticeably, indicating increased leak fluid quality. The cold leg suction piping in all the loops began to lose liquid at this time, and the loop A as well as the loop B hot leg levels began to increase.

The steam generator A primary level elevated above the steam generator at 252 minutes. The concurrent translation of loop fluid apparently caused the ATOG steam generator secondary pressure control to activate. Steam generator A was steamed beginning at 255 minutes (Figure 5.6.7), reducing its pressure from 455 to 365 psia at 266 minutes. The core minus steam generator A saturation temperature difference increased from 30 to 50F. The steam generator A feed became active at 261 minutes but, with loop flow interrupted and with the primary levels above the steam generators, primary system pressure was unresponsive to this steam generator activity (Figure 5.6.2). The gradual primary system depressurization continued from 660 psia at 240 minutes to 510 psia upon test termination at 300 minutes. The core flood tank became weakly active at 270 minutes as the primary system depressurized below 575 psia.

At test termination, the system was again relatively quiescent. The reactor vessel and downcomer collapsed liquid levels remained near the nozzle elevation, the RVVVs remained open, and the hot leg levels had virtually stabilized below the U-bends but above the steam generators. The loop was refilled after test termination.

Comparison

Reduced capacity HPI was used in Test 6, approximately one-half of the HPI flow rate at pressure used nominally (Figure 5.6.8). (The introduction of HPI was delayed somewhat in Test 6 because of the increased time required to pressurize the MIST HPI accumulators.) The comparison of Test 6 to Nominal Repeat Test 10 (311000 from Group 31) demonstrates an important system response -- the ability to adjust to imbalanced boundary conditions.

The RVVVs transported core steam to the reactor vessel downcomer where it was condensed by subcooled HPI. In the tests with full-capacity HPI, the heat capacity of the injected fluid was sufficient to condense the core-generated steam, offsetting the tendency of core steaming to pressurize the system. Furthermore, the transport of condensation-heated fluid to the break site obtained HPI-leak cooling sufficient to offset the core energy deposition. However, with reduced capacity HPI, the HPI heat capacity was initially insufficient to condense the entire core steam production. But the system responded to counter the excess steam production. The RVVVs continued to

discharge steam in excess of the HPI condensation capacity and the downcomer and cold leg discharge piping continued to void until the leak site fluid saturated (Figure 5.6.9 and 5.6.10). In response to the strong dependence of leak (critical) flow on fluid conditions, the leak mass flow rate decreased and the leak volumetric flow rate increased. In addition, the increased leak fluid enthalpy augmented leak-HPI cooling. These inherent adjustments occurred early in the Test 6 transient, at approximately 9 minutes. The leak fluid saturated, the measured leak fluid enthalpy indicated two-phase flow and, at 30 minutes, the leak fluid enthalpy increased toward that of saturated vapor (Figure 5.6.11). Upon the latter fluid state transition, the primary system pressure in Test 6 began to decrease continuously from 1350 psia (Figure 5.6.12). In the Nominal Repeat Test, on the other hand, the primary system depressurized up to 80 minutes, primarily through BCM heat transfer, then repressurized and stabilized when the hot leg levels attained intermediate elevations. In this manner, the primary system pressures in Tests 6 and 10 became approximately equal beyond 4 hours.

The primary system total fluid mass began to increase beyond 6 hours in test 6 (Figure 5.6.13) as the primary system depressurized sufficiently to activate the CFT. The mass still remained well below that of Test 10, however.

In summary, the decreased HPI flow rate of Test 6, much like the increased leak size of Test 2, demonstrated the inherent responsiveness of the system due primarily to the RVVVs. In both tests, the leak site fluid saturated, thus altering the system mass, energy, and volume balances toward equilibrium.

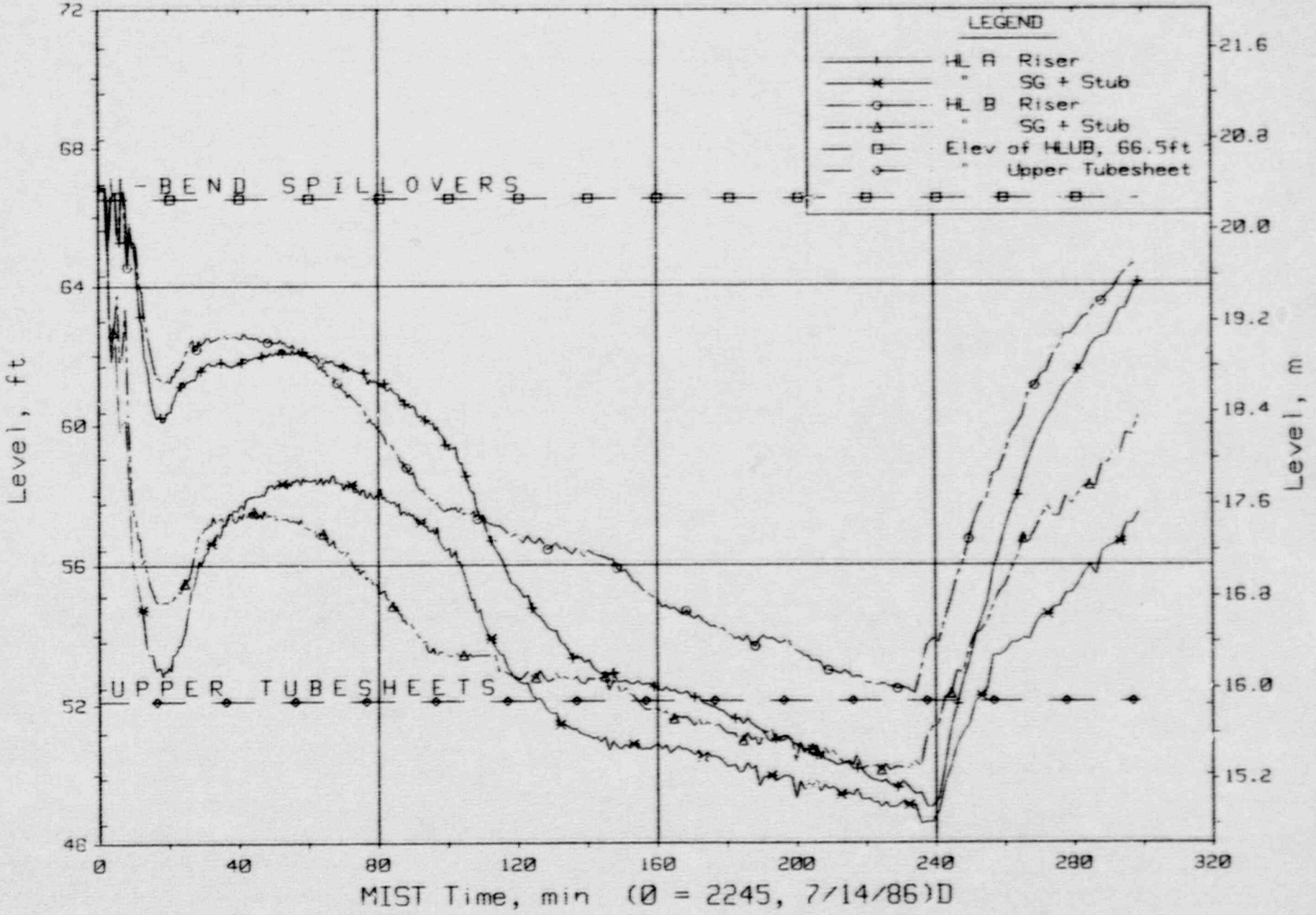

Figure 5.6.1. Hot Leg Riser and Stub Collapsed Liquid Levels

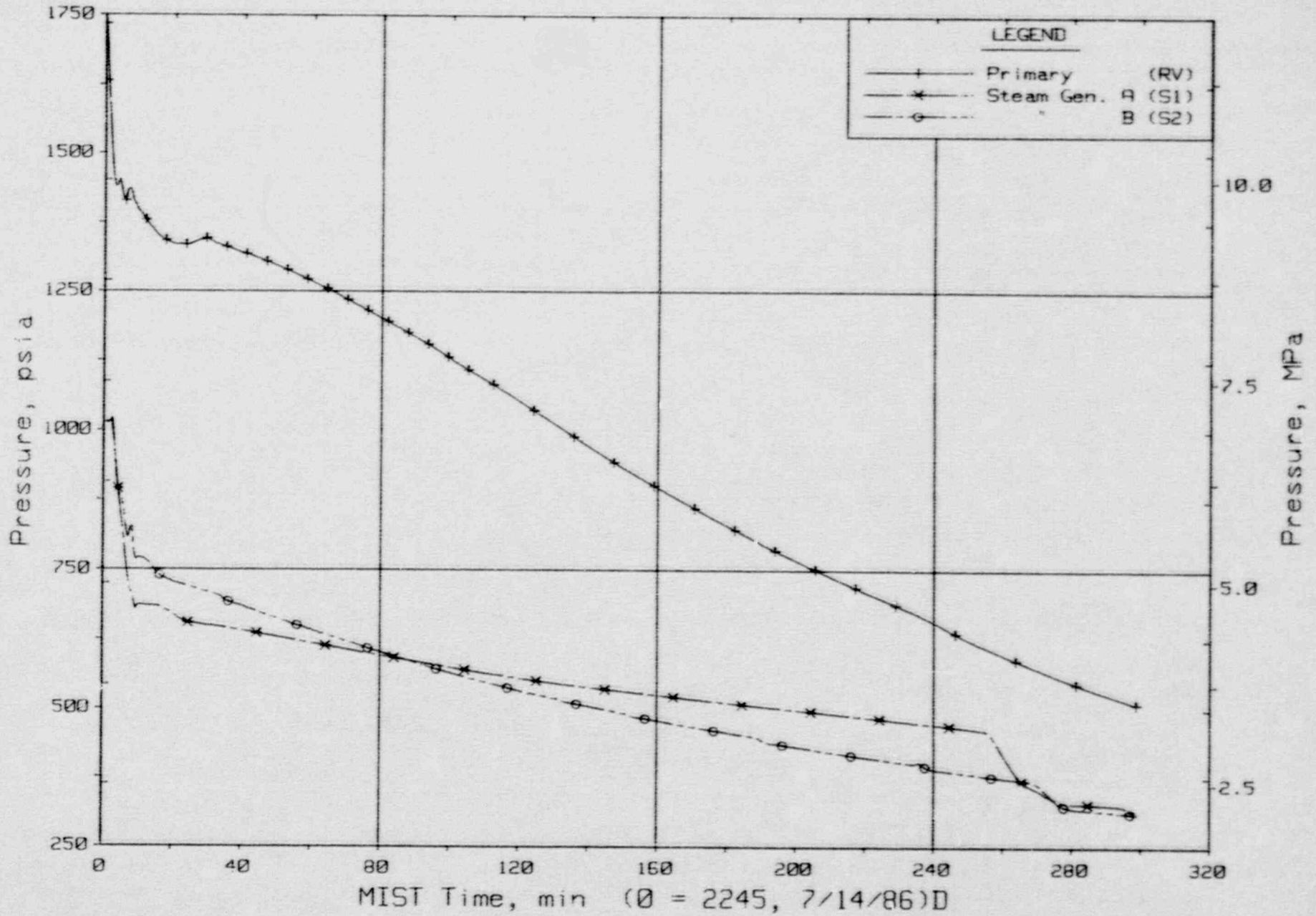

Figure 5.6.2. Primary and Secondary Pressures

Wed Jul 13 13:20:18 1988

PSGP1

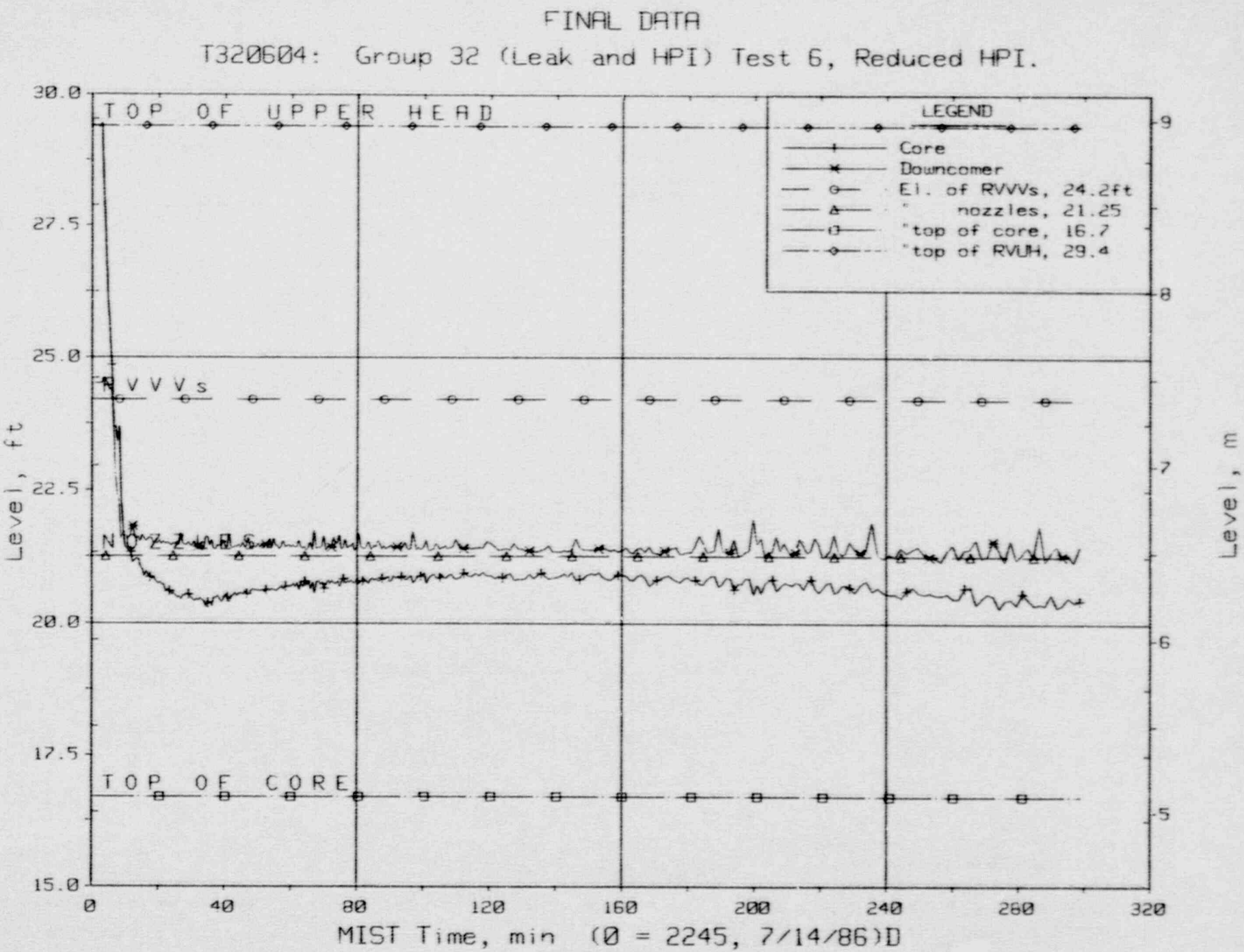

Figure 5.6.3. Core-Region Collapsed Liquid Levels

Wed Jul 13 13:23:14 1988

COLV1

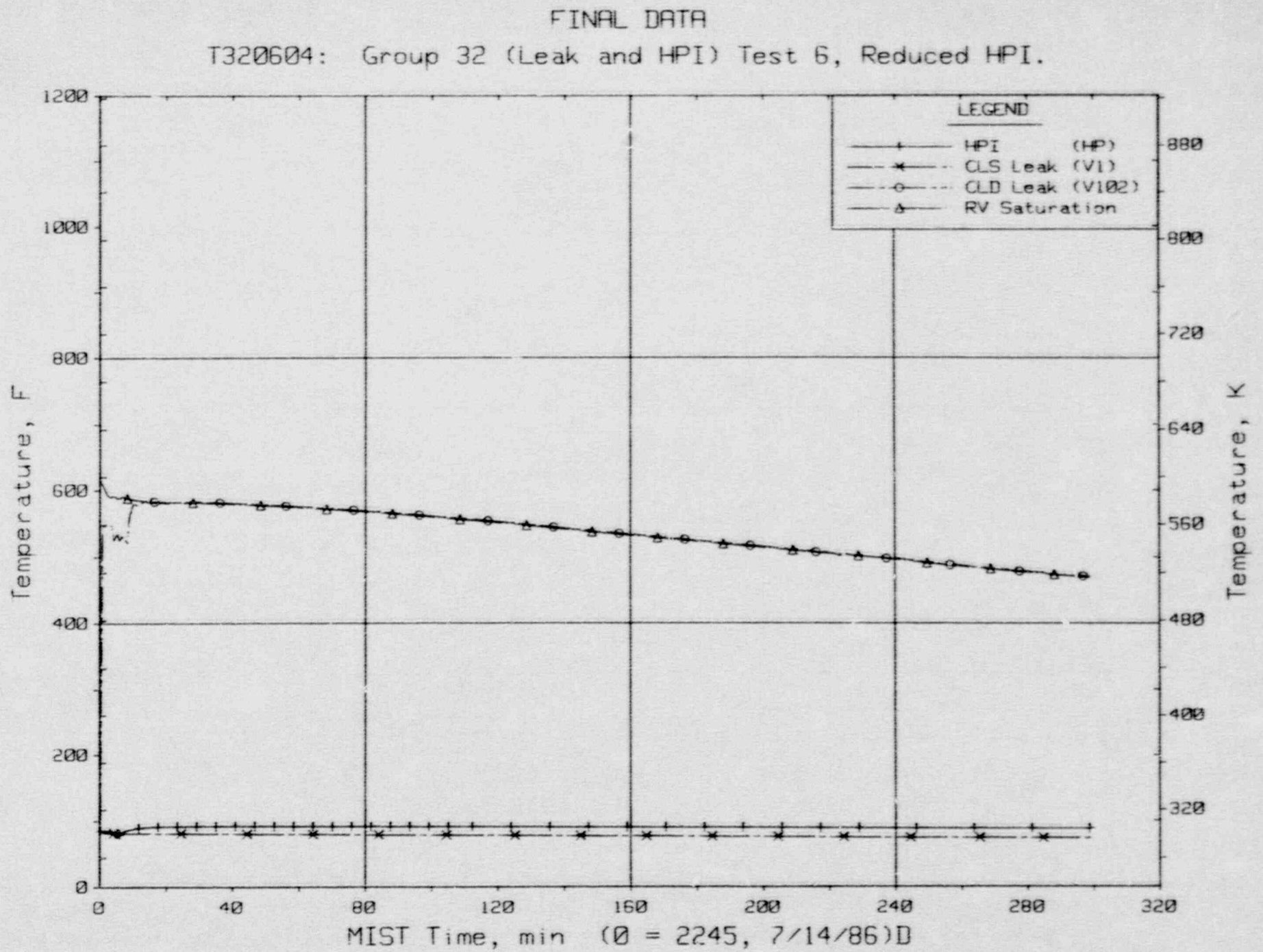

Figure 5.6.4. Single-Phase Discharge and HPI Fluid Temperatures

Wed Jul 13 13:25:58 1988

PRTC1

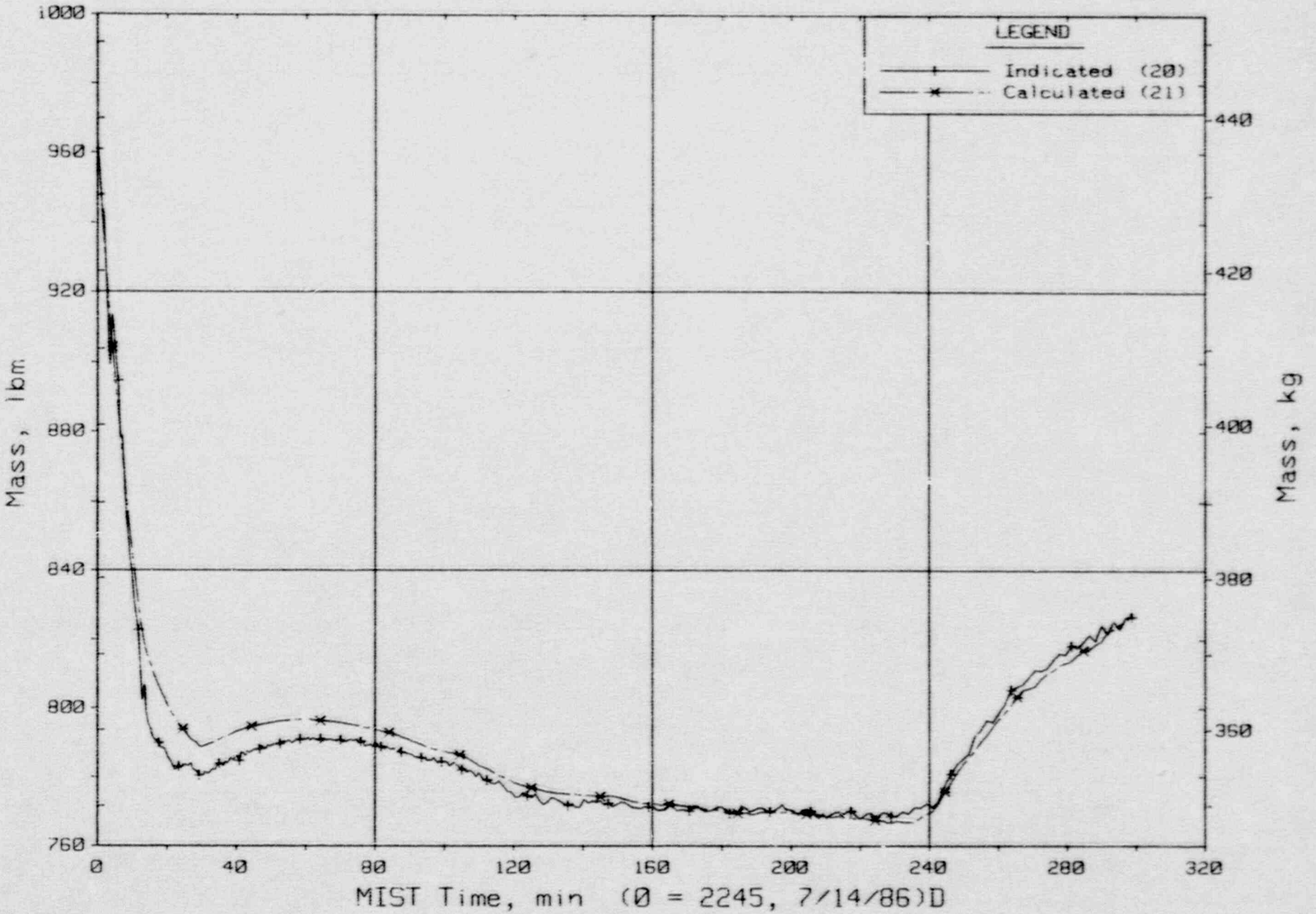

Figure 5.6.5. Total Primary Fluid Mass).

Wed Jul 13 13:28:12 1988

PRML1

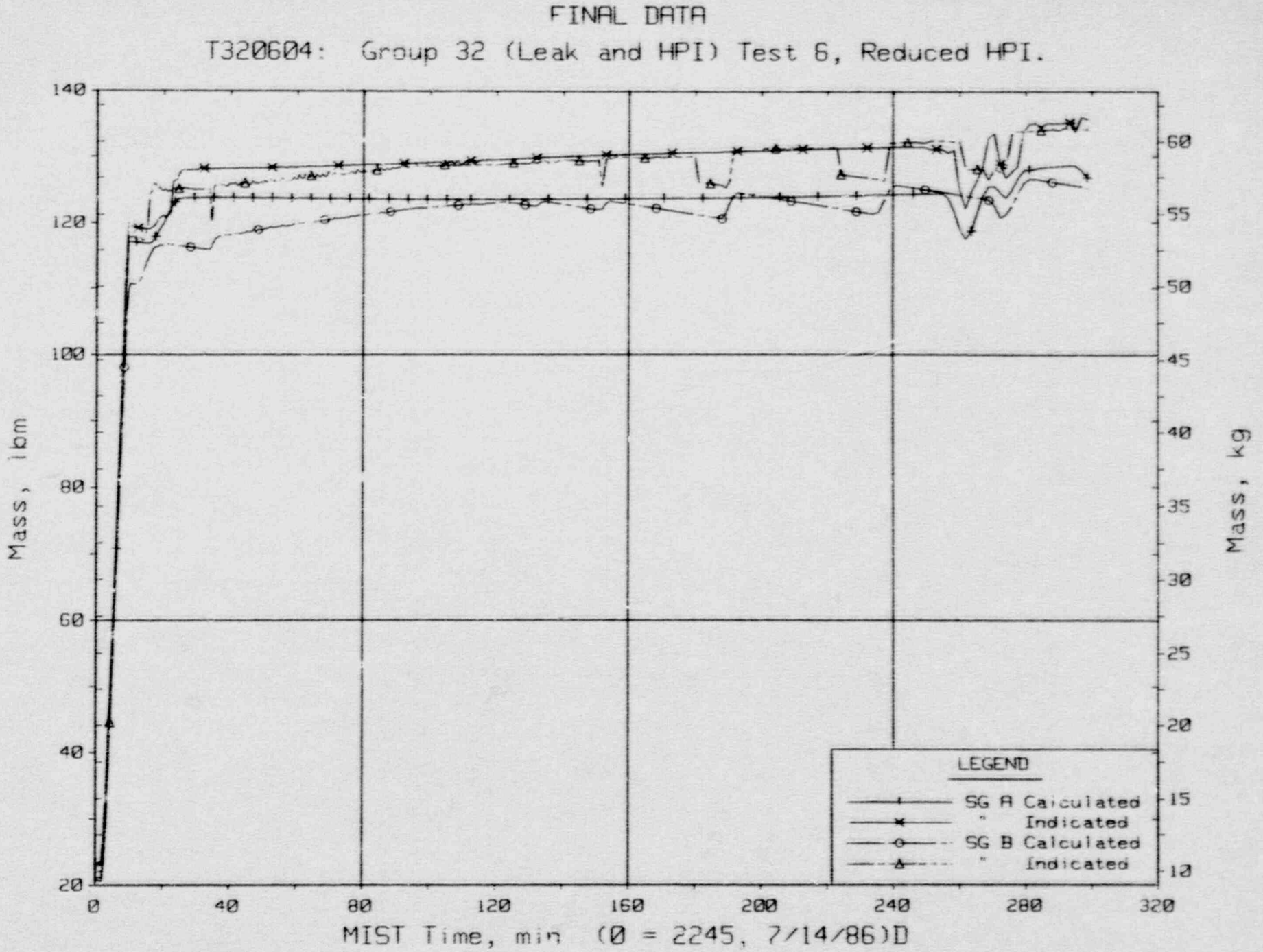

Figure 5.6.6. Steam Generator Secondary Mass Balances

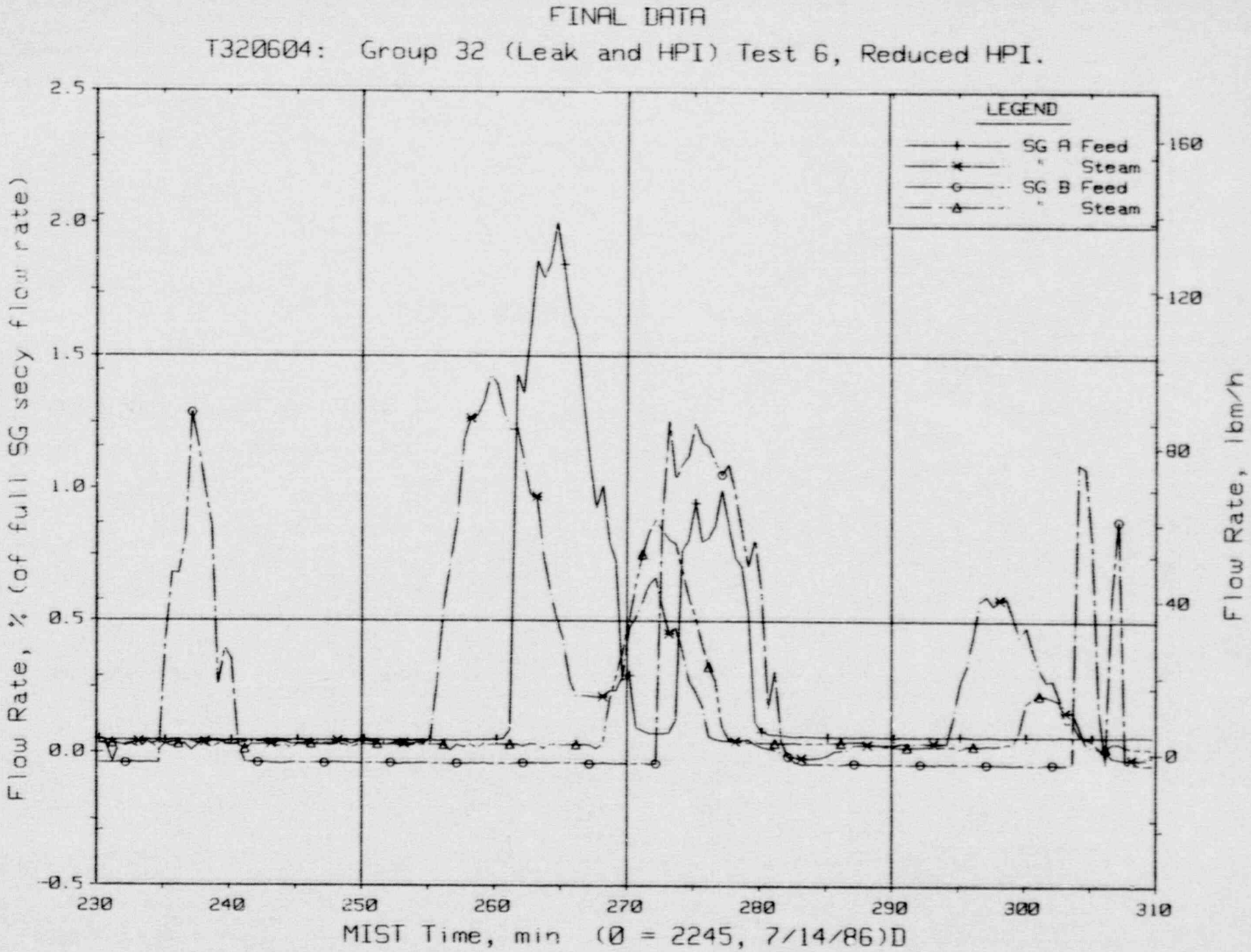

Figure 5.6.7. Secondary System Flow Rates

Wed Jul 13 14:57:56 1988

SGFL2

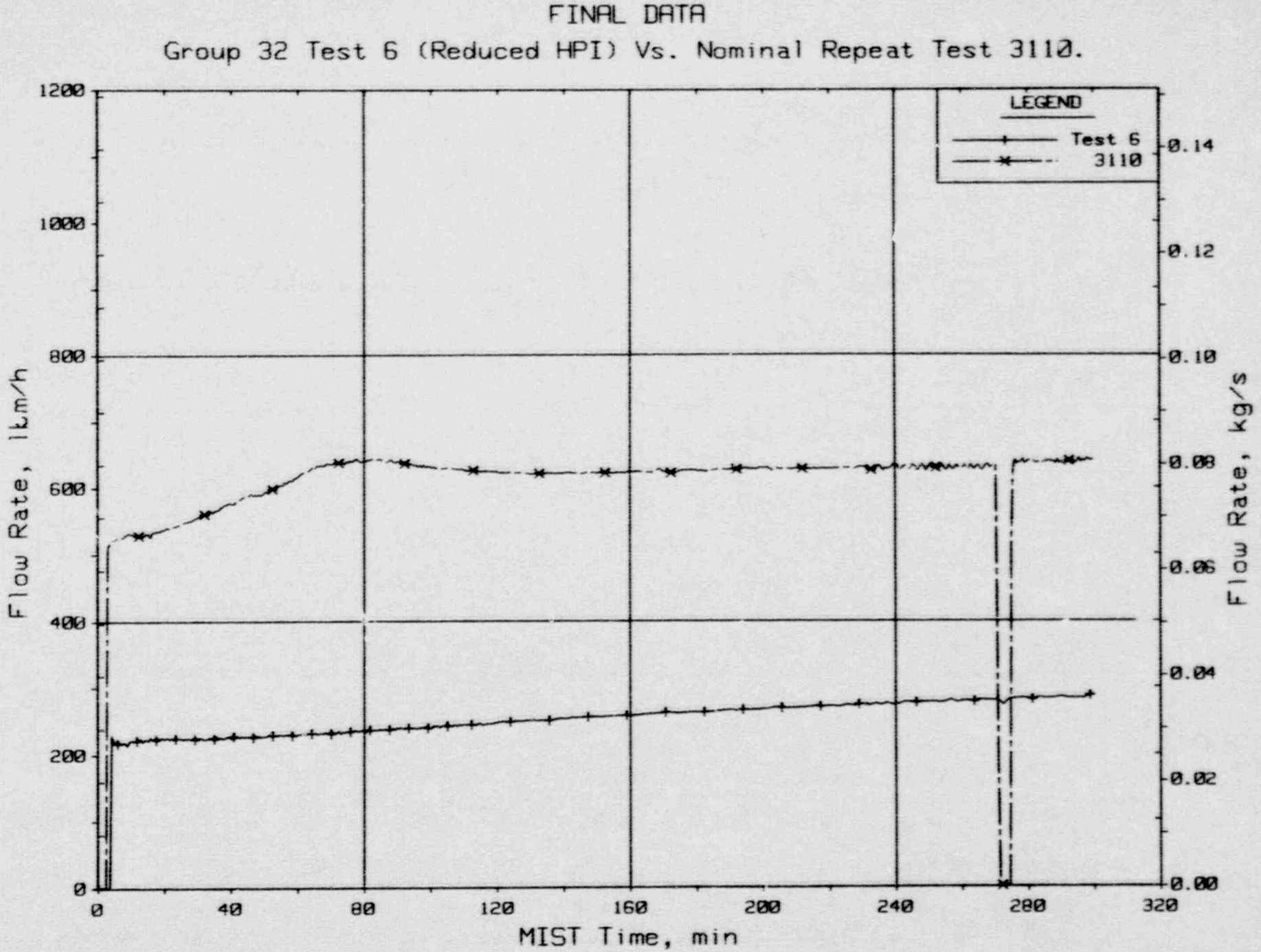

Figure 5.6.8. HPI Total Flow Rate (HPMM05)

Wed Jul 13 12:43:43 1988

6HPFL2

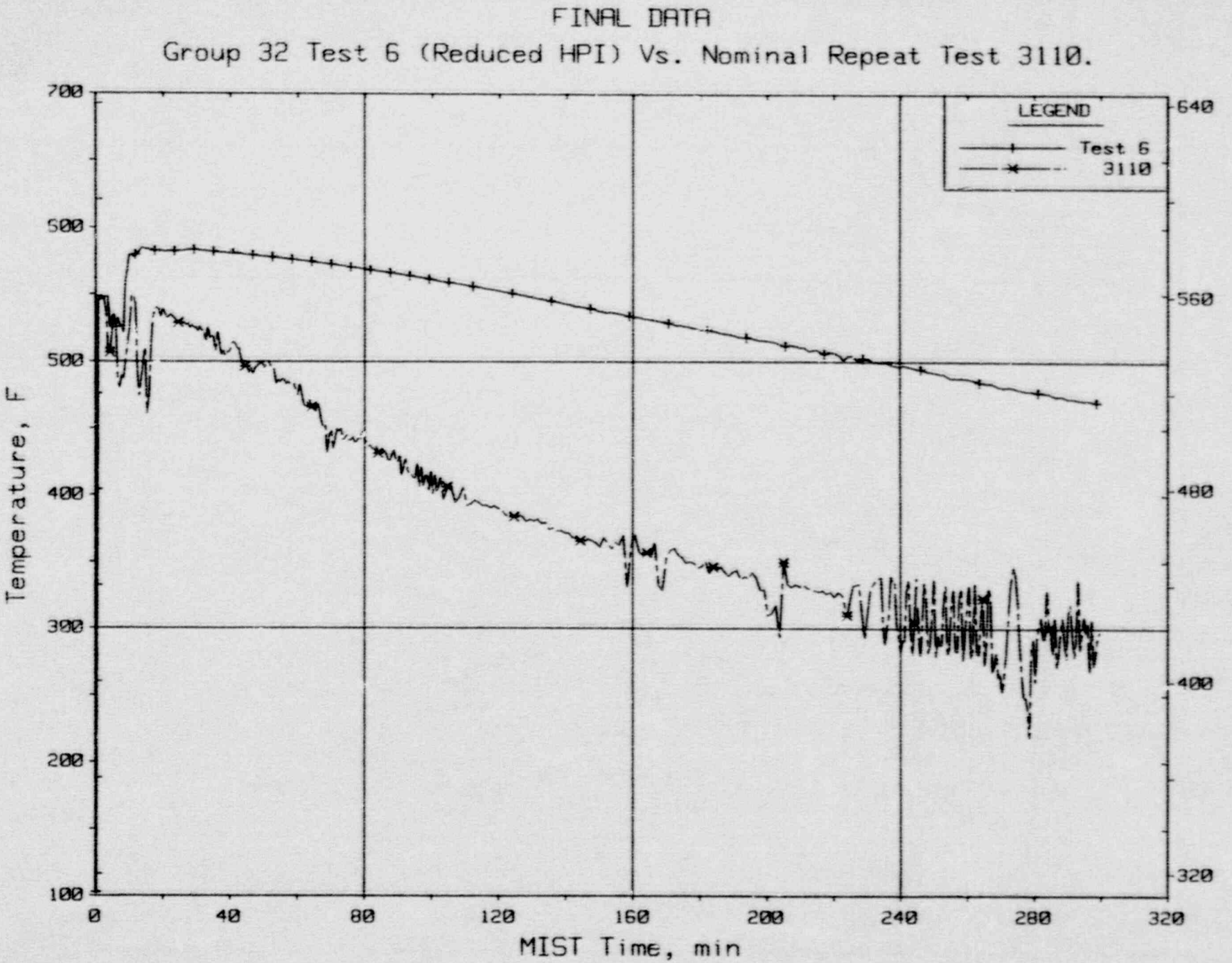

Figure 5.6.9. Leak Fluid Temperature (V1TC02)

Wed Jul 13 12:45:45 1988

6PRTC1

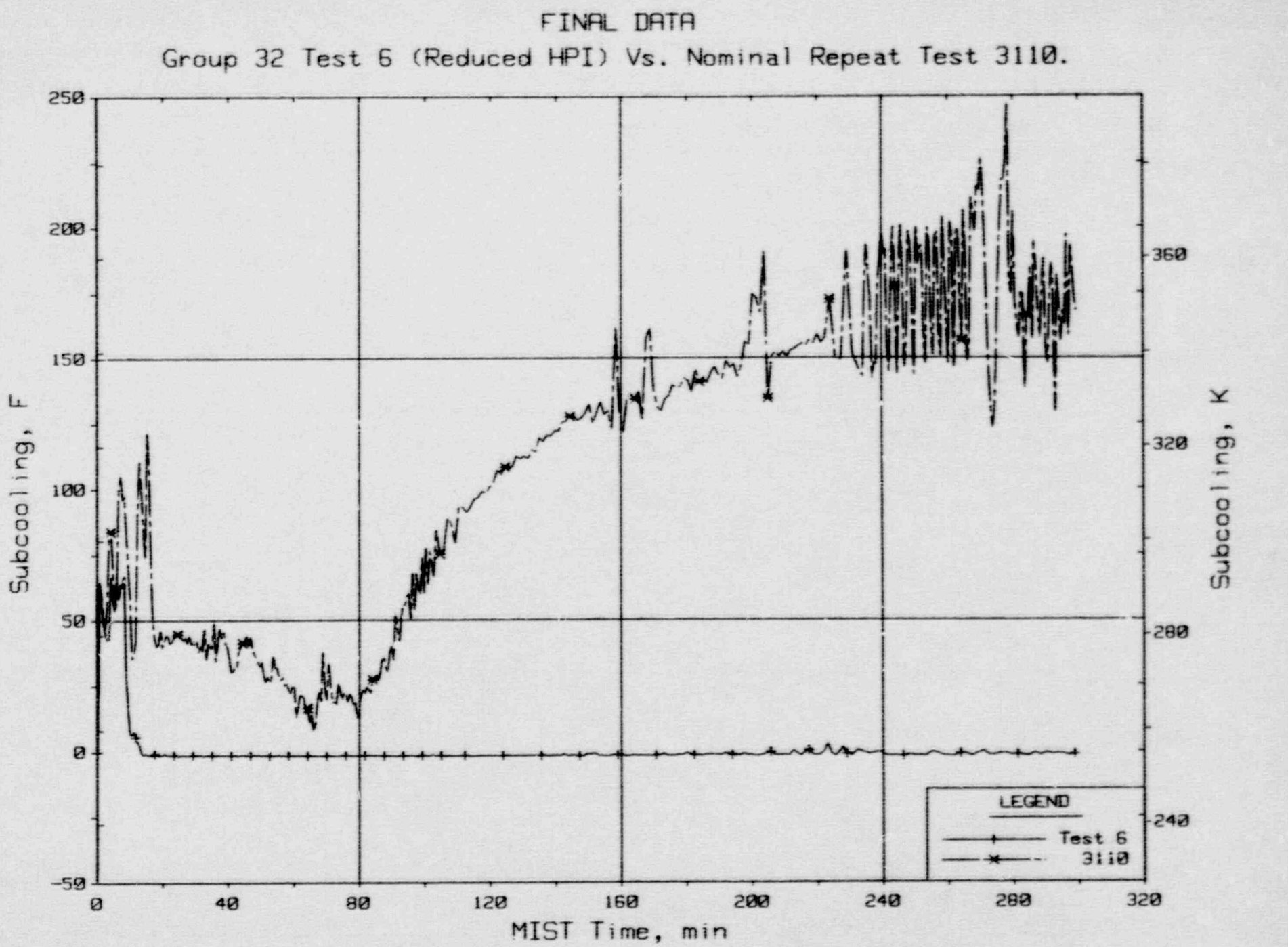

Figure 5.6.10. Leak Fluid Subcooling

Wed Jul 13 12:48:00 1988

6LKSUB

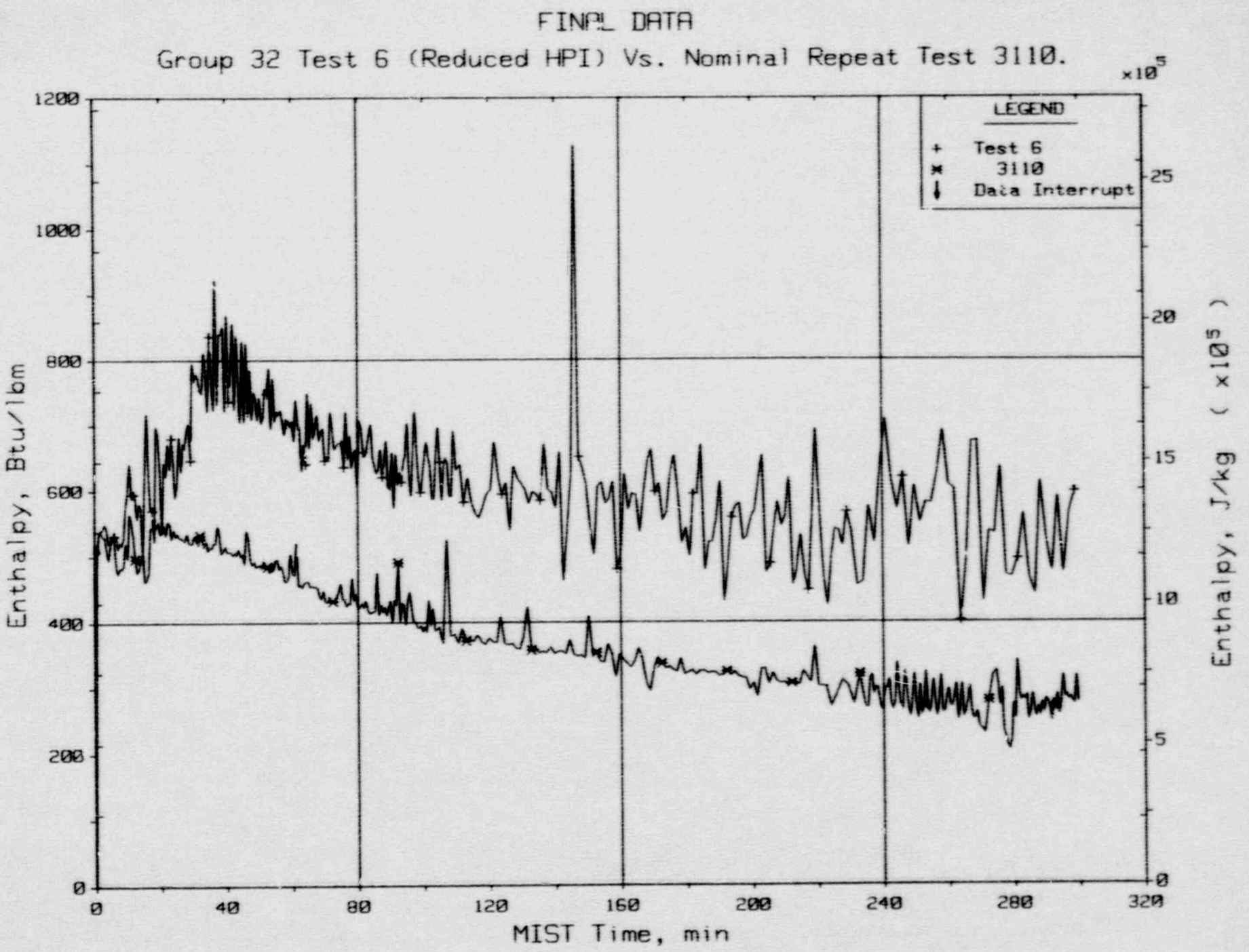

Figure 5.6.11. Single-Phase Leak Fluid Enthalpy

Wed Jul 13 12:50:21 1988

6V1EN1

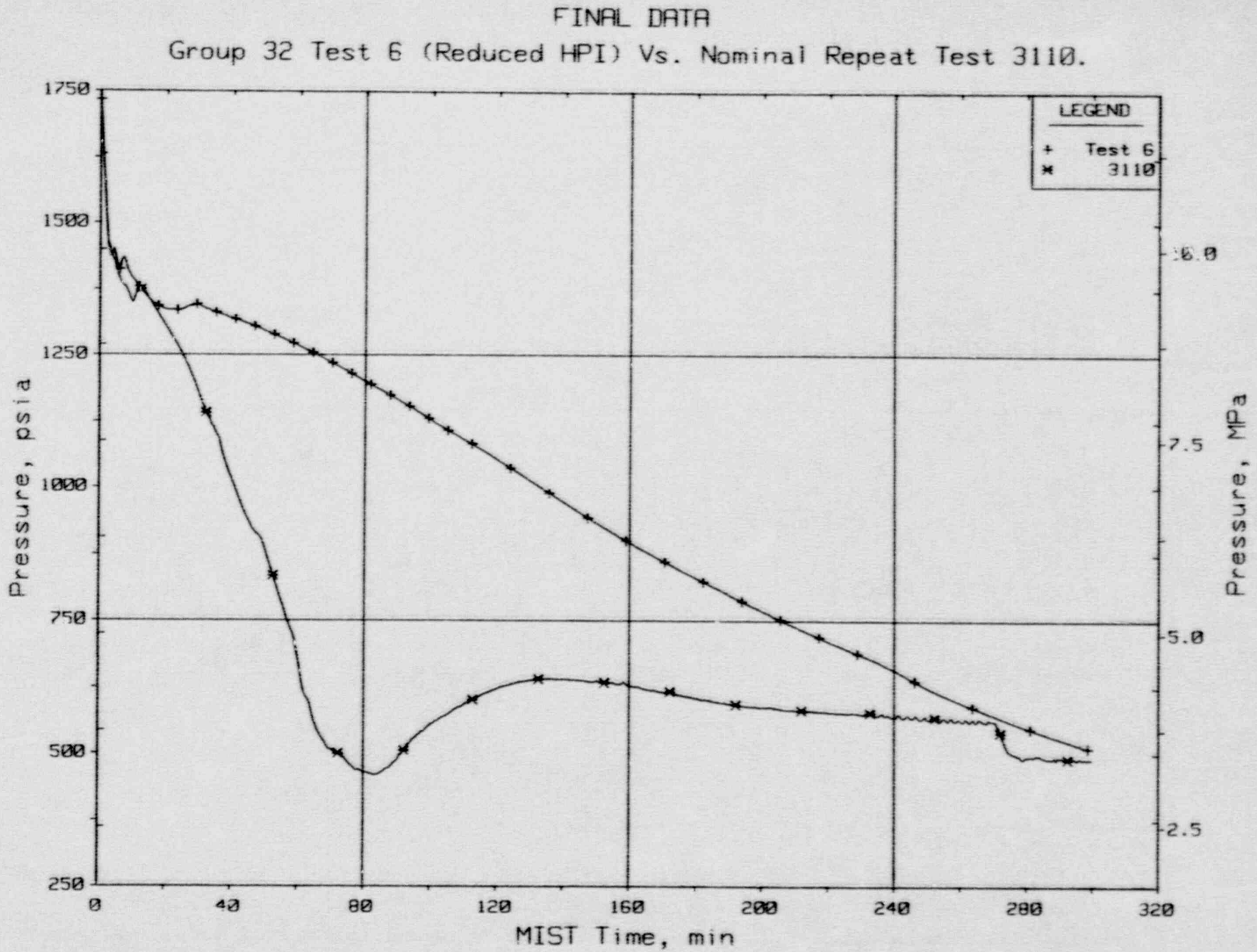

Figure 5.6.12. Reactor Vessel Pressure

Wed Jul 13 12:52:28 1988

6RVGP1

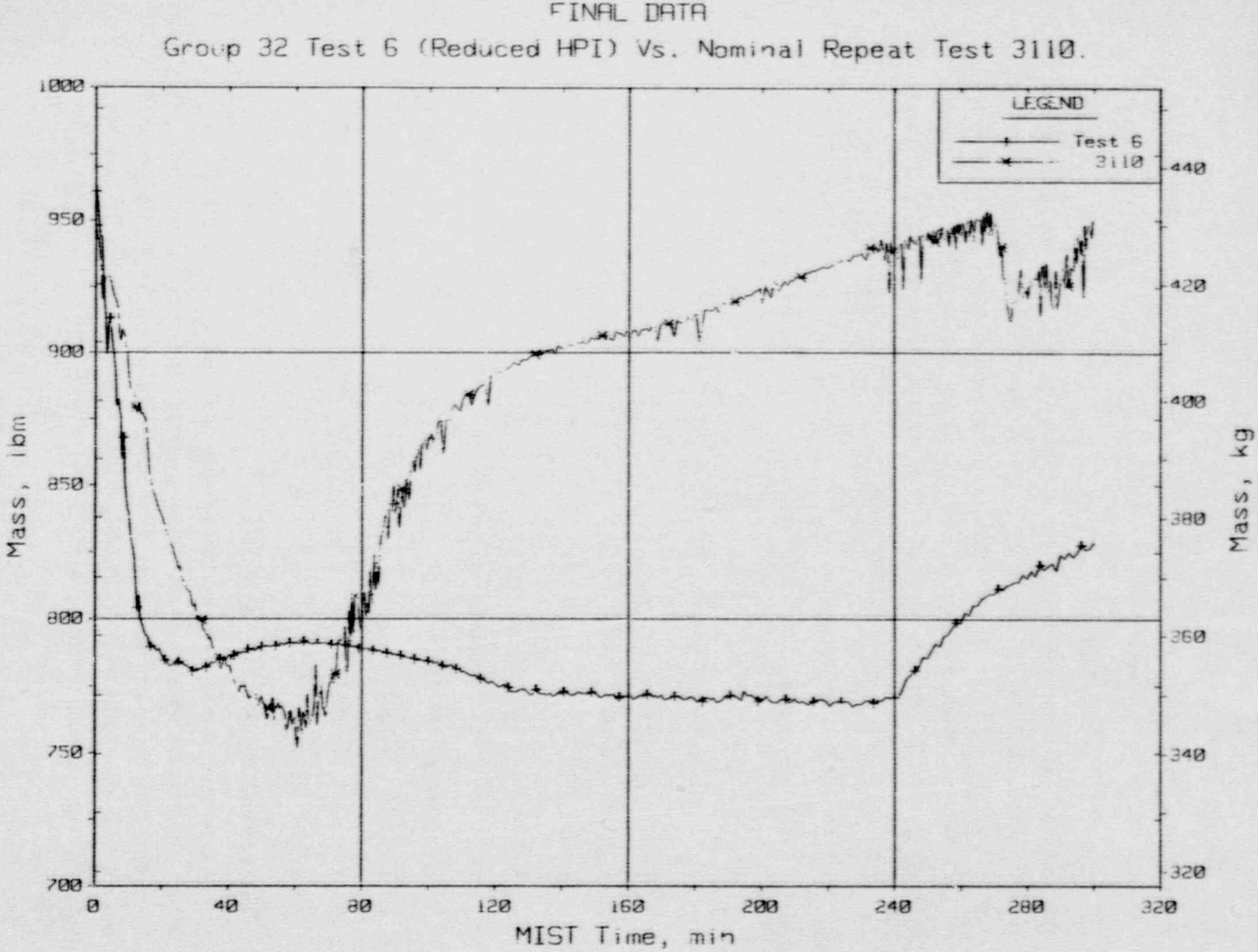

Figure 5.6.13. Primary System Total Fluid Mass (Indicated, PLML20s)

Fri Oct 28 15:25:32 1988

6PRML1

5.7. Summary of Observations

General observations, the effects of inter-test variations, and noteworthy interactions are provided herein.

5.7.1. General Observations

The Group 32 tests varying leak and HPI configurations used the same nominal boundary conditions as the Group 31 tests in which the individual boundary system controls were varied individually. The general observations of Group 32 thus parallel those of Group 31, and are described in detail in the Group 31 Report. The following general observations are outlined herein:

- Initial conditions and early events
- Interruption sequence
- Level adjustments
- Cold leg counterflow
- Intermittent loop flow
- RVVV activity
- Inter-cold leg flow
- RVVV effects
- Core inlet subcooling
- Hot leg liquid temperature profiles
- Asymmetric hot leg refill
- Refill spillover
- Restart of natural circulation and primary-to-secondary heat transfer
- Core cooling

Initial Conditions and Early Events

The initial conditions were virtually identical among the Group 32 tests. Slight inter-loop differences in steam generator heat removal existed. The downcomer flow rate was approximately 0.2% of scaled full flow less than the sum of the four cold leg flow rates. The timing of the test-initiating actions that were keyed to pressurizer draining varied among tests in a

manner that was consistent with the imposed leak and HPI variations. HPI delivery was noticeably delayed in Test 6 using half-capacity HPI.

Interruption Sequence

The saturation and interruption of loop A before loop B was caused by the initial outsurge of saturated pressurizer inventory to loop A. The effects of this outsurge presumably would have been dissipated had there been forced flow, therefore the A-versus-B sensitivity observed in MIST is traceable to the initialization of MIST in natural circulation.

Level Adjustments

The riser and stub levels of a loop realigned upon flow interruption to maintain the within-loop manometric balance with a diminishing hydraulic flow loss contribution.

Cold Leg Counterflow

Liquid-liquid counterflow commenced as the loop flow stagnated and RVVV-heated fluid descended to the elevation of the cold leg nozzles. Relatively warm fluid flowed upward (in backflow) along the top of the discharge piping, and HPI-cooled fluid flowed downward along the bottom of the piping.

Intermittent Loop Flow

The inverse relation between loop flow and core fluid temperature rise, and the accompanying response times, caused cyclic interruptions of the remaining active loop. For example, as loop flow diminished, the core fluid temperature rise increased, resulting in core exit saturation and voiding, and later in a resurgence of loop flow. (These interactions subsided upon completion of the initial refill of the steam generator secondaries.)

RVVV Activity

The RVVVs became active as the core exit fluid alternately subcooled and saturated, while the downcomer level had not yet descended to the elevation of the cold leg nozzles.

Inter-Cold Leg Flow

The cold leg fluid often flowed forward in one cold leg and backward in the adjacent cold leg during periods of otherwise stalled loop flow. The common

points of this intra-loop flow circuit were the steam generator primary outlet and the reactor vessel downcomer. The fluid density difference necessary to drive this natural circulation loop involved both fluid cooling and heating. HPI cooled the backward-flowing fluid, while the forward-flowing fluid was heated by mixing with the relatively warm steam generator outlet fluid.

RVVV Effects

The RVVVs discharged core steam to the downcomer where it was condensed by HPI. The heat capacity of the subcooled HPI, using full head-flow characteristics, was sufficient to condense the entire core heat input at more than 2% power. This decay power is achieved 13 minutes after reactor trip from extended operation at full power, thus the primary system generally gradually depressurized.

Core Inlet Subcooling

With loop flow interrupted, the core inlet fluid cooled in response to the excess of the HPI heat removal capacity over the core input. The subcooling of the core inlet fluid exceeded 200F.

Hot Leg Liquid Temperature Profiles

The hot leg liquid temperature profiles evidenced limited thermal inversions during hot leg refill. The uppermost liquid, in contact with the remaining vapor, was saturated. The remaining liquid reflected the preceding primary system pressure transient. Refill had started at a relatively low pressure, obtained through BCMs, but pressure increased as primary-to-secondary heat transfer was inhibited by intermediate levels. The core exit and hot leg fluid remained saturated through this pressure increase, thus the fluid being added at the bottom of the hot legs became successively warmer. In this manner, relatively cool fluid resided over the middle hot leg riser elevations whereas warmer fluid, saturated at the current pressure, resided at the top and bottom of the liquid columns.

The one-dimensionality of the MIST hot legs inhibited but did not preclude internal circulation such as would be driven by this thermal inversion. Also, the finite lengths of the guard heating zones may have sustained the liquid temperature variations such as by allowing a slight heat loss from the

middle elevations. Thus, the MIST liquid temperature gradients and their persistence may have been amplified atypically.

Asymmetric Hot Leg Refill

The hot leg levels achieved relatively equal intermediate elevations below the U-bend spillovers but with stub levels above the steam generators. The subsequent hot leg level trends were noticeably asymmetric, however. The loop A hot leg riser level gradually increased toward the spillover elevation while the loop B level remained nearly constant, apparently due to inter-loop asymmetries in guard heater control.

Refill Spillover

The quiescent system conditions quickly became responsive when a hot leg level was refilled to the U-bend spillover elevation. Of the multiple system changes, the core exit fluid temperature decrease was most influential. The core exit SCM increased sufficiently, from 0 to more than 100F in a few minutes, to trigger HPI throttling. The steam generator control temperature difference (core exit minus steam generator secondary saturation) dropped from more than 50F to less than zero, initiating a controlled rapid depressurization of the steam generator secondaries. Multiple spillovers occurred, spaced at about half-hour intervals, but of sequentially decreasing intensity.

Restart of Natural Circulation and
Primary-to-Secondary Heat Transfer

Natural circulation was reinitiated smoothly and rapidly upon sustained hot leg refill. The primary system was then cooled and depressurized through continuing primary-to-secondary heat transfer.

Core Cooling

The core remained completely covered throughout most of the tests, and remained cooled through all of the tests.

5.7.2. Effects of Altered Leak and HPI Configurations

The leak size, location, and isolation status and the HPI capacity were varied individually in the tests of Group 32. The effects of these inter-test variations are discussed according to the type of variations as follows:

- Break size (Tests 1 and 2)
- Break location (Tests 3 and 4)
- Break isolation status (Test 5)
- HPI capacity (Test 6)

Varied Leak Size: Leak Flow Rates

The initial leak flow rates varied directly with the leak flow areas; that is, the critical mass fluxes were initially approximately constant for (cold leg discharge) leak sizes of 5, 10, and 50 cm^2. The (modified) critical flow prediction appeared suitable for the two smaller break sizes but performed poorly for the 50-cm^2 break. With the larger break, the fluid at the break site was generally saturated; during the initial subcooled period, the break mass flow rate exceeded its metering capacity.

Varied Leak Size: System Response

The system remained full almost continuously with a 5-cm^2 break. Thus, the test transient evolved largely to a two-loop cooldown in single-phase natural circulation. The primary system pressure initially stabilized as the upper reactor vessel fluid approached saturation, decreased through continuing primary-to-secondary heat transfer during steam generator secondary refill, then repressurized to 1525 psia after secondary refill was completed. The core exit fluid remained subcooled, its subcooling increased with the continuing cooldown. The SCM achieved 75F, the setpoint of automatic throttling of HPI to maintain SCM, at 26 minutes. The subsequent HPI throttling reduced primary system pressure smoothly, and in parallel with the cooldown of the primary system. Although the decreasing primary system saturation temperature caused the upper reactor vessel voided volume to expand, the loop cooldown continued unabated. In summary, the 5-cm^2 leak was of insufficient size to interrupt loop flow. The primary system was depressurized primarily through automatic HPI throttling to maintain the SCM.

The dominant depressurization mechanism with a 10-cm^2 break was the HPI condensation of core steam. HPI-leak cooling was enabled by cold leg counterflow. BCMs effectively cooled and depressurized the primary system,

but were ultimately precluded by intermediate hot leg levels, i.e., above the steam generators but below the U-bend spillovers.

The primary system depressurized relatively rapidly with a 50-cm^2 leak, due to the increased leak volumetric flow. The cold leg discharge piping voided early in the transient, causing the leak site fluid to saturate and the critical mass flow rate to decrease. The mass flow rate with the 50-cm^2 leak thus approached the HPI flow rate and the (subcooled) leak flow rate observed with a 10-cm^2 break. The system conditions thus realigned to accommodate the increased break size. The primary system total fluid mass gradually increased towards the end of the 50-cm^2 break tests, but the hot leg levels remained well below the spillover point. Had the low-pressure injection (LPI) system been simulated in MIST, it would have been active for most of the test after approximately 50 minutes.

Varied Break Location

The following three break locations were tested: cold leg discharge (nominal), cold leg suction, and PORV. Each break used a scaled 10-cm^2 break flow area. Both the suction and discharge breaks were in cold leg B1, and the discharge break was the nominal configuration. The remaining boundary conditions were identical among the three tests.

The general system trends were similar among the three tests with differing leak locations. In all three tests, the primary system depressurized and the primary system total fluid mass approached equilibrium, but the mechanisms differed. Leak fluid heating was operative with both a cold leg suction and discharge leak, thus their interactions were quite similar until perturbed by the PORV actuation specified for the suction-break test. (The PORV actuation caused a BCM depressurization, but equilibrium was reachieved.)

The core exit fluid remained subcooled with the PORV break, the predominant mechanism of primary system depressurization was (automatic) HPI throttling to maintain the SCM, although the steam generators were also active -- steam generator A was active almost continuously and B was intermittently active.

The primary system gained fluid mass as soon as HPI was introduced with the PORV break, with vapor at the PORV. The primary system mass subsequently almost stabilized when the PORV site fluid subcooled. The start of primary

system refill was delayed with the cold leg breaks, however. Just before 1 hour, the primary system depressurizations were enhanced by BCMs, perturbing the HPI and leak flow rates sufficiently to reverse the mass loss.

Break Isolation Status (Test 5)

Test 5 repeated the nominal boundary conditions until leak isolation at 30 minutes. Test 5 was almost an exact replica of Nominal Repeat Test 10 until leak isolation.

The leak was isolated at 30 minutes. Based on the Nominal Test, the hot leg riser and stub levels were expected to be above the steam generators but below the spillover elevations, thus inhibiting primary-to-secondary heat transfer. These intermediate levels were obtained shortly after leak isolation. Leak isolation obtained a positive rate of change of both primary system mass and fluid volume. Also, the elimination of HPI-leak cooling caused the primary system total fluid energy to increase following leak isolation. As a result of these revised mass, volume, and energy trends, both the primary system pressure and the hot leg levels began to rise. Twenty minutes after leak isolation, with a primary system pressure of 1675 psia and rising, the hot leg levels achieved the U-bend spillover elevation. Natural circulation restarted, the steam generators reactivated, the primary system depressurized, and a two-loop cooldown ensued. The primary system depressurization was subsequently enhanced by HPI throttling for control of both pressurizer level and SCM.

Reduced HPI Capacity (Test 6)

Test 6 with reduced HPI capacity again demonstrated the inherent responsiveness of the system. Whereas the HPI flow rate and subcooling were sufficient to condense all the core steam production when using full HPI capacity, the HPI condensing capacity was insufficient in Test 6. The RVVVs continued to relieve steam to the downcomer, the cold leg discharge piping voided, and the resulting increase of the break volumetric discharge rate offset the excess core steam production. Similarly, the reduced HPI-leak cooling due to the reduced HPI flow rate was offset by the increased enthalpy of the leak site fluid. The primary system pressures using full HPI and half-capacity HPI merged after 4 hours of testing.

5.7.3. Noteworthy Interactions

The interactions addressed herein are perceived to be of intrinsic interest or to be useful to the code prediction of the test transients. Many of the noteworthy interactions of Group 32 parallel those of the Group 31 tests. Since these interactions have been discussed in detail in the Group 31 Report, they are only listed herein. These interactions are as follows:

- Initial interruption
- Counterflow
- Hot leg level differences
- RVVV effects
- Inter-cold leg flow
- BCM
- Equilibrium
- Spillover
- Restart of natural circulation
- Core cooling

The leak and HPI variations imposed in the Group 32 tests generated one additional noteworthy observation regarding RVVV effects and the system response to varied boundary conditions. Because the RVVVs link the core steam generation to the subcooled HPI and to the cold leg break sites, the system conditions change inherently toward depressurization and fluid mass equilibrium. With an increased break size, for example, the saturation of the break site fluid caused the break mass flow rate to decrease toward the HPI flow rate. As another example, the decreased condensing capacity with a reduced HPI flow rate was offset by an increased break volumetric discharge rate when the break site voided. Following a small break, the RVVV-equipped system thus has an inherent tendency to depressurize and to attain mass equilibrium.

6. SUMMARY

The six tests of Group 32 singly varied the leak size, location, and isolation status, and HPI capacity. The tests were conducted as specified. The results demonstrated a variety of system interactions and are useful for code benchmarking. The MIST interactions are of intrinsic interest because they may provide insight into expected plant behavior. MIST was necessarily atypical of a plant in certain important respects, however. The MIST interactions therefore are not to be applied directly to a plant.

The noteworthy interactions paralleled those of Group 31. In addition, the significance of the RVVVs was underscored by the observed tendency of the system conditions to offset imposed leak and HPI configuration changes. In each test, the primary system ultimately depressurized, the primary system total fluid mass stabilized and began to increase, and the core remained cooled.

The leak size variations demonstrated a variety of primary system depressurization mechanisms. The loop remained full throughout most of the 5-cm^2 leak transient. The primary system was cooled through continuing single-phase natural circulation heat transfer. The primary system was depressurized primarily through the automatic throttling of the high-pressure injection flow rate to maintain a subcooling margin of 75F at the core exit. Several modes of depressurization were encountered with a 10-cm^2 break. The most persistent mode was through the HPI condensation of the core steam production coupled with leak-HPI cooling. The 50-cm^2 leak transient, on the other hand, depressurized directly through the break volumetric discharge.

The test transients with varied leak locations were quite similar. HPI-leak cooling was operative with the cold leg suction break. This cooling mechanism offset core power by discharging relatively warm fluid out the break. The subcooled HPI fluid was heated as it condensed core steam (transported to

the downcomer through the RVVVs). The relatively warm fluid frequently traversed the cold leg piping in liquid-liquid counterflow; that is, the warmer fluid travelled backward along the top of the sloping cold leg discharge piping and the HPI-cooled fluid flowed forward along the bottom. One loop remained full and the core exit fluid remained subcooled with the simulated PORV break. The primary system thus depressurized through the PORV volumetric discharge, primary-to-secondary heat transfer in the full loop plus intermittent activity in the voided loop, and HPI throttling to maintain the core exit fluid subcooling margin.

The isolated leak test repeated the boundary system controls of the Nominal Repeat Test (311000) until leak isolation at 30 minutes. The initial transients were virtually identical. Upon leak isolation, the primary system abruptly began to refill and to repressurize. The repressurization was halted when the hot leg levels achieved the U-bend spillover elevation and a two-loop cooldown began.

The cold leg discharge piping voided in the test using half-capacity HPI. The break mass flow rate thus decreased towards the HPI flow rate, and the vapor discharged by the break offset the decreased condensation capability of the reduced HPI flow rate. This interaction was an example of the inherent system resiliency observed repeatedly in Test Group 32. The system conditions generally realigned to offset imposed boundary system changes. In each test, the primary system ultimately depressurized, the total primary system fluid mass stabilized and began to increase, and the core remained cooled.

7. REFERENCES

1. H. R. Carter and J. R. Gloudemans, "An Experimental Study of the Post-Small Break Loss-of-Coolant Accident Phenomena in a Scaled Babcock & Wilcox System," NUREG/CP-0058, Vol. 1, pp. 113-135. Proceedings of the U.S. Nuclear Regulatory Commission, Twelfth Water Reactor Safety Research Information Meeting, October 1984.

2. "Multi-Loop Integral System Test (MIST) Facility Specification," RDD:84:4091-01-01:01 (distributed November 1984, revision pending).

3. J. R. Gloudemans, "Simulation of Reactor Vessel Vent Valves," ASME Paper 85-WA/HT-29, 106th ASME Winter Annual Meeting, Miami, Florida, November 1985.

4. "Multi-Loop Integral System (MIST) Instrumentation -- Revision 3," RDD:84:4127-30-01:03, March 1987.

5. "MIST Test Specifications," BAW-1894, Rev. 1, March 1986.

6. L. S. Tong, Boiling Heat Transfer and Two-Phase Flow, Wiley & Sons, Inc., New York, 1965 (p. 110).

NRC FORM 335 (2-89) NRCM 1102, 3201, 3202

U.S. NUCLEAR REGULATORY COMMISSION

BIBLIOGRAPHIC DATA SHEET

(See instructions on the reverse)

1. REPORT NUMBER (Assigned by NRC, Add Vol., Supp., Rev., and Addendum Numbers, if any.)

NUREG/CR-5395, Vol. 4
EPRI/NP-6480
BAW-2062

2. TITLE AND SUBTITLE

Multiloop Integral System Test (MIST): Final Report
Test Group 32, SBLOCA with Altered Leak and HPI Configurations

3. DATE REPORT PUBLISHED

MONTH: July | YEAR: 1989

4. FIN OR GRANT NUMBER

B8909 & D1734

5. AUTHOR(S)

J. R. Gloudemans

6. TYPE OF REPORT

Technical

7. PERIOD COVERED (Inclusive Dates)

June 1986-March 1988

8. PERFORMING ORGANIZATION – NAME AND ADDRESS (If NRC, provide Division, Office or Region, U.S. Nuclear Regulatory Commission, and mailing address; if contractor, provide name and mailing address.)

Babcock & Wilcox
Nuclear Power Division
3315 Old Forest Road
Lynchburg, VA 24506-0935

Babcock & Wilcox
Research & Development Division
Alliance Research Center
1562 Beeson Street
Alliance, OH 44601

9. SPONSORING ORGANIZATION – NAME AND ADDRESS (If NRC, type "Same as above"; if contractor, provide NRC Division, Office or Region, U.S. Nuclear Regulatory Commission, and mailing address.)

Division of Systems Research
Office of Nuclear Regulatory Research
U. S. Nuclear Regulatory Commission
Washington, DC 20555

Electric Power Research Institute
P. O. Box 10412
Palo Alto, CA 94303

Babcock & Wilcox
Owners Group
P. O. Box 10935
Lynchburg, VA 24506-09354

10. SUPPLEMENTARY NOTES

11. ABSTRACT (200 words or less)

The Multiloop Integral System Test (MIST) is part of a multiphase program started in 1983 to address small-break loss-of-coolant accidents (SBLOCAs) specific to Babcock and Wilcox designed plants. MIST is sponsored by the U. S. Nuclear Regulatory Commission, the Babcock & Wilcox Owners Group, the Electric Power Research Institute, and Babcock and Wilcox. The unique features of the Babcock and Wilcox design, specifically the hot leg U-bends and steam generators, prevented the use of existing integral system data or existing integral facilities to address the thermal-hydraulic SBLOCA questions. MIST and two other supporting facilities were specifically designed and constructed for this program, and an existing facility--the Once Through Integral System (OTIS)--was also used. Data from MIST and the other facilities will be used to benchmark the adequacy of system codes, such as RELAP5 and TRAC, for predicting abnormal plant transients.

The MIST program is reported in 11 volumes. The program is summarized in Volume 1; Volumes 2 through 8 describes groups of tests by test type; Volume 9 presents inter-group comparisons; Volume 10 provides comparisons between the calculations of RELAP5/MOD2 and MIST observations, and Volume 11 presents the later Phase 4 tests. This Volume 4 pertains to Test Group 32, Altered Leak and HPI Configurations. The specifications, conduct, observations, and results of these tests are described.

12. KEY WORDS/DESCRIPTORS (List words or phrases that will assist researchers in locating the report.)

Multiloop Integral System Test (MIST), Babcock and Wilcox
Small break loss-of-coolant accident, transient testing, reactor safety
steam generator (once through), feed and bleed
steam generator tube rupture, station black out
Two-phase flow, SBLOCA without HPI injection, RELAP5/MOD2 calculations

13. AVAILABILITY STATEMENT

Unlimited

14. SECURITY CLASSIFICATION

(This Page)
Unclassified

(This Report)
Unclassified

15. NUMBER OF PAGES

16. PRICE

UNITED STATES
NUCLEAR REGULATORY COMMISSION
WASHINGTON, D.C. 20555

120555139531 1 1AN1R2
US NRC-OADM
DIV FOIA & PUBLICATIONS SVCS
TPS PDR-NUREG
P-209
WASHINGTON DC 20555


T320101

FINAL DATA

T320101: Group 32 SBLOCA Test 1, Reduced Leak Size - 5 cm2.

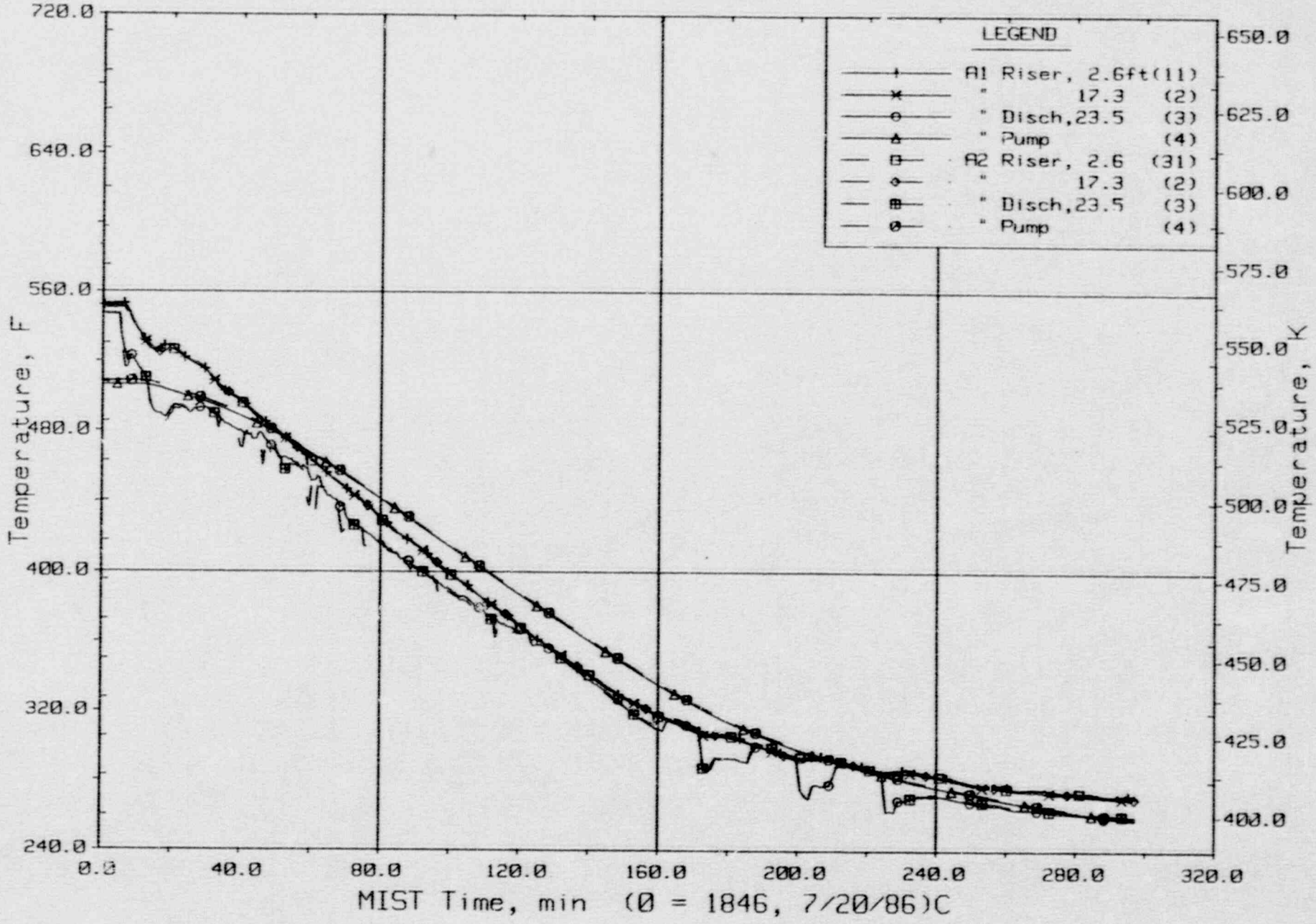

Loop A Cold Leg Metal Temperatures (C1,3MTs).

Mon May 16 10:33:42 1988

C1MT1

FINAL DATA

T320101: Group 32 SBLOCA Test 1, Reduced Leak Size - 5 cm2.

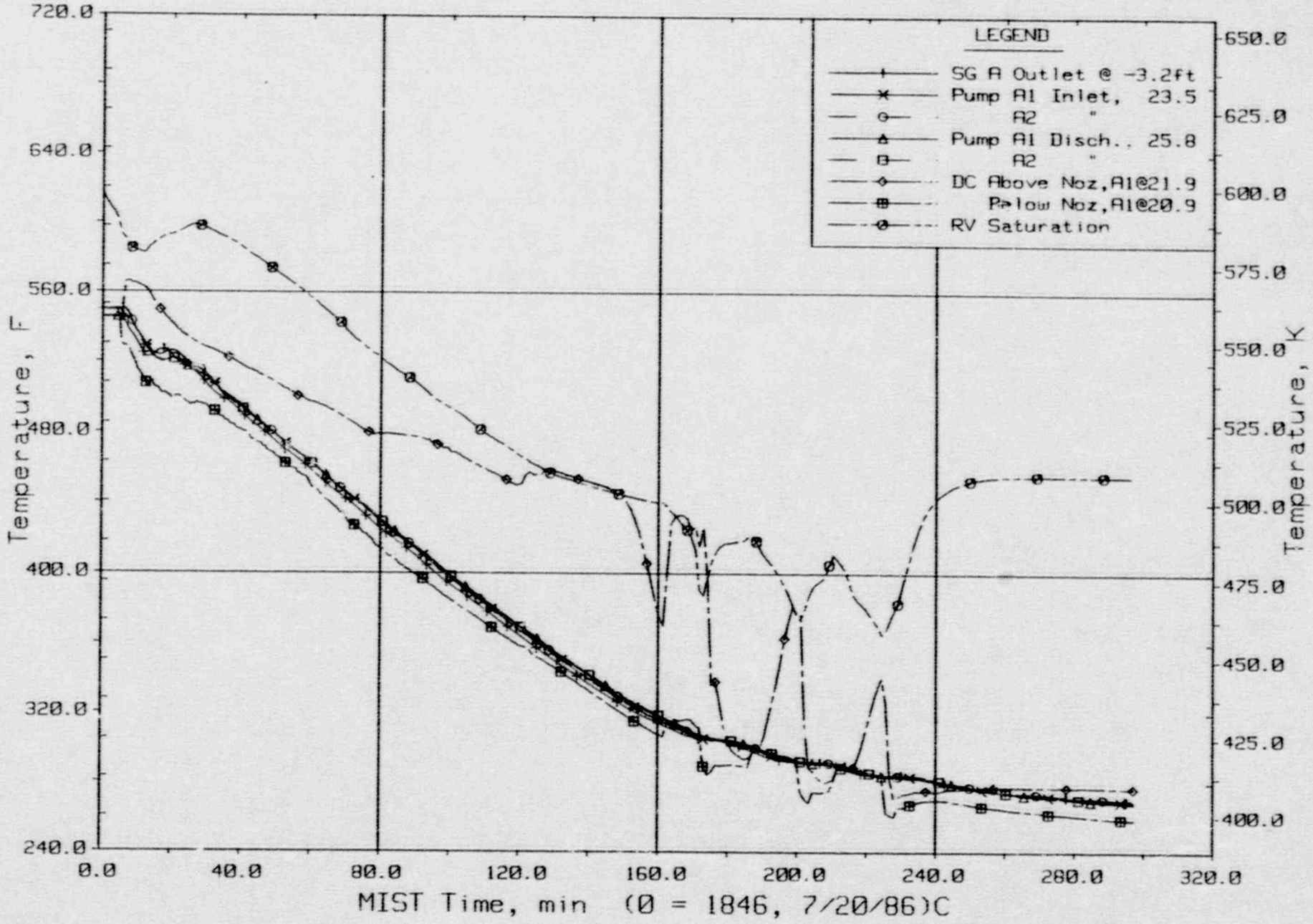

Loop A Cold Leg Fluid Temperatures (RTDs).

Mon May 16 18:43:01 1988

C1RT0

FINAL DATA

T320101: Group 32 SBLOCA Test 1, Reduced Leak Size - 5 cm2.

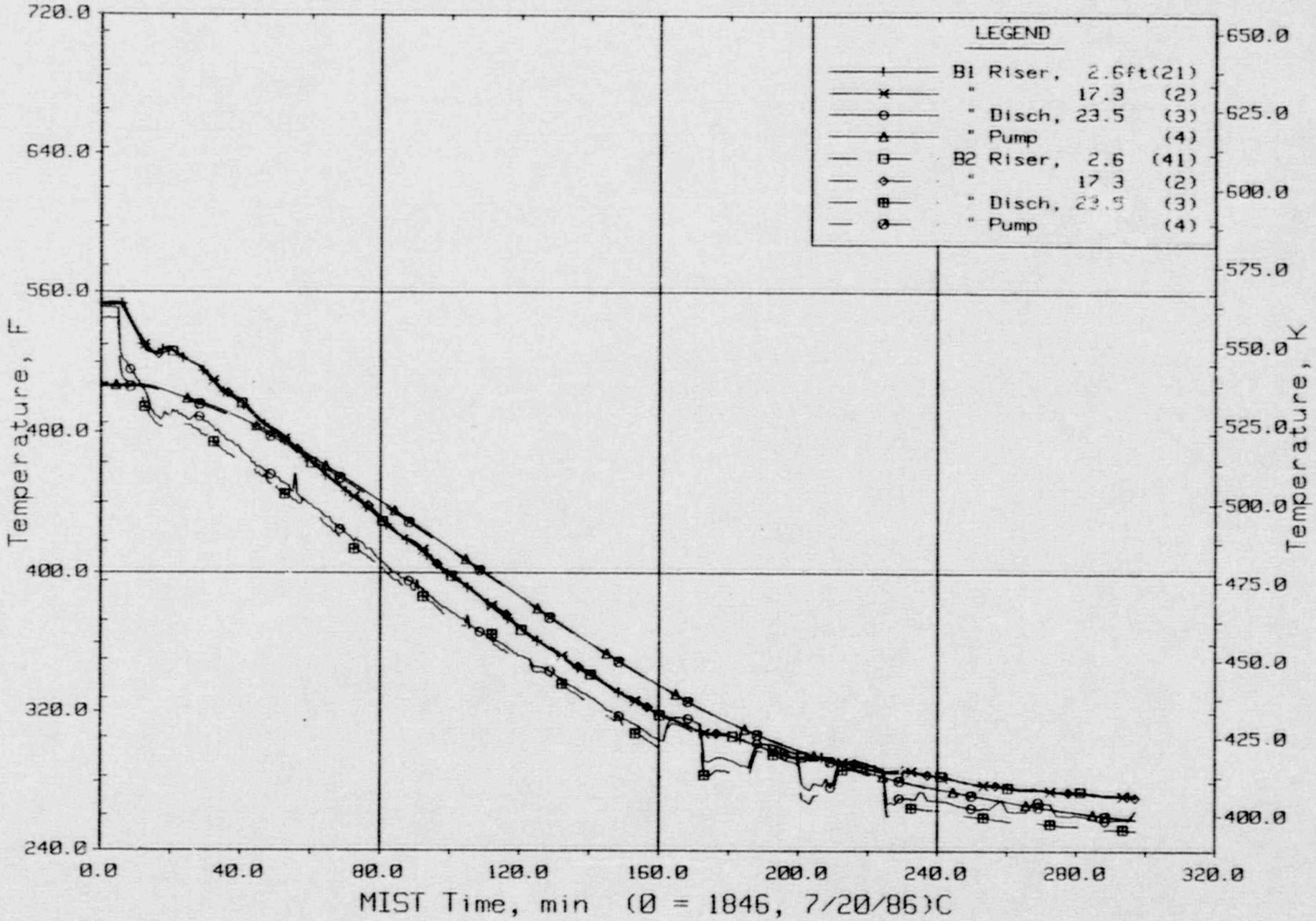

Loop B Cold Leg Metal Temperatures (C2,4MTs).

Mon May 16 18:37:58 1988

C2MT1

FINAL DATA

T320101: Group 32 SBLOCA Test 1, Reduced Leak Size - 5 cm2.

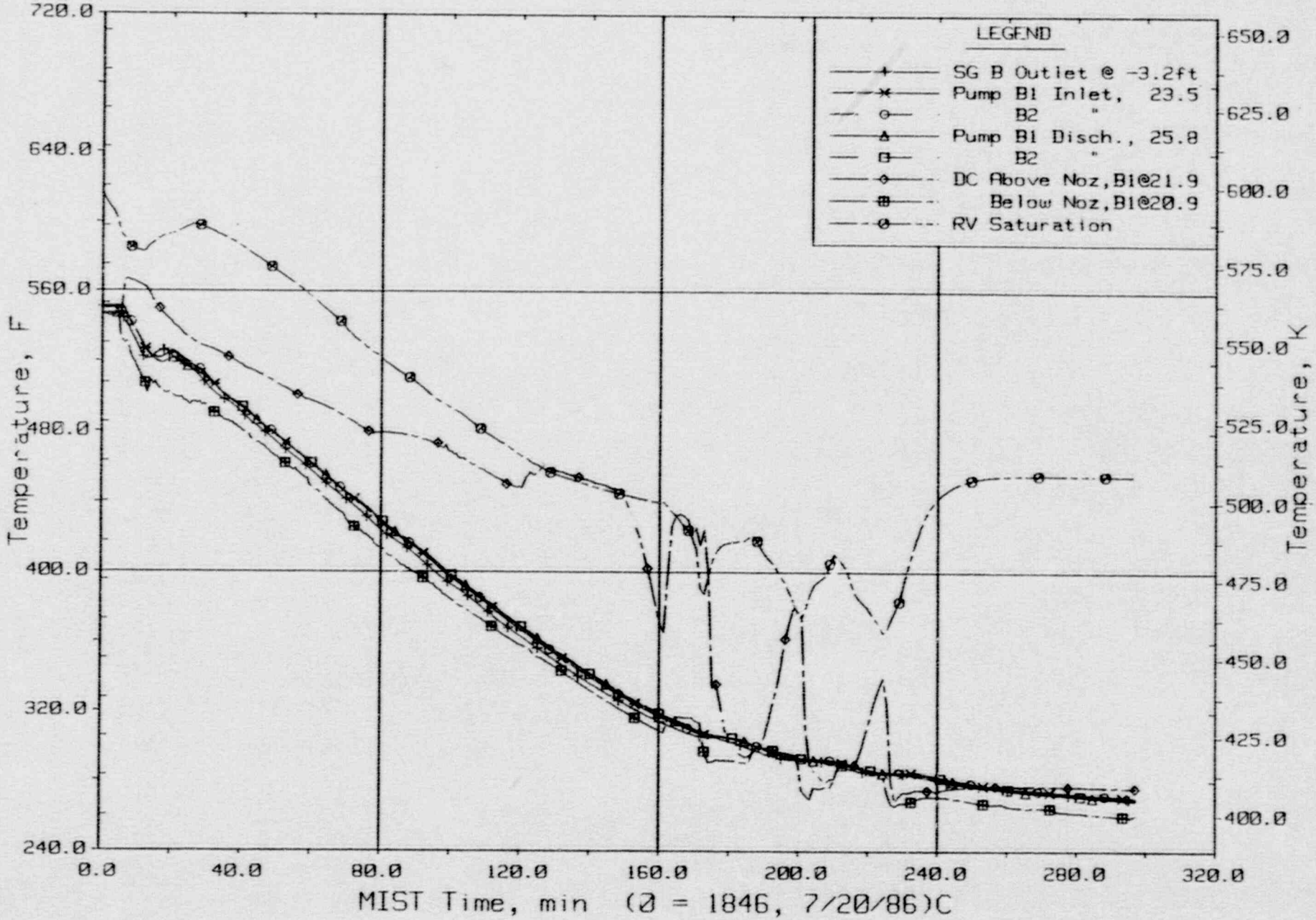

Loop B Cold Leg Fluid Temperatures (RTDs).

Mon May 16 18:47:04 1988

C2RTØ

FINAL DATA

T320101: Group 32 SBLOCA Test 1, Reduced Leak Size - 5 cm2.

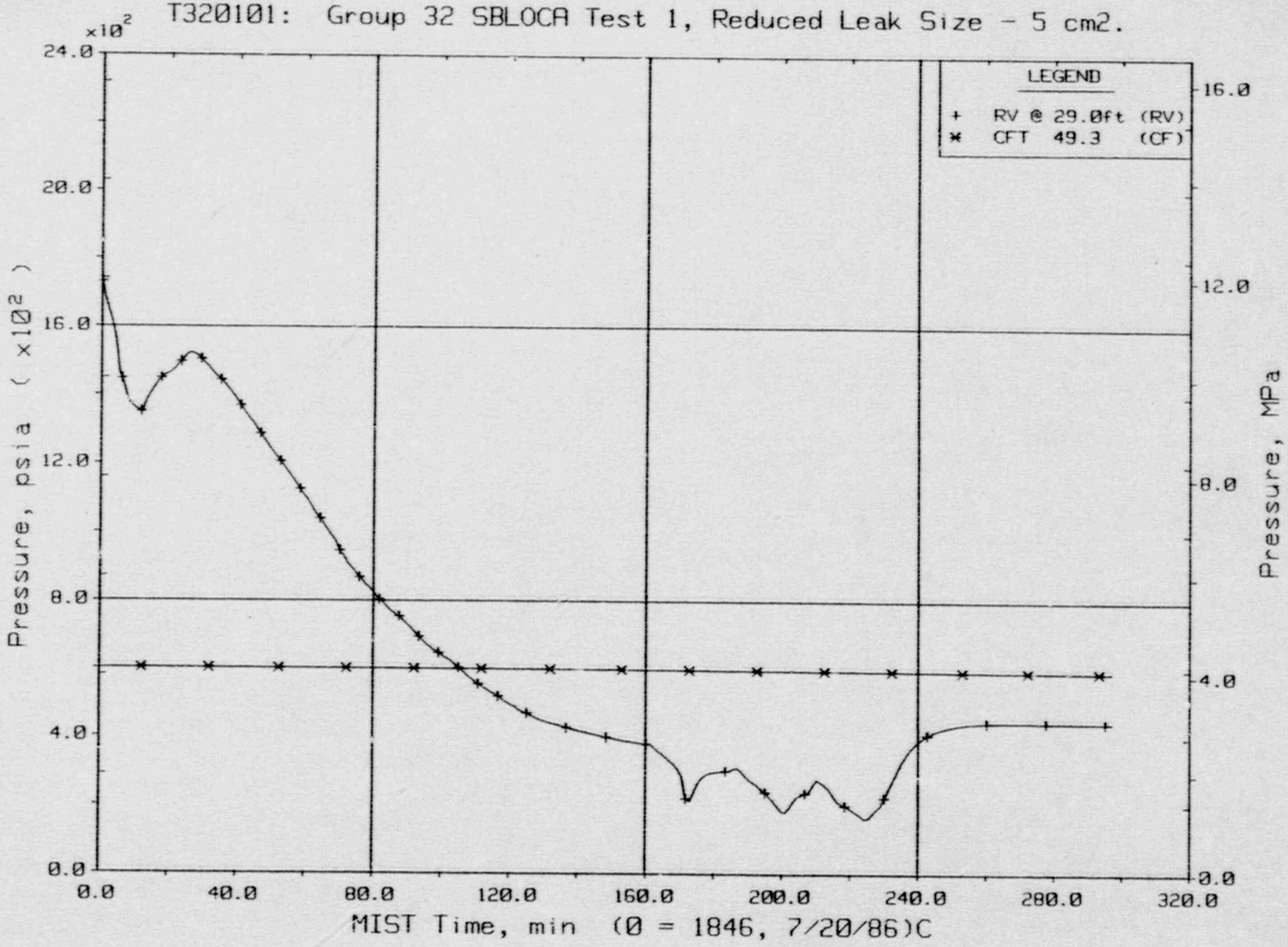

Primary System and Core Flood Tank Pressures (GP01s).

Mon May 16 18:49:44 1988

CFGP1

FINAL DATA

T320101: Group 32 SBLOCA Test 1, Reduced Leak Size - 5 cm2.

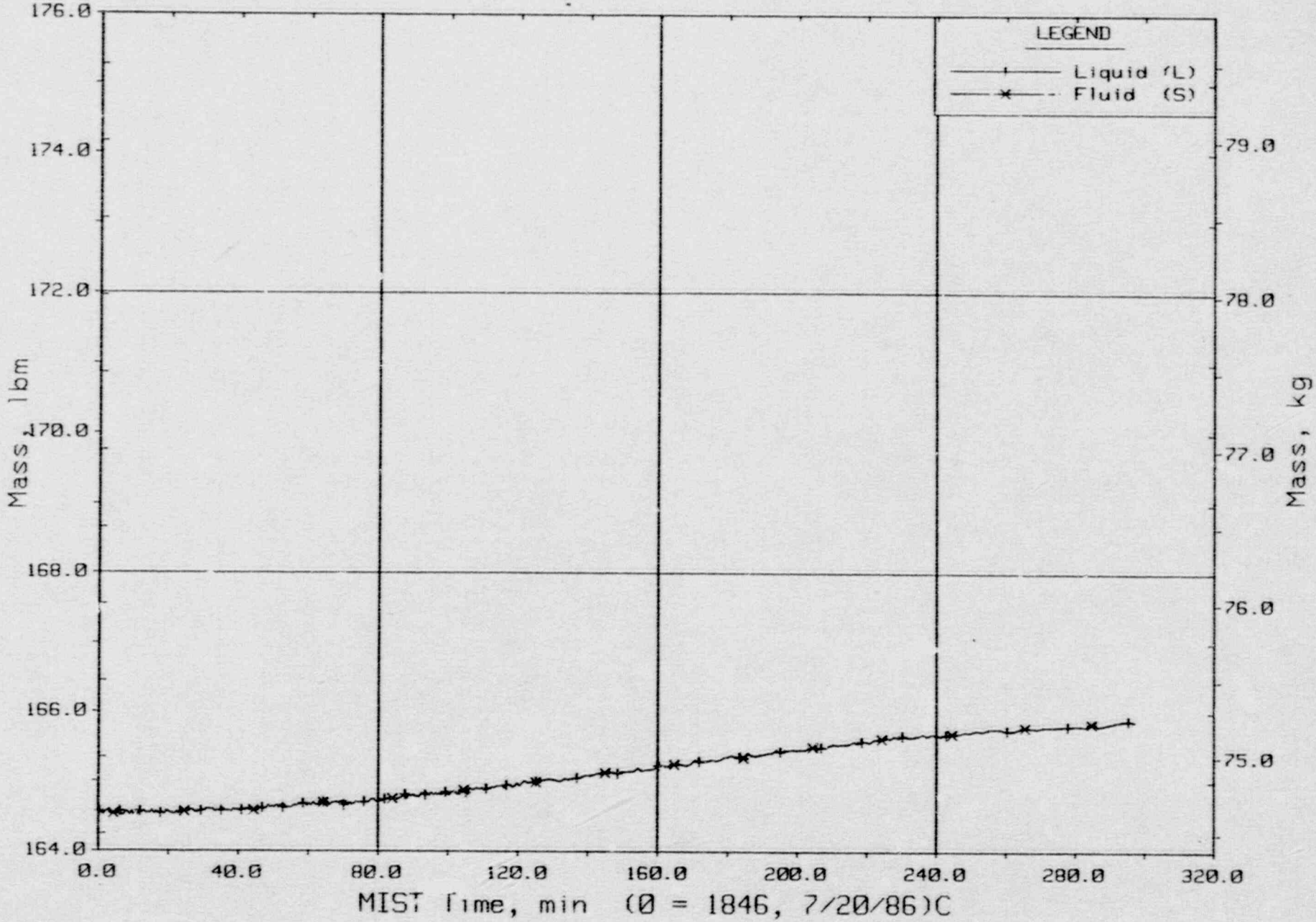

Core Flood Tank Liquid and Fluid Mass (CFMa20s).

Mon May 16 18:52:25 1988

CFML1

FINAL DATA

T320101: Group 32 Test 1, Reduced Leak Size.

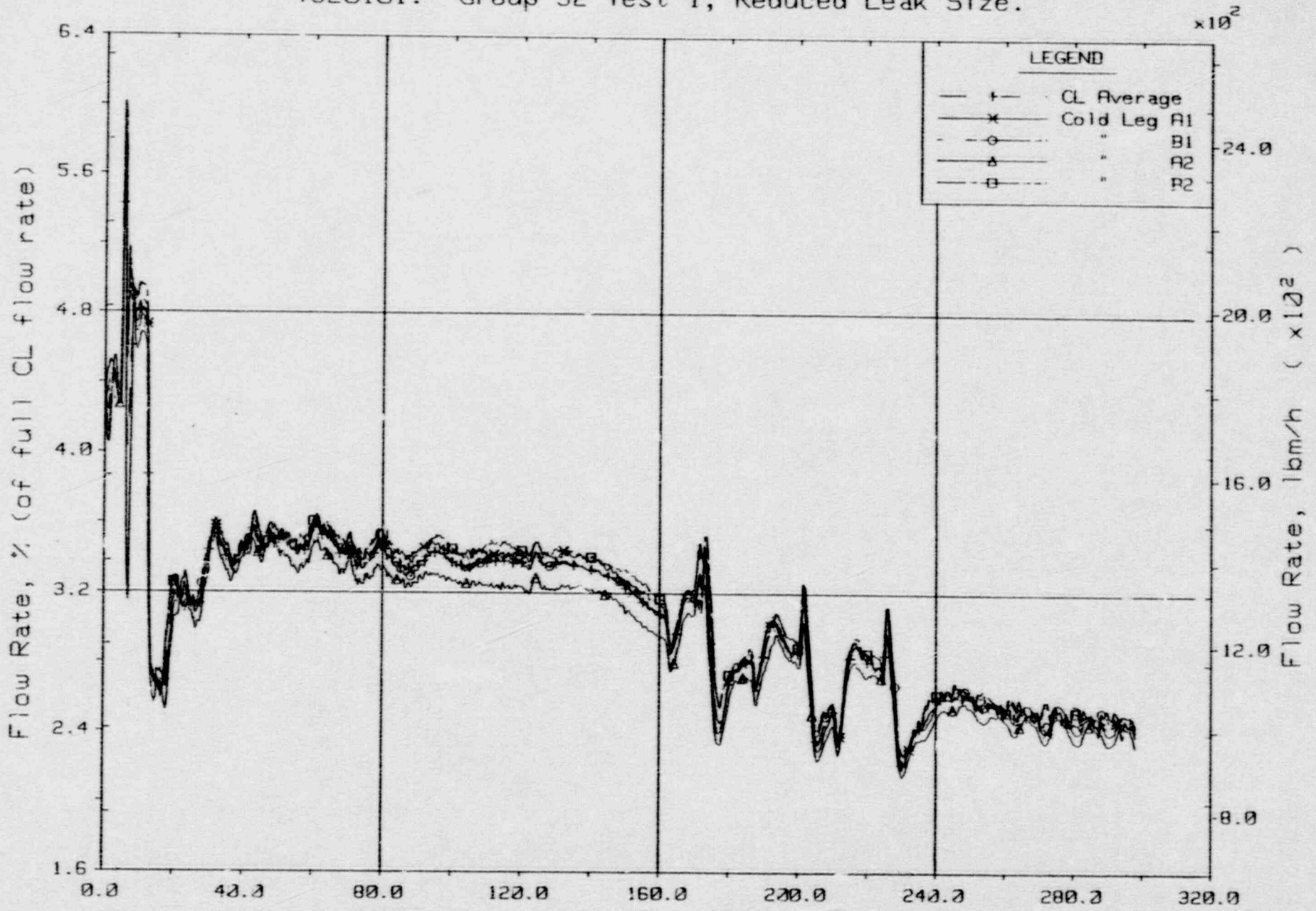

Cold Leg (Venturi) Flow Rates.

Mon Oct 31 14:20:29 1988

CLFL1

FINAL DATA

T320101: Group 32 SBLOCA Test 1, Reduced Leak Size - 5 cm2.

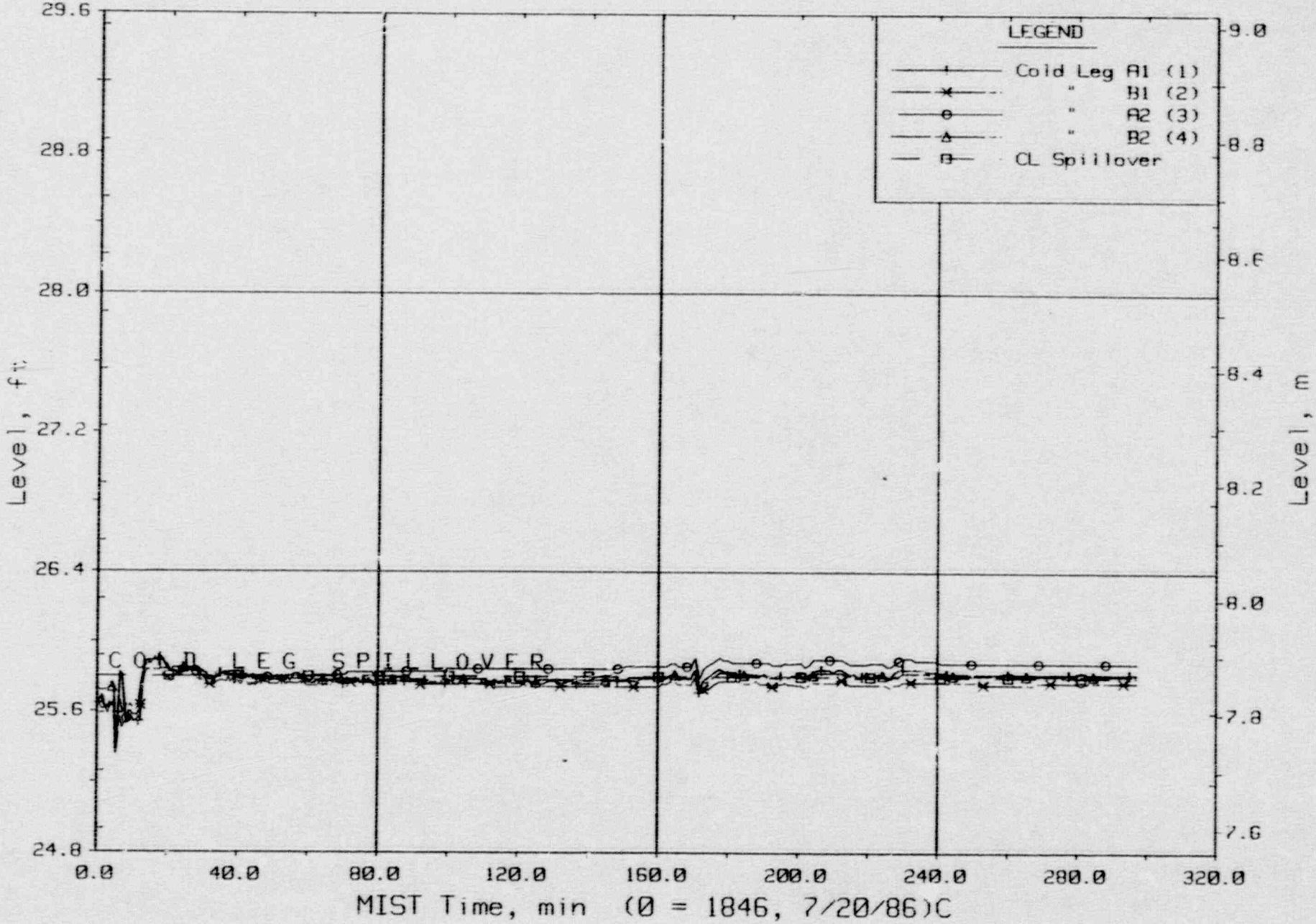

Cold Leg Suction Collapsed Liquid Levels (CnLV22s).

Mon May 16 18:55:49 1988

CLLV4

FINAL DATA

T320101: Group 32 SBLOCA Test 1, Reduced Leak Size - 5 cm2.

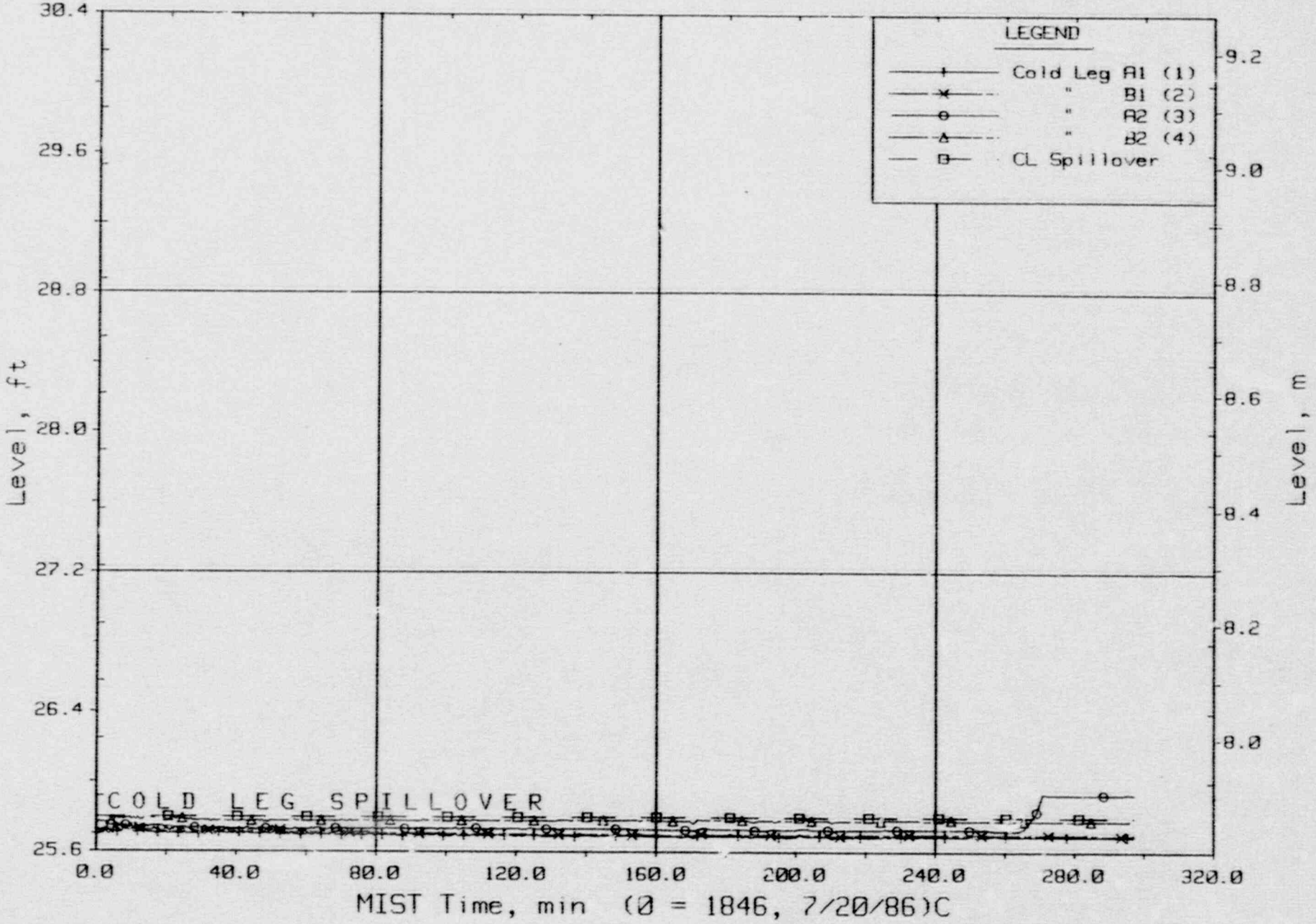

Cold Leg Discharge Collapsed Liquid Levels (CnLV23s).

Mon May 16 18:58:40 1988

CLLV5

FINAL DATA

T320101: Group 32 SBLOCA Test 1, Reduced Leak Size - 5 cm2.

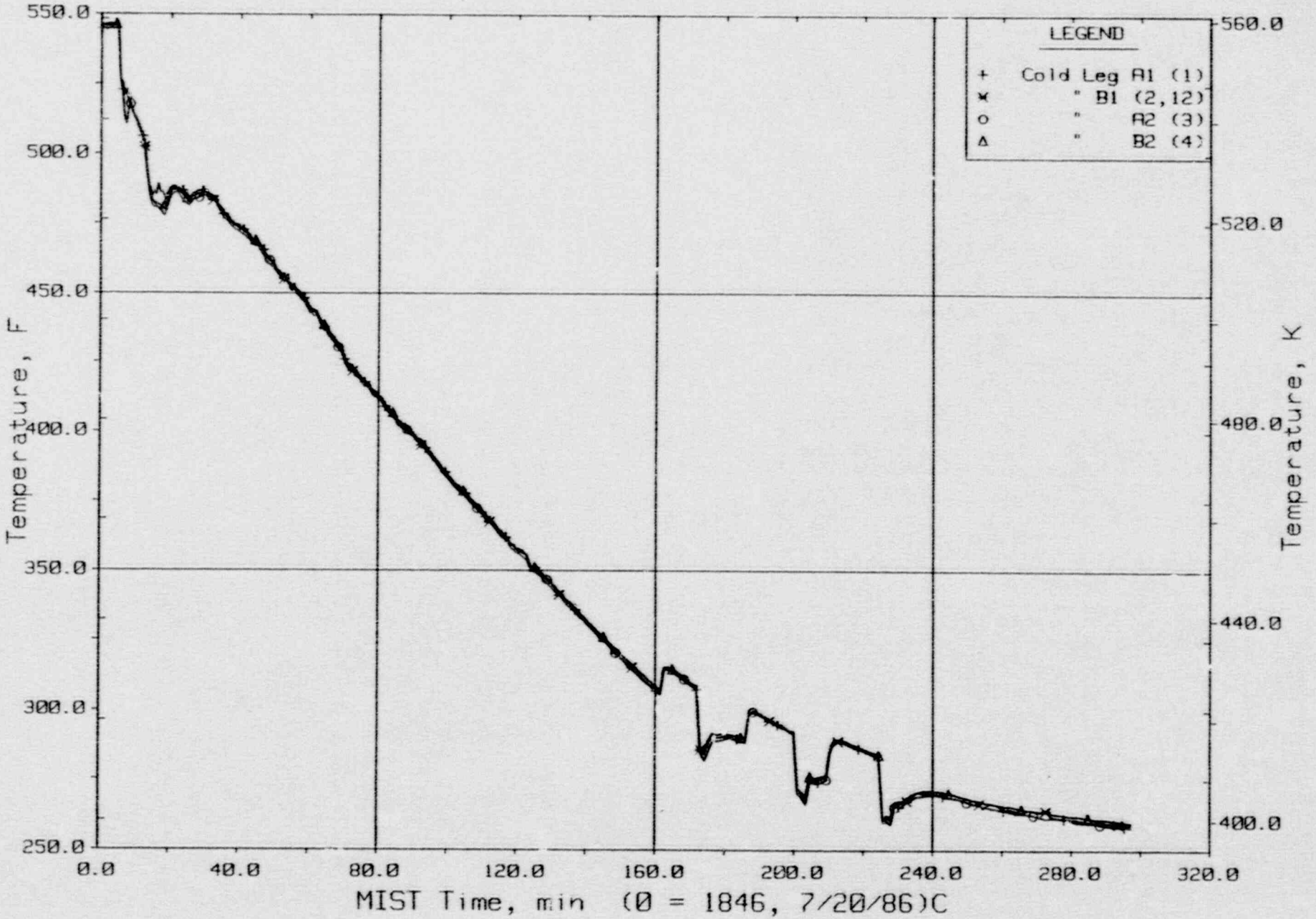

Cold Leg Nozzle Fluid Temperatures, Top of Rake (21.3ft, CnTC11s).

Mon May 16 19:03:31 1988

CLTC1

FINAL DATA

T320101: Group 32 SBLOCA Test 1, Reduced Leak Size - 5 cm2.

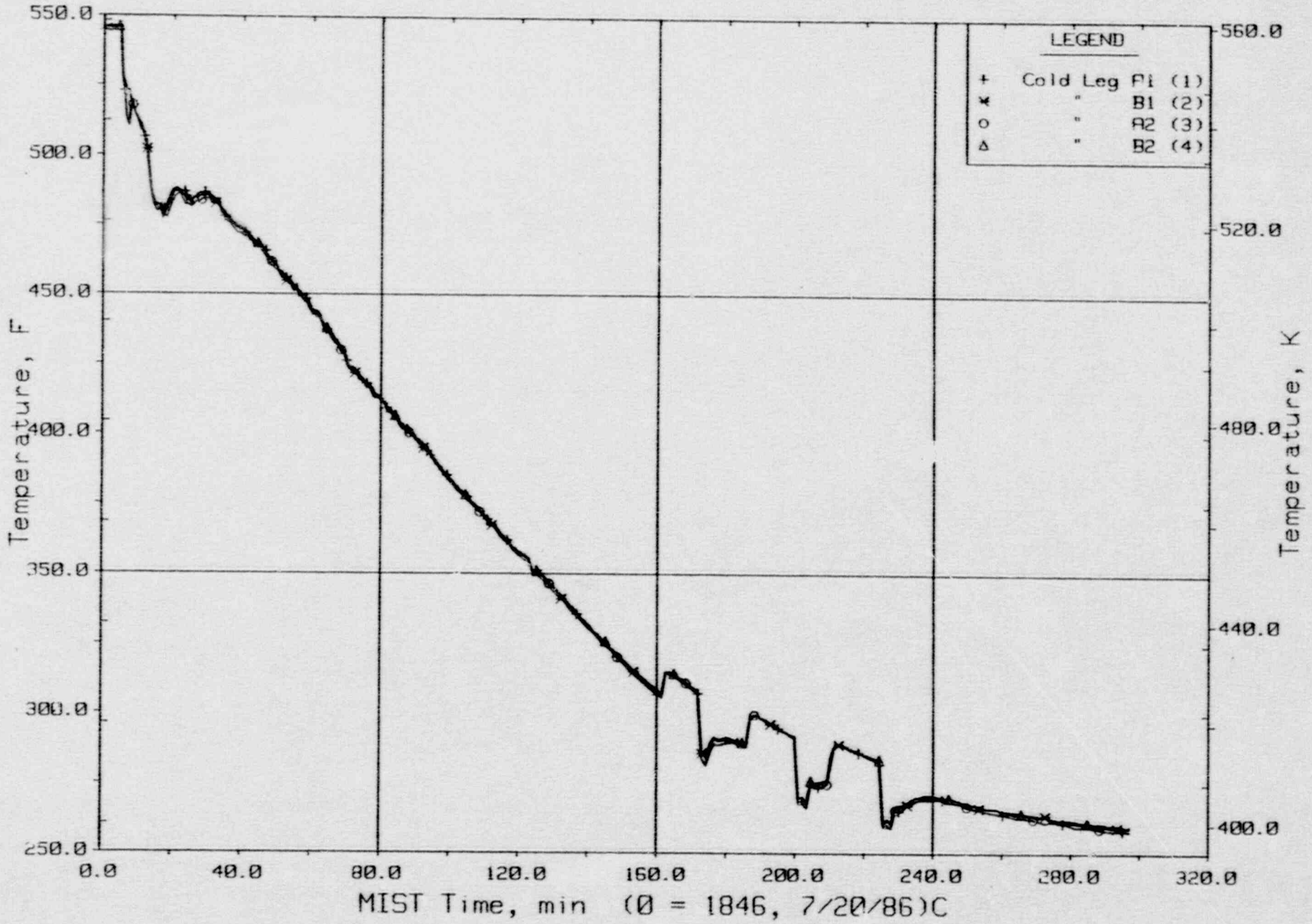

Cold Leg Nozzle Fluid Temperatures, Bottom of Rake (21.2ft, CnTC14s).

Mon May 16 19:06:01 1988

CLTC2

FINAL DATA

T?20101: Group 32 SBLOCA Test 1, Reduced Leak Size - 5 cm2.

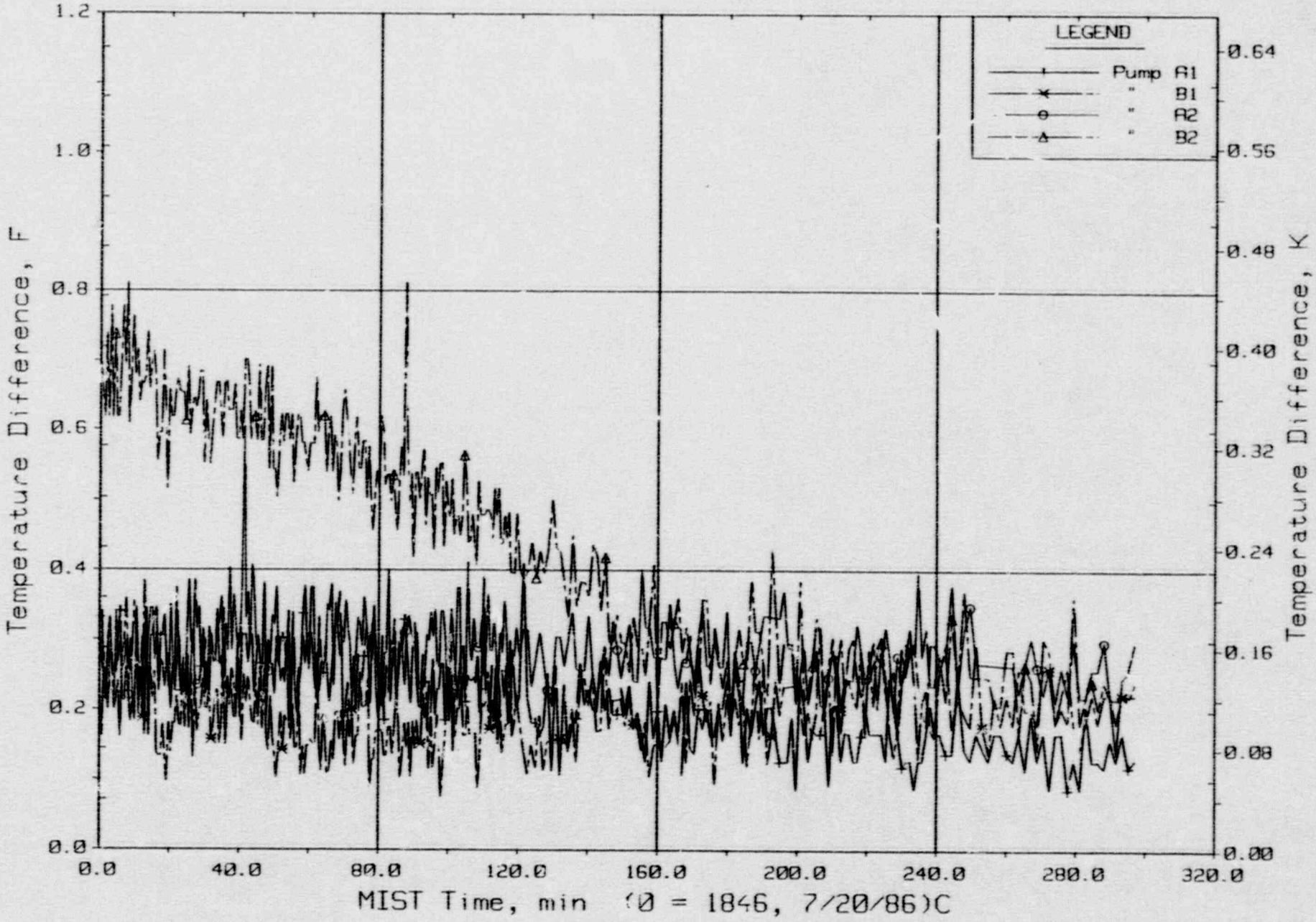

Maximum Differences Among RCP Rake FLuid Temperatures.

Mon May 16 19:09:08 1988

CLTD1

FINAL DATA

T320101: Group 32 SBLOCA Test 1, Reduced Leak Size - 5 cm2.

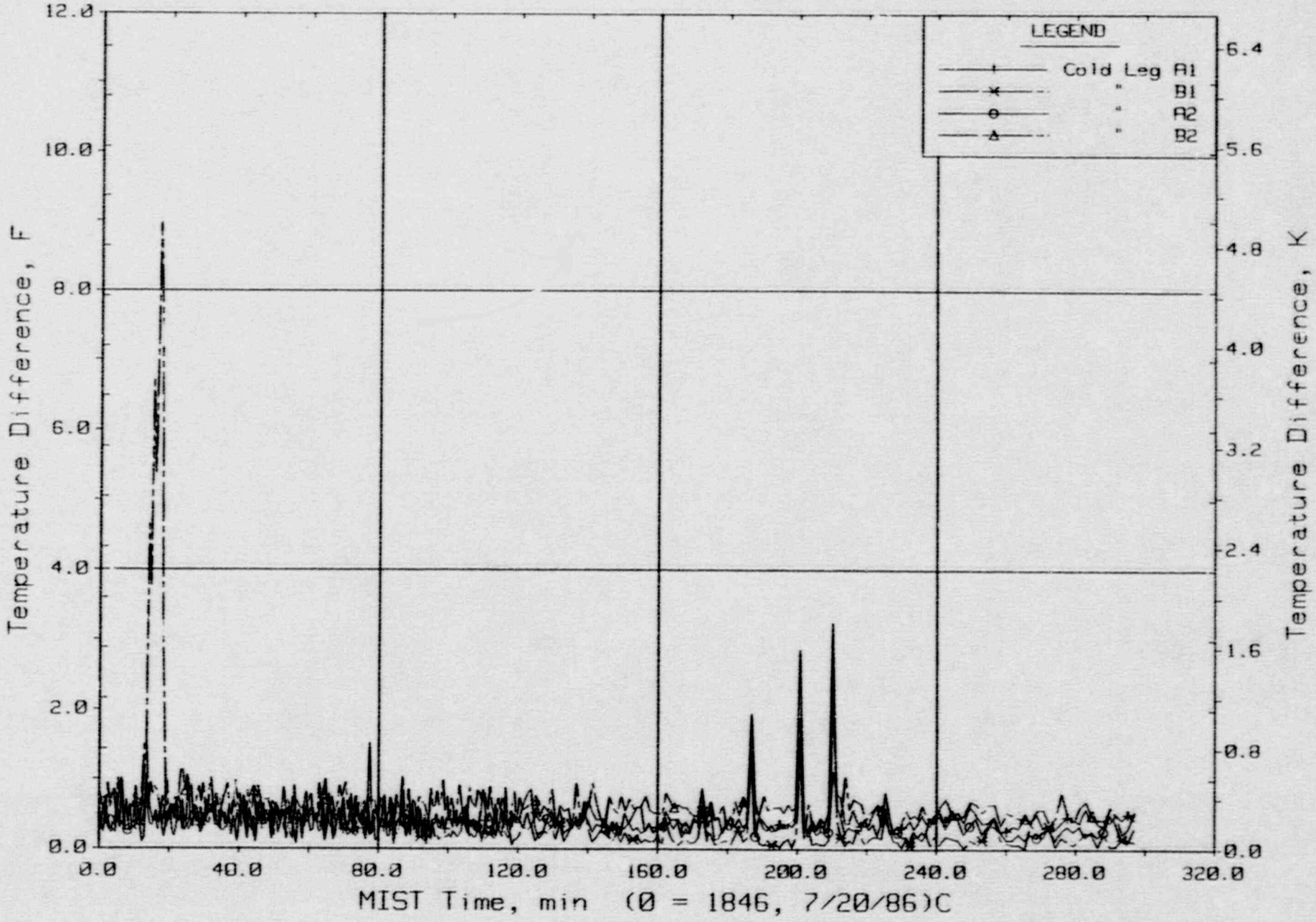

Maximum Differences Among CL Nozzle Rake Fluid Temperatures.

Mon May 16 19:12:31 1988

CLTD2

FINAL DATA

T320101: Group 32 SBLOCA Test 1, Reduced Leak Size - 5 cm2.

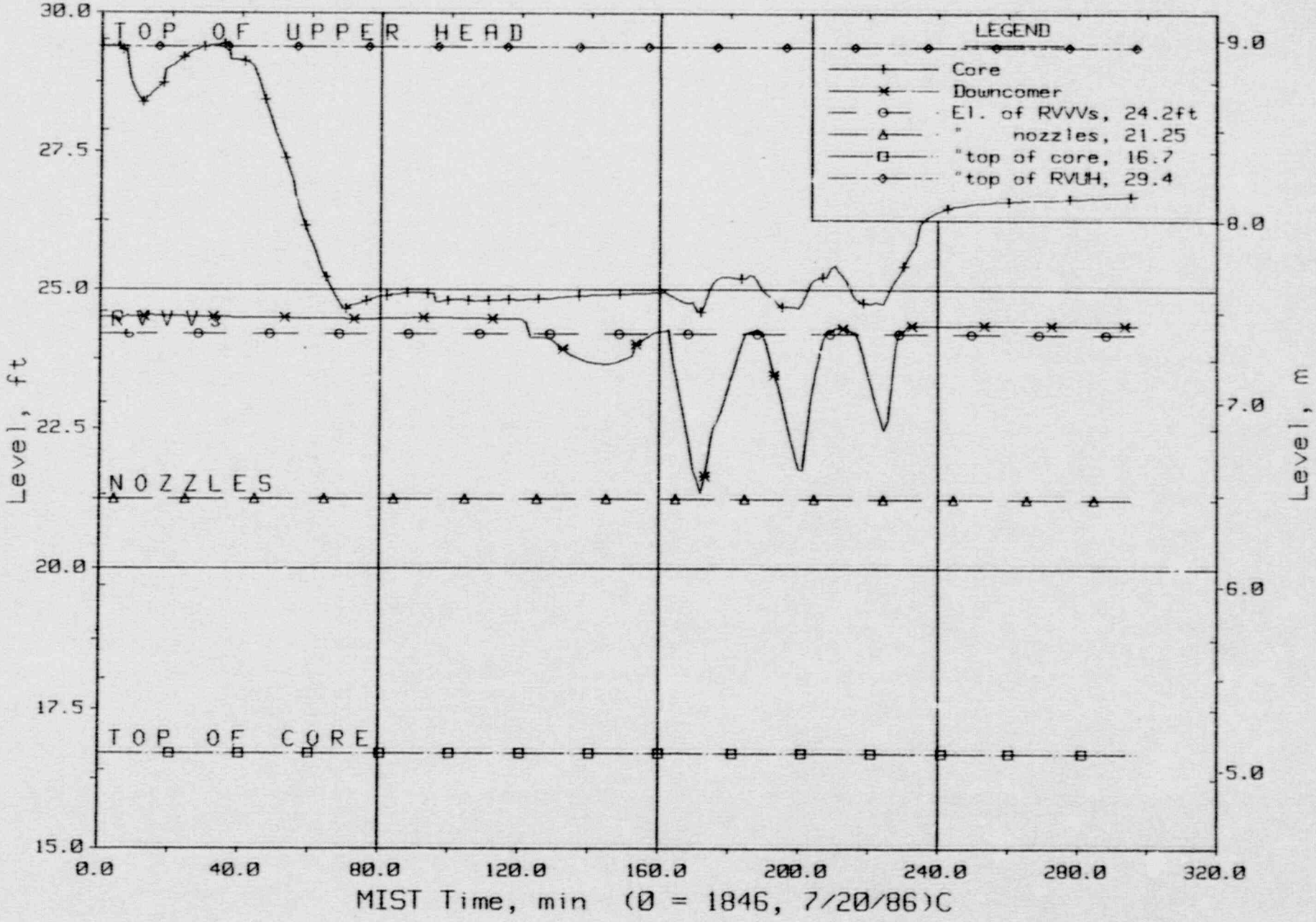

Core Region Collapsed Liquid Levels.

Mon May 16 19:15:49 1988

COLV1

FINAL DATA

T320101: Group 32 SBLOCA Test 1, Reduced Leak Size - 5 cm2.

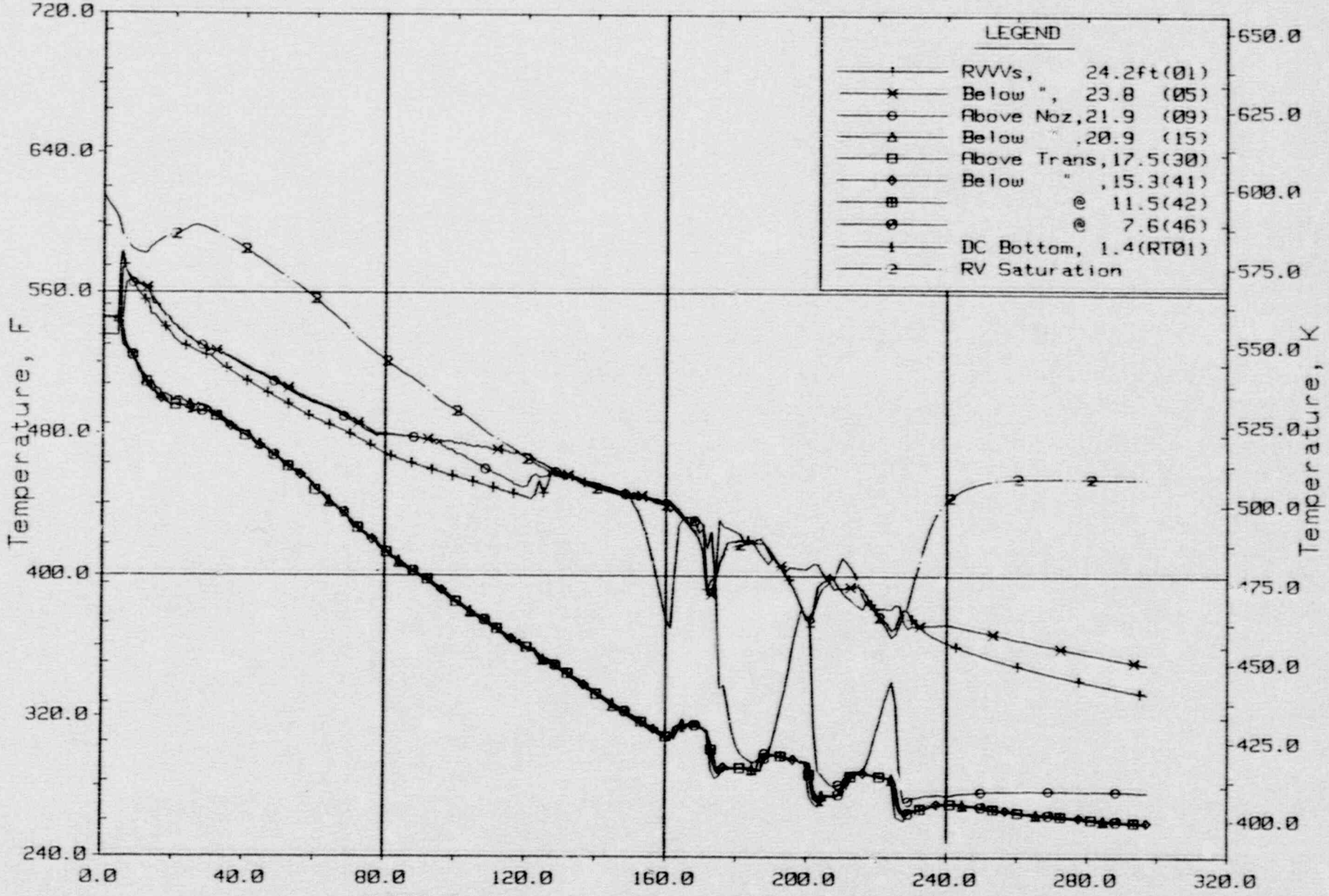

Downcomer Quadrant A1 Fluid Temperatures (DCTCs).

Mon May 16 19:21:10 1988

DCTC6

FINAL DATA

T320101: Group 32 SBLOCA Test 1, Reduced Leak Size - 5 cm2.

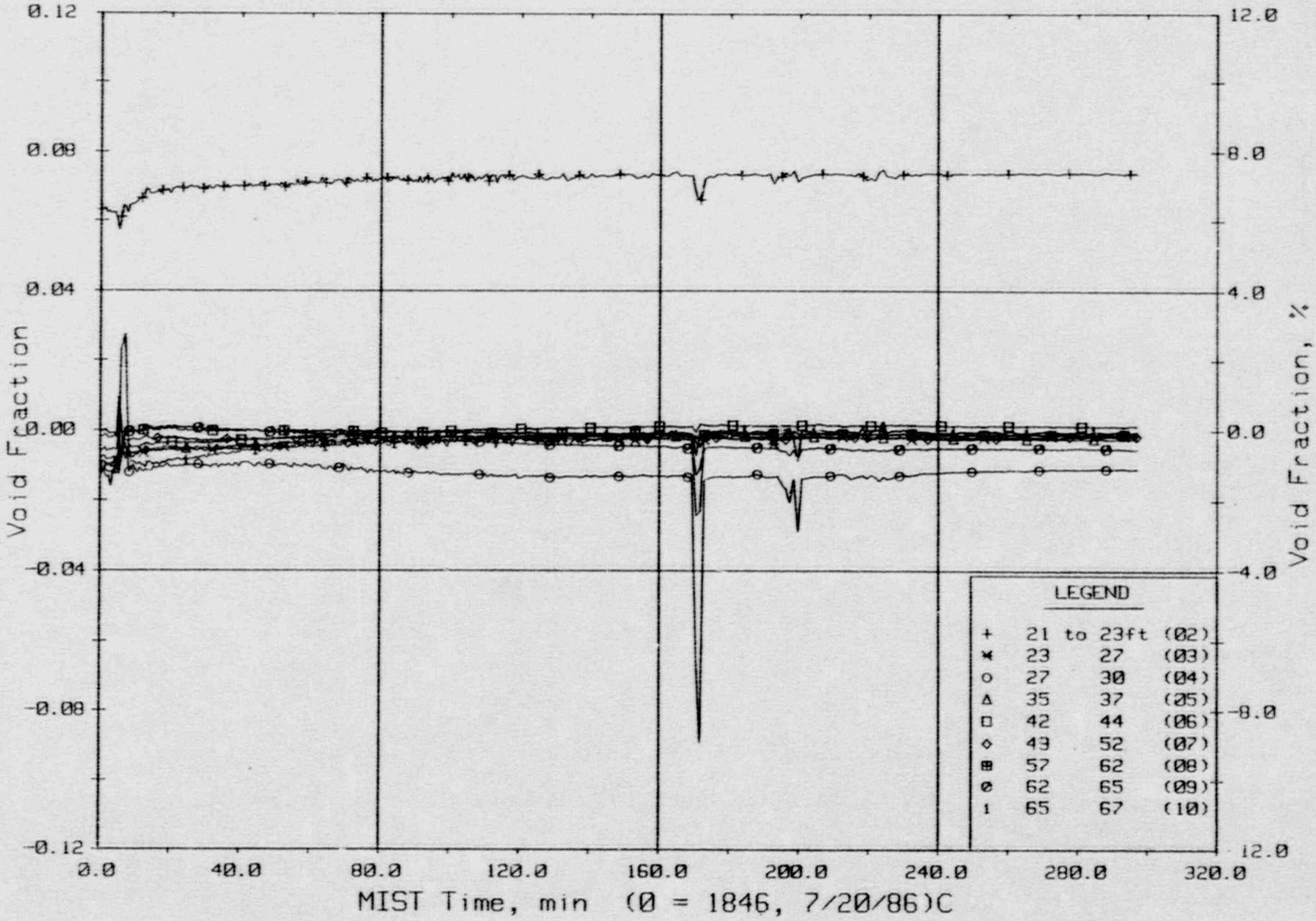

Hot Leg A Riser Void Fractions From Differential Pressures (HIVFs).

Mon May 16 19:25:03 1988

HIVF1

FINAL DATA

T320101: Group 32 SBLOCA Test 1, Reduced Leak Size - 5 cm2.

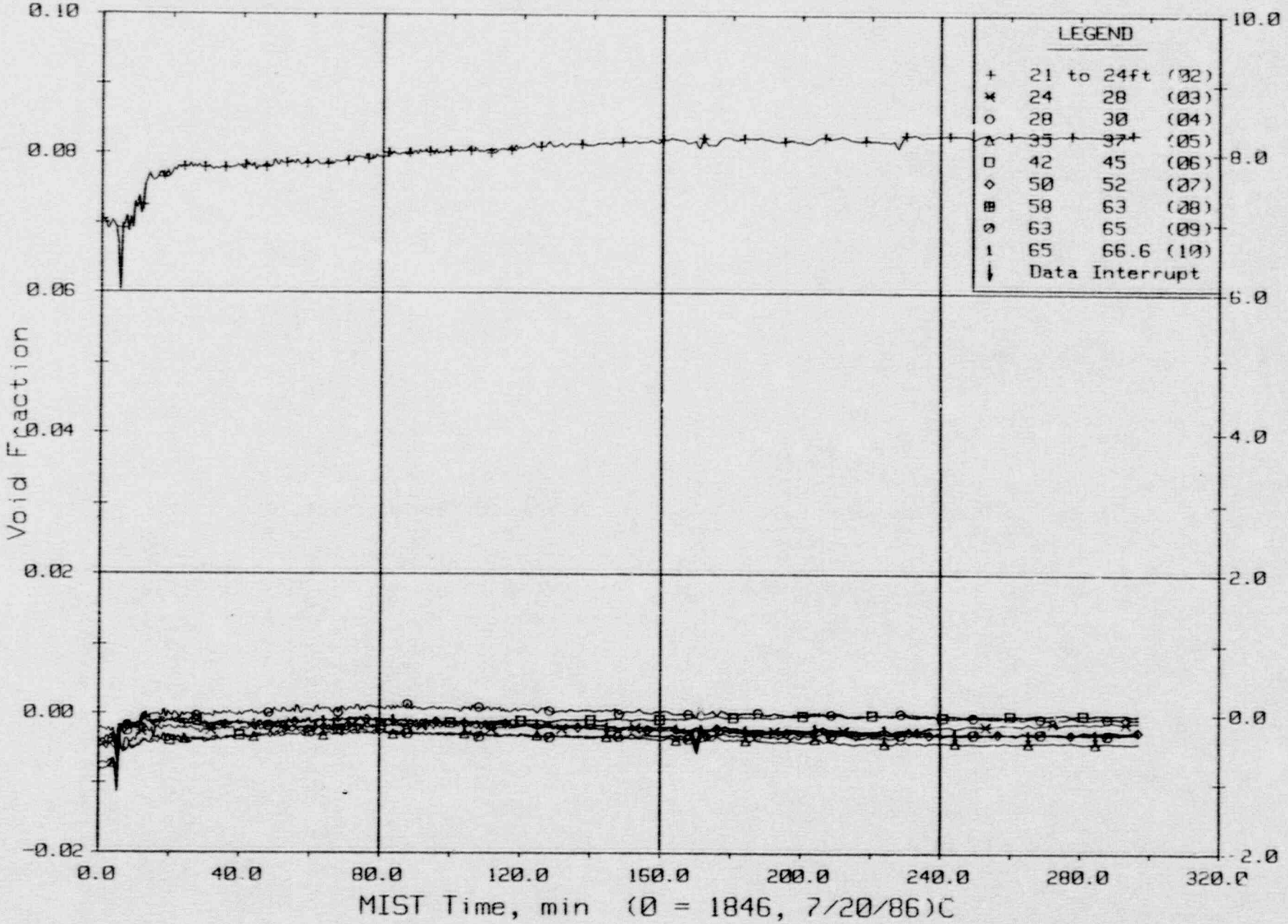

Hot Leg B Riser Void Fraction From Differential Pressures (H2VFs).

Mon May 16 19:28:24 1988

H2VF1

FINAL DATA

T320101: Group 32 SBLOCA Test 1, Reduced Leak Size - 5 cm2.

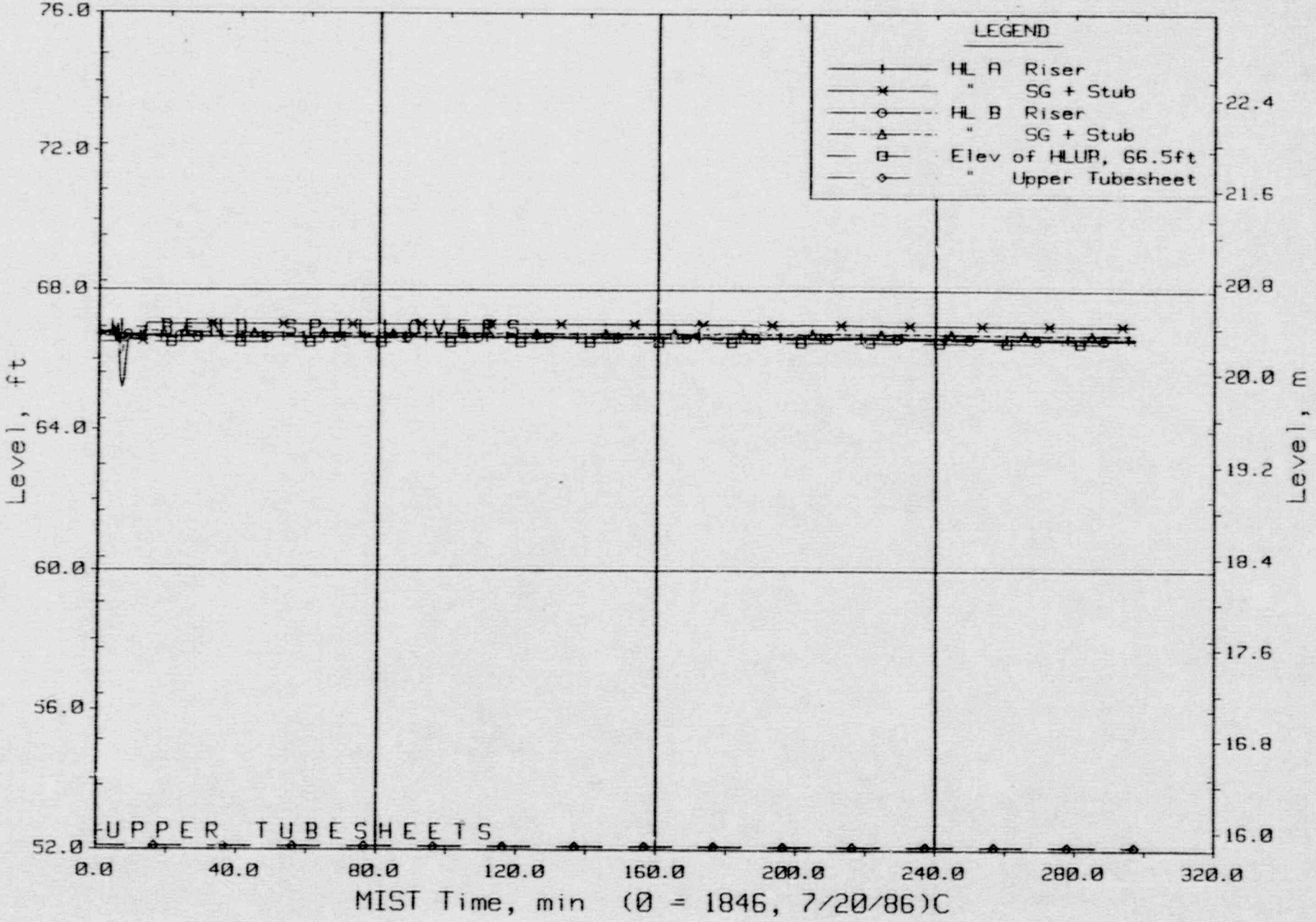

Hot Leg Riser and Stub Collapsed Liquid Levels.

Mon May 16 19:31:45 1988

HLLV1

FINAL DATA

T320101: Group 32 SBLOCA Test 1, Reduced Leak Size - 5 cm2.

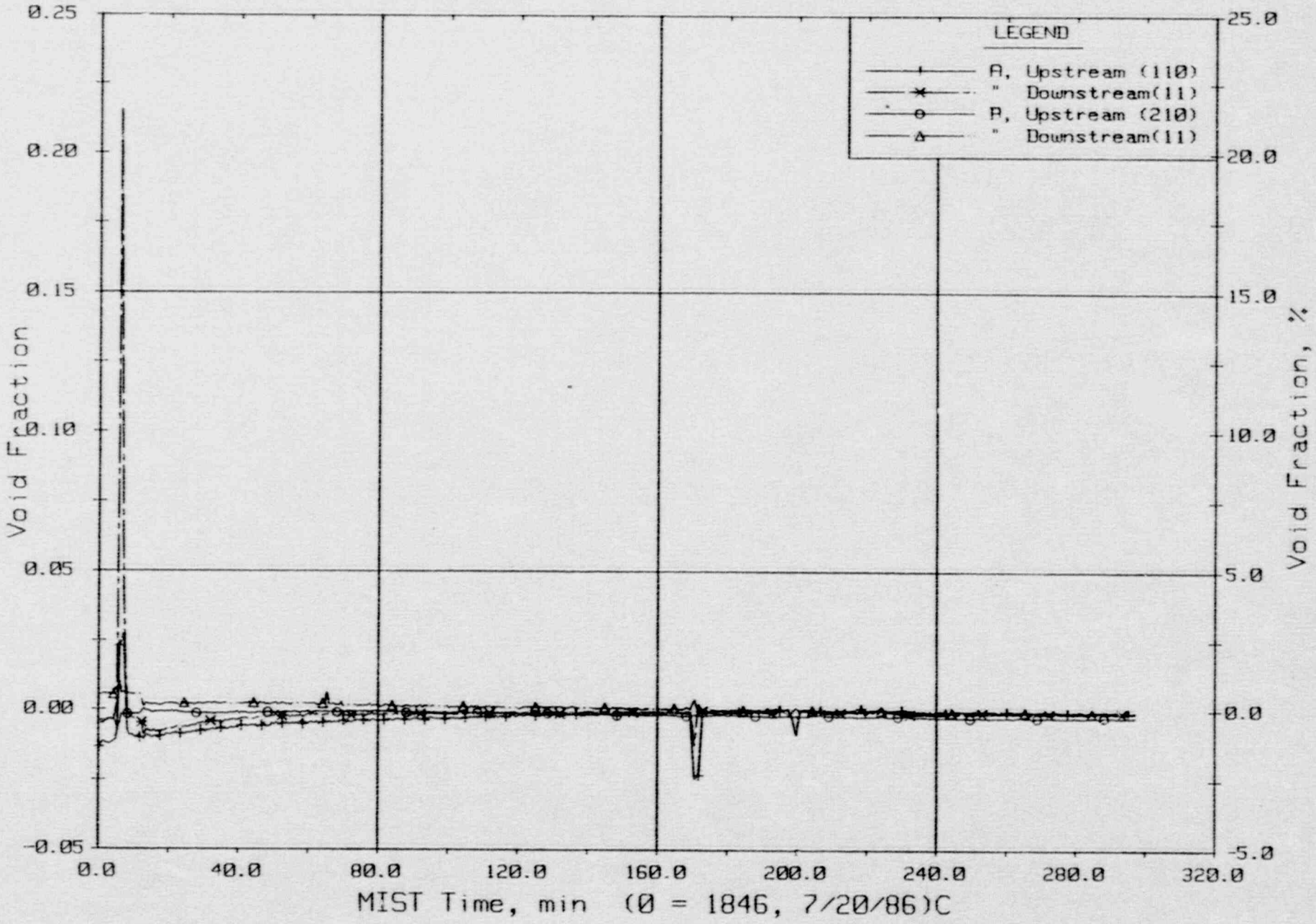

Hot Leg U-Bend Void Fractions From Diffl. Pressures (64.8 to 66.6 ft, HnVFs).

Mon May 16 19:34:44 1988

HLVF1

FINAL DATA

T320101: Group 32 SBLOCA Test 1, Reduced Leak Size - 5 cm2.

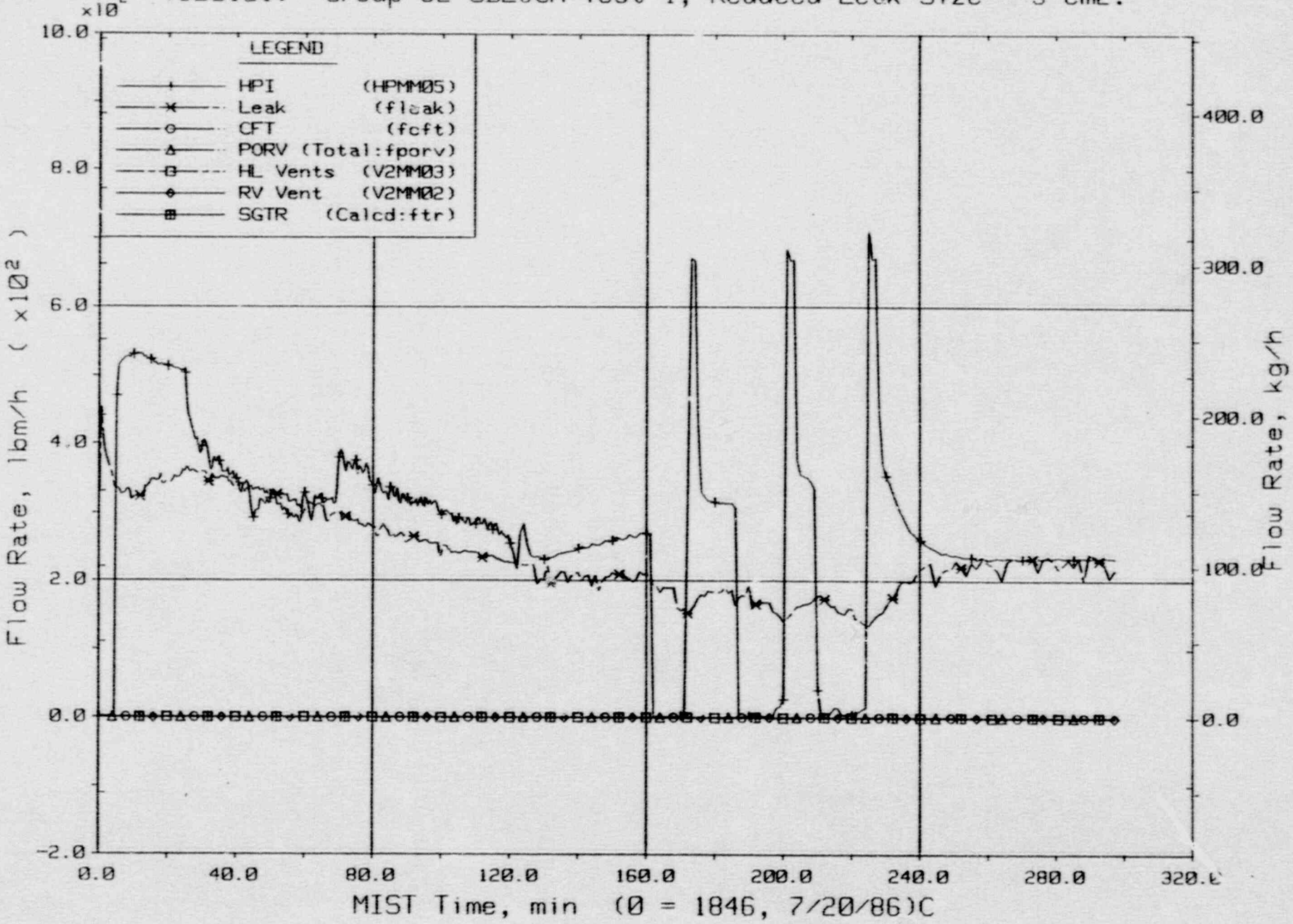

Primary System Boundary Flow Rates.

Fri May 20 11:35:44 1988

PBFL3

FINAL DATA

T320101: Group 32 SBLOCA Test 1, Reduced Leak Size - 5 cm2.

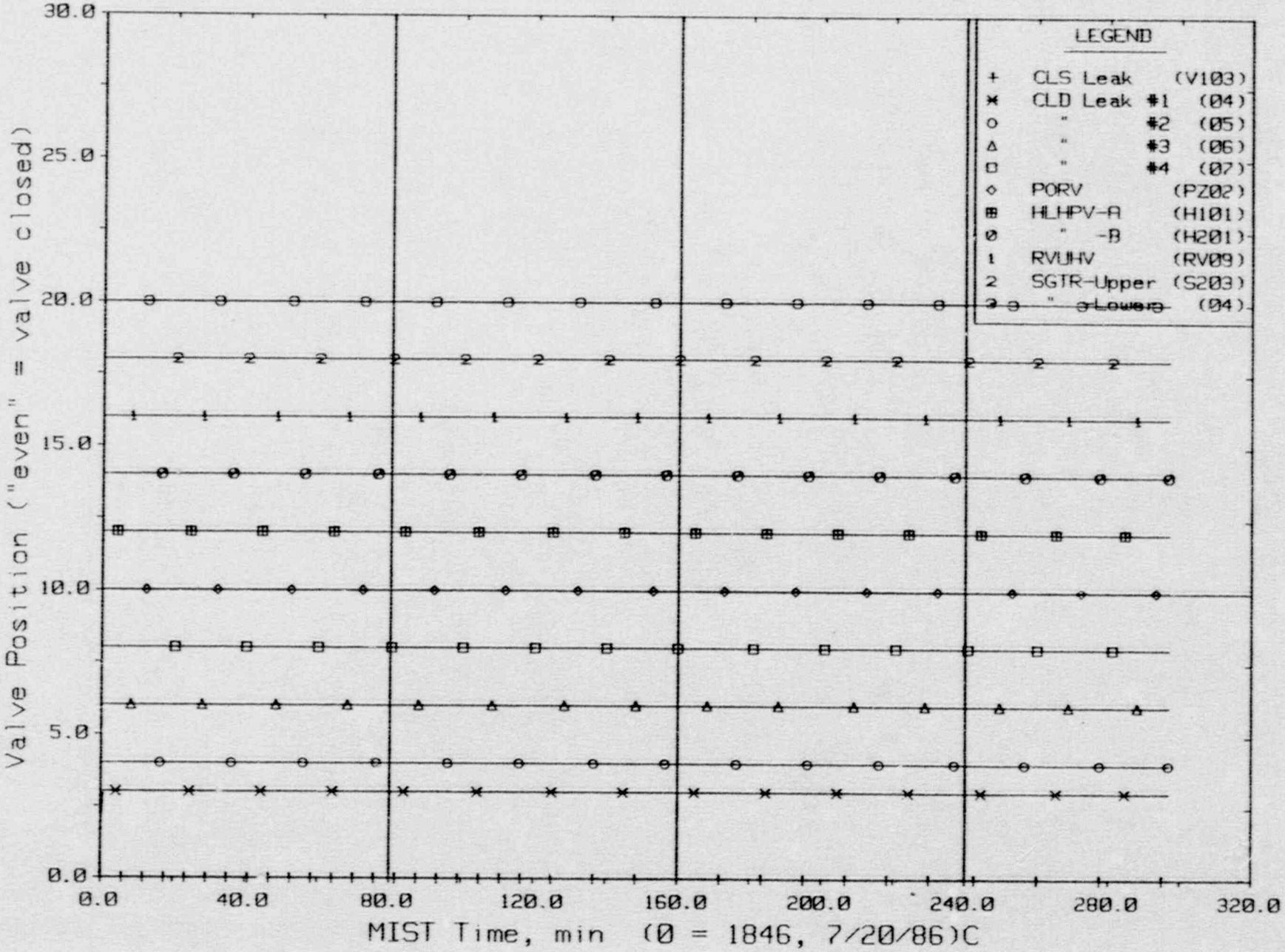

Primary System Discharge Limit Switch Indications (LSs).

Mon May 16 19:55:04 1988

PBLS1

FINAL DATA

T320101: Group 32 SBLOCA Test 1, Reduced Leak Size - 5 cm2.

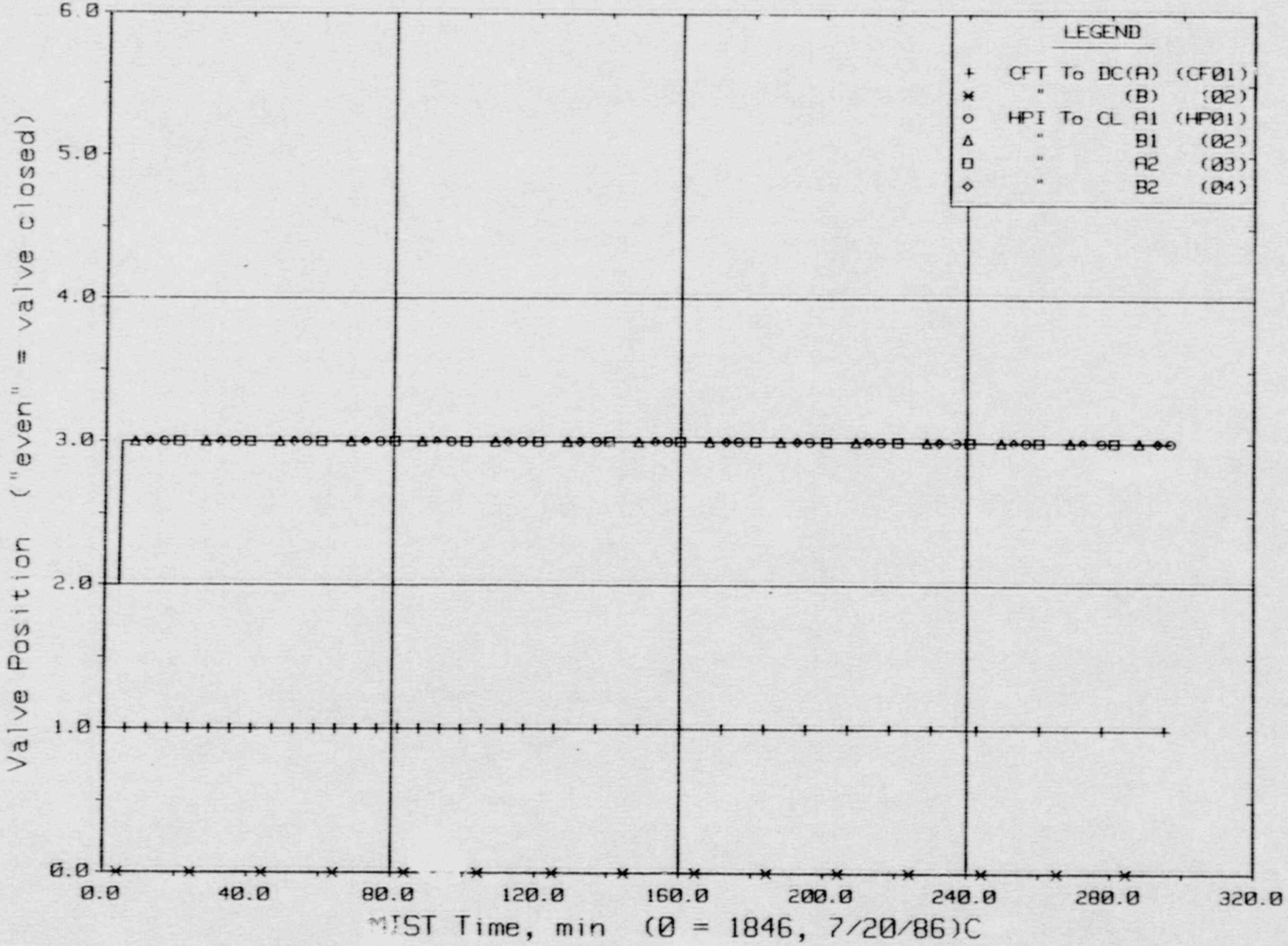

Primary System Injection Limit Switch Indications (LSs).

Mon May 16 19:58:01 1988

PBLS2

FINAL DATA

T320101: Group 32 SBLOCA Test 1, Reduced Leak Size - 5 cm2.

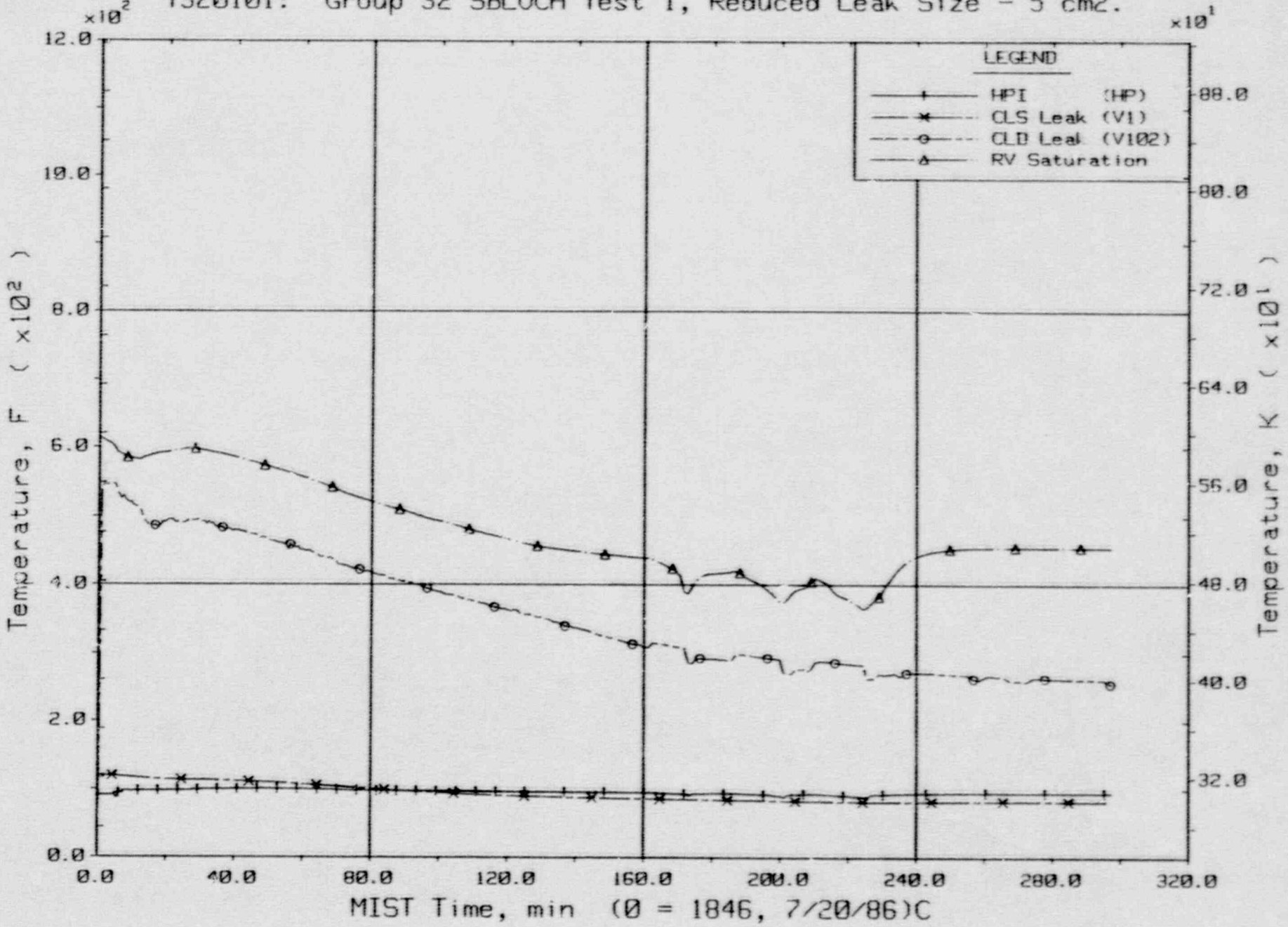

Single-Phase Discharge and HPI Fluid Temperatures (TC01s).

Mon May 16 19:43:22 1988

PBTC1

FINAL DATA

T320101: Group 32 SBLOCA Test 1, Reduced Leak Size - 5 cm2.

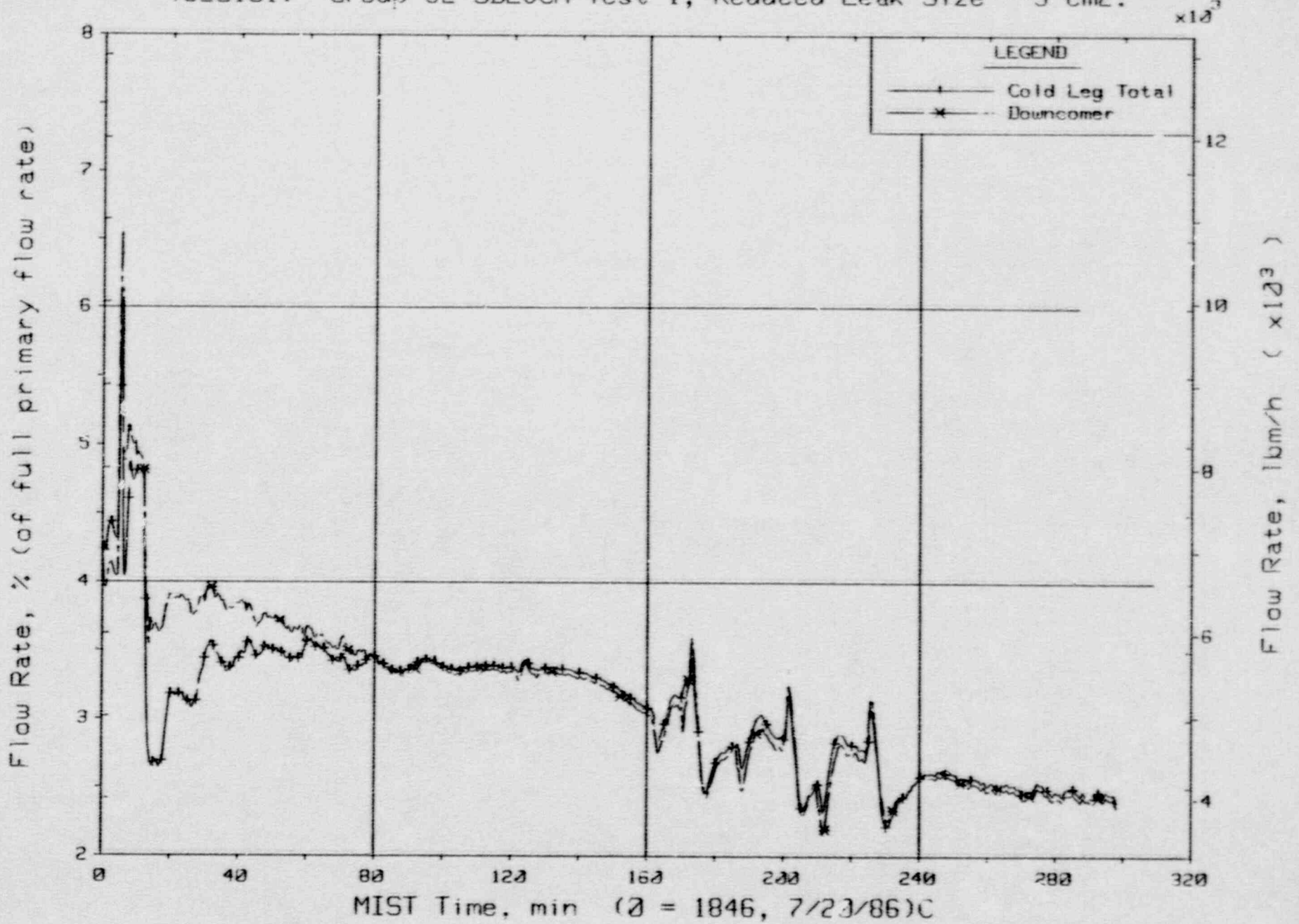

Primary System Venturi Flow Rates.

Mon Oct 31 14:35:02 1988

PRFL7

FINAL DATA

T320101: Group 32 SBLOCA Test 1, Reduced Leak Size - 5 cm2.

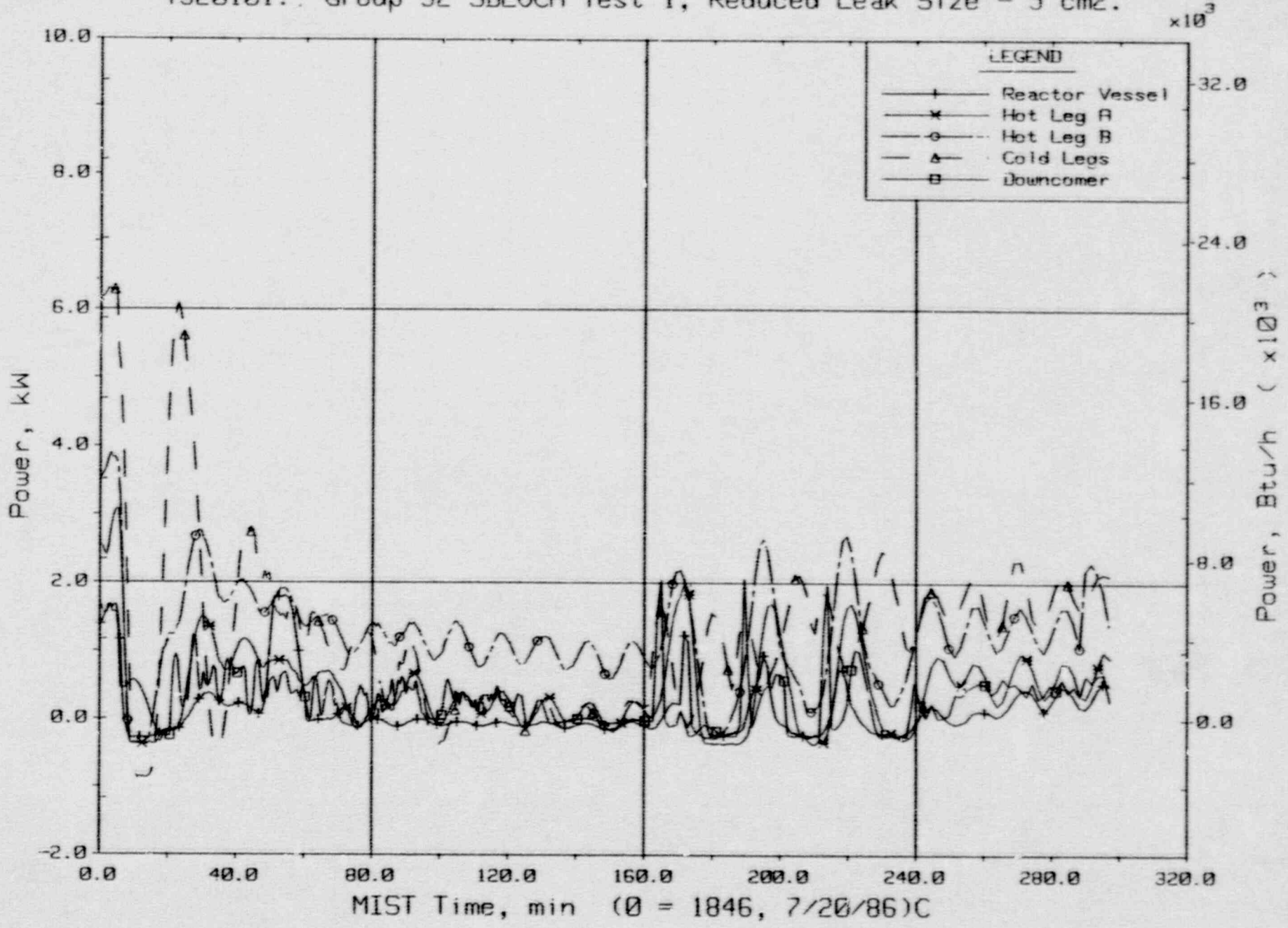

Guard Heater Specified Power Per Primary Component.

Mon May 16 19:46:33 1988

PRGQ1

FINAL DATA

T320101: Group 32 SBLOCA Test 1, Reduced Leak Size - 5 cm2.

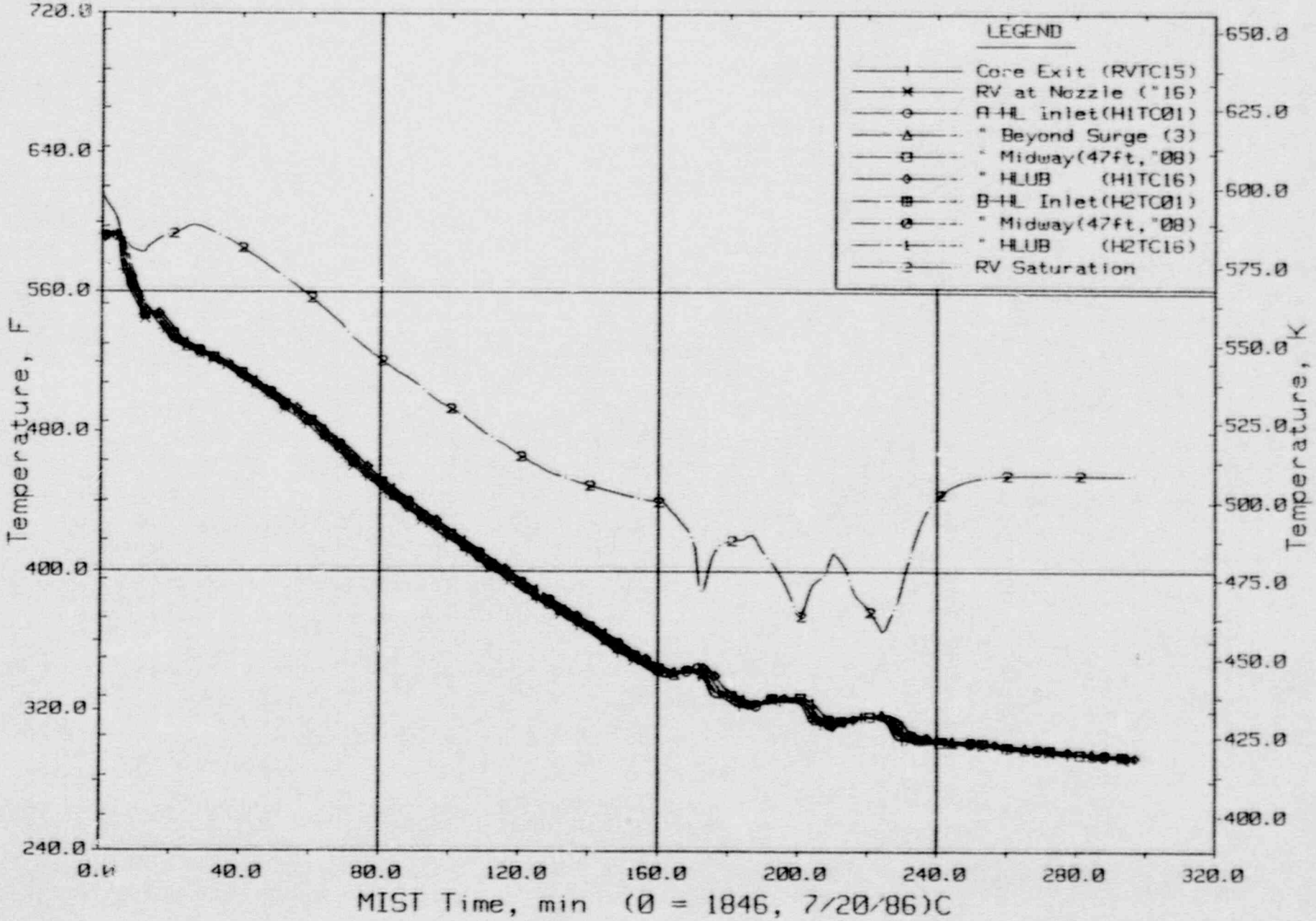

Composite Core Exit and Hot Leg Fluid Temperatures.

Mon May 16 19:50:42 1988

PRKT1

FINAL DATA

T320101: Group 32 SBLOCA Test 1, Reduced Leak Size - 5 cm2.

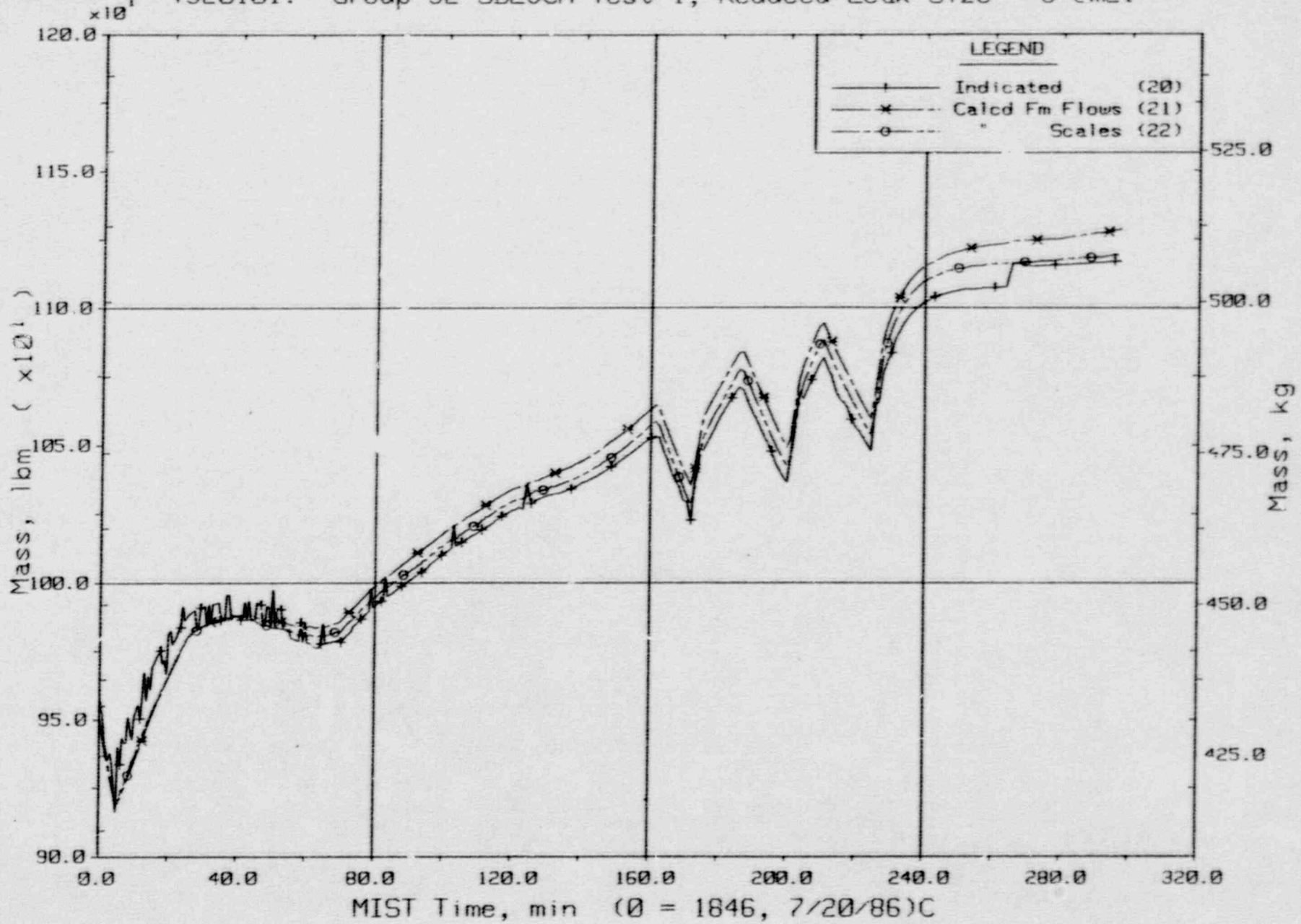

Primary System Total Fluid Mass (PLMLs).

Mon May 16 20:00:26 1988

PRML2

FINAL DATA

T32?101: Group 32 SBLOCA Test 1, Reduced Leak Size - 5 cm2.

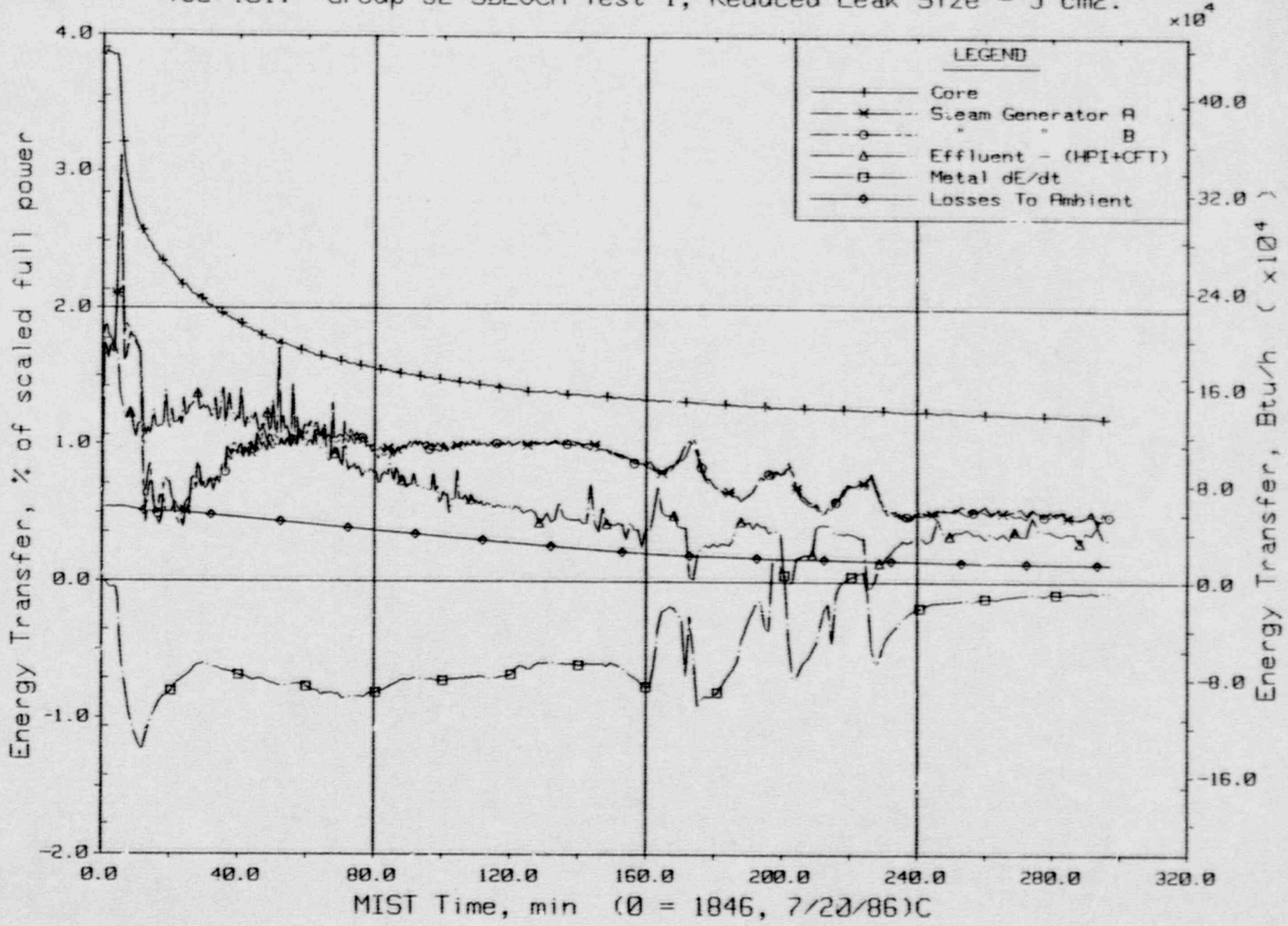

Primary System Energy Transfer.

Mon May 16 20:11:57 1988

PROE2

FINAL DATA

T320101: Group 32 SBLOCA Test 1, Reduced Leak Size - 5 cm2.

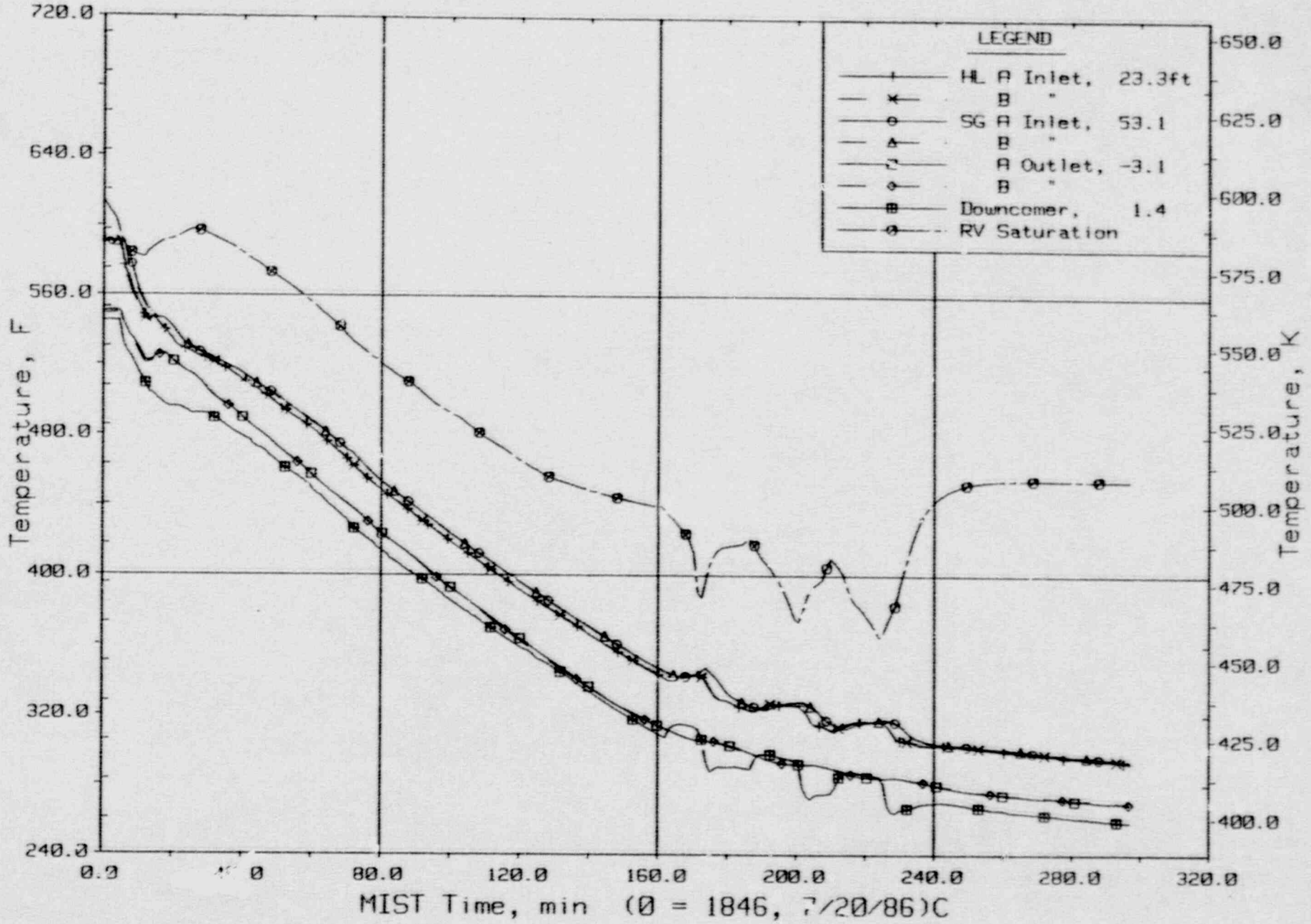

Primary System Fluid Temperatures (RTDs).

Mon May 16 20:15:30 1988

PRRT0

FINAL DATA

T320101: Group 32 SBLOCA Test 1, Reduced Leak Size - 5 cm2.

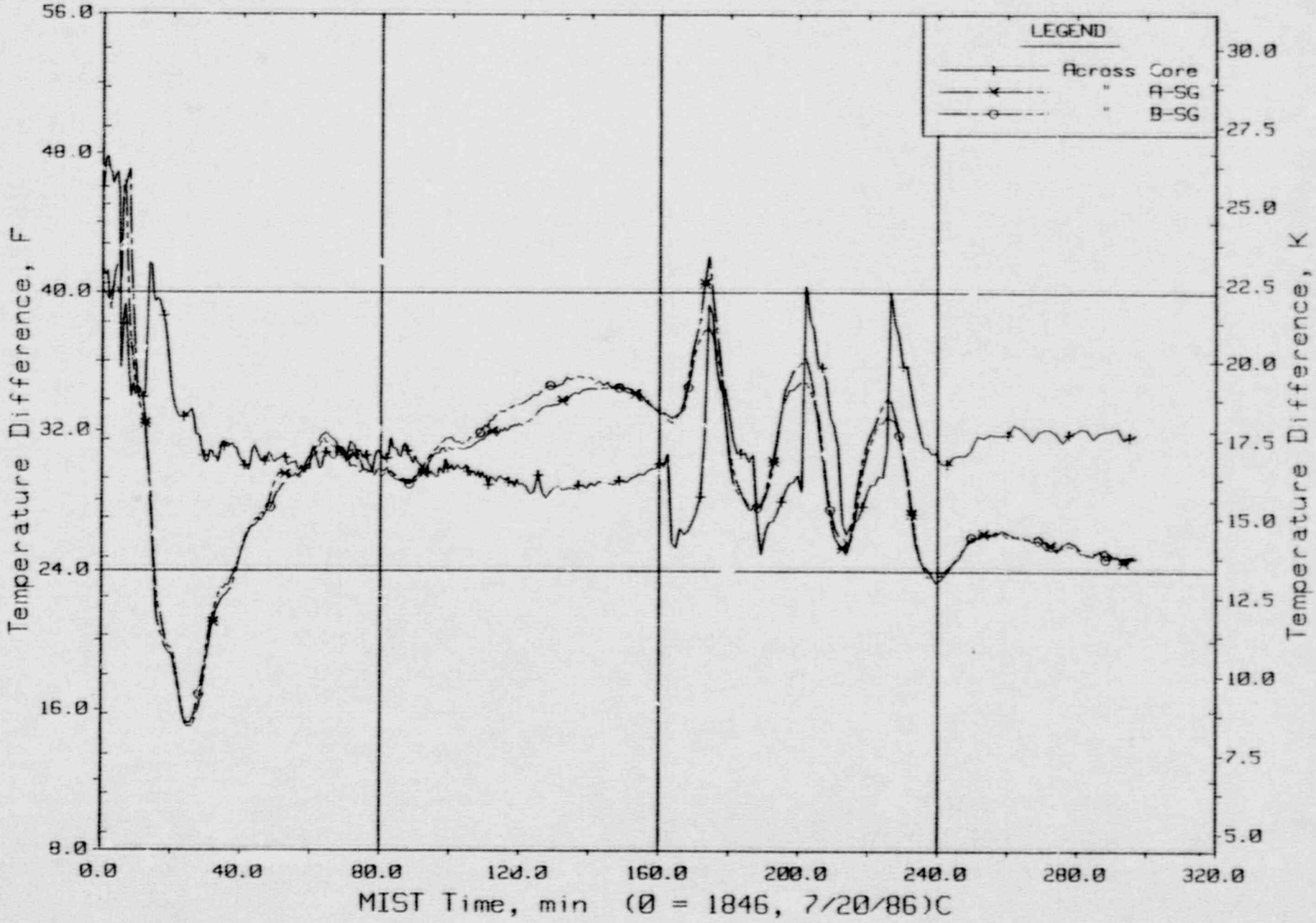

Key Temperature Differences.

Mon May 16 20:21:12 1988

PRTD2

FINAL DATA

T320101: Group 32 SBLOCA Test 1, Reduced Leak Size - 5 cm2.

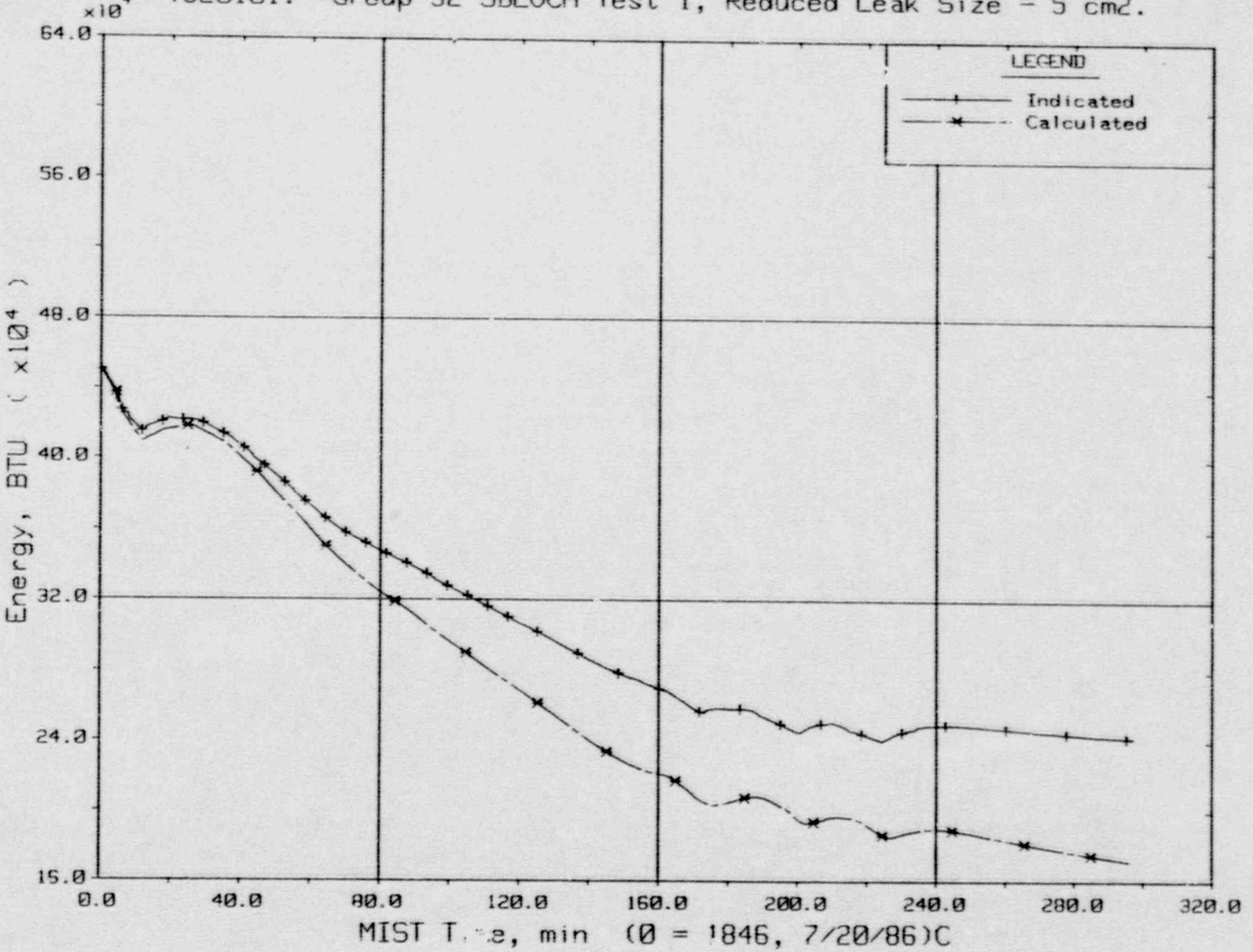

Primary System Total Fluid Energy.

Mon May 16 20:23:24 1988

PRTE2

FINAL DATA

T320101: Group 32 SBLOCA Test 1, Reduced Leak Size - 5 cm2.

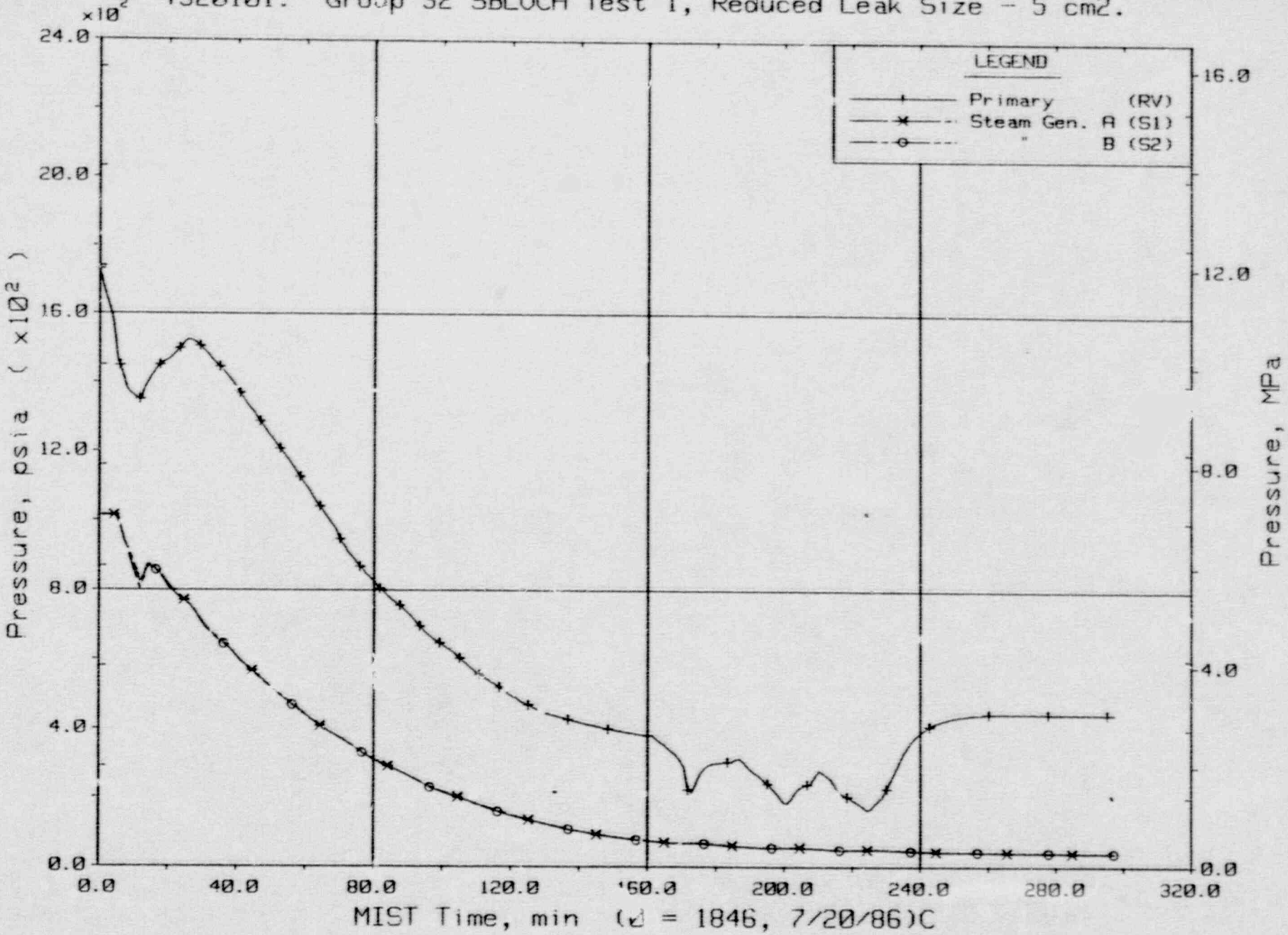

Primary and Secondary System Pressures (GP01s).

Mon May 16 20:25:39 1988

PSGP1

FINAL DATA

T320101: Group 32 SBLOCA Test 1, Reduced Leak Size - 5 cm2.

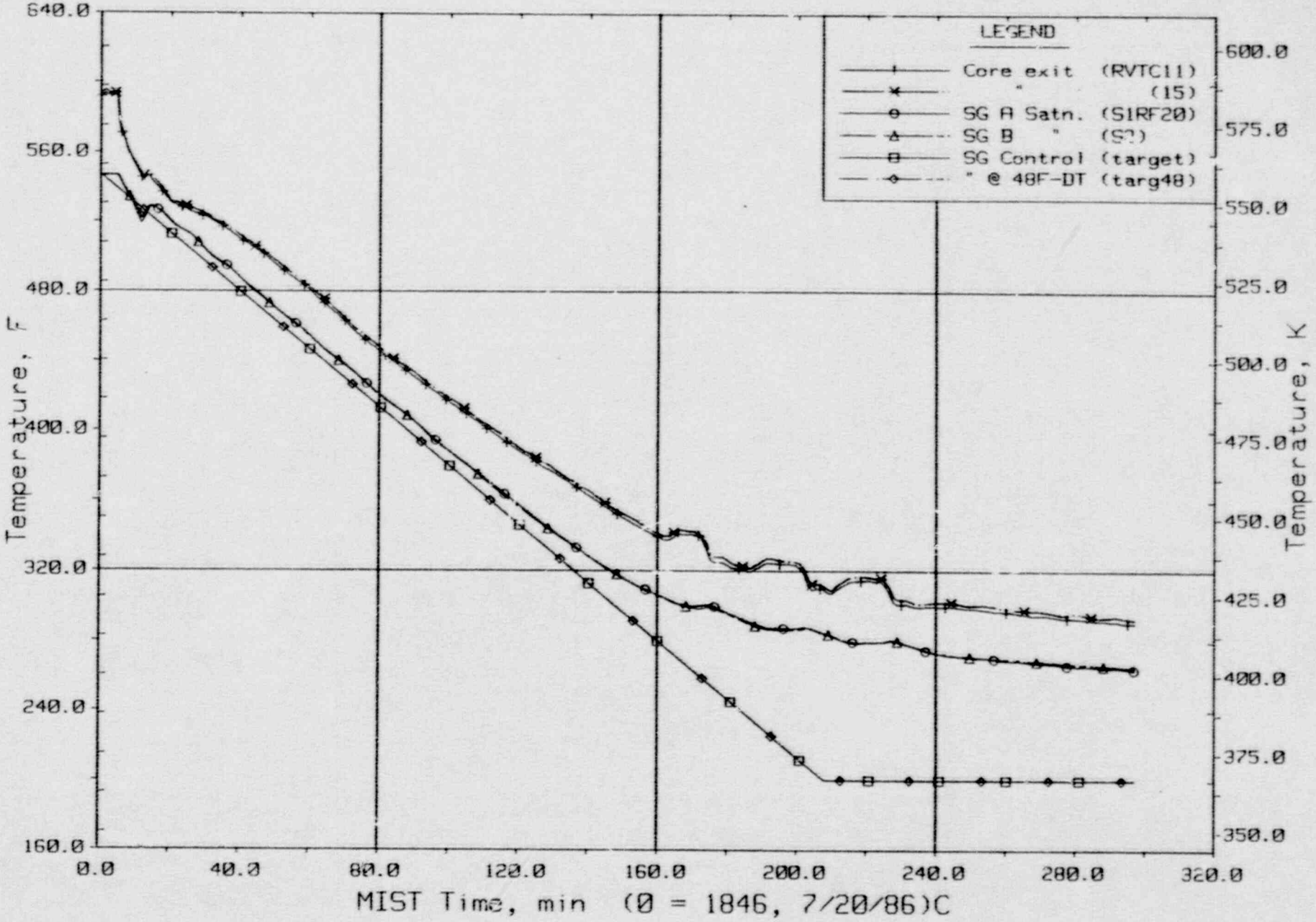

Steam Generator Secondary Saturation and Control Temperatures.

Mon May 16 20:28:36 1988

PSTC3

FINAL DATA

T320101: Group 32 SBLOCA Test 1, Reduced Leak Size - 5 cm2.

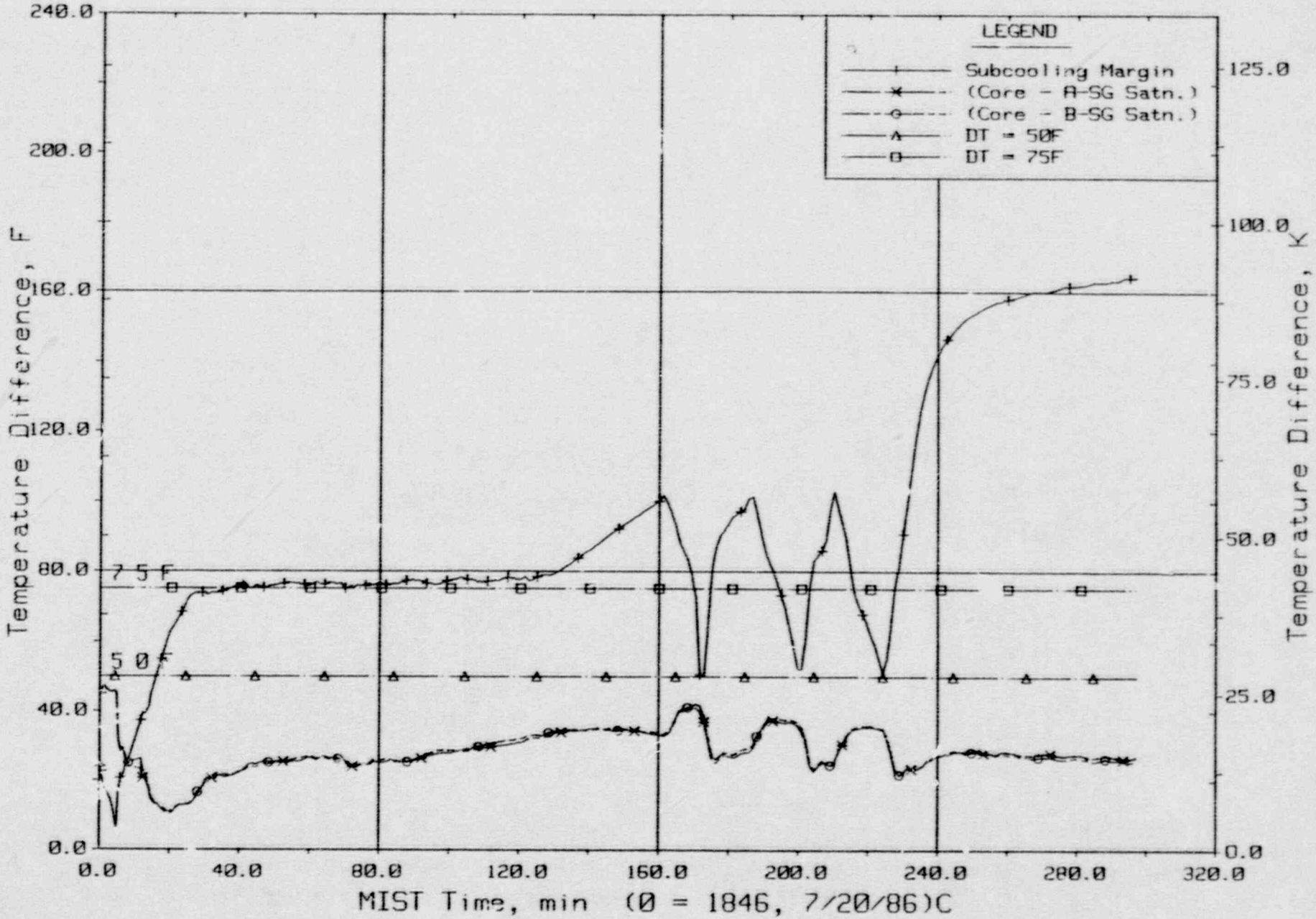

Control Temperature Differences

Mon May 16 20:18:38 1988

PCTD1

FINAL DATA

T320101: Group 32 SBLOCA Test 1, Reduced Leak Size - 5 cm2.

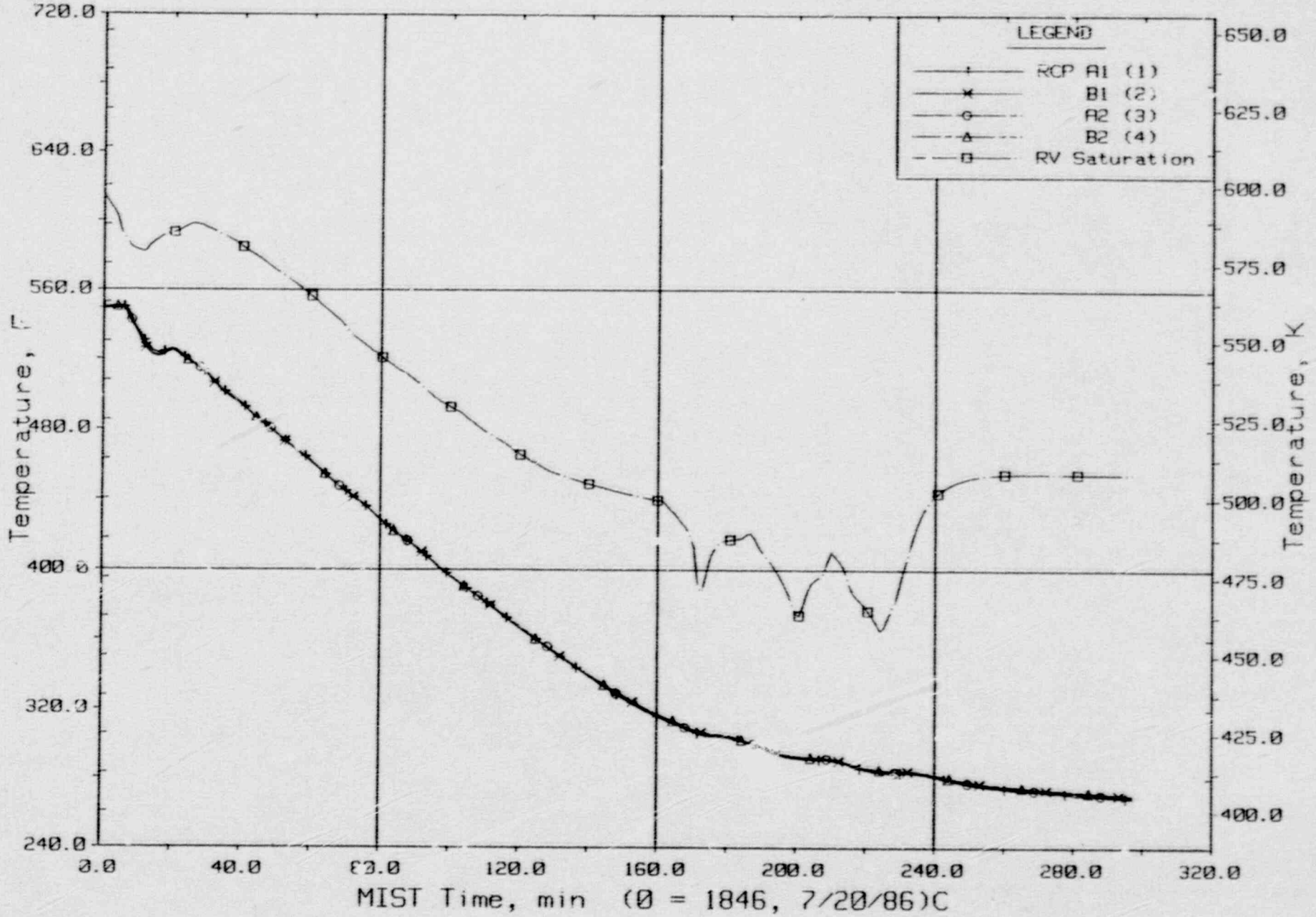

Pump Suction Fluid Temperature (CnRT01s).

Mon May 16 20:33:54 1988

PLOT10

FINAL DATA

T320101: Group 32 SBLOCA Test 1, Reduced Leak Size - 5 cm2.

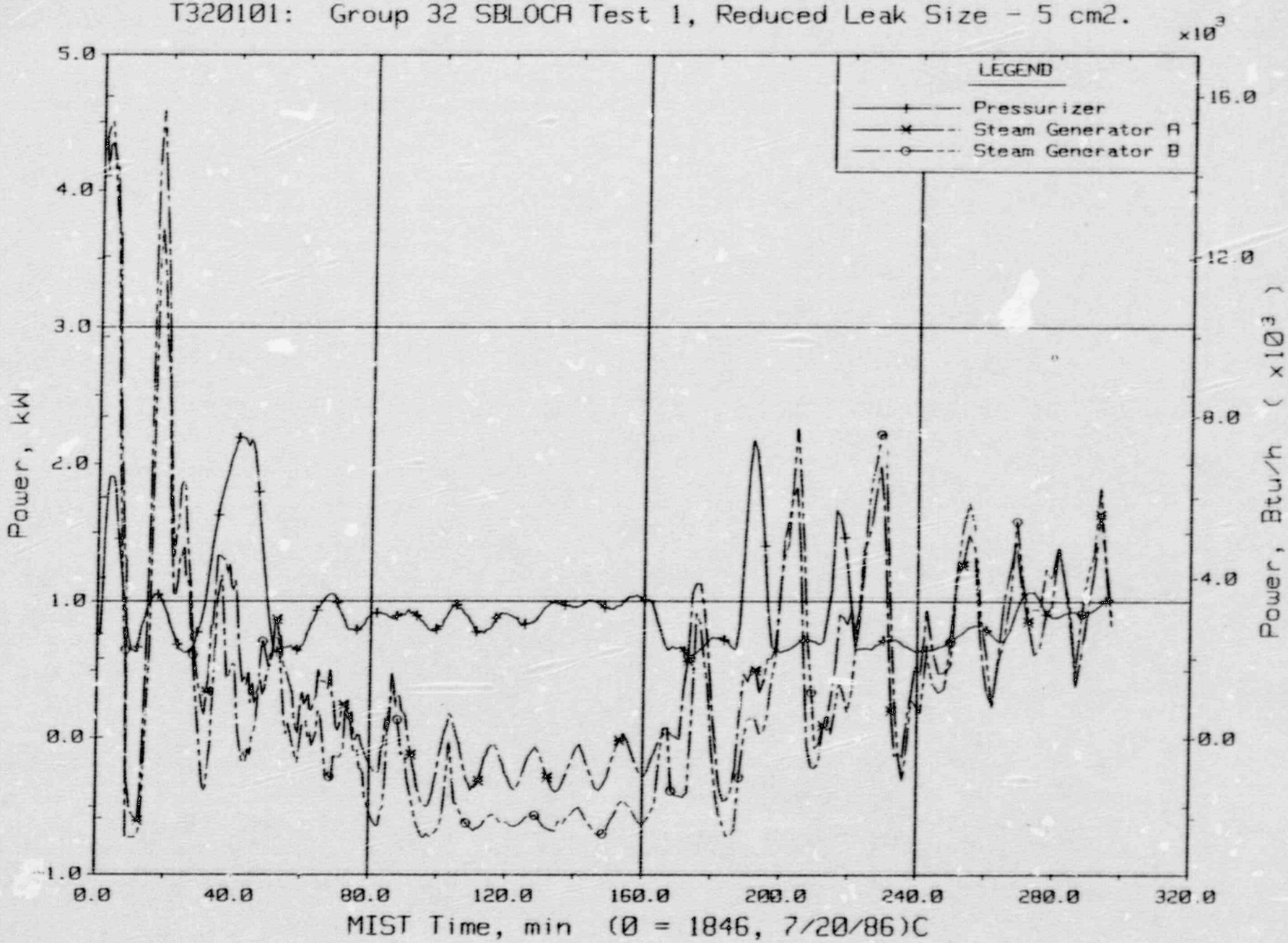

Guard Heater Specified Power, Pressurizer and Steam Generators.

Mon May 16 20:41:57 1988

PZG01

FINAL DATA

T320101: Group 32 SBLOCA Test 1, Reduced Leak Size - 5 cm².

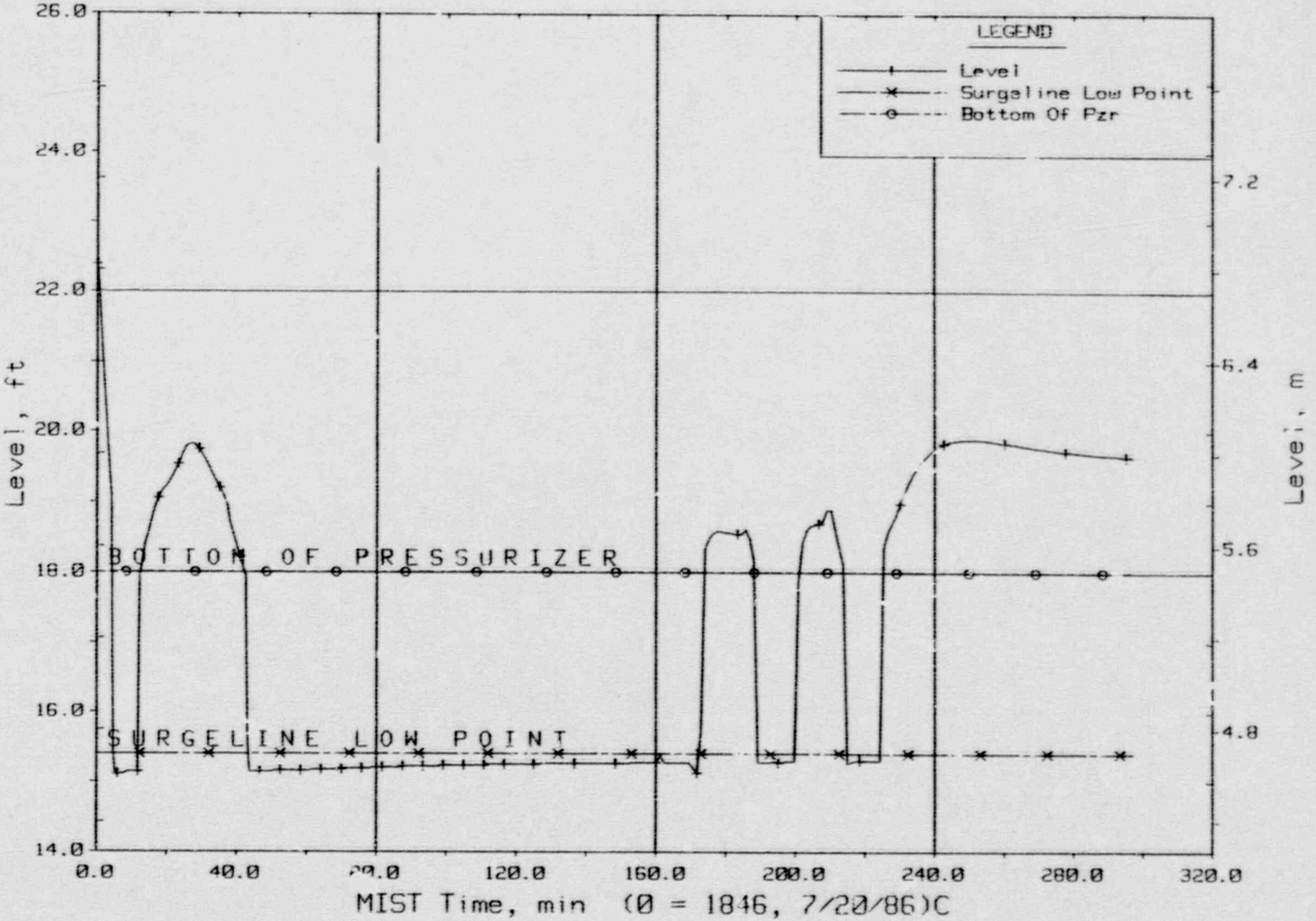

Pressurizer Collapsed Liquid Level (PZLV20).

Mon May 1F 20:44:35 1988

PZLV1

FINAL DATA

T320101: Group 32 SBLOCA Test 1, Reduced Leak Size - 5 cm2.

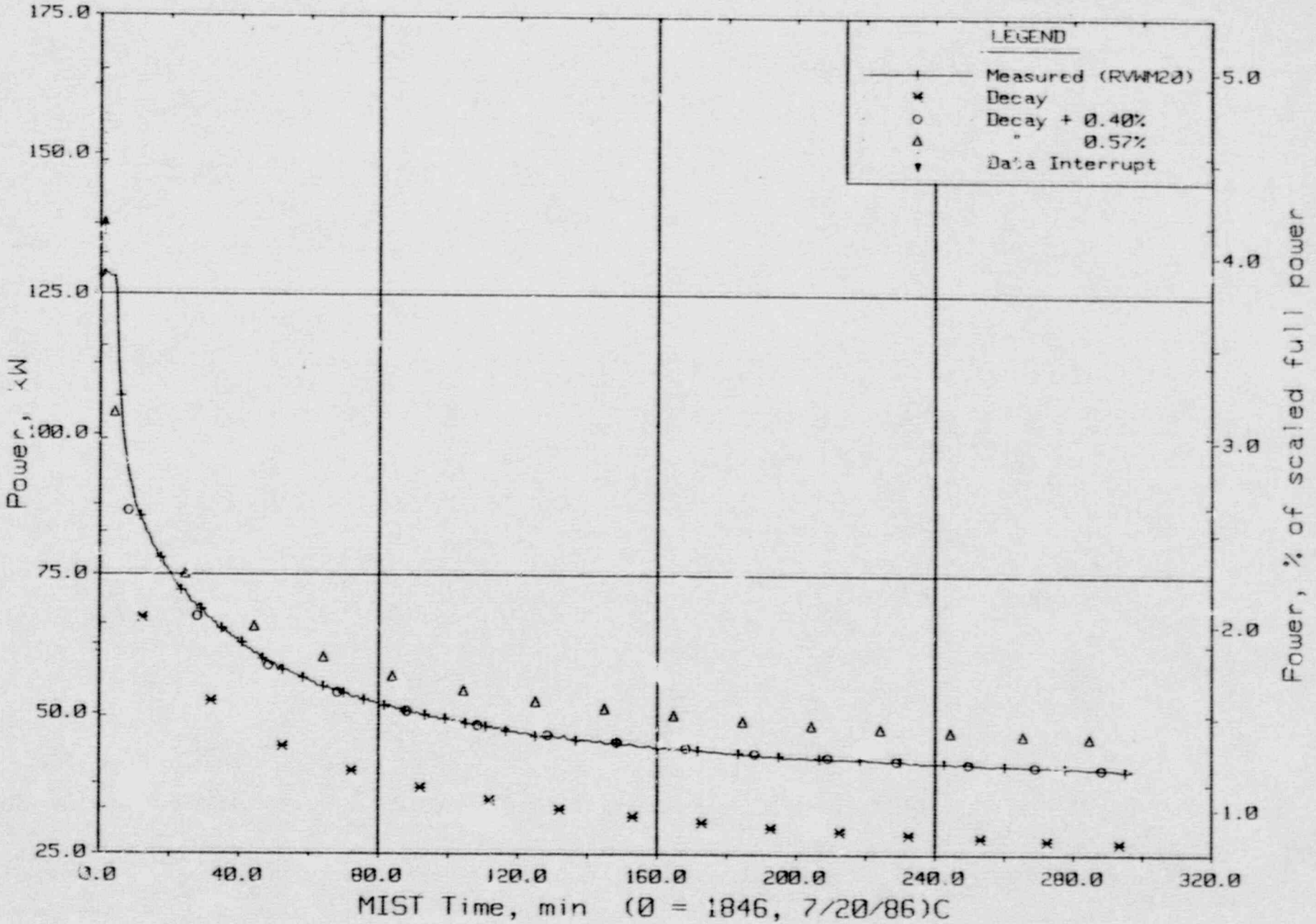

Core Power.

Mon May 16 20:47:11 1988

RV: 1.0

FINAL DATA

T320101: Group 32 SBLOCA Test 1, Reduced Leak Size - 5 cm2.

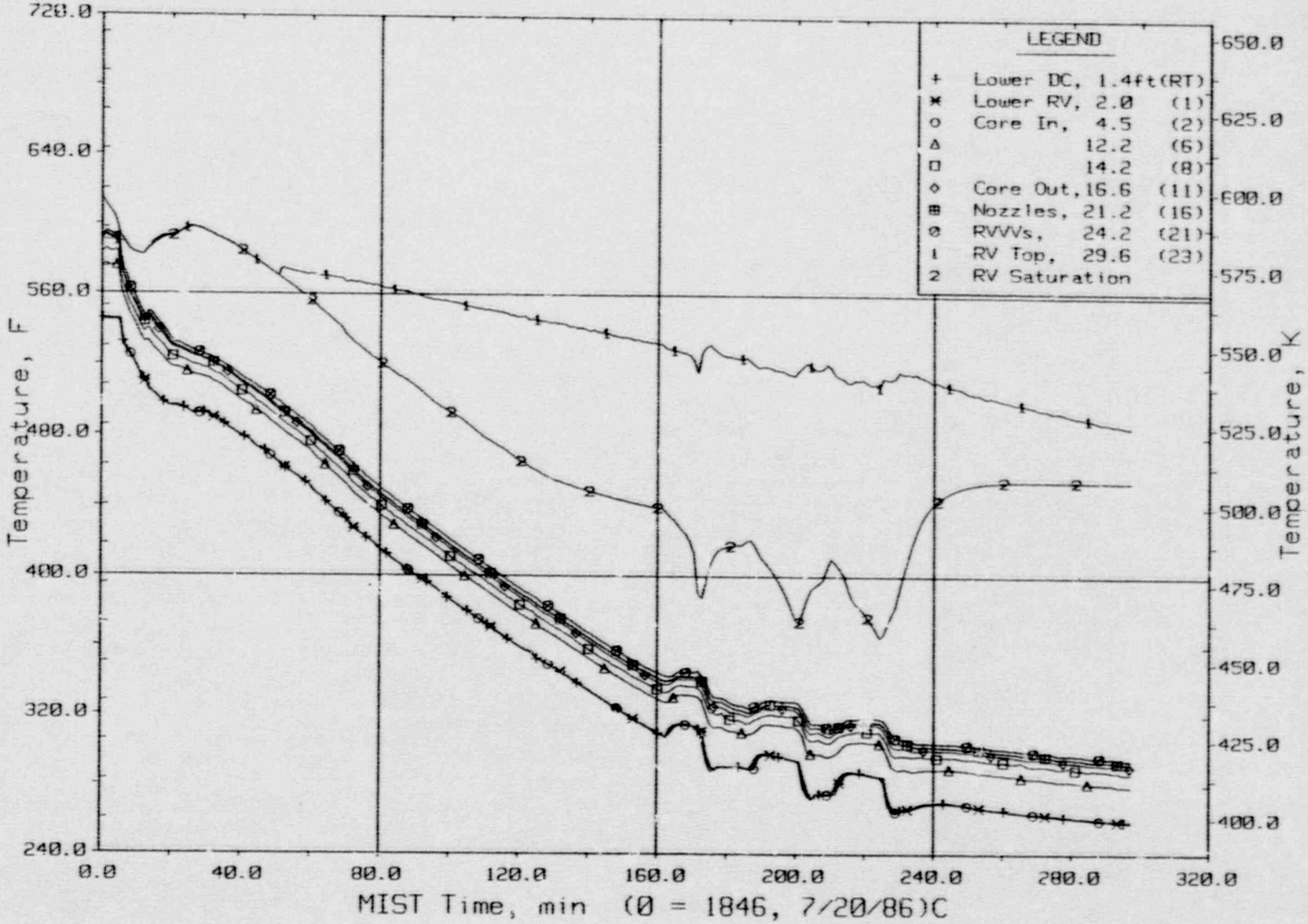

Core Unit Cell and Reactor Vessel Fluid Temperatures (RVTCs).

Mon May 16 20:56:41 1988

RVTC0

FINAL DATA

T320101: Group 32 SBLOCA Test 1, Reduced Leak Size - 5 cm2.

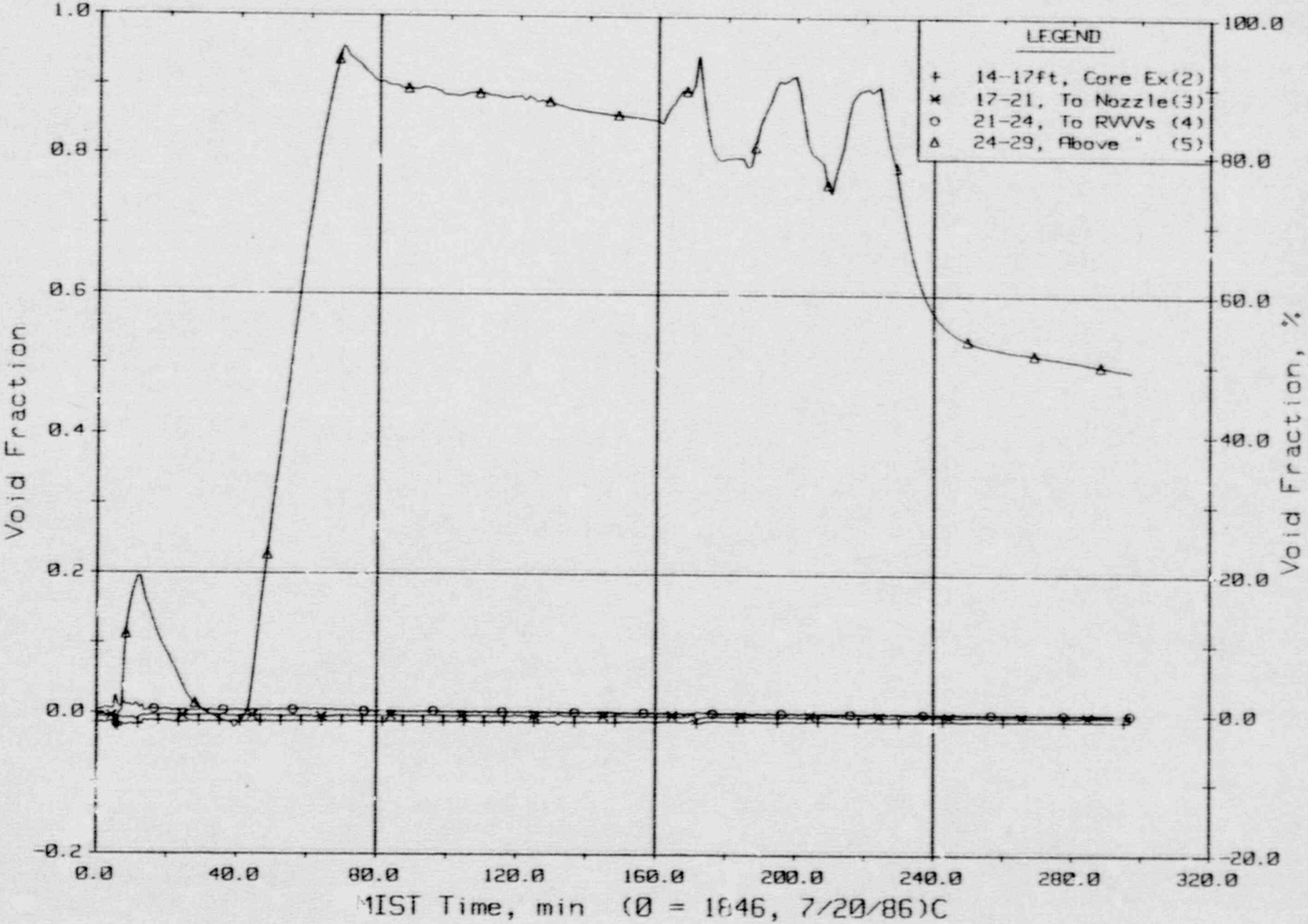

Reactor Vessel Void Fractions From Differential Pressures (RVVFs).

Mon May 16 20:53:34 1988

RVVF1

FINAL DATA

T320101: Group 32 SBLOCA Test 1, Reduced Leak Size - 5 cm2.

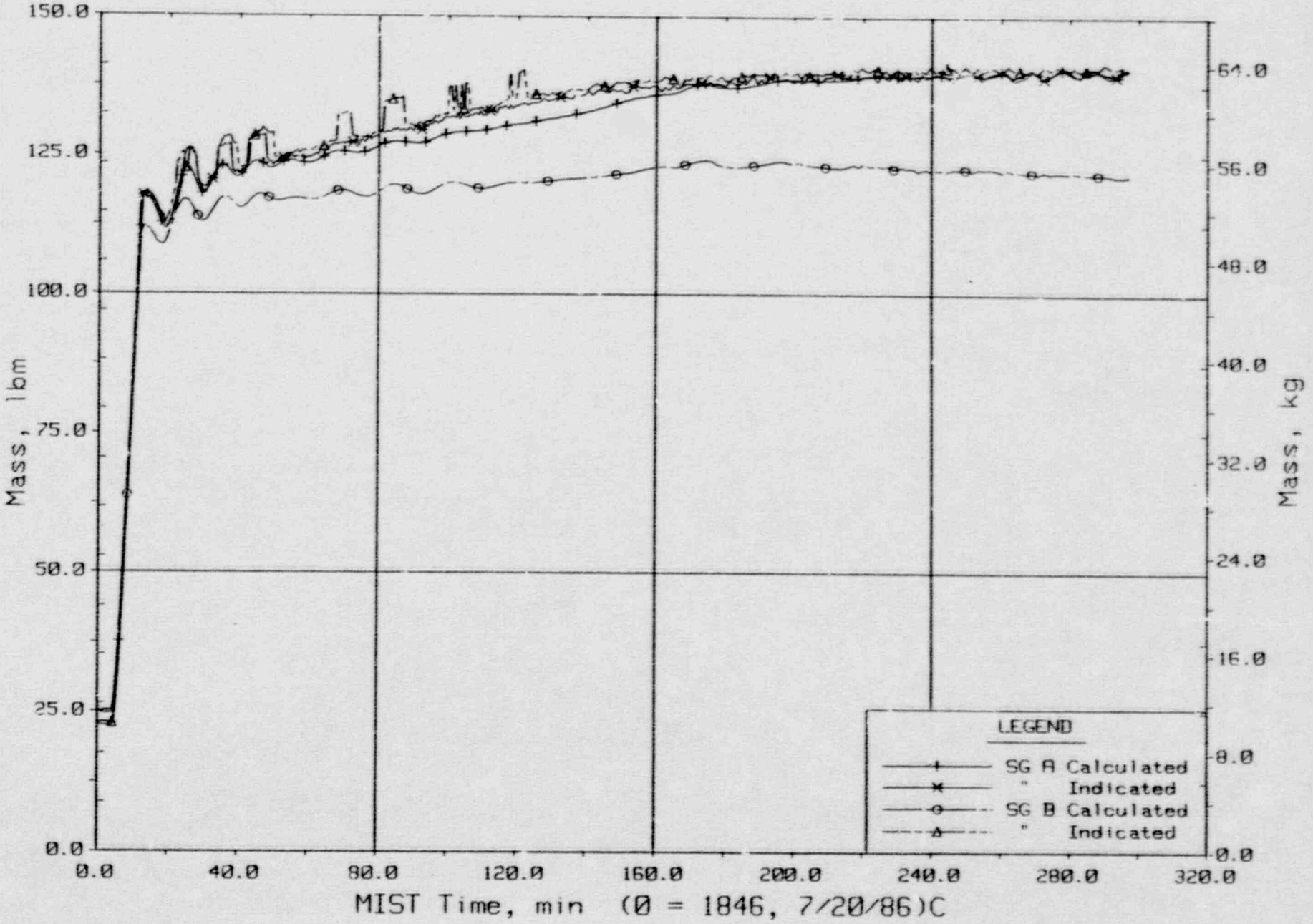

Steam Generator Secondary Fluid Mass Balances.

Mon May 16 21:02:30 1988

SCML2

FINAL DATA

T320101: Group 32 SBLOCA Test 1, Reduced Leak Size - 5 cm2.

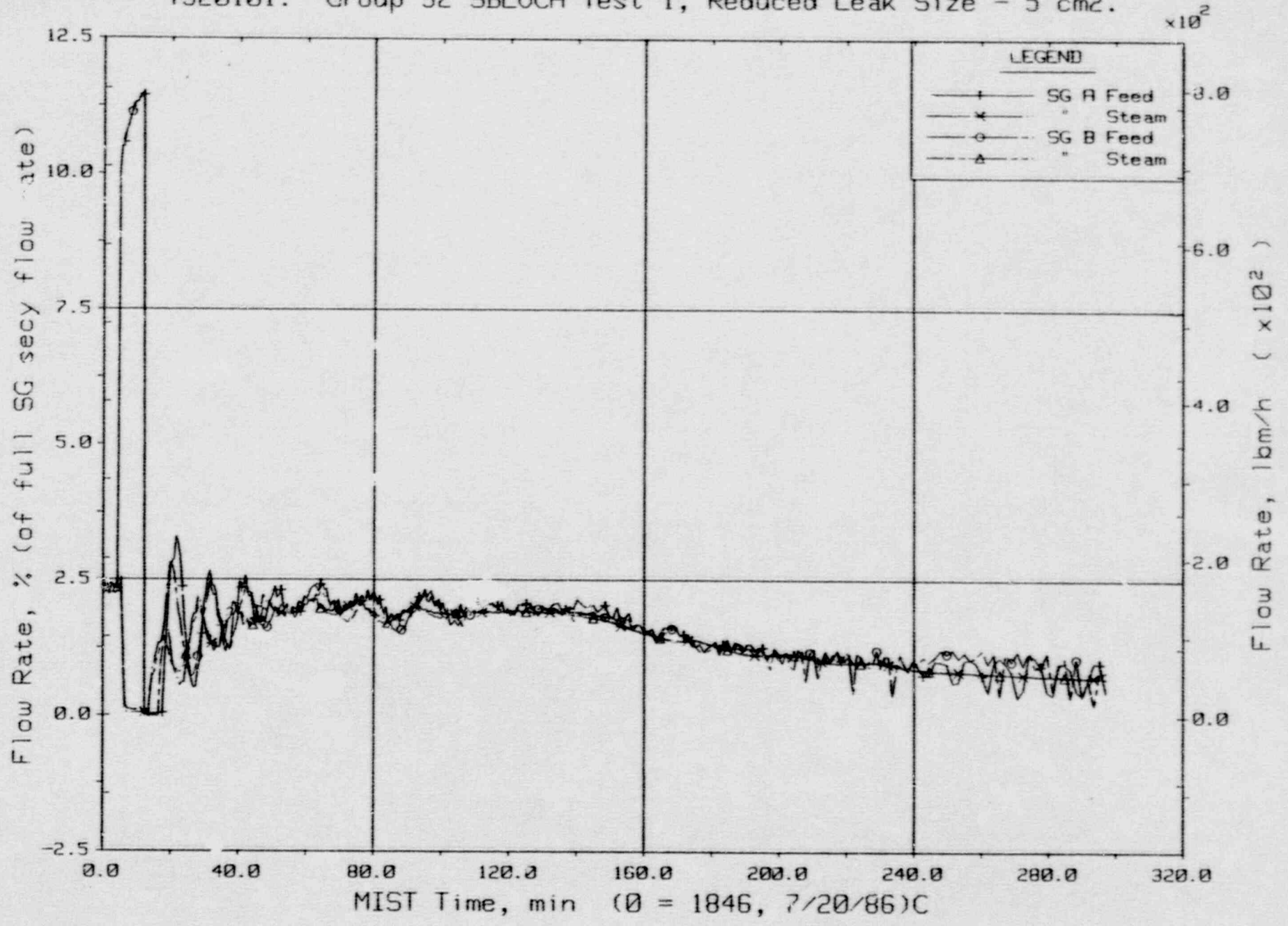

Steam Generator Secondary System Flow Rates.

Mon May 16 20:56:20 1988

SGFL2

FINAL DATA

T320101: Group 32 SBLOCA Test 1, Reduced Leak Size - 5 cm2.

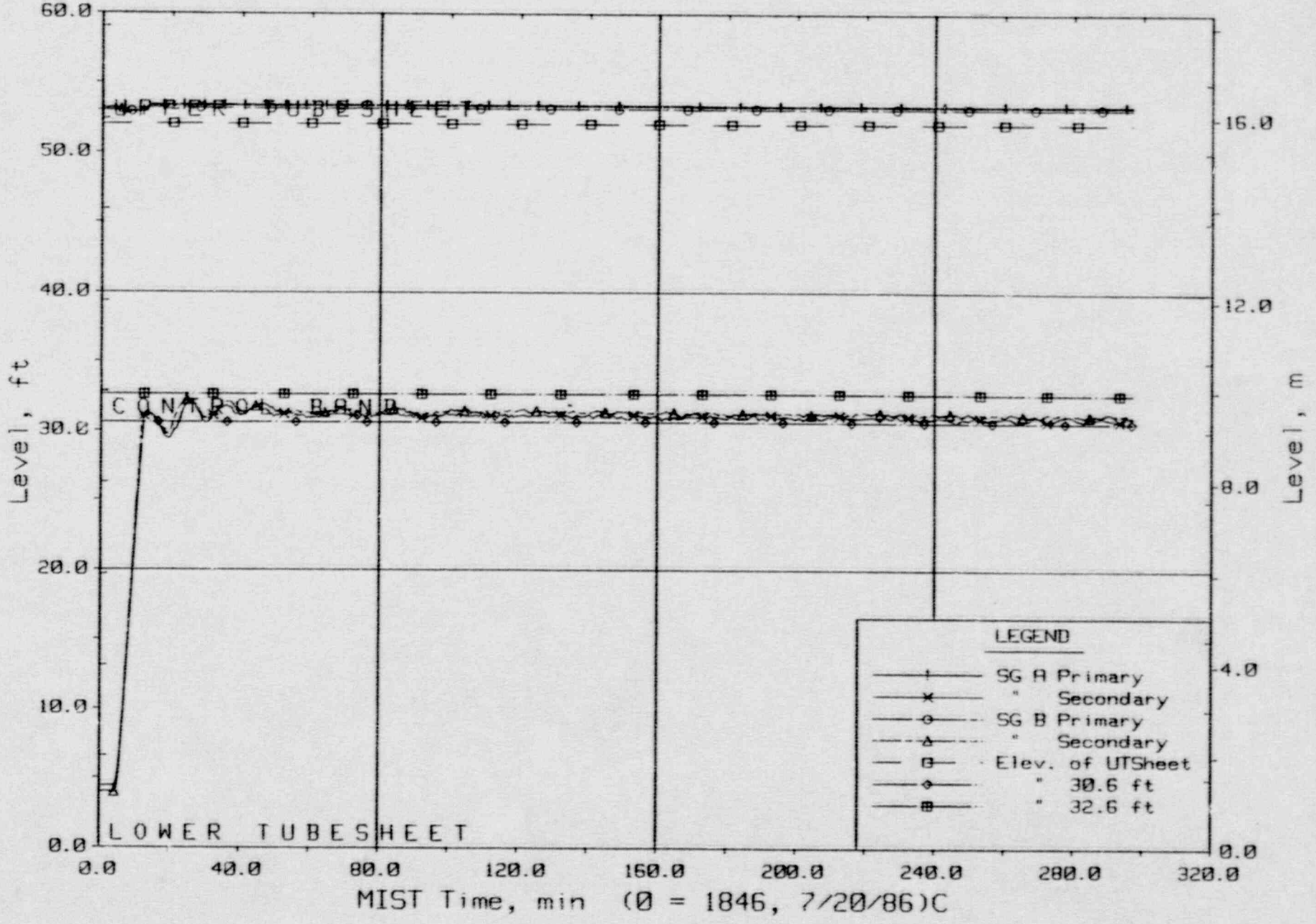

Steam Generator Collapsed Liquid Levels.

Mon May 16 20:59:33 1988

SGLV2

FINAL DATA

T320101: Group 32 SBLOCA Test 1, Reduced Leak Size - 5 cm2.

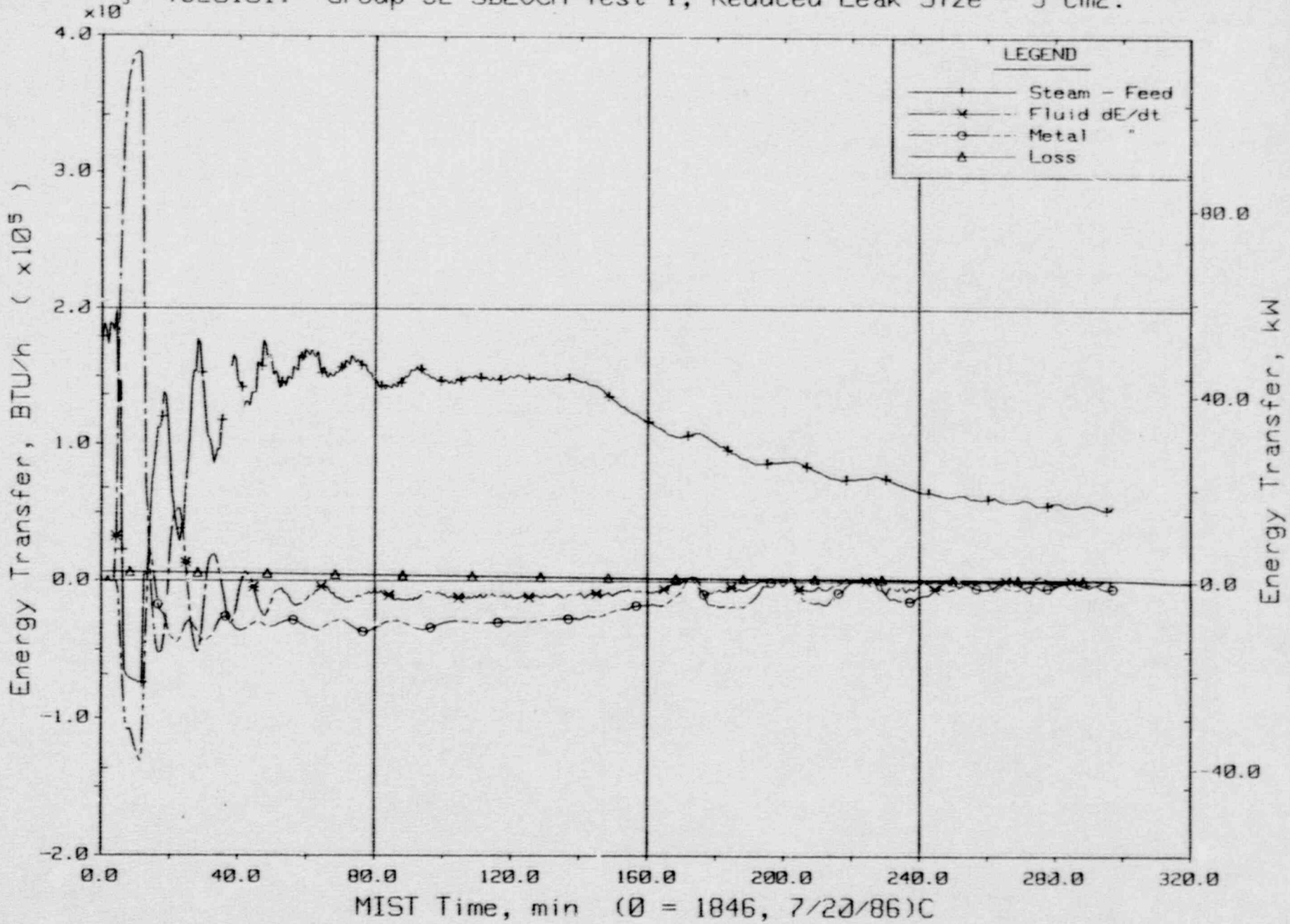

Steam Generator A Energy Transfer.

Mon May 16 21:11:49 1988

SGOE3

FINAL DATA

T320101: Group 32 SBLOCA Test 1, Reduced Leak Size - 5 cm2.

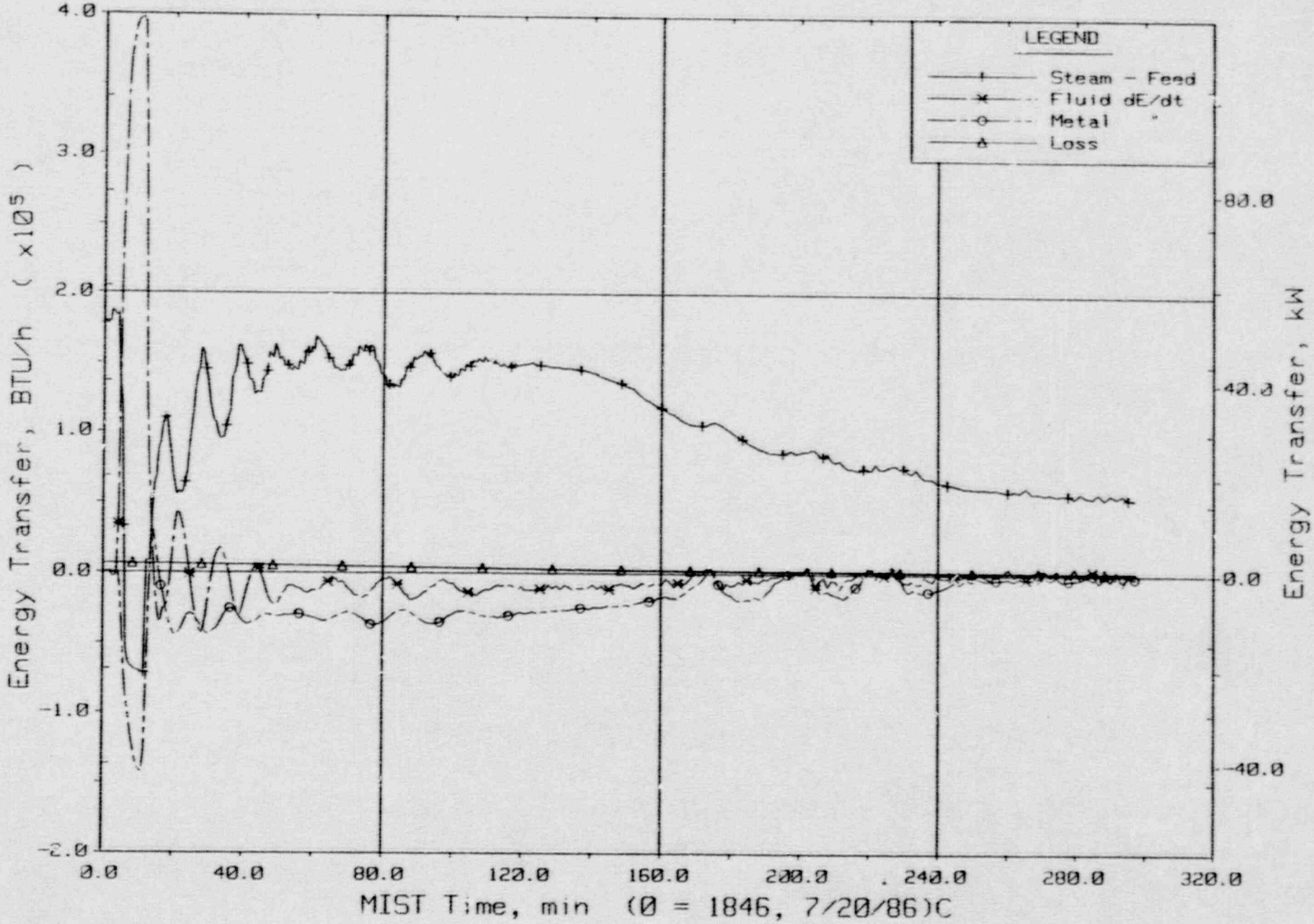

Steam Generator B Energy Transfer.

Mon May 16 21:14:42 1988

SGQE6

FINAL DATA

T320101: Group 32 SBLOCA Test 1, Reduced Leak Size - 5 cm2.

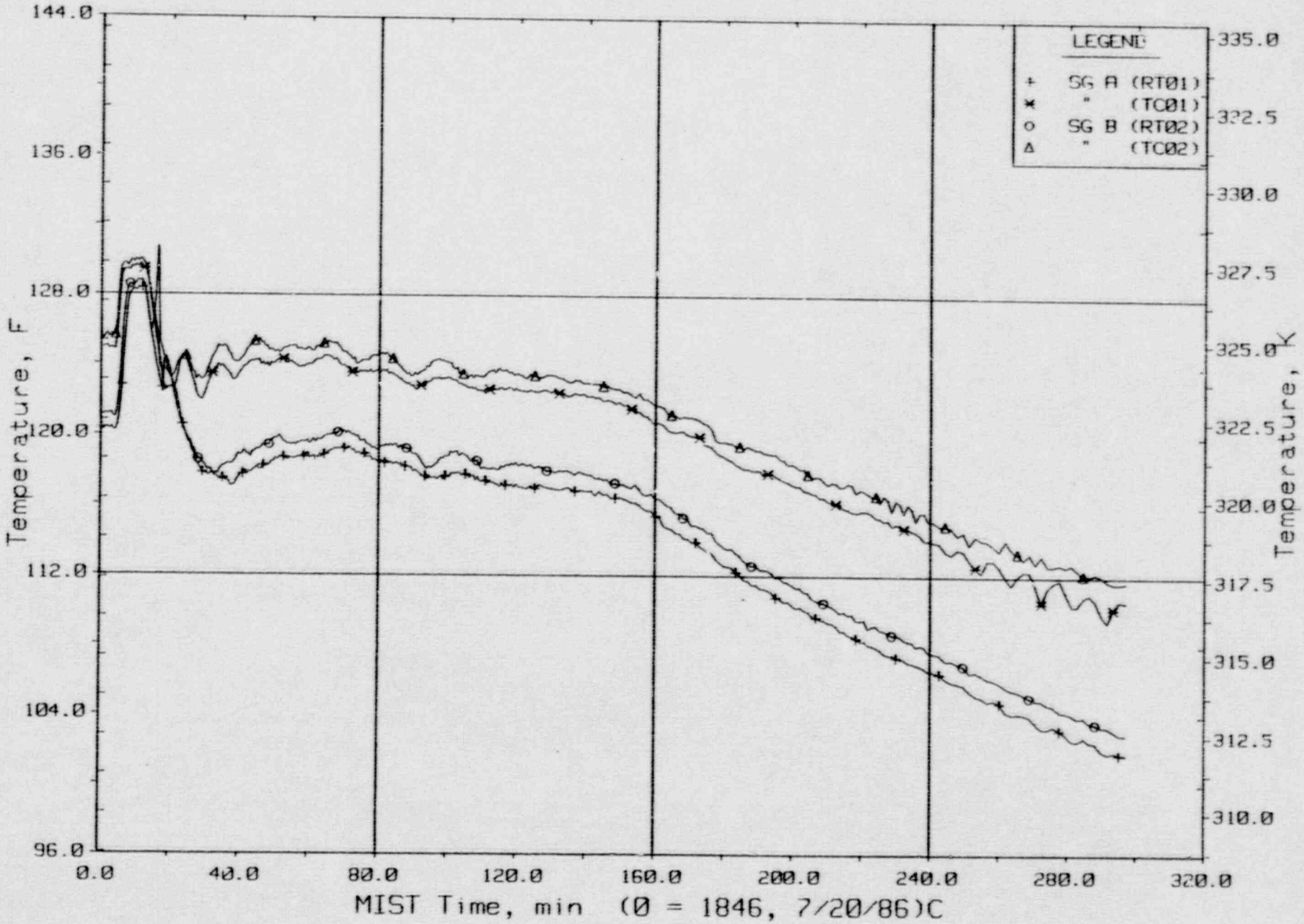

Feedwater Temperatures (SFs).

Mon May 16 21:05:10 1988

SGRT1

FINAL DATA

T320101: Group 32 SBLOCA Test 1, Reduced Leak Size - 5 cm2.

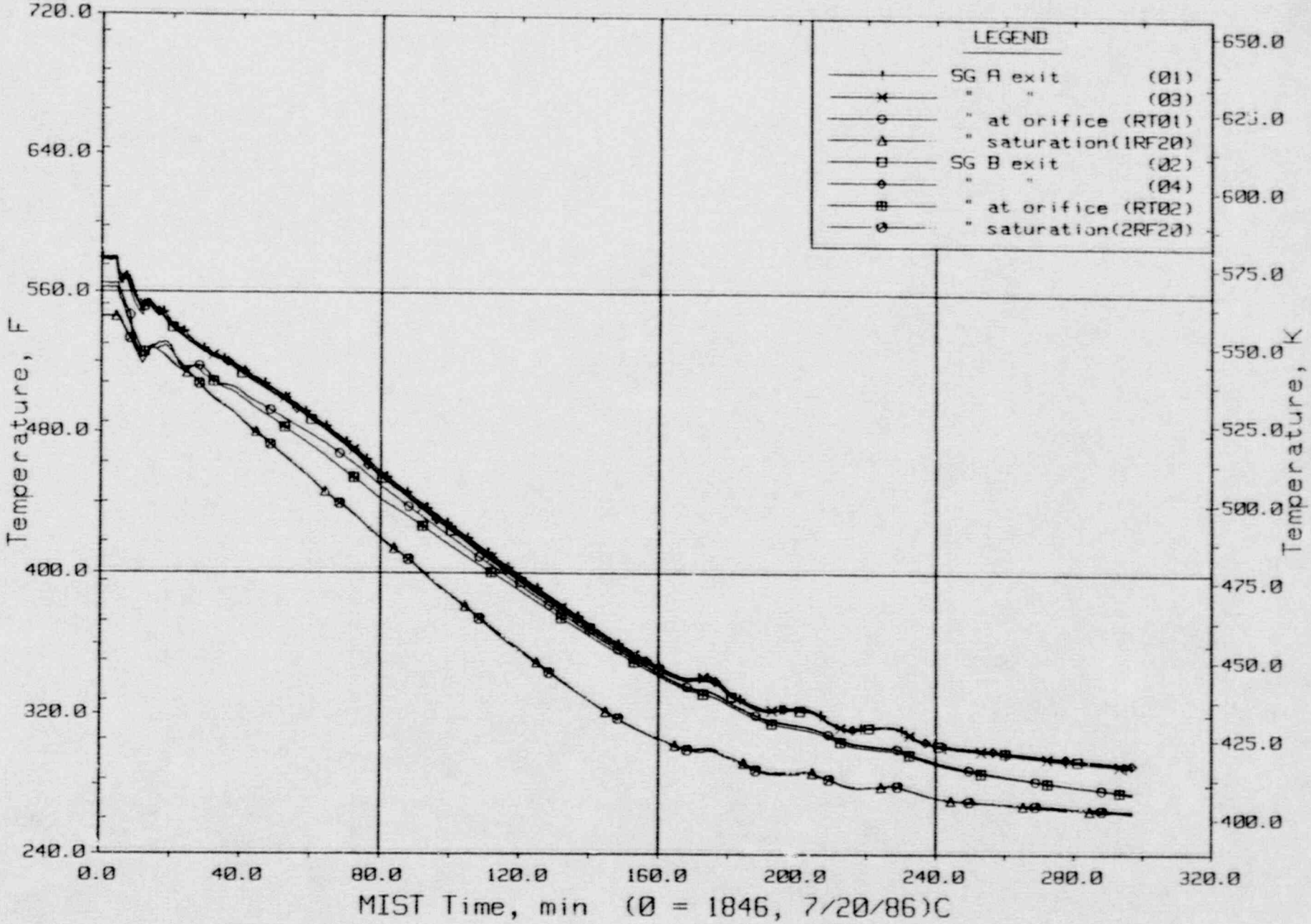

Steam Generator Steam Outlet Temperatures (SSTCs).

Mon May 16 21:08:32 1988

SGRT2

FINAL DATA

T320101: Group 32 SBLOCA Test 1, Reduced Leak Size - 5 cm2.

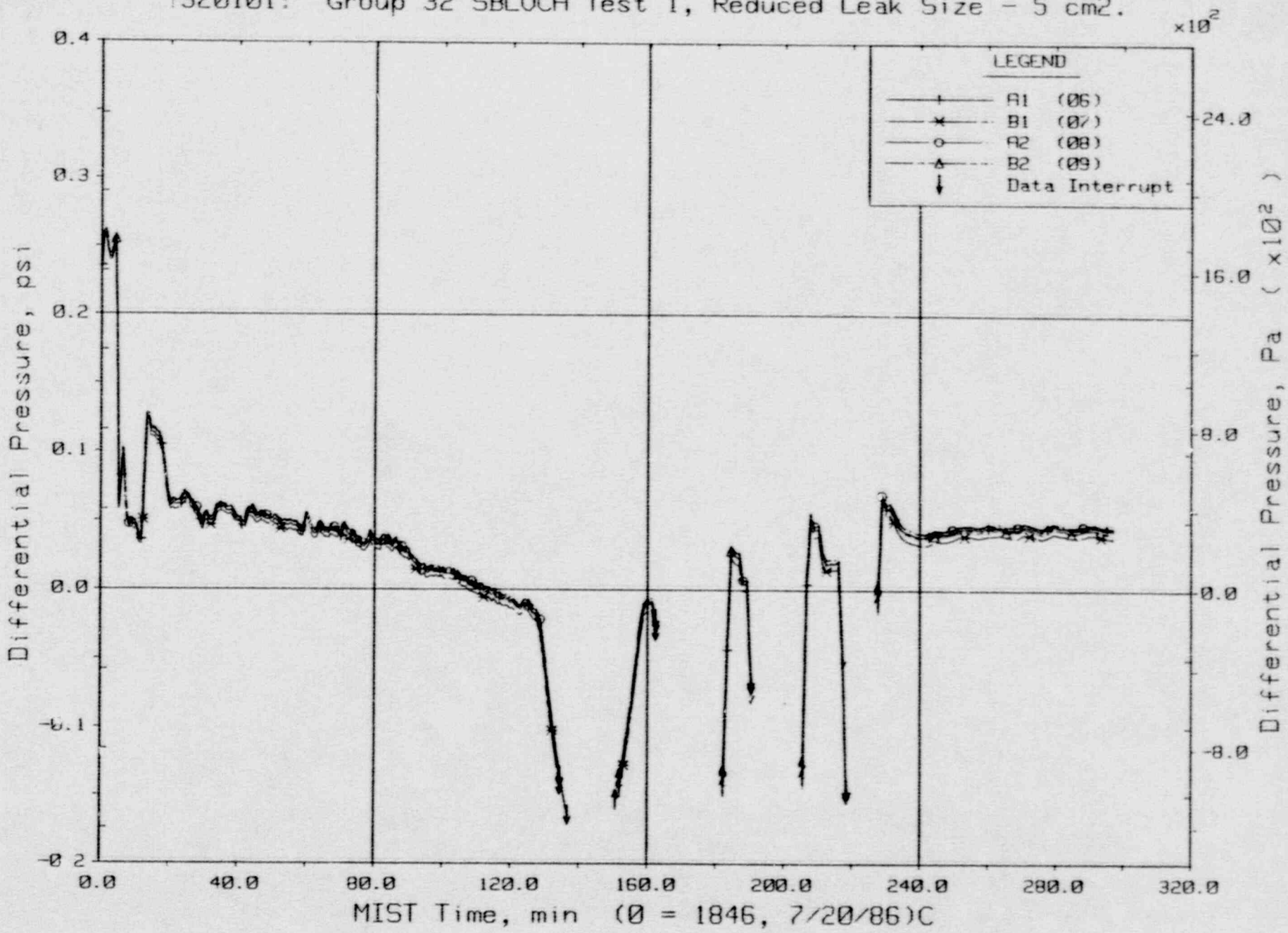

Reactor Vessel Vent Valve Differential Pressures (RVDPs).

Mon May 16 21:17:24 1988

VVDP1

FINAL DATA

T320101: Group 32 SBLOCA Test 1, Reduced Leak Size - 5 cm2.

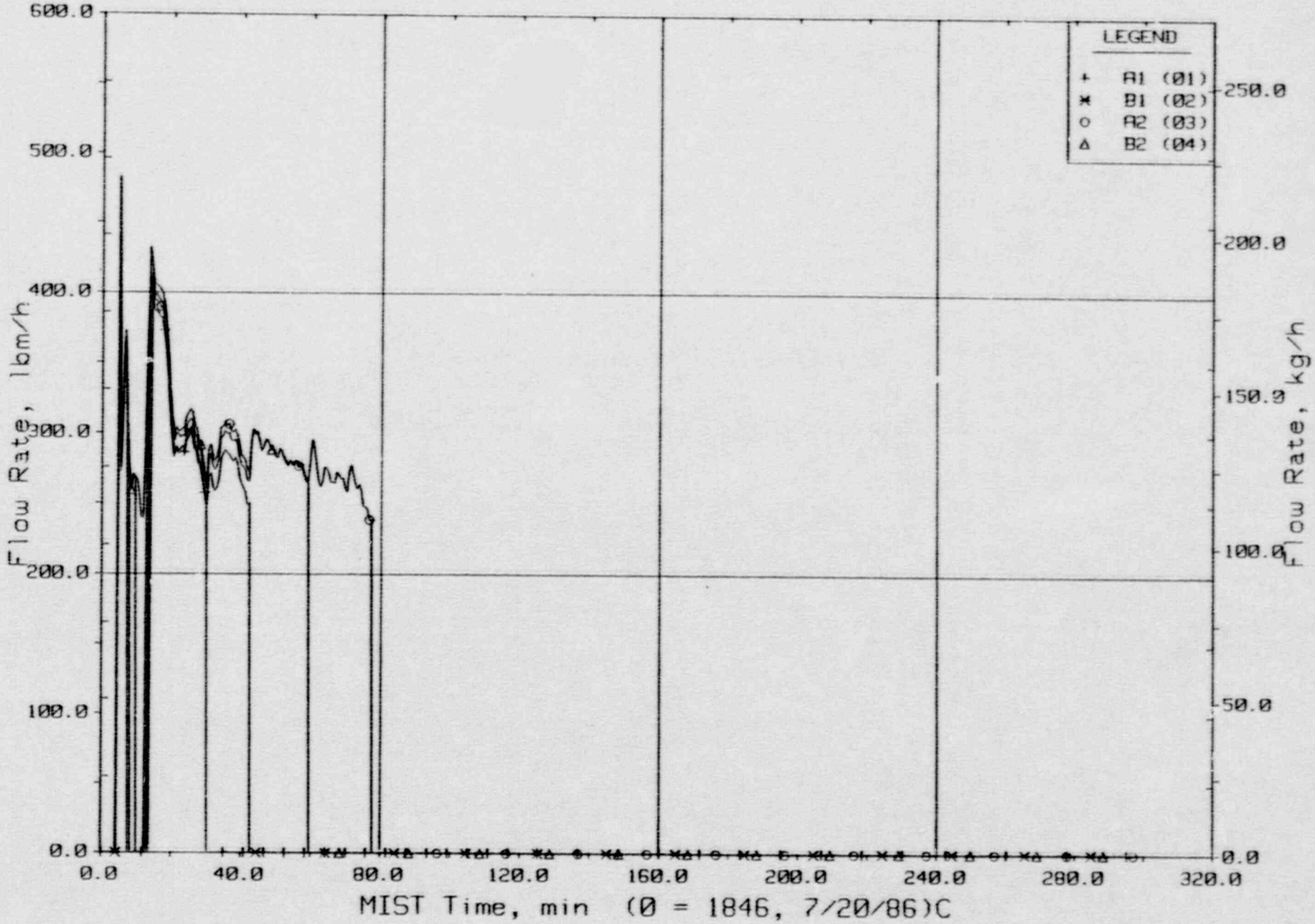

Reactor Vessel Vent Valve Flow Rates (RVORs).

Wed May 18 17:38:28 1988

VVFL1

FINAL DATA

T320101: Group 32 SBLOCA Test 1, Reduced Leak Size - 5 cm2.

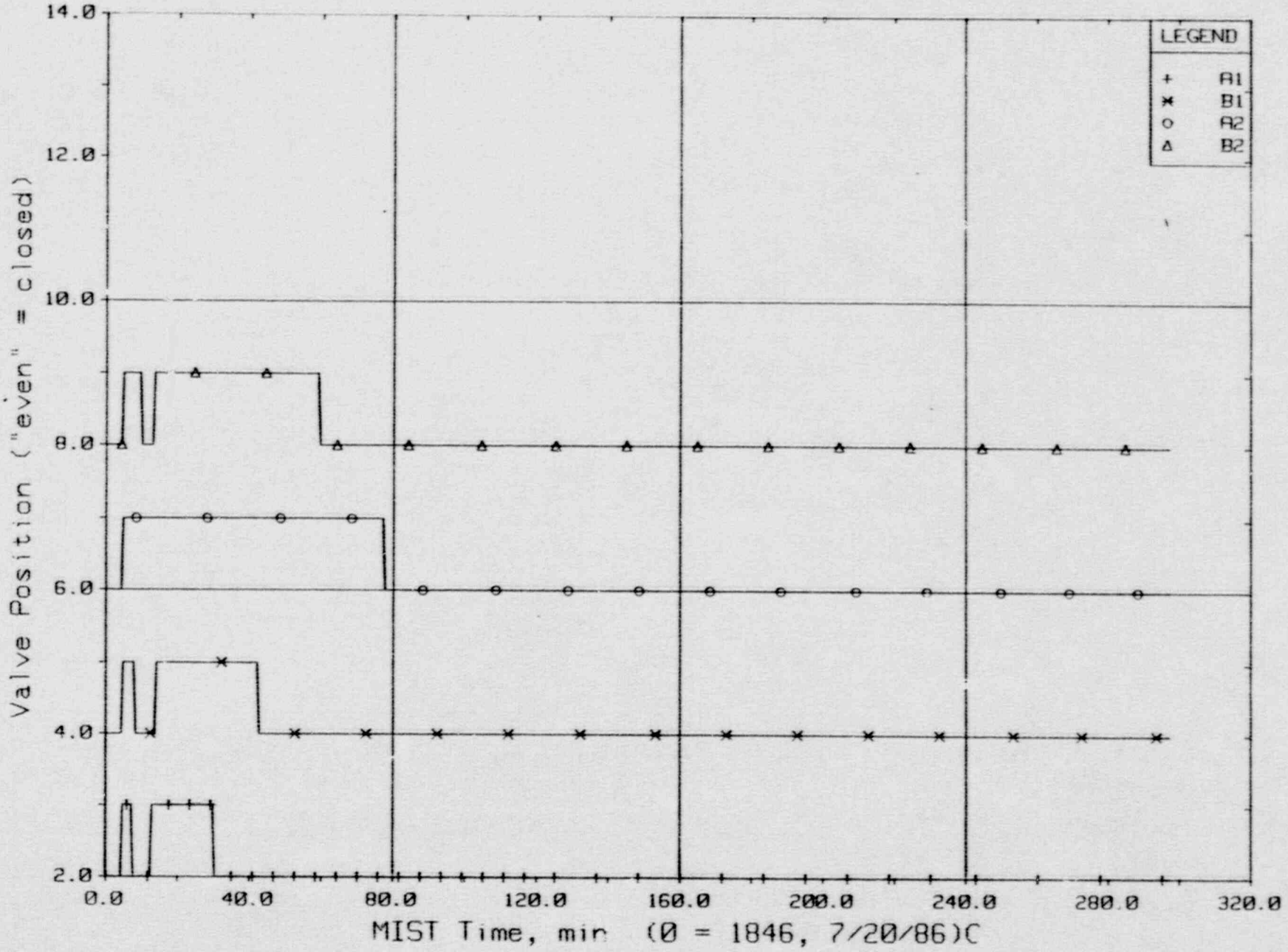

Reactor Vessel Vent Valve Positions.

Wed May 18 17:42:20 1988

VVLS1

FINAL DATA

T320101: Group 32 SBLOCA Test 1, Reduced Leak Size - 5 cm2.

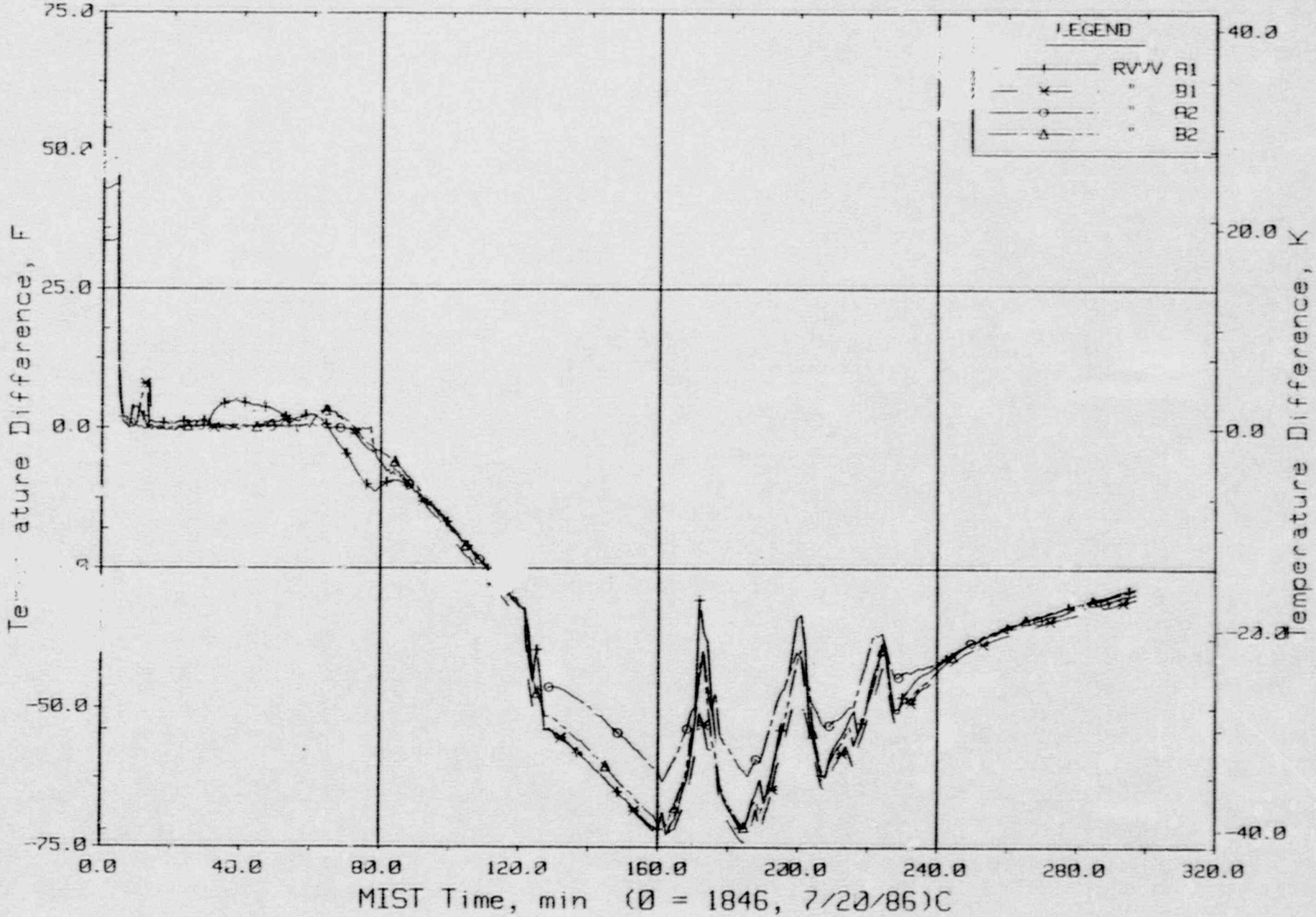

Temperature Differences Across Vent Valves.

Mon May 16 21:26:31 1988

VVTD1

T320201

FINAL DATA

T320201: Group 32 SBLOCA Test 2, Increased Leak Size -- 50 cm2.

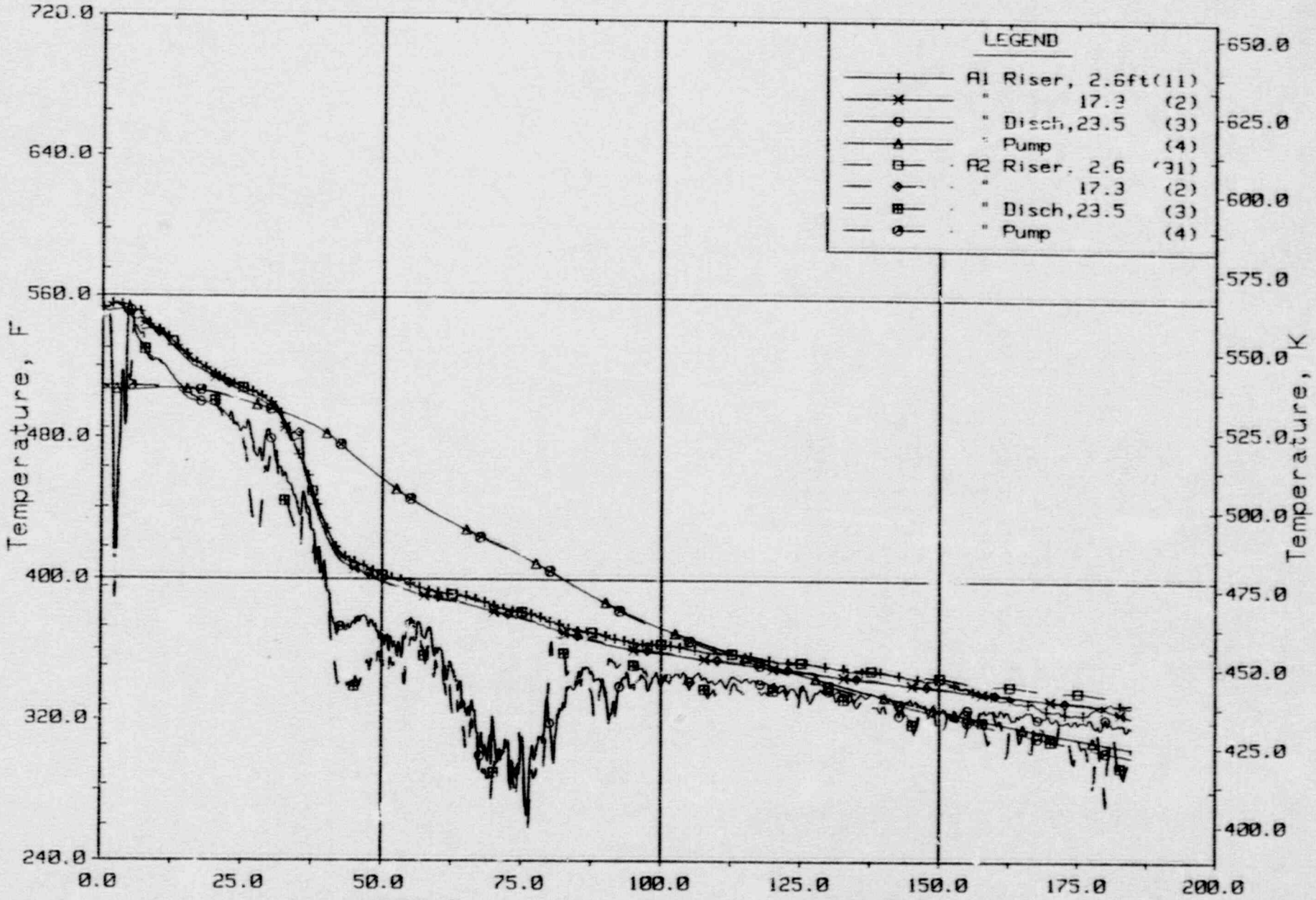

Loop A Cold Leg Metal Temperatures (C1,3M's).

Thu May 19 16:33:02 1988

C1MT1

FINAL DATA

T320201: Group 32 SBLOCA Test 2, Increased Leak Size - 50 cm2.

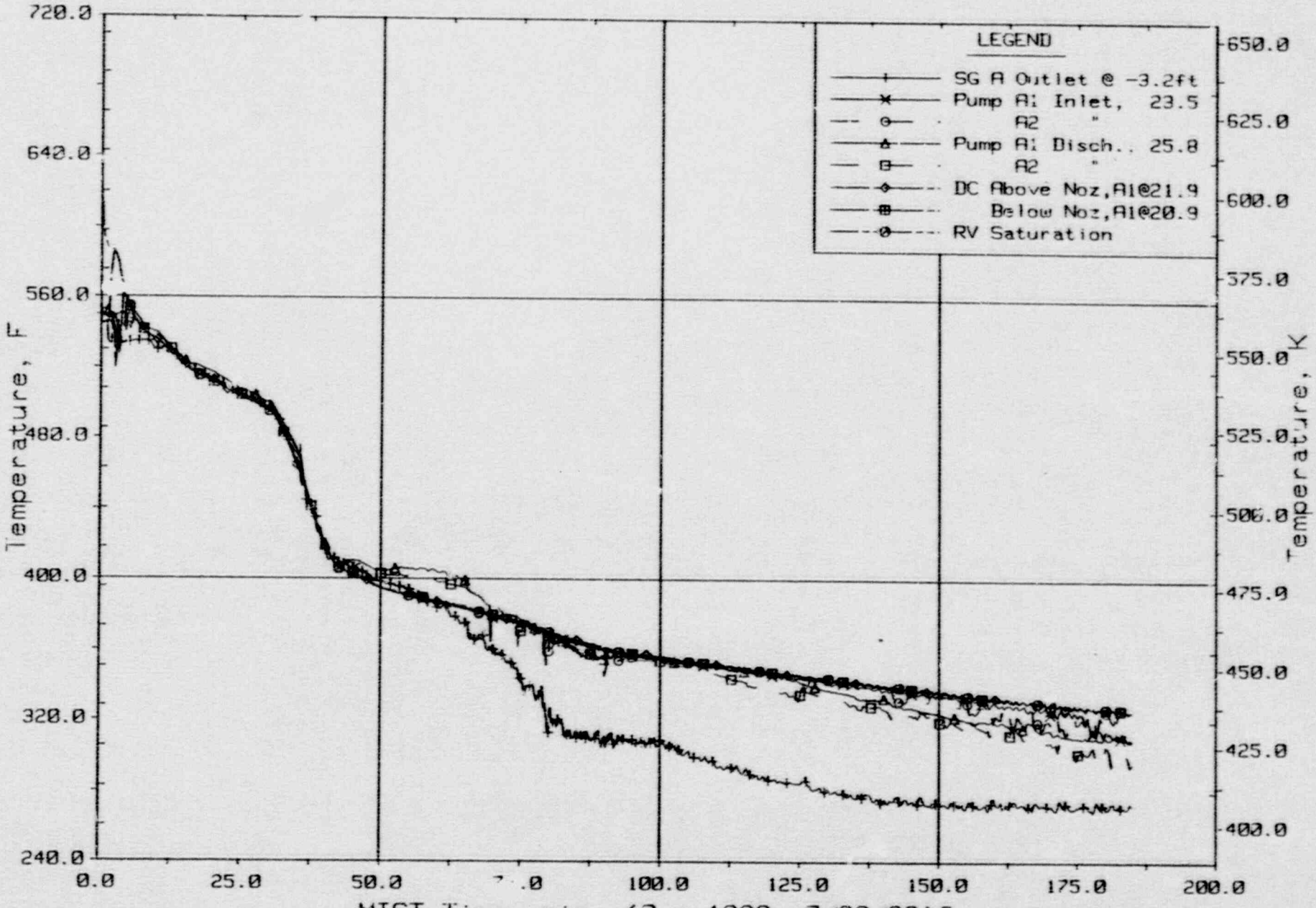

Loop A Cold Leg Fluid Temperatures (RTDs).

Thu May 19 16:45:13 1988

CIRT 0

FINAL DATA

T320201: Group 32 SBLOCA Test 2, Increased Leak Size -- 50 cm2.

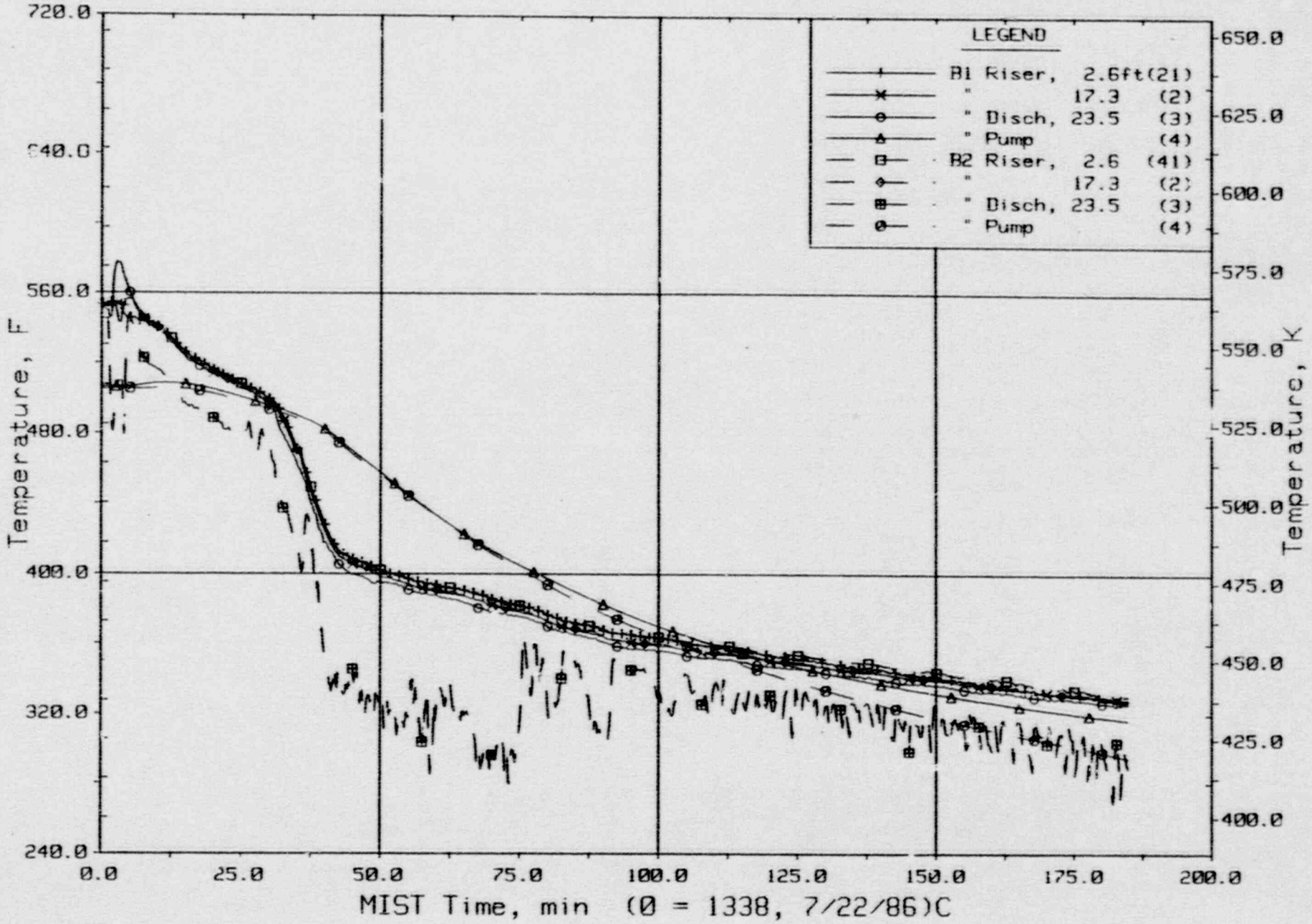

Loop R Cold Leg Metal Temperatures (C2,4MTs).

Thu May 19 16:38:27 1988

C2MT1

FINAL DATA

T320201: Group 32 SBLOCA Test 2, Increased Leak Size - 50 cm2.

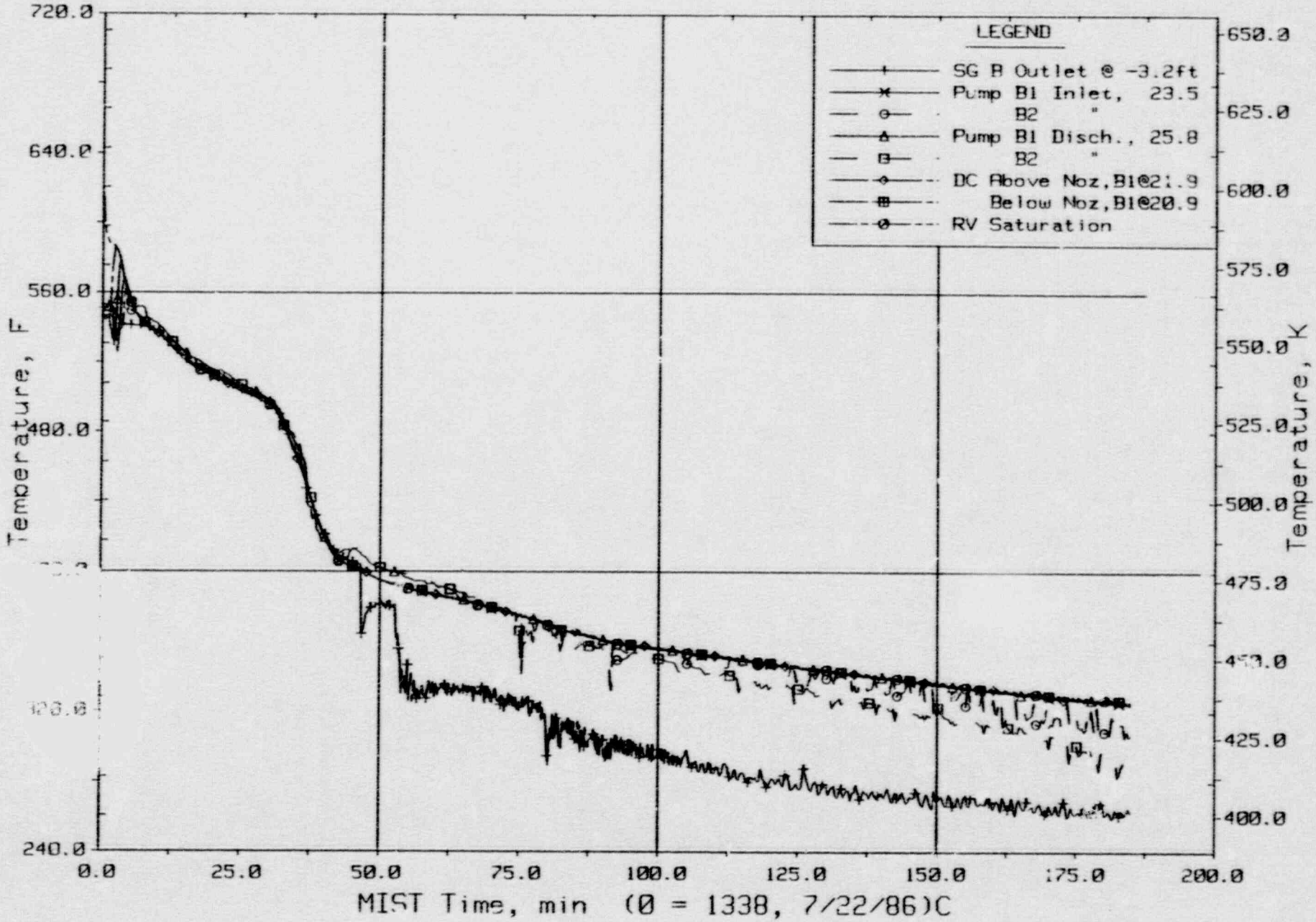

Loop B Cold Leg Fluid Temperatures (RTDs).

Thu May 19 16:50:48 1988

C25 3

FINAL DATA

T320201: Group 32 SBLOCA Test 2, Increased Leak Size - 50 cm2.

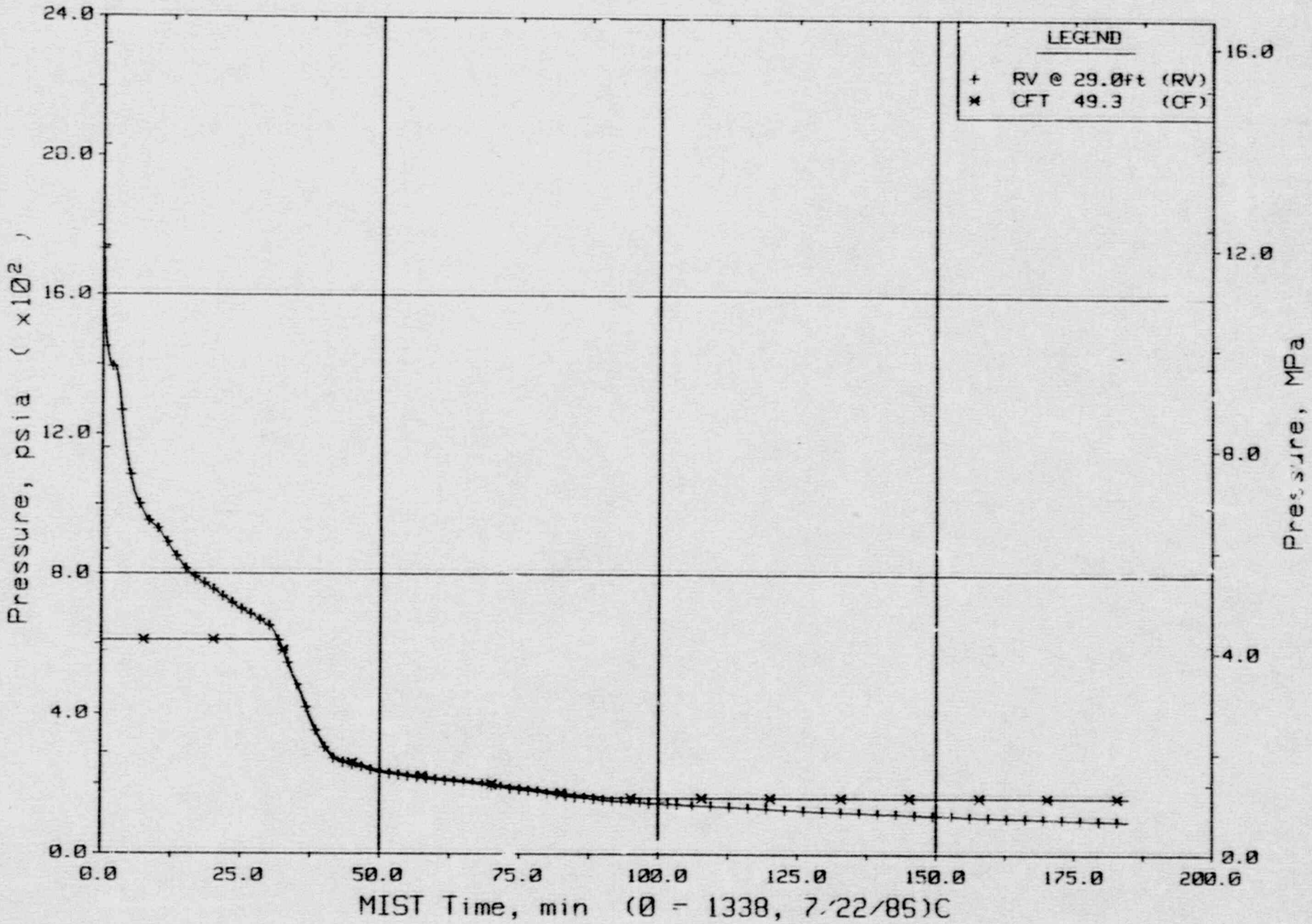

Primary System and Core Flood Tank Pressures (GP01s).

Thu May 19 16:53:47 1988

CFGP1

FINAL DATA

T320201: Group 32 SBLOCA Test 2, Increased Leak Size - 50 cm2.

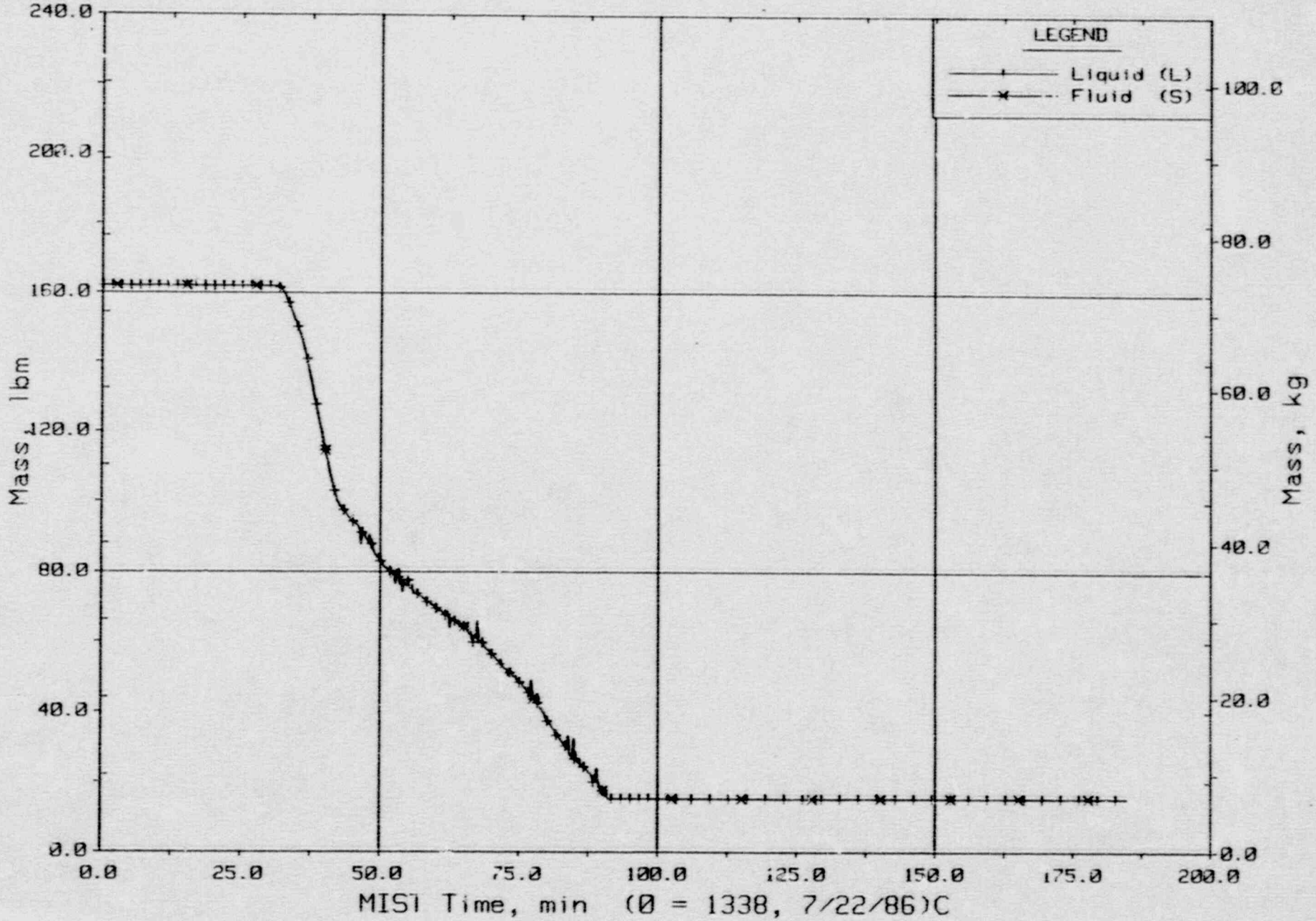

Core Flood Tank Liquid and Fluid Mass (CFMa20s).

FINAL DATA

T320201: Group 32 SBLOCA Test 2, Increased Leak Size - 50 cm2.

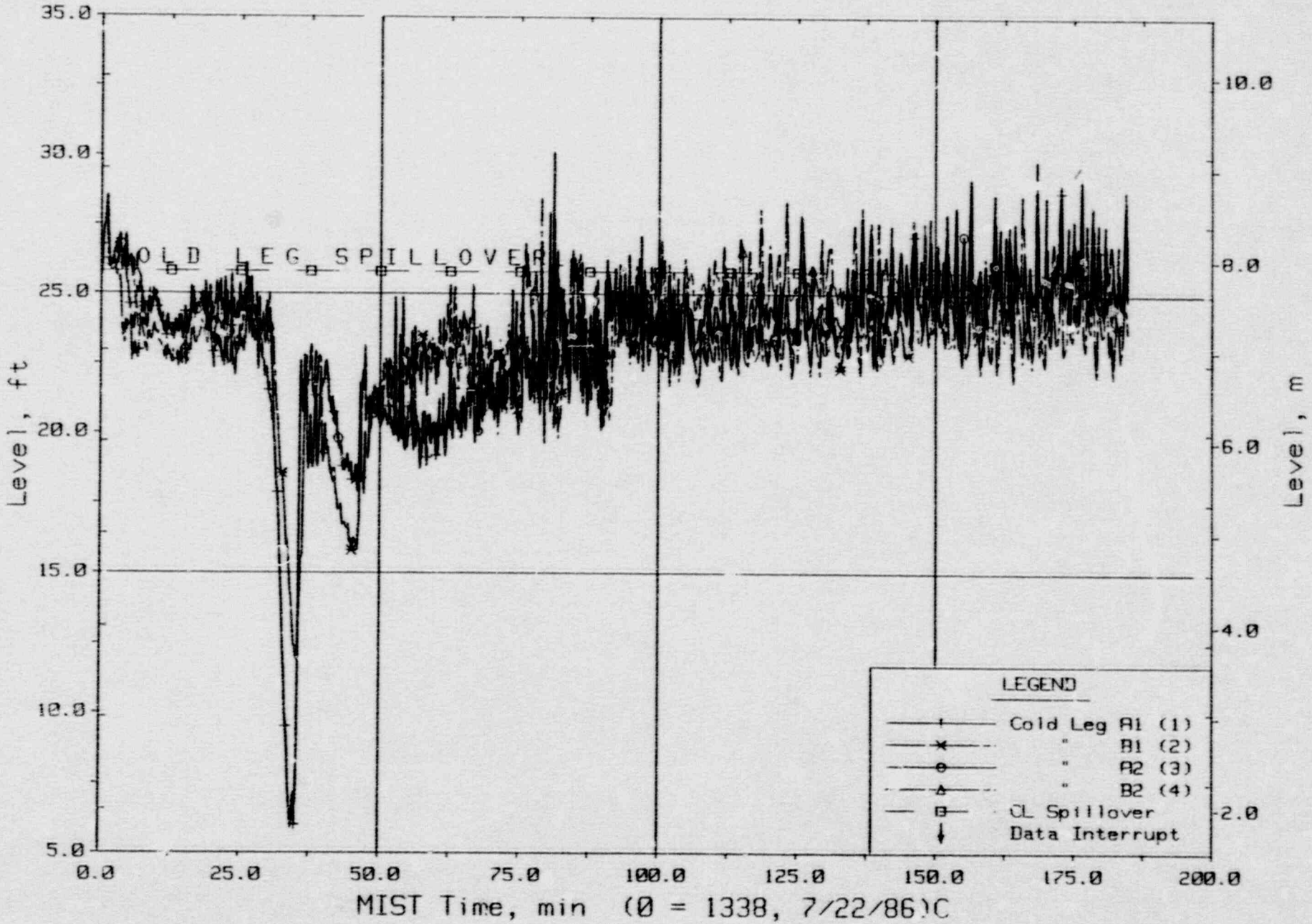

MIST Time, min (0 = 1338, 7/22/86)C

Cold Leg Suction Collapsed Liquid Levels (CnLV22s).

Thu May 19 17:01:41 1988

CLLV4

FINAL DATA

T320201: Group 32 SBLOCA Test 2, increased Leak Size - 50 cm2.

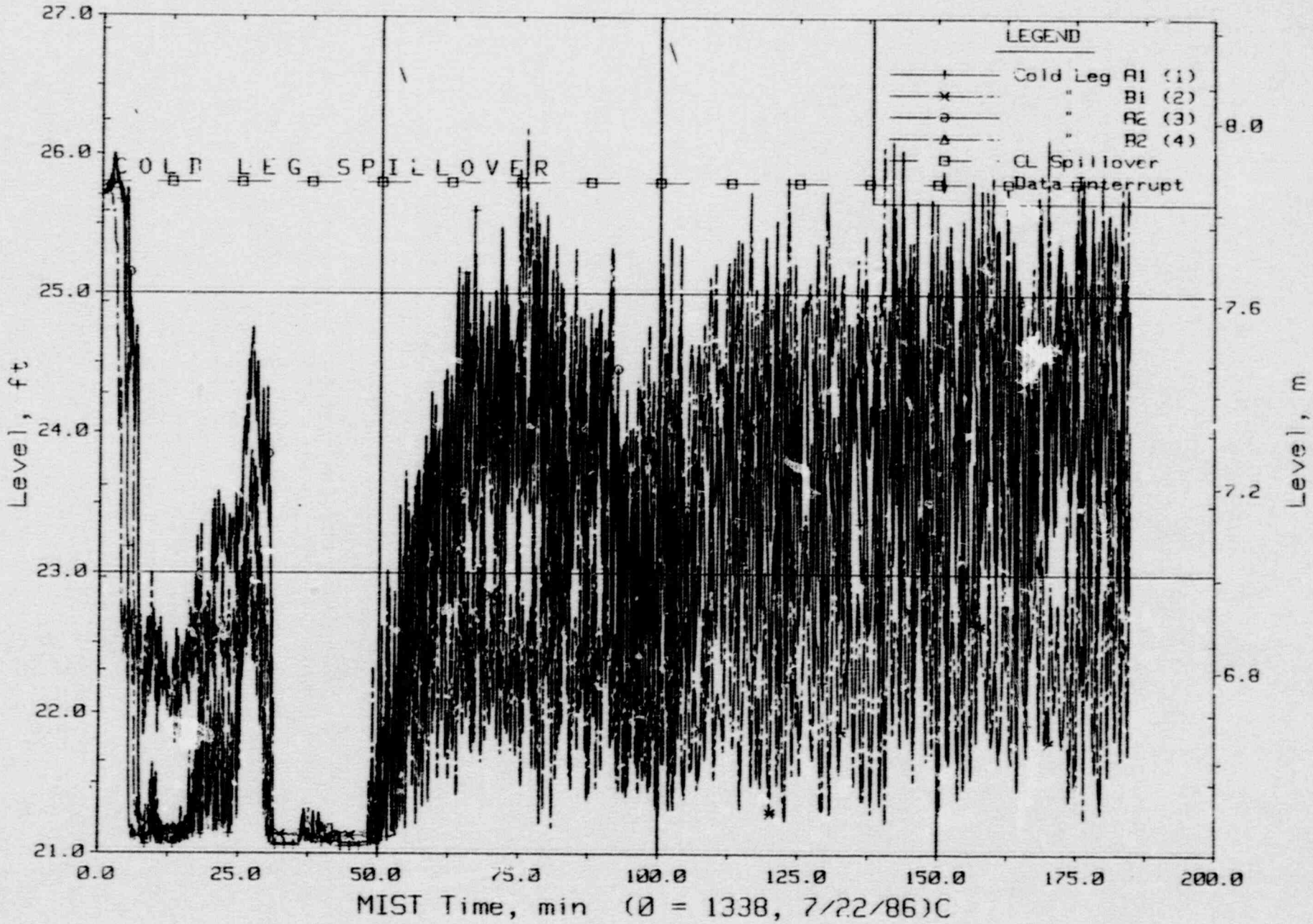

Cold Leg Discharge Collapsed Liquid Levels (CnLV23s).

Thu May 19 17:11:39 1988

CLLV5

FINAL DATA

T320201: Group 32 SBLOCA Test 2, Increased Leak Size - 50 cm2.

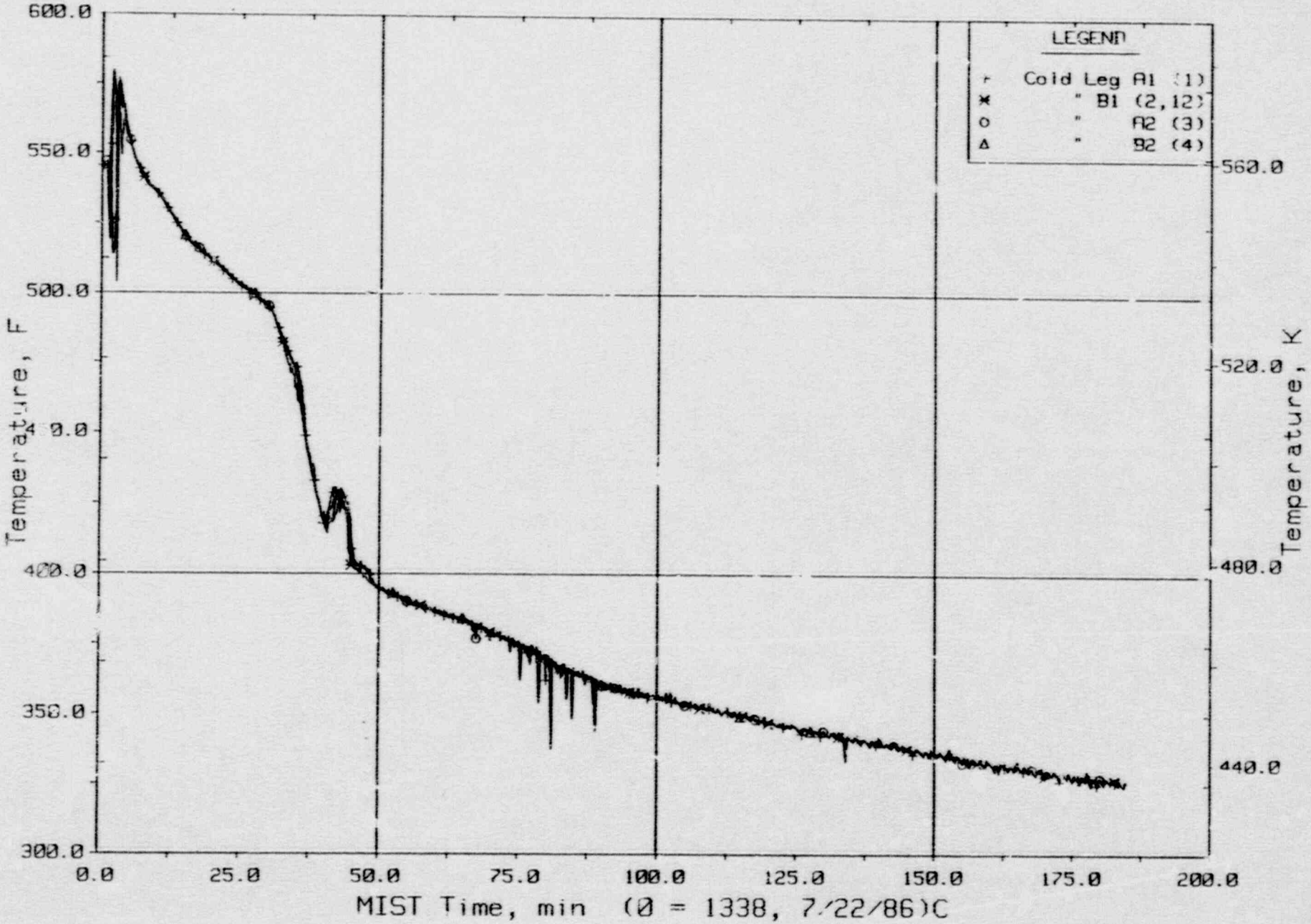

Cold Leg Nozzle Fluid Temperatures, Top of Rake (21.3ft, CnTC11s).

Thu May 19 17:16:58 1988

CLTC1

FINAL DATA

T320201: Group 32 SBLOCA Test 2, Increased Leak Size - 50 cm2.

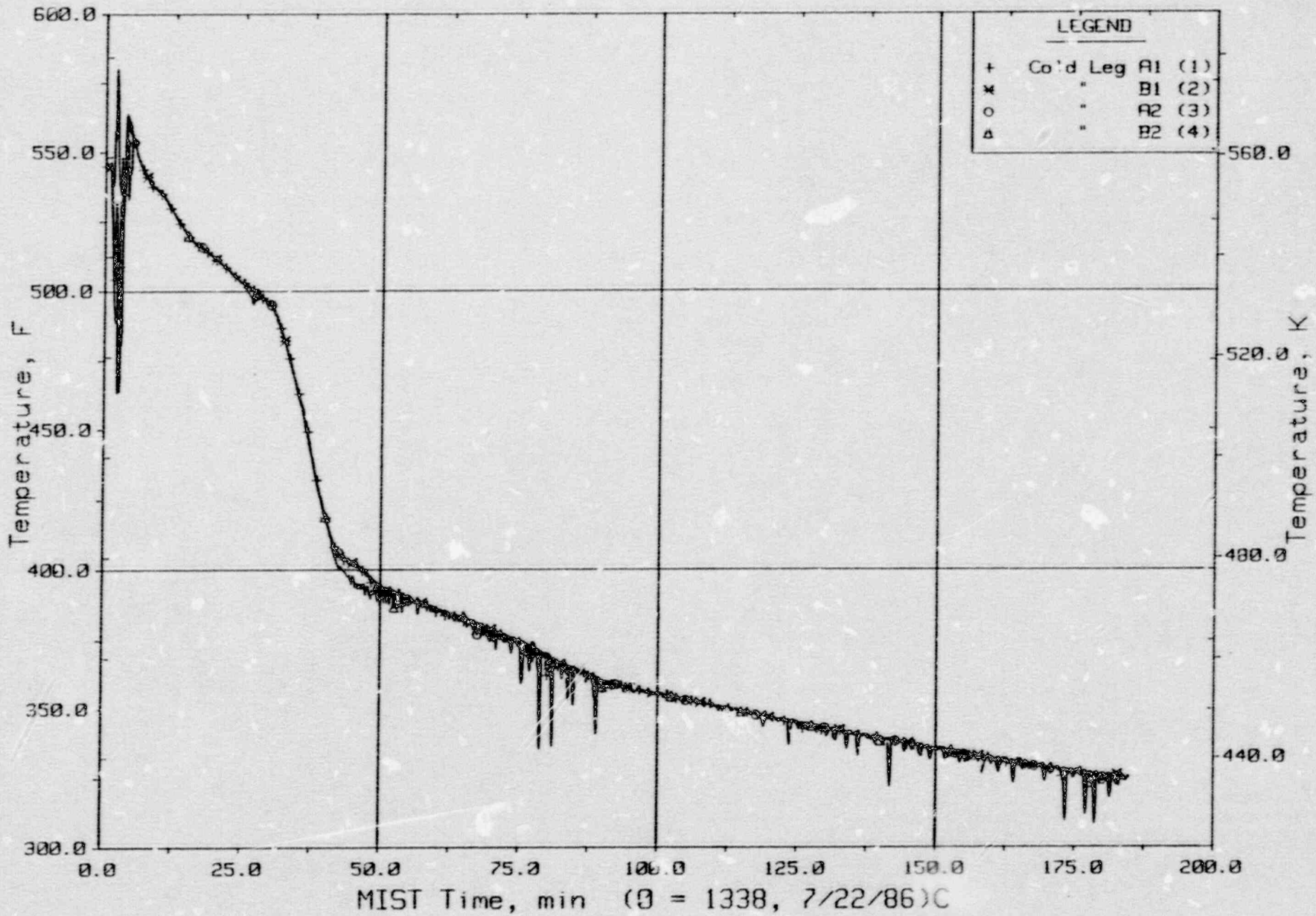

Cold Leg Nozzle Fluid Temperatures, Bottom of Rake (21.2ft, CnTC14s).

Thu May 19 17:20:00 1988

CLTC2

FINAL DATA

T320201: Group 32 SBLOCA Test 2, Increased Leak Size - 50 cm2.

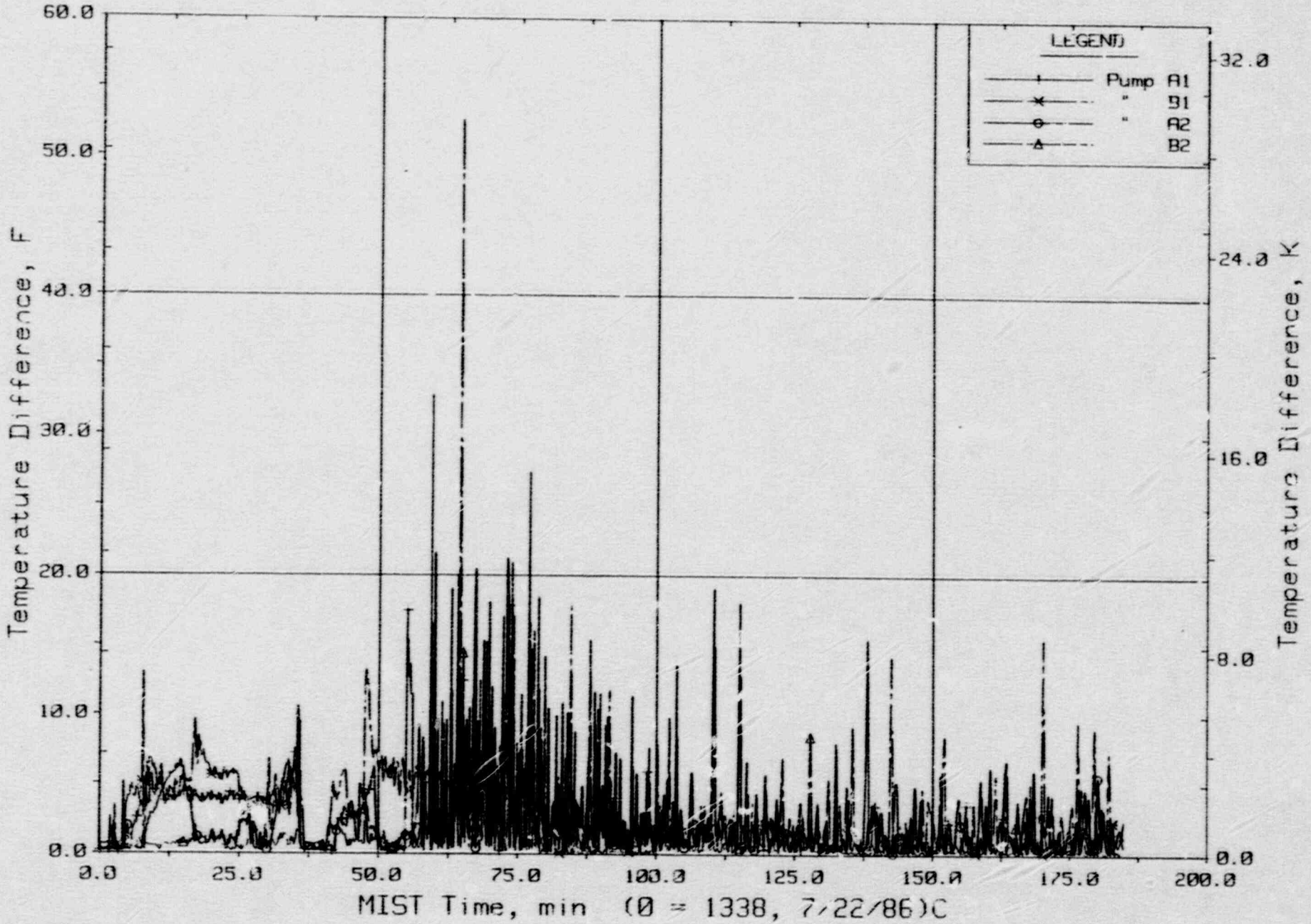

Maximum Differences Among RCP Rake Fluid Temperatures.

Thu May 19 17:24:38 1988

CLTD1

FINAL DATA

T320201: Group 32 SBLOCA Test 2, Increased Leak Size - 50 cm2.

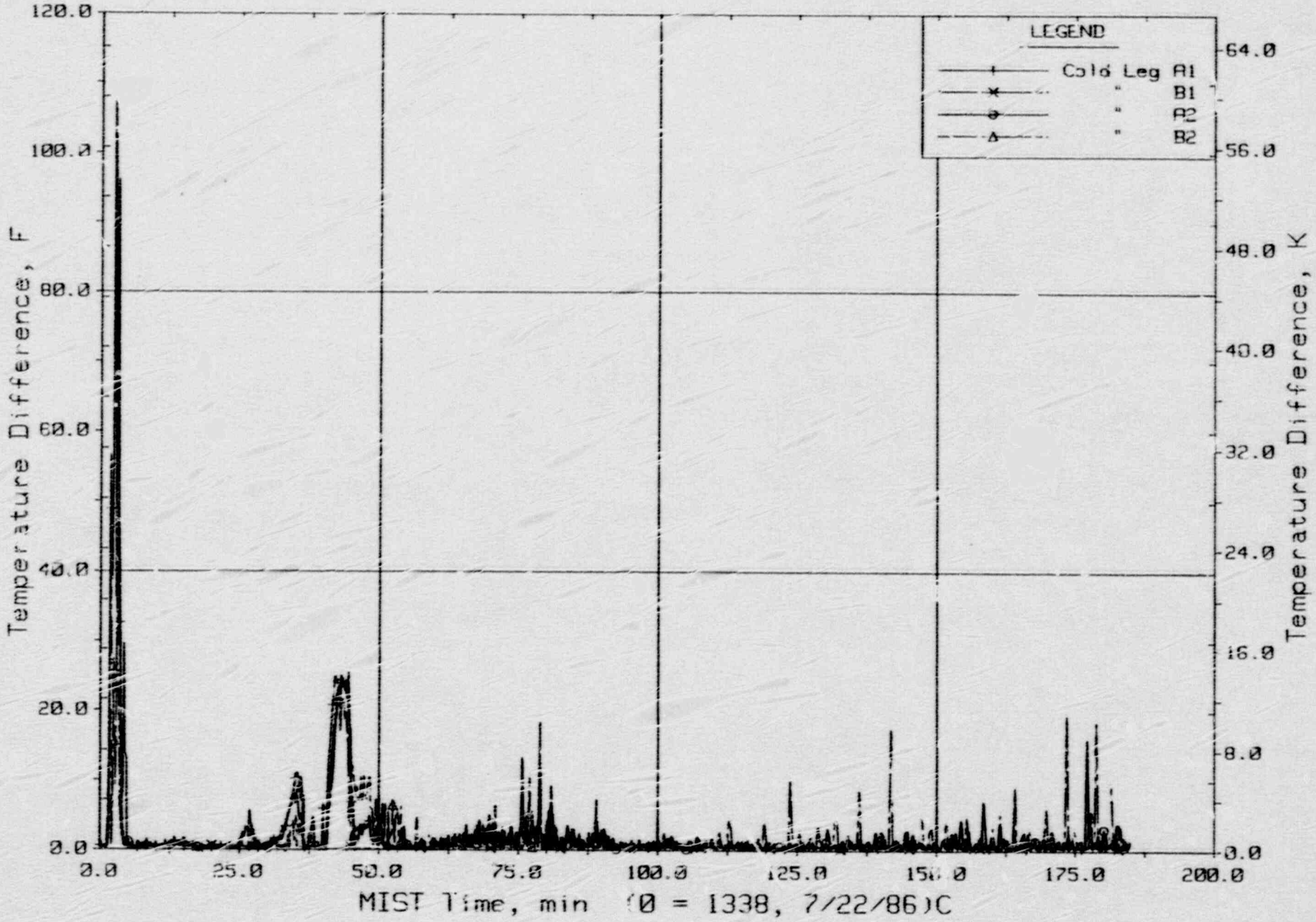

Maximum Differences among CL Nozzle Rake Fluid Temperatures.

Thu May 19 17:28:47 1988

CLTD2

FINAL JPTA

T320201: Group 32 SBLOCA Test ?, Increased Leak Size - 50 cm2.

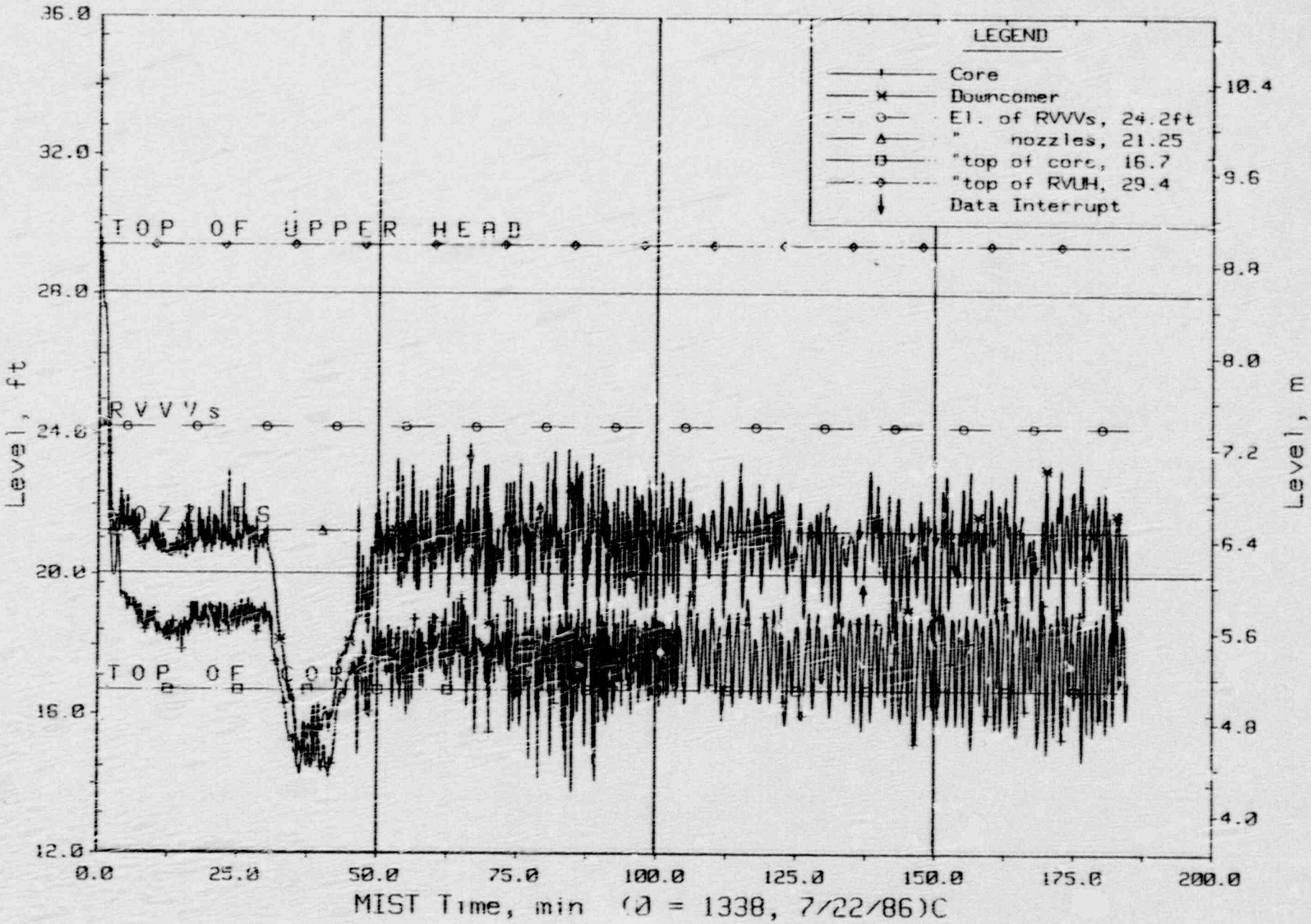

Core Region Collapsed Liquid Levels.

Thu May 19 17:33:26 1988

COLV1

FINAL DATA

T320201: Group 32 SBLOCA Test 2, Increased Leak Size - 50 cm2.

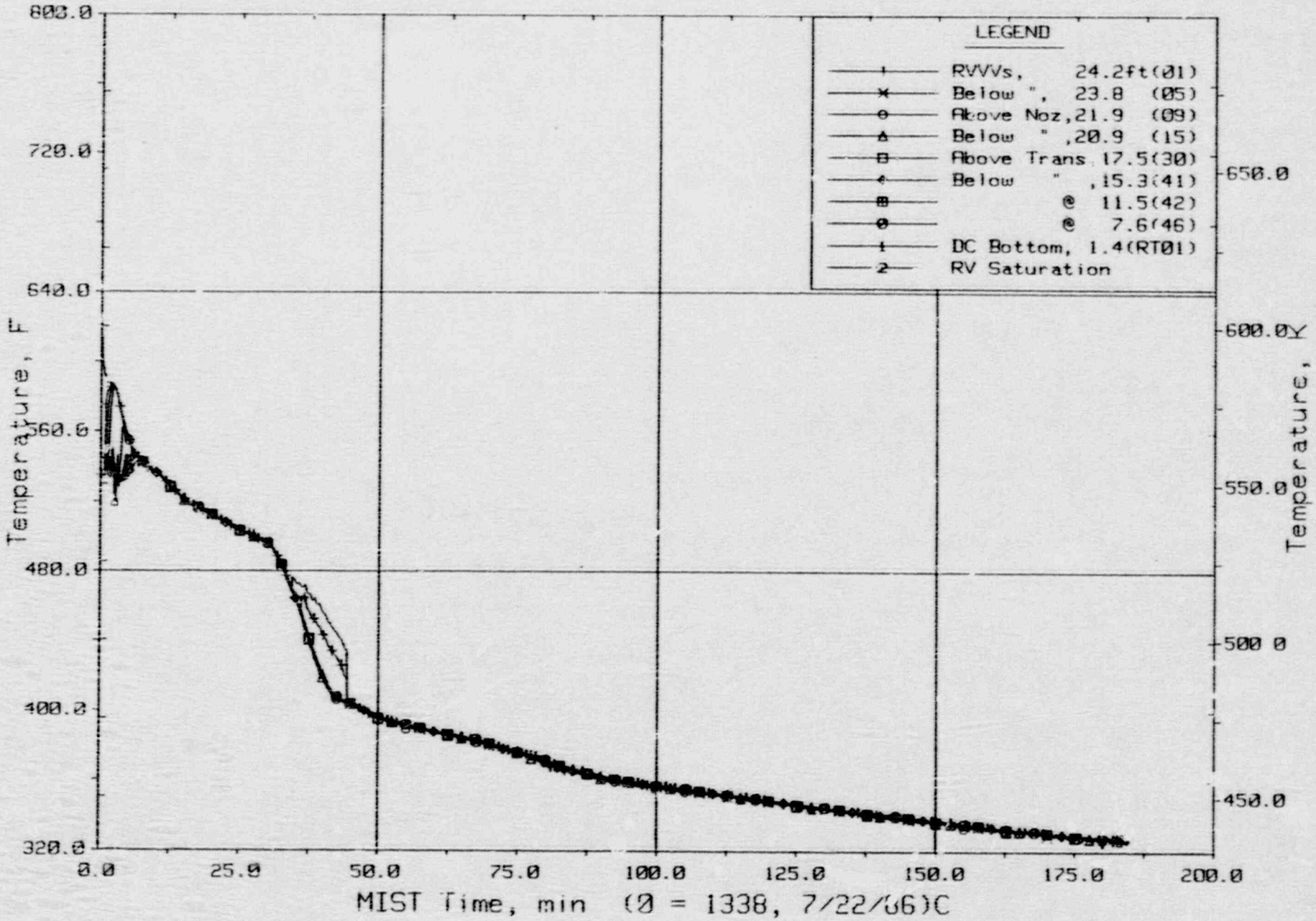

Downcomer Quadrant A1 Fluid Temperatures (DCTCs).

Thu May 19 17:41:46 1988

DCTC6

FINAL DATA

T320201: Group 32 Test 2, Increased Leak Size.

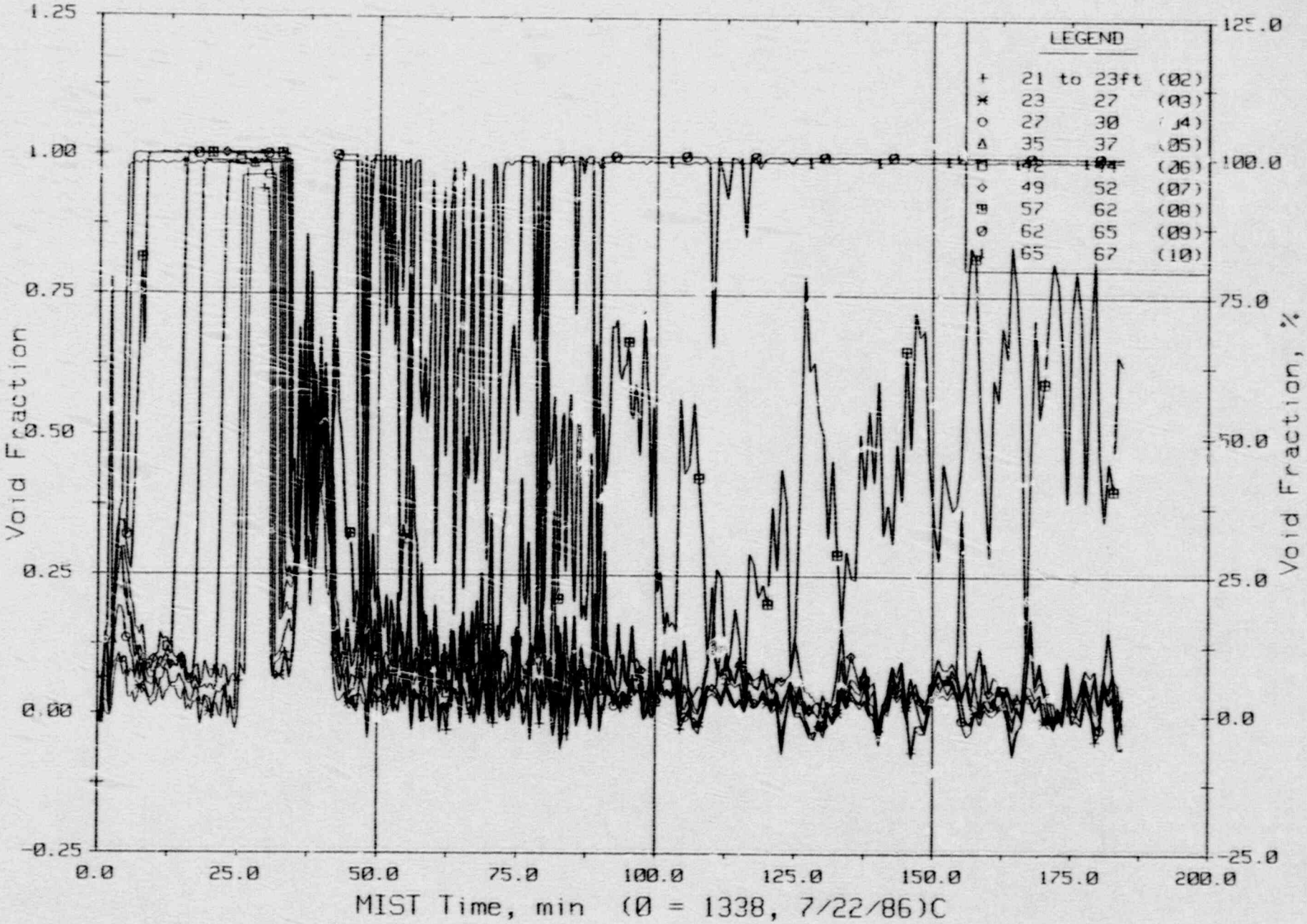

Hot Leg A Riser Void Fractions From Differential Pressures (HIVFs).

Tue Jun 7 09:06:26 1988

HIVF1

FINAL DATA

T320201: Group 32 SBLOCA Test 2, Increased Leak Size - 50 cm2.

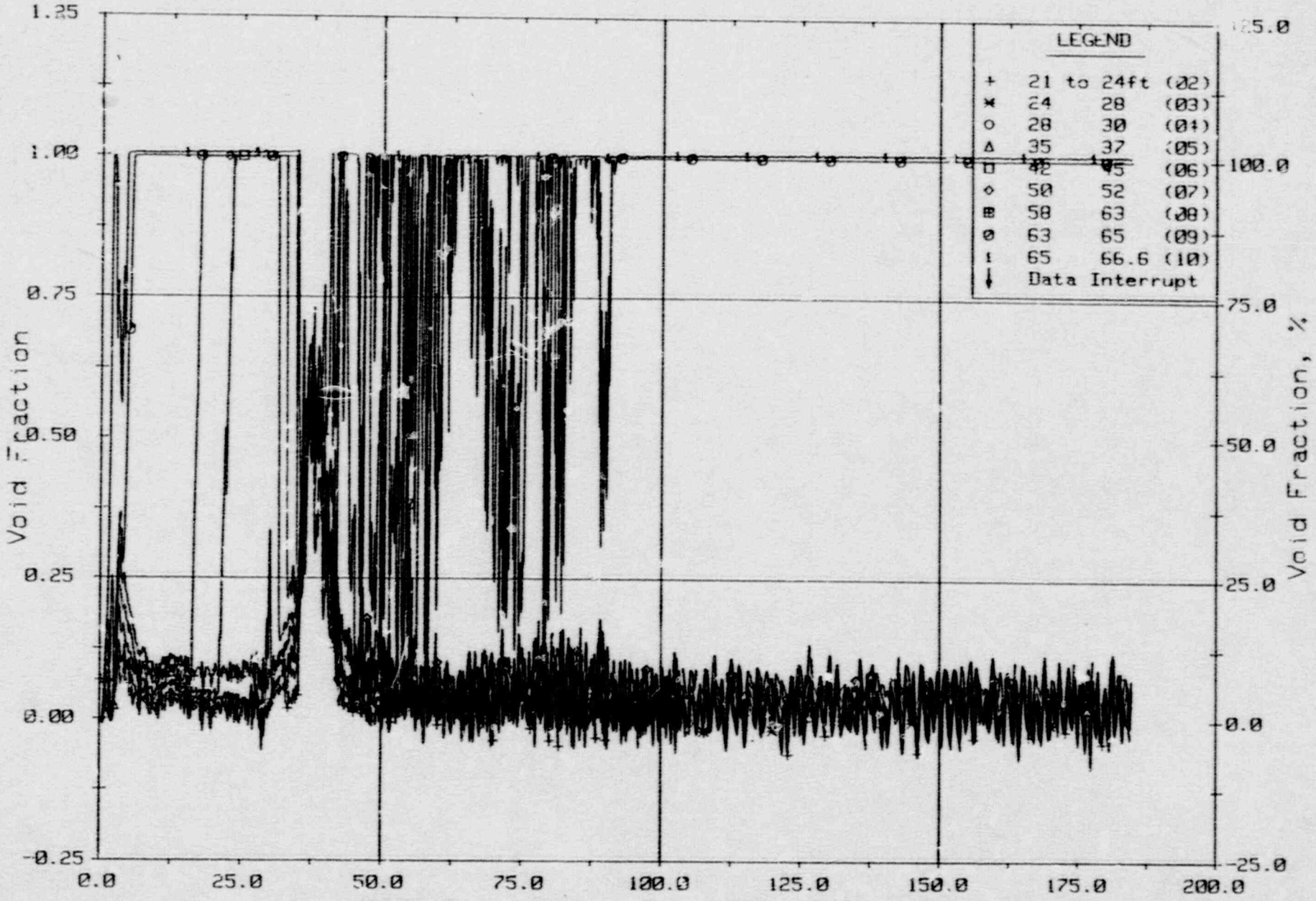

Hot Leg B Riser Void Fraction From Differential Pressures (H2VFs).

Thu May 19 17:53:59 1988

H2VF1

FINAL DATA

1320201: Group 32 SRLOCA Test 2, Increased Leak Size - 50 cm2.

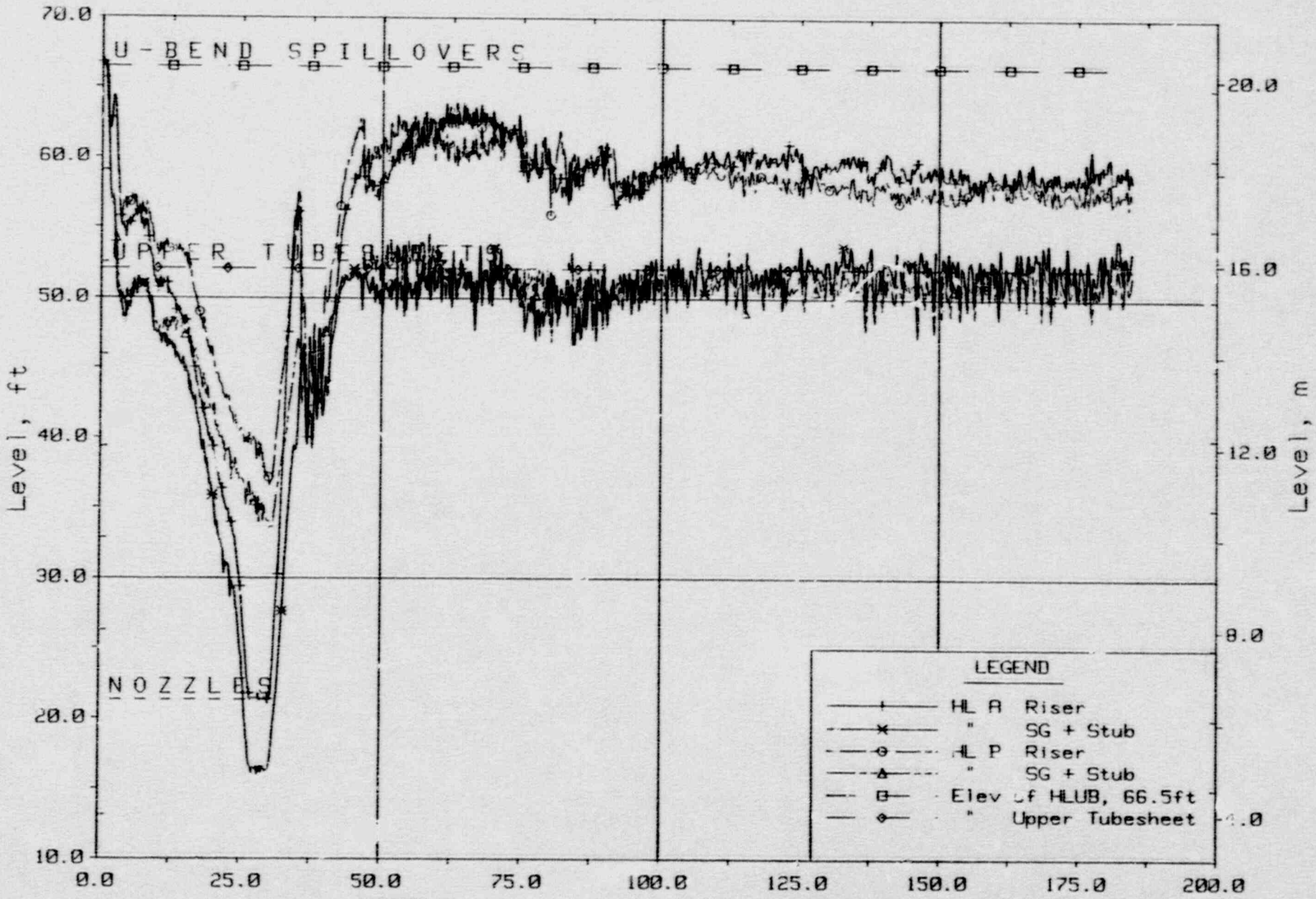

MIST Time, min (0 = 1338, 7/22/86)C

Hot Leg Riser and Stub Collapsed Liquid Levels.

Thu May 19 18:00:32 1988

HLLV1

FINAL DATA

T320201: Group 32 SBLOCA Test 2, Increased Leak Size - 50 cm2.

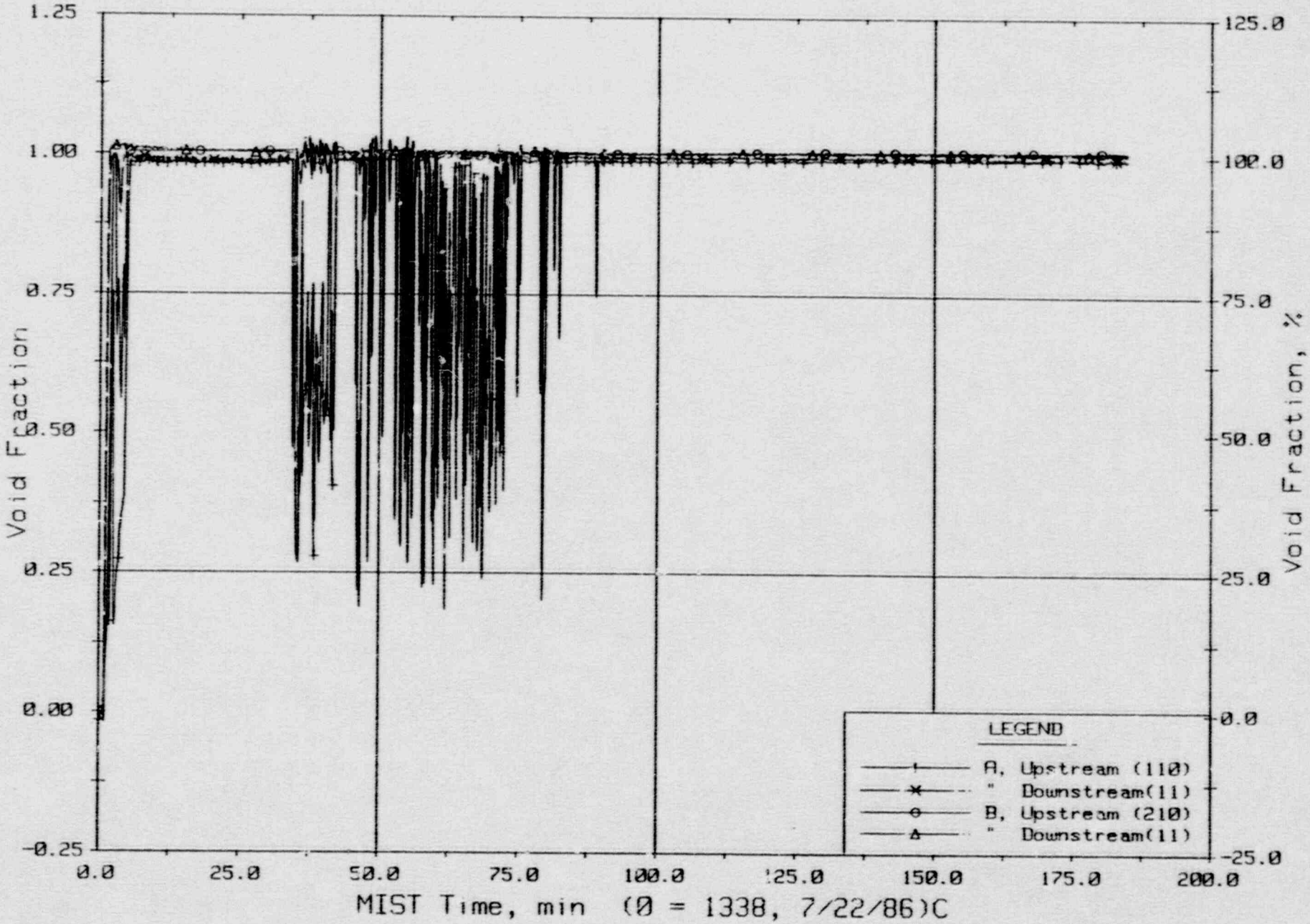

Hot Leg U-Bend Void Fractions From Diffl. Pressures (64.8 to 66.6 ft, HnVFs).

Thu May 19 18:04:30 1988

HLVF1

FINAL DATA

T320201: Group 32 SRLOCA Test 2, Increased Leak Size - 50 cm2.

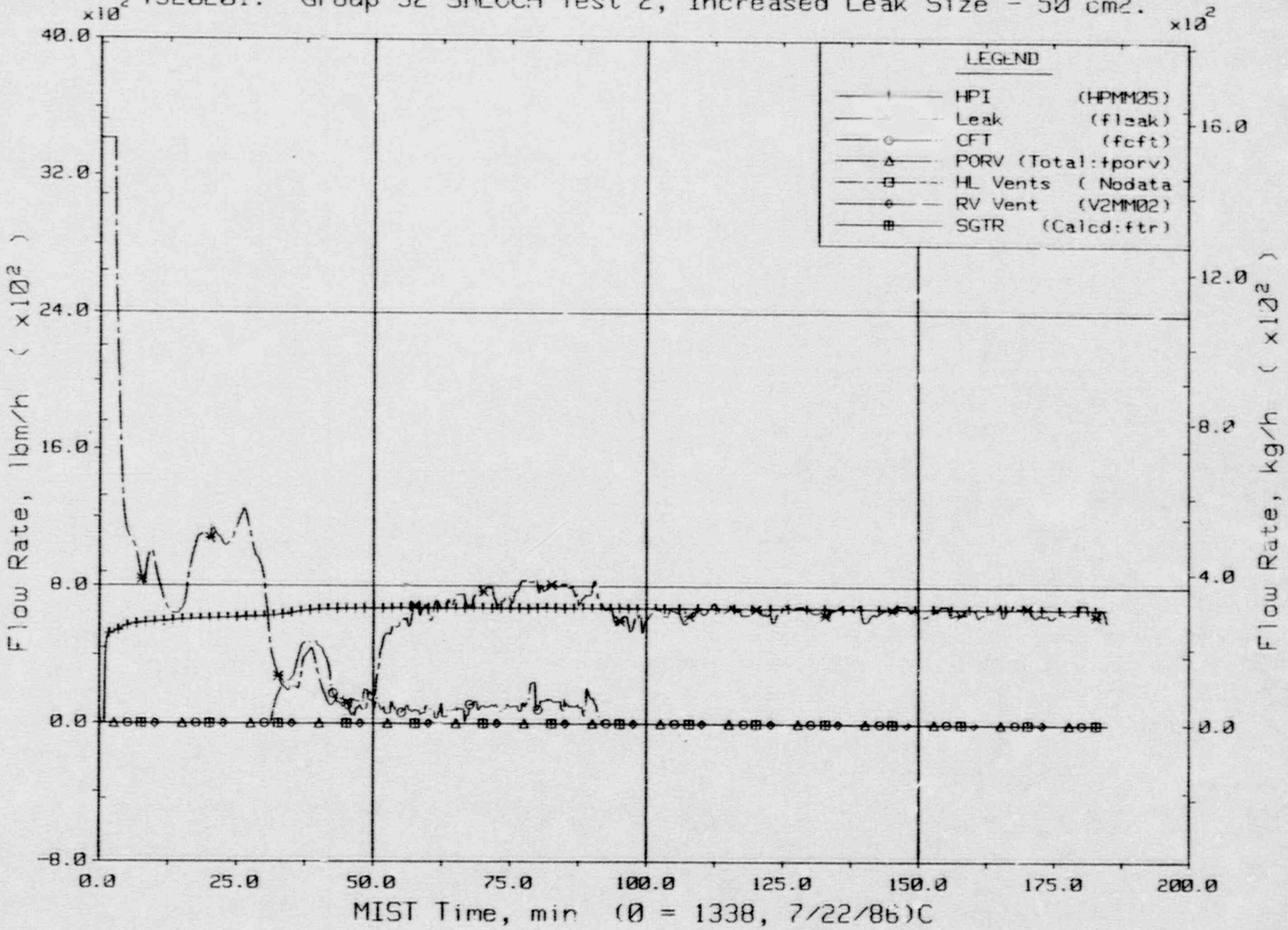

Primary System Boundary Flow Rates.

Thu May 19 18:11:31 1988

PB-L3

FINAL DATA

T320201: Group 32 SBLOCA Test 2, Increased Leak Size - 50 cm2.

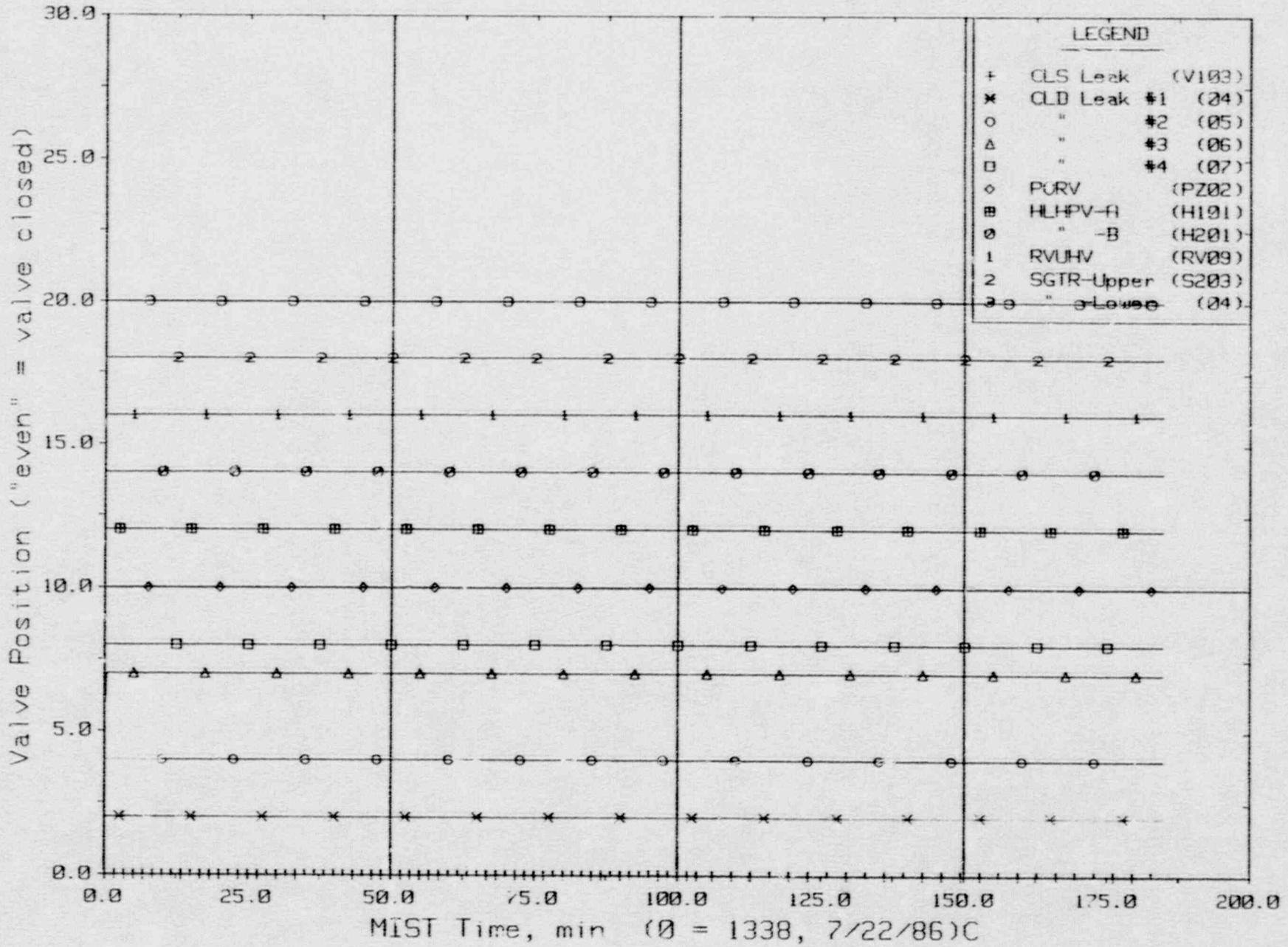

Primary System Discharge Limit Switch Indications (LSs).

Thu May 19 18:31:46 1988

PBLS1

FINAL DATA

T320201: Group 32 SBLOCA Test 2, Increased Leak Size - 50 cm2.

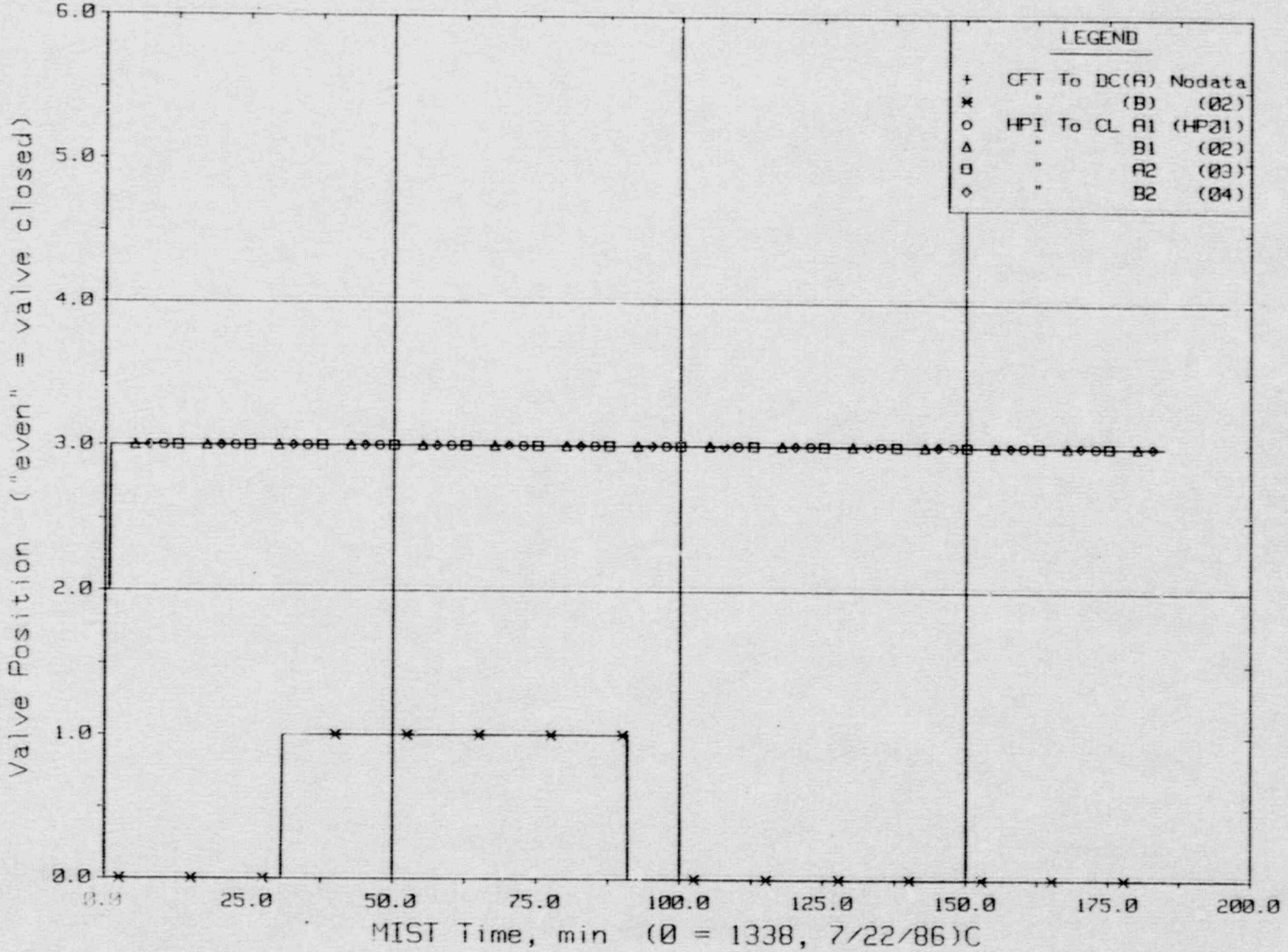

Primary System Injection Limit Switch Indications (LSs).

Thu May 19 18:34:59 1988

PBLS2

FINAL DATA

T320201: Group 32 SBLOCP Test 2, Increased Leak Size - 50 cm2.

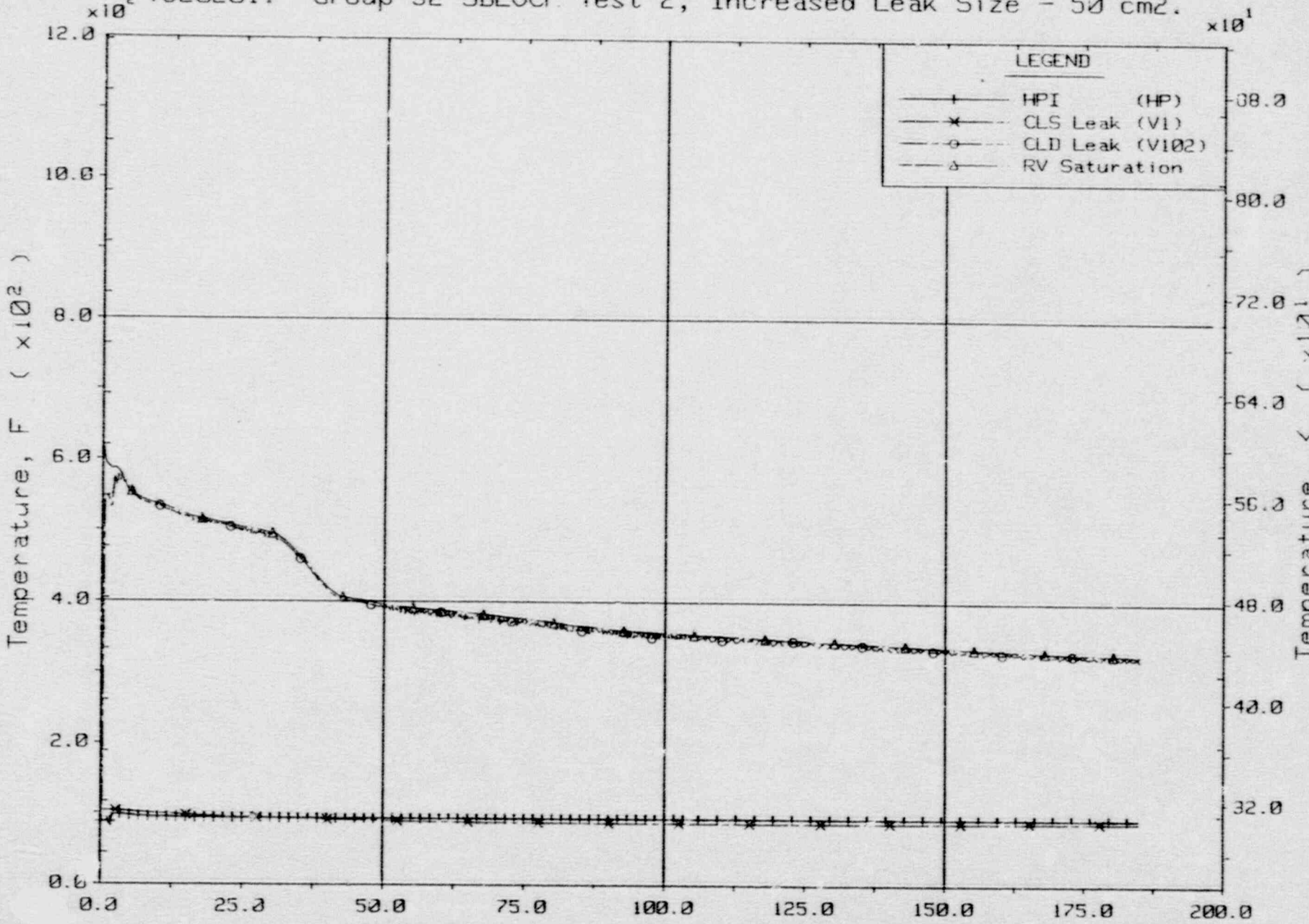

Single-Phase Discharge and HPI Fluid Temperatures (TC01s).

Thu May 19 18:15:09 1988

PPTC1

2

IMAGE EVALUATION TEST TARGET (MT-3)

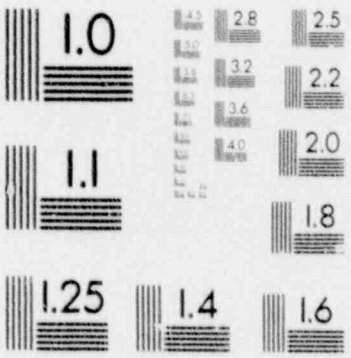

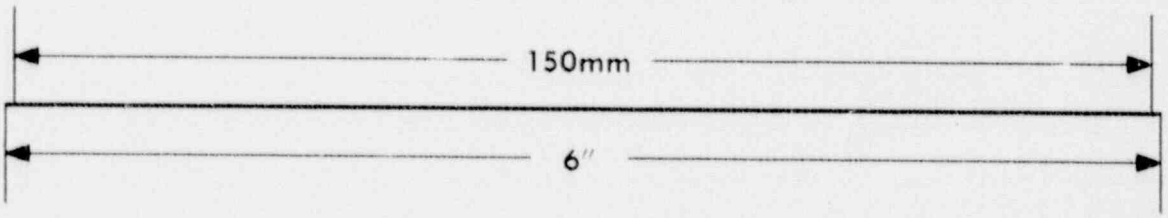

PHOTOGRAPHIC SCIENCES CORPORATION
770 BASKET ROAD
P.O. BOX 338
WEBSTER, NEW YORK 14580
(716) 265-1600

2

IMAGE EVALUATION TEST TARGET (MT-3)

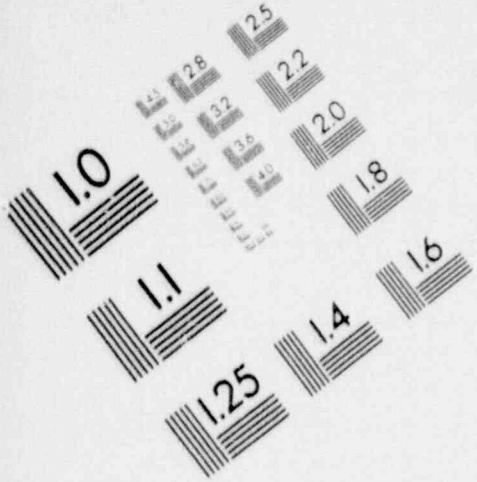

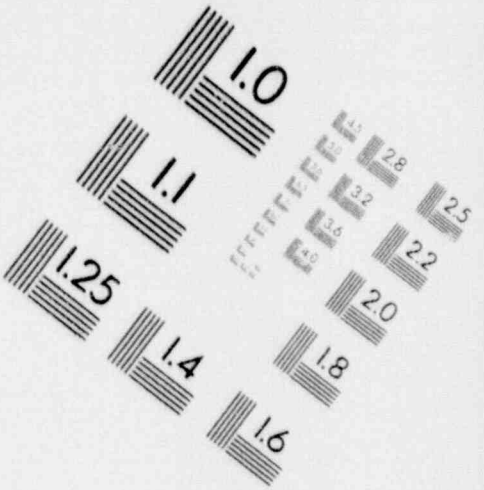

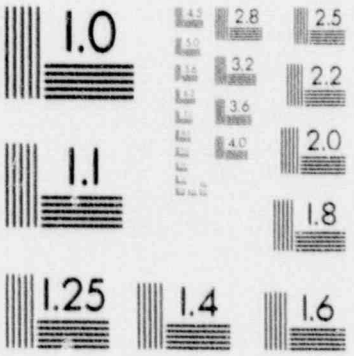

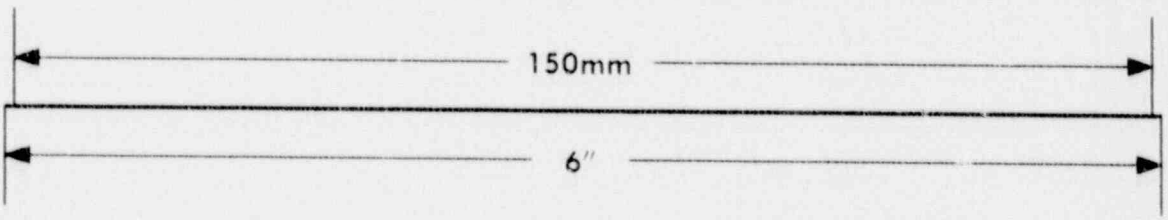

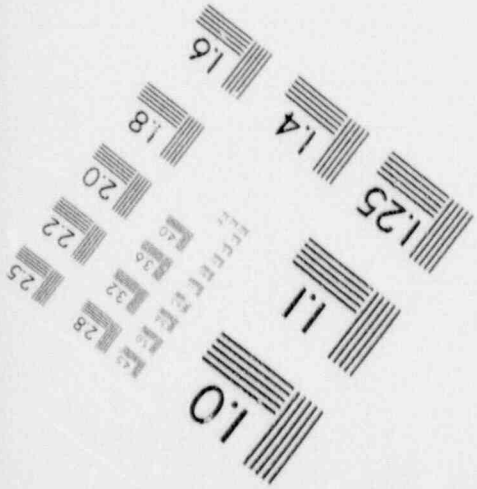

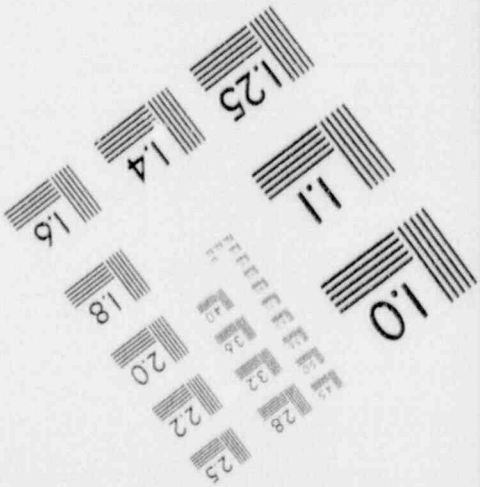

PHOTOGRAPHIC SCIENCES CORPORATION
770 BASKET ROAD
P.O. BOX 338
WEBSTER, NEW YORK 14580
(716) 265-1600

2

IMAGE EVALUATION TEST TARGET (MT-3)

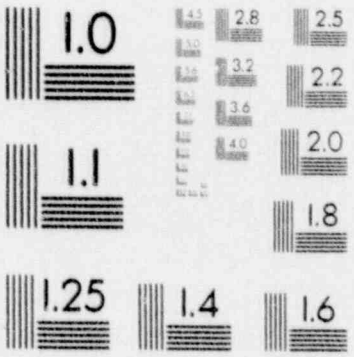

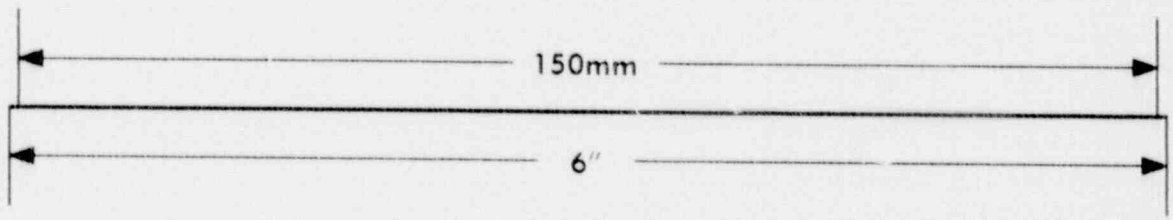

PHOTOGRAPHIC SCIENCES CORPORATION
770 BASKET ROAD
P.O. BOX 338
WEBSTER, NEW YORK 14580
(716) 265-1600

2

IMAGE EVALUATION TEST TARGET (MT-3)

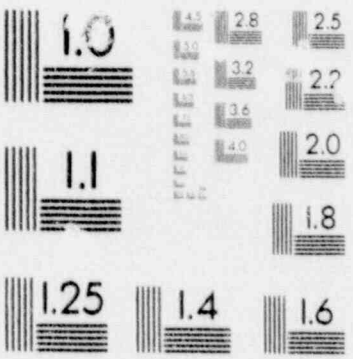

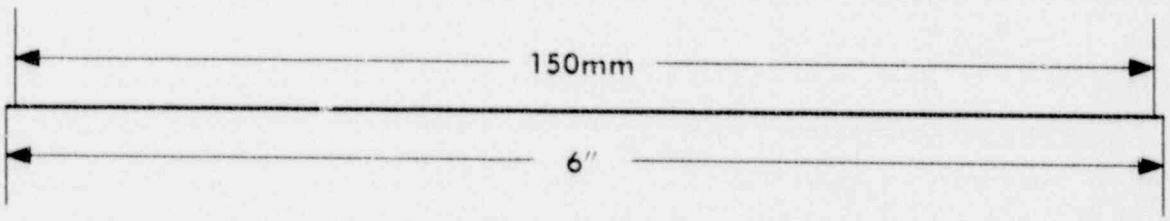

PHOTOGRAPHIC SCIENCES CORPORATION
770 BASKET ROAD
P.O. BOX 338
WEBSTER, NEW YORK 14580
(716) 265-1600

FINAL DATA

T320201: Group 32 SBLOCA Test 2, Increased Leak Size - 50 cm2.

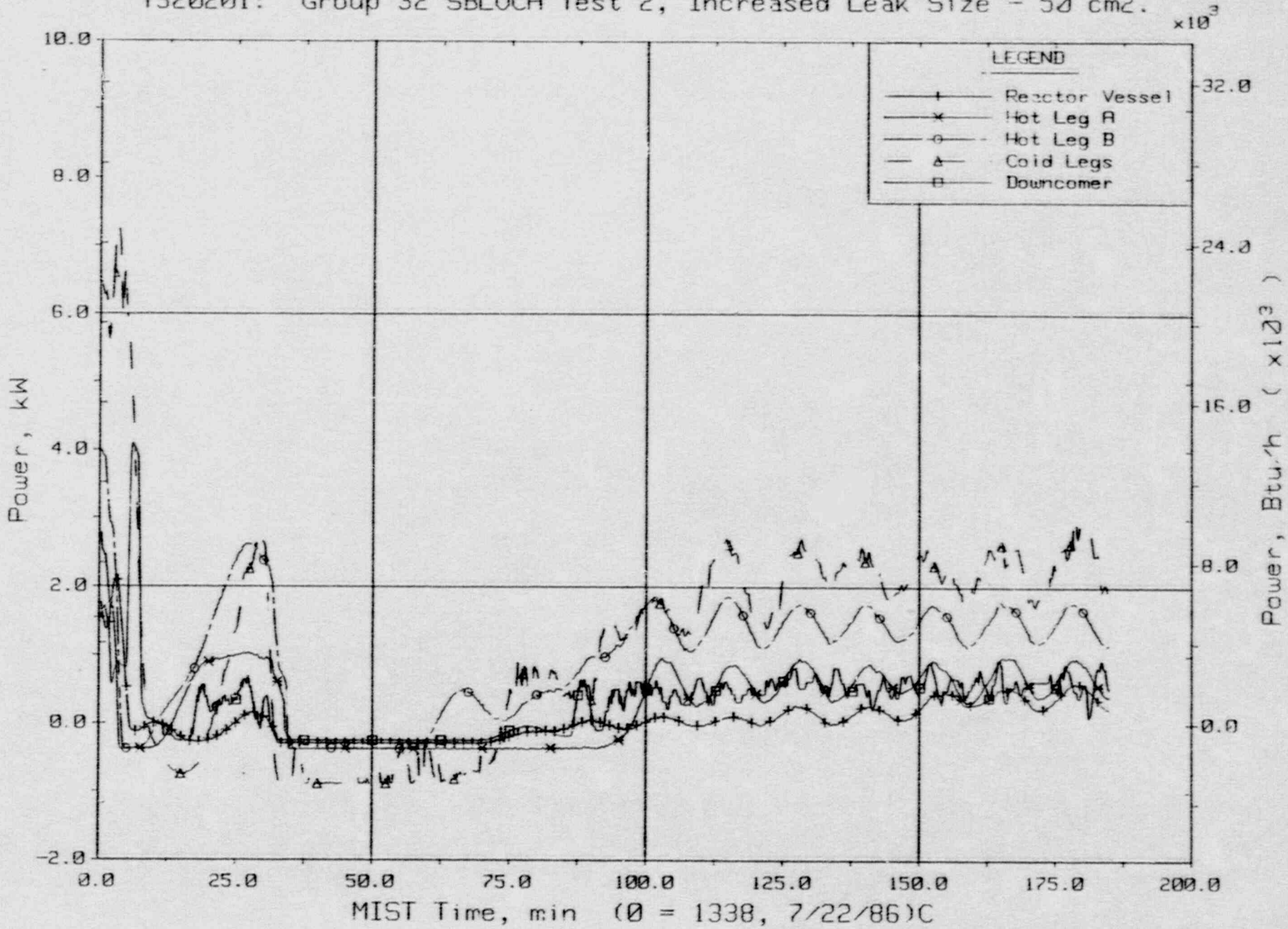

Guard Heater Specified Power Per Primary Component.

Thu May 19 18:19:10 1988

PRGQ1

FINAL DATA

T320201: Group 32 SBLOCA Test 2, Increased Leak Size - 50 cm2.

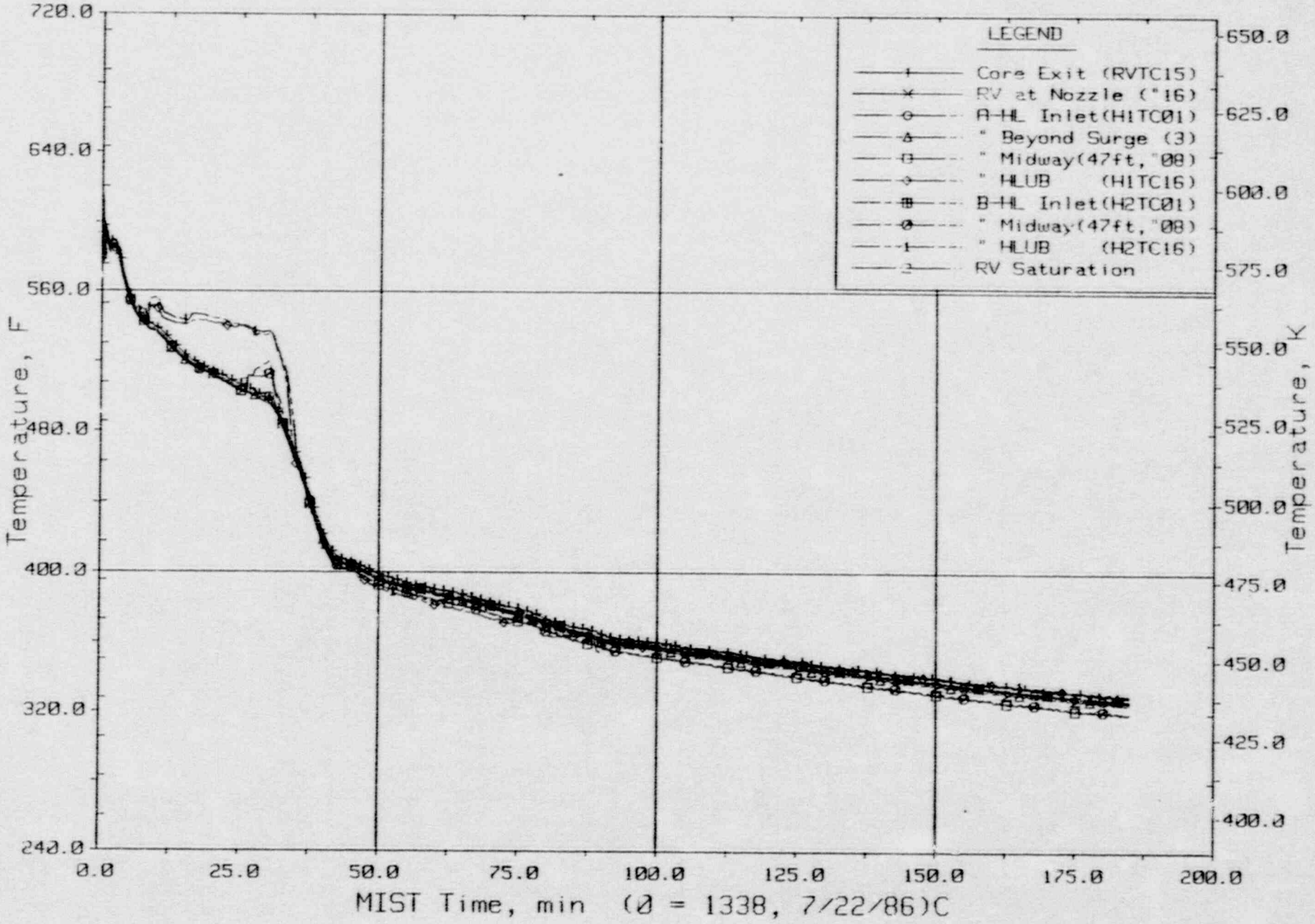

Composite Core Exit and Hot Leg Fluid Temperatures.

Thu May 19 18:26:02 1988

PRKT1

FINAL DATA

T320201: Group 32 SBLOCA Test 2, Increased Leak Size - 50 cm2.

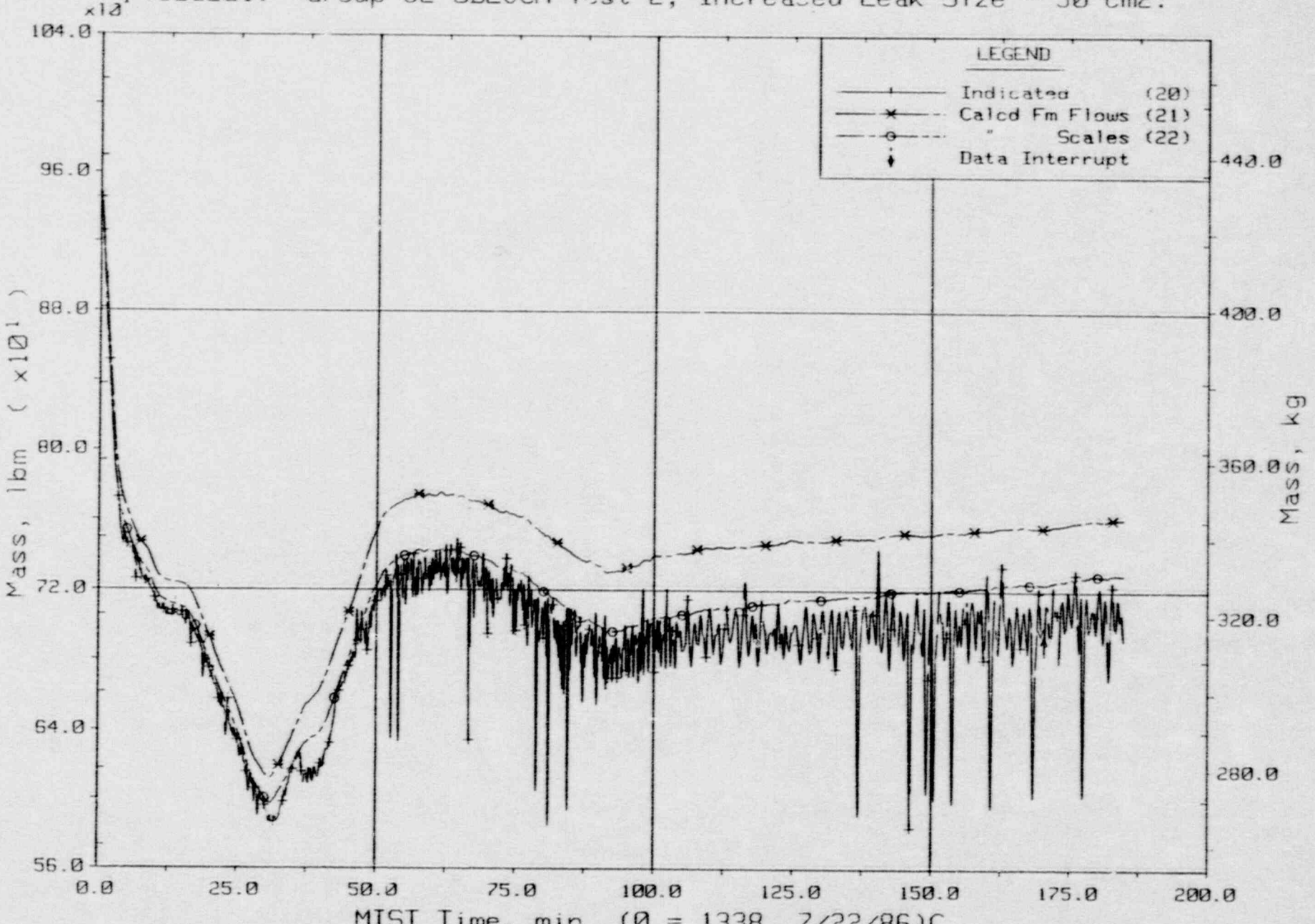

Primary Syster Total Fluid Mass (PLMLs).

Thu May 19 18:38:06 1988

PRML2

FINAL DATA

T320201: Group 32 SBLOCA Test 2, Increased Leak Size - 50 cm2.

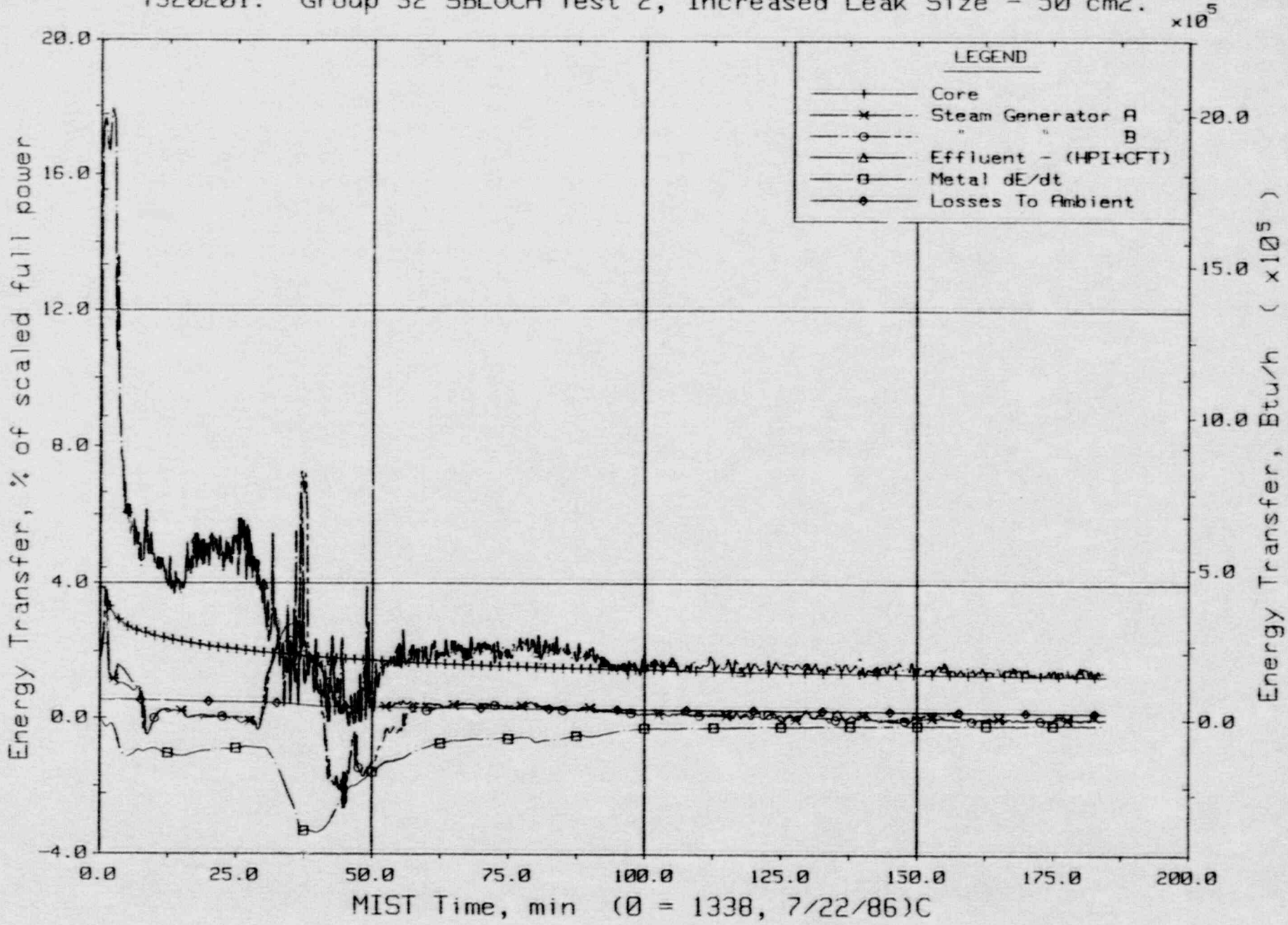

Primary System Energy Transfer.

Fri May 20 13:04:44 1988

PROE2

FINAL DATA

T320201: Group 32 SBLOCA Test 2, Increased Leak Size - 50 cm2.

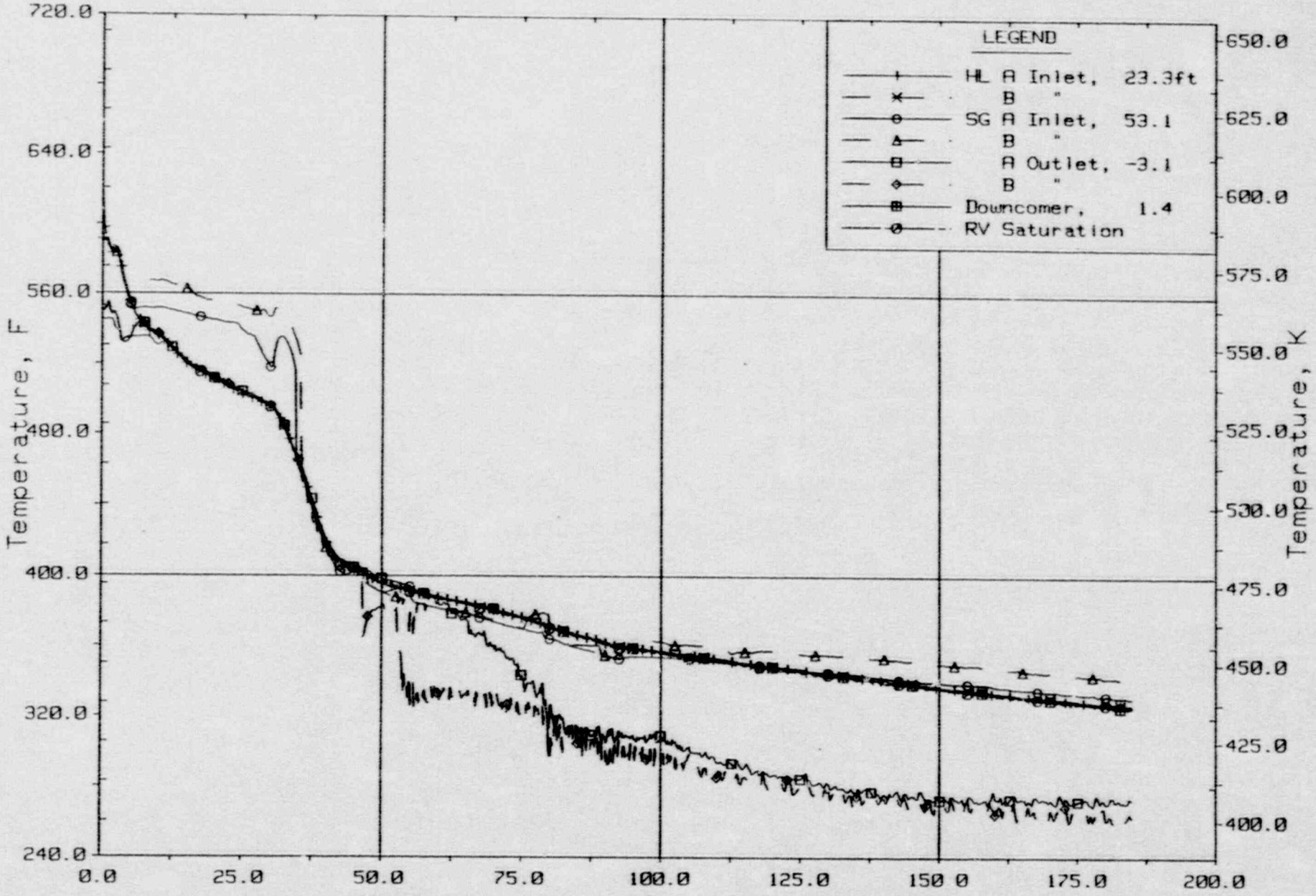

Primary System Fluid Temperatures (RTDs).

Fri May 20 13:09:51 1988

PRRT0

FINAL DATA

T320201: Group 32 SBLOCA Test 2, Increased Leak Size - 50 cm2.

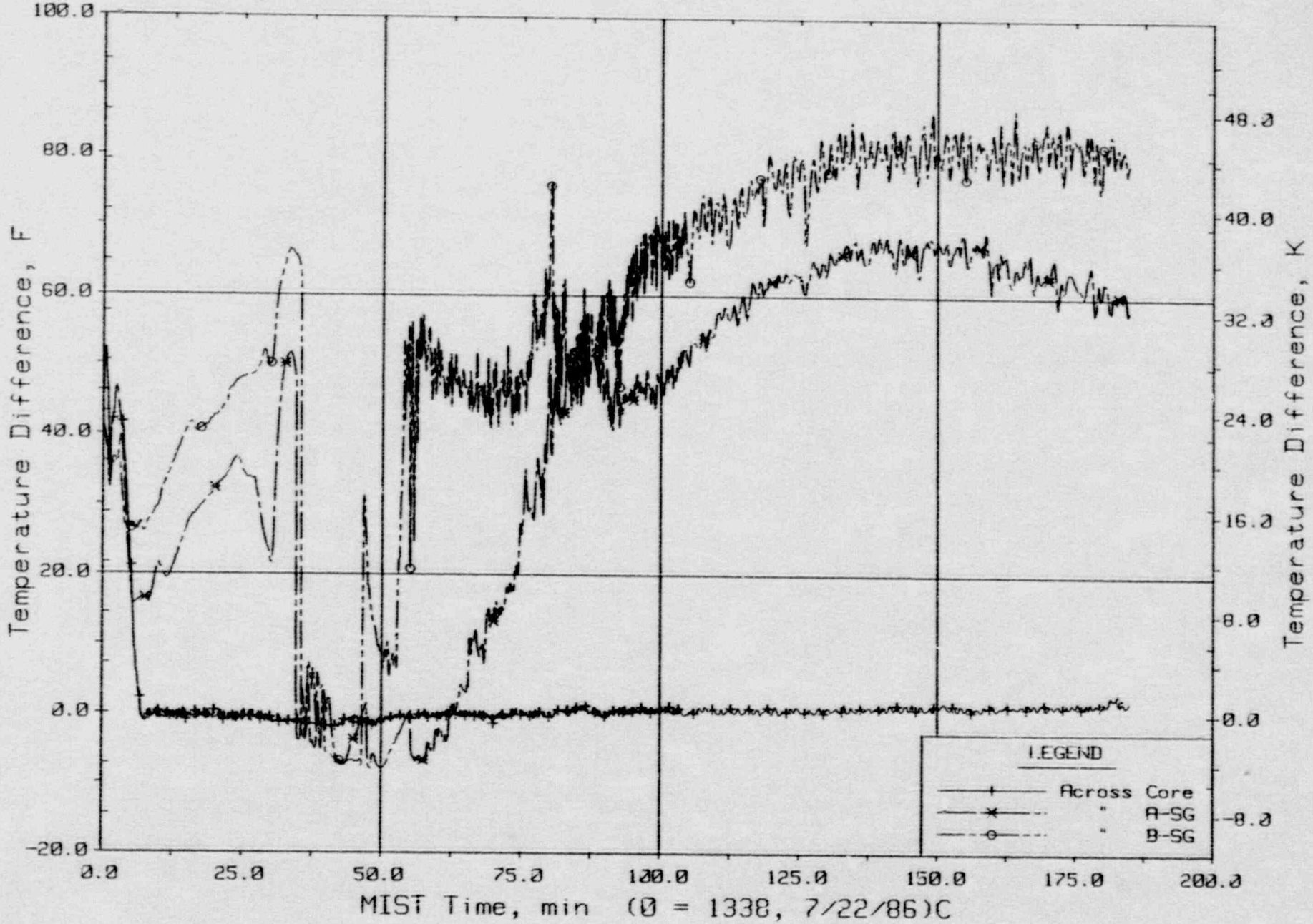

Key Temperature Differences.

Fri May 20 13:21:59 1988

PRTD2

FINAL DATA

T320201: Group 32 SBLOCA Test 2, Increased Leak Size - 50 cm2.

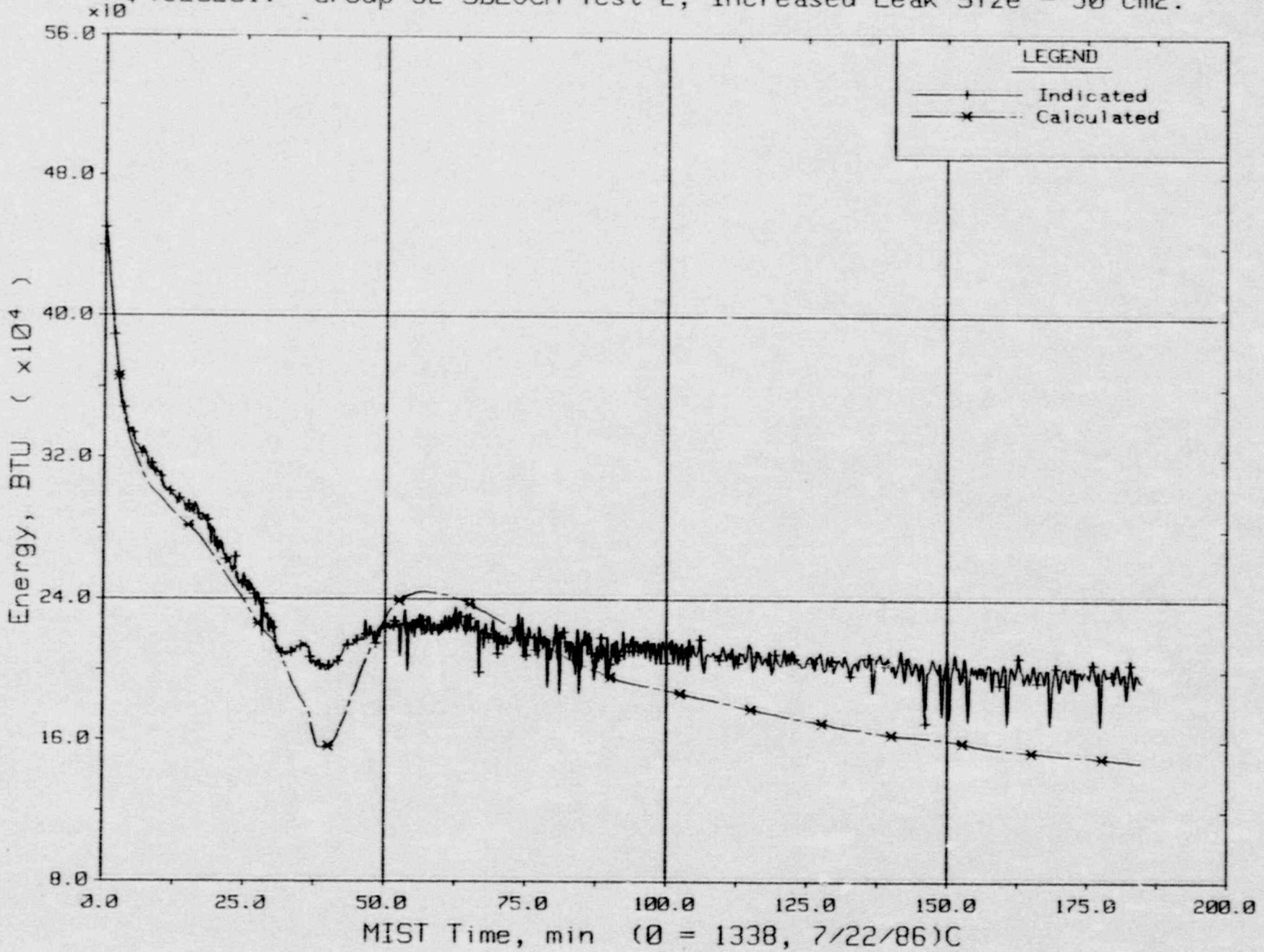

Primary System Total Fluid Energy.

Fri May 20 13:26:31 1988

PRTE2

FINAL DATA

T320201: Group 32 SBLOCA Test 2, Increased Leak Size - 50 cm2.

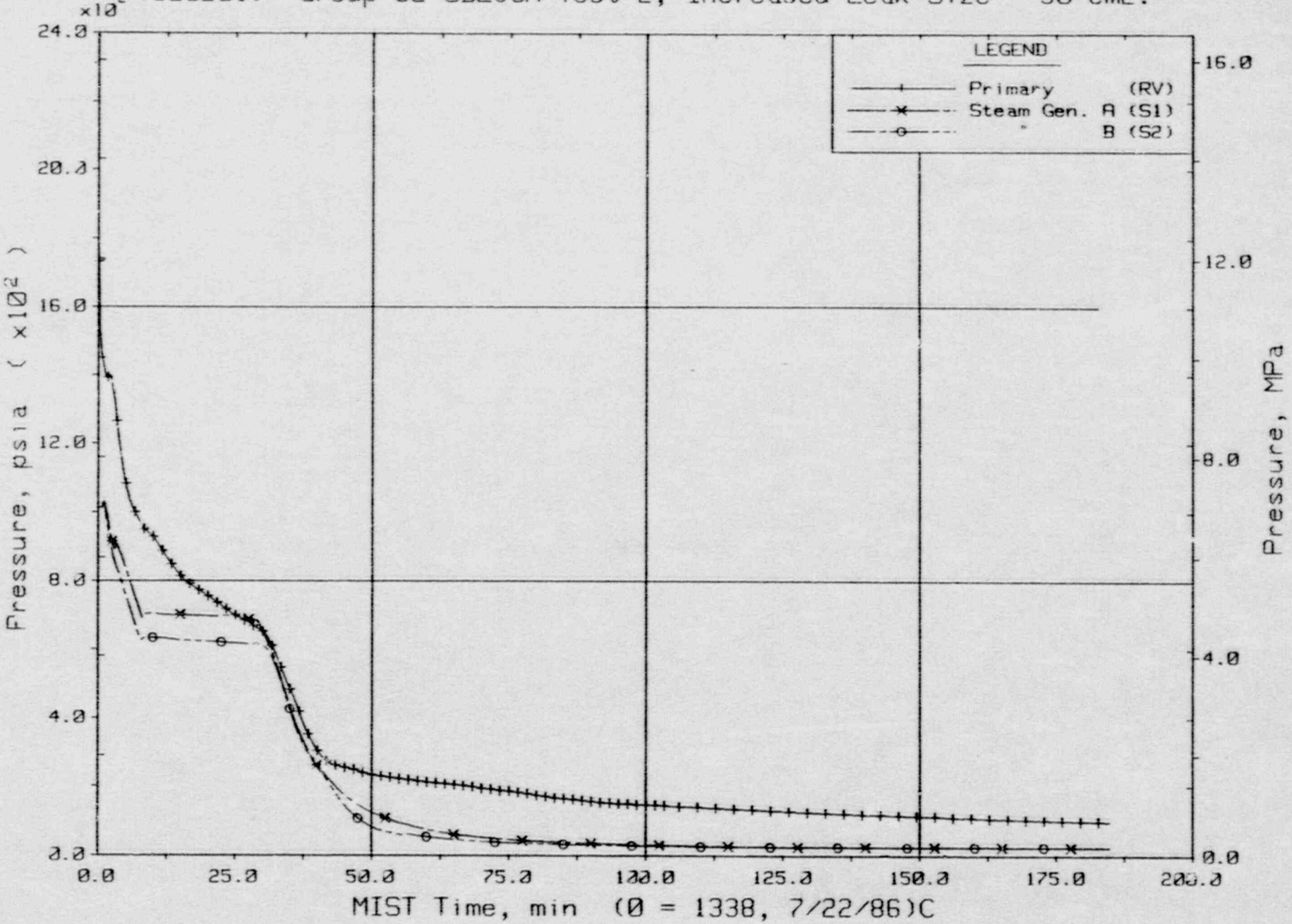

Primary and Secondary System Pressures (GP01s).

Fri May 20 13:29:35 1988

PSGP1

FINAL DATA

T320201: Group 32 SBLOCA Test 2, Increased Leak Size - 50 cm2.

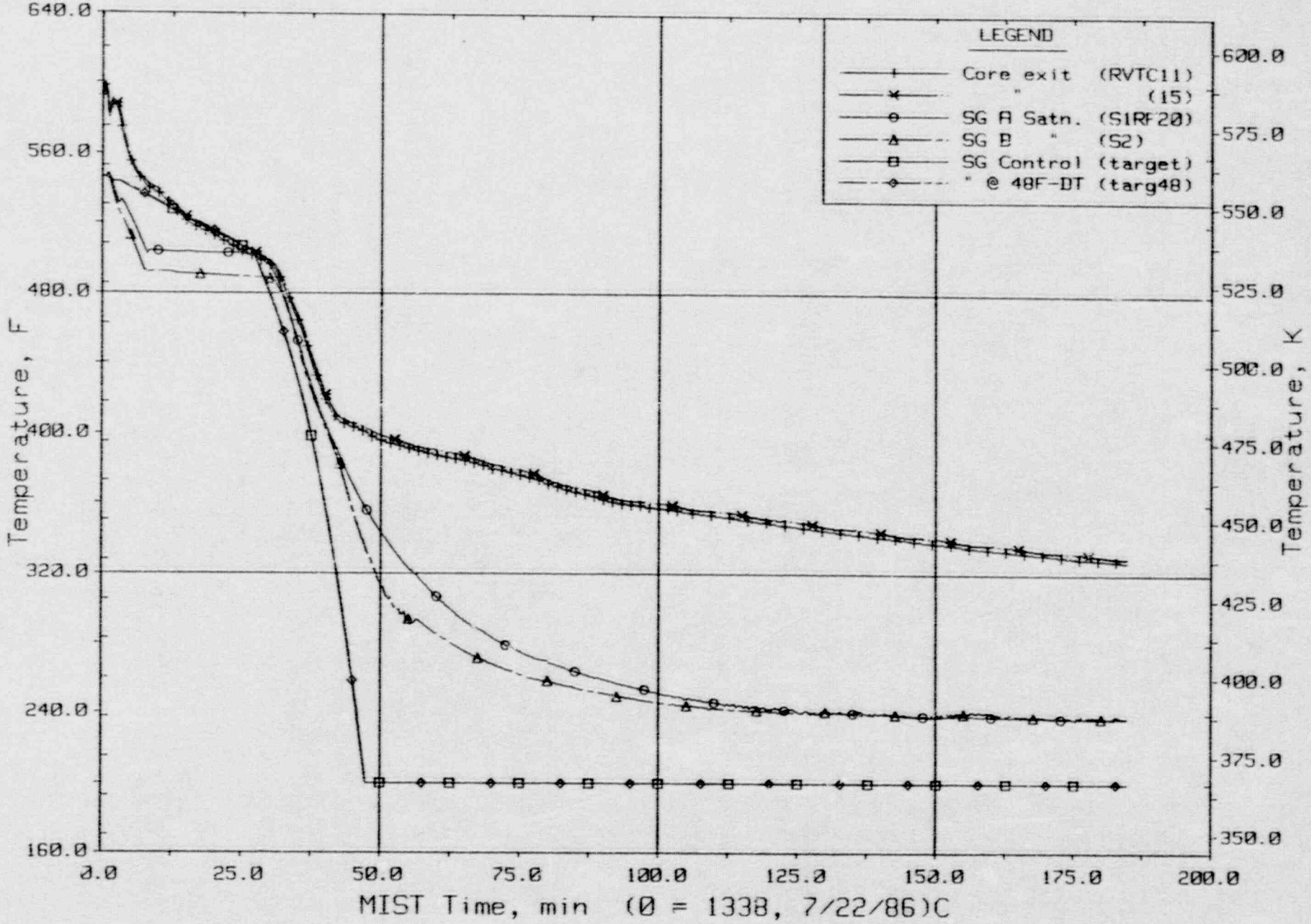

Steam Generator Secondary Saturation and Control Temperatures.

FINAL DATA

T320201: Group 32 SBLOCA Test 2, Increased Leak Size - 50 cm2.

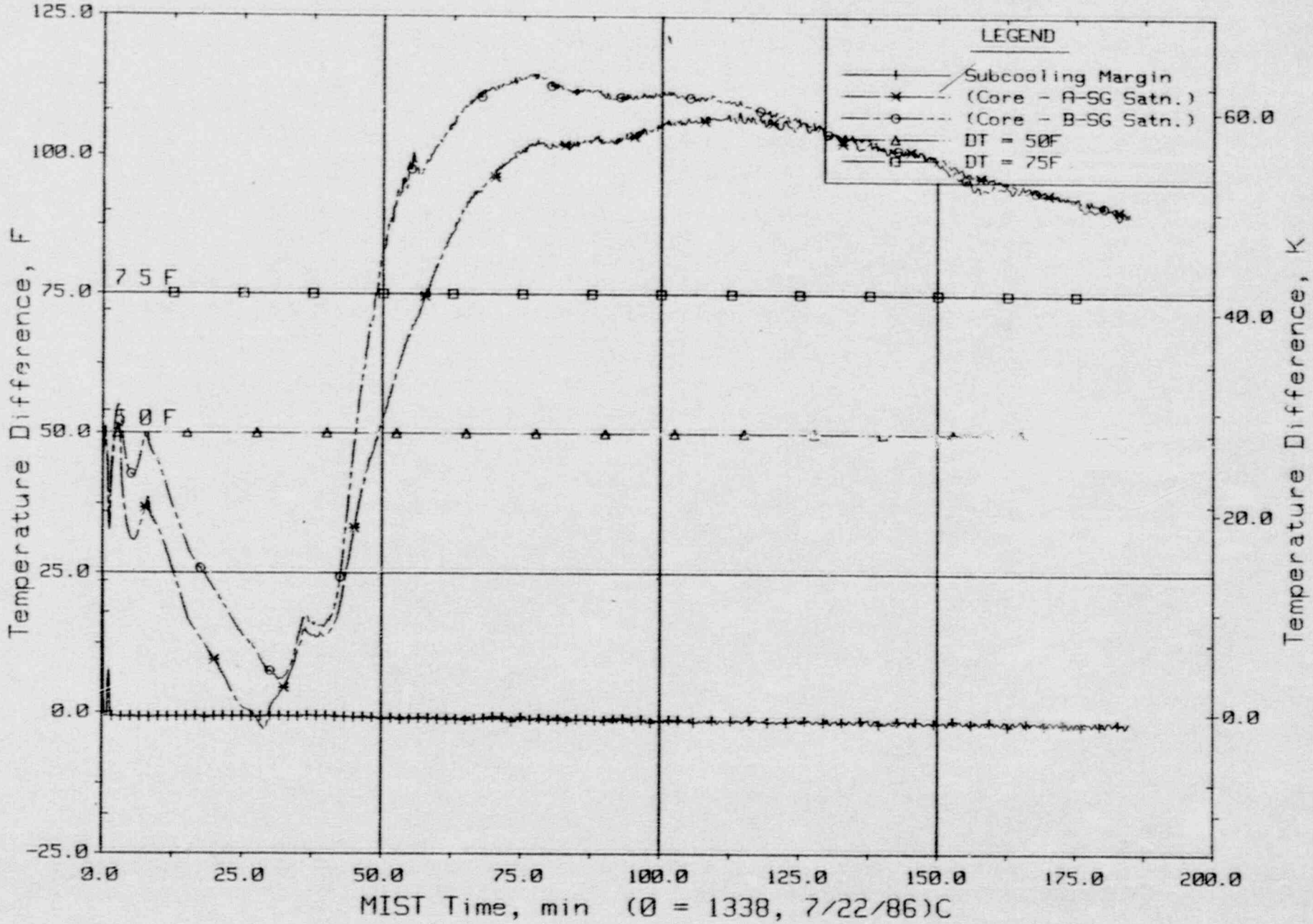

Control Temperature Differences.

Fri May 20 13:15:15 1988

PSTD1

FINAL DATA

T320201: Group 32 SBLOCA Test 2, Increased Leak Size - 50 cm2.

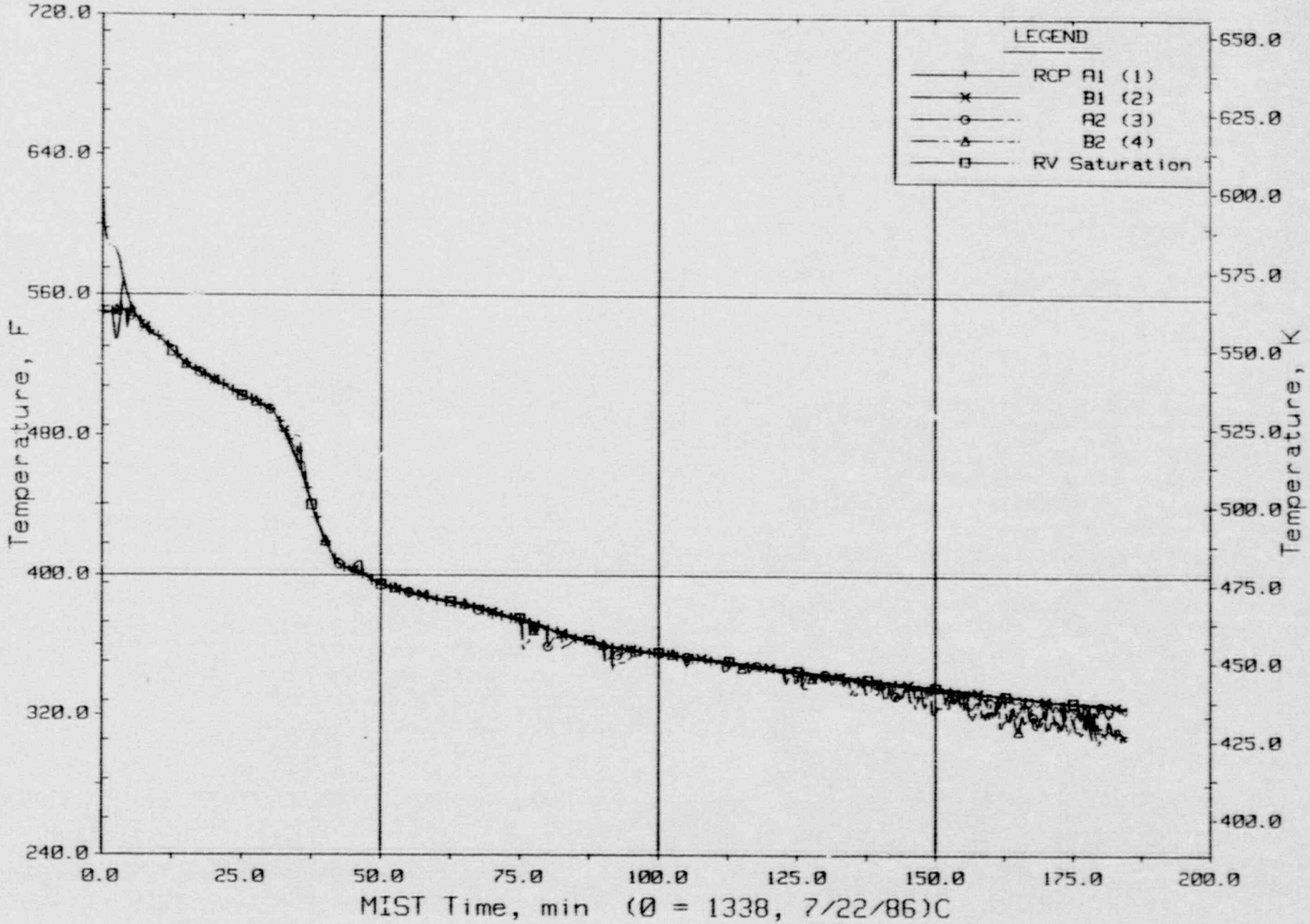

Pump Suction Fluid Temperature (CnRT01s).

Fri May 20 13:41:33 1988

PURT0

FINAL DATA

T320201: Group 32 SBLOCA Test 2, Increased Leak Size - 50 cm2.

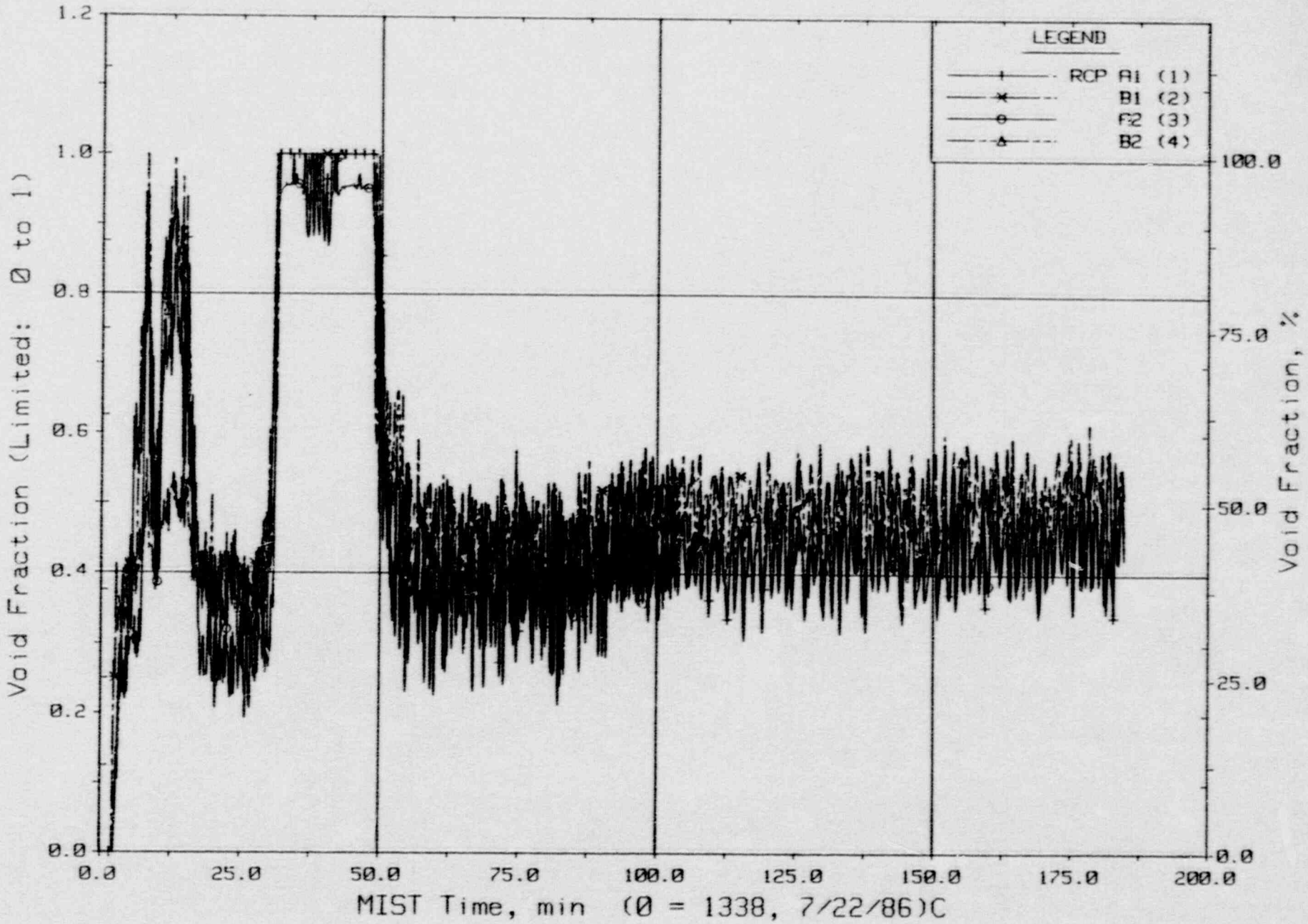

Pump Suction Void Fraction From Gamma Densitometers (CnGD21).

Fri May 20 13:47:54 1988

PUVF2

FINAL DATA

T320201: Group 32 SBLOCA Test 2, Increased Leak Size - 50 cm2.

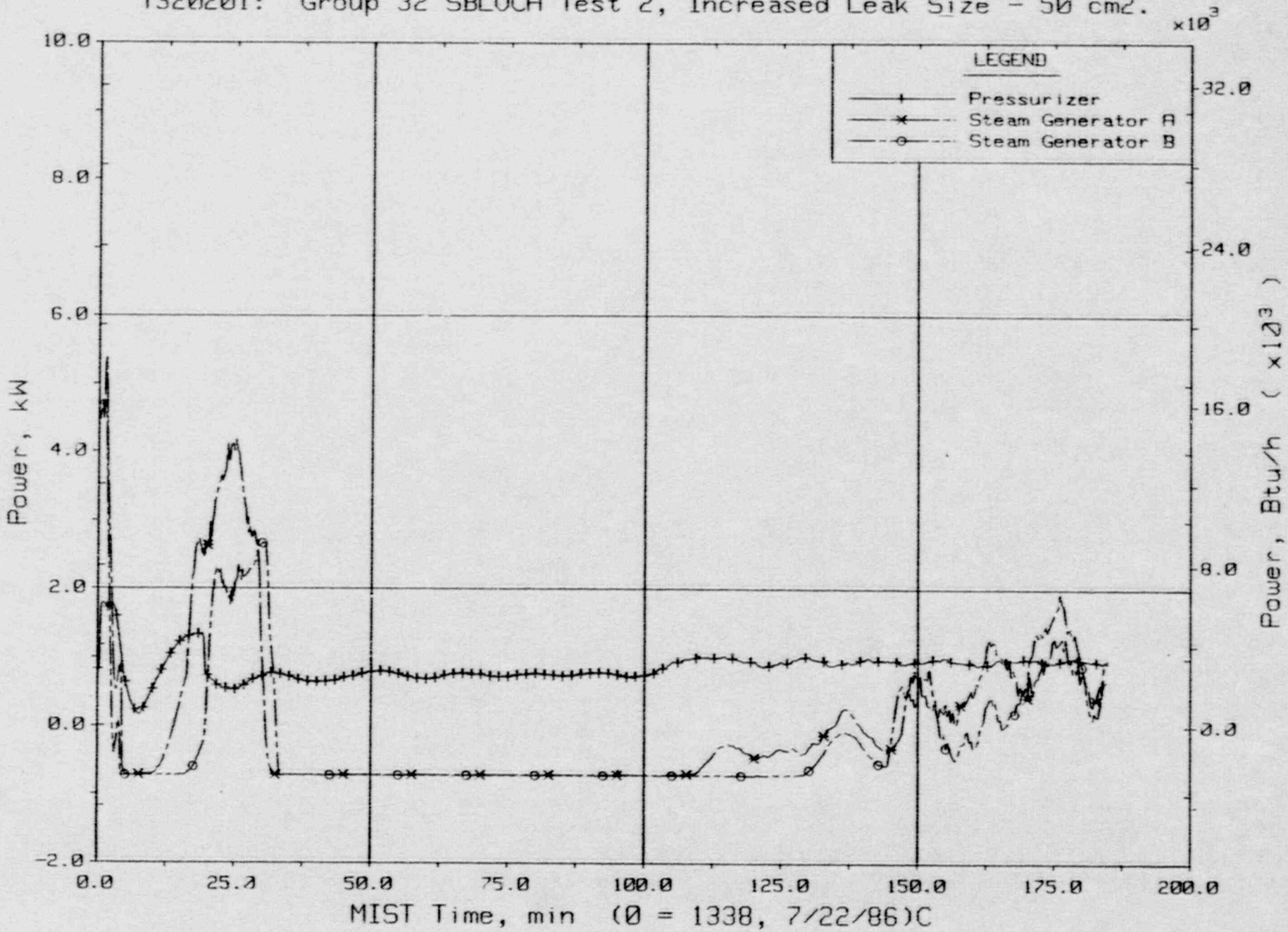

Guard Heater Specified Power, Pressurizer and Steam Generators.

Fri May 20 13:55:58 1988

PZGQ1

FINAL DATA

T320201: Group 32 SBLOCA Test 2, Increased Leak Size - 50 cm2.

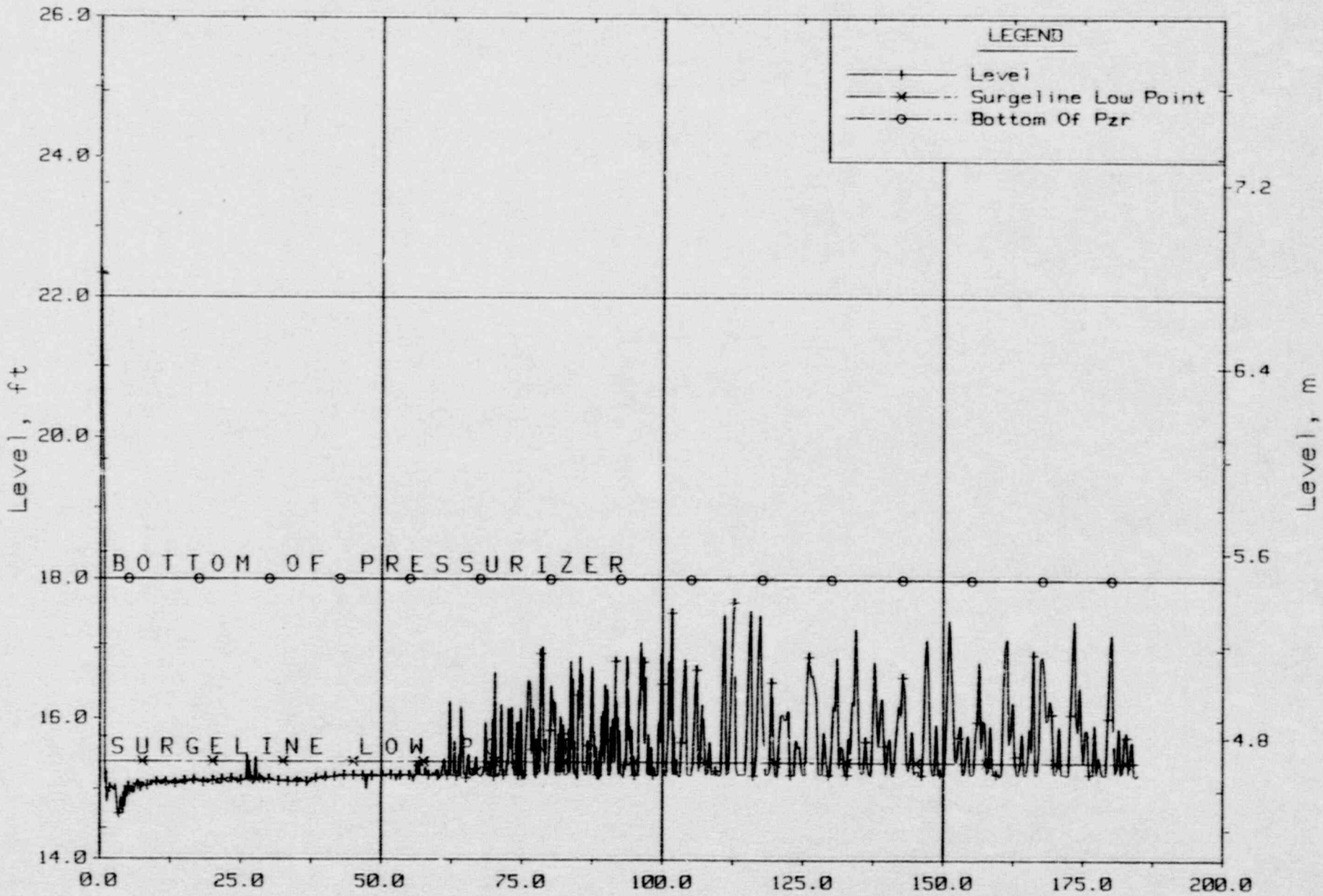

Pressurizer Collapsed Liquid Level (PZLV20).

Fri May 20 14:01:29 1988

PZLV1

FINAL DATA

T320201: Group 32 SBLOCA Test 2, Increased Leak Size - 50 cm2.

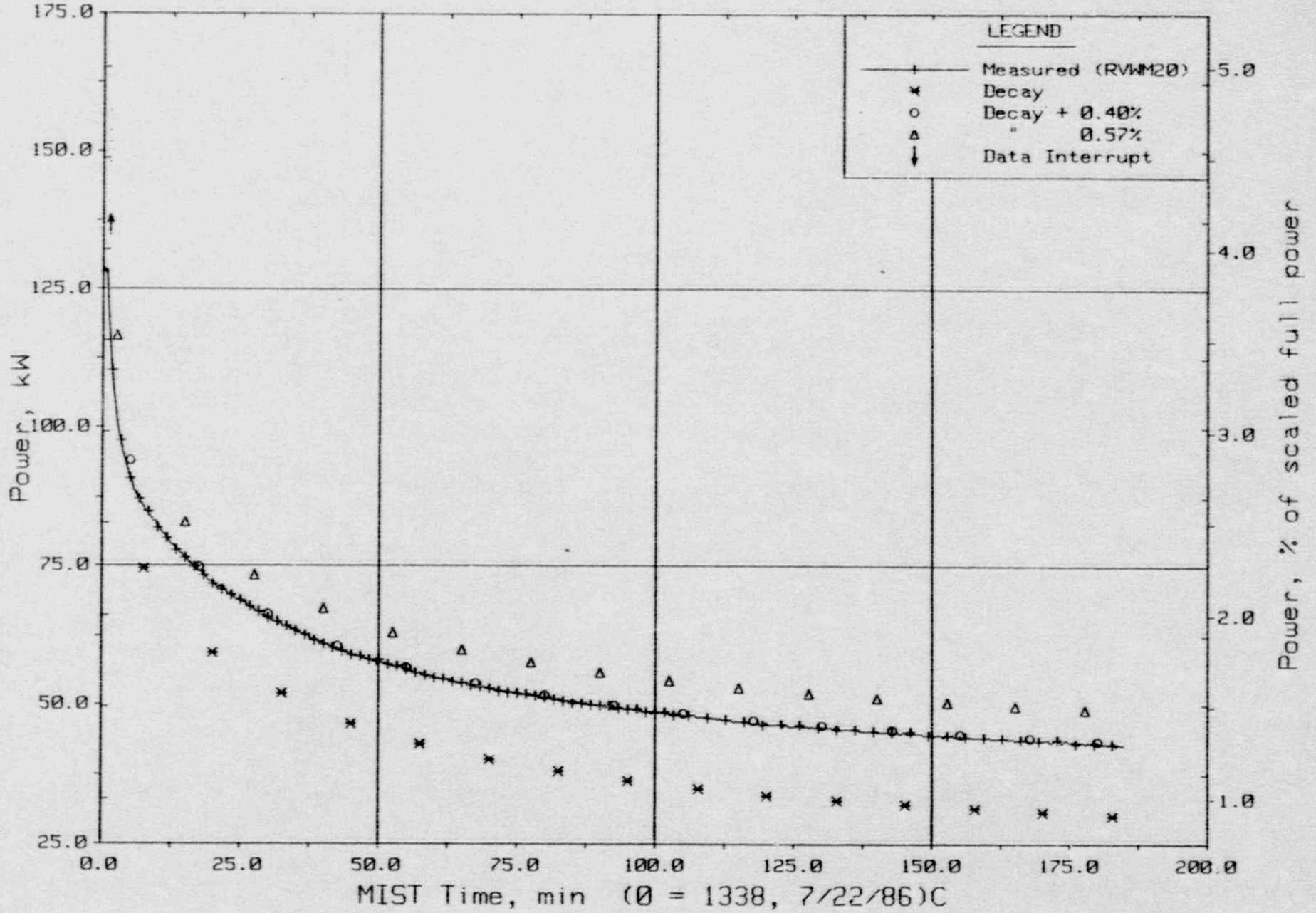

Core Power.

Fri May 20 14:15:30 1988

RVKW0

FINAL DATA

T320201: Group 32 SBLOCA Test 2, Increased Leak Size - 50 cm2.

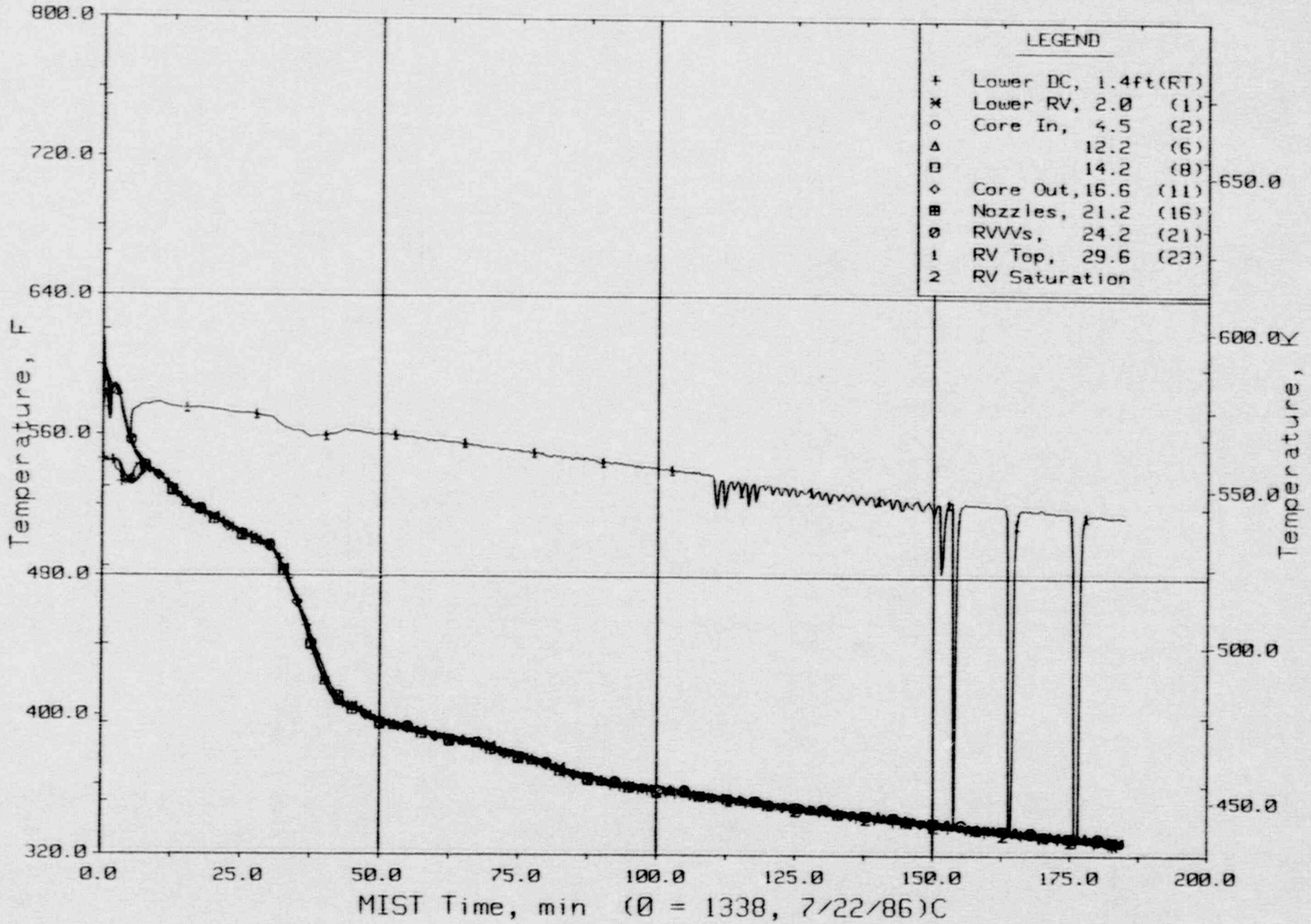

Core Unit Cell and Reactor Vessel Fluid Temperatures (RVTCs).

Fri May 20 14:33:39 1988

RVTCØ

FINAL DATA

T320201: Group 32 SBLOCA Test 2, Increased Leak Size - 50 cm2.

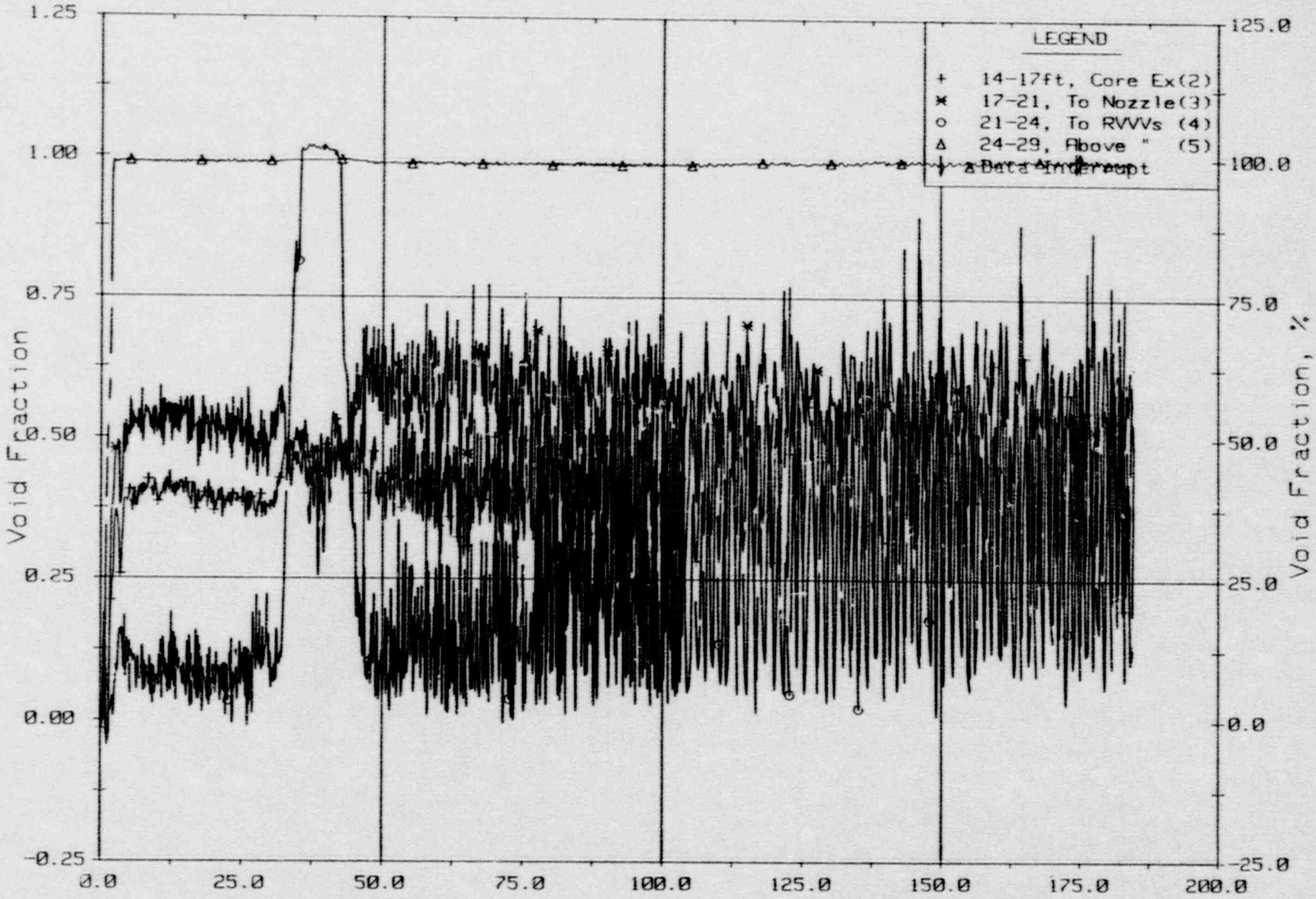

Reactor Vessel Void Fractions From Differential Pressures (RVVFs).

Fri May 20 14:41:06 1988

RVVF1

FINAL DATA

T320201: Group 32 SBLOCA Test 2, Increased Leak Size - 50 cm2.

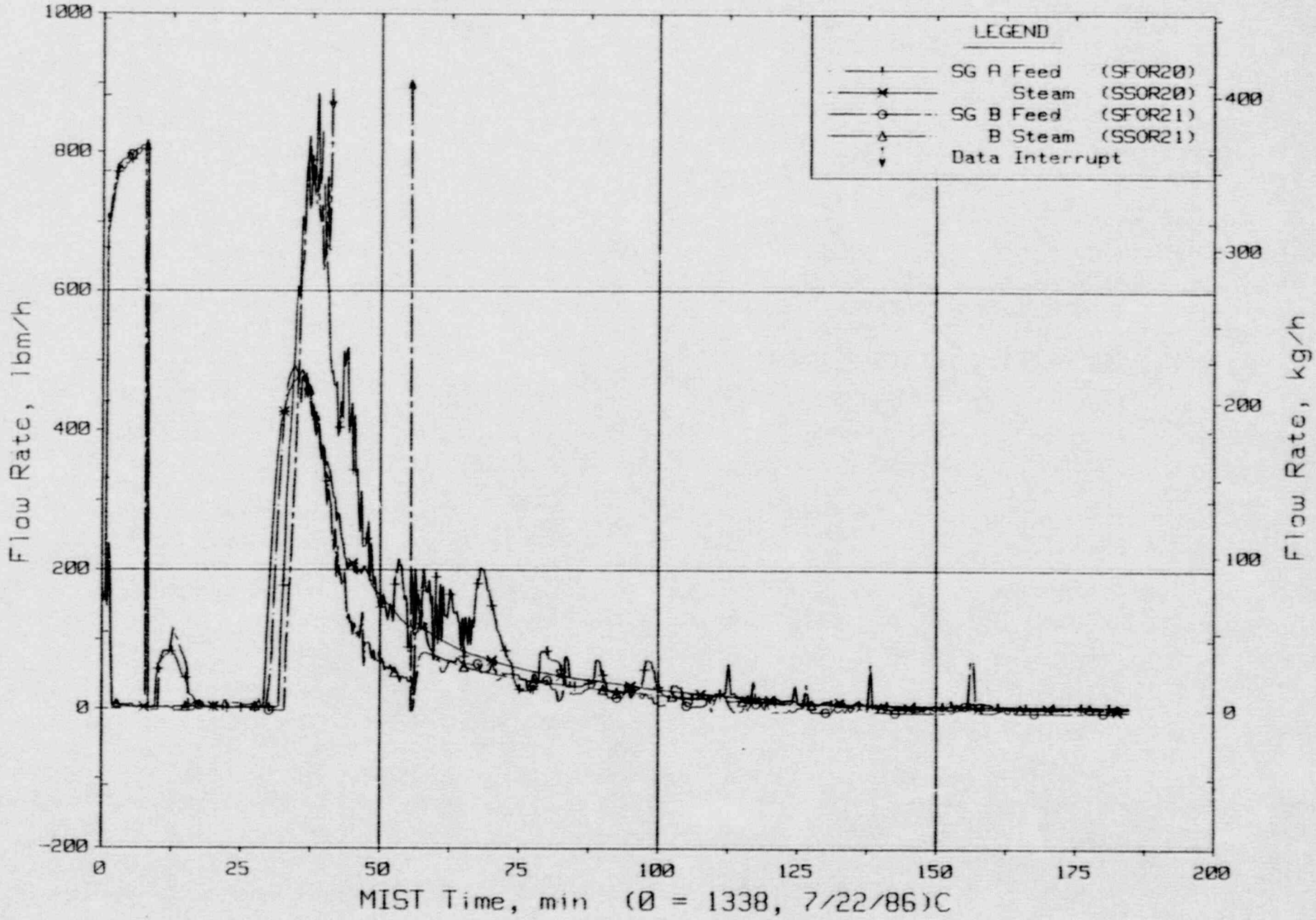

Steam Generator Secondary Flow Rates.

Thu Nov 3 14:19:15 1988

SGFL0

FINAL DATA

T320201: Group 32 SBLOCA Test 2, Increased Leak Size - 50 cm2.

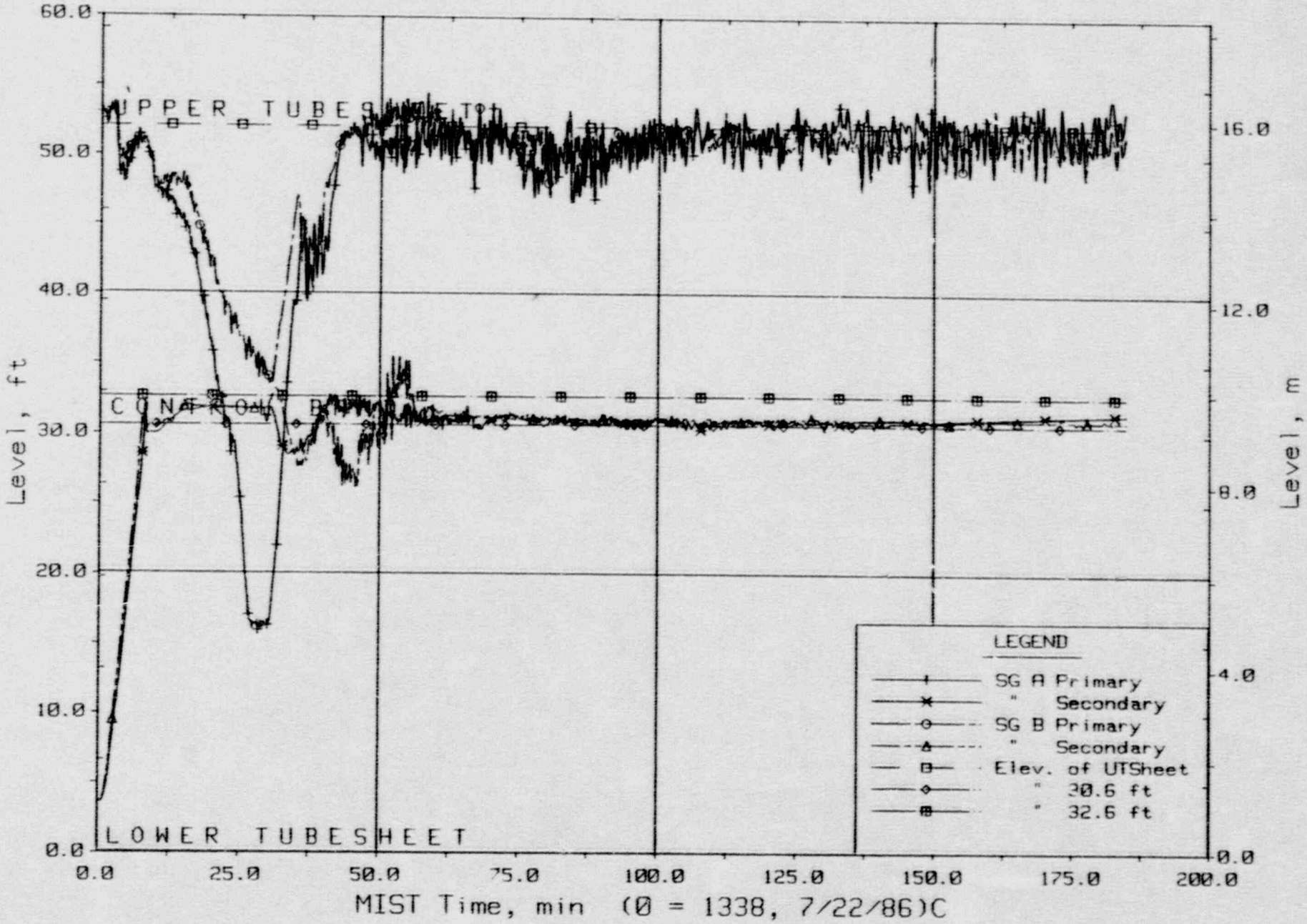

Steam Generator Collapsed Liquid Levels.

Fri May 20 15:06:56 1988

SGLV2

FINAL DATA

T320201: Group 32 SBLOCA Test 2, Increased Leak Size - 50 cm2.

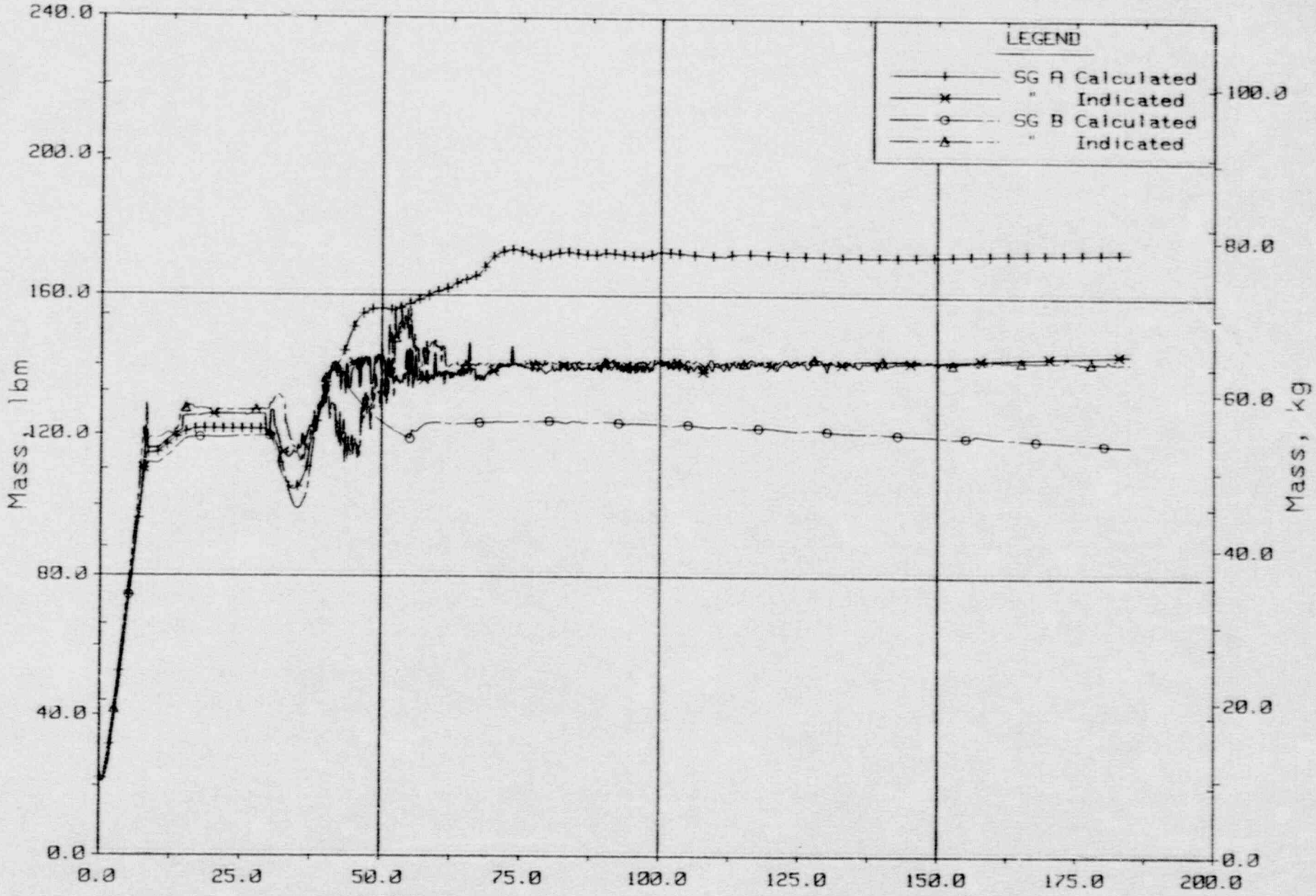

Steam Generator Secondary Fluid Mass Balances.

Fri May 20 15:18:00 1988

SGML1

FINAL DATA

T320201: Group 32 SBLOCA Test 2, Increased Leak Size - 50 cm2.

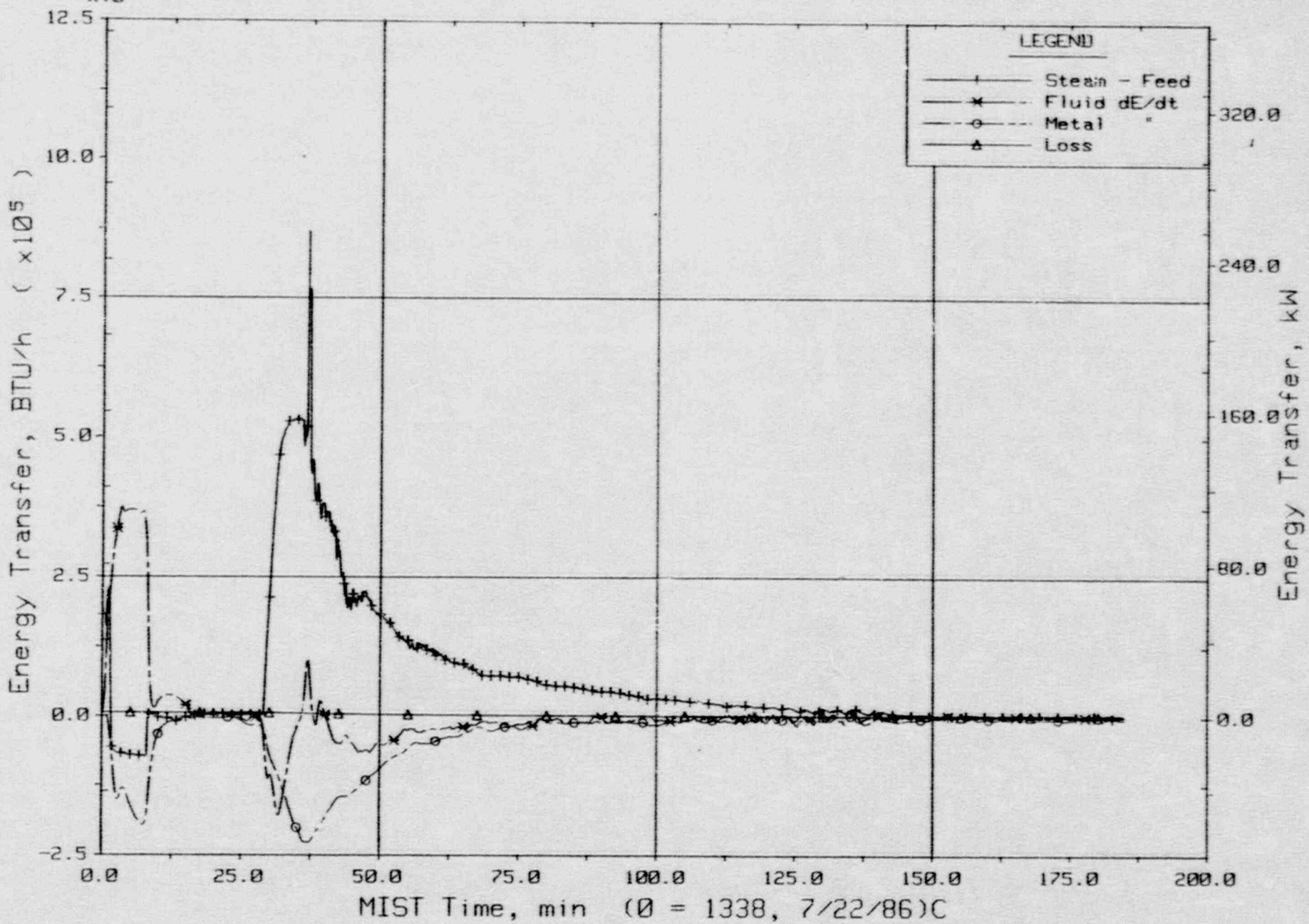

Steam Generator A Energy Transfer.

Fri May 20 15:32:24 1988

SGOE3

FINAL DATA

T320201: Group 32 SBLOCA Test 2, Increased Leak Size - 50 cm2.

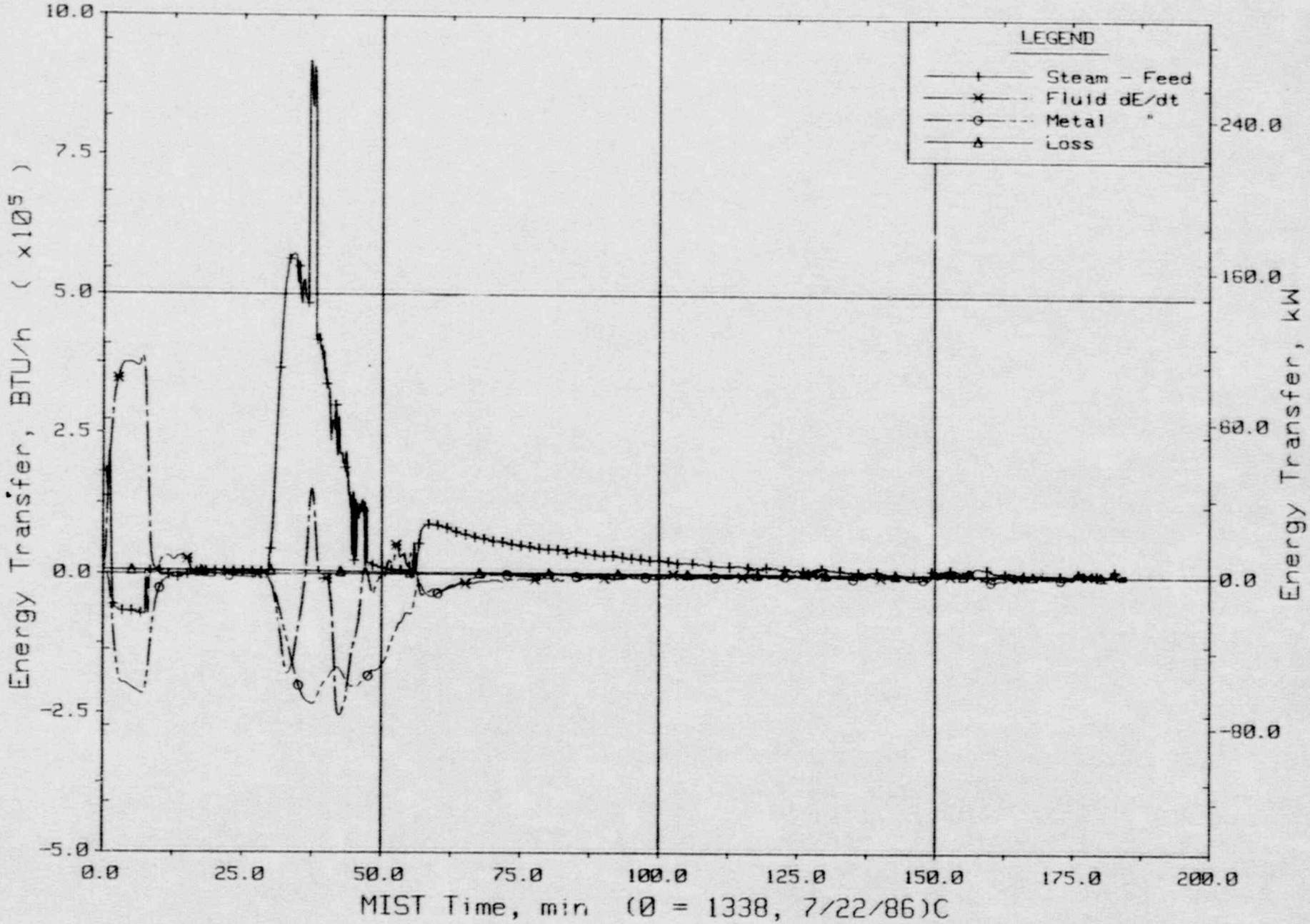

Steam Generator B Energy Transfer.

Fri May 20 15:36:38 1988

SGQE6

FINAL DATA

T320201: Group 32 SBLOCA Test 2, Increased Leak Size - 50 cm2.

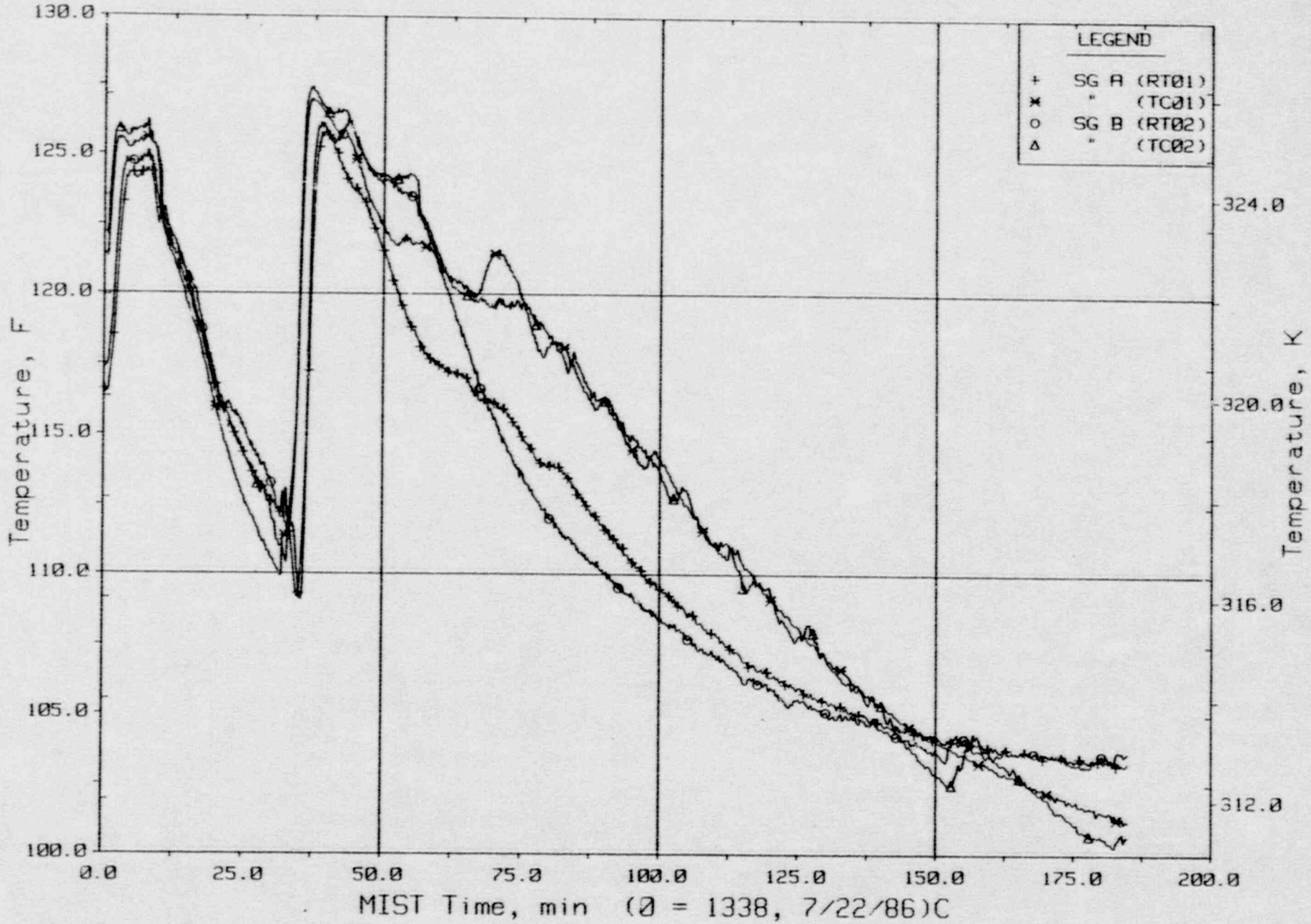

Feedwater Temperatures (SFs).

Fri May 20 15:22:11 1988

SGRT1

FINAL DATA

T320201: Group 32 SBLOCA Test 2, Increased Leak Size - 50 cm2.

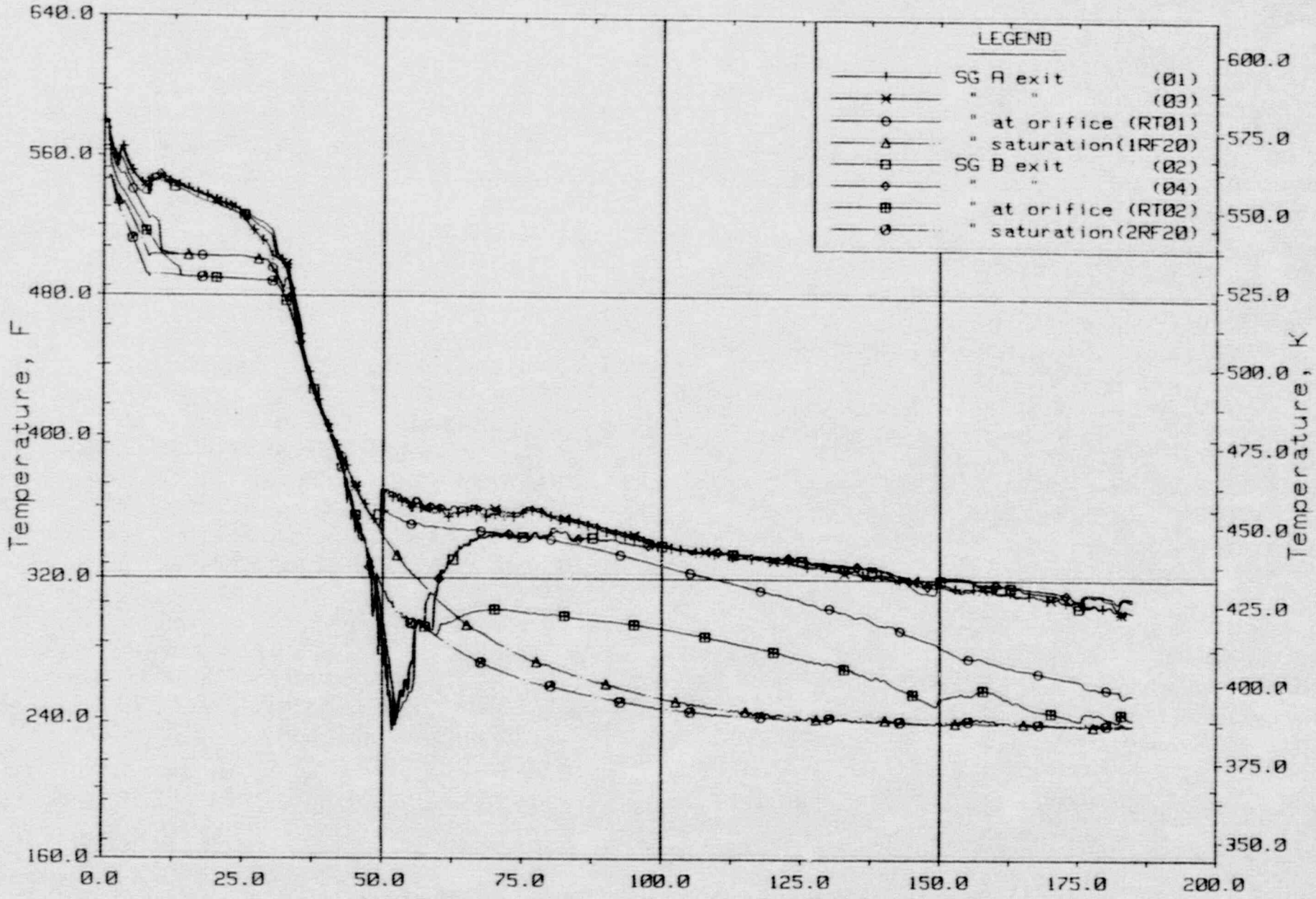

Steam Generator Steam Outlet Temperatures (SSTCs).

Fri May 20 15:27:33 1988

SGRT2

FINAL DATA

T320201: Group 32 SBLOCA Test 2, Increased Leak Size - 50 cm2.

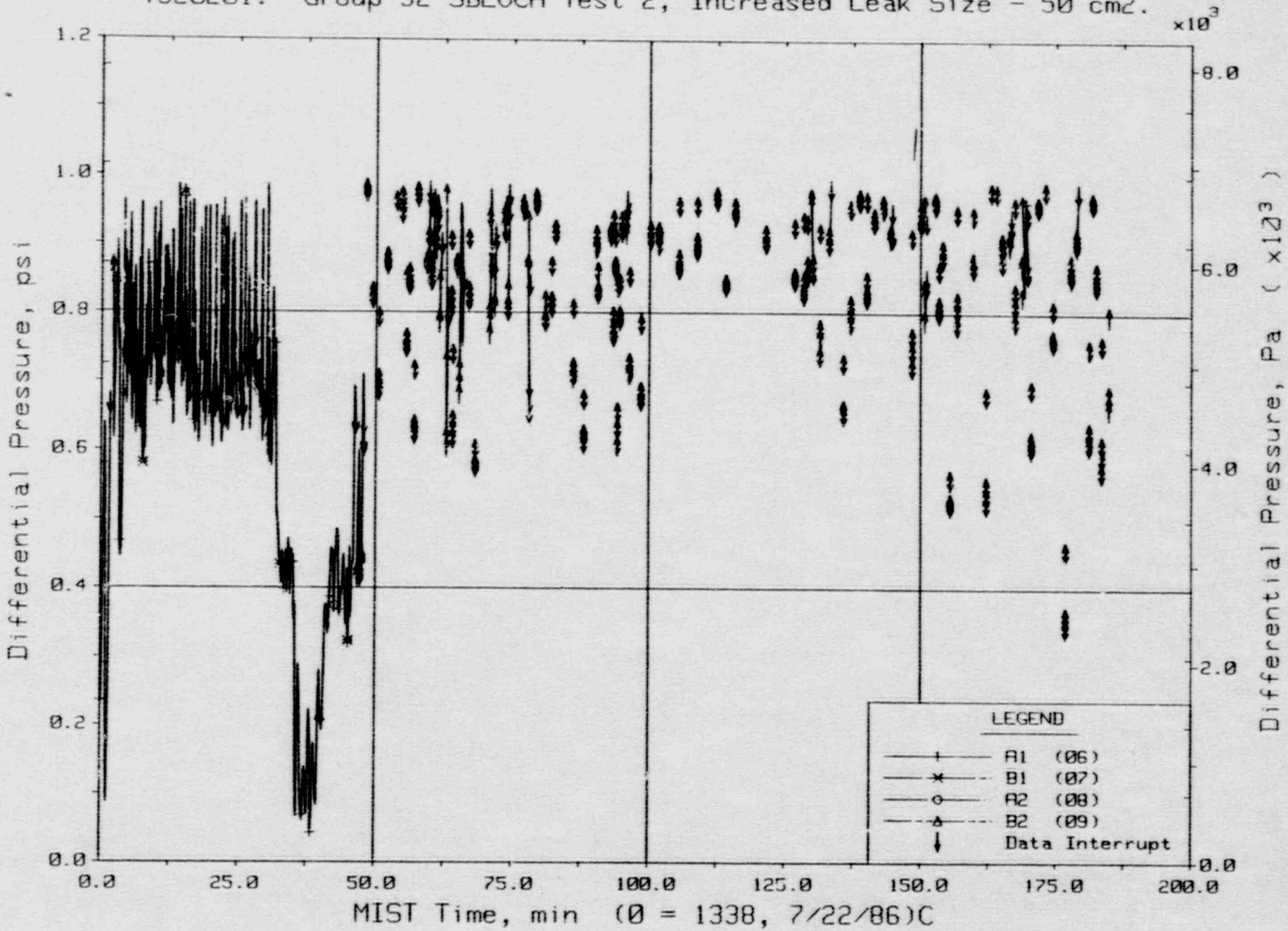

Reactor Vessel Vent Valve Differential Pressures (RVDPs).

Fri May 20 15:55:34 1988

VVDP1

FINAL DATA

T320201: Group 32 SBLOCA Test 2, Increased Leak Size - 50 cm2.

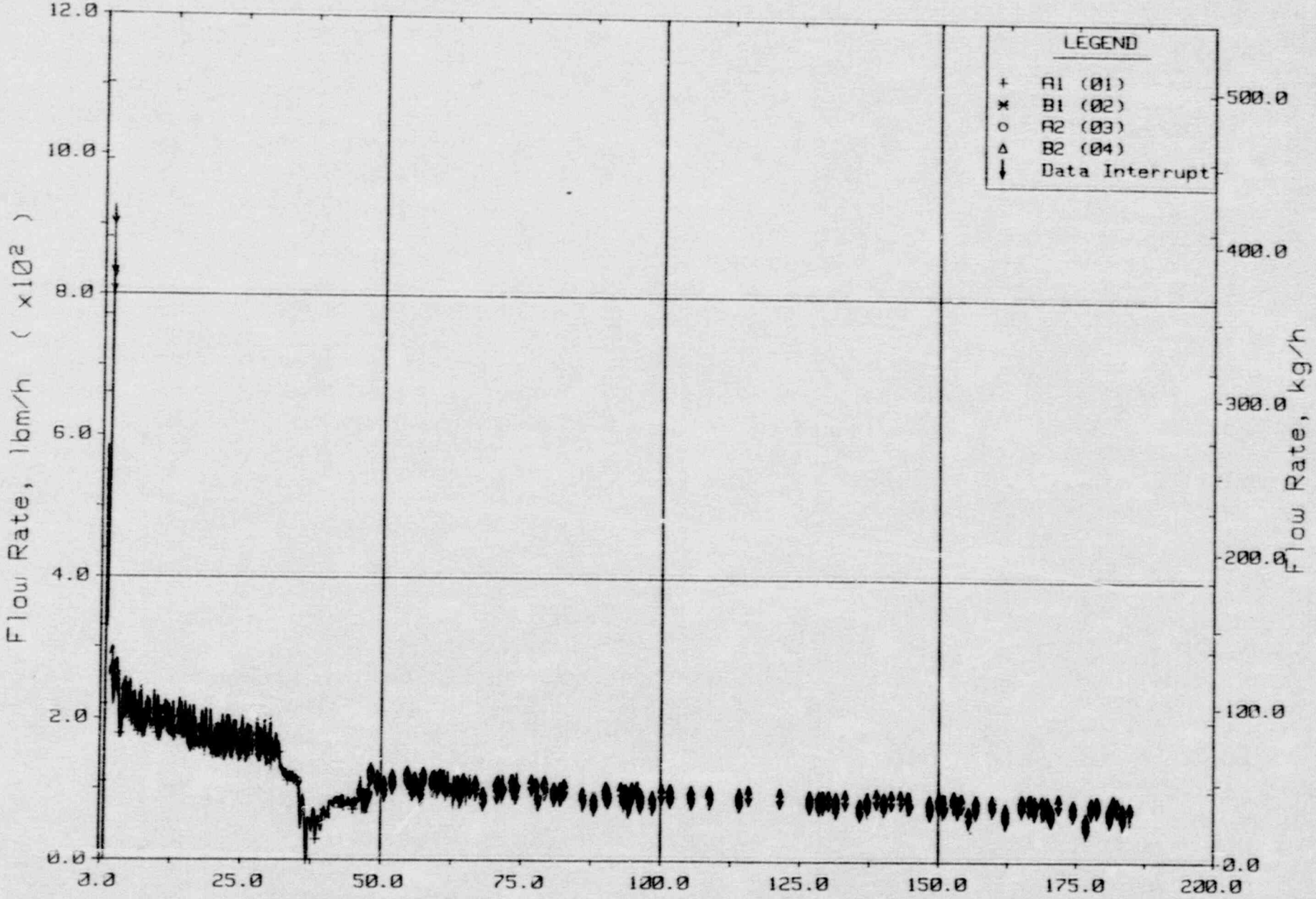

Reactor Vessel Vent Valve Flow Rates (RVORs).

Fri May 20 16:00:54 1988

VVFL1

FINAL DATA

T320201: Group 32 SBLOCA Test 2, Increased Leak Size - 50 cm2.

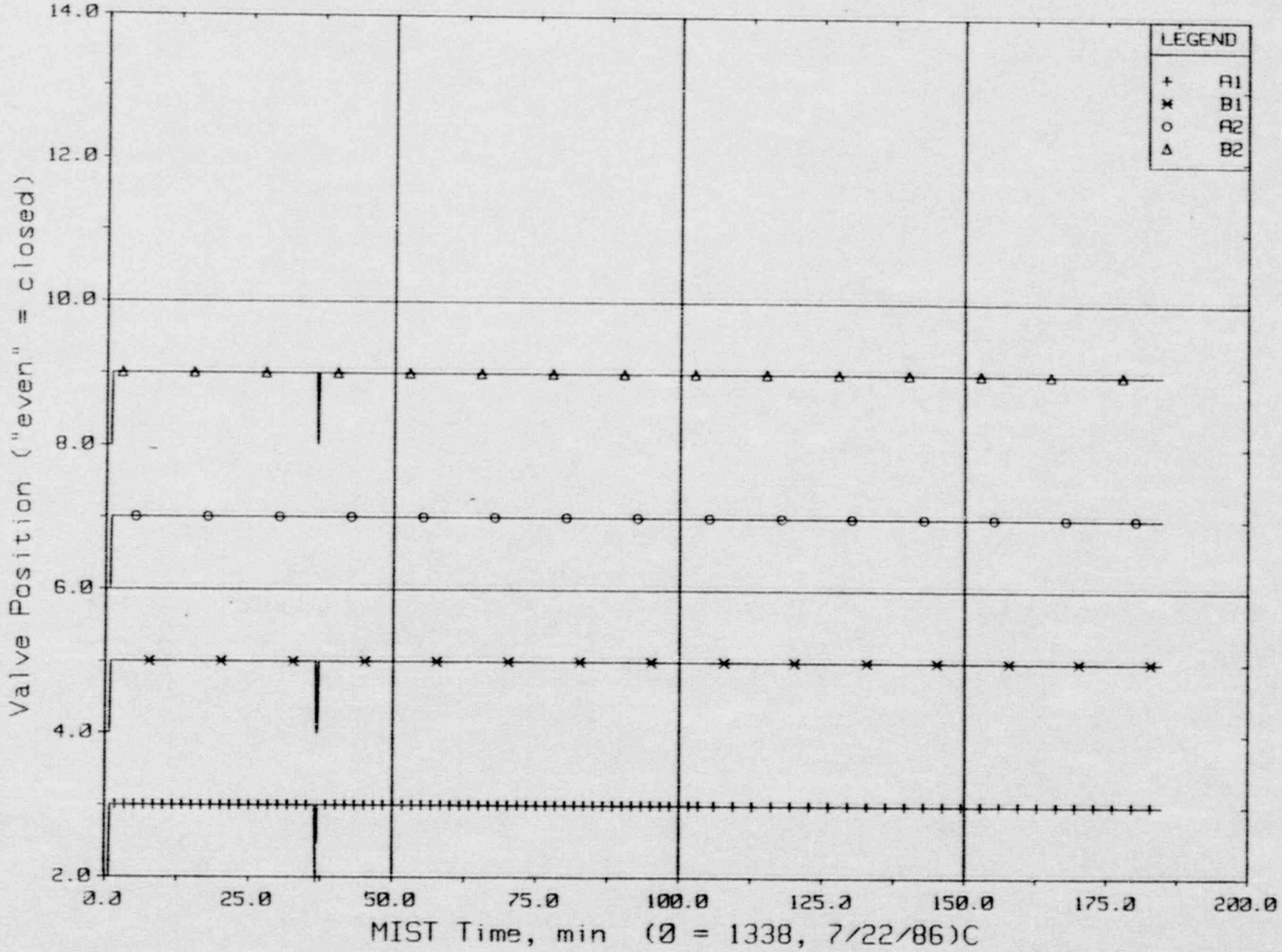

Reactor Vessel Vent Valve Positions.

Fri May 20 16:05:43 1988

VVLS1

FINAL DATA

T320201: Group 32 SBLOCA Test 2, Increased Leak Size - 50 cm2.

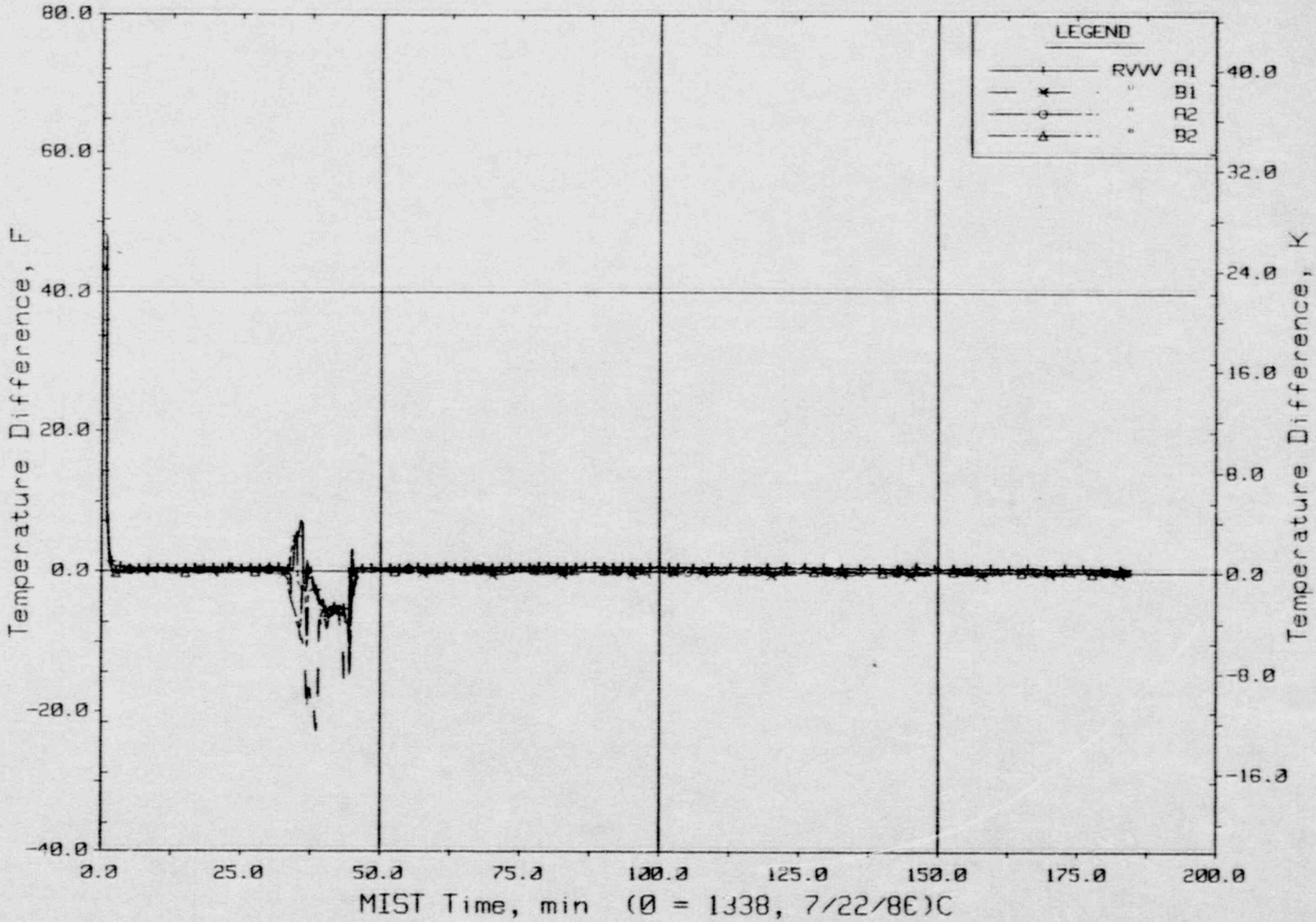

Temperature Differences Across Vent Valves.

Fri May 20 16:10:20 1988

VVTD1

T320302

FINAL DATA

T320302: Group 32 SBLOCA Test 3, Cold Leg Suction Leak.

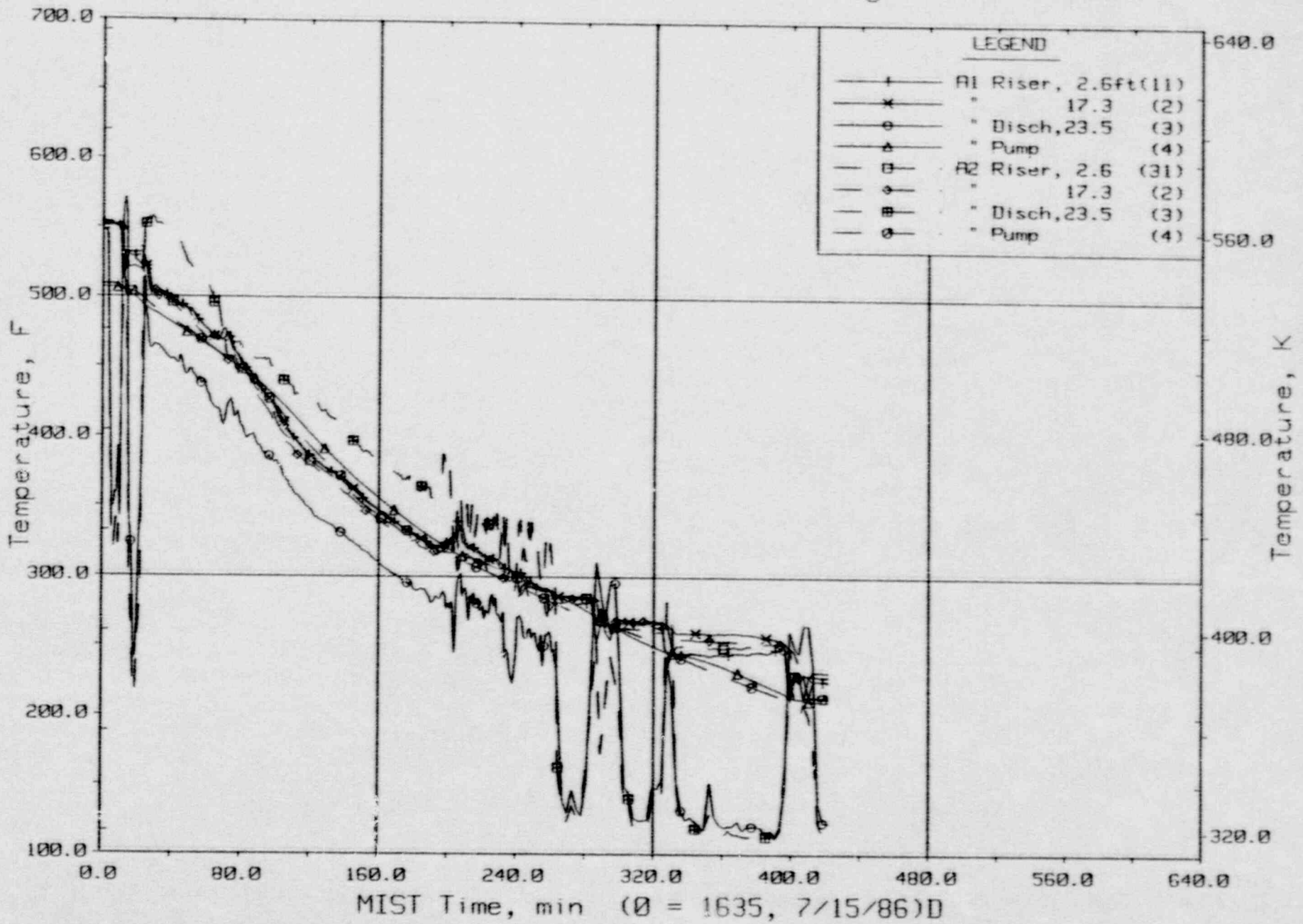

Loop A Cold Leg Metal Temperatures (C1,3MTs).

Wed Jun 8 11:25:28 1988

C1MT1

FINAL DATA

T320302: Group 32 SBLOCA Test 3, Cold Leg Suction Leak.

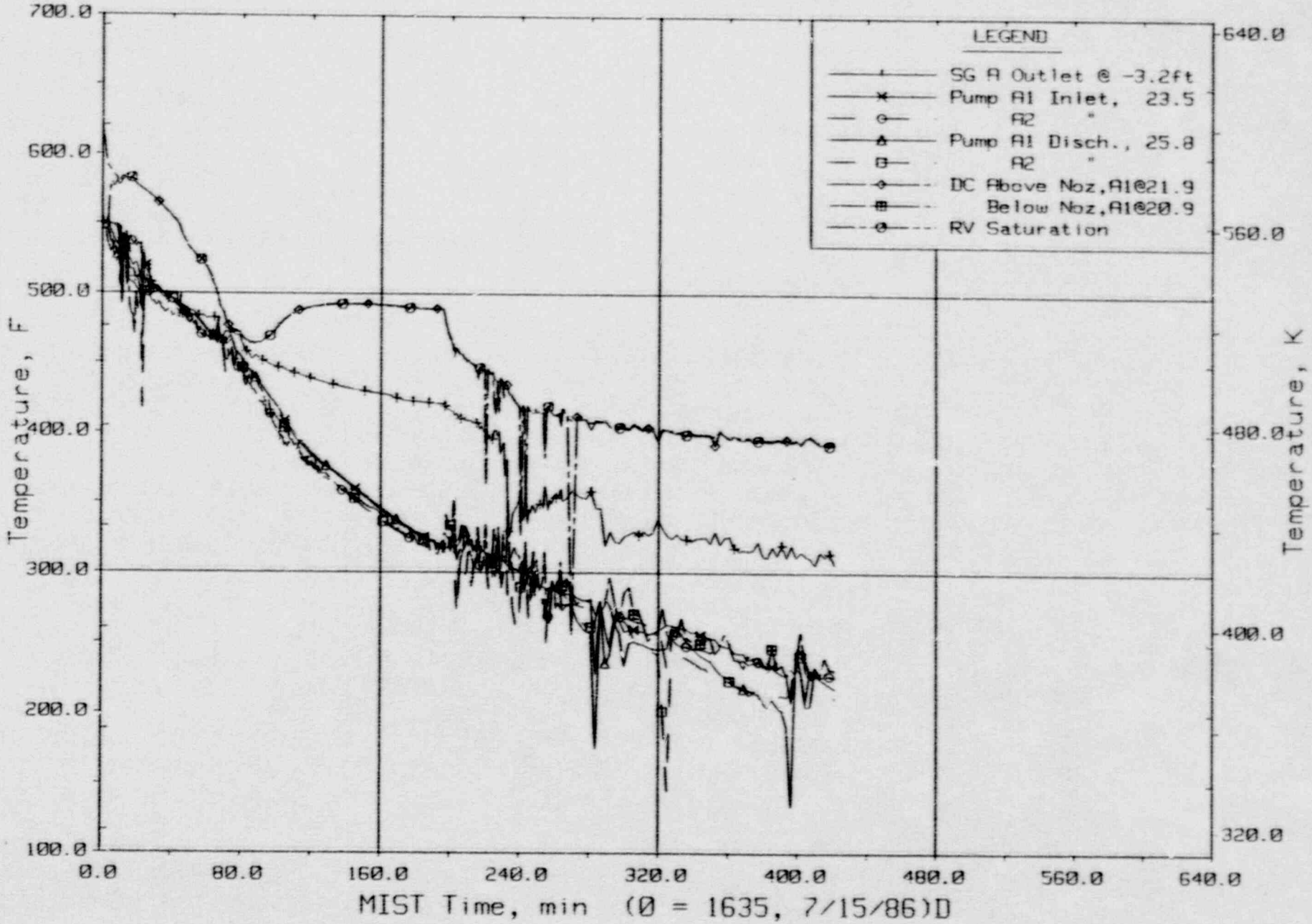

Loop A Cold Leg Fluid Temperatures (RTDs).

Wed Jun 8 11:30:39 1988

C1RT0

FINAL DATA

T320302: Group 32 SBLOCA Test 3, Cold Leg Suction Leak.

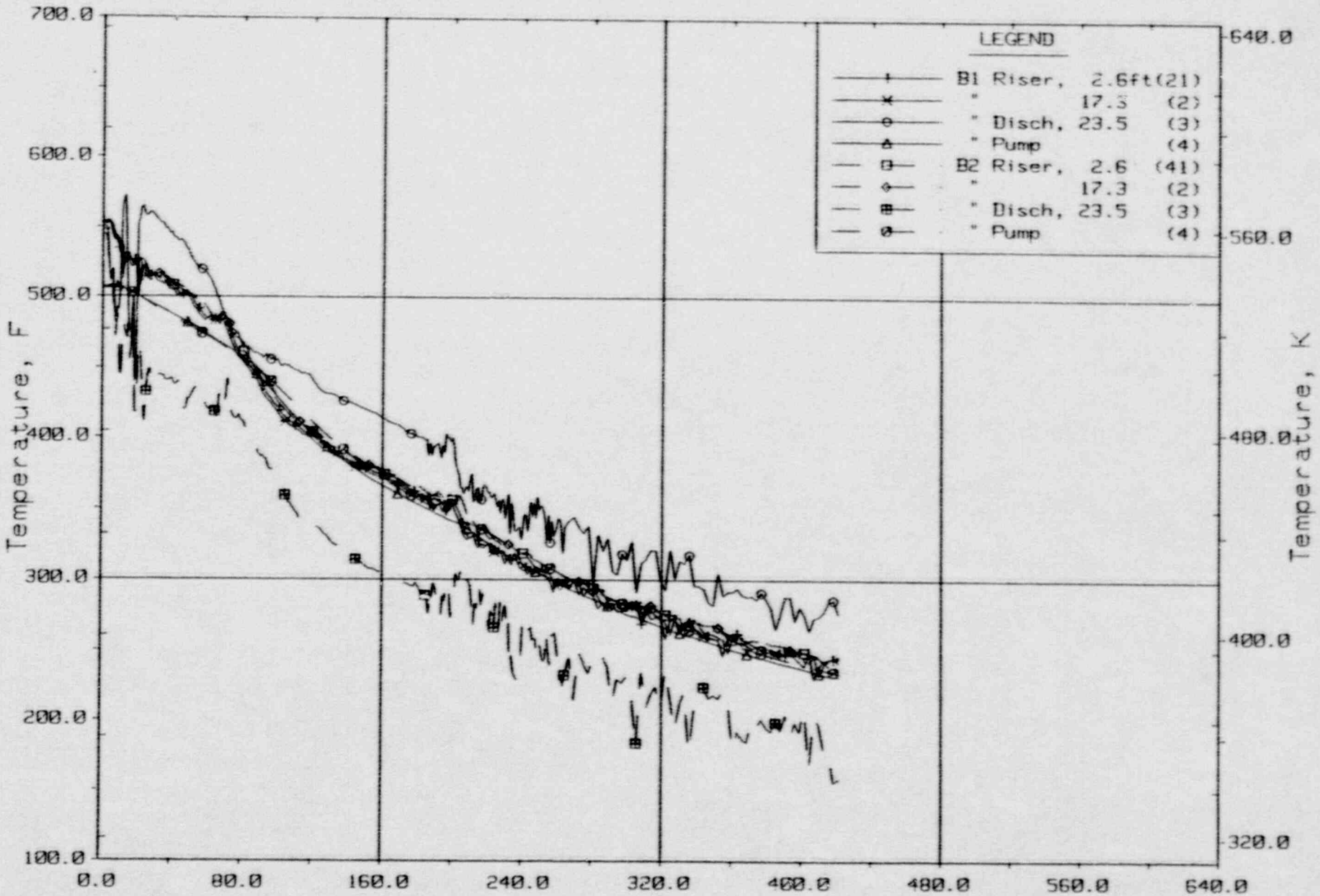

Loop B Cold Leg Metal Temperatures (C2,4MTs).

Wed Jun 8 11:37:16 1988

C2MT1

FINAL DATA

T320302: Group 32 SBLOCA Test 3, Cold Leg Suction Leak.

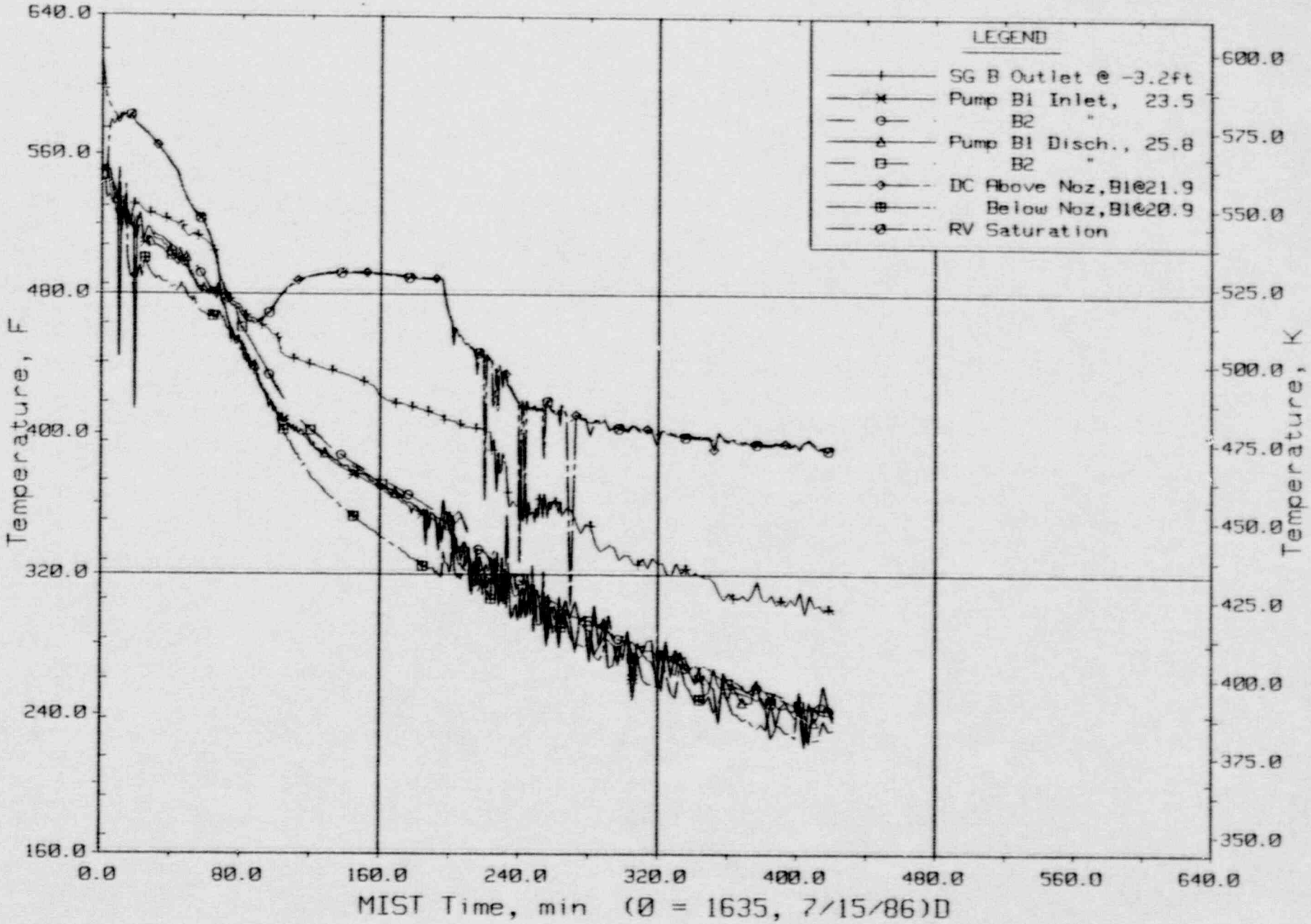

Loop B Cold Leg Fluid Temperatures (RTDs).

Wed Jun 8 11:41:13 1988

C2RTØ

FINAL DATA

T320302: Group 32 SBLOCA Test 3, Cold Leg Suction Leak.

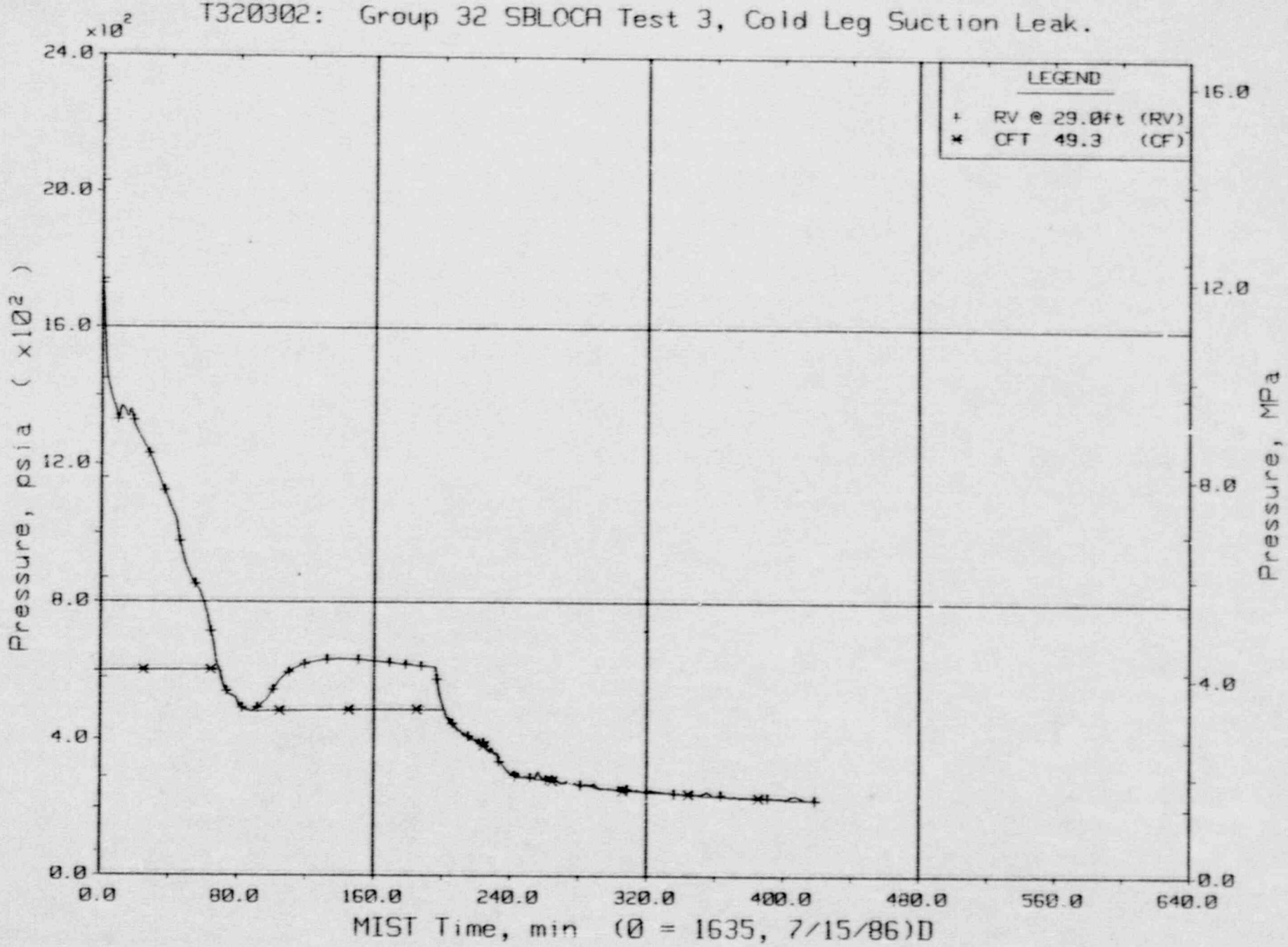

Primary System and Core Flood Tank Pressures (GP01s).

Wed Jun 8 11:44:42 1988

CFGP1

FINAL DATA

T320302: Group 32 SBLOCA Test 3, Cold Leg Suction Leak.

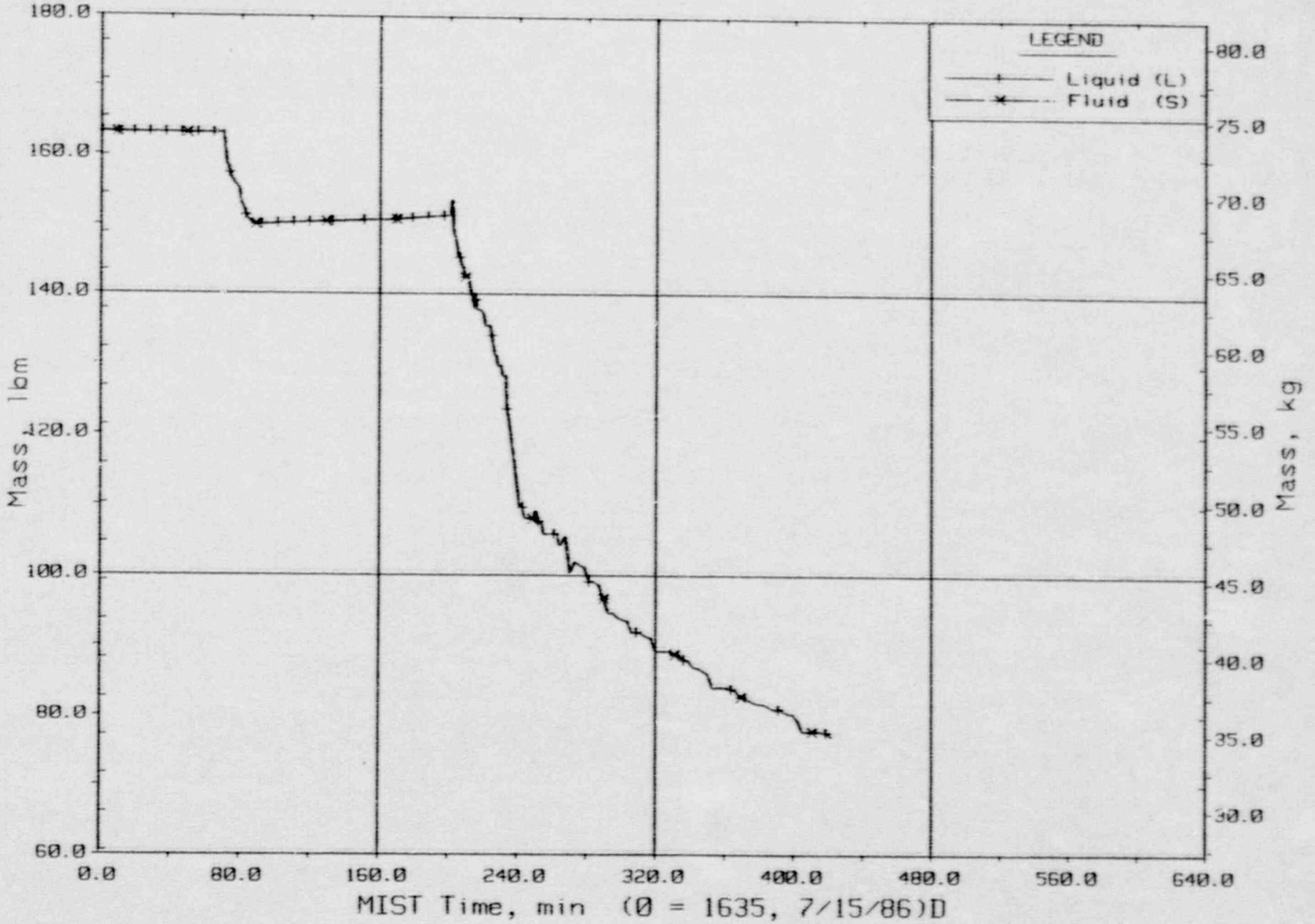

Core Flood Tank Liquid and Fluid Mass (CFMa20s).

Wed Jun 8 11:48:43 1988

CFML1

FINAL DATA

T320302: Group 32 SBLOCA Test 3, Cold Leg Suction Leak.

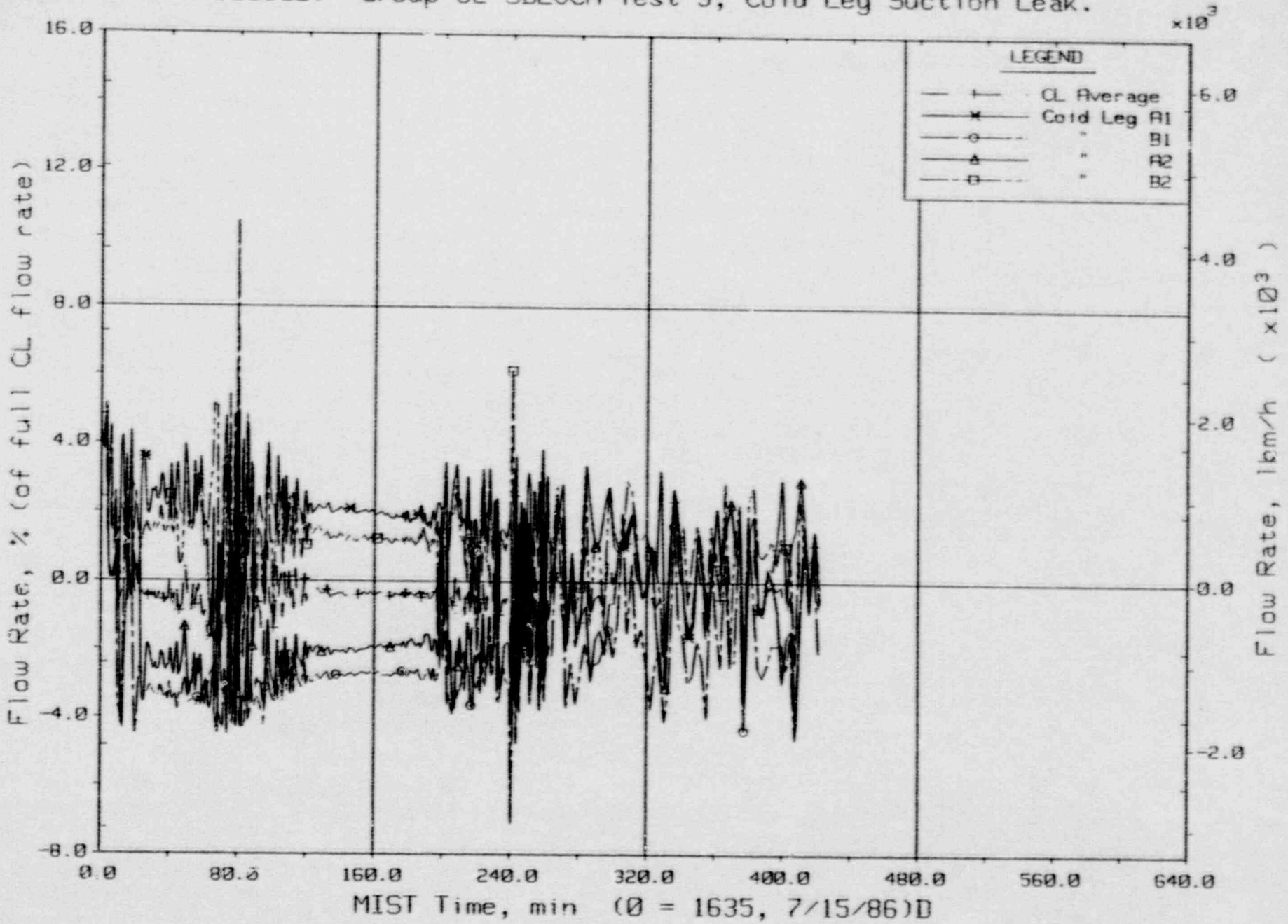

Cold Leg (Venturi) Flow Rates.

Wed Jun 8 11:52:51 1988

CLFL1

FINAL DATA

T320302: Group 32 SBLOCA Test 3, Cold Leg Suction Leak.

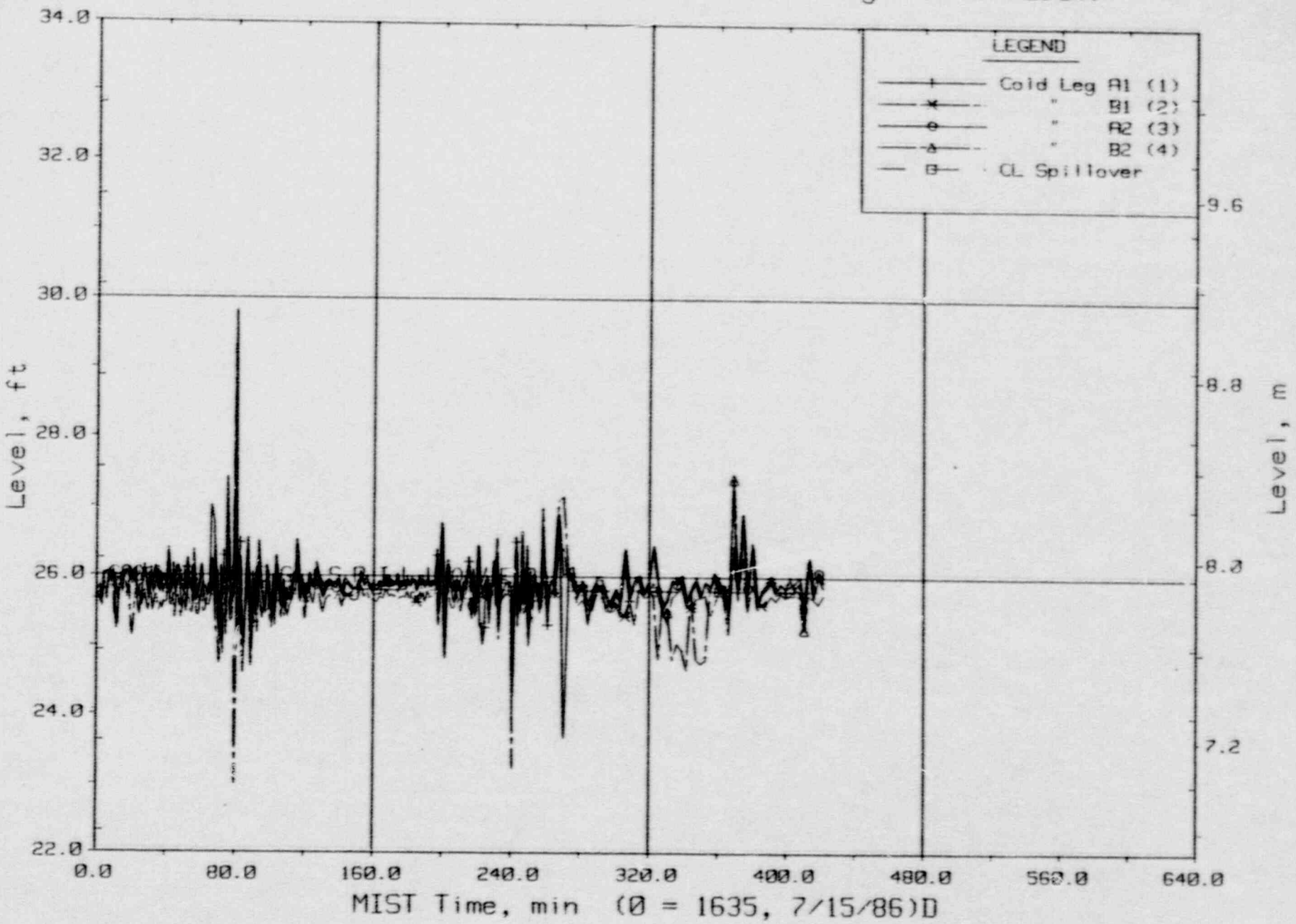

Cold Leg Suction Collapsed Liquid Levels (CnLV22s).

Wed Jun 8 11:58:12 1988

CLLV4

FINAL DATA

T320302: Group 32 SBLOCA Test 3, Cold Leg Suction Leak.

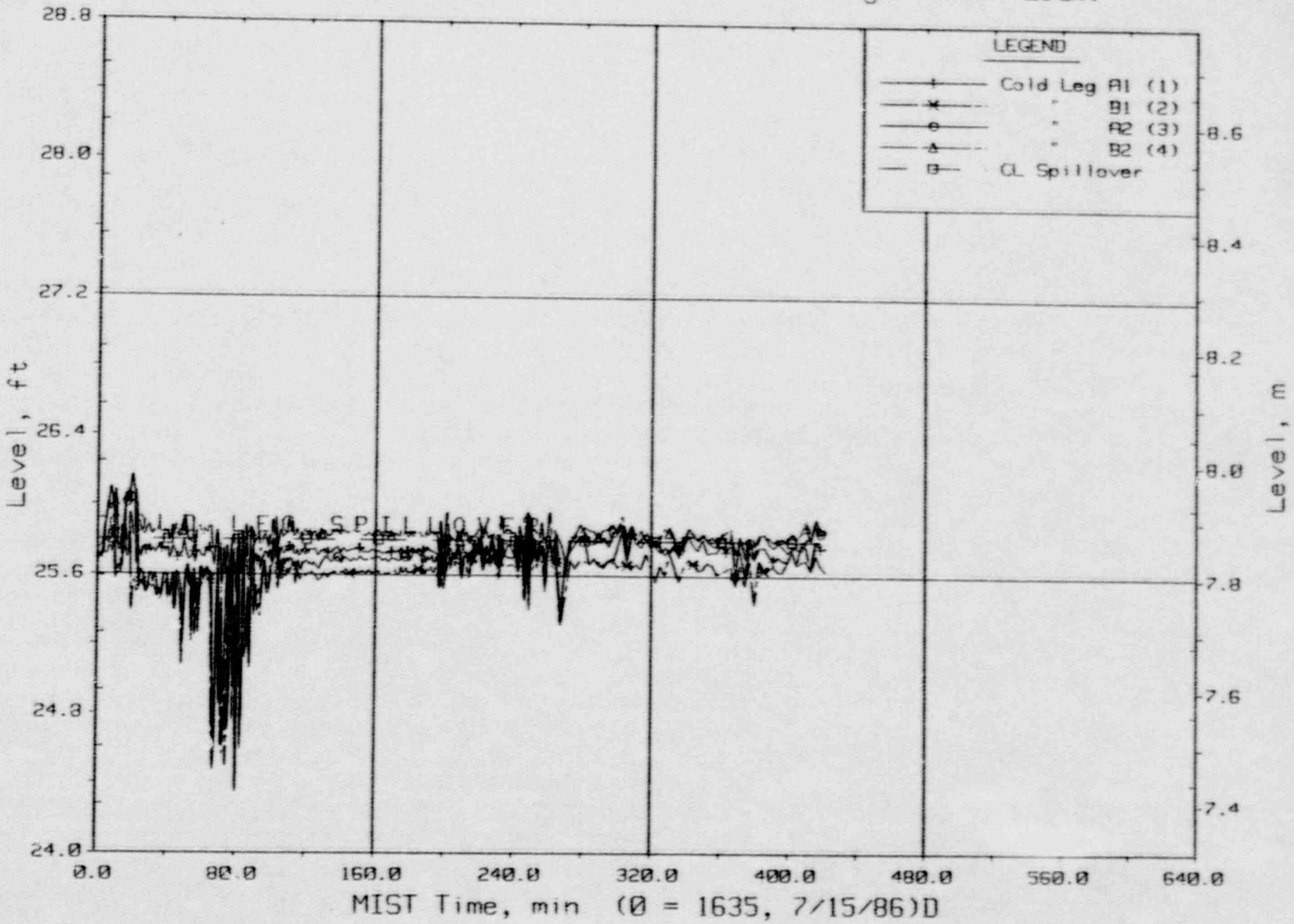

Cold Leg Discharge Collapsed Liquid Levels (CnLV23s).

Wed Jun 8 12:02:11 1988

CLLV5

FINAL DATA

T320302: Group 32 SBLOCA Test 3, Cold Leg Suction Leak.

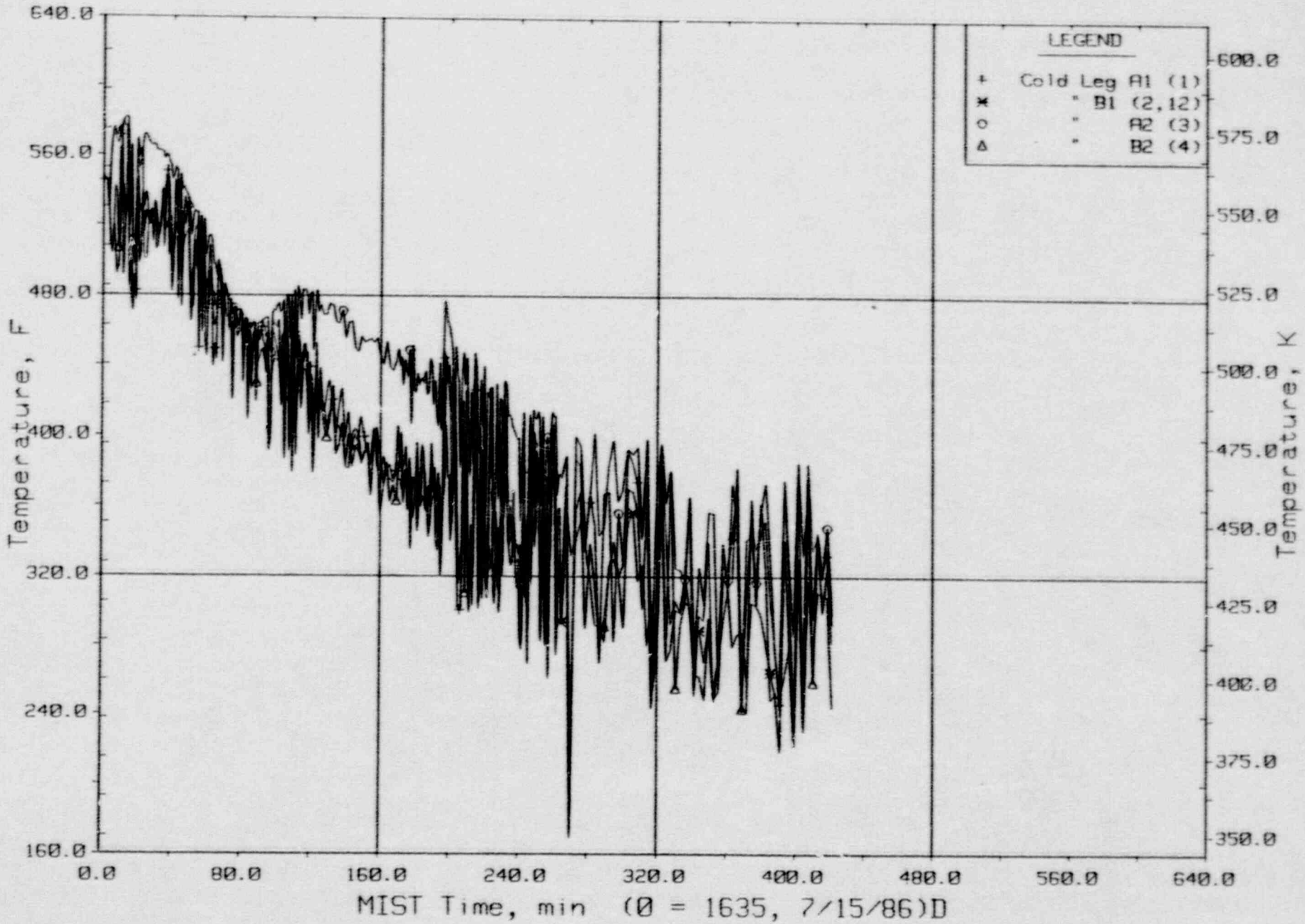

Cold Leg Nozzle Fluid Temperatures, Top of Rake (21.3ft, CnTC11s).

Wed Jun 8 12:06:47 1988

CLTC1

FINAL DATA

T320302: Group 32 SBLOCA Test 3, Cold Leg Suction Leak.

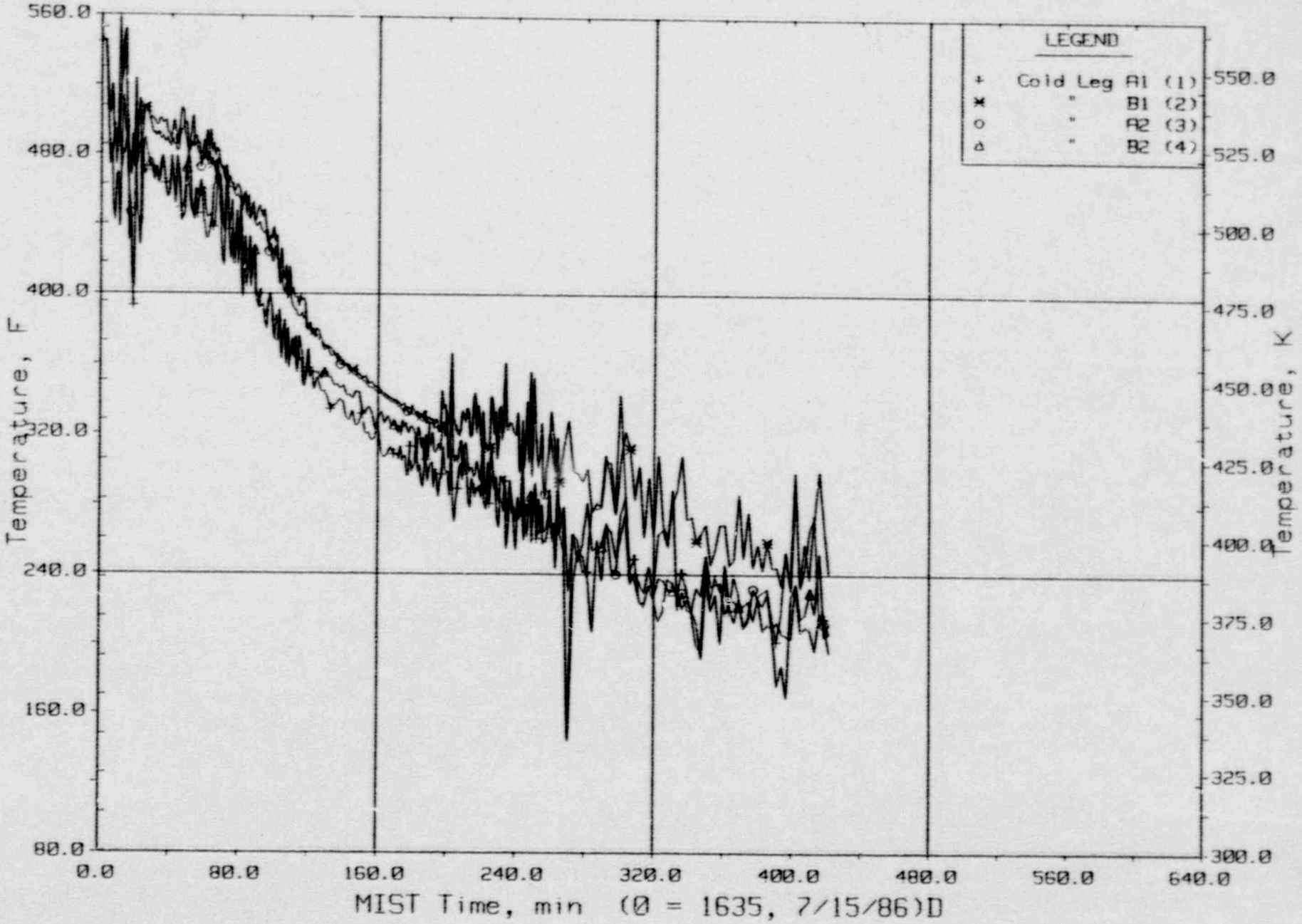

Cold Leg Nozzle Fluid Temperatures, Bottom of Rake (21.2ft, CnTC14s).

Wed Jun 8 12:09:29 1988

CLTC2

FINAL DATA

T320302: Group 32 SBLOCA Test 3, Cold Leg Suction Leak.

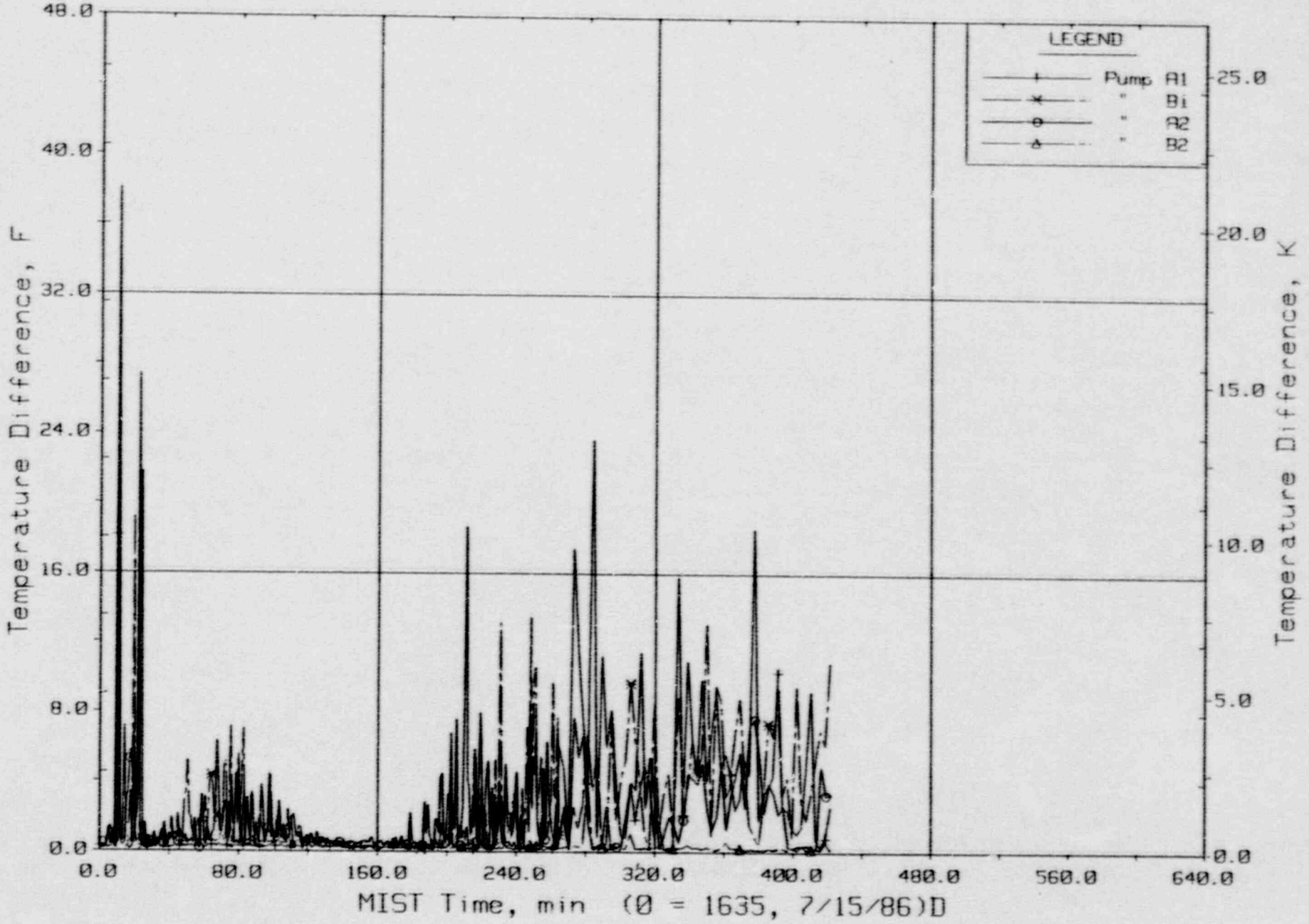

Maximum Differences Among RCP Rake Fluid Temperatures.

Wed Jun 8 12:12:37 1988

CLTD1

FINAL DATA

T320302: Group 32 SBLOCA Test 3, Cold Leg Suction Leak.

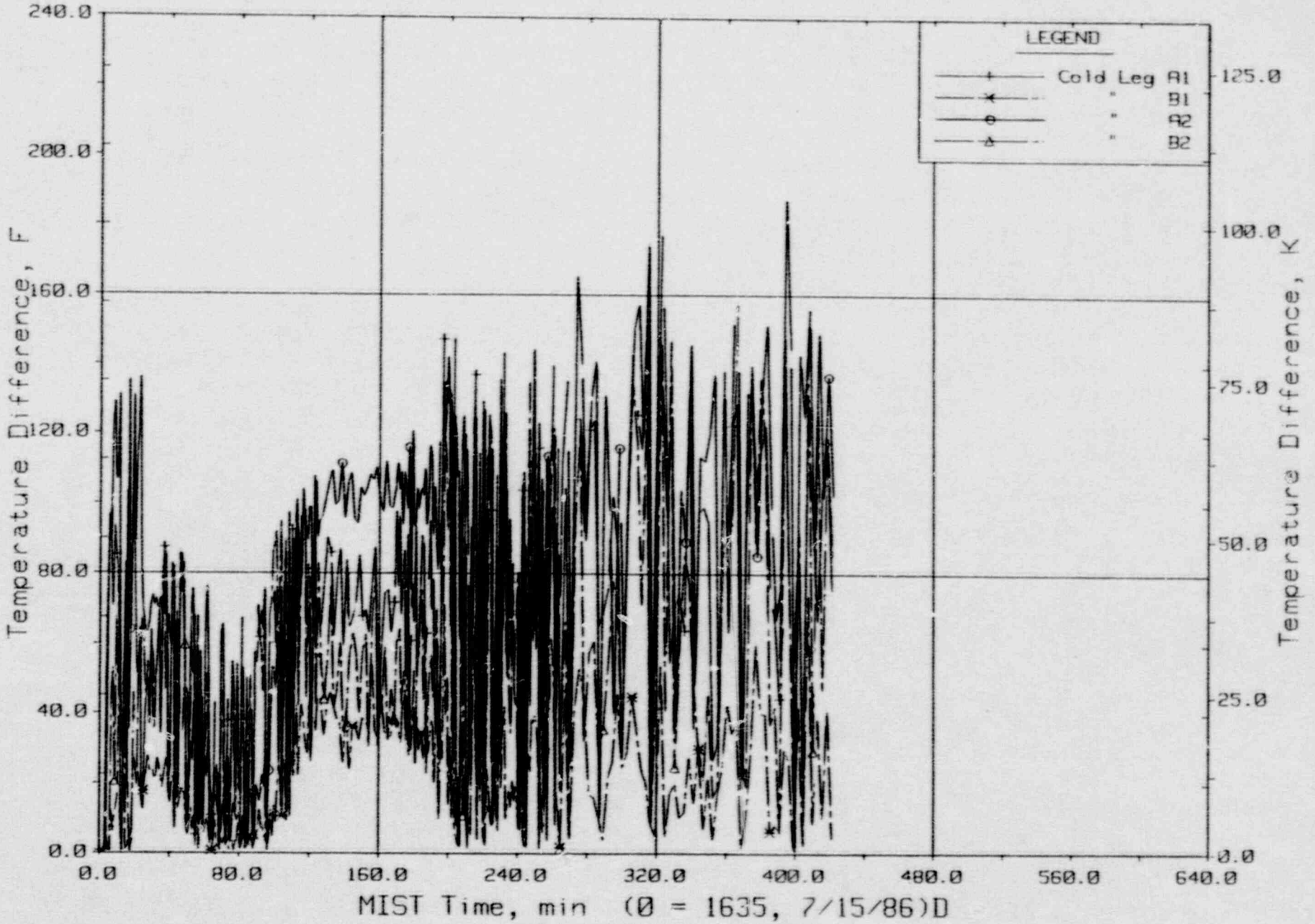

Maximum Differences Among CL Nozzle Rake Fluid Temperatures.

Wed Jun 8 12:15:26 1988

CLTD2

FINAL DATA

T320302: Group 32 SBLOCA Test 3, Cold Leg Suction Leak.

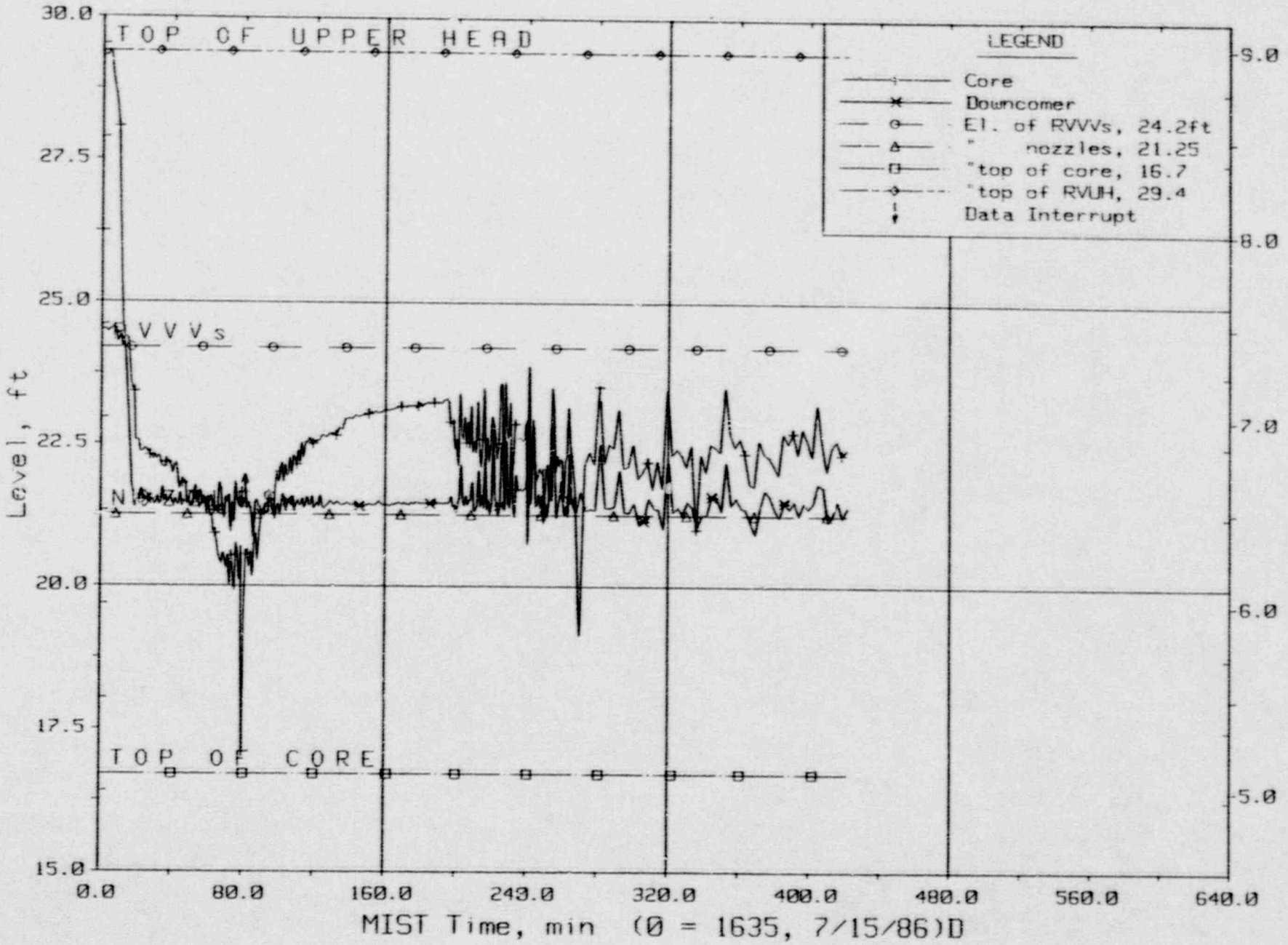

Core Region Collapsed Liquid Levels.

Wed Jun 8 12:20:57 1988

COLV1

FINAL DATA

T320302: Group 32 SBLOCA Test 3, Cold Leg Suction Leak.

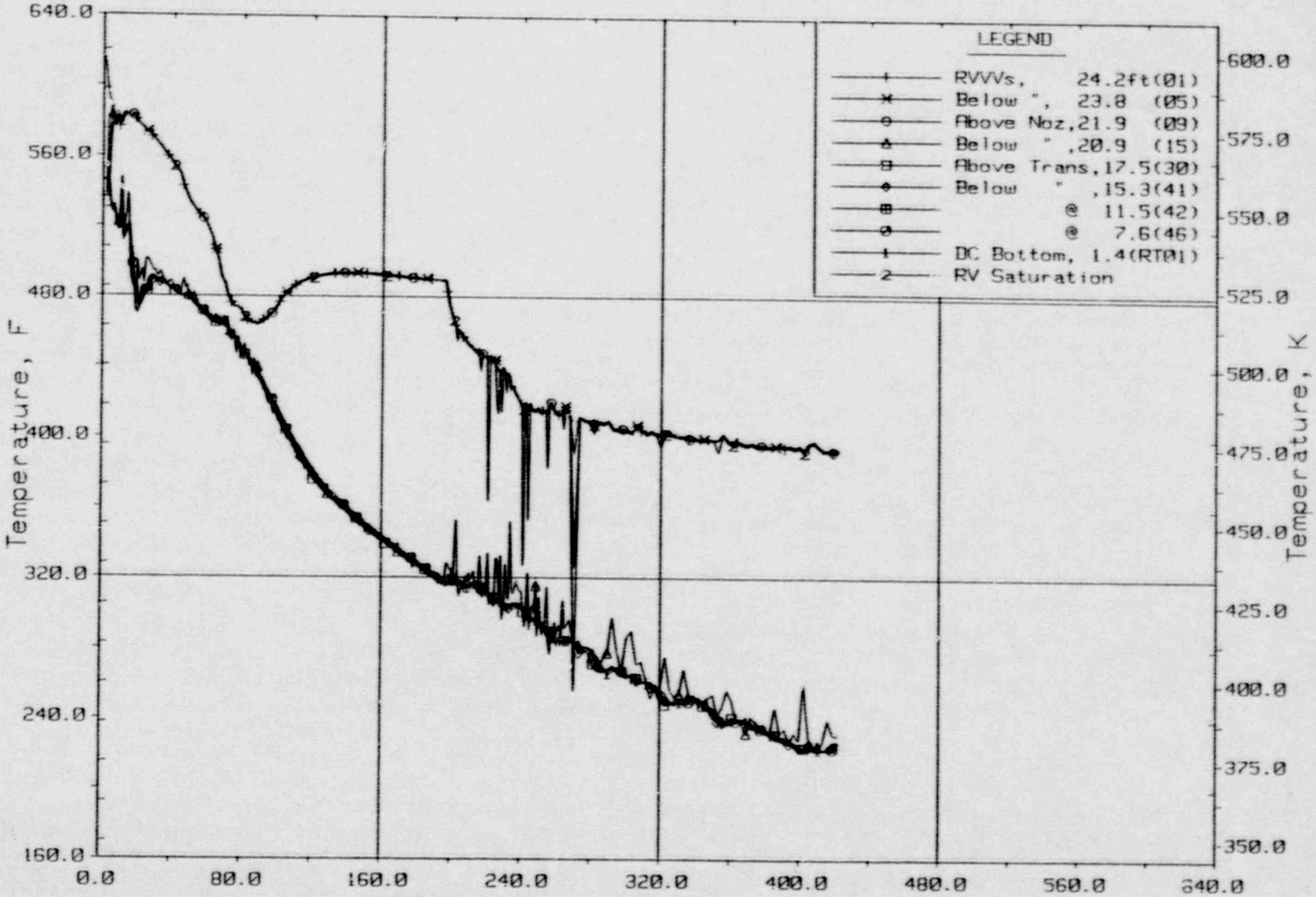

Downcomer Quadrant A1 Fluid Temperatures (DCTCs).

Wed Jun 8 12:27:49 1988

DCTC6

FINAL DATA

T320302: Group 32 SBLOCA Test 3, Cold Leg Suction Leak.

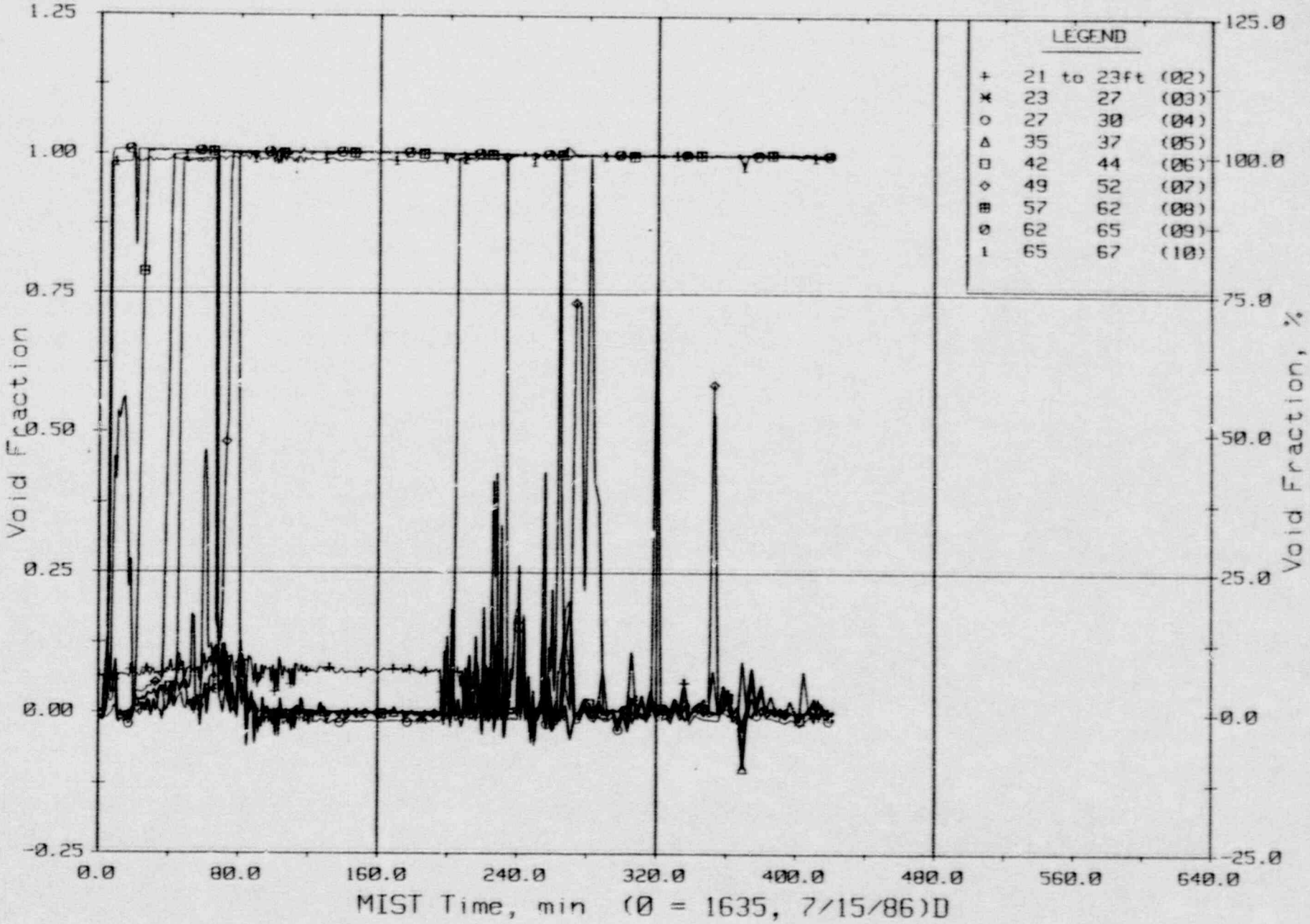

Hot Leg A Riser Void Fractions From Differential Pressures (HIVFs).

Wed Jun 8 12:31:35 1988

HIVF1

FINAL DATA

T320302: Group 32 SBLOCA Test 3, Cold Leg Suction Leak.

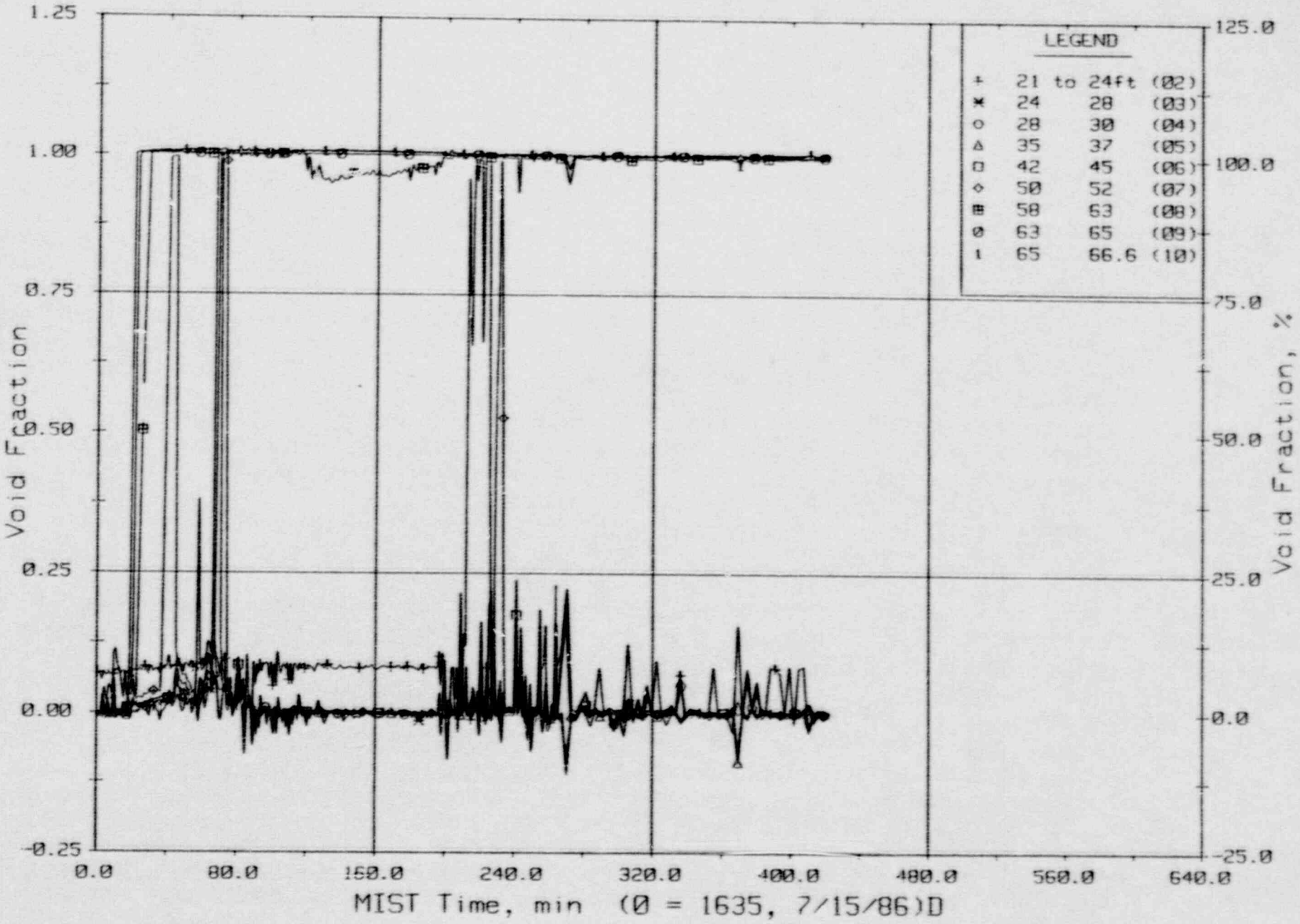

Hot Leg B Riser Void Fraction From Differential Pressures (H2VFs).

Wed Jun 8 12:35:03 1988

H2VF1

FINAL DATA

T320302: Group 32 SBLOCA Test 3, Cold Leg Suction Leak.

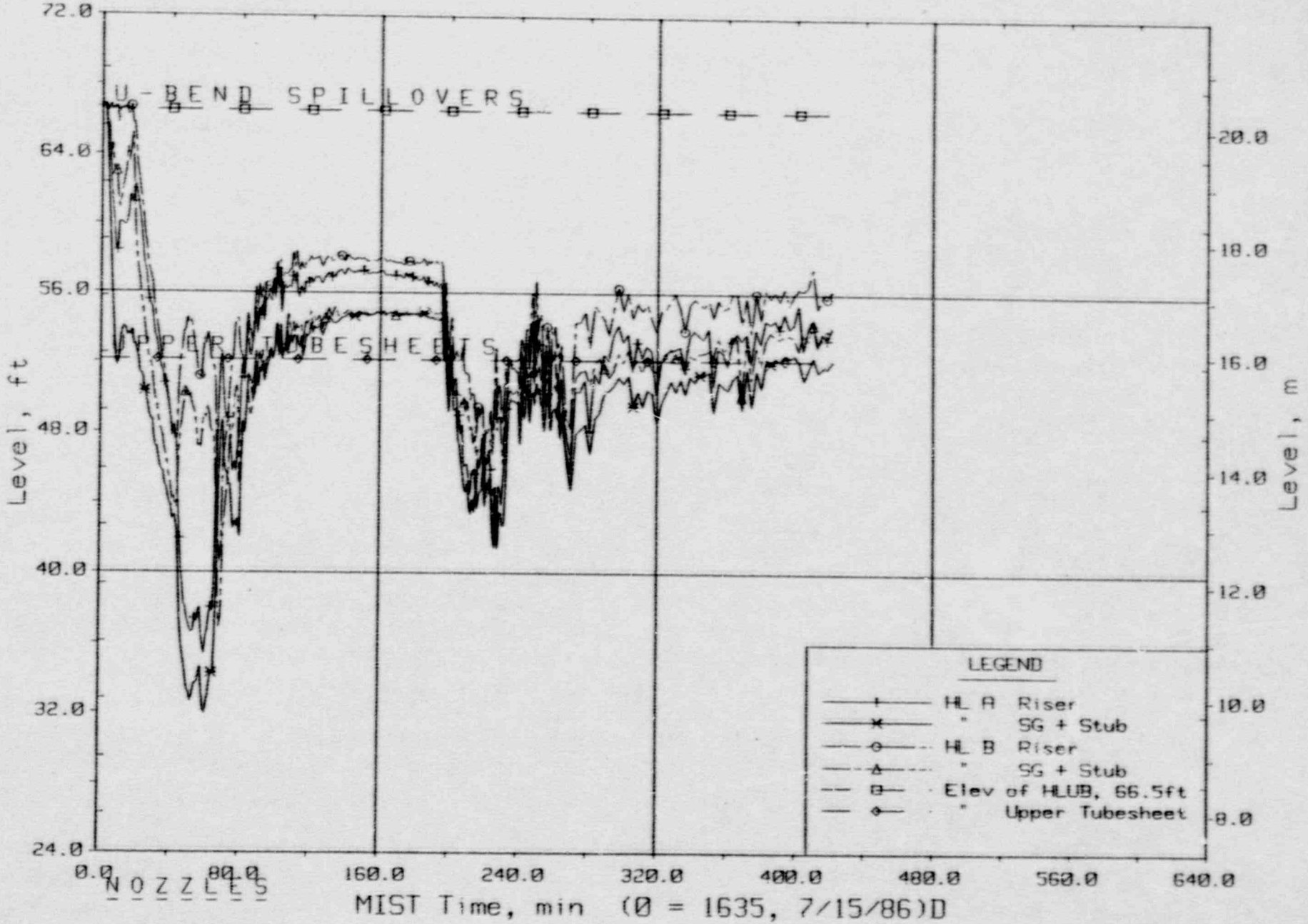

MIST Time, min (0 = 1635, 7/15/86)D

Hot Leg Riser and Stub Collapsed Liquid Levels.

Wed Jun 8 12:38:35 1988

HLLV1

FINAL DATA

T320302: Group 32 SBLOCA Test 3, Cold Leg Suction Leak.

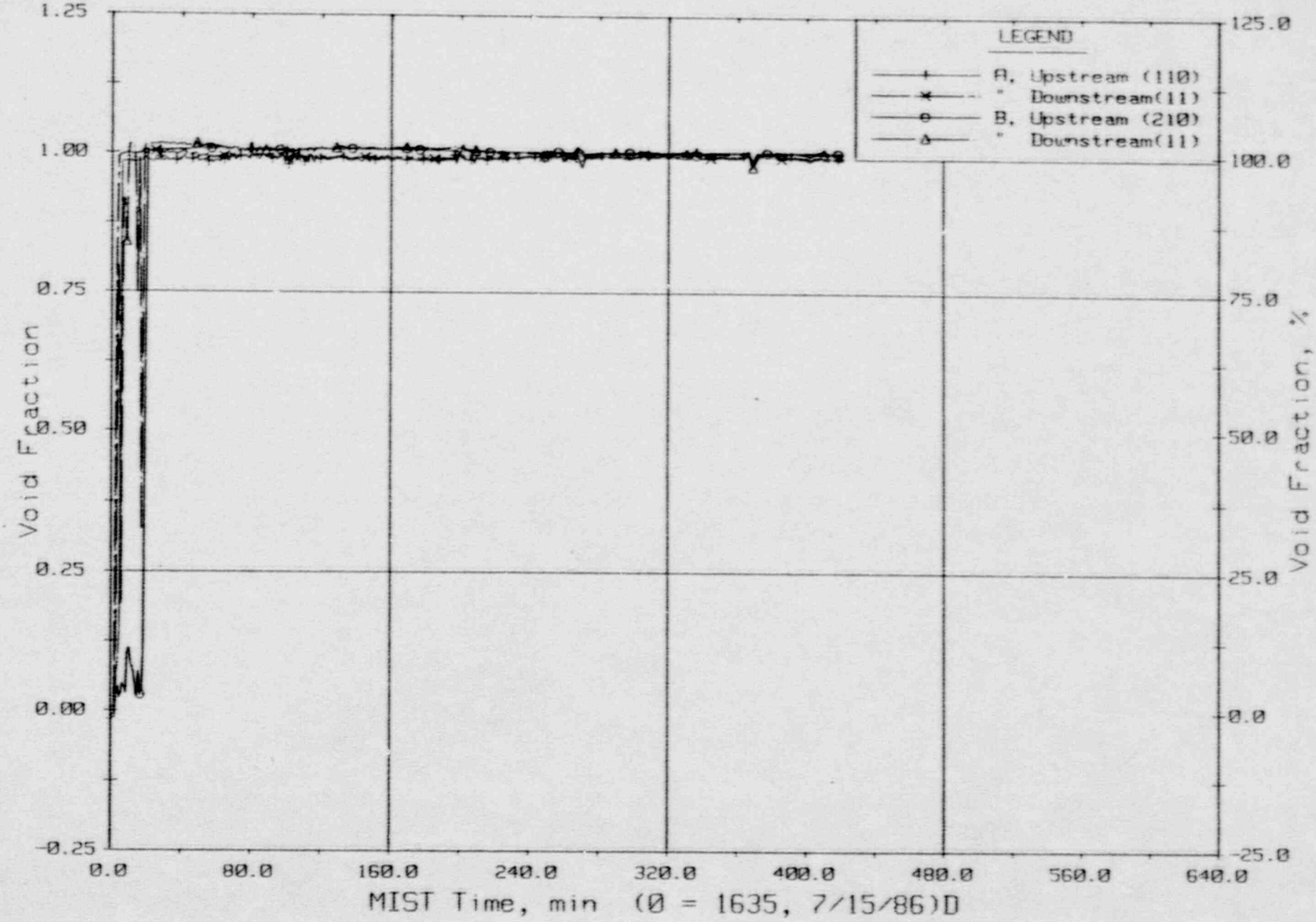

Hot Leg U-Bend Void Fractions From Diffl. Pressures (64.8 to 66.6 ft, HnVFs).

Wed Jun 8 12:41:29 1988

HLVF1

FINAL DATA

T320302: Group 32 SBLOCA Test 3, Cold Leg Suction Leak.

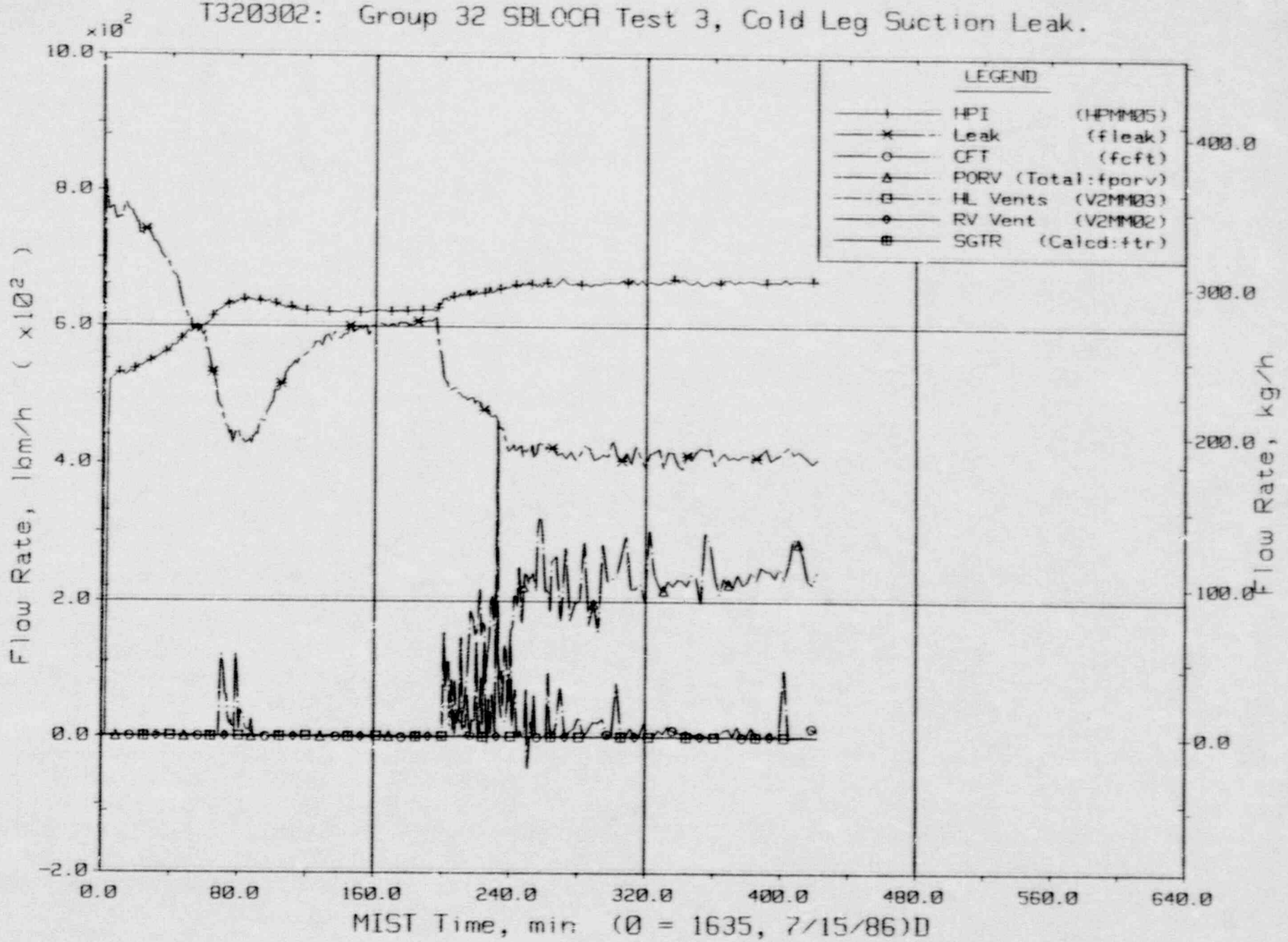

Primary System Boundary Flow Rates.

Wed Jun 8 12:45:03 1988

PBFL3

FINAL DATA

T320302: Group 32 SBLOCA Test 3, Cold Leg Suction Leak.

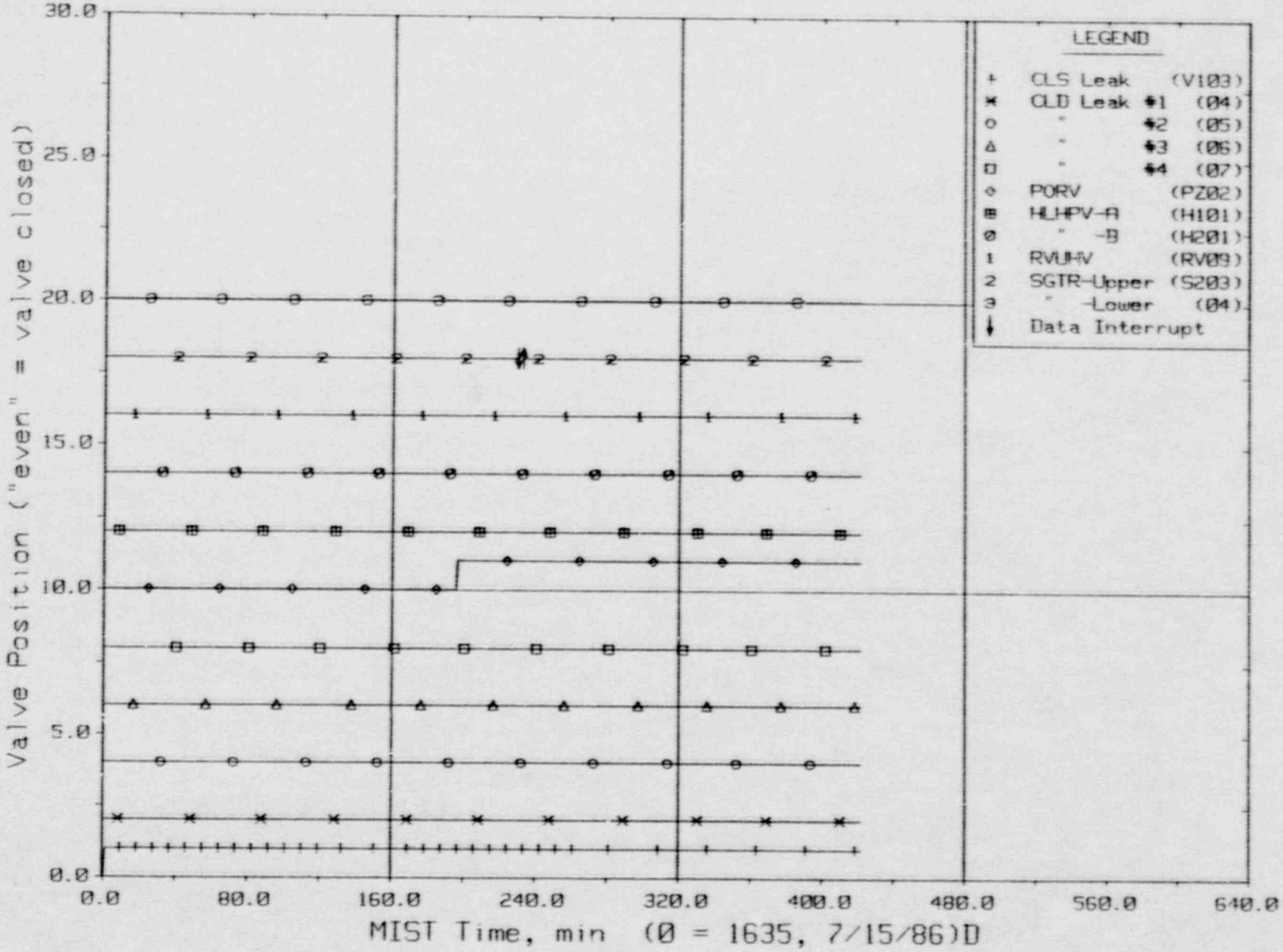

Primary System Discharge Limit Switch Indications (LSs).

Wed Jun 8 12:48:43 1988

PBLS1

FINAL DATA

T320302: Group 32 SBLOCA Test 3, Cold Leg Suction Leak.

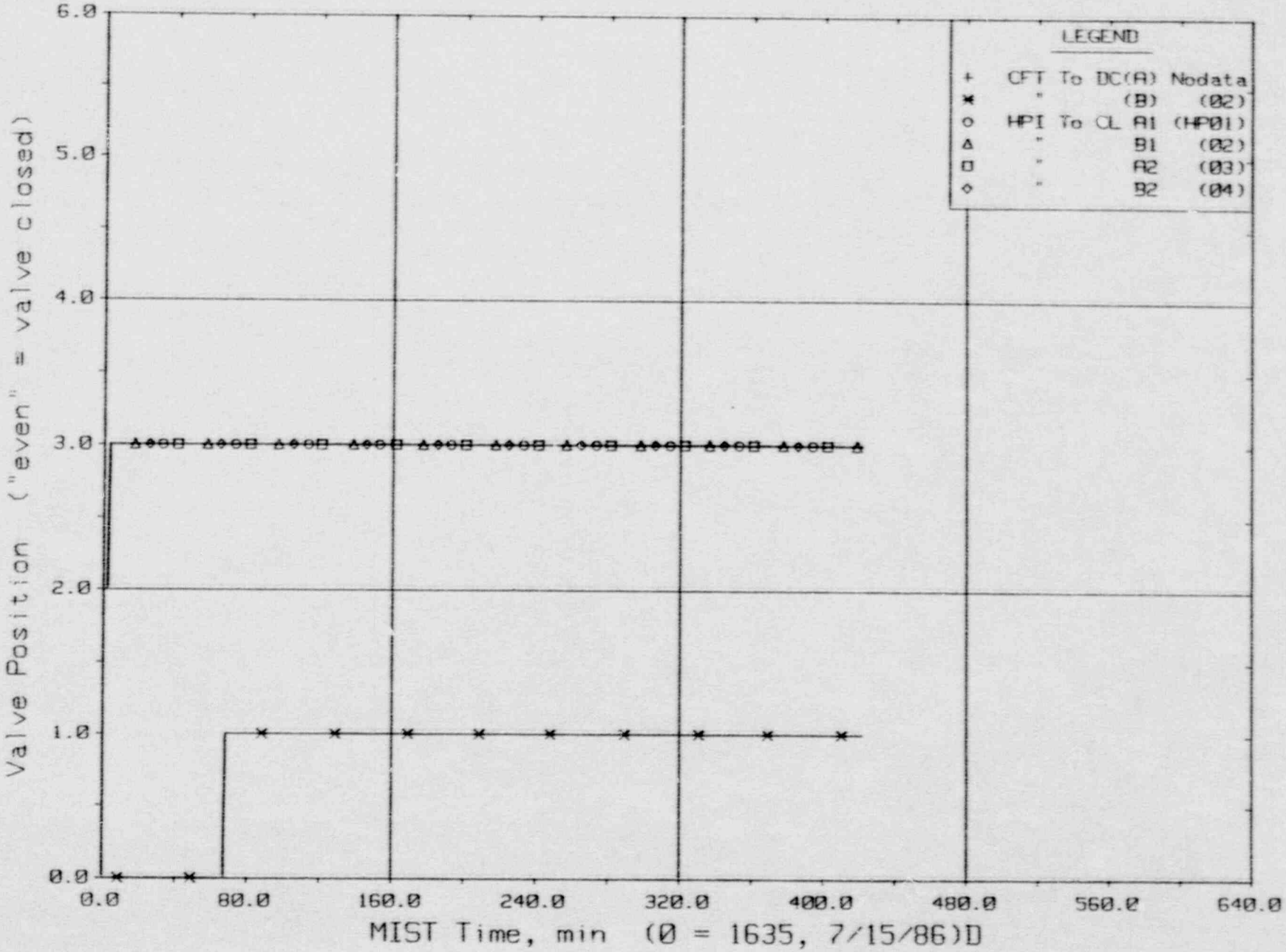

Primary System Injection Limit Switch Indications (LSs).

Wed Jun 8 12:51:21 1988

PBLS2

FINAL DATA

T320302: Group 32 SBLOCA Test 3, Cold Leg Suction Leak.

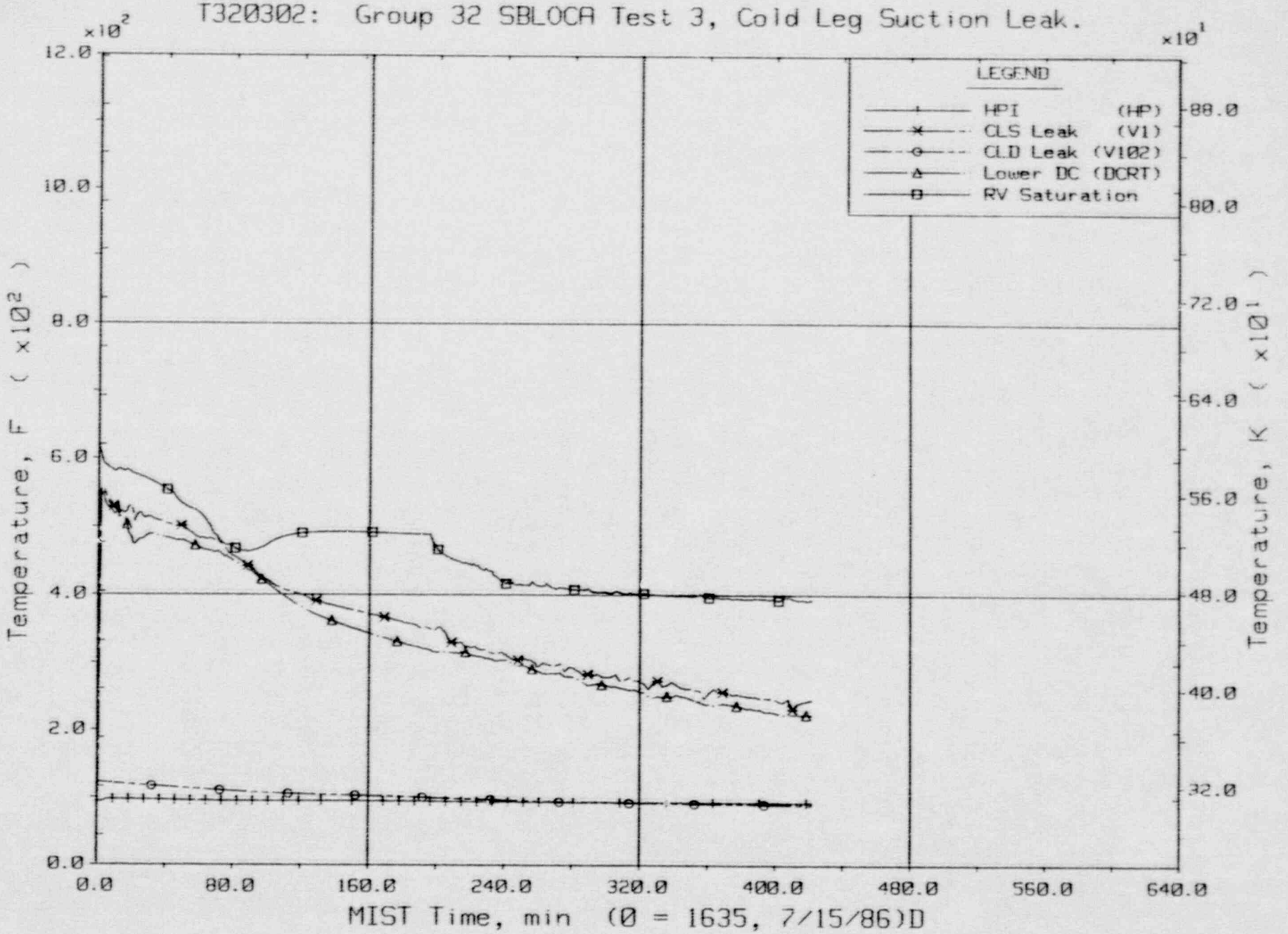

Single-Phase Discharge and HPI Fluid Temperatures (TC01s).

Wed Jun 8 12:54:00 1988

PBTC1p

FINAL DATA

T320302: Group 32 SBLOCA Test 3, Cold Leg Suction Leak.

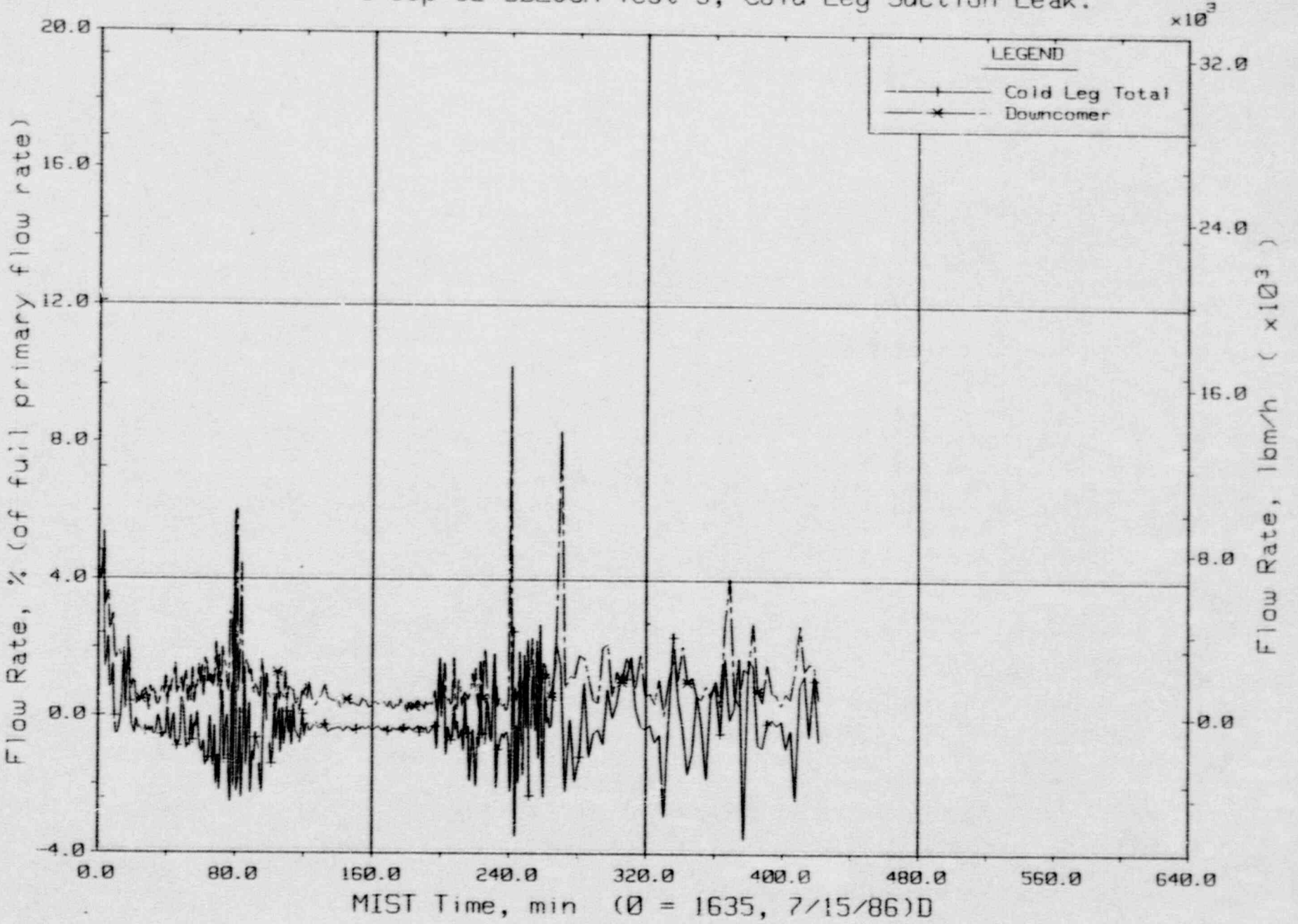

Primary System Venturi Flow Rates.

Wed Jun 8 12:56:17 1988

PRFL7

FINAL DATA

T320302: Group 32 SBLOCA Test 3, Cold Leg Suction Leak.

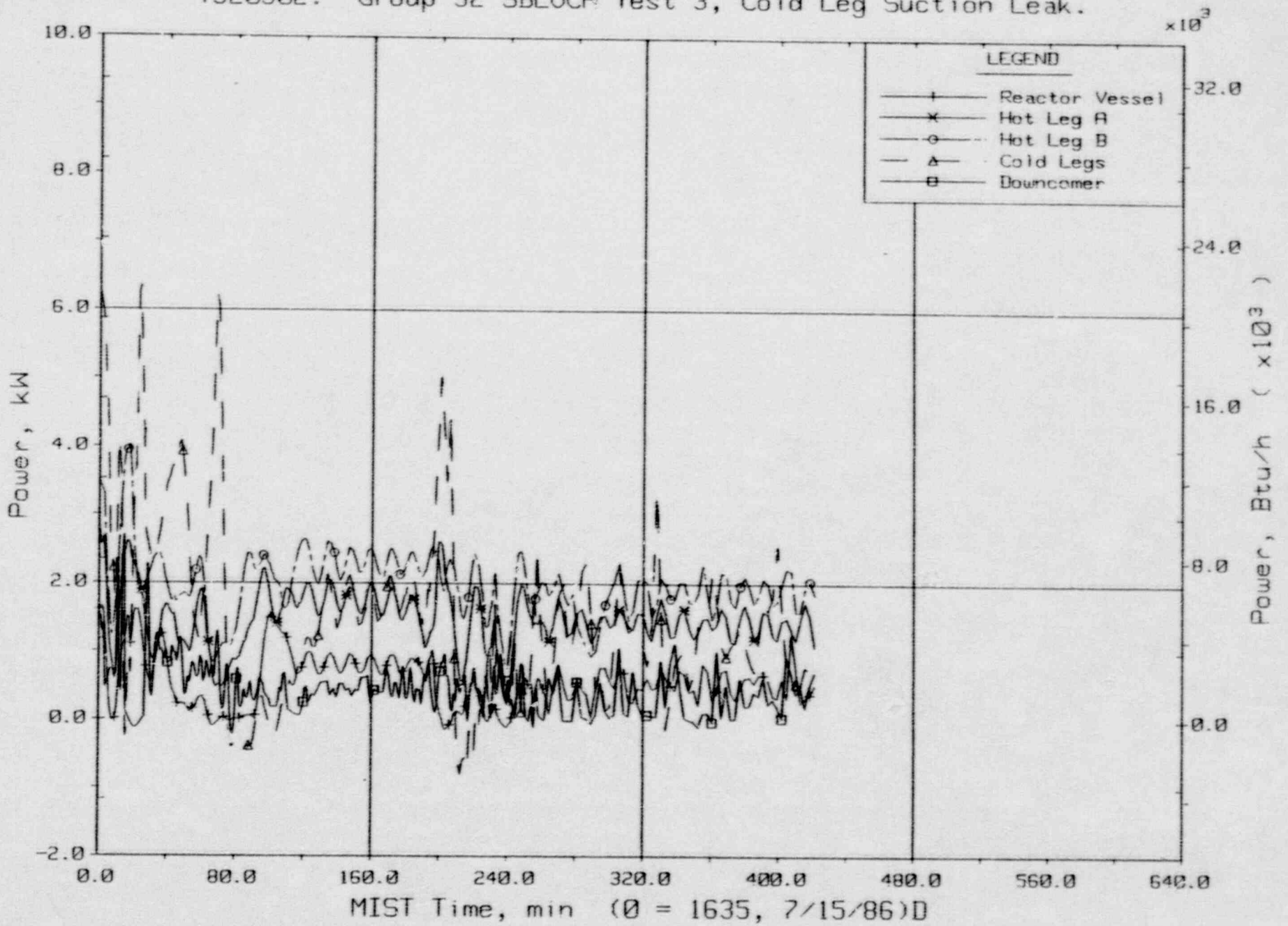

Guard Heater Specified Power Per Primary Component.

Wed Jun 8 12:59:24 1988

PRGQ1

FINAL DATA

T320302: Group 32 SBLOCA Test 3, Cold Leg Suction Leak.

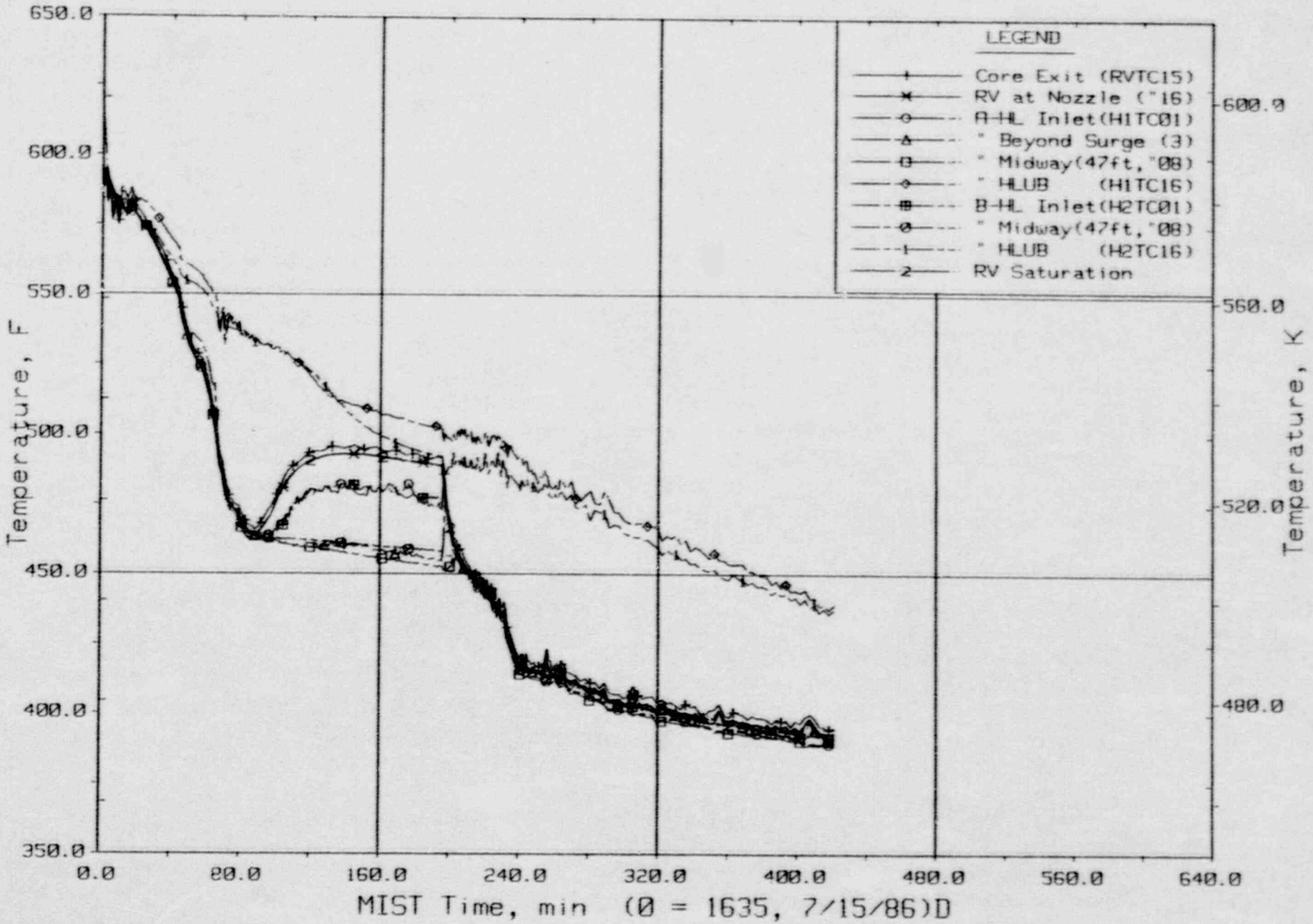

Composite Core Exit and Hot Leg Fluid Temperatures.

Wed Jun 8 13:03:28 1988

PRKT1

FINAL DATA

T320302: Group 32 SBLOCA Test 3, Cold Leg Suction Leak.

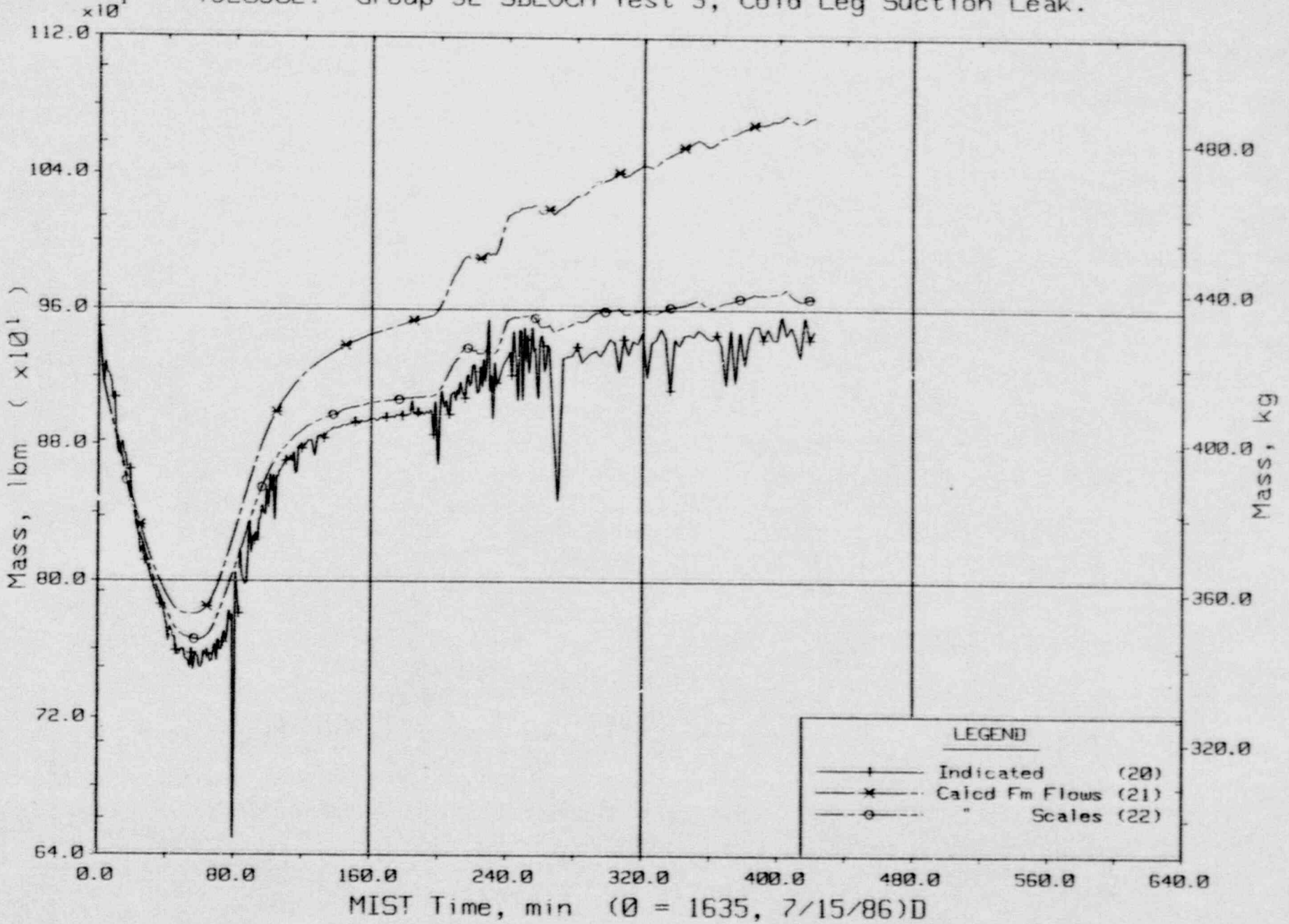

Primary System Total Fluid Mass (PLMLs).

Wed Jun 8 13:06:21 1988

PRML2

FINAL DATA

T320302: Group 32 SBLOCA Test 3, Cold Leg Suction Leak.

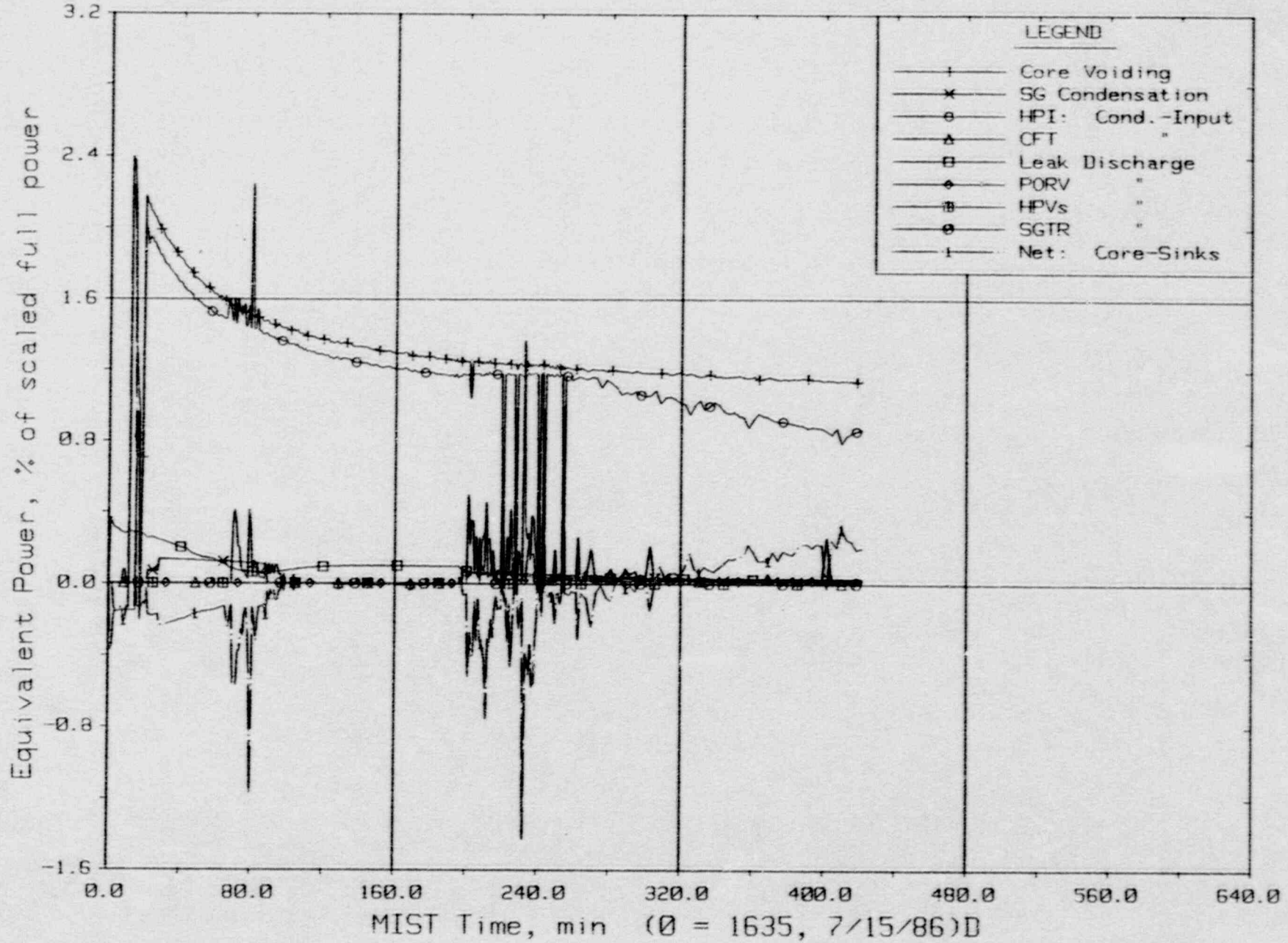

Primary Fluid Volume Changes By Components.

Wed Jun 8 13:09:37 1988

PRPA0

FINAL DATA

T320302: Group 32 SBLOCA Test 3, Cold Leg Suction Leak.

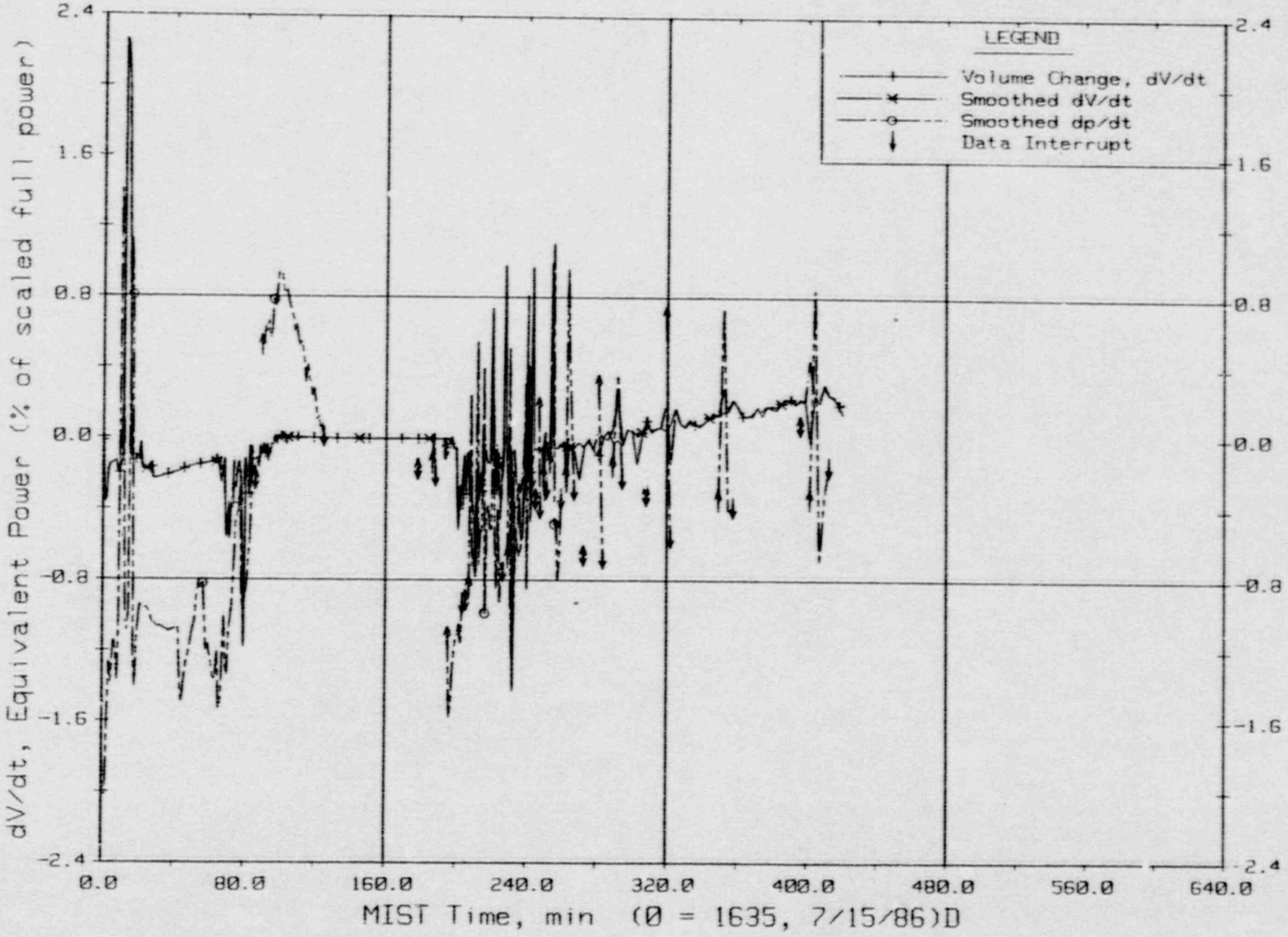

Primary Fluid Volume and Pressure Changes, dV/dt and dp/dt.

Wed Jun 8 13:12:40 1988

PRPA2

FINAL DATA

T320302: Group 32 SBLOCA Test 3, Cold Leg Suction Leak.

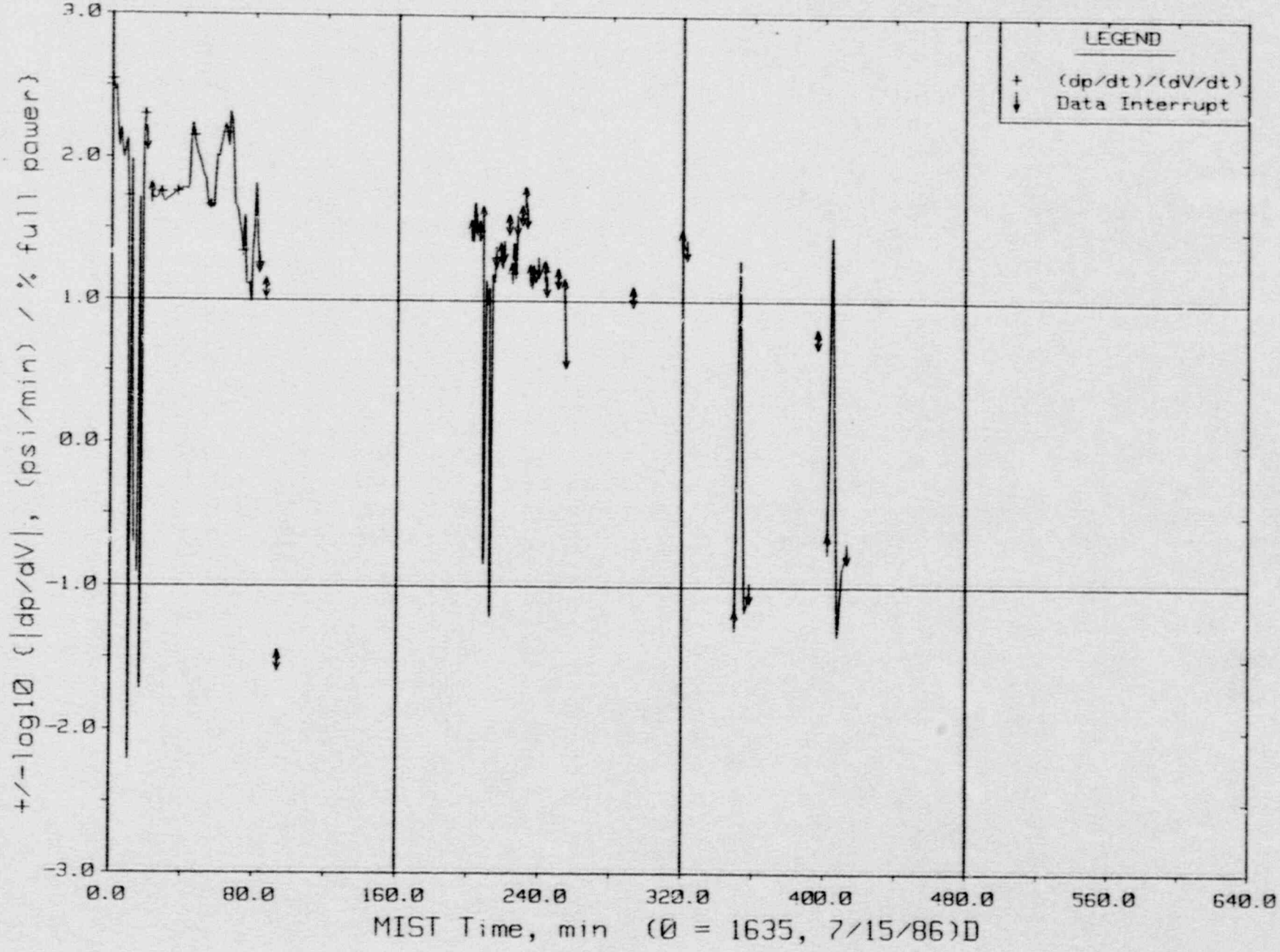

Primary System Response: " dp/dt divided by dV/dt.

Wed Jun 8 13:15:15 1988

PRPA3

FINAL DATA

T320302: Group 32 SBLOCA Test 3, Cold Leg Suction Leak.

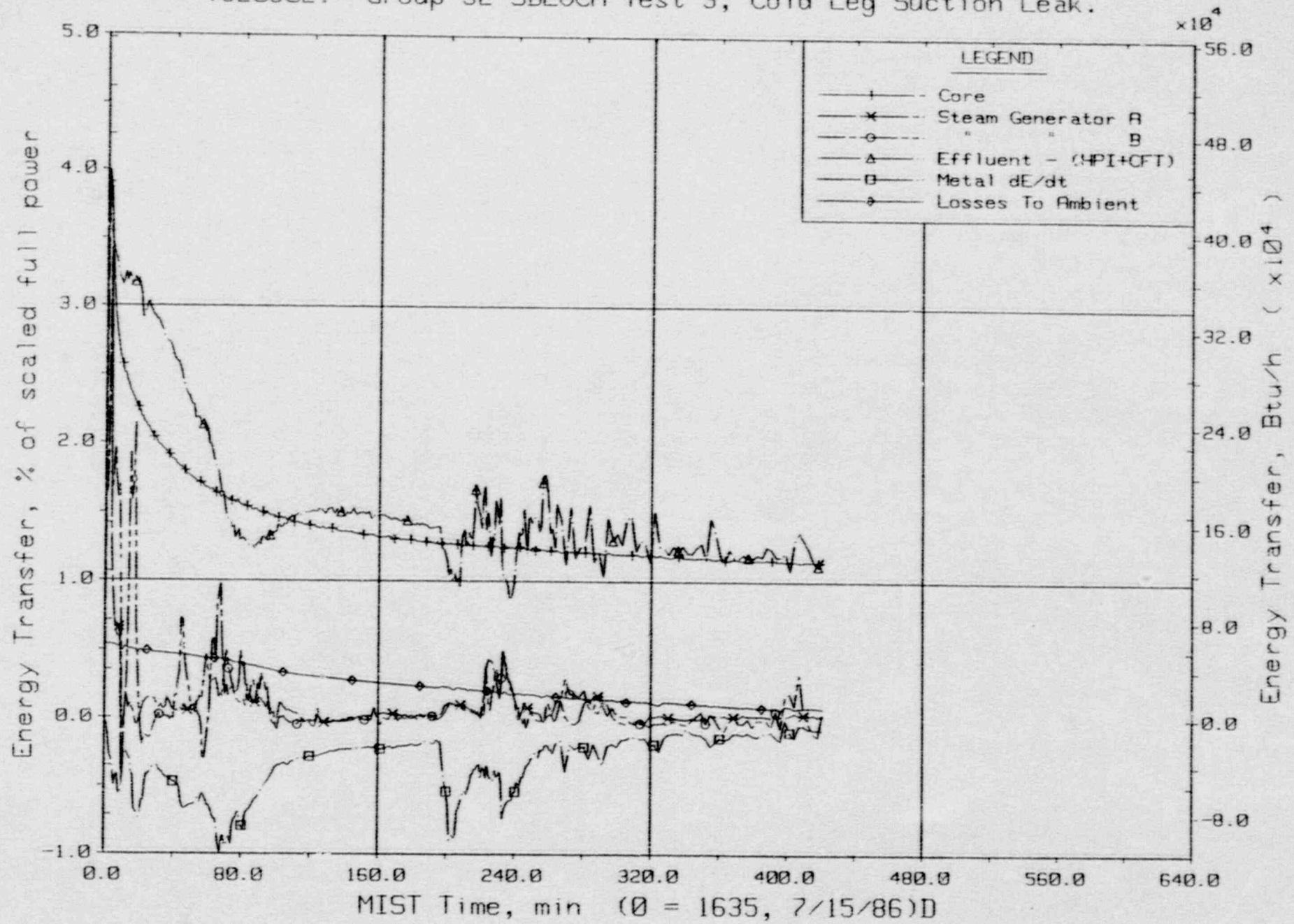

Primary System Energy Transfer.

Wed Jun 8 13:18:22 1988

PRQE2

FINAL DATA

T320302: Group 32 SBLOCA Test 3, Cold Leg Suction Leak.

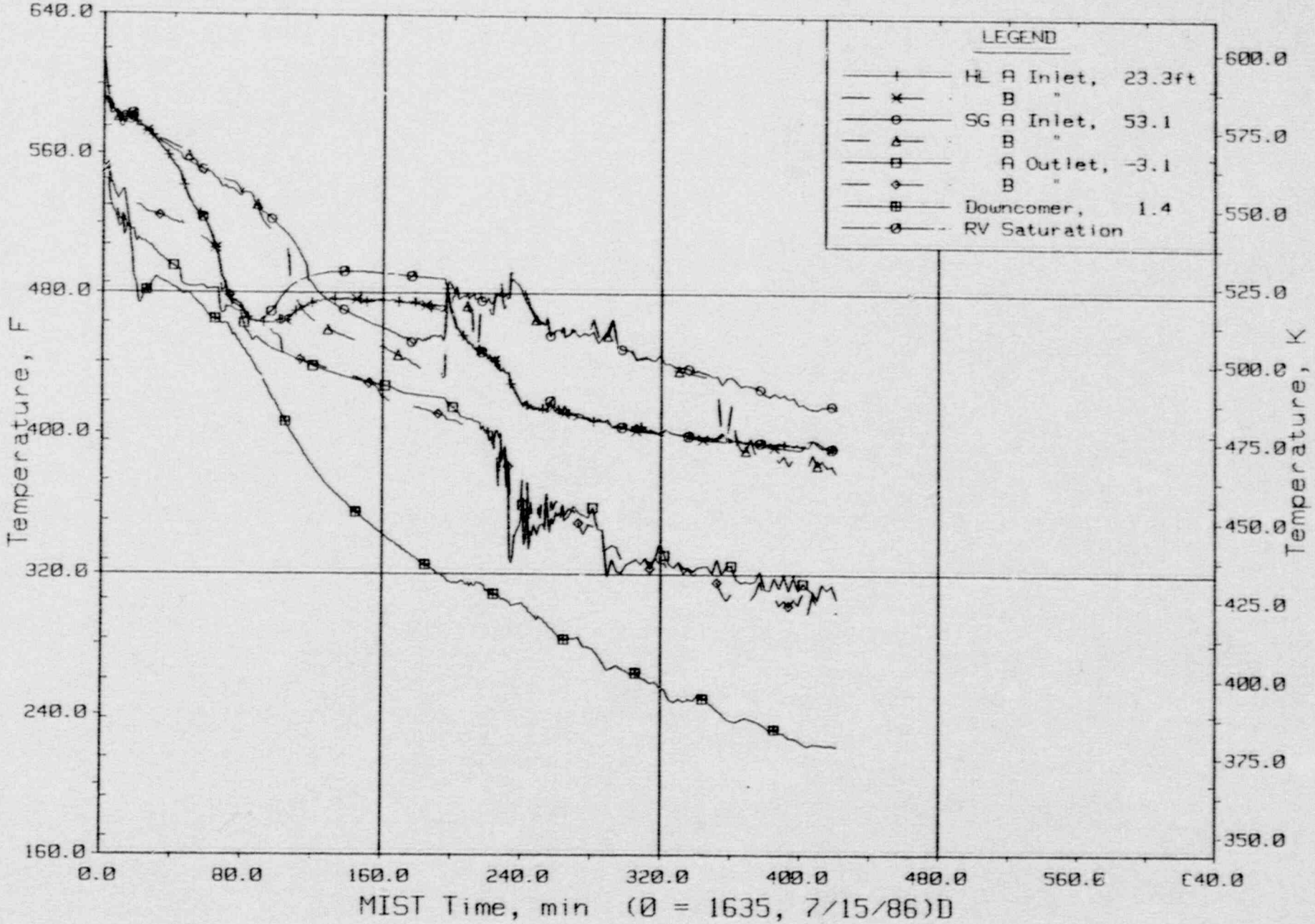

Primary System Fluid Temperatures (RTDs).

Wed Jun 8 13:22:43 1988

PRRT0

FINAL DATA

T320302: Group 32 SBLOCA Test 3, Cold Leg Suction Leak.

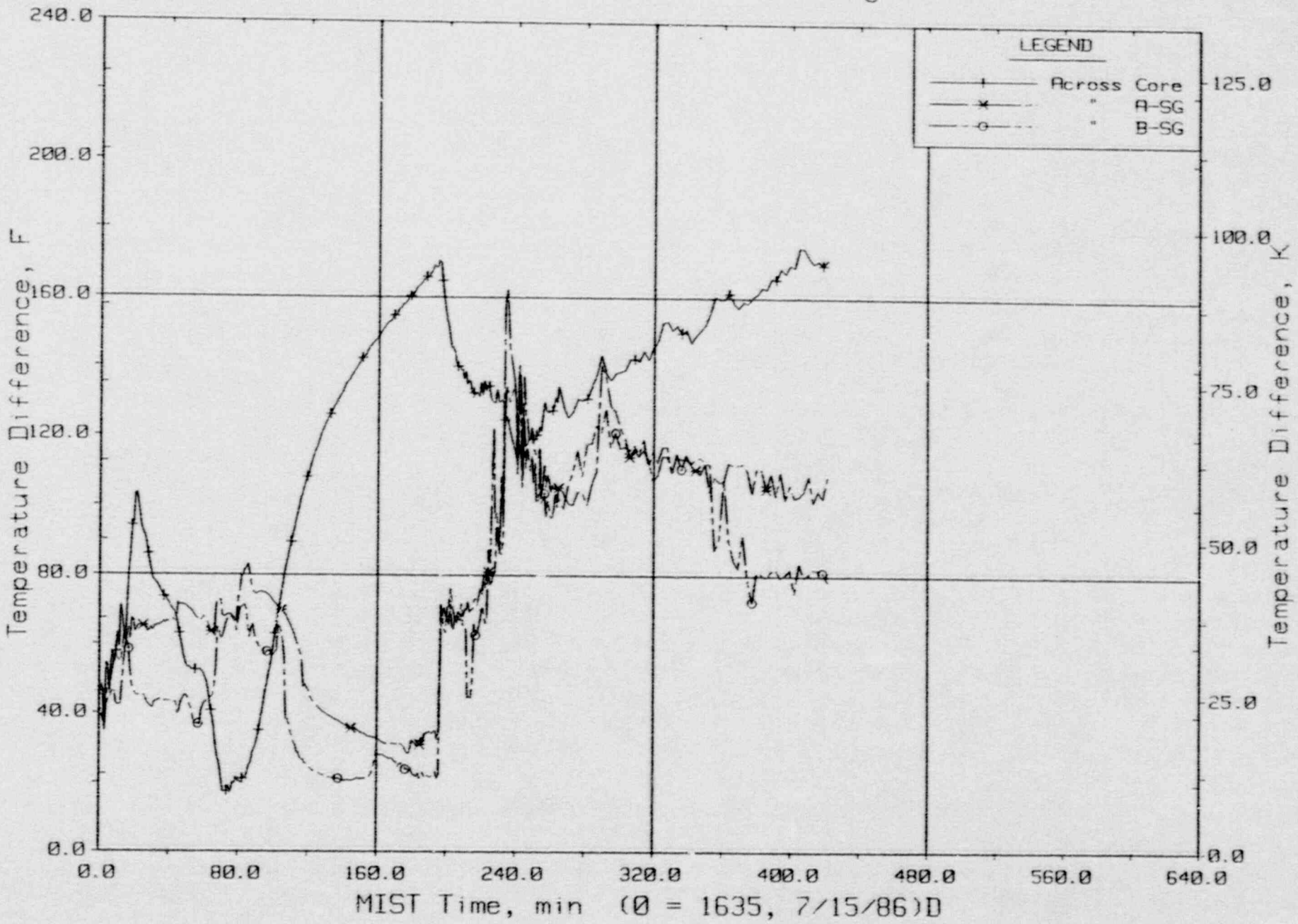

Key Temperature Differences.

Wed Jun 8 13:25:28 1988

PRTD2

FINAL DATA

T320302: Group 32 SBLOCA Test 3, Cold Leg Suction Leak.

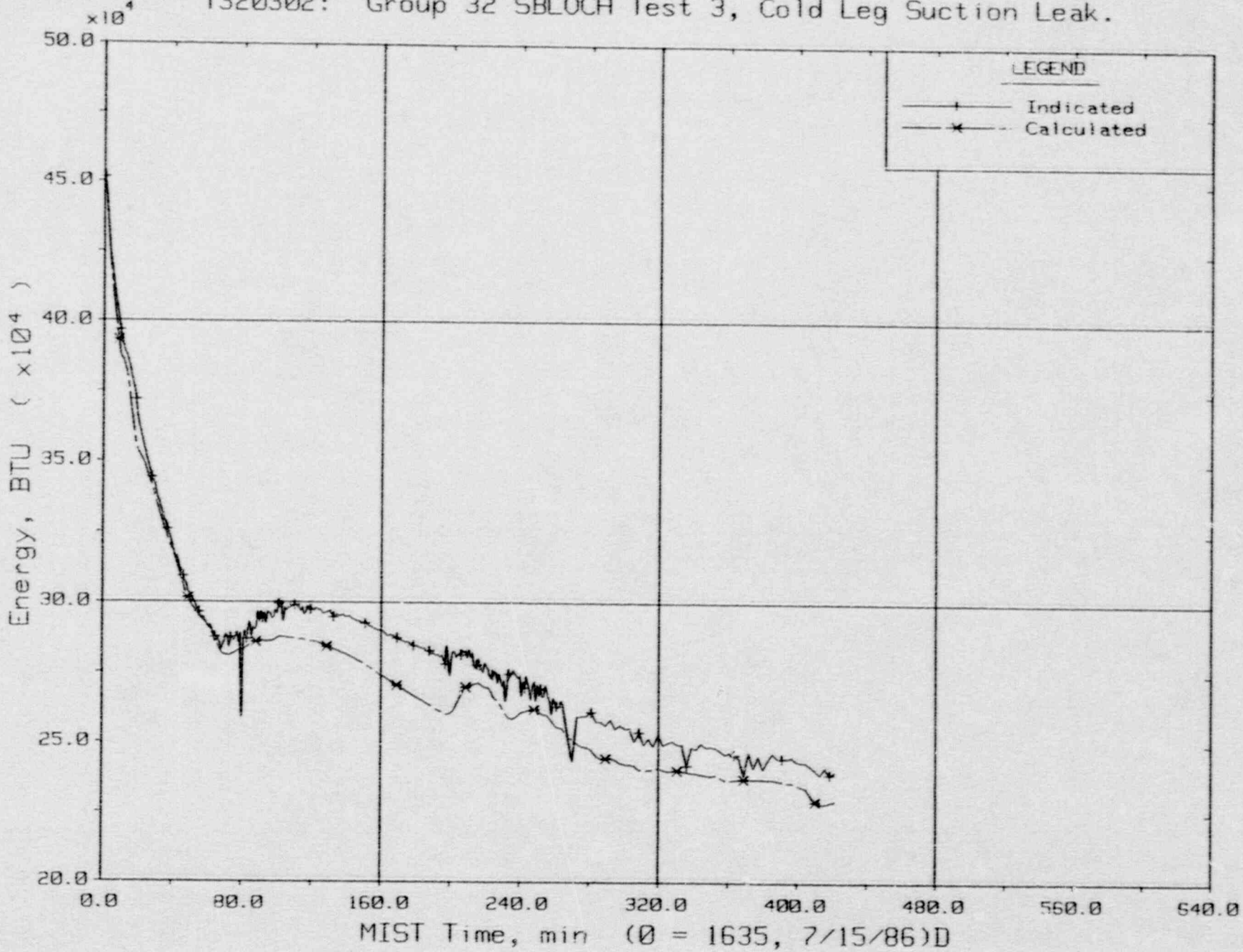

Primary System Total Fluid Energy.

Wed Jun 8 13:28:44 1988

PRTE2

FINAL DATA

T320302: Group 32 SBLOCA Test 3, Cold Leg Suction Leak.

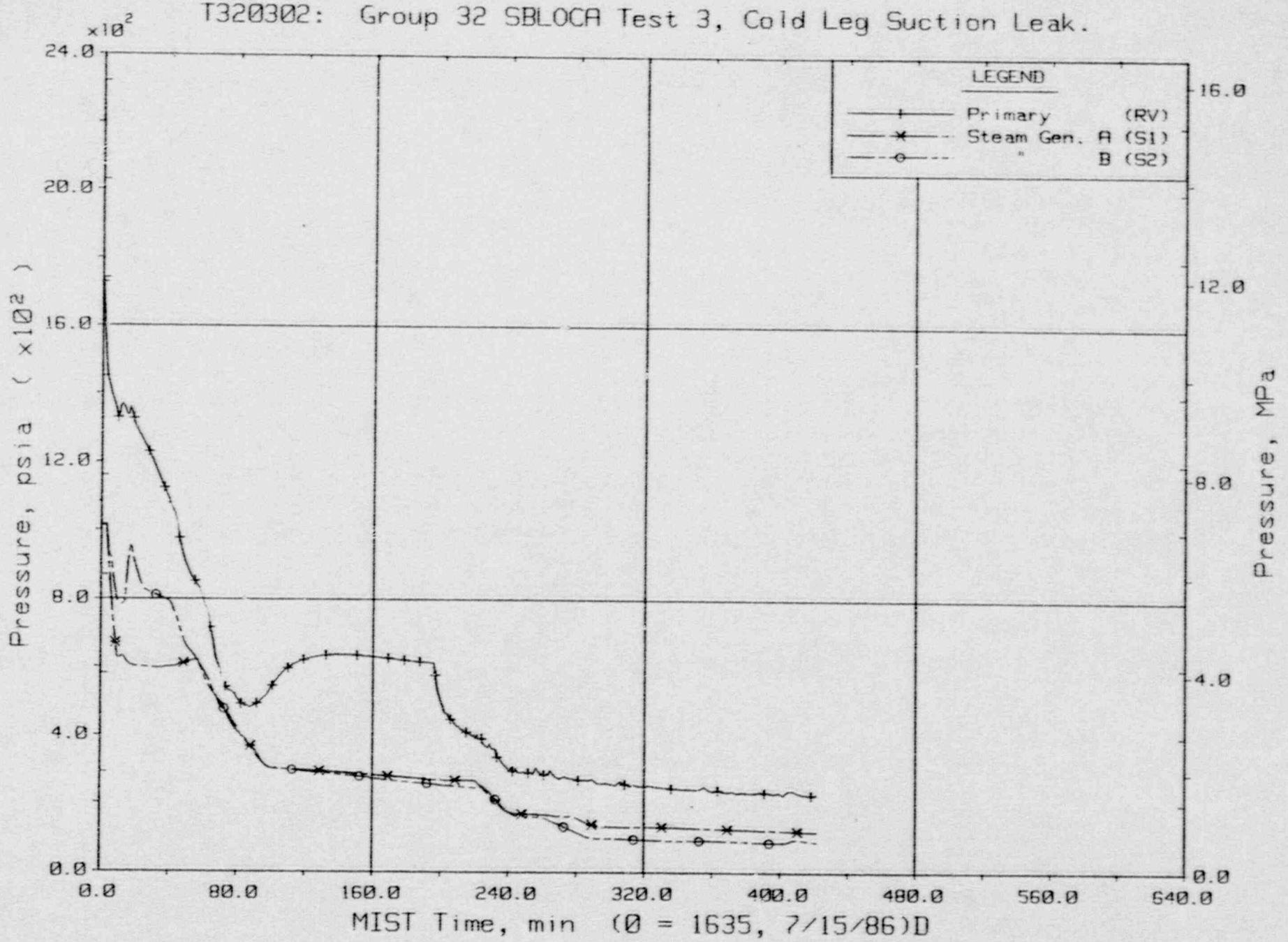

Primary and Secondary System Pressures (GP01s).

Wed Jun 8 13:32:20 1988

PSGP1

FINAL DATA

T320302: Group 32 SBLOCA Test 3, Cold Leg Suction Leak.

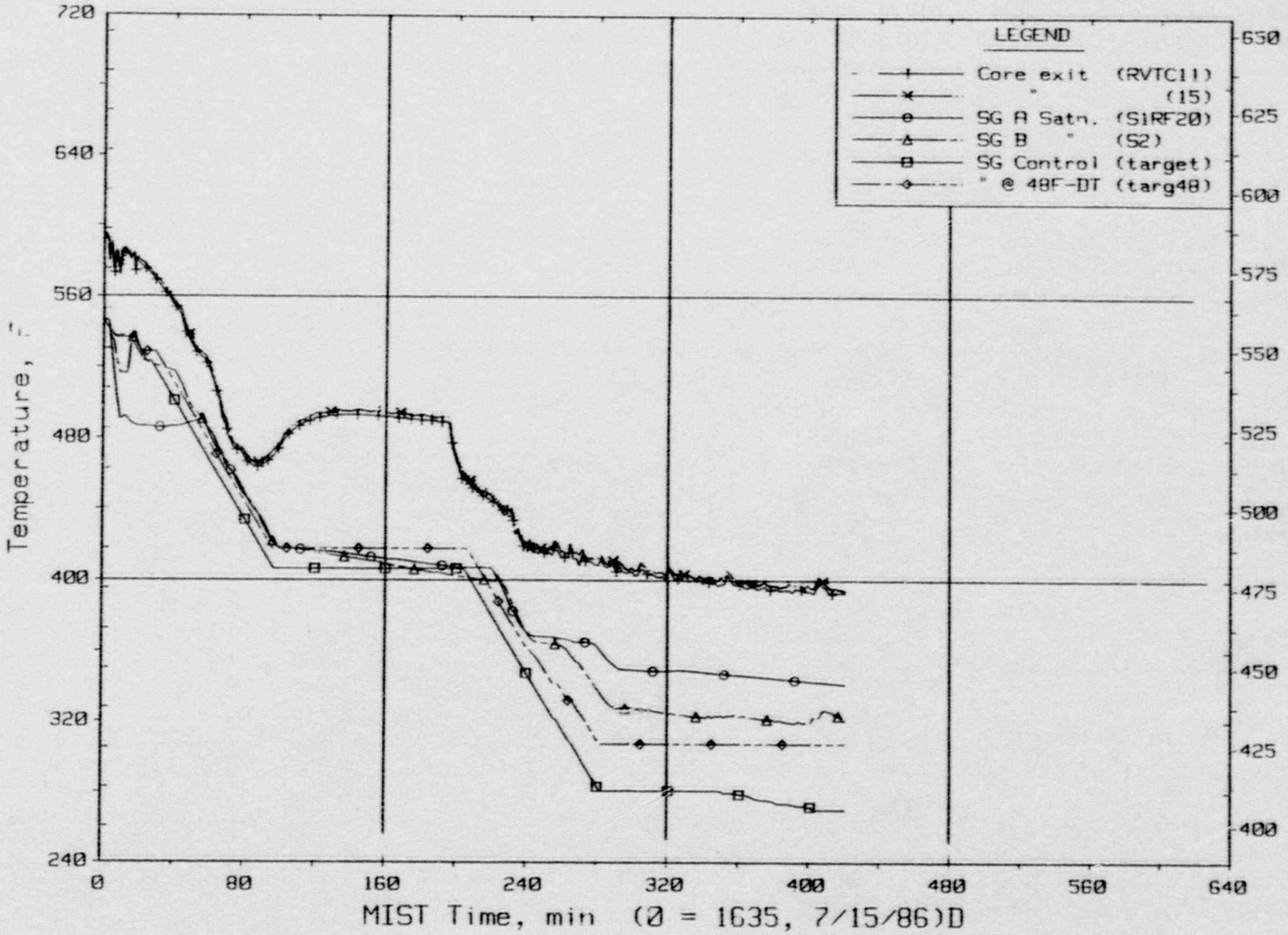

Steam Generator Secondary Saturation and Control Temperatures.

Thu Oct 27 11:26:22 1988

PSTC3

FINAL DATA

T320302: Group 32 SBLOCA Test 3, Cold Leg Suction Leak.

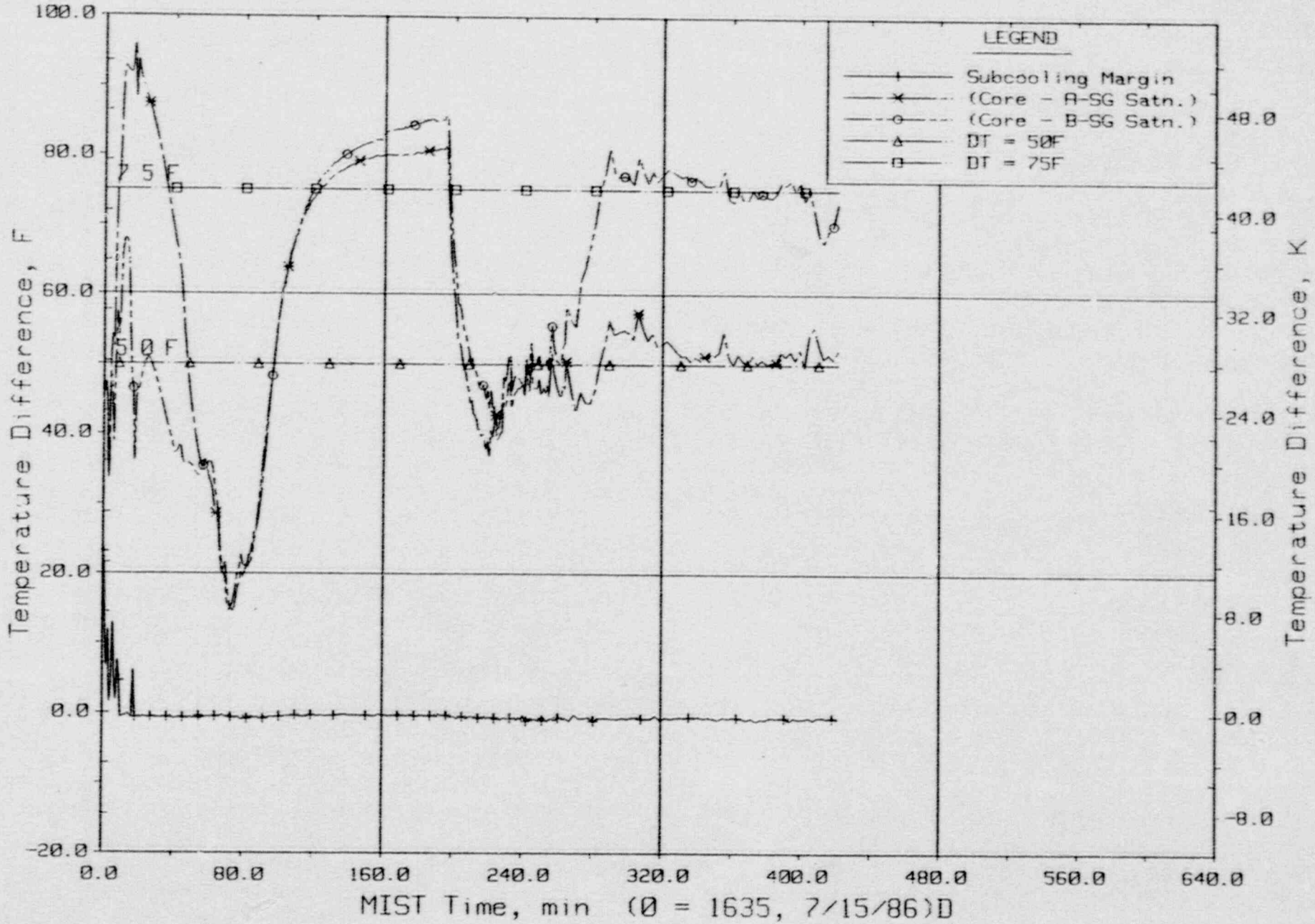

Control Temperature Differences.

Wed Jun 8 13:39:02 1988

PSTD1

FINAL DATA

T320302: Group 32 SBLOCA Test 3, Cold Leg Suction Leak.

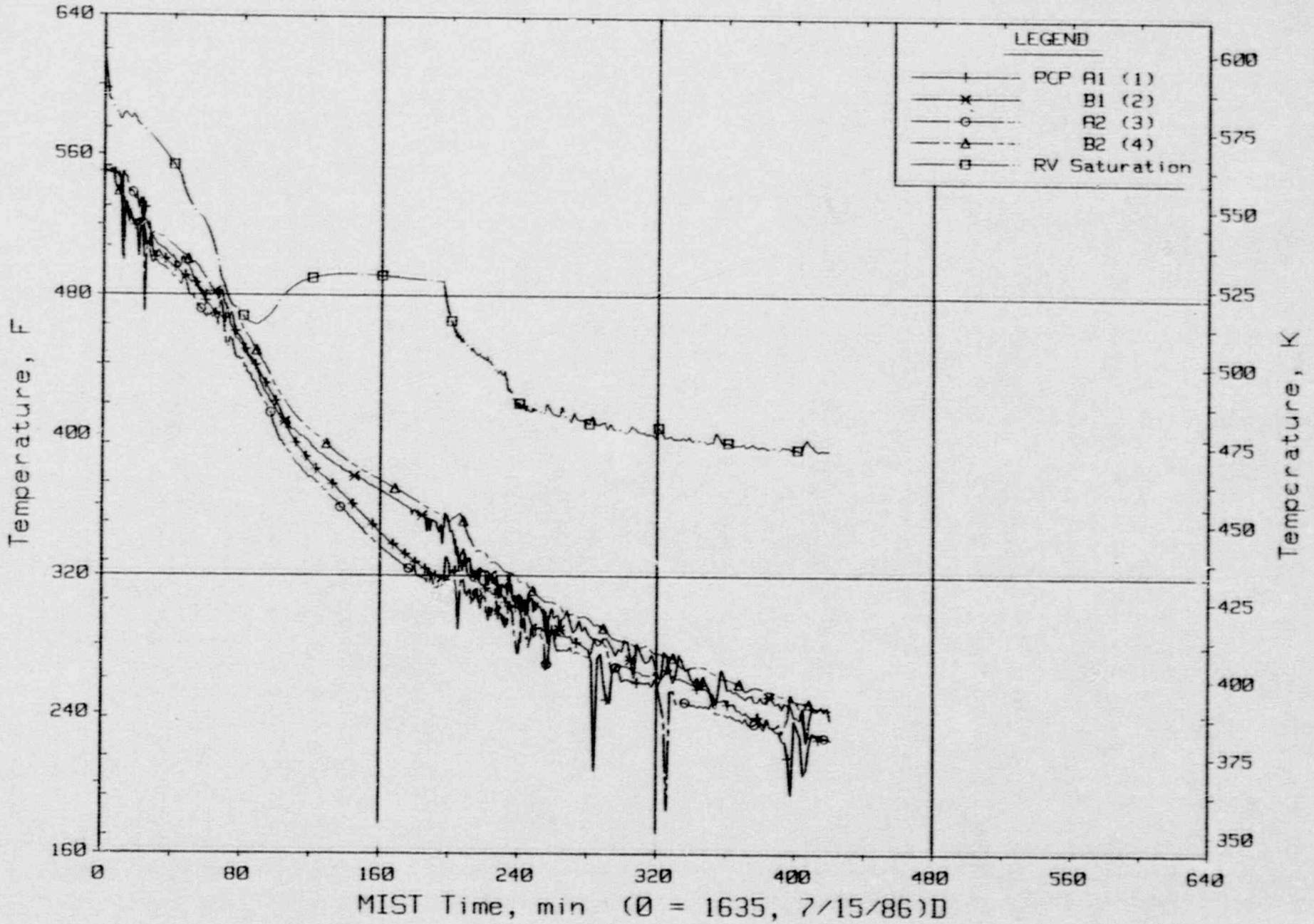

Pump Suction Fluid Temperature (CnRT01s).

Thu Oct 27 11:51:23 1988

PURT0

FINAL DATA

T320302: Group 32 SBLOCA Test 3, Cold Leg Suction Leak.

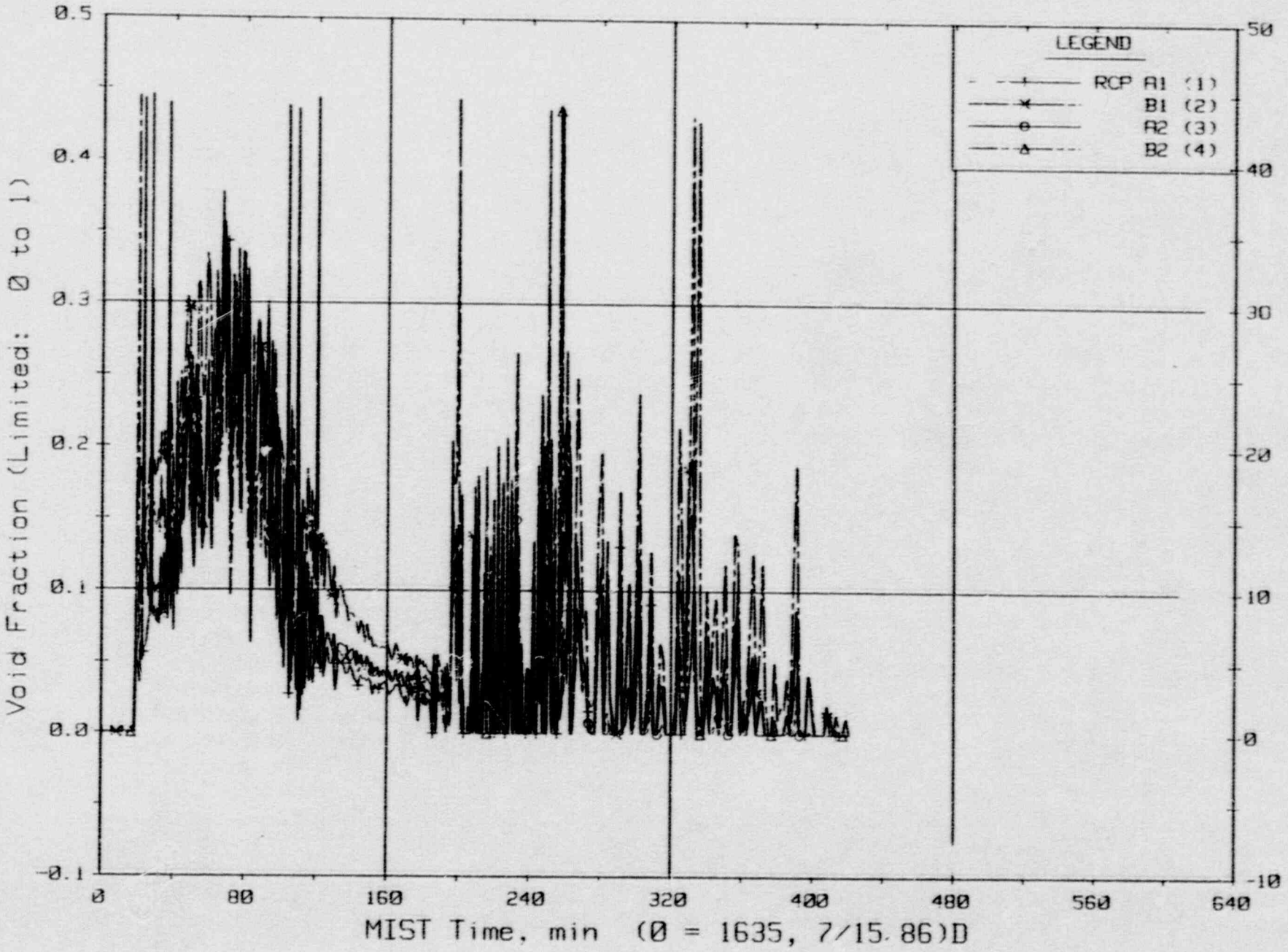

Pump Suction Void Fraction From Gamma Densitometers (CnGD21).

Thu Oct 27 11:55:46 1988

PUVF2

FINAL DATA

T320302: Group 32 SBLOCA Test 3, Cold Leg Suction Leak.

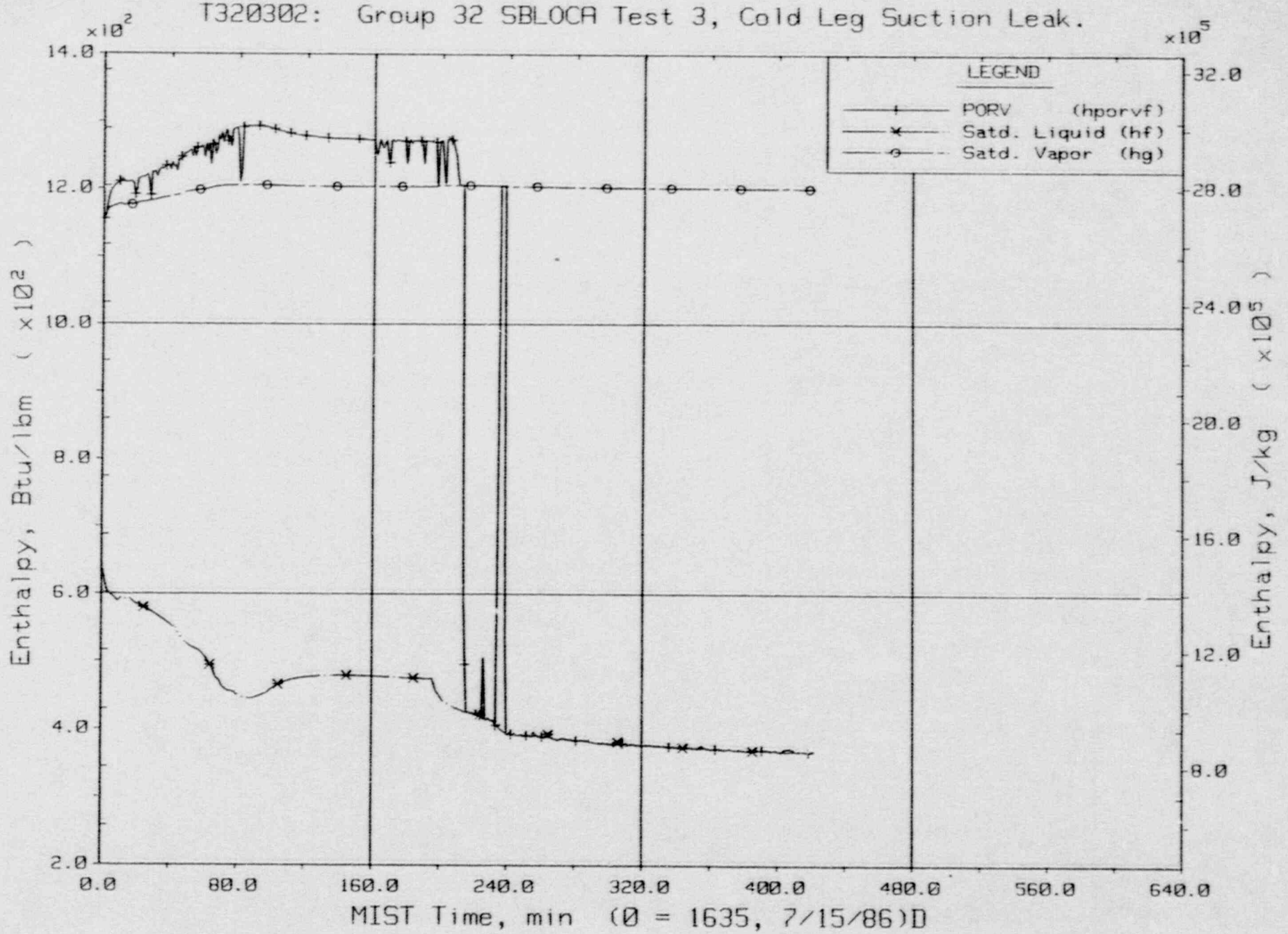

Power-Operated Relief Valve Enthalpy (Based On Flow Rate).

Wed Jun 8 13:42:53 1988

PZEN1

FINAL DATA

T320302: Group 32 SBLOCA Test 3, Cold Leg Suction Leak.

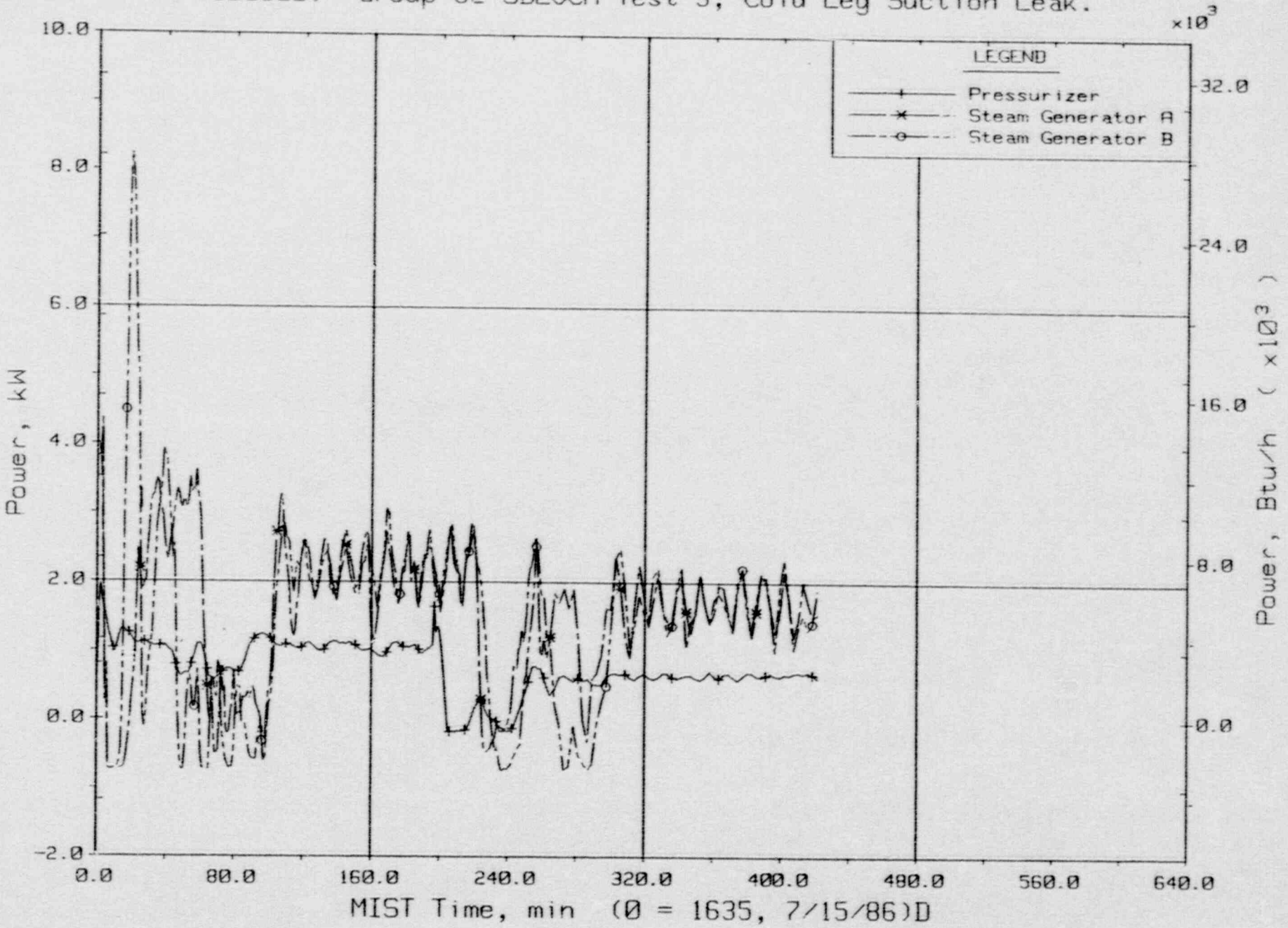

Guard Heater Specified Power, Pressurizer and Steam Generators.

Wed Jun 8 13:47:21 1988

PZGQ1

FINAL DATA

T320302: Group 32 SBLOCA Test 3, Cold Leg Suction Leak.

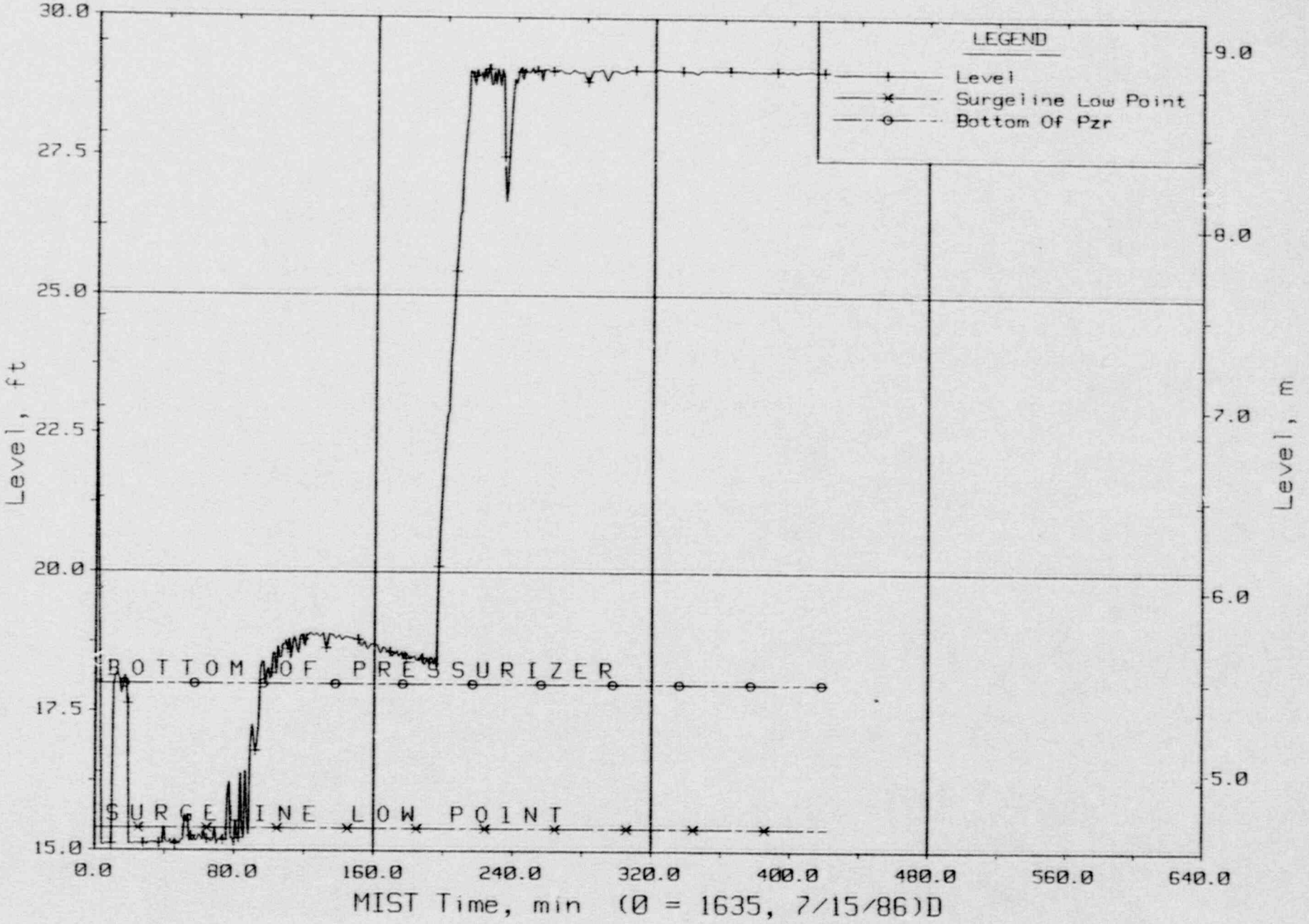

Pressurizer Collapsed Liquid Level (PZLV20).

Wed Jun 8 13:53:35 1988

PZLV1

FINAL DATA

T320302: Group 32 SBLOCA Test 3, Cold Leg Suction Leak.

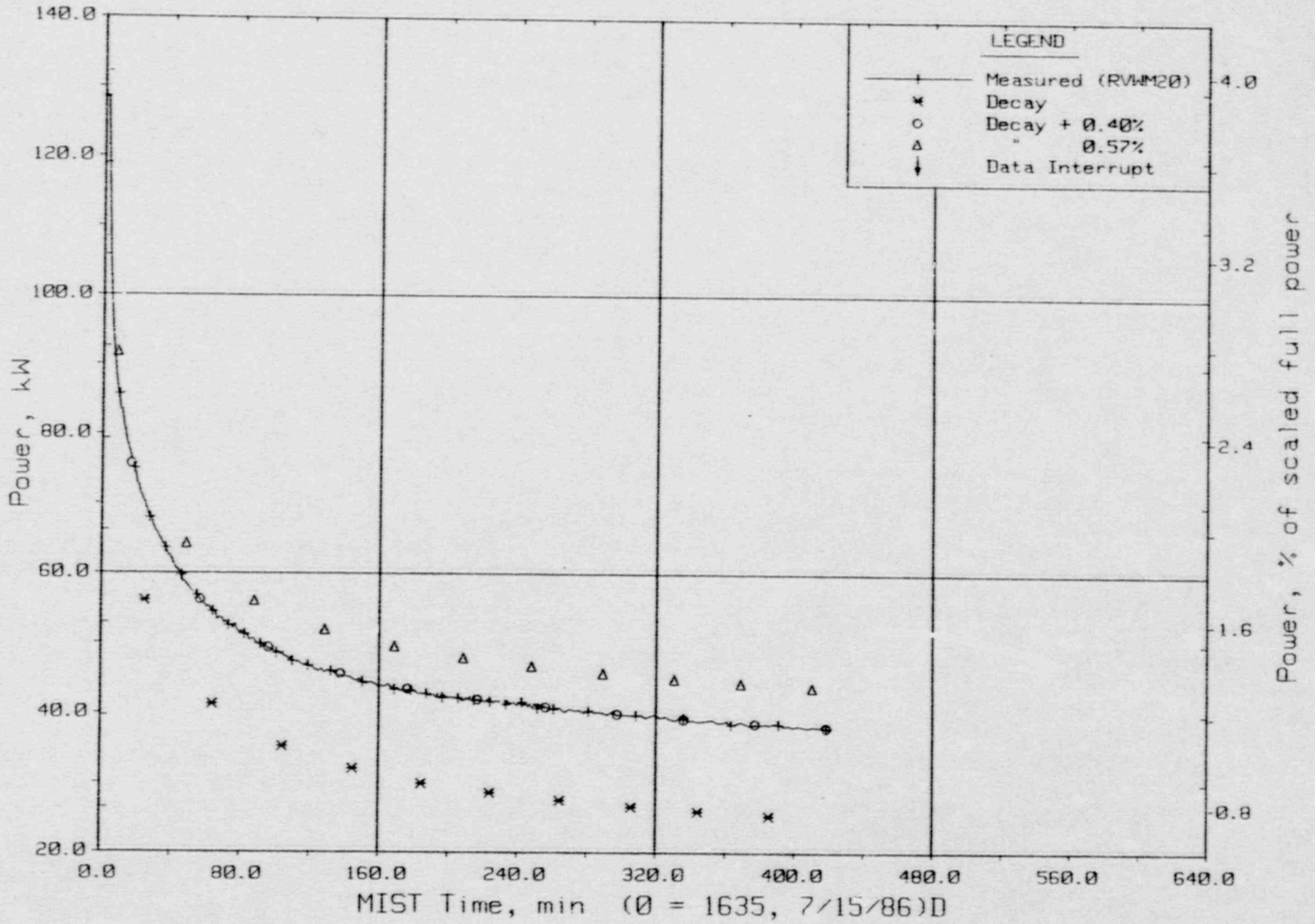

Core Power.

Wed Jun 8 13:57:27 1988

RVKW0

FINAL DATA

T320302: Group 32 SBLOCA Test 3, Cold Leg Suction Leak.

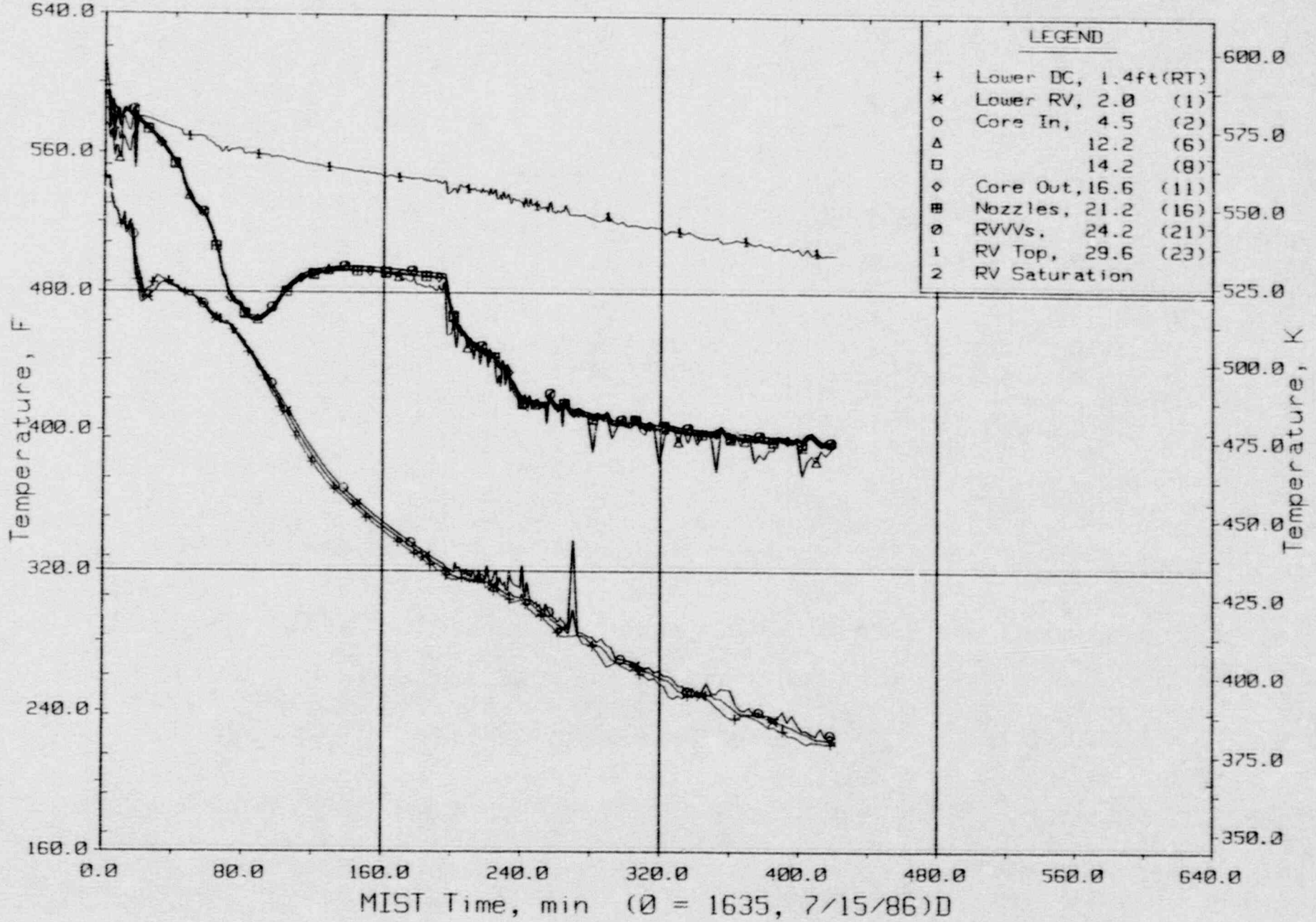

Core Unit Cell and Reactor Vessel Fluid Temperatures (RVTCs).

Wed Jun 8 14:04:46 1988

RVTC0

FINAL DATA

T320302: Group 32 SBLOCA Test 3, Cold Leg Suction Leak.

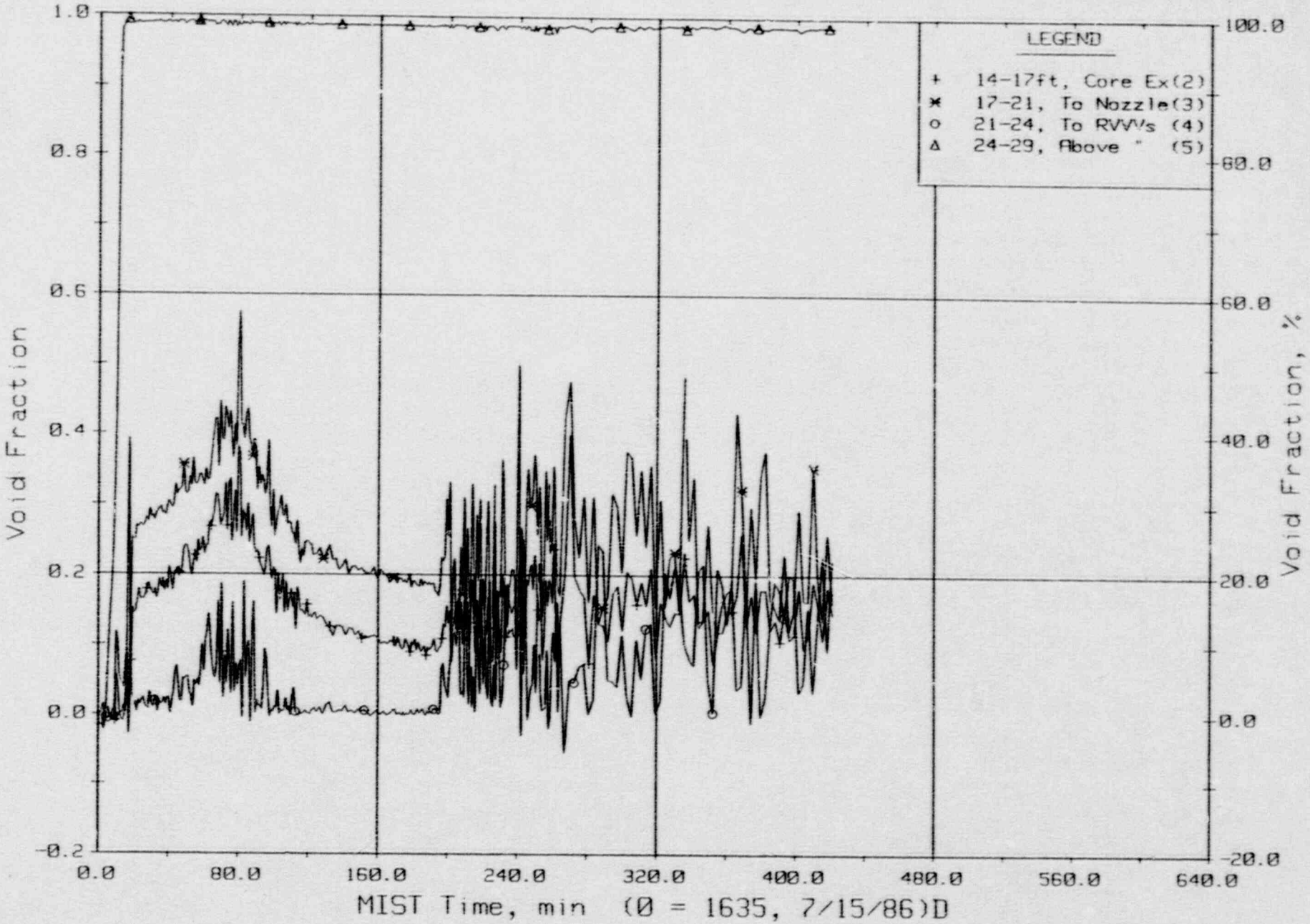

Reactor Vessel Void Fractions From Differential Pressures (RVVFs).

Wed Jun 8 14:10:09 1988

RVVF1

FINAL DATA

T320302: Group 32 SBLOCA Test 3, Cold Leg Suction Leak.

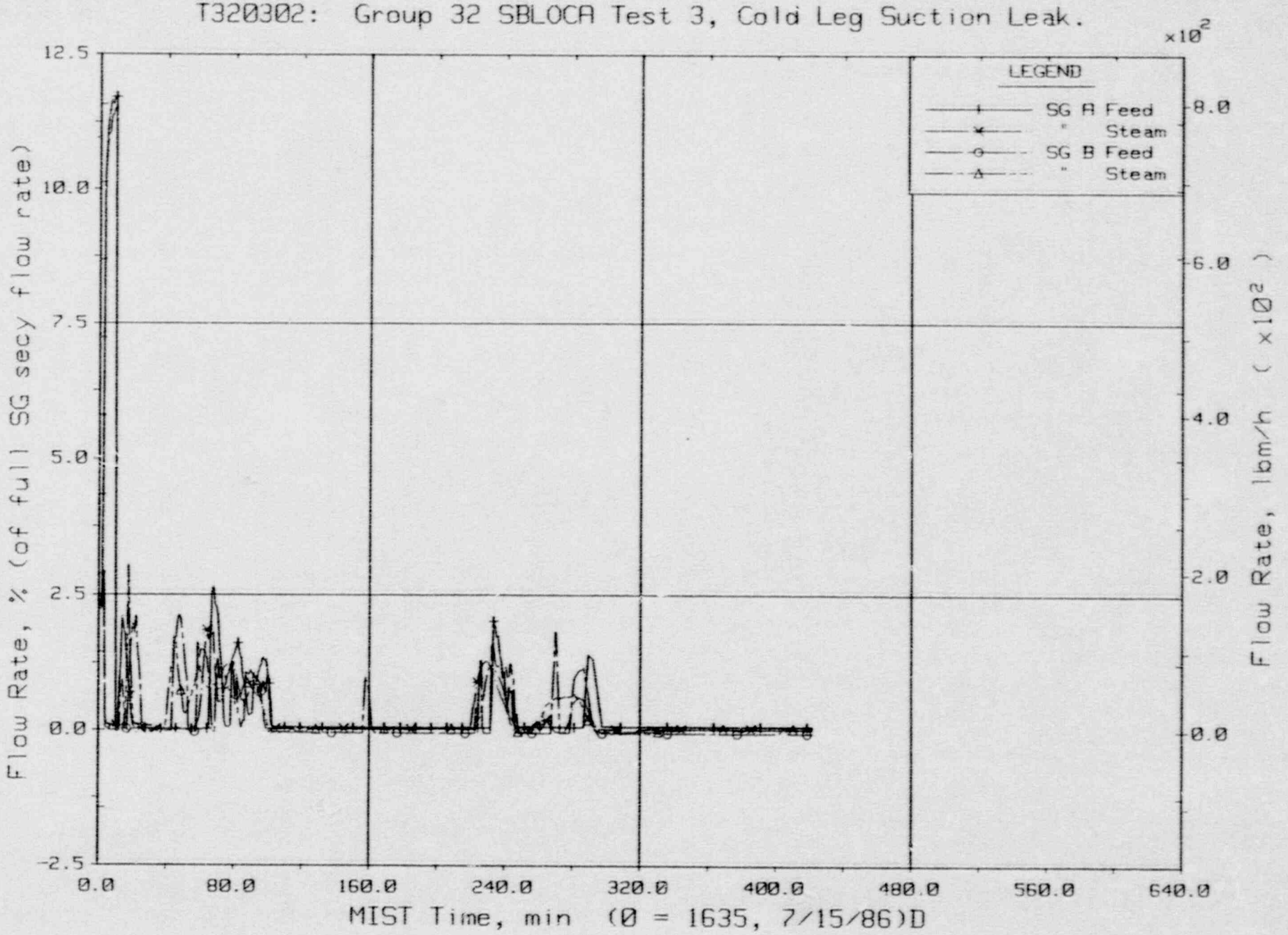

Steam Generator Secondary System Flow Rates.

Wed Jun 8 14:13:18 1988

SGFL2

FINAL DATA

T320302: Group 32 SBLOCA Test 3, Cold Leg Suction Leak.

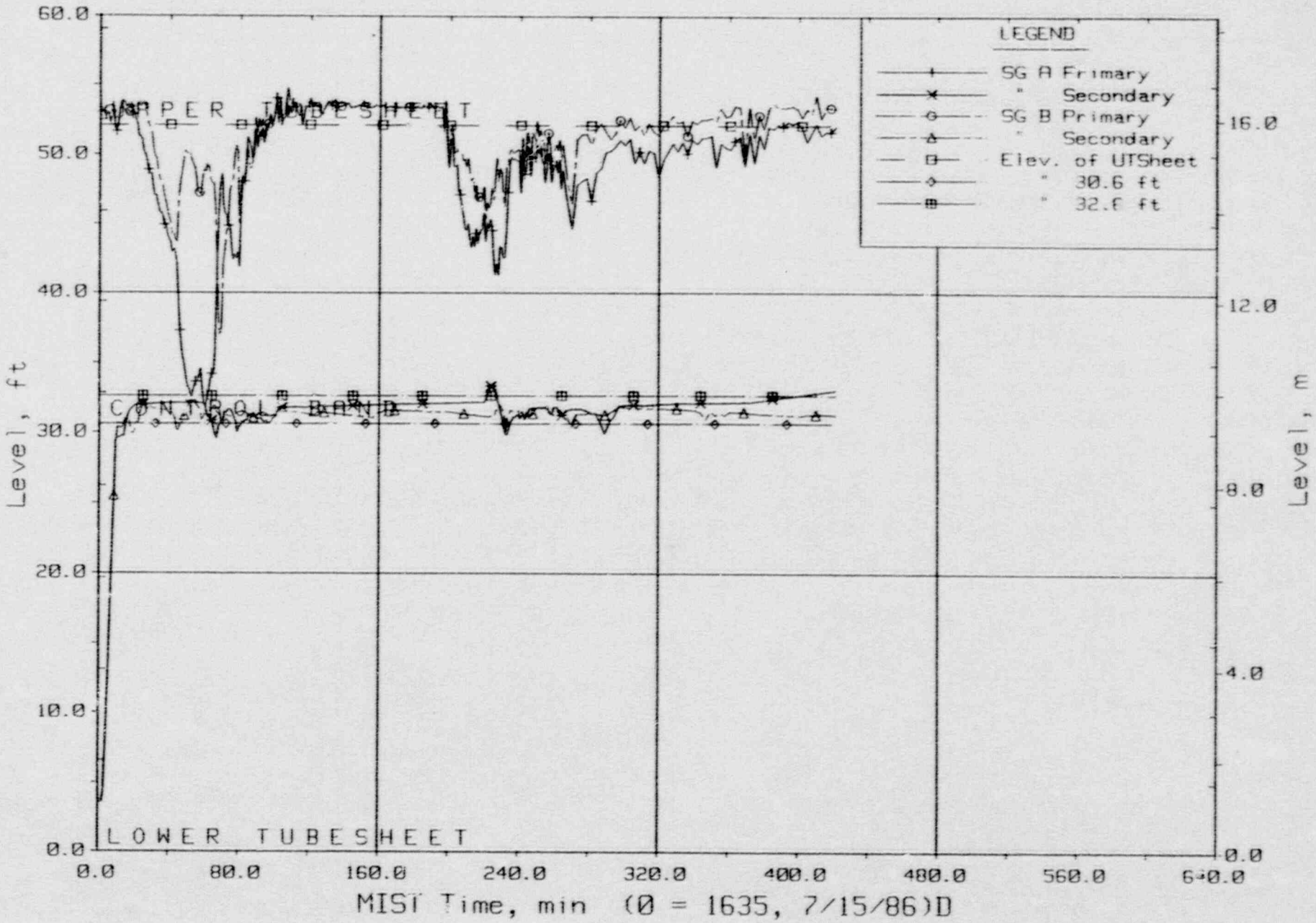

Steam Generator Collapsed Liquid Levels.

Wed Jun 8 14:16:50 1988

SGLV2

FINAL DATA

T320302: Group 32 SBLOCA Test 3, Cold Leg Suction Leak.

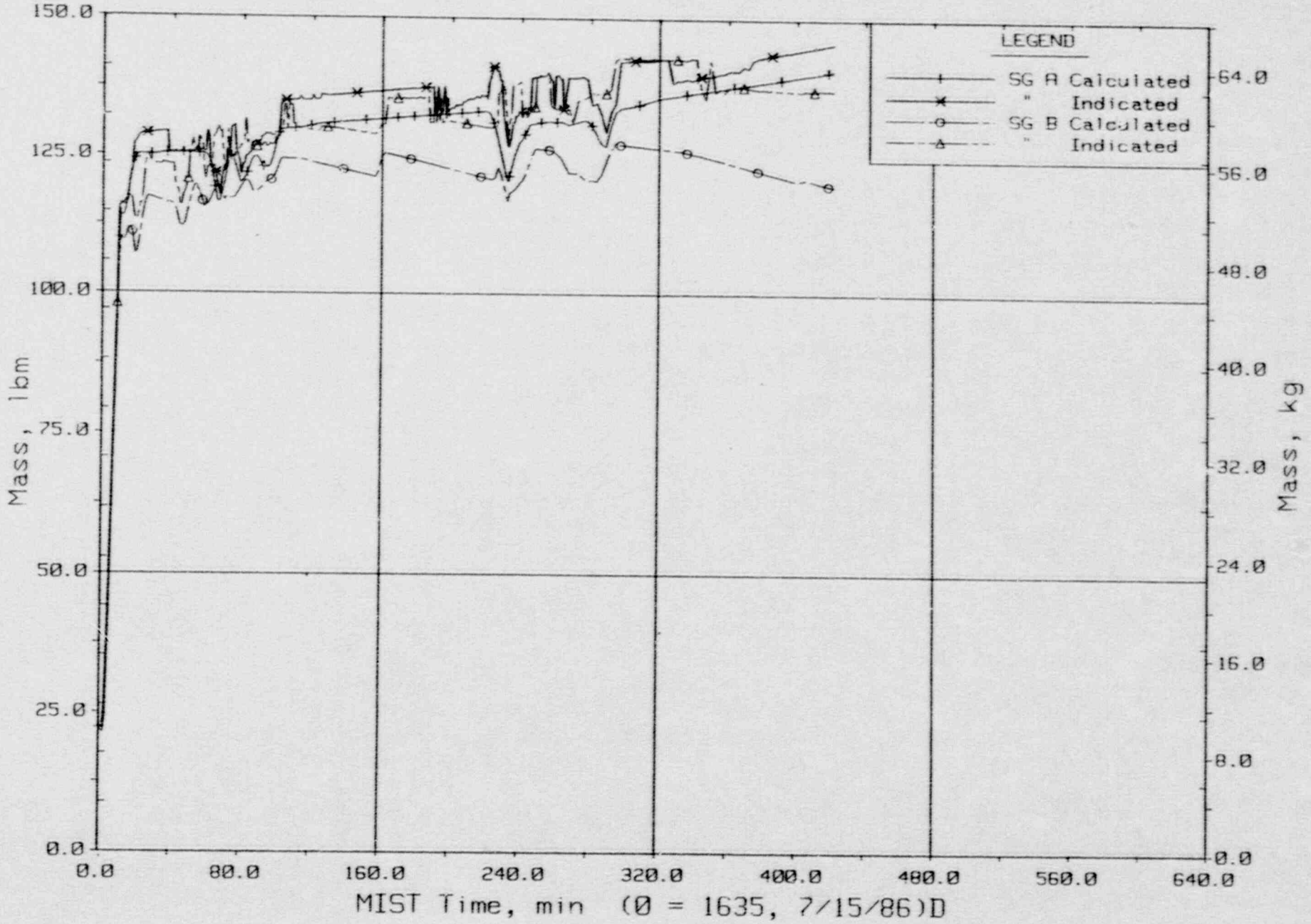

Steam Generator Secondary Fluid Mass Balances.

Wed Jun 8 14:20:20 1988

SGML1

FINAL DATA

T320302: Group 32 SBLOCA Test 3, Cold Leg Suction Leak.

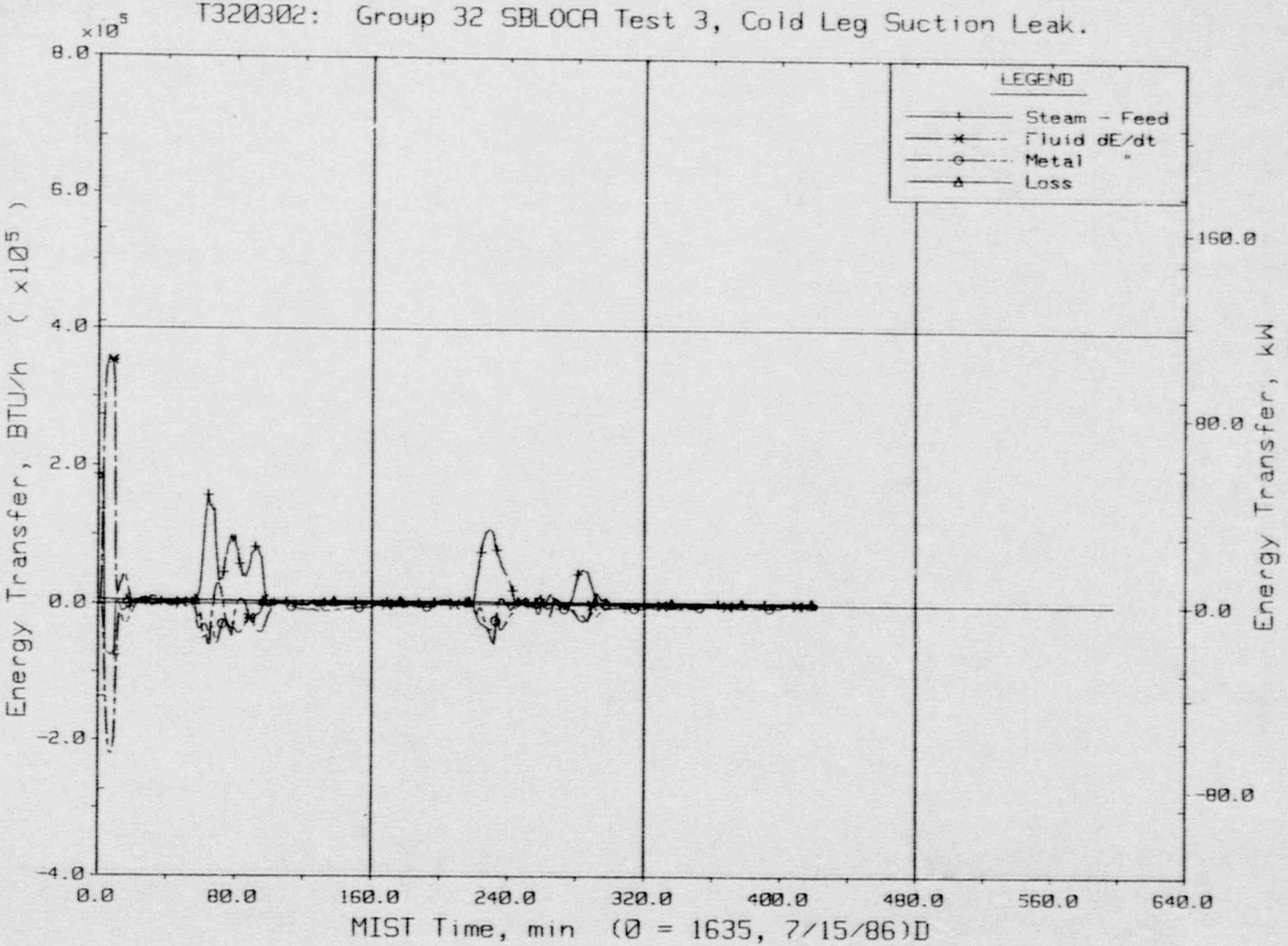

Steam Generator A Energy Transfer.

Wed Jun 8 14:23:29 1988

SGOE3

FINAL DATA

T320302: Group 32 SBLOCA Test 3, Cold Leg Suction Leak.

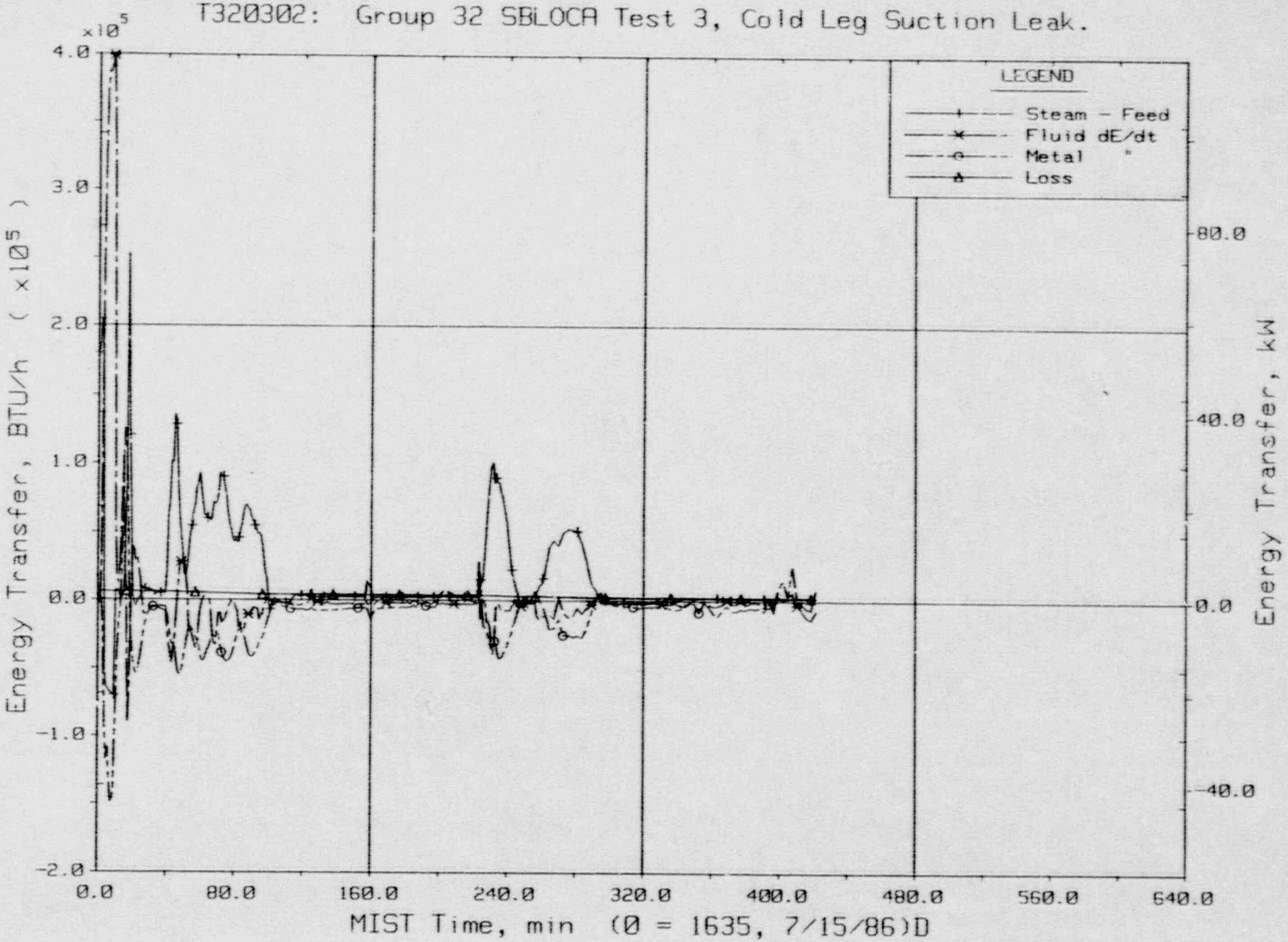

Steam Generator B Energy Transfer.

Wed Jun 8 14:26:27 1988

SGQE6

FINAL DATA

T320302: Group 32 SBLOCA Test 3, Cold Leg Suction Leak.

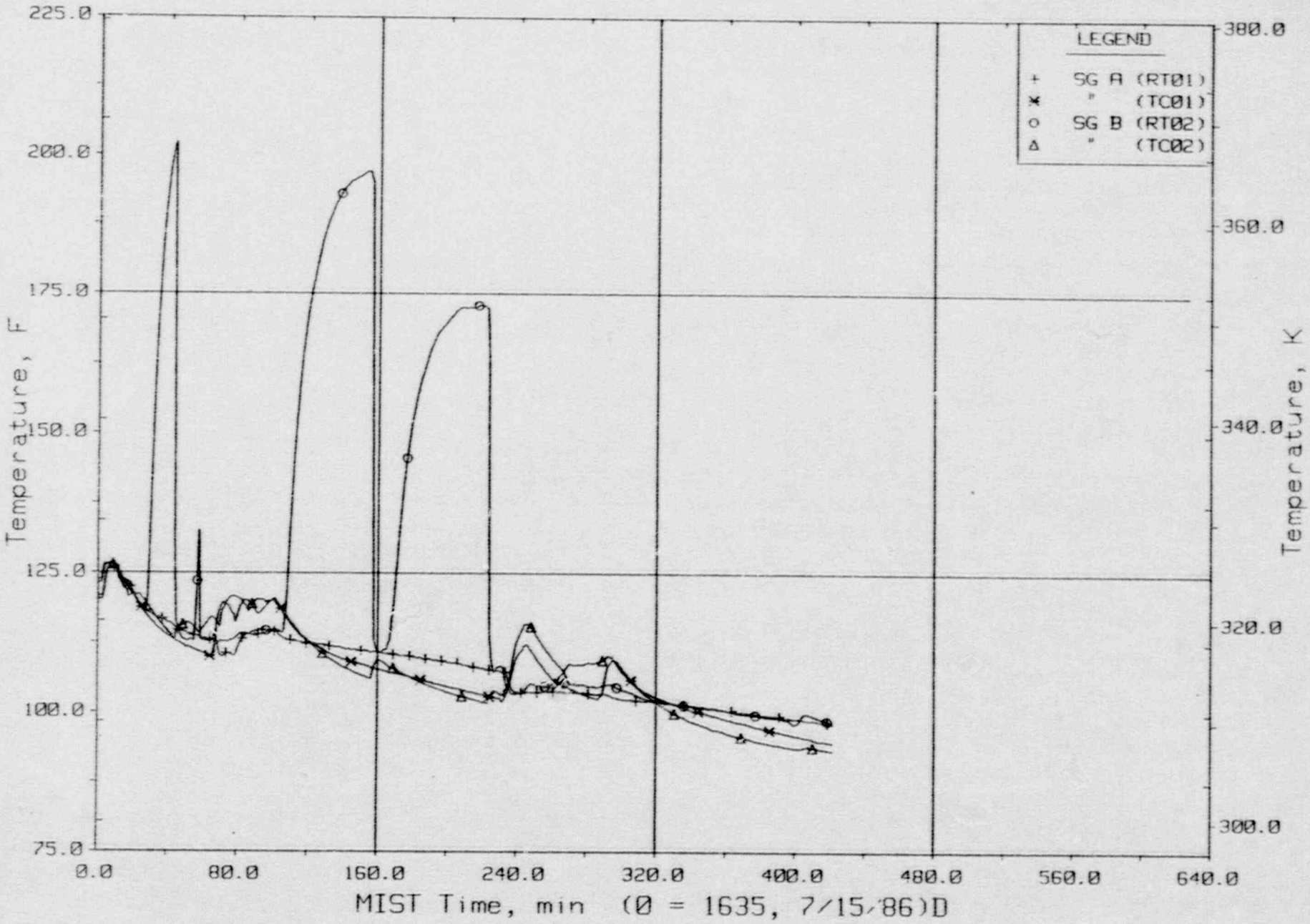

Feedwater Temperatures (SFs).

Wed Jun 8 14:28:56 1988

SGRT1

FINAL DATA

T320302: Group 32 SBLOCA Test 3, Cold Leg Suction Leak.

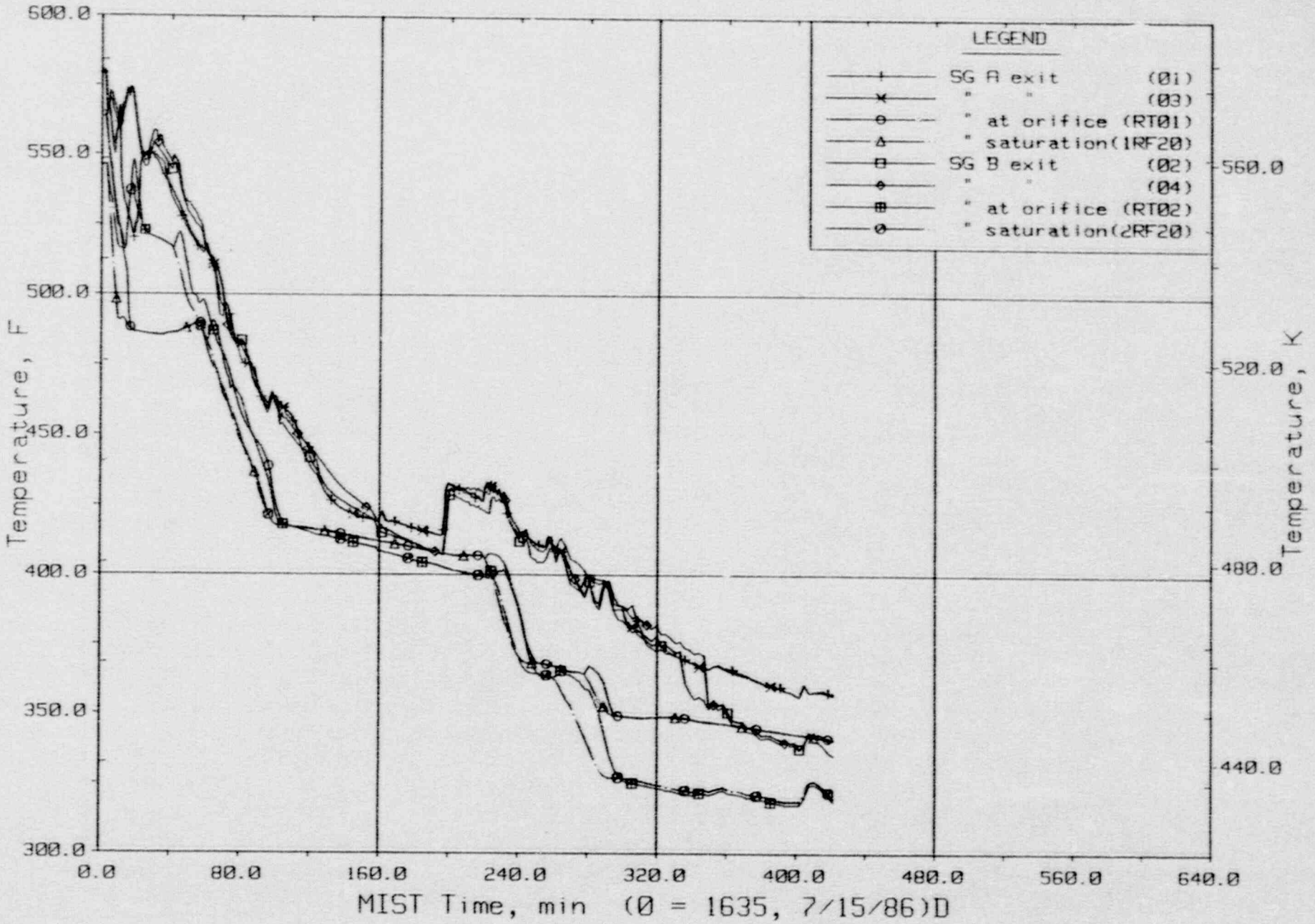

Steam Generator Steam Outlet Temperatures (SSTCs).

Wed Jun 8 14:32:02 1988

SGRT2

FINAL DATA

T320302: Group 32 SBLOCA Test 3, Cold Leg Suction Leak.

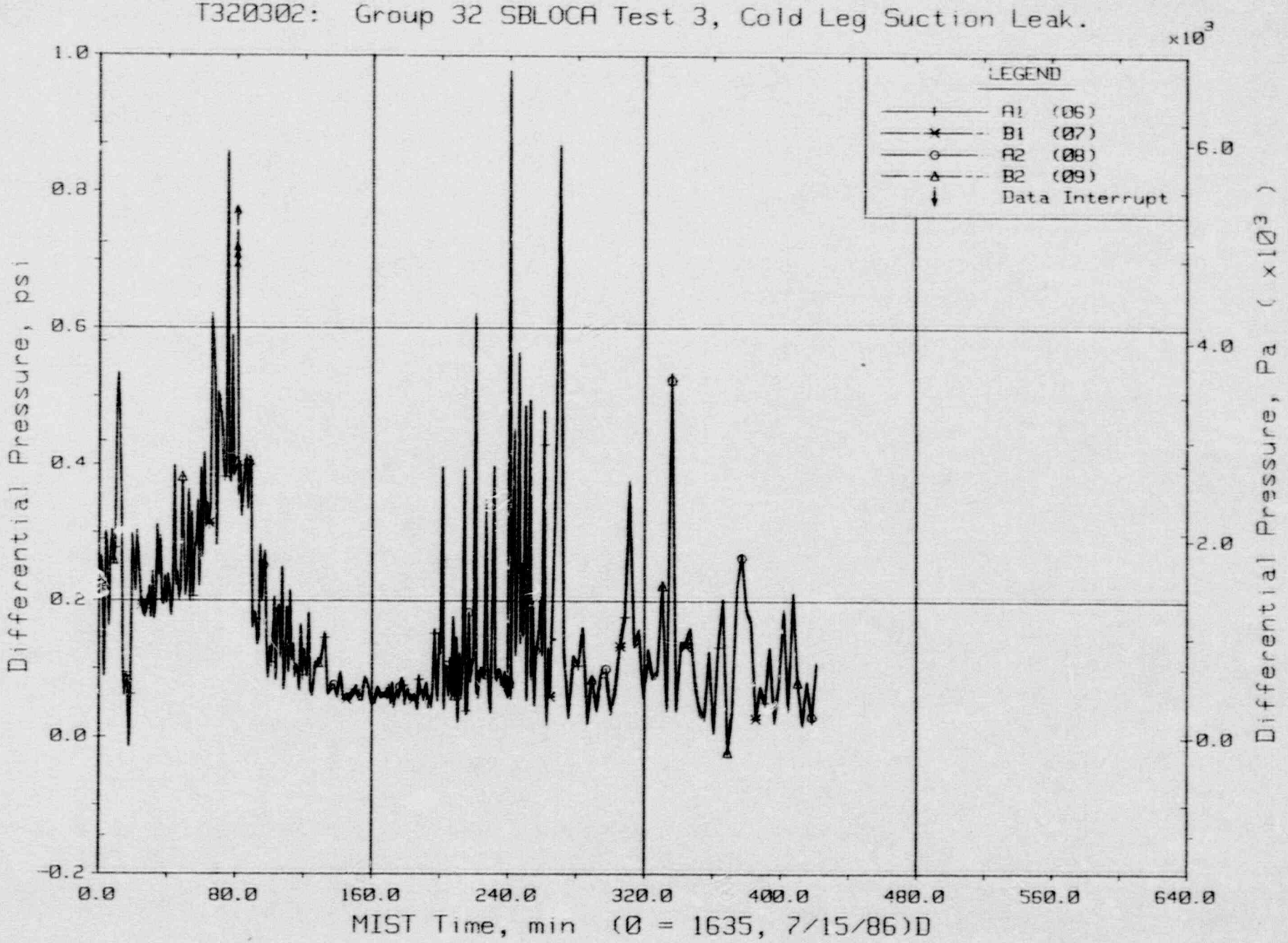

Reactor Vessel Vent Valve Differential Pressures (RVDPs).

Wed Jun 8 14:36:22 1988

VVDP1

FINAL DATA

T320302: Group 32 SBLOCA Test 3, Cold Leg Suction Leak.

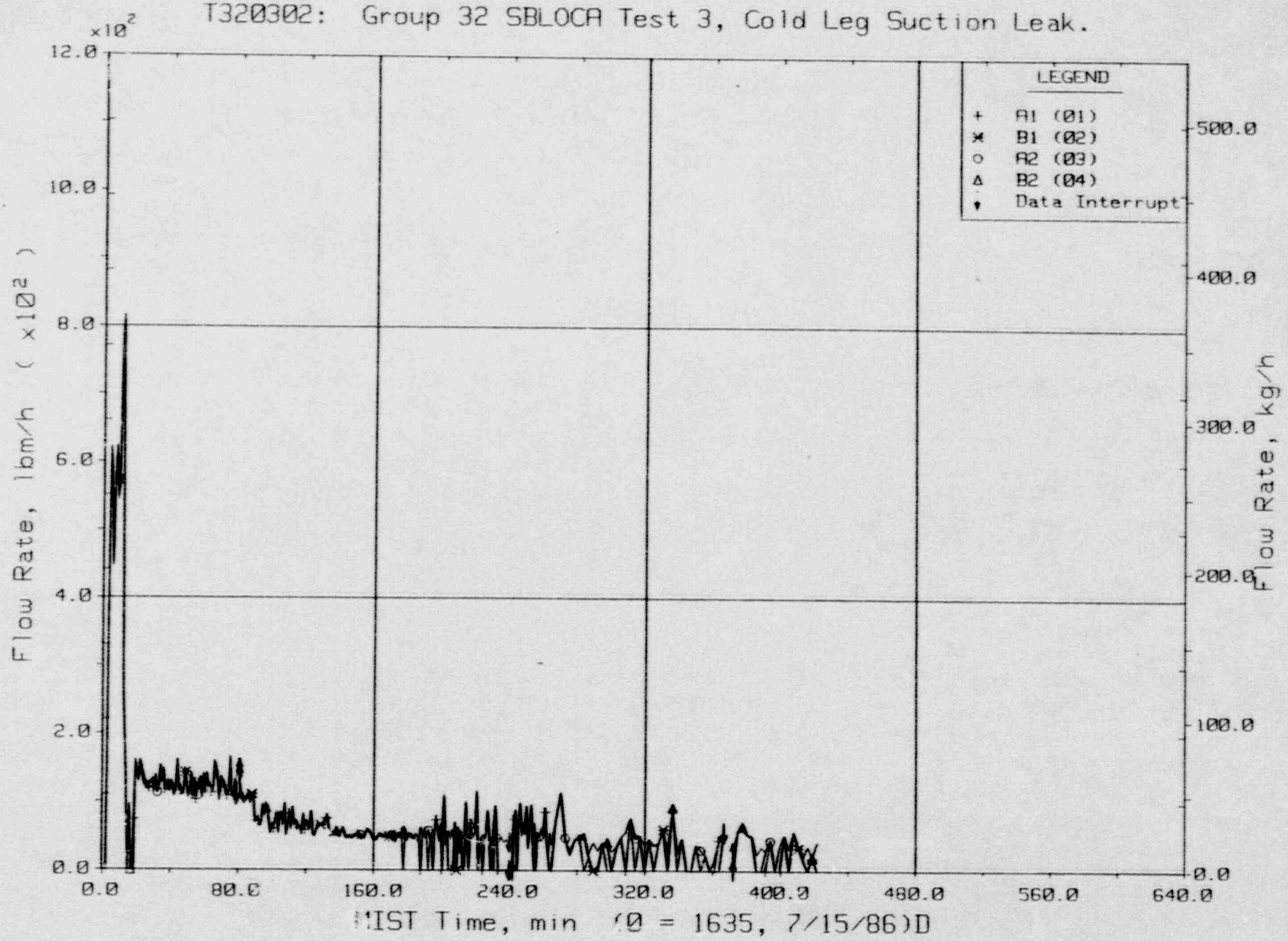

Reactor Vessel Vent Valve Flow Rates (RVORs).

Wed Jun 8 14:40:17 1988

VVFL1

FINAL DATA

T320302: Group 32 SBLOCA Test 3, Cold Leg Suction Leak.

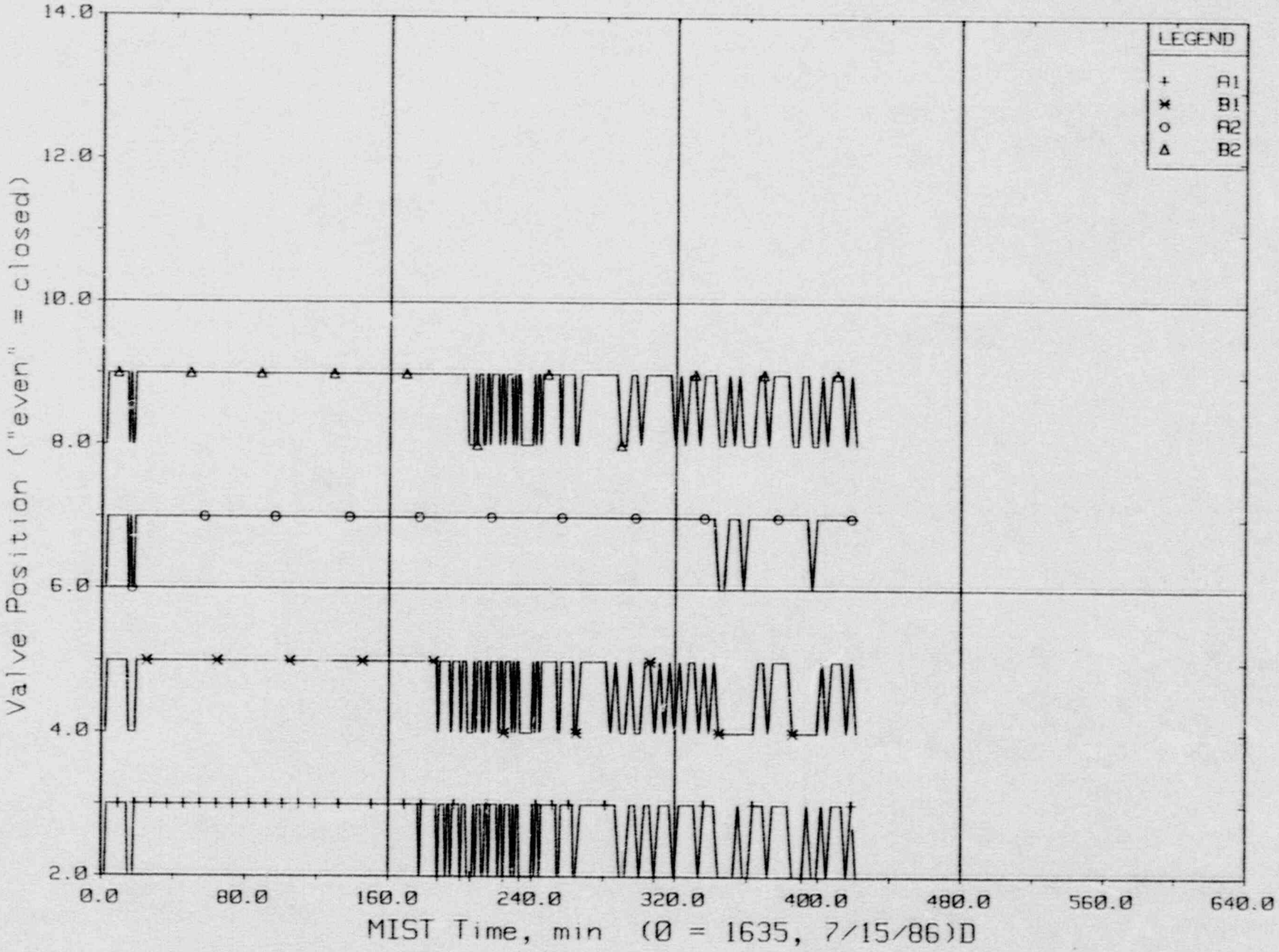

Reactor Vessel Vent Valve Positions.

Wed Jun 8 14:45:05 1988

VVLS1

FINAL DATA

T320302: Group 32 SBLOCA Test 3, Cold Leg Suction Leak.

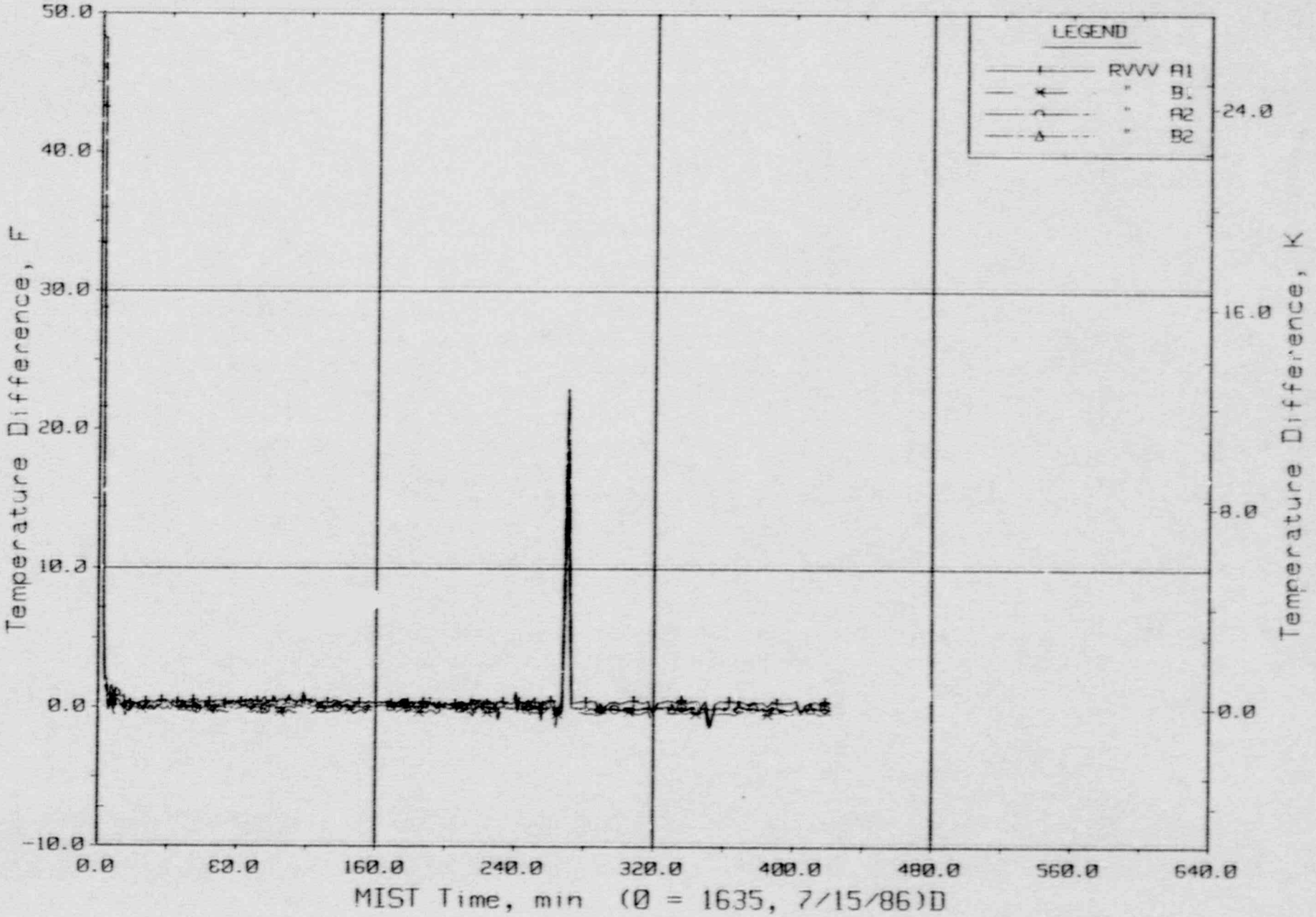

Temperature Differences Across Vent Valves.

Wed Jun 8 14:47:27 1988

VVTD1


T3204AA

FINAL DATA

T3204AA: Group 32 SBLOCA Test 4, PORV Break.

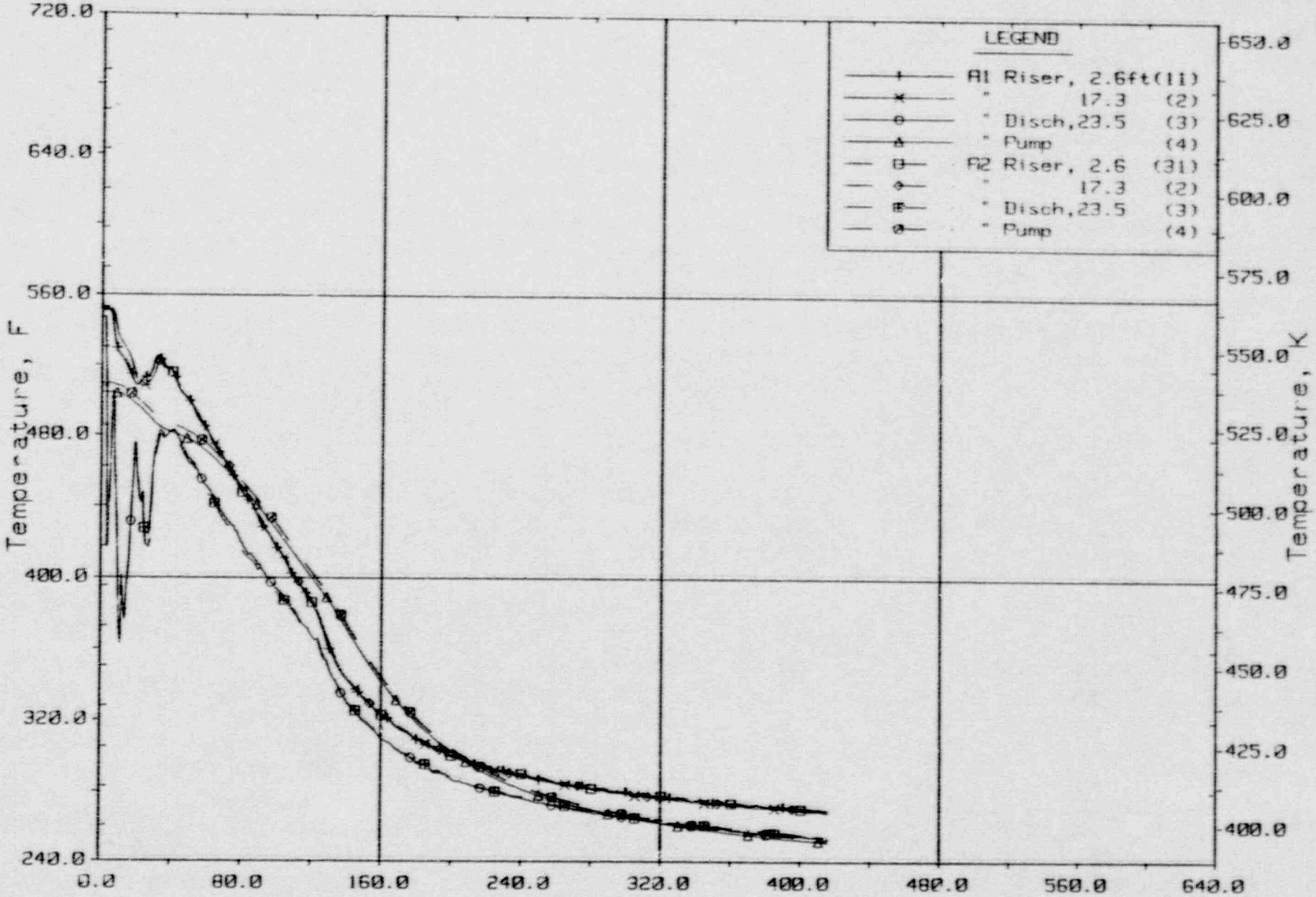

Loop A Cold Leg Metal Temperatures (C1,3MTs).

Wed Jun 8 16:19:14 1988

C1MT1

FINAL DATA

T3204AA: Group 32 SBLOCA Test 4, PORV Break.

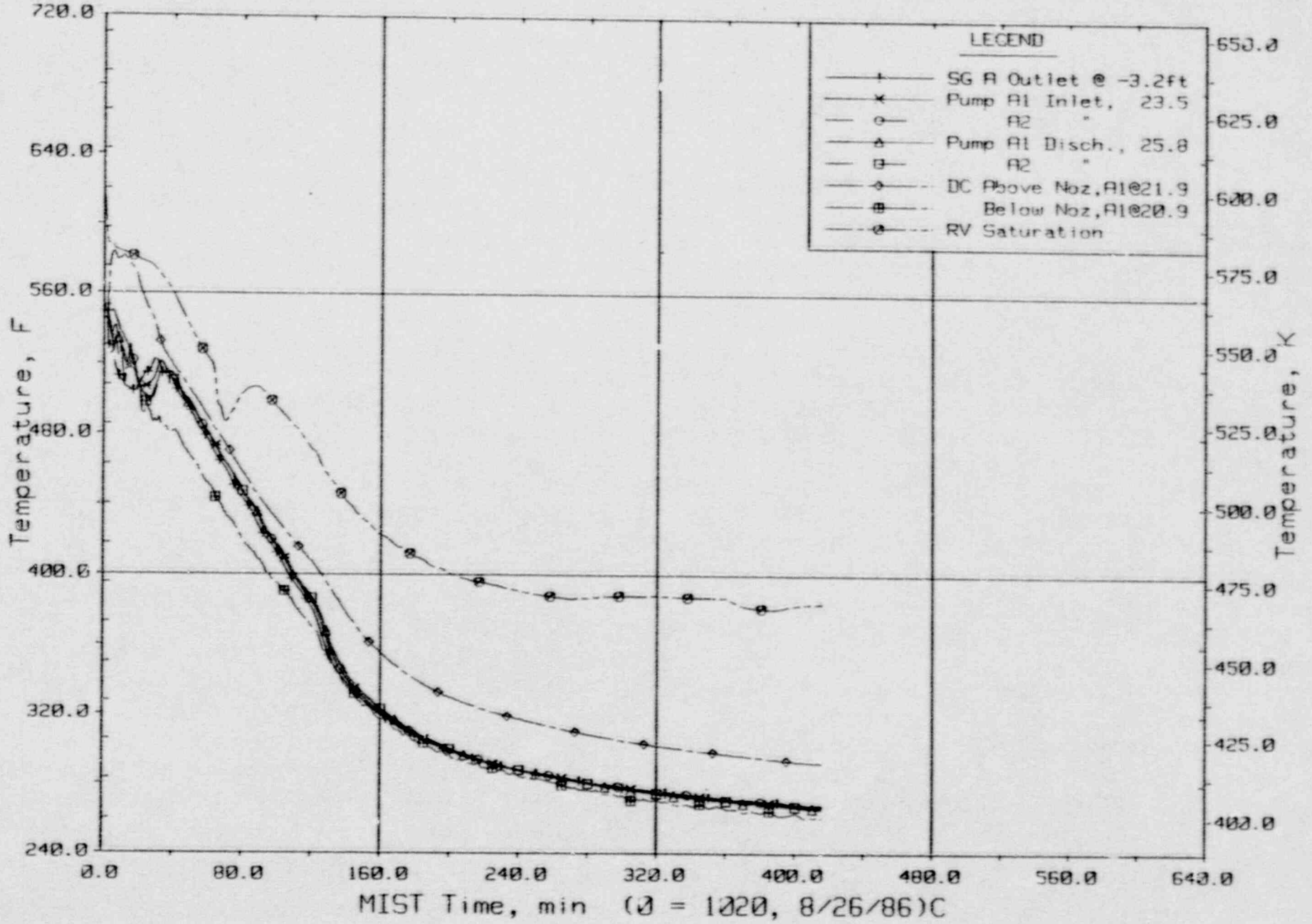

Loop A Cold Leg Fluid Temperatures (RTDs).

Wed Jun 8 16:23:24 1988

C1RTØ

FINAL DATA

T3204AA: Group 32 SBLOCA Test 4, PORV Break.

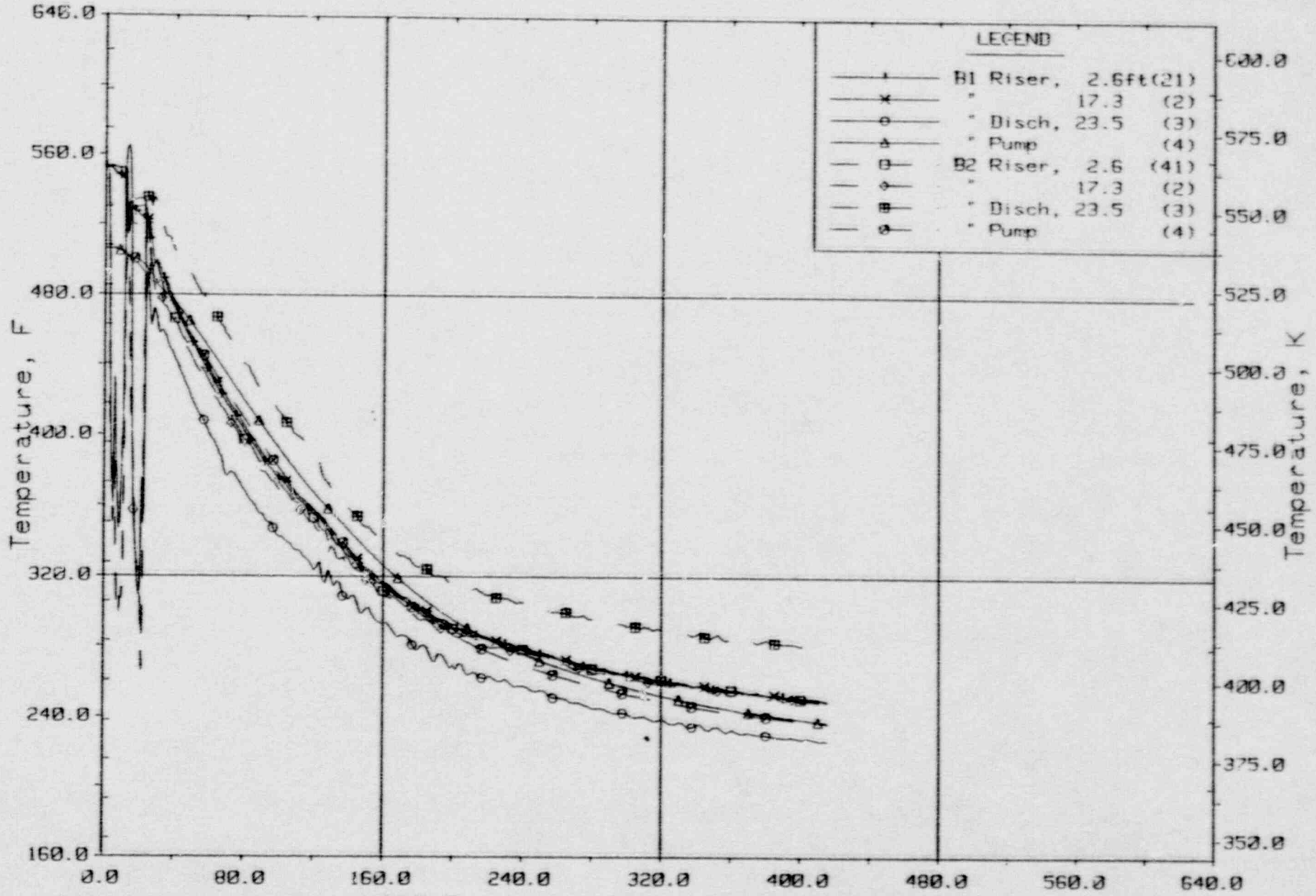

Loop B Cold Leg Metal Temperatures (C2,4MTs).

Wed Jun 8 16:28:17 1988

C2MT1

FINAL DATA

T3204AA: Group 32 SBLOCA Test 4, PORV Break.

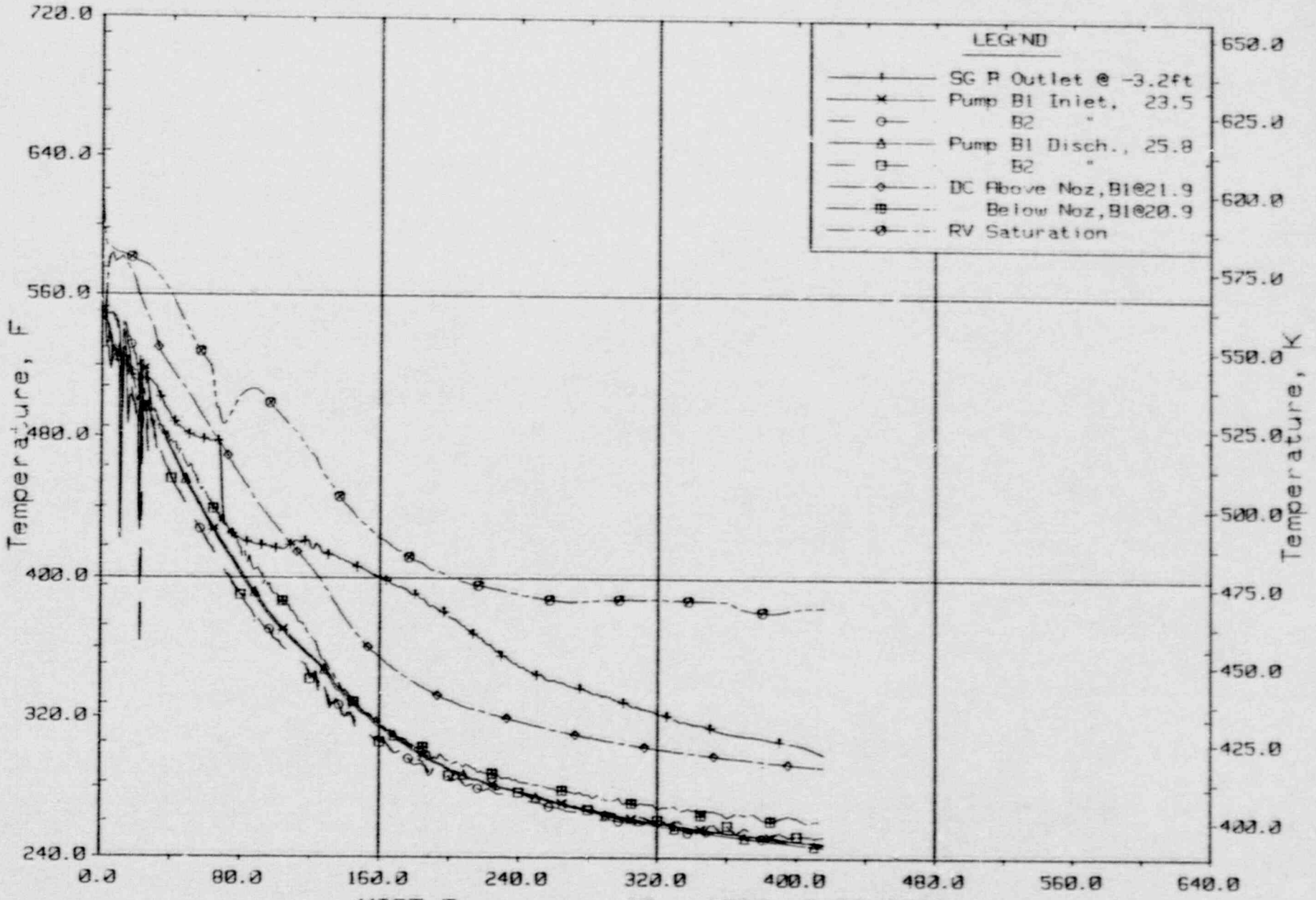

Loop B Cold Leg Fluid Temperatures (RTDs).

Wed Jun 8 16:33:38 1988

C2RT0

FINAL DATA

T3204AA: Group 32 SBLOCA Test 4, PORV Break.

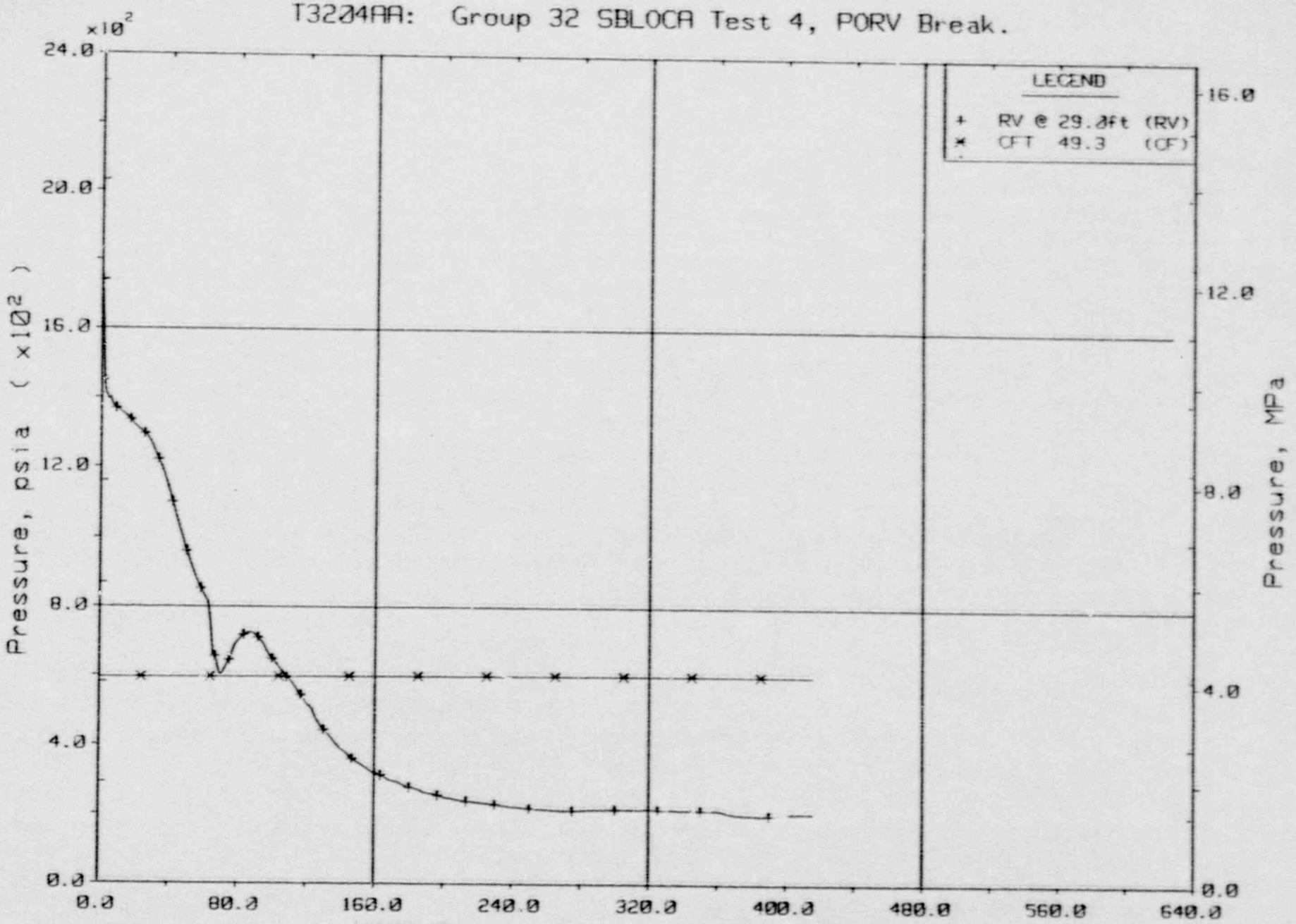

Primary System and Core Flood Tank Pressures (GP01s).

Wed Jun 8 16:36:32 1988

CFGP1

FINAL DATA

T3204AA: Group 32 SBLOCA Test 4, PORV Break.

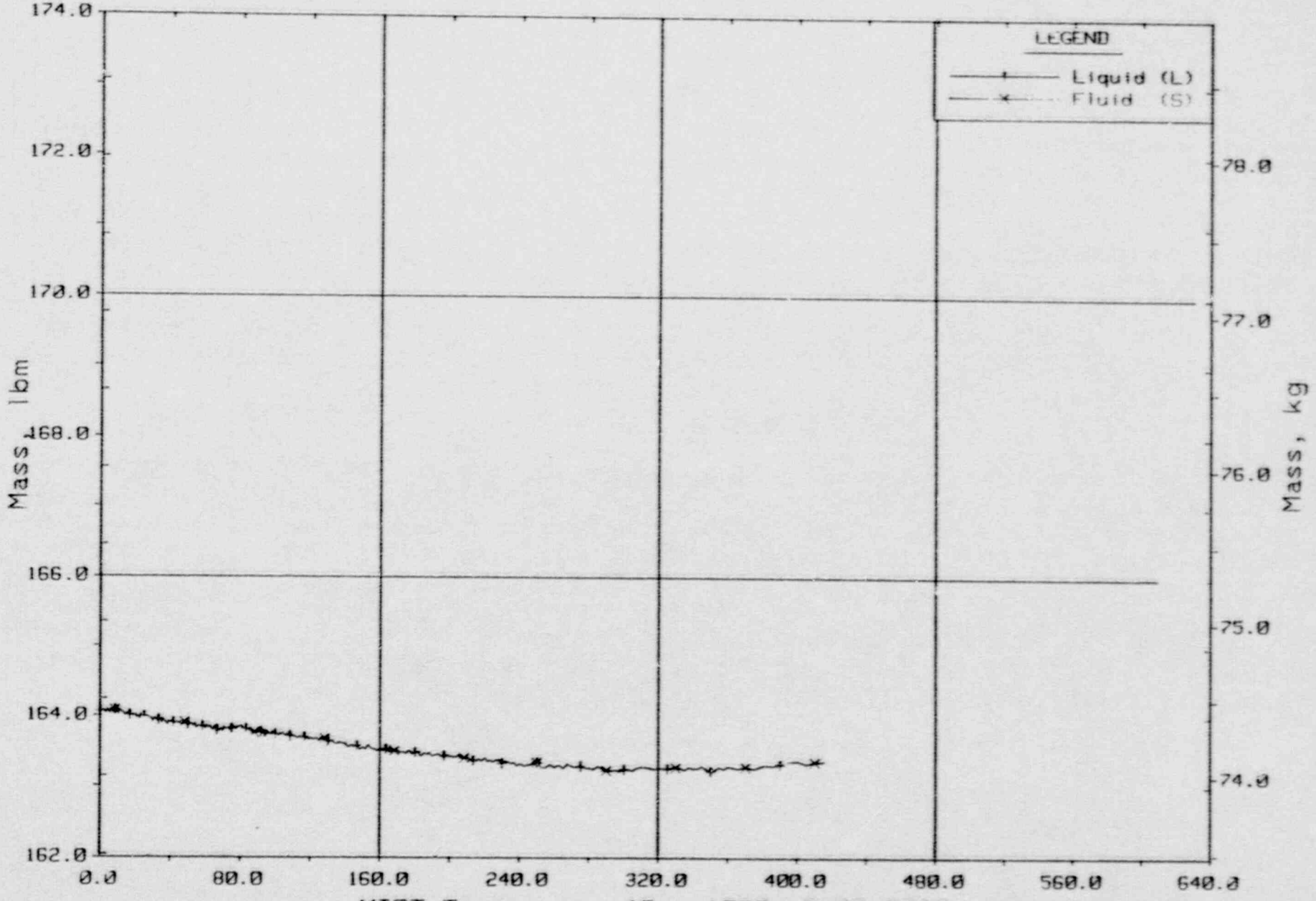

Core Flood Tank Liquid and Fluid Mass (CFMa20s).

Wed Jun 8 16:39:18 1988

CFML1

FINAL DATA

T3204AA: Group 32 SBLOCA Test 4, PORV Break.

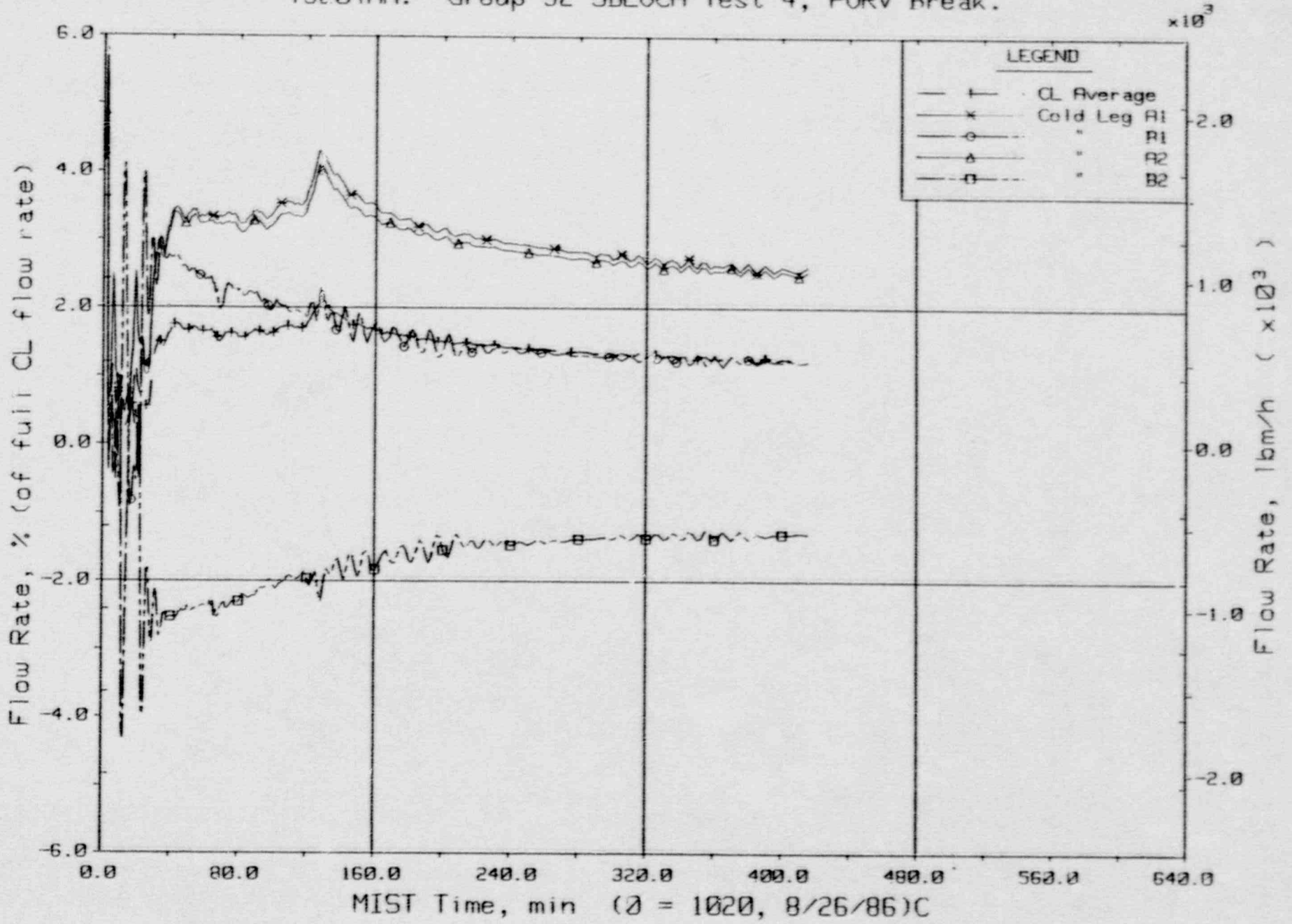

Cold Leg (Venturi) Flow Rates.

Wed Jun 8 16:43:57 1988

CLFL1

FINAL DATA

T3204AA: Group 32 SBLOCA Test 4, PORV Break.

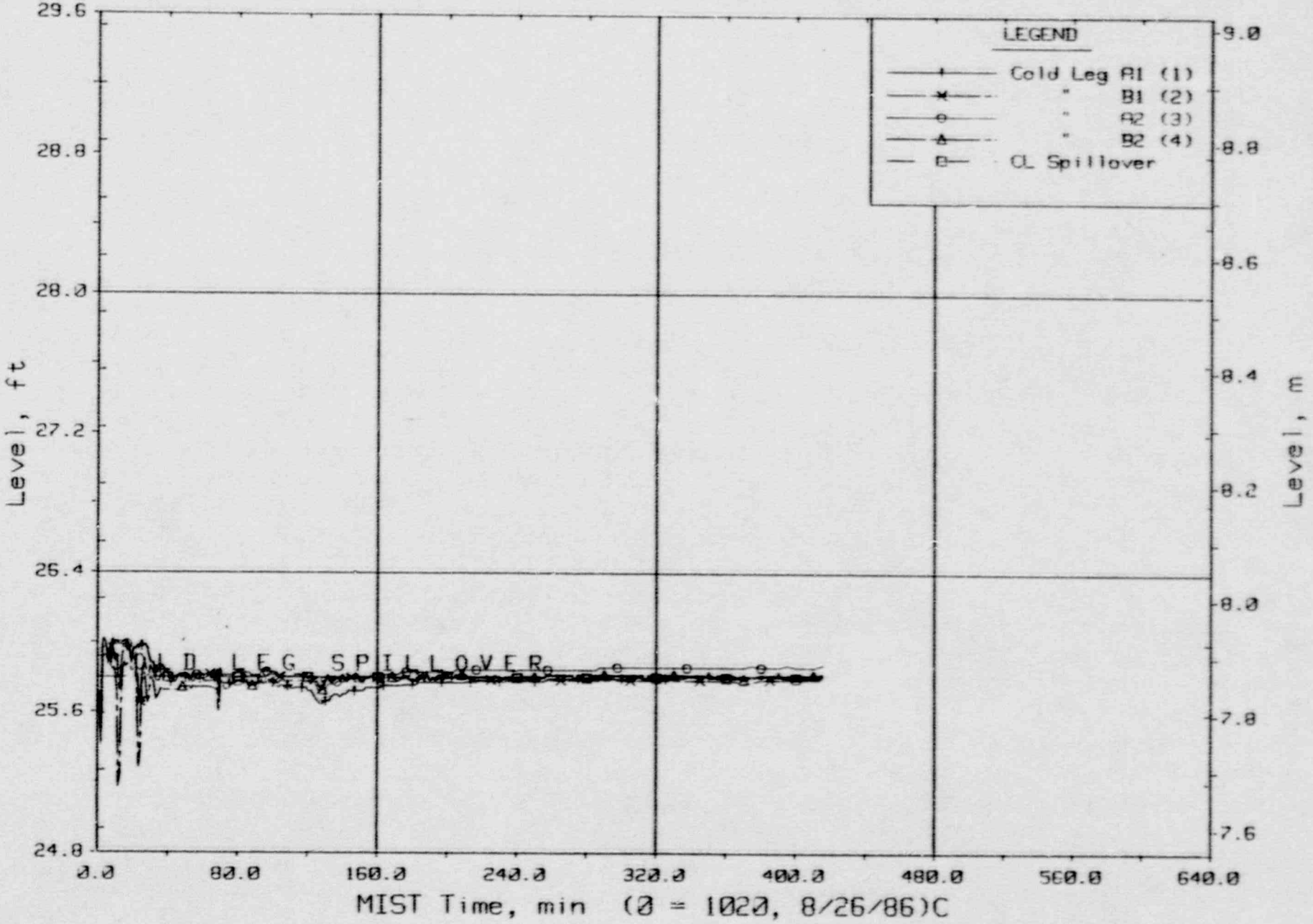

Cold Leg Suction Collapsed Liquid Levels (CnLV22s).

Wed Jun 8 16:50:17 1988

CLLV4

FINAL DATA

T3204AA: Group 32 SBLOCA Test 4, PORV Break.

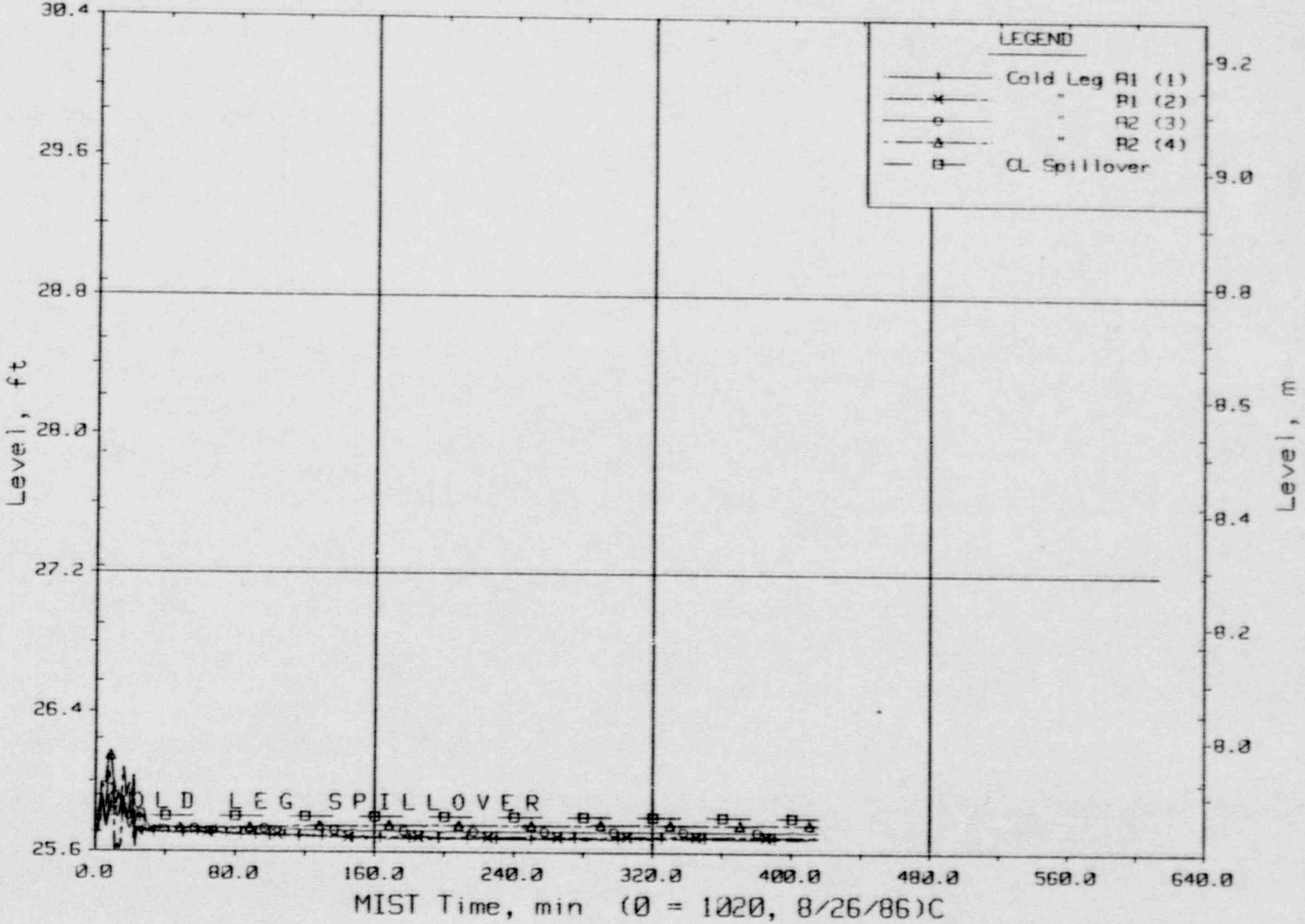

Cold Leg Discharge Collapsed Liquid Levels (CnLV23s).

Wed Jun 8 16:52:52 1988

CLLV5

FINAL DATA

T3204AA: Group 32 SBLOCA Test 4, PORV Break.

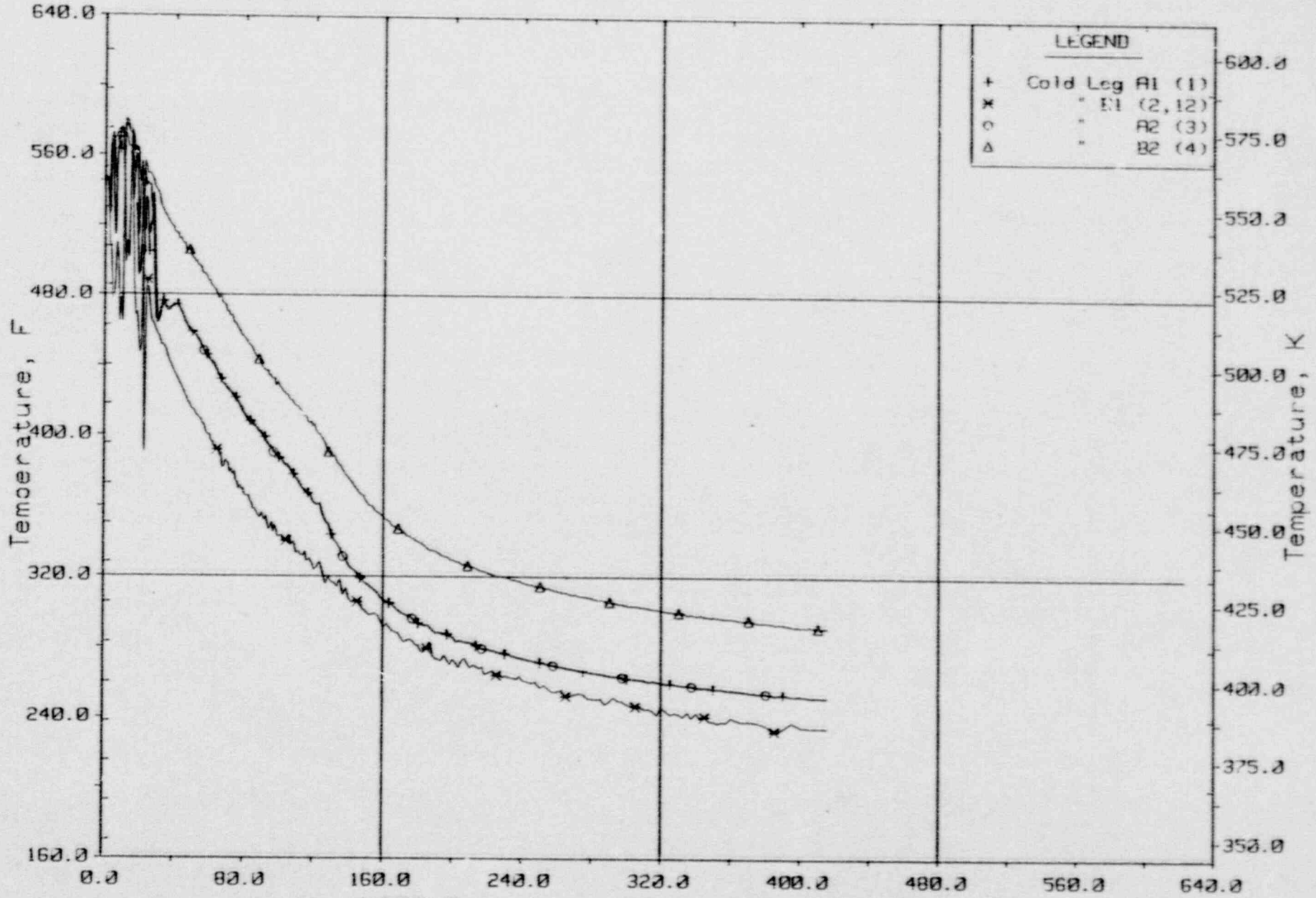

Cold Leg Nozzle Fluid Temperatures, Top of Rake (21.3ft, CnTC11s).

Wed Jun 8 15:57:01 1988

CLTC1

FINAL DATA

T3204AA: Group 32 SBLOCA Test 4, PORV Break.

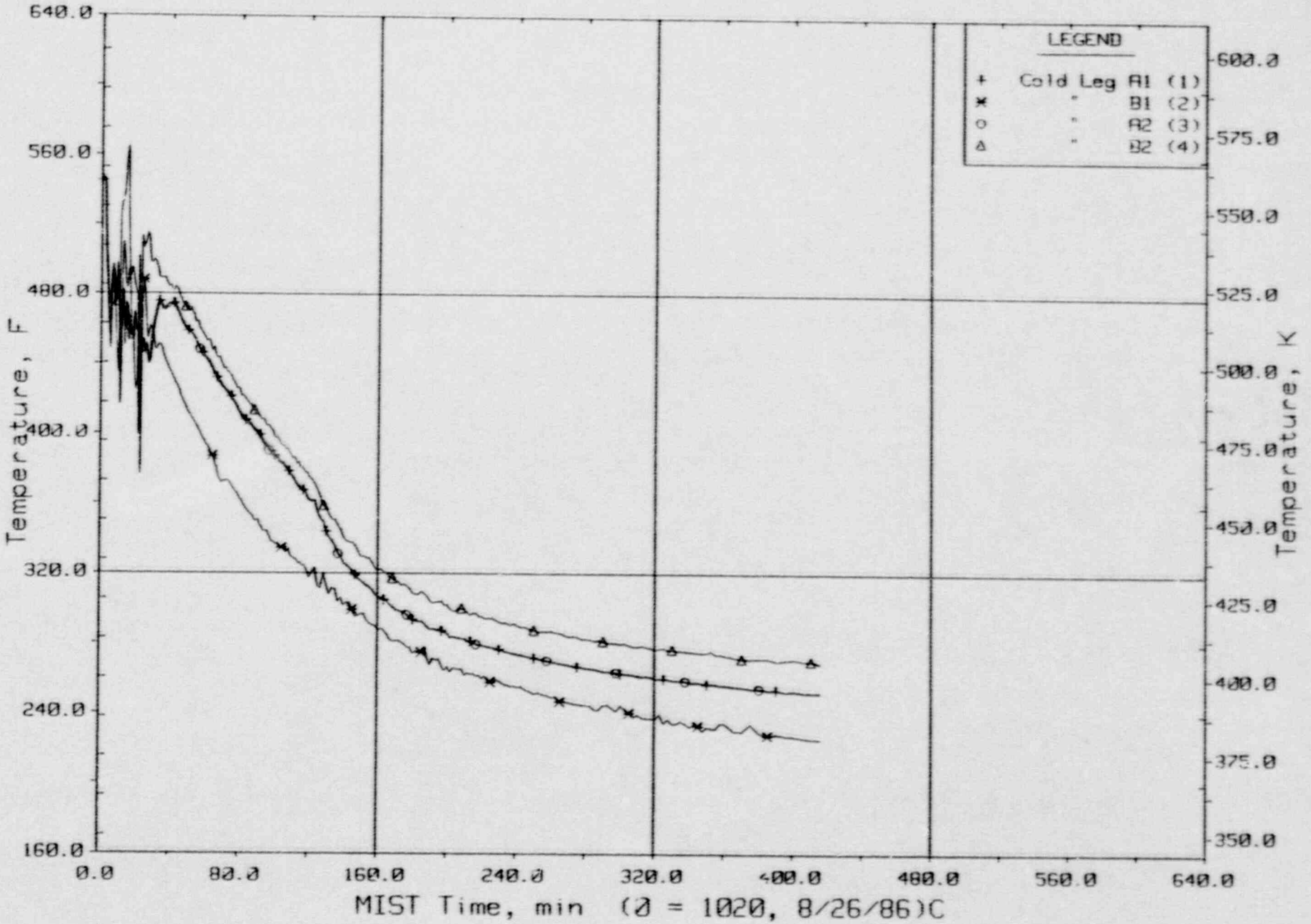

Cold Leg Nozzle Fluid Temperatures, Bottom of Rake (21.2ft, CnTC14s).

Wed Jun 8 16:59:24 1988

CLTC2

FINAL DATA

T3204AA: Group 32 SBLOCA Test 4, PORV Break

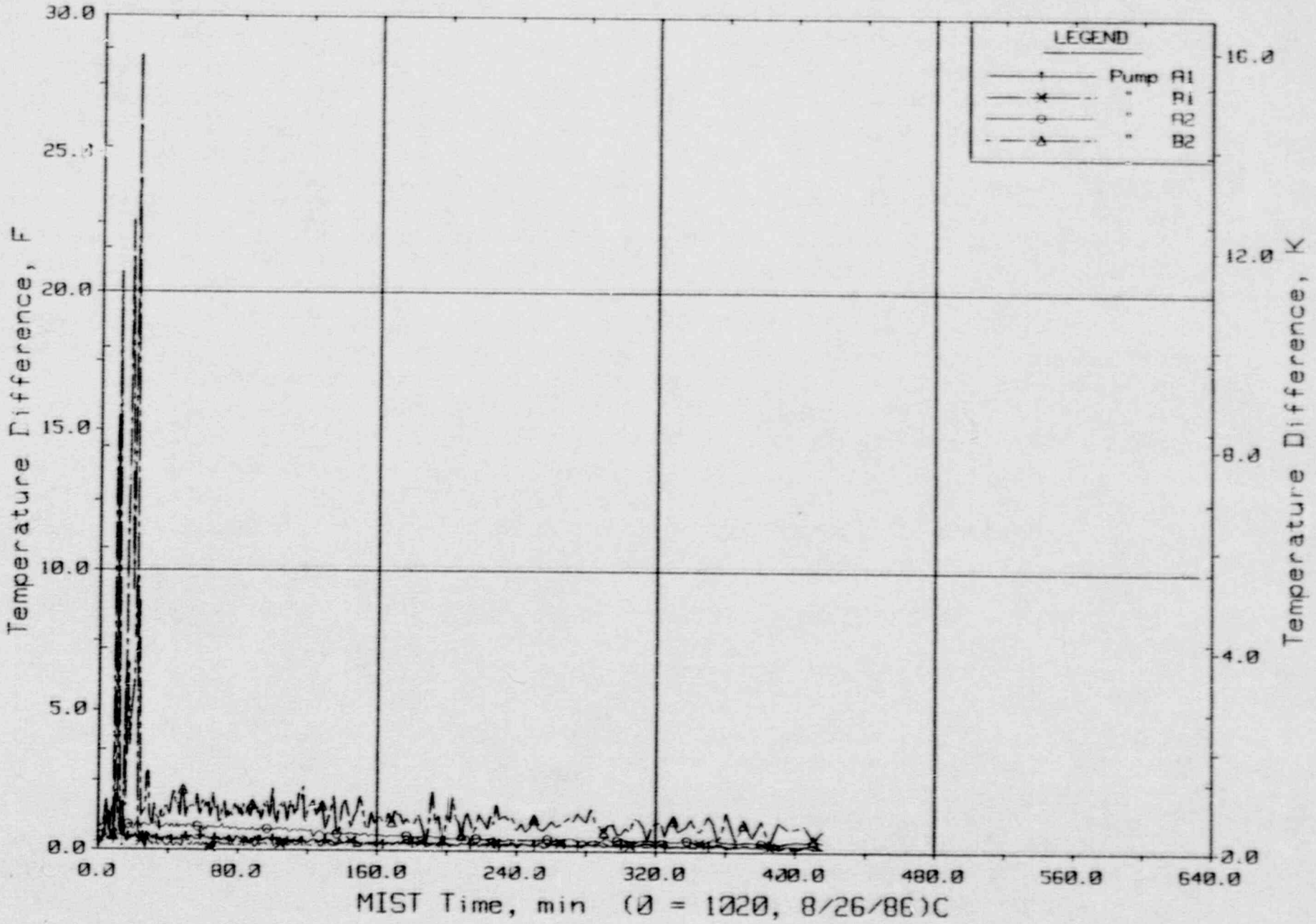

Maximum Differences Among RCP Rake Fluid Temperatures.

Wed Jun 8 17:01:57 1988

CLTD1

FINAL DATA

T3204AA: Group 32 SBLOCA Test 4, PORV Break.

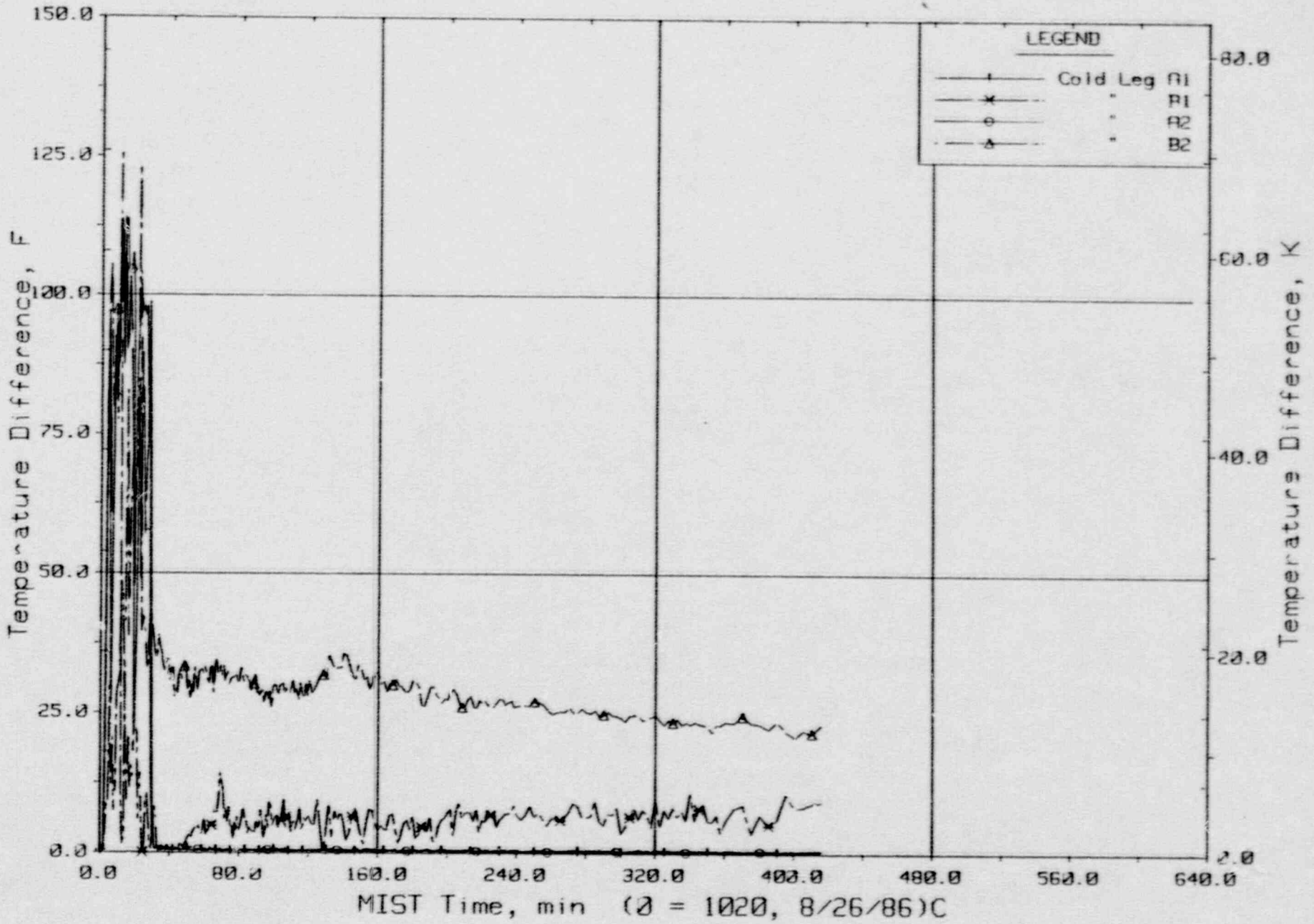

Maximum Differences Among CL Nozzle Rake Fluid Temperatures.

Wed Jun 6 17:04:45 1988

CLTD2

FINAL DATA

T3204AA: Group 32 SBLOCA Test 4, PORV Break.

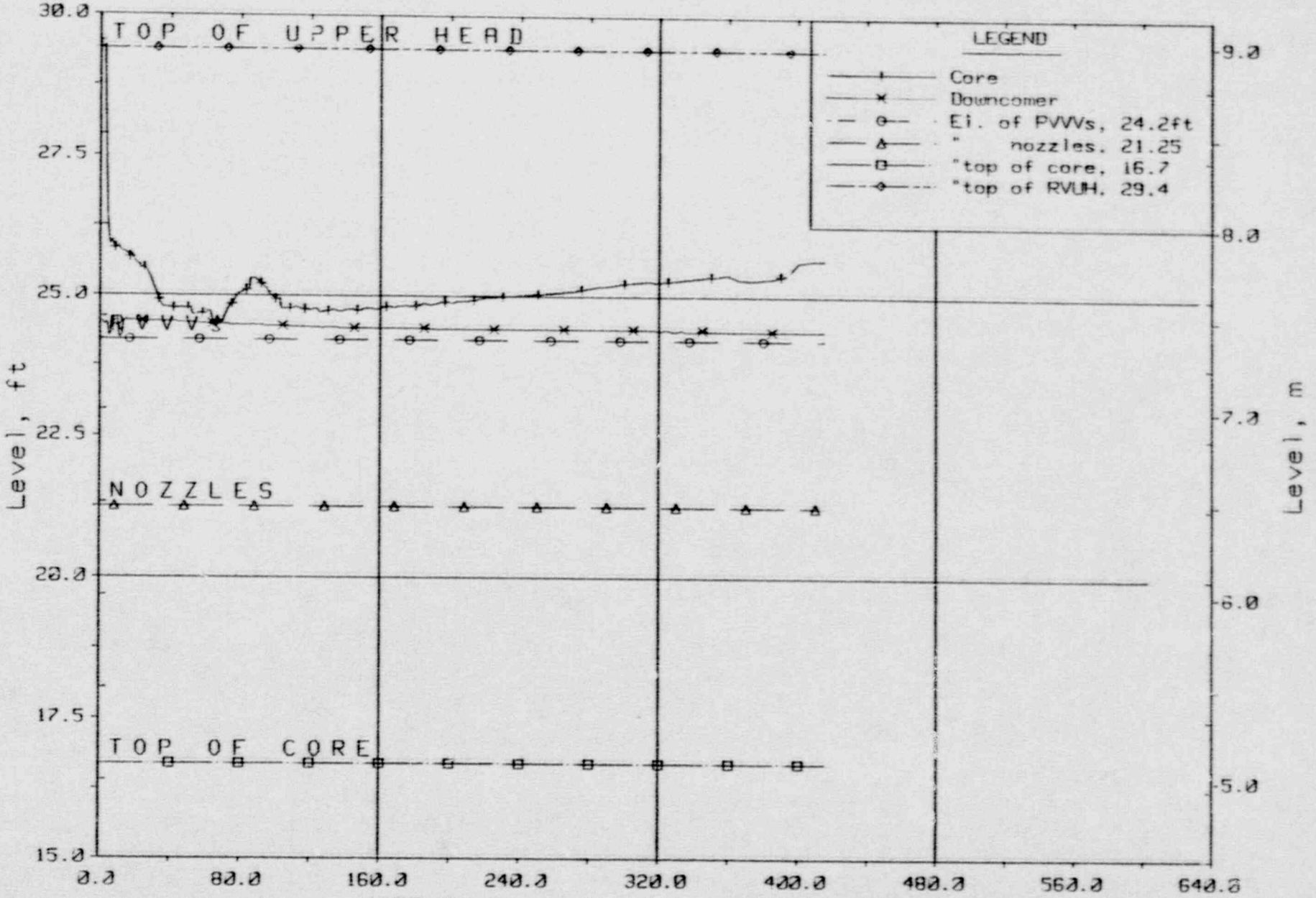

Core Region Collapsed Liquid Levels.

Wed Jun 8 17:08:05 1988

COLV1

FINAL DATA

T3204AA: Group 32 SBLOCA Test 4, PORV Break.

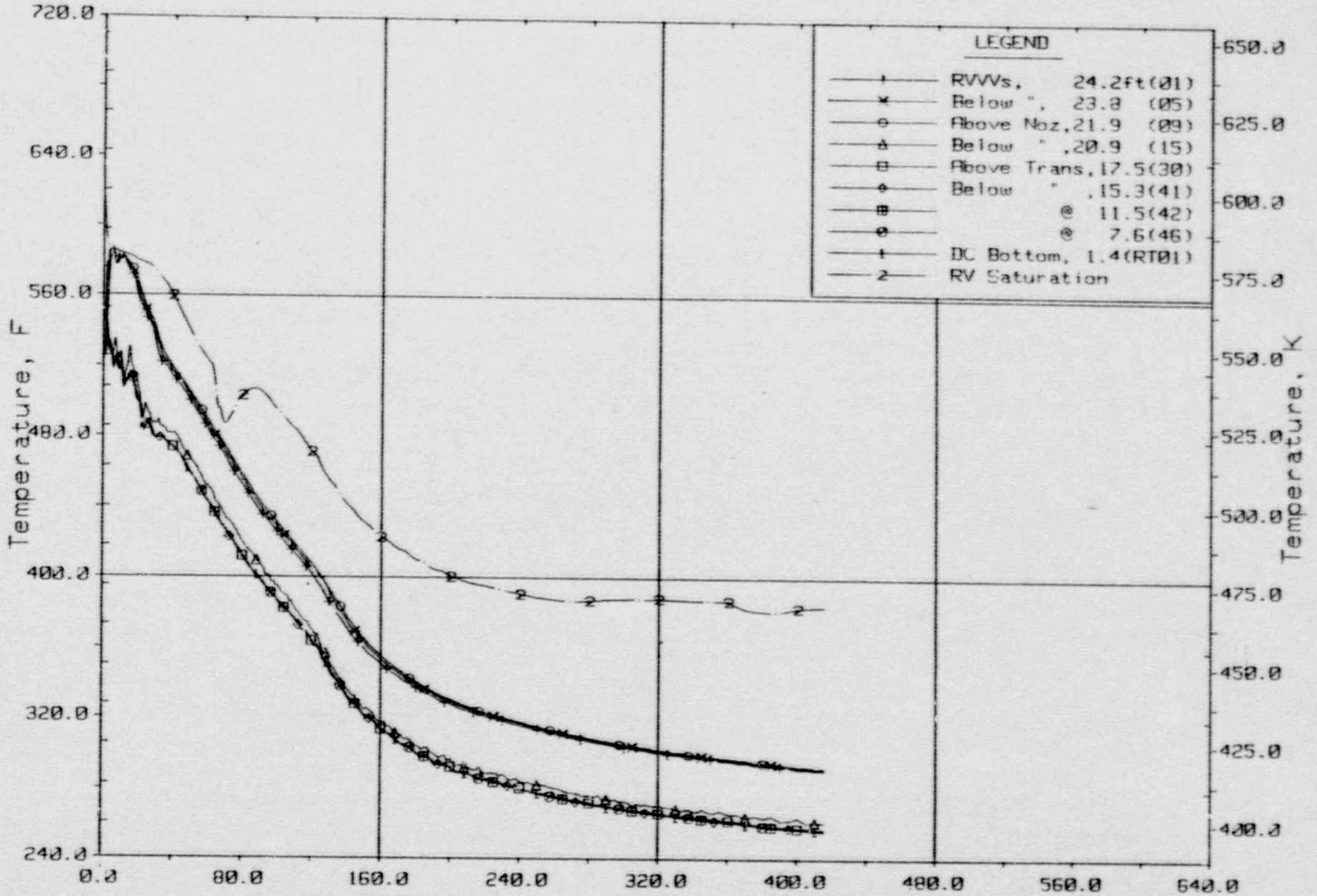

Downcomer Quadrant A1 Fluid Temperatures (DCTCs).

Wed Jun 8 17:15:02 1988

DCTC6

FINAL DATA

T3204AA: Group 32 SBLOCA Test 4, POPV Break.

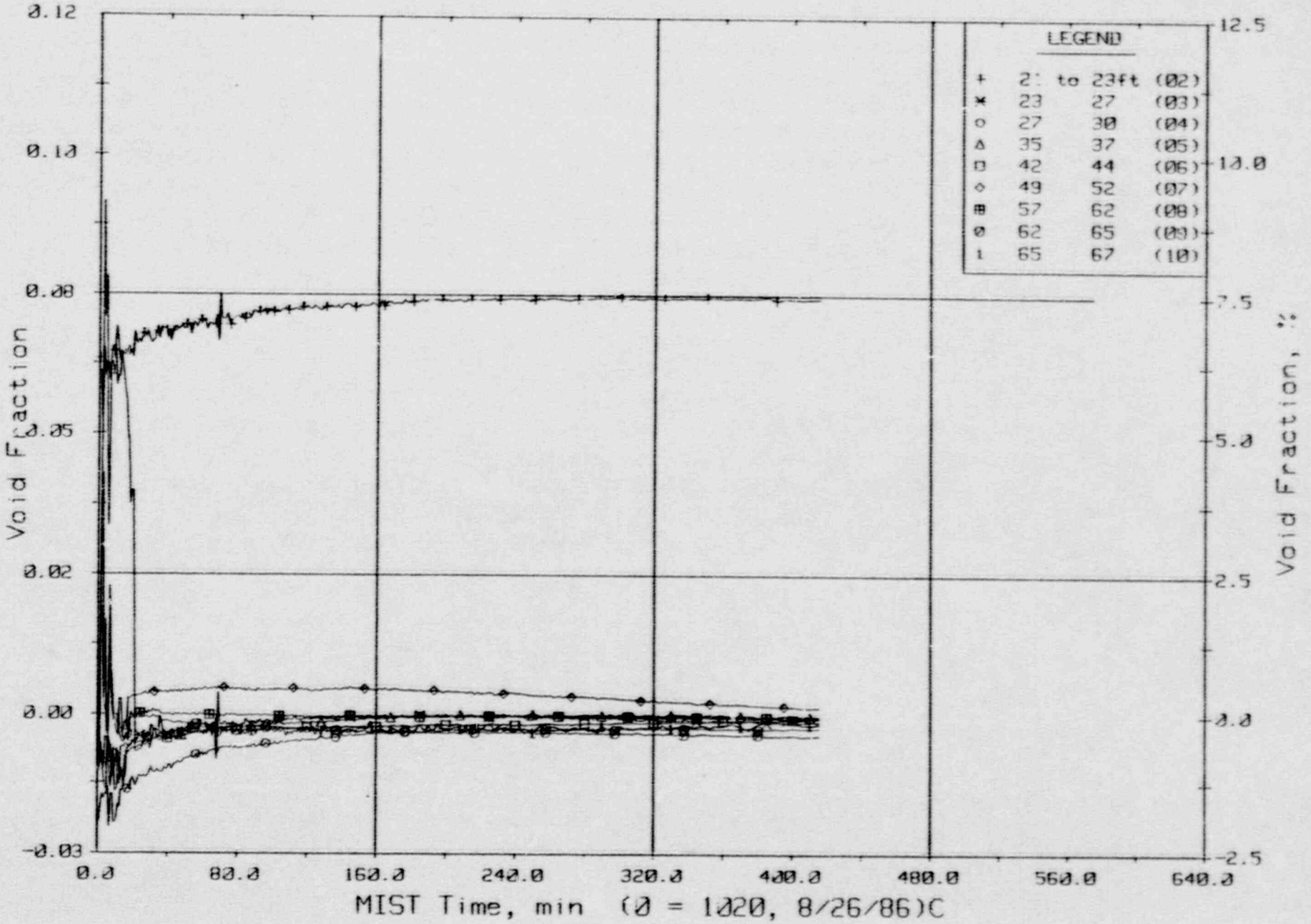

Hot Leg A Riser Void Fractions From Differential Pressures (HIVFs).

Wed Jun 8 12:19:16 1988

HIVF1

FINAL DATA

T3204AA: Group 32 SBLOCA Test 4, PORV Break.

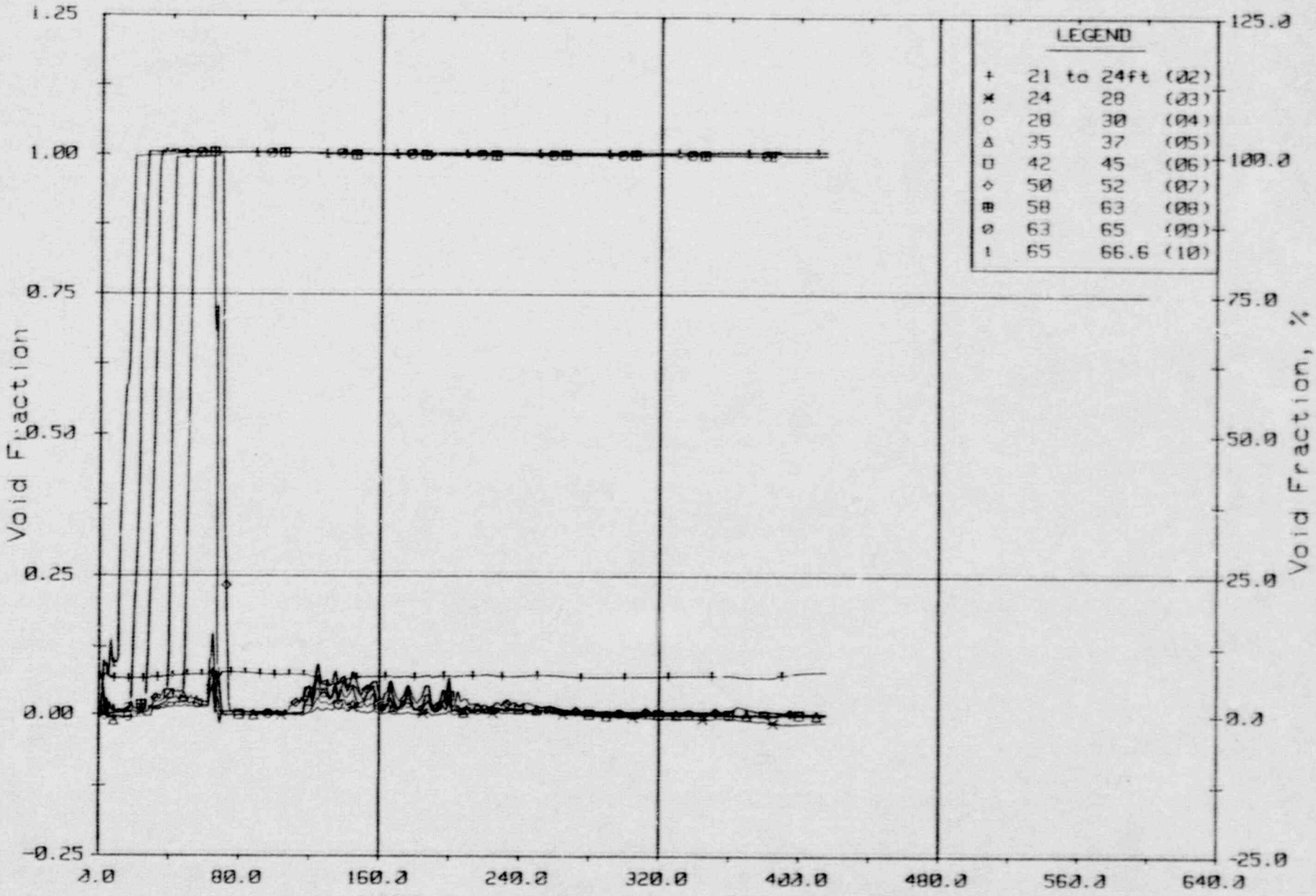

Hot Leg B Riser Void Fraction From Differential Pressures (H2VFs).

FINAL DATA

T3204AA: Group 32 SBLOCA Test 4, PORV Break.

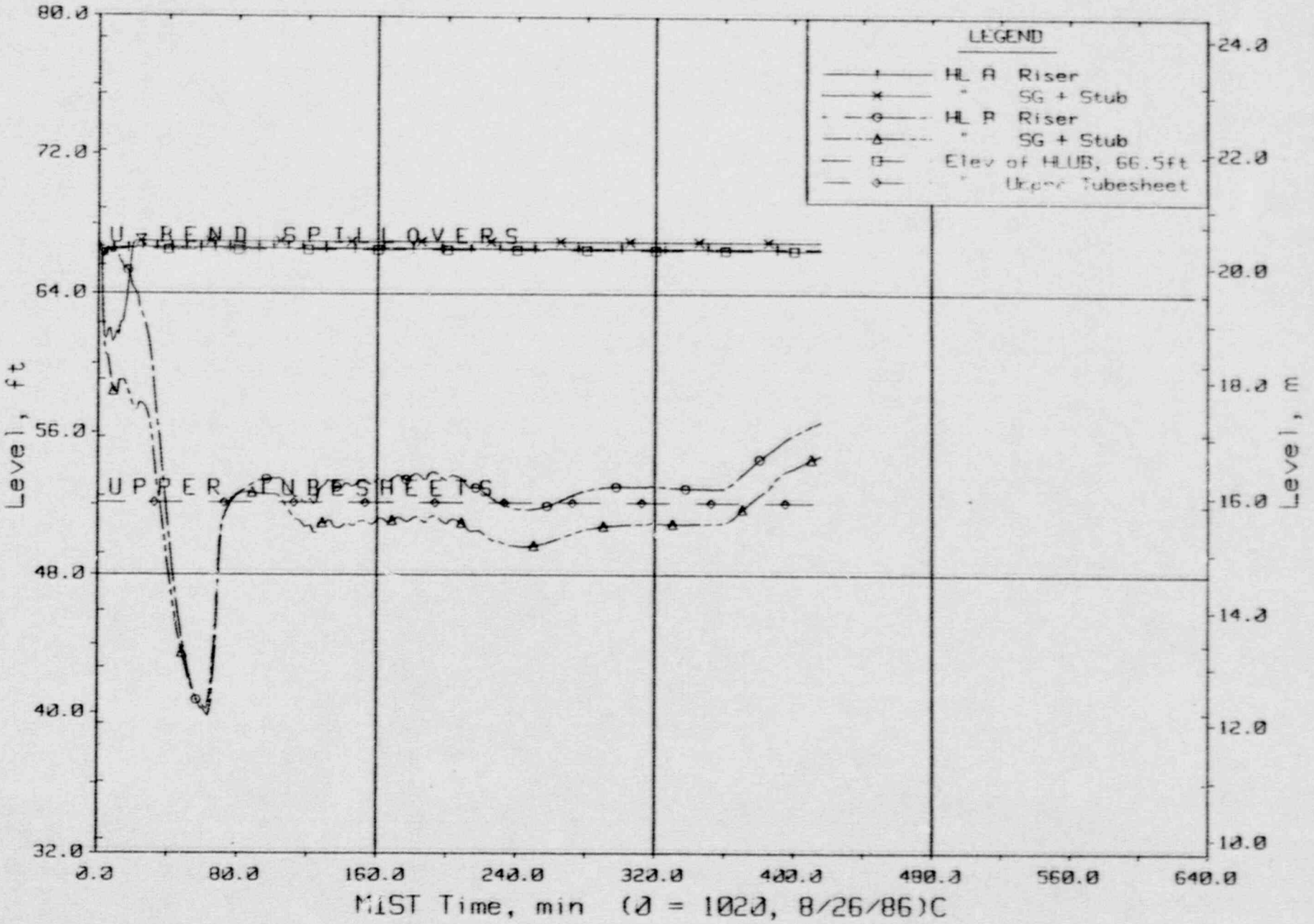

Hot Leg Riser and Stub Collapsed Liquid Levels.

Wed Jun 8 17:26:15 1988

HLLV1

FINAL DATA

T3204AA: Group 32 SBLOCA Test 4, PORV Break.

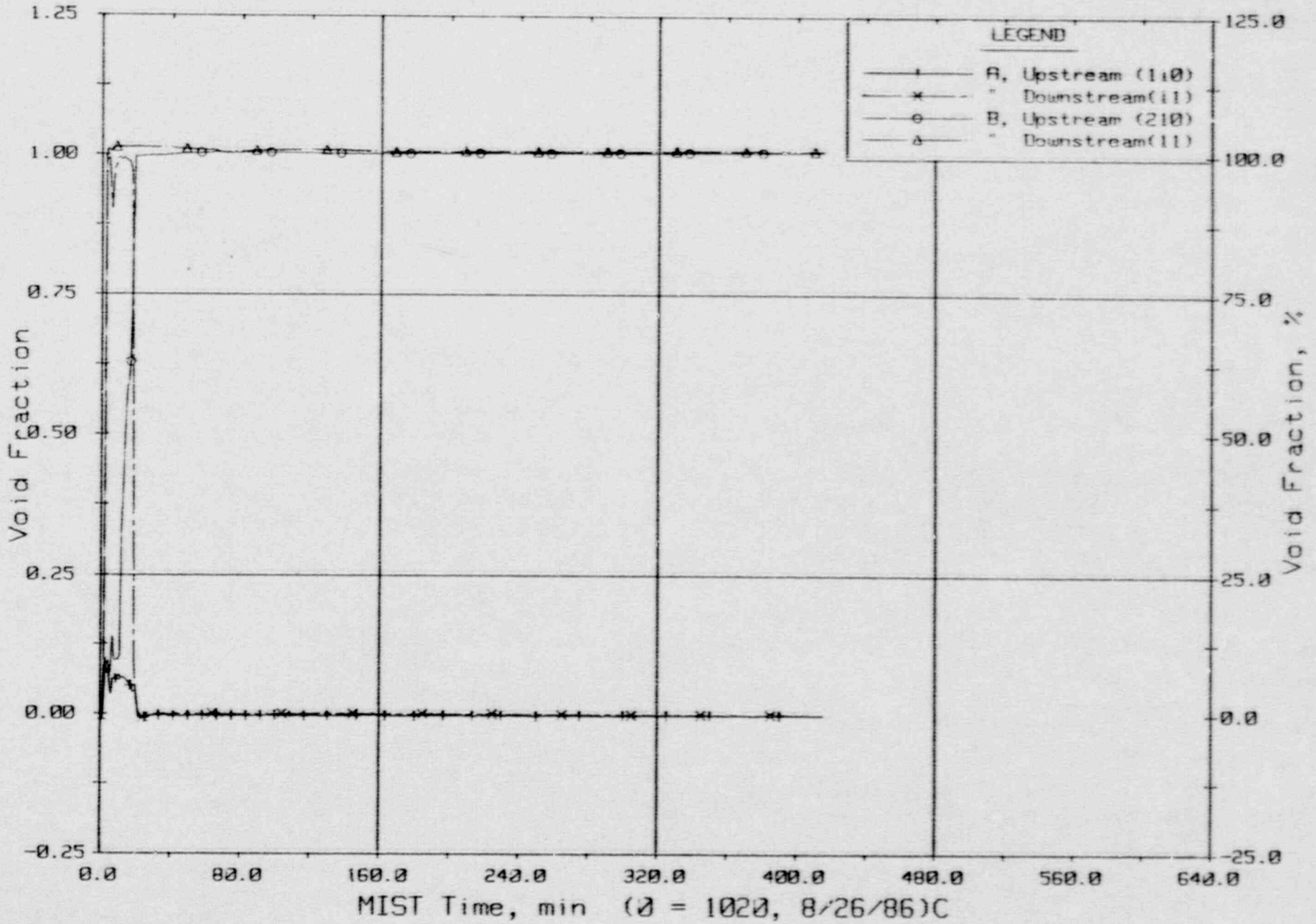

Hot Leg U-Bend Void Fractions From Diffl. Pressures (64.8 to 66.6 ft, HnVFs).

Wed Jun 8 17:29:52 1988

HLVF1

FINAL DATA

T3204AA: Group 32 SBLOCA Test 4, PORV Break.

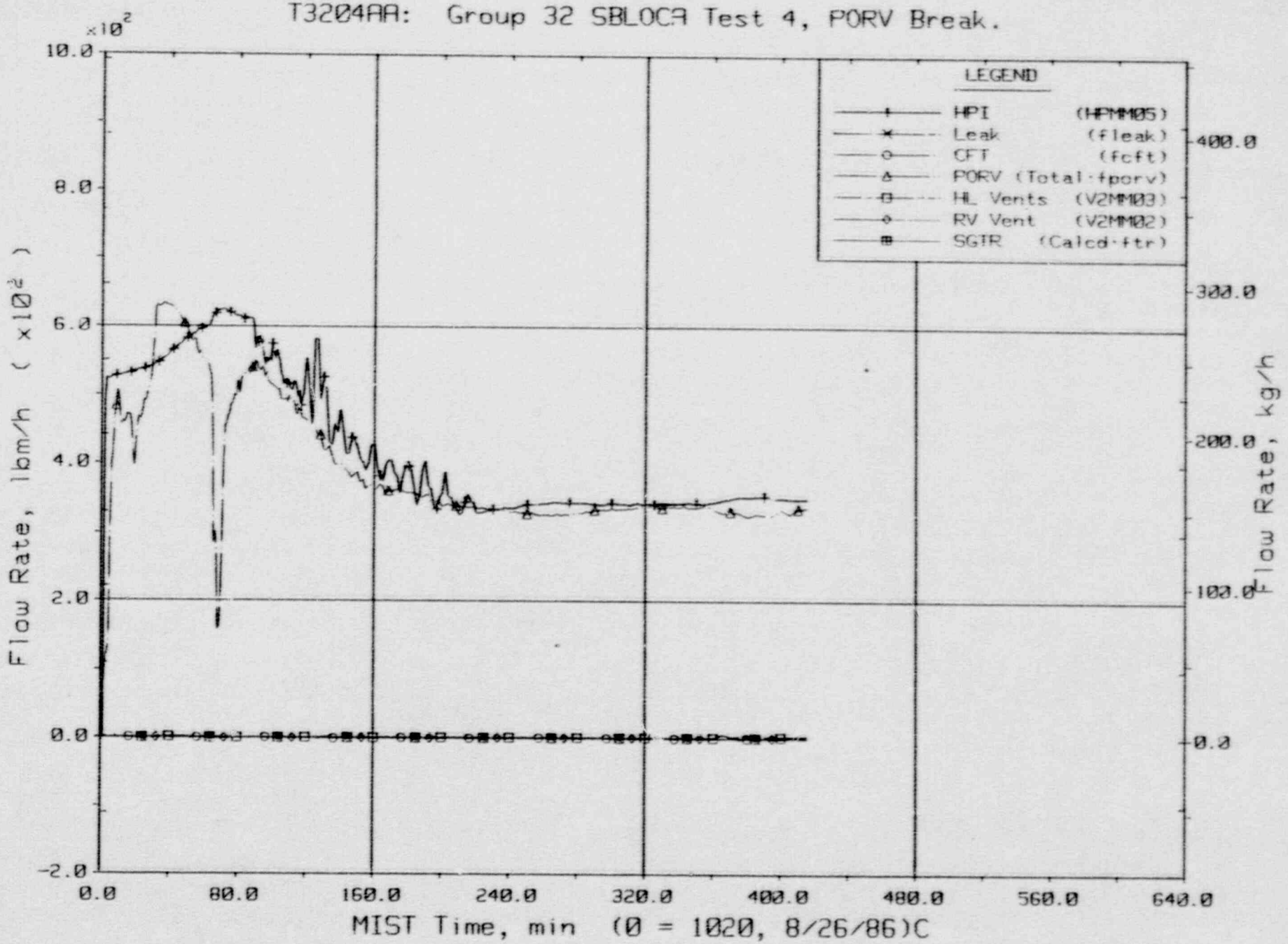

Primary System Boundary Flow Rates.

Wed Jun 8 17:34:01 1988

PBFL3

FINAL DATA

T3204AA: Group 32 SRLOCA Test 4, PORV Break.

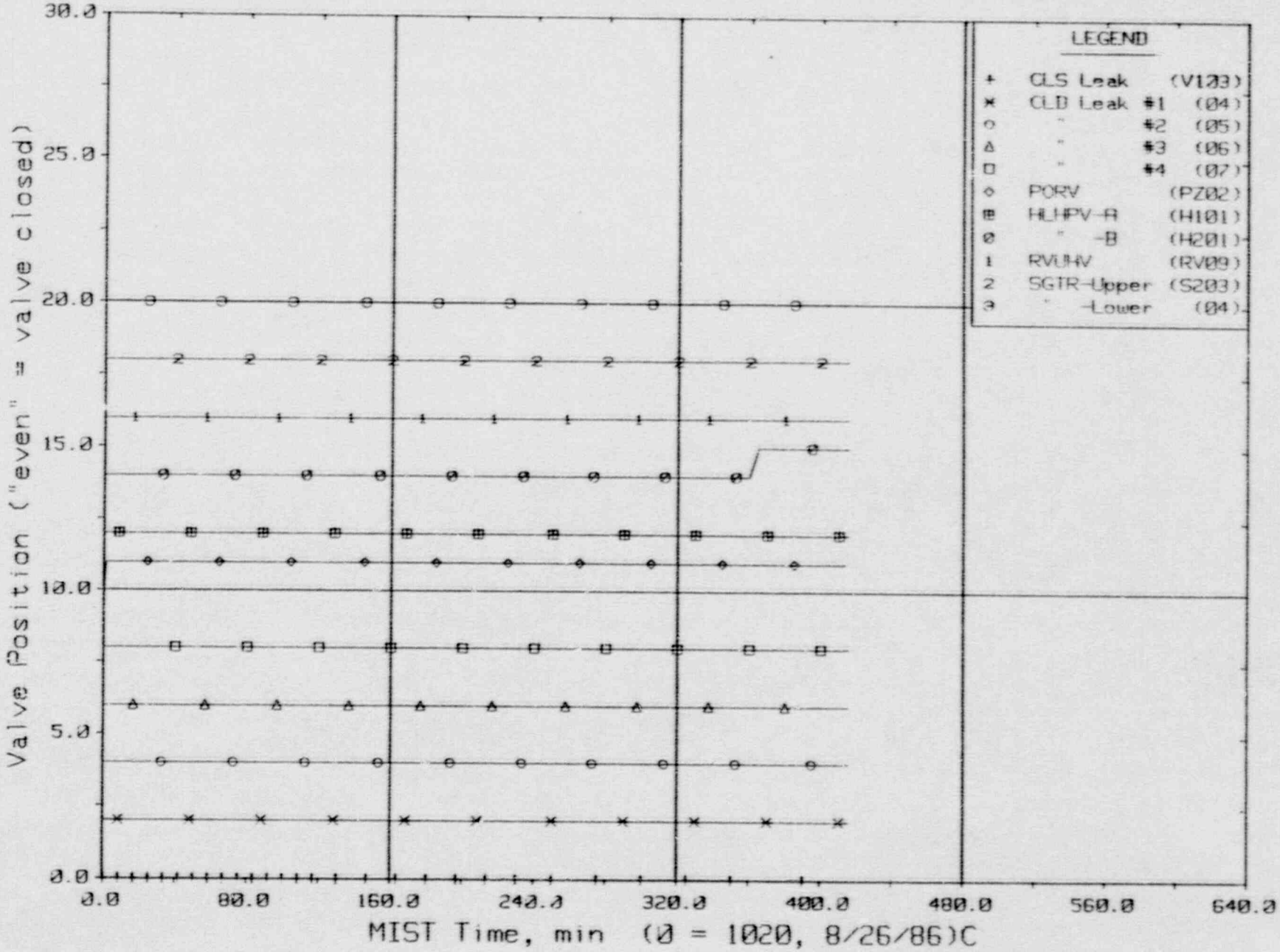

Primary System Discharge Limit Switch Indications (LSs).

Wed Jun 8 17:37:35 1988

PBLS1

FINAL DATA

T3204AA: Group 32 SRLOCA Test 4, PORV Break.

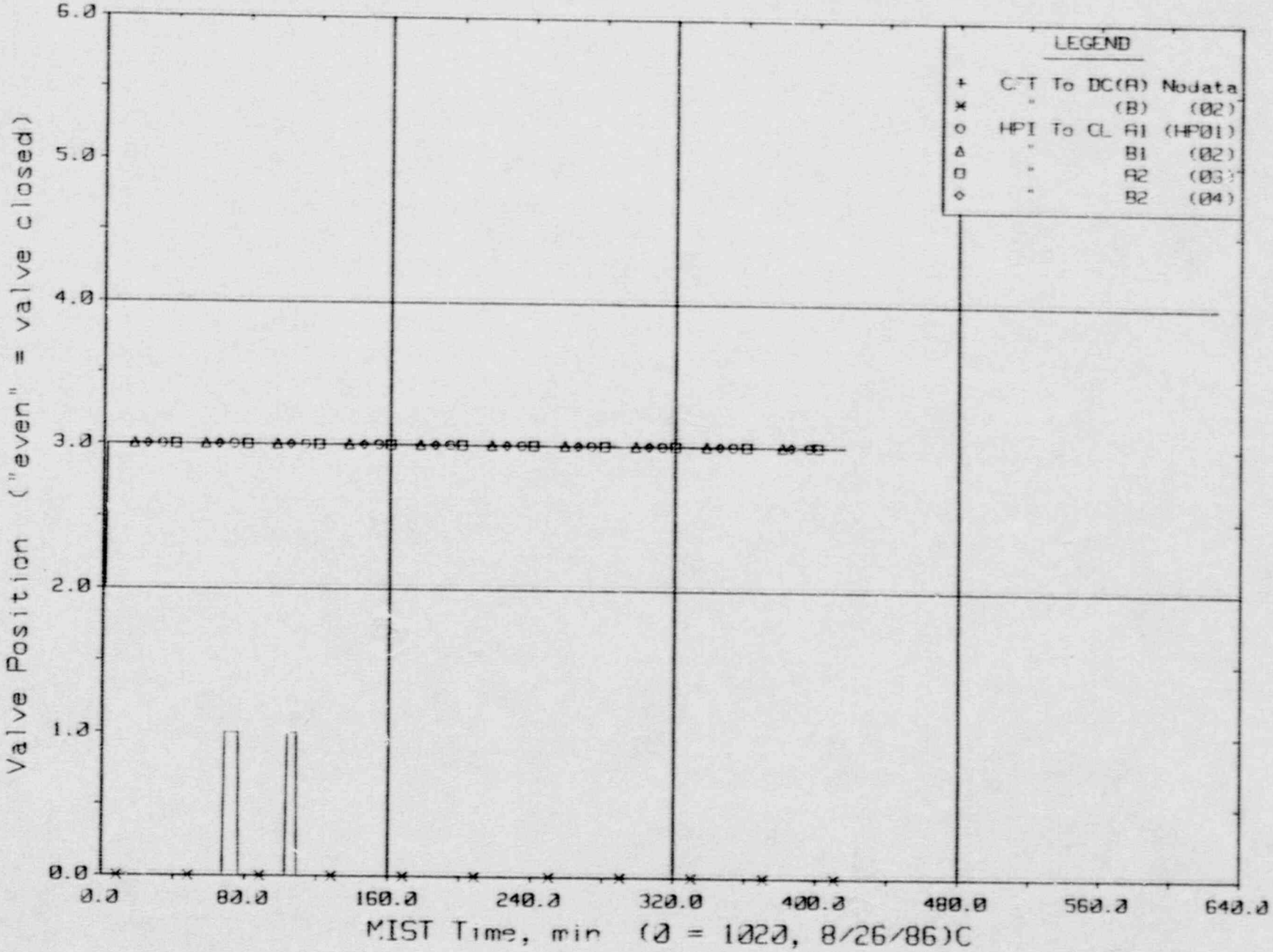

Primary System Injection Limit Switch Indications (LSs).

Wed Jun 8 17:40:42 1988

PHL32

FINAL DATA

T3204AA: Group 32 SBLOCA Test 4, PORV Break.

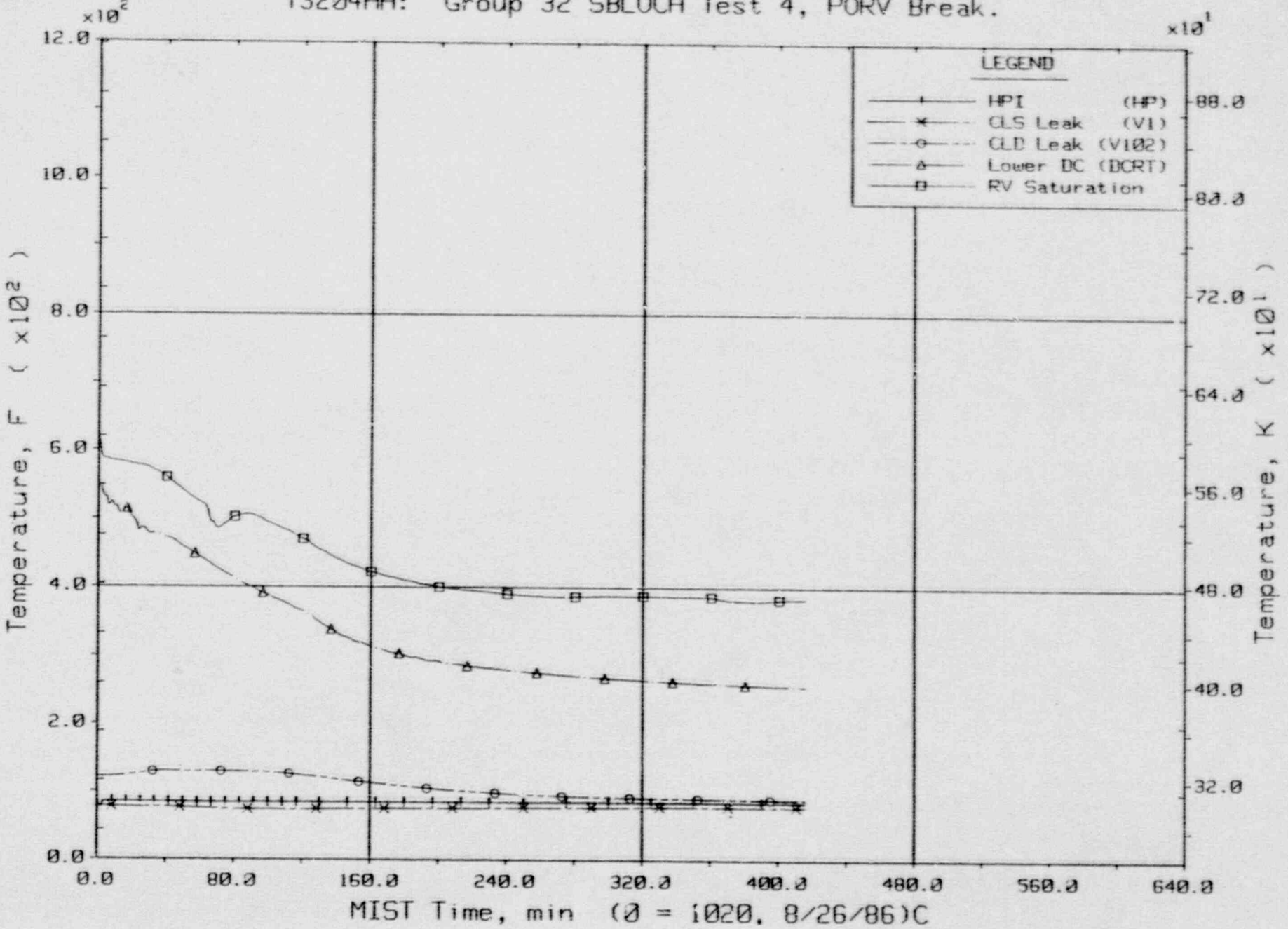

Single-Phase Discharge and HPI Fluid Temperatures (TC0ls).

Wed Jun 8 17:43:55 1988

PBTC1p

FINAL DATA

T3204AA: Group 32 SBLOCA Test 4, PORV Break.

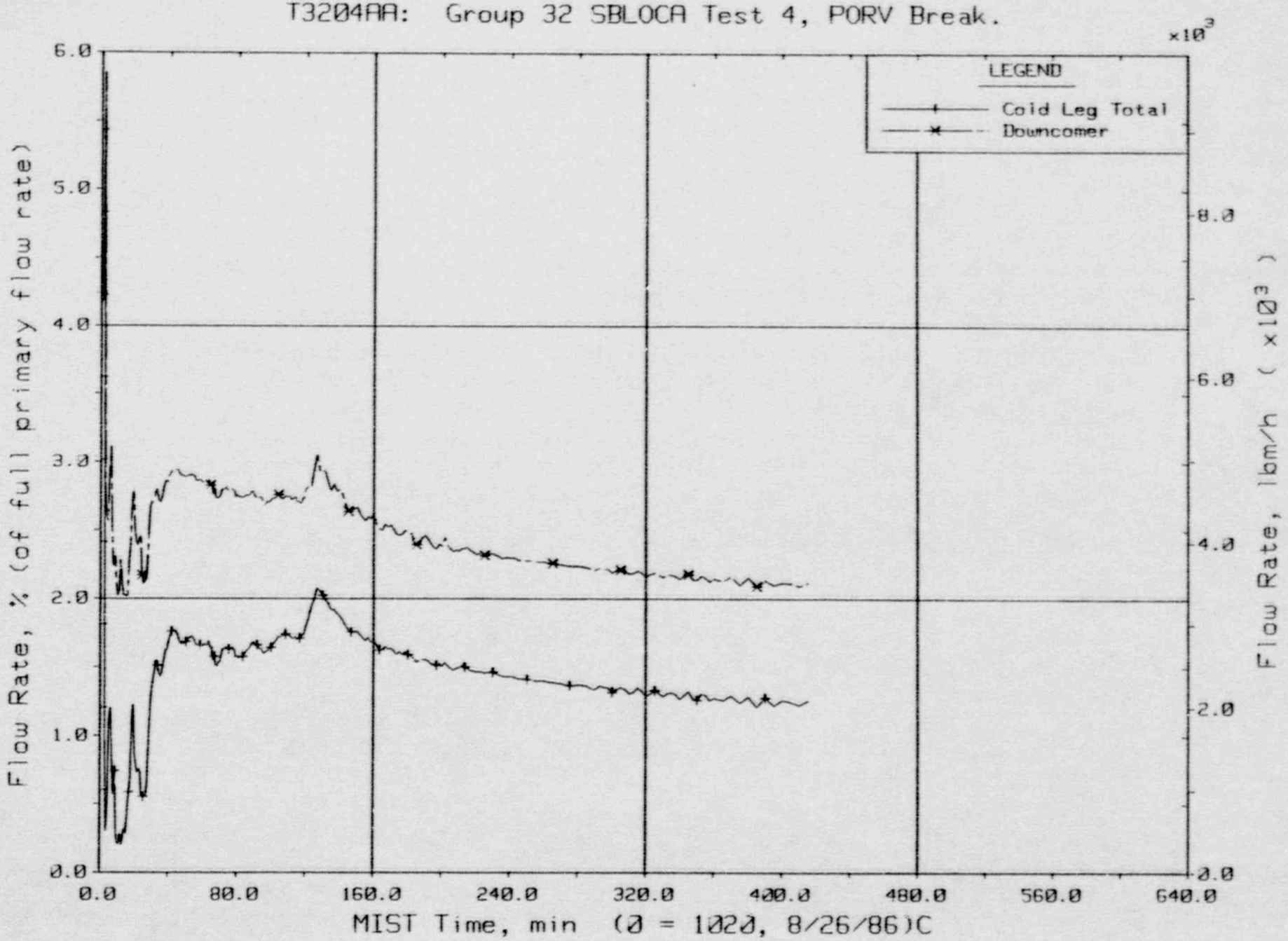

Primary System Venturi Flow Rates.

Wed Jun 8 17:46:26 1988

PRFL7

FINAL DATA

T3204AA: Group 32 SBLOCA Test 4, PORV Break.

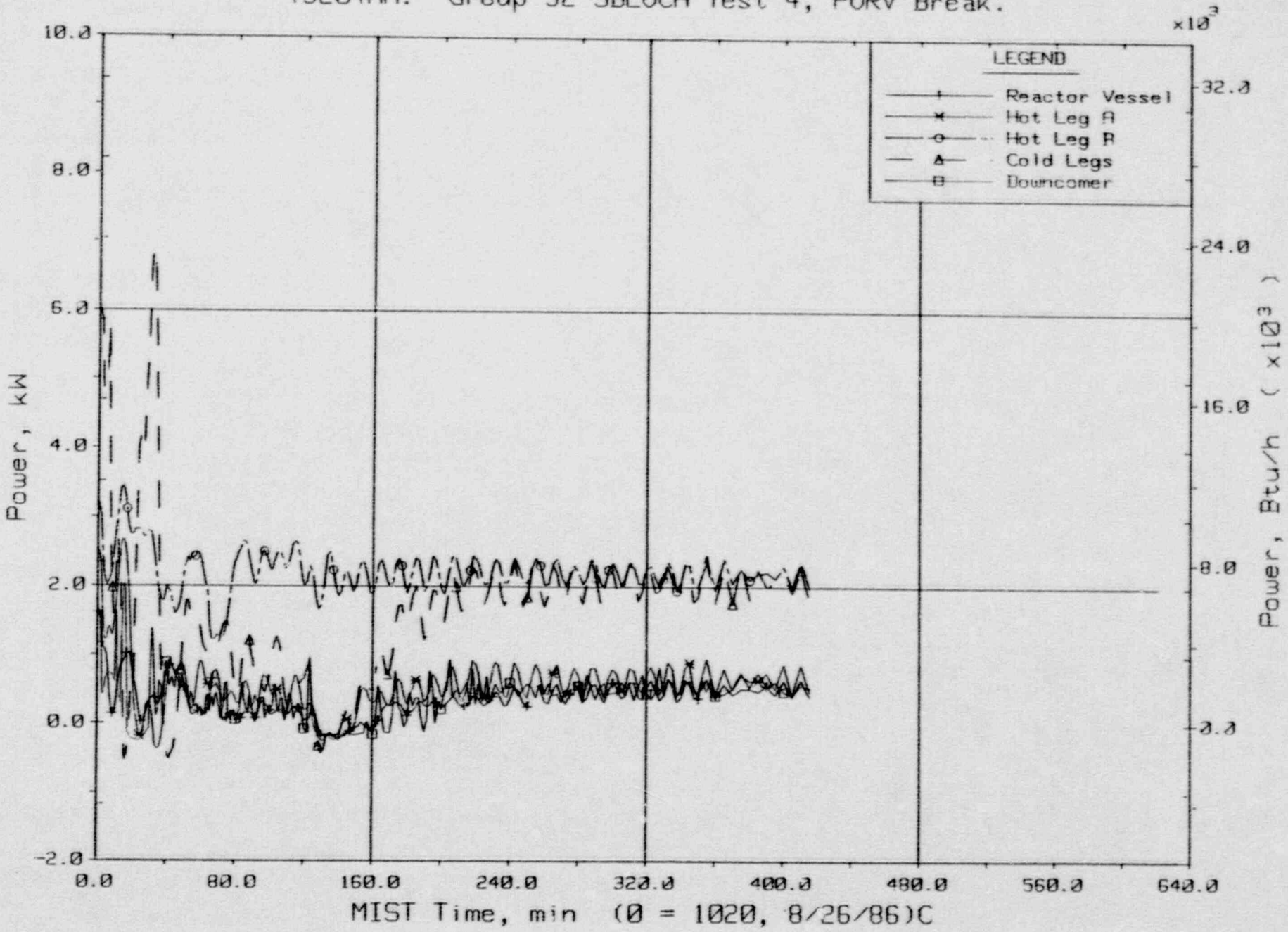

Guard Heater Specified Power Per Primary Component.

Wed Jun 8 17:49:18 1988

PRGQ1

FINAL DATA

T3204AA: Group 32 SBLOCA Test 4, PORV Break.

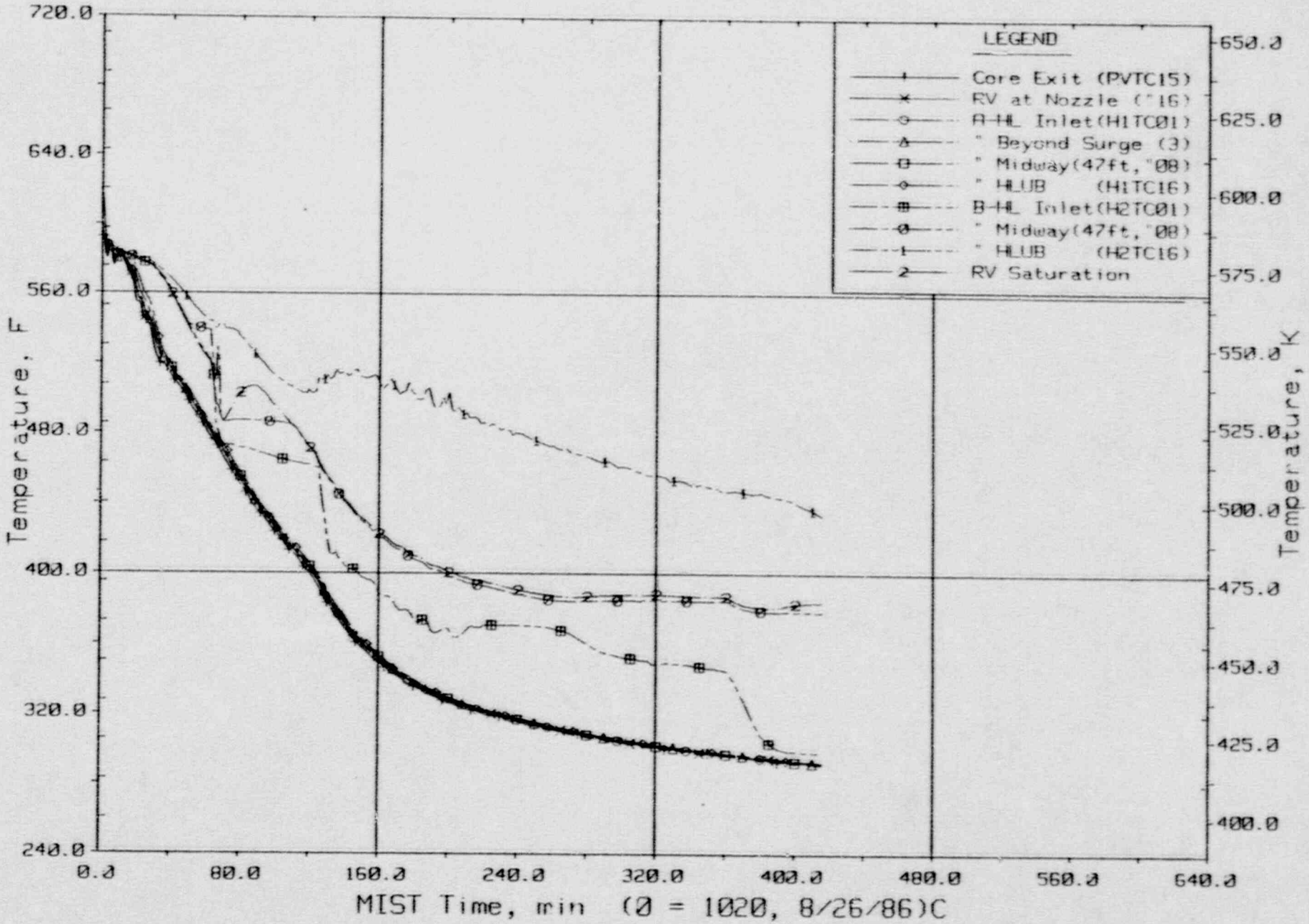

Composite Core Exit and Hot Leg Fluid Temperatures.

Wed Jun 8 17:52:56 1988

PRKT1

FINAL DATA

T3204AA: Group 32 SBLOCA Test 4, PORV Break.

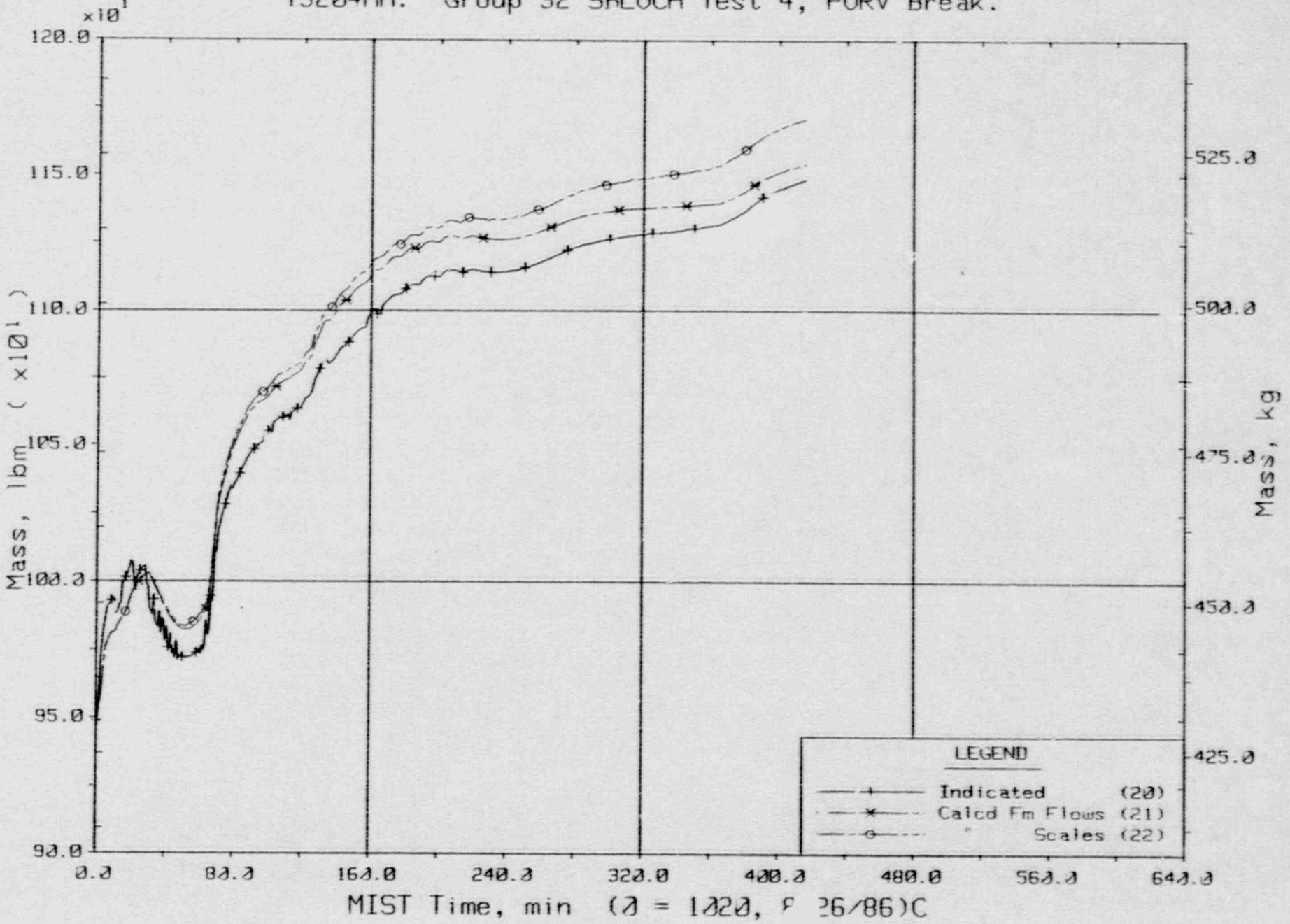

Primary System Total Fluid Mass (LMLs).

Wed Jun 8 17:55:47 1988

PRML2

FINAL DATA

T3204AA: Group 32 SBLOCA Test 4, PORV Break.

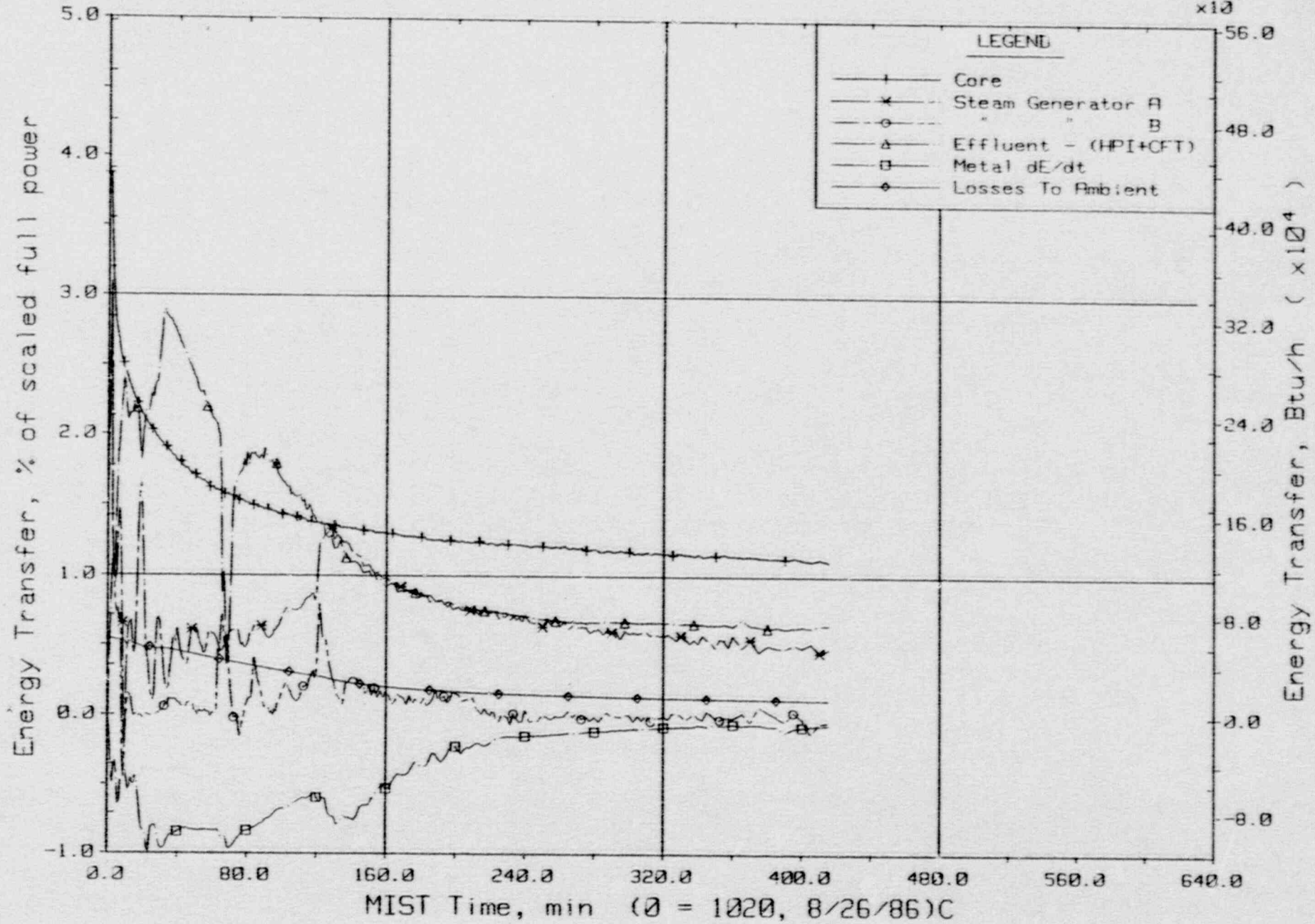

Primary System Energy Transfer.

Wed Jun 8 18:37:12 1988

PROE2

FINAL DATA

T3204AA: Group 32 SBLOCA Test 4, PORV Break.

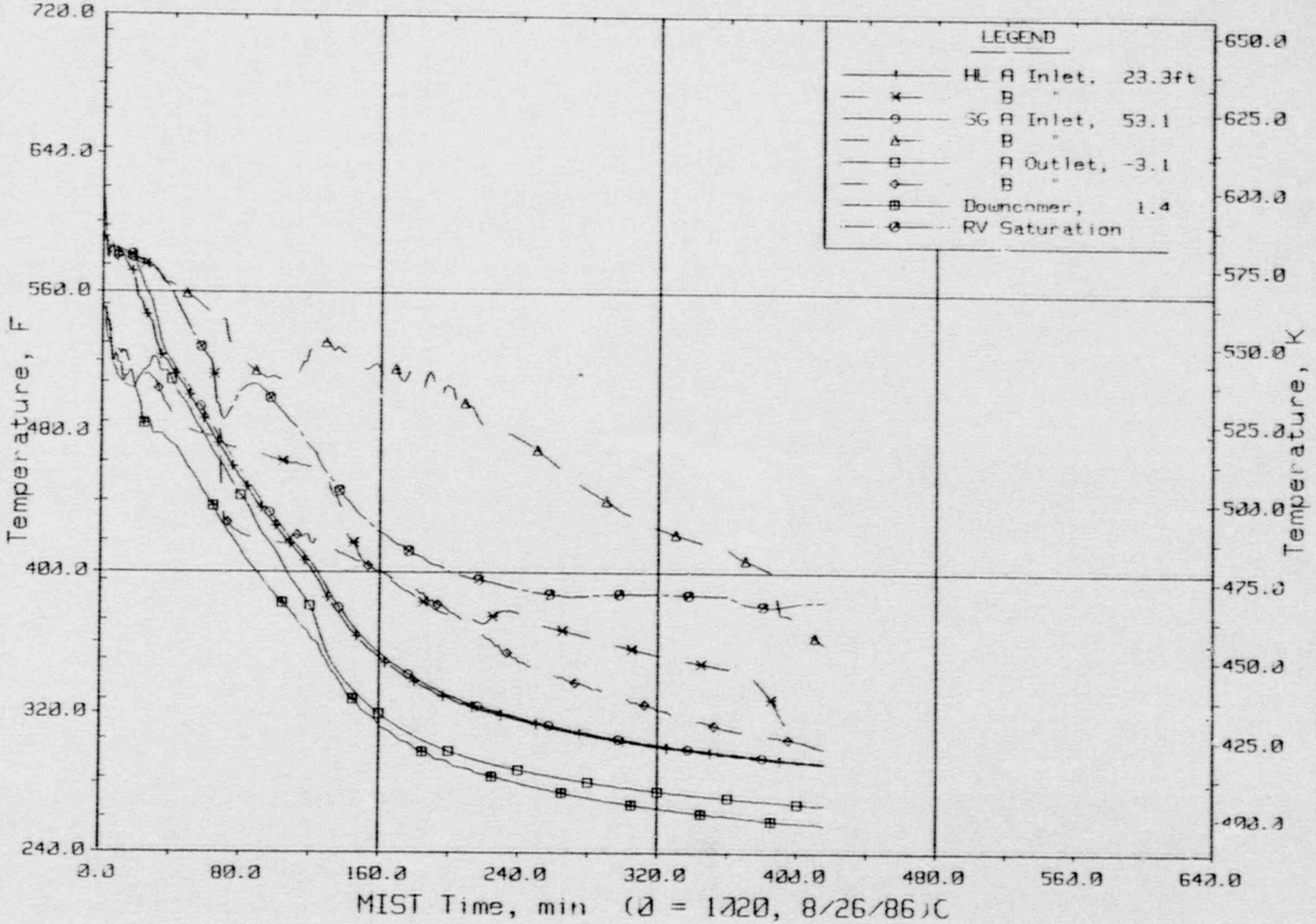

Primary System Fluid Temperatures (RTDs).

Wed Jun 8 18:10:20 1988

PRRT0

FINAL DATA

T3204AA: Group 32 SBLOCA Test 4, PORV Break.

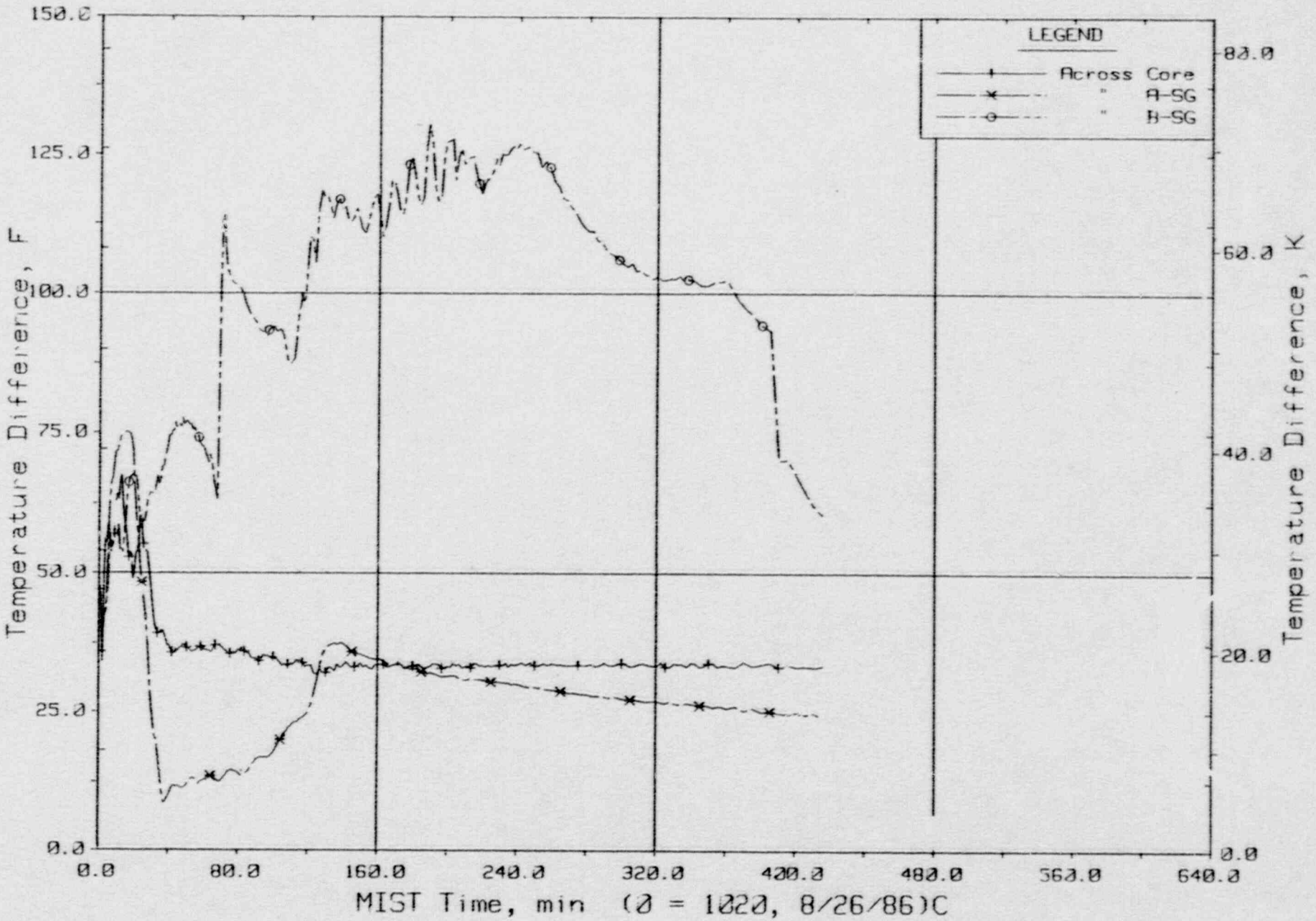

Key Temperature Differences.

Wed Jun 8 18:12:48 1988

PRTD2

FINAL DATA

T3204AA: Group 32 SBLOCA Test 4, PORV Break.

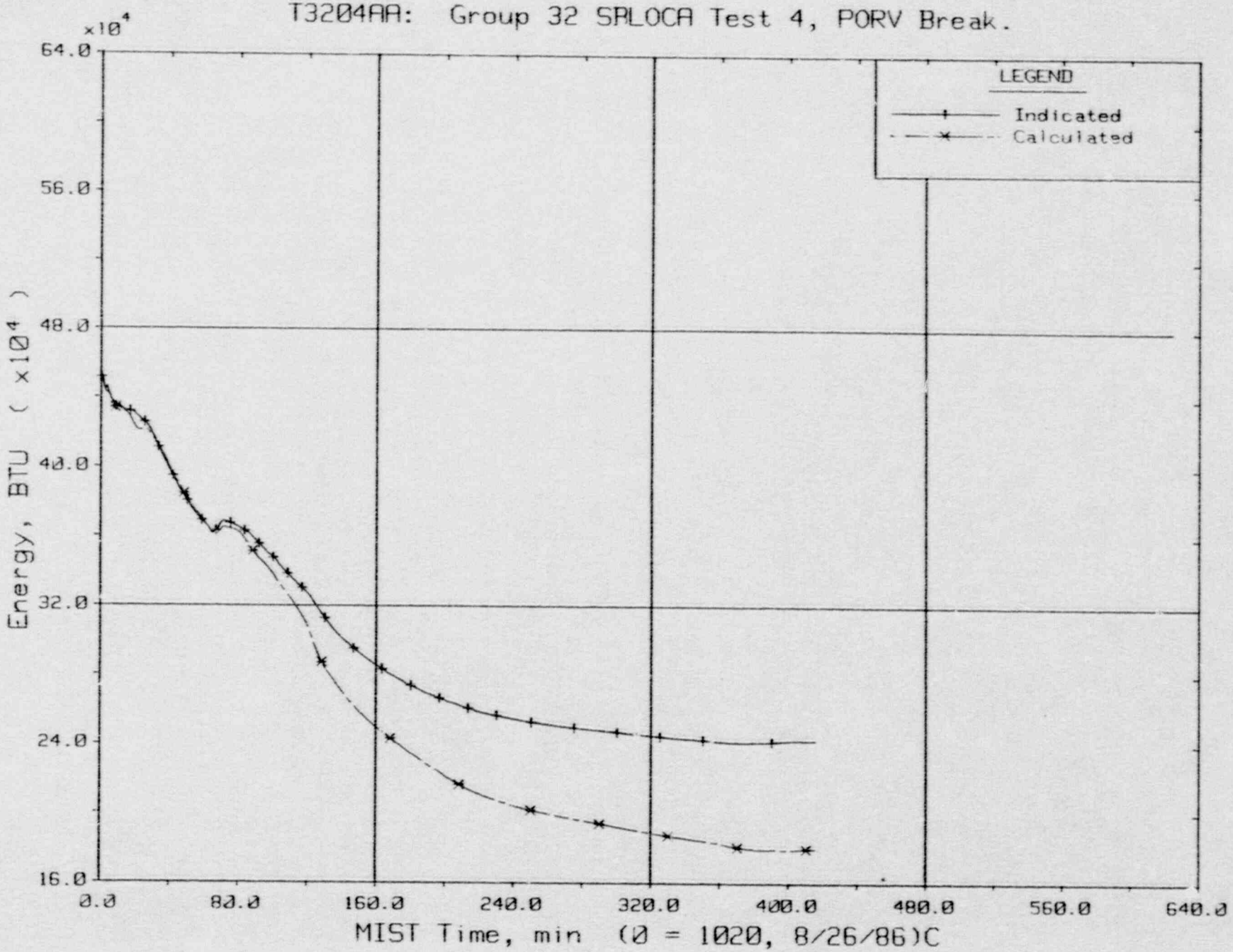

Primary System Total Fluid Energy.

Wed Jun 8 18:14:48 1988

PRTE2

FINAL DATA

T3204AA: Group 32 SBLOCA Test 4, PORV Break.

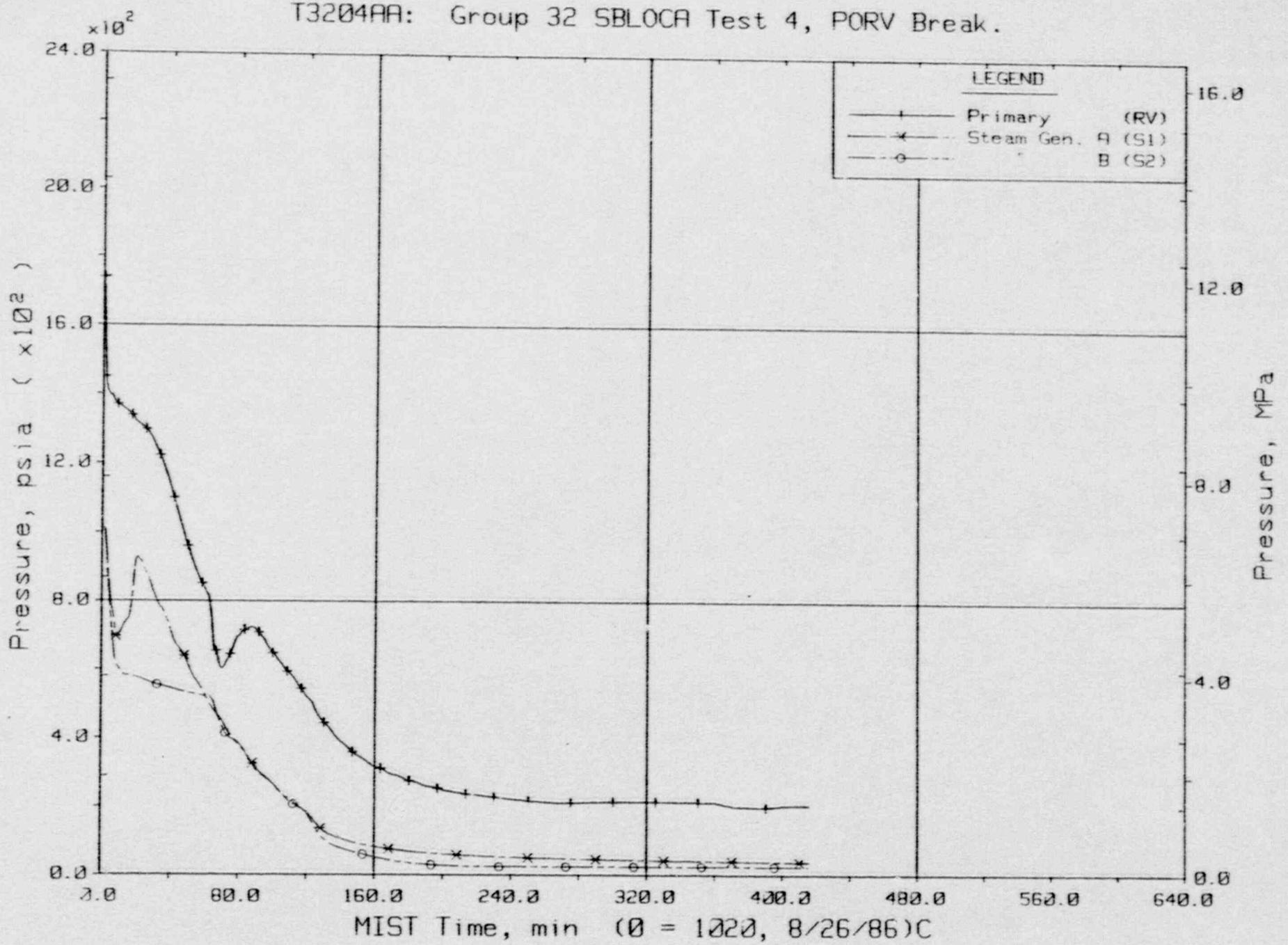

Primary and Secondary System Pressures (GP01s).

Wed Jun 8 18:16:53 1988

PSGP1

FINAL DATA

T3204AA: Group 32 SBLOCA Test 4, PORV Break.

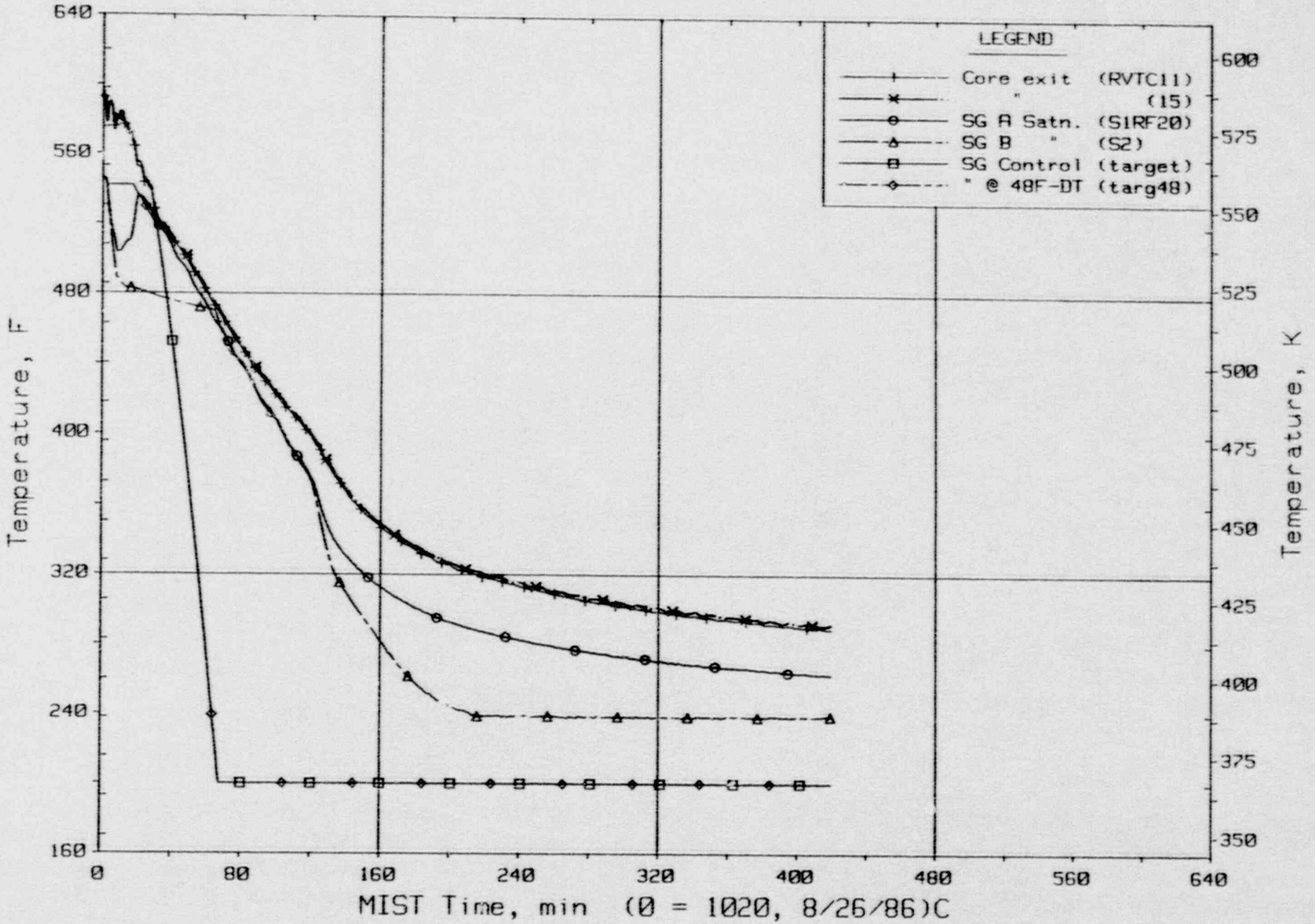

Steam Generator Secondary Saturation and Control Temperatures.

Mon Oct 31 14:34:08 1988

PSTC3

FINAL DATA

T3204AA: Group 32 SBLOCA Test 4, PORV Break.

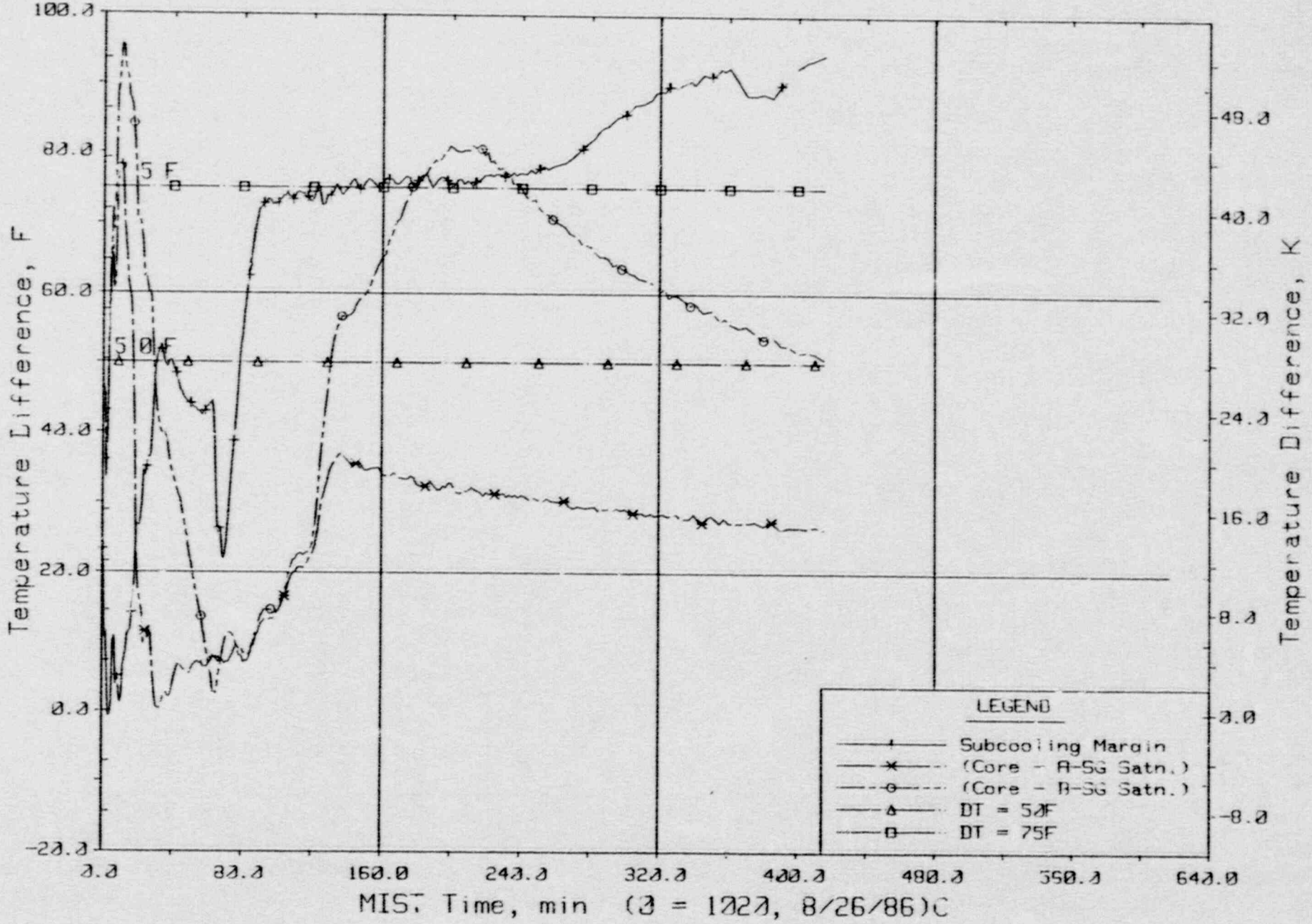

Control Temperature Differences.

Wed Jun 8 18:22:00 1988

PSTD1

FINAL DATA

T3204AA: Group 32 SBLOCA Test 4, PORV Break.

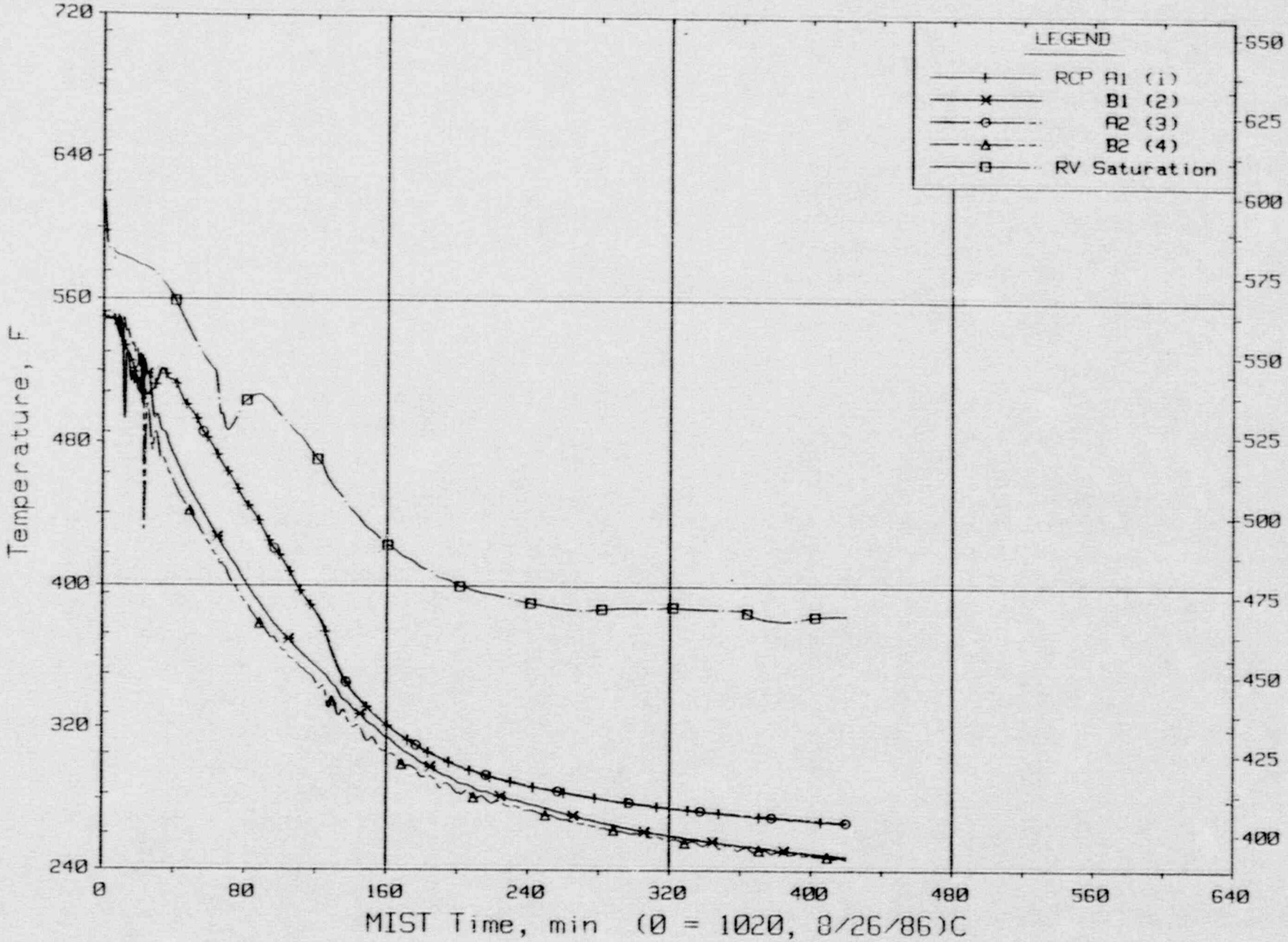

Pump Suction Fluid Temperature (CnRT0ls).

Mon Oct 31 14:49:43 1988

PURT0

FINAL DATA

T3204AA: Group 32 SBLOCA Test 4, PORV Break.

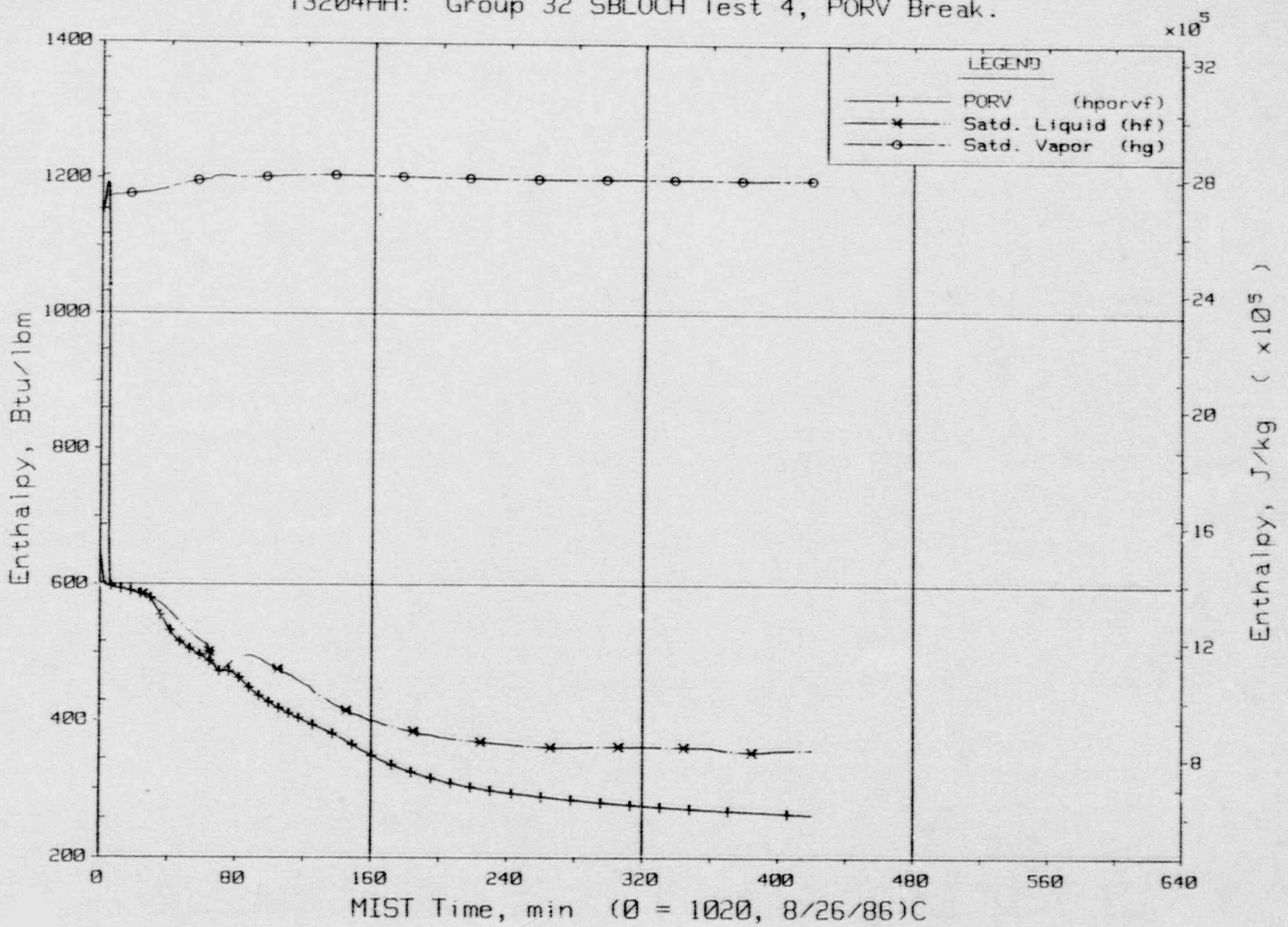

Power-Operated Relief Valve Enthalpy (Based On Flow Rate).

Mon Oct 31 14:42:28 1988

PZEN1

FINAL DATA

T3204AA: Group 32 SBLOCA Test 4, PORV Break.

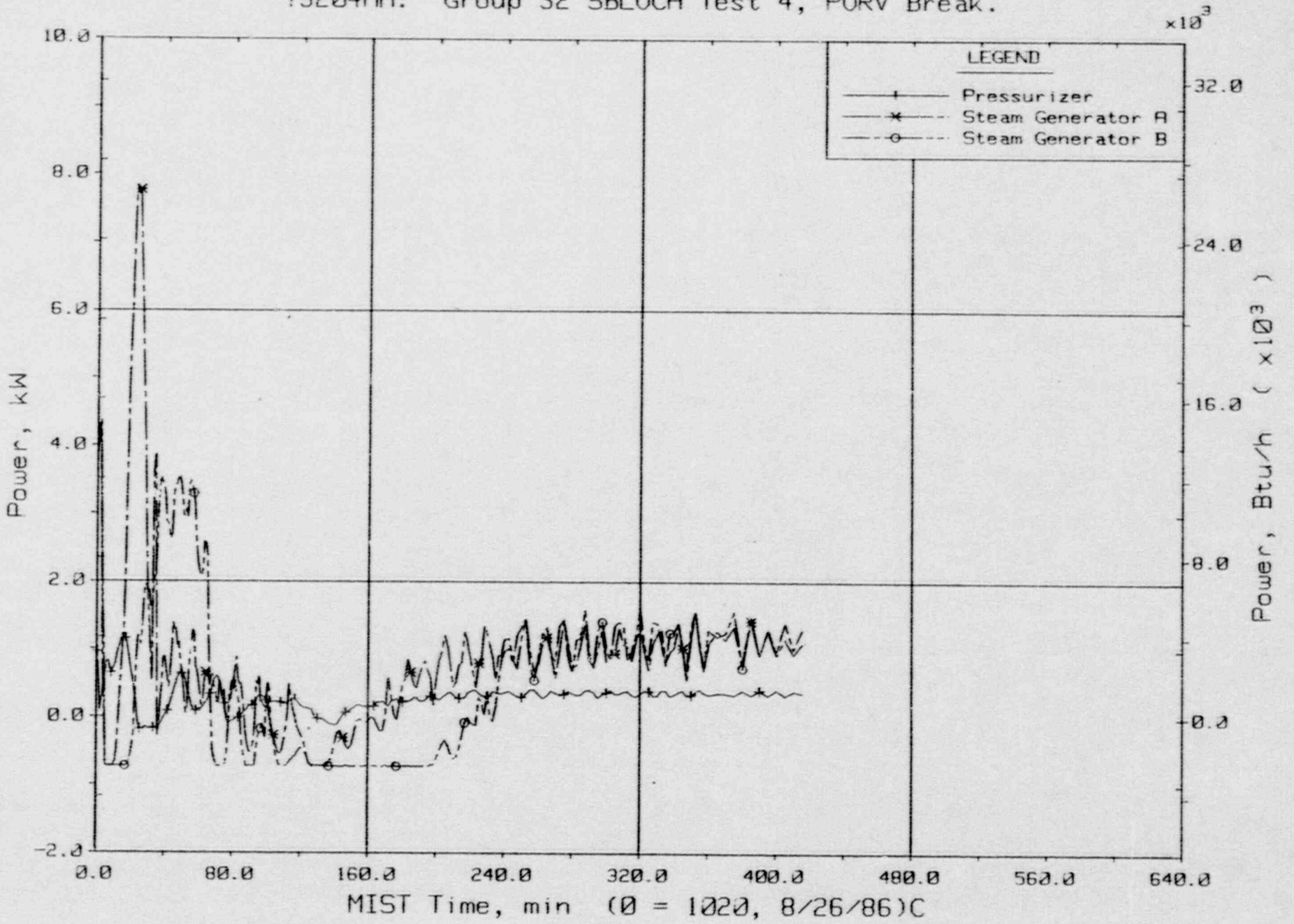

Guard Heater Specified Power, Pressurizer and Steam Generators.

Wed Jun 8 18:27:00 1988

PZGQ1

FINAL DATA

T3204AA: Group 32 SBLOCA Test 4, PORV Break.

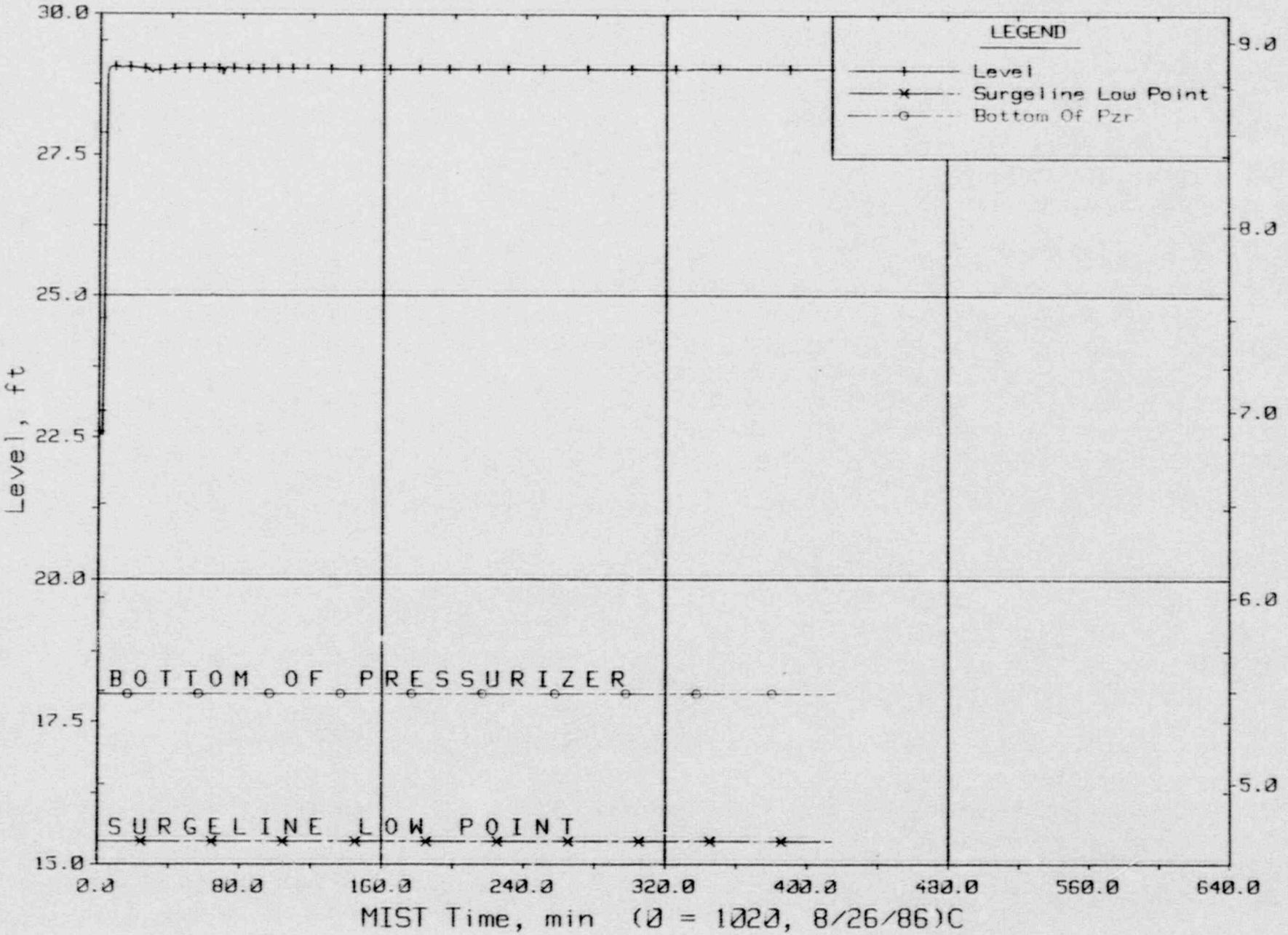

Pressurizer Collapsed Liquid Level (PZLV20).

Wed Jun 8 18:29:17 1988

PZLV1

FINAL DATA

T3204AA: Group 32 SBLOCA Test 4, PORV Break.

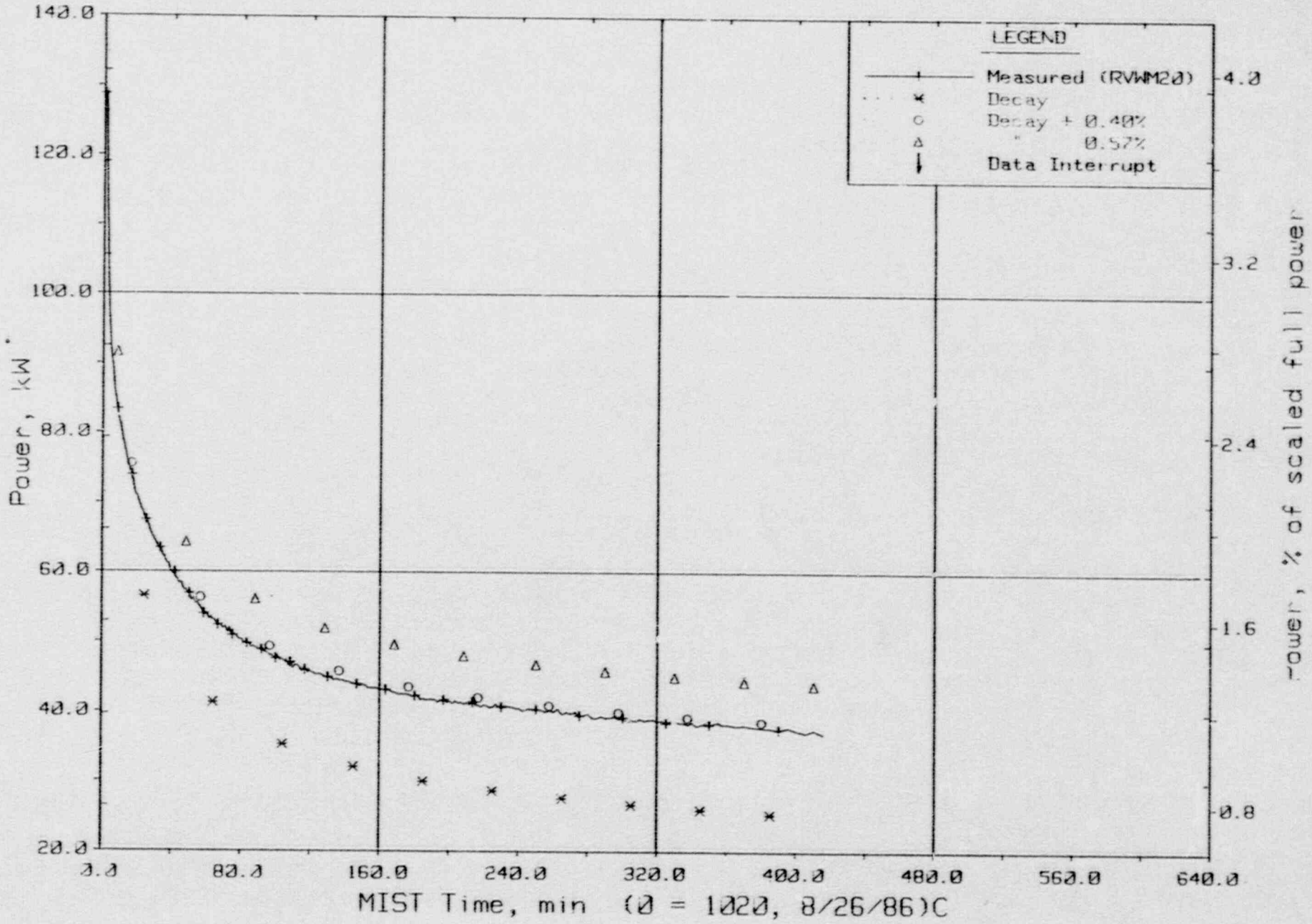

Core Power.

Wed Jun 8 18:32:29 1988

RVKW0

FINAL DATA

T3204AA: Group 32 SBLOCA Test 4, PORV Break.

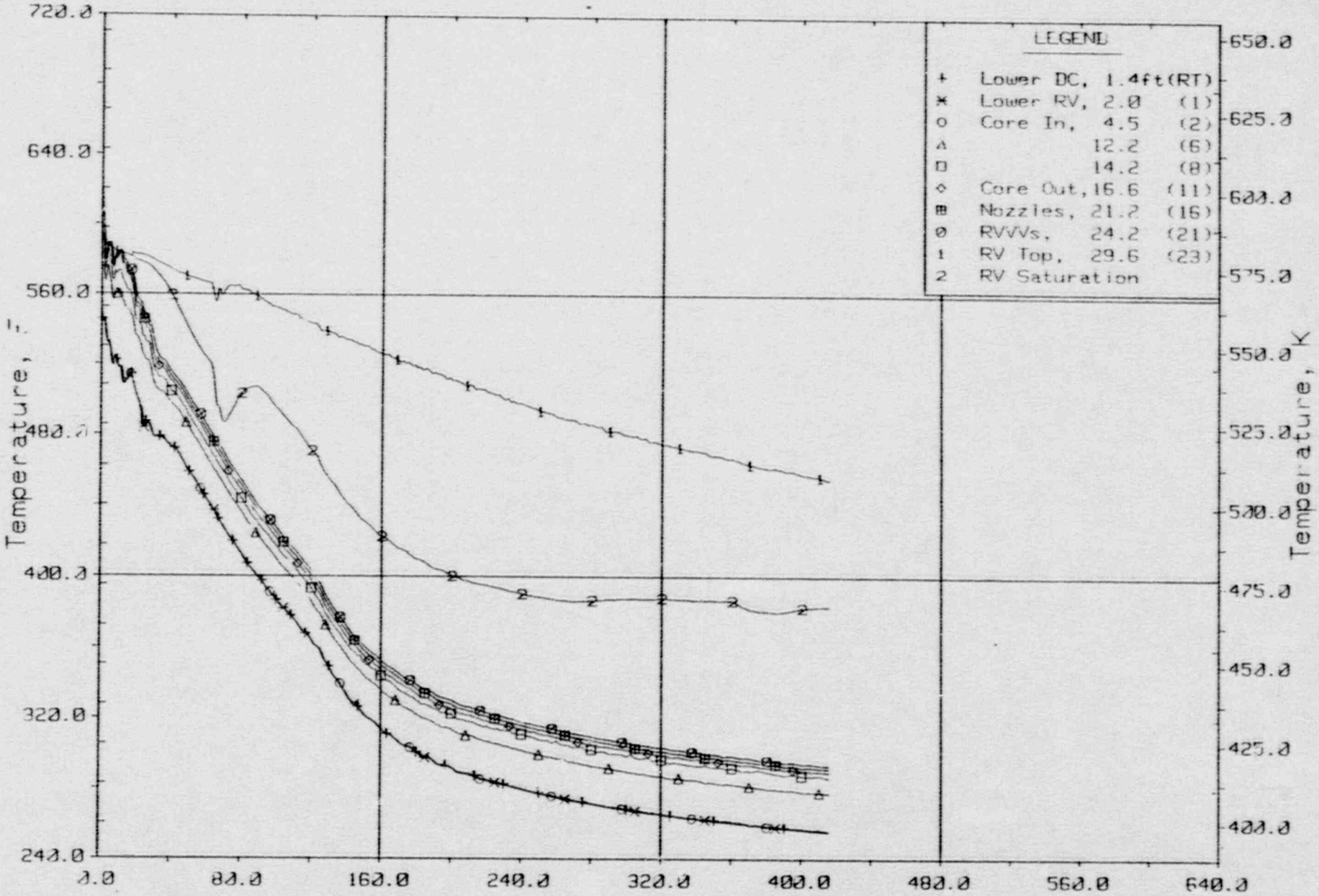

Core Unit Cell and Reactor Vessel Fluid Temperatures (RVTCs).

Wed Jun 8 18:35:51 1988

RVTC0

FINAL DATA

T3204AA: Group 32 SBLOCA Test 4, PORV Break.

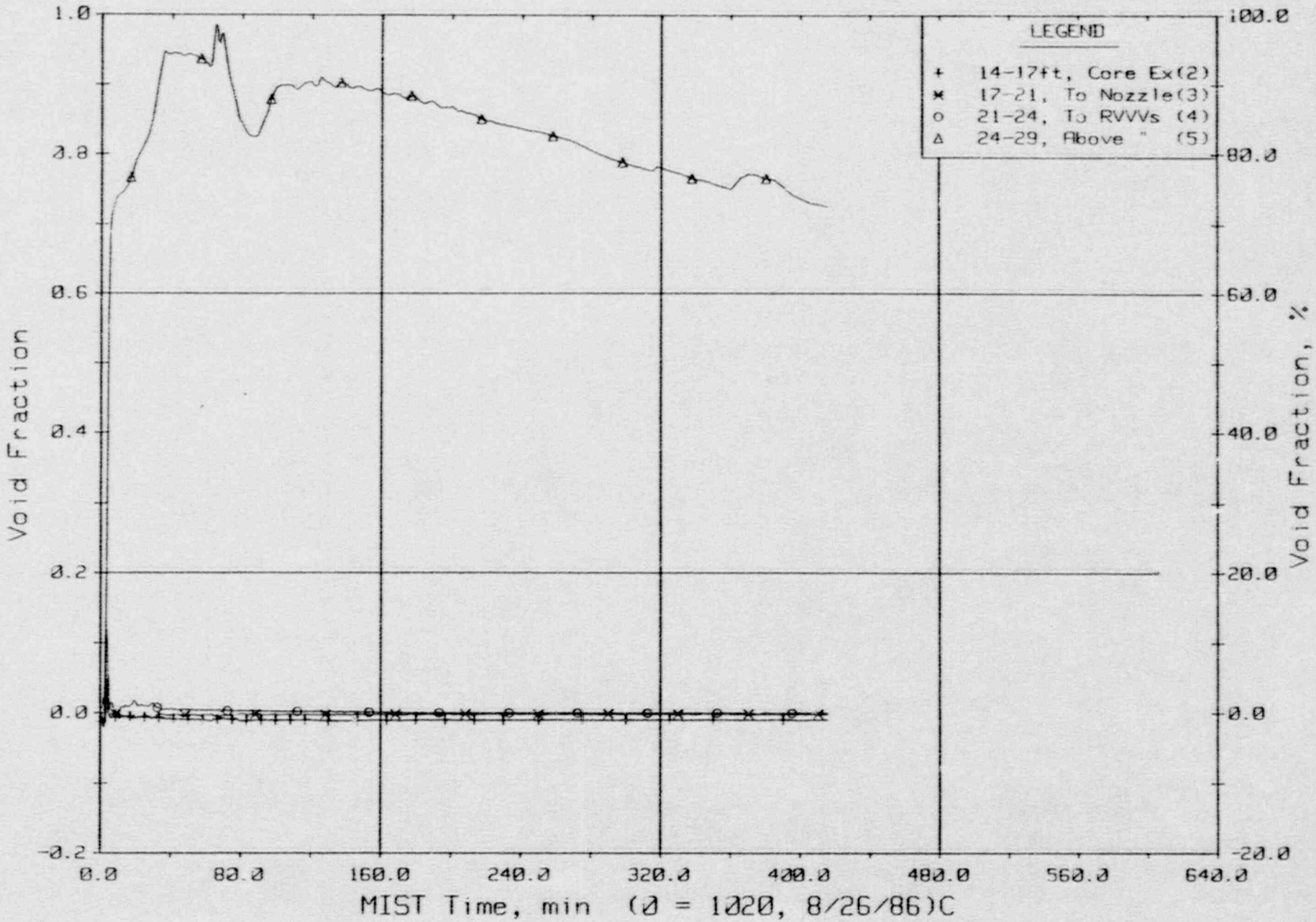

Reactor Vessel Void Fractions From Differential Pressures (RVVFs).

Wed Jun 8 10:38:31 1988

RVVF1

FINAL DATA

T3204AA: Group 32 SBLOCA Test 4, PORV Break.

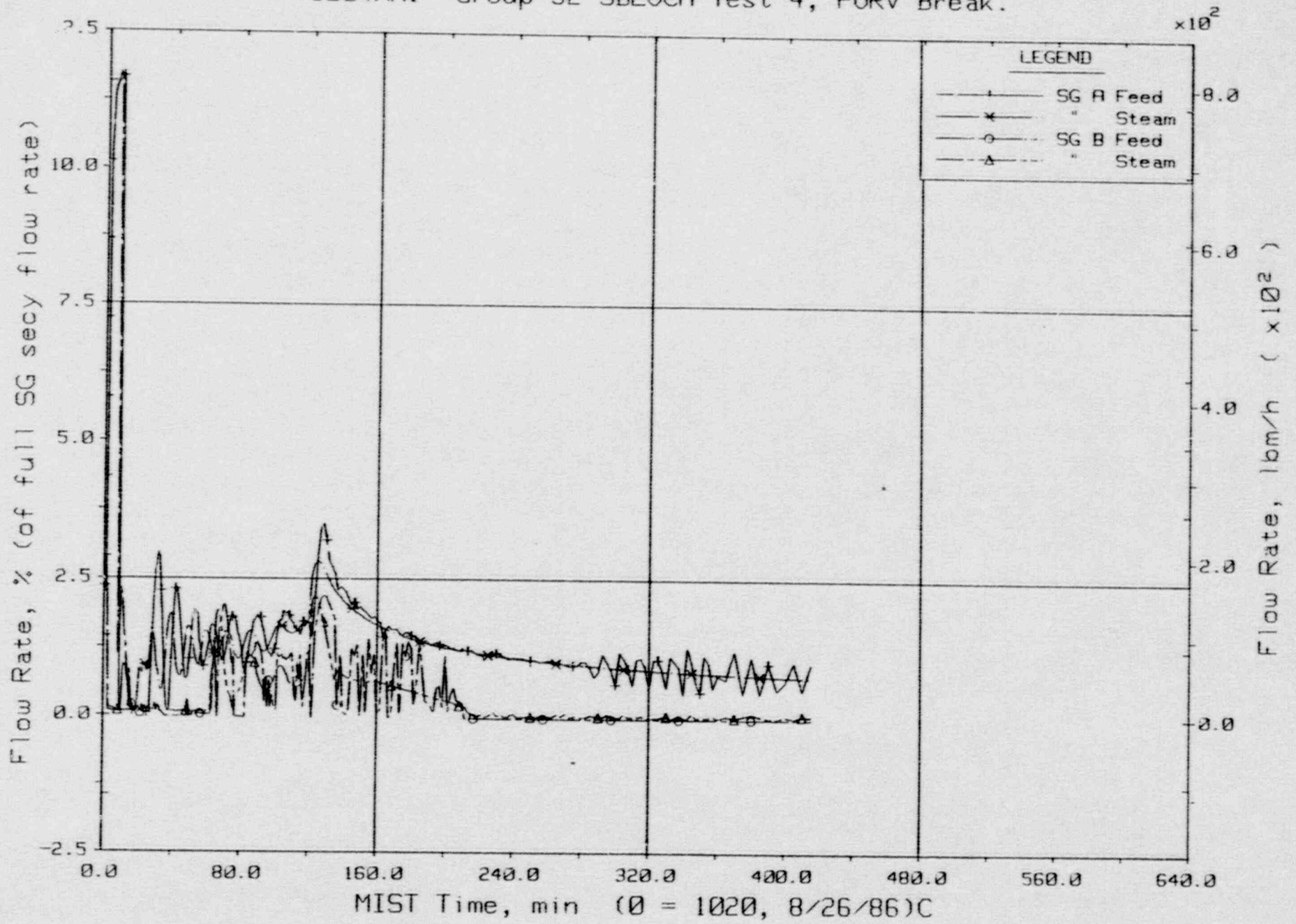

Steam Generator Secondary System Flow Rates.

Wed Jun 8 18:41:04 1988

SGFL2

FINAL DATA

T3204AA: Group 32 SBLOCA Test 4, PORV Break.

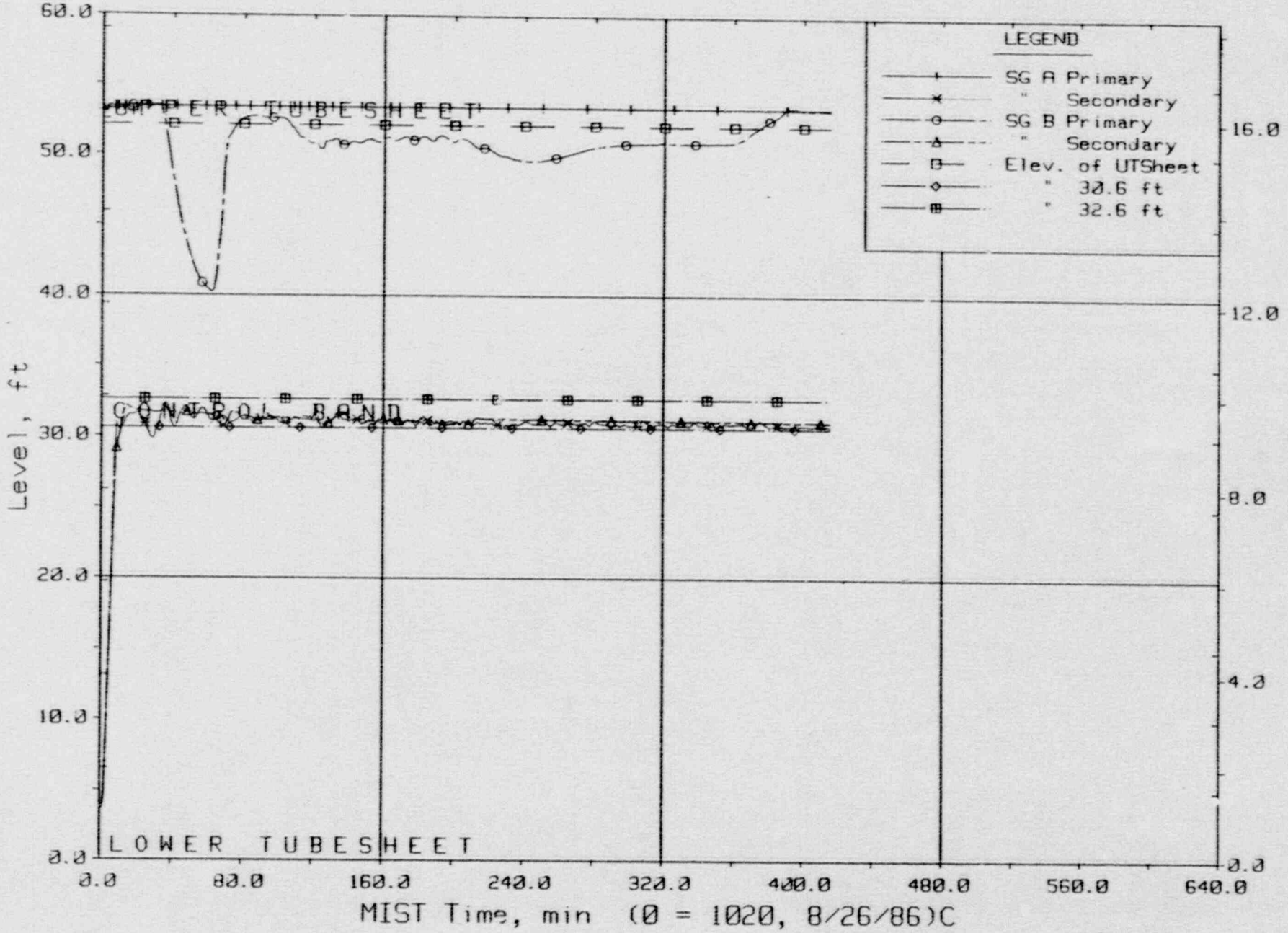

Steam Generator Collapsed Liquid Levels.

Wed Jun 8 10:43:57 1988

SGLV2

FINAL DATA

T3204AA: Group 32 SRLOCA Test 4, PORV Break.

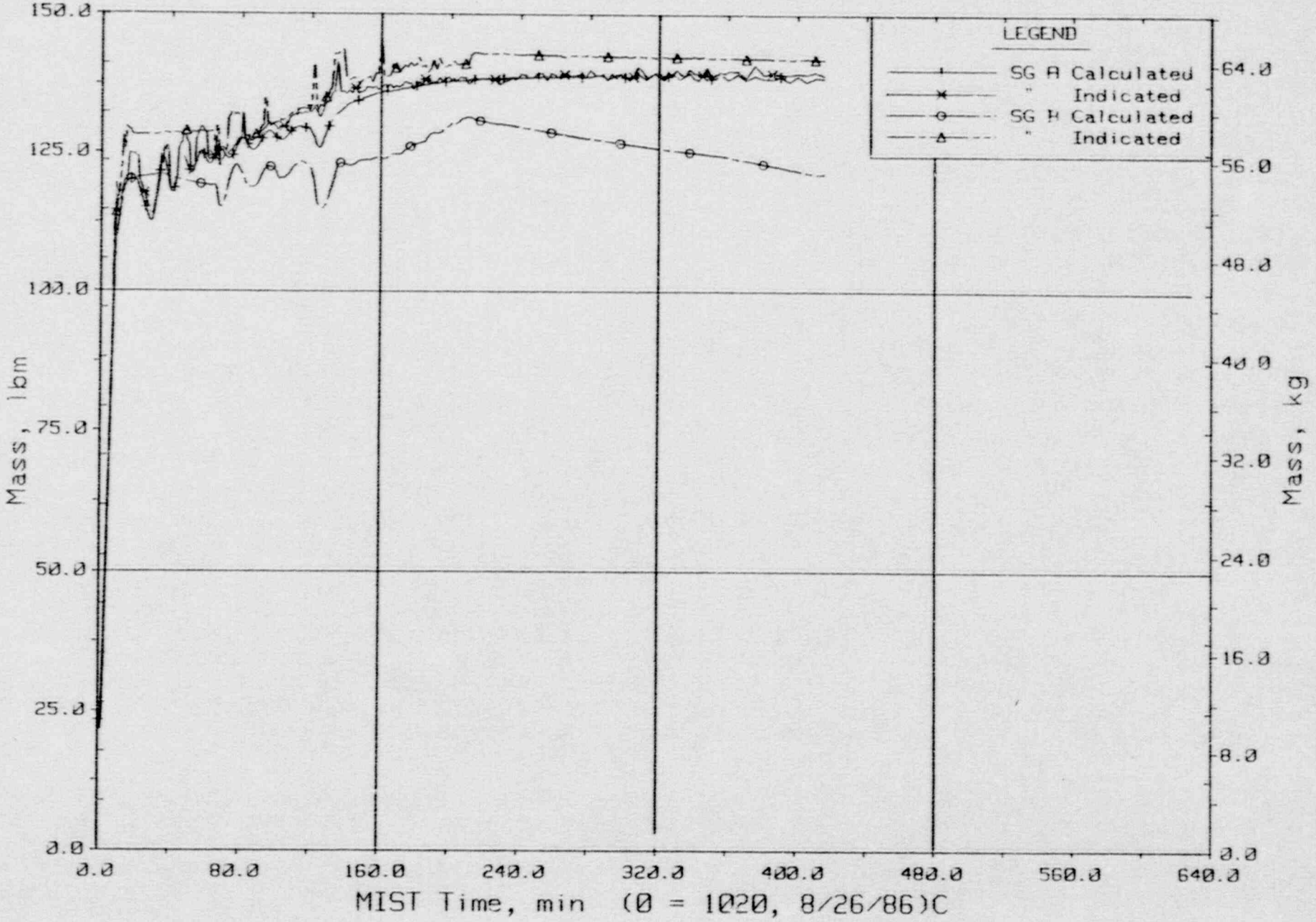

Steam Generator Secondary Fluid Mass Balances.

Wed Jun 8 10:46:33 1988

SGML1

FINAL DATA

T3204AA: Group 32 SBLOCA Test 4, PORV Break.

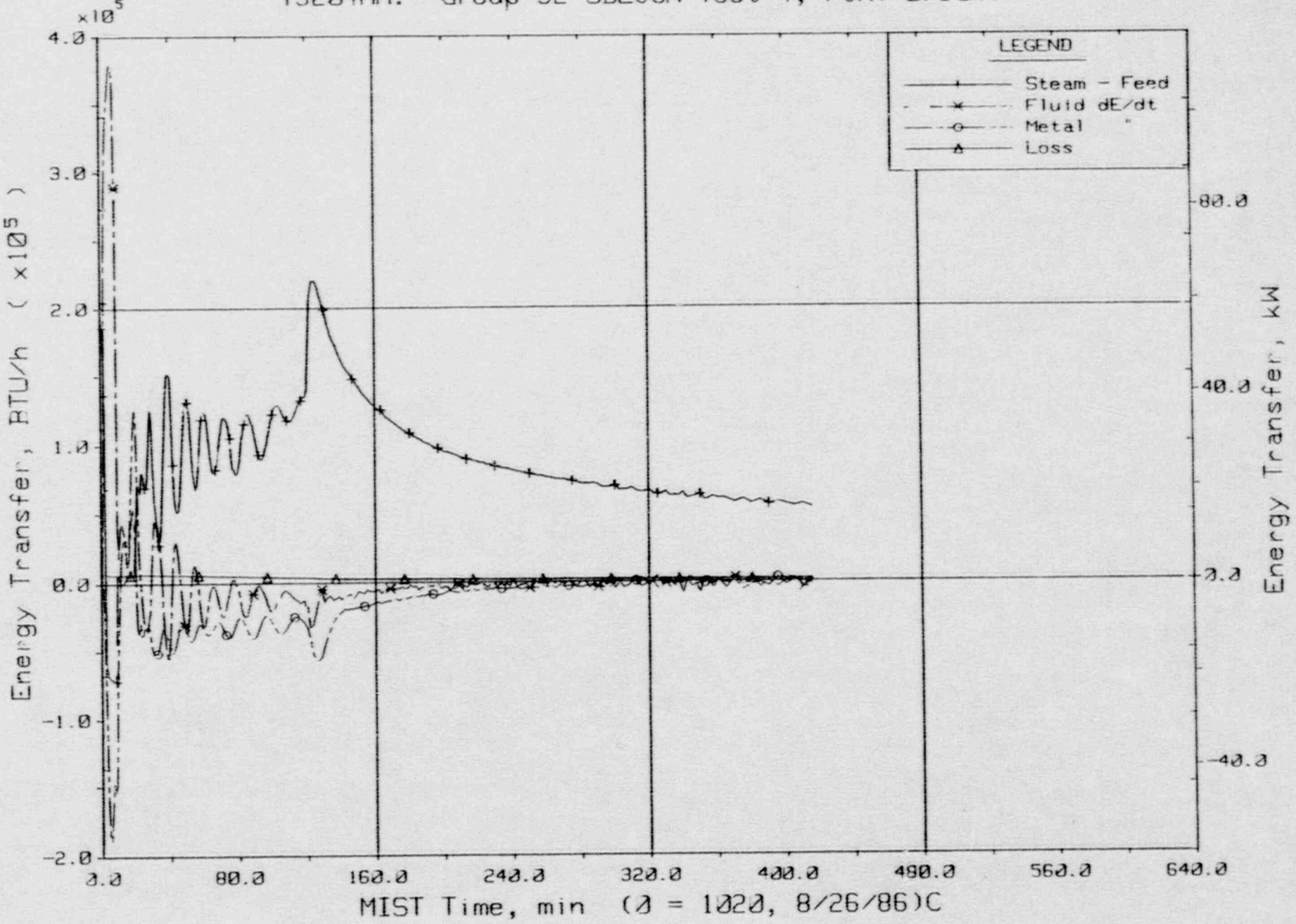

Steam Generator A Energy Transfer.

SGQE3

FINAL DATA

T3204AA: Group 32 SBLOCA Test 4, PORV Break.

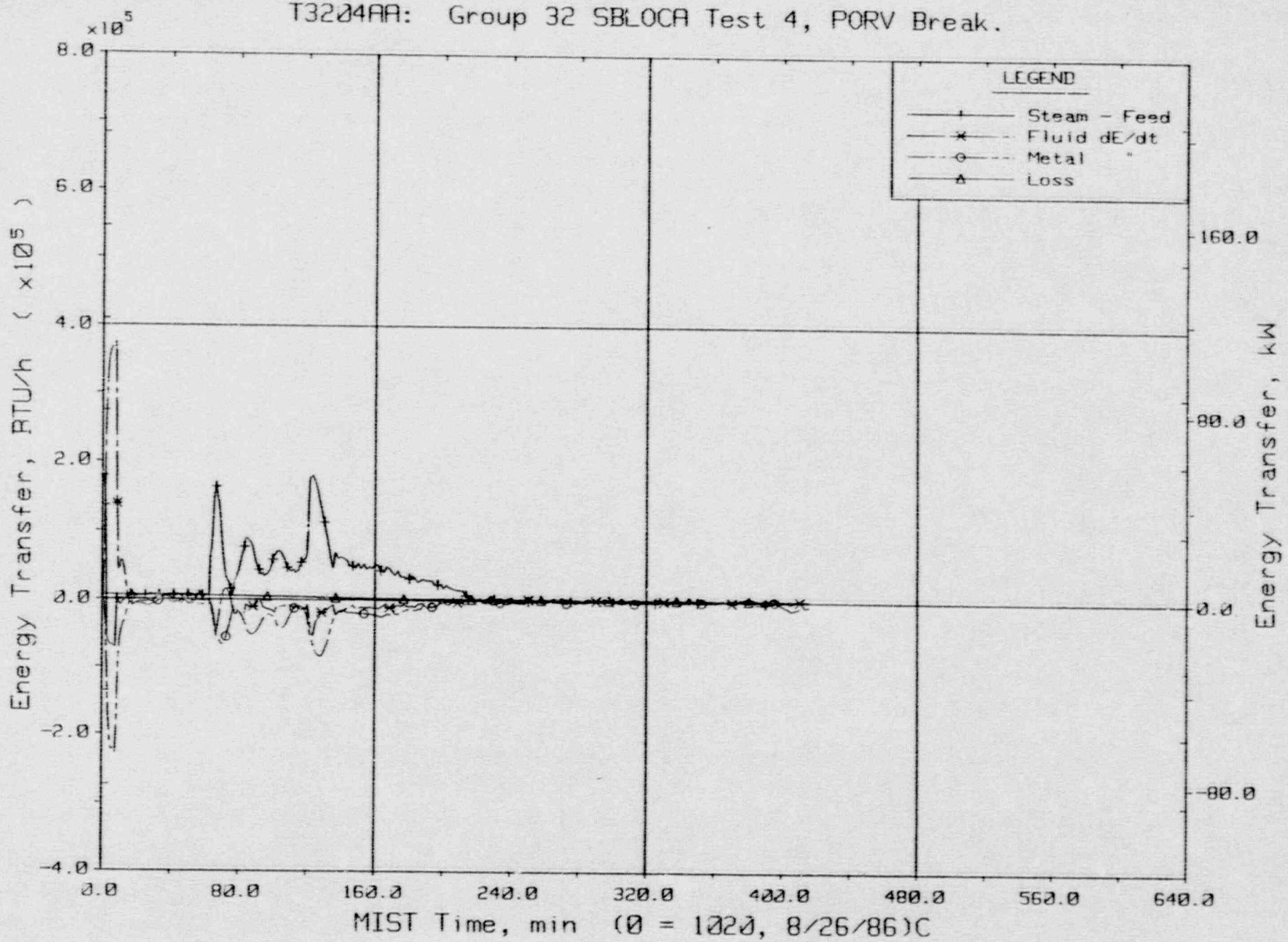

Steam Generator B Energy Transfer.

Wed Jun 8 10:51:50 1988

SGQE6

FINAL DATA

T3204AA: Group 32 SBLOCA Test 4, PORV Break.

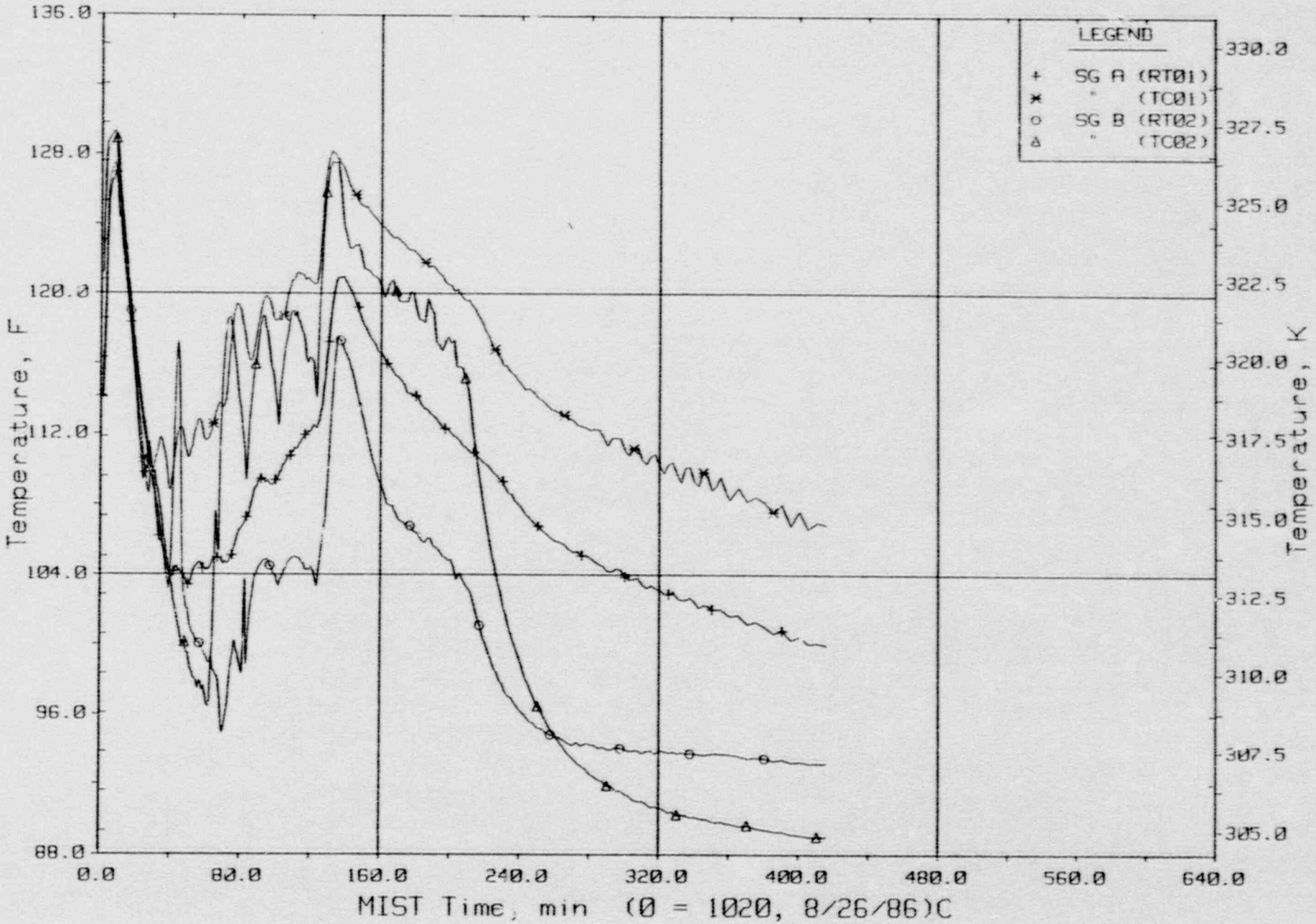

Feedwater Temperatures (SFs).

Wed Jun 8 18:54:06 1988

SGRT1

FINAL DATA

T3204AA: Group 32 SBLOCA Test 4, PORV Break.

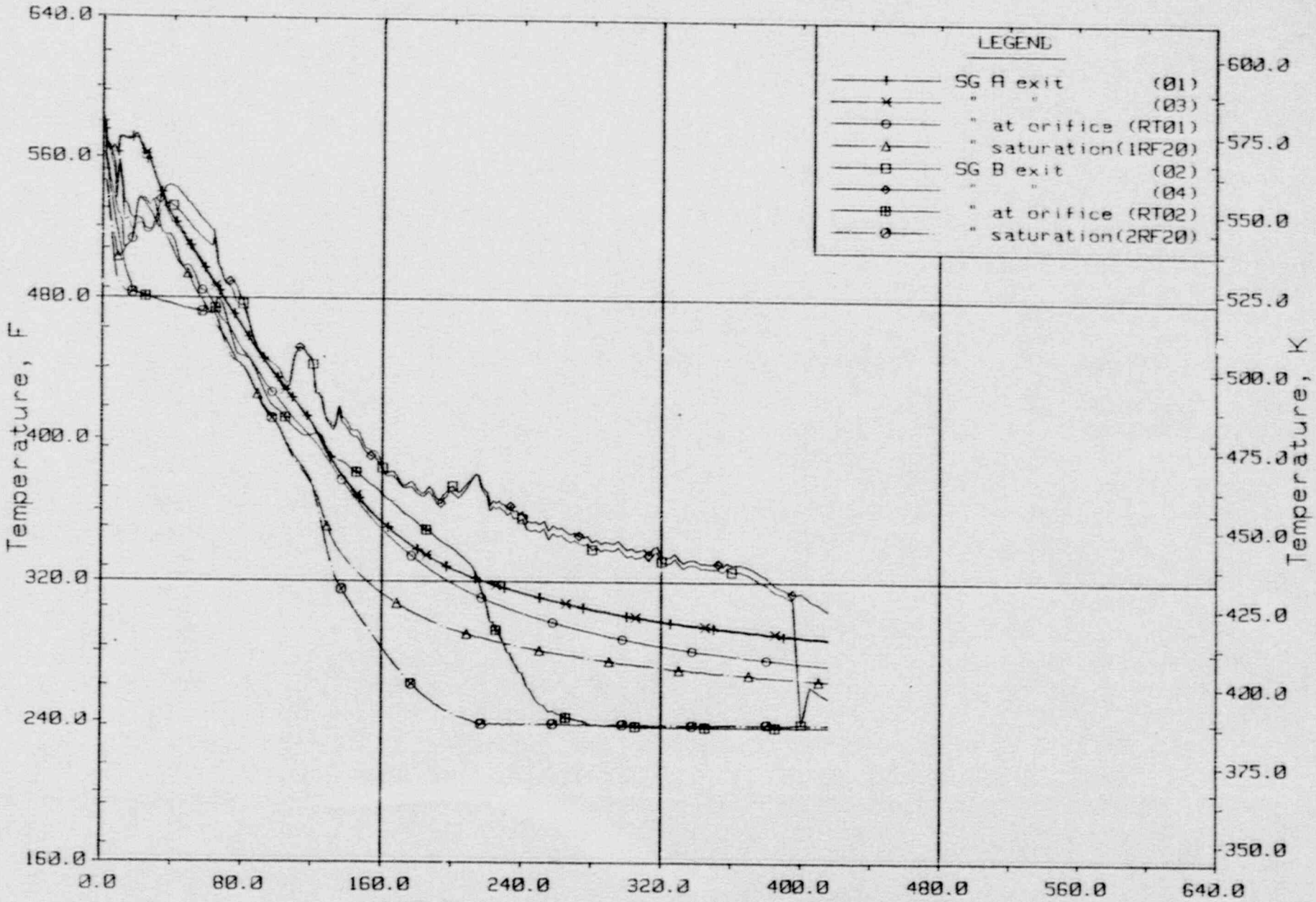

Steam Generator Steam Outlet Temperatures (SSTCs).

Wed Jun 8 10:57:00 1988

SGRT2

FINAL DATA

T3204AA: Group 32 SBLOCA Test 4, PORV Break.

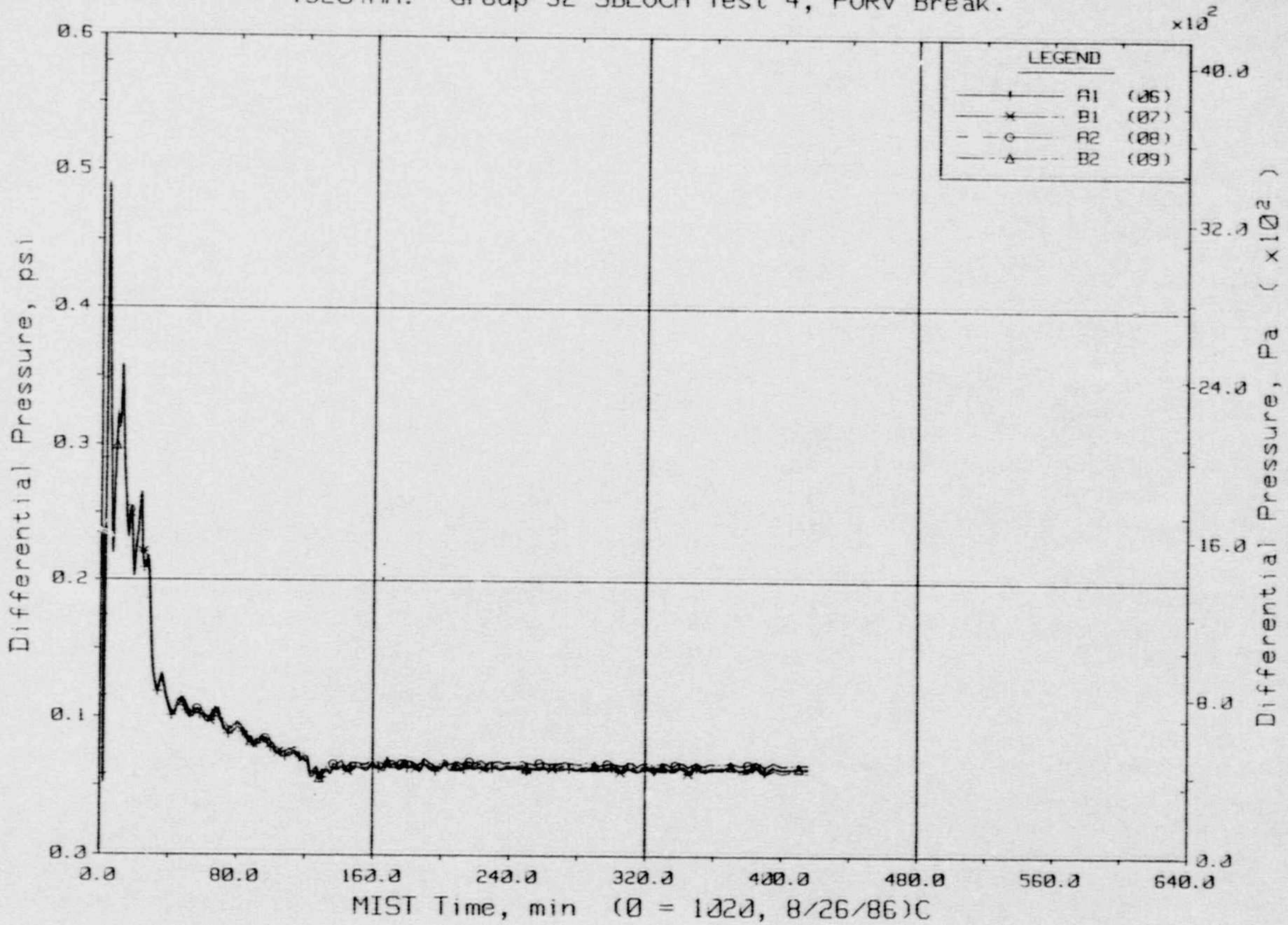

Reactor Vessel Vent Valve Differential Pressures (RVDPs).

Wed Jun 8 18:59:54 1988

VVDP1

FINAL DATA

T3204AA: Group 32 SBLOCA Test 4, PORV Break.

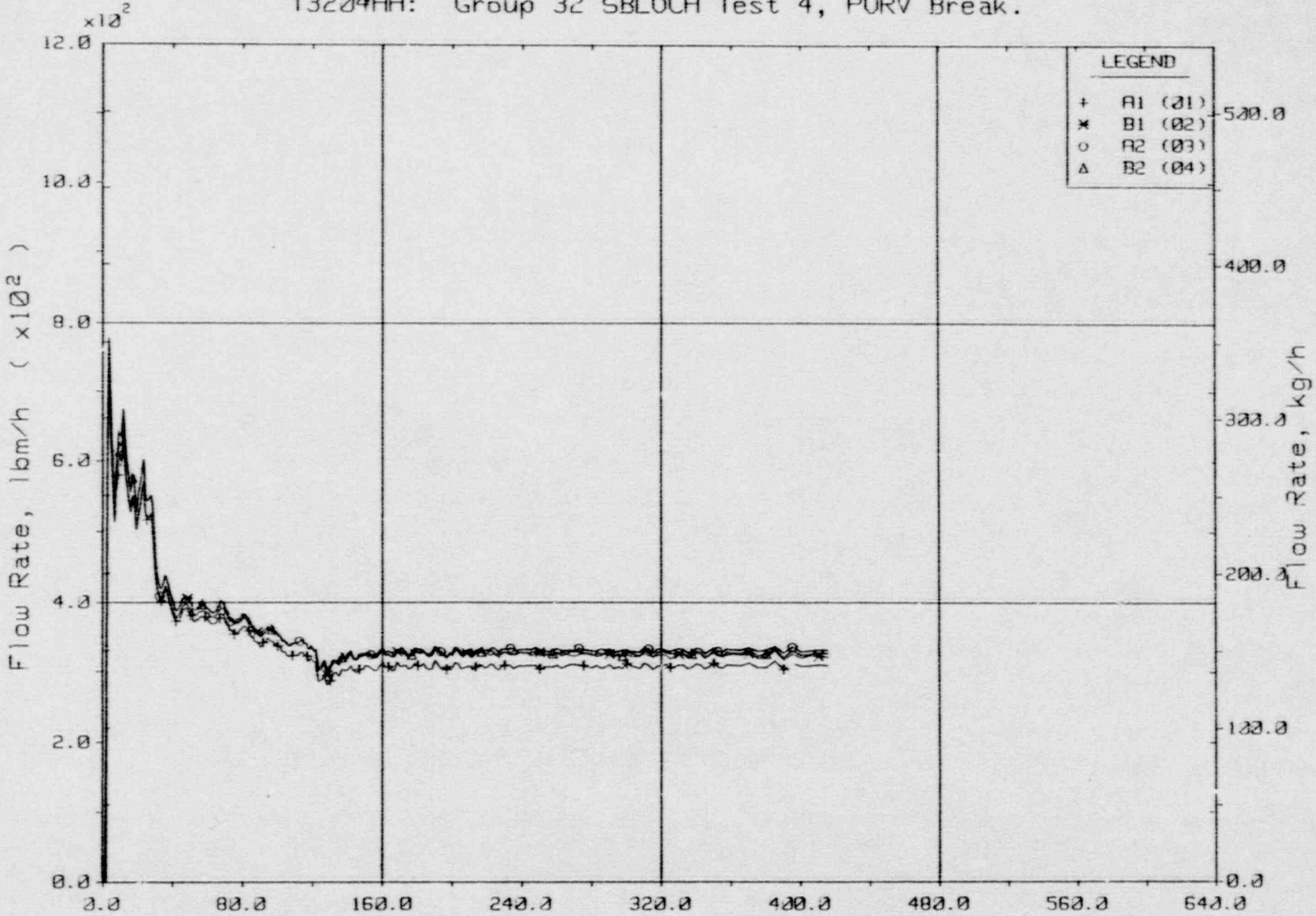

Reactor Vessel Vent Valve Flow Rates (RVORs).

Wed Jun 8 19:02:23 1988

VVFL1

FINAL DATA

T3204AA: Group 32 SBLOCA Test 4, PORV Break.

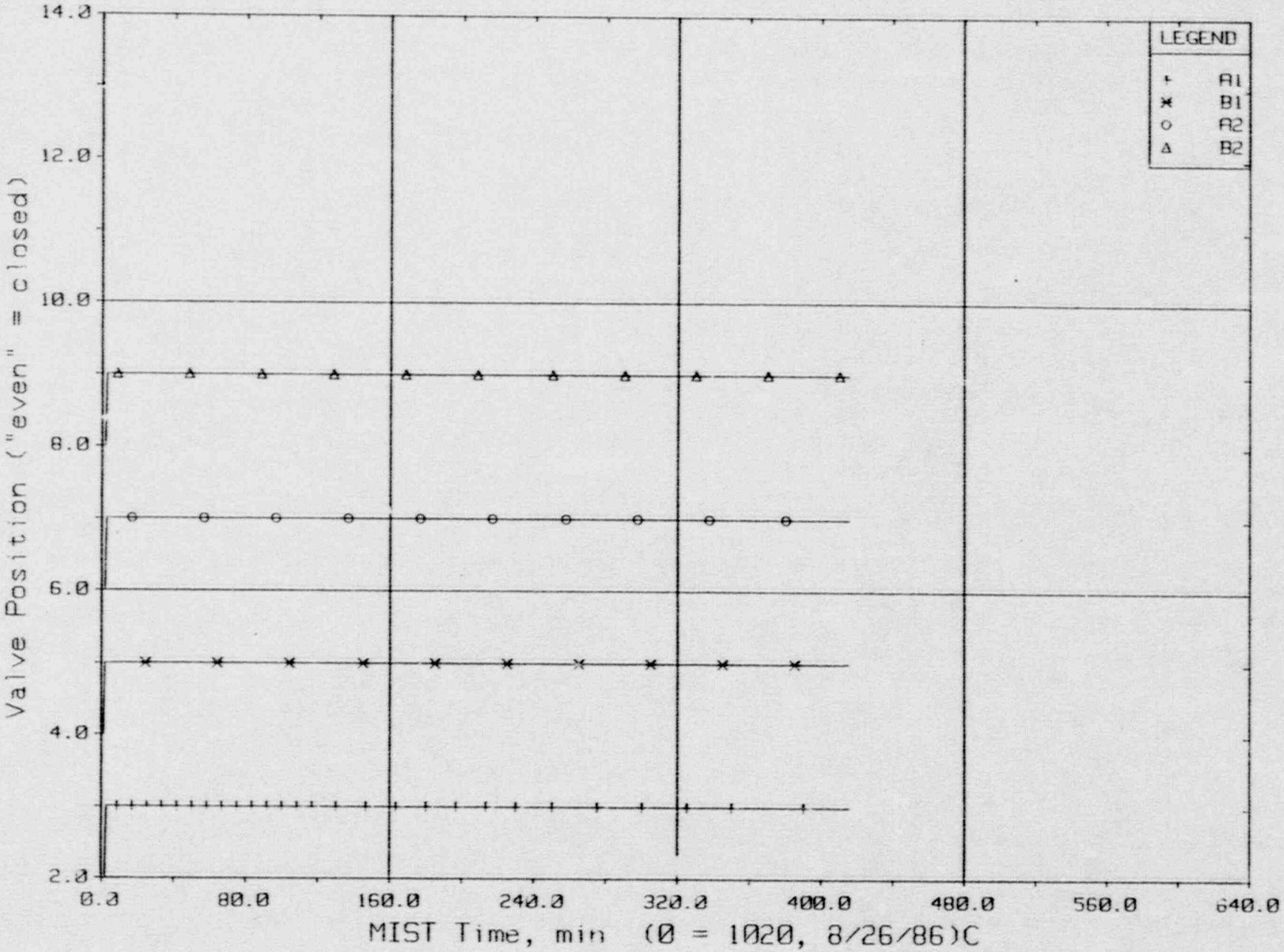

Reactor Vessel Vent Valve Positions.

Wed Jun 8 19:04:37 1988

VVLS1

FINAL DATA

T3204AA: Group 32 SBLOCA Test 4, PORV Break.

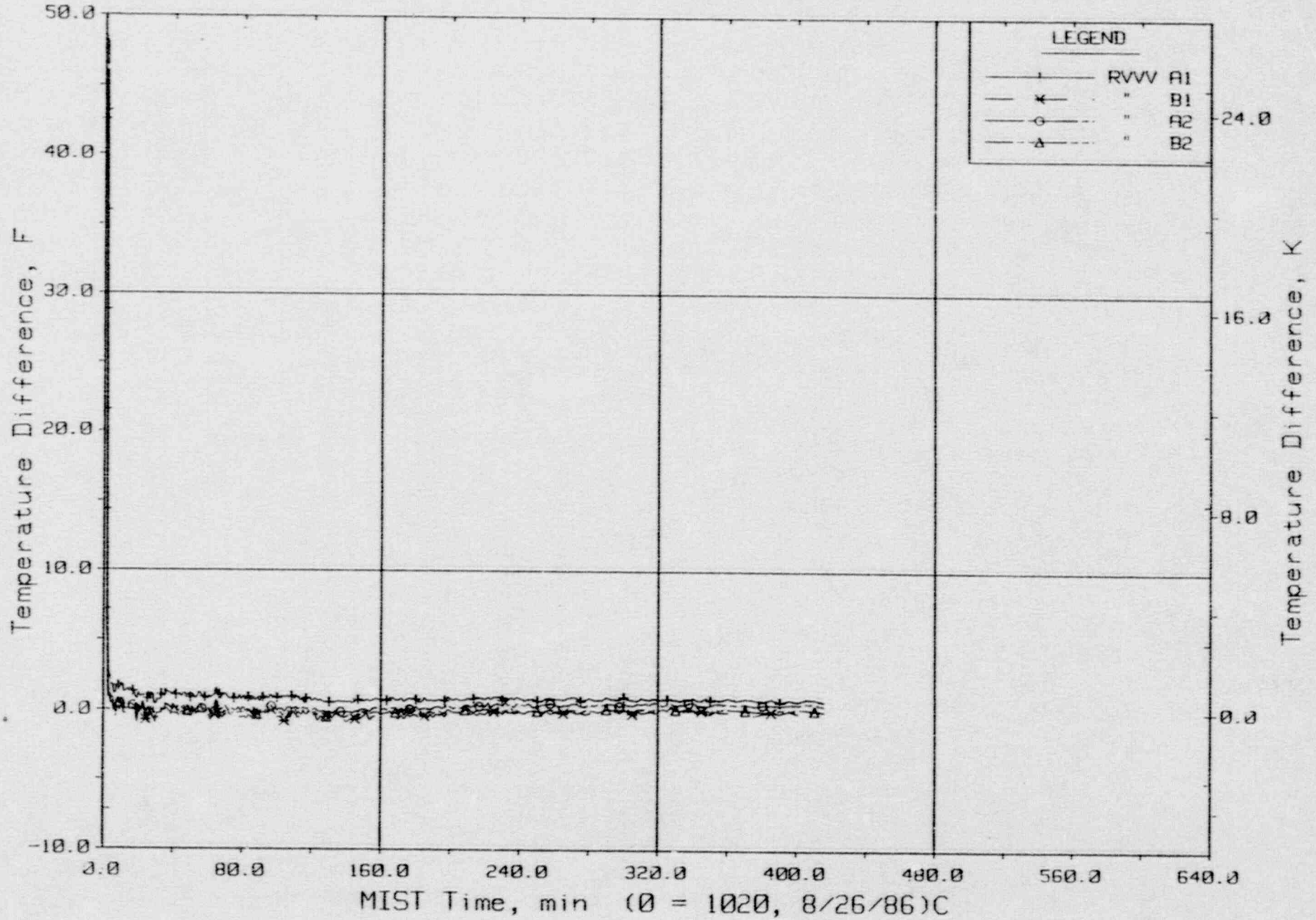

Temperature Differences Across Vent Valves.

Wed Jun 8 19:06:41 1988

VVTD1

T320503

FINAL DATA

T320503: Group 32 SBLOCA Test 5, Leak Isolated.

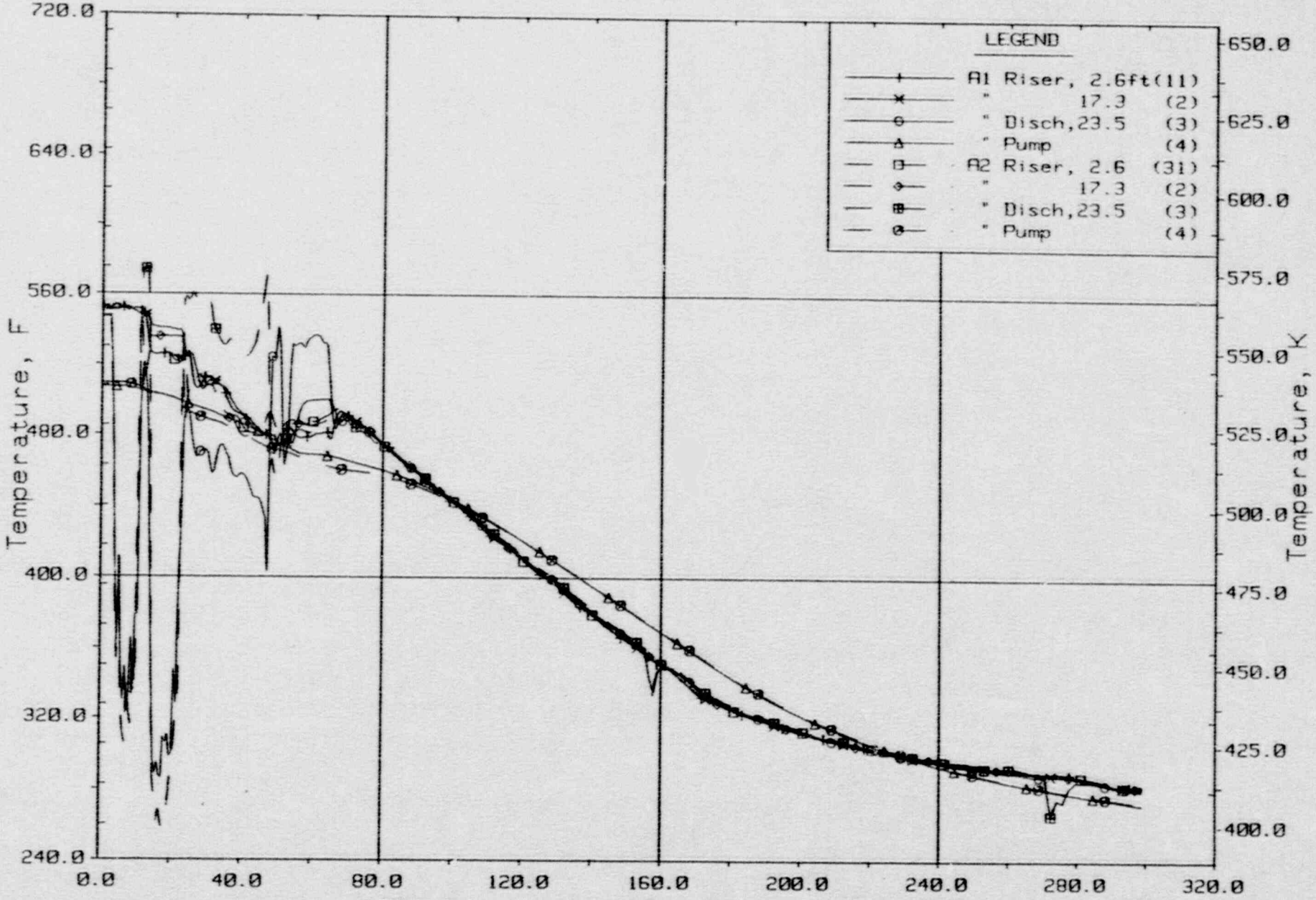

Loop A Cold Leg Metal Temperatures (C1,3MTs).

Thu Jun 9 09:02:29 1988

C1MT1

FINAL DATA

T320503: Group 32 SBLOCA Test 5, Leak Isolated.

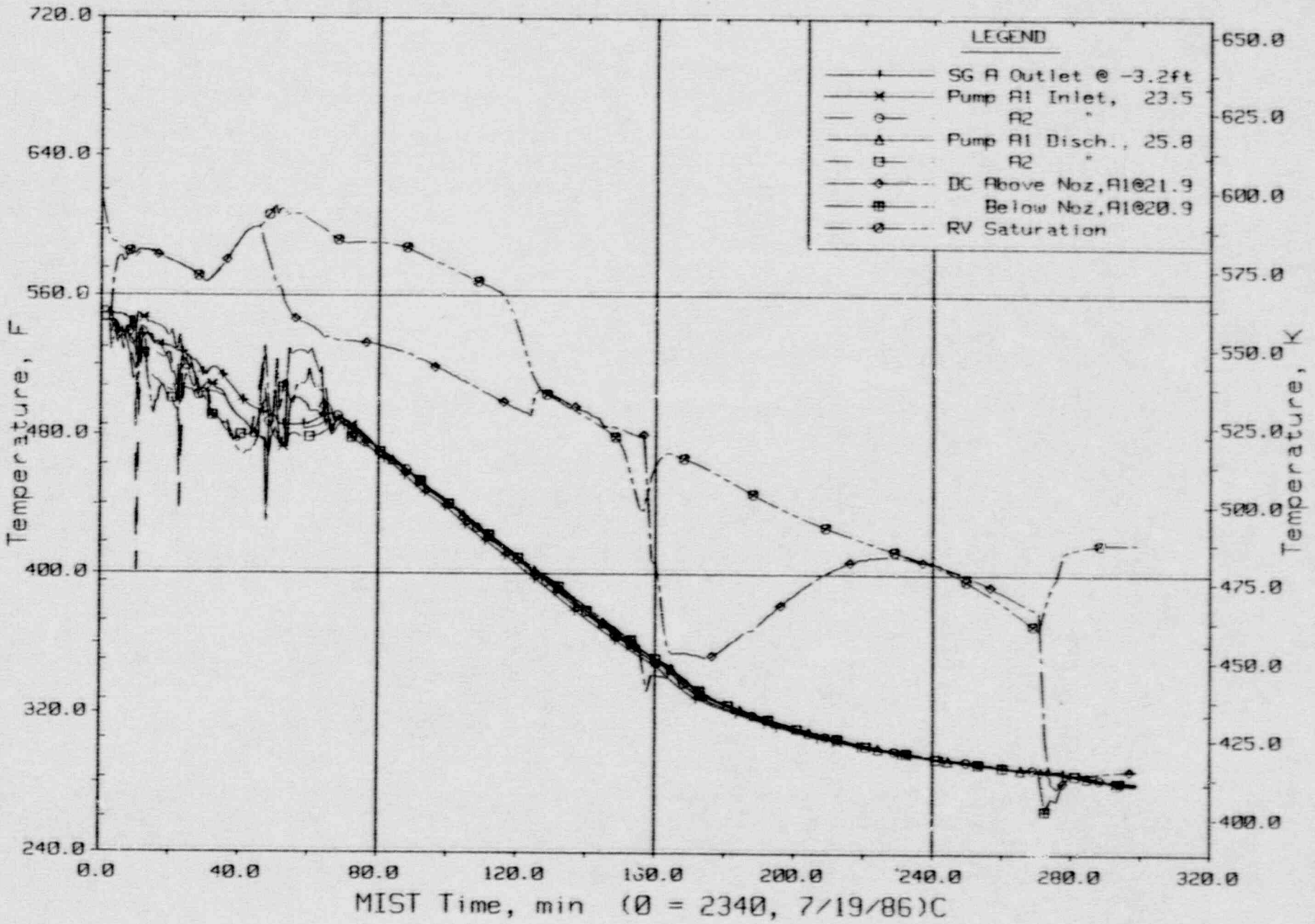

Loop A Cold Leg Fluid Temperatures (RTDs).

Thu Jun 9 09:07:12 1988

C:RT0

FINAL DATA

T320503: Group 32 SBLOCA Test 5, Leak Isolated.

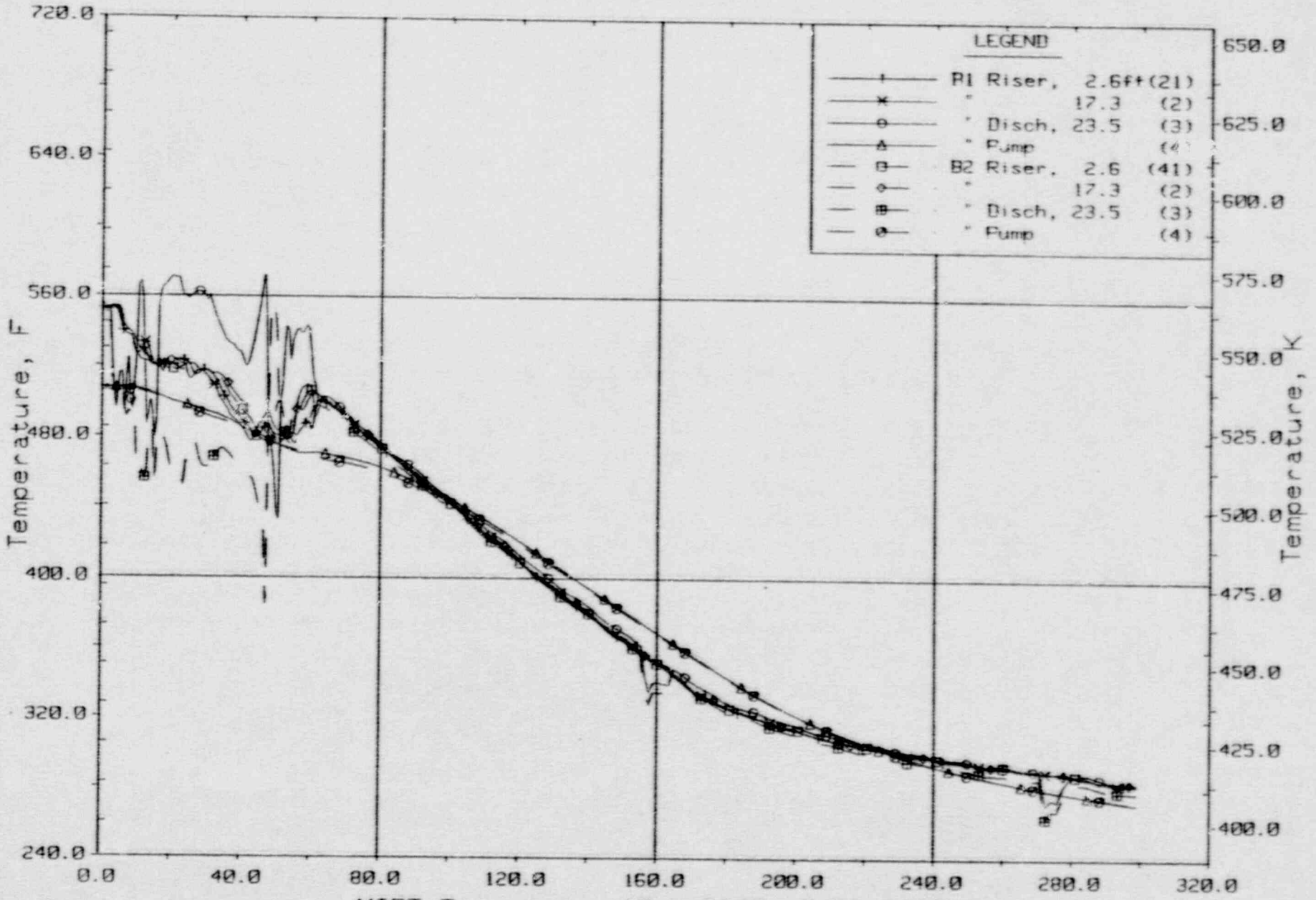

Loop B Cold Leg Metal Temperatures (C2,4MTs).

Thu Jun 9 09:11:49 1988

C2MT1

FINAL DATA

T320503: Group 32 SBLOCA Test 5, Leak Isolated.

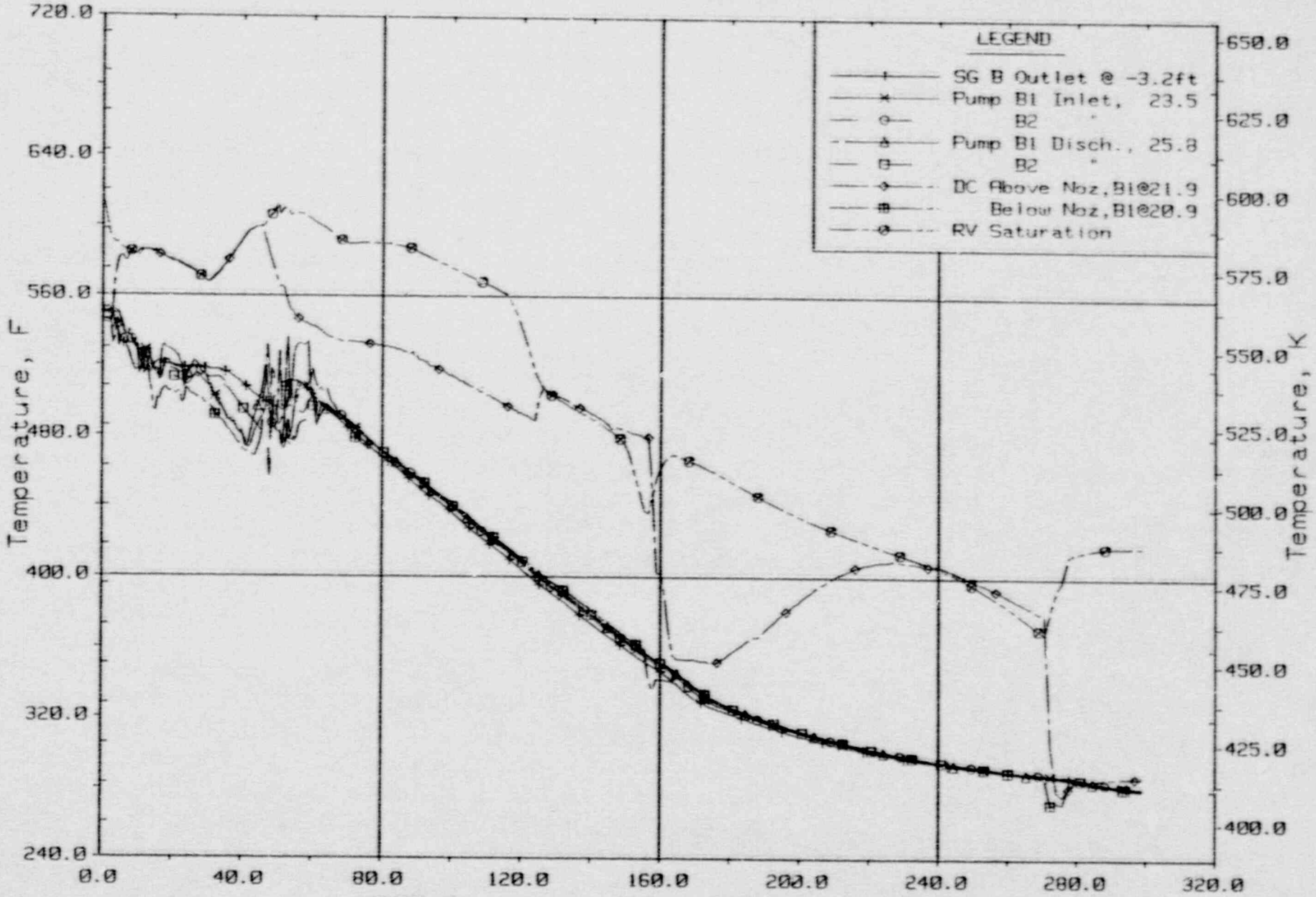

Loop B Cold Leg Fluid Temperatures (RTDs).

Thu Jun 9 09:17:53 1988

C2RT0

FINAL DATA

T320503: Group 32 SBLOCA Test 5, Leak Isolated.

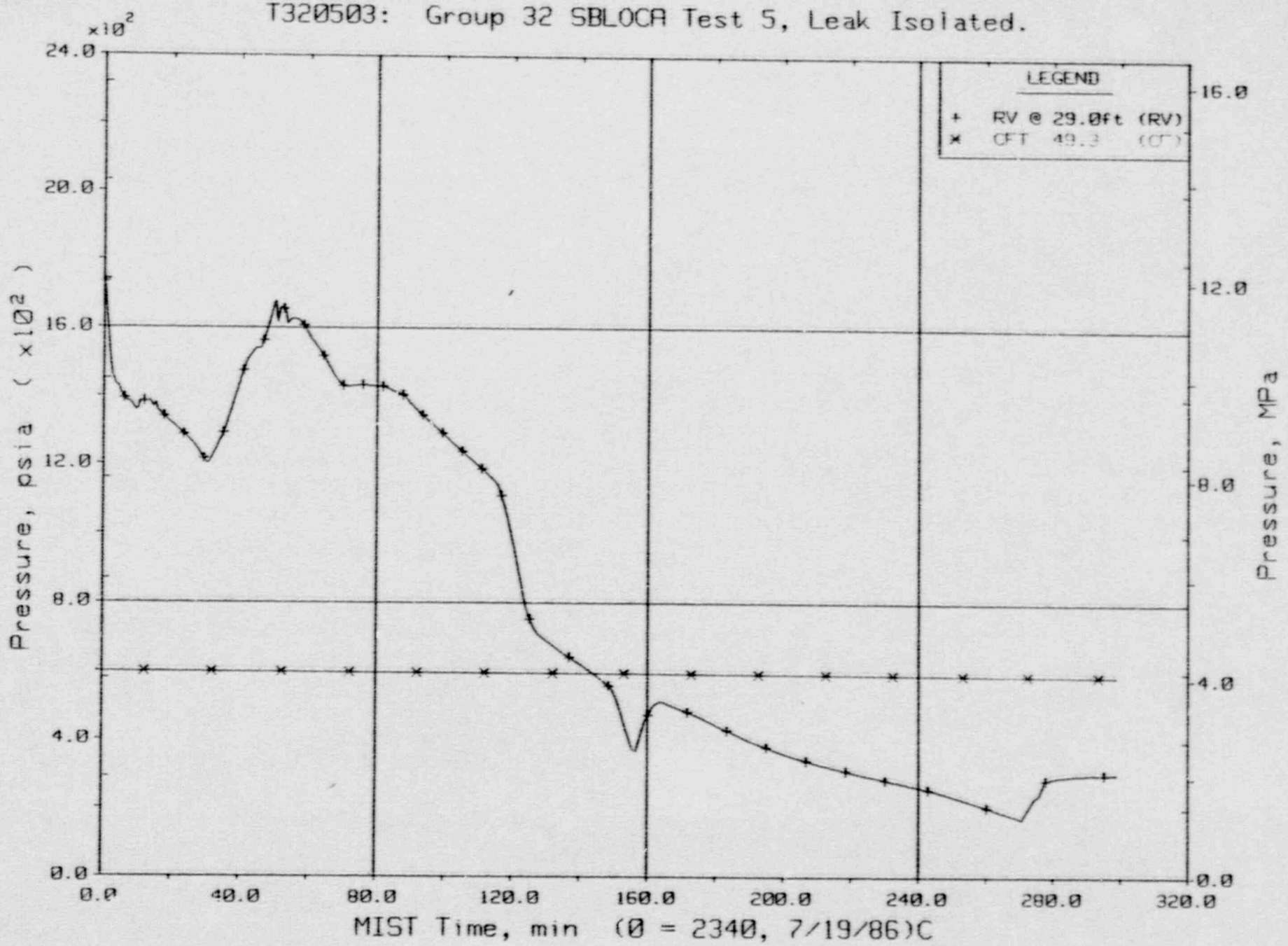

Primary System and Core Flood Tank Pressures (GP0ls).

Thu Jun 9 09:21:08 1988

CFGP1

FINAL DATA

T320503: Group 32 SBLOCA Test 5, Leak Isolated.

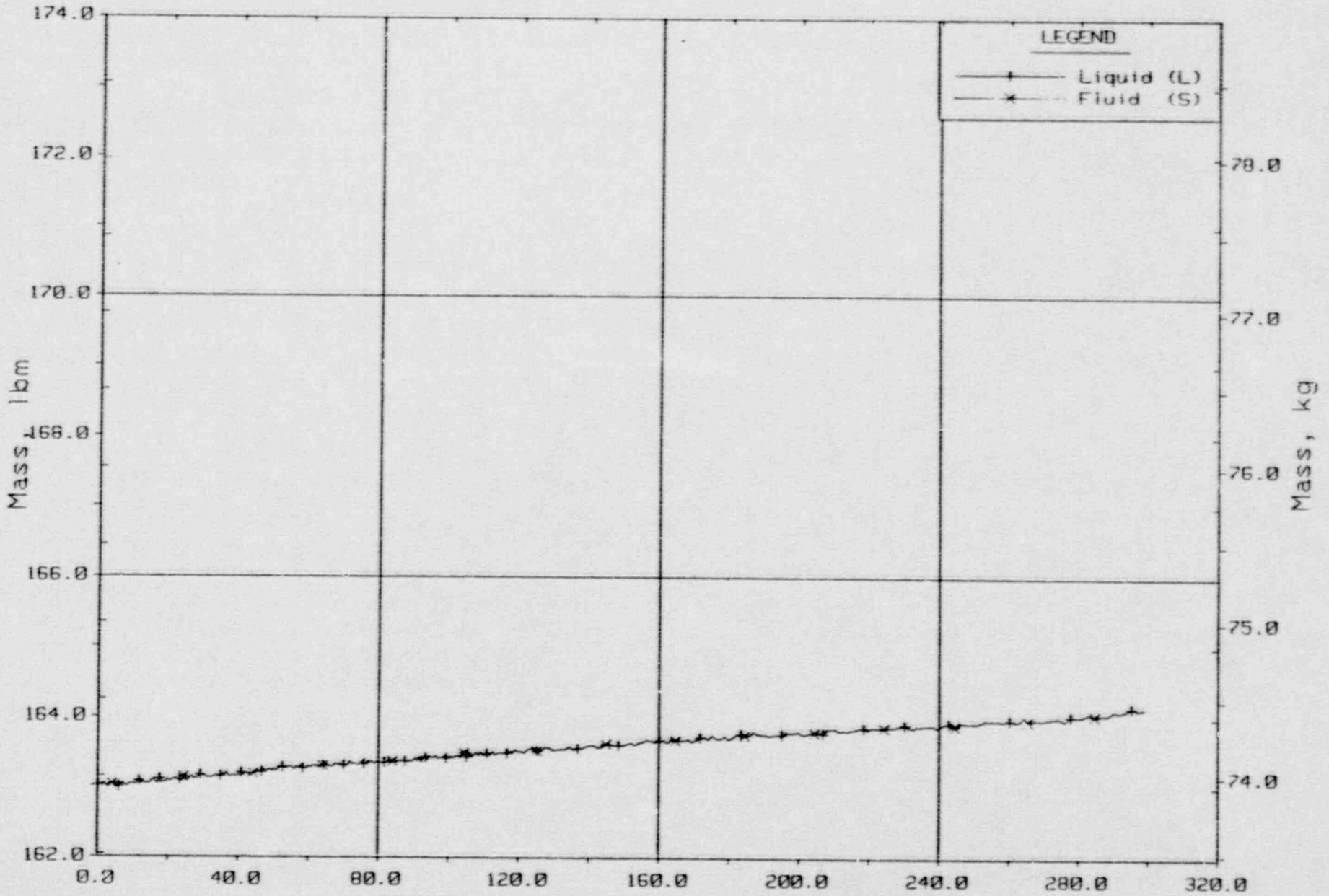

Core Flood Tank Liquid and Fluid Mass (CFMa20s).

Thu Jun 9 09:23:11 1988

CFML1

FINAL DATA

T320503: Group 32 SBLOCA Test 5, Leak Isolated.

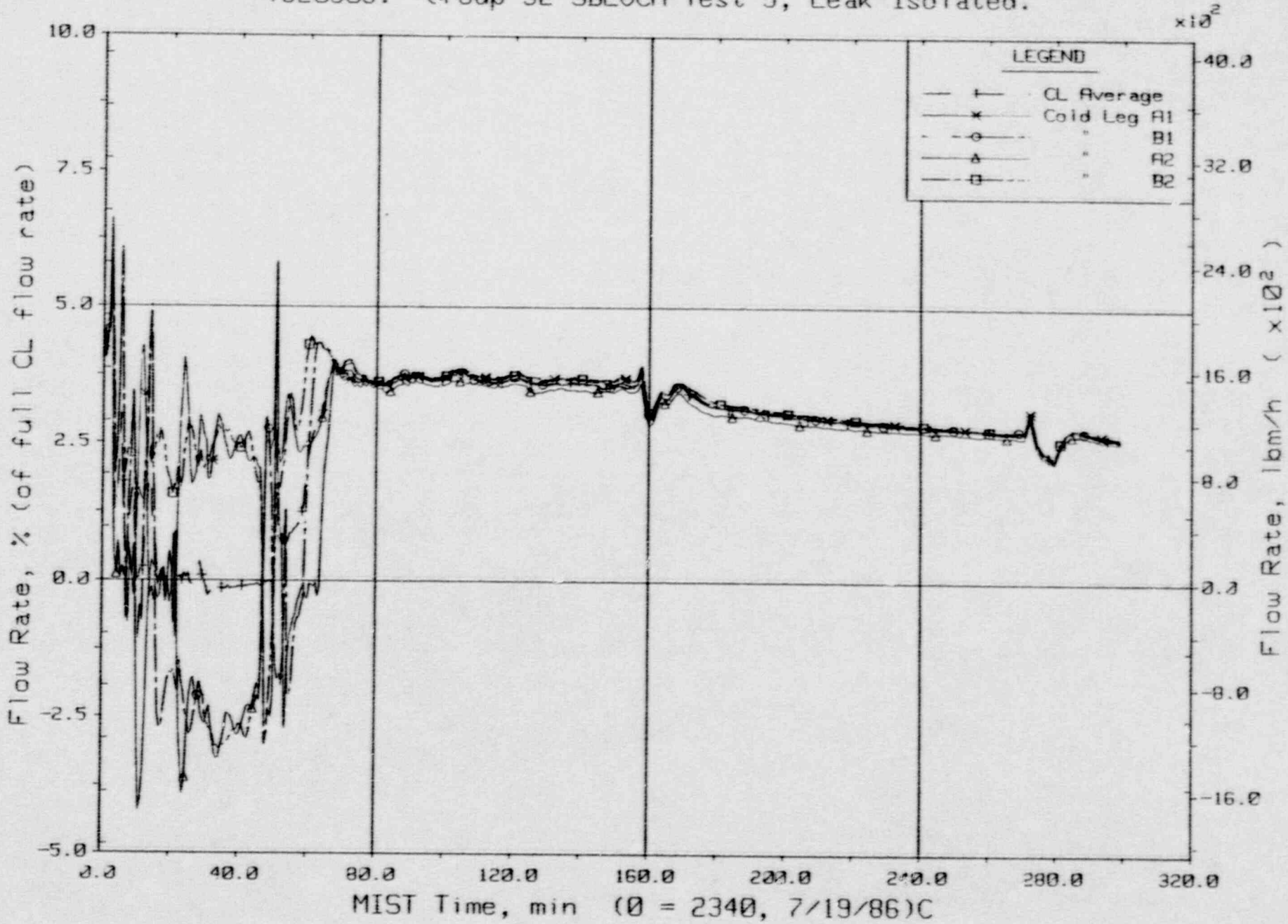

Cold Leg (Venturi) Flow Rates.

Thu Jun 9 09:26:13 1988

CLFL1

FINAL DATA

T320503: Group 32 SBLOCA Test 5, Leak Isolated.

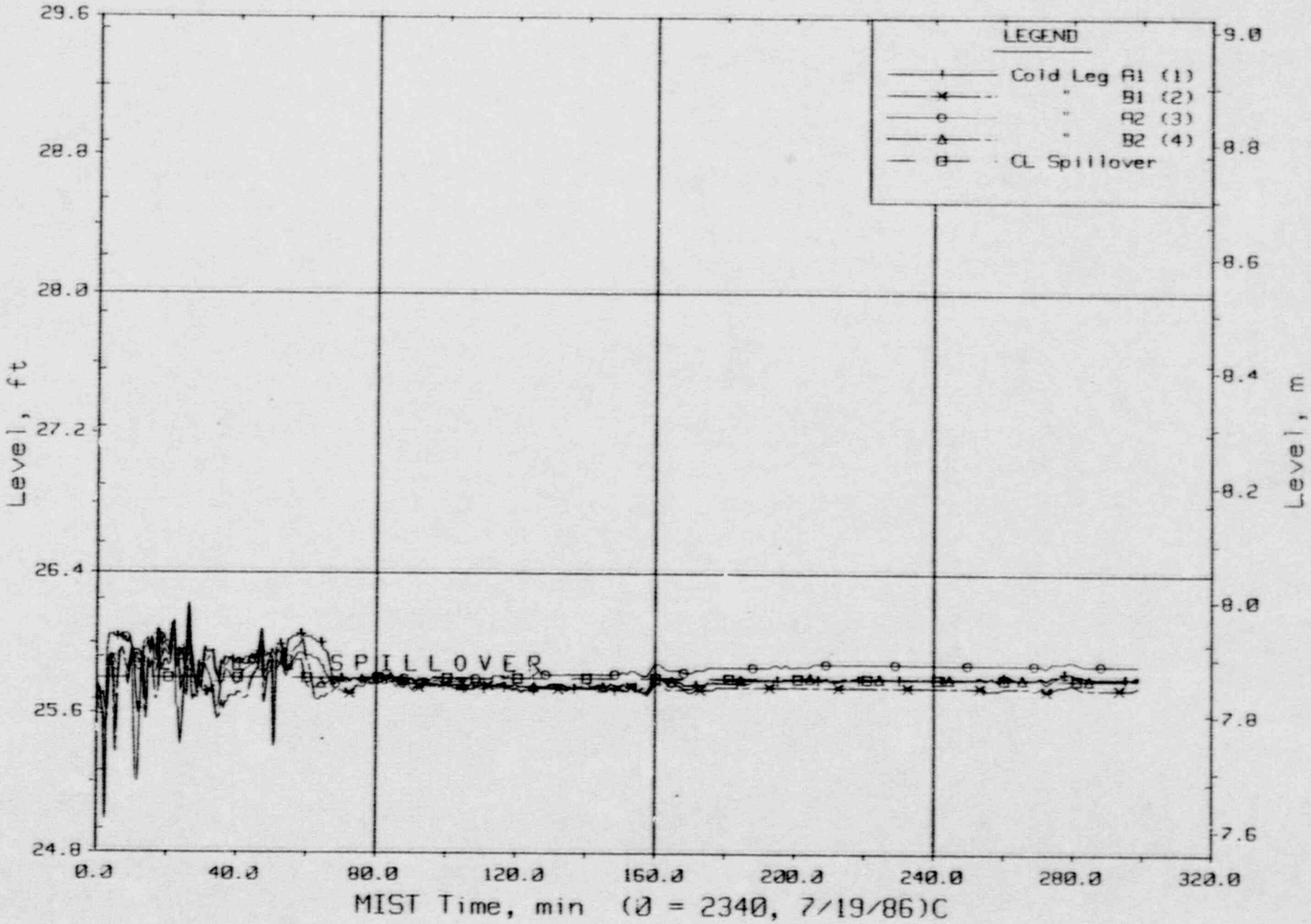

Cold Leg Suction Collapsed Liquid Levels (CnLV22s).

Thu Jun 9 09:29:44 1988

CLLV4

FINAL DATA

T320503: Group 32 SBLOCA Test 5, Leak Isolated.

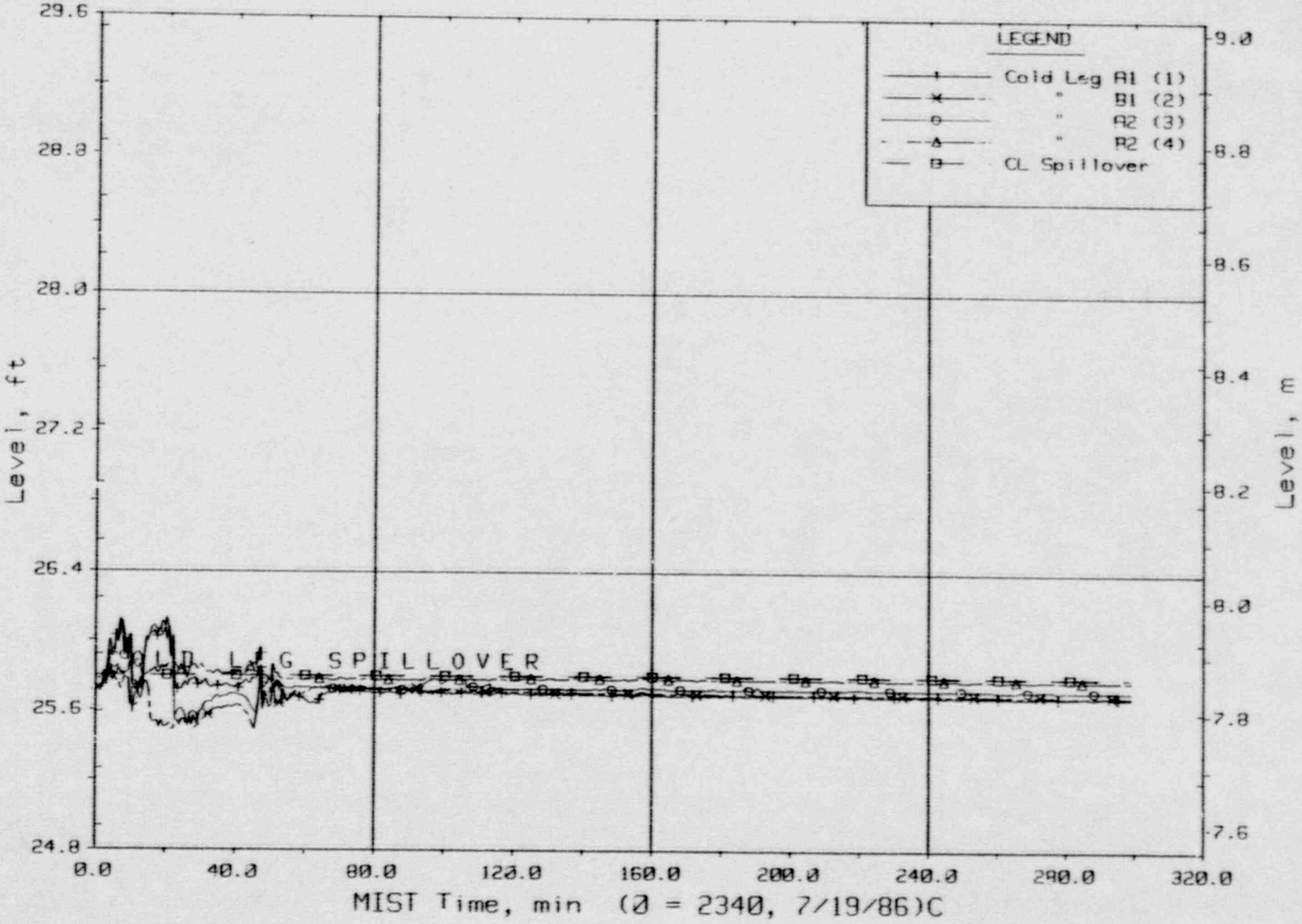

Cold Leg Discharge Collapsed Liquid Levels (CnLV23s).

Thu Jun 9 09:32:53 1988

CLLV5

FINAL DATA

T320503: Group 32 SBLOCA Test 5, Leak Isolated.

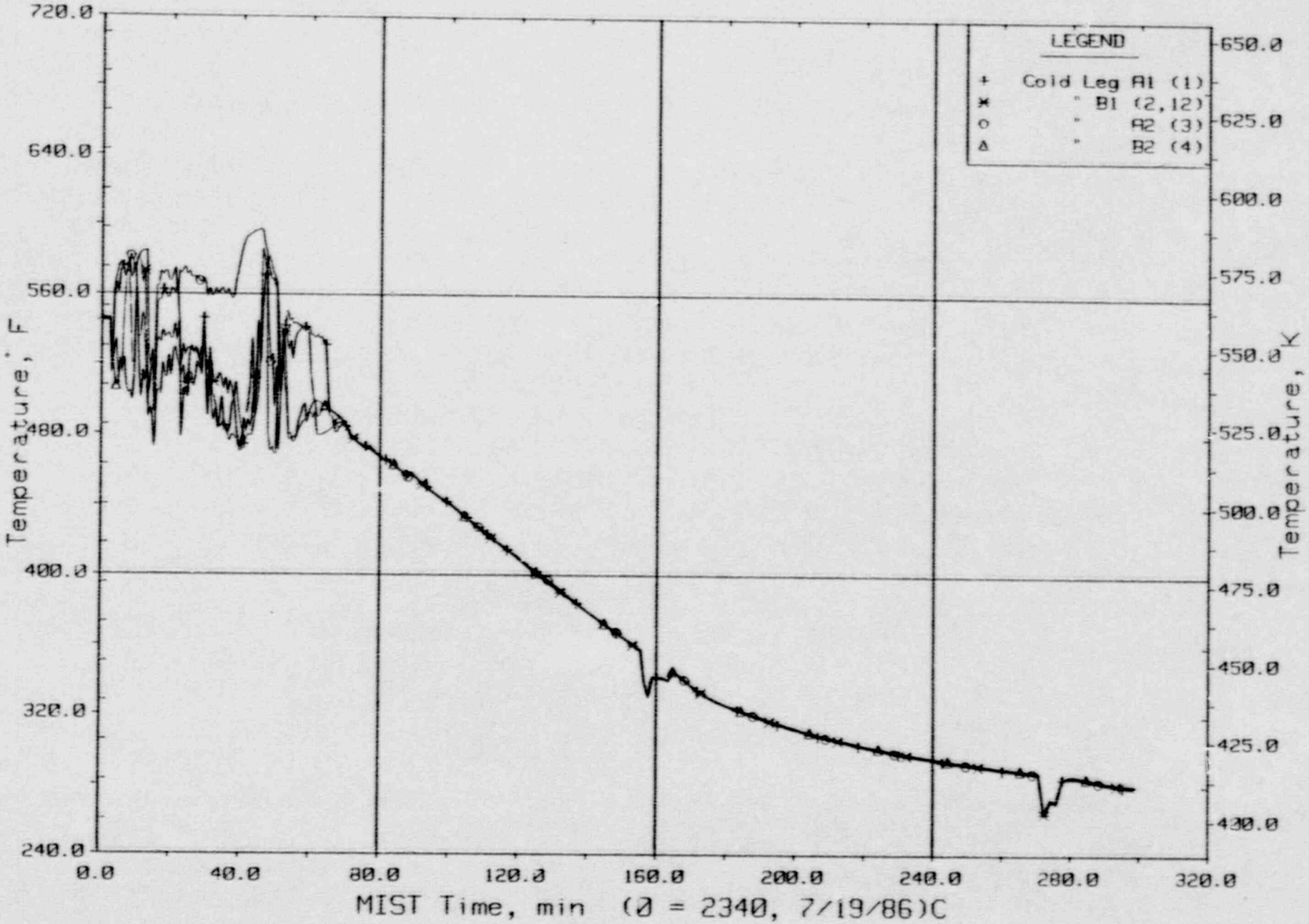

Cold Leg Nozzle Fluid Temperatures, Top of Rake (21.3ft, CnTC11s).

Thu Jun 9 09:37:15 1988

CLTC1

FINAL DATA

T320503: Group 32 SBLOCA Test 5, Leak Isolated.

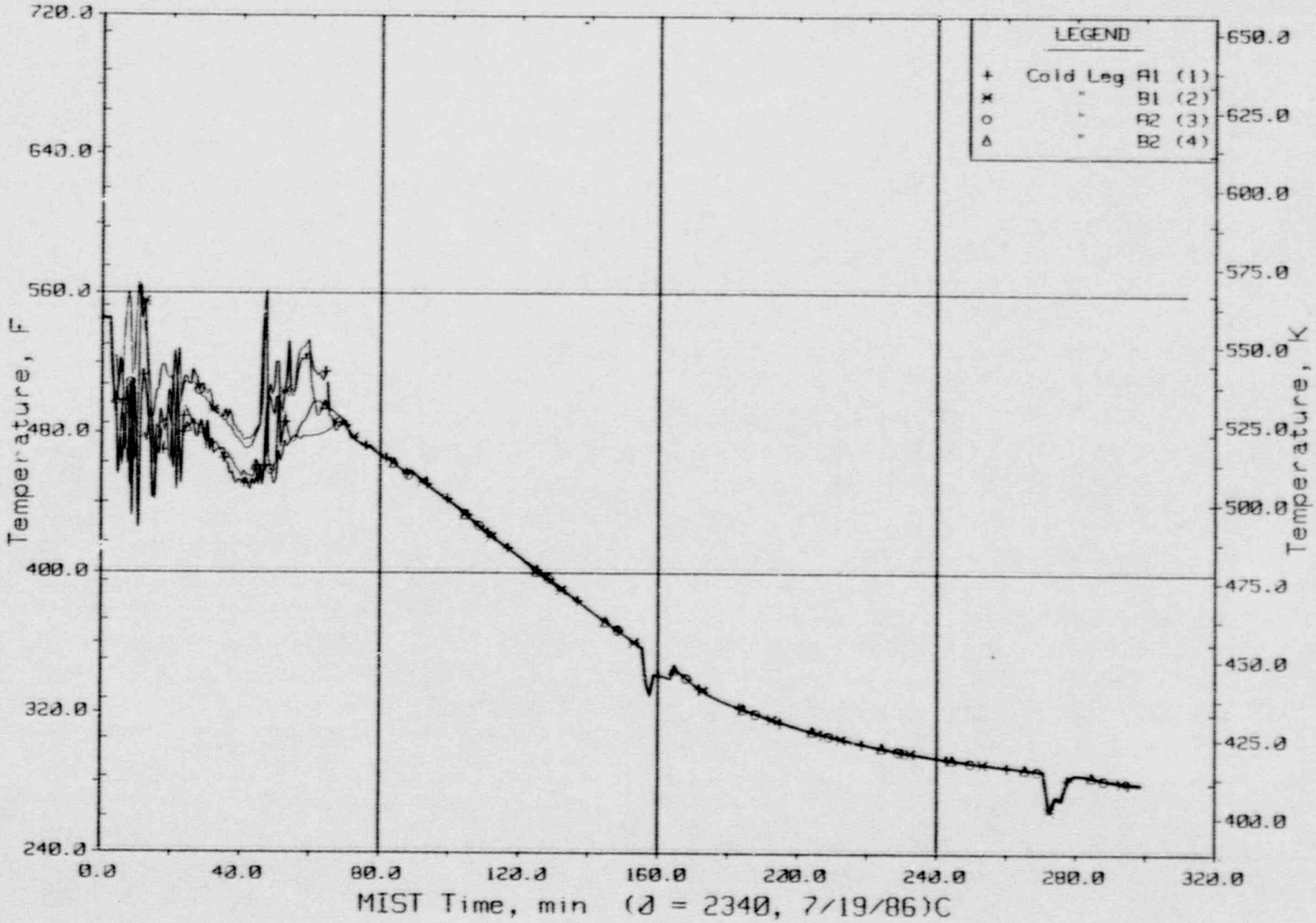

Cold Leg Nozzle Fluid Temperatures, Bottom of Rake (21.2ft, CnTC14s).

Thu Jun 9 09:39:55 1988

CLTC2

FINAL DATA

T320503: Group 32 SBLOCA Test 5, Leak Isolated.

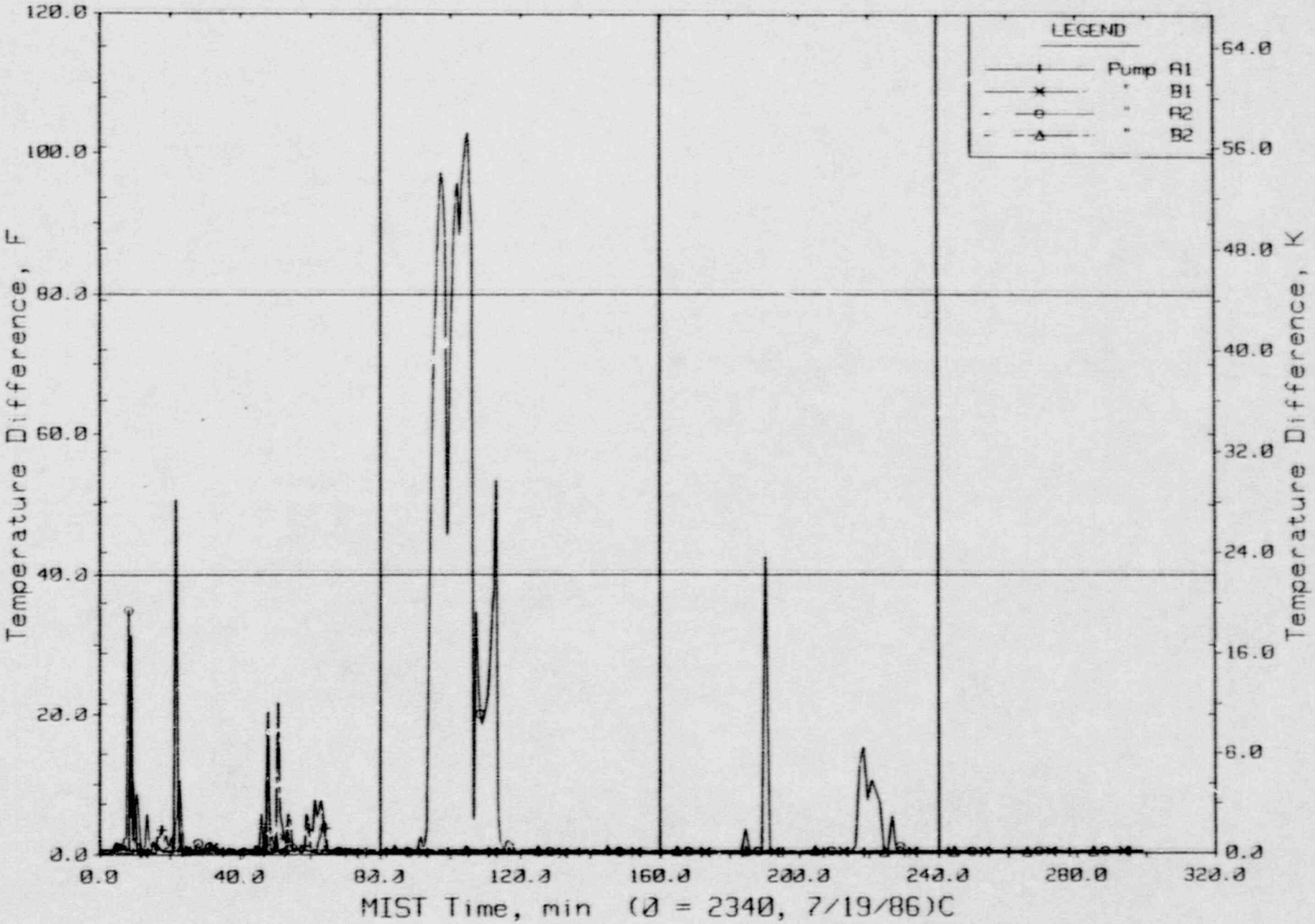

Maximum Differences Among RCP Rake Fluid Temperatures.

Thu Jun 9 09:43:22 1988

CLTD1

FINAL DATA

T320503: Group 32 SBLOCA Test 5, Leak Isolated.

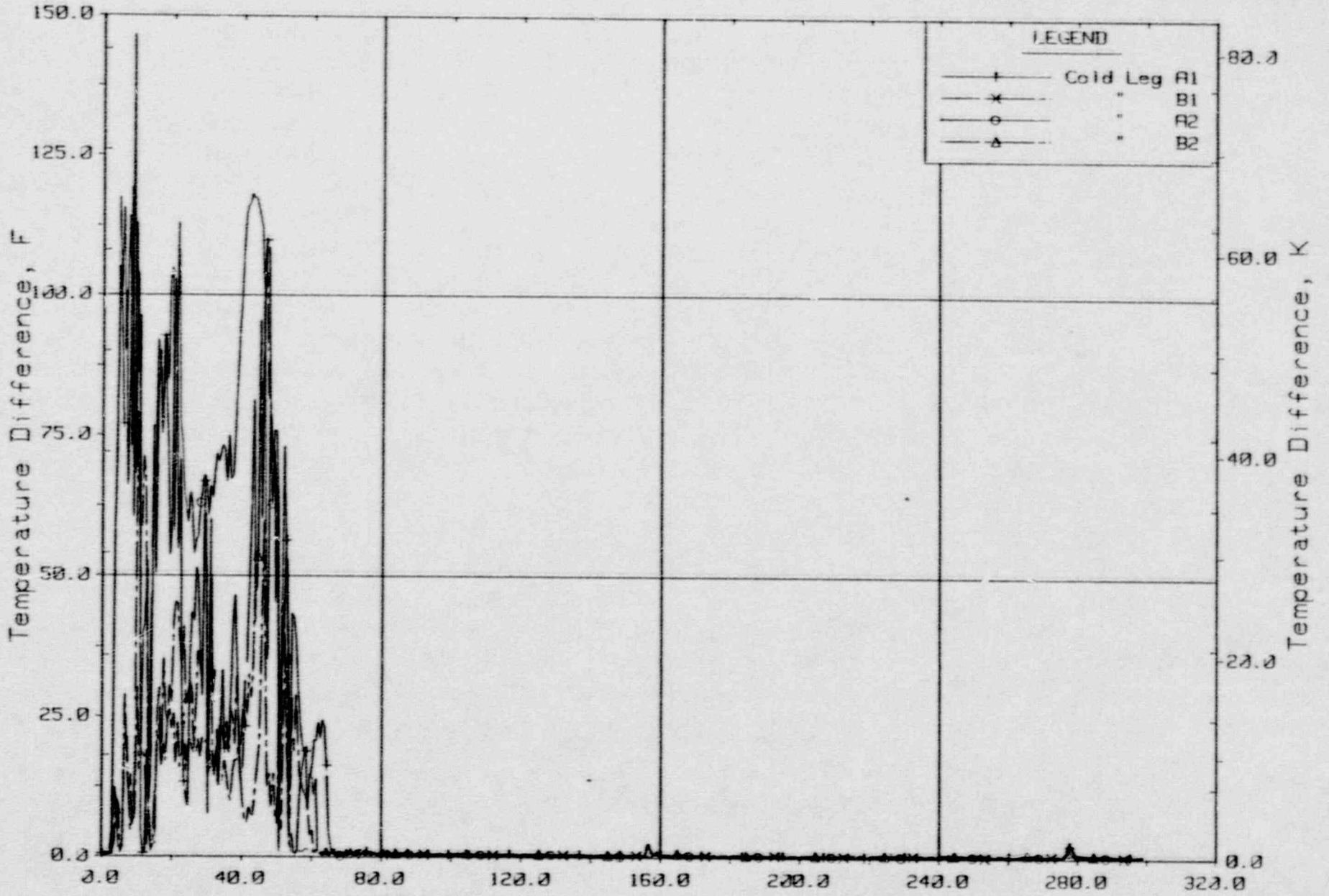

Maximum Differences Among CL Nozzle Rake Fluid Temperatures.

Thu Jun 9 09:46:24 1988

CLTD2

FINAL DATA

T320503: Group 32 SBLOCA Test 5, Leak Isolated.

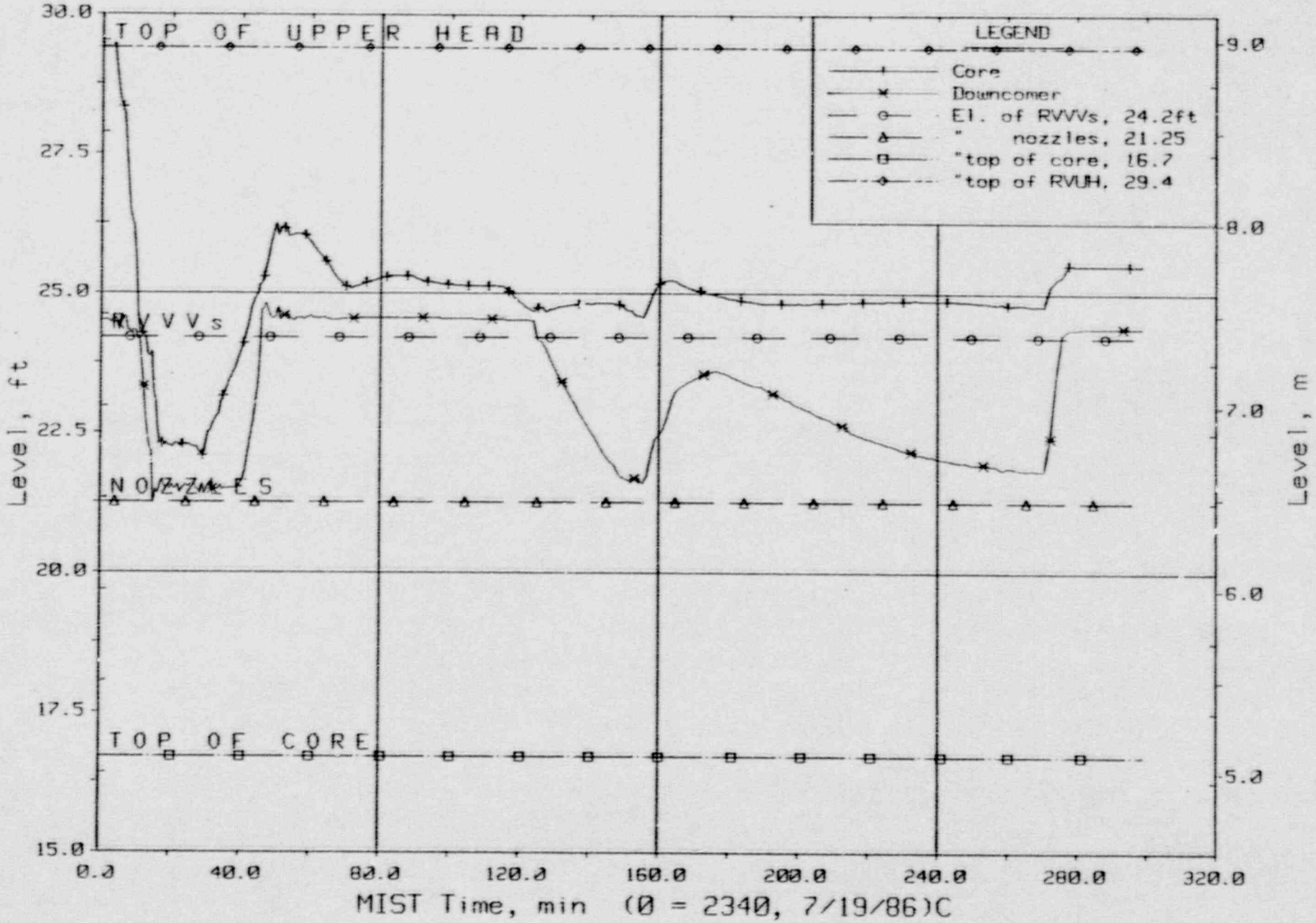

Core Region Collapsed Liquid Levels.

Thu Jun 9 09:51:17 1988

COLV1

FINAL DATA

T320503: Group 32 SBLOCA Test 5, Leak Isolated.

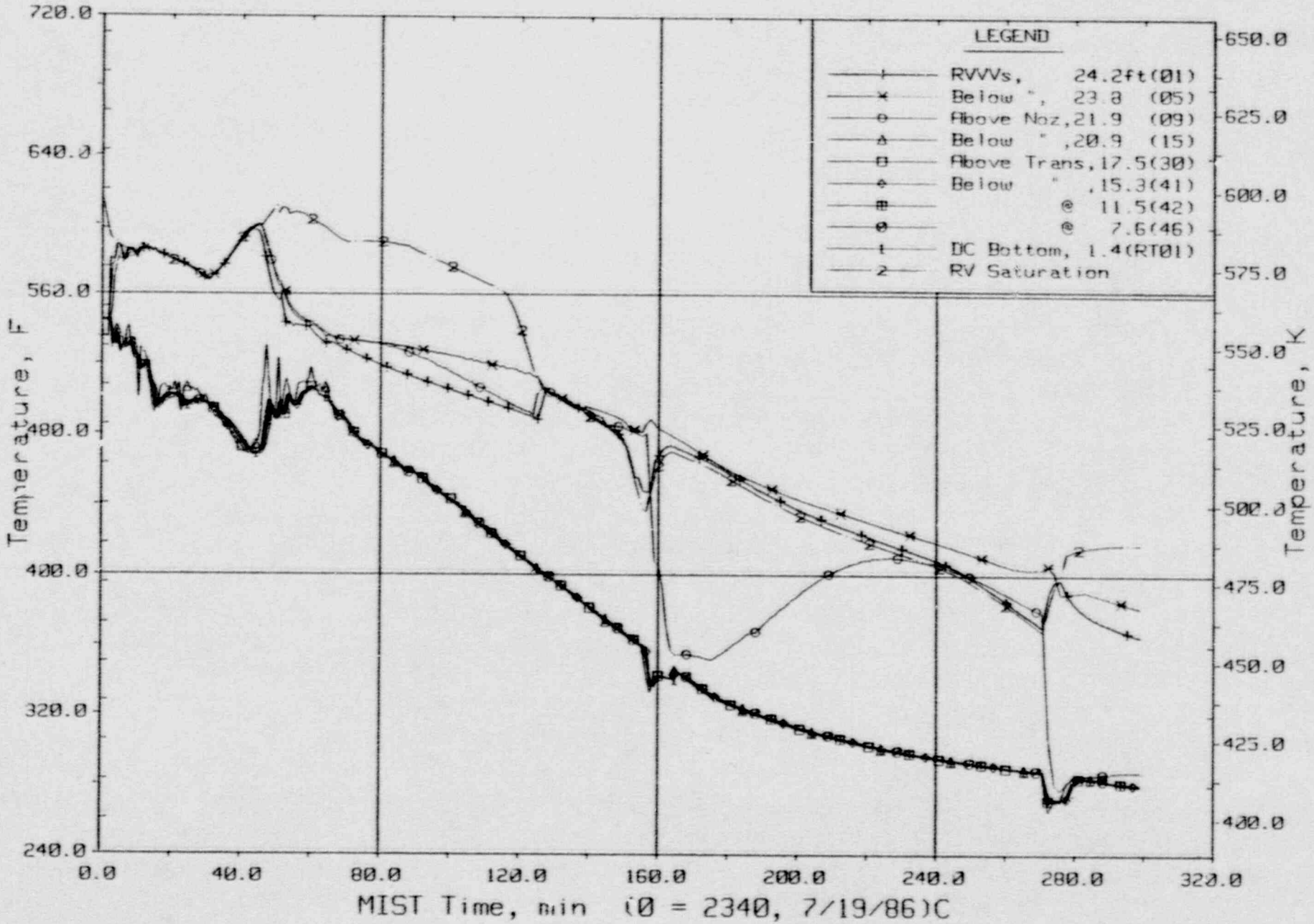

Downcomer Quadrant A1 Fluid Temperatures (DCTCs).

Thu Jun. 9 10:02:01 1988

DCTC6

FINAL DATA

T320503: Group 32 SBLOCA Test 5, Leak Isolated.

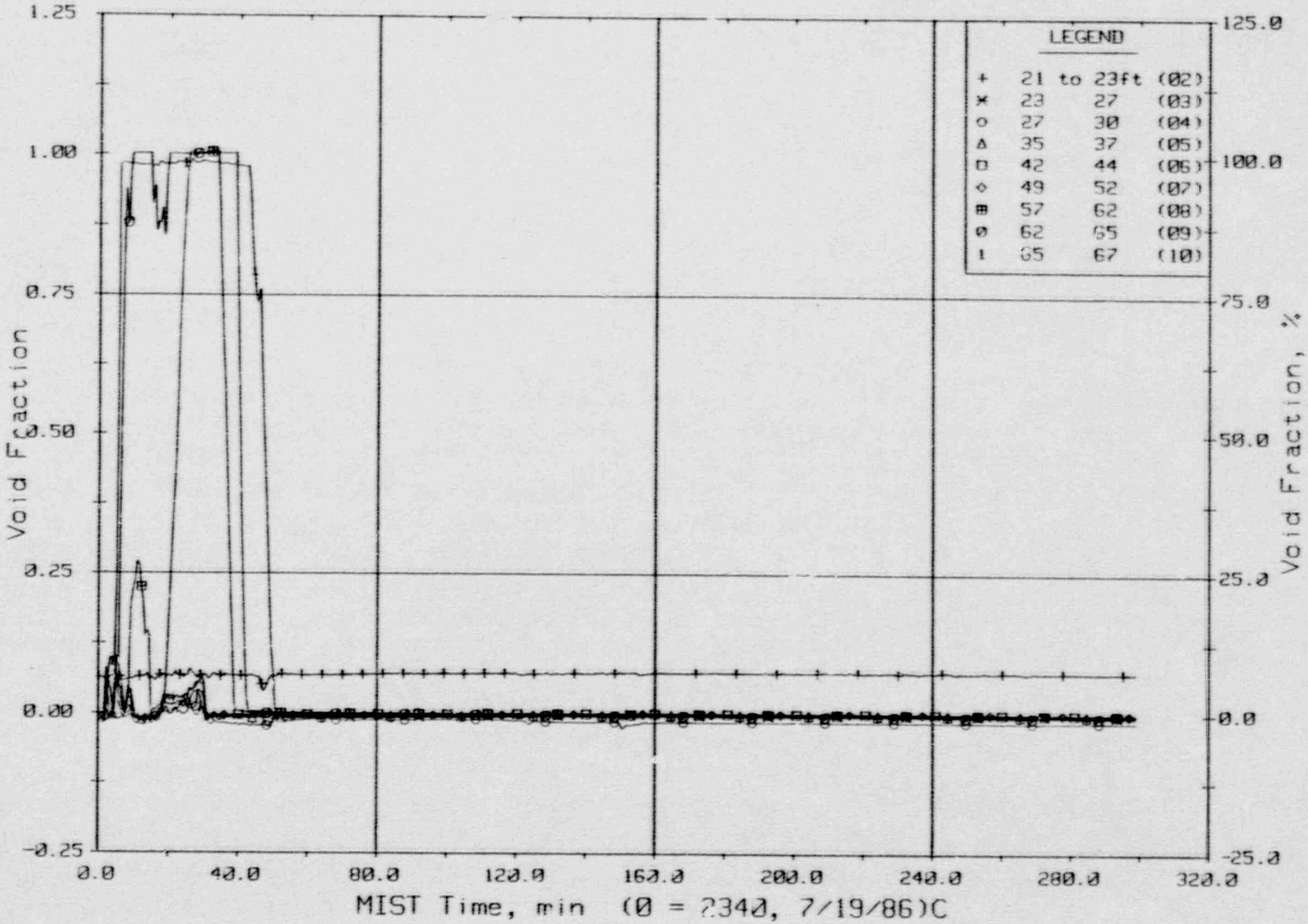

Hot Leg A Riser Void Fractions From Differential Pressures (HIVFs).

Thu Jun 9 10:06:24 1988

HIVF1

FINAL DATA

T320503: Group 32 SBLOCA Test 5, Leak Isolated.

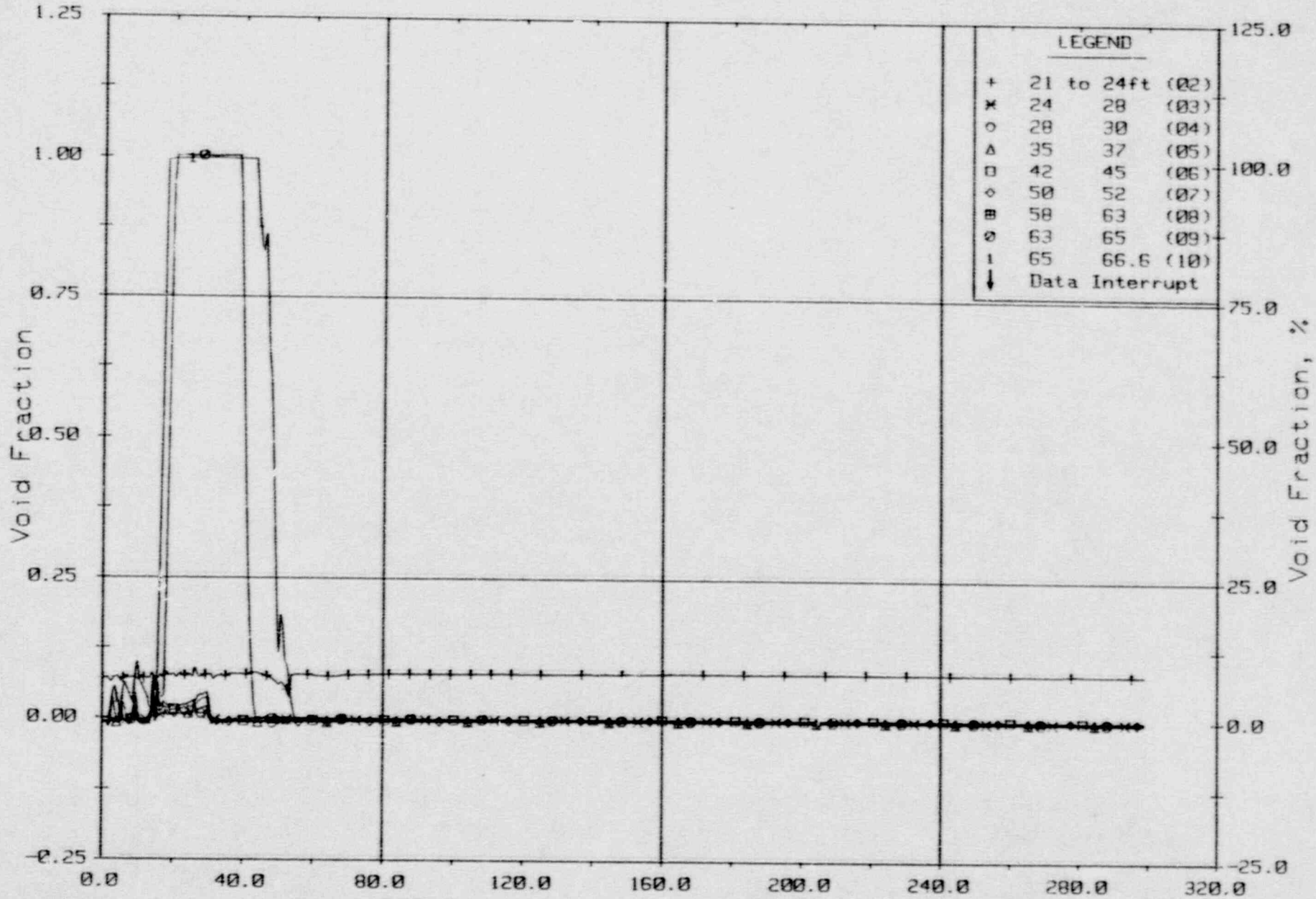

Hot Leg B Riser Void Fraction From Differential Pressures (H2VFs).

FINAL DATA

T320503: Group 32 SBLOCA Test 5, Leak Isolated.

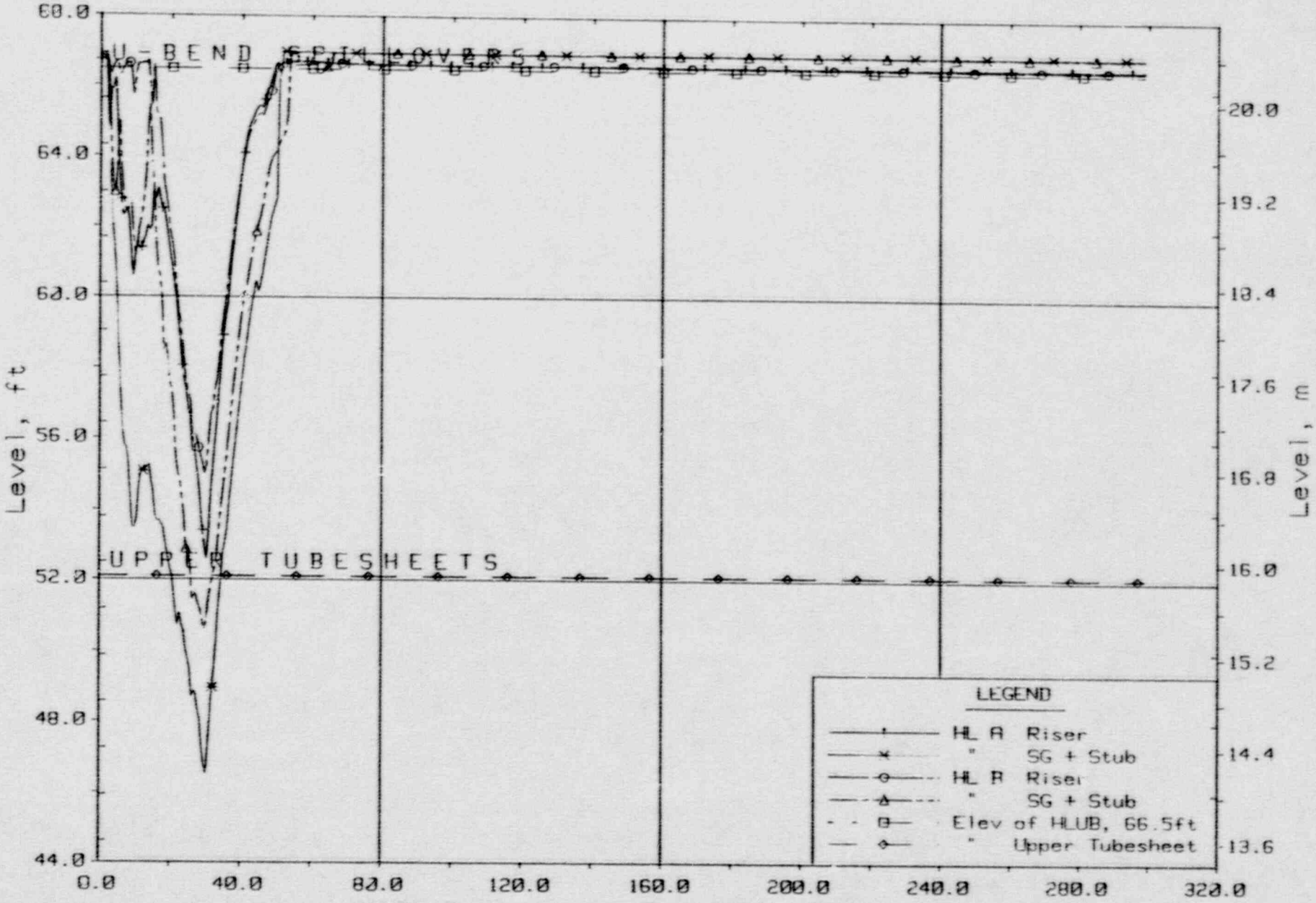

Hot Leg Riser and Stub Collapsed Liquid Levels.

Thu Jun 9 10:24:49 1988

HLLV1

FINAL DATA

T320503: Group 32 SBLOCA Test 5, Leak Isolated.

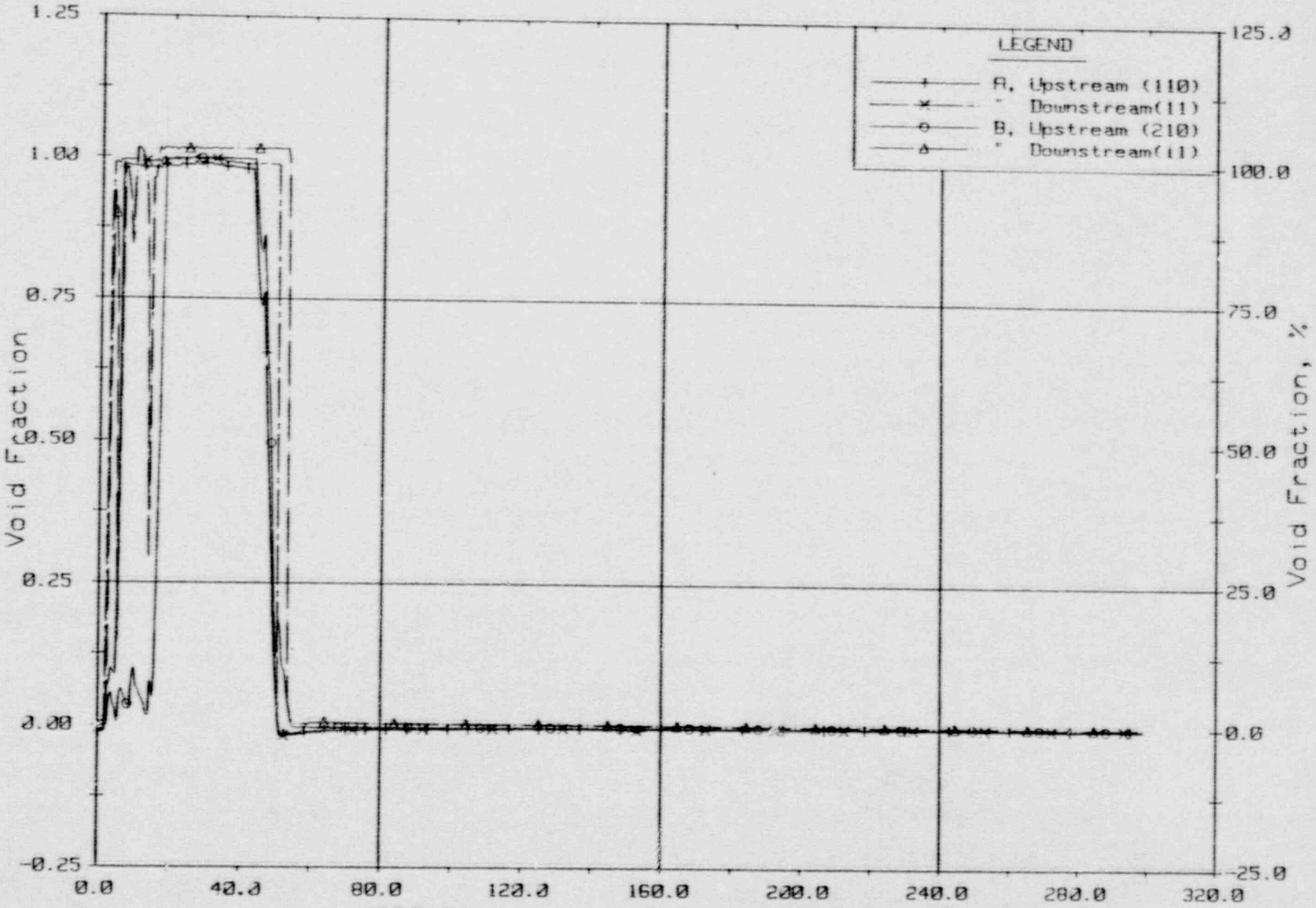

Hot Leg U-Bend Void Fractions From Diffl. Pressures (64.8 to 66.6 ft, HnVFs).

Thu Jun 9 10:31:02 1988

HLVF1

FINAL DATA

T320503: Group 32 SBLOCA Test 5, Leak Isolated.

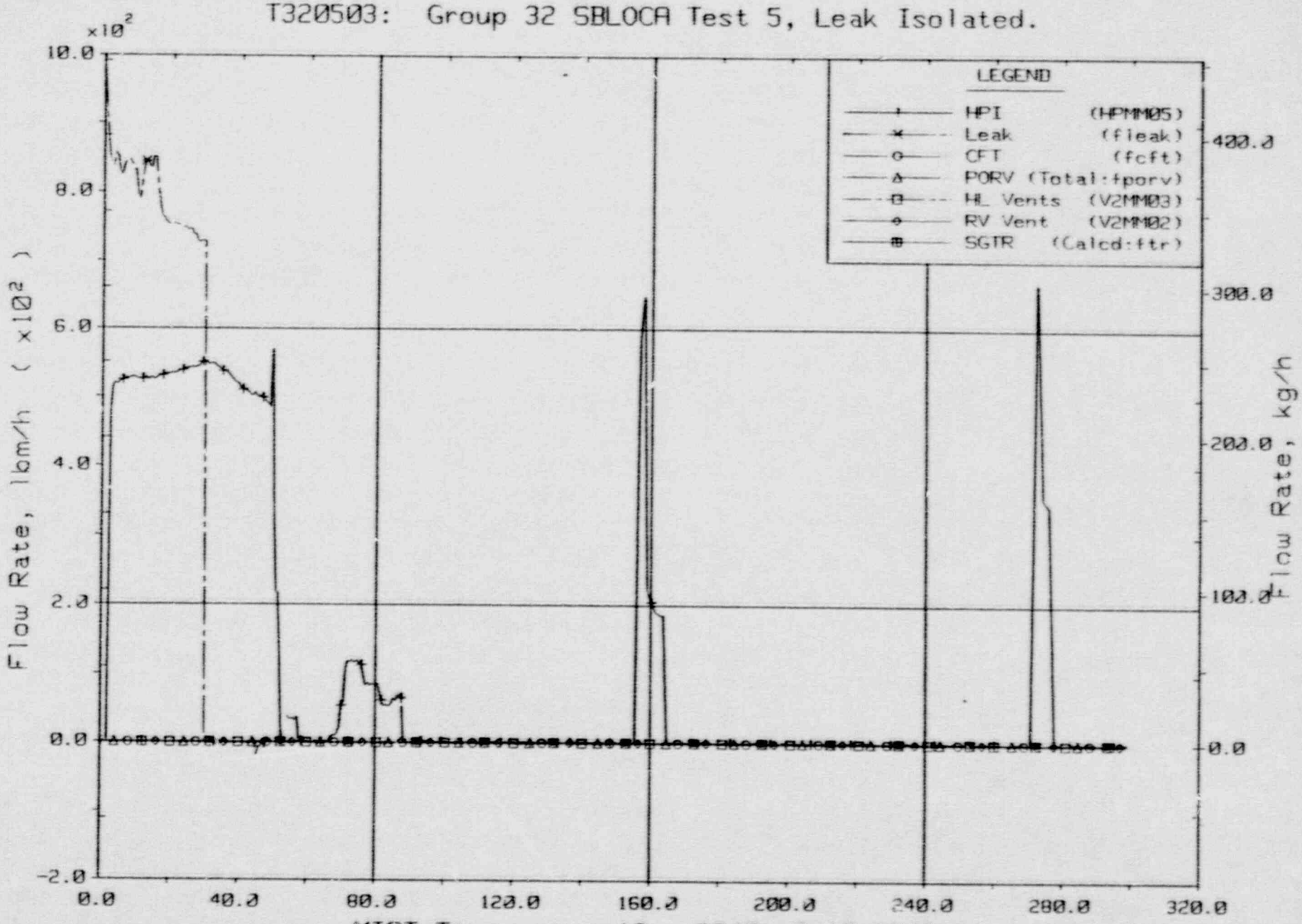

Primary System Boundary Flow Rates.

Thu Jun 3 10:52:38 1988

PBFL3

FINAL DATA

T320503: Group 32 SBLOCA Test 5, Leak Isolated.

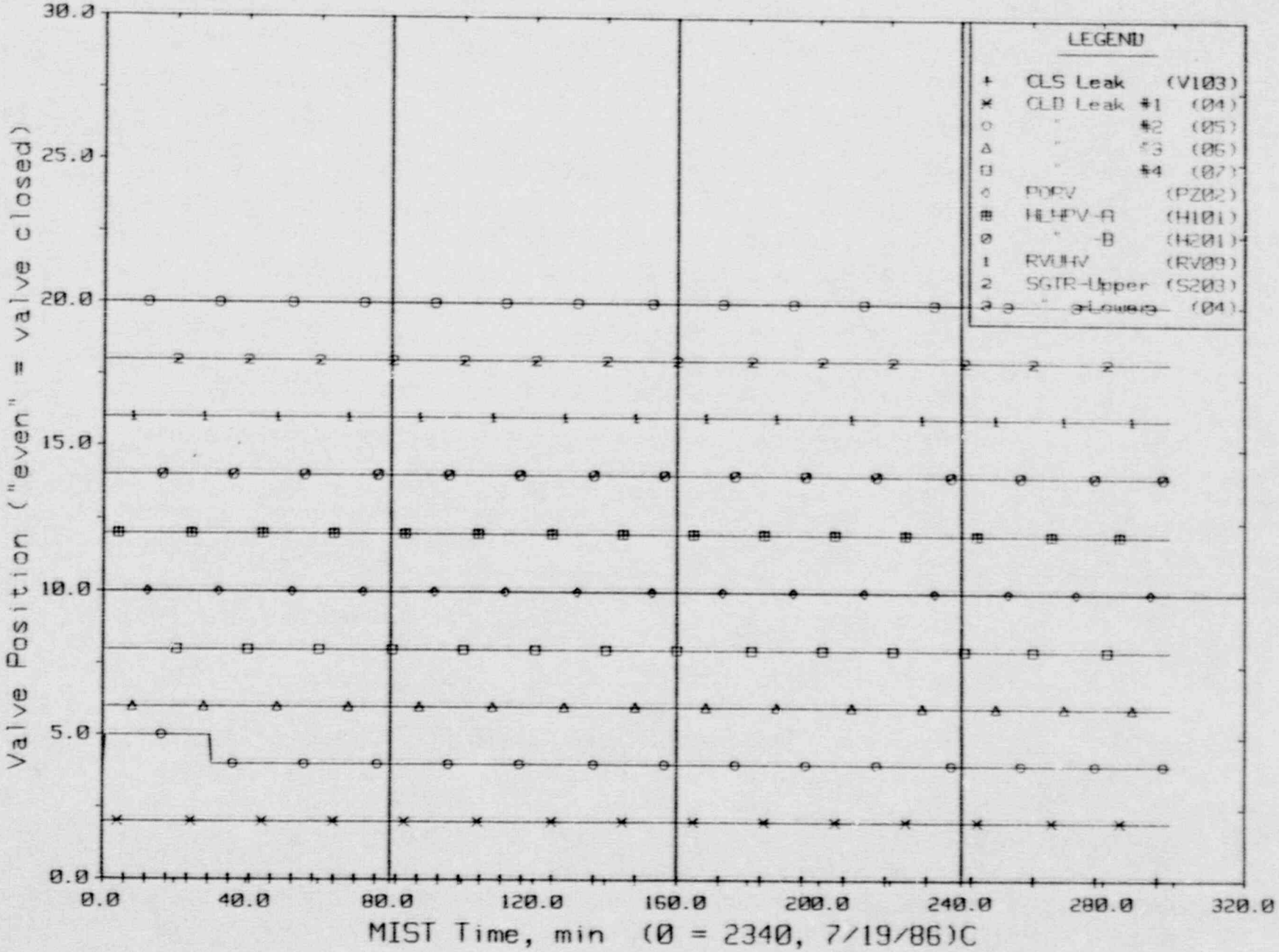

Primary System Discharge Limit Switch Indications (LSs).

Thu Jun 9 10:58:27 1988

PBLS1

FINAL DATA

T320503: Group 32 SBLOCA Test 5, Leak Isolated.

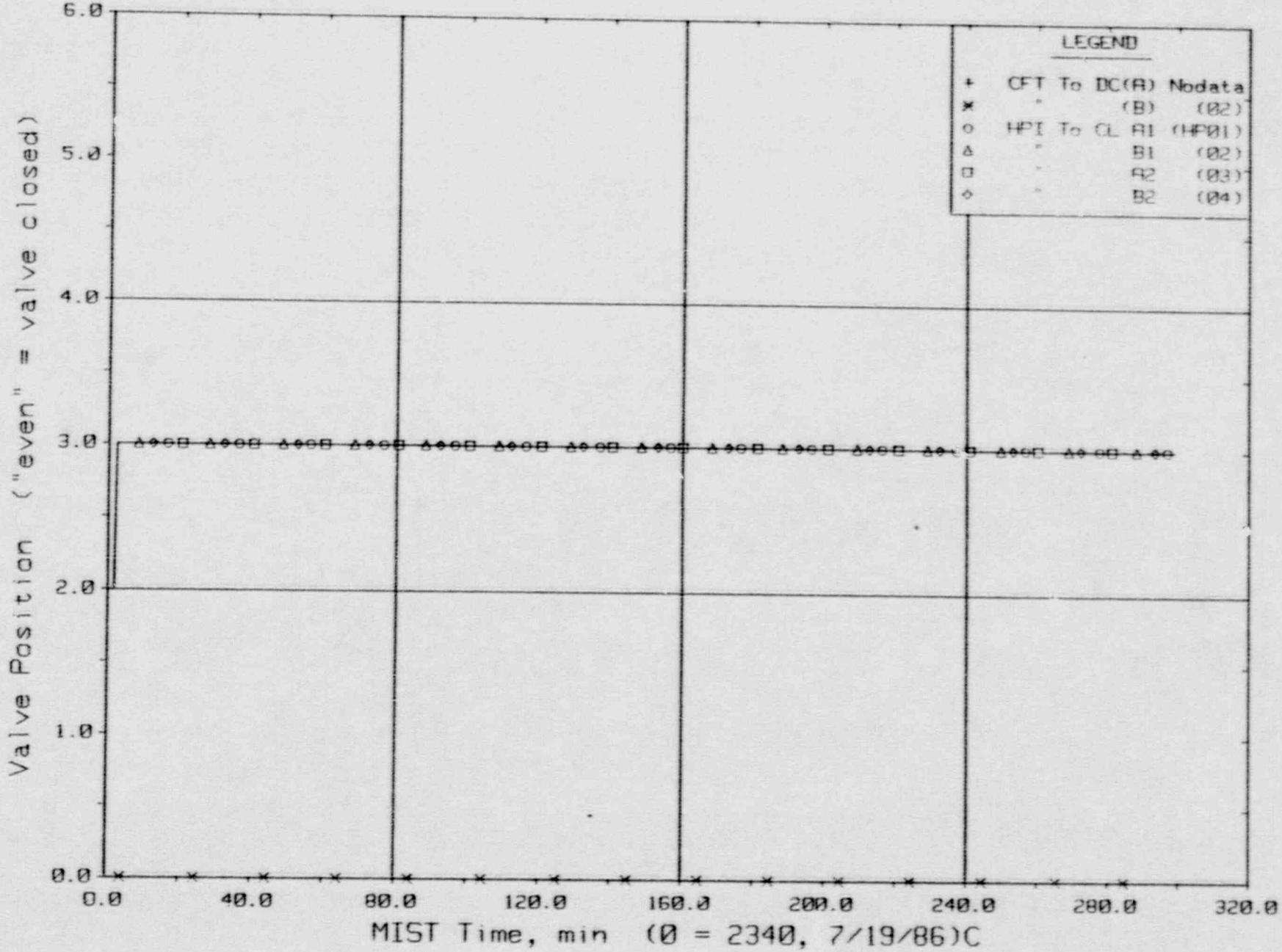

Primary System Injection Limit Switch Indications (LSs).

FINAL DATA

T320503: Group 32 SBLOCA Test 5, Leak Isolated.

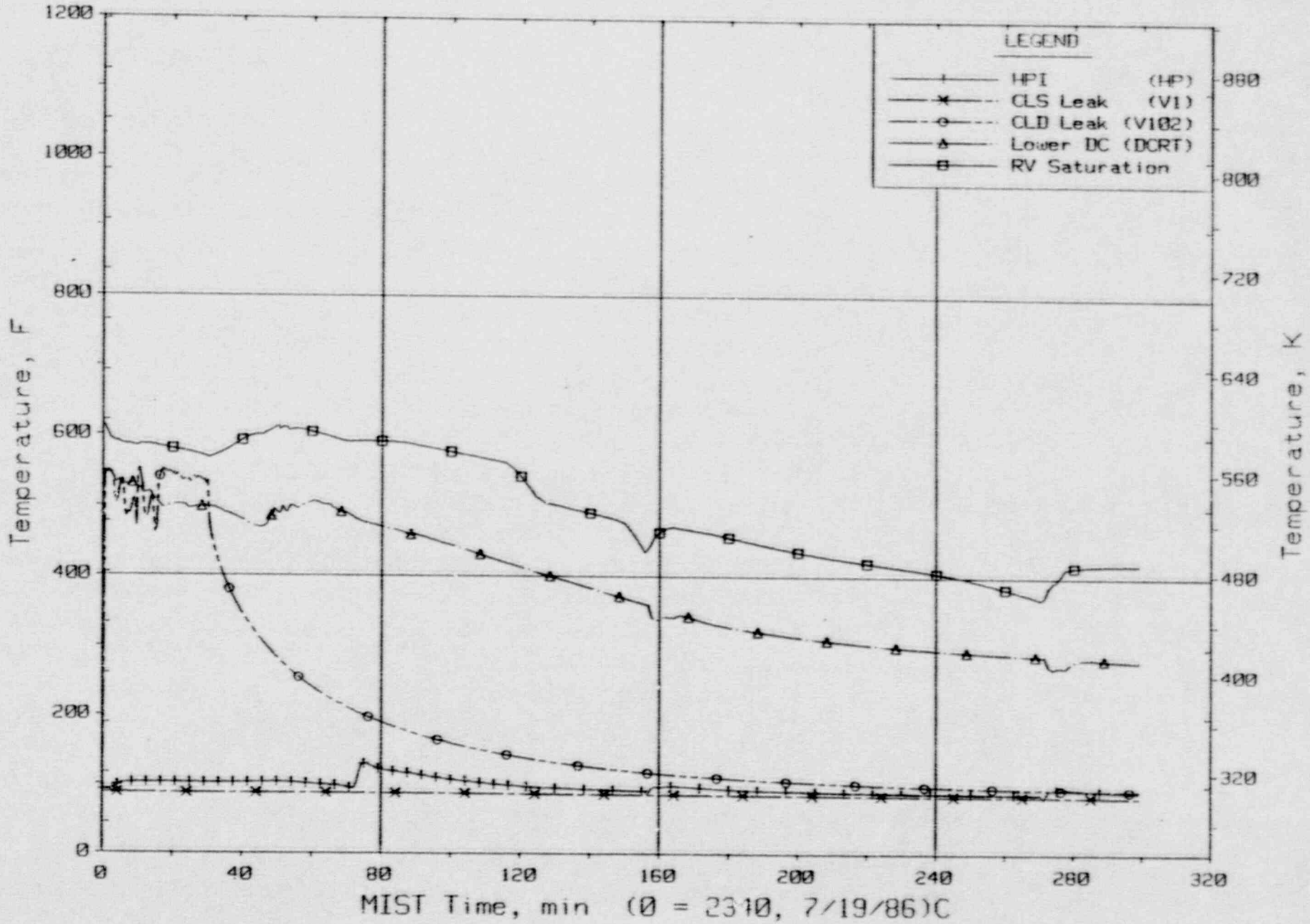

Single-Phase Discharge and HPI Fluid Temperatures (TC01s).

Mon Oct 31 15:58:16 1988

PBTC1p

FINAL DATA

T320503: Group 32 SBLOCA Test 5, Leak Isolated.

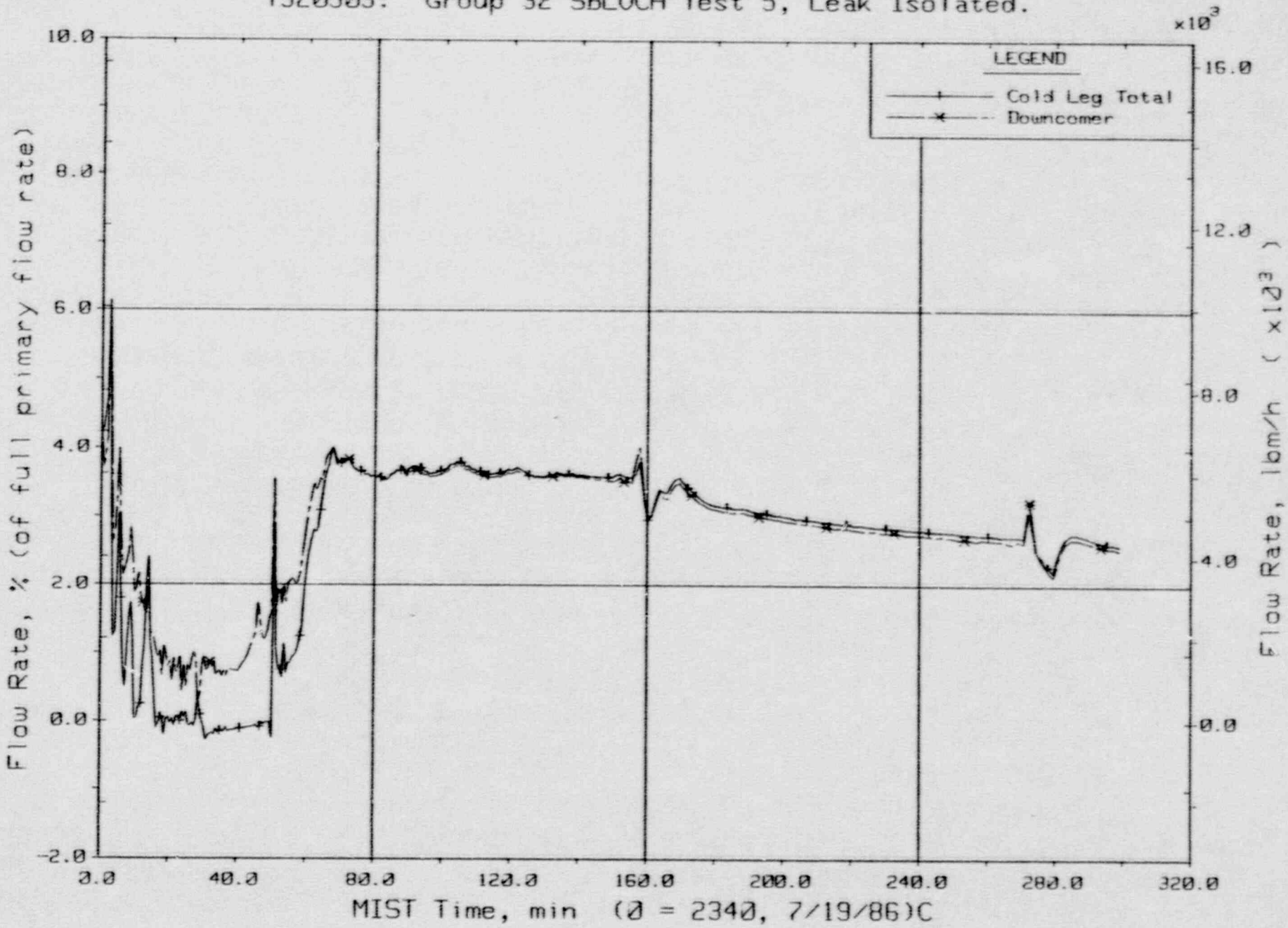

Primary System Venturi Flow Rates.

FINAL DATA

T320503: Group 32 SBLOCA Test 5, Leak Isolated.

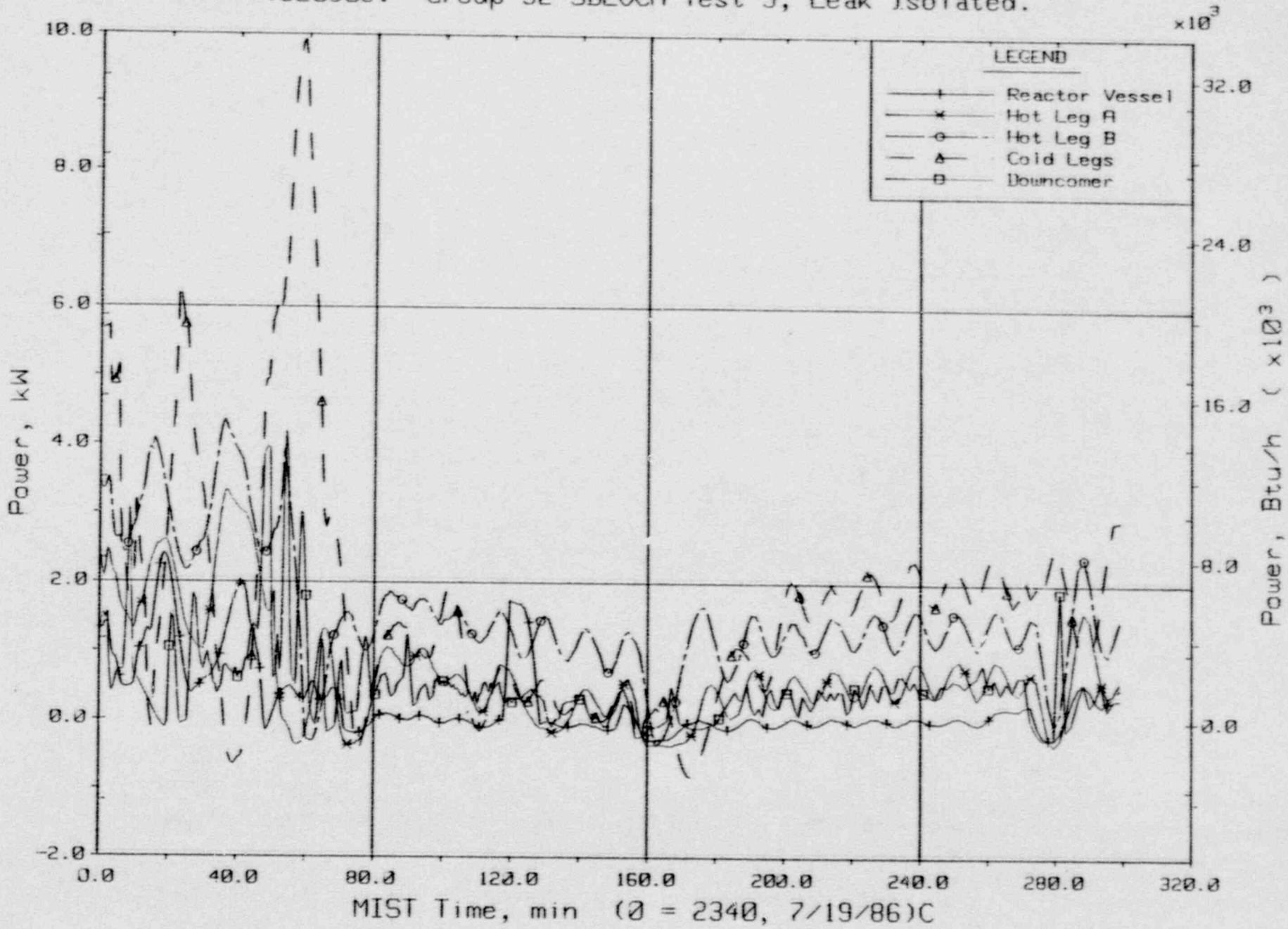

Guard Heater Specified Power Per Primary Component.

Thu Jun 9 11:10:42 1988

PRGQ1

FINAL DATA

T320503: Group 32 SBLOCA Test 5, Leak Isolated.

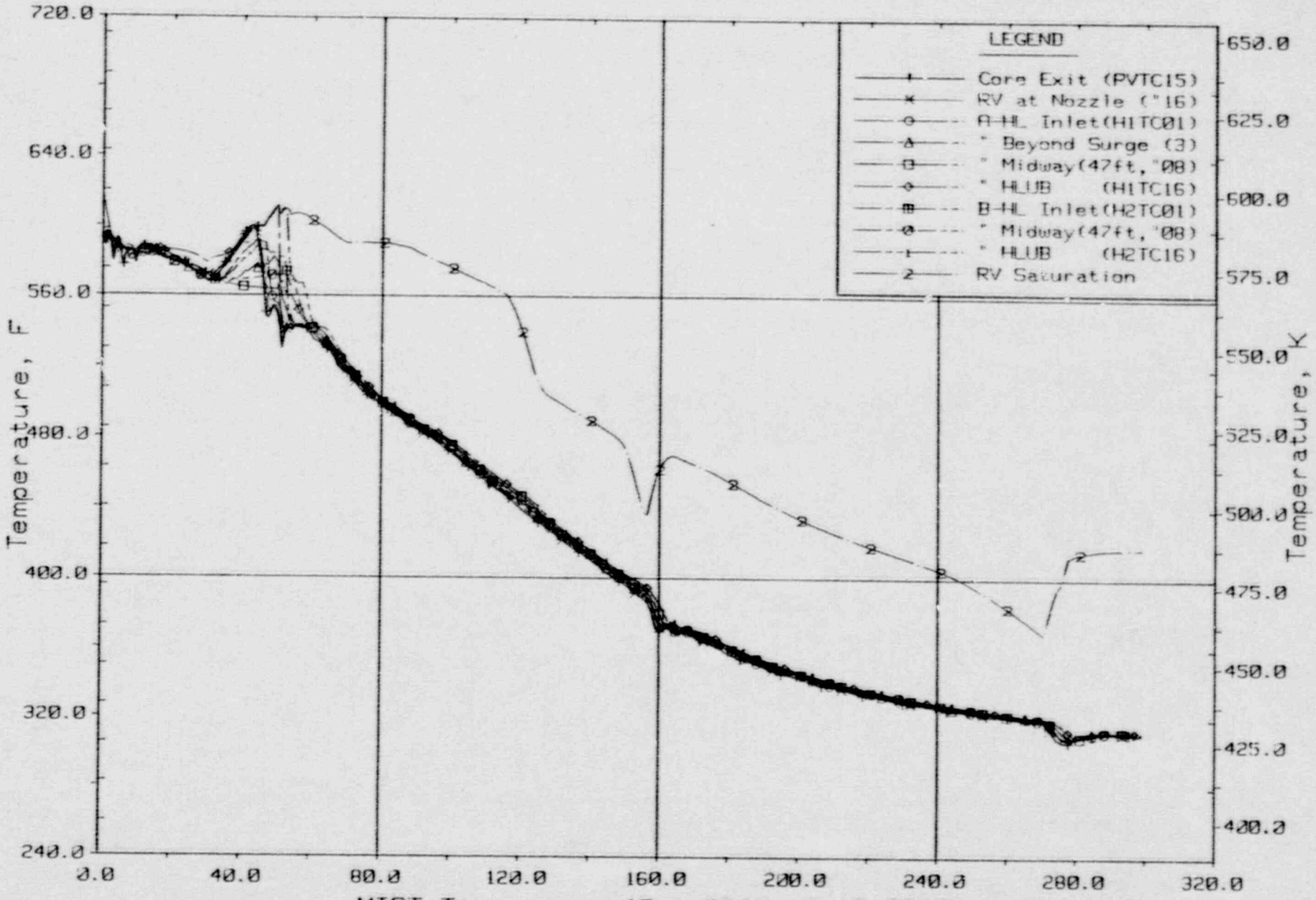

Composite Core Exit and Hot Leg Fluid Temperatures.

Thu Jun 9 11:14:48 1988

PRKT1

FINAL DATA

T320503: Group 32 SBLOCA Test 5, Leak Isolated.

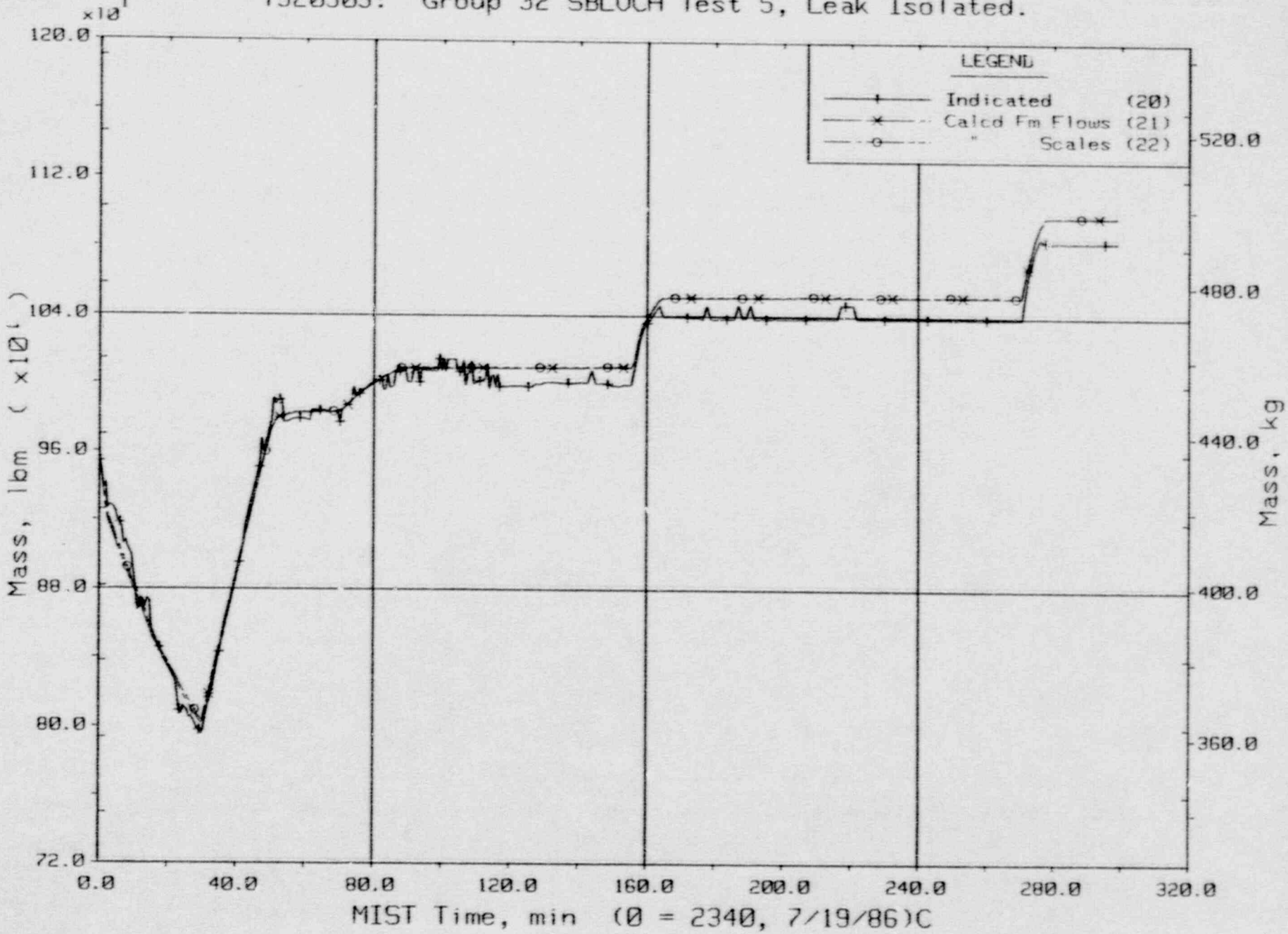

Primary System Total Fluid Mass (PLMLs).

Thu Jun 9 11:17:48 1988

PRML2

FINAL DATA

T320503: Group 32 SBLOCA Test 5, Leak Isolated.

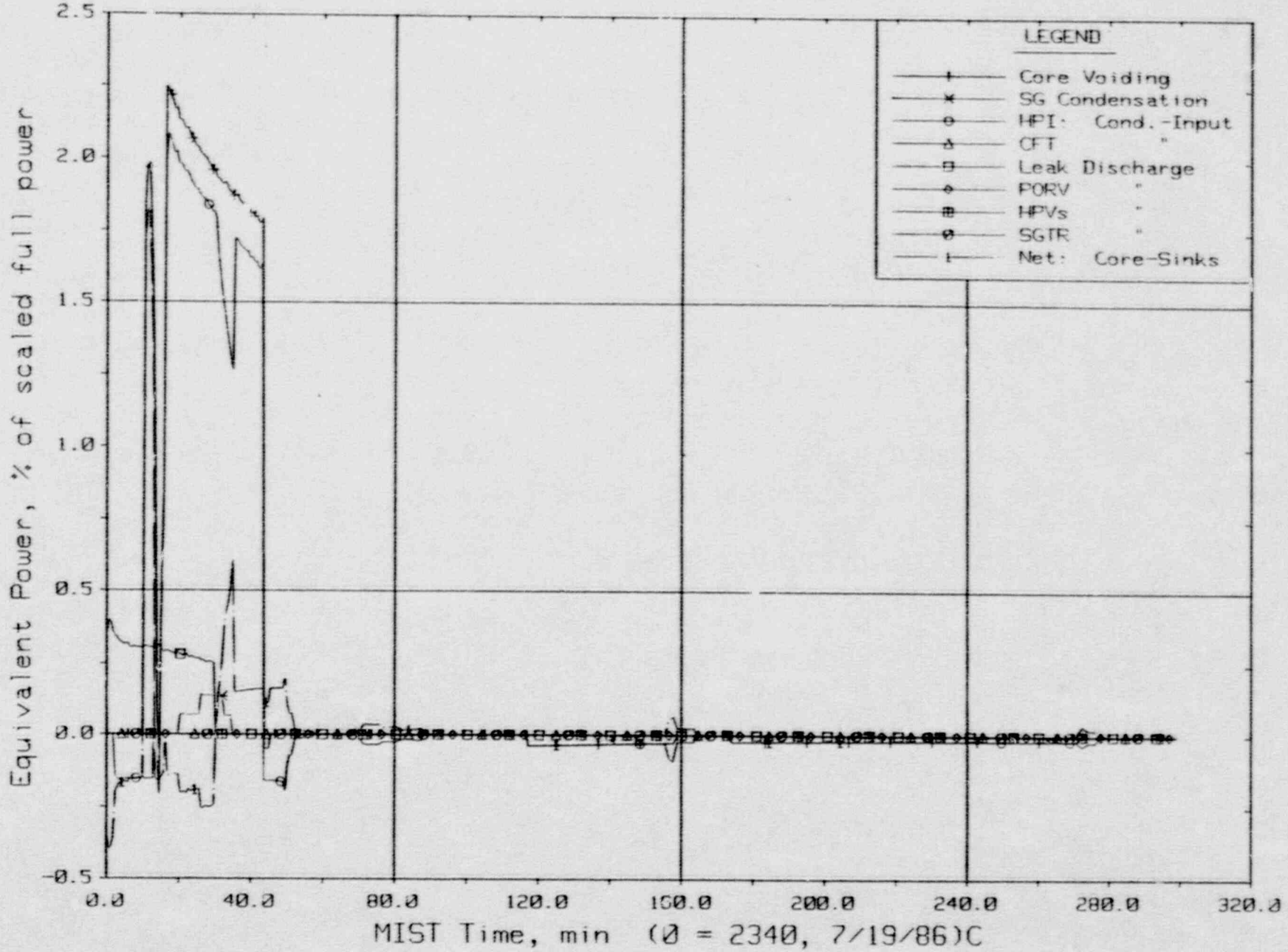

Primary Fluid Volume Changes By Components.

FINAL DATA

T320503: Group 32 SBLOCA Test 5, Leak Isolated.

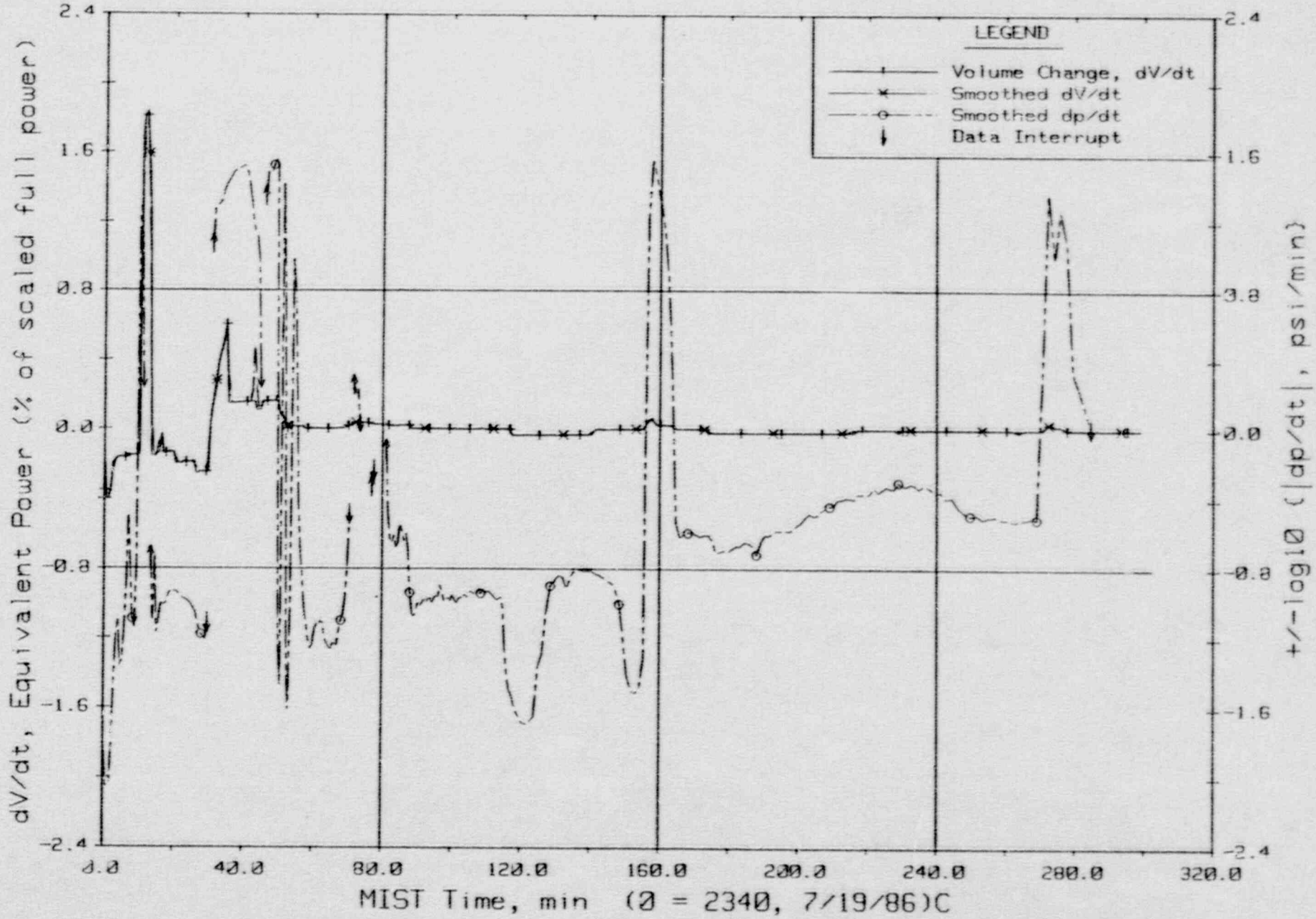

Primary Fluid Volume and Pressure Changes, dV/dt and dp/dt.

Thu Jun 9 11:24:03 1998

PRPA2

FINAL DATA

T320503: Group 32 SBLOCA Test 5, Leak Isolated.

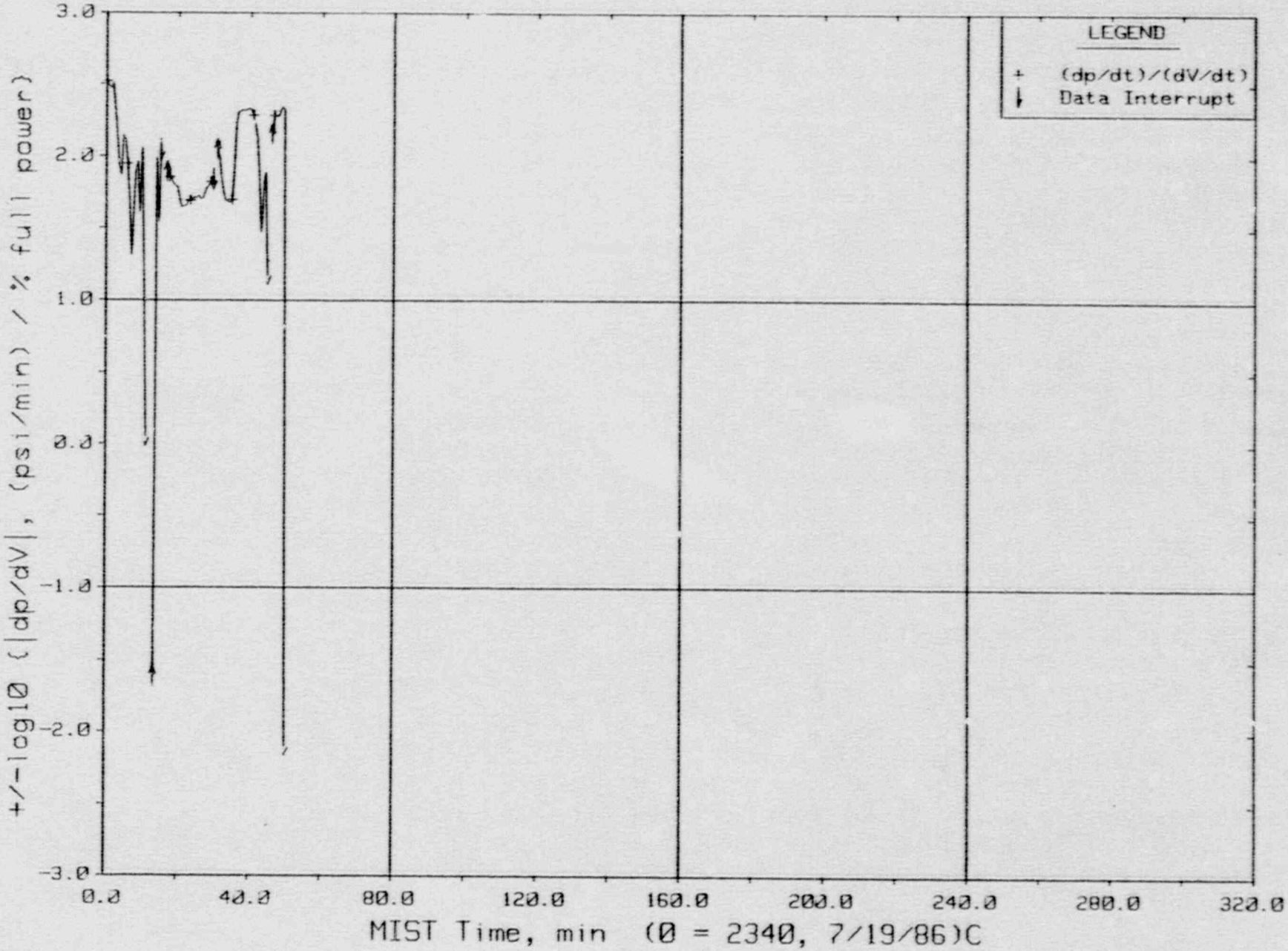

Primary System Response: dp/dt divided by dV/dt.

Thu Jun 9 11:26:24 1988

PRPA3

FINAL DATA

T320503: Group 32 SBLOCA Test 5, Leak Isolated.

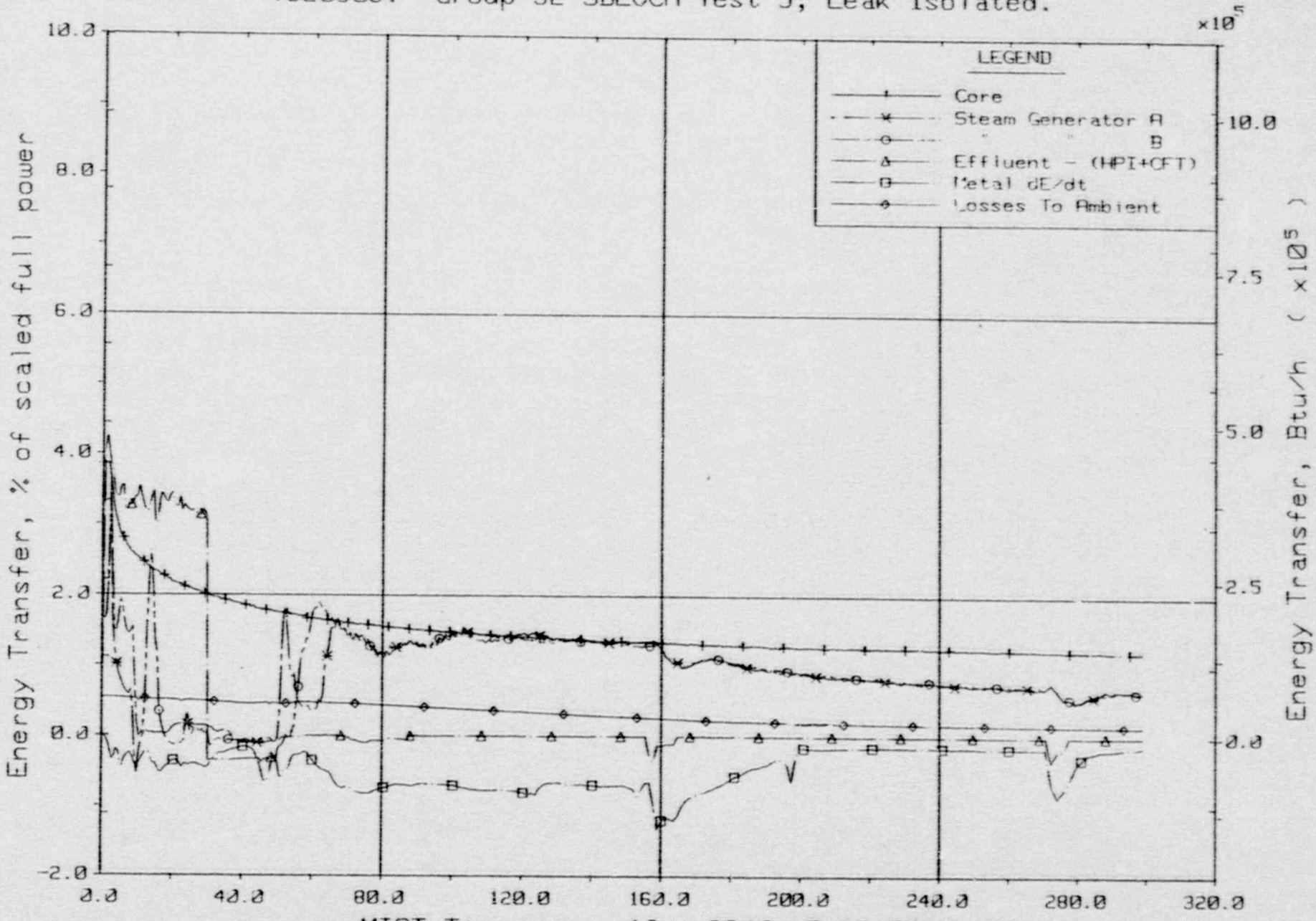

Primary System Energy Transfer.

Thu Jun 9 11:29:15 1988

PROE2

FINAL DATA

T320503: Group 32 SBLOCA Test 5, Leak Isolated.

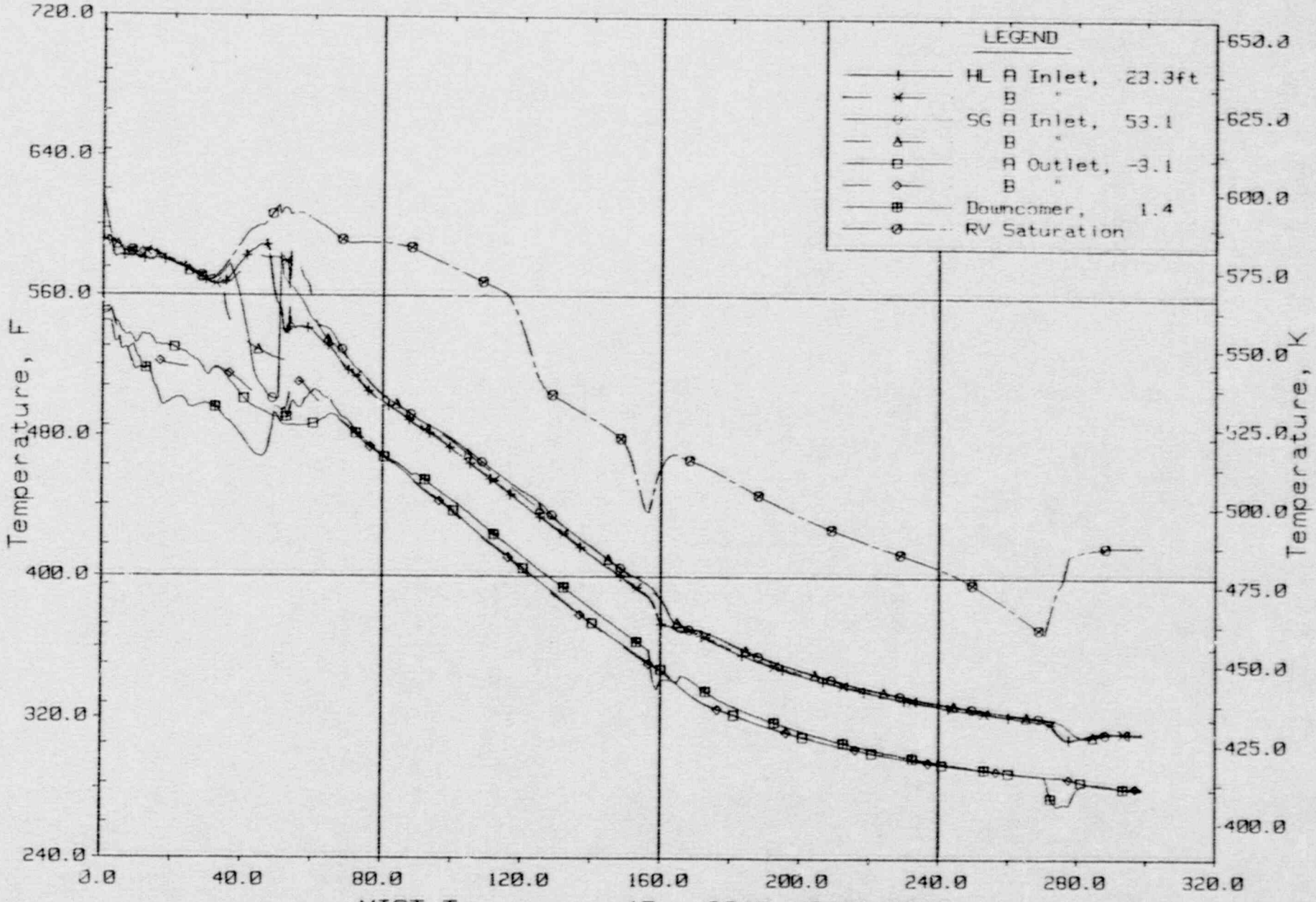

Primary System Fluid Temperatures (RTDs).

Thu Jun 9 11:32:51 1988

PRRT0

-INAL DATA

T320503: Group 32 SBLOCA Test 5, Leak Isolated.

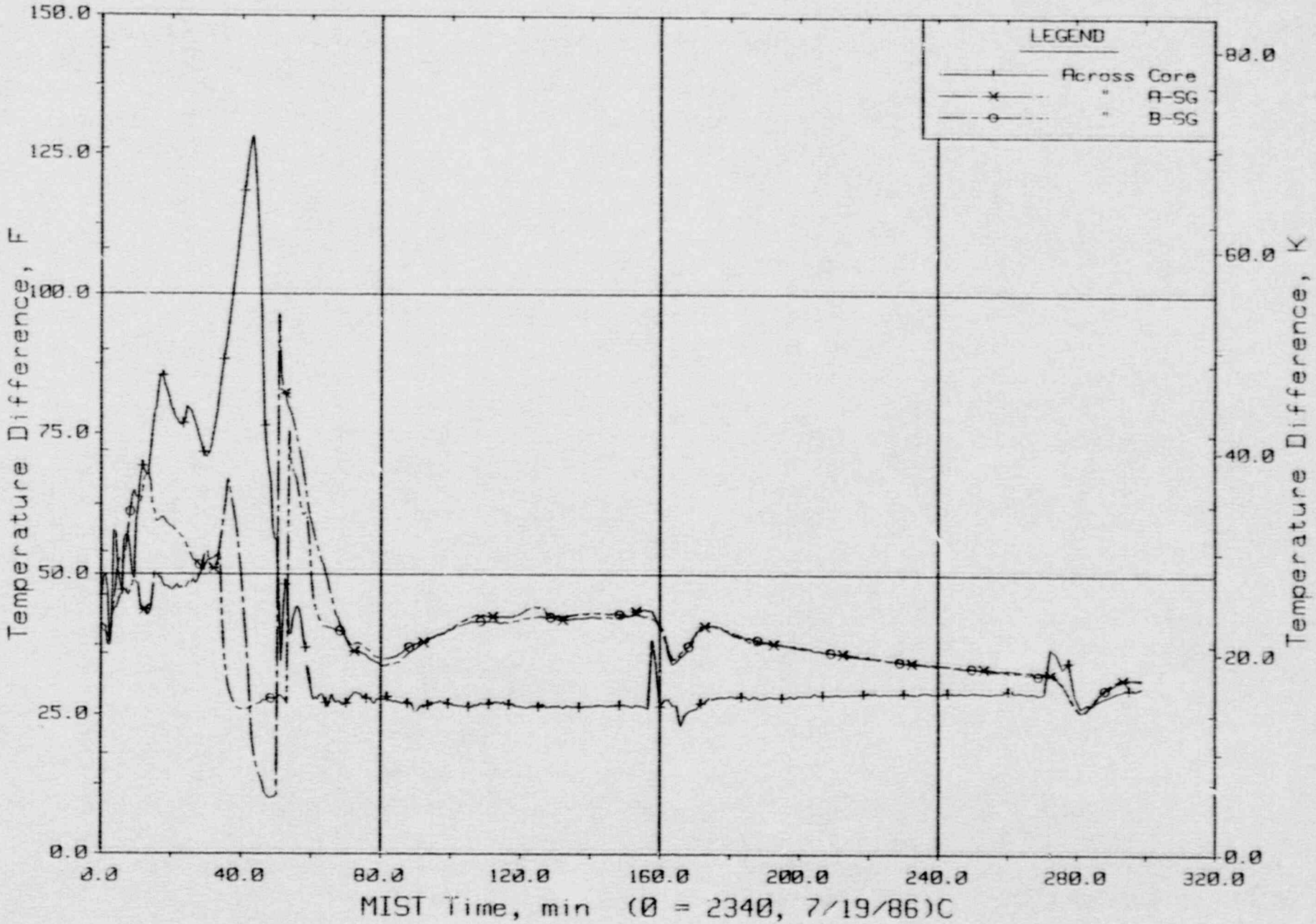

Key Temperature Differences.

Thu Jun 9 11:35:52 1988

PRTD2

FINAL DATA

T32Ø5Ø3: Group 32 SBLOCA Test 5, Leak Isolated.

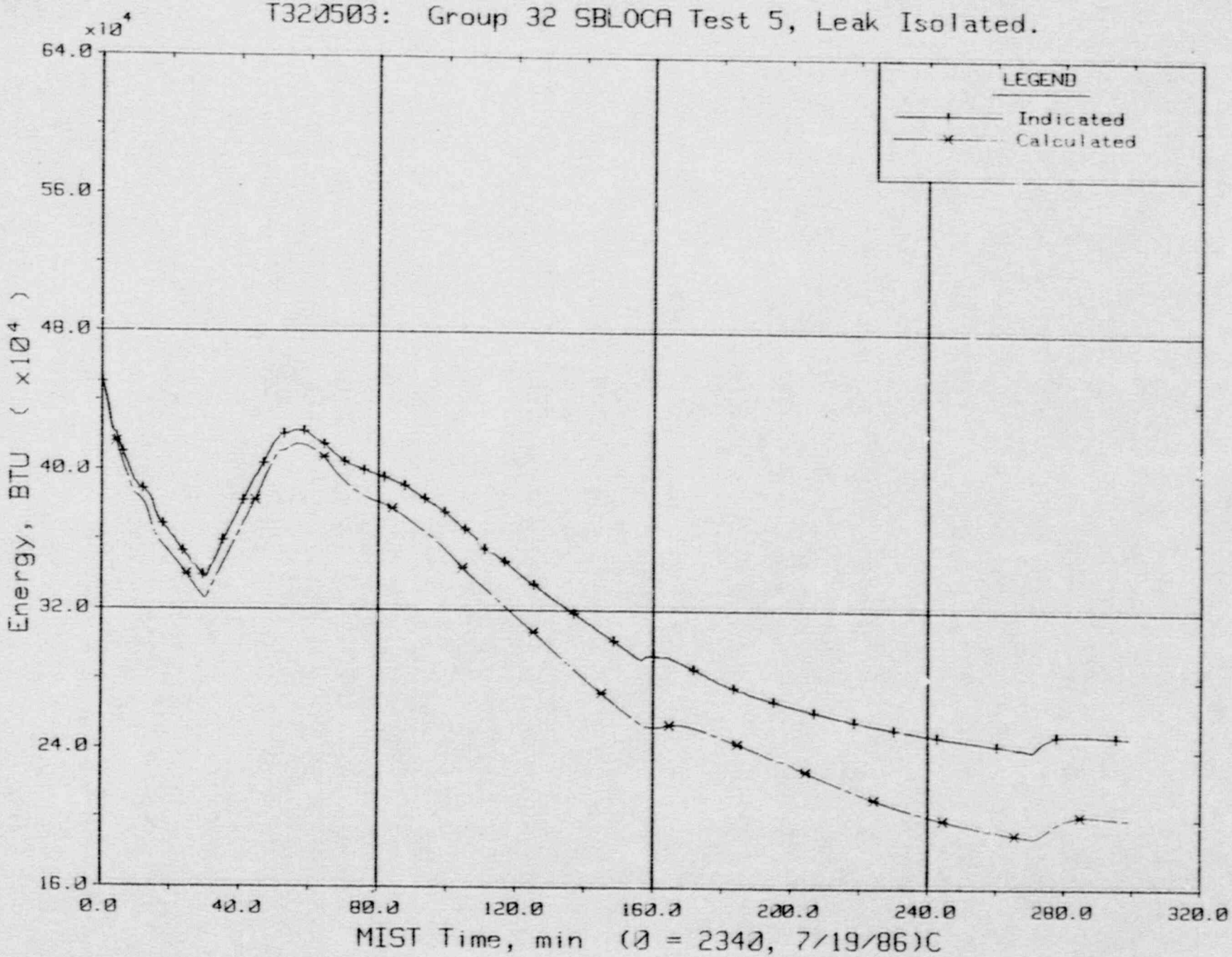

Primary System Total Fluid Energy.

FINAL DATA

T320503: Group 32 SBLOCA Test 5, Leak Isolated.

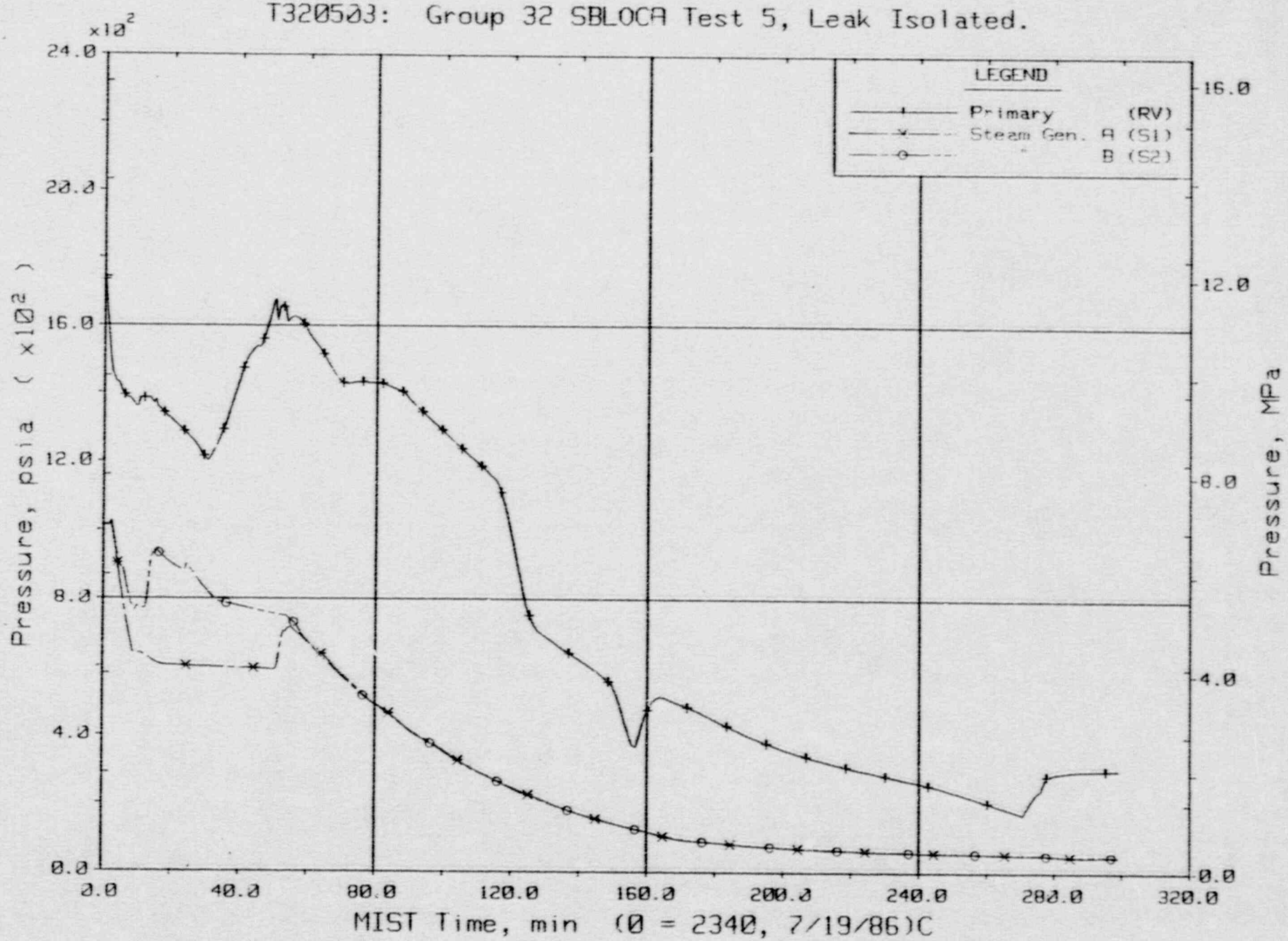

Primary and Secondary System Pressures (GP01s).

Thu Jun 9 11:41:38 1988

PSGP1

FINAL DATA

T320503: Group 32 SBLOCA Test 5, Leak Isolated.

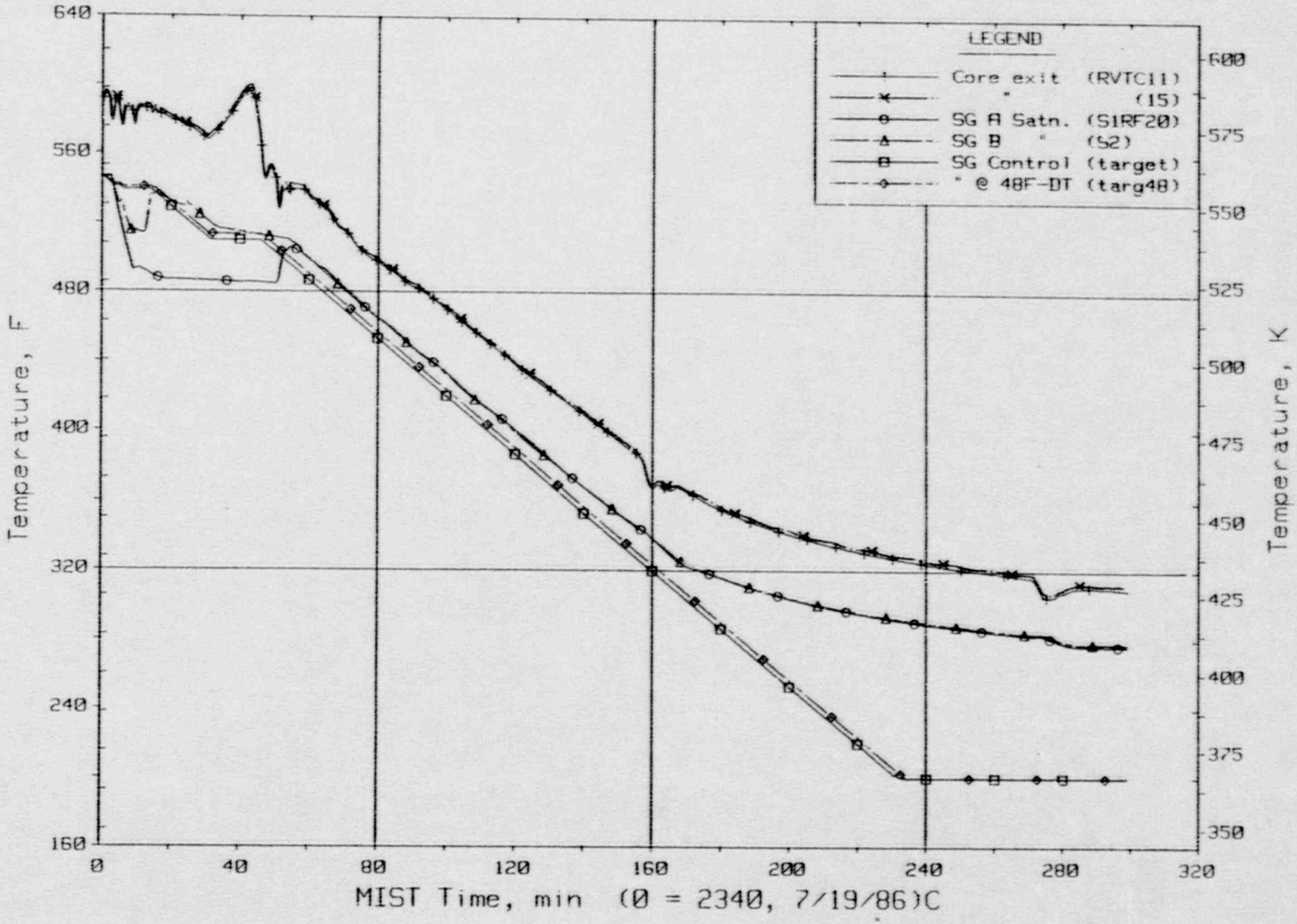

Steam Generator Secondary Saturation and Control Temperatures.

FINAL DATA

T320503: Group 32 SBLOCA Test 5, Leak Isolated.

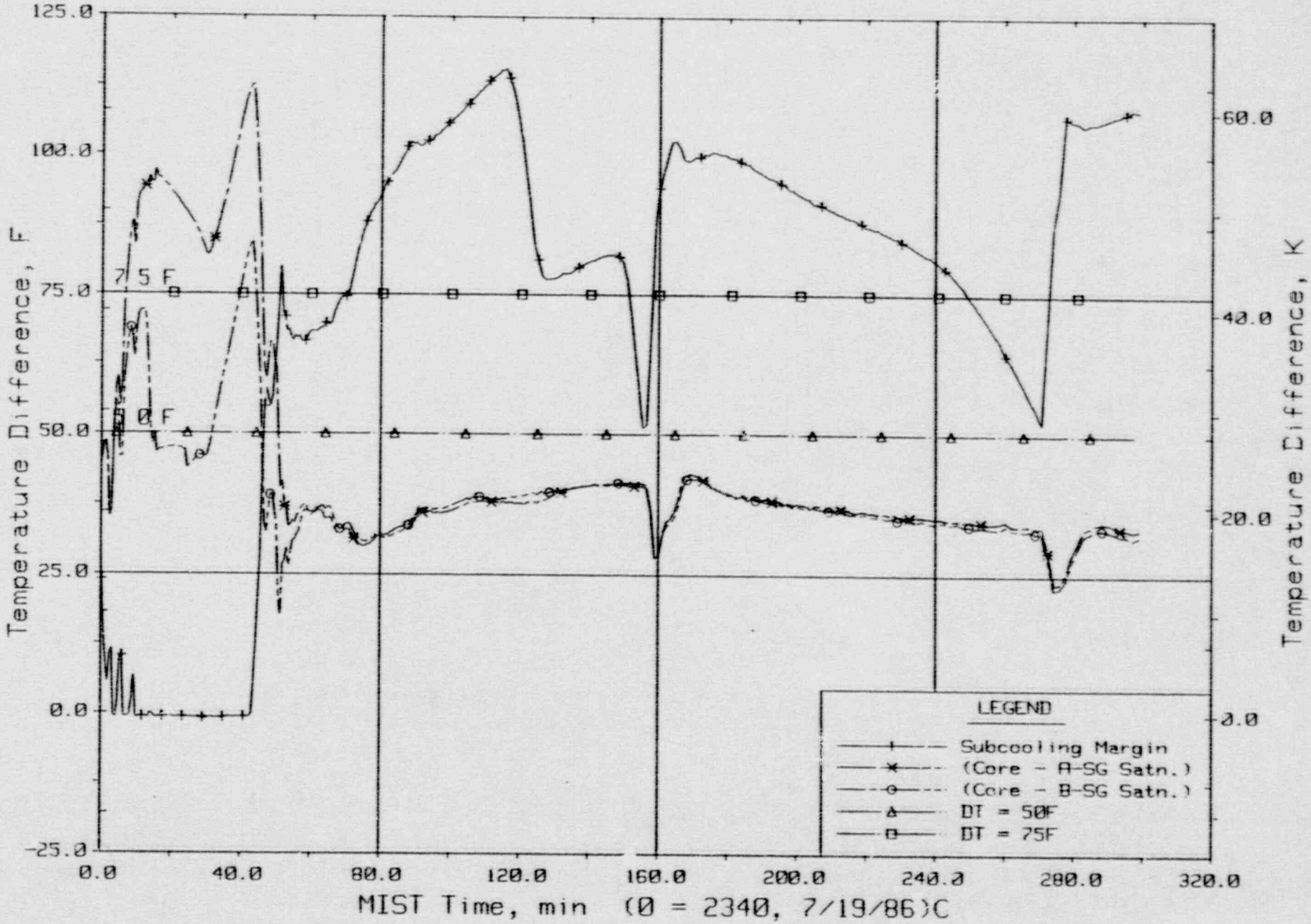

Control Temperature Differences.

Thu Jun 9 11:48:28 1986

PSTD1

FINAL DATA

T320503: Group 32 SBLOCA Test 5, Leak Isolated.

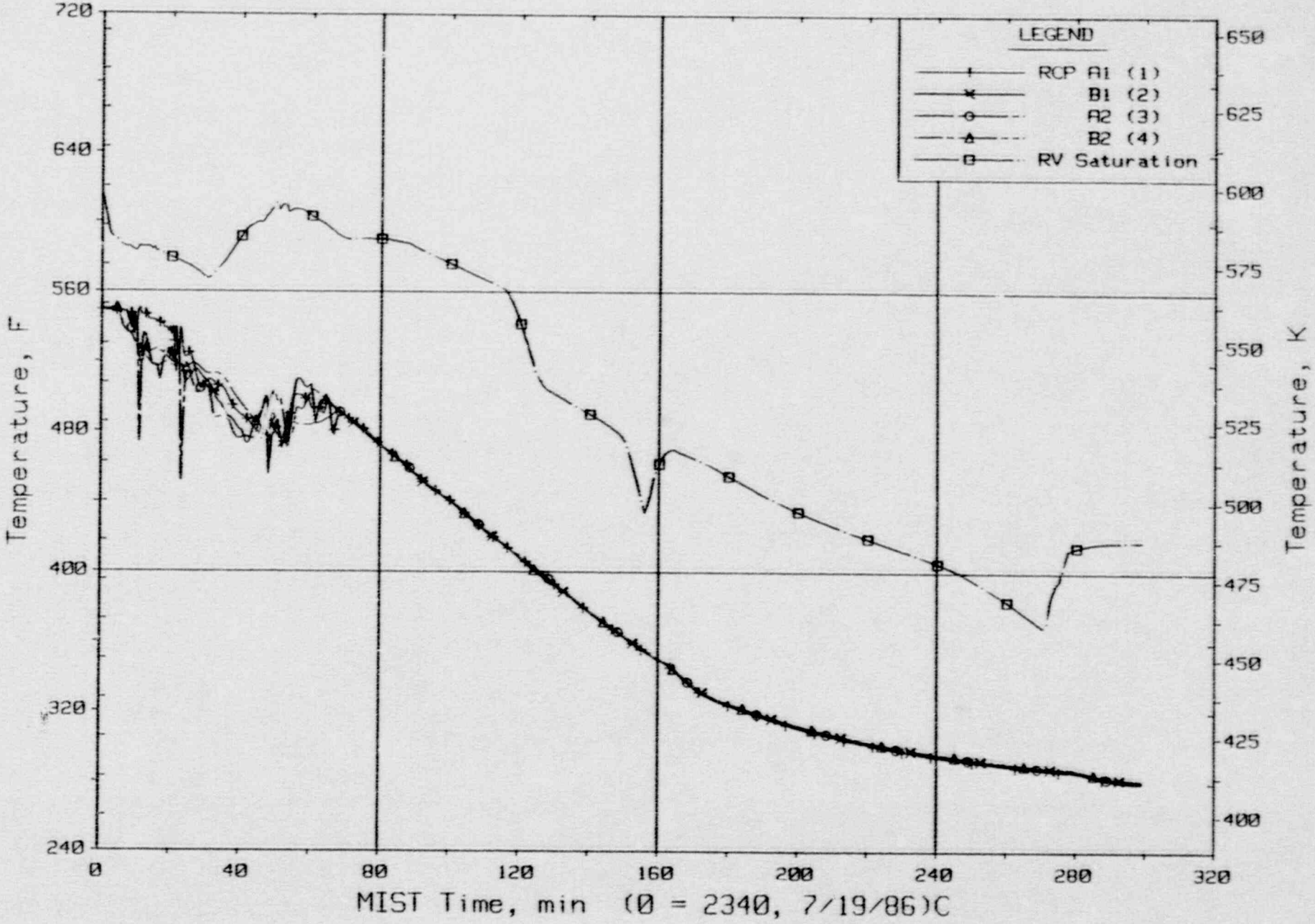

Pump Suction Fluid Temperature (CnRT01s).

Tue Nov 1 09:02:57 1988

PURT0

FINAL DATA

T320503: Group 32 SBLOCA Test 5, Leak Isolated.

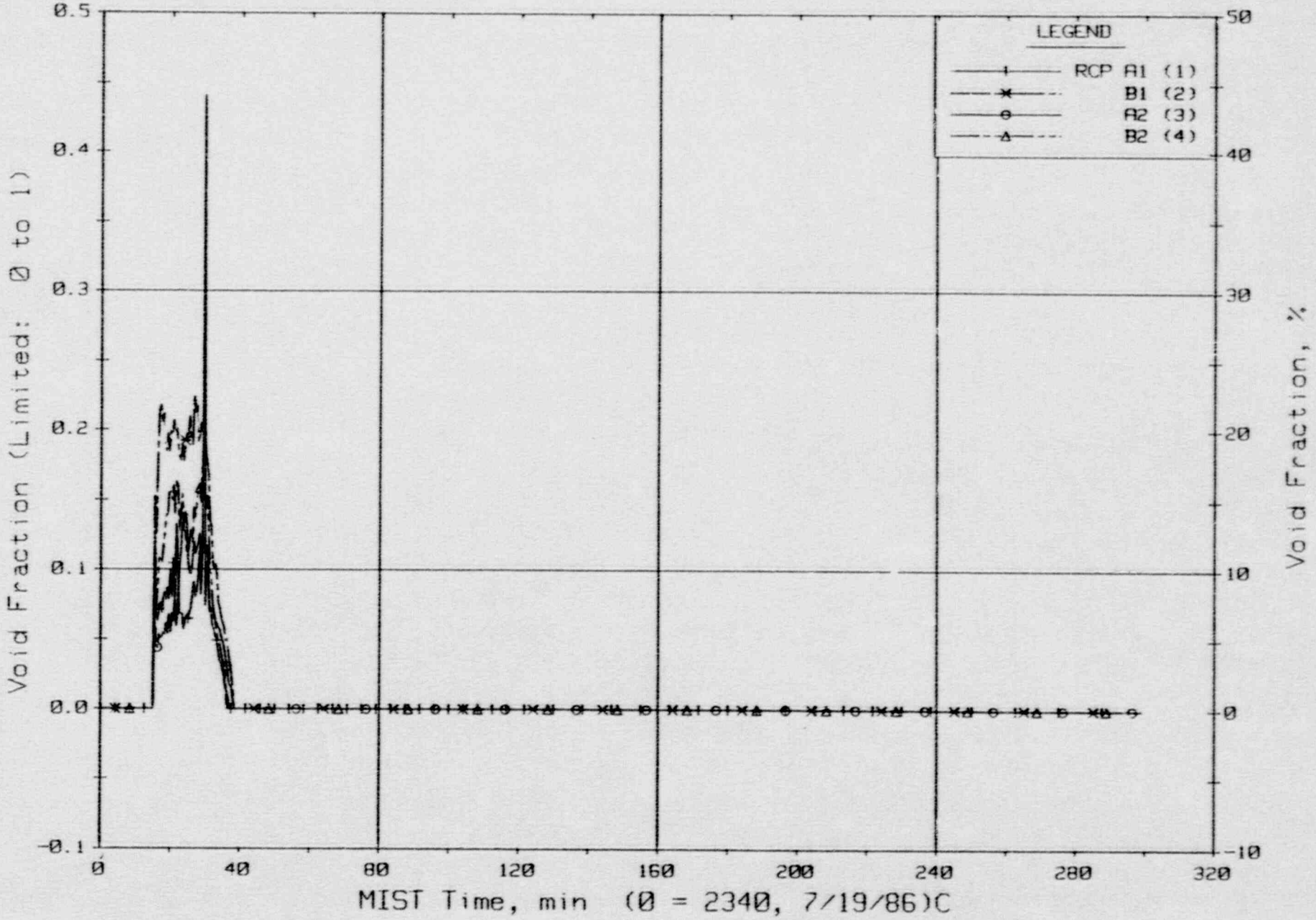

Pump Suction Void Fraction From Gamma Densitometers (CnGD21).

Tue Nov 1 09:06:21 1988

PUVF2

FINAL DATA

T320503: Group 32 SBLOCA Test 5, Leak Isolated.

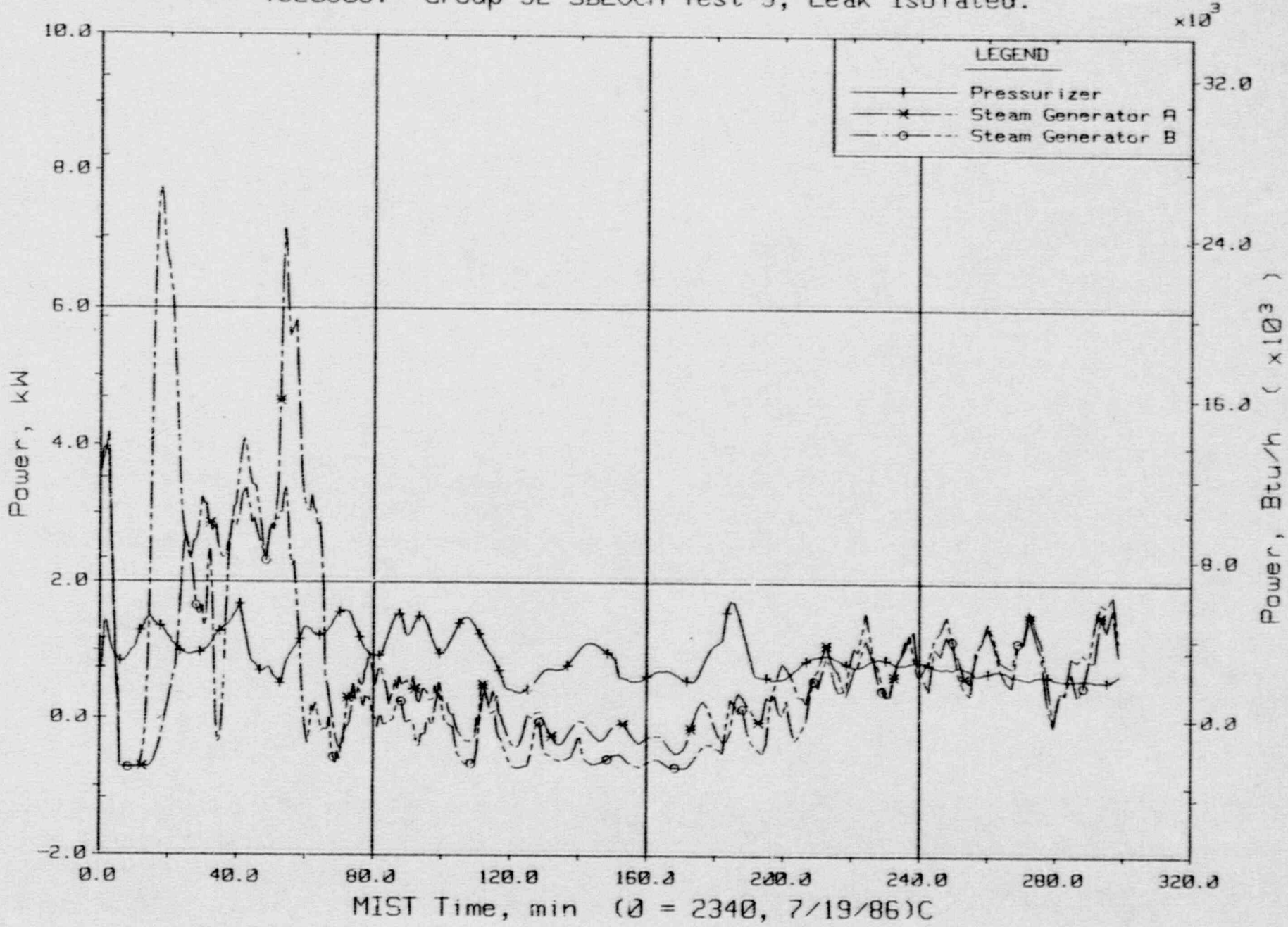

Guard Heater Specified Power, Pressurizer and Steam Generators.

Thu Jun 9 11:57:31 1988

PZG01

FINAL DATA

T320503: Group 32 SBLOCA Test 5, Leak Isolated.

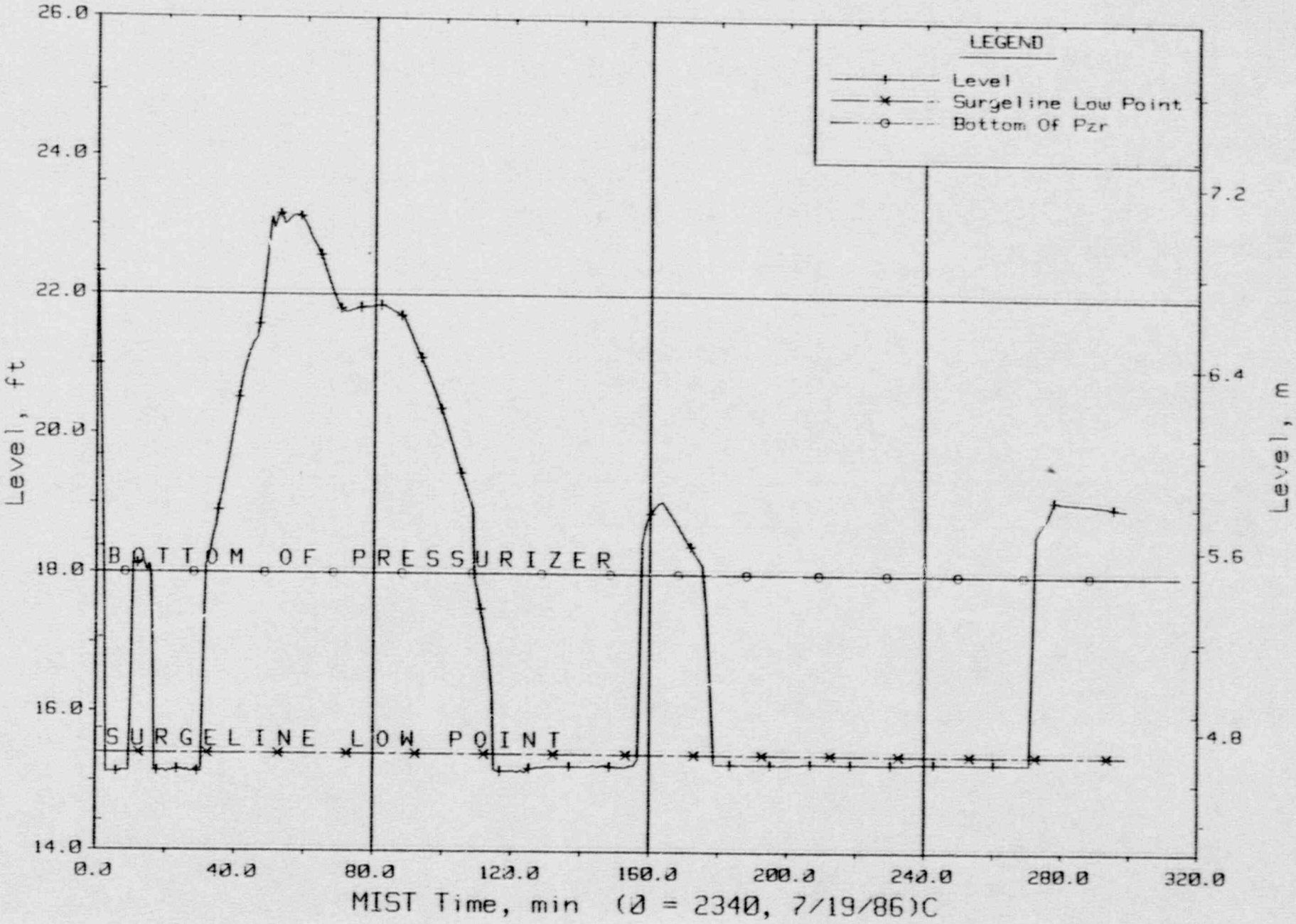

Pressurizer Collapsed Liquid Level (PZLV20).

Thu Jun 9 11:59:57 1988

PZLV1

FINAL DATA

T320503: Group 32 SBLOCA Test 5, Leak Isolated.

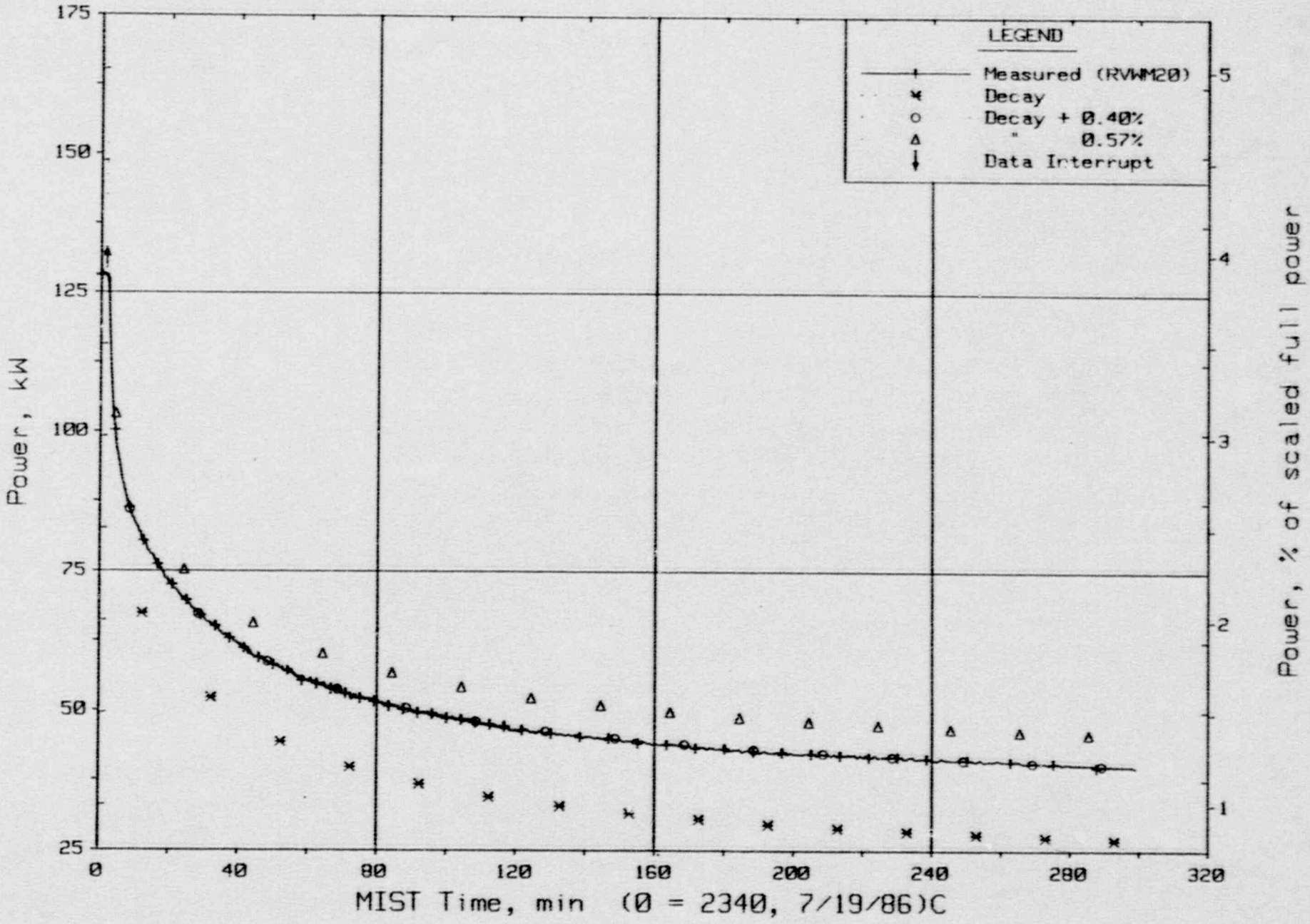

Core Power.

Tue Nov 1 08:54:20 1988

RVKW0

FINAL DATA

T320503: Group 32 SBLOCA Test 5, Leak Isolated.

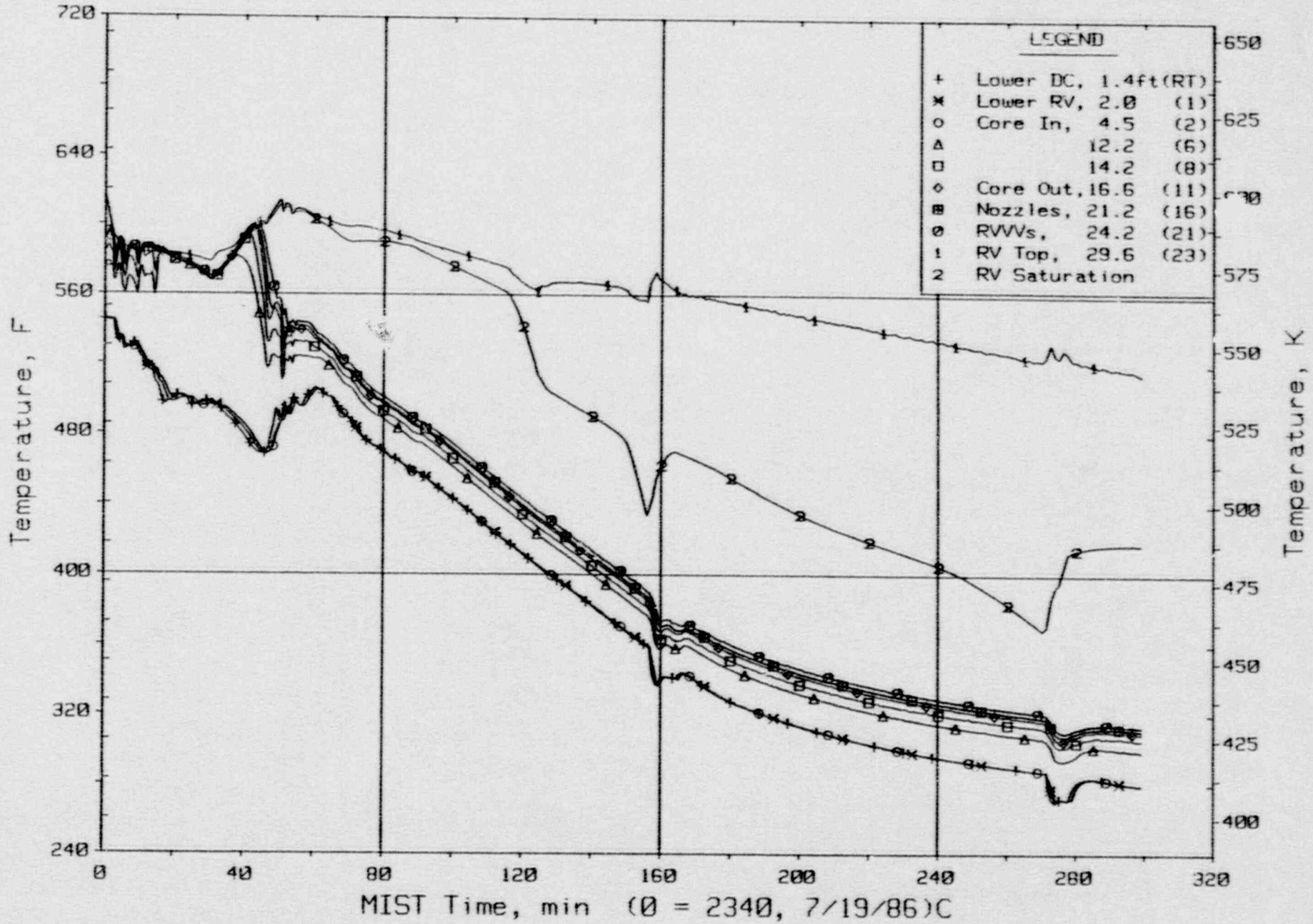

Core Unit Cell and Reactor Vessel Fluid Temperatures (RVTCs).

Tue Nov 1 00:59:00 1988

RVTC0

FINAL DATA

T320503: Group 32 SBLOCA Test 5, Leak Isolated.

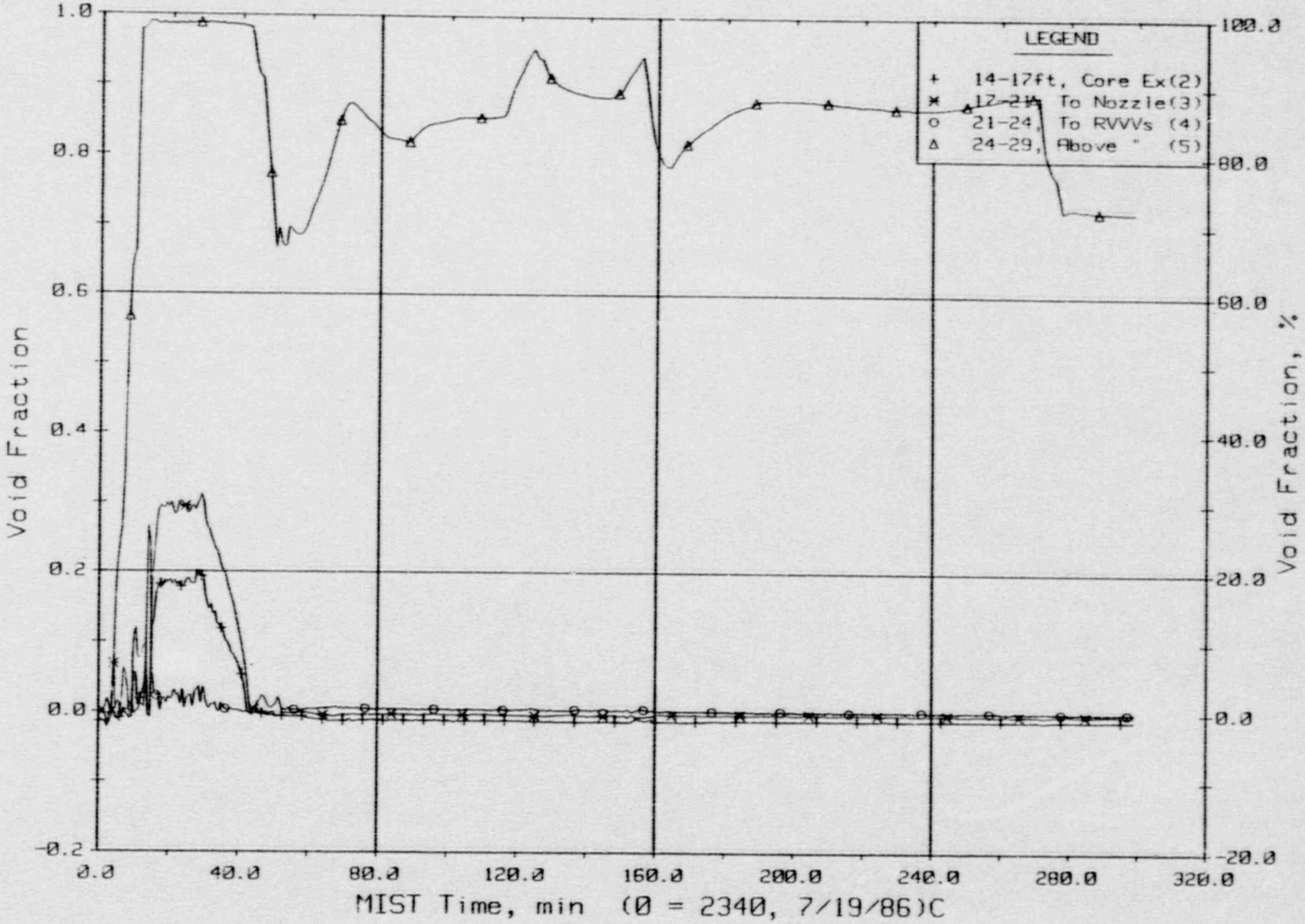

Reactor Vessel Void Fractions From Differential Pressures (RVVFs).

FINAL DATA

T320503: Group 32 SBLOCA Test 5, Leak Isolated.

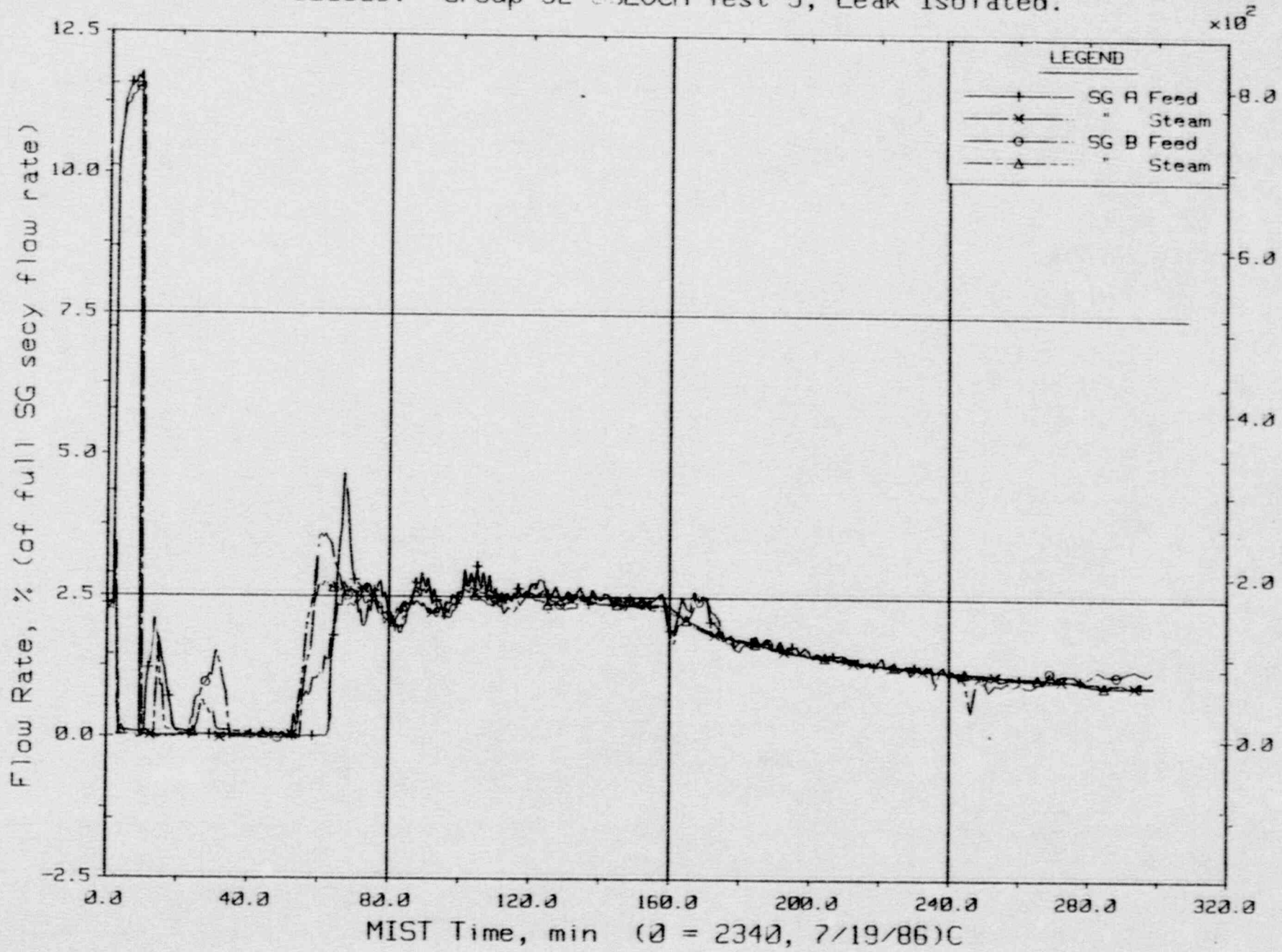

Steam Generator Secondary System Flow Rates.

Thu Jun 9 12:11:36 1988

SGFL2

FINAL DATA

T32∅503: Group 32 SBLOCA Test 5, Leak Isolated.

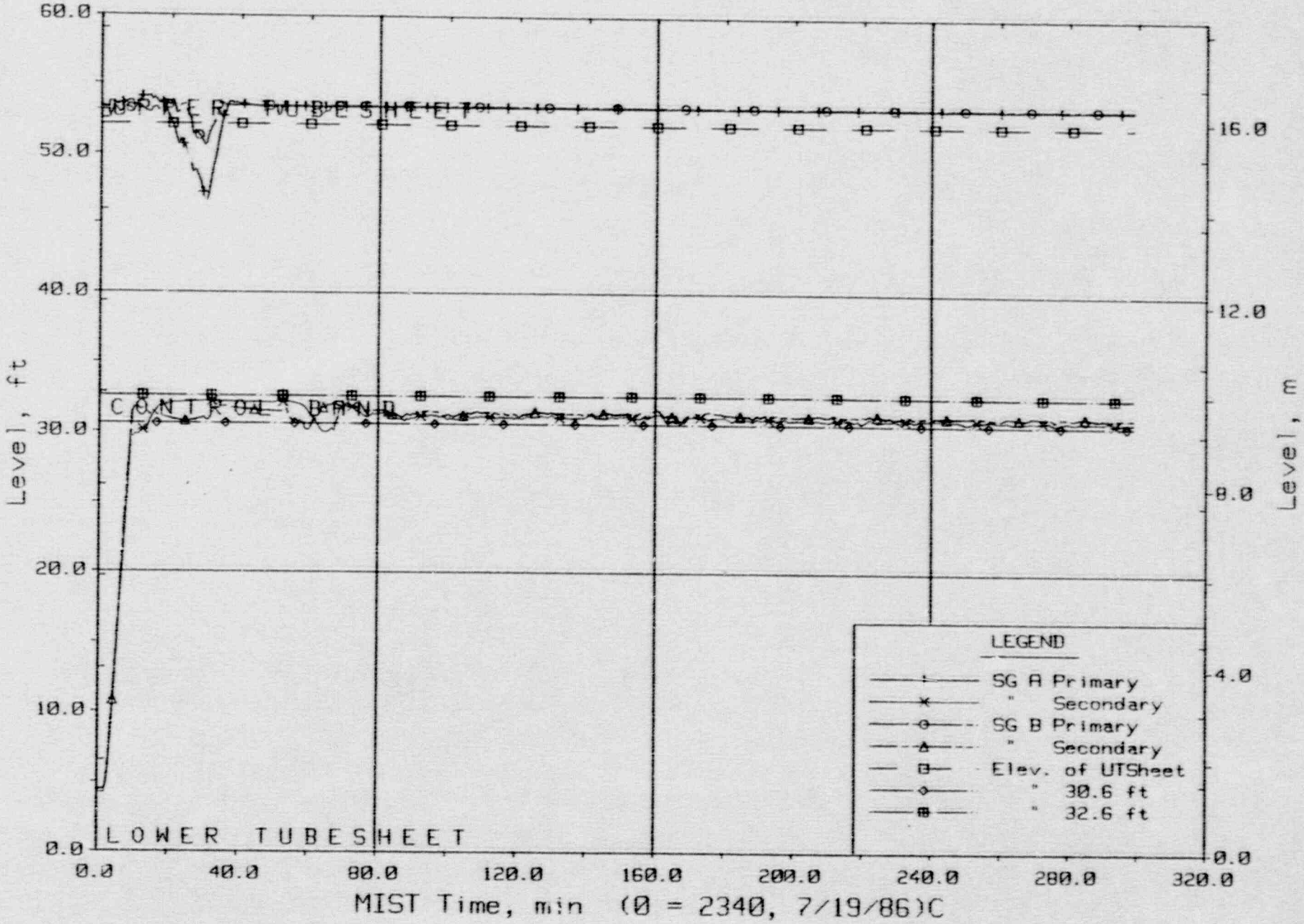

Steam Generator Collapsed Liquid Levels.

Thu Jun 9 12:14:51 1988

SGLV2

FINAL DATA

T320503: Group 32 SBLOCA Test 5, Leak Isolated.

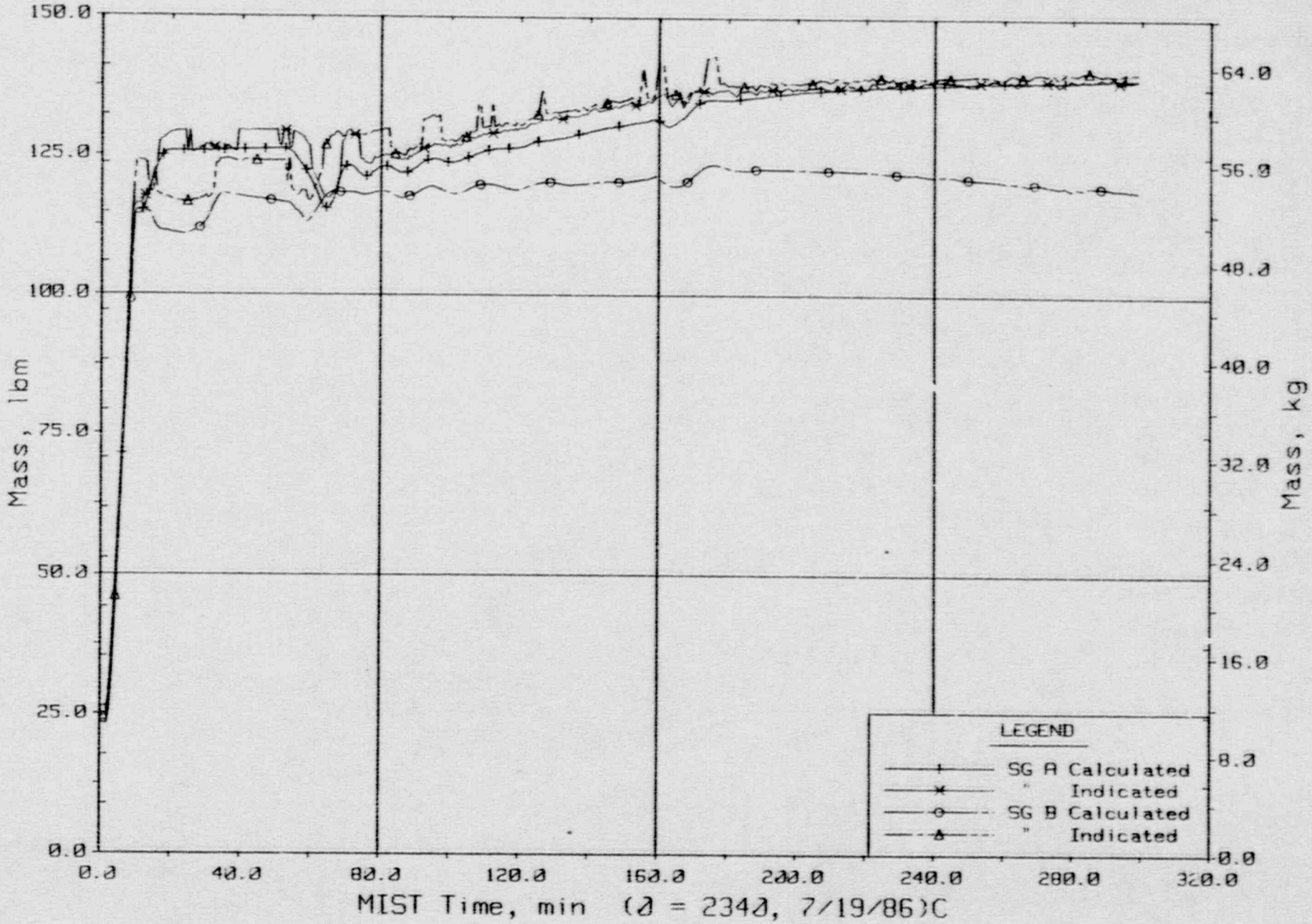

Steam Generator Secondary Fluid Mass Balances.

Thu Jun 9 12:17:46 1988

SGML1

FINAL DATA

T320503: Group 32 SBLOCA Test 5, Leak Isolated.

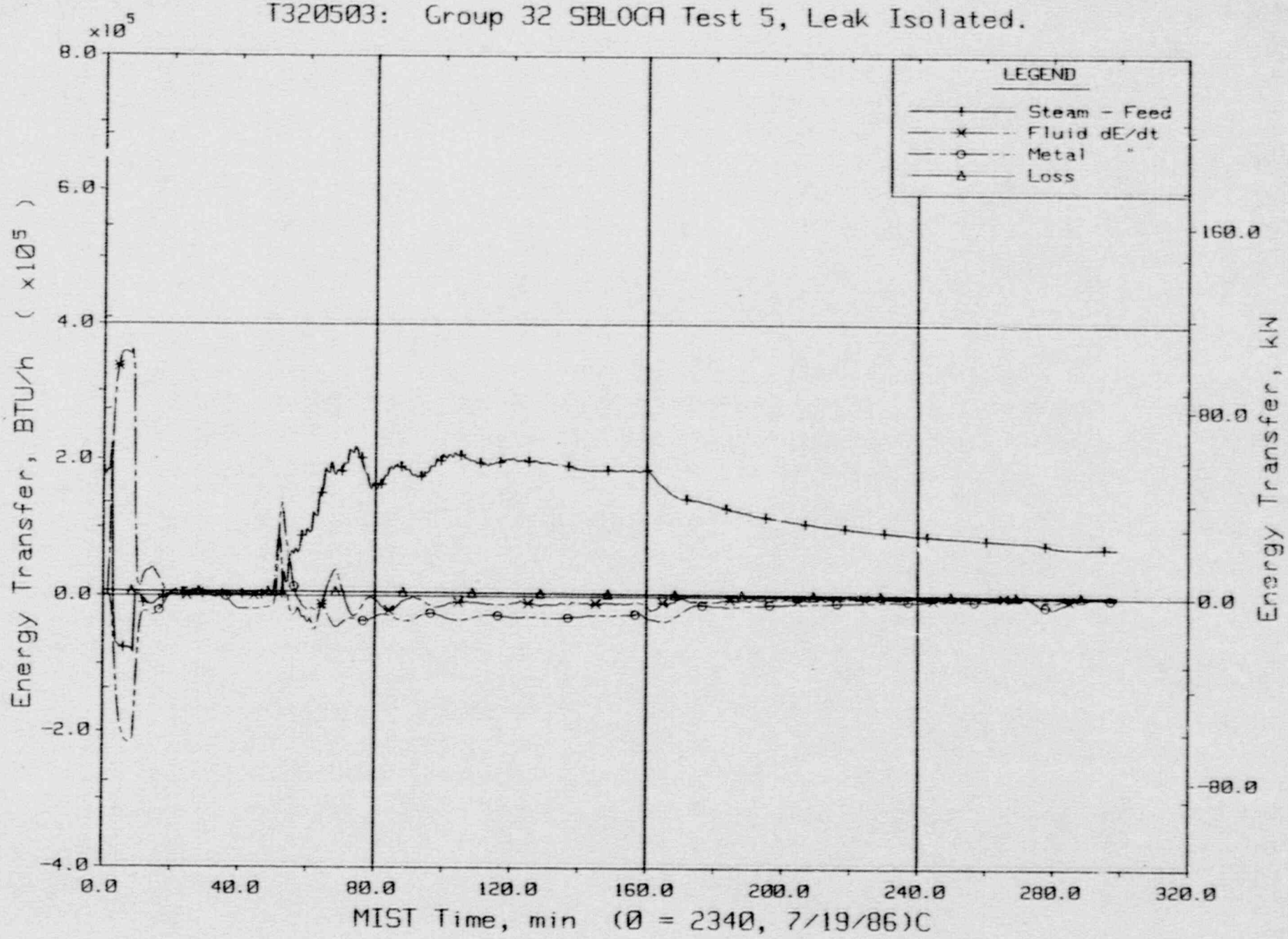

Steam Generator A Energy Transfer.

Thu Jun 9 12:24:53 1988

SGQE3

FINAL DATA

T320503: Group 32 SBLOCA Test 5, Leak Isolated.

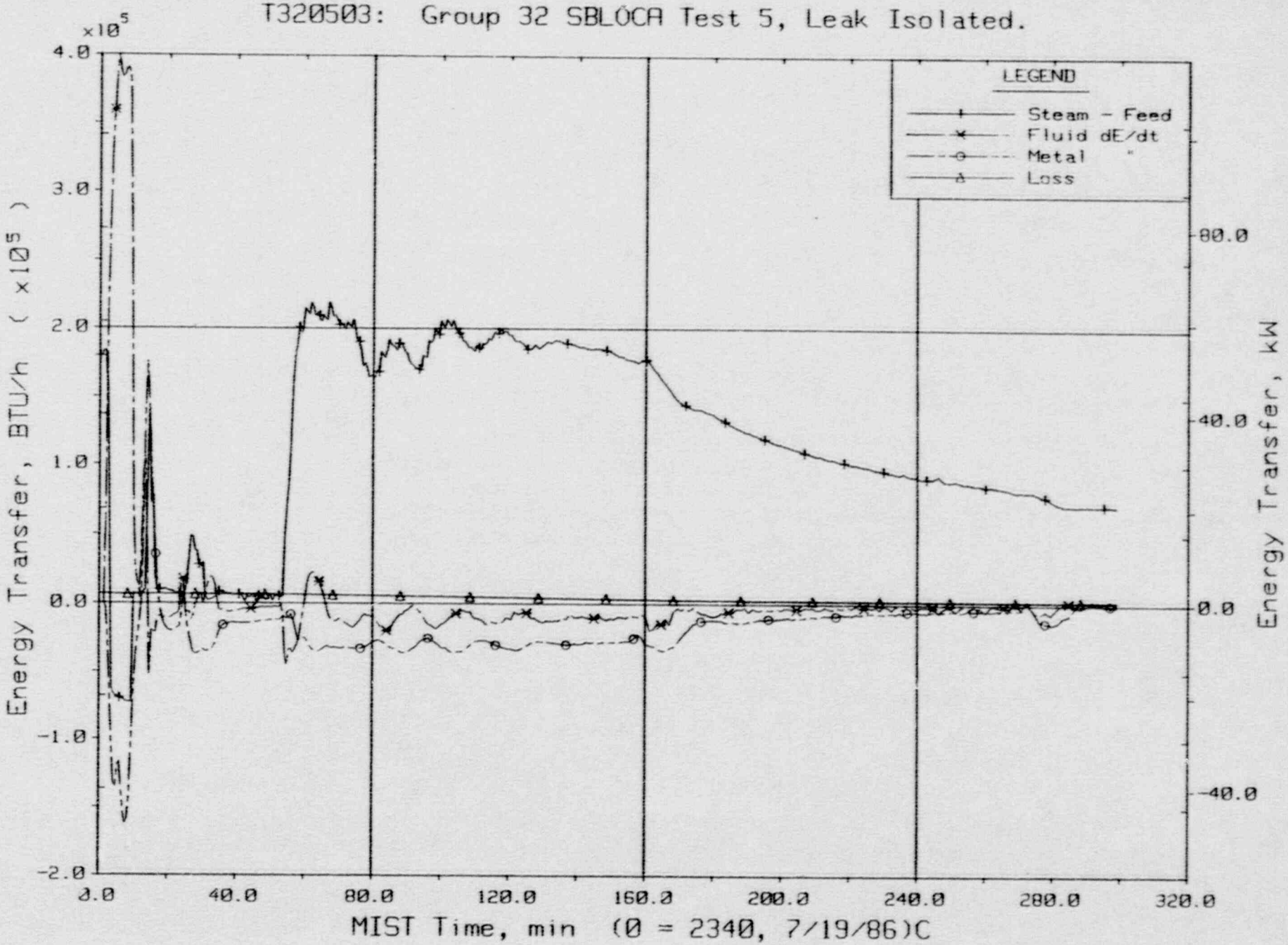

Steam Generator B Energy Transfer.

Thu Jun 9 12:30:15 1988

SGQE6

FINAL DATA

T320503: Group 32 SBLOCA Test 5, Leak Isolated.

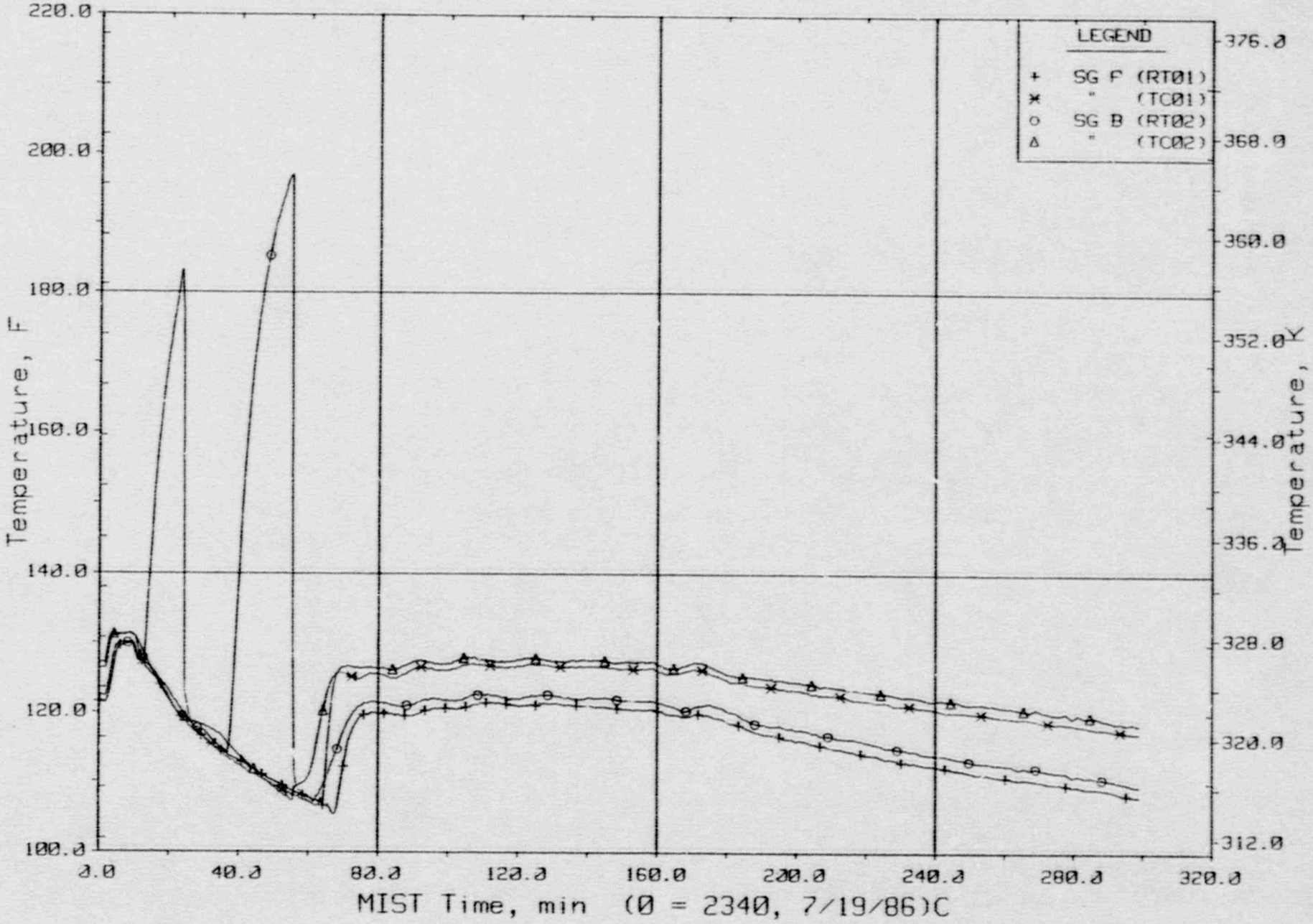

Feedwater Temperatures (SFs).

Thu Jun 9 12:32:45 1988

SGRT1

FINAL DATA

T320503: Group 32 SBLOCA Test 5, Leak Isolated.

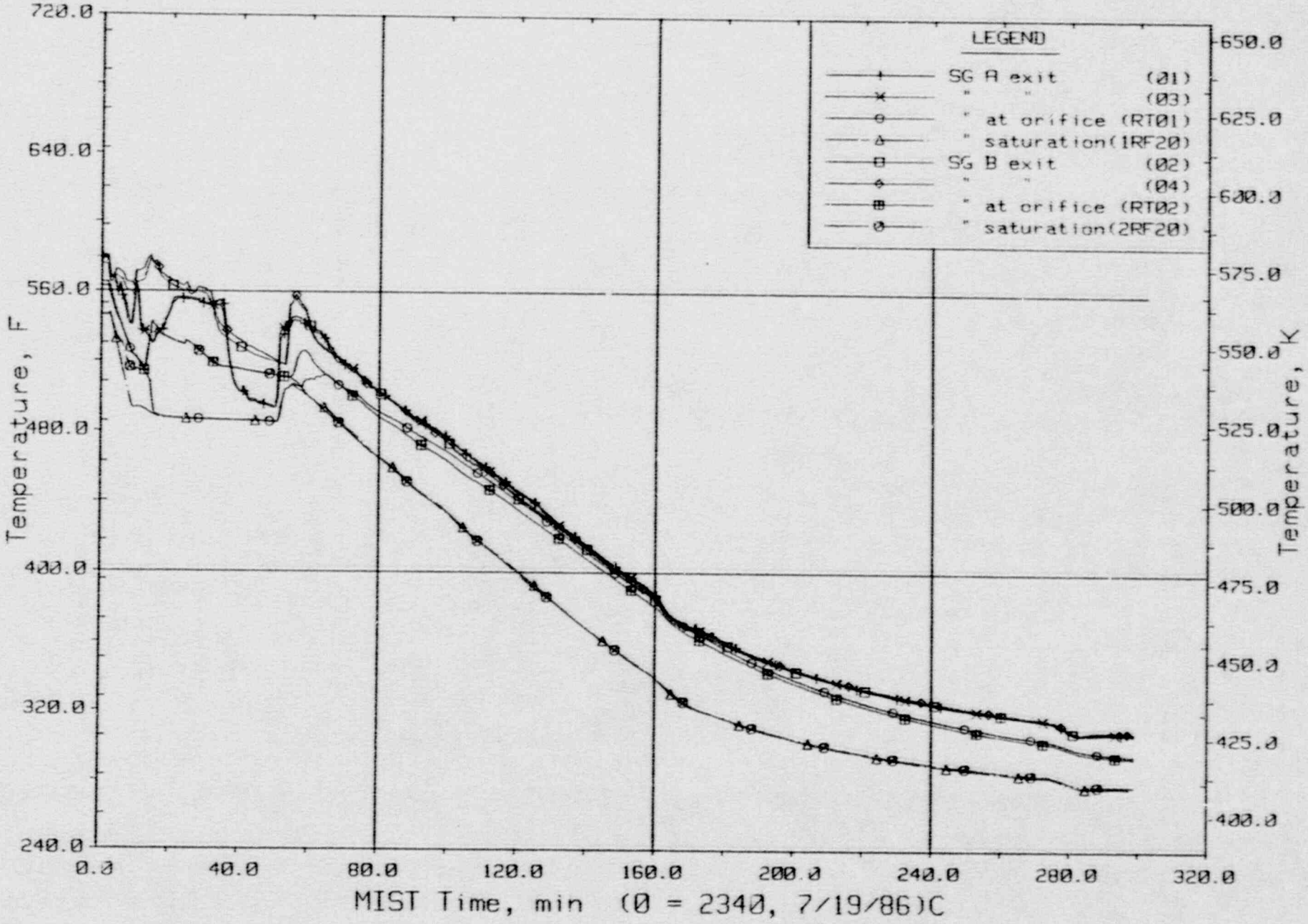

Steam Generator Steam Outlet Temperatures (SSTCs).

Thu Jun 9 12:36:07 1988

SGRT2

FINAL DATA

T320503: Group 32 SBLOCA Test 5, Leak Isolated.

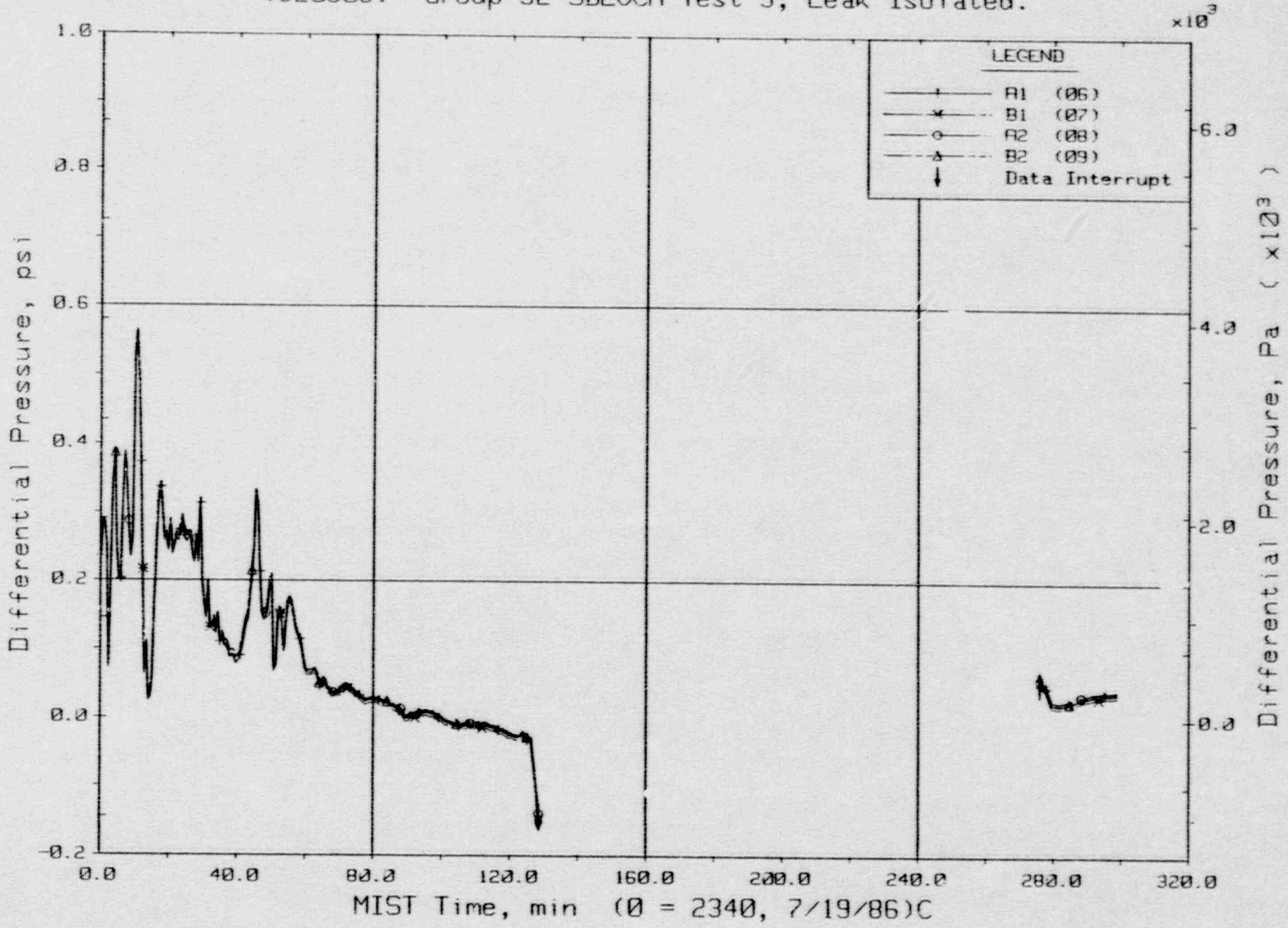

Reactor Vessel Vent Valve Differential Pressures (RVDPs).

Thu Jun 9 12:39:03 1988

VVDP1

FINAL DATA

T320503: Group 32 SBLOCA Test 5, Leak Isolated.

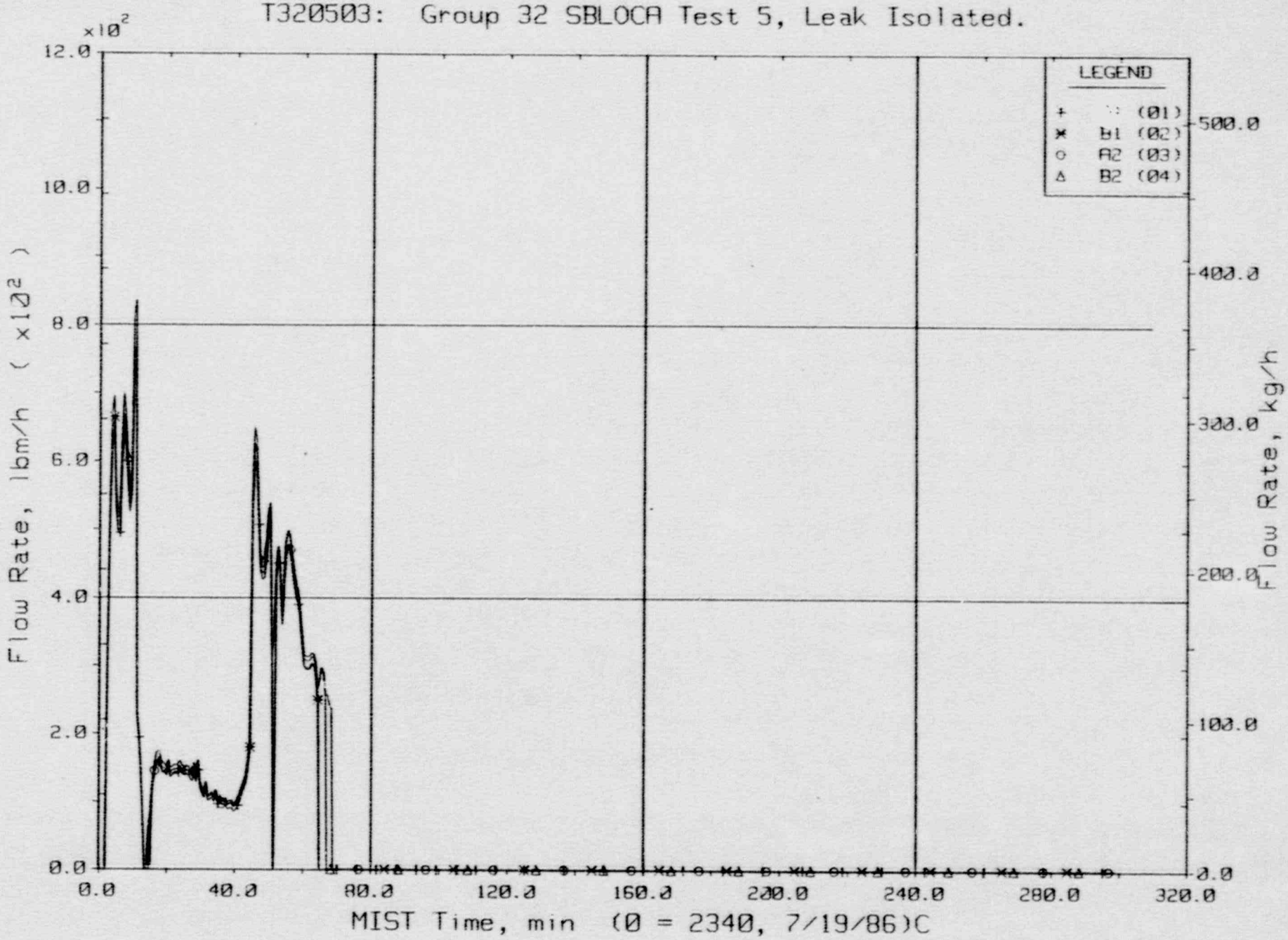

Reactor Vessel Vent Valve Flow Rates (RVORs).

Thu Jun 9 12:41:50 1988

VVFL1

FINAL DATA

T320503: Group 32 SBLOCA Test 5, Leak Isolated.

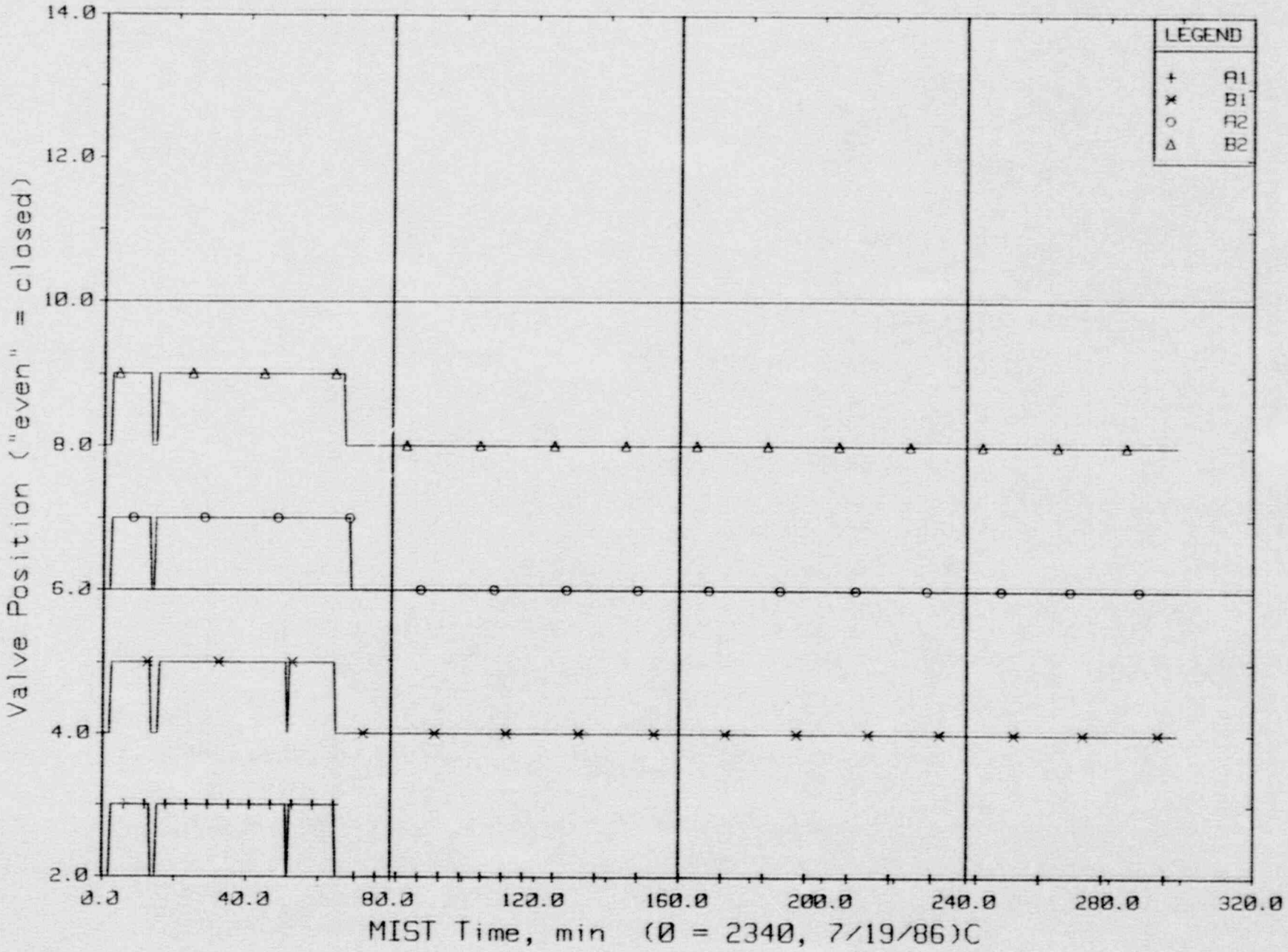

Reactor Vessel Vent Valve Positions.

Thu Jun 9 12:44:17 1988

VVLS1

FINAL DATA

T320503: Group 32 SBLOCA Test 5, Leak Isolated.

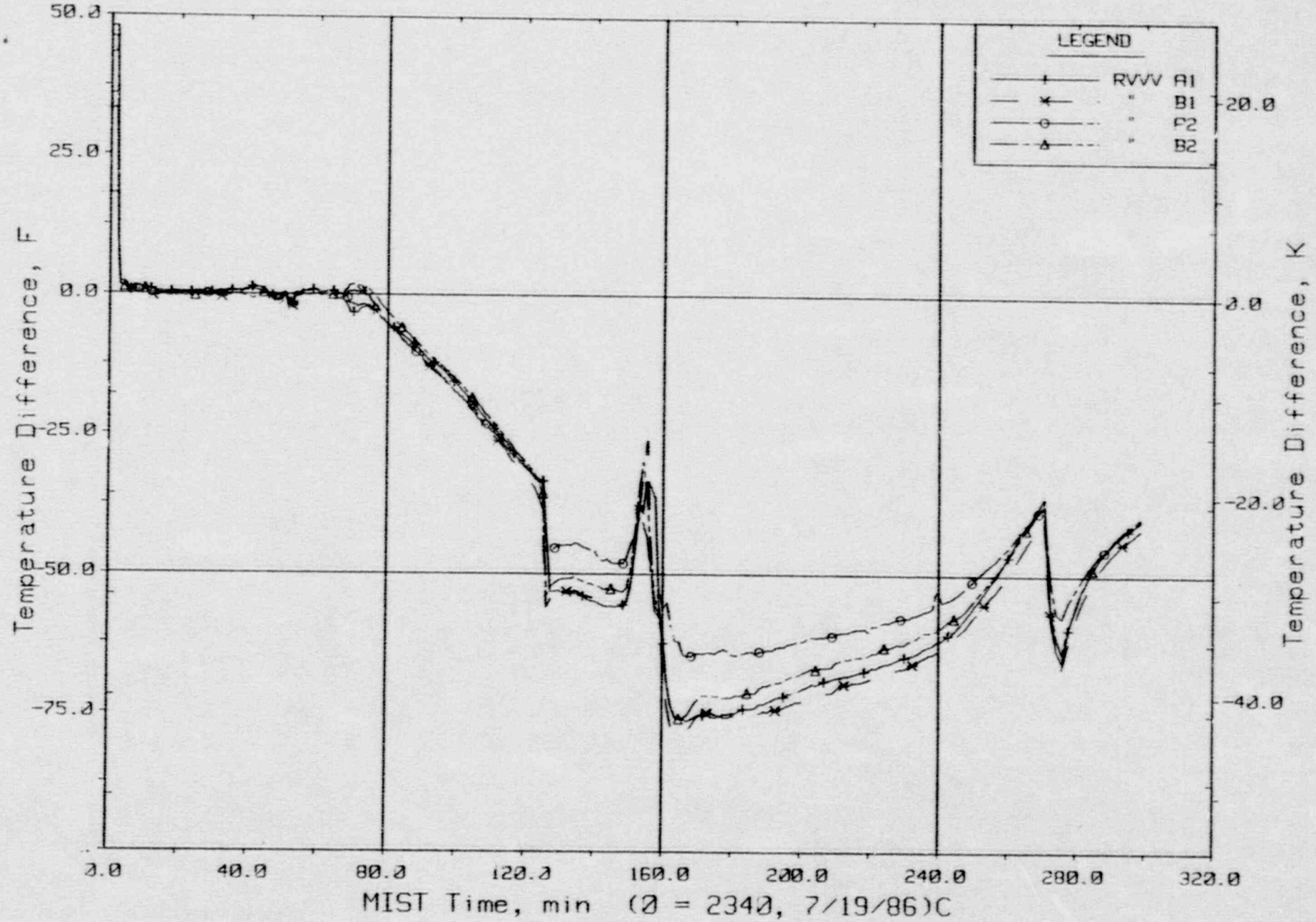

Temperature Differences Across Vent Valves.

Thu Jun 9 12:46:44 1988

VVTD1

T320604

FINAL DATA

T320604: Group 32 SBLOCA Test 6, Reduced-Capacity HPI.

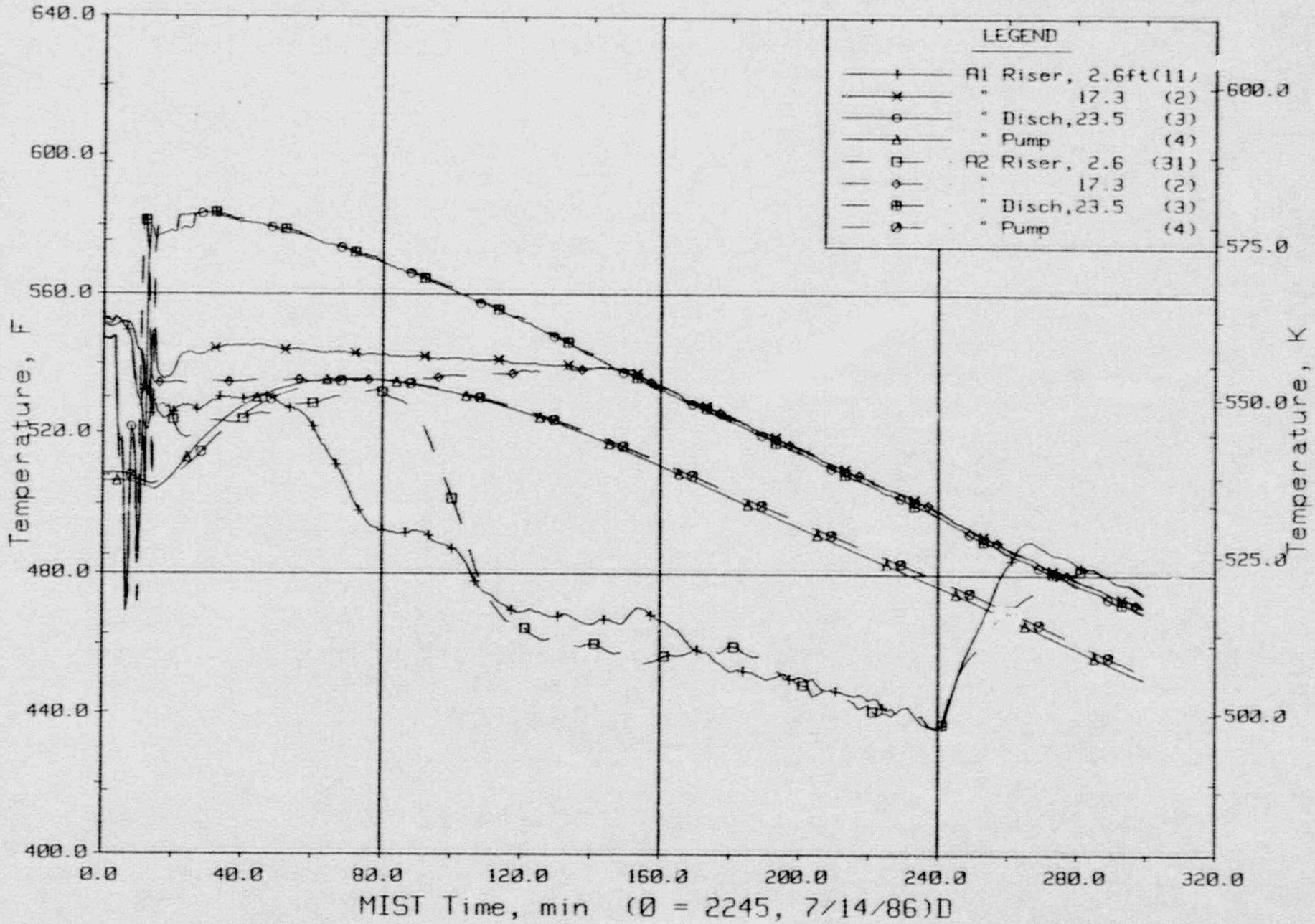

Loop A Cold Leg Metal Temperatures (C1,3MTs).

Thu Jun 9 16:43:34 1988

C1MT1

FINAL DATA

T320604: Group 32 SBLOCA Test 6, Reduced-Capacity HPI.

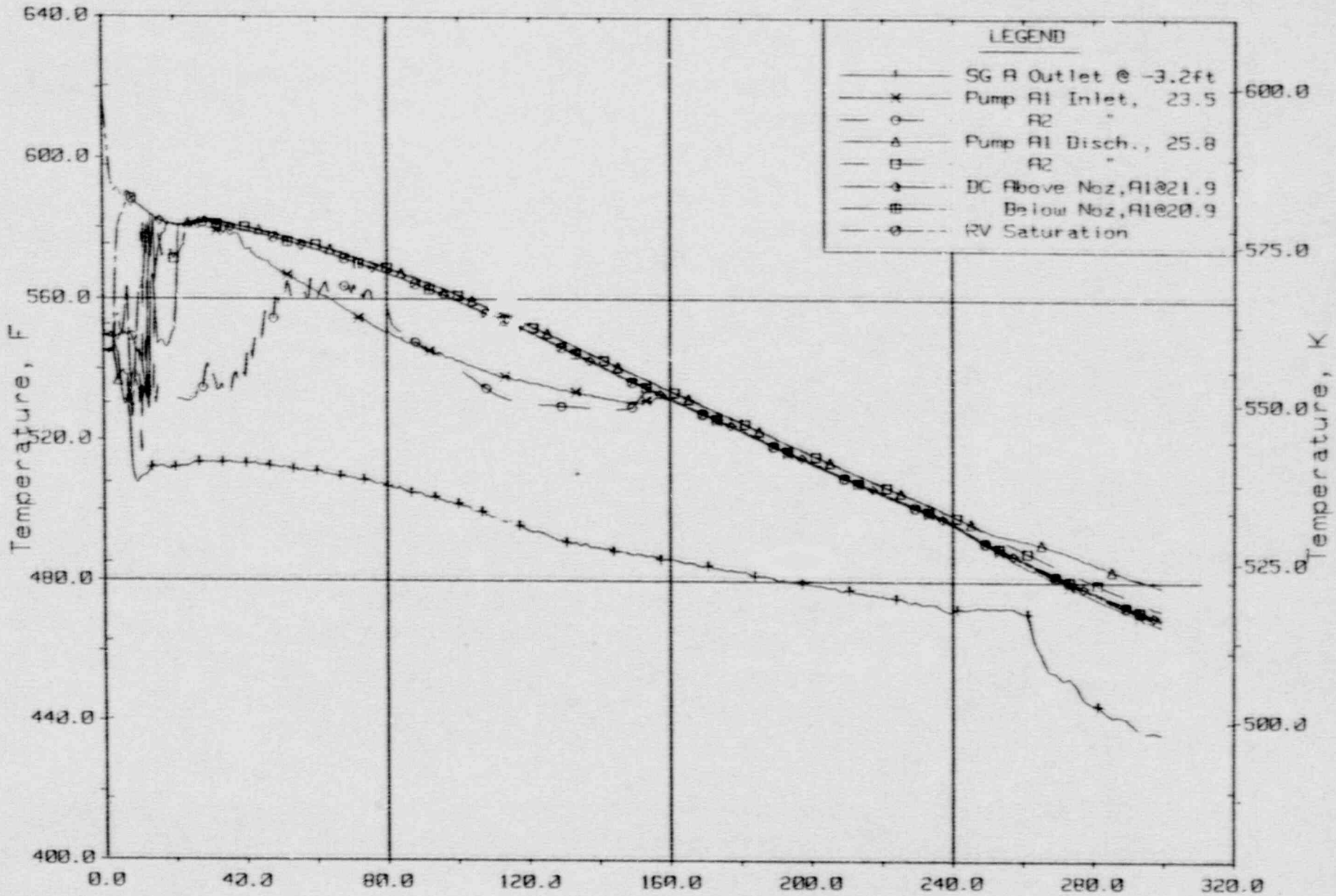

Loop A Cold Leg Fluid Temperatures (RTDs).

Thu Jun 9 16:46:59 1988

C1-RT0

FINAL DATA

T320604: Group 32 SBLOCA Test 6, Reduced-Capacity HPI.

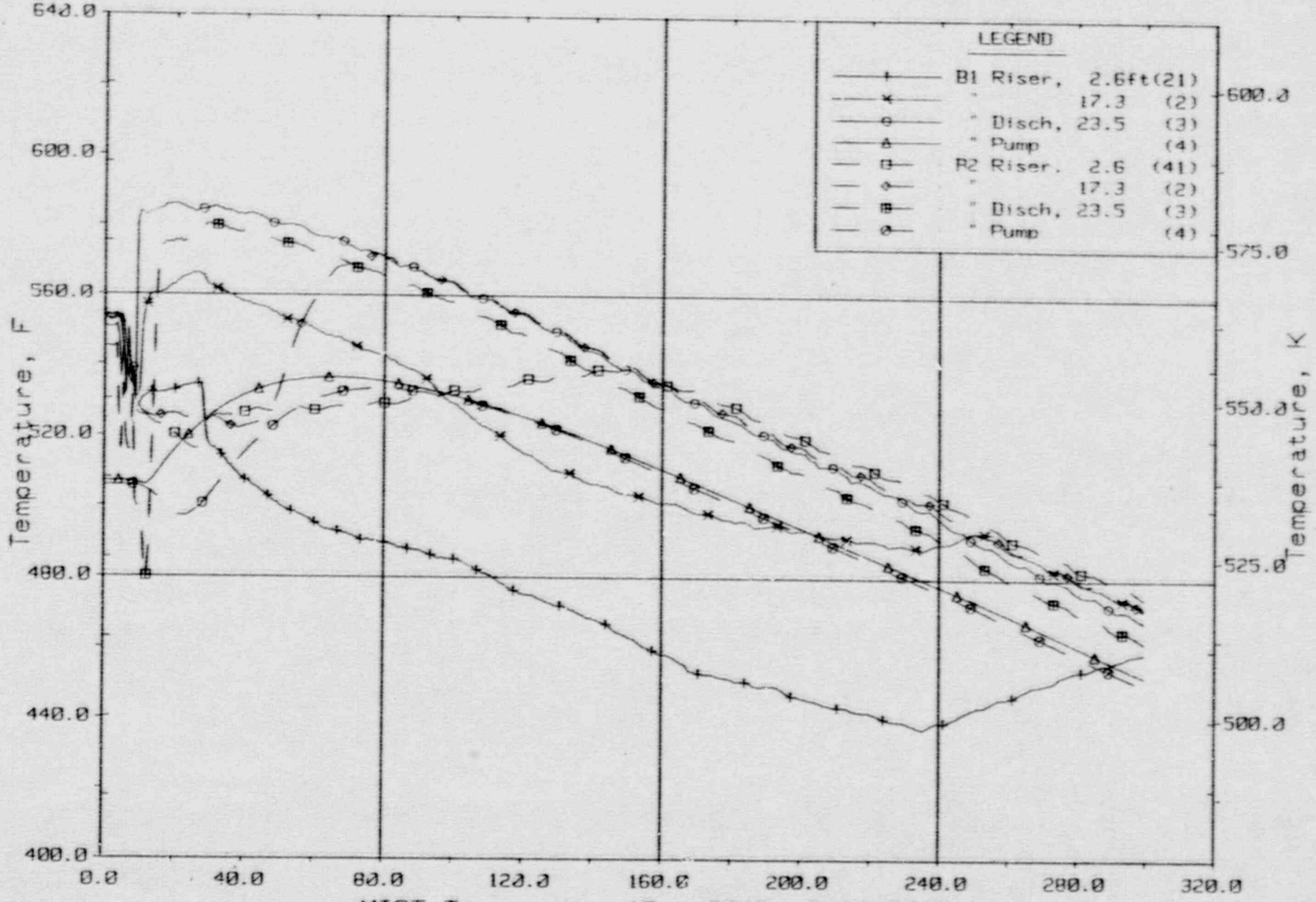

Loop B Cold Leg Metal Temperatures (C2,4MTs).

Thu Jun 9 16:50:28 1988

C2MT1

FINAL DATA

T320604: Group 32 SBLOCA Test 6, Reduced-Capacity HPI.

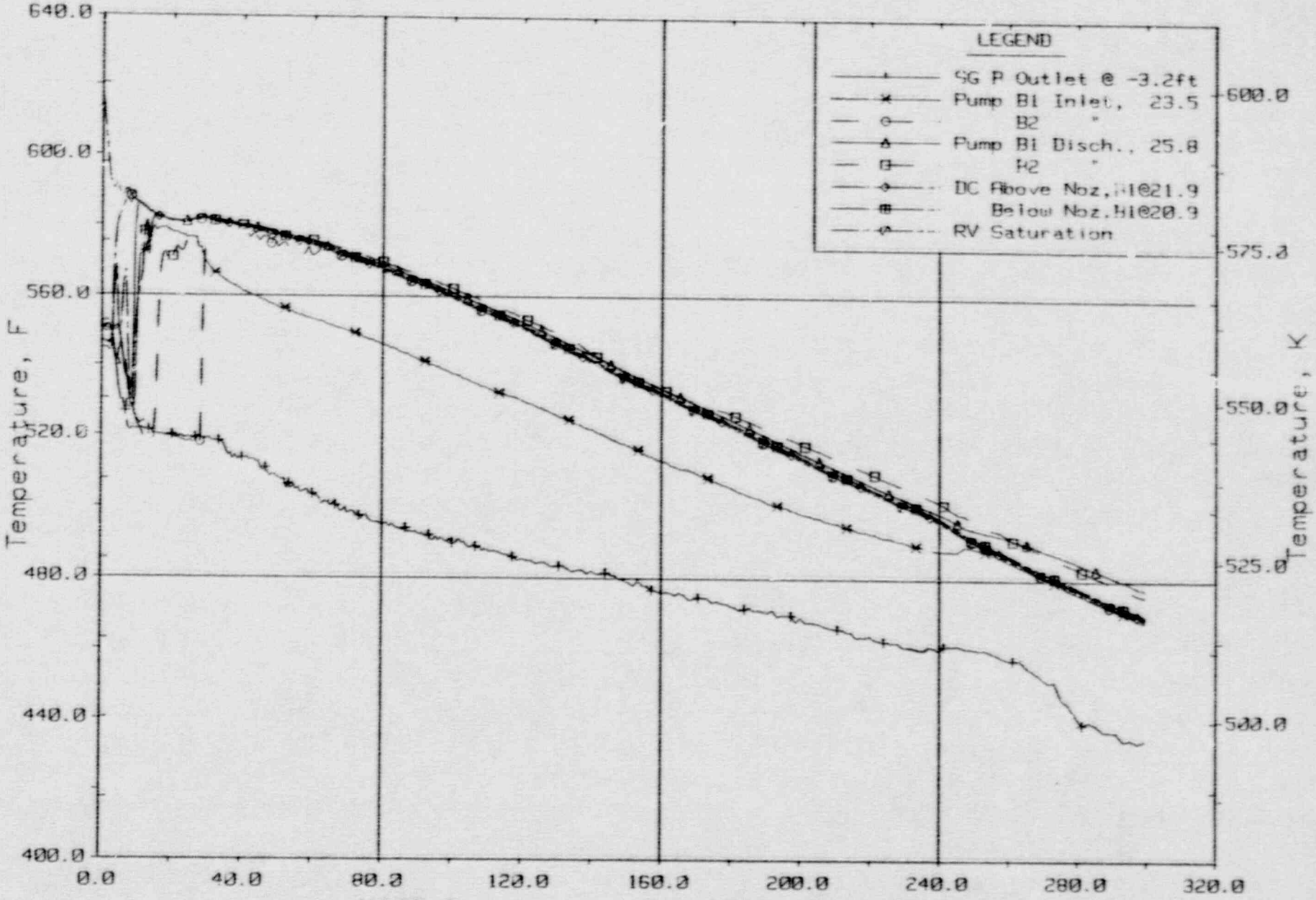

Loop B Cold Leg Fluid Temperatures (RTDs).

Thu Jun 9 16:54:05 1988

C2RT0

FINAL DATA

T320604: Group 32 SBLOCA Test 6, Reduced-Capacity HPI.

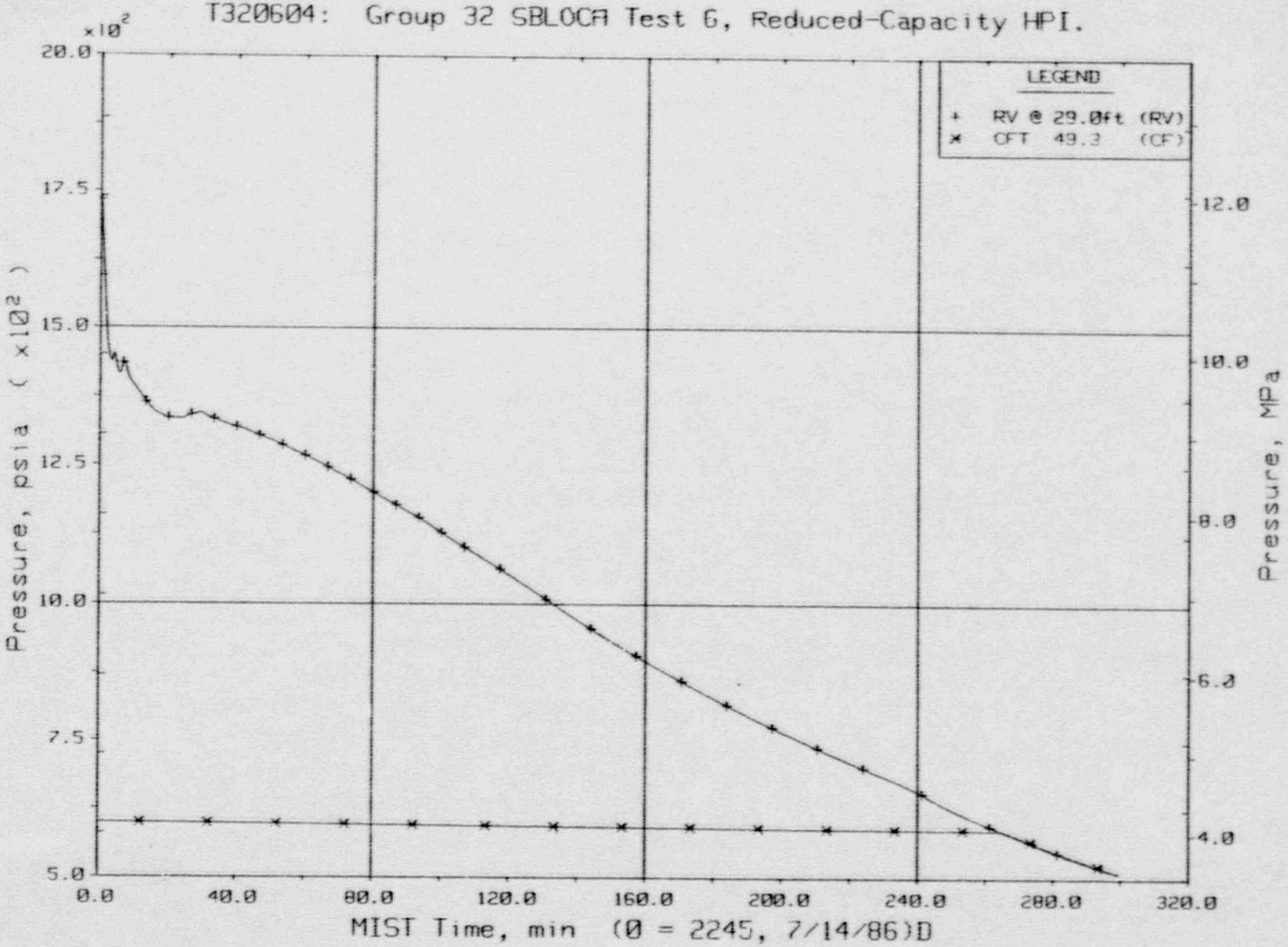

Primary System and Core Flood Tank Pressures (GP0ls).

Thu Jun 9 16:56:26 1988

CFGP1

FINAL DATA

T320604: Group 32 SBLOCA Test 6, Reduced-Capacity HPI.

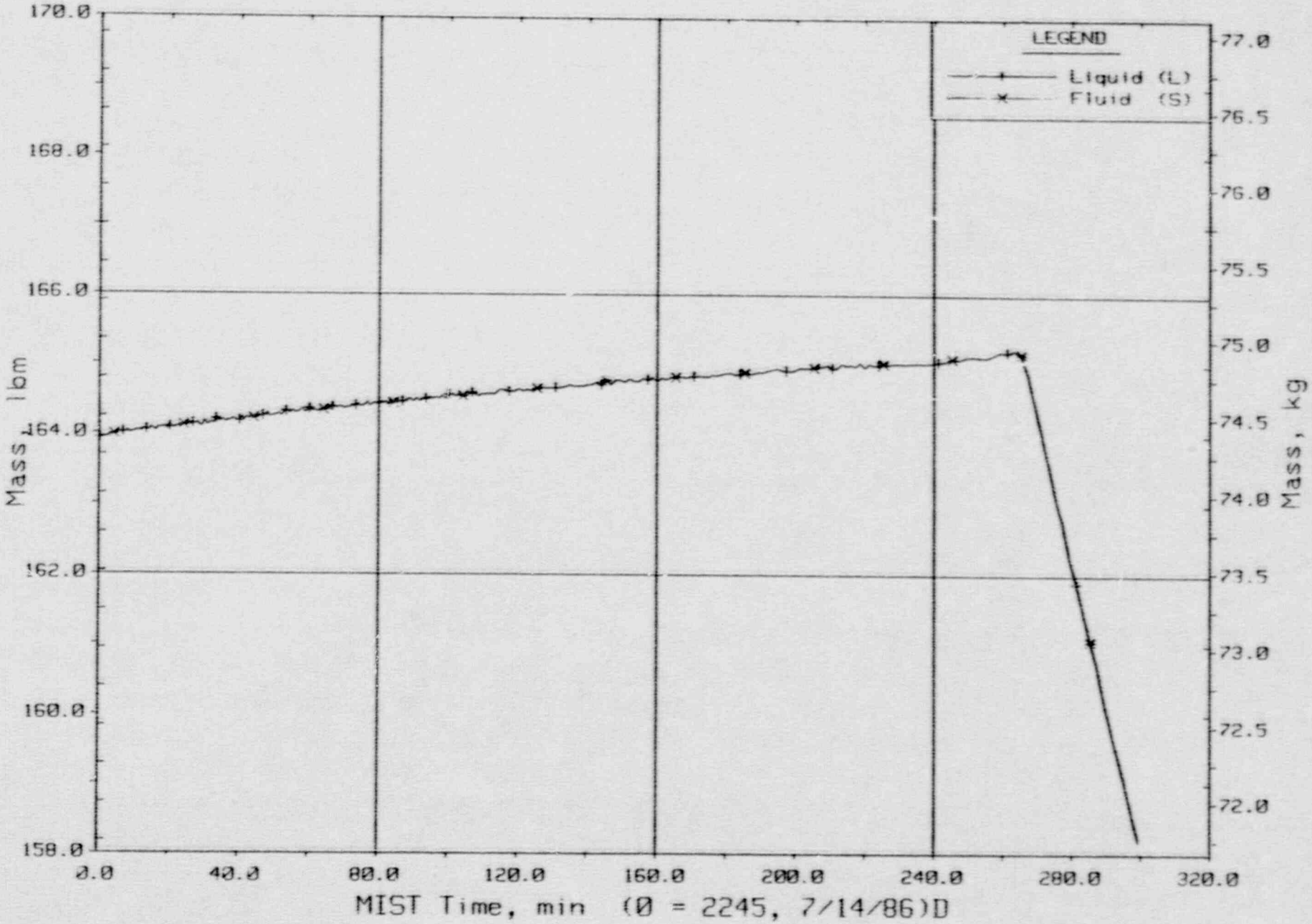

Core Flood Tank Liquid and Fluid Mass (CFMa20s).

FINAL DATA

T320604: Group 32 SBLOCA Test 6, Reduced-Capacity HPI.

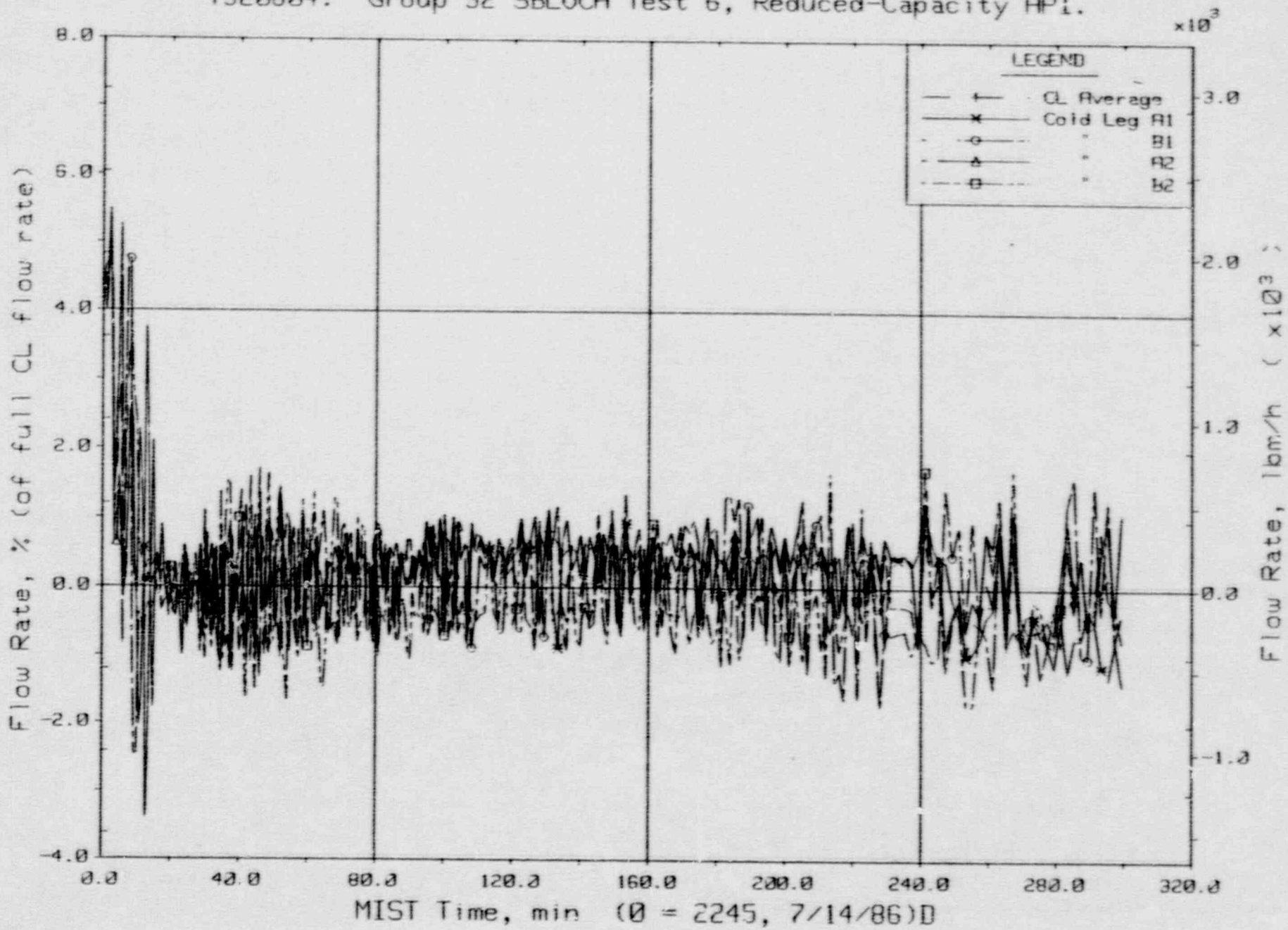

Cold Leg (Venturi) Flow Rates.

Thu Jun 9 17:02:20 1988

CLFL1

FINAL DATA

T320604: Group 32 SBLOCA Test 6, Reduced-Capacity HPI.

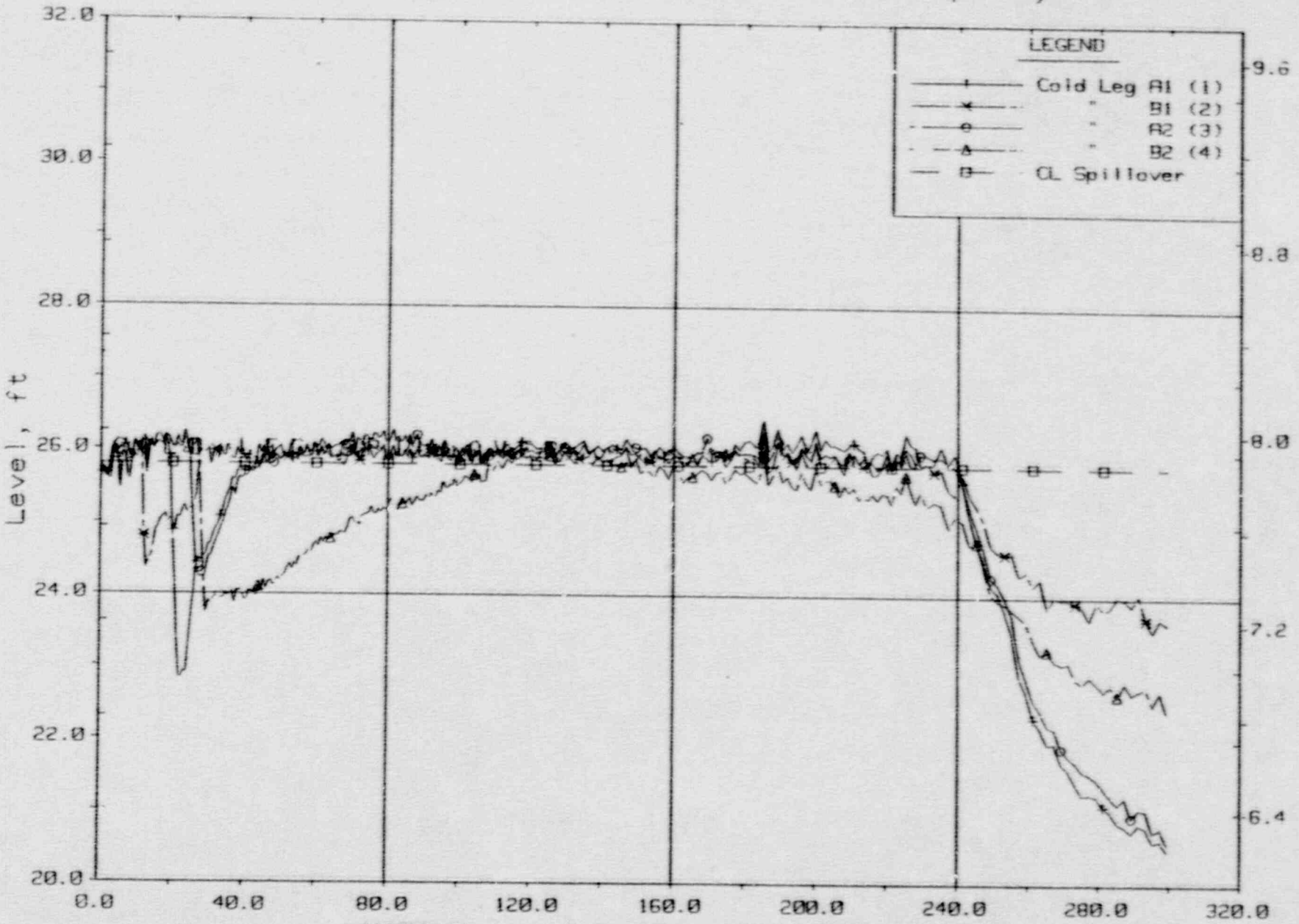

Cold Leg Suction Collapsed Liquid Levels (CnLV22s).

Thu Jun 9 1?:05:04 1988

CLLV4

FINAL DATA

T320604: Group 32 SBLOCA Test 6, Reduced-Capacity HPI.

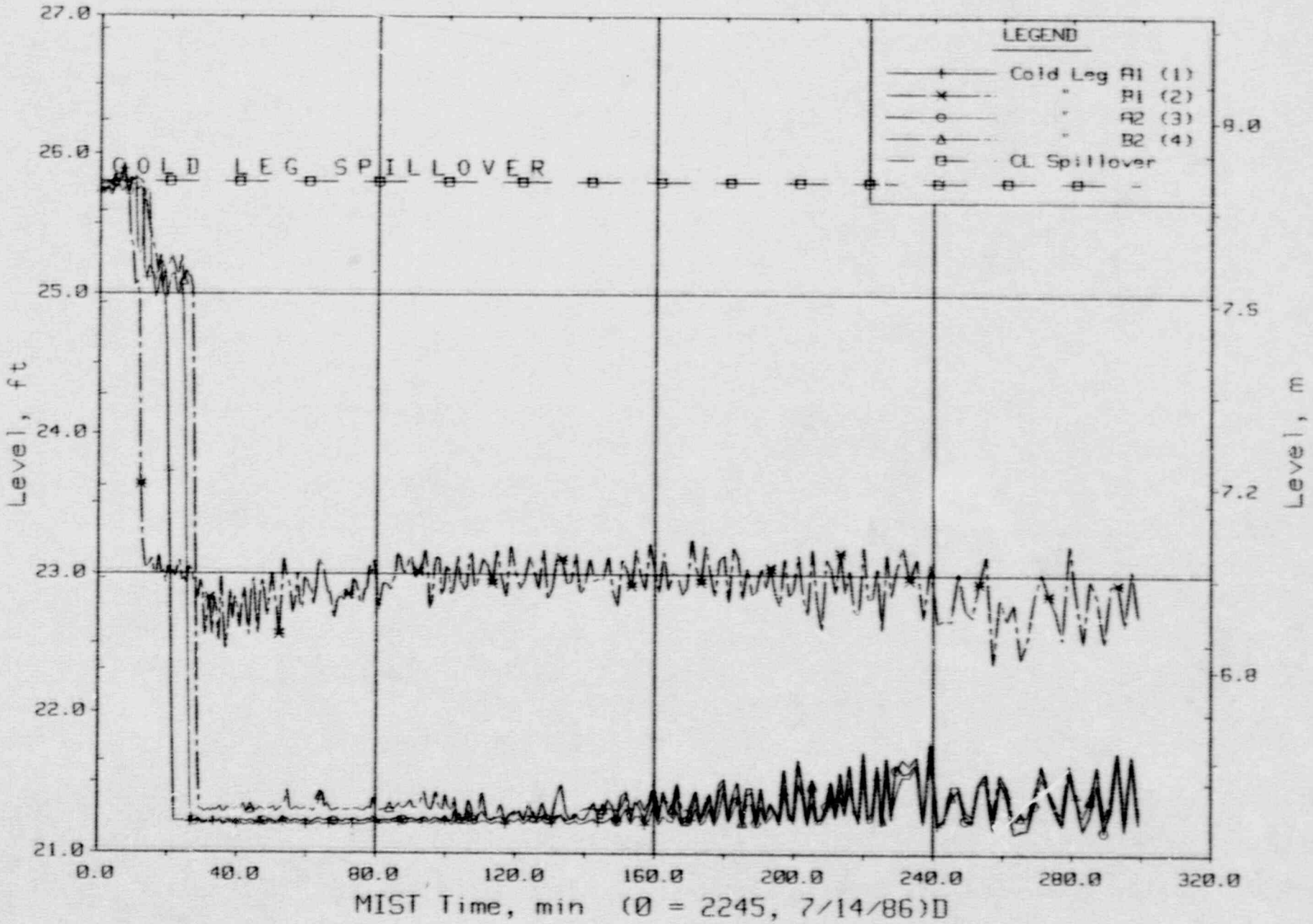

Cold Leg Discharge Collapsed Liquid Levels (CnLV23s).

Thu Jun 9 17:09:05 1988

CLLV5

FINAL DATA

T320604: Group 32 SBLOCA Test 6, Reduced-Capacity HPI.

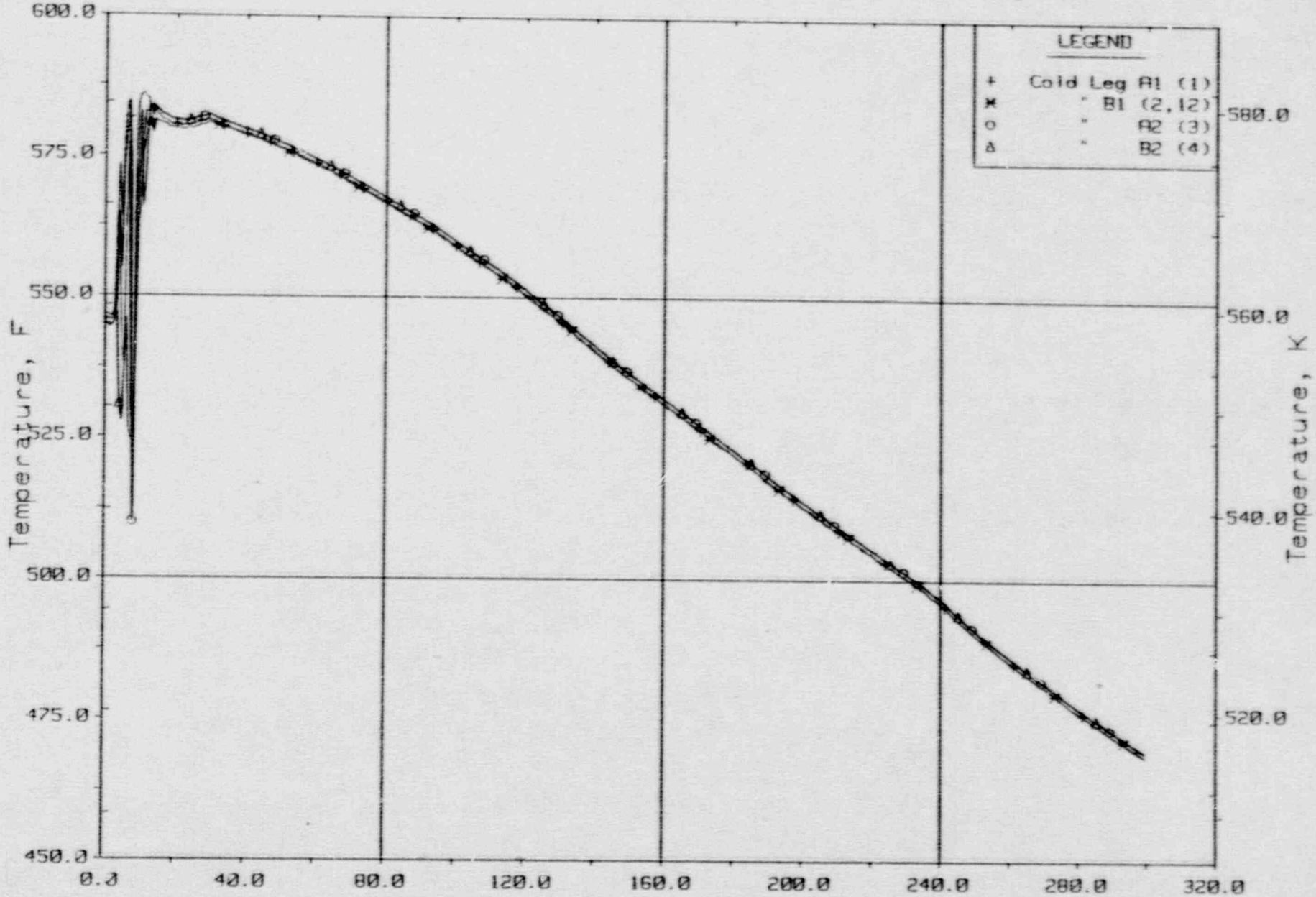

Cold Leg Nozzle Fluid Temperatures, Top of Rake (21.3ft, CnTC11s).

Thu Jun 9 17:13:34 1988

CLTC1

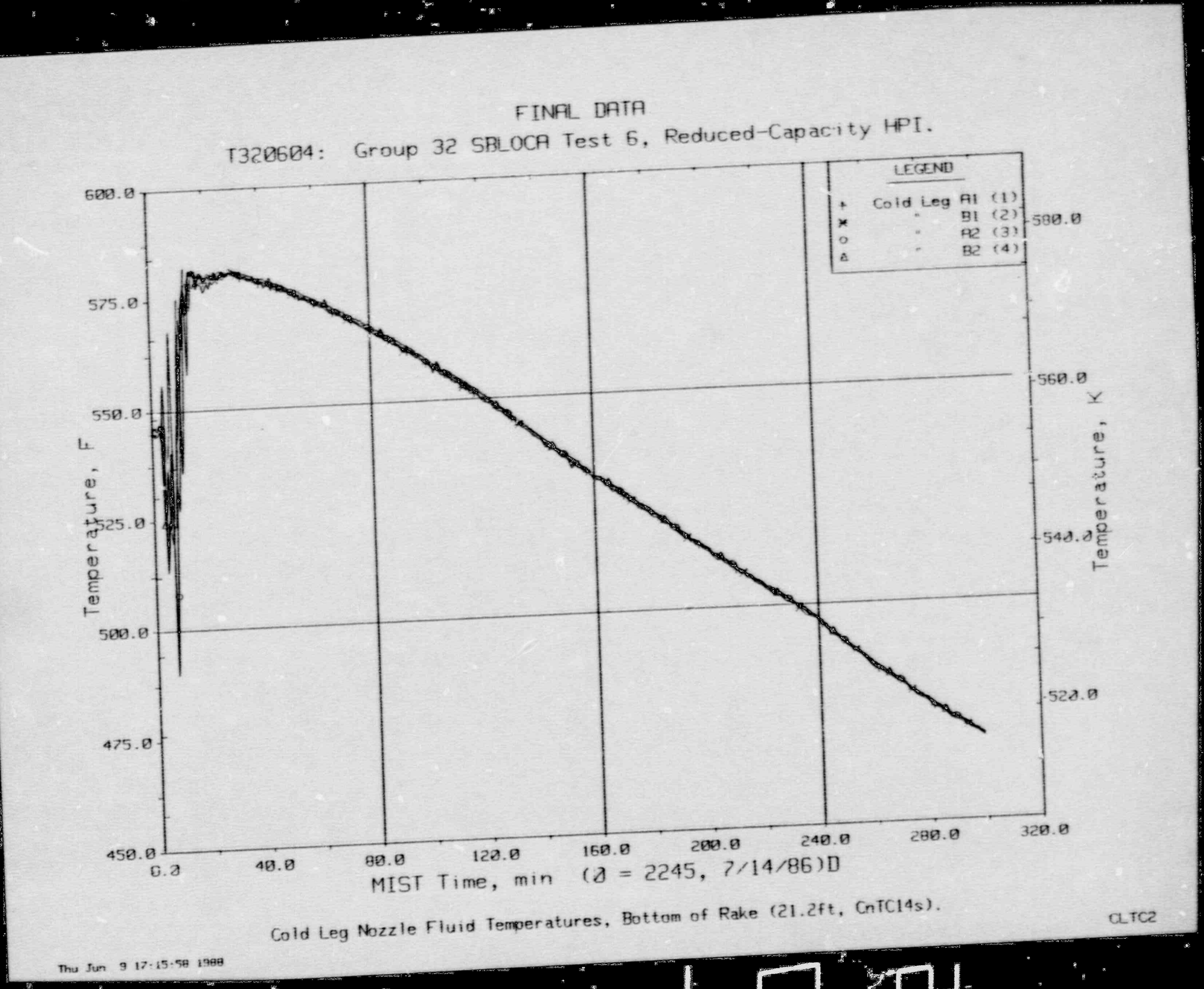
FINAL DATA
T320604: Group 32 SBLOCA Test 6, Reduced-Capacity HPI.
LEGEND
+ Cold Leg A1 (1)
× " B1 (2)
○ " A2 (3)
△ " B2 (4)
600.0
575.0
550.0
525.0
500.0
475.0
450.0
Temperature, F
580.0
560.0
540.0
520.0
Temperature, K
0.0
40.0
80.0
120.0
160.0
200.0
240.0
280.0
320.0
MIST Time, min (Ø = 2245, 7/14/86)D
Cold Leg Nozzle Fluid Temperatures, Bottom of Rake (21.2ft, CnTC14s).
CLTC2
Thu Jun 9 17:15:58 1988

FINAL DATA

T320604: Group 32 SBLOCA Test 6, Reduced-Capacity HPI.

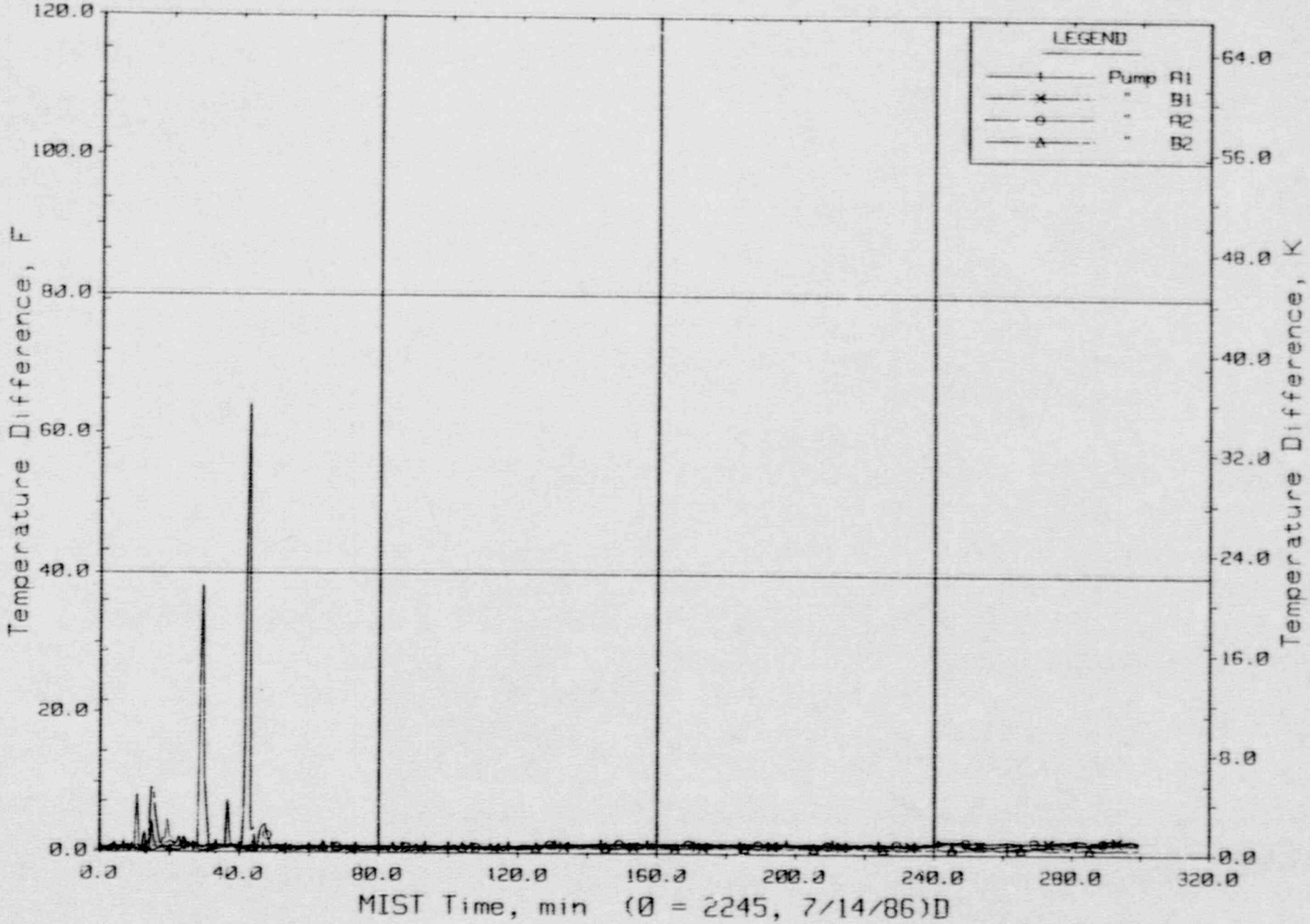

Maximum Differences Among RCP Rake Fluid Temperatures.

Thu Jun 9 17:18:38 1988

CLTD1

FINAL DATA

T320604: Group 32 SBLOCA Test 6, Reduced-Capacity HPI.

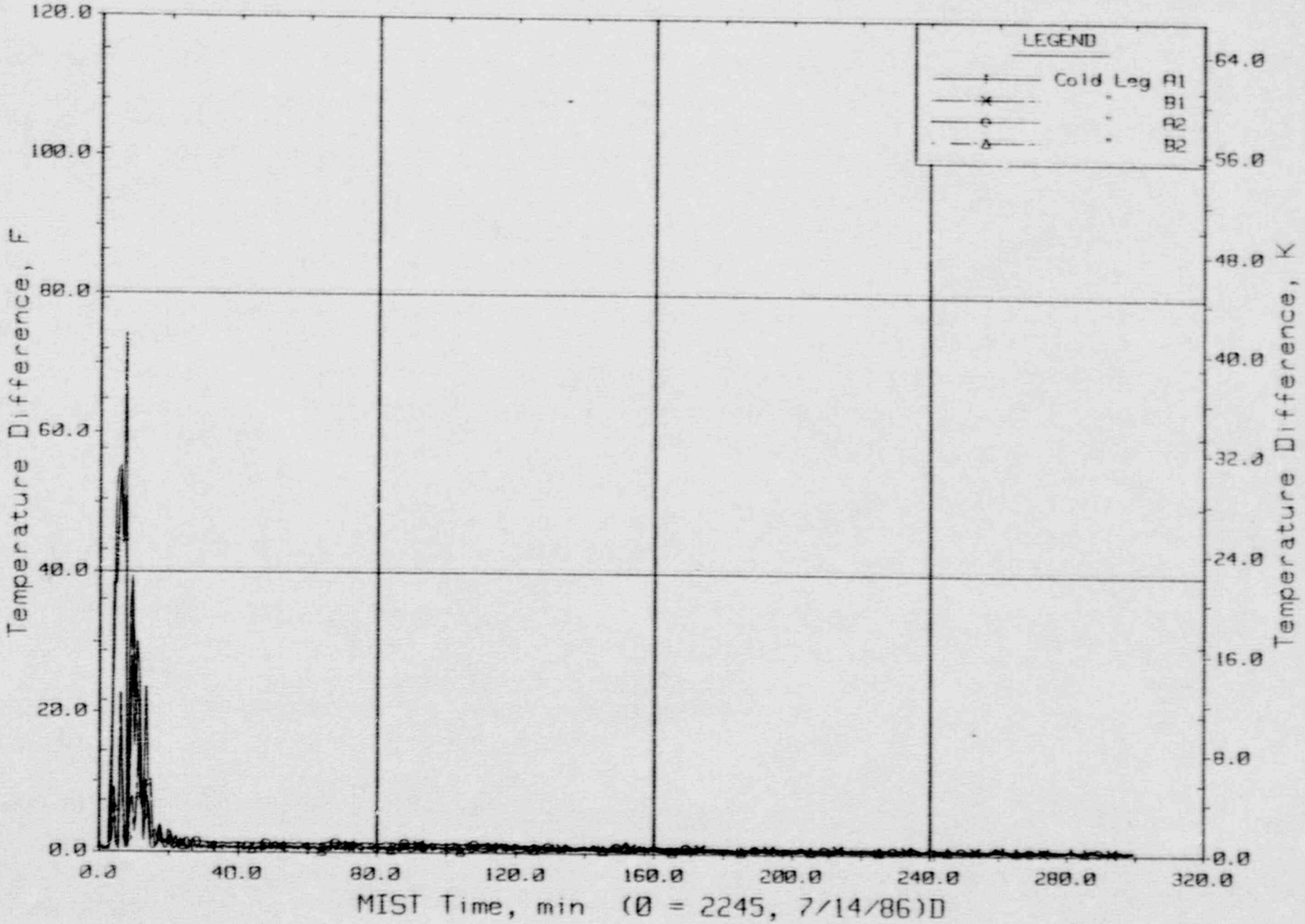

Maximum Differences Among CL Nozzle Rake Fluid Temperatures.

Thu Jun 9 17:21:22 1988

CLTD2

FINAL DATA

T320604: Group 32 SBLOCA Test 6, Reduced-Capacity HPI.

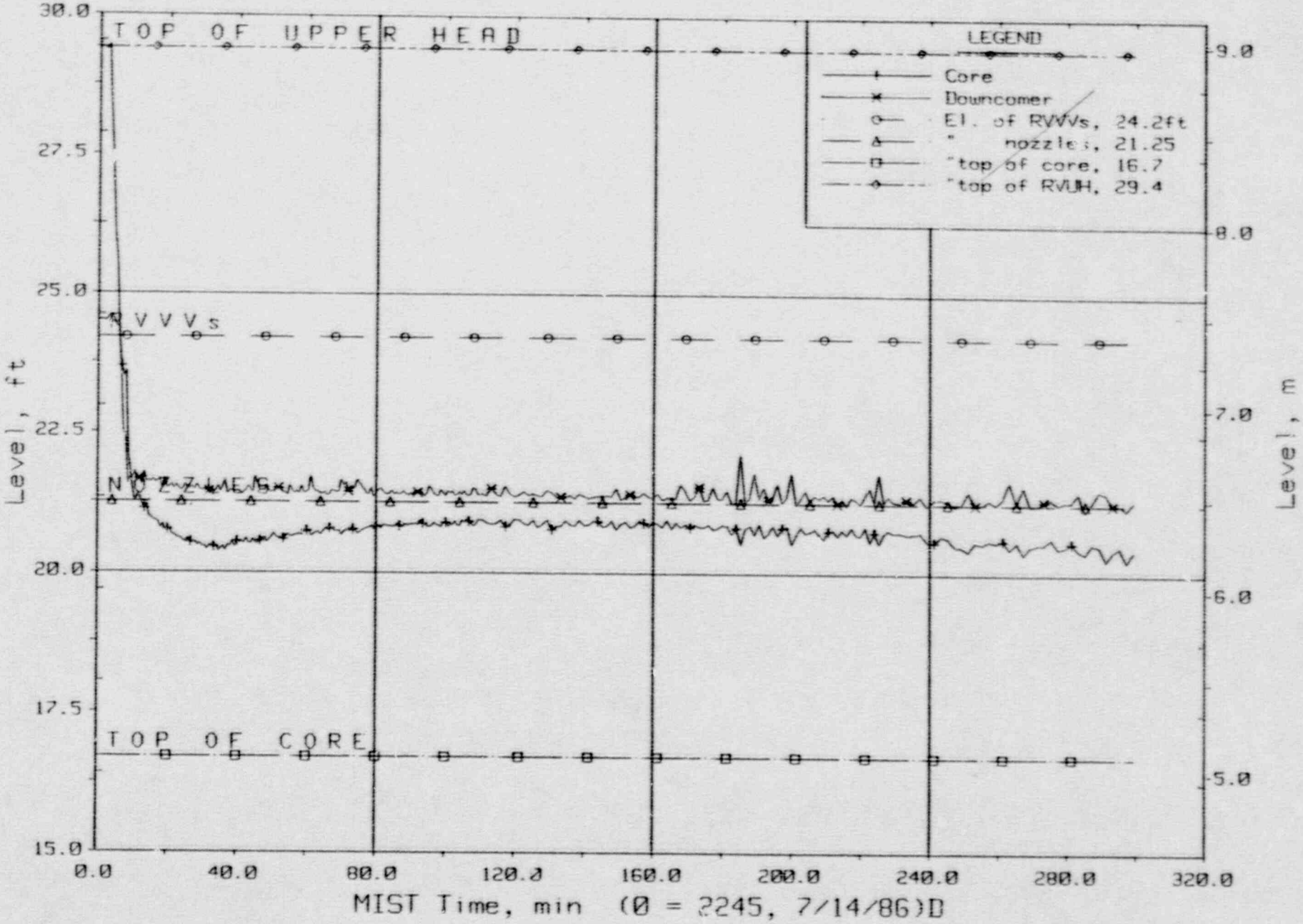

Core Region Collapsed Liquid Levels.

Thu Jun 9 17:24:38 1988

COLV1

FINAL DATA

T320604: Group 32 SBLOCA Test 6, Reduced-Capacity HPI.

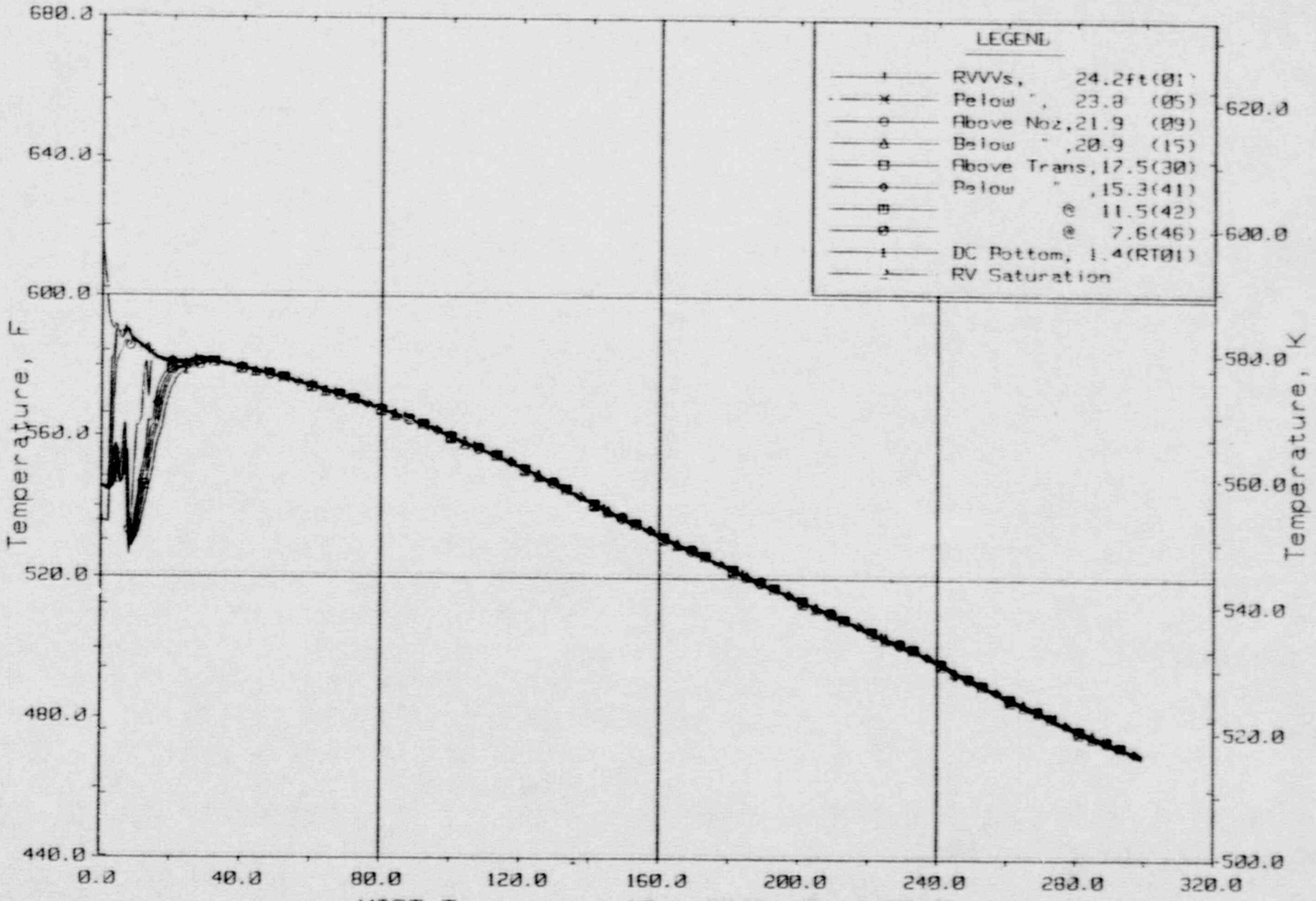

Downcomer Quadrant A1 Fluid Temperatures (DCTCs).

Thu Jun 9 17:33:28 1988

DCTC6

FINAL DATA

T320604: Group 32 SBLOCA Test 6, Reduced-Capacity HPI.

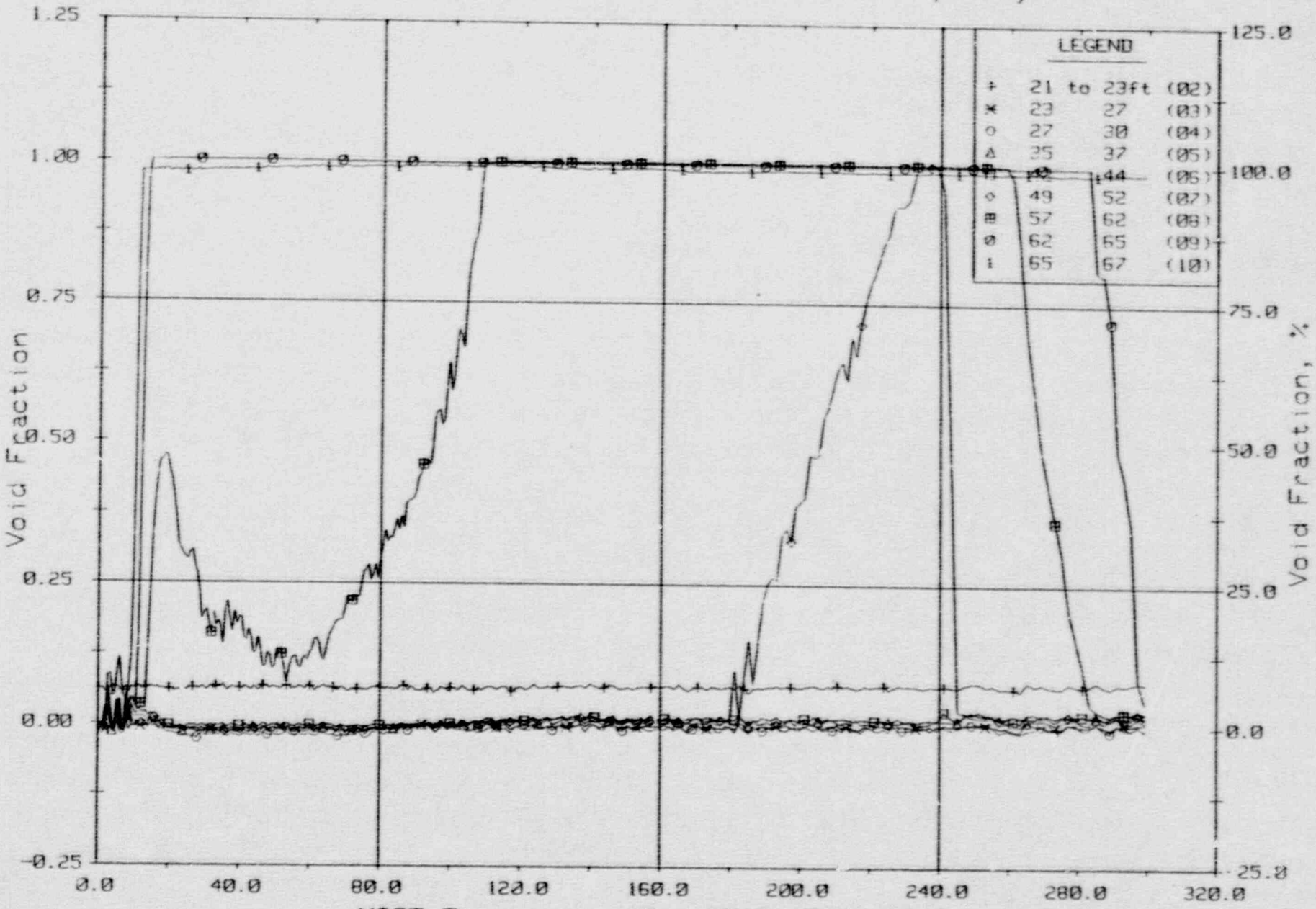

Hot Leg A Riser Void Fractions From Differential Pressures (HIVFs).

Thu Jun 9 17:37:02 1988

HIVF1

FINAL DATA

T320604: Group 32 SBLOCA Test 6, Reduced-Capacity HPI.

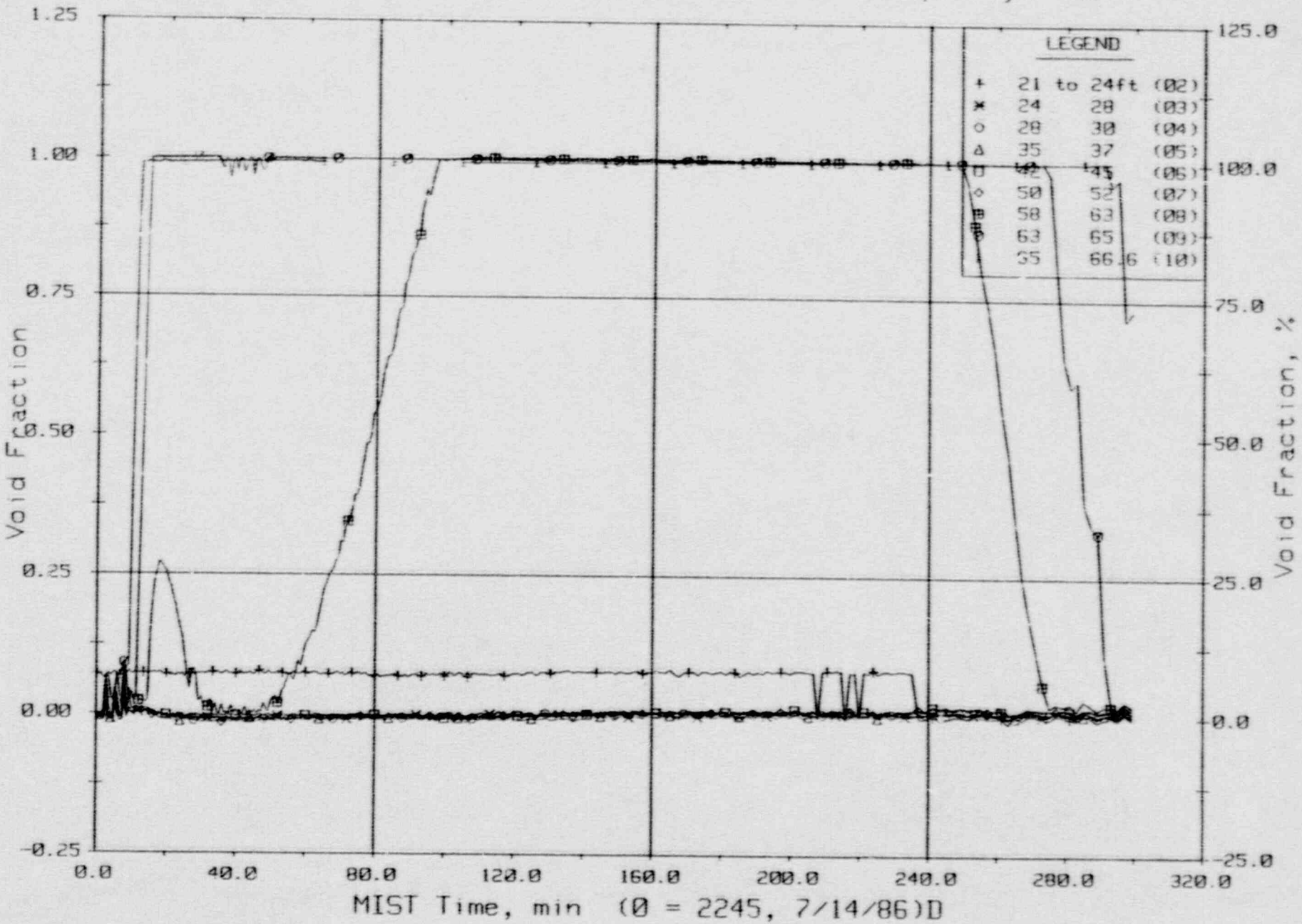

Hot Leg B Riser Void Fraction From Differential Pressures (H2VFs).

thu Jun 9 17:48:21 1988

H2VF1

FINAL DATA

T320604: Group 32 SBLOCA Test 6, Reduced-Capacity HPI.

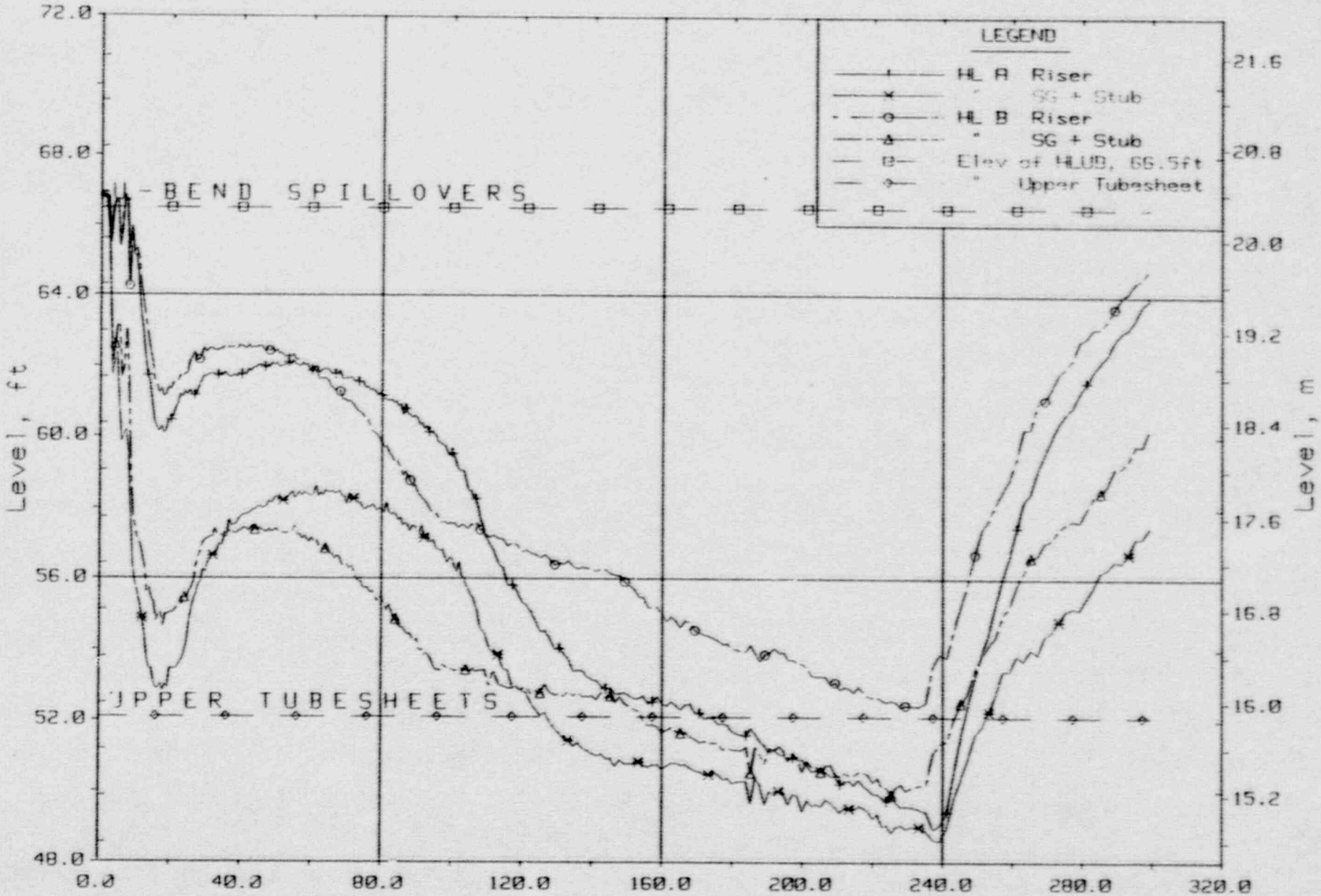

Hot Leg Riser and Stub Collapsed Liquid Levels.

Thu Jun 9 17:43:36 1988

HLLV1

FINAL DATA

T320604: Group 32 SBLOCA Test 6, Reduced-Capacity HPI.

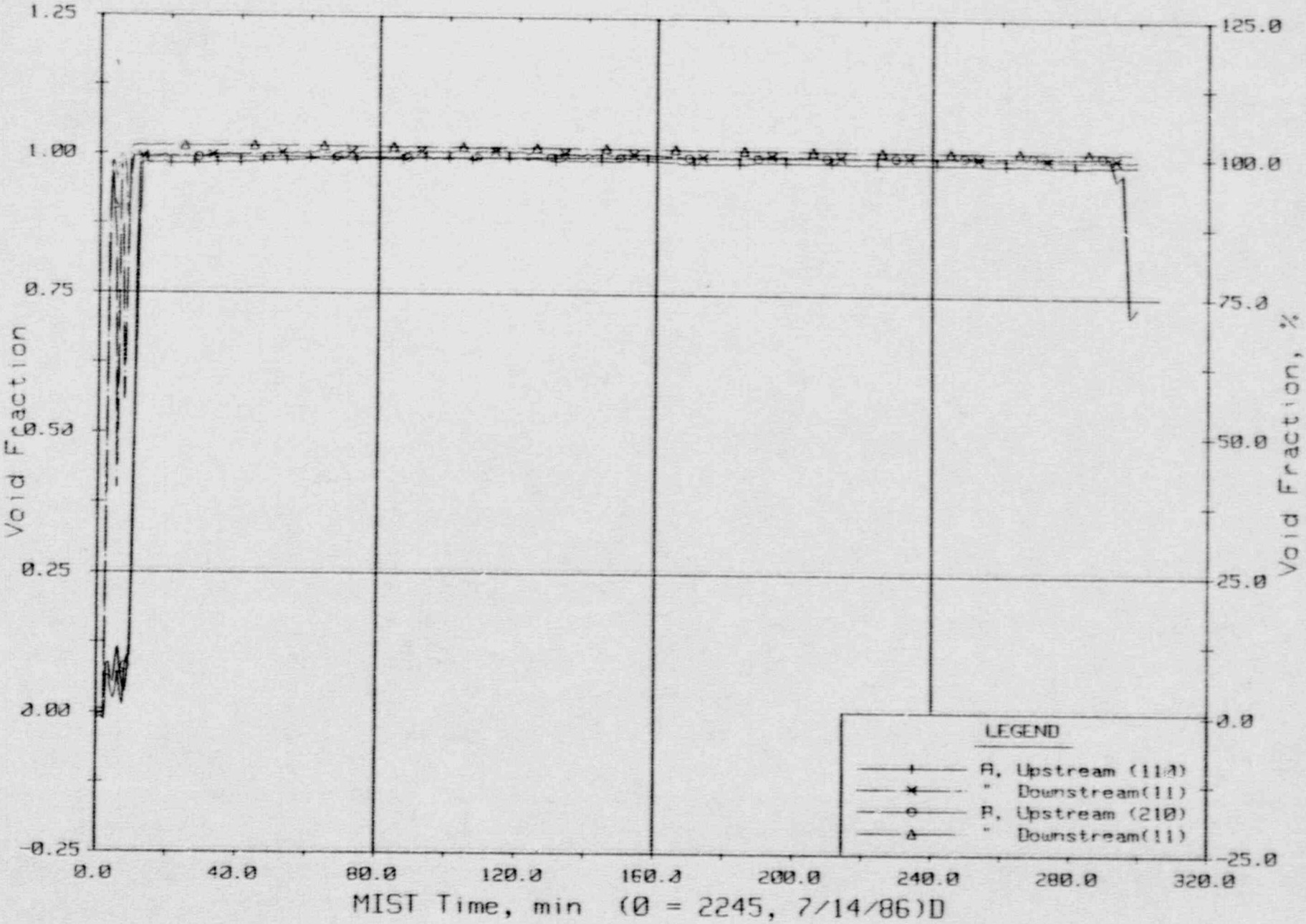

Hot Leg U-Bend Void Fractions From Diffl. Pressures (64.8 to 66.6 ft, HnVFs).

Thu Jun 9 17:46:28 1988

HLVF1

FINAL DATA

T320604: Group 32 SBLOCA Test 6, Reduced-Capacity HPI.

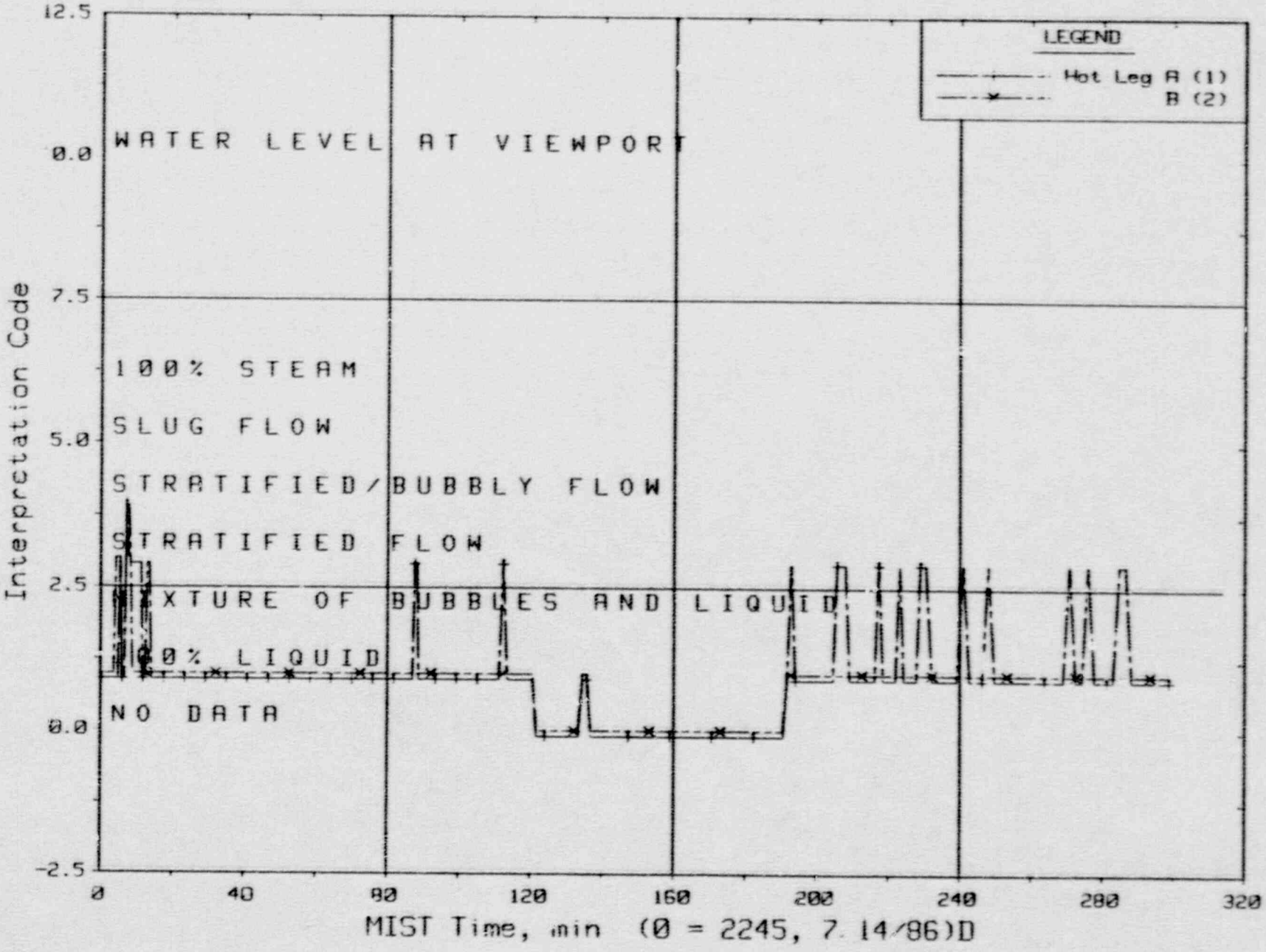

Hot Leg Horizontal Viewport Indications (HnMS01s).

Fri Oct 28 17:00:07 1988

HLVP2

FINAL DATA

T320604: Group 32 SBLOCA Test 6, Reduced-Capacity HPI.

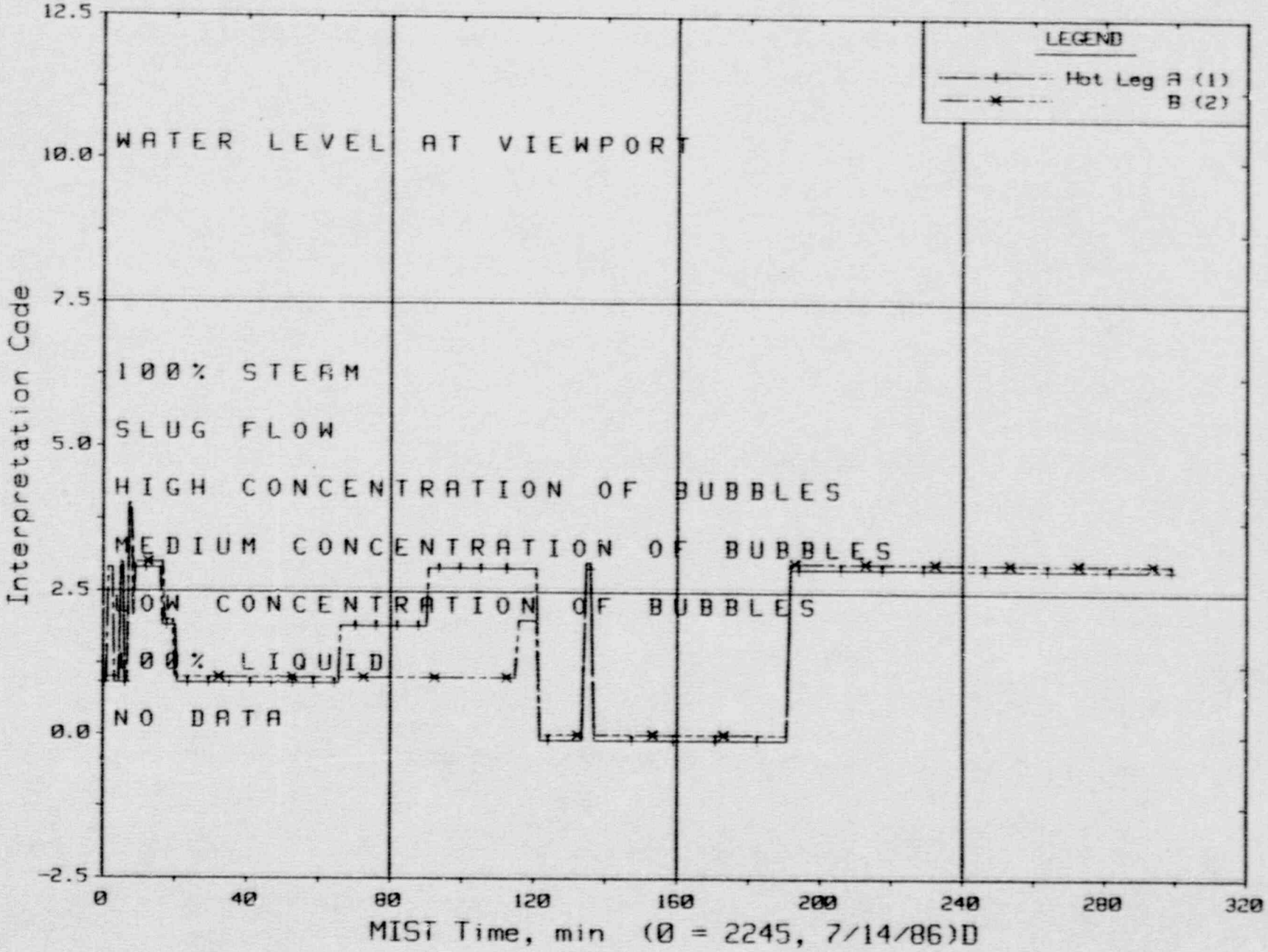

Hot Leg Riser Viewport Indications (HnMS02s).

Fri Oct 28 17:03:33 1988

HLVP3

FINAL DATA

T320604: Group 32 SBLOCA Test 6, Reduced-Capacity HPI.

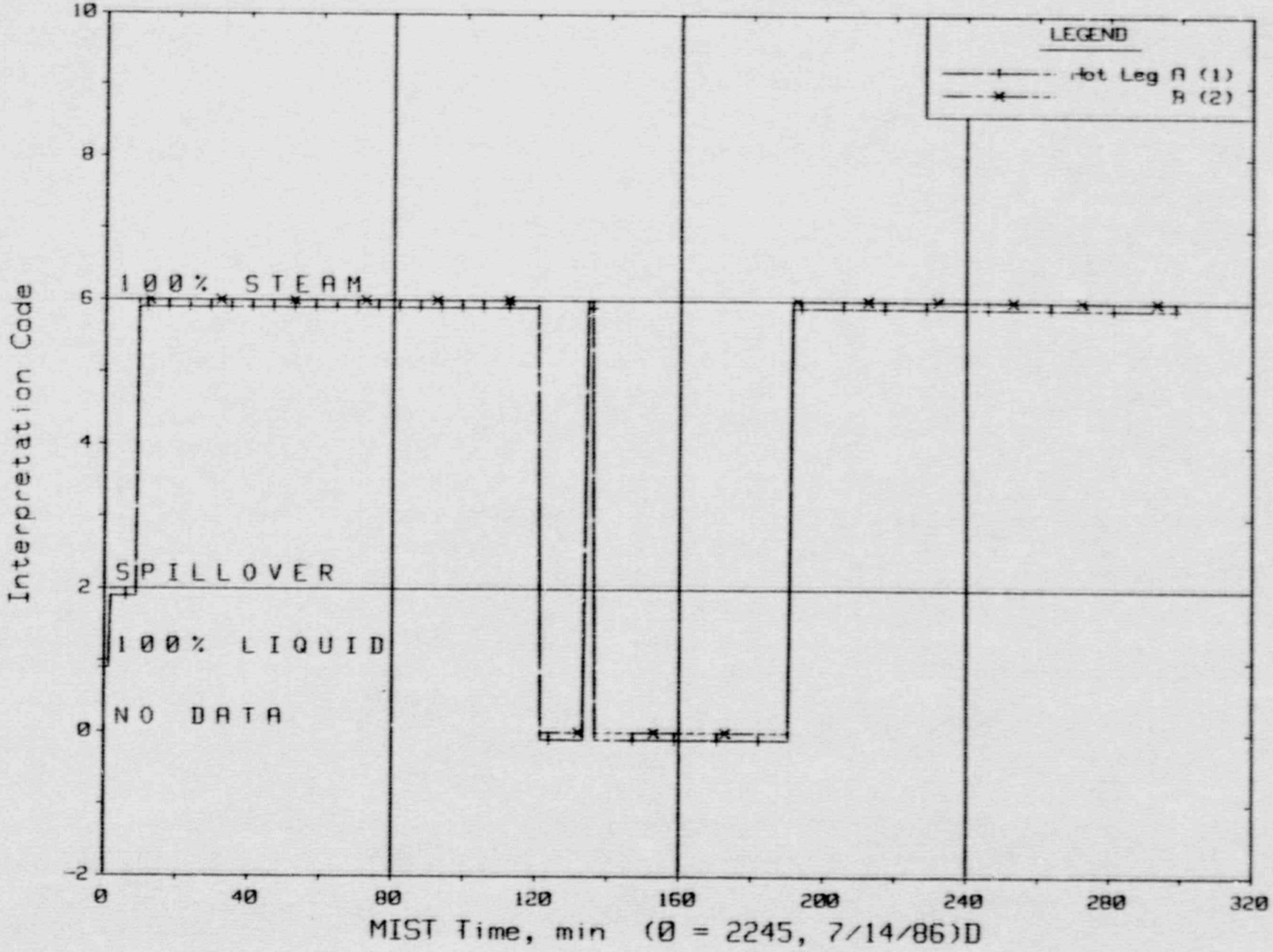

Hot Leg U-Bend Viewport Indications (HnMS03s).

Fri Oct 28 17:07:05 1988

HLVP4

FINAL DATA

T320604: Group 32 SBLOCA Test 6, Reduced-Capacity HPI.

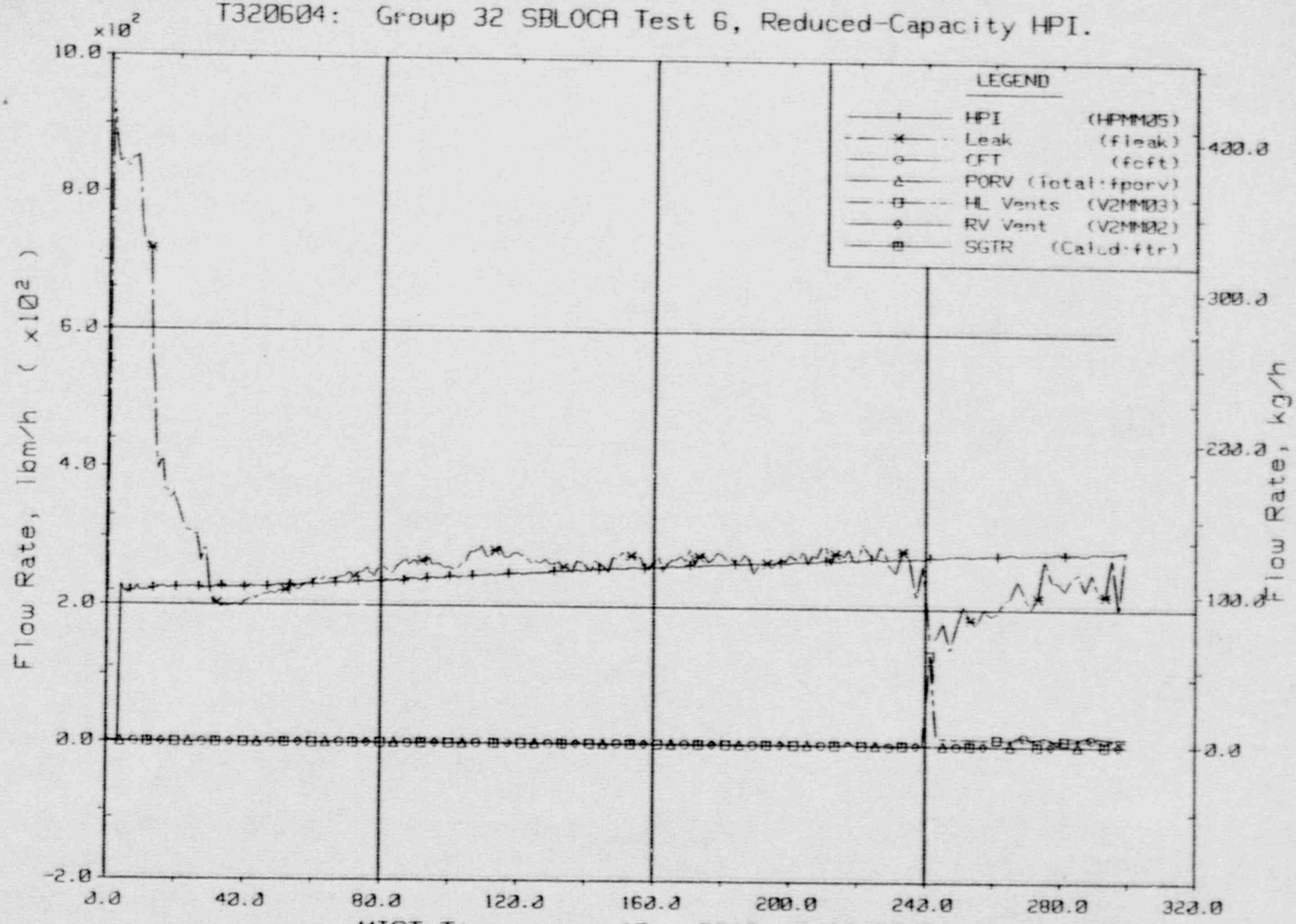

Primary System Boundary Flow Rates.

Thu Jun 9 17:49:52 1988

PBFL3

FINAL DATA

T320604: Group 32 SBLOCA Test 6, Reduced-Capacity HPI.

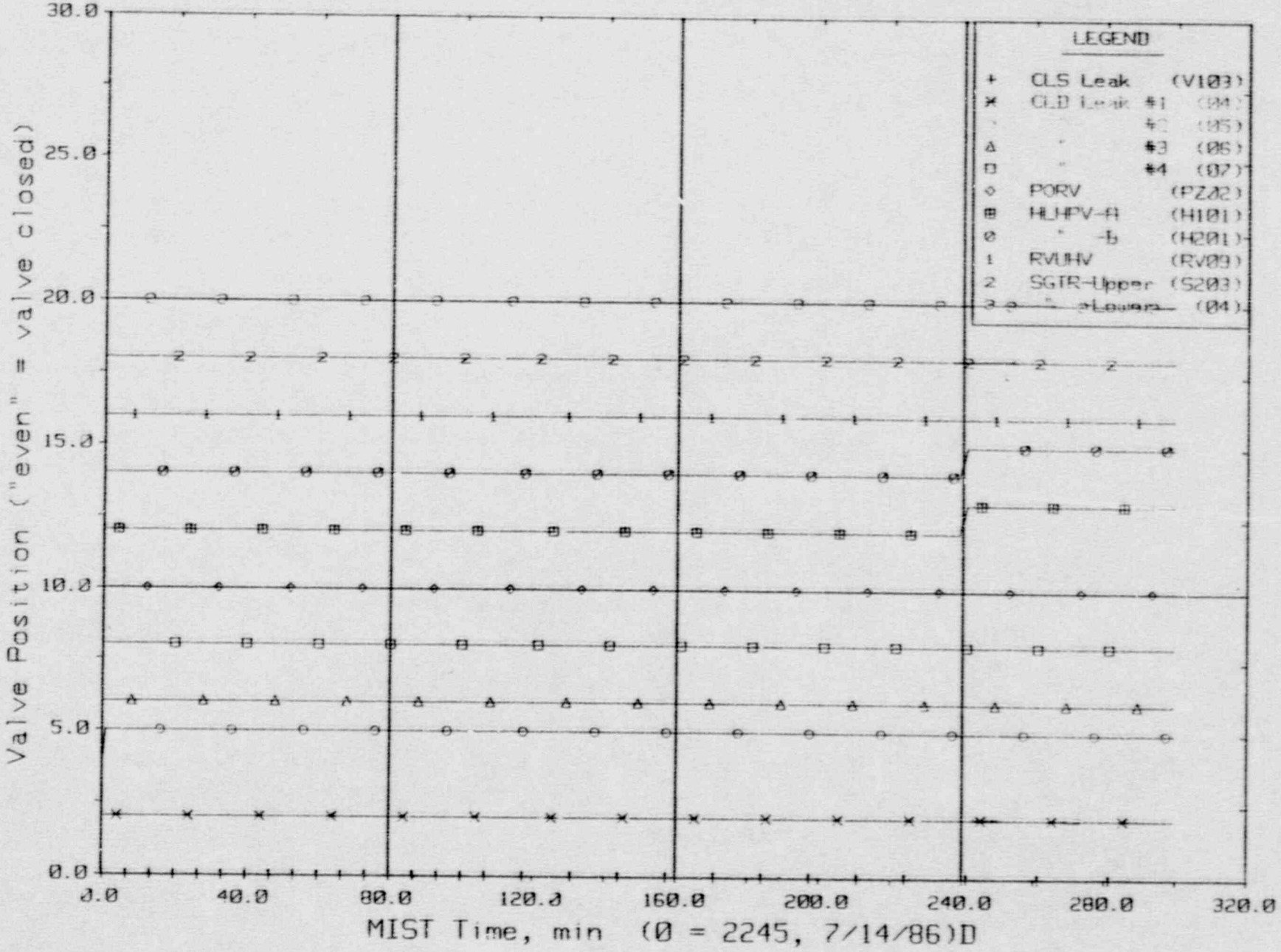

Primary System Discharge Limit Switch Indications (LSs).

Thu Jun 9 17:53:29 1988

PBLS1

FINAL DATA

T320604: Group 32 SBLOCA Test 6, Reduced-Capacity HPI.

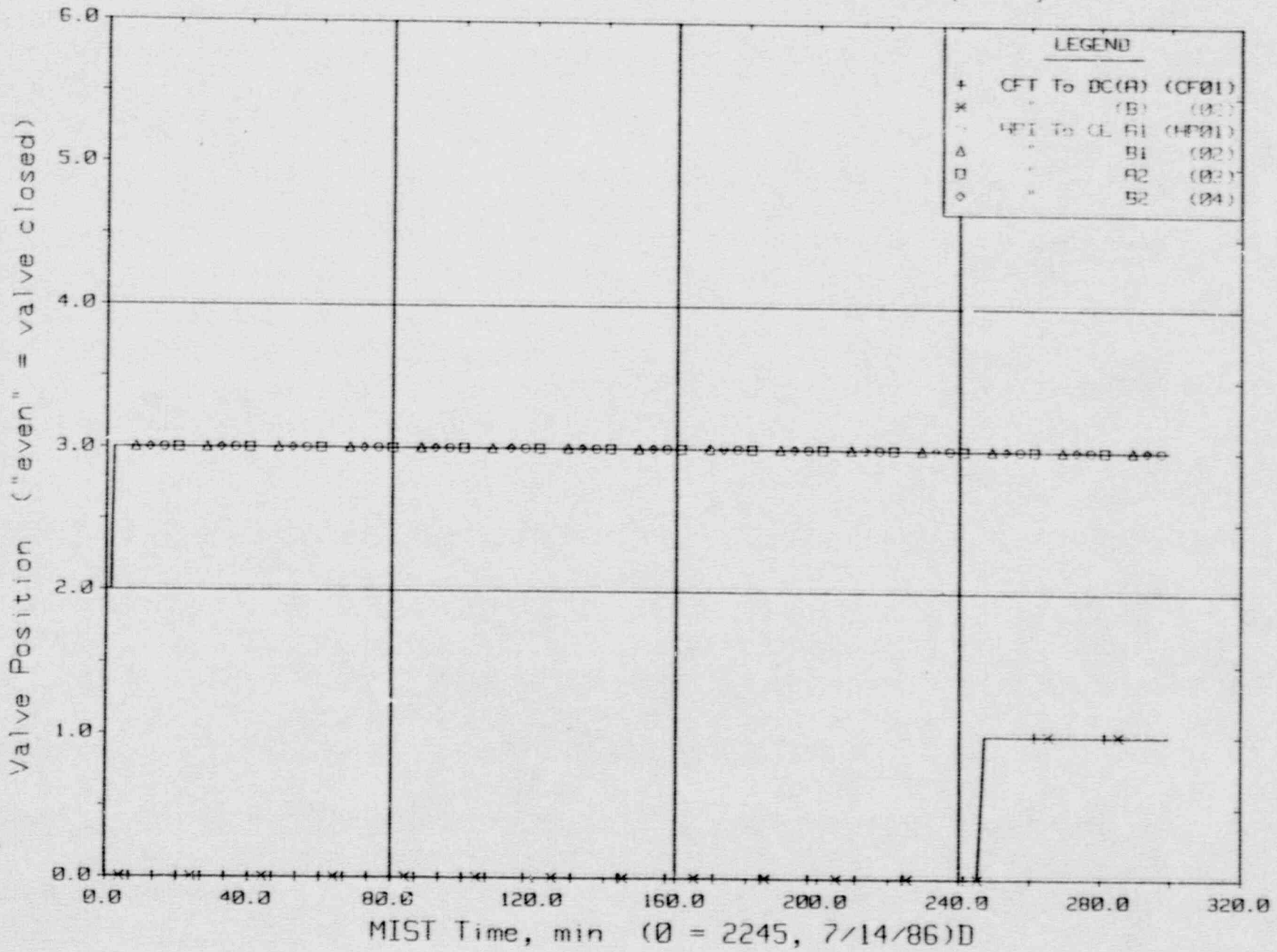

Primary System Injection Limit Switch Indications (LSs).

Thu Jun 9 17:56:14 1988

PBLS2

FINAL DATA

T320604: Group 32 SBLOCA Test 6, Reduced-Capacity HPI.

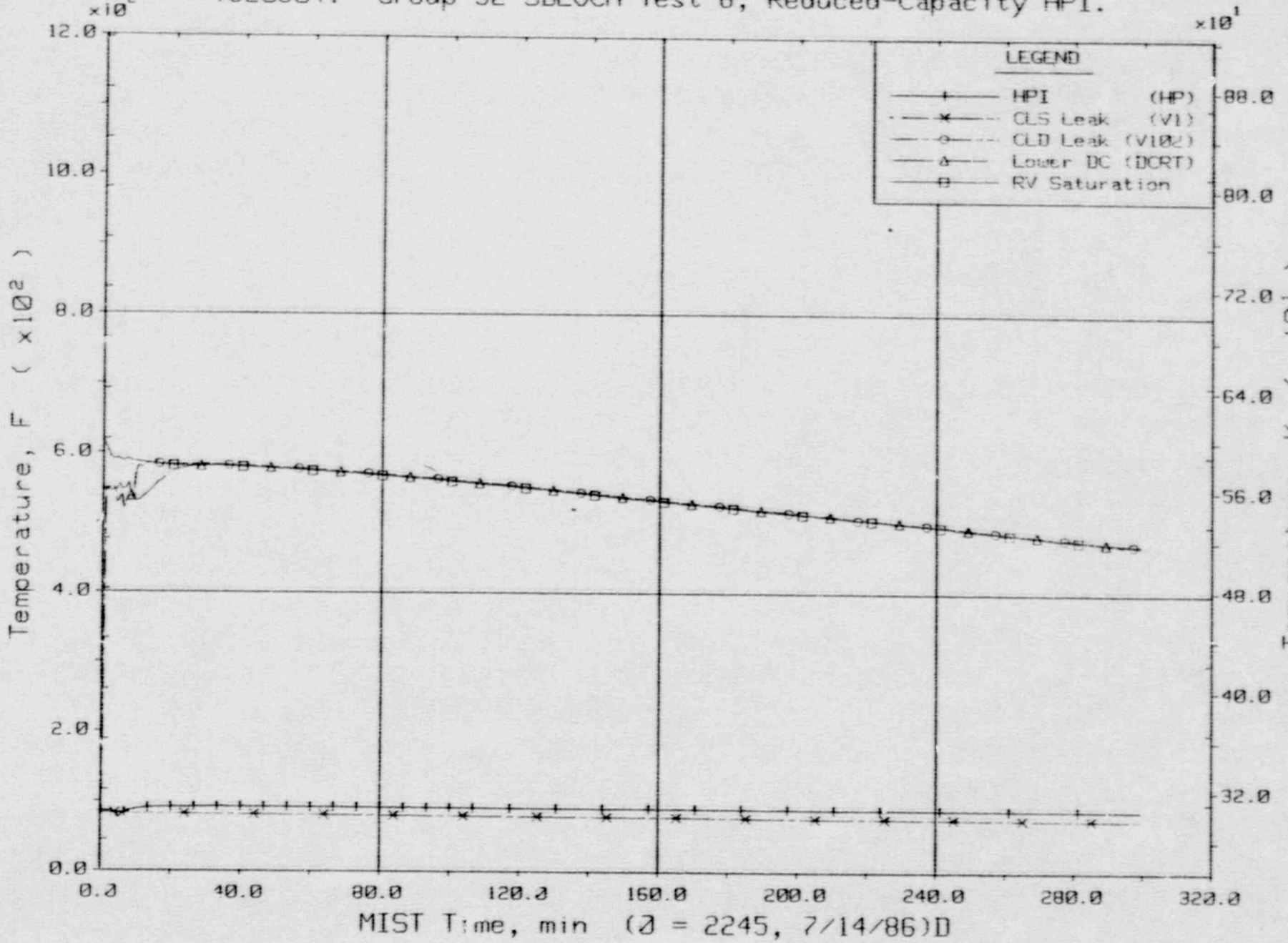

Single-Phase Discharge and HPI Fluid Temperatures (TC0ls).

Thu Jun 9 17:58:52 1988

PBTCip

FINAL DATA

T320604: Group 32 SBLOCA Test 6, Reduced-Capacity HPI.

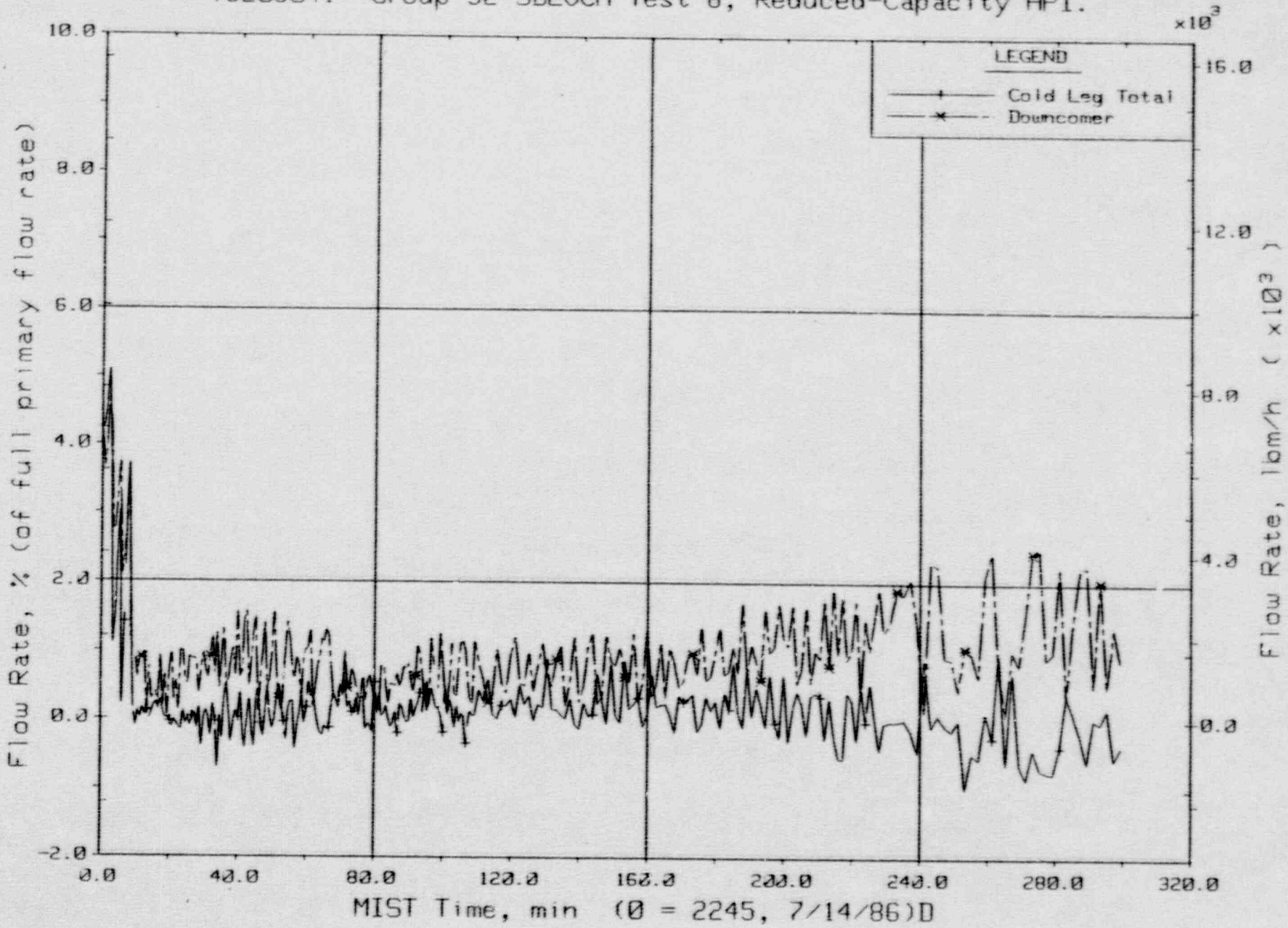

Primary System Venturi Flow Rates.

Thu Jun 9 18:01:07 1988

PRFL7

FINAL DATA

T320604: Group 32 SBLOCA Test 6, Reduced-Capacity HPI.

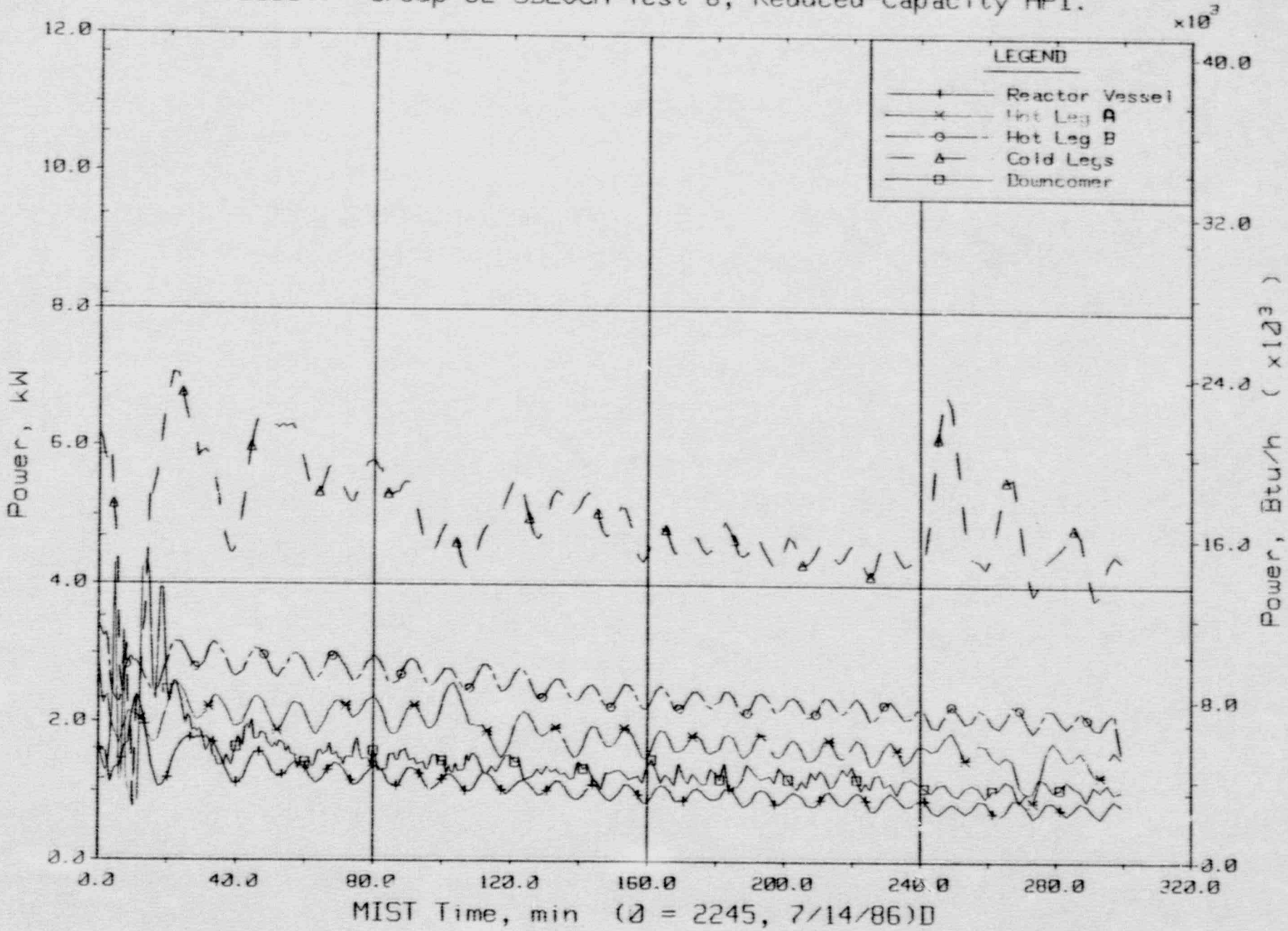

Guard Heater Specified Power Per Primary Component.

Thu Jun 9 18:04:08 1988

PRGQ1

FINAL DATA

T320604: Group 32 SBLOCA Test 6, Reduced-Capacity HPI.

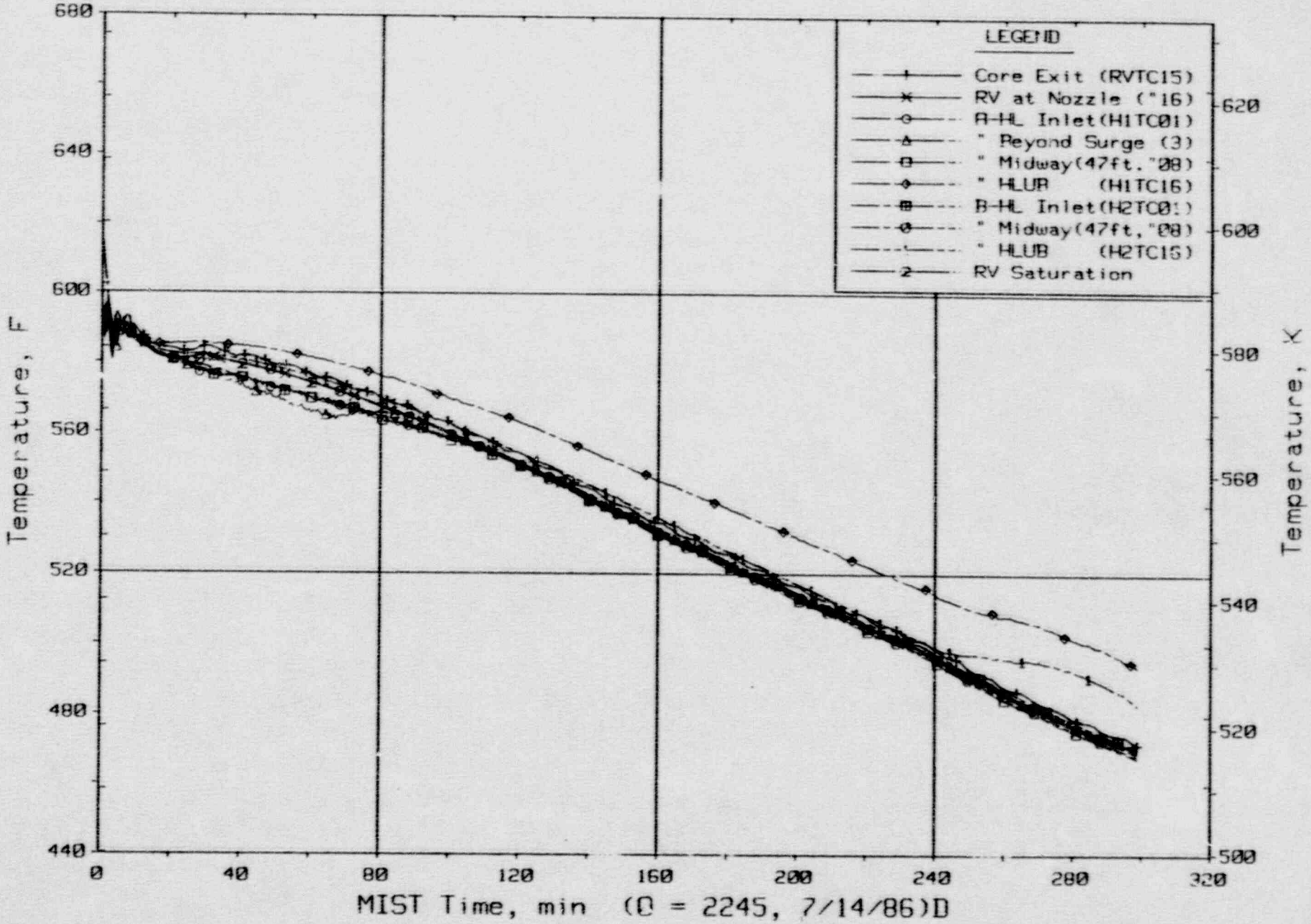

Composite Core Exit and Hot Leg Fluid Temperatures.

Fri Oct 28 16:37:34 1988

PRKT1

FINAL DATA

T320604: Group 32 SBLOCA Test 6, Reduced-Capacity HPI.

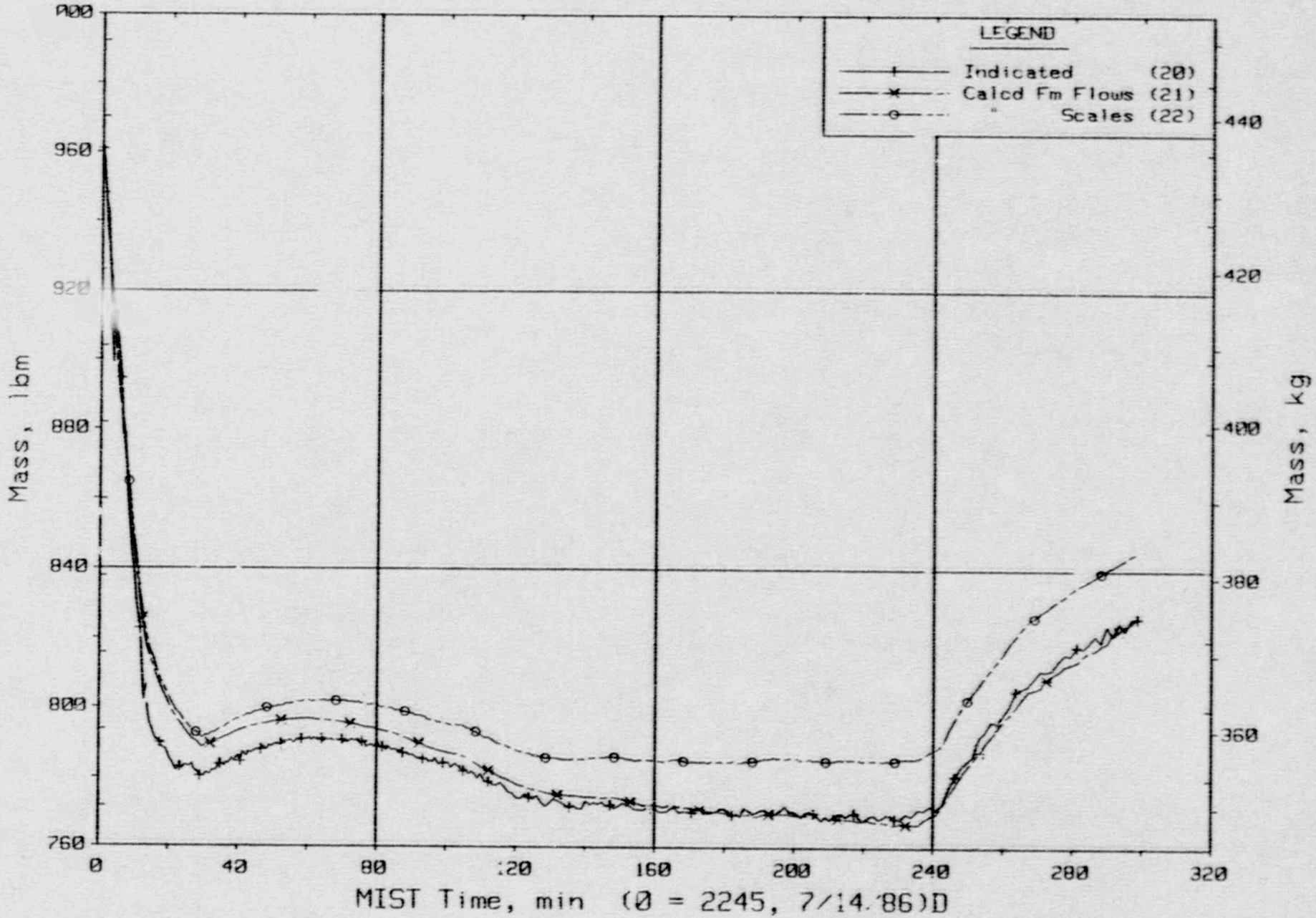

Primary System Total Fluid Mass (PLMLs).

Fri Oct 28 16:11:11 1988

PRML2

FINAL DATA

T32Ø6Ø4: Group 32 SBLOCA Test 6, Reduced-Capacity HPI.

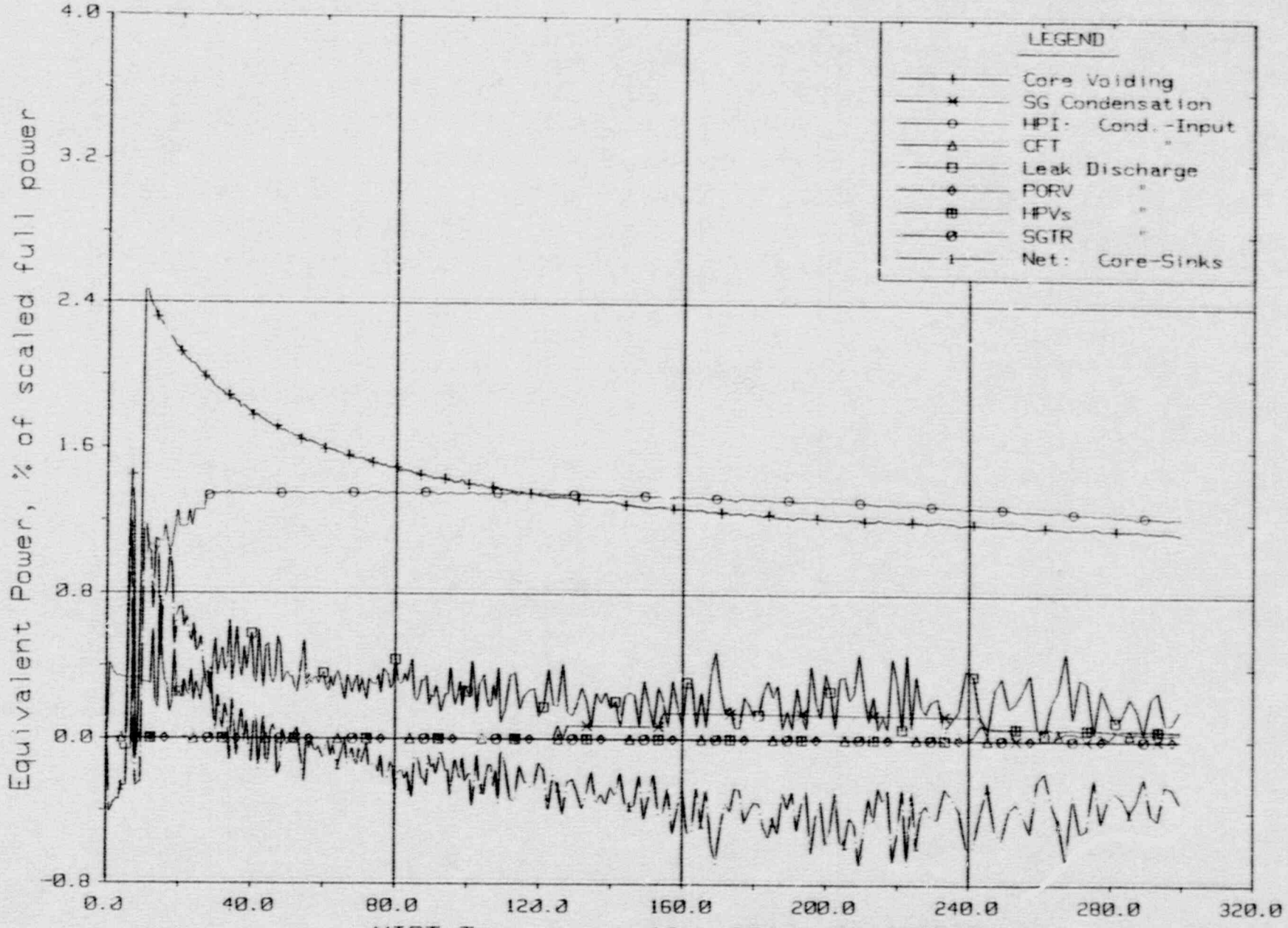

Primary Fluid Volume Changes By Components.

Fri Jun 10 08:54:11 1988

PRPA0

FINAL DATA

T320604: Group 32 SBLOCA Test 6, Reduced-Capacity HPI.

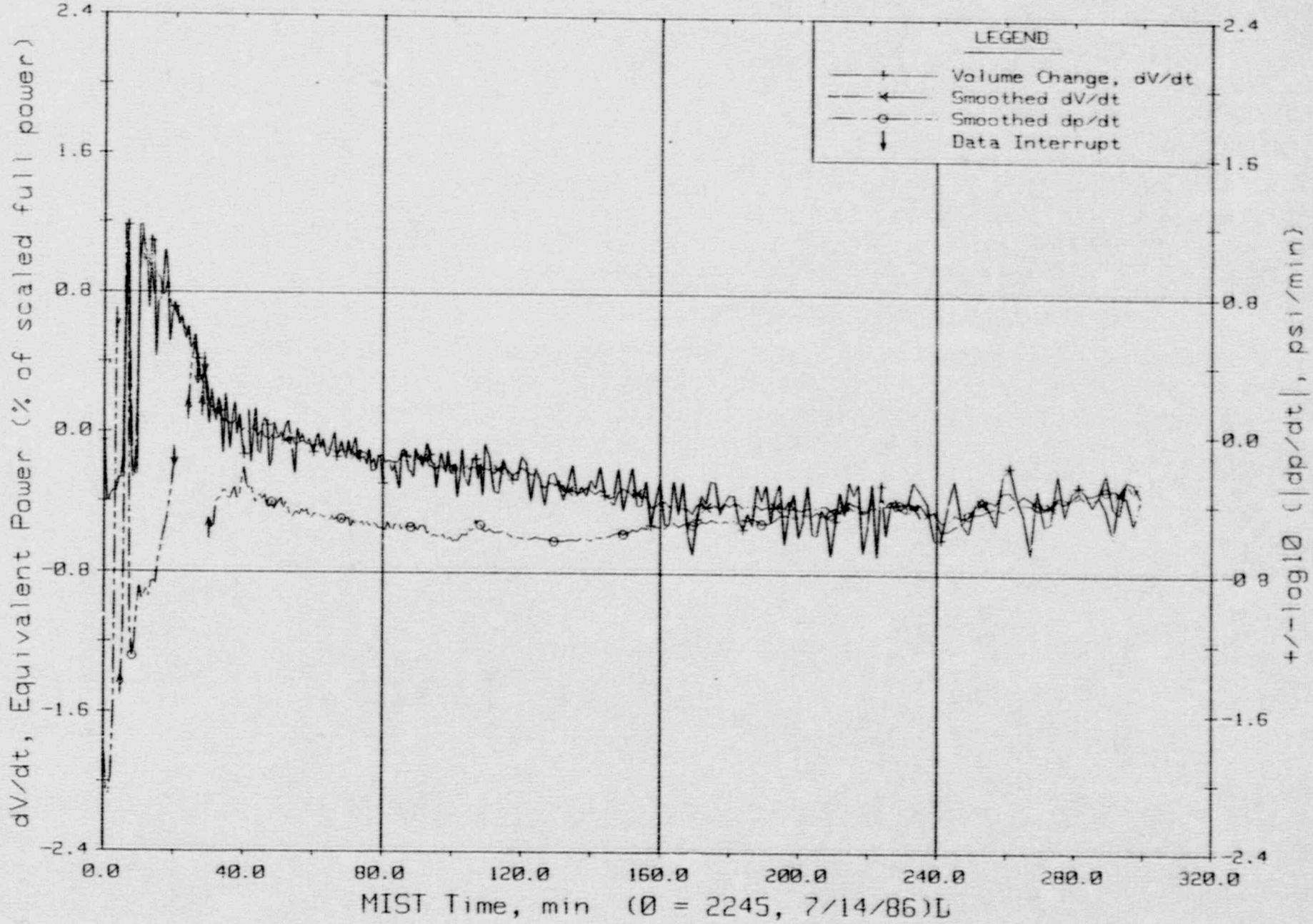

Primary Fluid Volume and Pressure Changes, dV/dt and dp/dt.

Fri Jun 10 08:57:21 1988

PRPA2

FINAL DATA

T320604: Group 32 SBLOCA Test 6, Reduced-Capacity HPI.

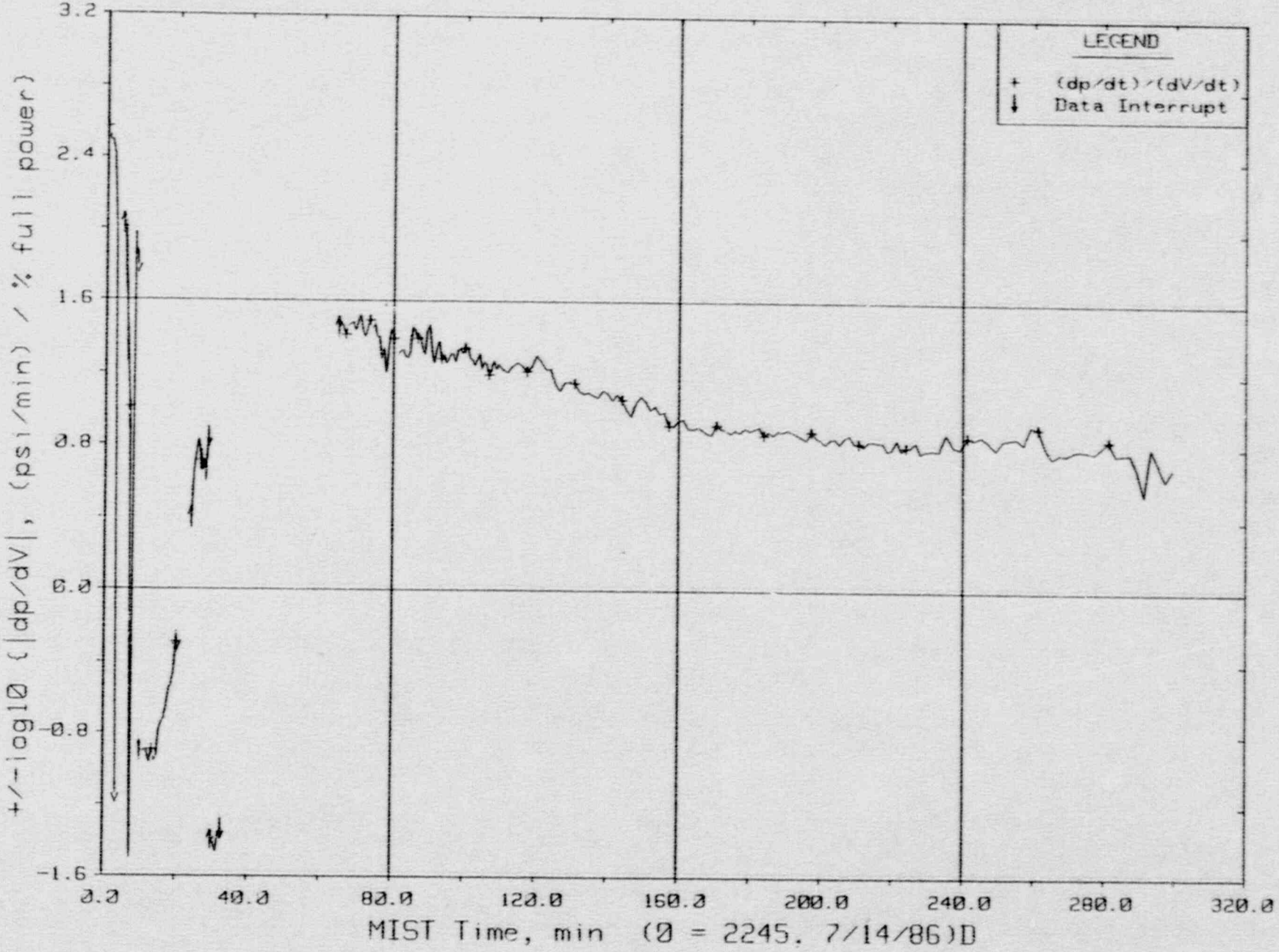

Primary System Response: dp/dt divided by dV/dt.

Thu Jun 9 18:19:32 1988

PRPA3

FINAL DATA

T320604: Group 32 SBLOCA Test 6, Reduced-Capacity HPI.

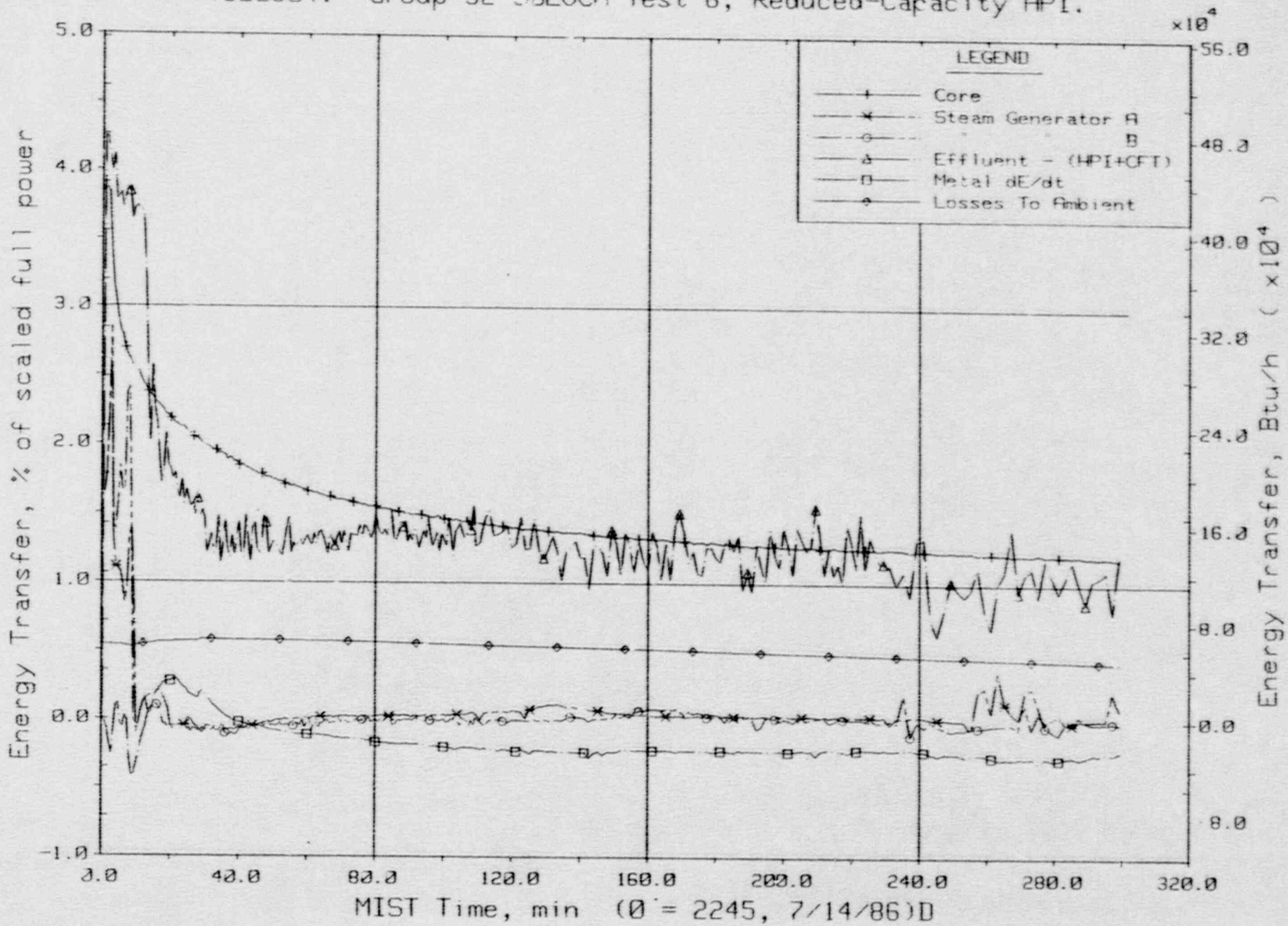

Primary System Energy Transfer.

Thu Jun 9 18:22:00 1988

PROE2

FINAL DATA

T320604: Group 32 SBLOCA Test 6, Reduced-Capacity HPI.

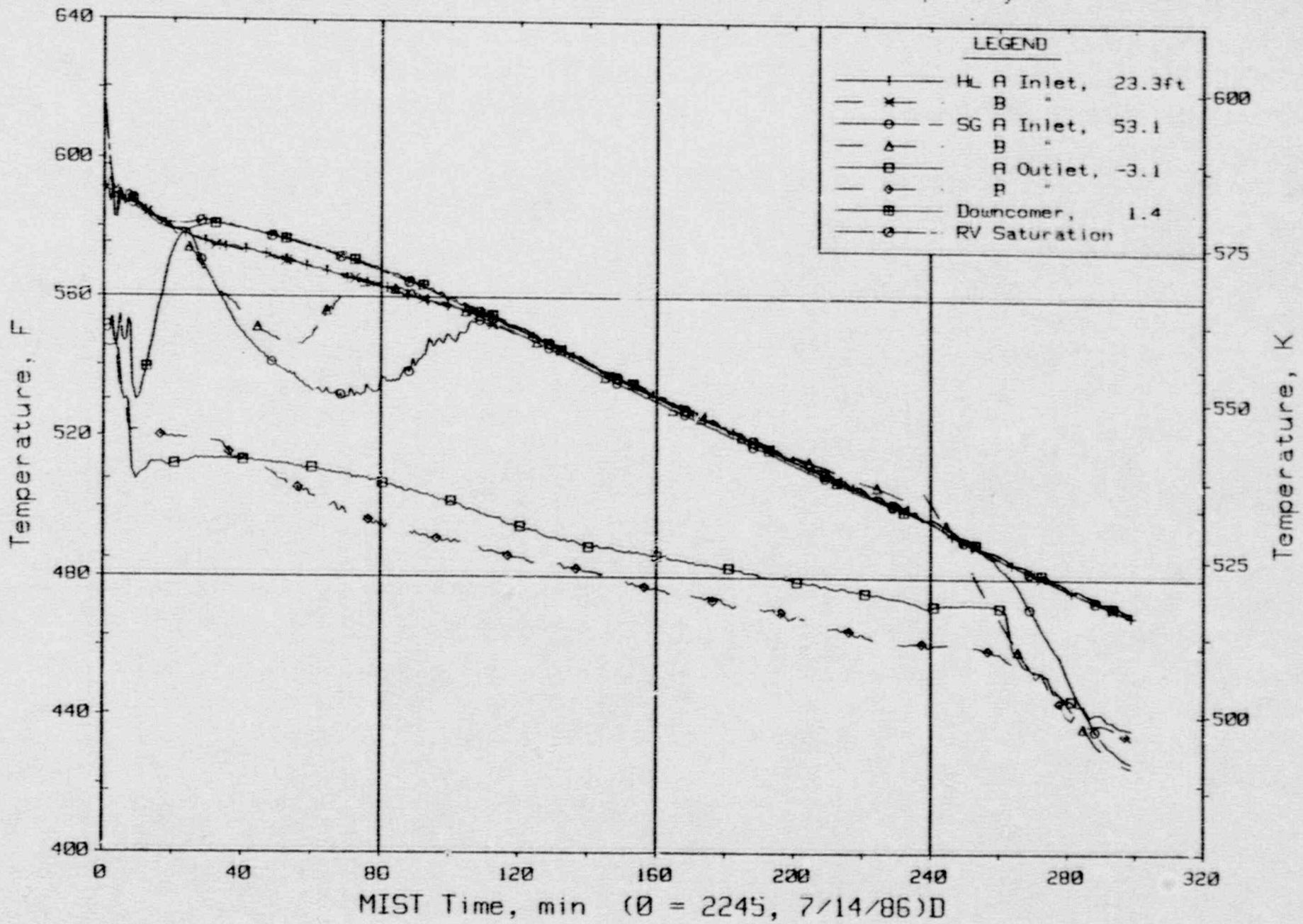

Primary System Fluid Temperatures (RTDs).

Fri Oct 28 16:14:59 1988

PRRT0

FINAL DATA

T320604: Group 32 SBLOCA Test 6, Reduced-Capacity HPI.

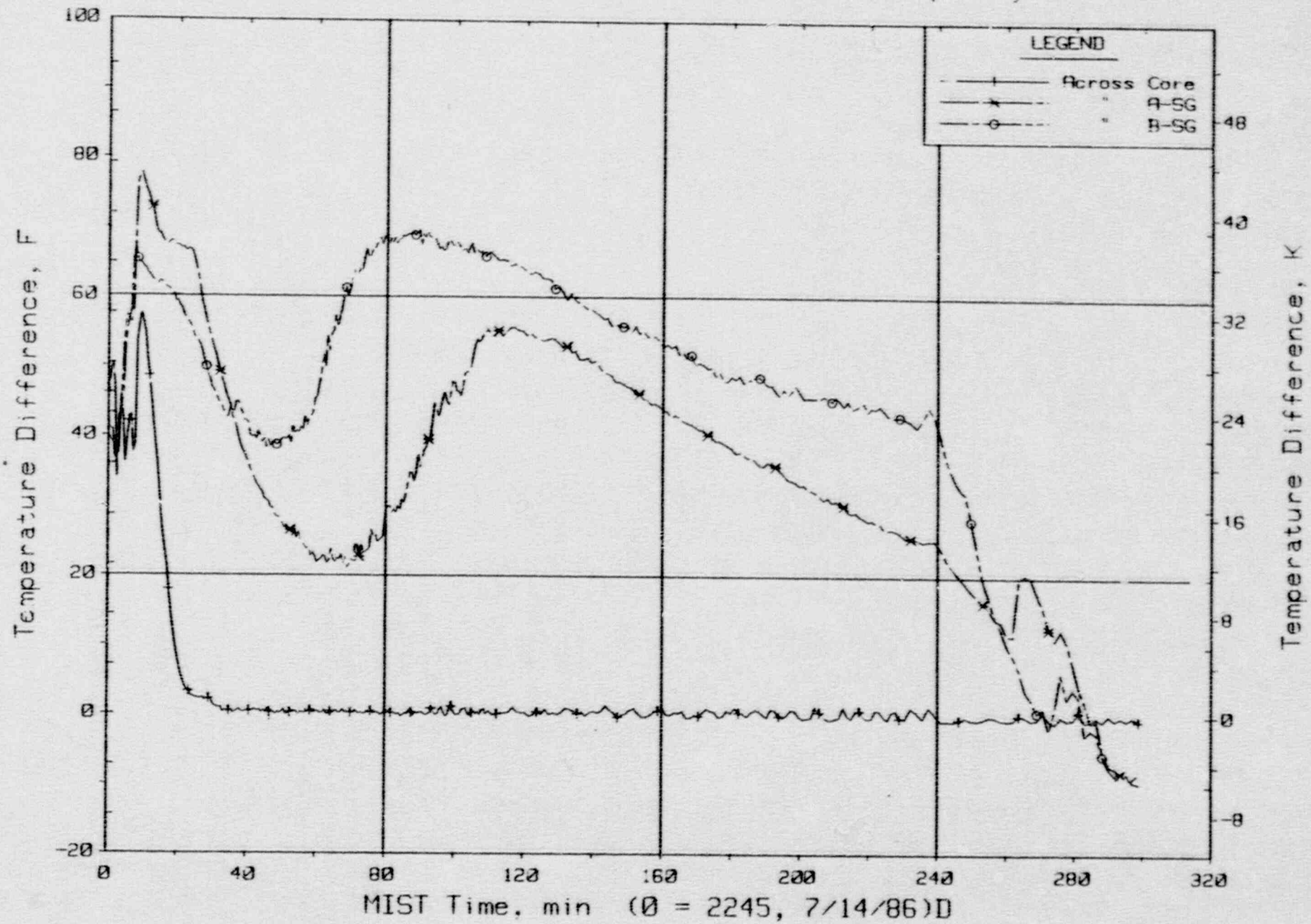

Key Temperature Differences.

Fri Oct 28 16:18:26 1988

PRTD2

FINAL DATA

T320604: Group 32 SBLOCA Test 6, Reduced-Capacity HPI.

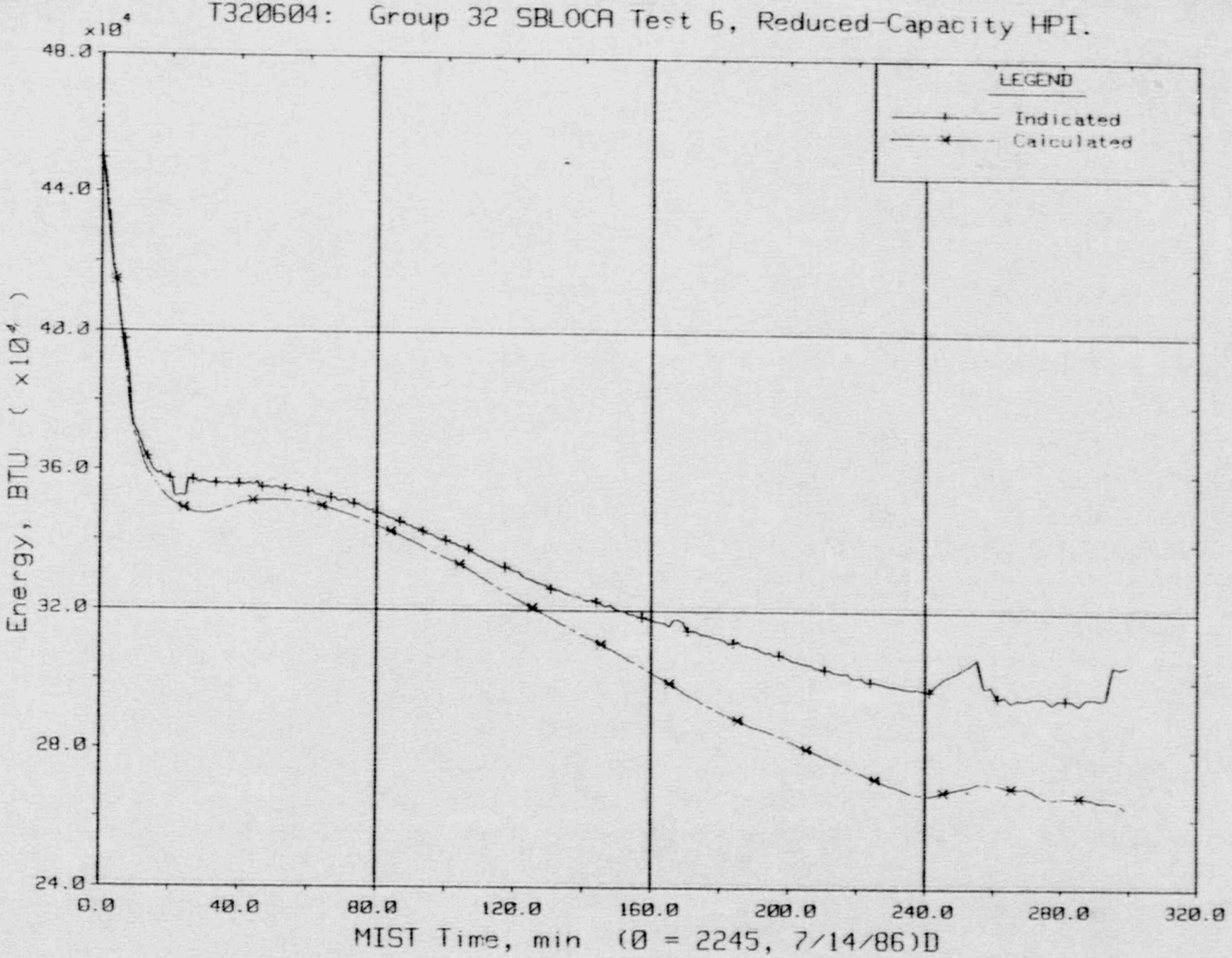

Primary System Total Fluid Energy.

Thu Jun 9 18:29:51 1988

PRTE2

FINAL DATA

T320604: Group 32 SBLOCA Test 6, Reduced-Capacity HPI.

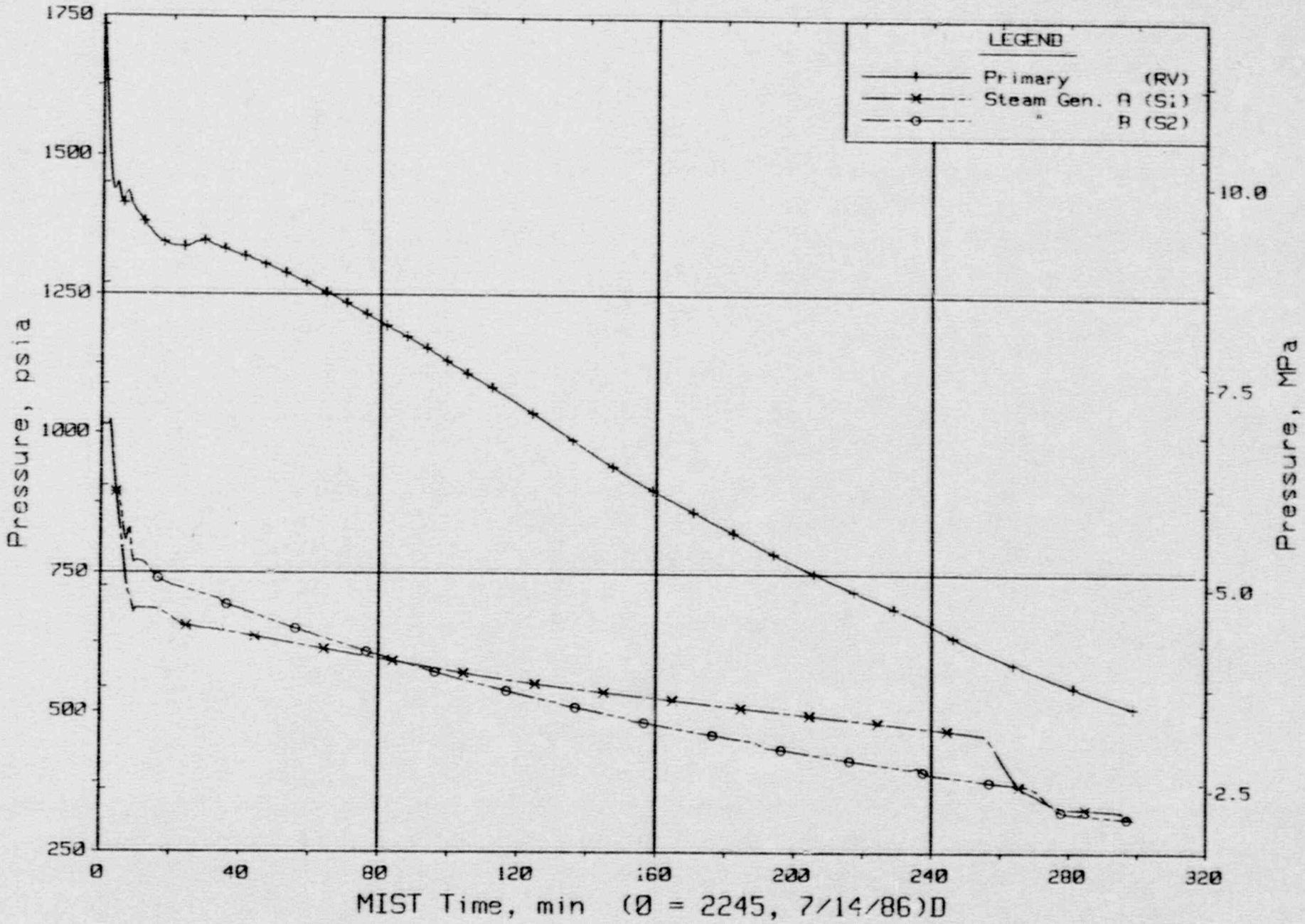

Primary and Secondary System Pressures (GP01s).

Fri Oct 28 16:22:10 1988

PSGP1

FINAL DATA

T320624: Group 32 SBLOCA Test 6, Peduced-Capacity HPI.

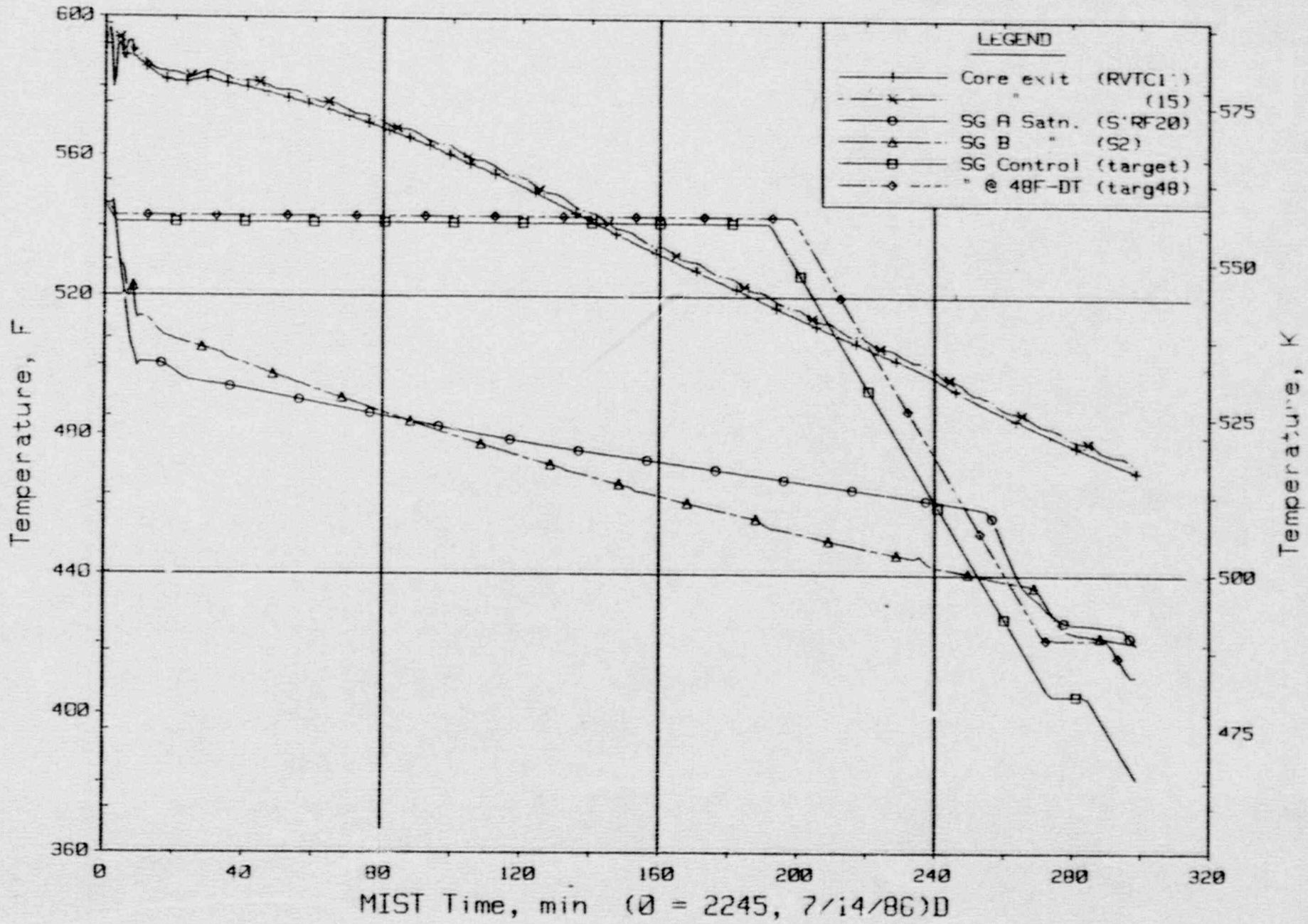

Steam Generator Secondary Saturation and Control Temperatures.

Fri Oct 28 16:27:35 1988

PSTC3

FINAL DATA

T320604: Group 32 SBLOCA Test 6, Reduced-Capacity HPI.

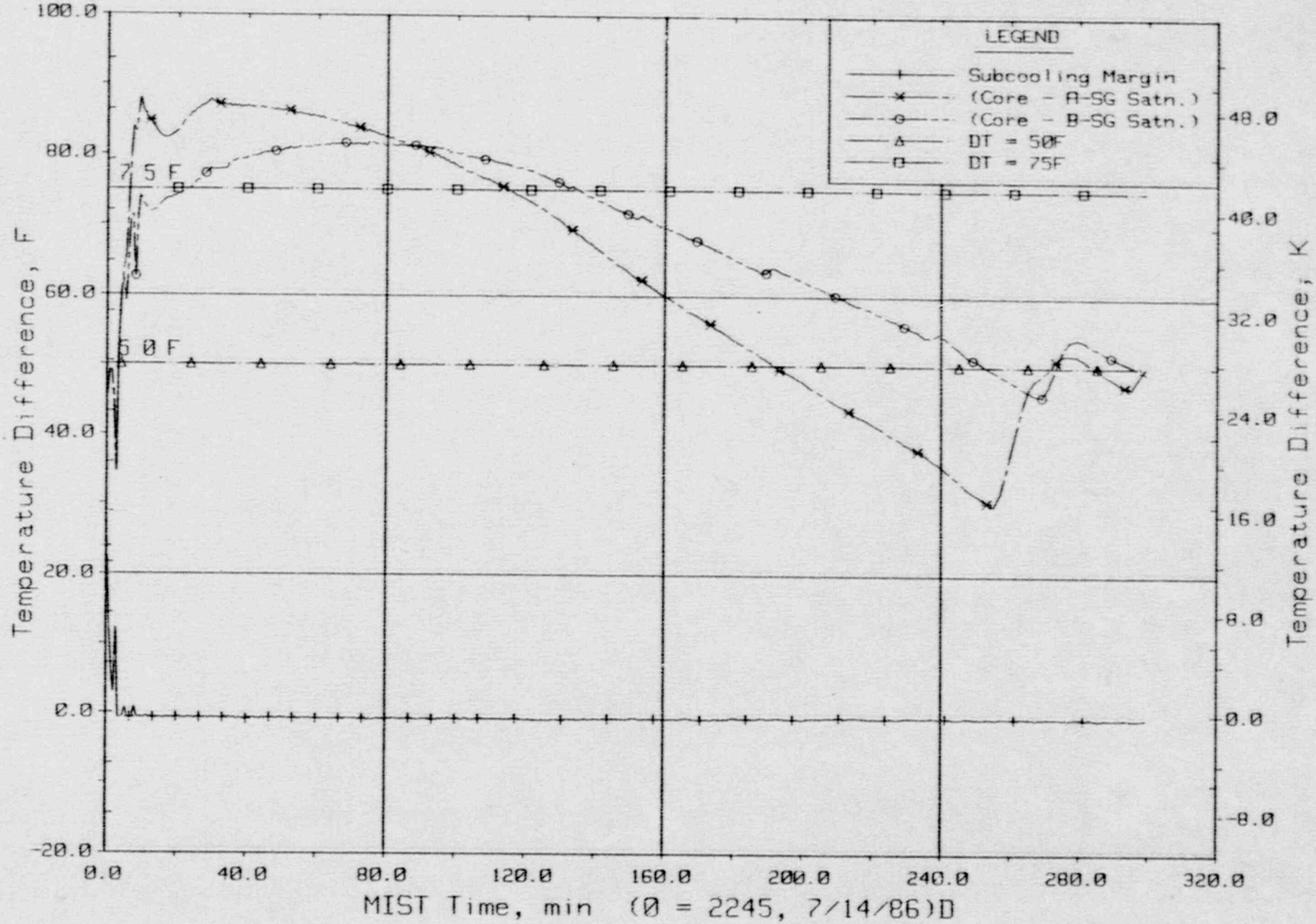

Control Temperature Differences.

Thu Jun 9 18:37:23 1988

PSTD1

FINAL DATA

T320604: Group 32 SBLOCA Test 6, Reduced-Capacity HPI.

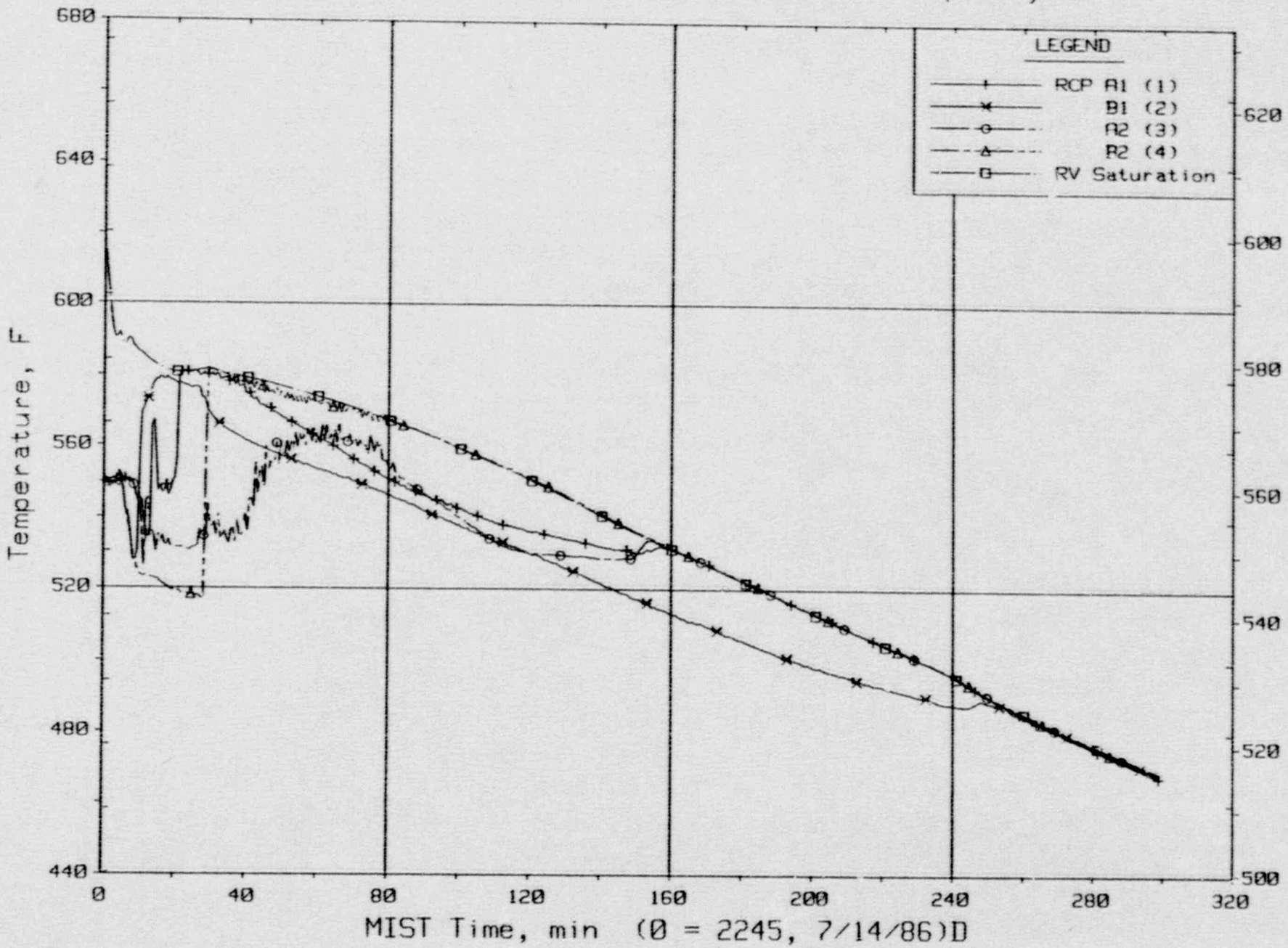

Pump Suction Fluid Temperature (CnRT01s).

Fri Oct 28 17:10:12 1988

PURT0

FINAL DATA

T320604: Group 32 SBLOCA Test 6, Reduced-Capacity HPI.

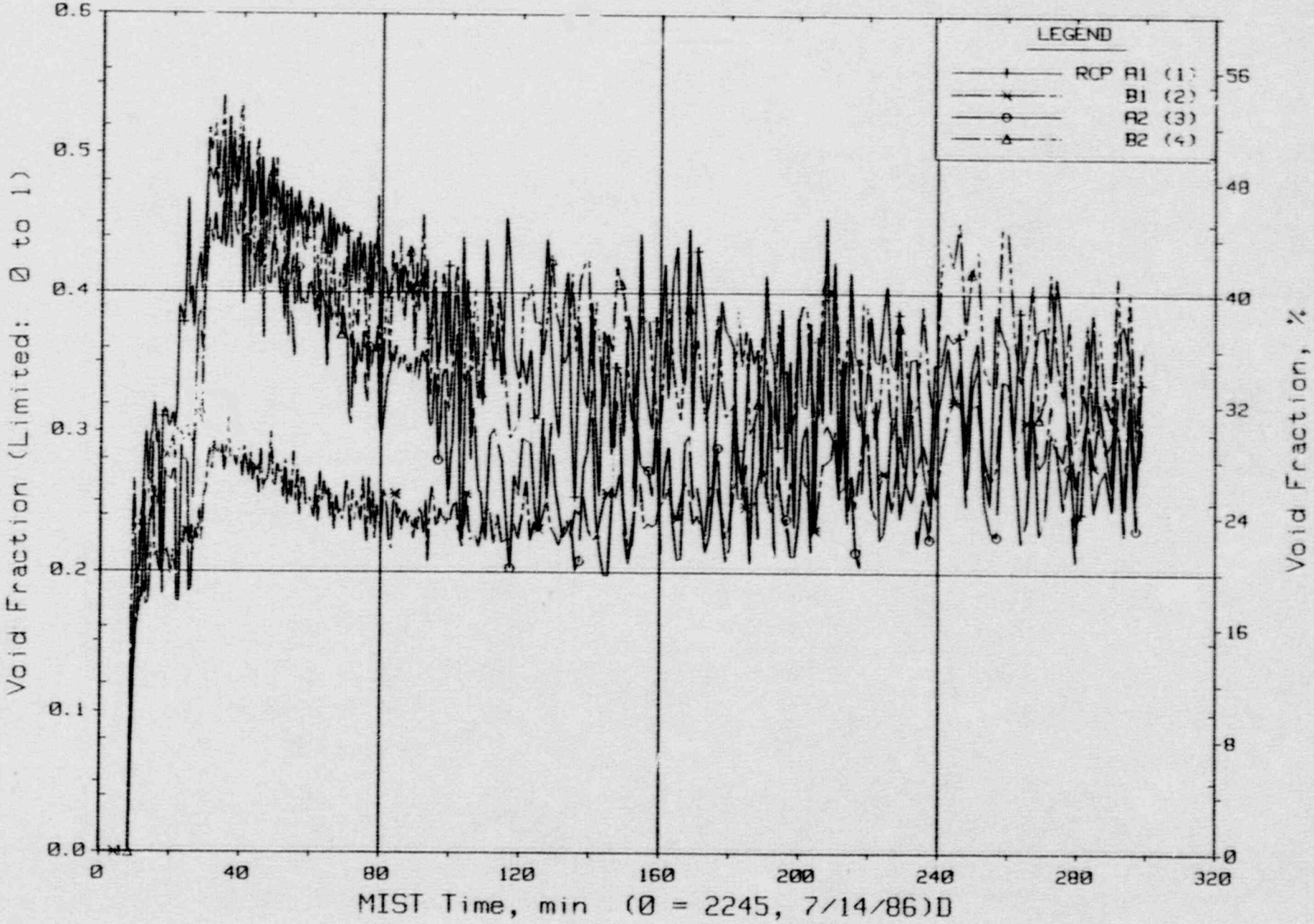

Pump Suction Void Fraction From Gamma Densitometers (CnGD21).

Fri Oct 28 17:13:57 1988

PUVF2

FINAL DATA

T320604: Group 32 SBLOCA Test 6, Reduced-Capacity HPI.

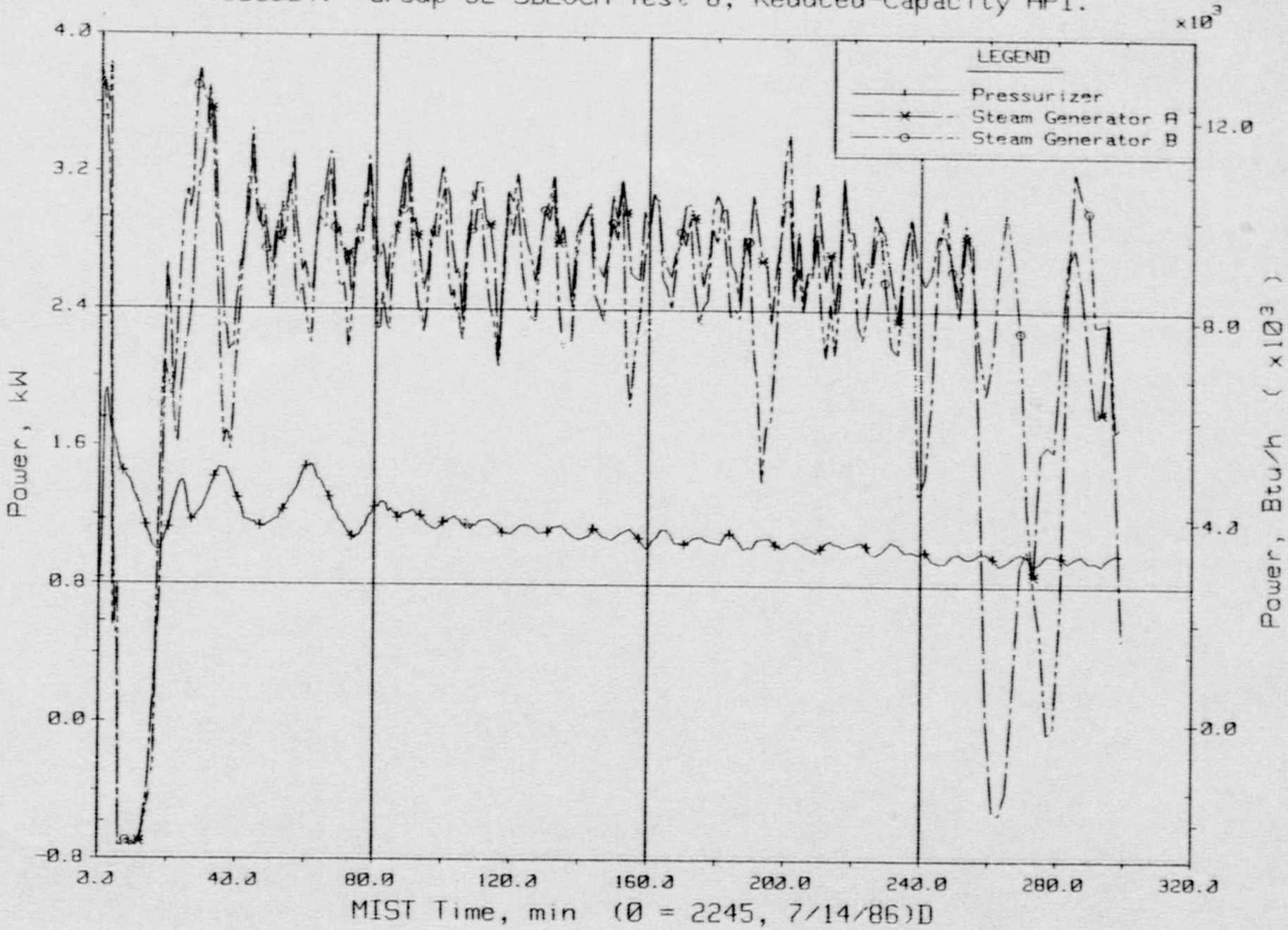

Guard Heater Specified Power, Pressurizer and Steam Generators.

Thu Jun 9 18:42:31 1988

PZGQ1

FINAL DATA

T320604: Group 32 SBLOCA Test 6, Reduced-Capacity HPI.

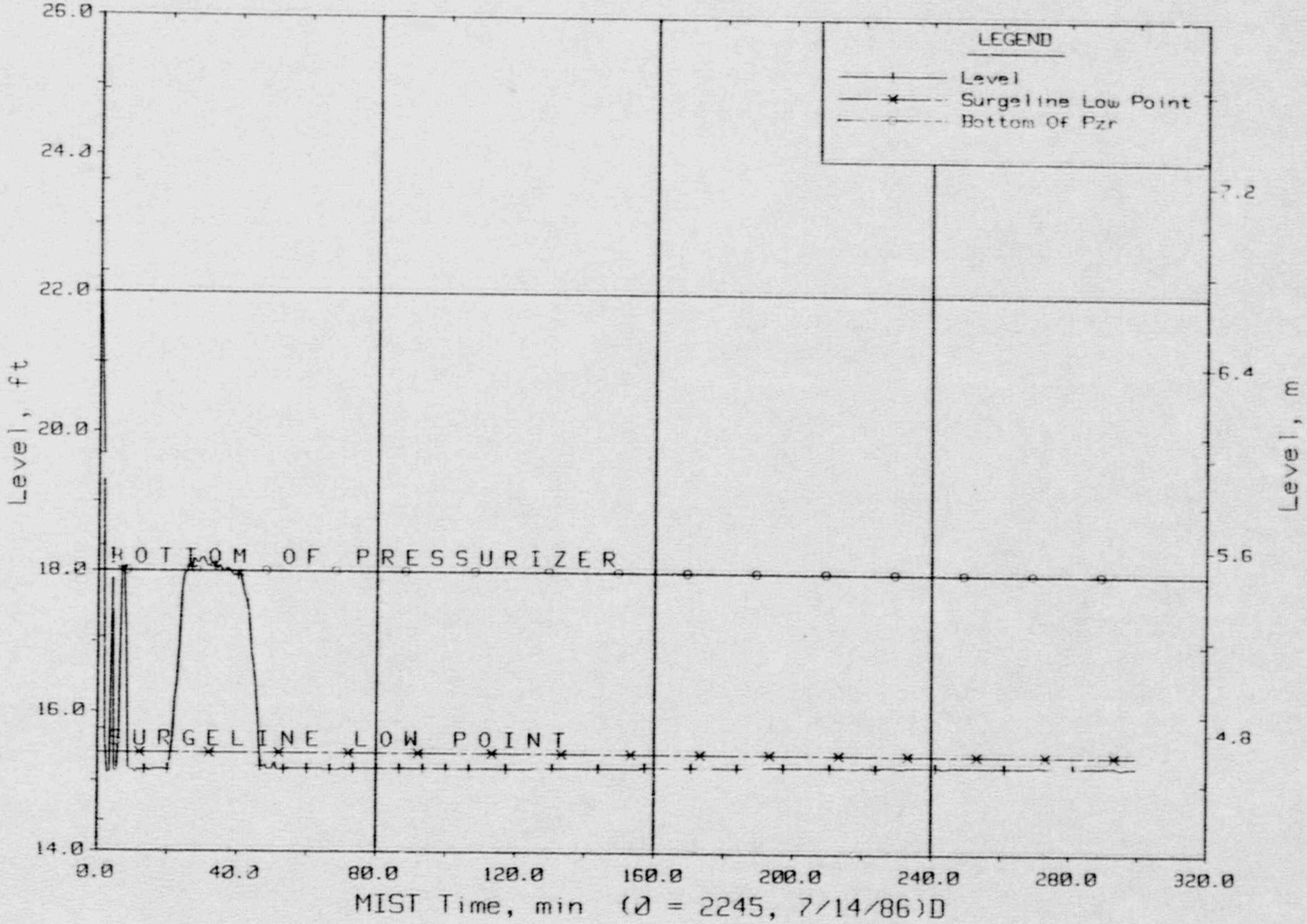

Pressurizer Collapsed Liquid Level (PZLV20).

Thu Jun 9 18:45:18 1988

PZLV1

FINAL DATA

T320604: Group 32 SBLOCA Test 6, Reduced-Capacity HPI.

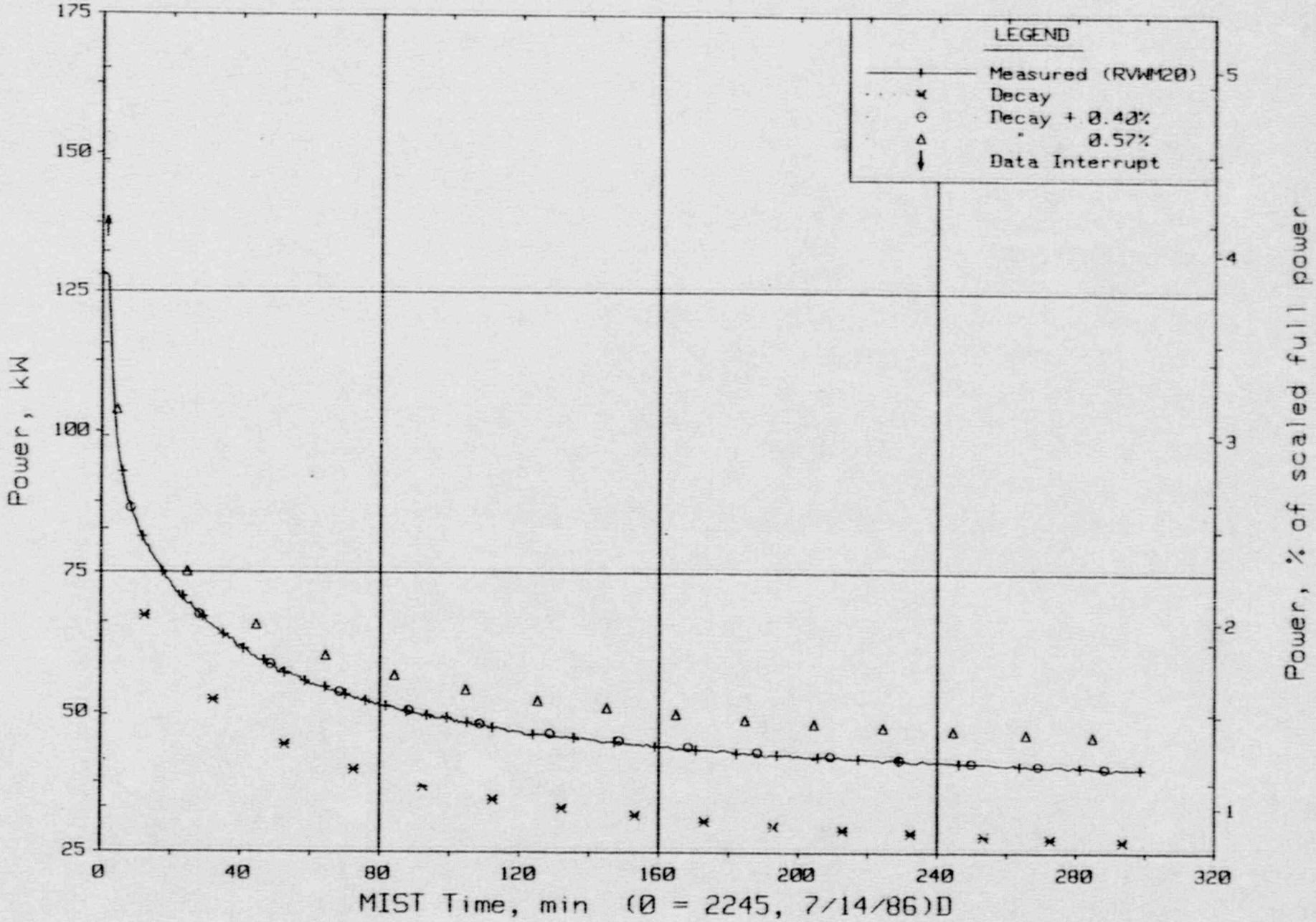

Core Power.

Fri Oct 28 17:17:16 1988

RVKW0

FINAL DATA

T320604: Group 32 SBLOCA Test 6, Reduced-Capacity HPI.

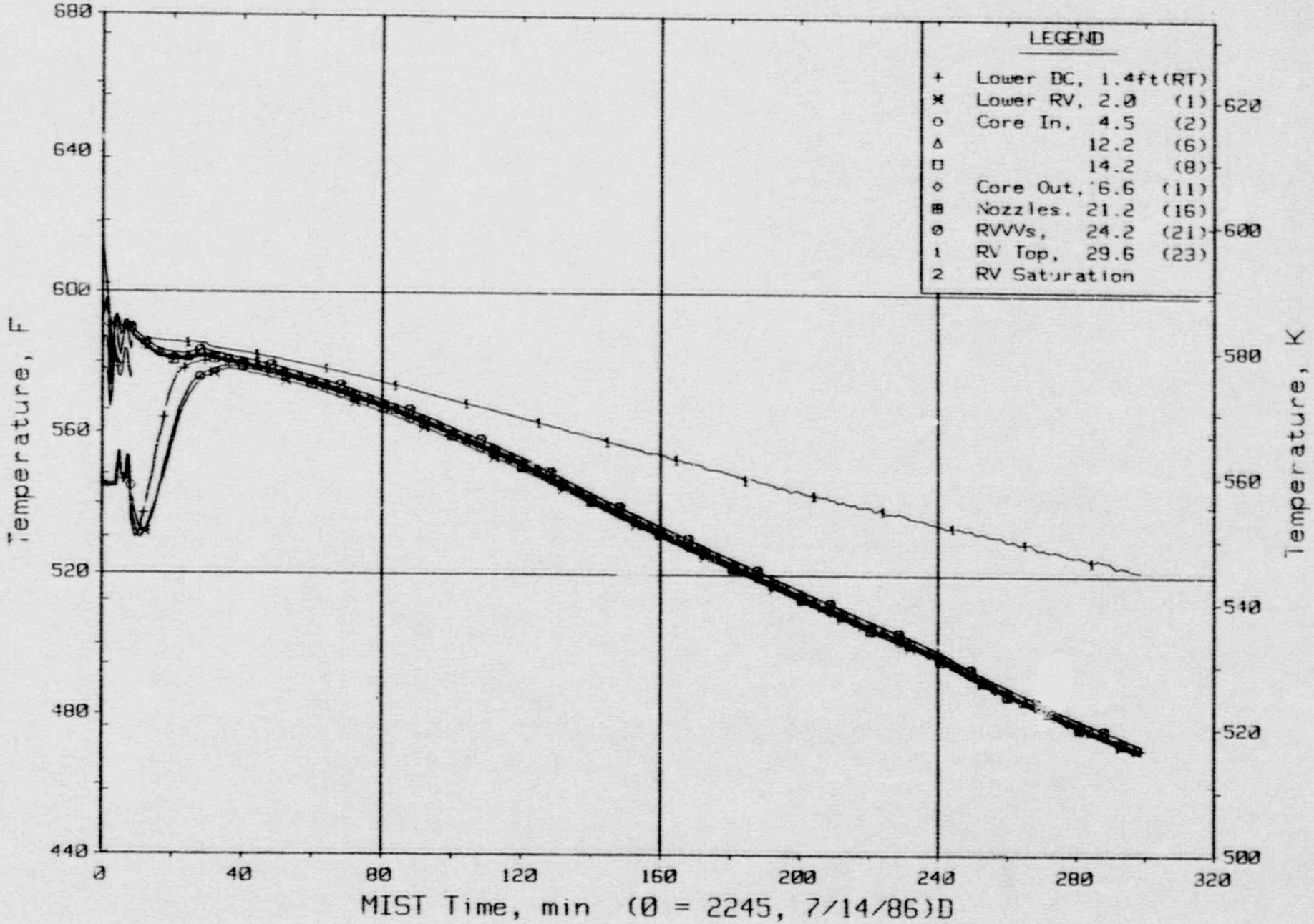

Core Unit Cell and Reactor Vessel Fluid Temperatures (RVTCs).

Fri Oct 28 16:40:20 1988

RVTC0

FINAL DATA

T320604: Group 32 SBLOCA Test 6, Reduced-Capacity HPI.

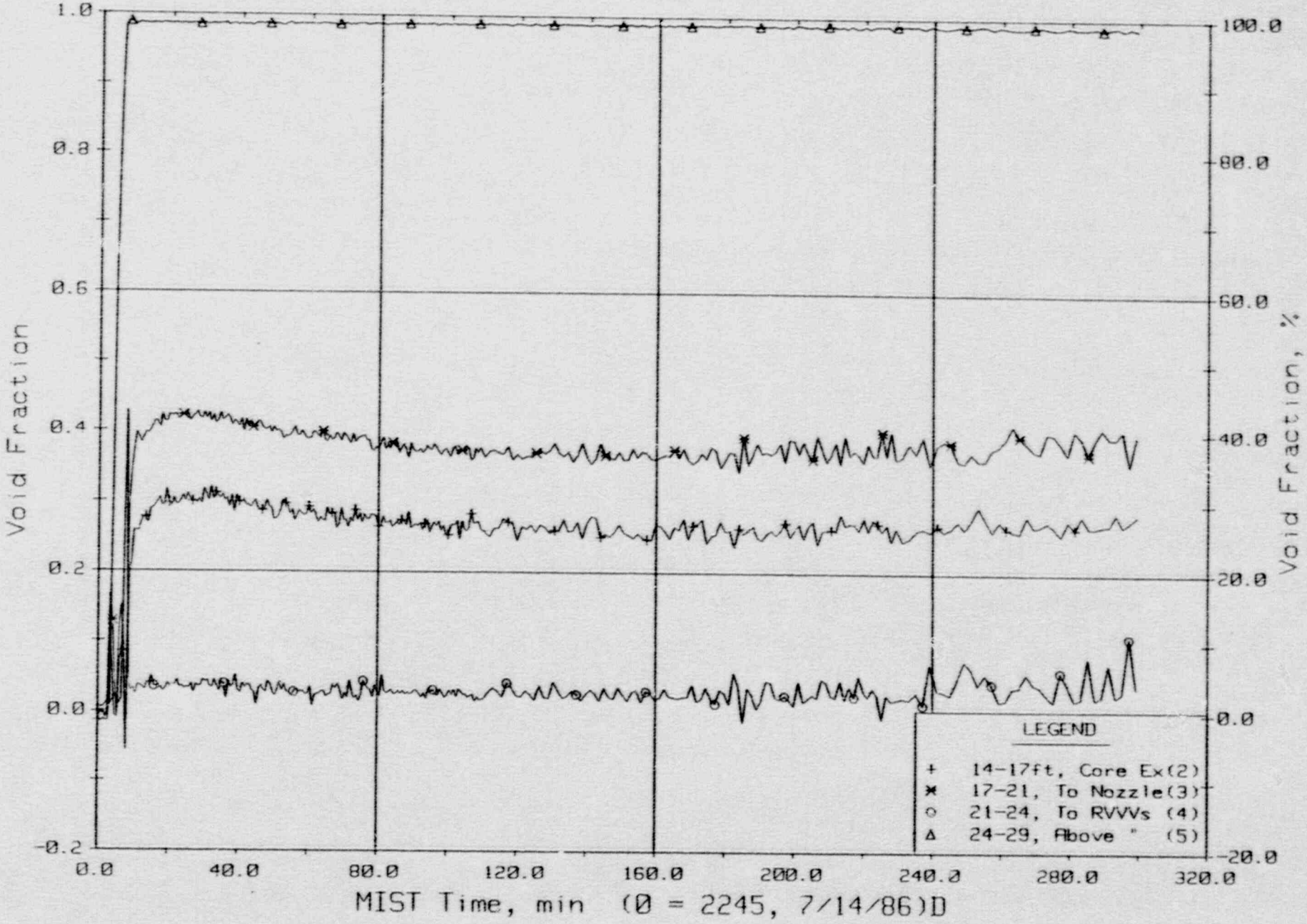

Reactor Vessel Void Fractions From Differential Pressures (RVVFs).

Thu Jun 9 18:53:45 1988

RVVF1

FINAL DATA

T320604: Group 32 SBLOCA Test 6, Reduced-Capacity HPI.

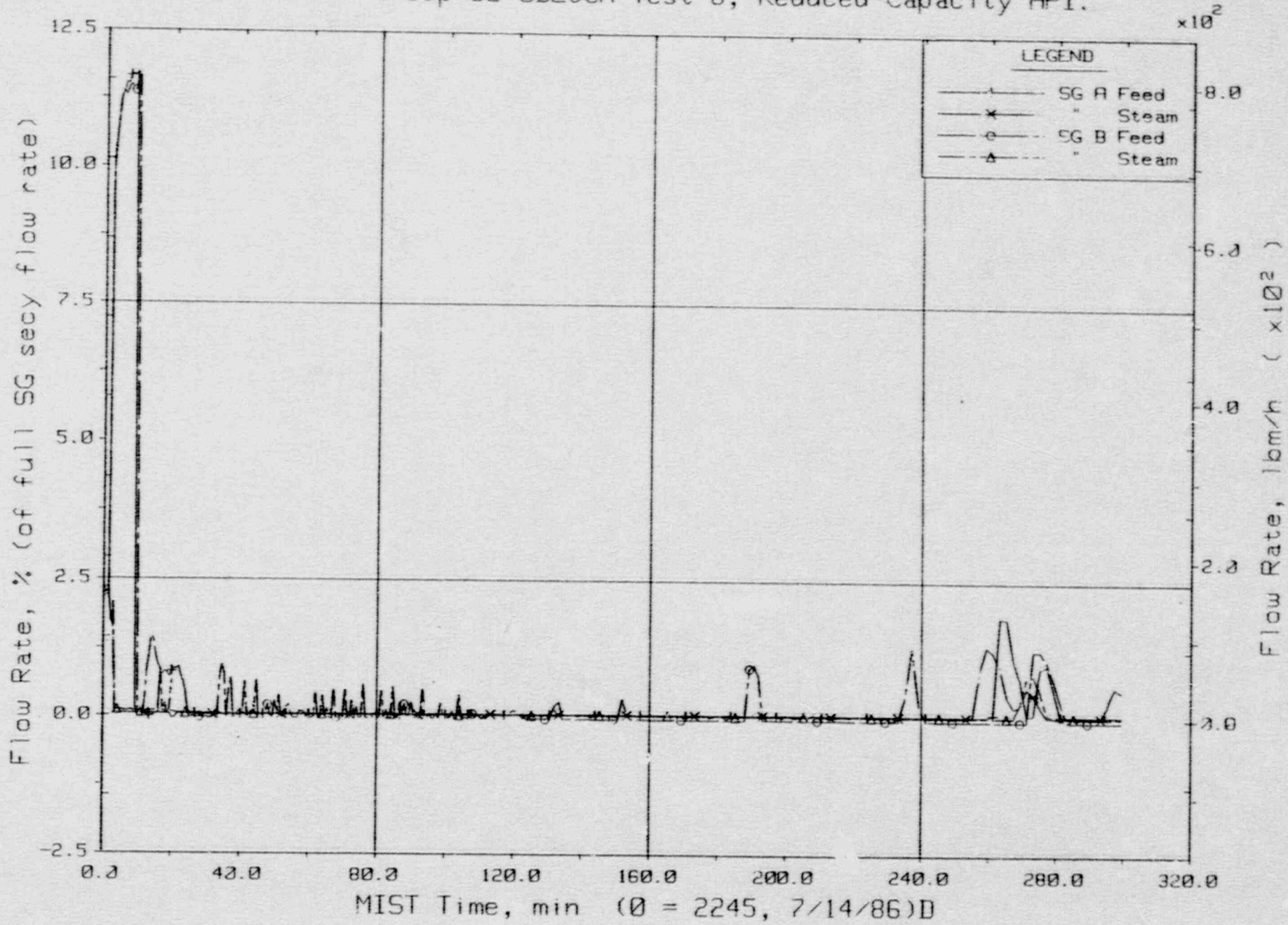

Steam Generator Secondary System Flow Rates.

Thu Jun 9 18:56:22 1988

SGFL2

FINAL DATA

T32Ø6Ø4: Group 32 SBLOCA Test 6, Reduced-Capacity HPI.

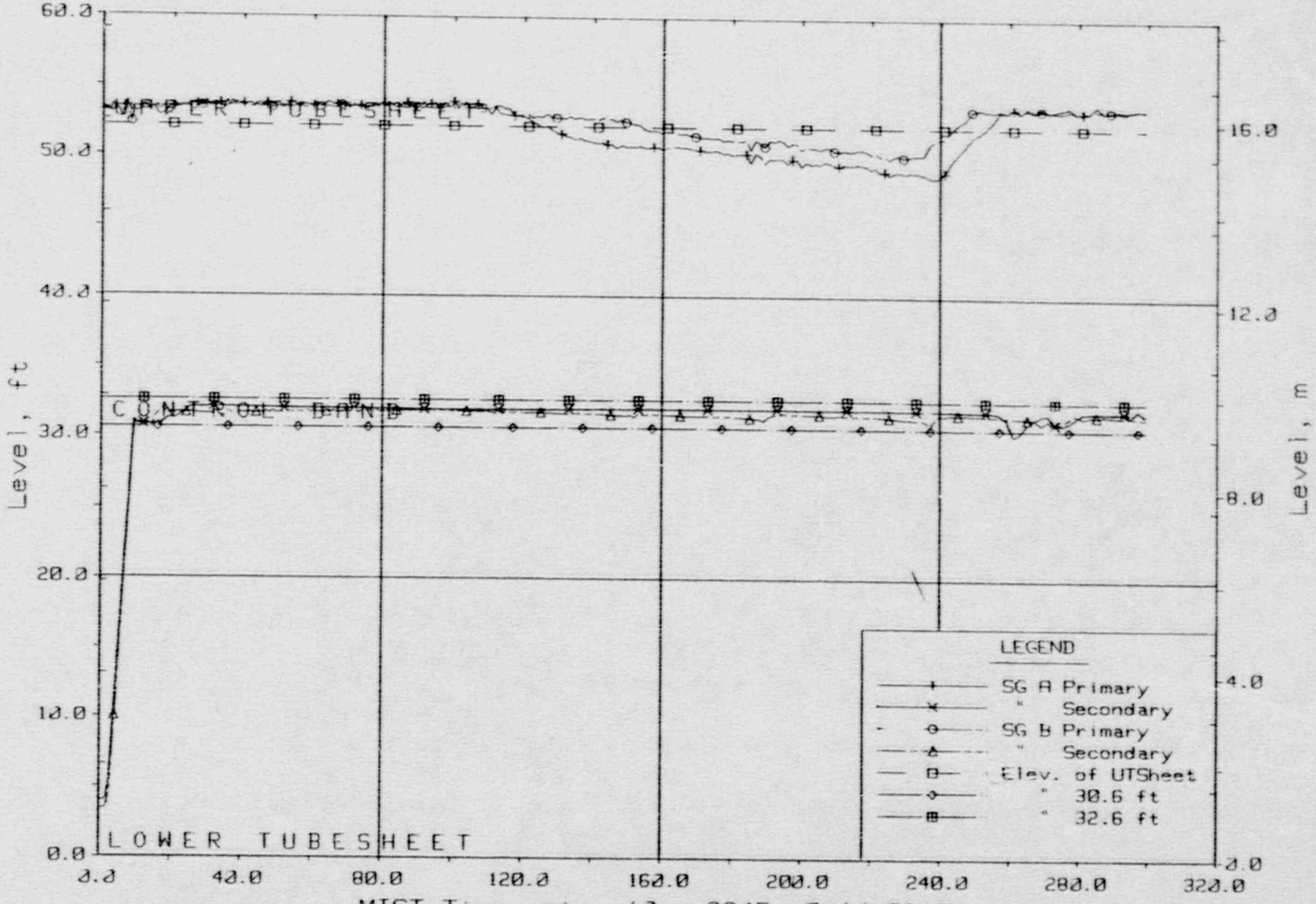

Steam Generator Collapsed Liquid Levels.

Thu Jun 9 18:59:30 1988

SGLV2

FINAL DATA

T320604: Group 32 SBLOCA Test 6, Reduced-Capacity HPI.

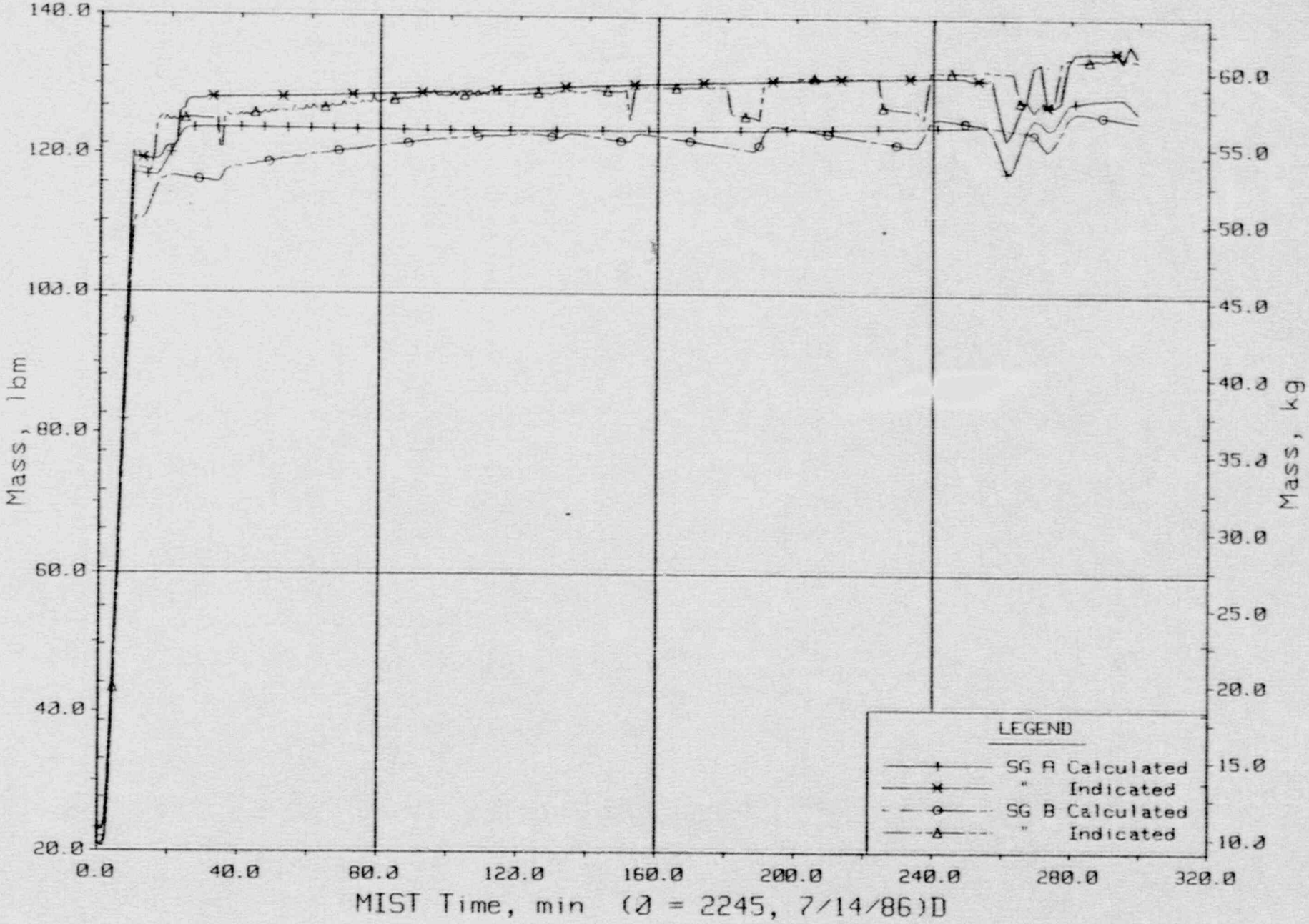

Steam Generator Secondary Fluid Mass Balances.

Thu Jun 9 19:02:13 1988

SGML1

FINAL DATA.

T320604: Group 32 SBLOCA Test 6, Reduced-Capacity HPI.

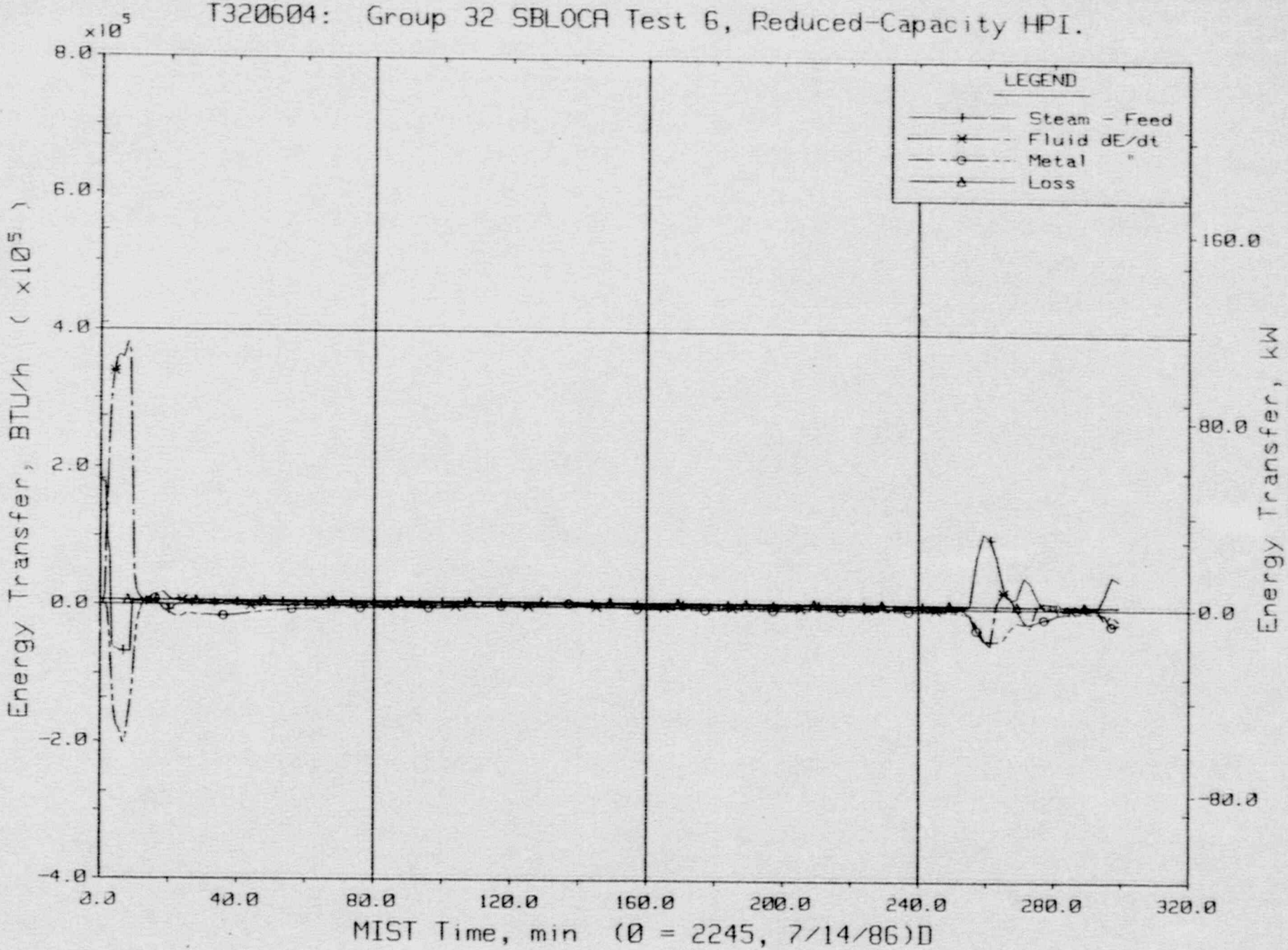

Steam Generator A Energy Transfer.

Thu Jun 9 19:05:06 1988

SGQE3

FINAL DATA

T320604: Group 32 SBLOCA Test 6, Reduced-Capacity HPI.

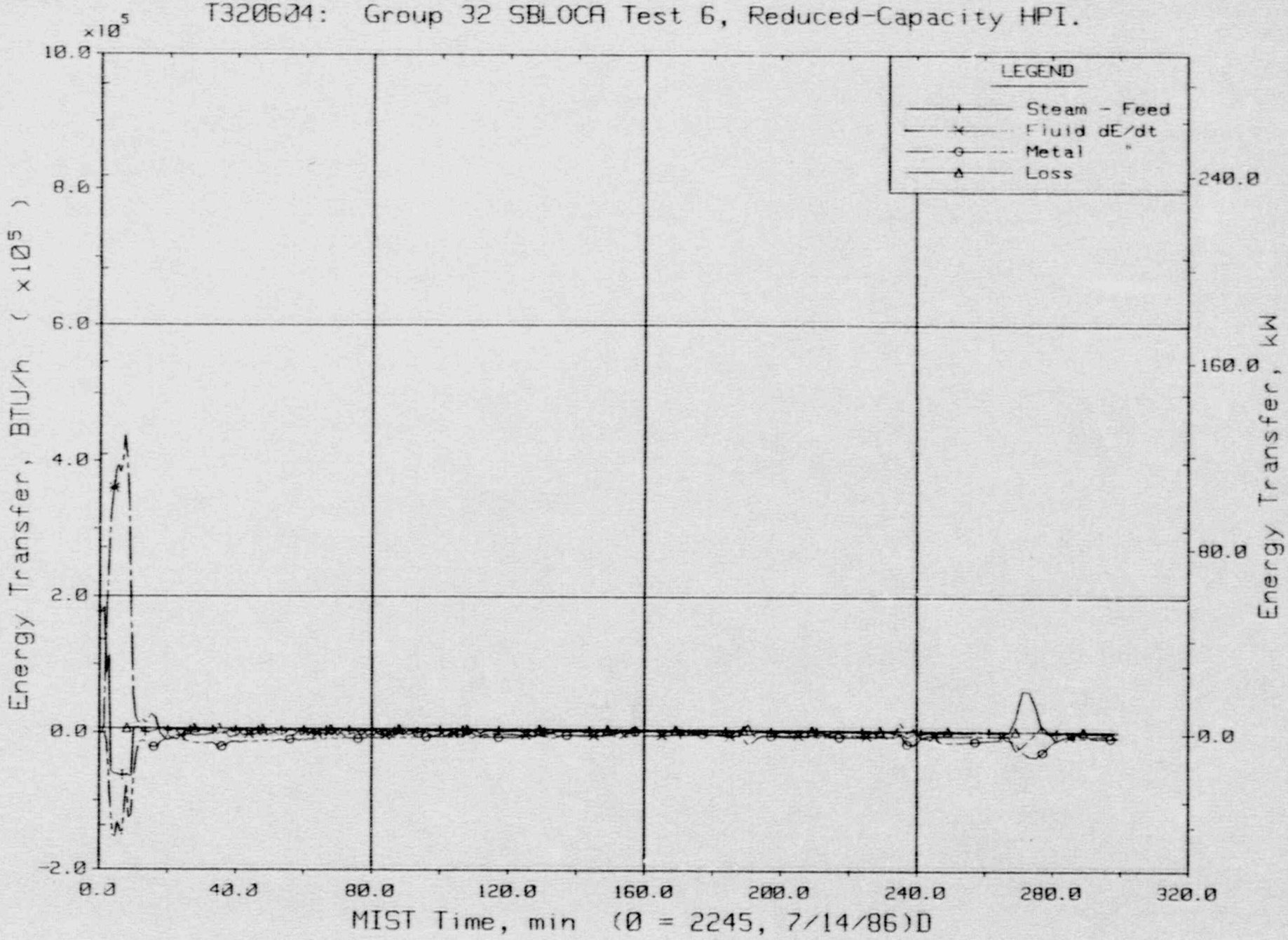

Steam Generator B Energy Transfer.

FINAL DATA

T322604: Group 32 SBLOCA Test 6, Reduced-Capacity HPI.

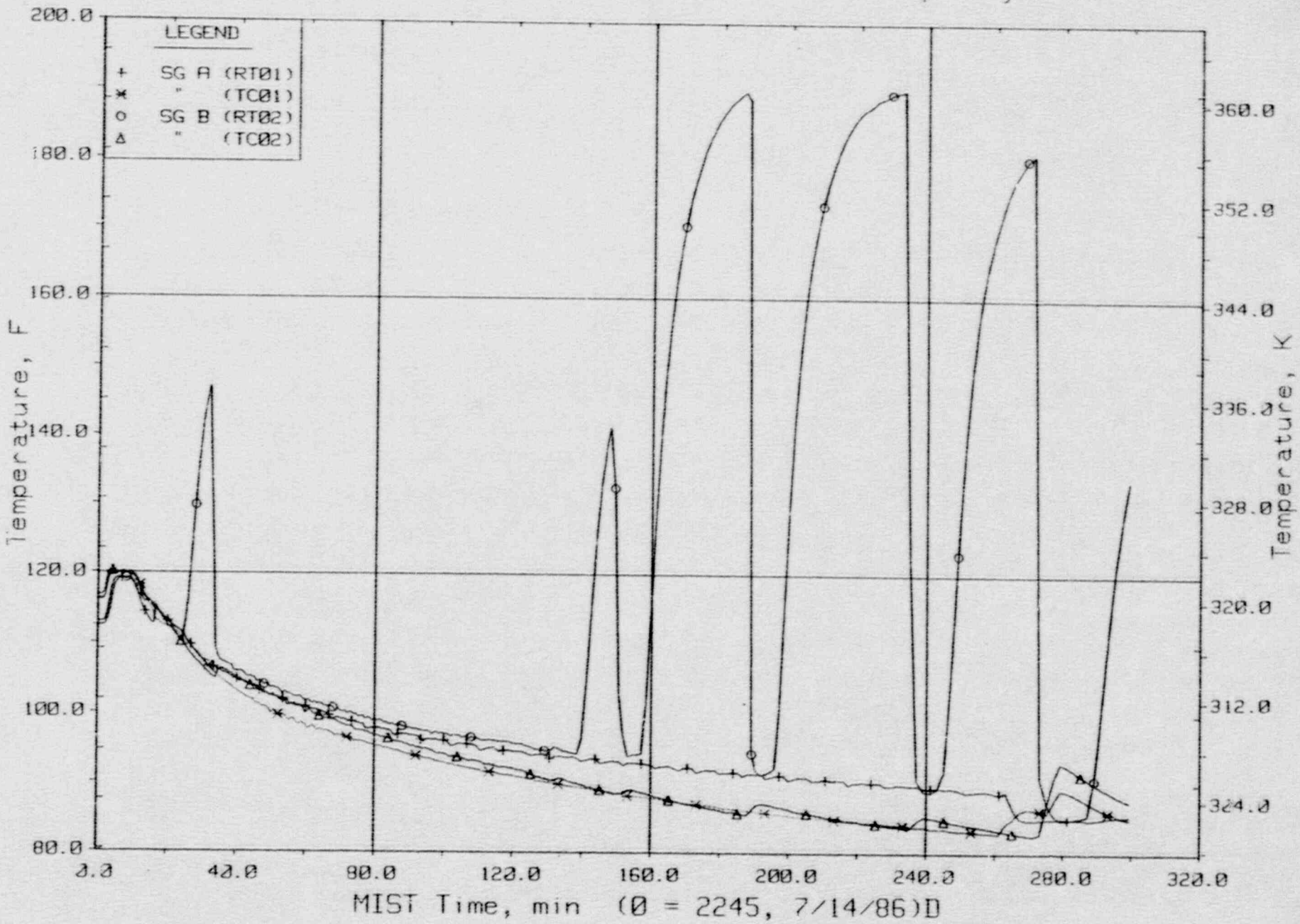

Feedwater Temperatures (SFs).

Thu Jun 9 19:10:08 1988

SGRT1

FINAL DATA

T320604: Group 32 SBLOCA Test 6, Reduced-Capacity HPI.

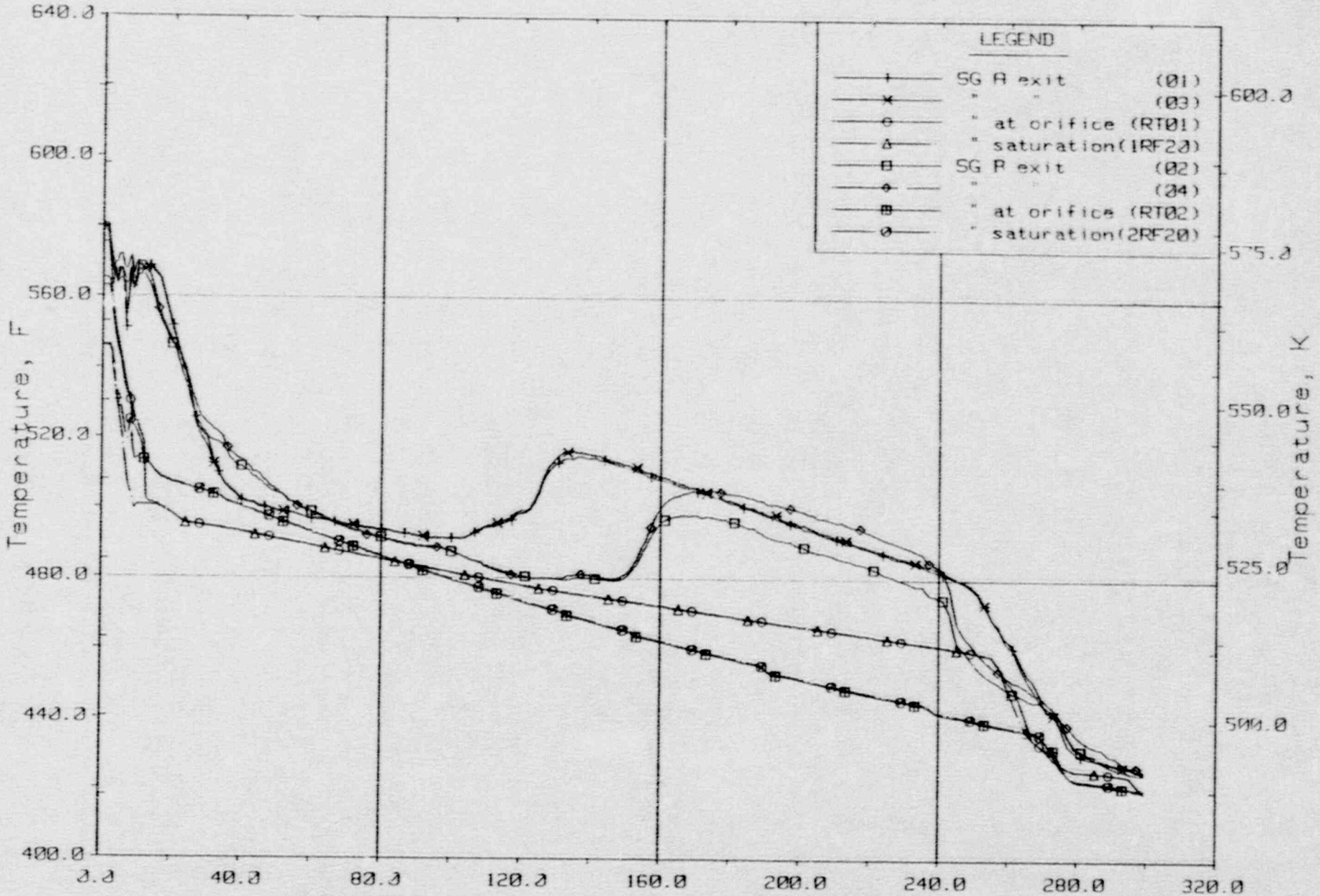

Steam Generator Steam Outlet Temperatures (SSTCs).

Thu Jun 9 19:13:15 1988

SGRT2

FINAL DATA

T320604: Group 32 SBLOCA Test 6, Reduced-Capacity HPI.

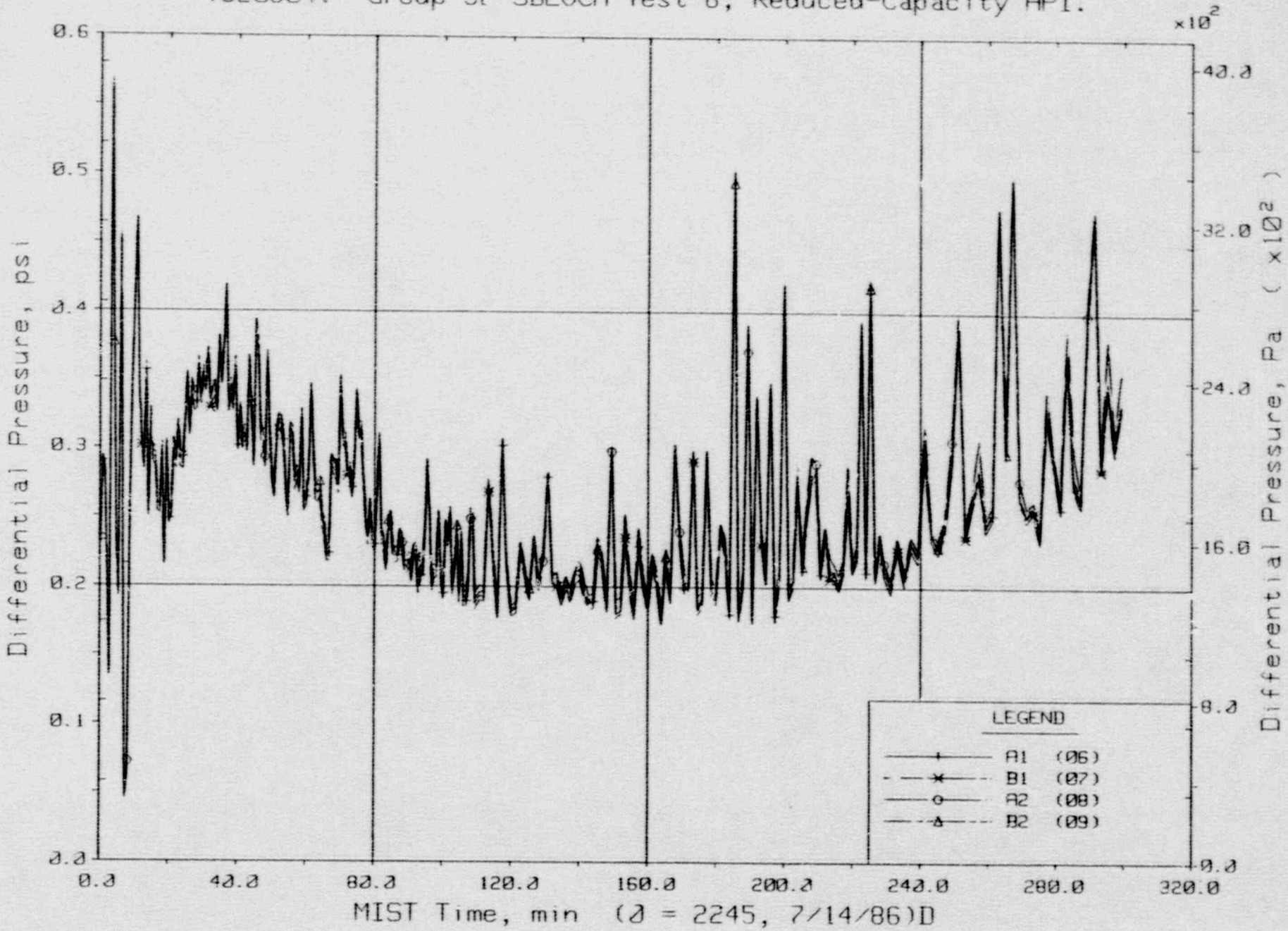

Reactor Vessel Vent Valve Differential Pressures (RVDPs).

Thu Jun 9 19:17:25 1988

VVDP1

FINAL DATA

T320604: Group 32 SBLOCA Test 6, Reduced-Capacity HPI.

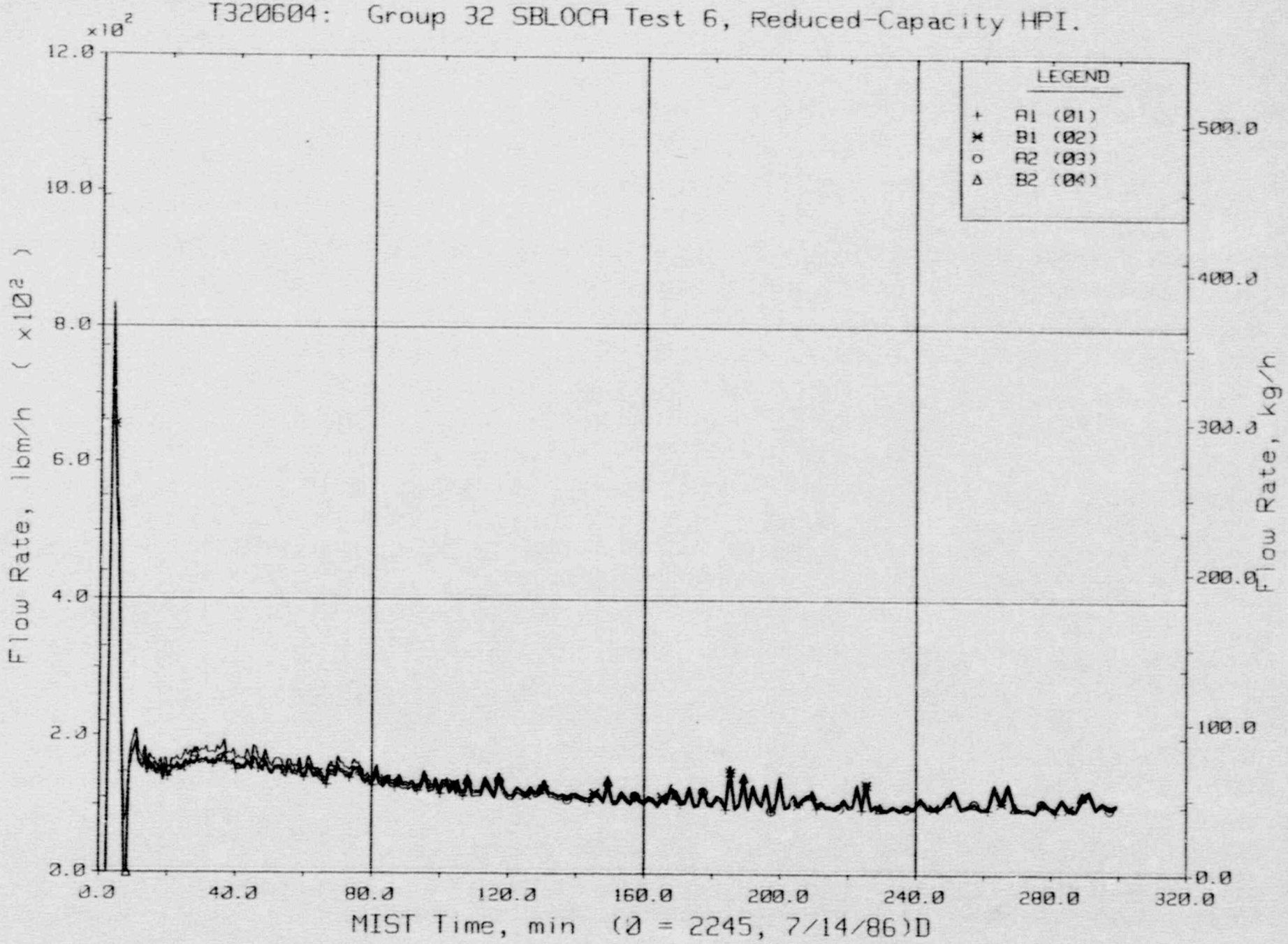

Reactor Vessel Vent Valve Flow Rates (RVORs).

Thu Jun 9 19:21:08 1988

VVFL1

FINAL DATA

T320604: Group 32 SBLOCA Test 6, Reduced-Capacity HPI.

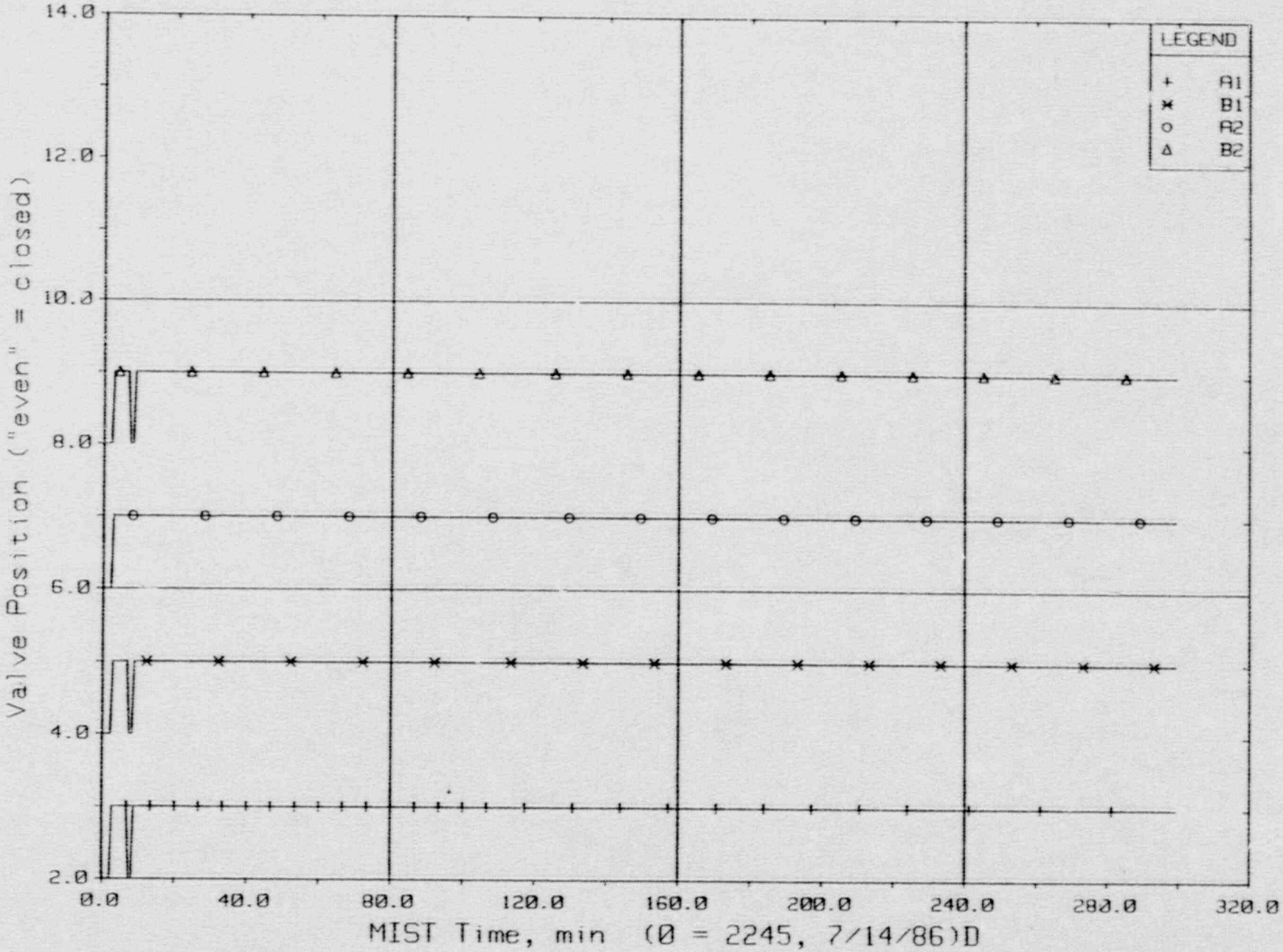

Reactor Vessel Vent Valve Positions.

Thu Jun 9 19:23:31 1988

VVL51

FINAL DATA

T320604: Group 32 SBLOCA Test 6, Reduced-Capacity HPI.

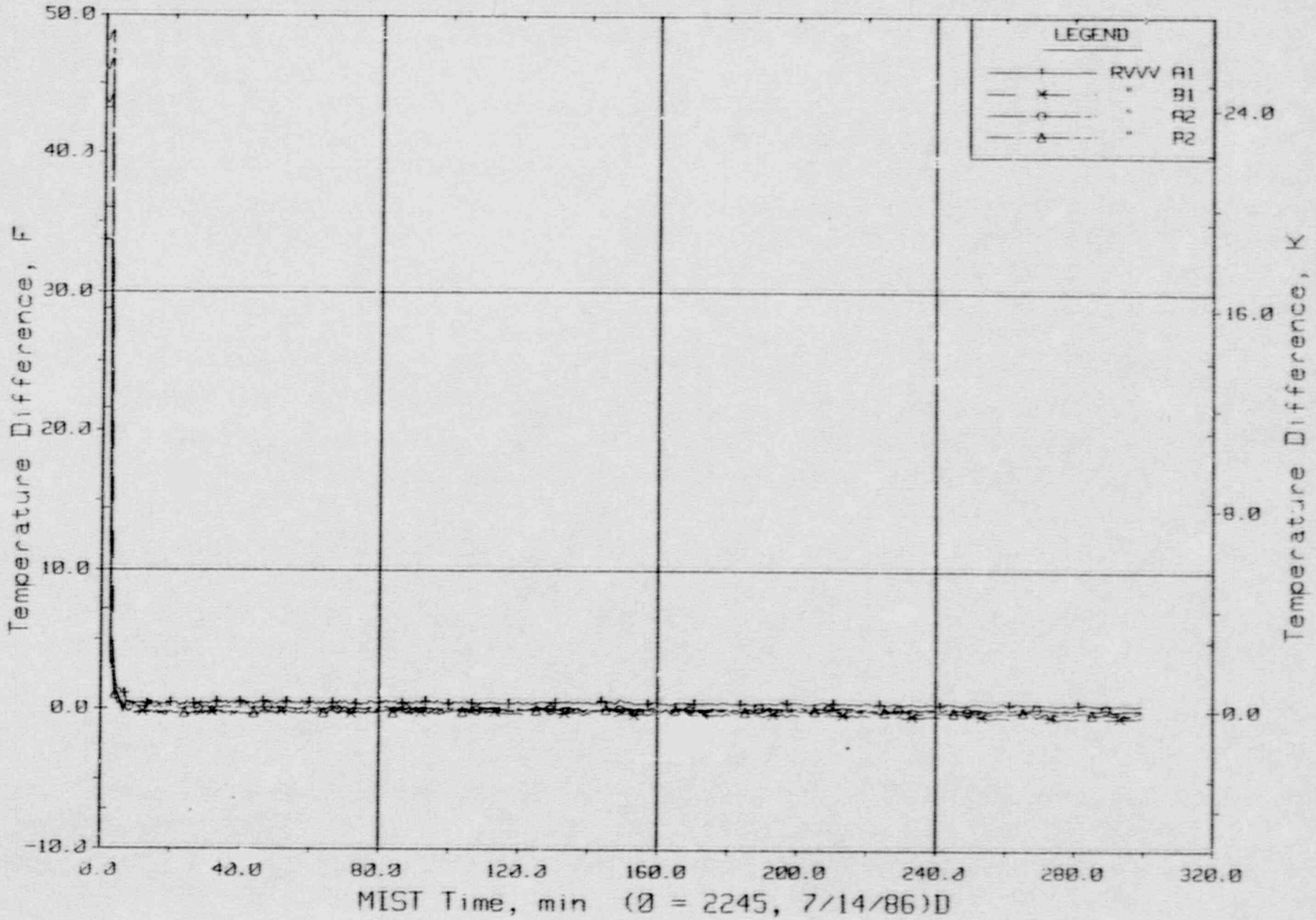

Temperature Differences Across Vent Valves.

Thu Jun 9 19:25:43 1988

VVTD1